

Small Molecules with Anti-trypanosomal and Anti-leishmanial Activity

Sebastian Siegfried Gehrke

A thesis submitted for the degree of Doctor of Philosophy

School of Pharmacy

University of East Anglia

October 2012

Acknowledgement

I must first acknowledge my supervisors Dr. Gerd K. Wagner, Dr. Dietmar Steverding, Dr. Richard Morris and Dr. Kevin Tyler who offered me this fantastic opportunity to develop a research project spanning the disciplines of medicinal chemistry, parasitology and computational biology. I specifically thank them for the stimulating discussions, suggestions and guidance towards a career as independent researcher.

I would like to thank Dr. Andre Tempone (Instituto Adolfo Lutz, Universidade de Sao Paulo, Sao Paulo, Brazil) for hosting a research visit and for giving me the opportunity to test my inhibitor libraries against *T.cruzi* and *Leishmania infantum*. Dr. Ed Tate and Megan Wright (Imperial College London) provided reagents essential for my target identification studies in a fruitful collaboration. Sincere thanks go to Prof. Robert Hider (King's College London) for providing iron chelating agents for the assessment of anti-parasitic activities, as well as advice and encouragement. Thanks go to Prof. Schlitzer (Phillip's University, Marburg, Germany), for the provision of additional molecular inhibitors.

I must thank the Norwich Research Park for a four year studentship and funding this research project. I also would like to thank King's College London (King's Brazil Initiative) and FAPESP Sao Paulo for financially supporting my three-week visit to Sao Paulo, Brazil. I further would like to thank King's College London and the John Innes Centre (Norwich) for additional financial support.

I am grateful for the scientific support I received, which enabled me to thrive both as a chemist and a biologist. I would like to thank Dr. Colin MacDonald (UEA, Norwich) and Dr. James Mason (King's College London) for the NMR support. I am also very grateful to Dr. David Hughes (UEA, Norwich) for recording the X-ray structures of small molecular inhibitors. I would like to thank the EPSRC national mass spectrometry service centre (Swansea University, Swansea, UK) for the recording of mass spectrometric data. I would like to also thank the tissue culture managers at UEA and KCL for providing a well organised working environment.

My lab colleagues have made my time at UEA, JIC and KCL very enjoyable. Particular thanks go to past and present members of the groups run by Gerd Wagner, Richard Morris, Kevin Tyler and Andre Tempone for the warm welcome, integration and friendship. A special thanks goes to the students Karin Pleban, Kathleen Adom, Afra Farook, Bill Smith, Sarah Seiberth, Adam Wiscombe, Cara Henwood, Riya Patel and Ben Young who contributed to the synthesis of several inhibitors.

I would like to thank Dr. Emma Sherwood for great support throughout my PhD, many good suggestions and proof reading of this thesis.

Of course I would never have got to where I am today without my family, whose unconditional love and support, gave me the confidence to pursue my dream to study science at the highest level.

Abstract

Parasitic diseases such as Human African Trypanosomiasis (HAT), Chagas disease and Leishmaniasis cause thousands of fatalities each year. Current chemotherapy is based on drugs discovered over 60 years ago that are expensive and difficult to administer. The drug-pipeline is virtually dry and the trickle of inhibitors that are in development are largely based on those that are already in use. Parasite resistance to these drugs is developing, underlining the urgent need for novel anti-parasitic drug therapies.

This study focused on the identification of novel small molecular inhibitors with anti-parasitic activities against *Trypanosoma brucei* spp. (HAT), *Trypanosoma cruzi* spp. (Chagas disease) and *Leishmania infantum* spp. (Leishmaniasis) with a particular focus on combining broad-spectrum activity with parasite-specificity.

A two-pronged approach was used to develop an effective chemotherapy through the optimisation of known inhibitors of glycosylphosphatidylinositol (GPI)-anchor biosynthesis and improving the specificity of iron chelators.

GPI anchor biosynthesis is a pathway essential for survival to all three parasites. Here, a rhodanine-N-acetic acid derivative served as the starting point for the development of a library of 379 thiazolidine-4-one and pyrazolone analogues. These were systematically screened against three species of parasitic protozoa and a mammalian cell line in order to identify inhibitors which demonstrate low- μ M anti-parasitic activity and a good selectivity profile.

Further target identification studies on the effect of these new inhibitors using *in vitro* assays confirmed inhibition of GPI anchor biosynthesis as a mode of action. This provides further evidence that the GPI anchor is a druggable target for the development of novel anti-parasitic agents against *T. brucei*, *T. cruzi* and *L. infantum*. Taken together, this work indicates that drugs targeting one feature common to all three protozoa can provide anti-parasitic activity with low toxicity against mammalian cells.

Contents

1	Introduction	1
1.1	Parasitic diseases	1
1.2	Current treatment for parasitic diseases	3
1.3	Current drug development	5
1.4	GPI-anchor biosynthesis as a prospective drug target	14
1.5	Rhodanine derivatives in drug discovery	17
1.6	Iron chelation as an anti-parasitic strategy	20
1.7	Parasite life cycles	22
2	Objectives	25
3	Rhodanine-N-acetic acid derivatives	26
3.1	Known biological activities of Rhodanine-N-acetic acid derivatives	26
3.2	Synthesis of inhibitor library	29
3.2.1	Synthesis of rhodanine-N-acetic acid derivatives	30
3.2.2	Knoevenagel reaction	31
3.2.3	Stereochemistry of the Knoevenagel reaction	33
3.2.4	Design of rhodanine-N-acetic acid derivatives with anti-parasitic activity .	36
3.2.5	Aromatic substitution strategies	37
3.2.6	Replacement of thiocarbonyl	39
3.2.7	Elongation of N3-sidechain	42
3.2.8	Esterification of carboxylic acid	45
3.2.9	Modification of the 3-benzyloxy group	49
3.2.10	Heterocyclic modifications	52
3.2.11	Reduction of the exo-cyclic double bond	56
3.2.12	Synthesis of photo-affinity label	57
3.3	Anti-trypanosomal activity	62
3.3.1	AlamarBlue & MTT activity/toxicity assays	62
3.3.2	Calculation of GI ₅₀ -values	65
3.3.3	Anti-Trypanosomal activity of rhodanine-N-acetic acid derivatives	65
3.3.4	Anti-trypanosomal activity of the rhodanine moiety	67
3.3.5	Derivatives with elongated N-3 side-chain linkers	69
3.3.6	N-1 ester modification and their anti-trypanosomal effect	71
3.3.7	Compounds with improved anti-parasitic activity after first optimisations .	75
3.3.8	Further optimisation of structure classes A,C and D	76

3.3.9	Heterocyclic modifications	80
3.3.10	Anti-trypanosomal effect of saturated rhodanine analogues	81
3.4	Anti-leishmanial activity	82
3.5	Target identification studies	86
3.5.1	Myristate labelling of GPI anchor biosynthesis	86
3.5.2	Flow cytometry analysis of <i>T. brucei</i> transferrin receptors	93
3.5.3	GPI cell-free radio-label assay	97
3.5.4	Target-based optimisation using homology modelling	102
3.5.5	Investigation of DPMS as a possible target for rhodanine inhibitors	108
3.6	Discussion	111
3.7	Summary	115
4	N-allyl rhodanine derivatives	116
4.1	previous biological activities of N-allyl rhodanine and analogues	116
4.2	Synthesis of inhibitor library	117
4.2.1	Aromatic Substitution	118
4.2.2	Replacement of the Thiocarbonyl X=O	119
4.2.3	Heterocyclic modifications	123
4.2.4	Reduction of the exo-cyclic double bond	127
4.3	Anti-parasitic activity	128
4.3.1	Anti-parasitic activity of N-allyl rhodanine derivatives	128
4.3.2	Modification of the thiocarbonyl	130
4.3.3	Modification of the 3-benzyloxy-substituent	131
4.3.4	Heterocyclic modifications	132
4.3.5	Effect of saturated N-propyl thiazolidine-2,4-dione derivative	133
4.4	Target identification studies	135
4.4.1	Myristate labelling of GPI anchor biosynthesis	135
4.4.2	Flow cytometry analysis of <i>T. brucei</i> transferrin receptors	138
4.4.3	GPI cell-free radio-label assay	142
4.5	Discussion	145
4.6	Summary	147
5	Rhodanine derivatives	148
5.1	Rhodanine derivatives with an anti-parasitic application	148
5.2	Synthesis of inhibitor library	149
5.2.1	Synthesis of rhodanine and thiazolidine-2,4-dione derivatives	151
5.2.2	Synthesis of 3-amino rhodanine derivatives	156
5.2.3	Synthesis of N-phenyl rhodanine derivatives	156

5.2.4	Synthesis of heterocyclic-modified rhodanine derivatives	159
5.2.5	Alkylation of the thiocarbonyl in rhodanine derivatives	161
5.2.6	Replacement of thiocarbonyl group in rhodanine derivatives	167
5.2.7	Reduction of exo-double-bond	169
5.3	Anti-parasitic activity	171
5.3.1	Anti-parasitic activity of rhodanine derivatives	171
5.3.2	Anti-parasitic activity of thiazolidine-2,4-dione derivatives	173
5.3.3	Anti-parasitic activity of N-phenyl rhodanine derivative	175
5.3.4	Anti-parasitic activity of N-amino rhodanine derivatives	175
5.3.5	Anti-parasitic activity of heterocyclic modified analogues	178
5.3.6	Anti-trypanosomal effects of 3-benzyloxy modified analogues	179
5.3.7	Activity of reduced rhodanine and thiazolidine-2,4-dione derivatives . . .	179
5.3.8	Modifications of the thiocarbonyl and anti-parasitic activity	180
5.4	Target identification studies	182
5.4.1	GPI cell-free radio-label assay	182
5.5	Discussion	187
5.6	Summary	188
6	Pyrazolone derivatives	190
6.1	Introduction	190
6.2	Synthesis of inhibitor library	191
6.2.1	Synthetic strategies towards anti-parasitic pyrazolone derivatives	191
6.2.2	Stereochemistry of pyrazole derivatives	191
6.2.3	Synthesis of pyrazolone derivatives via Route A	193
6.2.4	Synthesis of pyrazolone derivatives via Route B	195
6.2.5	Improved reaction conditions for pyrazolone derivatives	196
6.2.6	Synthesis of ester-analogues	202
6.2.7	Reduction of exo-cyclic double bond in pyrazolone derivatives	203
6.2.8	Synthesis of heterocyclic modified pyrazole derivatives	203
6.2.9	Synthesis of N-1 aliphatic modified pyrazolone	205
6.3	Anti-parasitic activity	208
6.3.1	Anti-parasitic activity of phenyl pyrazolones	208
6.3.2	Anti-parasitic activity of 3-benzoic acid pyrazolones	210
6.3.3	Anti-trypanosomal effect of the reduction of the exo-cyclic double bond .	211
6.4	Discussion	211
6.5	Summary	212
7	Iron chelating agents - hydroxypyridinones	213

7.1	Introduction	213
7.2	Synthesis of iron chelating agents	216
7.2.1	Previous synthesis of HPO iron chelators	216
7.2.2	Synthesis of CQ-HPO conjugated derivatives	216
7.3	Anti-parasitic activity	218
7.3.1	Anti-parasitic activity of simple aliphatic HPO iron chelators	219
7.3.2	Improved selectivity through CQ conjugation strategy	219
7.4	Target identification studies	220
7.4.1	Transferrin uptake in <i>T. brucei</i>	220
7.4.2	Fe(III) saturation experiments	221
7.5	Discussion	222
7.6	Summary	223
8	Conclusion and outlook	224
9	Methods	231
9.1	Reagents, Materials and Equipment	231
9.2	Synthesis of 5-benzylidene rhodanine N-acetic acid derivatives	231
9.3	Synthesis of 5-benzylidene thiazolidine-2,4-diones N-acetic ester derivatives	239
9.4	Synthesis of elongated N-3 side chain analogues	244
9.5	Synthesis of ester derivatives	249
9.6	Synthesis of modified benzyloxy benzaldehydes	263
9.7	Synthesis of 2-amino substituted pyridine carboxaldehyde derivatives	270
9.8	Synthesis of heterocyclic derivatives	274
9.9	Reduction of rhodanine and thiazolidine-2,4-dione derivatives	277
9.10	Synthesis of N-allyl rhodanine and thiazolidine-2,4-dione derivatives	278
9.11	Reduction of N-allyl thiazolidine-2,4-dione derivatives	297
9.12	Synthesis of rhodanine derivatives	298
9.13	Synthesis of heterocyclic modified rhodanine derivatives and analogues	319
9.14	Reduction of the rhodanine derivative	321
9.15	Reduction of thiazolidine-2,4-dione derivatives	323
9.16	Alkylation of the thiocarbonyl in rhodanine derivatives	323
9.17	Synthesis of photo-label affinity probe	331
9.18	Synthesis of pyrazole derivatives	335
9.19	Synthesis of CQ-HPO conjugated iron chelators	349
9.20	Preparation of media	356
9.21	Culturing of parasites and mammalian cells	357
9.22	Anti-parasitic activity and toxicity assays	358

9.23 Metabolic labelling of GPI-anchor proteins with myristate analogues	361
9.24 Transferrin uptake after iron starvation	364
9.25 Flow cytometry	364
9.26 Fluorescence microscopy	365
9.27 Photo-labelling of <i>T. brucei</i> proteins	365
10 References	369
11 Appendices	392

List of Figures

1	Current chemotherapy against HAT	4
2	Current chemotherapy against Chagas disease	5
3	Current chemotherapy against Leishmaniasis	6
4	Current drugs in clinical development	8
5	New drugs for chemotherapy of Leishmaniasis	9
6	Anti-fungal azole derivatives as anti-parasitic agents	11
7	The cysteine-peptidase inhibitor K-777 against Chagas disease	12
8	Schematic representation of GPI-anchored proteins	15
9	General structure of rhodanine-N-acetic acid derivatives	17
10	Epalrestat, a rhodanine-N-acetic acid derivatives	19
11	The bacterial siderophore Deferoxamine	21
12	Molecular structure of the iron chelator ortho-Phenanthroline	21
13	The iron chelating agent Deferiprone	21
14	Life cycle of <i>T. brucei</i> in Tsetse fly and man	23
15	Life cycle of <i>T. cruzi</i> in Triatomine bug and man	24
16	Life cycle of <i>Leishmania infantum</i> in sand fly and man	24
17	Previous examples of rhodanine-N-acetic acid derivatives	26
18	Examples of rhodanine and thiazolidine-2,4-dione derivatives in clinical use	29
19	Strategies to improve anti-trypanosomal activity of identified lead structure	36
20	¹ H- and ¹³ C-NMR spectra showing long range coupling between CH and CF ₃	43
21	Molecular orbital model of overlapping 2p and 1s orbitals from F and H	44
22	Retrosynthesis of improved rhodanine-N-acetic acid derivatives	50
23	Photo-affinity label for the identification of possible targets in parasites	58
24	Reaction mechanism of aryl azides after UV-activation	59
25	Photo-affinity strategy to identify molecular targets	60
26	Colorimetric activity-/ toxicity assays	62

27	Intracellular reduction of blue resazurin to purple resorufin	63
28	Intracellular reduction of yellow tetrazole salt MTT to its purple formazan	64
29	Plot of log(C) against normalised parasite survivals and structure of Melarsoprol	66
30	Possible effects of the meta-CF ₃ group on the activity of rhodanine derivatives	71
31	Correlation of logP and increasing anti-leishmanial activity	84
32	Myristate analogue for metabolic labelling	87
33	Tag for visualisation of metabolic labelling of YnC fatty acids	88
34	Myristate labelling results, SDS gels after 3 h incubation	89
35	Myristate labelling results, YnC12 labelling after 24 h pre-incubation	91
36	Pentadecylic acid YnC15	92
37	Myristate labelling results, YnC15 labelling after 24 h pre-incubation	93
38	Myristate labelling in HL60 cells with YnC12 labelling after 24 h pre-incubation	94
39	Mean fluorescence intensity of FITC-labelled transferrin	95
40	Flow-cytometry analysis of FITC labelled transferrin uptake	96
41	Flow-cytometry analysis of rhodanine-N-acetic ester derivatives	97
42	Substrates of cell-free GPI-synthesis assay	98
43	Sequence alignment of DPMS amino acid sequences	103
44	Ramachandran plots of Robetta homology models 1-5	105
45	Docking of GDP-mannose into the active site of Homology model 4	106
46	Overlay of homology model 4 and mannosyl-3-phosphoglycerate synthase	107
47	Docking simulations of rhodanine-N-acetic acid derivatives	109
48	Interactions within the active site of homology model 4	110
49	Long-range ⁵ J _{H,F} coupling	112
50	Rhodanine-N-acetic derivatives and analogues identified as leads	113
51	Examples of previously N-allyl rhodanine derivatives	116
52	Synthetic strategy for N-allyl rhodanine and analogues	118
53	X-ray structure of rhodanine-N-allyl derivative	120
54	SDS gels after 3 h incubation wit YnC12 and N-allyl rhodanine derivatives	137
55	SDS gels after 24 h incubation wit YnC12 and N-allyl rhodanine derivatives	138
56	SDS gels after 24 h incubation wit YnC15 and N-allyl rhodanine derivatives	139
57	YnC12 labelling of HL60 cells in the presence of N-allyl rhodanine derivatives	139
58	Fluorescence intensity of FITC-transferrin with N-allyl rhodanine derivatives	140
59	Flow cytometry analysis of N-allyl rhodanine derivatives	141
60	Examples of previous rhodanine and thiazolidine-2,4-dione derivatives	148
61	Strategy towards synthesis of rhodanine derivatives and analogues	150
62	Resonance structures of rhodanine derivatives	153
63	Newan-projection for E-isomer	155

64	Resonance structures to explain razemisation of double bond	161
65	Electrophilic substitution of the thiocarbonyl group in rhodanine derivatives . . .	162
66	Rhodanine derivatives, their anti-parasitic activity and correlation to logP . . .	171
67	Pyrazolone derivatives as alternative inhibitor template.	190
68	Synthetic strategies towards pyrazole-derivatives with anti-parasitic activity. . .	192
69	Z- and E-isomer of pyrazolone derivatives	194
70	Measurement of distances of CH-proton and CF ₃ -group	197
71	2D-NMR for confirmation of the Z-configuration of double bond	202
72	Comparison of logP values for pyrazolone derivatives	206
73	Iron chelators and their Fe(III)-complexes	213
74	Conjugation strategy towards improved anti-parasitic HPO derivatives.	215
75	HPO-CQ at different pH values	215
76	Mean Fluorescence Intensity of fluorescein labelled transerrin	221
77	Overview of rhodanine derivatives with anti-parasitic activity	225
78	Pipette scheme for AlamarBlue assay in 24 well plate	359
79	Pipette scheme for AlamarBlue/MTT assay in 96 well plate	360
80	SDS gel visualised with Tamra-Channel settings, YnC12 3 h inhibitor incubation	392
81	SDS gel visualised with Coomassie stain, YnC12 24 h inhibitor incubation . . .	392
82	in-gel fluorescence after 24 h incubation with inhibitors and YnC12 labelling . .	393
83	Coomassie stain after 24 h incubation with inhibitors and 4 h YnC12 labelling . .	393
84	in-gel fluorescence: Tamra settings, YnC15	394
85	Coomassie staining, YnC15	394
86	in-gel fluorescence: Tamra setting, YnC12 HL60 cells	395
87	Coomassie stain, YnC12 HL60 cells	395
88	HPTLC of GPI synthesis radio-label assay (Plate 1)	396
89	HPTLC of GPI synthesis radio-label assay (Plate 2)	396
90	HPTLC of GPI synthesis radio-label assay (Plate 3)	397
91	HPTLC of GPI synthesis radio-label assay (Plate 4)	397
92	HPTLC of GPI synthesis radio-label assay (Plate 5)	398
93	HPTLC of GPI synthesis radio-label assay (Plate 6)	398

List of Tables

1	Summary of parasitic diseases discussed in this thesis	13
2	Rhodanine derivatives with DPMS inhibitory effect	30
3	Synthesis of 5-benzylidene rhodanine-N-acetic acid derivatives	38
4	Synthesised thiazolidine-2,4-dione ester derivatives	41

5	Rhodanine-N-acetic acid derivatives and their R substituents	45
6	Rhodanine carboxylic ester derivatives	47
7	Synthesis of modified 3-benzyloxy-benzaldehyde derivatives	51
8	Synthesis of modified 3-benzyloxybenzaldehyde derivatives	52
9	Synthesis of heterocyclic rhodanine-N-acetic acid derivatives	53
10	Synthesis of amino-substituted aldehydes, yield and method	55
11	Synthesis of heterocyclic rhodanine-N-acetic acid/ ester derivatives	56
12	Reduction of rhodanine-N-acetic ester analogues	57
13	Comparison of residual <i>T. brucei</i> DPMS activity and trypanocidal activity	67
14	Anti-trypanosomal activity of rhodanine-N-acetic acid derivatives	68
15	Activity of starting rhodanine-N-acetic acid derivatives	69
16	Anti-trypanosomal activities of derivatives with elongated side chain.	70
17	Anti-trypanosomal activity of ester analogues and their toxicity	72
18	Inhibitor classes A-D as anti-trypanosomal agents	76
19	3rd generation optimisation of compound classes A, C and D.	77
20	Optimisation of compounds from class B	79
21	Heterocyclic modified rhodanine-N-acetic acid and there ester analogues.	81
22	Reduced rhodanine-N-acetic ester analogues and their anti-trypanosomal activity	83
23	Rhodanine ester and analogues with anti-leishmanial activity	85
24	Anti-parasitic activity of compounds chosen for target identification studies.	90
25	cell-free GPI assay for rhodanine-N-acetic acid derivatives	100
26	cell-free GPI assay for rhodanine-N-acetic acid derivative 2	101
27	Cell-free GPI assay for rhodanine-N-acetic acid derivatives 3	102
28	Knoevenagel condensation reaction of N-allyl rhodanine derivatives	121
29	Synthesis of N-allyl thiazolidine-2,4-dione derivative	122
30	Synthesis of N-allyl thiazolidine-2,4-dione derivates	124
31	Synthesis of modified N-allyl rhodanine and thiazolidine-2,4-dione derivatives .	125
32	Anti-parasitic activity of N-allyl rhodanine derivatives	129
33	N-allyl thiazolidine-2,4-dione derivatives and their anti-parastic activity.	131
34	Activity of 3-benzyloxy modified N-allyl rhodanine derivatives.	132
35	Activities of heterocyclic modified N-allyl rhodanine and analogous derivatives .	133
36	Anti-trypanosomal activity of saturated N-propyl thiazolidine-2,4-dione derivative	134
37	Glutathione reactivity of N-allyl rhodanine derivatives	134
38	Anti-parasitic activity of chosen N-allyl rhodanine derivatives	136
39	Cell-free GPI assay results for N-allyl rhodanine derivatives-1	143
40	Cell-free GPI assay results for N-allyl rhodanine derivatives-2	144
41	Synthesis of rhodanine derivatives	152

42	Synthesis of thiazolidine-2,4-dione derivatives	154
43	Synthesis of 5-benzylidene modified N-amino rhodanine derivatives	157
44	Synthesis of 5-benzylidene modified N-phenyl rhodanine derivatives	158
45	Synthesis of heterocyclic and 3-benzoyloxy modified rhodanine derivatives	160
46	Alkylation of the thiocarbonyl group in benzylidene rhodanine derivatives	164
47	Synthesis of S-modified acetic ester analogues	167
48	Anti-parasitic activity of rhodanine derivatives	172
49	Anti-parasitic activity of thiazolidine-2,4-dione derivatives.	174
50	Screening results of N-phenyl rhodanine derivatives	176
51	Anti-parasitic activity of N-amino rhodanine derivatives	177
52	Anti-parasitic activity of heterocyclic modified rhodanine derivatives	178
53	Anti-trypanosomal effect of 3-benzoyloxy modifications.	179
54	Comparison of Anti-parasitic activity of reduced rhodanine derivatives	180
55	Anti-parasitic activity of S-modified and S-substituted rhodanine analogues.	181
56	cell-free GPI assay for rhodanine derivatives	183
57	cell-free GPI assay for N-amino rhodanine derivatives-1	184
58	cell-free GPI assay for N-amino rhodanine derivatives-2	185
59	cell-free GPI assay for N-phenyl rhodanine derivatives	186
60	Synthesis of pyrazolone derivatives through synthetic Route A	196
61	Synthesis of pyrazole derivatives using route B	198
62	Improved reaction conditions towards pyrazolone derivatives	200
63	Synthesis of heterocyclic modified pyrazolone derivatives	205
64	Knoevenagel condensation of N-1-aliphatic modified pyrazolone derivatives	208
65	Anti-parasitic activity of phenyl pyrazolones derivatives.	209
66	Anti-parasitic activity of 3-benzoic acid pyrazole derivatives.	210
67	Anti-trypanosomal effect on the reduction of the exo-cyclic double bond.	211
68	Simple N-Alkyl HPO derivatives	218
69	Anti-parasitic activity of simple N-alkyl modified HPO derivatives	219
70	Chloroquine-conjugated iron chelator and their anti-parasitic activity	220
71	Importance of catechol-modified inhibitors on antitrypanosomal activity	227
72	Reagents for Baltz-Media preparation	356
73	Reagents for Baltz-Media-completion	356
74	Reagents for RPMI-media	357
75	Parasite concentration for metabolic labelling	362
76	Cell density for labelling experiment	362

List of Schemes

1	Synthesis of 5-Benzylidene rhodanine N-acetic acid derivatives	30
2	Mechanism of the Knoevenagel reaction.	31
3	Michael acceptor reactivity of Knoevenagel product	32
4	Zimmerman-Traxler transition state of Knoevenagel reaction	35
5	Synthesis of 5-Benzylidene rhodanine N-acetic acid derivatives	37
6	Synthesis N-acetic acid thiazolidine-2,4-dione analogue	39
7	Synthesis of thiazolidine-2,4-dione ester derivatives	40
8	Synthesis of elongated N-3 sidechain linkers	42
9	Synthesis of N-3 elongated rhodanine acid derivatives	44
10	Synthesis of Ester derivatives of rhodanine-N-acetic acids	46
11	Racemization of exo-cyclic double bond configuration	49
12	Synthesis of modified 3-benzyloxy benzaldehydes	50
13	Synthesis of 3-benzyloxy-modified analogues	52
14	Synthesis of heterocyclic rhodanine-N-acetic acid derivatives	53
15	Synthesis of amino-substituted aldehydes	54
16	Synthesis of heterocyclic derivatives	56
17	Synthesis of reduced analogues	57
18	Synthesis of phosphorochloridate	59
19	Synthesis of photo-label-aldehyde	61
20	Synthesis of rhodanine-N-acetic ethyl ester photo-affinity label	61
21	Catechol reactivity to react with biological nucleophiles or cross-link proteins . .	73
22	Knoevenagel condensation reaction of N-allyl rhodanine derivatives	118
23	Synthesis of N-allyl thiazolidine-2,4-dione derivative	122
24	Synthesis of N-allyl thiazolidine-2,4-dione derivatives	123
25	Synthesis of modified N-allyl rhodanine and thiazolidine-2,4-dione derivatives .	124
26	Synthesis of reduced N-allyl thiazolidine-2,4-dione analogue	127
27	Alternative strategy toward reduced N-allyl thiazolidine-2,4-dione derivatives . .	128
28	Synthesis of rhodanine and thiazolidine-2,4-dione derivatives	151
29	Synthesis of 5-benzylidene modified N-amino rhodanine derivatives	156
30	Synthesis of 5-benzylidene modified N-phenyl rhodanine derivatives	159
31	Synthesis of heterocyclic and 3-benzyloxy modified rhodanine derivatives	162
32	Two approaches towards alkylated thiocarbonyl derivatives	163
33	Alkylation of the thiocarbonyl group in benzylidene rhodanine derivatives	163
34	Alkylation of the thiocarbonyl group	165
35	Synthesis of S-modified acetic ester analogues	166

36	Substitution of S-alkyl analogues	168
37	Synthesis of thiocarbonyl substituted analogues	168
38	Attempts to alkylate N-substituted rhodanine derivatives	168
39	Reduction of the exo-cyclic double bond in rhodanine derivatives	170
40	Reduction of exo-cyclic double bond using the Hantzsch-ester approach	171
41	Two approaches pyrazole-derivatives	193
42	Synthesis of pyrazolone derivatives through synthetic Route A	195
43	Synthesis of pyrazolone derivatives using route B	198
44	Side-reaction in the microwave assisted one-pot reaction	199
45	Improved reaction conditions towards pyrazolone derivatives	199
46	Esterification reaction of pyrazolone derivatives	203
47	Reduction of pyrazole derivatives	204
48	Synthesis of furanyl-carbaldehyde	204
49	Synthesis of heterocyclic modified pyrazolone derivatives	205
50	Synthesis of N-1 unsubstituted pyrazolone precursor	207
51	Knoevenagel condensation reaction of N-1-aliphatic modified pyrazolones	207
52	Synthesis of simple N-1-substituted HPO derivatives	216
53	Synthesis of CQ-HPO conjugate derivatives	217

1 Introduction

1.1 Parasitic diseases

Neglected parasitic diseases such as Human African Trypanosomiasis (HAT), Chagas disease and Leishmaniasis are major health threats in significant areas of the population.^[1] People affected by these parasites live mainly in the developing countries, resulting in major health threats, as most of these diseases are fatal if untreated.^[2–4] Combined, these diseases threaten a total of 500,000 million people worldwide, of which 20 million people are actually infected, and more than 100,000 of whom die annually due to diseases caused by *Trypanosoma brucei* spp. (*T. brucei*), *Trypanosoma cruzi* sp. (*T. cruzi*) and *Leishmania* sp.^[2–7] The current chemotherapy is based on drugs discovered over 60 years ago to which resistance is developing.^[1] The drug-pipeline is virtually empty and new drugs in development are mostly based on established drugs, that are expensive and difficult to administer.^[8–12] There is an urgent need for new and novel anti-parasitic drug therapies.

These tropical parasitic diseases are caused by kinetoplastid protozoan parasites, such as *Trypanosoma* spp. and *Leishmania* spp., which are characterised by the presence of mitochondrial DNA contained within a kinetoplast.^[13] These parasites are well adapted to the biological environment in their hosts and have evolved different strategies to ensure survival and rapid propagation by binary fission.^[13] A particularly interesting feature is a highly decorated plasma membrane that is essential for the survival of these parasites.^[13] Due to similarities in cellular biology, it is not surprising that recent genomic data showed that out of 8,000 genes in each kinetoplastid genome, more than 6,000 orthologous genes have been found in *Trypanosoma brucei*, *Trypanosoma cruzi* and *Leishmania infantum*.^[13] Despite these similarities, each of these kinetoplastid protozoa cause distinct human diseases transmitted by different insect vectors.^[13] Furthermore, all of these protozoa are found in different compartments within their human host, complicating the discovery of a general treatment against these parasites.^[14]

T. b. gambiense and *T. b. rhodesiense* are the etiological origin of Human African Trypanosomiasis (HAT).^[3] In 2002, the combined fatality rate of Chagas disease and HAT was estimated at 48,000 deaths.^[3] After extensive efforts, both in vector control and patient surveillance, the number of new infections has dropped below 10,000 (9878) people in 2009, with 7139 reported causes in 2010, but the actual number of infected people is estimated at 30,000, all of whom will die from HAT if left untreated.^[6] A total of 70 million people living in 36 sub-Saharan countries are at risk of infection with HAT.^[6] HAT is transmitted by the bite of an infected tsetse fly, limiting the disease distribution to its breeding grounds.^[6] Three particular strains of *T. brucei* spread HAT and the animal disease Nagana; *T. b. gambiense* causes the

severe chronic disease in human, whereas *T. b. rhodesiense* is responsible for the acute disease.^[6] *T. b. brucei* is the etiological agent for animal trypanosomiasis (Nagana disease) in domestic animals like cattle, with huge economical consequences for the country.^[6] However, animal infection by *T. b. rhodesiense* has also been reported and plays an essential role as a parasite reservoir in the distribution of HAT.^[15] *T. b. brucei* is morphologically indistinguishable to *T. b. gambiense* and *T. b. rhodesiense*, the parasites causing HAT in humans, so serves as a model for HAT.^[16] HAT presents itself in two stages; in the first stage trypanosomes infect subcutaneous tissue, blood and lymph, resulting in fever, joint pain and itching.^[5] In the second stage, the parasites penetrate the blood brain barrier, causing infection of the central nervous system and manifesting neurological and psychiatric disorders, including the disturbance of the sleep cycle, hence this disease is also known as african sleeping sickness.^[5]

Chagas disease is caused by the parasite *T. cruzi* and is transmitted through the faeces of an infected triatomine bug, which is involuntary smeared in bite wounds, mouth or eyes.^[2] Contaminated food, blood transfusions, organ transplantations, passage from mother to newborn and lab accidents are further transmission routes.^[2] In the human host, *T. cruzi* trypomastigotes infect human cells, where they transform to amastigotes in order to reproduce by binary fission.^[17] Chagas disease is endemic in 26 Latin American countries, putting 25 million people at risk of infection, of which 10 million people are estimated to be currently infected, resulting in death of 10,000 people in 2008.^[2,5] Chagas disease is curable if treatment is commenced shortly after infection (2 months), however disease diagnosis is difficult, resulting in chronic infection where patients develop cardiac and neurological alterations (30 % and 10 % of patients, respectively).^[2] For many of these patients a heart transplant is the last life-prolonging measure,¹ however infection of the new heart is likely to reoccur. In the first two months after infection, patients commonly present mild fever and headaches, symptoms easily associated with bacterial or viral infections.^[2] However in 50 % of the cases, skin lesions around the bite wound of the triatomine bug are observed in combination with a purplish swelling of one eyelid.^[2] Chagas disease is not confined to Latin American, as cases have been reported in the United States of America, Canada and even European and Western Pacific countries, however these cases are thought to be due to increased population mobility.^[2] Nevertheless, the outbreak of Chagas disease in non-endemic countries is considered as a serious public health challenge.^[5]

The parasite *Leishmania sp.* causes Leishmaniasis in humans and accounts for the majority of casualties reported by these three parasitic diseases.^[4] *Leishmania sp.* causes death in 51,000 people living in 88 countries around the world, affecting a total of 0.2 % of the worlds population. An estimate of 12 million people are currently infected and 1.5-2 million individuals are newly infected annually.^[3,4,7] Overall 350 million people are at risk of infection worldwide.^[13]

¹personal communication with physicians at the heart transplantation centre in Sao Paulo, Brazil

Leishmaniasis is caused by the bite of an infected female sandfly,^[5] transmitting the promastigote form of *Leishmania spp.* into the human host, where the parasite transforms into the amastigote form and infects intracellular macrophages.^[8] There are 23 species of *Leishmania spp.*, of which 20-21 species cause two forms of Leishmaniasis in humans.^[13,18] Visceral Leishmaniasis is the most severe form as the parasite is found in internal organs, causing death within 2 years if untreated.^[5] Cutaneous Leishmaniasis is the common form, causing skin ulcers and in the worst case disfigurement by destruction of the soft tissue around the nose, mouth and throat (mucocutaneous Leishmaniasis).^[5] All *Leishmania spp.* show different drug sensitivities and need different drug applications, making treatment extremely difficult.^[8] In this study only one of these 23 *Leishmania spp.*, *Leishmania infantum* will be the focus for development of anti-parasitic compounds. *L. infantum* belongs to the class of *Leishmania donovani*,^[19] causing the fatal visceral Leishmaniasis in humans.^[8]

1.2 Current treatment for parasitic diseases

The current treatment of HAT, Chagas disease and Leishmaniasis is based on drugs which were developed decades ago and are difficult to administer as well as causing severe side effects.^[8,20,21]

There are currently four drugs registered for the treatment of HAT, of which three were developed more than 60 years ago.^[6] For the first stage of HAT infection with *T. b. gambiense* and *T. b. rhodiense*, Pentamidine is the front line drug.^[20] Pentamidine (Figure 1) has been widely used and although resistance is shown to be inducible in laboratory strains, no resistance has been observed during 60 years of clinical use.^[20] Suramin (Figure 1) is an alternative first line drug, but is of limited use due to its high affinity to proteins in blood plasma (resulting in undesired pharmacokinetics), furthermore resistance has also been reported.^[20] The treatment of the second stage of HAT relies on the ability of the drug to penetrate the blood-brain barrier in order to reach parasitic compartments in humans.^[20] The first line treatment is the arsenical drug Melarsoprol (Figure 1), administered parenterally it is able to treat both *T. b. gambiense* and *T. b. rhodiense* infections, but unfortunately treatment is also very toxic and causes death in 5 % of patients, showing symptoms similar to arsenic poisoning.^[20,22] A more recent drug, introduced in 1990 for the treatment of stage 2 HAT caused by *T. b. gambiense* is Eflornithine (Figure 1) an irreversible inhibitor of ornithine decarboxylase.^[20] However, the production of Eflornithine is very expensive and administration via intravenous injection over a course of 14 days limits its use in rural Africa.^[23] Since 2009, a combination therapy of Nifurtimox and Eflornithine is in clinical use, benefiting from the oral availability and cheap production of Nifurtimox.^[20] Cross-resistance in particular against the chronic stage of HAT has been reported in the treatment with Melarsoprol, leaving Eflornithine, which is difficult to administer under field

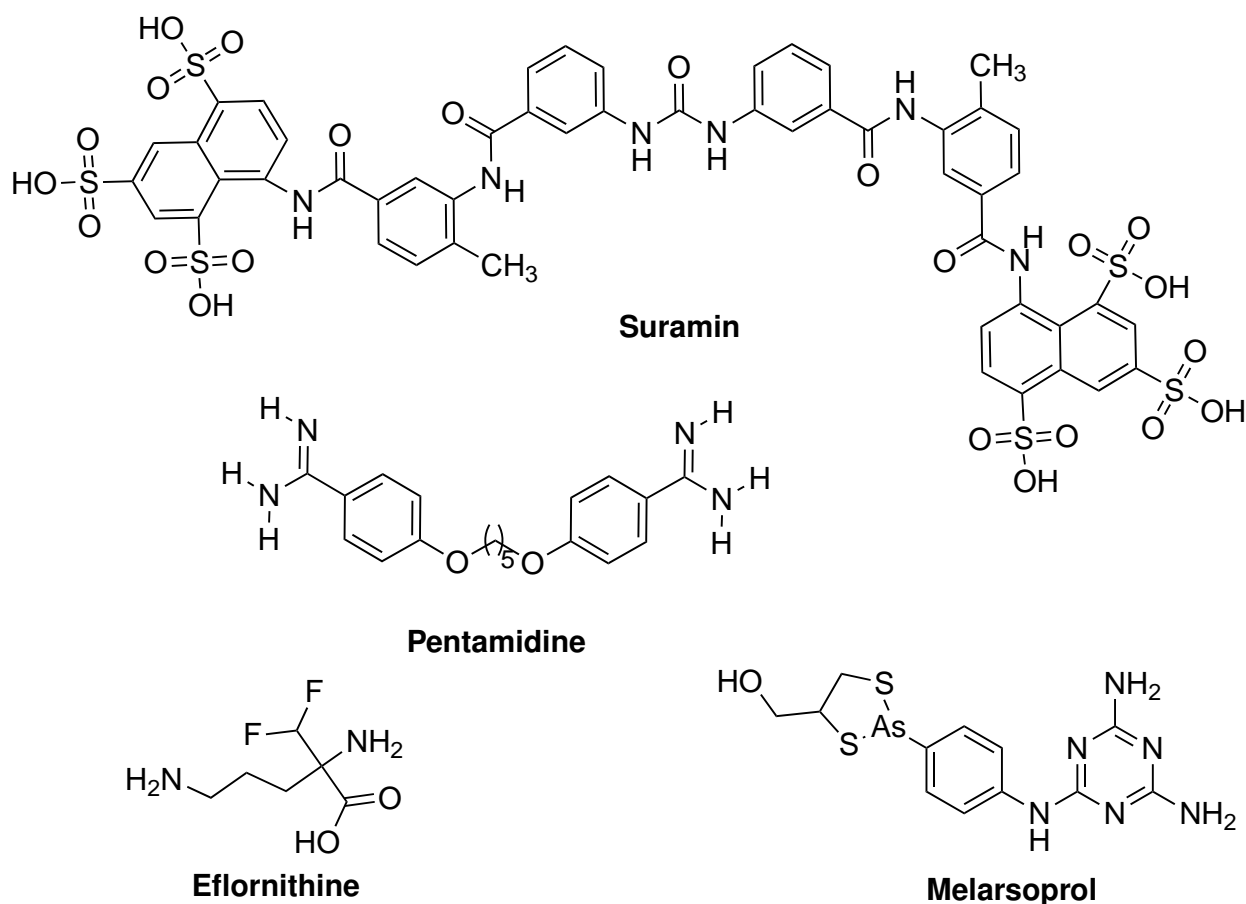


Figure 1: Current drugs against first and late stage HAT.

conditions, as the last resort.^[20]

The first line treatment against Chagas disease is vector control and the screening of blood transfusions, which has reduced the number of people at risk of infection from 100 million to 40 million people in 2003.^[21] Therapeutically, Chagas disease is treated with Benznidazole and Nifurtimox (Figure 2) which has been reported to cure 100 % of patients in the early stage. However these drugs are less effective against the chronic stage of the disease and the adverse toxic side effects (CNS toxicity and peripheral neuropathy) outweigh their beneficial effect.^[2,21] Benznidazole and Nifurtimox (Figure 3) belong to the class of nitro-heterocycles, commonly reported to be associated with mutagenicity.^[24] Indeed Benznidazole has been shown to induce mitotic recombination events in diploid strains of *Aspergillus nidulans*, whereas Nifurtimox tested positive for mutagenesis, based on somatic mutation and recombination tests in *Drosophila melanogaster* and the bacterium *Salmonella typhimurium*.^[24,25]

The first line treatment for Leishmaniasis, both visceral and cutaneous (mucocutaneous) forms are the pentavalent antimonial drugs Pentostam and Meglumine antimoniate (Figure 3), both administered by parenteral injection and introduced more than 50 years ago.^[8] But,

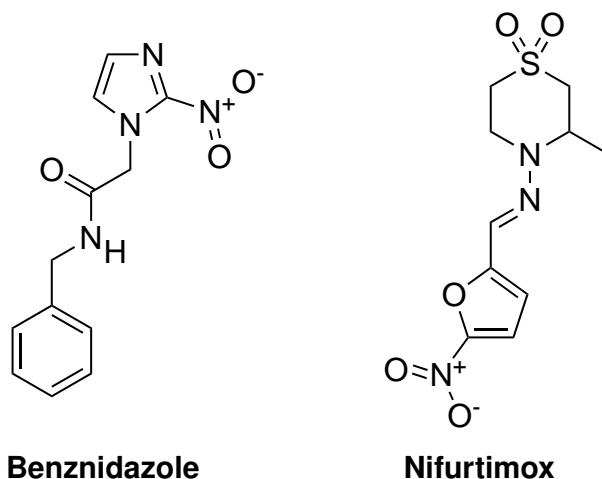


Figure 2: Current drugs against acute and chronic Chagas disease.

widespread resistance against pentavalent antimonial drugs limit their use.^[8] The antimicrobial diamidine Pentamidine (Figure 1) is used as second line drug for these resistant strains, but is of limited use due to its toxicity.^[8]

The anti-fungal polyene antibiotic Amphotericin B (Figure 3) and its lipid-formulated AmBiosome are highly effective drugs against antimonial resistant visceral and mucocutaneous Leishmaniasis, however its prolonged parenteral administration (up to 28 days) and the severe side effects for amphotericin B (nephrotoxicity) restrict their application.^[8]

1.3 Current drug development

The current drug treatments against HAT, Chagas disease and Leishmaniasis are unsatisfactory, due to resistance and severe toxic side effects.^[26] There is an urgent need for novel anti-parasitic agents in order to treat these diseases and evade resistance to established drug therapies.^[26] In the years from 1975 to 1999 less than 1 % (13 drugs) of new chemical entities released to the market (1393 drugs) were indicated for tropical diseases (Malaria, Leishmaniasis, Lymphatic Filariasis, Chagas disease, and Schistosomiasis).^[26] Economically this reflects the lowest investment (10.1 % of \$35.3 billion) for development of drugs against tropical diseases by the pharmaceutical industry.^[26] The private sector and government contributions were as low as \$70 million in 1999.^[26] Despite the wealth of genetic information available (the genomes of all three protozoa have been sequenced) there has been little improvement in the field of anti-parasitic research.^[26] After a long innovation gap in the development of drugs to treat tropical diseases, non-profit public private partnership programmes between industry and academia have been established. (e.g. Drugs for Neglected Diseases initiative (DNDi))

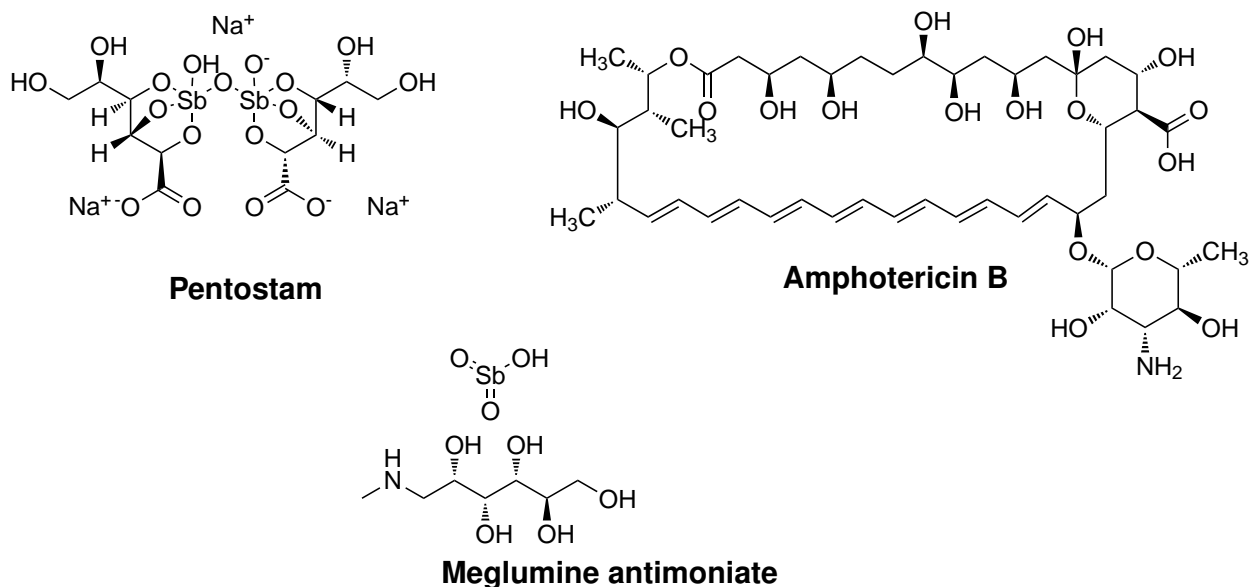


Figure 3: Current drugs against visceral and/or cutaneous (mucocutaneous) Leishmaniasis.

<http://www.dndi.org>, Medicines for Malaria Venture (MMV): <http://www.mmv.org>).^[12] There are currently no vaccines against Leishmaniasis, Chagas disease or HAT and antigenic variation in trypanosomes will make the prospect for vaccination very unlikely, leaving chemotherapy as the only treatment.^[7,22]

The current drug treatments against HAT are considered out-dated and unacceptable, as many drugs were developed >60 years ago and Melarsoprol fatality rates are reported to be as high as 5%.^[20] Currently only disease control by case detection and treatment prevent an endemic outbreak of HAT.^[27] In 2009, diamidine Pafuramidine (DB289), a derivative of Pentamidine, was the first drug in clinical phase III for the second stage of HAT, until liver and renal-toxicity discontinued its development.^[28,29] The related aza-analogue DB829 is currently in preclinical development, but already shows good oral availability and was able to cure a central nervous system (CNS) mouse model of HAT (*in vitro* activity 19 nM, SI > 10,000).^[12] DB829 belongs to the class of diamidines, which are readily accumulated in mM concentrations within DNA-containing organelles, such as the kinetoplast or nucleus, but accumulation was observed in acidocalcisomes, suggesting DNA binding as possible mode-of-action, although accumulation in other cell compartments could contribute to the trypanocidal activity.^[30,31] Moreover, aza-analogues of furamidine have been shown to cross the blood-brain barrier through an active transport.^[32] Although this is also true for other pentamidine derivatives, uptake studies have shown that the pyridine-nitrogens in DB829, slow down the efflux transporter, which clears the drug from the cerebral fluid.^[32] In September 2009, the nitroim-

²Personal communication with Xavier Ding, research scientist at MMV, Cancun, Mexico

idazole Fexinidazole (DNDi supported) entered first human phase I trials as drug against *T. b. gambiense* and *T. b. rhodesiense*.^[11] The orally available Fexinidazole (41 % oral availability), a derivative of Megazol,^[12,30] has shown nM activity *in vitro* (IC₅₀ 0.16-0.93 µg/mL) and *in vivo* (100 mg/day/kg over 4 days or 200 mg/day/kg for 5 days, 100 % cure rate in mice, *in vitro* SI >100), with promising results against both drug-sensitive and drug-resistant strains of *T. brucei* spp.^[11,33] Metabolic studies in mice, rats, dogs and humans have identified two active metabolites of Fexinidazole (a sulfoxide and sulfone), which are most likely responsible for anti-trypanosomal activity.^[11,34] Fexinidazole is not a new discovery, but a re-evaluation of a drug shown to be mutagenic as shown by Ames tests in bacteria.^[11] However, further mutagenic evaluations on human lymphocytes, mouse bone marrow cells and *ex vivo* unscheduled DNA synthesis in rats showed no genotoxicity.^[11] The mechanism of action is unknown, but is proposed to involve bio-reductive activation by nitro-reductases in *T. brucei*, generating nitro-anion radicals, which cause DNA damage.^[35,36] In mammalian cells Fexinidazole is thought not to be reducible under aerobic conditions,^[11] however nitro-anion generation from bacteria in humans can not be ruled out. *Leishmania donovani* possesses a similar type I nitro-reductase and indeed *in vitro* studies with Fexinidazole in a mouse model of visceral Leishmaniasis have shown a 98.4 % reduction of parasitaemia and complete clearance of *Leishmania donovani* amastigotes from macrophages *in vitro*.^[37]

The other drug against HAT, currently in clinical phase I, is the oxaborole SCYX-7158 (DNDi supported).^[12] SCYX-7158 was discovered through the screening of a oxaborole library against *T. b. rhodisiense* and *T. b. gambiense*, which revealed a sub-µM inhibitor (IC₅₀ 0.29 µM and 0.07-0.36 µM, respectively).^[12,38] SCYX-7158 has been shown to actively be transported into the brain, making SCYX-7158 a candidate for the treatment of the late stage of HAT.^[38] The mechanism of action is unknown, but SCYX-7158 has been shown to localise near the flagella pocket region in *T. brucei*.^[38,39] SCYX-7158 passed absorption, distribution, metabolism, and excretion (ADME) studies (55 % oral availability) and toxicity studies (SI *in vitro* >100) and is currently in Phase I clinical trials by DNDi.^[12,40]

A very recent example of the development of a drug against both visceral and cutaneous Leishmaniasis is Miltefosine (Figure 5), which has been used since 2002 in India.^[41] Miltefosine is the first orally available treatment for Leishmaniasis and was included in the World Health Organisation (WHO) medical repertoire in 2010.^[41] Miltefosine is an analogue of phosphatidylcholine and was first described in 1980, independently as both an anti-cancer drug and anti-leishmanial drug with excellent oral availability.^[42,43] The mode of action in both cancer cells and *Leishmania* is considered to have a similar molecular basis, as both result in apoptosis and disturbance of lipid-dependant cell signalling pathways.^[41] Detailed studies on the mode of action in *Leishmania* have shown that Miltefosine interferes with lipid metabolism (affecting membrane composition), DNA fragmentation during apoptosis and cytochrome c

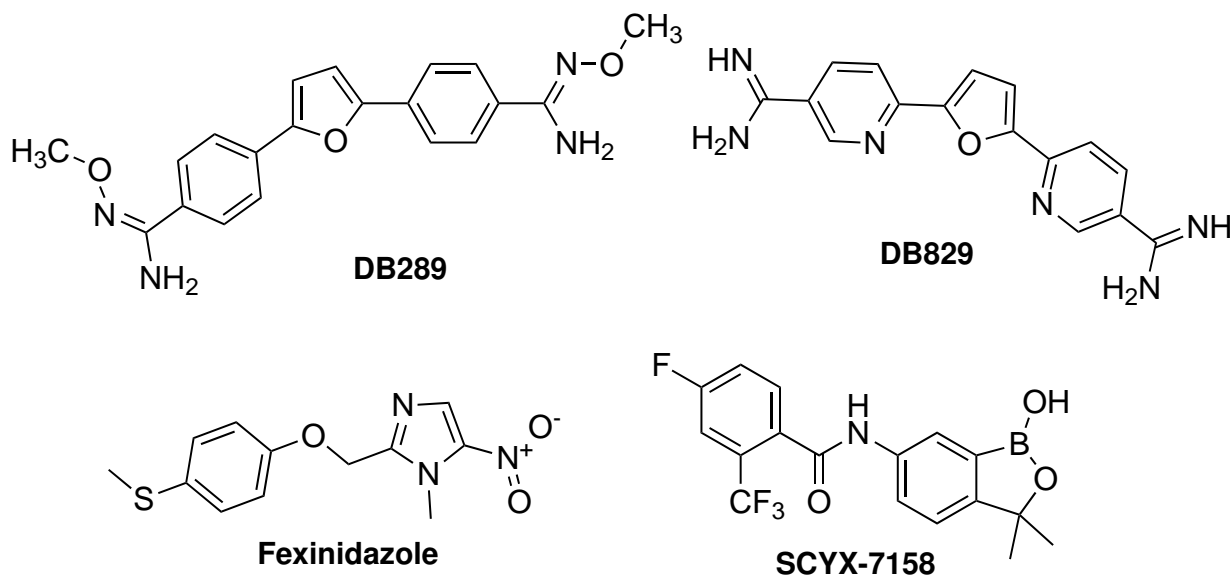


Figure 4: Current drugs in clinical development; DB289 failed clinical trials, DB829 currently in preclinical trials, Fexinidazole and SCYX-7158 are currently in clinical phase 1.

oxidase activity in mitochondria, however the exact mode of action is unknown and multiple targets in *Leishmania spp.* are proposed.^[41] Miltefosine has been shown to be particularly active against *Leishmania donovani* strains (EC_{50} 3.3-4.6 μ M in an amastigote model of infected macrophages),^[41] however there is uncertainty about efficacy in *L. infantum*, the parasite discussed in this study.^[8] The current problem with Miltefosine medication is its high cost of production compared to cheap antimonials, therefore several combination therapies with Paromomycin and liposomal Amphotericin B are currently in clinical trials.^[41] Miltefosine is also currently investigated for the treatment of Chagas disease, as it shows comparable activities to Benznidazole.^[44] Although there are as yet no reported cases of Miltefosine resistant *Leishmania*, drug uptake was shown to be transporter mediated and resistance is easily induced in laboratory strains.^[41] Treatment with Miltefosine is further limited due to its teratogenicity,^[8] highlighting the need for safer and cheaper drugs for the medication of *Leishmaniasis*.

Sitamaquine (Figure 5), an 8-amino-quinoline derivative is the first drug developed against the visceral form of *Leishmaniasis* and entered clinical trials in March 2002 (currently in clinical phase 2b).^[45–48] First reports on the efficacy of Sitamaquine have shown a 80 % cure rate of patients, but only at doses high enough to also cause nephrotoxicity.^[49] Therefore, combination therapies with Sitamaquine are currently explored to overcome liver toxicity and improve anti-leishmanial activity.^[49] The exact mode of action is unknown, however studies have indicated that Sitamaquine uptake is mediated in an electrical and concentration dependant manner, causing accumulation in the cytosol,^[50] where it accumulates in the acidocalcisome. But accumulation in this organelle may not responsible for anti-leishmanial activity, as activity has

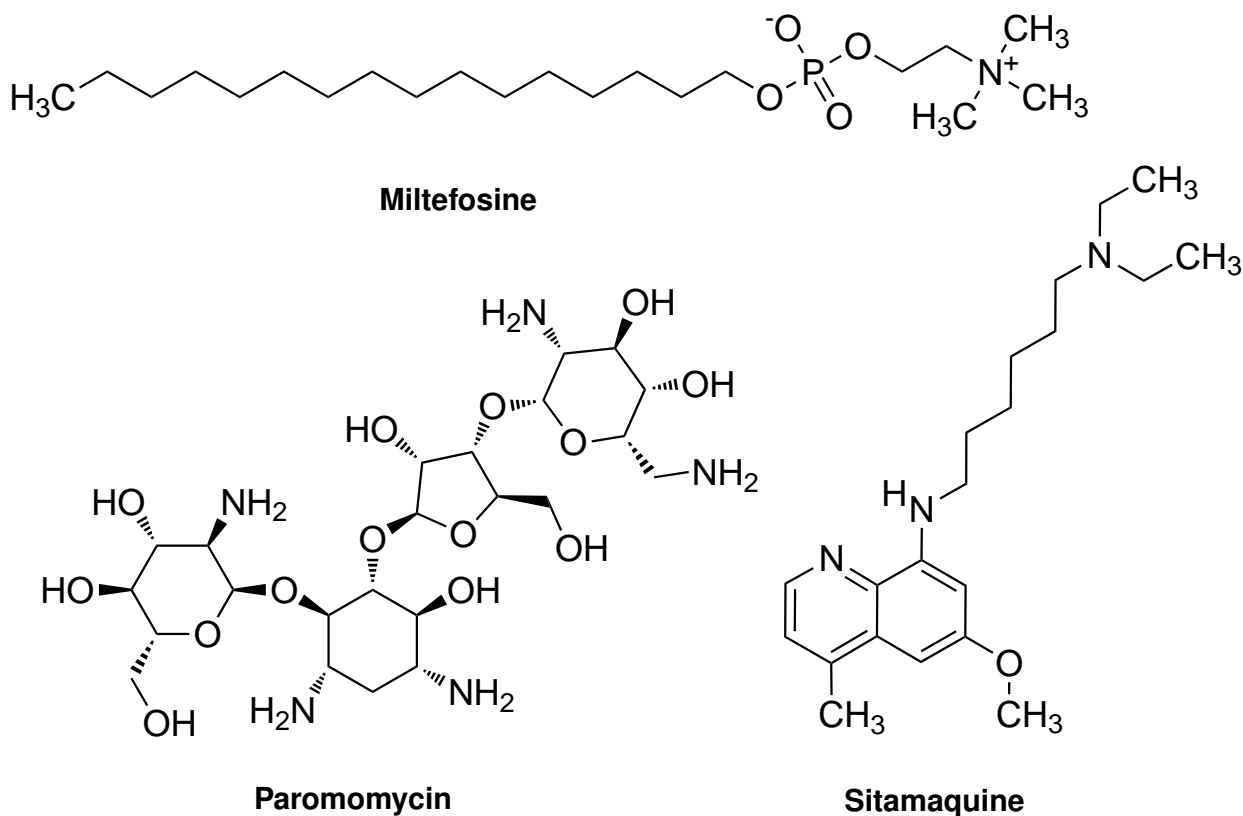


Figure 5: Current drugs in clinical trials as anti-leishmanial agents.

been shown against acidocalchosome null mutants in *Leishmania major*.^[46] Currently, changes in the membrane potential in the parasitic mitochondria and interactions with membrane lipids are believed to be the mode-of-action.^[9,46,51]

Paromomycin (Figure 5), an anti-bacterial amino-glycoside antibiotic is the latest anti-leishmanial drug registered for visceral Leishmaniasis in India.^[9] Paromomycin causes a depolarisation of the leishmanial mitochondrial membrane, interferes with the protein biosynthesis (ribosomes) and causes respiratory dysfunction.^[9,48] However, Paromomycin efficacy is inferior to Amphotericin B, injection pains have frequently being reported and distribution problems of Paromomycin make this drug unavailable for endemic regions.^[9,48]

The anti-fungal drugs Ketoconazole, Itraconazole and Fluconazole (Figure 6) have been assessed in various clinical trials against visceral and cutaneous Leishmaniasis with varying success rates.^[8] These azole derivatives are inhibitors of the 14- α -demethylase in sterol biosynthesis, however *Leishmania spp.* have the ability to survive reduced sterol availability by using metabolised sterols from the human host, possibly explaining the variations in clinical trials.^[48,49] Inhibition of the sterol pathway and in particular 14- α -demethylase is an interesting anti-parasitic target, as this pathway is conserved between *L. infantum*, *T. cruzi* and *T. brucei*.^[52] Indeed, the azole derivative Posaconazole (Figure 6) has been shown to inhibit

epimastigote proliferation in *T. cruzi* by reducing the ergosterol synthesis, due to inhibition of 14- α -lanosterol demethylase.^[21,53]

T. cruzi and other parasites are dependent on *de novo* synthesis of sterols, in particular ergosterol-like 24-alkyl-sterols as found in fungi and plants, presenting essential lipid components of membranes.^[54]

Posaconazole has been shown to be more effective than Benznidazole and Nifurtimox (in the treating both early and late stages of Chagas disease). Subsequently Posaconazole has recently entered clinical phase II against both stages of Chagas disease together with other 14- α -lanosterol demethylase inhibitors, such as TAK-187 (Phase I) and Ravuconazole (phase 1).^[55,56] These azole derivatives bind within the lanosterol binding site of 14- α -lanosterol demethylase, where the azole-nitrogen atoms chelate the heme iron in the active site, interrupting oxidation and substrate binding.^[57]

The drugs presented to this point are all derived from those used in other clinical applications (Table 1, also shows general overview of all three parasitic diseases). In contrast, one drug specifically designed against Chagas disease is the cysteine peptidase inhibitor K-777 (Figure 7), which has been shown to cure acute and chronic Chagas disease mouse models and is currently in preclinical development.^[10,58] The major cysteine peptidase, also known as Cruzipain, is an essential enzyme associated with induced host tissue damage in the proliferation of the parasite and is furthermore suggested to digest human IgG proteins to escape the host immune response.^[59,60]

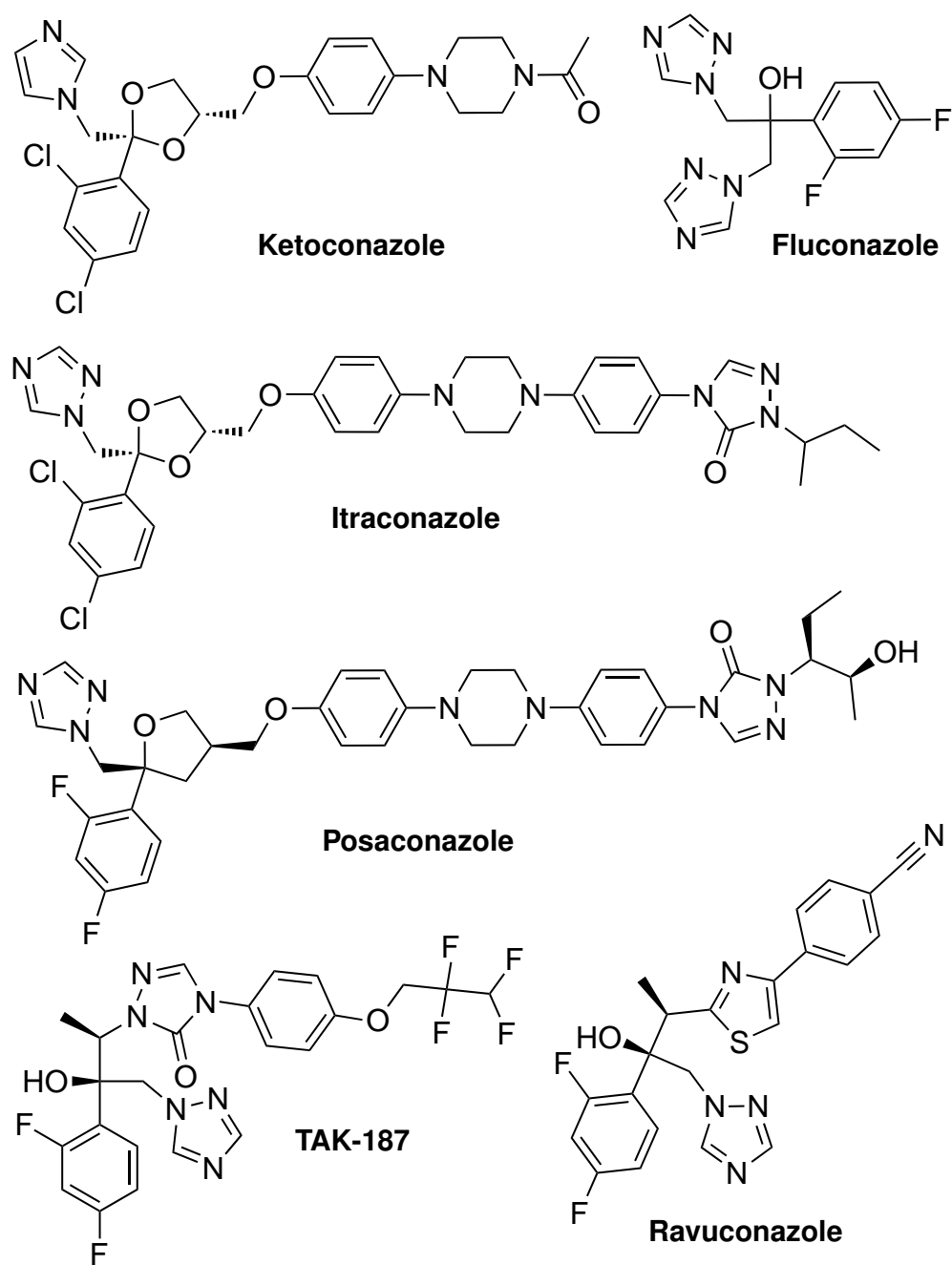


Figure 6: Anti-fungal azole derivatives against the 14- α -demethylase sterol pathway in *T. cruzi* and *L. infantum*.

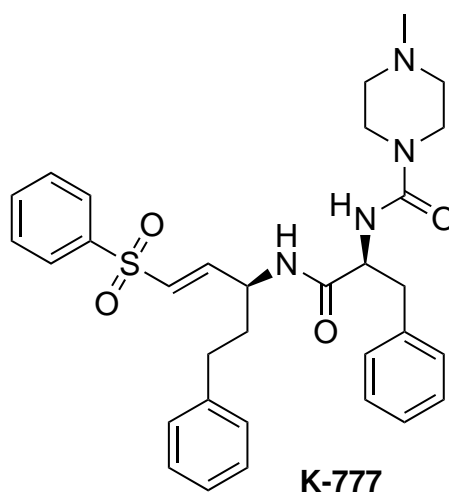


Figure 7: The cysteine-peptidase inhibitor K-777 against Chagas disease, currently in pre-clinical development.

Table 1: Summary of parasitic diseases discussed in this thesis and their current treatment and drugs in clinical development.

	HAT	Cagas Disease	Leishmaniasis
Disease form	First stage and late stage ^[5]	acute phase and chronic stage ^[2]	Visceral, cutaneous and mucocutaneous ^[4]
Etiological agent	<i>T. b. gambiense</i> , <i>T. b. rhodesiense</i> ^[3]	<i>T. cruzi</i> ^[2]	21 <i>Leishmania sp.</i> ^[3,4,7]
Host distribution	subcutaneous tissue, blood and lymph, cerebral spinal fluid ^[6]	intracellular, in cytoplasm of heart smooth muscle, gut, CNS ^[17]	intracellular in phagolysosomes of macrophages ^[8]
Vectors	Tsetse fly ^[6]	Triatamine bug ^[2]	female sandfly ^[5]
Transmission	bite of infected Tsetse fly ^[6]	feces of triatamine bug, blood transfusion, organ transplantation ^[2]	bite of infected infected sandfly ^[5]
Geographic distribution	sub-Saharan countries in Africa ^[6]	26 Latin American ^[2,5] countries	South and Central America Europe, Africa, Asia ^[13]
Population at risk	70,000,000 people ^[6]	25,000,000 people ^[2,5]	350,000,000 people ^[13]
Infections	7,139 people ^[6]	10,000,000 people ^[2,5]	12,000,000 people ^[3,4,7]
Deaths per annum	30,000 people ^[6]	10,000 people ^[2,5]	51,000 people ^[3,4,7]
Current chemotherapy	Pentamidine , Suramin, Melarsoprol, Eflornithine ^[20]	Benznidazole, Nifurtimox ^[24]	Pentostam, Meglumine antimoniate, Pentamidine, Amphotericin B ^[8]
Drugs in the pipeline	Nifurtimox/Eflornithine DB829 (preclinical) ^[12] Fexinidazole (phase I) ^[11] SCYX-7158 (Phase I) ^[12,38]	Posaconazole (phase 2) ^[21,53] TAK-187 (phase I) ^[55,56] Ravuconazole (phase 1) ^[55,56] K-777 (preclinical) ^[10,58]	Miltefosine (approved 2010) ^[41] Sitamaquine (phase 2b) ^[45–48] Paromomycin (licensed in India) ^[9] Ketoconazole, Itraconazole Fluconazole (anti-fungal drugs) ^[48,49]

layout of table modified from Stuart et al.^[13]

1.4 GPI-anchor biosynthesis as a prospective drug target

Most of the drugs in the pipeline for treating HAT, Chagas disease and Leishmaniasis were initially developed for other applications. Although this a good approach to identify drugs quickly,^[8] analysis of the kinetoplastid genome has allowed the identification of common targets essential for parasite survival which have yet to be exploited.^[13] Particularly interesting anti-parasitic targets essential for all three protozoa include biosynthetic pathways in fatty acid biosynthesis, glycoposphatidylinositol (GPI) anchor biosynthesis, sterol biosynthesis (ergosterol and isoprenoids), cysteine proteases, protein kinases and iron chelation therapy.^[13,61–63] However, the path towards broad anti-parasitic agents is difficult, as all three parasites are found within different compartments in the human organism and efforts to find anti-trypanosomal agents against *T. brucei* and *T. cruzi* have been described as "frustrating".^[14]

GPI-anchor biosynthesis has been shown to be essential for the survival of *T. brucei*, *T. cruzi* and *L. infantum*, using chemical and or genetic approaches (Figure 8).^[18,64–67] In *T. brucei*, the GPI-anchor serves to attach essential proteins to the plasma membrane of the parasite, particularly the variant surface glycoprotein (VSG) protein to confer protection and the transferrin-receptor needed for iron uptake.^[69,70] *T. brucei* is covered in a dense-cell surface coat of VSG proteins,^[71] which undergoes constant anti-genetic variation from 1,000 immunologically distinct VSG genes.^[72,73] Although only one VSG gene is expressed at a time, tight regulation of gene expression enables temporal changes in the VSG coat, allowing the parasite to evade the human host immune system.^[72,73]

The related kinetoplastid *Leishmania sp.* is also known to express GPI-anchored glycoproteins and GPI-related lipophosphoglycan and glycoinositolphospholipid structures on its surface, suggesting that GPI-anchor synthesis inhibition could lead to anti-parasitic agents with anti-trypanosomal and anti-leishmanial activity.^[71] However, *Leishmania mexicana* has been shown to survive without GPI-anchored glycoproteins and GPI related structures, whereas *Leishmania major* displayed dependencies on these structures for survival.^[71] Recently, GPI-anchor biosynthesis inhibition in *Leishmania spp.* has been reviewed, highlighting the importance of GPI-anchored glycoconjugates for survival and virulence and suggesting similar targets as discussed in this thesis for *T. brucei*.^[18] Genetic studies on a knockout *T. brucei* strain deficient in *TbGPI10*, the gene that encodes the third mannosyltransferase (MT-III) in *T. brucei*-GPI synthesis, has been shown not to be viable in the bloodstream form *in vitro*.^[70] Although, the protective coat, which is associated with the GPI-anchor, would theoretically not be essential for *T. brucei in vitro*, the loss of the VSG-coat is thought to change cell-morphology and this combined with the loss of the GPI- bound trypanosome transferrin receptor could explain the observed trypanocidal effects.^[70] In addition to genetic validations of GPI-anchor synthesis as an anti-trypanosomal target, the enzymes involved in the GPI-anchor biosynthe-

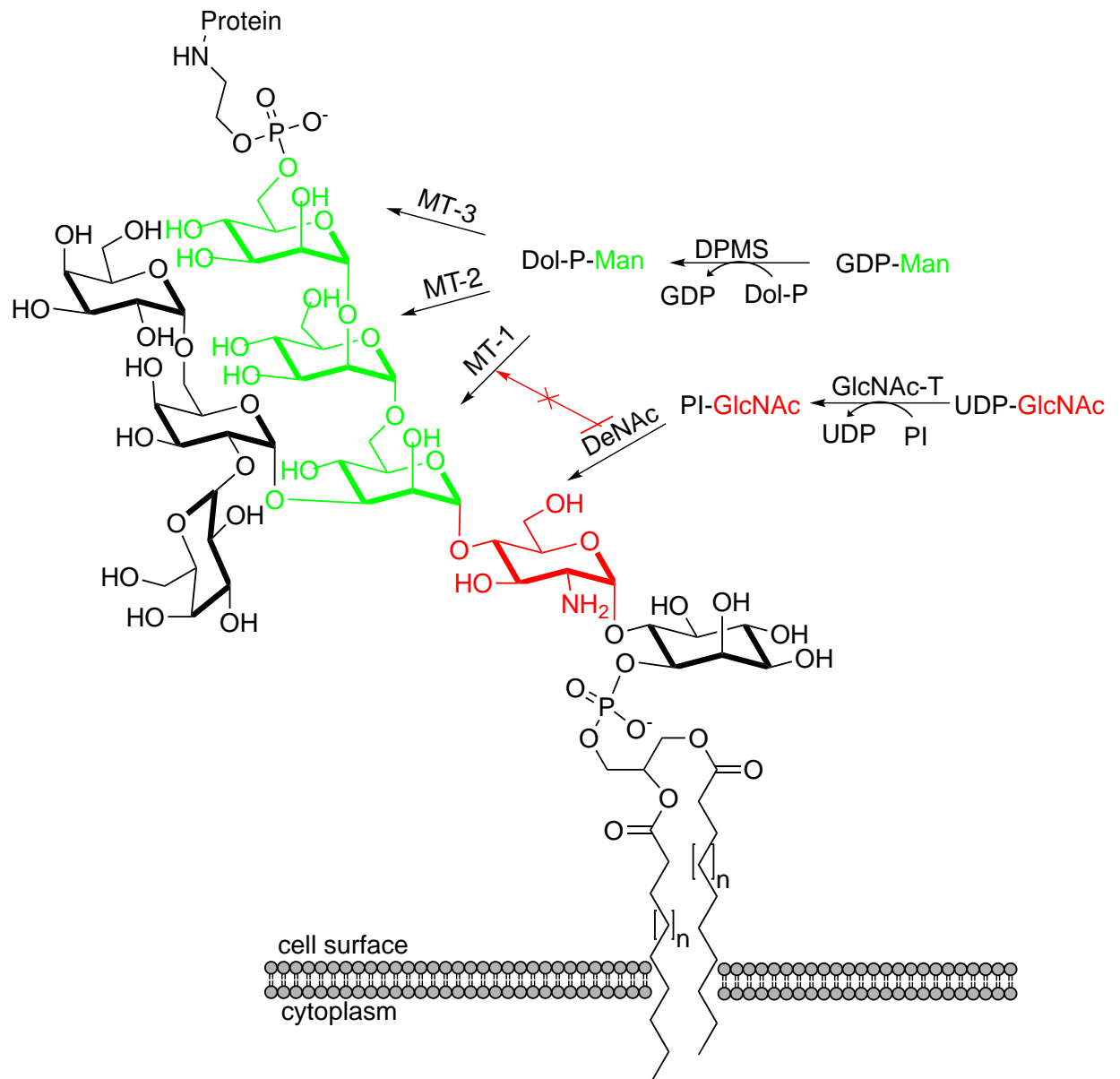


Figure 8: Schematic representation of GPI-anchored VSG protein and key steps in the GPI-anchor biosynthesis; MT I-III: mannosyltransferases; DPMS: dolichol-phosphate mannose synthase; GlcNAc-T: N-acetylglucosaminyltransferase complex; DeNAc: GlcNAc-PI de-N-acetylase.^[68]

sis pathway have been evaluated as potential targets for the development of anti-trypanosomal agents.^[64,74] Chemical and genetic studies confirmed inhibition of GPI anchor biosynthesis as a validated target of the bloodstream form of *T. brucei*.^[64,65,75] Although mammalian and trypanosomal GPI-biosynthesis are very similar, there are essential differences which can be exploited in potential drugs against *T. brucei*, *T. cruzi* and *L. infantum*.^[70] The mannosylation and acylation steps in the GPI-anchor synthesis in *T. brucei*, *T. cruzi* and *L. infantum* are of particular interest, as their substrate specificity and order of action differ from the mammalian analogues.^[64] In protozoa such as *T. brucei*, *T. cruzi* and *L. infantum* the 2-OH of inositol is acylated with a fatty acid after addition of the first mannose and detailed investigations have shown that without this fatty acid, the ethanol-amine phosphate is not added to the third mannose residue, resulting in the loss of GPI-anchors for attachment of proteins.^[64] Whereas in mammalian cells the acylation occurs prior to the transfer of the first mannose, the differing substrate specificities of both mammalian and *T. brucei* enzymes have been exploited through the use of modified substrate analogues.^[64] The first step of GPI-anchor biosynthesis is the transfer of N-acetylglucosamine (GlcNAc) from UDP-GlcNAc to phosphatidylinositol (PI). This step is catalysed by the N-acetylglucosaminyl transferase complex (GlcNAc-T) (Figure 8).^[64] In the consecutive step of the GPI-anchor biosynthesis, the N-acetyl group of PI-GlcNAc is removed by the Zn-metalloprotease GlcNAc-PI de-N-acetylase (DeNAc).^[64,76] DeNAc has been genetically validated as a target for the development of anti-trypanosomal agents.^[71] Inhibition studies with modified substrates suggested substrate-channeling between DeNAc and MT-I could prevent GlcN-PI from accessing the active site of MT-I.^[77] This implies that successful inhibition of DeNAc will prevent the incorporation of the tri-mannoside core structure (Figure 8 displayed in green). The incorporation of this tri-mannoside core structure is catalysed by three mannosyltransferases MT-I-III using Dol-P-Man as the common donor substrate.^[64] Dol-P-Man is a key substrate in GPI-anchor biosynthesis, as it is used by the mannosyltransferases MTI-III and furthermore for four more mannosyltransferases for the formation of N-linked glycans.^[78–80] The formation of Dol-P-Man is catalysed by dolichol-phosphate mannosase synthase (DPMS) from dolicholphosphate (Dol-P) and the sugar-nucleotide GDP-mannose (GDP-Man).^[80] Inhibition of DPMS would prevent formation of key substrate Dol-P-Man, therefore it has an essential role in GPI-anchor biosynthesis and is an attractive target (Figure 8).^[68] Indeed, inhibition of DPMS by small molecular inhibitors has been shown to result in moderate anti-trypanosomal activity in *T. brucei*.^[68]

T. cruzi is also dependant on GPI-anchor biosynthesis to attach trans-silidases on its membrane surface, allowing the parasite to invade cells and ensuring parasite survival.^[66] GPI-deficient *T. cruzi* amastigotes fail to develop into infective trypomastigotes within host cells,^[67] suggesting that GPI-anchor biosynthesis in *T. cruzi* is a valid drug target.

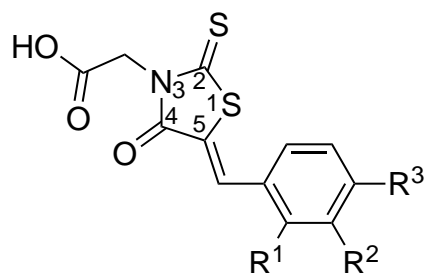


Figure 9: General structure of rhodanine-N-acetic acid derivatives with inhibitory activity against DPMS, R^1 - R^3 variable

1.5 Rhodanine derivatives in drug discovery

Recently, rhodanine-N-acetic acid derivatives (Figure 9) have been discovered as inhibitors of DPMS, with possible inhibitory effects on other enzymes essential for GPI-anchor biosynthesis in *T. brucei*.^[68] However these derivatives showed no inhibitory effect on parasitic growth at 100 μM .^[68] Thus further optimisation of this scaffold might be a good starting point for the development of anti-parasitic agents. Rhodanine derivatives are known to bind to a diverse set of targets, explaining their significant appearance in the literature (299 publications in the years 2010-2011).^[81] Consequently, this compound class has recently been classified as an undesirable scaffold for screening against molecular targets.^[82] However, there is continued discussion about the usefulness of the rhodanine scaffold. Supporters insist the rhodanine scaffold benefits from its ability to bind to a broad range of molecular targets,^[83] while others would avoid rhodanine derivatives at any cost in a drug discovery program.^[82,84] A detailed analysis of the rhodanine scaffold in protein crystallographic structures, identified the thiocarbonyl as major contributor to polar and intermolecular interactions in molecular targets.^[83] Density functional theory calculations on rhodanine derivatives have shown that the highest occupied molecular orbital (HOMO)-orbital is localised at the exo-cyclic sulphur atom.^[83] In addition, the electrostatic potential has been calculated and mapped on the surface-accessible molecular surface, showing localisation of a negative potential on the thiocarbonyl.^[83] These calculations give an explanation for the observed polar and intermolecular interactions of the thiocarbonyl moiety in protein X-ray structures.^[83]

However, this is not the only reason for controversy regarding their use. The exo-cyclic double bond in rhodanine-5-benzylidene derivatives is part of a Michael acceptor system and therefore prone to nucleophilic attack and covalent binding to molecular targets.^[81–83] The ability of rhodanine derivatives to react as Michael acceptors have been shown in a X-ray structure of hepatitis C virus (HCV) RNA polymerase NS5B with a 5-benzylidene rhodanine covalently bound to the Cys366 residue, although pre-incubation and dilution experiments suggest re-

versible binding *in vitro*.^[85] Using ultra-violet spectroscopy another rhodanine derivative has been shown to act as a Michael acceptor with dithiothreitol (DTT) under physiological conditions (a decrease of absorbance, due to interruption of the conjugated aromatic system was observed).^[86] Here too, Michael acceptor reactivity was described as reversible, shown by complete restoration of the conjugated aromatic system after exposure to oxidative conditions.^[86] But this experiment is questionable, as rhodanine derivatives have been found to undergo light-induced binding to nucleophiles, which in the absence of light were found to be of a reversible nature.^[87] Alternative methods to show Michael acceptor reactivity in rhodanine derivatives include the La antigen protein reactive species Nuclear Magnetic Resonance (NMR) assay.^[88] Out of 19 rhodanine compounds screened for Michael acceptor reactivity against the human La antigen protein, an important component of the ribonucleoprotein complex,^[89] 8 compounds were shown to react as Michael acceptors.^[90] The Michael acceptor reaction of rhodanine with nucleophiles results in the loss of the conjugated aromatic system, energetically disfavours this kind of reaction,^[83] which could explain the lack of general Michael acceptor reactivity of rhodanine derivatives and the reversibility of the reaction.

A third and possible main reason for the controversial reputation of rhodanine derivatives in screening campaigns is their interference with many biological assays due to their intense colour and ability to chelate transition metals.^[81,82] The impact of a publication on rhodanine as Pan assay interference compounds in screening of libraries, describing rhodanine derivatives as "pollutants of the scientific literature", is significant.^[82] Researchers who previously published a number of papers and reviews about the benefits of the rhodanine scaffold, praising its distinct biological activity, subsequently changed opinion and would now only use the rhodanine scaffold in drug development combined with X-ray crystallography and even then, only as probes.^[81,82,91–96] Despite debates on the status of rhodanine derivatives as promiscuous binders or privileged scaffolds, many have made it successfully through clinical trials. Epalrestat (Figure 10), is a rhodanine-N-acetic derivative with Michael acceptor system and is currently the only available aldose reductase inhibitor against diabetic retinopathy/nephropathy in Japan.^[97]

The rhodanine class seems to be an ideal starting point to achieve inhibition of one or multiple pathways common to *T. brucei*, *T. cruzi* and *L. infantum*. Rhodanine derivatives have been reported as inhibitors of bacterial, fungal and recently parasitic glycosyltransferases,^[86,92–95,98–100] making them particularly interesting for the development of inhibitors against GPI-anchor synthesis in parasites. This is further supported by reports about rhodanine derivatives as mimics for phosphate groups,^[68,86,100–105] as many of the glycosyltransferases involved in the GPI-anchor biosynthesis have sugar nucleotide donors (GDP-Man), for which the rhodanine-scaffold would be an ideal mimic.^[68]

The rhodanine class could also potentially be an important scaffold for the development of

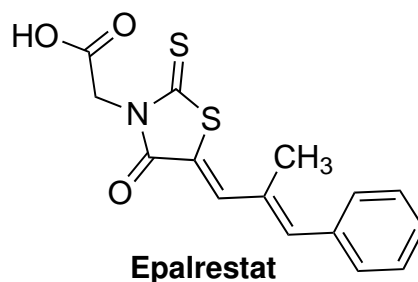


Figure 10: Epalrestat, a rhodanine-N-acetic acid derivatives used against long term diabetic complications.

inhibitors against the sterol pathway in parasitic organisms, as they have been found to inhibit many NAD(P)H processing enzymes,^[106–110] in particular aldose reductases similar to 14- α -demethylase CYP51.^[111] Here a catechol moiety on the 5-position of the rhodanine-scaffold has been reported as mimic for NAD(P)H in bacterial enzymes.^[107,108] This combination of a catechol motif and a rhodanine moiety has been shown to successfully inhibit type II fatty acid biosynthesis in *Plasmodium falciparum* by inhibiting the enoyl acyl carrier protein reductase.^[112] However none of these derivatives have been assessed for their anti-trypanosomal and anti-leishmanial activity.

Rhodanine derivatives have been identified as inhibitors against hepatitis C virus proteases,^[113,114] but only with moderate activities and poor selectivity for viral proteases compared to the mammalian equivalent^[114]. However this could potentially be exploited, as mammalian protease inhibitors showed surprising selectivities and activities against the trypanosome proteasome.^[115] Therefore rhodanine derivatives might be potential candidates for inhibitors against parasitic proteases.

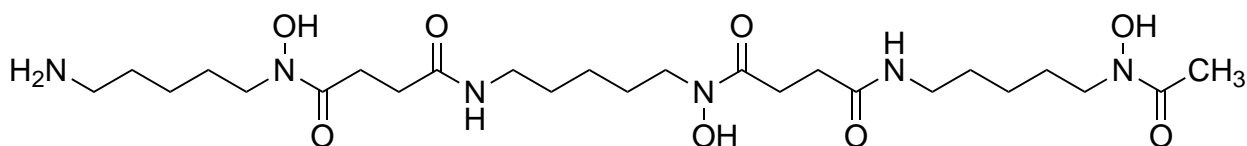
The thiazolidine-2,4-dione derivative AS605240, an inhibitor of phosphoinositide 3-kinase- γ (PI3K γ) has been found to be as effective against cutaneous Leishmaniasis as the pentavalent antimonial stibogluconate in *Leishmania mexicana* infected mice (15 mg/kg dose).^[116] Genetic knockout experiments of PI3K γ in mice caused a suppression of parasite entry into the phagocytes,^[116] confirming the role of host PI3K γ in parasite infection. AS605240 was first explored against neuroblastoma, rheumatoid arthritis and systemic lupus erythematosus, diseases affected by PI3K γ inhibition.^[117,118] But recently PI3K γ has been suggested as target against kinetoplastids such as *T. brucei*, *T. cruzi* and *Leishmania spp.* as genomic data has identified 12 proteins belonging to the PI3K γ protein superfamily, with some of them unique to these parasites.^[119] *TbVps34*, the *T. brucei* equivalent of PI3K γ has been shown to be important for membrane trafficking and Golgi segregation during binary fission.^[120] Various kinase inhibitors have been assessed for their anti-parasitic activity *in vitro* and in *T. brucei* spp., *T. cruzi* and *Leishmania major* infected mice.^[119] Although no benefit was conferred

on *T. cruzi* and *Leishmania major* infected mice, *T. brucei* infected mice showed an extended survival of 10.8 ± 2.4 days.^[119] Kinase inhibitors are promising starting points for combating trypanosomal infection,^[119] however the PI3K γ inhibitor AS605240 and other thiazolidine-2,4-dione derivatives have not yet been assessed for their anti-parasitic activity.

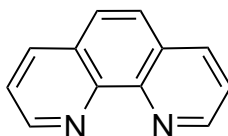
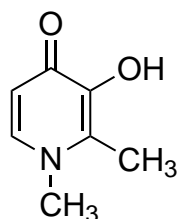
The rhodanine compound class has been chosen as a lead structure due to its previously reported biological activities, in particular its ability to inhibit glycosyltransferases, such as DPMS in the GPI-anchor biosynthesis.^[68] Rhodanine and rhodanine-like compounds, such as thiazolidine-2,4-dione and pyrazolones were among the few reported small molecular inhibitors for glycosyltransferases.^[86,92–95,98–100] The majority of glycosyltransferase inhibitors are carbohydrate analogues mimicking essential transition states.^[99,121] Although the use of the rhodanine scaffold may pose potential problems in the drug discovery process, recent examples have shown that this scaffold can serve as a lead for enzymes such as the tyrosyl-DNA Phosphodiesterase I, for which there are no alternative templates available.^[122] Another potential problem of rhodanine derivatives is selectivity towards a molecular target, but here too a recent report on proviral (integration site for moloney murine leukemia virus) kinases have shown that non-specific thiazolidine-2,4-dione derivatives can be optimised to be selective inhibitor candidates with low nM target affinity.^[123]

1.6 Iron chelation as an anti-parasitic strategy

A further main focus of this project was the investigation of iron chelation therapy against protozoan diseases like HAT, Chagas disease and Leishmaniasis. Iron is an essential element in all living organisms, including *T. brucei*, *T. cruzi* and *L. infantum*.^[61–63] Iron, due to its oxide-reductive properties and high affinity to oxygen is an important co-factor in numerous enzymes, such as ribonucleotide reductase which is involved in DNA synthesis.^[124,125] The bloodstream form of *T. brucei* does not have a conventional respiratory chain, instead oxidation and electron transport for energy production is carried out by the iron-dependent alternative oxidase (TAO).^[126] Genetic alterations of the heme binding site in TAO have validated iron dependency for catalytic function.^[127] Furthermore, the iron chelator ortho-Phenanthroline (Figure 12) has been shown to inactivate the TAO-complex.^[127] The main source of iron in *T. brucei* is host transferrin, which is transported through the trypanosomal receptor for transferrin uptake (*TbTfR*) in order to reach the interior of the parasite.^[128] Intracellular amastigotes of *L. infantum* salvage iron from host macrophages.^[126] Whereas *T. cruzi* has been shown to rely on transferrin uptake, but the exact mechanism is unknown.^[126] Iron depletion in parasites has been shown to induce oxidative stress, prevent J-base synthesis, decrease DNA synthesis and inevitably cause death.^[126] Consequently, iron chelation has been suggested as a potential strategy to combat infectious diseases.^[126] While iron chelation would cause

**Deferoxamine****Figure 11:** The bacterial siderophore Deferoxamine.

general cytotoxicity, iron chelators with possible parasite selectivity, without interfering with the host iron status, would be of particular interest. Deferoxamine (Figure 11) is a bacterial siderophore that has been shown to reduce parasitemia *in vivo* in *L. infantum* and *T. cruzi* infected mice, without interfering with the host iron metabolism.^[62,63] However, a complete cure of parasitemia was not achieved, highlighting the need for novel parasite selective iron chelators.^[62,63] Deferoxamine has also been shown to inhibit *T. brucei* growth *in vitro*,^[61] however no *in vivo* studies have been performed yet.^[126] Few iron chelating agents besides Deferoxamine have been investigated as anti-parasitic agents.^[126]

**ortho-Phenanthroline****Figure 12:** Molecular structure of the iron chelator ortho-Phenanthroline.**Deferiprone****Figure 13:** The iron chelating agent Deferiprone.

In this study the anti-parasitic activity of iron chelators derived from the clinically used Deferiprone (Figure 13) were investigated. Deferiprone is an orally available iron chelator for the treatment of thalassemia in humans.^[129] Deferiprone and simple N-alkyl substituted analogues have previously been assessed for anti-plasmodial activity against *Plasmodium falciparum* and showed promising activities *in vivo*.^[130–132] But these Deferiprone derivatives also

showed increased toxicity in mice and *in vitro* against mammalian K-562 cells.^[130–132] Further modification in particular on the N-1 position of Deferiprone would be an interesting starting point for anti-parasitic activity with increased selectivity. Additionally the oral availability is very interesting as most of the previously mentioned anti-parasitic agents relied on parenteral administration.

1.7 Parasite life cycles

T. brucei ssp., *T. cruzi* (Y-strain) and *L. infantum* exist in different stages of the life cycle depending on time of infection and host.^[2–4] Individual life cycle stages differ in regards to the metabolism and ecology of the parasite,^[133] therefore it is important to screen against relevant stages of the parasites.

Anti-parasitic activity screens against *T. brucei* ssp. were performed using *T. brucei brucei* trypomastigotes (Figure 14) which cause the animal disease Nagana, but are not pathogenic to humans.^[16] *T. b. brucei* is commonly used as model for *T. b. gambiense* and *T. b. rhodiense*, the parasite causing HAT in humans.^[33,134,135] Previously the first line drug Pentamidine has been tested against *T. b. brucei*, showing an anti-trypanosomal activity of 14 nM.^[134] Furthermore, the anti-trypanosomal activity of Fexinidazole against *T. brucei brucei* ($2.38 \pm 0.88 \mu\text{M}$), *T. brucei rhodesiense* ($2.17 \pm 0.29 \mu\text{M}$) and *T. brucei gambiense* ($1.84 \pm 1.13 \mu\text{M}$) showed similar activities.^[33] In the same study the standard drugs Melarsoprol, Pentamidine and Diminazene have been shown to have comparable anti-parasitic activity,^[33] further validating that screens against *T. b. brucei* are indicative for the activity against other *T. brucei* ssp. causing HAT in humans.

Anti-parasitic activity screens against *T. cruzi* were performed using trypomastigotes (Figure 15), which are found in the mammalian host during the acute phase of Chagas disease.^[136] *T. cruzi* trypomastigotes are responsible for continuation of the intracellular infection and are commonly used in anti-parasitic drug screens for Chagas disease.^[17,136,137] In these screening campaigns Benznidazole was used as a standard and reference drug ($172.4 \mu\text{M}$).^[137]

Anti-parasitic activity screens against *L. infantum* were performed using promastigotes (Figure 16). Screening against the promastigote form reduced the cost and time for evaluation of the anti-leishmanial activity of inhibitors. The promastigote form of *T. cruzi* is found extracellularly in the sand fly vector and the parasites can be grown in high densities.^[133] Therefore screens against the promastigote form are very popular,^[133] although metabolism and ecology of the promastigote form differ from the amastigote stage.^[133] In order to overcome this hurdle, active compounds against the promastigote stage were assayed against growth of the intracellular *Leishmania* amastigote form.^[133] But screens against *Leishmania* amastigotes are very expensive in terms of the maintenance of lab animals and varying success of infectivity with

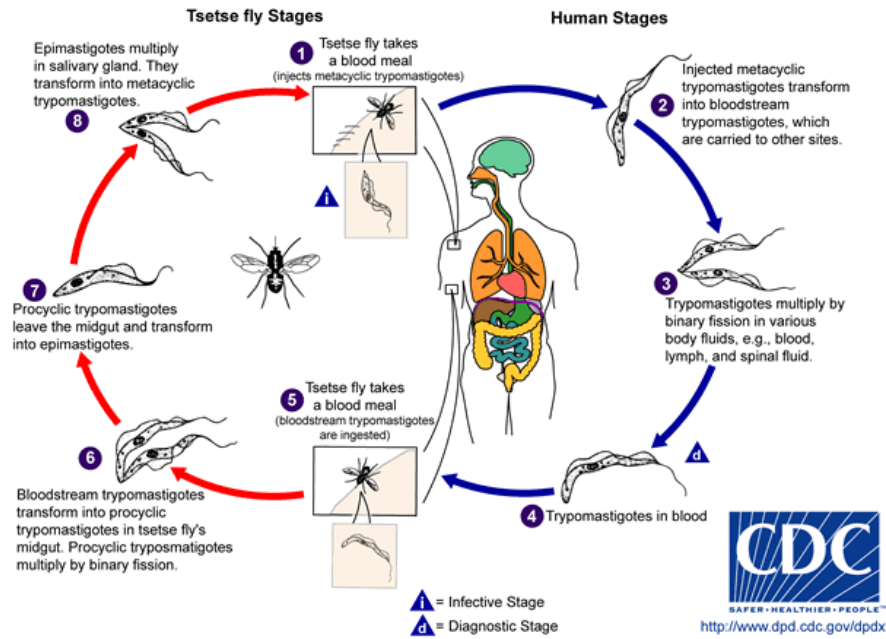


Figure 14: Life cycle of *T. brucei* in Tsetse fly and man; picture taken from <http://www.dpd.cdc.gov>.

macrophages.³ It has been found that the promastigote stage is less sensitive towards small molecular inhibitors as compared to the intracellular amastigote form.^[138] Although screening results against the promastigote form are therefore of limited value as indicator for activity against the infective mammalian form,^[138] it was chosen as fast evaluation of a large set of inhibitors in short time. However, drugs such as Amphotericin B and Miltefosine which affect membrane integrity have been shown to have comparable activities in the vector and mammalian stage of the parasite,^[138] possibly validating the approach for screening of inhibitors against *Leishmania* promastigotes to identify potent inhibitors of the amastigote growth.

³Personal communication with Dr. Andre Tempone

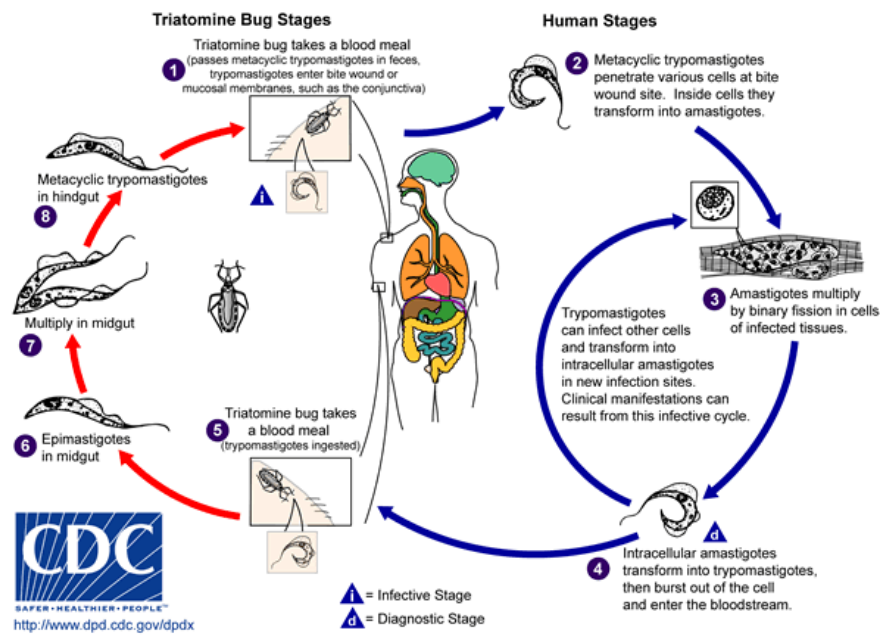


Figure 15: Life cycle of *T. cruzi* in Triatomine bug and man; picture taken from <http://www.dpd.cdc.gov>.

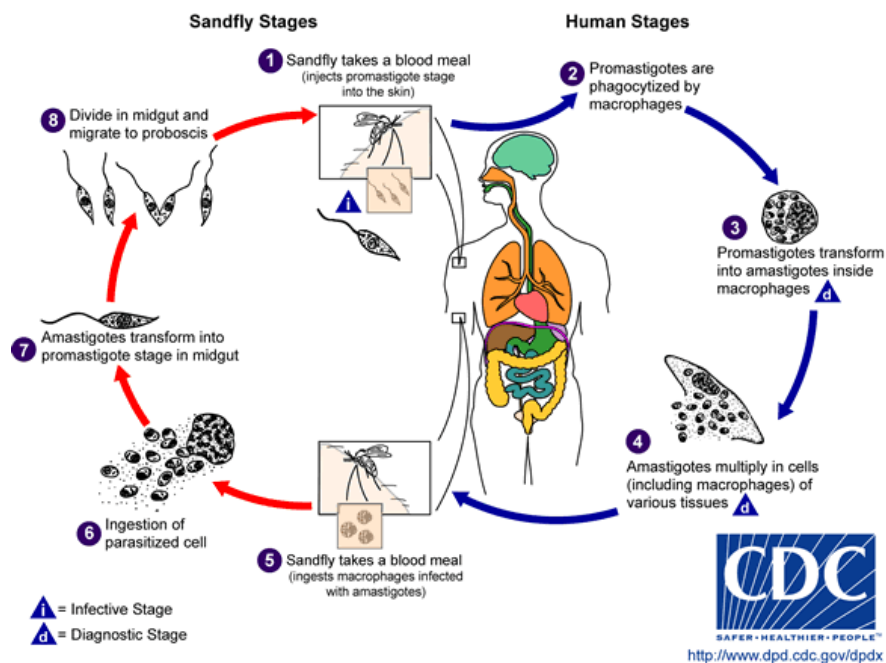


Figure 16: Life cycle of *Leishmania infantum* in sand fly and man; picture taken from <http://www.dpd.cdc.gov>.

2 Objectives

The main goal of this study was the identification of novel small molecular inhibitors against the parasitic protozoa *T. brucei*, *T. cruzi* and *L. infantum*. Of particular interest was the identification of inhibitors with simultaneous activity against all three parasites and low mammalian toxicity. In order to identify such potential broad-spectrum and parasite-selective inhibitors, whole-parasite cytotoxicity assays were used as primary screening assays. These anti-parasite assays were complemented by toxicity assays against mammalian cell lines in order to assess the selectivity profile of inhibitor candidates.

As chemical starting points, known inhibitors of *T. brucei* GPI-anchor biosynthesis on the one hand side, and known iron chelators on the other, were selected. Chemical synthesis of analogue libraries was carried out in order to improve the anti-parasitic activity of these starting compounds and to explore their applicability to *T. cruzi* and *L. infantum*.

Inhibitor candidates were evaluated for their activity against the bloodstream form of *T. brucei brucei*. The evaluation against *T. cruzi* was performed with the trypomastigote form, found in human blood, whereas the evaluation against Leishmania was executed against the promastigote form (insect vector) of *L. infantum* with testing of active candidates against the amastigote form in mice macrophages.

These whole-parasite assays do not provide information about the molecular target or mode-of-action of active compounds. It was therefore another goal of this study to carry out target identification studies with selected inhibitors. These experiments included additional biological assays as well as computational approaches and the development and application of chemical probes. Results from these target identification experiments were expected to also inform the rational design of optimized inhibitor analogues.

3 Rhodanine-N-acetic acid derivatives

3.1 Known biological activities of Rhodanine-N-acetic acid derivatives

Rhodanine-N-acetic acid derivatives are known for their broad biological activity as anti-viral, anti-bacterial, anti-fungal, anti-malarial, anti-tumor, anti-inflammatory and cardiotoxic agents.^[91] Recently, rhodanine-N-acetic acid derivatives have also been reported as anti-trypanosomal agents against the bloodstream form of *T. brucei*.^[68]

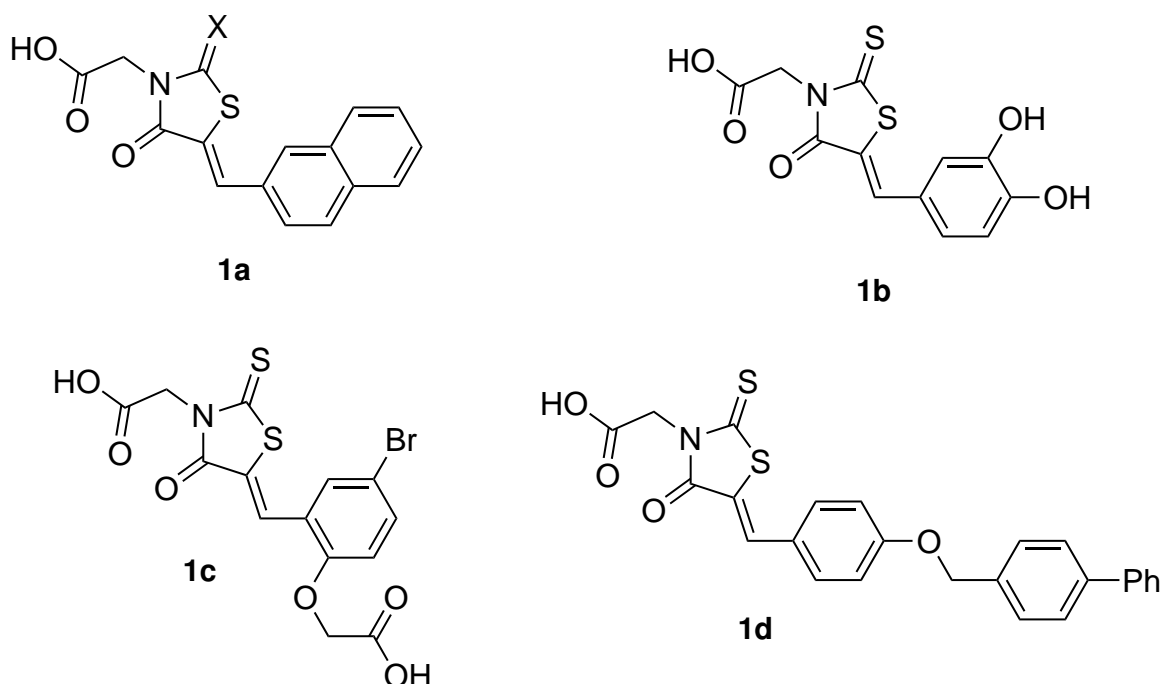


Figure 17: Previous examples of rhodanine-N-acetic acid derivatives and their corresponding thiazolidine-2,4-dione derivatives with anti-parasitic potential; X=O,S.

Rhodanine-N-acetic acid derivatives (Figure 17, **1a–d**) have been reported as aldose reductase and/or oxidoreductase inhibitors and in particular as NAD(P)H cofactor mimics.^[106–110] The rhodanine-N-acetic acid derivative **1a** was the first rhodanine-like inhibitor discovered for bovine aldose reductase.^[106] In a different study, aldose reductase activity was explained by the ability of rhodanine-N-acetic acid derivatives to function as a NAD(P)H cofactor mimic, leading to the use of this compound class as a proteomic tool for oxidoreductases.^[107,108]

Recently, compounds **1c** and **1d** have been identified as potent aldose reductase inhibitors.^[107,110] Parasitic kinetoplastids, such as *Trypanosoma ssp.* and *Leishmania sp.* are sensitive to oxidative stress,^[139] the flavoenzyme trypanothione reductase has been validated as essential for growth and virulence of these parasites.^[140–142] Rhodanine-N-acetic acid derivatives and in particular catechol derivatives that are thought to resemble the NAD(P)H cofac-

tor,^[107,108] might be very interesting candidates for inhibitors against flavoenzyme reductases in parasites. Indeed, rhodanine-N-acetic acid derivatives have been identified as moderate inhibitors of trypanosomal 14 α demethylase CYP51 (45 μ M (*T. brucei*) and 38 μ M (*T. cruzi*)), a NAD(P)H dependant enzyme of the cytochrome P450 family, essential for sterol-biosynthesis in *T. cruzi* and *T. brucei*.^[111] Although, each protozoon has different sterol requirements (sterols play a structural role in *T. cruzi* membrane formation and a functional role for life cycle regulation in *T. brucei*), inhibition of 14 α demethylase CYP51 caused anti-trypanosomal activity in both *T. brucei* and *T. cruzi*.^[111] Sterol biosynthesis in trypanosomes is a particularly interesting target as several azole CYP51 inhibitors, such as E1224, Posaconazole and Tak-187 are currently in clinical trials as anti-trypanosomal agents against Chagas disease (further details see Chapter 1.3).^[55] Rhodanine-N-acetic acid derivatives could potentially present an alternative scaffold to these azole derivatives in order to develop new anti-trypanosomal agents against both *T. brucei* and *T. cruzi*.

Besides their role as oxidoreductase inhibitors, rhodanine-N-acetic acid derivatives have been studied as inhibitors for UDP-galactopyranose mutase (UGM).^[86,100] UGM catalyses the formation of UDP-galactopyranose, a precursor for the assembly of galactofuranose, which is a key substrate for lipophosphoglycan synthesis in many pathogenic prokaryotes and protozoans, such as *L. infantum* and *T. cruzi*.^[86,100] Therefore, inhibition of UGM has been suggested as strategy for anti-leishmanial drugs, in particular against the visceral form of Leishmaniasis.^[100] In addition, rhodanine-N-acetic acid derivatives have been studied as inhibitors against MurB and MurG bacterial glycosyltransferases.^[101,103,143] This significant accumulation of reports about the inhibitory activity against bacterial glycosyltransferases was hypothesised to originate from the ability of the rhodanine moiety to function as a mimic for diphosphate bonds of sugar nucleotide substrates.^[86,100–104,143] The reported activity against glycosyltransferases and the possible ability to mimic phosphate bonds ultimately led to the discovery of novel inhibitors for dolichol phosphate mannanose synthase (DPMS), an essential sugar nucleotide glycosyltransferase in *T. brucei*.^[68] DPMS catalyses the formation of Dolicholphosphate mannanose (Dol-P-Man) from dolicholphosphate (Dol-P) and the sugar-nucleotide GDP-mannose (GDP-Man).^[80]

GDP-Man was proposed to have structural similarity to 5-benzylidene rhodanine-N-acetic acid derivatives.^[68] The most active DPMS inhibitor in the reported rhodanine-N-acetic acid series had a residual DPMS-activity of 10 %, however the same inhibitor only displayed moderate anti-trypanosomal activity at 338 μ M.^[68] In contrast, the most promising anti-trypanosomal activity in this series was observed at 96 μ M, with a residual DPMS activity of only 23 %, ^[68] suggesting other mode of actions for these inhibitors, as DPMS activity did not correlate with the shown *in vitro* results against *T. brucei*. Indeed, using a free-cell assay of the Glycosylphosphatidylinositol (GPI)-synthesis in *T. brucei*, the inhibitor with the most promising

anti-trypanosomal activity has been shown to inhibit other enzymes in addition to DPMS in the GPI-anchor biosynthesis, therefore possibly explaining the additional contribution to anti-trypanosomal activity.^[68]

The inhibition of one or possibly multiple steps in the described biosynthesis pathway will interrupt the formation of GPI-anchors, having lethal effects on the bloodstream form of *T. brucei*.^[64] Another potential target in the GPI-anchor biosynthesis is the Zn-metalloprotease GlcNAc-PI de-N-acetylase (DeNAc), where zinc-binding substrates have been postulated to inhibit DeNAc.^[76] Indeed, carboxylic acids or hydroxamic acid as zinc-binding groups have been shown to inhibit DeNAc, confirming this hypothesis.^[77] Coincidentally, rhodanine-N-acetic acid derivatives have previously been identified as zinc-chelating agents and potent inhibitors of the Anthrax-Zn-metalloproteinase.^[144,145] Furthermore, rhodanine-N-acetic acid derivatives have been studied as fungal mannosyltransferase 1 inhibitors in *Candida albicans* and other bacterial UDP-glycosyl transferases.^[98,99] The ability to chelate zinc and to bind numerous glycosyl processing enzymes make rhodanine-N-acetic acid derivatives excellent candidates for the development of multi-targeted inhibitors of the GPI-anchor biosynthesis pathway, particularly as these derivatives have already been shown to inhibit DPMS, an early essential enzyme in the GPI-anchor biosynthesis.^[68] Recently, rhodanine-N-acetic acid derivatives have been studied as drugs against Alzheimer's disease (AD), inhibiting tau aggregation in the brain of AD patients *ex vivo*, demonstrating their capabilities to penetrate the blood-brain barrier.^[146,147] Therefore, rhodanine-N-acetic acid derivatives, if sufficiently active against *T. brucei*, could potentially be applied as drugs for stage 2 human african trypanosomiasis (HAT) in the central nervous system.

Rhodanine-N-acetic acid derivatives have been found to have interesting inhibition properties against Hepatitis C Virus (HCV) chymotrypsin-like protease.^[113,114] However, most of these derivatives have been identified as unspecific inhibitors for HCV proteases and significantly inhibit other mammalian serine proteases, such as chymotrypsin, trypsin, plasmin and elastase.^[113,114] This lack of specificity can potentially be exploited, as substrates with mammalian proteasome trypsin-like activity have previously been assessed for their anti-trypanosomal activity against *T. brucei*, showing interesting selectivities for *T. brucei* as compared to the mammalian proteasome.^[115] Therefore, it would be of interest to study rhodanine-N-acetic acid derivatives with trypsin-like activity for their anti-trypanosomal potential.

Although, rhodanine-N-acetic acid derivatives show a lot of beneficial characteristics for the development of anti-parasitic agents, several draw-backs have been reported.^[82] Rhodanine derivatives were reported to interfere with assay read-outs in colorimetric assays.^[82] Indeed coloured rhodanine derivatives have been applied as chromogenic agents to monitor bacterial colony growth.^[148,149]

Furthermore, rhodanine-N-acetic acid derivatives have been reported to undergo nonspe-

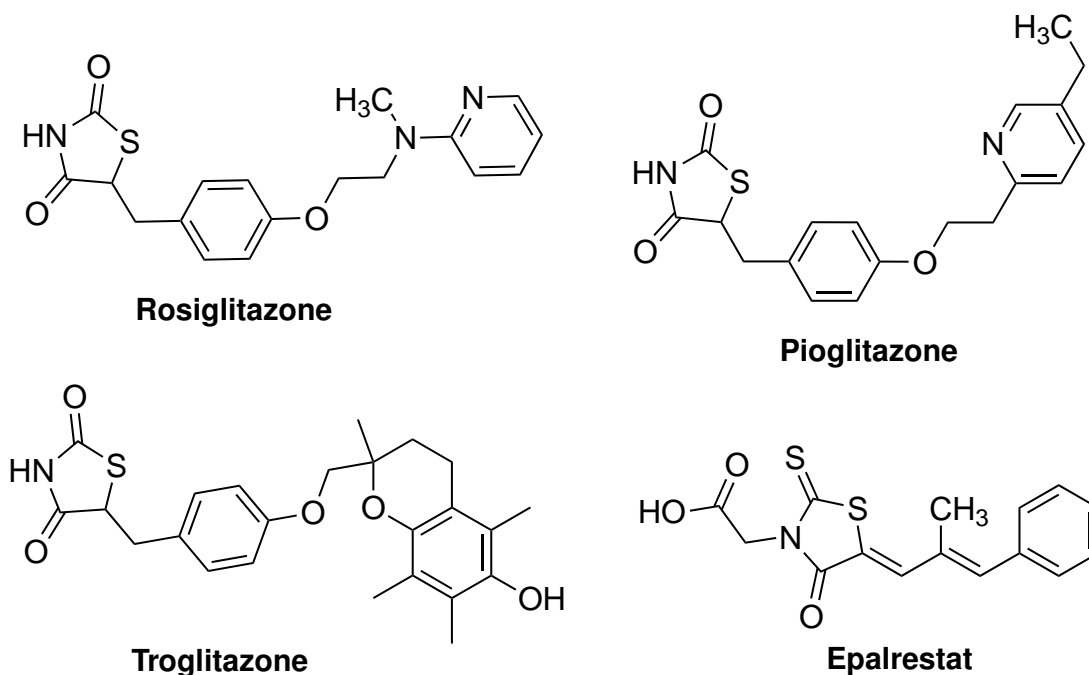


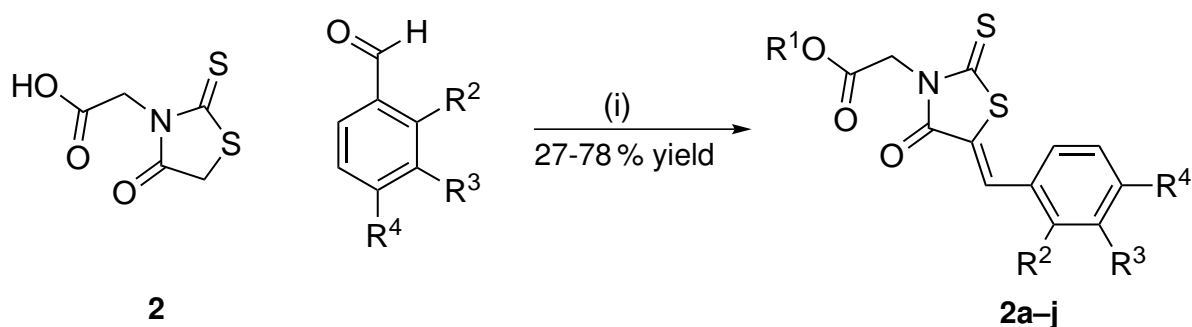
Figure 18: Examples of rhodanine and thiazolidine-2,4-dione derivatives in clinical use

cific binding to proteins and therefore decrease their activity towards the target protein.^[150] This unspecific binding most likely occurred through Michael acceptor systems within the rhodanine structure, making them susceptible to nucleophiles such as thiols in various proteins.^[82,86] Indeed, rhodanine derivatives have been shown to undergo Michael addition reactions with dithiothreitol (DTT) under reducing conditions and physiological pH, however the binding to DTT of the rhodanine-moiety was described as reversible under oxidative conditions.^[86]

Besides these undesired side-effects of rhodanine derivatives, there are examples of rhodanine derivatives or analogues which are successfully used as drugs. Rosiglitazone, Pioglitazone and Troglitazone represent examples of thiazolidine-2,4-dione derivatives, which are used in the treatment of type II diabetes mellitus.^[91] Epalrestat is a rhodanine derivative that is used as aldose-reductase inhibitor for the treatment of diabetic complications.^[91]

3.2 Synthesis of inhibitor library

In this chapter the synthesis of rhodanine-N-acetic acid derivatives is described. Following these descriptions, the underlying reaction mechanism of the Knoevenagel condensation and a possible side-reaction (Michael addition) will be discussed. Next a detailed analysis of the underlying stereo-chemistry is presented in order to understand the formation of double bond isomers, as well as to determine the double bond configuration of rhodanine-N-acetic acid derivatives.



Scheme 1: Synthesis of 5-Benzylidene rhodanine N-acetic acid derivatives **2a–j**; (i) NH_4OAc , DMF, 80°C , 3h (**2a**) or EtOH, piperidine, 80°C , 3-6 h (**2b–j**). For substituents $\text{R}^1\text{--R}^4$ see Table 2.^[68]

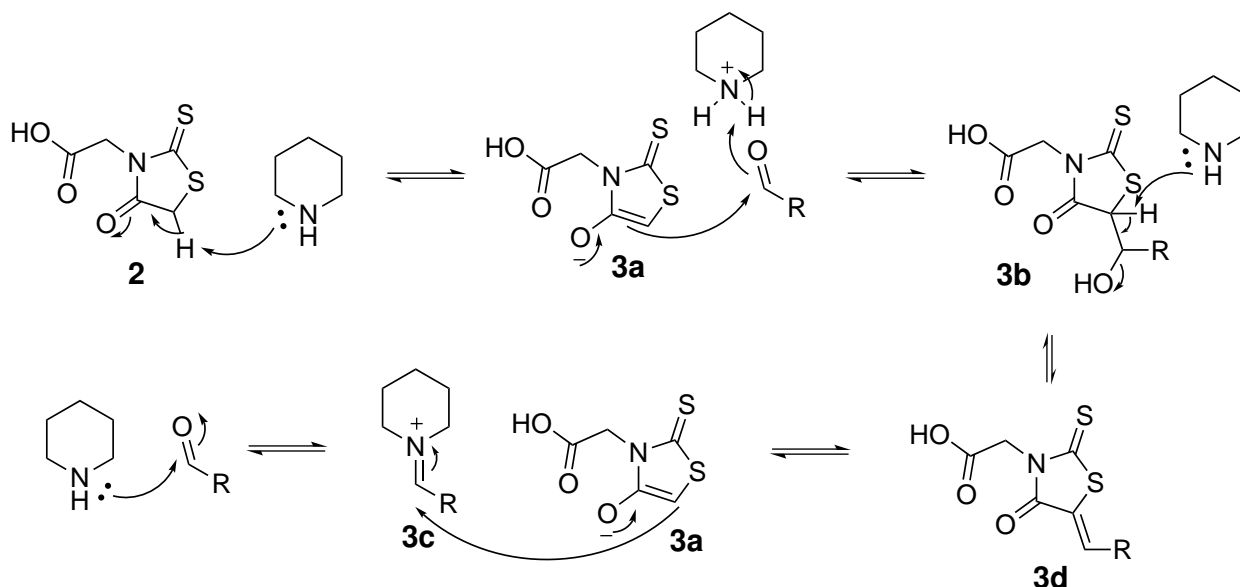
Table 2: Library of rhodanine-N-acetic acid derivatives identified as inhibitors against DPMS, see Scheme 1 for structures.^[68]

#	R^1	R^2	R^3	R^4
2a	H	H	H	H
2b	H	H	H	OBn
2c	H	H	OBn	H
2d	Piperidine	H	OBn	OBn
2e	H	OH	H	H
2f	H	H	OH	H
2g	H	H	H	OH
2h	H	H	H	Cl
2i	H	H	H	CN
2j	H	H	H	CCH

3.2.1 Synthesis of rhodanine-N-acetic acid derivatives

Rhodanine-N-acetic acid derivatives have been reported as inhibitors for DPMS, an essential enzyme for GPI-anchor biosynthesis in *T. brucei*, *T. cruzi* and *L. infantum*.^[68,151] This study was chosen as the starting point for the synthesis of rhodanine-N-acetic acid derivatives with anti-parasitic activity. These rhodanine-N-acetic acid derivatives were synthesised by Knoevenagel condensation reaction of rhodanine-N-acetic acid and various benzaldehyde derivatives (Scheme 1, see Table 2).^[68] Different solvent systems and base catalysts have been explored to optimise the reaction conditions and piperidine in ethanol has been identified as a preferable system, resulting in short reaction times and simple product isolation by filtration.^[68]

In order to optimise the condensation reaction further, the underlying mechanism of the Knoevenagel reaction is studied in further detail (Chapter 3.2.2) and different reaction condi-



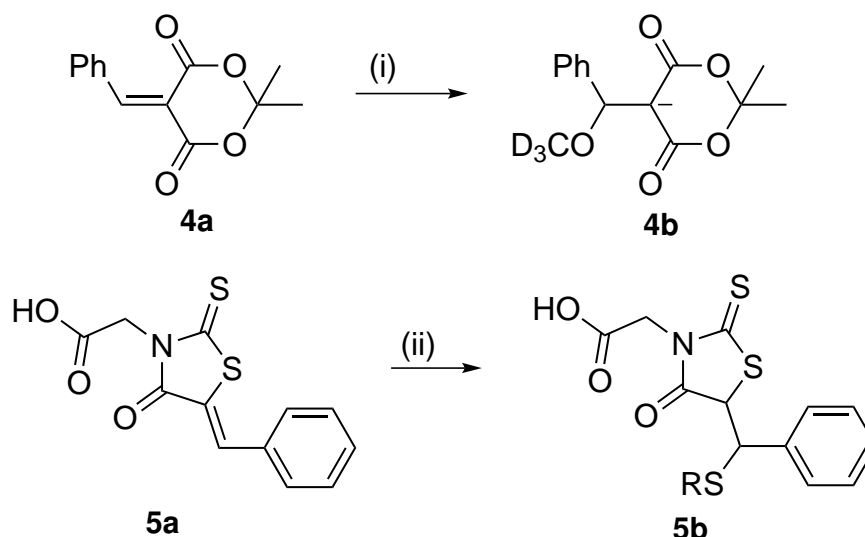
Scheme 2: Mechanism of the Knoevenagel reaction.

tions are discussed.

3.2.2 Knoevenagel reaction

The Knoevenagel reaction, first described by Emil Knoevenagel, is a special form of the aldol condensation reaction.^[152] The Knoevenagel reaction describes the reaction of an activated methylene compound with ketones or aldehydes in the presence of a weak base.^[152,153] An example for such an activated methylene group can be found in the rhodanine derivative **2** (Scheme 1). The methylene group in compound **2** is activated by the electron withdrawing effect of a thio-ester and a carbonyl group. The first step of the Knoevenagel reaction is the formation of the enolate **3a** (Scheme 2), using a weak base such as piperidine. The most common catalyst for the Knoevenagel reaction is piperidine acetate (piperidine in acetic acid).^[152]

In the proceeding step the enol **3a** can either react directly with the aldehyde to form the β -hydroxy carbonyl **3b** or can react with the imine **3c**.^[152] Both reaction mechanisms lead to the formation of the elimination product **3d**. If the reaction proceeds via the β -hydroxy carbonyl **3b**, it follows the Hann-Lapworth reaction mechanism.^[152] Otherwise, the mechanism follows the Knoevenagel mechanism, with the addition of the enol to the imine to form the corresponding β -amino intermediate.^[152] In order for the reaction to proceed via the Knoevenagel mechanism, an imine has to be formed prior to nucleophilic attack of the enol. The formation of the imine intermediate **3c** depends on the steric demands of the amine and the carbonyl compound, as well as the concentration of amine.^[154] Catalytic amounts of amine favour the



Scheme 3: Michael acceptor reactivity of Knoevenagel products; (i) NaOCD_3 ; (ii) R-SH .

Hann-Lapworth mechanism and the reaction proceeds over the β -hydroxy carbonyl **3b**.^[152] The second common step in both mechanism is the 1,2-elimination of water or amine.

Both reactions, the nucleophilic addition and the 1,2-elimination are strongly solvent dependant.^[152] While the addition reaction is facilitated by solvents with high polarity, the second step proceeds best in aprotic solvents.^[152] Therefore, solvents like dimethylformamide (DMF) would be ideal for the Knoevenagel reaction.^[155] However polar protic solvents, such as ethanol are preferable for the synthesis of rhodanine derivatives due to facile product isolation by precipitation of the elimination product **3d**.^[68]

The elimination product **3d** possesses an exo-cyclic double bond in conjugation to a carbonyl, this 1,4-electrophilic system is also known as a Michael acceptor system. Michael acceptor systems are known to undergo reaction with nucleophiles, 1,4-nucleophilic additions to this $\alpha\beta$ -unsaturated carbonyl system are therefore known as Michael addition.^[152] There is a strong correlation between the Michael acceptor reactivity and the Lewis acidity of the Knoevenagel product.^[156] The Lewis acidity and therefore Michael acceptor reactivity of neutral organic lewis acid increases with electron-withdrawing groups and planarity of the molecule.^[152] An example of an excellent Michael acceptor is displayed in Scheme 3. This Knoevenagel product **4a**, also known as Meldrum's acid possesses two strong electron-withdrawing carboxylic ester groups which form a planar structure.^[152] Upon addition of base to the Michael acceptor system, a labile pseudo base adduct is formed.^[152] The existence of this base adduct, also known as abaddon **4b** has been confirmed by NMR and UV spectroscopy.^[152] The rhodanine-N-acetic derivative **5a** can react with nucleophiles in a similar way, but here the abaddon has never been reported and the reaction proceeds to the protonated form **5b** (Scheme 3), as similar derivatives of **5a** have been reported as reversible ac-

ceptors of DTT under physiological conditions.^[86] Furthermore, the Michael acceptor reactivity of rhodanine-N-acetic acid derivatives has been confirmed by a X-ray structure of hepatitis C virus RNA polymerase showing the Michael addition product of a cysteine residue covalently attached to the rhodanine-benzylidene moiety.^[85]

But the Michael acceptor reactivity of rhodanine derivative is considered to be rare, as the conjugated aromatic system between the rhodanine core and the benzylidene moiety would be interrupted.^[83] This is even more pronounced in 5-benzylidene thiazolidine-2,4-dione derivatives, where the thiocarbonyl is substituted with a carbonyl group, as there are no reports about Michael reaction adducts.^[81,83] Thiazolidine-2,4-dione derivatives have been shown to inhibit autotaxin, which similar to hepatitis C virus RNA polymerase has a cysteine residue in its active side, in a reversible (non-covalently) manner, as 97 % of substrate could be recovered after enzymatic reaction with complete retention of enzymatic activity.^[157]

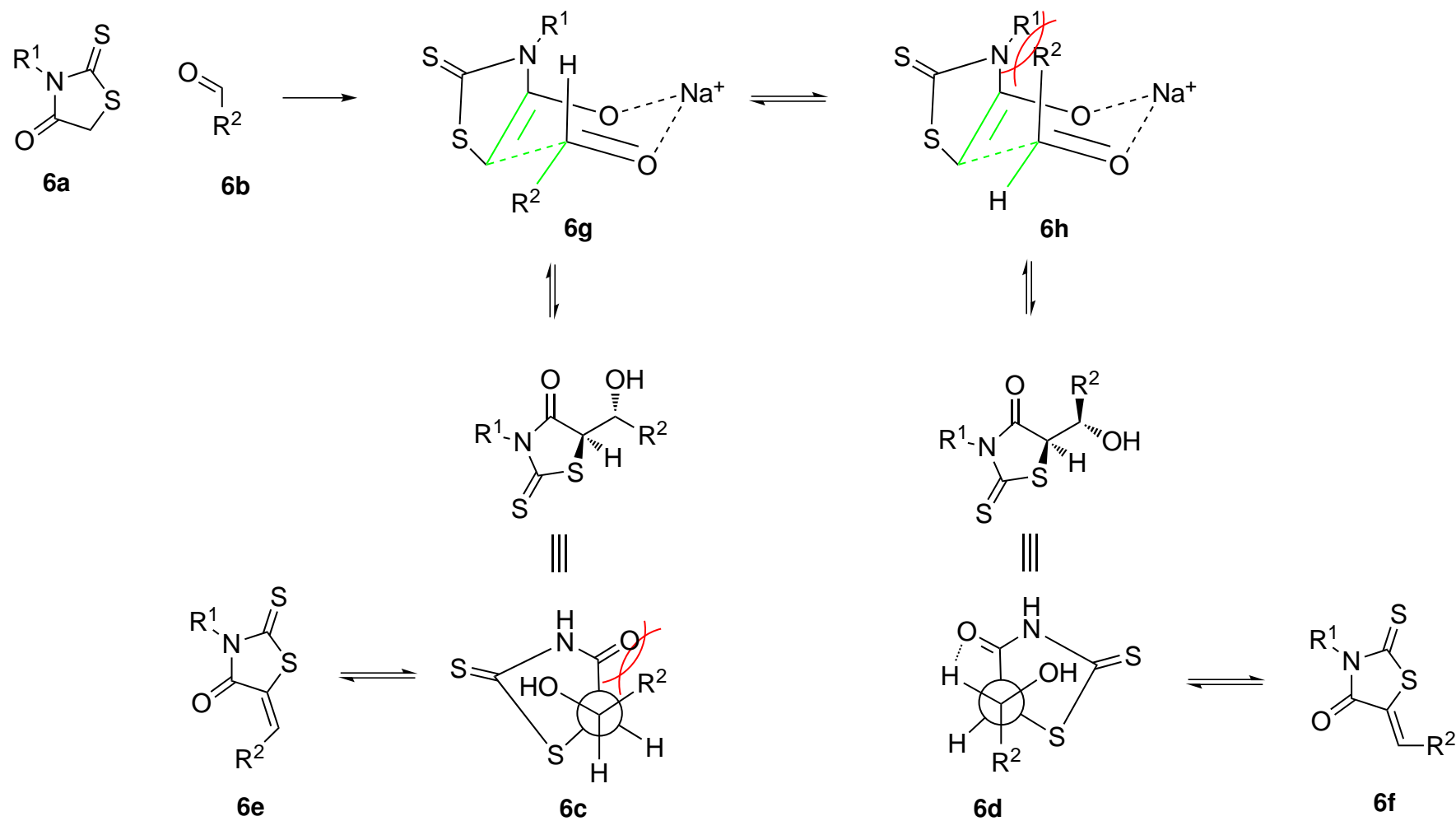
3.2.3 Stereochemistry of the Knoevenagel reaction

The Knoevenagel reaction, depending on the nature of the substrates, can give rise to different diastereoisomers, which differ in the configuration of the exo-cyclic double bond. In order to understand the biological activity of rhodanine derivatives it is therefore crucial to know the exact configuration of the double bond to differentiate both isomers.

To understand the formation of these different isomers, the reaction of a rhodanine derivative **6a** (Scheme 4) and an aldehyde **6b** is examined in further detail. The stereospecific outcome of this reaction is mostly dependant on steric considerations. In the following discussions, the Hann-Lapworth mechanism over the β -hydroxy intermediate will be used to explain the different diastereoisomers. The aldol reaction between **6a** and **6b** can form two aldol-products **6c** and **6d**. In the following elimination reaction two diastereoisomers are formed, the E-isomer (**6e**) and the Z-isomer (**6f**). The Z-isomer **6f** has been described as the thermodynamically more stable product.^[158] All reactions are reversible, so that only one diastereoisomer could preferably be formed. Previous studies on the mechanism of the aldol-condensation reaction, proposed a Zimmerman-Traxler like transition state of the rhodanine **6a** and the aldehyde **6b**.^[158] In this study, the chelating agent for the electrophilic carbonyl and the enol was suggested to be H^+ .^[158] However, metal ions such as lithium or boron are known to be primarily involved in Zimmerman-Traxler transition states.^[159] The Zimmerman-Traxler transition state is aimed at avoiding syn-pentane interactions of axial substituents in chair-like transition states.^[159] In other words, Z-enolates react to syn-aldol product, while E-enolates lead to the anti-aldol product.^[159] In the Zimmerman-Traxler transition state of rhodanine **6a** and aldehyde **6b**, sodium ions are proposed as chelating agents, as sodium acetate is a commonly used as weak base in combination with acetic acid in Knoevenagel reactions.^[160,161] In the transition states for the E-isomer **6g** and the Z-isomer **6h**, the syn-pentane interactions are minimised

for the E-isomer **6g**. The Z-isomer **6h** shows 1,3-diaxial interactions between R^2 and NR^1 . Assuming anti-periplanar elimination of water, the product **6e** is formed over the intermediate **6c**. The Newman-projection shows an unfavourable interaction between R^2 and the carbonyl group. This steric interaction was thought to be the reason for the formation of the thermodynamically stable Z-isomer.^[158] Following the reaction pathway starting from the Zimmerman-Traxler transition state for the Z-isomer **6h**, an aldol product is formed, which is favoured by less steric interactions between R^2 and the sulphur group.^[158] Assuming the reaction proceeds via an anti-periplanar elimination of water, a favourable hydrogen bond interaction between the carbonyl group and the methylene proton could be hypothesised. As mentioned before, it will be very unlikely that the reaction proceeds via strict Zimmerman-Traxler transition states, so that regio-selectivity is mainly governed by steric interactions, which are most easily displayed in the appropriate Newman-projection rather than cyclic transition states as proposed earlier.^[158] Considering only steric considerations, the Z-isomer is under less steric strain with the R^2 substituent facing towards the sulphur group. However, the introduction of additional substituents on R^2 , especially hydrogen bond donors could affect the preference for formation of the E-isomer as will be shown later in this thesis.

The stereo-configuration of the methylene (CH) proton in rhodanine derivatives is easily determined by X-ray structure analysis or NMR spectroscopy. The chemical shift of the CH signal in 1H -NMR or ^{13}C -NMR spectra depends on the alkenic substituents. This observation is particularly useful, with highly anisotropic substituents like carbonyl groups. The chemical shifts of the CH signals can be calculated and compared to the experimentally determined values in order to determine the stereochemistry of the products.^[162] Methylene protons in proximity to a carbonyl group are more deshielded and appear further downfield in the 1H -NMR spectra. The Z-methylene proton chemical shift of a thiazolidine-2,4-dione derivative has been reported to be 7.74 ppm while the E-form had a chemical shift of 7.30 ppm.^[162] In the case of di- or tri-substituted Knoevenagel products (electrophile is an aldehyde (di) or a ketone (tri)), the $^3J_{C=O,H}$ coupling between the carbonyl group and the methylene proton of compounds with known stereochemistry can be measured and then compared to unknown derivatives.^[106,163] Vicinal $^3J_{C=O,H}$ coupling constants between 3.7-6.8 Hz indicate the Z-isomer, while coupling constants between 10.0-12.3 Hz are indicative for the E-isomer.^[163] This approach was applied for elucidation of the double bond configuration of pyrazolone derivatives in chapter 6.



Scheme 4: Zimmerman-Traxler transition state and Newman projections of Knoevenagel reaction intermediates, comparison of the formation of E- and Z- double bond isomers.

3.2.4 Design of rhodanine-N-acetic acid derivatives with anti-parasitic activity

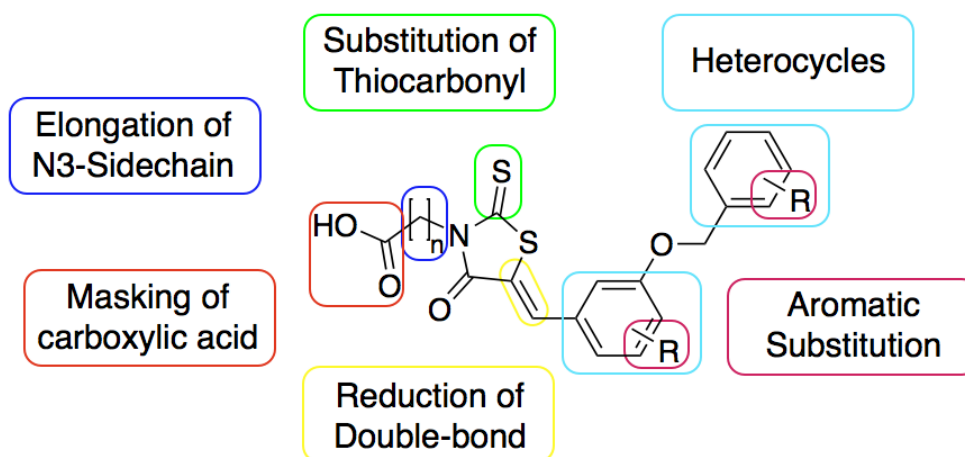
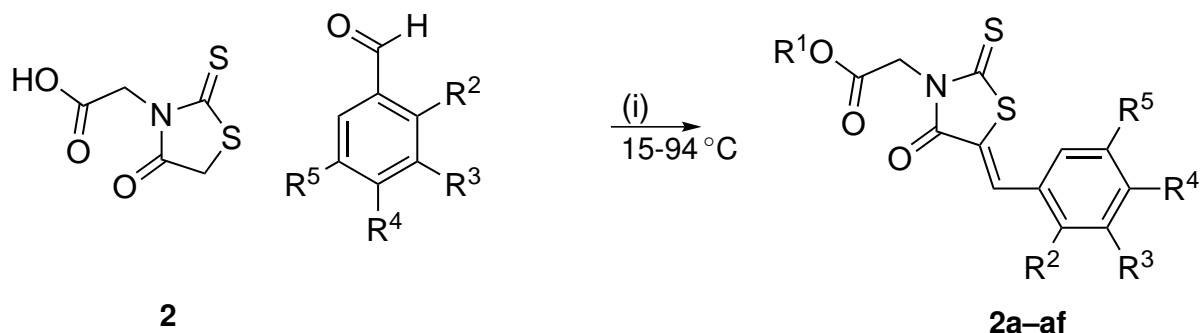


Figure 19: Strategies to improve anti-trypanosomal activity of identified lead structure.

One of the most active inhibitors of *T. brucei* growth and the DPMS enzyme is the rhodanine-N-acetic acid derivative **2c**.^[68] Compound **2c** has a 5-benzylidene derivative with a benzyloxy substituent in the meta position. This compound was chosen as lead structure for further modifications to increase the *in vitro* activity.^[68] The optimised rhodanine-N-acetic acid derivatives have been designed according to Lipinski's rule of five.^[164] Therefore, the new derivatives have a molecular weight less than 500 g/mol, less than 5 hydrogen-bond donors, less than 10 hydrogen-bond acceptors and an octanol-water partition coefficient logP value of less than 5.^[164] The molecular weight of compound **2c** is relatively low (385 g/mol), allowing further optimisation. The rhodanine N-acetic acid starting structure shows large scope for modifications to improve activity (Figure 19).

Inhibitors were designed for broad anti-parasitic activity (*T. brucei*, *T. cruzi*, *L. infantum*). Therefore the activity of these inhibitors as anti-trypanosomal and anti-leishmanial agents was evaluated against the whole organism. This phenotypic assay allows to screen for compounds with broad spectrum activity, already optimized for cell membrane penetration and activity against the whole parasites. Once compounds with interesting anti-parasitic activity are found, further target identification via labelling experiments will allow the elucidation of the molecular target. This target identification is essential in order to optimize activity and selectivity of inhibitor candidates. Rhodanine-N-acetic acid derivatives have been chosen primarily for their previous anti-parasitic activity and in particular for their ability to act as substrates in glycosyltransferases for GPI-anchor biosynthesis inhibition.^[68,86,111] This could potentially lead to multiple drug targets, making resistance less likely to evolve.

In order to improve the activity of future inhibitors, modifications were carried out to as-



Scheme 5: Synthesis of 5-Benzylidene rhodanine N-acetic acid derivatives **2a–ai**; (i) EtOH, 80 °C; for bases used for synthesis and R^{1–5} substituents see Table 3.

sess the structural requirements for anti-parasitic compounds. To establish a structure activity relationship (SAR), different 5-benzylidene substituted analogues were synthesised. This approach helped to identify electronic and spacial requirements. Next, the role of the thiocarbonyl was assessed by substitution strategies with a carbonyl. To study the effect of the N-3-acetic acid moiety, longer side-chain analogues were synthesised. The effect of the carboxylic acid under physiological conditions has been studied by converting the free acid to its ester to mask the negative charge. The role of the exo-cyclic double bond was studied by the synthesis of saturated analogues. And lastly the influence of heterocyclic modifications in the 5-position of the rhodanine core was examined.

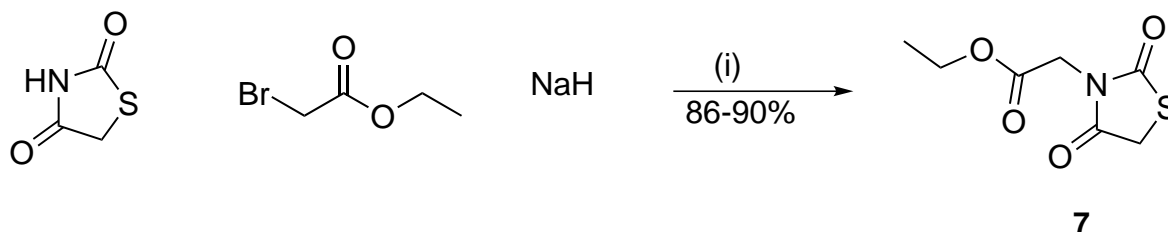
3.2.5 Aromatic substitution strategies

The modification on the 5-position of the initial rhodanine-N-3-acetic acid library was not extensive enough to draw conclusions about electronic or spacial requirements for activity against the bloodstream form of *T. brucei*. The derivatives were synthesised via base-catalyst Knoevenagel condensation reactions using conventional heating (Scheme 5),^[153] and piperidine or sodium acetate as weak bases in ethanol as the solvent. The products were obtained after simple filtration. The choice of bases seemed to have no effect on the overall yield of Knoevenagel condensation products, but the use of piperidine resulted in the formation of piperidine salts in **2d** and **2y**. To convert the piperidine salt to the free carboxylic acid, the salts were dissolved in 1 N hydrochloric acid (HCl) and the free carboxylic acids were extracted with ethyl acetate (EtOAc). The conversion of the salt to the free acid represented a further step in the synthesis. Whereas then using sodium acetate (NaOAc) as base, the corresponding acetate salts were not obtained, therefore sodium acetate is the preferable base for the synthesis of rhodanine-N-acetic acid derivatives. Furthermore, piperidine proved to be more difficult to separate from the products and recrystallisations had to be performed or more solvent had to be used to wash the excess piperidine in the filtration step. Sodium acetate on the other hand

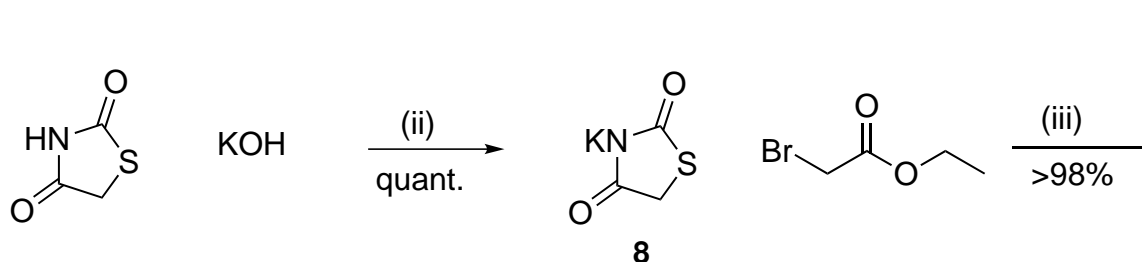
Table 3: Synthesised Rhodanine-N-acetic acid derivatives; yield; chemical shift for CH signal (both ^1H and ^{13}C); n.a.: not available; **2a–r**: piperidine as base; **2s–ae**: NaOAc as base; **2y** δ in MeOD- d_4 otherwise DMSO- d_6 , see Scheme 5.

#	R^1	R^2	R^3	R^4	R^5	yield [%]	NMR shifts of CH	
							δ_{H}	δ_{C}
2a	H	H	H	H	H	72	7.91	134.0
2b	H	H	H	OBn	H	24	7.86	134.1
2c	H	H	OBn	H	H	82	7.86	134.2
2d	Piperidine	H	OBn	OBn	H	54	7.74	133.5
2e	H	OH	H	H	H	45	8.04	129.9
2f	H	H	OH	H	H	84	7.77	134.2
2g	H	H	H	OH	H	45	7.79	134.7
2h	H	H	H	Cl	H	93	7.85	132.4
2i	H	H	H	CN	H	78	7.91	131.4
2j	H	H	H	CCH	H	87	7.85	132.5
2k	H	H	NO_2	H	H	67	8.02-8.18	135.8
2l	H	H	Br	OMe	H	75	7.87	n.a.
2m	H	H	CH_3	H	H	76	7.85	131.7
2n	H	H	H	CH_3	H	78	7.87	134.1
2o	H	CH_3	H	H	H	78	7.96	139.5
2p	H	H	CF_3	H	H	94	8.03	132.1
2q	H	H	H	CF_3	H	73	7.99	131.7
2r	H	CF_3	H	H	H	81	7.89	127.8
2s	H	H	H	SO_2Me	H	29	7.99	137.5
2t	H	H	H	NMe_2	H	87	7.75	135.5
2u	H	H	OH	OH	H	76	7.65	126.7-137.9
2v	H	H	COOH	H	H	17	7.80	n.a.
2w	H	OH	H	OH	H	52	7.99	n.a.
2x	H	CF_3	H	H	CF_3	27	7.77-8.17	n.a.
2y	Piperidine	H	H	tBu	H	20	7.70	133.5
2z	H	H	H	tBu	H	79	7.68	134.7
2aa	H	COOH	H	H	H	15	8.79	136.0
2ab	H	CF_3	H	CF_3	H	27	7.77	124.6
2ac	H	H	H	OMe	H	31	7.55-7.88	n.a.
2ad	H	H	H	NHAc	H	85	7.82	133.9
2ae	H	H	CF_3	H	CF_3	40	8.00	n.a.

Method 1:



Method 2:

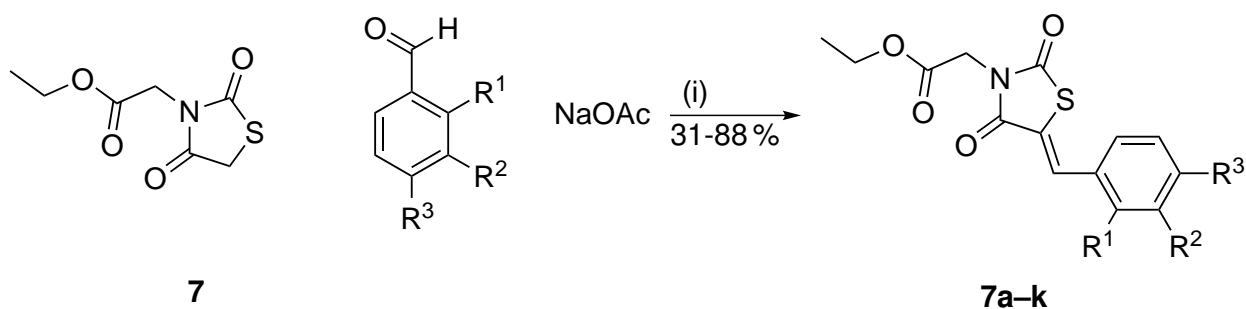


Scheme 6: Synthesis N-acetic acid thiazolidine-2,4-dione analogue; (i) DMF, 0 ° C to rt; (ii) EtOH, 80 ° C; (iii) acetone, 70 ° C.

is easily removed after the first washing step in the filtration or after extraction with EtOAc. The stereochemistry of the exo-cyclic double bond was determined by comparisons of the chemical shift of the methylene-CH signal in ^1H - and ^{13}C -NMR experiments. The chemical shifts (δ_{H} , δ_{C}) were in good correlation with previously reported chemical shifts for the thermodynamically stable Z-isomer.^[162,163]

3.2.6 Replacement of thiocarbonyl

Rhodanine-like compounds are known as promiscuous binders to a range of molecular targets.^[83] An analysis of rhodanine derivatives in protein X-ray structures have shown that the exo-cyclic thiocarbonyl group is involved in multiple molecular interactions such as hydrogen bonding and electrostatic effects.^[83] Although thiocarbonyl hydrogen bonds are less favoured compared to carbonyl hydrogen bond interactions, it has been suggested that water dissociation from thiocarbonyl residues is facilitated and this is a major factor in the formation of hydrogen bonds in thiocarbonyl groups.^[83] Therefore, substitution of the thiocarbonyl to a carbonyl group could increase the selectivity towards anti-parasitic targets through the formation of specific hydrogen bond interactions with the carbonyl group, possibly reducing unwanted interactions. The substitution will also reveal the importance of a exo-cyclic thiocarbonyl group for anti-parasitic activity. The synthetic strategy towards N-acetic acid thiazolidine-2,4-dione analogues is outlined in Scheme 6.



Scheme 7: Synthesis of thiazolidine-2,4-dione ester derivatives **7a-k**; (i) EtOH, 80 °C, for R¹-R³ see Table 4.

Initially, thiazolidine-2,4-dione was subjected to alkylation conditions with iodo- and bromo-acetic acid sodium salts (X=Br,I and R=Na) in the presence of sodium hydride in DMF (Scheme 6 Method 1). The reaction protocol was adapted from Bhat et al. The solvent was substituted with DMF for better solubility of the starting thiazolidine-2,4-dione (technical grade, 90 %).^[165] However, the alkylation did not occur under these reaction conditions and only starting material was recovered. Using the adapted protocol with ethyl-2-bromoacetate as the alkylating agent yielded the desired ethyl ester **7**. The yield was dependant on the use of anhydrous solvents, varying from 86-90 % after column chromatography. At the same time a different protocol was explored for the synthesis of the ethyl ester **7** (Scheme 6 Method 2). Treating thiazolidine-2,4-diones with potassium hydroxide in ethanol resulted in the formation of the potassium salt **8** after simple filtration in quantitative yields.^[166] The following alkylation was carried out in the presence of ethyl-2-bromoacetate to afford the product **7** in excellent yields (>98 %) after simple extraction. Both methods gave access to the ester derivative **7**, but the synthesis of the free carboxylic acid was not achieved. Instead of hydrolysing the ester under basic or acidic conditions, **7** was chosen for subsequent Knoevenagel reactions with various aldehydes. The ester **7** can be seen as the pro-drug of the free carboxylic acid. Similar ester-modified compounds have been shown to improve membrane diffusion and consequently improve anti-parasitic activity.^[167] Within the parasite, the ester derivative could be hydrolysed and release the active free carboxylic acid, or the ester derivative binds directly to the desired target. The capability of hydrolysing ester analogues to free acids has previously been shown in *T. brucei*.^[167]

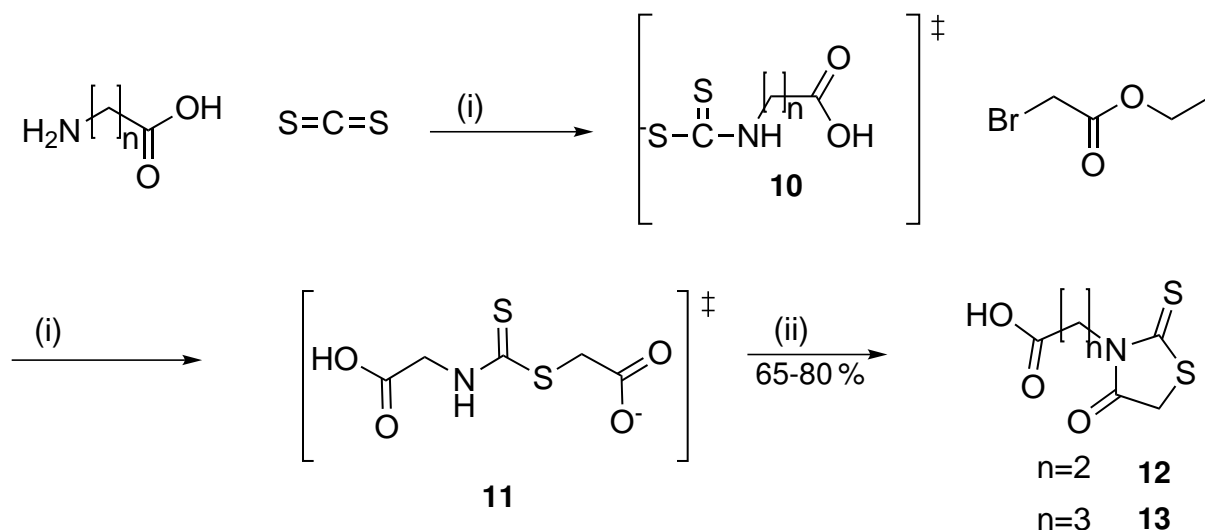
Derivatives of **7a-l** were synthesised via Knoevenagel condensation with various benzaldehydes and sodium acetate as the base (Scheme 7). The synthesised analogues **7a-l** showed improved solubility in ethanol. Because of this improved solubility only **7j** and **7a** were afforded after simple filtration from ethanol, all other derivatives (**7c**, **7d**, **7e**, **7f**, **7l**, **7i**, and **7k**) were purified by column chromatography, explaining the particularly low yields of 31 % for **7k**. The synthesis of the para-trifluoromethyl substituted derivative **7g** did not succeed under these

Table 4: Synthesised thiazolidine-2,4-dione ester derivatives **7a–k** including yields and NMR chemical shifts of CH signal (both ^1H and ^{13}C); $\text{R}^1\text{--R}^3$; yield; δ_{C} for **7k** in MeOD otherwise all δ in CDCl_3 ; n.a.: not available.

#	R^1	R^2	R^3	[%] yield	NMR shifts of CH	
					δ_{H}	δ_{C}
7a	H	H	H	46	7.95	n.a.
7b	CH_3	H	H	69	8.07	132.8
7c	H	CH_3	H	71	7.91	135.1
7d	H	H	CH_3	71	7.75	134.8
7e	CF_3	H	H	87	8.20	130.6
7f	H	CF_3	H	52	7.94	132.7
7g	H	H	CF_3	no reaction		
7h	H	OBn	H	88	7.86	134.6
7i	H	H	OBn	50	7.89	134.7
7j	H	OBn	OBn	67	7.79	134.8
7k	H	OH	OH	31-58	7.78	136.2

conditions. TLC showed complete consumption of starting **7**, but also the formation of multiple decomposition products. All products were afforded as the Z-isomer, which was confirmed by the chemical shifts of the methylene signal in ^1H - and ^{13}C -NMR experiments. The chemical shifts of the CH signal were in the same range as for the corresponding rhodanine derivatives **9**. A particularly interesting compound with respect to the configuration of the double bond was the ortho-trifluoromethyl substituted derivative **7e**. The chemical shift in the ^1H -NMR experiment for the CH-signal was further downfield at 8.20 ppm, while all other derivatives were in the range of 7.75-8.07 ppm. The closest chemical shift was that of **7b**, with a chemical shift of 8.07 ppm. Both structures are related through substitution of the ortho-position in the 5-benzylidene moiety. Thus, indicating that the ortho-substituent is in proximity of the CH-group, deshielding it to appear further downfield compared to meta- and para-substituted analogues.

The three dimensional coordinates of **7e** were prepared with the MOE2009.10 software package (Merck molecular force field 94x (MMFF94x)) and distances between the CH group and the trifluoromethyl group were calculated. The fluorine atoms of the trifluoromethyl group are only 0.2 Å further apart from the CH-group than the carbonyl group (Figure 20). This results suggested that the trifluoro-methyl group was indeed responsible for the change of the chemical shift in the CH-signal in the ^1H - and ^{13}C -NMR experiments. But even more remarkable was the observation of a $^5J_{\text{H},\text{F}}$ -coupling constant of 1.9 Hz, between the proton of the CH-group and the fluorines in the trifluoromethyl (CF_3) group. The intramolecular distance between the CH-proton and the trifluoromethyl group was estimated to be 2.8 Å and therefore just out of the van der Waals-radii of the participating fluorine and hydrogen atoms (2.7 Å).^[168] However,



Scheme 8: Synthesis of elongated N-3 sidechain linkers in rhodanine-N-acetic acid analogues **12** and **13**; (i) NaOH_{aq} , rt; (ii) HCl , 100°C .

the distance measurement was only estimated, assuming a slightly shorter intramolecular distance within the van der Waals-radii would allow the overlap of the 1s orbital of the proton and 2p orbital of the fluorine, generating a one-center molecular orbital (Figure 21).^[169–171] All atomic orbitals (the bonding and anti-bonding) will be filled, so that covalent bonds cannot be formed. These orbital interactions might explain the observed $^5J_{H,F}$ coupling of 1.9 Hz. However, the exact mechanism of this long range coupling constant is unknown, but has been shown to be dependant on the intramolecular distance between both coupling partners.^[172]

Furthermore such coupling constants have previously been used to reveal intramolecular interactions, such as hydrogen-bonds of participating groups.^[173] For example fluorine-groups participating in hydrogen-bonding to an intermolecular amide (NH) showed $^5J_{H,F}$ coupling constants in the range of 1.7-2.0 Hz.^[173] It can be concluded that a value of 1.9 Hz for the $^5J_{H,F}$ coupling constant in **7e** was dependant on the through space distance and or intermolecular interaction of the hydrogen (CH) and fluorine group (CF_3), thus suggesting possible hydrogen-bonding interaction between the trifluoromethyl group and the CH moiety. Interestingly, the ^{13}C -NMR experiment showed a similar long range $^4J_{C,F}$ coupling constant of 1.9 Hz between the $\underline{\text{CH}}$ and the $\underline{\text{CF}_3}$ group.

3.2.7 Elongation of N3-sidechain

To study the influence of the N-3 side chain length, derivatives with a propionic and butyric acid function were synthesised (Scheme 8). Therefore, a one-pot reaction sequence starting from β -alanine or γ -aminobutyric acid was pursued.^[174] The one-pot-reaction sequence was

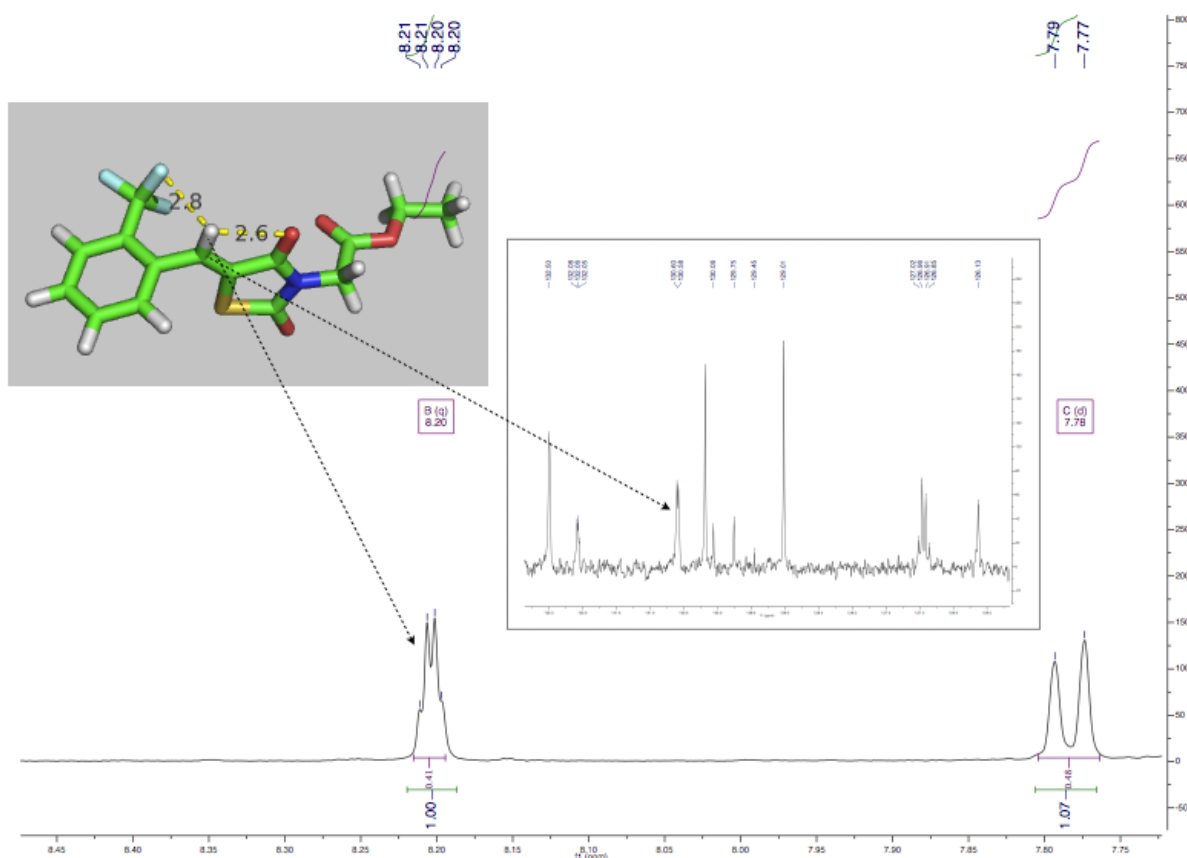
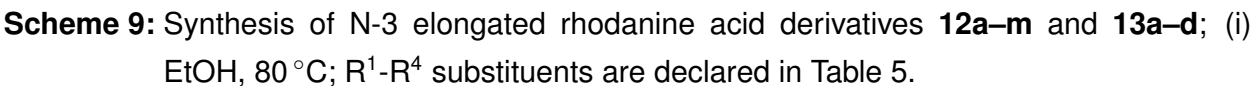
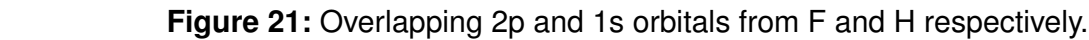


Figure 20: ^1H - and ^{13}C -NMR spectra of **7e** showing long range coupling between CH and CF_3 ; the stick representation of **7e** showing distances between CH and CF_3 and $\text{C}=\text{O}$.

slightly modified in order to optimise the product isolation and yield of the reaction. Carbon disulphide was added to an aqueous solution of the corresponding acid in the presence of sodium hydroxide. In the following reaction sequence, bromo acetic acetate was added to intermediate **10**. The substitution product **11** is subjected to acidic conditions to catalyse the formation of the desired five-membered heterocycles **12** and **13** (Scheme 8). The products were afforded after recrystallization and simple filtration as red crystals. In this reaction sequence the chloro-acetic acetate was substituted with the corresponding bromo-derivative and reaction times were slightly varied to allow products **12** and **13** time for the crystallisation process, whereas in the previously published procedure, the products were afforded after column chromatography.^[174] The yields of the reaction varied from 65-80 % for **12** and 68 % for **13**. Each reaction step was accompanied with a change of colour of the reaction mixture. A bright red colour in the last step was indicative of complete consumption of bromo acetic acetate as confirmed by TLC.

The modified rhodanine precursors **12** and **13** were subjected to Knoevenagel condensa-



All compounds had chemical shifts of the CH group indicating the Z-configuration, with the only exception of compound **12j**, which had a slightly lower chemical shift for δ_H at 7.42 ppm. Unfortunately, the ^{13}C chemical shift could not be measured because of the poor solubility of **12j** in DMSO- d_6 . It would have been expected, that the chemical shift of **12j** would be slightly lower (>7.70 ppm) because of the combined deshielding of the carbonyl and the hydroxy group, if the Z-configuration would have been present. This result indicated that the double bond in **12j** might have been in the E-configuration. Indeed, the presence of a trifluoromethyl group in ortho-position of the 5-benzylidene moiety in compounds **12e** and **12g** resulted in a chemical shift of >7.70 ppm. The proximity in space of the trifluoromethyl group could be seen by a large $^5J_{H,F}$ -coupling of the CH- and the CF_3 -group (see Figure 20), confirming the Z-configuration

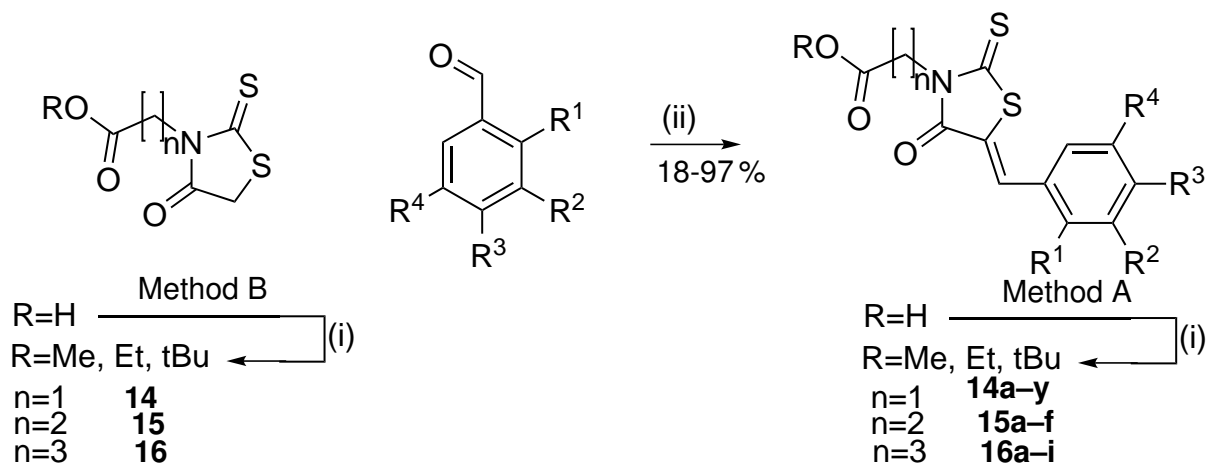
Table 5: Rhodanine derivatives **12a–m** and **13a–d** and their R substituents, yields and chemical shifts ($\delta_{H,C}$); n.a.: not available; see Scheme 9.

#	n	R ¹	R ²	R ³	R ⁴	[%] yield	NMR shifts of CH [ppm]	
							δ_H	δ_C
12a	2	H	H	H	H	80	7.81	132.7
12b	2	CH ₃	H	H	H	87	7.88	130.3
12c	2	H	CH ₃	H	H	98	7.75	133.1
12d	2	H	H	CH ₃	H	97	7.77	133.0
12e	2	CF ₃	H	H	H	58	7.80	126.2
12f	2	H	CF ₃	H	H	69	7.92	130.7
12g	2	CF ₃	H	H	CF ₃	19	7.77	124.9
12h	2	H	H	NMe ₂	H	80	7.67	134.4
12i	2	H	H	Cl	H	83	7.81	131.1
12j	2	OH	H	H	H	21	7.42	n.a.
12k	2	H	OH	H	H	79	7.69	133.0
12l	2	H	H	OH	H	85	7.68	133.9
12m	2	H	OH	OH	H	91	7.51	135.2
13a	3	H	H	H	H	90	7.80	132.7
13b	3	CH ₃	H	H	H	61	7.88	130.4
13c	3	H	CH ₃	H	H	71	7.73	132.8
13d	3	H	H	CH ₃	H	72	7.76	132.9

of the double bond.

3.2.8 Esterification of carboxylic acid

The efficiency of carboxylic acid compounds to penetrate membranes can potentially be improved by the synthesis of ester derivatives, as mentioned in section 3.2.6.^[167] Derivatives of **2** were converted to esters using standard esterification conditions with N',N'-dicyclohexylcarbodiimide (DCC), 4-dimethylaminopyridine (DMAP) and the desired alcohol (methanol, ethanol or *tert*-butanol). Two strategies have been applied to achieve this transformation. In the first strategy (Method A), the previous synthesised analogues **2m**, **2p**, **2o**, and **2d** were subjected to standard esterification conditions. The yield of the reaction varied from 18-78%. There, compound **14f** gave the lowest yield by showing only 18% conversion to the *tert*-butyl ester after 16 h. The trend seemed to be that the ethyl ester resulted in a higher yield (78%), than the methyl ester (41%), followed by the *tert*-butyl ester (18%). However, a major factor for the decreased yield was the purification method. Derivatives **14a–h** were purified by column chromatography, the major by-product of the esterification reaction was dicyclohexylurea (DCU) and the catalyst DMAP. Both of these molecules, but in particular DCU are very unpo-



Scheme 10: Synthesis of Ester derivatives; **14a-h**: Method A; **14i-y**, **15a-f**, and **16c-i**: Method B (i) DCC, DMAP, ROH (R=Me, Et, tBu), rt, 4-16 h; (ii) NaOAc, 80 °C, EtOH; R and R¹-R³ are declared in Table 6.

lar molecules and had similar retention times as the esters. Separation of these by-products proved to be difficult and multiple purification steps had to be performed.

For these reasons, a second approach towards ester derivatives was investigated (Method B). The starting rhodanine derivatives **2**, **12**, and **13** were converted to their esters prior to subjecting them to the Knoevenagel reaction. The esterification was carried out with methanol, ethanol and *tert*-butanol as the nucleophilic reagents. The esterification using ethanol yielded the desired ethyl ester **14** in almost quantitative yields (64-99 %) after purification. Improvements of the purification protocol had a significant role in increased yields. In the first purification step, DCU is precipitated with the addition of dichloromethane to the EtOH/CHCl₃ (10:1) solution. DCU was filtered as a white solid from the crude reaction mixture, improving consecutive purification efforts via flash column chromatography. The ethyl ester of **14** was afforded as yellow oil, which solidified upon exposure to air. Applying the improved purification protocol to the crude methyl ester of **14** afforded the product in 78 % yield. Lastly, *tert*-butanol was used for the esterification reaction and yielded only 17 % after purification. Similarly as described above, the ethyl ester of **14** was afforded in the highest yield of 99 %, followed by the methyl ester with 78 % and the *tert*-butyl ester with 17 %. For the following esterification reaction with **12** and **13**, ethanol was chosen to afford the corresponding ethyl esters **15** and **16**.

Interestingly, the yield of the esterification reaction for **12** was only 21-39 % and even prolonged reaction times did not affect the isolated yields. However, applying the esterification on **13** resulted in the formation of the butyl ester **16** in good yields of 72-77 %. The rhodanine ester derivatives **14**, **15**, and **16** were subjected to various aldehydes in a Knoevenagel reaction with NaOAc as base. The yield of the reaction ranged from 32-97 %. Impurities from the pre-

Table 6: Rhodanine ester derivatives **14a–ab**, **15a–f**, and **16a–j**; R and R¹-R³; yield; chemical shift of CH ($\delta_{H,C}$), see Scheme 10.

#	n	R	R ¹	R ²	R ³	R ⁴	[%]		NMR shifts of CH [ppm]	
							yield	δ_{solvent}	δ_H	δ_C
14a	1	Et	H	CH ₃	H	H	53	CDCl ₃	7.14, 7.76	134.5, 138.7
14b	1	tBu	H	CH ₃	H	H	72	CDCl ₃	7.75	134.3
14c	1	Me	H	CH ₃	H	H	41	DMSO	7.86	n.a.
14d	1	Et	H	H	CF ₃	H	69	DMSO	8.00	n.a.
14e	1	Me	H	H	CF ₃	H	71	DMSO	8.00	n.a.
14f	1	tBu	H	OBn	OBn	H	18	DMSO	7.81	n.a.
14g	1	Et	CH ₃	H	H	H	78	DMSO	8.00	n.a.
14h	1	tBu	CH ₃	H	H	H	49	DMSO	7.99	n.a.
14i	1	Et	H	H	H	H	73	CDCl ₃	7.79	134.2
14j	1	tBu	H	H	H	H	77	CDCl ₃	7.78, 7.79	133.4, 133.9
14k	1	Et	CF ₃	H	H	H	86	CDCl ₃	7.45, 8.05	129.4, 132.6
14l	1	Et	H	CF ₃	H	H	51	CDCl ₃	7.79	131.8
14m	1	Et	CF ₃	H	H	CF ₃	62	CDCl ₃	8.00	127.1
14n	1	Et	H	H	CH ₃	H	90	CDCl ₃	7.77	n.a.
14o	1	Et	H	H	tBu	H	55	CDCl ₃	7.71	134.3
14p	1	Et	OH	H	H	H	84	CDCl ₃	8.19	130.1
14q	1	Et	H	OH	H	H	86	CDCl ₃	7.55	133.9
14r	1	Et	H	H	OH	H	89	CDCl ₃	7.61	134.3
14s	1	Me	H	OH	OH	H	32	MeOD	7.65	136.0
14t	1	Et	H	OH	OH	H	58	MeOD	7.55	136.0
14u	1	Et	OH	H	OH	H	86	DMSO	8.00	130.6
14v	1	Et	H	OBn	H	H	54	CDCl ₃	7.73	134.0
14w	1	Et	H	H	OBn	H	67	CDCl ₃	7.74	134.1
14x	1	Et	H	OBn	OBn	H	87	CDCl ₃	7.64	134.3
14y	1	Et	H	OMe	OH	OMe	64	CDCl ₃	7.65	134.7
15a	2	Et	H	H	H	H	72	CDCl ₃	7.73	133.5
15b	2	Et	CH ₃	H	H	H	35	CDCl ₃	7.97	131.5
15c	2	Et	H	CH ₃	H	H	61	CDCl ₃	7.72	133.9
15d	2	Et	H	H	CH ₃	H	57	CDCl ₃	7.73	133.9
15e	2	Et	H	H	OH	H	93	CDCl ₃	7.61	133.8
15f	2	Et	H	OH	OH	H	52	DMSO	7.65	134.3
16a	3	Et	H	H	H	H	91	DMSO	7.80	n.a.
16b	3	Et	CH ₃	H	H	H	92	CDCl ₃	7.94	131.0
16c	3	Et	H	CH ₃	H	H	97	CDCl ₃	7.68	133.5
16d	3	Et	H	H	CH ₃	H	55	CDCl ₃	7.71	133.6
16e	3	Et	CF ₃	H	H	CF ₃	91	CDCl ₃	7.92-7.96	126.2
16f	3	Et	OH	H	H	H	94	CDCl ₃	8.29	129.6
16g	3	Et	H	OH	H	H	94	CDCl ₃	7.64	133.4
16h	3	Et	H	H	OH	H	71	CDCl ₃	7.81	132.7
16i	3	Et	H	OH	OH	H	85	CDCl ₃	7.62	134.1

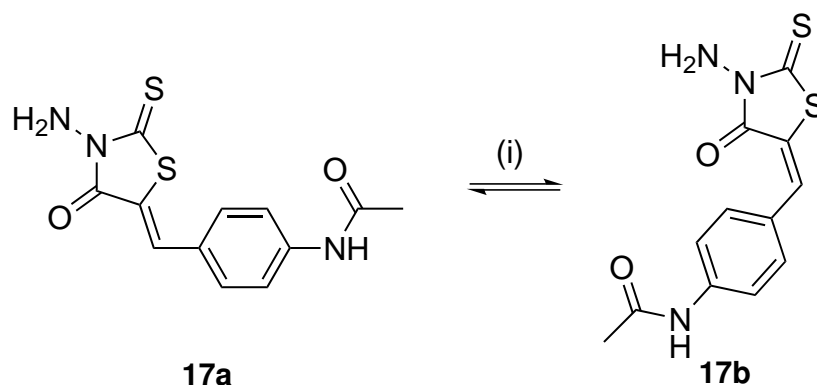
vious esterification reaction (DCC, DCU, or DMAP) improved yields and reaction times of the condensation reaction. The products **14a–ab**, **15a–f**, and **16a–j** were afforded after column chromatography.

The ester derivatives **14a–ab**, **15a–f**, and **16a–j** were almost all obtained as a single stereoisomer. The chemical shift δ 7.55–8.29 ppm of the CH signal identified these molecules as the Z-configured diastereoisomer. The NMR spectra were recorded mainly in CDCl_3 , or DMSO-d_6 and MeOD-d_4 , if the solubility of the compound did not allow recording in CDCl_3 . The usage of different deuterated solvents was useful in order to study the influence of the solvent on the chemical shift of the CH-signal. DMSO-d_6 , as a dipolar aprotic solvent resulted in a further deshielding (8.00 ppm) of the CH-signal in ^1H -NMR experiments compared to CDCl_3 (7.75 ppm). On the other hand, MeOD-d_4 resulted in a upfield-shift of the CH-signal to 7.55 ppm. MeOD-d_4 , as polar-protic solvent, has the capability to form hydrogen bond interactions with the CH-signal, therefore lowering the chemical shift to appear upfield.

Compounds **14a**, **14j**, and **14k** were afforded as mixtures of the Z- and E-diastereoisomers. Compound **14a** was afforded as a mixture of predominantly the Z-isomer, in a ratio of 5:1 (Z:E). The E-isomer had a chemical shift of the CH signal of 7.14 ppm in the ^1H -NMR experiment, while the Z-isomer, deshielded by the neighbouring carbonyl group, showed a chemical shift of 7.76 ppm. The trend was very similar in the ^{13}C -NMR experiment, where the E-isomer had a chemical shift of the CH-signal at 134.5 ppm, while the Z-isomer peak appeared at 138.7 ppm.

The *tert*-butyl ester **14j** was afforded in a Z:E ratio of 3:1. The chemical shift of the Z- and E-isomer in both ^1H -NMR (Z:7.79 ppm, E:7.78 ppm) and ^{13}C -NMR (Z:133.9 ppm, E:133.4 ppm) experiments was very similar and less distinguished than **14a**. The ethyl ester **14k** showed a Z:E ratio of 2:1 and additional long range $^5J_{\text{H(C)},\text{F}}$ -coupling constants. The coupling constants in the ^1H -NMR experiment showed similar values of 2.2 Hz then compared to **7e** (1.9 Hz). This is not surprising, as the distance of the trifluoromethyl group in the E-isomer was predicted to be 2.7 Å (MOE, MacPymol-distance measuring) and therefore both isomers have the same distance between the CH-group and the trifluoromethyl group (Figure 20). Also the 2,5-di-trifluoromethyl derivative **14m** and **16e** showed a long-range $^5J_{\text{C},\text{F}}$ coupling constant of 1.9 Hz, but here only the Z-isomers (δ_{H} 7.92–8.00 ppm) have been observed. The chemical-shift of the CH-proton in **14k** showed the usual tendency, with the E-isomer having a chemical shift of the CH-signal at 7.45 ppm, whereas the Z-isomer showing a peak further downfield at 8.05 ppm.

So far, all Knoevenagel condensation reactions yielded only the thermodynamically more stable Z-isomer as the major product.^[158] The combination of a Knoevenagel reaction followed by an esterification (Method A: **14a**) or an esterification followed by a Knoevenagel condensation (Method B: **14j** and **14k**) gave rise to the E-isomer, but with the Z-isomer still as the predominant product. It was interesting to observe that both methods gave access to both isomers, however only the ethyl ester of **14** which showed impurities of the esterification re-



Scheme 11: Racemization of exo-cyclic double bond configuration; (i) Ph-SH, DIPEA, toluene, 100 °C.

action, reacted to the corresponding E-isomer. It is thought that DMAP might be responsible for the reaction towards to the E-isomer. DMAP could possibly attack the Michael acceptor system and the product could isomerize and eliminate the base again to react to the corresponding E-isomer. A similar type of reaction has been observed with rhodanine derivatives and thiophenol in refluxing benzene (Scheme 11).^[85]

In the previous study, a 3-amino rhodanine derivative was chosen for the reaction with thiophenol in benzene.^[85] In order to show that thiophenol does induce racimerization of the exo-cyclic double bond in rhodanine derivatives, a similar rhodanine derivative **17a** was chosen for the isomerization reaction. The reaction was performed as described in the previous study, however the solvent was substituted with toluene as a replacement for carcinogenic benzene. Unfortunately the desired E-isomer **17b** was not observed. Benzene might have been essential for this type of reaction, or toluene may have caused the isomerization to the Z-isomer, as described in the same study for methanol, water or buffer.^[85]

3.2.9 Modification of the 3-benzyloxy group

The originally investigated rhodanine-N-acetic acid derivative (R=H, n=1, X=S, Y=O, Z=CH, A=C=H, Figure 19) had a 3-benzyloxy-substituent on the 5-benzylidene moiety. In order to study the importance of this 3-benzyloxy substituent, two modifications were introduced (Figure 22). The first modification was aimed at examining the spacial requirement of the 3-benzyloxy substituent through the synthesis of methoxy-substituted analogues. Furthermore, several pyridine substituents were installed in the 3-benzyloxy-moiety (Figure 22, green). For the second modification, the 3-benzyloxy substituent was replaced by a heterocyclic modification. The N-benzylpyridine-2-amine group was chosen to replace the benzyloxy(benzene) moiety (Figure 22, blue). The modifications on the 3-benzyloxy substituent derived from aldehydes,

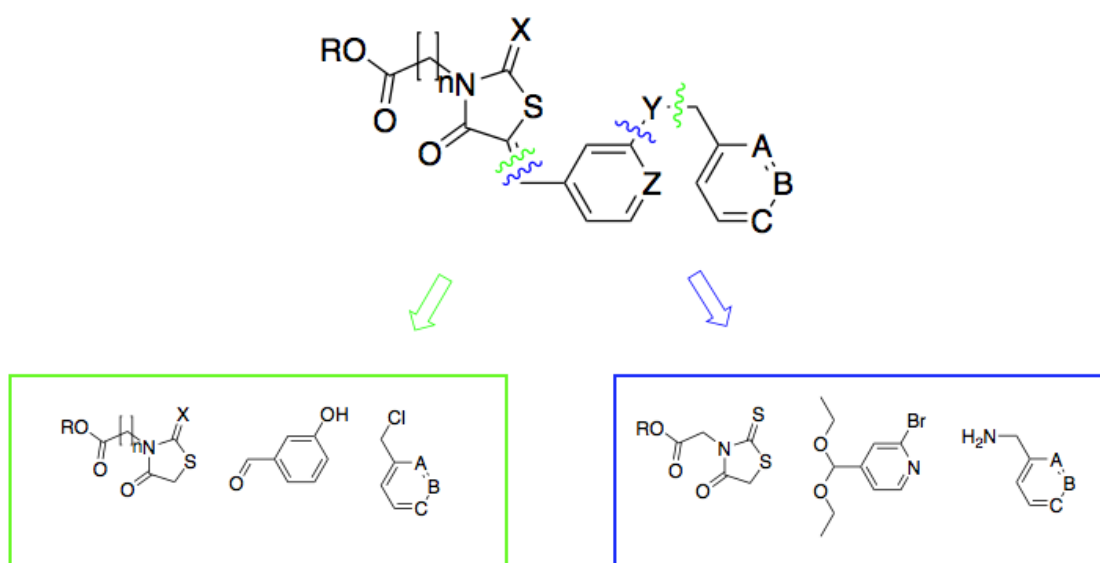
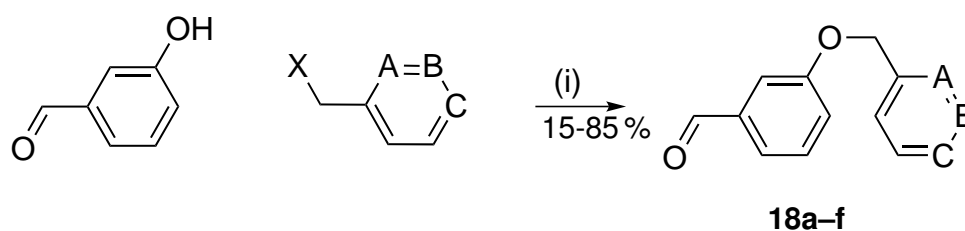


Figure 22: Retrosynthesis of improved rhodanine-N-acetic acid derivatives; R=H,Et; X=O,S; n=1,2; Y=O,NH; Z=CH, N; A=N,C-R¹, B=N,CR², C=N,CR³.



Scheme 12: Synthesis of modified aldehydes **18a-f** (i) K₂CO₃, 50-90 °C, DMF, NaI ; A, B, C, X see Table 7.

not commercially available. These aldehydes were synthesised by nucleophilic substitution reactions between 3-hydroxybenzaldehyde and various benzylic chlorides (Scheme 12) with potassium carbonate (K₂CO₃) as base. The reaction was carried out in DMF, a dipolar aprotic solvent, in order to stabilise the charged intermediate of the S_N2 reaction.

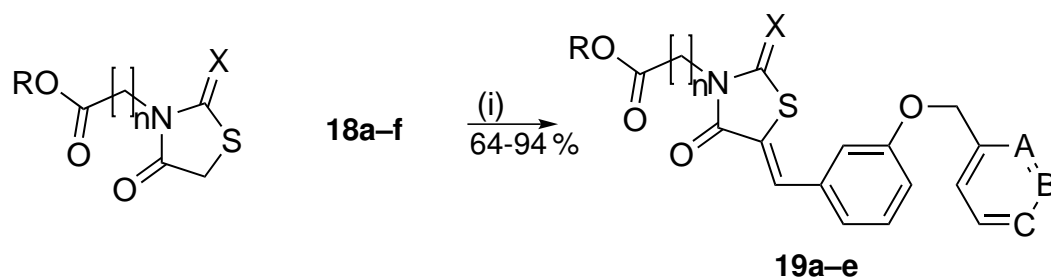
Although benzaldehyde **18a** was commercially available, it was synthesised to test the reaction protocol for the synthesis of the modified aldehydes **18b-f**. The reaction of 3-hydroxybenzaldehyde and benzylbromide proceeded with an excellent yield of 84% after column chromatography and 4 h reaction time. In the following substitution reactions benzylchloride (Scheme 12, X=Cl) derivatives were used for the substitution reaction. Initially, aldehyde **18b** was synthesised using the reaction protocol described above (K₂CO₃, DMF, 90 °C), but after 8 h only 18% was converted to the desired product. In order to improve the yield and possible

Table 7: Synthesis of modified 3-benzyloxy-benzaldehyde derivatives; A,B,C,X for modified aldehydes **18a–f**; catalyst and yield, see Scheme 12.

#	X	A	B	C	Temperature	catalyst	yield [%]
18a	Br	CH	CH	CH	90	none	84
18b	Cl	CH	COMe	CH	90	none	15
	Cl	CH	COMe	CH	90	NaI	82
18c	Cl	CH	CH	COMe	90	none	30-53
	Cl	CH	CH	COMe	90	NaI	85
18d	Cl	N	CH	CH	50	none	55
18e	Cl	CH	N	CH	50	none	16
	Cl	CH	N	CH	50	NaI	59
18f	Cl	CH	CH	N	50	none	33
	Cl	CH	CH	N	50	NaI	50

the reaction time, sodium iodide was added as a catalyst, mediating the reaction to the corresponding benzyliodide derivatives. These derivatives are equipped with a good iodide leaving group and therefore react preferably in S_N2 reactions with the 3-hydroxy-benzaldehyde. Indeed, in the presence of sodium iodide the yield of **18b** improved to 82 % with similar reaction times. The uncatalysed reaction, without sodium iodide, of **18b–f** resulted in low yields of 15-55 %. Whereas the reaction in presence of sodium iodide proceeded in high yields of 50-85 %. The low yield of 50 % was due to decomposition of the starting pyridyl-chloride derivatives or the aldehydes **18d–f** at high temperatures over 50 °C.

The modified aldehydes **18a–f** were subjected to Knoevenagel condensation conditions to yield the desired derivatives **19a–i** (Scheme 13). The Knoevenagel reaction proceeded with an excellent yields of 64-94 % after column chromatography. However, the reaction with the ethyl ester of **14** and the pyridinyl-aldehydes **18d–f** did not result in the formation of the desired product. Instead only decomposition products were observed. It was most likely that the aldehydes decomposed under the reaction conditions and lower temperatures might have led to the formation of products **19j–k**. The reaction times of the Knoevenagel reaction varied from 1-8 h. In particular the short reaction times of only 1 h for **19a** and **19e** were very surprising, as for all previous Knoevenagel reactions an average of 4 h was observed for the complete consumption of starting materials. The chemical shift of the CH-signal in $^1\text{H-NMR}$ (7.63-7.87 ppm) and $^{13}\text{C-NMR}$ (133.4-134.7 ppm) experiments confirmed the formation of the Z-isomer as the only product.



Scheme 13: Synthesis of 3-benzyloxy-modified analogues **19a–a**; (i) NaOAc, EtOH, 80 °C, see Table 8.

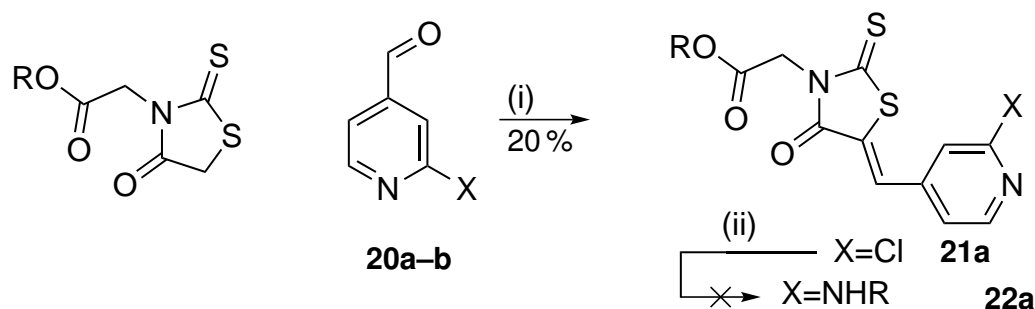
Table 8: Synthesis of condensation products with modified 3-benzyloxybenzaldehyde derivatives; R, n, X, A, B and C for 3-benzyloxy modified derivatives **19a–l**; δ_{CDCl_3} , see Scheme 13.

#	R	n	X	A	B	C	yield [%]	NMR shifts of CH [ppm]	
								δ_H	δ_C
19a	Et	2	S	CH	COMe	CH	82	7.66	133.4
19b	Et	1	O	CH	COMe	CH	94	7.86	134.6
19c	Et	1	S	CH	CH	COMe	64	7.63	134.0
19d	Et	1	O	CH	CH	COMe	94	7.87	134.7
19e	Et	2	S	CH	CH	COMe	80	7.65	133.4
19j	Et	1	S	N	CH	CH	30	7.65	133.6
19l	Et	1	S	CH	N	CH	38	7.66	133.7
19k	Et	1	S	CH	CH	N	50	7.64	133.5
19f	H	2	S	N	CH	CH	75	7.76	132.5
19g	H	2	S	CH	N	CH	69	7.77	132.3
19h	H	2	S	CH	CH	N	82	7.77	132.4

3.2.10 Heterocyclic modification on the 5-position of the rhodanine-N-acetic acid

For the introduction of the second modification on the 3-benzyloxy lead structure, an 3-amino-benzylidene group was chosen to replace the benzyloxy-substituent. The substitution of the oxygen linker with an amino-linker might show improved activity, possibly indicating hydrogen bond donor activity of this moiety. On the other hand the amino-benzylidene group is in theory easily introduced by simple nucleophilic substitution of the corresponding 2-halogen-pyridine analogues.

Initially, the introduction of the amino-benzylidene substituent should occur after Knoevenagel condensation with the appropriate 2-substituted pyridine aldehyde. A good leaving group in ortho-position next to the pyridine nitrogen was thought to facilitate nucleophilic aromatic substitution reactions with amino-benzylidene derivatives (Scheme 14). Therefore, rhodanine-

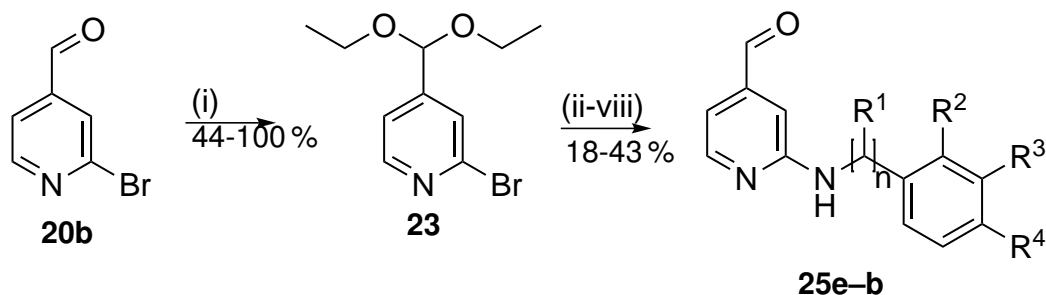


Scheme 14: Synthesis of heterocyclic derivatives **22a** as replacement for the 3-benzyloxygroup; (i) R=Et (**14**), X=Cl (**20a**), NaOAc, 80 °C, EtOH; (ii) neat benzylamine, 190 °C, see Table 9.

Table 9: Synthesis of heterocyclic modified rhodanine-N-acetic acid derivatives; of R, X for the synthesis of **21a–c**; yield and chemical shift of CH-signal, see Scheme 14.

#	R	X	yield [%]	$\delta_{\text{DMSO}-d_6}$
21a	Et	Cl	20	7.88
21b	H	Cl	no reaction	
21c	Et	Br	decomposition	
22a	Et	NHBn	no reaction	

N-acetic ethyl ester (R=Et, **14**) was subjected to Knoevenagel condensation condition with 2-chloro substituted isonicotinaldehyde **20a** (Scheme 14). The reaction yielded the desired Knoevenagel product **21a** in moderate yields of 20 % after simple filtration. The chemical shift of δ_H 7.88 ppm of the CH-signal identified the product as the Z-isomer. Attempts to synthesise the free carboxylic analogue **21b** failed and no reaction was observed. Also the attempt to install the 2-bromo-leaving group on the pyridine moiety failed and only decomposition was observed in the synthesis of derivative **21c**. After having installed the chloro-leaving group on the pyridine moiety of the derivative **21a**, the compound was subjected to aromatic substitution conditions in neat benzylamine solution. The reaction mixture was refluxed at 190 °C. However, no reaction between the amino-benzylidene group and the 2-chloro-aminopyridine **21a** was observed. The lack of reactivity is most likely explained by the poor chloro leaving group compared to a bromo-substituent in 2-position of the pyridine ring. In order to repeat the reaction with the better bromo-leaving group, the Knoevenagel reaction with the 2-bromopyridine aldehyde **20b** was carried out at room temperature and under a nitrogen gas protection atmosphere to prevent decomposition of the aldehyde. None of these efforts resulted in the formation of the bromo-derivative of **21a**. In order to overcome the decomposition of the starting aldehyde **20b** under Knoevenagel condensation conditions, a different strategy had



Scheme 15: Synthesis of amino-substituted aldehydes **25a–g**; (i) TFA, EtOH, CHCl_3 , $80\text{ }^\circ\text{C}$, 2 h; (ii) $\text{NH}_2\text{-R}$ (neat), reflux ($150\text{-}190\text{ }^\circ\text{C}$); (iii) Cs_2CO_3 , DMF, $\text{NH}_2\text{-R}$; (iv) Cs_2CO_3 , ACN, $\text{NH}_2\text{-R}$; (v) $\text{NH}_2\text{-R}$, NaOtBu; (vi) $\text{Pd}(\text{OAc})_2$, NaOtBu, DPPF, dioxane/toluene (1:1); (vii) $\text{NH}_2\text{-R}$, CuI, CsOAc, toluene, $110\text{ }^\circ\text{C}$; (viii) H_2O , TFA, rt; for substituents of $n, \text{R}^1\text{-R}^4$ see Table 10.

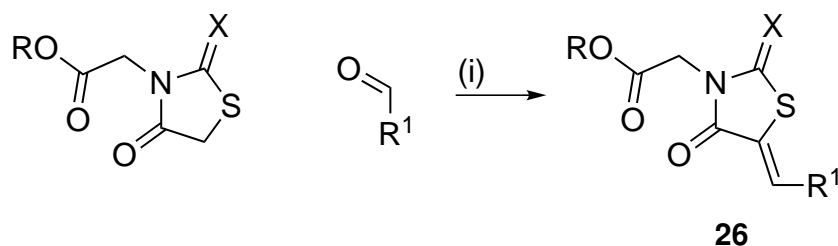
to employed. Analysing the aldehyde **20b** in closer detail identified the aldehyde functional group as the most sensitive functional group. For this reason the aldehyde functional group was protected as its acetal (Scheme 15). By applying this strategy the order of the reaction could be reversed. The nucleophilic aromatic substitution reaction could be carried out prior to the Knoevenagel reaction.

The acetylation of the aldehyde functional group was carried out in ethanol in the presence of TFA. The reaction mixture was heated to reflux to form the full acetal in quantitative yields. The full acetate **23** was obtained after simple basic extraction as clear oil. The crude was sufficiently pure (NMR $>95\%$) for the following substitution reaction. Different reaction conditions have been explored for the nucleophilic aromatic substitution of the 2-bromo-pyridine derivative **23** (Scheme 15, Table 10). At the beginning, the amination was carried out in neat benzylamine solution at boiling point of the corresponding amine ($100\text{-}190\text{ }^\circ\text{C}$) (method (ii) in Scheme 15). However, the desired nucleophilic substitution did not occur and the starting material could be recovered. Next, bases were added to increase the nucleophilicity of the benzylamine derivatives. Here, caesium carbonate was used in dimethylformamide or acetonitrile, however the substitution product was not observed and the starting materials were recovered after column chromatography (methods (iii-iv), Scheme 15). Using sodium *tert*-butoxide as a strong base, resulted in the successful formation of the desired 2-amino-pyridine **24i** and **24j** in moderate yields of 21-36% (method (v), Scheme 15). But the trifluoromethyl substituted analogue **24b** could not be synthesised under these reaction conditions. Different conditions for the substitution were explored in order to improve the nucleophilicity of the amines, but reaction yields did not improve. A different approach for the substitution reaction was the palladium catalyst amination reaction using $\text{Pd}(\text{OAc})_2$ as palladium source (method (vi), Scheme 15). The reaction proceeded to the desired product **24k**, but the yields were not satisfactory (18%), reflect-

Table 10: Synthesis of amino-substituted aldehydes, yield and method; n, R¹-R⁴ for amino-substituted acetals **24a–n** and aldehydes **25a–g**; reaction conditions used and yields; see Scheme 15.

#	n	R ¹	R ²	R ³	R ⁴	method	yield [%]	aldehyde	
								#	yield [%]
24a	1	H	H	H	CH ₃	(ii)	no reaction		
24b	1	H	H	H	CF ₃	(ii)	no reaction		
24c	1	H	H	H	H	(ii)	no reaction		
24d	1	CH ₃	H	H	H	(ii)	no reaction		
24e	2	H	H	H	H	(ii)	no reaction		
24f	2	H	H	H	OH	(ii)	no reaction		
24g	1	H	H	H	CH ₃	(iii)	no reaction		
24h	1	H	H	H	CH ₃	(iv)	no reaction		
24b	1	H	H	H	CF ₃	(v)	no reaction		
24i	2	H	H	H	H	(v)	21-32	25a	44-100
24j	1	H	H	H	CH ₃	(v)	36	25b	100
24k	1	H	H	H	H	(vi)	18	25c	100
24l	1	H	H	H	CH ₃	(vii)	43	25f	43
24m	1	H	H	H	CF ₃	(vii)	n.a.	25d	100
24n	1	H	H	H	H	(vii)	65	n.a.	n.a.

ing the poor reactivity of substituted aldehydes/ acetals from type **20a–b** with benzylamine derivatives.^[175] In order to overcome the lack of reactivity an Ullman-type coupling reaction with Cu(I) has been used for the formation of the acetals **24l**, **24m**, and **24n** (Method (d) in Scheme 15).^[175] Therefore, a modified version of the amination protocol of Frey et al. has been applied to the acetal **23**.^[175] Copper iodide has been used as source for Cu(I) and caesium acetate served as the base. The reaction proceeded in excellent yields (43-65 %) and has been chosen as the preferred approach for the synthesis of derivatives of the type **24**. In all cases, the desired 2-amino aldehydes **25a**, **25b**, **25c**, **24l**, and **25d** were obtained after acidic hydrolysis of the acetal with TFA at room temperature. Compound **26a** was chosen for the further Knoevenagel reaction with the ethyl ester of **14** (Scheme 16). The reaction proceeded in good yields of 75 %. In addition to these heterocyclic modification several other pyridine-carboxaldehydes, furanyl-aldehydes as well as cinnamonyl-aldehydes were chosen for the Knoevenagel reaction with rhodanine-N-acetic acid **2** and thiazolidine-2,4-dione derivatives and their ethyl-ester analogues **7** and **14** (Scheme 16). The yields of the reactions varied from 14-100 % and the chemical shift of the CH-signal in ¹H-NMR experiments showed only formation of the thermodynamically more stable *Z*-isomer.^[160] The chemical shift for the CH-signal in DMSO-d₆ (7.05-7.96 ppm) were observed further downfield than for CDCl₃ (7.29-7.75 ppm).



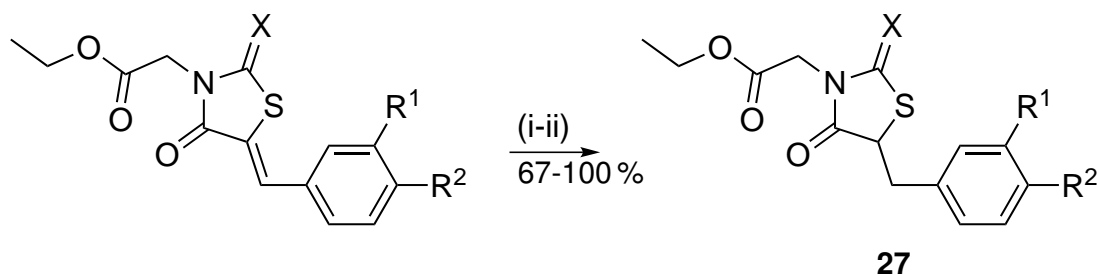
Scheme 16: Synthesis of heterocyclic derivatives **26a–j**; X=S,O; R=H,Et, R¹=**25f**, 2-pyridine, 3-pyridine, 4-pyridine, furan, cinnamonaldehyde (i) NaOAc, EtOH, 80 °C, see Table 11.

Table 11: Synthesis of heterocyclic rhodanine-N-acetic acid/ ester derivatives; R¹-R² and X of heterocyclic compounds **26a–j**; yield and chemical shift of CH-signal, see Scheme 16.

#	R ¹	X	R ²	yield [%]	NMR shift of CH [ppm]		
					δ_{solvent}	δ_H	δ_C
26a	Et	S	25f	75	CDCl ₃	7.53	131.6
26b	H	S	2-pyridinyl	54	DMSO-d ₆	7.92	129.4
26c	H	S	3-pyridinyl	74	DMSO-d ₆	7.96	130.6
26d	H	S	4-pyridinyl	82	DMSO-d ₆	7.90	n.a.
26e	H	S	phenylallylidene	20	DMSO-d ₆	7.71-7.75	n.a.
26f	Et	S	2-pyridinyl	100	CDCl ₃	7.67	128.6
26g	Et	S	3-pyridinyl	14	CDCl ₃	7.75	129.9
26h	Et	S	4-pyridinyl	28	DMSO-d ₆	7.05	n.a.
26i	Et	O	4-pyridinyl	21	CDCl ₃	7.29	n.a.
26j	Et	S	2-furanyl	38	CDCl ₃	7.51	119.1-119.2

3.2.11 Reduction of the exo-cyclic double bond in rhodanine-N-acetic acid derivatives

The exo-cyclic double bond within the rhodanine or thiazolidine-2,4-dione derivatives are part of a Michael acceptor system. The double bond is conjugated to a carbonyl group, making it potentially prone to 1,4-nucleophilic attack from biological nucleophiles such as glutathione.^[82,83] Previous examples of nucleophilic attacks to the Michael acceptor system in rhodanine and thiazolidine-2,4-dione derivatives have been discussed in section 3.2.2 (Scheme 3). In order to study the effect of the double bond on the activity against various protozoa, a range of saturated analogues have been synthesised. There are essentially three methods to reduce the double bond in rhodanine-like derivatives.^[104,176,177] Derivatives with an exo-cyclic sulphur group can be reduced by LiBH₄ in the presence of pyridine or via the Hantzsch-ester method.^[104,176,177] The reported yields for the LiBH₄ in pyridine reduction for rhodanine deriva-



Scheme 17: Synthesis of reduced analogues **27a–c**; for X=S, R^{1,2}=OH,H (i) Hantzsch ester **28**, activated SiO₂ gel, toluene, 85 °C, dark; for X=O, R^{1,2}=OH,H (i) Pd/C, H₂, dioxane, see Table 12.

Table 12: Reduction of rhodanine-N-acetic ester analogues; X and R¹-R² of reduced analogues **27a–c**; yield, chemical shift of CH-signal, see Scheme 17.

#	X	R1	R2	method	yield
27a	S	H	H	(i)	67
27b	O	H	H	(ii)	98
27c	O	OH	OH	(ii)	100

tives were only 26 %.^[161] For this reason, the second approach, the Hantzsch-ester reduction, was chosen for the reduction of rhodanine derivatives. The Hantzsch ester is a milder reducing agent compared to LiBH₄.^[177] Compounds with an exo-cyclic carbonyl group were reduced by catalytic hydrogenation with Pd/C and H₂ (Scheme 17). The Hantzsch ester reduction of the exo-cyclic double bond in **27a** proceeded in good yields of 67 %. The reduced analogue **27a** was easily purified by direct application of the crude silica to column chromatography. The hydrogenation of the compounds from the type **7** worked very well, yielding the products **27b** and **27c** after simple filtration over celite.

3.2.12 Synthesis of photo-affinity label for identification of target proteins

Introduction

The rhodanine N-acetic acid inhibitors **2a–ai**, the thiazolidine-2,4-dione derivatives **7a–l**, their ester analogues **14a–ab**, **21a**, 3-benzyloxy-modified analogues **19a–l**, the heterocyclic modified analogues **26a–j** and the reduced analogues **27a–c** were designed as inhibitors for parasitic growth. Therefore all inhibitors were screened against parasitic organism and mammalian cells to evaluate their activity and toxicity profile (Chapter 3.2.5, 3.2.6, 3.2.7, 3.2.8, 3.2.9, 3.2.10 and 3.2.11) . This approach helped in the identification of potent inhibitors against parasitic growth, without prior optimisation towards a specific target protein. However, in later opti-

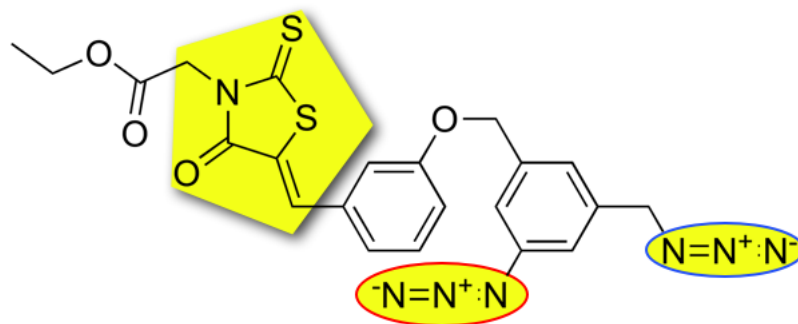


Figure 23: Photo-affinity label for the identification of possible targets in parasites (*T. brucei*, *T. cruzi*, *L. infantum*) and mammalian cells (HL60 cells); five-membered ring (yellow): affinity probe; red circle: photo-label group; blue circle: Click-chemistry tag.

misation steps it is important to know the molecular target protein(s) of the designed inhibitors. In order to identify possible target proteins, a photo-affinity probe with three major components was designed (Figure 23). The first important component was the rhodanine affinity ligand (yellow five-membered ring, Figure 23). The affinity ligand ensures target-specificity by tight binding to its molecular target. The second component is a UV-sensitive aromatic-azide-tag (red circle, Figure 23). Aromatic azides are widely used in protein photo-affinity labelling.^[178] Under UV-activation (254 nm), aromatic azides from the type **29** form highly reactive intermediates (Figure 24),^[179] such as singlet nitrenes, which are converted to triplet nitrenes at higher temperatures.^[180] Otherwise at low temperatures (< 77 K), singlet nitrenes react to ketenimines (azepine **30**). These reactive intermediates, the triplet nitrenes or the ketenimine azepines **30** can react with nucleophiles in the receptor protein which are in close proximity.^[180] The third component of the photo-affinity probe (Figure 23) is an alkyl azide group (blue circle, Figure 23), which is stable under UV-irradiation conditions.^[178] This alkyl azide served as an additional tag for the introduction of fluorescence- or biotin-probes via Click-Chemistry reaction.

The designed probe with all three components (affinity-, photo-label, click-chemistry-group) will be applied to protein mixtures of parasitic or mammalian origin (Figure 25). The affinity group will provide the selectivity for the individual target protein or target proteins. After a short incubation time, the ligand-probe receptor-protein complex will be exposed to UV-irradiation, to promote the formation of covalent bonds between the ligand and the receptor. In the final step click-chemistry will be applied to the covalently bonded ligand-receptor complex and an identification tag, for example a fluorophore or biotin-moiety is introduced via the free alkyl-azide linker of the ligand. If biotin is chosen for the tagging of the protein-ligand complex, a

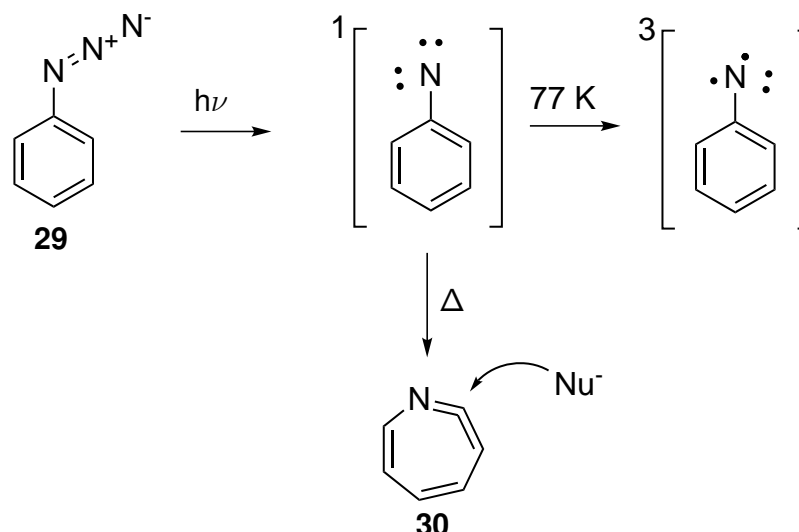


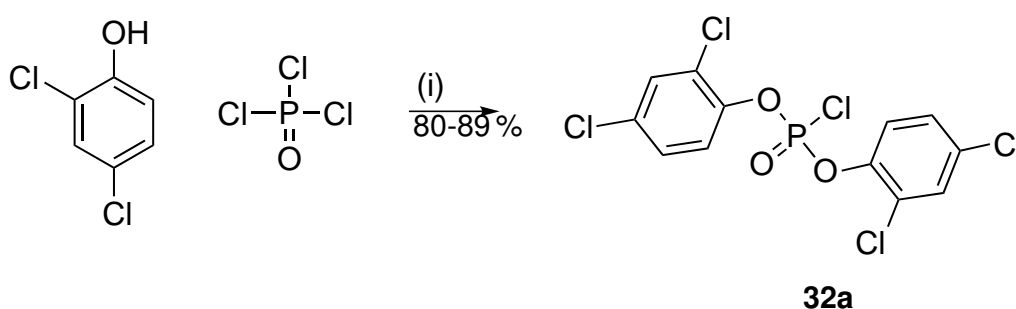
Figure 24: Reaction mechanism of aryl azides after UV-activation.

purification step via streptavidin beads can be performed, otherwise the fluorescence of the protein-ligand-complex can directly be read from a SDS-gel.

Synthesis of the photo-affinity label probe

The synthesis of the photo-affinity probe (Figure 23) was performed according to previous reports.^[178,181] The only difference in the synthetic procedure was the introduction of a different affinity group on the photo-label-alkylazide moiety.^[181]

The bis-(2,4-dichlorophenyl) phosphorochloridate **31a** was synthesised via esterification reaction of phosphoryl trichloride and 2 eq of 2,4-dichlorophenol.^[182] The product **31a** was afforded in excellent yields of 80-89 % after simple distillation (Scheme 18).^[182] The major by-



Scheme 18: Synthesis of phosphorochloridate **31**; (i) magnesium turnings, rt \rightarrow 120 °C, 3 h at 120 °C, 3 h at 160 °C.

product of the esterification was the dichloro-monoester **31b**, but this by-product was fractionated by distillation and re-reacted with 2,4-dichlorophenol. The stated yield was the combined yield of both reactions.

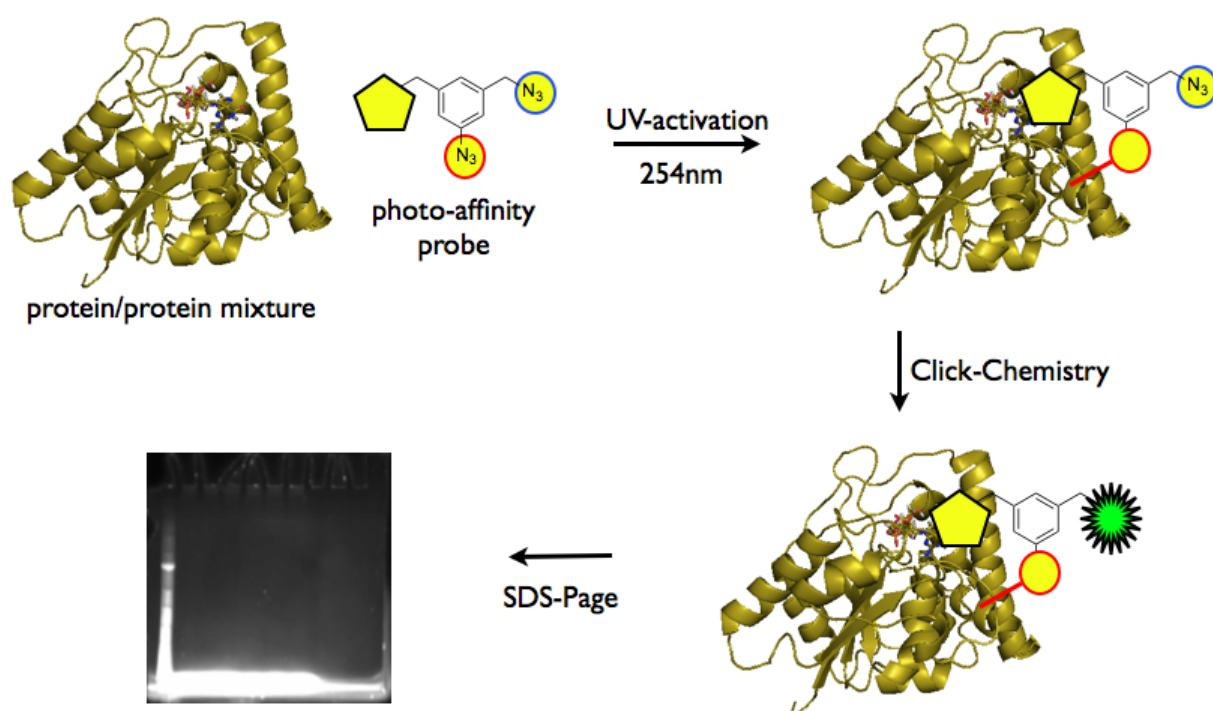
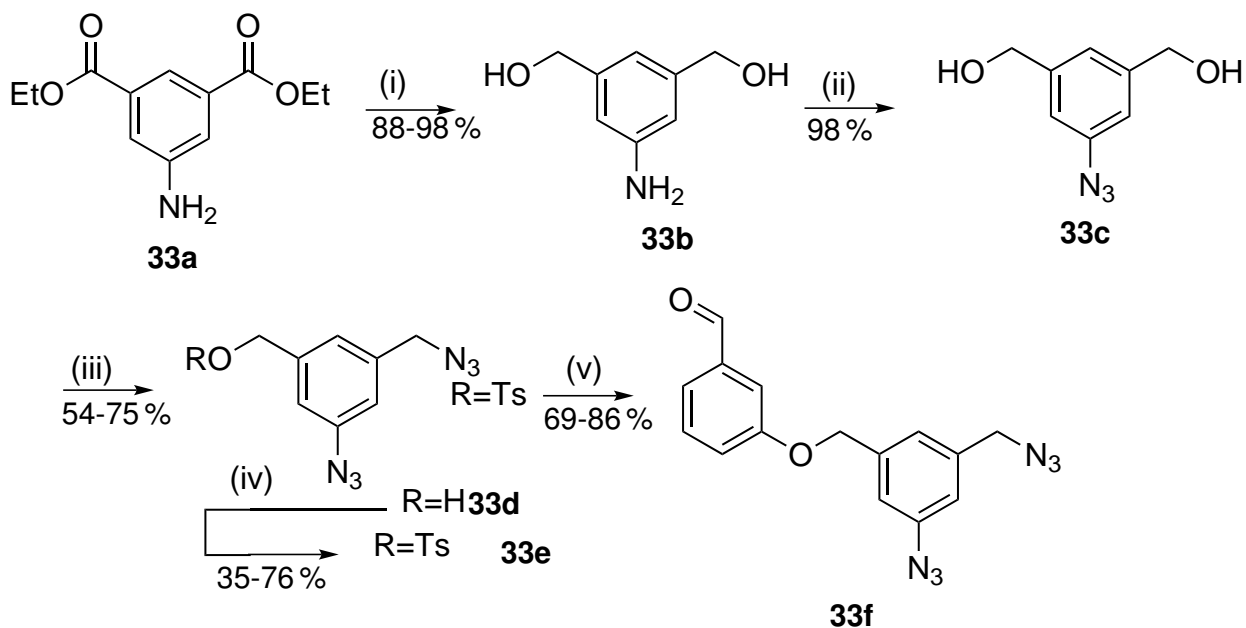


Figure 25: Photo-affinity strategy to identify molecular targets; five-membered ring (yellow): affinity probe; red circle: photo-label group; blue circle: Click-chemistry tag; green: Alexa-Fluor 488 or biotin-tag.

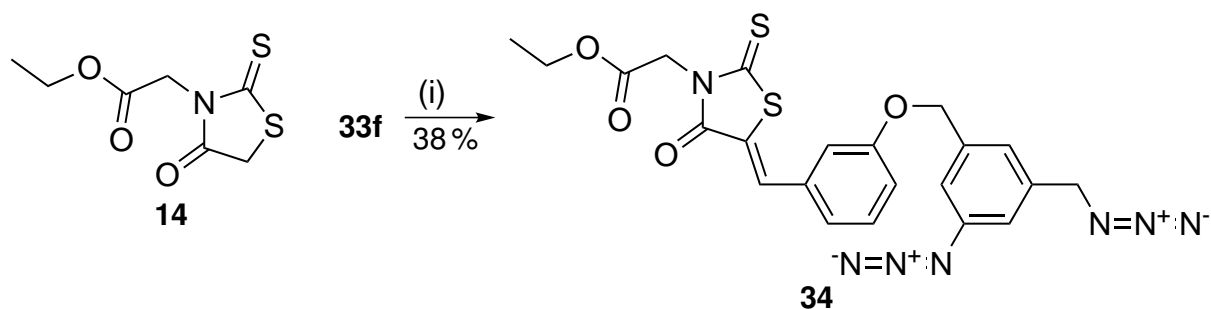
The synthesis towards the photo-affinity probe **34** started from dimethyl 5-aminoisophthalate **33a**. The diester **33a** was reduced with excess lithium aluminium hydride (LiAlH_4) in THF ((i) in Scheme 19).

The reduced amino-diol **33b** was obtained in excellent yields of 88-98 %. The following amino to azido transformation was performed with *tert*-butyl nitrite (tBuONO) and TMS-N_3 in acetonitrile to obtain the desired azido-diol **33c** with a 98 % yield ((ii) in Scheme 19). The conversion of one of the alcohols in **33c** to an azide functionality was achieved by a one-pot reaction with **31a**, DMAP and sodium azide (NaN_3) in dimethylformamide ((iii) in Scheme 19). The conversion of only one of the primary alcohols was achieved by using 1.1 eq of **31a**. Under these conditions less than 10 % of the azido-diol **33c** were converted to the tri-azido analogue. The desired di-azido-alcohol **33d** was afforded after column chromatography in yields of 54-75 %. The free primary alcohol of **33d** was tosylated with tosyl chloride (TsCl) and triethylamine (NEt_3). For this substitution, it was important to keep the reaction temperature under 0°C , otherwise decomposition was observed. Tosylated di-azide **33e** was afforded in moderate yields of 35-76 %. The 3-benzyloxy modified aldehyde **33f** was synthesised by nucleophilic substitution reaction between 3-hydroxybenzaldehyde and the tosyl di-azide **33e**. The photo-



Scheme 19: Synthesis of photo-label-aldehyde **33f**; (i) LiAlH_4 , THF $0^\circ\text{C} \rightarrow \text{rt}$, 8 h; (ii) $t\text{-BuONO}$, TMS-N_3 , ACN, $0^\circ\text{C} \rightarrow \text{rt}$, 2 h; (iii) **31a**, DMAP, NaN_3 , DMF, rt, 4 h; (iv) Ts-Cl , NEt_3 , 0°C , 2 h; K_2CO_3 , DMF, 50°C .

affinity aldehyde **33f** was reacted with rhodanine-N-acetic ethyl ester **14** in a Knoevenagel reaction to afford the desired photo-affinity-probe in moderate yields of 38 % (Scheme 20). The Knoevenagel reaction was carried out at lower temperatures of 50°C to ensure that the photo-affinity label does not decompose.



Scheme 20: Synthesis of rhodanine-N-acetic ethyl ester photo-affinity label **34**; (i) NaOAc , EtOH, 50°C , 2 h.

3.3 Anti-trypanosomal activity

3.3.1 AlamarBlue & MTT activity/toxicity assays

In this section the whole cell assays against trypanosomes and mammalian cells are described in detail. The detailed description is important in order to understand the possible problems which can arise with the screening of rhodanine compounds. Rhodanine derivatives were mostly afforded as yellow to red solids after filtration, in solution these derivatives caused an intense colour change in the aqueous assay media. This colour can interfere with the assay readout, as the measured absorbance wavelengths of indicator dye and compound absorbance could overlap. In this study, the activity of growth inhibitors was evaluated with colorimetric assays, such as the AlamarBlue assay (Figure 26, (a)) or the MTT-assay (Figure 26, (b)).^[183,184] The cell viability dye AlamarBlue was used for determination of activity data against *T. brucei* and toxicity data against HL60 cells. MTT was used for the acquisition of the activity data against *T. cruzi*.

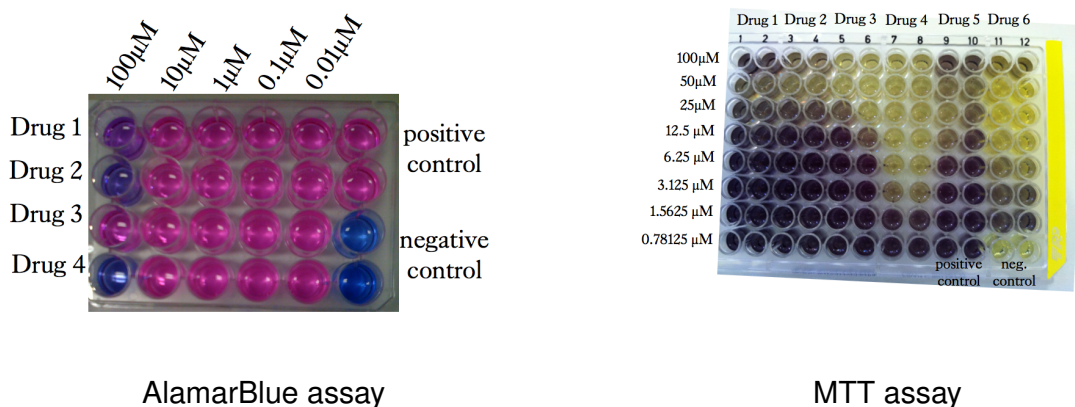


Figure 26: Colorimetric activity-/ toxicity assays. Left: Outline of 24 well plate assay for estimation of GI_{50} values for *T. brucei* and HL60 cell growth after 72 h of incubation. Right: Outline of 96 well plate assay for determination of GI_{50} values for *T. cruzi* and *L. infantum* after 24 h of incubation.

The AlamarBlue assay is an one-step assay, which does not require any washing or extraction steps prior to read out of cell viability, as compared to the MTT analogous assay.^[185] The cell viability can be determined by simple linear correlation between cell density and the absorbance or fluorescence intensity of AlamarBlue.^[183] Living cells are able to reduce the blue AlamarBlue (also known as resazurin) to the pink resorufin (Figure 27).^[183] In mammalian cells, the reduction of resazurin is dependant on the activity of dehydrogenases in the respira-

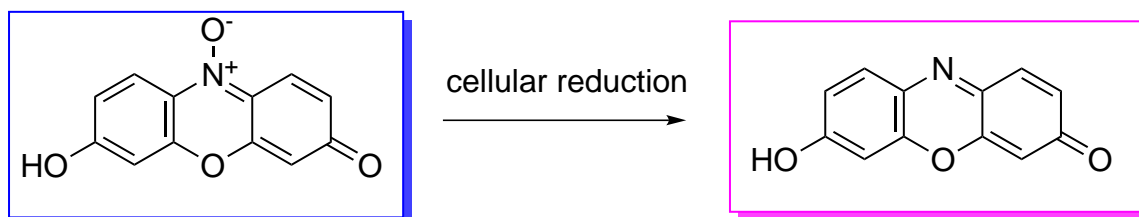


Figure 27: Intracellular reduction of blue resazurin to purple resorufin.

tory chain of mitochondria.^[185] In *T. brucei* the reductions are believed to occur in the glycolytic pathway.^[185]

The activity assay for *T. b. brucei* TC211 was performed in a 24 well plate format (Figure 26, (a)). Therefore, *T. brucei* was cultured in Baltz medium supplemented with 16.7% heat-inactivated foetal bovine serum (FBS) at a final concentration of 10^4 cells in 1 mL media. Controls were performed in the presence of 0.5% DMSO, without showing any toxic effects. Inhibitors were tested at five concentrations (100, 10, 1, 0.1, 0.01 μ M) in a final DMSO-concentration of 0.5%. The cells were incubated for 24 h in the presence of the inhibitor prior to addition of AlamarBlue (10% solution). After a further 48 h the resazurin indicator dye has been reduced by living parasites and the absorbance at 570 nm was read, using 630 nm as the reference wavelength for the absorbance of proteins in the media. Each assay was performed at least in duplicate with more replicates added.

As previously mentioned, AlamarBlue can also be used to monitor the viability of mammalian cells. Here Human myeloid leukaemia (HL60) cells were used for the evaluation of the toxicity of anti-parasitic compounds. The cell line was first isolated from a patient with acute promyelocytic leukemia.^[186] HL60 cells are easy to maintain, grow in suspension and reproduce faster than normal cells, therefore they can easily be applied to high throughput assays in order to screen for general cytotoxicity.^[187,188] HL60 cells are commonly used as reference for general cytotoxicity in drug discovery for HAT, Chagas disease^[189,190] and Leishmaniasis.^[191] Screening results obtained with immortal cancer cell lines for toxicity correlate well with toxicity against primary cells if the drug affects common basal functions of cells.^[187,188] In general the cytotoxicity data obtained with HL60 cells is lower compared to screening results against primary cell lines.⁴

Similar to the activity assay against *T. brucei*, HL60 cells were seeded in 24 well plate at a final concentration of 10^5 cells in 1 mL RPMI 1640 medium supplemented with 2 mM L-glutamine and 16.7% FBS. HL60 cells were challenged with five concentrations of each inhibitor over a time period of 24 h, prior to addition of AlamarBlue (10% solution). Following the read out procedure described for *T. brucei*, the absorbance at 570 nm was acquired. Al-

⁴oral communication with Dr. Dietmar Steverding

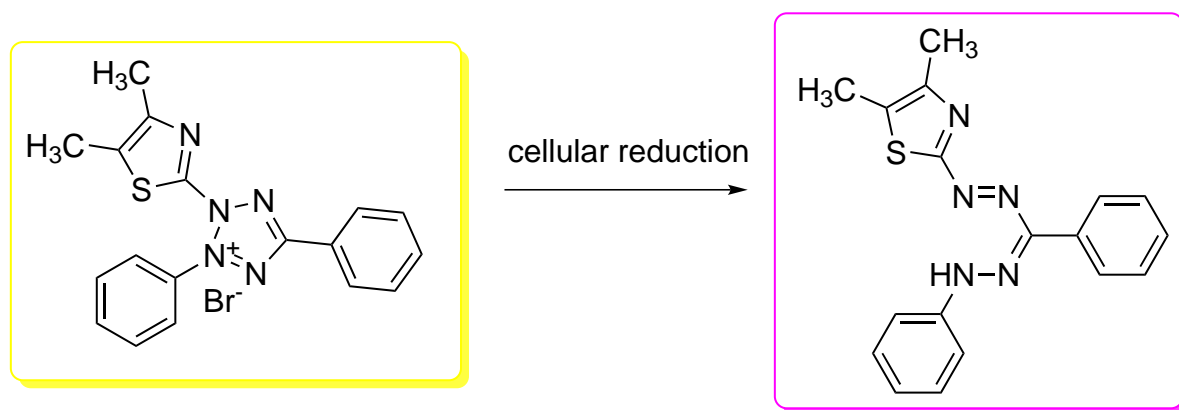


Figure 28: Intracellular reduction of yellow tetrazole salt MTT to its purple formazan.

ternatively, the toxicity assay was performed in a 96 well format with a total volume of 200 μL media and a cell density of $10^5 \frac{\text{cells}}{\text{mL}}$. HL60-cells were challenged with 8 different inhibitor concentrations (100, 50, 25, 12.5, 6.25, 3.125, 1.5625, 0.78125 μM) over a period of 44 h. After which AlamarBlue was added and the cells were incubated for another 4 h. The fluorescence of resorufin was read at 585 nm (emission) with excitation at 570 nm. Using the fluorescence intensity instead of the absorbance had the advantage of less interference of yellow coloured inhibitors in the toxicity assay. Furthermore, performing the toxicity assay in a 96 well plate allowed the screening of 2 additional drugs per plate with three additional concentrations (Figure 26).

For the evaluation of inhibitory activity against *T. cruzi* the MTT-assay variant was pursued. MTT, 3-[4,5- dimethylthiazol-2-y1]-2,5-diphenyl-tetrazolium bromide is a similar indicator dye for cell viability to AlamarBlue. Yellow tetrazolium salt (MTT) is reduced by mitochondrial enzymes to its purple furazan salt. The progress of this reduction can be followed by measuring the absorbance at 550 nm.^[136] The assay is performed in a 96 well plate, with *T. cruzi* trypanomastigote densities of $10^6 \frac{\text{cells}}{\text{mL}}$. After 24 h, MTT was added and formazan extraction was carried out with 10% (v/v) SDS over a time period of 18 h. The total formazan concentration and therefore the number of viable *T. cruzi* was obtained by measuring the absorbance at 550 nm. Unfortunately most rhodanine inhibitors also absorbed at a similar region as the MTT viability dye, resulting in missing activity data against *T. cruzi* throughout this thesis. The AlamarBlue viability dye was not available for the whole cell assays against *T. cruzi*.

The minimum inhibitory concentration (MIC) for all inhibitors was determined by visual inspection with a light microscope. The MIC is defined as the minimum drug concentration, where all parasites or mammalian cells were lysed.

3.3.2 Calculation of GI₅₀-values

All assays were performed in the presence of a positive and a negative control in order to accurately define 0 % and 100 % parasite survival. This was essential for normalisation of the obtained absorbance or fluorescence intensity data. Here, the steps for calculation of growth inhibition constants (GI₅₀) are described for the arsenical drug Melarsoprol. Melarsoprol has been evaluated against *T. brucei* and HL60 cell growth in the AlamarBlue assay (Figure 29, (b)). The raw absorbance data was normalised and plotted against the logarithm of Melarsoprol concentrations (log(C)) (Figure 29). Growth inhibition constants GI₅₀, the concentration needed to reduce cell growth by 50 %, was calculated by the following equation

$$Y = \frac{100}{1 + 10^{(LogGI_{50} - X) \cdot HillSlope}} \quad (1)$$

where Y is the parasite concentration, X is log(C) and the Hill-Slope is variable. Applying this formula in the integrated settings of Prism GraphPad v5.0a for Mac OS X resulted in GI₅₀-values of 1.70 nM and 1.76 nM for each individual assay. Next the average of the GI₅₀ values together with their standard deviation was calculated (1.73 ± 0.04 nM, MIC 10 nM). The calculated GI₅₀-value for Melarsoprol was very similar to previously published GI₅₀ against *T. b. rhodesiense* (1.7 nM) and *T. brucei brucei* (3.7 nM).^[185,189] The toxicity of Melarsoprol against HL60 cells was calculated to 14.53 ± 1.27 µM (MIC 100 µM), slightly less toxic than previously reported (3.26 µM).^[189] The calculated GI₅₀ values for Melarsoprol for *T. brucei* and HL60 cells not only validate the AlamarBlue assay, but also validate the chosen model for the estimation of GI₅₀ values. The standard drug for *T. cruzi* was Benznidazole and GI₅₀ was estimated to 440.7 nM (CI95 % 406.2-478.4 nM).

3.3.3 Anti-Trypanosomal activity of rhodanine-N-acetic acid derivatives

Anti-trypanosomal activity of rhodanine-N-acetic acid derivatives 2a–ai

The previously identified DPMS inhibitors **2a–j** were re-synthesised and screened against *T. brucei* and *T. cruzi*.^[68] Previously **2a–j** showed activities against the bloodstream form of *T. brucei* of >100 µM (Table 13).^[68] Therefore, it was expected that derivatives **2a–j** would not show any trypanocidal activity against the *T. brucei* variant TC211. However, surprisingly compounds **2a** and **2d** showed activities of 56.0 µM and 12.7 µM, respectively. The increased activity of the piperidine salt **2d** was particularly interesting, as this derivative showed the highest GI₅₀-value of 492 µM.^[68] However, these results may reflect the poor solubility of rhodanine derivatives in aqueous media, as previous reports had shown that salts of rhodanine-N-acetic acids improve water solubility.^[192] Alternatively, the salt adduct **2d** may improve diffusion through biological membranes. Improved membrane permeability would also explain

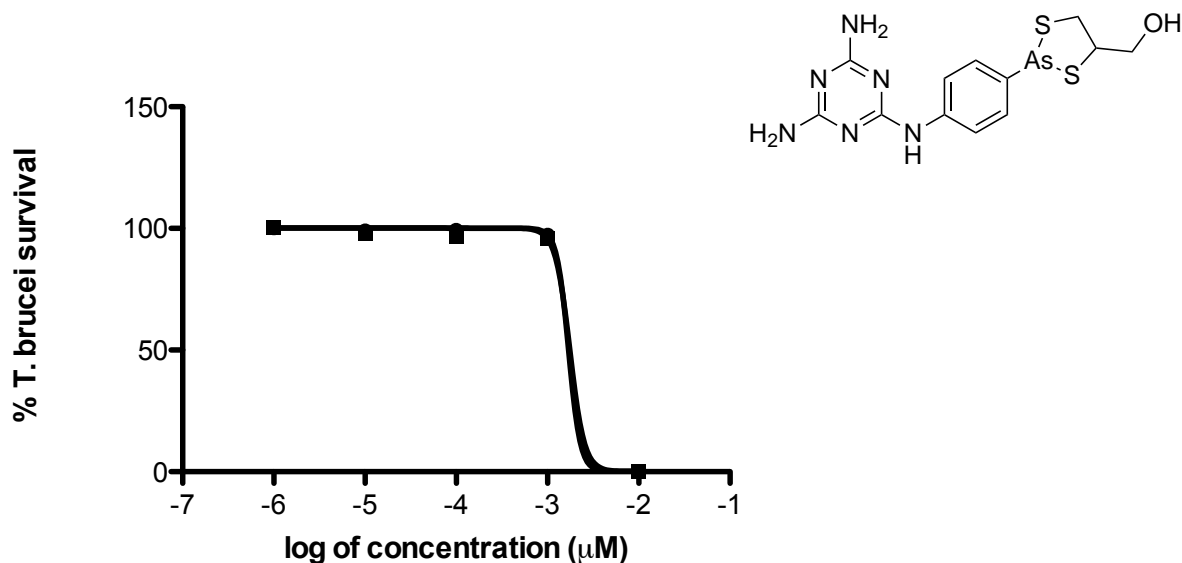
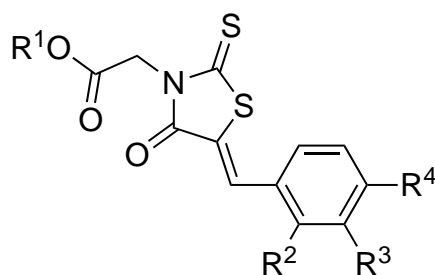


Figure 29: Plot of log(C) against normalised parasite survivals and structure of Melarsoprol.

the relatively high toxicity (45.2 μM) of the piperidine-salt **2d**. Overall, activity against *T. brucei* correlated well with previous results (Table 13).^[68] However, the residual DPMS activity in the previous study, generally did not correlate with its *in vitro* activity against *T. brucei*.^[68] This observation indicates that the salt adduct improved the compounds ability to penetrate biological plasma membranes. In the case of **2d**, this would mean that the two very lipophilic benzylsubstituents facilitate the diffusion through the parasite membrane. Once inside the cytosol, **2d** can diffuse to its potential target (e.g. DPMS). In order to support the hypothesis that increased lipophilicity improves anti-parasitic activity (Table 14), the library of rhodanine-N-acetic acid derivatives was enlarged through the addition of lipophilic substituents such as methyl, trifluoromethyl or *tert*-butyl-groups. Initially, the activity of the starting rhodanine-N-acetic acid **2** was assessed and was found inactive against *T. brucei*. Indeed, none of the derivatives showed activity against *T. brucei* and *T. cruzi* at 100 μM. Similarly to **2d**, the piperidine salt of compound **2y** (R⁴=*tert*-butyl) was prepared and tested. But in this case the activity of the piperidine salt **2y** and the free acid **2z** did not affect trypanosomal activity. Di-trifluoromethyl substituted derivatives **2ab** and **2ae** were not active at 100 μM, but showed some trypanocidal activity at the highest concentration of 100 μM. Interestingly, the catechol derivative **2u** (R¹=OH) did not show any anti-parasitic activity, but its slightly modified analogue **35a** (R¹=NH₂) inhibited *T. brucei* growth at GI₅₀ 17.1 μM. These results suggested modifications on position N-1 to be important for anti-trypanosomal activity. All derivatives had minimum inhibitory concentration of >100 μM.

Table 13: Comparison of residual *T. brucei* DPMS activity and trypanocidal activity; Pip: piperidine salt.

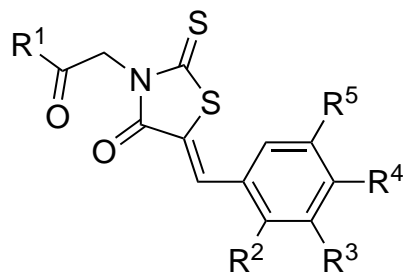
compounds

#	R ¹	R ²	R ³	R ⁴	[%] DPMS ^(a)	GI ₅₀ [μM]			
						<i>T. brucei</i> ^(a)	<i>T. brucei</i>	<i>T. cruzi</i>	HL60
2a	H	H	H	H	42 ± 5	232 ± 12	56.0 ± 3.3	>100	>100
2b	H	H	H	OBn	10 ± 2	338 ± 31	>100	>100	>100
2c	H	H	OBn	H	23 ± 3	96 ± 5	>100	>100	>100
2d	Pip	H	OBn	OBn	20 ± 4	492 ± 24	12.7 ± 0.2	n.a.	45.2 ± 2.1
2e	H	OH	H	H	23 ± 8	107 ± 12	>100	>100	124.1 ± 6.6
2f	H	H	OH	H	70 ± 4	427 ± 19	>100	>100	>100
2g	H	H	H	OH	90 ± 5	345 ± 23	>100	>100	>100
2h	H	H	H	Cl	73 ± 6	244 ± 17	>100	>100	>100
2i	H	H	H	CN	86 ± 5	398 ± 19	>100	>100	>100
2j	H	H	H	CCH	94 ± 7	>1000	>100	>100	>100

(a) Data published by Smith et al.^[68]

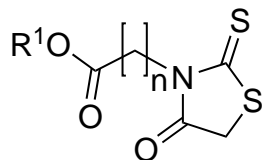
3.3.4 Anti-trypanosomal activity of the rhodanine moiety

It has been established, that anti-parasitic activity might vary with N-1 substitutions. In order to further elucidate the role of the N-1-substituent on the rhodanine moiety, several N-1-modified aliphatic acids were screened against *T. brucei* (Table 15, (a)). Firstly, rhodanine-N-acetic acid **2** was evaluated against *T. brucei*, but showed only weak anti-trypanosomal effects (around 100 μM), although the exact value was not measured as it was beyond the highest concentration in the screen. Furthermore, the ester derivatives **14** have been screened against *T. brucei* and showed promising trypanocidal effects of GI₅₀ 11.1 and 13.2 μM against *T. brucei*. Analogues with an elongated N-side linker (**12** and **13**) showed increased activity against *T. brucei* with longer linker lengths. The logP values of all derivatives were calculated (MarvinSketch) and compared to the anti-trypanosomal activity. With the exception of the methyl ester analogue **14**, a linear relationship between the logP value and anti-trypanosomal activity was observed (Table 15, (b)). Although the methyl ester **14** had a logP of 0.46, its activity was higher (11.1 μM) compared to **12** (50.6 μM) which had a logP value of 0.55. This result sug-

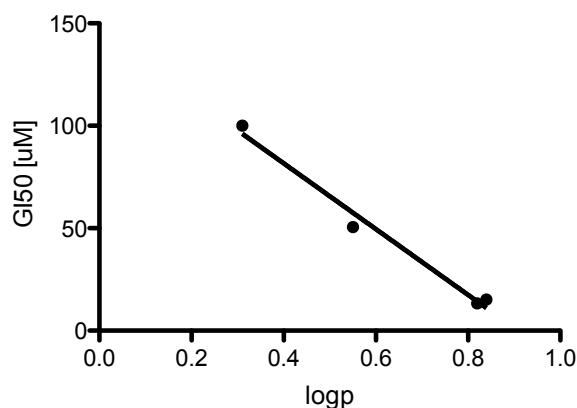
Table 14: Anti-trypanosomal activity of rhodanine-N-acetic acid derivatives **2**, **2k–ae**, and **35a**.**2a–ae**

#	R ¹	R ²	R ³	R ⁴	R ⁵	GI ₅₀ [μM]		
						<i>T. brucei</i>	<i>T. cruzi</i>	HL-60
2	OH	n.a.	n.a.	n.a.	n.a.	>100	n.a.	n.a.
2k	OH	H	NO ₂	H	H	>100	>100	>100
2l	OH	H	Br	OMe	H	>100	>100	>100
2m	OH	H	CH ₃	H	H	>100	>100	>100
2n	OH	H	H	CH ₃	H	>100	>100	>100
2o	OH	CH ₃	H	H	H	>100	n.a.	>100
2p	OH	H	CF ₃	H	H	>100	>100	>100
2q	OH	H	H	CF ₃	H	>100	>100	>100
2r	OH	CF ₃	H	H	H	>100	>100	>100
2ag	OH	CF ₃	H	CF ₃	H	>100	>100	n.a.
2s	OH	H	H	SO ₂ Me	H	>100	>100	>100
2t	OH	H	H	NMe ₂	H	>100	>100	>100
2u	OH	H	OH	OH	H	>100	>100	n.a.
2v	OH	H	COOH	H	H	>100	>100	>100
2w	OH	OH	H	OH	H	>100	>100	>100
2x	OH	CF ₃	H	H	CF ₃	>100	>100	>100
2y	C ₅ H ₁₁ N	H	H	tBu	H	>100	>100	>100
2z	OH	H	H	tBu	H	>100	>100	>100
2aa	OH	COOH	H	H	H	>100	>100	n.a.
2ab	OH	CF ₃	H	CF ₃	H	185.6 ± 3.54	>100	>100
2ac	OH	H	H	OMe	H	>100	>100	n.a.
2ad	OH	H	H	NHAc	H	>100	>100	>100
2ae	OH	H	CF ₃	H	CF ₃	109.7 ± 10.61	>100	n.a.
35a^(a)	NH ₂	H	OH	OH	H	17.7 ± 0.1	>100	n.a.

(a) received from Prof. Dr. M. Schlitzer, Phillips University, Marburg, Germany.

Table 15: Activity of starting rhodanine-N-acetic acid derivatives and correlation to logP ($Y=145.9-160.5 \cdot x$, $r^2=1.0$).**(a)** Activity of starting rhodanine

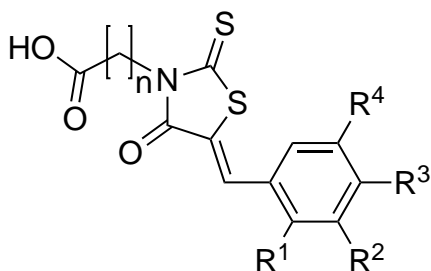
#	n	R	logP ^(a)	GI ₅₀ [μM]	
				<i>T. brucei</i>	HL60
2	1	H	0.31	100	n.a.
14	1	Me	0.46	11.1 ± 0.1	n.a.
12	2	H	0.55	50.6 ± 1.2	>100
14	1	Et	0.82	13.3 ± 0.5	>100
13	3	H	0.84	15.2 ± 3.3	>100

^(a)calculated with ChemAxon MarvinSketch**(b)** Correlation of logP and GI₅₀ (*T. brucei*)

gested that the anti-trypanosomal activity went beyond simple correlation to logP and other factors had to be considered. Under physiological pH the analogue **12** is negatively charged, potentially resulting in repulsion from the parasitic membrane, whereas the negative charge in the methyl ester analogue **14** is masked, facilitating diffusion to the plasma membrane. In the case of the ethyl ester analogue **14** and the charged analogue **13** the effect is less dominant, possibly due to similar logP values (0.82 and 0.84). The two additional methylene-linker groups might contribute more to membrane diffusion than the ethyl ester moiety. Thus increased linker length and ester functionalities resulted in low μM inhibitors of *T. brucei* growth, without showing toxicity against mammalian cells (HL60 cells, Table 15 (a)). The methyl and ethyl esters **14** as well as the elongated analogue **13** cleared parasitaemia at 100 μM (MIC 100 μM). Therefore, it was of interest if additional substituents in position 5 of the rhodanine moiety would further enhance their anti-parasitic activity.

3.3.5 Derivatives with elongated N-3 side-chain linkers

Increasing lipophilicity of the rhodanine-moiety led to increased potency against *T. brucei* (Table 15). In this chapter, the effect of the increased linker-length of derivatives **12** and **13** was studied. In particular their condensation products on position 5 were of interest to increase anti-parasitic activity. And indeed, the simple condensation product of **12** and benzaldehyde was almost 4 times as potent against *T. brucei* (**12a**, GI₅₀ 13.0 μM) as the unsubstituted rhoda-

Table 16: Anti-trypanosomal activities of derivatives with elongated side chain.

#	n	R ¹	R ²	R ³	R ⁴	MIC [μ M]		GI ₅₀ [μ M]	
						<i>T. brucei</i>	<i>T. brucei</i>	<i>T. cruzi</i>	HL60
12a	2	H	H	H	H	100	13.0 \pm 0.7	>100	>100
12l	2	H	H	OH	H	n.a.	n.a.	>100	>100
12k	2	H	OH	H	H	>100	>100	>100	n.a.
12m	2	H	OH	OH	H	100	14.2 \pm 2.3	>100	>100
12h	2	H	H	NMe ₂	H	>100	60.8 \pm 8.9	>100	>100
12i	2	H	H	Cl	H	>100	60.6 \pm 2.0	>100	>100
12b	2	CH ₃	H	H	H	100	13.0 \pm 0.6	>100	>100
12c	2	H	CH ₃	H	H	>100	72.8 \pm 1.9	>100	>100
12d	2	H	H	CH ₃	H	100	12.3 \pm 0.9	>100	>100
12e	2	CF ₃	H	H	H	100	11.5 \pm 0.1	>100	>100
12f	2	H	CF ₃	H	H	100	13.9 \pm 1.4	>100	>100
12g	2	CF ₃	H	H	CF ₃	100	9.0 \pm 0.3	>100	>100
13a	3	H	H	H	H	100	13.3 \pm 0.6	>100	>100
13b	3	CH ₃	H	H	H	100	13.0 \pm 1.6	>100	>100
13c	3	H	CH ₃	H	H	100	13.6 \pm 1.8	>100	>100
13d	3	H	H	CH ₃	H	100	16.7 \pm 0.3	>100	>100

nine precursor **12** (50.6 μ M, Table 16). The derivative **13a** with an additional methylene-group in the linker moiety of the rhodanine showed similar activity of GI₅₀ 13.3 μ M against *T. brucei*. But compared to its parent rhodanine (**13**, GI₅₀ 15.2 μ M) the condensation had only a minor effect on the overall activity. Substitutions in ortho-position on the 5-benzylidene moiety were well tolerated by methyl and trifluoromethyl groups (GI₅₀ 11.5-13.0 μ M). In the case of the propyl-linked derivatives **12a–g** a trifluoromethyl group in meta-position increased anti-trypanosomal activity (GI₅₀ 13.9 μ M). The corresponding meta-hydroxy or meta-methyl substituted analogues were 5 times less active. It is possible, that the trifluoromethyl acts as a hydrogen-bond acceptor through negative hyper conjugation of the aromatic π -system, or the bulky trifluoromethyl group might fill a lipophilic pocket within the active site of a protein (Figure 30).^[193,194] It is also possible that the increased activity was merely a result of increased solubility through the trifluoromethyl substitution.^[195] Trifluoromethyl substituents are known to

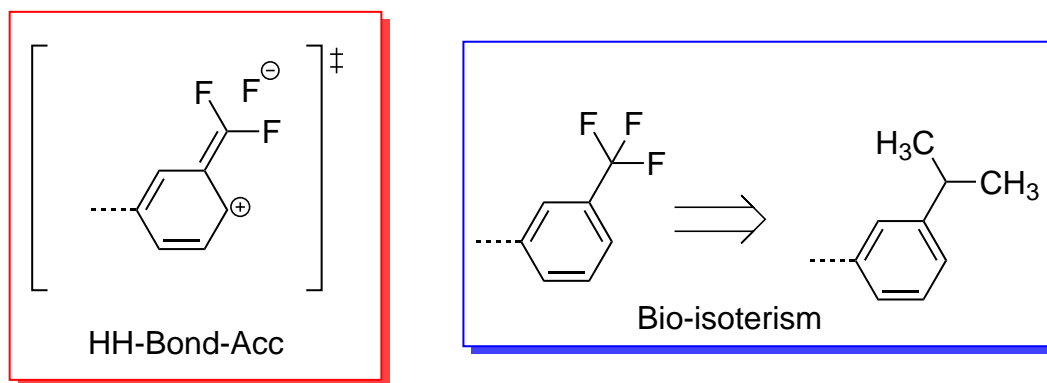


Figure 30: Possible effects of the meta- CF_3 group on the activity of rhodanine derivatives.

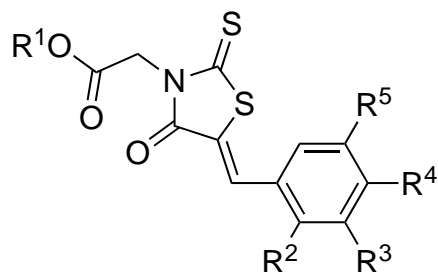
act as hydrogen-bond acceptors, but they also have been used as replacements for isosteric OH groups.^[193,196] However, in compound **12e**, the reason for increased activity cannot be explained by mimicking hydroxyl groups, as the meta-hydroxy analogue **12k** did not show any anti-trypanosomal activity. But it was interesting to observe that anti-trypanosomal activity was restored through installing an additional para-hydroxy substituent (**12m**, GI_{50} 14.2 μM). The bis-trifluoromethyl substituted compound **12g** might benefit from improved solubility and was therefore the most active anti-parasitic compound in this series (GI_{50} 9.0 μM).^[196] But other effects of the trifluoromethyl group, such as resemblance to bulky propyl groups or hydrogen-bond acceptor functionality or indeed attraction to electropositive regions (Asn, Glu, Arg) of receptor sites may be responsible for increased activity.^[195] Almost all derivatives of this series were able to lyse *T. brucei* *in vitro* at 100 μM (MIC 100 μM) and did not show toxicity against mammalian HL60 cells at 100 μM (Table 16).

3.3.6 N-1 ester modification and their anti-trypanosomal effect

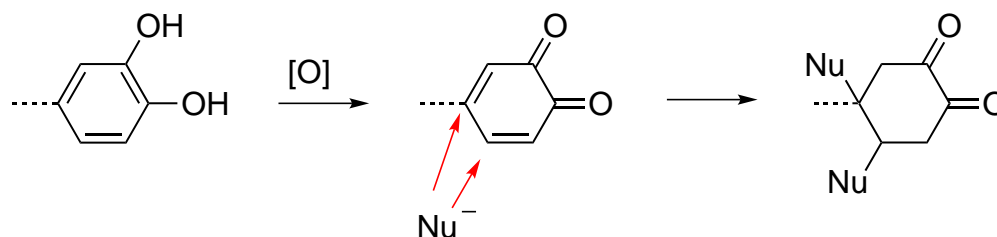
In Table 15, a linear relationship between logP and the starting rhodanine derivatives was observed. Following this trend, elongated N-1-sidechain rhodanines showed similar activities to ester derivatives due to similar logP values. However, a methyl ester did not follow this trend; although the logP (0.46) was relatively low, its activity was better than compounds with higher logPs (0.82, 0.84). Thus far, it has been established that elongated derivatives with a free carboxylic acid had activities against *T. brucei* in the range of 9.0-72.8 μM . In this chapter, ester derivatives of rhodanine-N-acetic acid were screened for their trypanocidal activity (Table 17).

Hydroxy-modified ester analogues

The most potent compound against *T. brucei* growth was the catechol modified ethyl ester **14t** (Table 17). **14t** had an activity of GI_{50} 1.6 μM against *T. brucei*, without showing any

Table 17: Anti-trypanosomal activity of ester analogues and their toxicity, sorted by activity and toxicity.

#	R ¹	R ²	R ³	R ⁴	R ⁵	GI ₅₀ [μM]			
						<i>T. brucei</i>	SI (<i>T. brucei</i>)	<i>T. cruzi</i>	HL60
14t	Et	H	OH	OH	H	1.6 ± 0.1	>62.5	n.a.	>100
14o	Et	H	H	tBu	H	1.7 ± 0.1	>59	>100	>100
14v	Et	H	OBn	H	H	4.4 ± 1.1	>23	>100	>100
14j	tBu	H	H	H	H	9.6 ± 0.8	>10	>100	>100
14a	Et	H	CH ₃	H	H	1.5 ± 0.3	21	>100	31.0 ± 0.8
14b	tBu	H	CH ₃	H	H	1.8 ± 0.1	14	5.1 ± 0.5	25.0 ± 1.6
14g	Et	CH ₃	H	H	H	1.3 ± 0.1	10	>100	12.7 ± 0.9
14c	Me	H	CH ₃	H	H	1.3 ± 0.1	9	>100	12.0 ± 1.7
14h	tBu	CH ₃	H	H	H	5.2 ± 0.3	9	>100	48.2 ± 7.0
14d	Et	H	H	CF ₃	H	1.4 ± 0.1	8	n.a.	11.8 ± 0.5
14e	Me	H	H	CF ₃	H	1.4 ± 0.1	7	17.4 ± 1.1	9.9 ± 1.8
14k	Et	CF ₃	H	H	H	1.4 ± 0.1	7	n.a.	9.3 ± 3.7
14l	Et	H	CF ₃	H	H	1.7 ± 0.1	7	n.a.	11.3 ± 3.7
14m	Et	CF ₃	H	H	CF ₃	1.8 ± 0.1	n.a.	n.a.	n.a.
14w	Et	H	H	OBn	H	17.0 ± 0.9	6	>100	>100
14i	Et	H	H	H	H	8.3 ± 0.7	5	94.6 ± 1.8	38.0 ± 1.8
14y	Et	H	OMe	OH	OMe	11.7 ± 1.8	3	46.6 ± 0.5	38.1 ± 6.4
14p	Et	OH	H	H	H	1.7 ± 0.1	2	n.a.	4.1 ± 0.7
14s	Me	H	OH	OH	H	11.1 ± 0.1	2	n.a.	23.6 ± 1.1
14n	Et	H	H	CH ₃	H	15.6 ± 1.4	2	n.a.	29.3 ± 8.3
14q	Et	H	OH	H	H	4.8 ± 0.9	2	n.a.	9.9 ± 0.5
14f	tBu	H	OBn	OBn	H	>100	n.a.	>100	n.a.
14x	Et	H	OBn	OBn	H	>100	>1	>100	>100
14u	Et	OH	H	OH	H	1.7 ± 0.1	n.a.	4.7 ± 0.6	n.a.
35b	Me	H	OH	OH	H	10.1 ± 1.6	n.a.	n.a.	n.a.
14r	Et	H	H	OH	H	17.6 ± 0.1	n.a.	>100	n.a.



Scheme 21: Catechol reactivity to react with biological nucleophiles or cross-link proteins, adapted scheme by Stanwell et. al^[198].

toxicity against HL60 cells at 100 μM . This was a surprising observation, since the analogous catechol modified free acid **2u** did not show any trypanocidal activity. The simple esterification resulted in the transformation of an inactive compound against *T. brucei* growth to one of the most active inhibitors both in terms of anti-trypanosomal activity and selectivity against HL60 cells (SI >63, Table 17). In particular the missing toxicity against HL60 cells was significant, since similar compounds, such as the N-1-unmodified catechol rhodanine **36a** (Table 41, page 152) has previously been reported as potent inhibitor of HL60 cell growth.^[197] Compound **37** has been shown to inhibit oncoprotein aggregation of c-Myc Max, therefore preventing DNA binding and leading to apoptosis in HL60 cells.^[197] Indeed, **36a** showed a GI_{50} value of 45 μM against HL60 cells growth, confirming the previously reported IC_{50} of 23 μM .^[197] The additional substituent in position N-1 in compound **14t** led to complete loss of toxicity against HL60 cell growth, potentially showing that c-Myc Max aggregation was not inhibited. However, the ethyl ester modification was essential for retaining the selectivity as the corresponding methyl ester **14s** had only a selectivity index (SI) of 2 and displayed a ten-fold reduction in anti-parasitic activity (GI_{50} 11.1 μM). This indicates the potential problem of catechol-containing molecules in medicinal chemistry.^[198] The cytotoxicity of catechol derivatives is believed to derive from oxidation of the hydroxyl groups to quinones, which can react with biological nucleophiles such as glutathione or cross-link proteins (Scheme 21).^[198,199]

However, this mode-of-action cannot be generalised, as the free acid of **14t** has previously been reported as non-covalent ("affinity-based") probe for the NAD(P)H site of dehydrogenases.^[107,108] Indeed, similar catechol derivatives showed nM activity against the NAD(P)H-dependant enoyl acyl carrier protein reductase of *Plasmodium falciparum* (PfENR).^[112] The catechol moiety has been found to be essential for PfENR inhibition and thus for type II fatty acid biosynthesis inhibition.^[112] *T. brucei* uses a related elongase pathway for *de novo* synthesis of myristate, an essential building block for GPI anchor biosynthesis,^[200] (further details in section 5.1) possibly explaining the low μM anti-trypanosomal activity.

A third possible mode of action was derived during the evaluation of the activity and toxicity assays against *T. brucei* and HL60 cells. Stock solutions of catechol derivatives **14t**, **14s**, and

35b in DMSO are distinguished by their bright yellow-orange colour. However, in aqueous solutions these compounds were bright red. Catechol rhodanine **36a** has previously been found to form brown complexes with Fe(III) ions.^[201] In addition, Mn(II) and Mg(II) formed purple-red complexes with catechol rhodanine under basic conditions.^[201] It seemed evident that **14t**, **14s**, and **35b** formed metal-complexes in the assay medium. Although the red colour might have indicated Mn(II) or Mg(II) chelation, the neutral pH of the assay medium made Fe(III) more likely.

Other hydroxy-substituted methyl and ethyl ester derivatives (**14p**, **14s**, **14q**, **14u**, **35b**, **14r**, and **14y**) showed good activity against *T. brucei* growth (GI₅₀ 1.7-17.6 µM), however the selectivity indices were less preferable for derivatives **14p**, **14s**, and **14q** (SI 2). A particularly interesting inhibitor was **14u**, as it showed activity in the lower µM range for both *T. brucei* and *T. cruzi* (GI₅₀ 1.7 and 4.7 µM). The previously mentioned formation of bright red colours in the assay medium interfered with the MTT formazan readout, therefore derivatives **14p**, **35b**, and **14r** could not be assessed against *T. cruzi*, although the MIC value was 100 µM.

Methyl-, trifluoromethyl- and *tert*-butyl-substituted benzylidene derivatives and their trypanocidal activity

Methyl- and trifluoromethyl-substituted ester derivatives **14a–l** and **14n** had low µM activity against *T. brucei* with GI₅₀ values ranging from 1.3-15.6 µM and had SI of 2-21. These derivatives showed general cytotoxic effects against *T. brucei* and HL60 cells. Different ester modifications (methyl, ethyl or *tert*-butyl) had no effect on the activity against *T. brucei* or toxicity against HL60 cells. However, modification of the ester moieties resulted in an increased activity against *T. cruzi*. The ethyl ester derivative **14a** did not show any trypanocidal activity against *T. cruzi* at 100 µM, while the methyl ester substitution increased activity by a factor of 20 (GI₅₀ 5.1 µM). Modification of the ester group also proved beneficial for the unsubstituted benzylidene derivatives **14i** and **14j**. The ethyl ester modification in **14i** increased activity against *T. brucei* by a factor of 7 (GI₅₀ 8.3 µM) compared to the free acid analogue **2a** (GI₅₀ 56.0 µM), but **14i** also showed increased toxicity against HL60 cells (GI₅₀ 38 µM). Substitution of the ethyl to a bulky *tert*-butyl ester had no effect on the anti-trypanosomal activity against *T. brucei*, but has proven beneficial in terms of its toxicity. The *tert*-butyl ester derivative **14j** retained activity at GI₅₀ 9.6 µM and did not show any toxicity against HL60 cells at 100 µM. A similar conclusion could be drawn by comparing the 5-benzylidene modifications in para position. The bulky lipophilic trifluoromethyl derivatives **14d** and **14e** displayed low µM activity against *T. brucei*, but also demonstrated significant toxicity against HL60 cells (SI 7). Bio-isosteric replacement of the trifluoromethyl group (Taft E value -2.4), to the only slightly larger *tert*-butyl group (Taft E value -2.78) resulted in complete loss of toxicity at 100 µM against HL60 cells, while activity against *T. brucei* was retained at GI₅₀ 1.7 µM.^[193] The retention in activity might suggest that the trifluoromethyl group served as a lipophilic substituent in para-position of the 5-benzylidene

moiety.

Benzyloxy-modified 5-benzylidene ester derivatives and their anti-trypanosomal activity

Benzyloxy-modified rhodanine-N-acetic acid derivatives **2b**, **2c**, and **2d** were of particular interest, as they showed promising activity against DPMS (residual activity 10-23 %), an essential enzyme in the GPI-anchor biosynthesis.^[68] It was pleasing to observe, that the 3-benzyloxy-modified ethyl ester **14v** showed low μM activity against *T. brucei* (GI_{50} 4.4 μM) and most importantly did not reveal any toxicity against HL60 cells at 100 μM . These results might indicate a correlation between the *in vitro* anti-trypanosomal activity against *T. brucei* and the enzymatic activity of DPMS. The ester modification could facilitate membrane diffusion, allowing a higher concentration of the inhibitor to reach the enzymatic site for effective inhibition. Interestingly the 4-benzyloxy-ethyl ester was four times less active *in vitro* against *T. brucei*, although it showed two times better DPMS inhibition (Table 13, 10 % residual activity) than **14v** (23 % residual activity).^[68] However, it is not known if the active inhibitor of DPMS is the free acid or its ester analogue. Moreover, potentially multiple targets in *T. brucei* could be affected by the modified analogues **14v** and **14w**. The 3,4-bis-benzyloxy ester modified analogues **14f** and **14x** did not demonstrate any trypanosomal activity at 100 μM . These analogues might have been too lipophilic to pass through the parasitic plasma membrane and therefore demonstrate the limits of increasing lipophilicity to gain anti-trypanosomal activity.

3.3.7 Compounds with improved anti-parasitic activity identified after first generation of optimisation

The first round of optimisations of rhodanine-N-acetic acid derivatives led to compounds with low μM activity (GI_{50} 1.6-14.2 μM) against *T. brucei* and *T. cruzi* with low toxicity against HL60 cells (Table 18). The first class of derivatives (Class A, Table 18) was composed of the catechol modified rhodanine derivatives **14t** and **12m**. Possible further optimisations include the combination of an elongated side-linker and an ester functionality.

Benzyloxy-modified esters and in particular compound **14v** showed good activity against *T. brucei* (GI_{50} 4.4 μM) while revealing no toxicity against HL60 cells. This derivative (Class B, Table 18) was interesting, as its parent free acid has been identified as good DPMS inhibitor.^[68] Further optimisation of this derivative would include modifications on the 3-benzyloxy moiety.

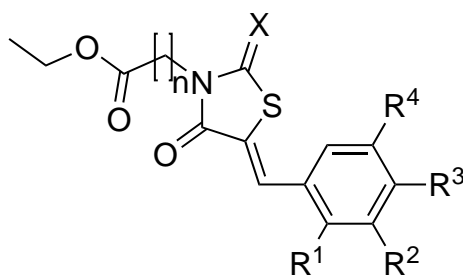
The ester derivatives **14o** and **14b** represent the other identified class of compounds with improved anti-parasitic activity (Class C and D, Table 18). They had low μM activity against *T. brucei* (**14o** and **14b**) and *T. cruzi* (**14b**). Further modifications of the thiocarbonyl group in the rhodanine moiety might improve their toxicity profile, as the carbonyl group has been shown to undergo more specific interaction compared to the thiocarbonyl, which has a diffuse HOMO orbital, favouring multiple polar and intermolecular interactions.^[83]

Table 18: 2nd generation inhibitor classes A-D as anti-trypanosomal agents against *T. brucei* and *T. cruzi*.

#	Class	R ¹	n	R ²	R ³	GI ₅₀ [μM]			
						<i>T. brucei</i>	SI <i>T. brucei</i>	<i>T. cruzi</i>	HL60
14t	A	Et	1	OH	OH	1.6 ± 0.1	>62.5	n.a.	>100
12m		H	2	OH	OH	14.2 ± 2.3	>7	>100	>100
14v	B	Et	1	OBn	H	4.4 ± 1.1	>23	>100	>100
14o	C	Et	1	H	tBu	1.7 ± 0.1	>59	>100	>100
14b	D	tBu	1	CH ₃	H	1.8 ± 0.1	14	5.1 ± 0.5	25.0 ± 1.6

3.3.8 Further optimisation of structure classes A,C and D

In the next round of inhibitor optimisation, the free carboxylic acid of the elongated analogues was masked as its ethyl ester. This modification resulted in low μM active compounds for the simple N-acetic ester modified series. The thiocarbonyl in the rhodanine was replaced by a carbonyl group. A recent review about rhodanine derivatives suggested that this thiocarbonyl group is a major contributor to the ubiquitous binding of rhodanine derivatives.^[83] The interactions of the thiocarbonyl group in rhodanine derivatives in protein X-ray structures in the PDB database has been analysed and revealed that this group undergoes a significant amount of polar and intermolecular interactions.^[83] Therefore, replacement of this thiocarbonyl might increase selectivity towards a particular target, possibly simultaneously reducing toxicity against HL60 cells. The modifications on the 5-benzylidene moiety were chosen based on previous results. Hydroxy, methyl and trifluoromethyl substituents resulted in low μM trypanocidal compounds, if combined with an ester moiety on the N1-side of the rhodanine core structure (Table 17). The results of the screening of these inhibitors against *T. brucei*, *T. cruzi* and HL60 cells is summarised in Table 19. The entries in the table were sorted by increasing activity against *T. brucei* and decreasing toxicity against HL60 cells. Not surprisingly, the top entries of Table 19 constituted catechol derivatives (**7k**, **15f**, and **16i**). Substitution of the thiocarbonyl did not effect activity against *T. brucei*. The dione derivative **7k** had a GI₅₀ of 1.4 μM against *T. brucei*, whilst showing no toxicity against HL60 cells. Alkylation of the 3,4-dihydroxy motif with benzyl groups totally abolished anti-trypanosomal activity. This might indicate that the catechol moiety could be involved in hydrogen bonding interactions. Alterna-

Table 19: 3rd generation optimisation of compound classes A, C and D.

#	X	n	R ¹	R ²	R ³	R ⁴	GI ₅₀ [μM]			
							<i>T. brucei</i>	SI <i>T. brucei</i>	<i>T. cruzi</i>	HL60
7k	O	1	H	OH	OH	H	1.4 ± 0.2	>71	>100	>100
15f	S	2	H	OH	OH	H	0.9 ± 0.1	35	n.a.	31.2 ± 2.8
16i	S	3	H	OH	OH	H	1.4 ± 0.3	21	n.a.	29.0 ± 4.2
16a	S	3	H	H	H	H	7.4 ± 5.2	>14	n.a.	>100
16e	S	3	CF ₃	H	H	CF ₃	9.5 ± 0.1	5	>100	47.9 ± 4.6
15a	S	2	H	H	H	H	4.5 ± 0.3	4	>100	16.5 ± 1.2
16f	S	3	OH	H	H	H	1.3 ± 0.1	n.a.	10.9 ± 0.1	n.a.
15c	S	2	H	CH ₃	H	H	10.2 ± 0.2	2	>100	17.6 ± 2.5
15b	S	2	CH ₃	H	H	H	10.6 ± 0.3	3	>100	35.6 ± 2.9
16b	S	3	CH ₃	H	H	H	11.5 ± 0.1	4	>100	40.5 ± 3.3
16c	S	3	H	CH ₃	H	H	12.0 ± 1.1	3	>100	31.5 ± 1.6
7e	O	1	CF ₃	H	H	H	13.0 ± 1.2	>8	>100	>100
15d	S	2	H	H	CH ₃	H	13.1 ± 2.4	3	>100	44.4 ± 5.6
7f	O	1	H	CF ₃	H	H	13.3 ± 0.4	>8	>100	>100
7c	O	1	H	CH ₃	H	H	14.7 ± 1.7	>7	>100	>100
16d	S	3	H	H	CH ₃	H	15.1 ± 2.2	>7	>100	>100
7b	O	1	CH ₃	H	H	H	15.2 ± 2.3	>7	>100	>100
7d	O	1	H	H	CH ₃	H	16.3 ± 1.8	>6	>100	>100
16g	S	3	H	OH	H	H	16.8 ± 1.0		21.4 ± 4.2	n.a.
15e	S	2	H	H	OH	H	17.4 ± 0.5	1	>100	9.2 ± 2.0
7j	O	1	H	OBn	OBn	H	>100	>1	n.a.	>100

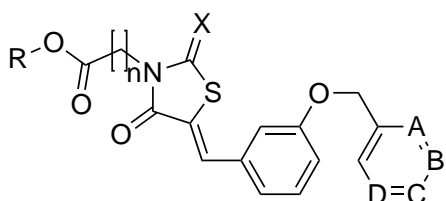
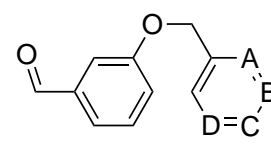
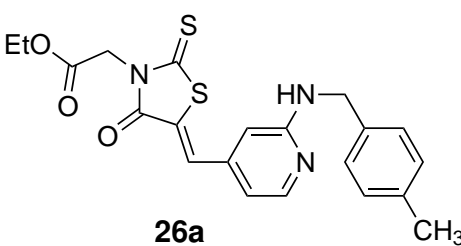
tively the 3,4-benzyloxy substituent may be too bulky to be accommodated in the active site, or it may have been too lipophilic to pass through the parasite membrane. The elongation of the side-chain in N-1 position in the rhodanine moiety combined with the ester modification and a catechol motif in position five resulted in the first inhibitor against *T. brucei* growth in the sub- μM range. The elongated analogue **15f** had a GI_{50} value of $0.9\ \mu\text{M}$ and displayed a SI of 35 towards HL60 cells. Increasing the methylene linker even further, as shown in compound **16i** did not improve activity against *T. brucei*. Interestingly, the combination of an elongated side chain ($n=3$) combined with a hydroxy substituent on the 5-benzylidene moiety resulted in compounds **16f** and **16g**, which displayed moderate activities against *T. cruzi* (GI_{50} 10.9–21.4 μM). However, the shorter ($n=2$) linker analogue did not show any activity against *T. cruzi*, but toxicity in the lower μM range against HL60 (GI_{50} 9.2 μM).

Applying the elongation and esterification strategy on methyl or trifluoromethyl benzylidene modified rhodanine derivatives did not improve their anti-parasitic activity (GI_{50} 9.5–16.3 μM) or toxicity against HL60 cells (SI 2–8) compared to derivatives **14a–l**. The substitution of the thiocarbonyl to a carbonyl group improved their toxicity profile and none of the inhibitors displayed any toxicity against HL60 cells at 100 μM . But the replacement also reduced the anti-parasitic activity by a factor of 10 (GI_{50} 13.0–16.3 μM).

Optimisation of compound class B

In the first screening of rhodanine derivatives, a 5-(benzylidene-3 benzyloxy) rhodanine-N-acetic acid derivative (**2c**, Table 20) has been identified as DPMS inhibitor of *T. brucei*, but did not display any activity against *T. brucei* *in vitro*.^[68] The introduction of an ethyl ester moiety as replacement for the free acid resulted in low μM activity against *T. brucei* (**14v**, Table 20). In order to improve the anti-trypanosomal activity, various substituents on the 3-benzyloxy moiety were introduced. Furthermore, the side-chain linker was elongated by an additional methylene-unit, and the thiocarbonyl was substituted with a carbonyl group. Lastly prolonged N-1-side-chain analogues with a free acid moiety were compared to ester analogues. The assessed inhibitors are displayed in increasing order of activity against *T. brucei* and decreasing toxicity against HL60 cells (Table 20). Indeed, substitution of the 3-benzyloxy substituent improved activity against *T. brucei* by a factor of 3 compared to the unsubstituted analogue **14v**. The inhibitor **19c** displayed low μM activity against *T. brucei* (GI_{50} 1.5 μM) and only minor toxicity against HL60 cells (SI 59). The derivative **14v** is equipped with a para-methoxy substituent on the 3-benzyloxy-moiety. Using this modification and replacing the thiocarbonyl to a carbonyl group furnished **19e**, revealing a 10-fold decrease in activity against *T. brucei*. Similarly, increasing the length of the N-1 side-linker in compound **19e** caused a 10-fold drop in anti-trypanosomal activity against *T. brucei*, this is similar to previous reports that substitution to the carbonyl group results in loss of activity.^[81] It was interesting to observe that the starting para-methoxy substituted aldehyde **18c** did not display any anti-trypanosomal activity

Table 20: Optimisation of compounds from class B, substitution of the 3-benzyloxy-substituent.

															
19c–f, 14v, 7h, 2c, and 34								18d–c				26a			
#	n	X	R	A	B	C	D	GI ₅₀ [μM]							
								<i>T. brucei</i>	SI	<i>T. cruzi</i>	HL60				
19c	1	S	Et	CH	CH	COMe	CH	1.5 ± 0.3	59	>100	88.8 ± 8.5				
14v	1	S	Et	CH	CH	CH	CH	4.4 ± 1.1	>23	>100	>100				
7h	1	O	Et	CH	CH	CH	CH	11.1 ± 0.3	>9	>100	>100				
19k	1	S	Et	CH	CH	N	CH	1.7 ± 0.1	9	n.a.	15.5 ± 1.7				
19j	1	S	Et	N	CH	CH	CH	1.7 ± 0.1	9	n.a.	14.7 ± 2.7				
19l	1	S	Et	CH	N	CH	CH	1.7 ± 0.1	7	n.a.	11.5 ± 4.8				
19d	1	O	Et	CH	CH	COMe	CH	9.9 ± 4.2	n.a.	>100	n.a.				
34	1	S	Et	CH	CN3	CH	CN3	12.9 ± 4.6	>8	>100	>100				
19b	1	O	Et	CH	COMe	CH	CH	13.1 ± 2.7	n.a.	>100	n.a.				
19e	2	S	Et	CH	CH	COMe	CH	13.9 ± 3.4	n.a.	n.a.	n.a.				
19a	2	S	Et	CH	COMe	CH	CH	14.8 ± 0.4	n.a.	>100	n.a.				
18b		n.a.		CH	COMe	CH	CH	15.5 ± 3.0	n.a.	n.a.	n.a.				
18e		n.a.		CH	N	CH	CH	17.4 ± 0.2	n.a.	n.a.	n.a.				
19h	2	S	H	CH	CH	N	CH	60.7 ± 3.3	2	n.a.	>100				
19g	2	S	H	CH	N	CH	CH	66.9 ± 2.0	1	n.a.	>100				
19f	2	S	H	N	CH	CH	CH	68.3 ± 0.7	1	n.a.	>100				
18f		n.a.		CH	CH	N	CH	>100	n.a.	n.a.	n.a.				
18d		n.a.		N	CH	CH	CH	>100	n.a.	n.a.	n.a.				
18c		n.a.		CH	CH	COMe	CH	>100	n.a.	n.a.	n.a.				
2c	1	S	H	CH	CH	CH	CH	>100	>1	>100	>100				
26a	not applicable							1.6 ± 0.1	6	21.6 ± 4.0	10.0 ± 3.8				

at 100 μM . While the analogous meta-methoxy substituted aldehyde **18b** had a moderate effect on trypanosomal growth (GI_{50} 15.5 μM). However, the corresponding condensation product **19a** was 10-fold less active than the para-substituted analogue **19c**.

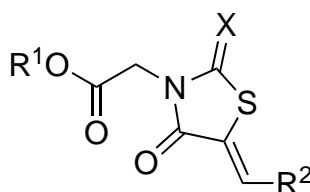
The introduction of a pyridine-moiety in compounds **19k**, **19j**, and **19l** resulted in low μM active inhibitors of *T. brucei* growth (GI_{50} 1.7 μM). But these derivatives displayed less selectivity between *T. brucei* and HL60 cells (SI 7-9), compared to the methoxy substituted derivative **19c** (SI 59). Similar to the methoxy-substituted analogues, the meta-pyridine substituted aldehyde **18e** showed moderate anti-trypanosomal activity while the ortho- and para-substituted analogues did not display any activity against *T. brucei* at 100 μM . The combination of a free carboxylic acid and an elongated side-chain with the pyridine-substitution furnished compounds **19h**, **19g**, and **19f**, which displayed only moderate activity against *T. brucei* (GI_{50} 60.7-68.3 μM).

Compound **34** was a protein-reactive photo-labelling probe. This probe was designed to bind to its target protein via an aryl-azide moiety, while a second photo-stable aliphatic azide serves as a tag for biotin or fluorophores (such as AlexaFluor 488). It was pleasing to observe that although relatively large azide substituents were introduced, the probe **34** retained most of its anti-trypanosomal activity (GI_{50} 12.9 μM) compared to the original lead structure **14v** (GI_{50} 4.4 μM).

In order to study the importance of the oxygen-linker in the benzyloxy-substituted analogues, the heterocycle **26a** was assessed for its anti-trypanosomal potential. The 5-(benzylidene-3-benzyloxy) moiety has been replaced with a 2-amino(benzylidene)-pyridine group in compound **26a**. This derivative was the first inhibitor in this series to display a trypanocidal effect both in *T. brucei* and *T. cruzi*, however the activity against *T. cruzi* might correlate to the toxicity towards HL60 cells. Yet this inhibitor was a good starting point for the development for more potent and in particular less toxic inhibitors of *T. brucei* and *T. cruzi* growth.

3.3.9 Heterocyclic modifications on position 5 of N-1-substituted rhodanine and thiazolidine-2,4-dione derivatives

Heterocyclic analogues, such as the rhodanine-N-acetic ester derivative **26a** (Table 20) has been identified as low μM growth inhibitor of *T. brucei* and *T. cruzi*, but also displayed high toxicity against HL60 cells (GI_{50} 10.0 μM). In this chapter, several 5-pyridine modifications have been assessed for their anti-trypanosomal activity (Table 21). The most active inhibitor in this series had a 3-pyridinyl modification on the 5-position of the rhodanine-N-acetic ester moiety. Compounds **26g** and **26f** displayed anti-trypanosomal activity against *T. brucei* in the low μM range (GI_{50} 1.5 μM) and against *T. cruzi* at 100 μM (MIC 100 μM). The exact GI_{50} values could not be obtained due to interference of the derivatives with the viability dye MTT used in the growth inhibition assay for *T. cruzi*. Furthermore, both inhibitors **26g** and **26f** possessed a

Table 21: Heterocyclic modified rhodanine-N-acetic acid and there ester analogues.

#	x	R ¹	R ²	GI ₅₀ [μM]			
				<i>T. brucei</i>	SI <i>T. brucei</i>	<i>T. cruzi</i>	HL60
26g	S	Et	3-pyridinyl	1.5 ± 0.2	34	n.a.	51.5 ± 2.5
26f	S	Et	2-pyridinyl	1.5 ± 0.3	>67	n.a.	>100
21a	S	Et	2-cl-4-pyridinyl	1.7 ± 0.1	n.a.	6.9 ± 0.6	n.a.
26c	S	H	3-pyridinyl	116.0 ± 6.4	>1	>100	>100
26i	O	Et	4-pyridinyl	16.4 ± 1.7	>6	n.a.	>100
26b	S	H	2-pyridinyl	>100	>1	>100	>100
26h	S	Et	4-pyridinyl	>100	>1	>100	>100
26d	S	H	4-pyridinyl	>100	>1	>100	>100
26j	S	Et	2-furanyl	7.4 ± 2.1	7	n.a.	48.1 ± 2.4

good toxicology profile (SI 34-(>67)). The anti-parasitic effect against *T. brucei* could already be observed in the free carboxylic acid derivative **26c**, which inhibited growth of *T. brucei* at 100 μM by 55 % (data not shown) and resulted in a GI₅₀ 116 μM. The transformation of the acid to the ethyl ester resulted in a compound with low μM activity and a good selectivity profile.

A 4-pyridinyl-modification on position 5 of the rhodanine-N-acetic acid (**26d**) and ester (**26h**) resulted in a complete loss of anti-trypanosomal activity against both *T. brucei* and *T. cruzi*. However, substituting the thiocarbonyl to a carbonyl-group in compound **26i** restored some of the anti-trypanosomal activity against *T. brucei* (GI₅₀ 16.4 μM). In addition the introduction of a 2-chloro-substituent next to 4-pyridinyl-moiety restored activity. Indeed, compound **21a** was equipotent against *T. brucei* and *T. cruzi* as the 2- and 3-pyridinyl substituted inhibitors **26g** and **26f** (GI₅₀ 1.5 μM).

3.3.10 Anti-trypanosomal effect of saturated rhodanine analogues

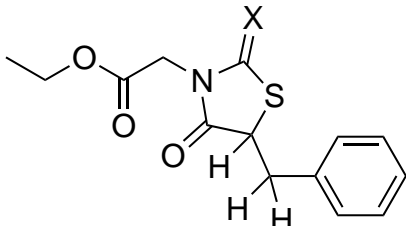
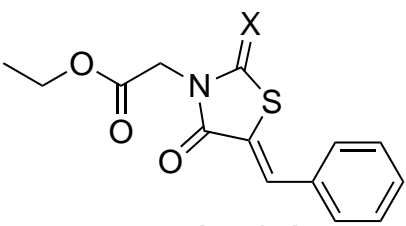
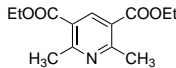
The inhibitor with the highest anti-trypanosomal activity against *T. brucei* was the catechol derivative **7k**, which had a GI₅₀ of 1.4 μM against *T. brucei* growth and did not show any toxicity against HL60 cells (Table 22). Similarly, the unsubstituted 5-benzylidene rhodanine-N-acetic acid ester **14i** displayed low μM activity against *T. brucei* (GI₅₀ 8.3 μM). In order to study the growth inhibition of these derivatives in more detail, the exo-cyclic double bond was reduced and evaluated for their trypanocidal activity (Table 22). The double bond in rhoda-

nine and thiazolidine-2,4-dione derivatives is part of a Michael acceptor system and therefore susceptible to nucleophilic attack by glutathione or similar biological nucleophiles. If inhibitors in this series could covalently bind over this Michael acceptor system to the target protein, reduction of this double bond should abolish its activity. The reduction of the benzylidene rhodanine-N-acetic ester **14i** furnished the saturated analogue **27a**. The reduction of the double bond in derivative **27a** improved its anti-trypanosomal activity towards *T. brucei*. This result not only suggested that the inhibitor did not covalently bind to its target, it also revealed possible strategies to increase its anti-parasitic activity against *T. brucei*. It is possible that reduction of the double bond in compound **27a** increased flexibility and solubility compared to its non-reduced analogue **14i**. Substitution of the thiocarbonyl to a carbonyl functionality reduced the anti-trypanosomal activity to 50.3 μM . **27b** was 50 times less active against *T. brucei* and HL60 cells. These promising results on the reduction of the unsubstituted rhodanine-N-acetic ester derivative **14i** encouraged the reduction of the double bond in the catechol derivative **7k**. This thiazolidine-2,4-dione derivative was one of the most active inhibitor against *T. brucei* growth and displayed no toxicity against HL60 cells. The reduction of the double bond furnished a compound 11 times less active against *T. brucei*. However, the reduced analogue **27c** still possessed a GI_{50} value of 16 μM . It is possible that the catechol moiety in **27c** is involved in hydrogen-bonding interactions. Increased flexibility resulting from the reduction of the double bond might weaken these interactions. Furthermore, the non-reduced analogue **7k** might resemble a conformation that preferably binds to its molecular target, whereas the reduction of the double bond results in multiple possible conformers. The only side-product of the reduction of the rhodanine-derivatives, a Hantzsch ester **28**, has been purified and tested for anti-trypanosomal activity. The Hantzsch ester did not show any activity at 100 μM on *T. cruzi* growth.

3.4 Anti-leishmanial activity

The complete set of compounds, previously assessed for their anti-trypanosomal activity, were screened against *Leishmania infantum* promastigotes. Initially, *L. infantum* promastigotes were screened against the whole inhibitor library at a fixed concentration of 100 μM in a 96 well plate format. Each inhibitor was evaluated for its anti-leishmanial effects by visual inspection under a light microscope. Derivatives which killed *L. infantum* at 100 μM (MIC 100 μM) were further evaluated. These pre-selection steps narrowed the focus onto the analysis of compounds with interesting anti-leishmanial activity to maximise efficiency during the limited time available for the execution of these activity screens (data not shown). For compounds with MIC values at 100 μM , a complete inhibition curve was recorded using the MTT 96 well format assay previously described (chapter 3.3.1).

Table 22: Reduced rhodanine-N-acetic ester analogues and their anti-trypanosomal activity.

 27a, 27b, and 27c				 14i and 7k			
#	X	R ¹	R ²	GI ₅₀ [μM]			
				<i>T. brucei</i>	SI <i>T. brucei</i>	<i>T. cruzi</i>	HL60
27a	S	H	H	1.3 ± 0.1	14	n.a.	18.1 ± 3.6
27b	O	H	H	50.3 ± 4.0	>2	>100	>100
14i	S	H	H	8.3 ± 0.7	5	94.6 ± 1.8	38.0 ± 1.8
27c	O	OH	OH	16.0 ± 2.5		n.a.	n.a.
7k	O	OH	OH	1.4 ± 0.2	>71	>100	>100
28				n.a.	n.a.	>100	n.a.

A total of 14 compounds showed anti-leishmanial effects and their GI₅₀ values were assessed (Table 23). All these derivatives displayed anti-trypanosomal activity against *T. brucei* in the low μM range (GI₅₀ 0.9-16.8 μM). The most active inhibitor was the rhodanine-N-acetic *tert*-butyl ester derivative **14b**. Derivative **14b** stood out for its broad anti-parasitic activity against *T. brucei*, *T. cruzi* and *L. infantum*. The GI₅₀ of **14b** against the tested protozoa was in the range of 1.8-5.1 μM and the SI ranged from 5-14. It is worth noticing that the methyl and ethyl ester derivative of **14b** displayed no activity against *L. infantum*, suggesting that the bulky and lipophilic *tert*-butyl ester was necessary for anti-leishmanial activity. It would be possible that a high logP-value and therefore a high lipophilicity may facilitate the uptake of the inhibitor resulting in increased anti-leishmanial activity.

In order to analyse this hypothesis further, the logP of anti-leishmanial inhibitors (Table 23) was plotted against their GI₅₀ values (Figure 31). The red spots in the graph represent hydroxy-modified inhibitors, whereas the yellow colour indicates lipophilic substituents such as methyl, trifluoromethyl and *tert*-butyl groups on the 5-benzylidene moiety. The green colour represents inhibitors of the heterocyclic modified series or derivatives with a reduced exocyclic double bond. Excluding the last mentioned green labelled analogues, a negative trend between the logP and GI₅₀ was observed. Increasing logP values in inhibitors in this series resulted in low μM active compounds against *L. infantum*.

However, with the exception of compound **14b**, all inhibitors in this series were equal or

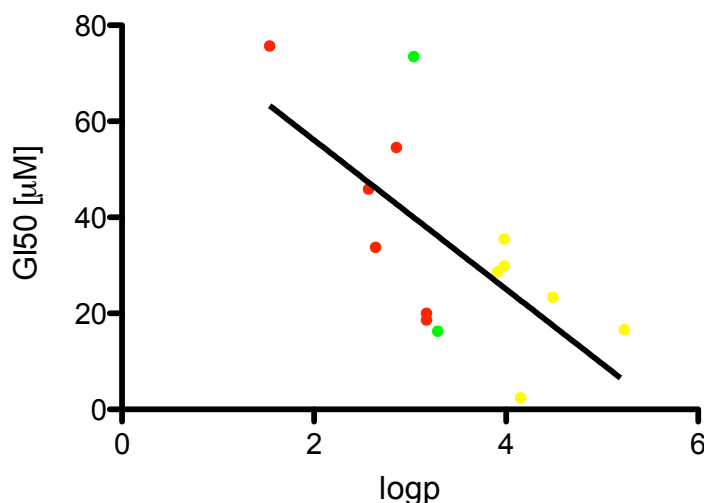
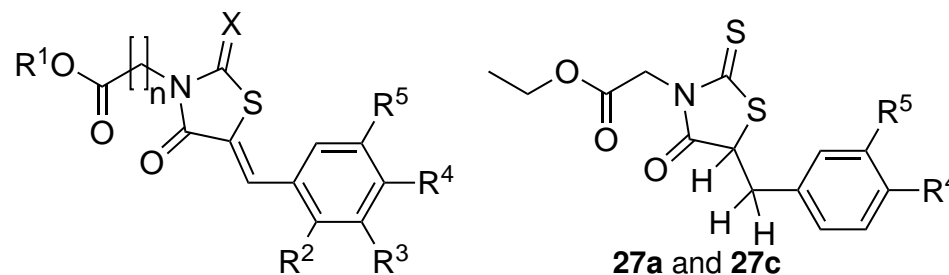


Figure 31: Correlation of logP and increasing anti-leishmanial activity ($Y=87.2-15.5 \cdot x$, $r^2=0.4$); red: hydroxy substituted inhibitors; yellow: lipophilic; green: reduced or heterocyclic modified derivative.

more toxic against HL60 cells than their anti-leishmanial activity ($SI < 1 \rightarrow > 4$).

It also seemed that this inhibitor series was more selective towards *L. infantum* and *T. brucei* than against *T. cruzi*. Although many GI_{50} in Table 23 were not recorded against *T. cruzi*, their MIC value was either 100 or $>100 \mu M$. A MIC value in this range would result in GI_{50} values in the range of 50–200 μM . Inhibitors have been screened against *T. cruzi*, but GI_{50} values could not be determined due to colorimetric interference of the inhibitor with the MTT viability dye. However the reduced analogues could be tested, as reduction of the exocyclic double bond in **27a** and **27c** caused a decrease in colour intensity. The reduction of the double bond disrupts the conjugated aromatic system and therefore inhibitors appeared less coloured in solution. The derivative **14b** was also tested for its anti-leishmanial activity against *L. infantum* amastigotes, as this is the standard assay for evaluation against Leishmaniasis,^[202] however these experiments were inconclusive as infection of mice macrophages with *L. infantum* amastigotes failed, a common problem with this assay.^[202]

Table 23: Rhodanine- and thiazolidine-2,4-dione-N-ester derivatives with anti-leishmanial activity; logP calculated with instantchem (ChemAxon).

#	n	X	R ¹	R ²	R ³	R ⁴	R ⁵	logP	GI ₅₀ [μM]				
									<i>L. infantum</i>	SI <i>L. infantum</i>	<i>T. brucei</i>	<i>T. cruzi</i>	HL60
14b	1	S	tBu	H	CH ₃	H	H	4.15	2.4 ± 0.3	10	1.8 ± 0.1	5.1 ± 0.5	25.0 ± 1.6
19k	1	S	Et					3.29	16.3 ± 6.9	1	1.7 ± 0.1	n.a.	15.5 ± 1.7
16e	3	S	Et	CF ₃	H	H	CF ₃	5.23	16.6 ± 2.5	3	9.5 ± 0.1	>100	47.9 ± 4.6
16g	3	S	Et	H	OH	H	H	3.17	18.6 ± 10.6	n.a.	16.8 ± 1.0	21.4 ± 4.2	n.a.
16f	3	S	Et	OH	H	H	H	3.17	20.0 ± 1.5	n.a.	1.3 ± 0.1	10.9 ± 0.1	n.a.
14o	1	S	Et	H	H	tBu	H	4.49	23.4 ± 2.8	>4	1.7 ± 0.1	>100	>100
14m	1	S	Et	CF ₃	H	H	CF ₃	3.91	28.7 ± 1.1	n.a.	1.8 ± 0.1	n.a.	n.a.
16b	3	S	Et	CH ₃	H	H	H	3.98	29.9 ± 0.9	1	11.5 ± 0.1	>100	40.5 ± 3.3
14p	1	S	Et	OH	H	H	H	2.64	33.8 ± 1.7	<1	1.7 ± 0.1	n.a.	4.1 ± 0.7
16c	3	S	Et	H	CH ₃	H	H	3.98	35.5 ± 0.1	1	12.0 ± 1.1	>100	31.5 ± 1.6
15f	2	S	Et	H	OH	OH	H	2.57	45.9 ± 15.1	1	0.9 ± 0.1	n.a.	31.2 ± 2.8
16i	3	S	Et	H	OH	OH	H	2.86	54.6 ± 0.4	<1	1.4 ± 0.3	n.a.	29.0 ± 4.2
27a	1	S	Et	H	H	H	H	3.04	73.5 ± 5.5	<1	1.3 ± 0.1	n.a.	18.1 ± 3.6
27c	1	O	Et	H	OH	OH	H	1.54	75.7 ± 4.8	n.a.	16.0 ± 2.5	n.a.	n.a.

3.5 Target identification studies

The anti-parasitic activity data to this point were obtained through whole cell activity assays. Although this type of assay allowed the optimisation of the inhibitors in this series to low μM activity, more insight in the molecular target(s) is needed in order to further optimise the anti-parasitic activity. The initial objective was the identification of anti-parasitic agents with potential activity against enzymes in the GPI-anchor biosynthesis, therefore several assays have been designed to validate inhibition of this pathway. Two derivatives with interesting anti-parasitic activity were chosen for further target validation studies. The first of these compounds was the 3-benzyloxy rhodanine ethyl ester **14v** (Table 24). This compound was chosen for its low μM activity against *T. brucei* growth (GI_{50} 4.4 μM) and high selectivity ($\text{SI} > 23$). Furthermore the free acid analogue had been shown to inhibit DPMS in previous studies.^[68] The second compound was the meta-methyl rhodanine ethyl ester **14a** (Table 24), which was also chosen for its low activity against *T. brucei* (GI_{50} 1.5 μM). One further consideration was that the analogous *tert*-butyl ester showed broad anti-parasitic activity against *T. brucei*, *T. cruzi* and *L. infantum* (GI_{50} 1.8, 5.1, 2.4 μM , SI 14, 5, 10). This compound was assumed to have a similar target than the ethyl ester analogue **14a**, as activity against *T. brucei* was very similar. The target identification studies were carried out on *T. brucei*, as this parasite was the main focus of this study and other parasites were not accessible at this point.

3.5.1 Myristate labelling of GPI anchor biosynthesis

Introduction to myristate role in GPI anchor biosynthesis

The bloodstream form of *T. brucei* is covered in a dense coat of variant surface glycoproteins (VSG), which are attached via a conserved GPI anchor to the plasma membrane of the parasite.^[69,203] This VSG coat serves as a barrier for components of the host immune system and undergoes constant antigenetic variation, thus evading the host immune system.^[70,204]

The GPI structure constitutes two myristates, that are embedded into the lipid bilayer of the parasite membrane, anchoring the GPI-VSG construct.^[69,203] Therefore, myristate has an essential role in GPI anchor biosynthesis, as it is the sole fatty acid component integrated within this construct in *T. brucei*.^[205] Myristate is readily taken up from the host serum and used in GPI-anchor biosynthesis, as has been shown by incorporation of radio-labelled [^3H]-myristate.^[203,205] Myristate is incorporated within the GPI structure through both fatty acid remodelling of the GPI precursor and myristate exchange, although the latter was thought to function in repair to ensure myristate incorporation.^[205]

In this research study, a myristic acid analogue bearing an alkyne moiety (Figure 32) for the introduction of a fluorescent biotin tag via Click-Chemistry was used for the metabolic labelling

of the GPI-VSG structure in live trypanosomes.^{[206]5}

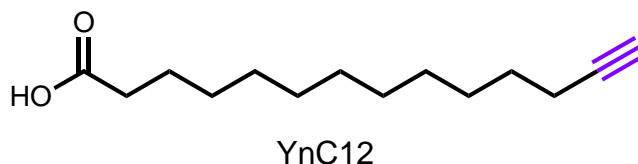


Figure 32: Myristate analogue bearing an alkyne functionality for labelling with TAMRA-fluorophore and biotin-tag, provided by Megan Wright and Dr. Ed Tate (Imperial College London, London, UK).^[206]

Effect of inhibitors **14v** and **14a** on myristate labelling after an incubation period of 3 h

Initially, **14v** and **14a** were used at a concentration slightly under the minimum inhibitory concentration, in order to allow parasite survival, whilst observing the maximum effect on GPI-anchor biosynthesis. Derivatives **14v** and **14a** have been chosen for this study, because of their low μM anti-trypanosomal effect in *T. brucei*. *T. brucei* was incubated with **14v** and **14a** over a time period of 3 h, after which the cells were counted and adjusted to similar concentrations. The myristic acid analogue **YnC12** was added to the parasites and incubation was continued for another 4 h to ensure good incorporation of the myristate analogue in the GPI-anchor of *T. brucei*. After incubation, the cells were lysed and the proteins purified by precipitation from acetone. Next, the fluorescent/ biotin-tag was introduced by Click-chemistry between the alkyne-fatty acid analogue and the azide tag in **38** (Figure 33). This crude extract was used without further purification and applied to a SDS gel. After fixation of the sodium dodecyl sulphate (SDS)-gel, the in-gel fluorescence was measured under TAMRA-setting in a fluorescence plate reader (Figure 34). Indeed, the positive control with DMSO and **YnC12** showed two fluorescently labelled bands. One very intense band at a molecular weight around 50 kDa and the expected band for the GPI-VSG proteins at 57 kDa.^[207] A possible explanation for the additional band, would be that **YnC12** inhibits some steps in the *de novo* synthesis or recycling of GPI-VSG proteins, resulting in low-molecular weight analogues of 50 kDa with a small proportion of **YnC12** still incorporated in the full GPI-VSG construct. Previously, radioactive labelling with [^3H]-myristate in the presence of tunicamycin, an inhibitor of N-linked glycosylation, resulted in the appearance of two bands at 55 and 57 kDa, with the 55 kDa band representing the N-linked glycosylation deficient GPI-VSG proteins.^[207] In this study, the lower band at 50 kDa might represent newly synthesised GPI-VSG proteins, where glycosylation steps are inhibited by **YnC12**, whereas the weaker fluorescent band at 57 kDa represent the

⁵The myristic analogue YnC12 was kindly provided by Megan Wright (Research group: Prof. Dr. Ed Tate, Imperial College London, London, UK)

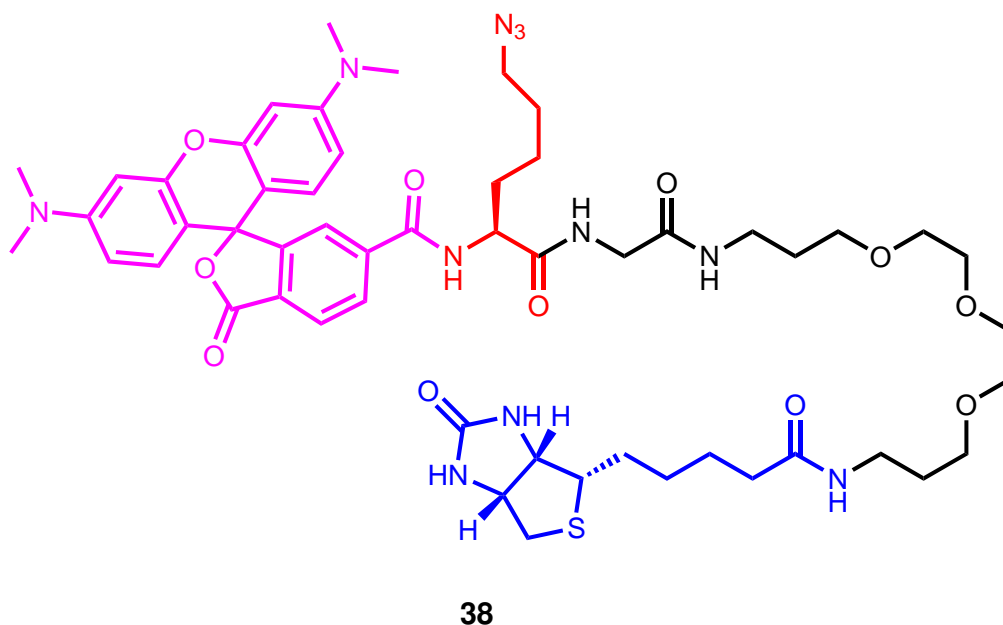


Figure 33: Tag **38** for visualisation of metabolic labelling of YnC fatty acids, provided by Megan Wright and Dr. Ed Tate (Imperial College London, London, UK).^[206]

recycled GPI-VSG proteins with all modification already in place. However, this hypothesis requires confirmation through mass spectrometric analysis of the corresponding bands.

Next, the effect of pre-incubation with the inhibitors **14v** and **14a** (lane:1 and 2 in Figure 34) on myristic labelling of the GPI-anchored VSG proteins was studied. Both inhibitors **14v** and **14a** resulted in reduction in the fluorescent signal in the 50 kDa band, while the higher band 57 kDa appeared at similar intensities compared to the control with DMSO only. In particular, the 3-benzyloxy derivative **14v** caused a significant reduction in fluorescent signal after only 3 h of incubation compared to the positive control. This observation was further supported by Coomassie staining of the same gel, indicating that equal or indeed slightly more protein was applied in lane 1 for the derivative **14v**. Since *T. brucei* has two distinct pathways to incorporate myristate in the GPI-VSG structure (remodelling of fatty acids or exchange in complete GPI-VSG constructs).^[207] It might be possible that derivative **14z** only inhibits *de novo* synthesis via remodelling, possibly explaining the reduction of the fluorescent band at 50 kDa. Coomassie staining identified the 57 kDa band as the major protein in the crude protein mixture. This may explain the weak fluorescent intensity of the 57 kDa band, as only recycled GPI-VSG proteins are myristylated. The bloodstream form of *T. brucei* has a high rate of endocytosis and is therefore able to change its VSG-coat every 12 min,^[208] and this should lead to a reduction of the 57 kDa band if only **YnC12** is present as the sole source for myristate. However **YnC12** was not the sole source for myristate and this might explain the higher intensity of the 57 kDa band compared to the weak fluorescence signal. The methyl derivative **14a**

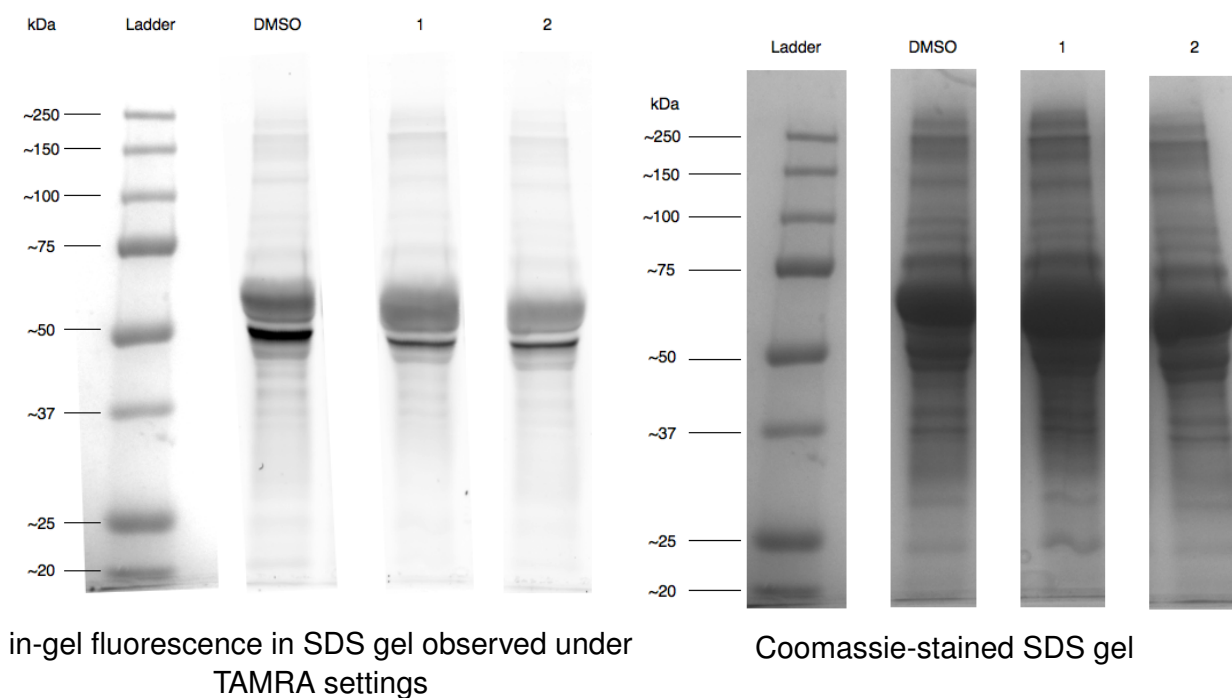


Figure 34: SDS gels after 3 h incubation with **14v** and **14a**; lane 1: **14v**, lane 2: **14a**, full gels see Chapter 11.

also showed a reduction of the 50 kDa fluorescent band, confirmed by Coomassie staining, but seemed to be less active than **14v**. Interestingly, **14v** and **14a** also had low μM activity against *T. brucei* *in vitro*, suggesting that indeed GPI anchor biosynthesis inhibition could be responsible for the anti-trypanosomal effect. Although the 3-methyl derivative **14a** resulted only in a small reduction of myristate incorporation, it was slightly more active against *T. brucei* than **14v**, but unfortunately it was also more toxic against mammalian cells (Figure 34).

Effect of inhibitors **14v** and **14a** on myristate labelling after an incubation period of 24 h

The initial experiment confirmed that the myristate analogue **YnC12** is incorporated in the full (57 kDa) GPI-VSG structure and an unknown protein (50 kDa), most likely a VSG-precursor, as the protein was very abundant (Figure 34). However, in order to validate the labelling a negative control with *T. brucei* proteins without **YnC12** and the fluorescent tag **38** has been performed. Although, a reduction of fluorescent signal for the derivatives **14v** and **14a** was observed after 3 h, longer incubation times with the inhibitors have not been investigated yet. Therefore, the initial labelling experiment was repeated with longer incubation times and an additional negative control. The incubation time was chosen to be 24 h, as at this time activity against the parasites was observed. Assays to determine the effective doses for the labelling were performed against *T. brucei*. Next, *T. brucei* was incubated with concentrations of inhibitors which did not display any toxicity against the parasites over a time course

Table 24: Anti-parasitic activity of compounds chosen for target identification studies.

GI ₅₀ [μM]					
#	R	<i>T. brucei</i>	<i>T. cruzi</i>	<i>L. infantum</i>	HL60
14v	OBn	4.4 ± 1.1	>100	>100	>100
14a	CH ₃	1.5 ± 0.3	>100	>100	31.0 ± 0.8

of 24 h. Although the benzyloxy derivative **14v** previously did not show toxicity at 50 μM (MIC 100 μM), reduced parasite densities were observed after 24 h. However, the number of live trypanosomes after 24 h was still sufficient for the following labelling experiment with myristate **YnC12**. Therefore, the parasite density was adjusted to $3.7 \times 10^6 \frac{\text{cells}}{\text{mL}}$ and **YnC12** and fresh inhibitors (**14v** and **14a**, respectively) were added at a final concentration of 100 μM and incubation was continued for another 4 h. After 4 h, parasites were lysed, proteins precipitated with acetone and subsequently subjected to click-chemistry with the tag **38**. Finally, 10 μg crude labelled protein was loaded on a SDS gel and separated. The fluorescent protein bands were visualised under TAMRA settings and stained with Coomassie blue (Figure 35).

Pleasingly, the negative control in the absence of **YnC12** did not show unspecific labelling of the tag **38** with trypanosomal proteins. Interestingly, the Coomassie stained SDS gel showed the same two protein bands at 50 and 57 kDa as described previously (Figure 34). This result does suggest that most likely a GPI-VSG precursor at 50 kDa is present in the crude protein composition in *T. brucei*, possibly a precursor before N-linked glycosylation. As expected the positive control in the presence of DMSO resulted in an intense fluorescent signal at 50 kDa, with only minor amounts of a higher 57 kDa protein band. Prolonging the incubation time of derivative **14v** from 3 h to 24 h resulted in a complete loss of the fluorescent band at 50 kDa and therefore in no incorporation of **YnC12** in this GPI-VSG precursor. However, the faint 57 kDa band still remained, further supporting that **14v** inhibits incorporation of **YnC12** almost solely in the precursor at 50 kDa. Indeed, the Coomassie stain did not show any remnants of the 50 kDa protein, but an abundant 57 kDa band for the full GPI-VSG proteins. This observation can be explained in the light of previous work, where VSG RNAi silencing caused cell cycle arrest, blocking further cell division.^[209] Although *T. brucei* unable to synthesise new VSG proteins could survive *in vitro*, an inability to vary the VSG coat led to clearance by the immune system (*in vivo*).^[209] Here, inhibitors of GPI anchor synthesis prevent the par-

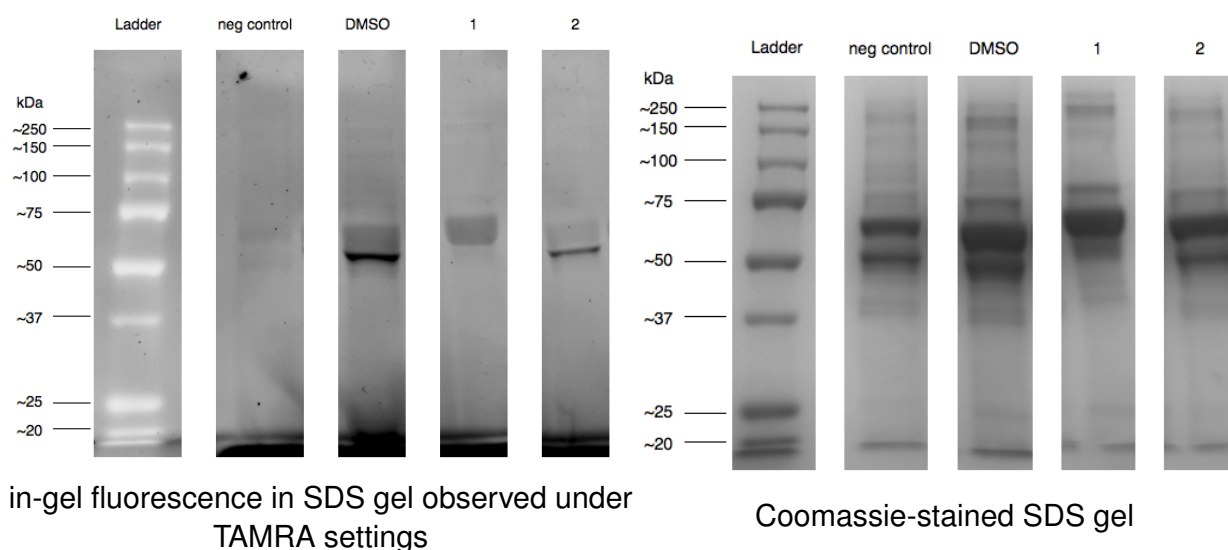


Figure 35: YnC12 labelling after 24 h pre-incubation with **14v** and **14a**; lane 1: **14v**, lane 2: **14a**; full gels see Chapter 11.

asite from recycling VSG proteins, but retain a minimal protective coat, which could explain the residual 57 kDa GPI-VSG proteins for **14v** in the Coomassie stained gel (Figure 35). This previous study would explain the proposed idea that *T. brucei* has the ability to monitor VSG synthesis or VSG-coverage of the cell surface.^[210] VSG has been shown to have a half life time of 33 ± 9 h,^[211] less than the time used for the evaluation of anti-trypanosomal activity (72 h) of **14v**. The methyl derivative **14a** also showed a significant reduction of the fluorescent intensity of the 50 kDa protein by approximately 50 %. Coomassie staining confirmed this reduction of the lower 50 kDa band compared to the positive control. The upper band at 57 kDa for **14a** was weakly labelled in the fluorescent channel, but Coomassie staining revealed a large amount of 57 kDa proteins.

Effects on fatty acid labelling of GPI-anchored proteins using the pentadecylic fatty acid YnC15 and the inhibitors **14v** and **14a**

The metabolic labelling with the myristate analogue YnC12 resulted in incorporation into the full (57 kDa) and partially (50 kDa) synthesised GPI-VSG proteins. The ester derivatives **14v** and **14a** have been shown to inhibit this incorporation, resulting in reduction and/ or loss of GPI-VSG proteins. Next, the myristic acid probe YnC12 was exchanged with the pentadecylic fatty-acid analogue YnC15 (Figure 36).⁶ *T. brucei* exclusively uses myristic acid for the full GPI-VSG construct, however other fatty acids can be incorporated in GPI-precursors and will be exchanged by myristate in the final GPI-VSG adduct.^[205] Incorporation of the pentadecylic fatty-acid analogue YnC15 could potentially answer the question if the protein band at 50 kDa

⁶YnC15 was kindly provided by Megan Wright and Dr. Ed Tate (Imperial College London, London, UK).

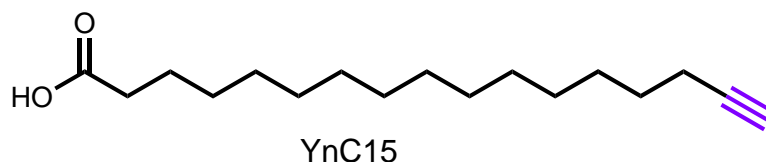


Figure 36: Pentadecylic acid **YnC15**

is a fatty acid precursor of the partially synthesised GPI-VSG proteins. Therefore, *T. brucei* was incubated with the derivatives **14v** and **14a** over a period of 24 h. After which the parasites were counted and subjected to metabolic labelling with the elongated fatty acid analogue **YnC15** for a further 4 h. Unfortunately, the elongated fatty acid **YnC15** showed some toxicity against *T. brucei* and caused cell death in combination with **14v**. However, the ester analogue **14a** in combination with **YnC15** showed less toxicity and could further be subjected to fluorescent labelling with the fluorophore **38** under Click-chemistry conditions. The crude proteins of the negative control (without **YnC15**), the positive control (DMSO) and **14a** were separated on a SDS gel and the bands were visualised using in-gel fluorescence and Coomassie staining (Figure 37). The negative control in the absence of **YnC15** showed minor unspecific binding of the fluorophore **38** with proteins at 57 kDa, which is most likely the full GPI-VSG-protein band. In contrast, labelling in the presence of **YnC15** resulted in a weak additional band just below the 57 kDa band (55 kDa). Coomassie staining showed the 50 kDa band for the negative and positive control, but under in-gel fluorescence analysis these bands did not appear. It might be possible that the additional weak band at 55 kDa is further unspecific binding of the fluorophore with the GPI-VSG-construct. The inhibition with the rhodanine derivative **14a** resulted in similar protein band intensities than for the positive control with DMSO only. There were two bands at 55 and 57 kDa with the former being very weak. Coomassie staining showed that slightly less proteins were loaded onto the SDS gel for derivative **14a**, but the staining showed diffuse bands ranging from 50-57 kDa. In conclusion, labelling with the elongated analogue resulted only in minor incorporation into the GPI-VSG-proteins as expected by exclusivity of myristate in this construct.^[205]

Fatty acid labelling in HL60 cells and effect of pre-incubation with selected rhodanine inhibitors

The derivatives **14v** and **14a** have been shown to inhibit enzymes of the GPI-anchor biosynthesis through reduction of myristate uptake into the GPI-anchor. In order to investigate the mode of action of the derivatives **14v** and **14a** on HL60 cells, the myristate labelling with **YnC12** was repeated in the presence of these inhibitors. In particular for derivative **14a**, this was an important question as it showed toxicity against HL60 cells at GI_{50} 31.0 μ M. HL60 cells were incubated for 24 h in the presence of **14v** and **14a** at inhibitor concentrations of 50 and 7.5 μ M

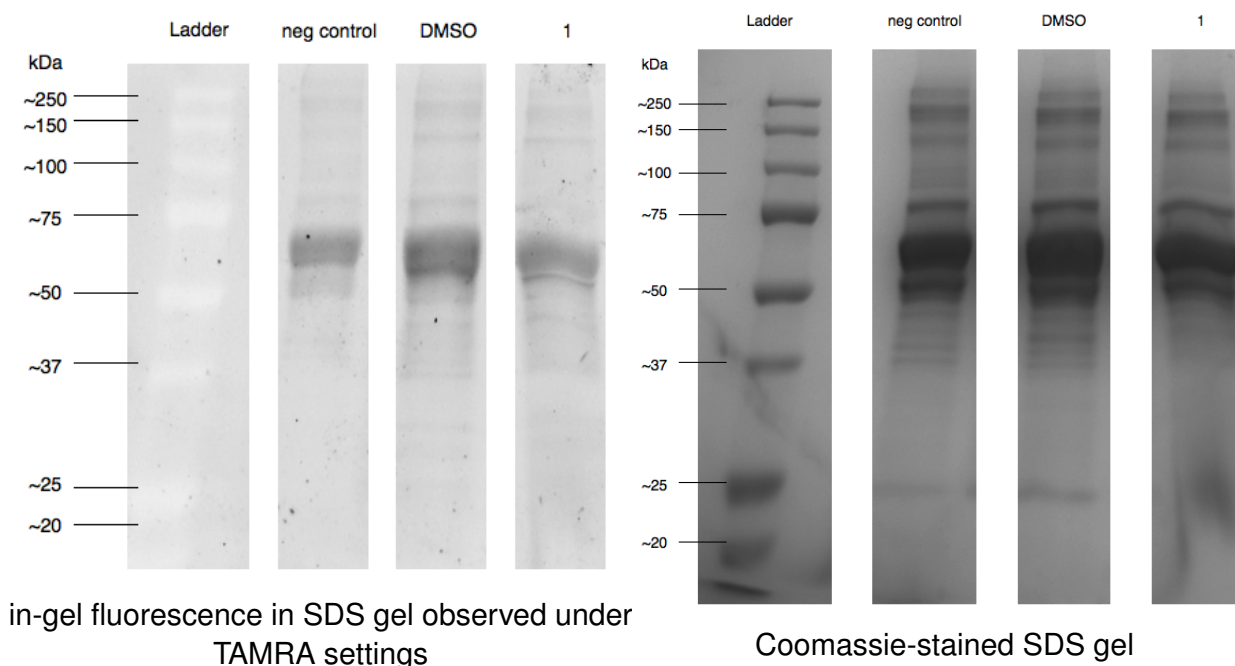


Figure 37: YnC15 labelling after 24 h pre-incubation with **14a**; lane 1: **14a**; full gels see Chapter 11.

respectively. After the incubation period the cells were counted and subjected to YnC12 over a time period of 4 h, crude proteins were precipitated and modified with a fluorophore using Click-chemistry. In-gel fluorescence of the separated crude proteins and Coomassie staining showed that YnC12 did not specifically label proteins in HL60 cells. In the negative control in the absence of YnC12 the in-gel fluorescence showed a weak band at 80 kDa, Coomassie staining on the same gel displayed only one major protein band at 80 kDa. The fluorescence intensity of these 80 kDa band was increased in the positive control with DMSO and in the cases for **14v** and **14a**, however the increasing intensity correlated with increasing amounts of protein loaded to the gel as shown in the Coomassie stained gel (Figure 38). In conclusion, fatty acid metabolism might not be affected by the derivatives **14v** and **14a** in HL60 cells, suggesting a different mode of action.

3.5.2 Flow cytometry analysis of *T. brucei* transferrin receptors for GPI anchor biosynthesis inhibition studies

In the previous section, inhibition of GPI anchor biosynthesis has been demonstrated to be a possible mode-of-action of inhibitors **14v** and **14a**, using a myristic acid analogue to label myristate incorporated proteins in *T. brucei* and observe in-gel fluorescence on SDS gels (Figure 35). This method was excellent to identify GPI-anchor biosynthesis as possible target of the derivatives **14v** and **14a**.

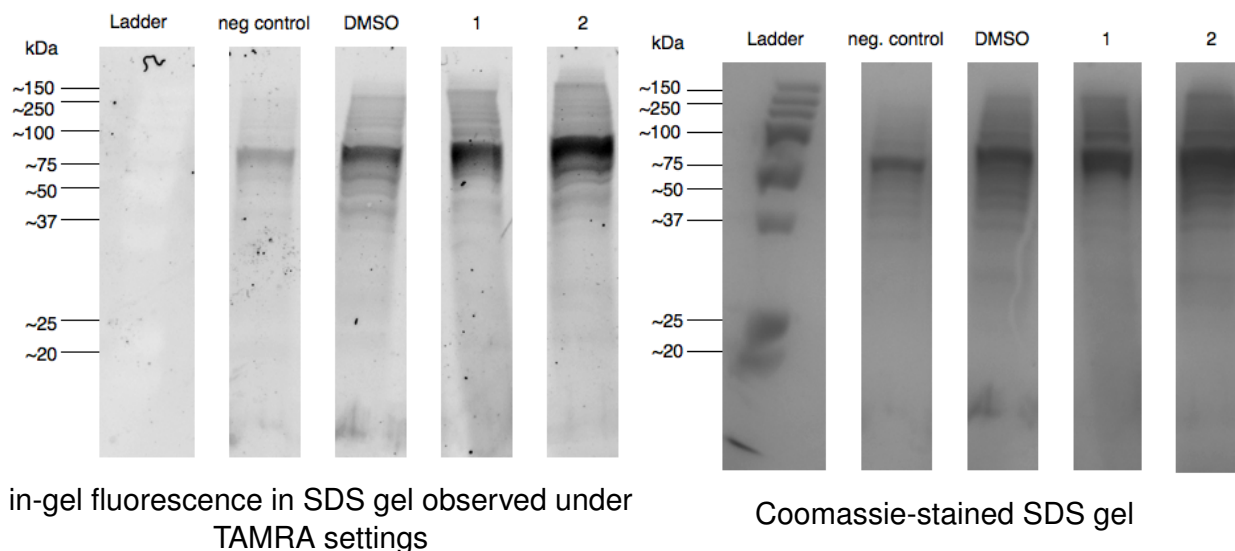


Figure 38: YnC12 labelling after 24 h pre-incubation with **14aa** and **14a**; lane 1: **14v**, lane 2: **14a**; full gels see Chapter 11.

In order to further support the hypothesis, that the trypanocidal effect of **14v** and **14a** derives from GPI-anchor synthesis inhibition, quantified and unambiguous experiments needed to be performed. An experiment to monitor the quantified inhibition of GPI-anchor biosynthesis is the use of flow-cytometry to measure the uptake of Fluorescein IsoThioCyanate (FITC)-conjugated bovine transferrin. *T. brucei* like all living cells is dependant on iron for growth.^[128] The major source for iron in *T. brucei* is host transferrin, which is bound to the trypanosomal receptor for transferrin uptake (*TbTfR*) in order to reach the interior of the parasite.^[128] The *TbTf* receptor shows a significant sequence similarity to VSG proteins (60-76 %) and both are attached via a GPI anchor to the plasma-membrane of the bloodstream form of *T. brucei*.^[128]

Thus, *TbTf* receptor iron uptake directly depends on GPI-anchor biosynthesis and inhibition thereof will affect the parasites ability to uptake transferrin. Furthermore, subjecting *T. brucei* to iron starvation conditions has been shown to upregulate the synthesis of GPI-anchored *TbTf* receptors and indeed this up regulation could be quantified by measuring the uptake of radioactive labelled holo-transferrin.^[212] In this research study, FITC-conjugated bovine transferrin was used as direct indicator for the iron status in *T. brucei* and therefore the parasites ability to synthesis GPI-anchored *TbTfRs*.

T. brucei was incubated with the rhodanine derivatives **14v** and **14a** for 24 h, after which the media was exchanged to transferrin-free media in order to cause iron-starvation and therefore increased expression of *TbTfRs*. After 2 h of incubation, the FITC-labelled transferrin was added and fluorescence intensity was quantified using flow-cytometry (Figure 39). The positive control with DMSO only showed a high fluorescence intensity signal (13,874.8 FU),

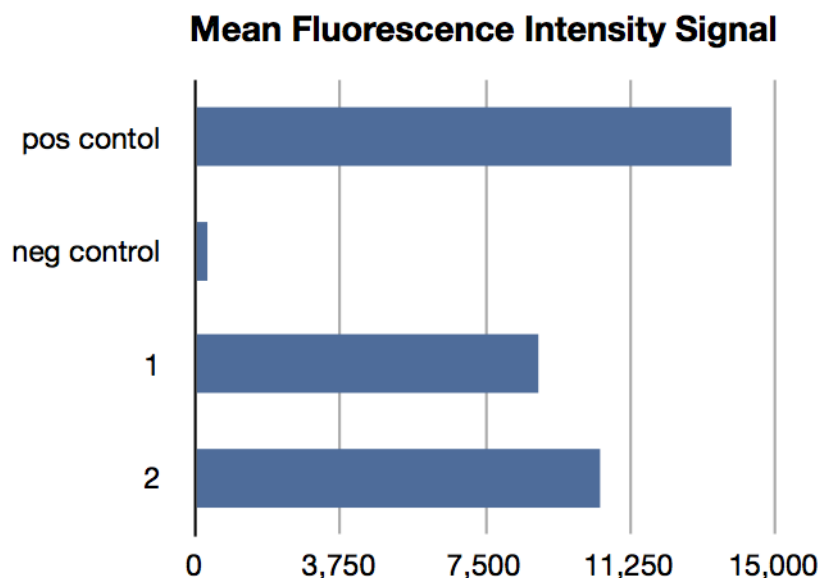


Figure 39: Mean fluorescence intensity of FITC-labelled transferrin after incubation with 1: **14v**, 2: **14a**.

whereas the negative control without the FITC-labelled transferrin showed a negligible mean fluorescence (312.5 FU). Analysis of the side-scattered light showed that the majority of trypanosomes were intact (Figure 40, SSC-A vs Fluorescent intensity) The FITC-labelled trypanosomes were further stained with DAPI and analysed by fluorescence microscopy. The fluorescently labelled trypanosomes showed a bright DAPI (blue) stained kinetoplast and nucleus and if treated with FITC-labelled transferrin (green) an additional fluorescent signal was detected (Figure 40). In the absence of FITC-labelled transferrin (in the negative control), no fluorescence signal for FITC was detected under the fluorescent microscope (Figure 40).

Interestingly, the 3-benzyloxy derivative **14v** resulted in a 36 % decrease in fluorescent signal compared to the positive control (Figure 39). Analysis of the side-scattered light and the fluorescence intensity indicated lysed trypanosomes, which might explain the drop in fluorescent intensity. But although the number of parasites was decreased, the intact trypanosomes showed a decrease in transferrin uptake, confirming the hypothesis that GPI-anchor is indeed inhibited by this derivative. Indeed, further analysis under fluorescence microscopy showed that the FITC-labelled transferrin content in parasites treated with **14v** was decreased compared to the positive control (Figure 41 and Figure 40, respectively). The fluorescent microscopy picture in Figure 41 shows a sample of the three different populations of *T. brucei* if treated with **14v**. The first type of parasite showed normal uptake of transferrin, while another displayed no presence of the FITC fluorophore and the last type showed a lysed parasite with diffuse DAPI staining. The observation of the second type of parasite was in agreement with

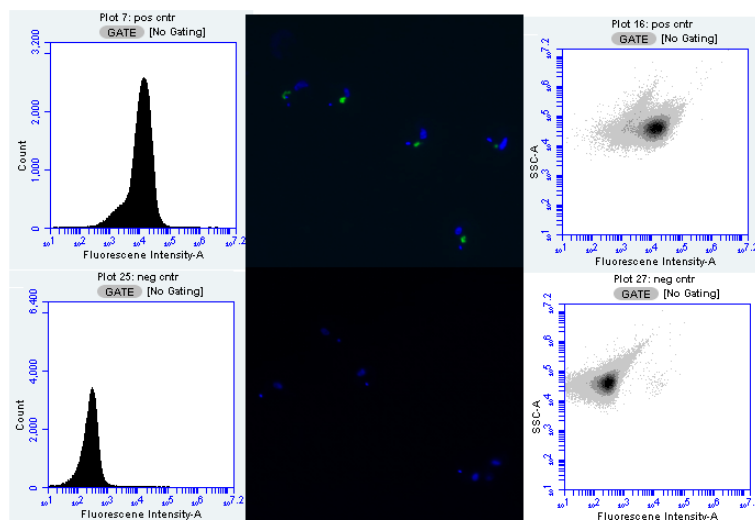


Figure 40: Flow-cytometry analysis of cell morphology (SSC-A vs. Fluorescent intensity) and uptake of FITC labelled transferrin; Fluorescence microscopy images with DAPI co-staining.

the myristic acid labelling experiment, where a decreased amount of GPI-VSG proteins were observed after incubation with **14v**. In order to visualise the effects in more detail it would be necessary to repeat the experiment with lower doses of inhibitor.

Then parasites were treated with **14a**, cells with and without FITC-label were detected under the fluorescent microscope (Figure 41). Indeed, the mean fluorescent intensity of parasites treated with **14a** was slightly higher (10,476.3 FU) compared to treatment with **14v** (8,878.4 FU), indicating **14a** weaker inhibition of the GPI-anchor biosynthesis. Treatment with **14a** caused a 25 % deduction of FITC fluorescent signal compared to the positive control (Figure 39). The combination of flow-cytometry with fluorescence microscopy was very well suited to study and quantify the influence of **14v** and **14a** on GPI-anchor biosynthesis.

The flow-cytometry analysis of transferrin uptake confirmed the previous experiment with the metabolic labelling with myristate **YnC12**. The meta-benzyloxy ethyl ester **14v** showed the strongest inhibition of myristate incorporation and in the flow-cytometry experiment, reduced GPI anchor biosynthesis was confirmed by a reduced uptake of FITC-labelled transferrin. The reduction in fluorescence intensity correlated directly to the expressed GPI-anchored *TbTf* receptors. The meta-methyl rhodanine ethyl ester **14a** showed similar results in both assays, but was a slightly weaker inhibitor of GPI-anchor biosynthesis, as could be seen in the flow-cytometry experiment. The two studies combined strengthened the hypothesis that GPI-anchor synthesis was inhibited by **14v** and **14a**.

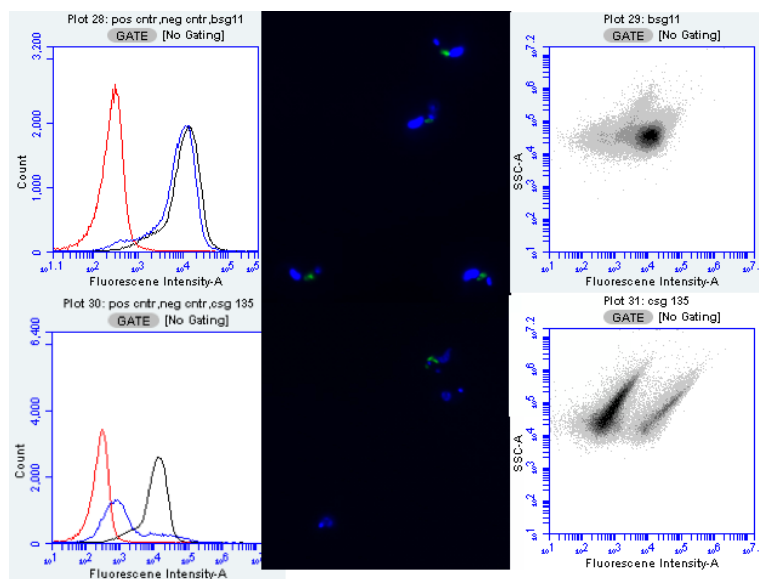


Figure 41: Flow-cytometry analysis of derivatives **14v** and **14a**; Side-scattered light vs fluorescent intensity and Number of cells vs fluorescent intensity and fluorescence microscopy pictures of treated parasites.

3.5.3 GPI cell-free radio-label assay

Introduction to cell-free GPI-synthesis assay

Initially the DPMS inhibitors in Table 2 were screened to evaluate their trypanocidal activity against *T. brucei* (Table 25).^[68] With the exception of the unsubstituted 5-benzylidene derivative **2a** (GI_{50} 56.0 μ M) none of the other inhibitors showed any effect on *T. brucei* growth at 100 μ M, although they inhibited DPMS, a validated anti-trypanosomal protein, with good to moderate residual activities.^[68] In addition to these studies a cell free-GPI synthesis assay on trypanosome enzymes was performed.⁷ Briefly, radio-labelled GDP-[³H]-Man was subjected to cell-free membranes of *T. brucei* in the presence of 1 mM of rhodanine-inhibitor.^[68] This membrane layer contains all enzymes involved in GPI anchor biosynthesis and is able to synthesise the GPI-anchor until the substrate ethanolamine-P-Man α 1-2Man α 1-6Man α 1-4GlcNH₂-PI.^[68] Intermediates of the GPI-anchor synthesis can be extracted and separated by high performance thin layer chromatography (HPTLC).^[68] The radio-labelled intermediates of the GPI-anchor synthesis can be visualised by fluorography and this TLC-plate can be analysed by comparison of substrate band intensities (Table 25).^[68] In order to explain GPI-anchor synthesis in the cell-free system, individual steps will be explained in further detail for the control (DMSO, Table 25). The first band on the HPTLC is representing Dol-P-Man, whose synthesis is catalysed by DPMS from GDP-[³H]-Man and dolichylphosphate. A weak

⁷This assays were performed by Dr. Terry Smith from the University of St. Andrews, St Andrews, Scotland, UK

intensity of this band in combination with weaker consecutive bands is indicative for DPMS inhibition. However, frequently this band will appear with a decreased fluorescent intensity, but is accompanied by intensive consecutive bands, indicating that the substrate Dol-P-Man is faster consumed than re-synthesised.⁸ In the consecutive step the mannosyltransferase 1 (MT-1) catalyses the transfer of Dol-P-Man onto GlcNH₂-PI, resulting in the formation of the second band (M1) on the HPTLC.^[65] The next mannose residue is installed by the α 1-6 mannosyltransferase (MT-2) resulting in the formation of Man α 1-6Man α 1-4GlcNH₂-PI (M2) on the HPTLC plate.^[65] The third mannose is transferred by an α 1-2-mannosyl transferase from Dol-P-Man to generate Man α 1-2Man α 1-6Man α 1-4GlcNH₂-PI (M3).^[65] Next the inositol acyltransferase acylates M3 to generate the substrate Man α 1-2Man α 1-6Man α 1-4GlcNH₂-(acyl)PI (aM3).^[65] The final step performed by the cell-free system is the ethanol amine phosphate transfer to form the substrate ethanolamine-P-Man α 1-2Man α 1-6Man α 1-4GlcNH₂-PI (A') (Figure 42). Inhibition of individual enzymes by rhodanine derivatives will lead to accumulation of

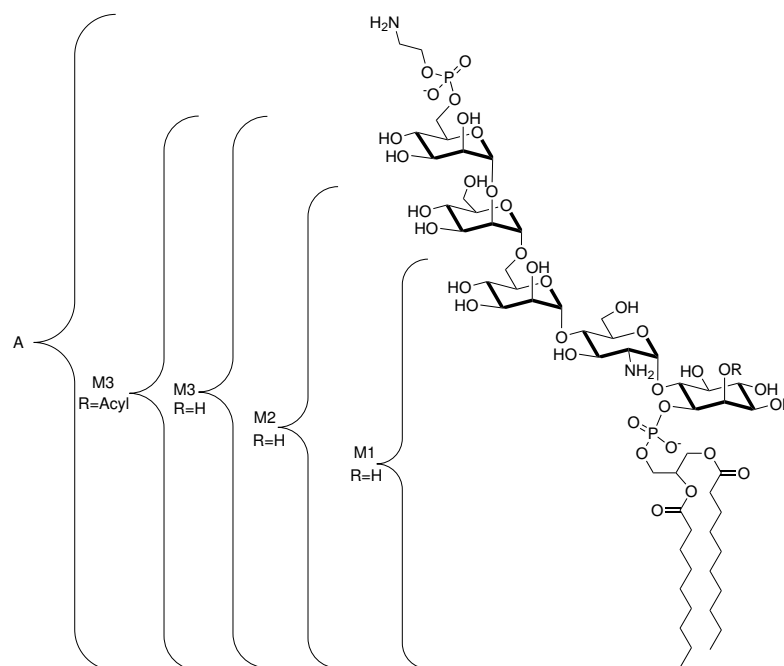


Figure 42: Substrates of cell-free GPI-synthesis assay, M1: Man α 1-4GlcNH₂-PI; M2: Man α 1-6Man α 1-4GlcNH₂-PI; M3: Man α 1-2Man α 1-6Man α 1-4GlcNH₂-PI (M3); aM3: Man α 1-2Man α 1-6Man α 1-4GlcNH₂-(acyl)PI; A': ethanolamine-P-Man α 1-2Man α 1-6Man α 1-4GlcNH₂-PI.

the individual substrates of that particular enzyme and can therefore be identified by this cell-free assay.

⁸Oral communication with Dr. Terry Smith, St. Andrews University

Comparison of DPMS activity and activity in cell-free GPI-synthesis assay and *in vitro* activity

A chosen subset of rhodanine-N-acetic acid derivatives was screened in this cell-free assay of GPI-anchor synthesis in order to identify potential targets within the GPI-anchor biosynthesis pathway. Particularly interesting were the derivatives shown in Table 25, as residual DPMS activity data was already available.^[68] The DPMS activity correlated well with the cell-free assay, as low residual DPMS activity resulted in weak substrate bands upstream from Dol-P-Man. The high intensity of the Dol-P-Man band might be explained by accumulation of substrate over time, as none of the inhibitors abolished DPMS synthesis completely. This hypothesis is supported by derivative **2f**, a weak DPMS inhibitor, resulting in a diminished Dol-P-Man band followed by a weak M1 band. While **2f** inhibits DPMS weakly, less Dol-P-Man substrate is accumulated, resulting in a weak band. However, it may also be possible that the derivatives inhibit additionally the first mannosyltransferases MT-1 and therefore cause decrease in subsequent substrate bands. To this point it is unclear if one or more enzymes were inhibited by these rhodanine-N-acetic acid derivatives. However, particularly exciting was the observation that **2c**, the free acid analogue of the ester derivative **14v**, which has been shown by myristate labelling and flow cytometry analysis to inhibit GPI-anchor biosynthesis, indeed is a good DPMS and possible MT-1 inhibitor.

It is likely, that the ester derivative has the same molecular target, as the ester moiety potentially serves as a pro-drug and increases membrane diffusion, while being hydrolysed within the cell. This hypothesis was supported by low μM activity of the ester derivatives against the bloodstream form of *T. brucei* *in vitro* (Table 25). Indeed, the most promising inhibitor was **14v** as it showed a good selectivity index of $\text{SI} > 23$, while most of the other ester-derivatives showed increased toxicity towards HL60 cells.

Methyl and trifluoromethyl substituted rhodanine-N-acetic acid and their activity in the cell-free GPI-synthesis assay

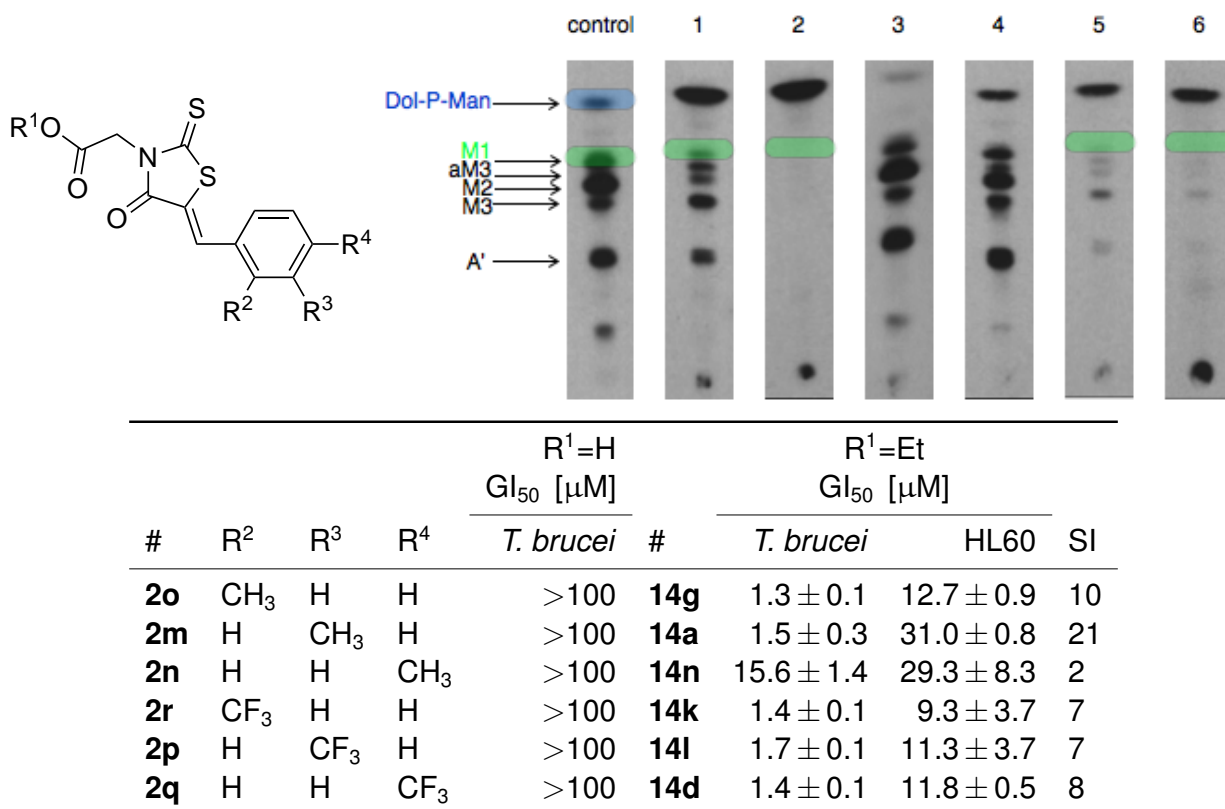
Previously, the rhodanine-N-acetic ester derivative **14a** has been shown by myristate labelling and flow cytometry analysis to inhibit GPI-anchor biosynthesis. In the following research study, the activity against isolated enzymes of the GPI-anchor synthesis is narrowed down and should allow the identification of the molecular target(s) within the GPI-anchor biosynthesis. The free carboxylic acid derivative **2m** was screened in the cell-free GPI-synthesis assay as it is assumed that the ester moiety is cleaved upon entering into the parasitic cell. However, it may also be likely that the ester derivative is the active agent. The free acid analogue **2m** showed the strongest inhibition in this series, resulting in complete inhibition of the first mannosyltransferase (MT-1) and possible also DPMS (Table 26). This radio-labelled assay possibly identified the enzymes inhibited in the GPI-anchor biosynthesis, resulting in

Table 25: cell-free GPI assay for rhodanine-N-acetic acid derivatives; lane 1: **2a**, lane 2: **2ah**, lane 3: **2c**, lane 4: **2e**, lane 5: **2g**, lane 6: **2f**; *in vitro* activity against *T. brucei*; Blue highlighted bands: DPMS inhibition; Green highlighted bands: MT-1 inhibition.

#	R ²	R ³	R ⁴	R ¹ =H		#	R ¹ =Et	
				GI ₅₀ [μM]			GI ₅₀ [μM]	
				res. DPMS ^[68] [%]	<i>T. brucei</i>		<i>T. brucei</i>	HL60
2e	OH	H	H	23 ± 8	>100	14p	1.7 ± 0.1	4.1 ± 0.7
2c	H	OBn	H	23 ± 3	>100	14v	4.4 ± 1.1	>100
2f	H	OH	H	90 ± 5	>100	14q	4.8 ± 0.9	9.9 ± 0.5
2a	H	H	H	42 ± 5	56.0 ± 3.3	14i	8.3 ± 0.7	38.0 ± 1.8
2ah	H	H	OBn	10 ± 2	>100	14w	17.0 ± 0.9	>100
2g	H	H	OH	70 ± 4	>100	14r	17.6 ± 0.1	n.a.

decreased incorporation of myristate in metabolic labelling experiments and a reduction in uptake of FITC-labelled transferrin. All three assays showed similar results, but the radio-label assay narrowed the inhibition of GPI-anchor biosynthesis down to MT-1 and DPMS. Shifting the methyl group on the 5-benzylidene moiety in para-position (**2n**) abolished its activity against MT-1. There was a weak band for DPMS, but this was not indicative for DPMS inhibition, as Dol-P-Man has been synthesised but was used in subsequent steps, explaining the intense bands of consecutive substrates. Transferring the methyl substituent in ortho-position in derivative **2o** decreased MT-1 inhibition. Interestingly, in the trifluoromethyl series the meta- and para-substituted analogues showed good MT-1 inhibition, whereas the ortho substituent did not show any inhibition of GPI-anchor synthesis. The anti-trypanosomal activity against *T. brucei* *in vitro* correlated well with GPI-anchor synthesis inhibition. However, trifluoromethyl substituted analogues showed increasing toxicity against HL60 cells. The most promising candidate in this series was the meta-methyl substituted ester analogue **14a** as it showed low μM activity against *T. brucei*, while having a good SI of 21.

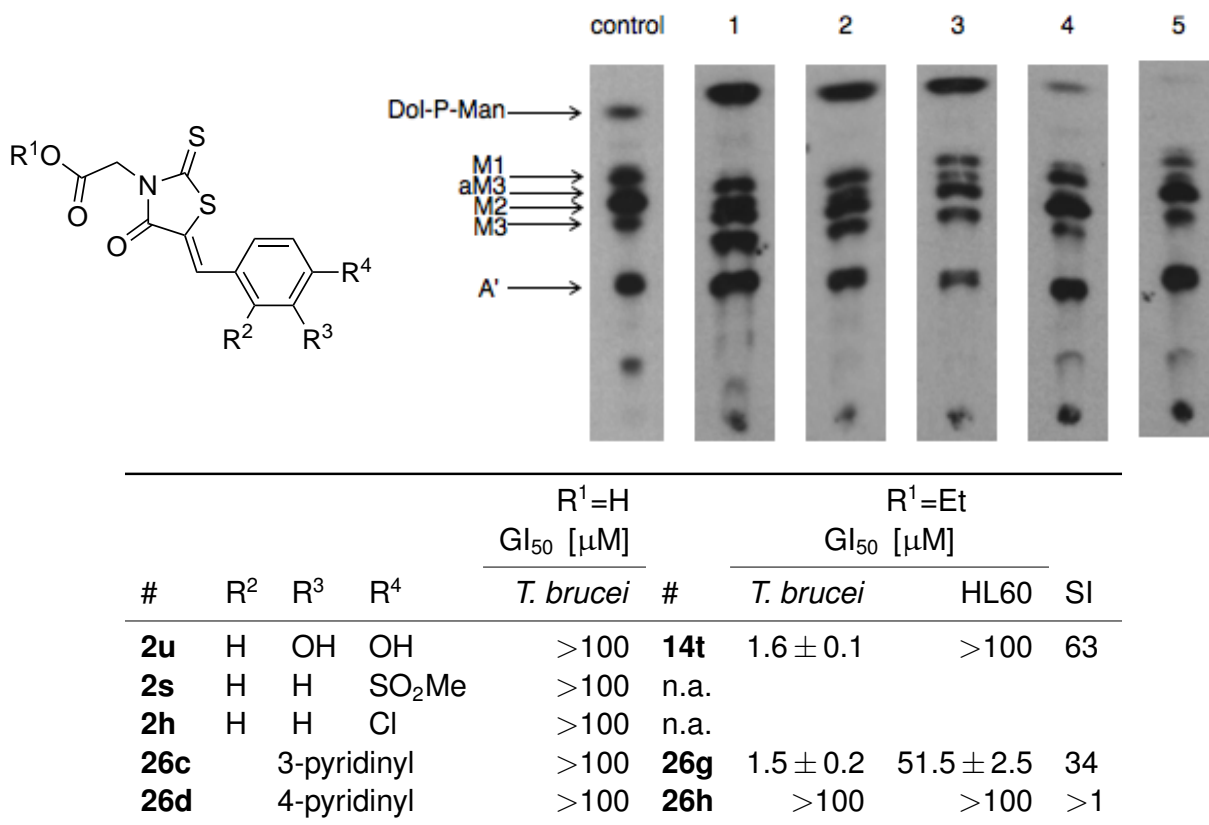
Table 26: cell-free GPI assay for rhodanine-N-acetic acid derivative-2; lane 1: **2o**, lane 2: **2m**, lane 3: **2n**, lane 4: **2r**, lane 5: **2p**, lane 6: **2q**; *in vitro* activity against *T. brucei*; Blue highlighted bands: DPMS inhibition; Green highlighted bands: MT-1 inhibition.



Anti-trypanosomal rhodanine-N-acetic acid derivative with no activity in cell-free GPI-synthesis

Interestingly, one of the most potent inhibitors against *T. brucei* growth *in vitro* did not show any effect on enzymes of the GPI-anchor biosynthesis as is to be seen in the results of the cell-free GPI-synthesis assay with **2u** (structural analogue of **14t**, Table 27). Also, the pyridine derivative **26d** was inactive in the GPI-synthesis assay, whereas its structural ethyl ester analogue **26h** displayed anti-trypanosomal activity in the low μM range. The catechol derivative **14t** may inhibit oxide-reductases in parasites, as several other rhodanine-catechol derivatives have been reported as molecular probes for bacterial NAD(P)H-dependant oxidoreductases.^[107,108] However, the exact mode of action of these derivatives is unknown at the present time, but using the fluorescence properties of **2u** in combination with native protein gels (western blots), the molecular target could potentially be identified.^[108]

Table 27: Cell-free GPI assay for rhodanine-N-acetic acid derivatives-3; R¹=H; lane 1: **2u**, lane 2: **2s**, lane 3: **2h**, lane 4: **26c**, lane 5: **26d**; *in vitro* activity against *T. brucei*; Blue highlighted bands: DPMS inhibition; Green highlighted bands: MT-1 inhibition.



3.5.4 Target-based optimisation using homology modelling

The target identification assays discussed in the previous chapters identified DPMS and/ or MT-1 as possible targets of the the inhibitors **14v** and **14a**. In particular the meta-benzyloxy derivative **14v** was interesting for DPMS inhibition, as the free acid analogue has previously been shown to inhibit DPMS with a residual activity of 23 %.^[68] In order to improve activity against DPMS, it would be beneficial to know the exact binding mode within the active site.

However, the rational design of inhibitors against DPMS is complicated by the absence of crystallographic data to date. DPMS with its crucial role in Dol-P-Man synthesis plays an important role in several glycosylation pathways among eukaryotic organisms.^[213] Therefore it was not surprising to observe high sequence similarities among *T. brucei*, *T. cruzi*, *L. infantum* and *Saccharomyces cerevisiae* (*S. cerevisiae*) DPMS (Figure 43). Furthermore, *T. brucei* DPMS has been shown to complement a DPM deficient clone of *S. cerevisiae* (yeast strain dpm1-6), causing rescue of this phenotype if grown on plates.^[213]

However, features characteristic to *T. brucei* DPMS, such as the missing dolichol binding site, essential for DPMS functionality in hamsters,^[214] have been highlighted as possible strate-

1	-----MSIEYSVIVPAYHEKLNKPLTTRLFAGMSPEN--AKK	36	P14020	DPM1_YEAST
1	-----MAVKYSIIVPAYKECGNLSHLQAG-VDR LADDGFSKNE	37	Q26732	Q26732_TRYBB
1	-----MQYSIIVPAYKECGNLEPLIRRVFAAVTEQGLPTQN	36	A4ICW5	A4ICW5_LEIIN
1	-----MPINYTIVVPAYKECGNLEALTRKRVFDATCDAGFAKND	38	K2MKX4	K2MKX4_TRYCR
1	MASLEVSRSPPRRSRRELEVRSPRQNKYSVLLPTYNERENLPLIVWLLVKFSFSESG---IN	57	O60762	DPM1_HUMAN
	: * : : : * : * * : : .			
37	TELIFVDDNSQDGSVEEVDALAHQGYNVRIIV--RTNERGLSSAVLKGFYEAKQYLVCM	94	P14020	DPM1_YEAST
38	VEMVIIVDDNSRDGSVEVVEKVRNEGYGVRIEV--RTNDRGLSSAVIHGISVSKGSFILVM	95	Q26732	Q26732_TRYBB
37	VEMLIVDDNSRDGSKEVVERLHEEGFNVHMDV--RTTERGLSSAVIHGLRHTSGAYKLVCM	94	A4ICW5	A4ICW5_LEIIN
39	VEMLIVDDNSQDGSVEVVKLQTEGYGVRIIDV--RTKERGLSSAVIHGISVSKGSFILVM	96	K2MKX4	K2MKX4_TRYCR
58	YEIIIIIDGSPDGTDRVAEQLEKIYGS DRILLRPREKKLGLGTAYIHGMKHATGNYIIIM	117	O60762	DPM1_HUMAN
	* : : : : * * * * * : . . : : : : * . . * * . : * : : : : : . * : : * :			
95	DADLQHPPE TVPKLFESLHDH--AFTLGTTRYAPGVGIDKDWPMYRRVISSTARMMARPL-	151	P14020	DPM1_YEAST
96	DADLQHPPE TVPKLLRALEKPGVEFVCGTRYGAGVEIDKDWPLHRRFISWGARLLARPL-	154	Q26732	Q26732_TRYBB
95	DADLQHPPE CVPALFKALCRDGVFVCGTRYGAGIEIDKNWPAHRR LISWGARLLARPL-	153	A4ICW5	A4ICW5_LEIIN
97	DADLQHPPE AVPRLLRALERPGVDFVCGTRYGAGVAIDGDWPIHRRVISWGARVLARPL-	155	K2MKX4	K2MKX4_TRYCR
118	DADLSHHPKF IPEFIRKQKEGNFDIVSGTRYKGNGG-VYGWDLKRKIIISRCANFLTQILL	176	O60762	DPM1_HUMAN
	. * * : * : : . : . * * * : . * * * . . : : : * :			
152	TIASDPMSGFFGLQKKYLENCNPRDINSQGFKIALELLAKLPLRPDRVAIGEVPTTFGV	211	P14020	DPM1_YEAST
155	TPLSDPMSGFFGPSRSMFFNNGGREVVNPIGYKIALELFVKCAVR-----KYEEVGFNFAT	209	Q26732	Q26732_TRYBB
154	TTLSDPMSGFFGIRDGVFKRHA-GEVNSIGYKIALELFVKCRVQ-----CFEEVGFNFAT	207	A4ICW5	A4ICW5_LEIIN
156	TPLSDPMSGFFGLRKEVFORGV-RELSPIGYKIALELFVKCRVQ-----NYEEVGFNFAT	209	K2MKX4	K2MKX4_TRYCR
177	RPGASDLTGSRFLYRKEVLEKLEKCVSKGYVFMEMIVRARQ---LNYTIGEVPISEVD	233	O60762	DPM1_HUMAN
	: . : : * * . . * : : : : : : : * * : . *			
212	RTEGESKLSGKVIIQYLQQLKELYVFKFGANNLILFITFSWILFFYVCYQLYHLVF---	267	P14020	DPM1_YEAST
210	RTVGESKLTGKVIINYLEHLKLLYFYVYGTALTGSTR-AVAGLFTVFTFFSTHLSLA	267	Q26732	Q26732_TRYBB
208	RTYGESKLTGKVIIFHYLEHLYALYLFKLGRLFYVFFV-VAVMFAMYLVAFLYHSLF---	262	A4ICW5	A4ICW5_LEIIN
210	RMVGESKLTGKVIIHLYLKLRLALYLYAFGKVVLLIPL-VMIFIFLWAVKQFF-----	260	K2MKX4	K2MKX4_TRYCR
234	RVYGESKLGNEIVSFLKGLLTFLFATT-----	260	O60762	DPM1_HUMAN
	* ***** * : * . : : * * * :			

Figure 43: Sequence alignment of DPMS amino acid sequence of *S. cerevisiae*, *T. brucei*, *T. cruzi*, *L. infantum* and human DPM1 using uniprot align functionality; 37 % sequence similarity between *S. cerevisiae*, *T. brucei*, *T. cruzi*, *L. infantum* and 69 % similarity between *T. brucei* and *S. cerevisiae* DPMS.

gies for the development of *T. brucei* specific inhibitors.^[213] Fluorescence resonance energy transfer studies on *S. cerevisiae* DPMS in conjunction with the use of the Robetta homology modelling server has been used to establish a structural model for yeast DPMS.^[215] Taking into consideration that *S. cerevisiae* DPMS shows a high sequence similarity to *T. brucei* (Figure 43), the primary amino acid sequence of *T. brucei* DPMS was submitted to the Robetta full-chain protein structure prediction server in order to obtain a homology model, which may help the rational improvement of the previous found rhodanine-N-acetic acid derivatives.^[216]

Homology-Modelling of DPMS using Robetta

The Robetta full-chain protein structure prediction server is a fully automated tool to predict the atomic coordinates of proteins with unknown 3D structure.^[216] Starting from the primary amino acid sequence of the unknown protein, a search for proteins with similar amino acid sequences is performed.^[216] This initial step, classified as "Ginzu", uses BLAST and psi-BLAST

searches to identify structural homologous proteins in the PDB database^[217], generating individual domains of the primary amino acid sequence, which can be applied to a further neural network based search (Pcons2)^[218] in order to identify further structural homologous proteins and/or models of already predicted proteins.^[216] Fragment domains, which cannot be assigned to a homologue, are *de novo* modelled and assembled with all other fragments to generate the final full-chain homology model.^[216] The closest structural homologue identified by psi-BLAST (34.10) was a mannosyl-3-phosphoglycerate synthase (MPGS) from *Rubrobacter xylanophilus* (3F1Y).^[219] Both, DPMS and MPGS both have GDP-mannose as common donor substrate, indeed the X-ray structure of GDP-mannose bound to MPGS has already been solved (3O3P), allowing the comparison of both GDP-binding sites of the models and the parent.^[219] The Robetta server generated five homology models of DPMS, based on the primary amino acid sequence and the parent MPGS. The models were submitted to model evaluation servers such as PROSA II, VERIFY_3D and ProQ,^[220–222] however the results were not conclusive and no model could be ruled out based on these results (data not shown). Therefore, Ramachandran plots of the models were generated (Figure 44)^[223] and based on these results models 1, 3 and 5 could be eliminated as they showed disfavoured conformations of amino acid residues. Both homology model 2 and model 4 were further evaluated as potential models for DPMS.

Docking of the natural substrate GDP-mannose

To further evaluate the potential of these models to serve as a model for DPMS, docking simulations of the natural substrate GDP-mannose were performed using Gold Suite 4.12 (CCDC, Cambridge, UK). The binding site was defined over the whole protein and 50 docking runs were performed. The docking poses were analysed and compared to known interactions of GDP-mannose within the active site of yeast DPMS (Tyr12, Asp44, Asp97, Arg212), as all these residues are conserved through all DPMS structures of *T. brucei*, *T. cruzi*, *L. infantum* and *S. cerevisiae*, they may indicate their importance for catalytic activity.^[215] The docking simulation for GDP-mannose were carried out for all five homology models, but only homology model 4 showed the expected interactions of GDP-mannose within the active site of the homology model (Figure 45). Although not all interactions are displayed in the interaction diagram in Figure 45, the ligand is placed in proximity of the expected amino acid residues. As the 3D coordinates of the homology model for yeast DPMS were not available for comparison with the generated homology model 4, the mannosyl-3-phosphoglycerate synthase (MPGS) from *Rubrobacter xylanophilus* (3O3P) was chosen for this purpose. Therefore, homology model 4 was aligned with 3O3P, showing that many of the modelled residues were similar to the active site of 3O3P, as can be seen Figure 46. Although many of the residues, such as the Tyr11 are different in 3O3P, the interactions and placement of docked GDP-mannose was very similar compared to the homology model of yeast DPMS.^[215] However, this results should be han-

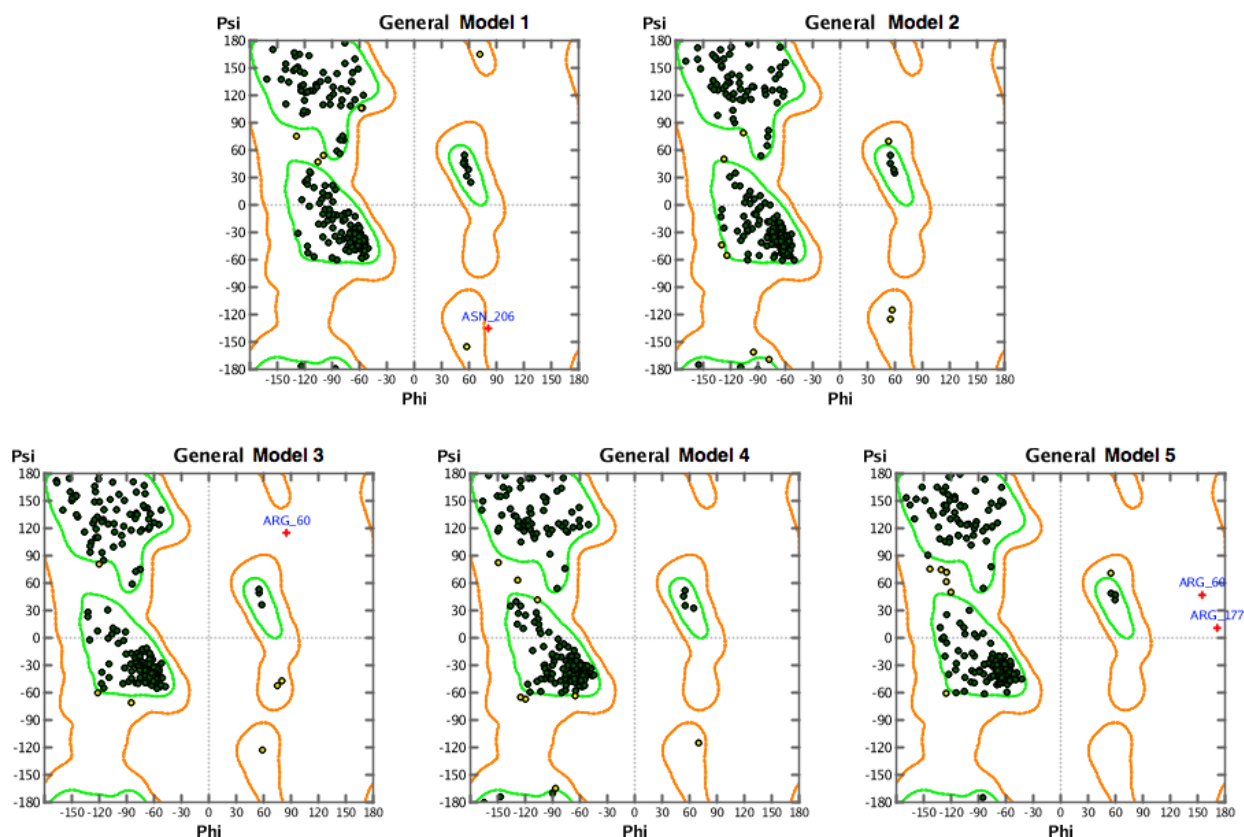


Figure 44: Ramachandran plots of Robetta homology models 1-5; generated with MOE2009.10.^[223]

dled with care, as the homology model is not based on experimental evidence as compared to the yeast DPMS homology model and the closest psi-BLAST hit showed a similarity of only 34.10 %.^[215]

Docking of rhodanine-N-acetic acid derivatives

Homology model 4 has been chosen as the model for the potential DPMS structure, based on re-docking experiments of GDP-mannose to the active site and similar molecular interactions of this substrate as described for yeast DPMS.^[215] In order to investigate the hypothetical binding mode of rhodanine-N-acetic acid derivatives, three-dimensional structures were generated and energy minimised using the MMF94 forcefield option in MOE2009.10.^[223] One of the most active rhodanine-N-acetic acid derivatives against DPMS was the 3-benzyloxy derivative **2c** (23 % residual DPMS activity)^[68], its ethyl ester analogue **14v** has been shown to inhibit GPI-anchor biosynthesis *in vitro* as could be observed by myristate labelling and flow cytometry experiments (Figure 35 and Figure 41 respectively). The energy-minimised ligand **2c** was docked into the active site of the DPMS homology model (HM 4) and consecutively compared

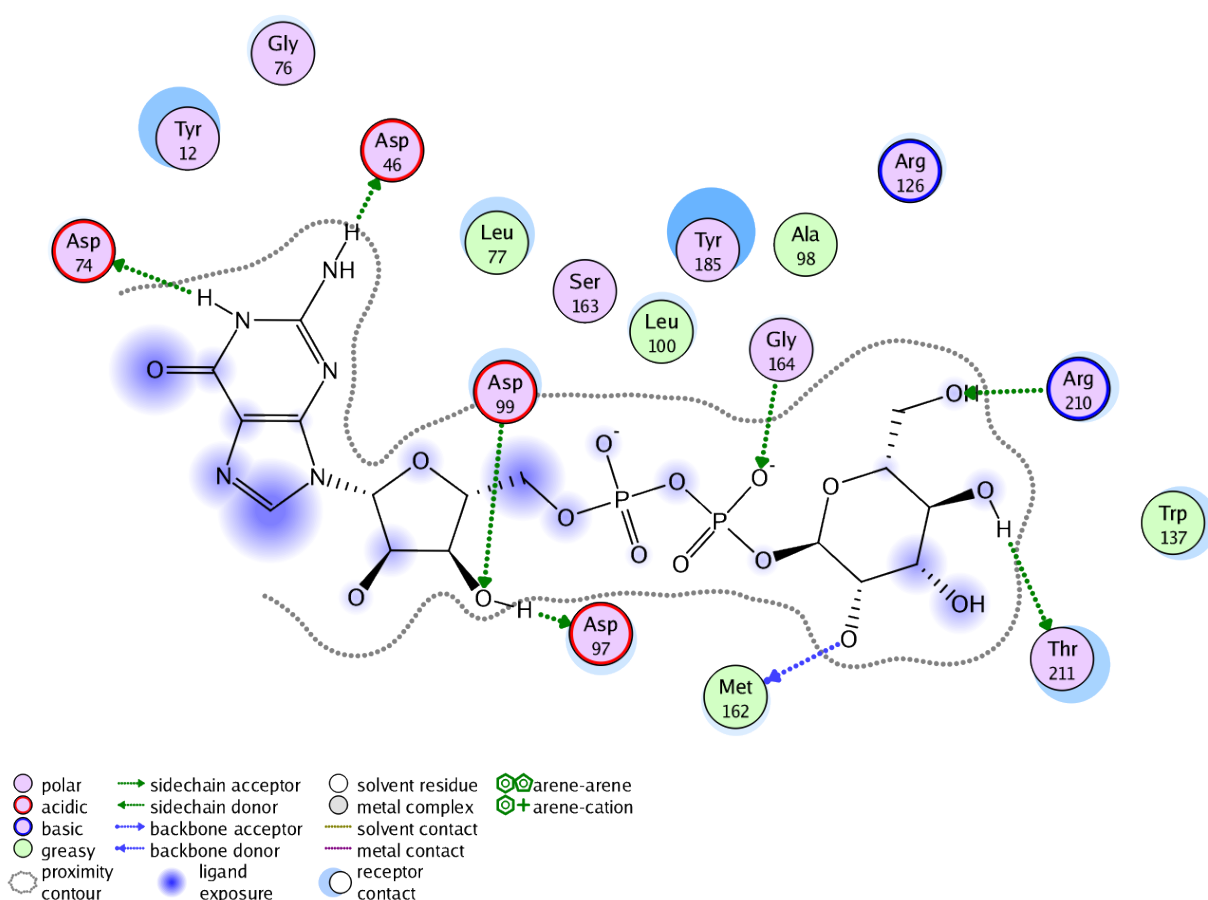


Figure 45: Docking of GDP-mannose into the active site of Homology model 4 using Gold Suite 4.12 (CCDC, Cambridge, UK) and MOE2009.10^[223] for graphical visualisation.

to the proposed binding of GDP-mannose (Figure 47). The predicted docking pose for **2c** was within the mannose and phosphate site of the previously docked GDP-mannose. The 3-benzyloxy substituent fills a small lipophilic pocket within the binding site, possibly explaining the structural requirements of this moiety. However, two arginine residues (Arg126 and Arg210) contribute the most to the binding of **2c** in the active site. Both residues were modelled to undergo close hydrogen-bond interactions (1.9 and 2.2 Å) with carbonyl groups of the rhodanine-moiety and the N-1-carboxylic side-chain. Interestingly, this binding mode was conserved for other docking experiments with rhodanine-N-acetic acid derivatives independent of the 5-benzylidene substitution (data not shown). Rhodanine derivatives were frequently described as phosphate mimics^[68,100,101,103] and this proposed binding mode would be in agreement with this hypothesis. However, here the 5-benzylidene moiety would be in proximity to the phosphate binding site, rather than the rhodanine-moiety as previously hypothesised.^[100]

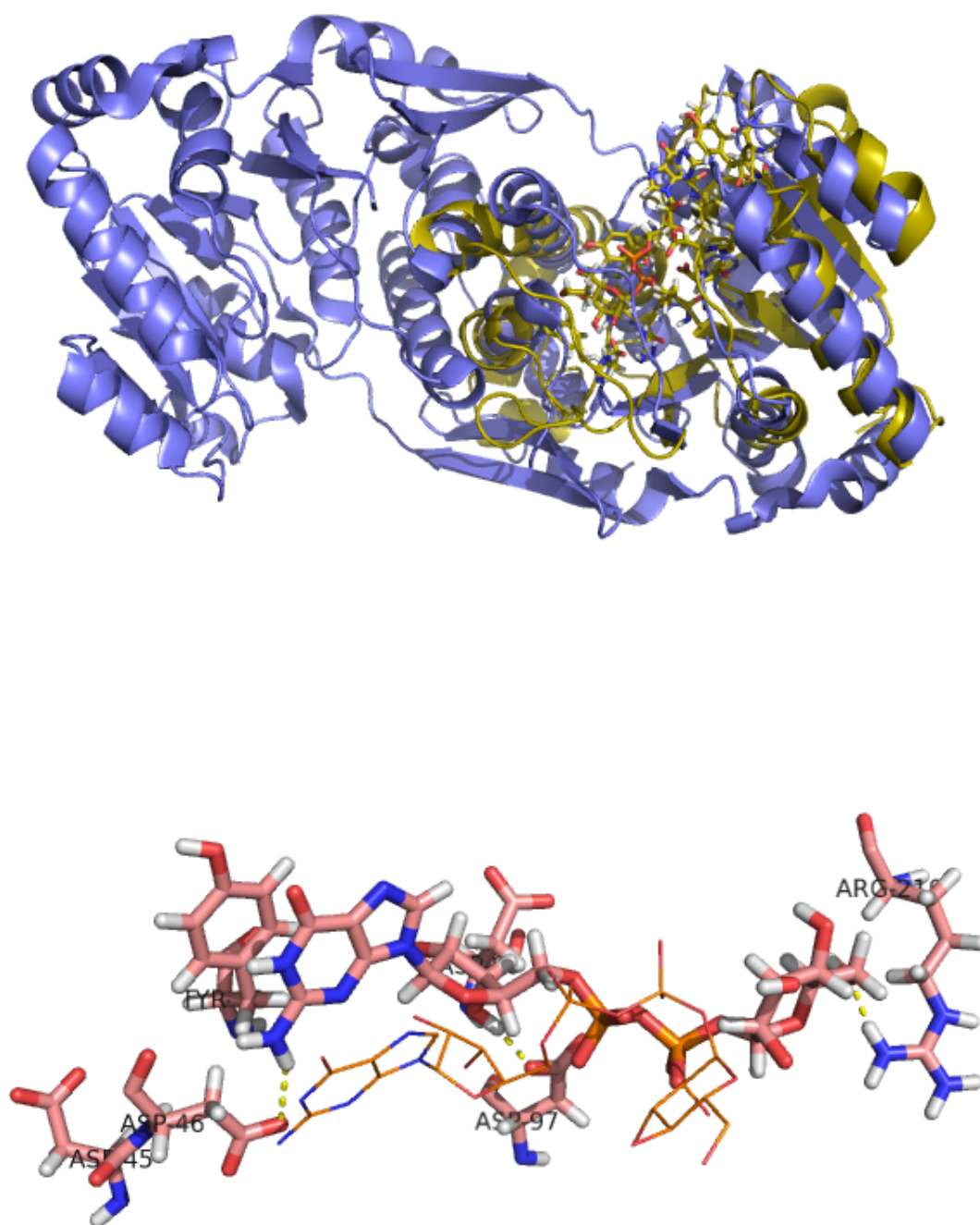


Figure 46: Overlay of homology model (HM) 4 and parent mannosyl-3-phosphoglycerate synthase (MPGS) from *Rubrobacter xylophilus* (3F1Y); in the active site the GDP-mannose substrate from MPGS is displayed as lines, while the re-docked substrate for the HM 4 is shown as sticks together with active site residues of the HM.

Next, with the assumption that the homology model for DPMS is valid, a molecular probe for DPMS has been designed to verify the molecular target *in vitro*. The proposed binding mode of this rhodanine probe **34** is shown in Figure 48. The arginine Arg126 in this proposed binding mode undergoes hydrogen bonding interactions with the N-1-carboxylic side chain, while the rhodanine moiety is placed in close proximity to the phosphate binding side (Asp97 and Asp99). In contrast to previous docking solutions the modified 3-benzyloxy moiety is modelled to undergo pi-stacking interaction with Tyr12, a residue believed to undergo π -stacking interactions with the GDP-nucleotide.^[215]

3.5.5 Investigation of DPMS as a possible target for rhodanine inhibitors

The final step for the target identification was to confirm binding to DPMS and to identify its exact binding mode. Therefore a rhodanine photo-affinity probe (**34**) was designed with the capability to covalently bind to proteins in close proximity upon UV-activation. In this chapter, the experimental setup and results of this target identification study is described. The photo-affinity probe **34** showed activity against *T. brucei* at GI_{50} 12.9 μ M, however compared to the unsubstituted 3-benzyloxy analogue **14v** (GI_{50} 4.4 μ M), the activity decreased by a factor of 3. Both **34** and **14v** did not show any toxicity against HL60 cells at 100 μ M. Further details about the photo-affinity label are described in section 3.2.12. The labelling was carried out in 24 well plates with incubation times varying from 4 to 24 h in the presence of photo-affinity probe **34** and *T. brucei*. Initially a tubular low-pressure mercury-vapour discharge lamp from Phillips with a UV maximum irradiation at 365 nm, a wavelength ideally for initiation of photo-cross-linking to proteins was used.^[179] After UV-activation, the parasites were lysed and proteins precipitated and subjected to Click-chemistry conditions with an alkyne-AlexaFluor488 tag. However, SDS-gel analysis did not show any fluorescent tagged protein bands (results not shown). After this initial experiment it was assumed that the photo-induced coupling to proteins is insufficient. In order to improve the experimental setup, the experiment was repeated as described above, but this time a portable UV-lamp at 254 nm maximum UV-irradiation was used for the photo-cross linking of the probe and the molecular target. Furthermore, this time the fluorescent tag was exchanged with an alkyne-biotin tag, in order to increase sensitivity by concentration of biotin-tagged proteins with streptavidin beads. However, SDS-gel analysis after Coomassie staining did not show any protein bands other than in the negative control without **34**. It seemed that although rhodanine derivatives are described as promiscuous binders,^[82] **34** did not interact with any proteins. As this was rather unlikely considering its biological activity, the problem has to be the photo-cross-linking procedure. Indeed a recent communication with Prof. Keith A. Stubbs (The University of Western Australia) suggested that 24 well plates might not be suitable for the UV-cross linking step and that quartz spectrophotometric cuvettes might increase efficiency of the photo-labelling step due to better light exposure. In order to increase

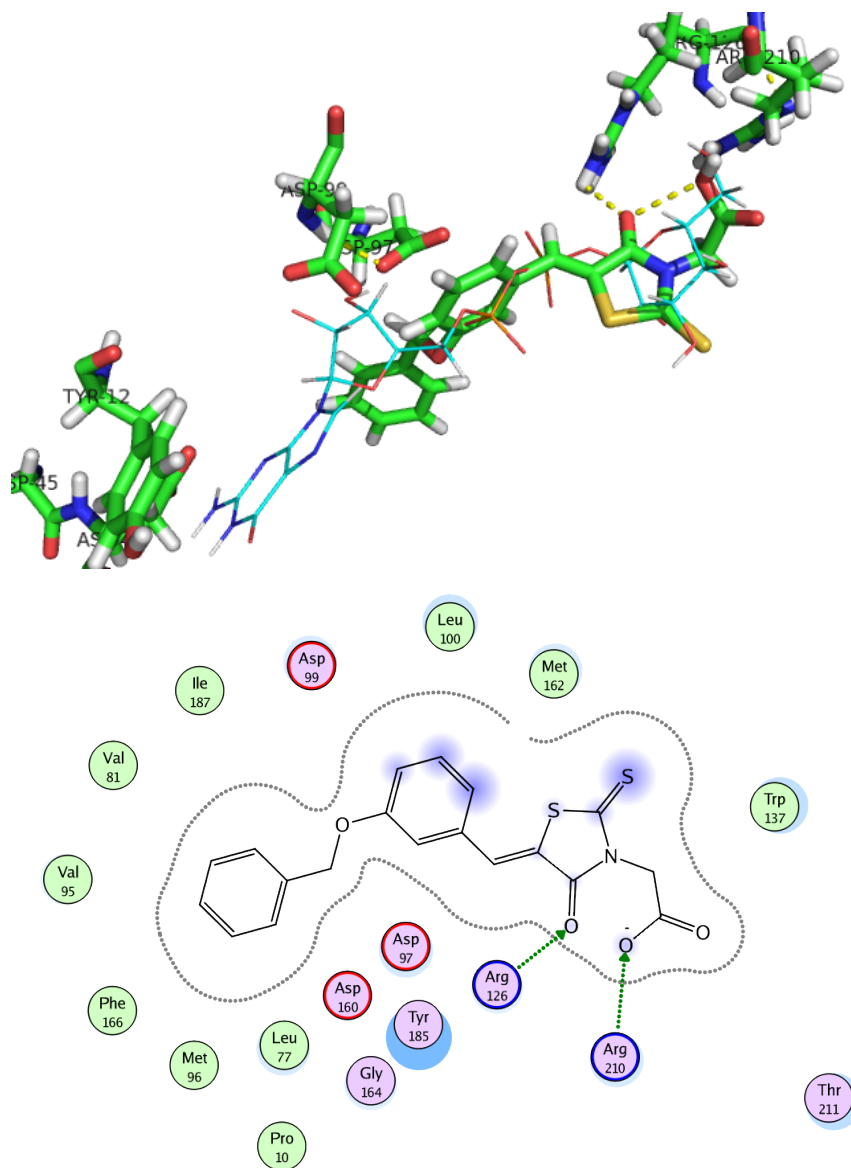


Figure 47: Representative docking result of rhodanine-N-acetic acid derivatives within the active site of homology model 4, upper figure shows the alignment of GDP-Man (lines) with the rhodanine inhibitor (stick); lower figure shows interactions within the active site; pictures were created with MacPymolX11 and MOE.2009.10.

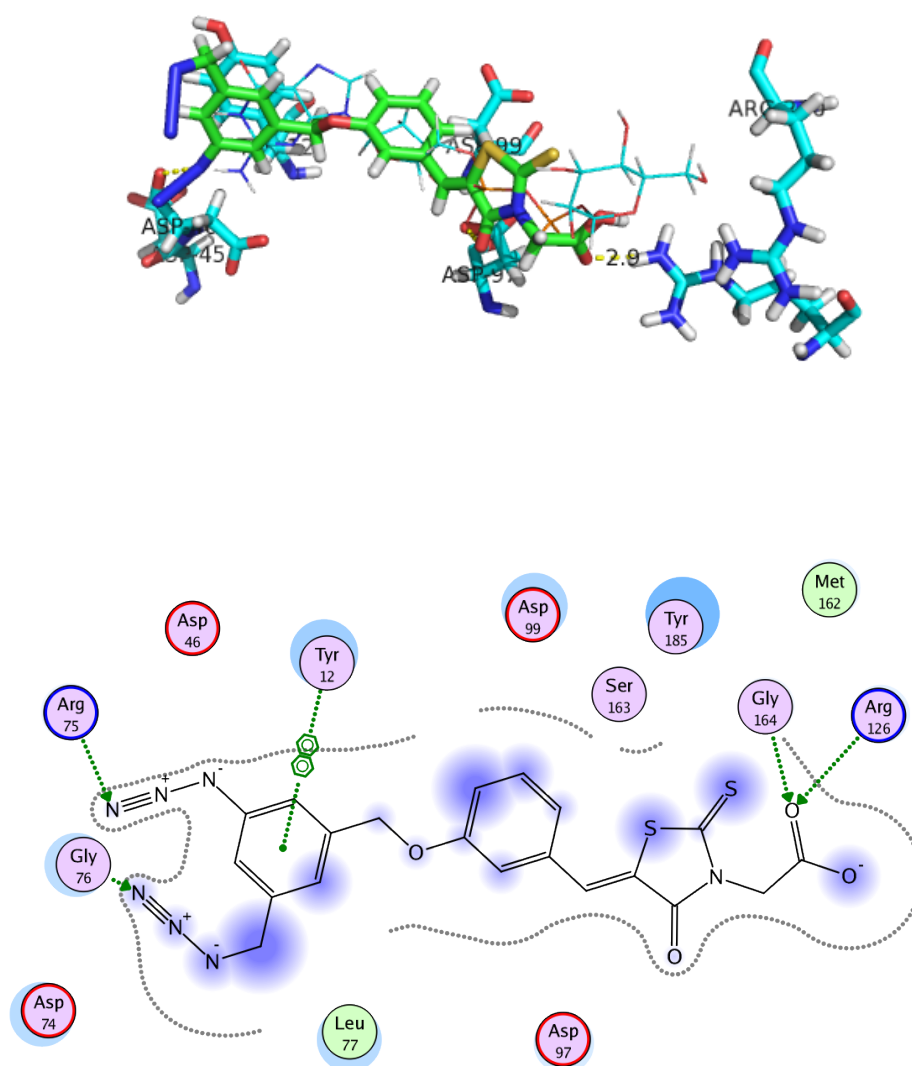


Figure 48: Interactions of rhodanine-probe within the active site of homology model 4, overlaid with GDP-Man (lines); pictures were created with MacPymolX11 and MOE.2009.10.

the sensitivity even further it is planned to lyse the parasite prior to addition of the photo-affinity probe and to initiate the cross-linking within the crude protein mixture.

3.6 Discussion

The rhodanine-N-acetic acid and the related thiazolidine-2,4-dione scaffold are an interesting starting point for the development of broad-spectrum anti-parasitic agents. Numerous biological applications of rhodanine and related compounds have been reported, often this scaffold is described as privileged for its ability to undergo multiple interactions with proteins.^[81,83,91,224] However, recently rhodanine derivatives were suggested to be promiscuous binders and therefore it was crucial in this study to evaluate the anti-parasitic activity always based on previous toxicity studies against HL60 cells.^[82] While in many clinical applications it would be desirable to minimise side-effects, hitting multiple targets in parasites would be beneficial, as resistance is less likely to occur.

The investigations towards anti-parasitic agents started with a report of rhodanine-N-acetic acid derivatives as inhibitors of trypanosomal DPMS, an essential enzyme in GPI-anchor biosynthesis in *T. brucei*.^[68] However none of these derivatives inhibited DPMS completely (at best 10 % residual activity) or showed trypanocidal activity beyond ED₅₀ 96 µM.^[68] Various derivatives of the previously found inhibitors were synthesised in order to increase *in vitro* anti-parasitic activity. A synthetically interesting derivative was the ortho-trifluoromethyl derivative **7e** (Figure 49), as it showed a long range ⁵J_{H,F} coupling constant of 1.9 Hz in ¹H-NMR and ¹³C-NMR experiments. This long range coupling is most likely explained via orbital interactions (Figure 49) of the 1s orbital of H and the 2p orbital of F through-space. The long range coupling was used to determine the double bond configuration as the thermodynamically more stable Z-isomer.^[162] The interaction of the trifluoromethyl group and the CH group and therefore the ⁵J_{H,F} coupling could potentially be used as diagnostic tool for the measurement of intermolecular interaction of **7e** and a target protein. Where disruption of the coupling would indicate binding of the protein towards the probe. A similar experiment has been performed previously with a 5-fluoropyrimidine substituted RNA, where the ⁵J_{F,H} long-range coupling was diagnostic for nucleic acid conformations.^[225] Isomerisation of the exo-cyclic double bond could be induced via a reaction sequence of esterification followed by a Knoevenagel reaction, giving access to various E- and Z-isomer mixtures with the Z-isomer as major product. This racemisation was most likely DMAP induced, as traces of DMAP have been observed.

Various modifications on the 5-benzylidene moiety in rhodanine-N-acetic acid derivatives have been explored, but none of these modifications resulted in improved anti-parasitic activity (GI₅₀ >100). Modifications on the N-3 position of the rhodanine scaffold, such as elongation of the side-linker, have been identified as essential for low µM activity against *T. brucei* (GI₅₀ 9.0-

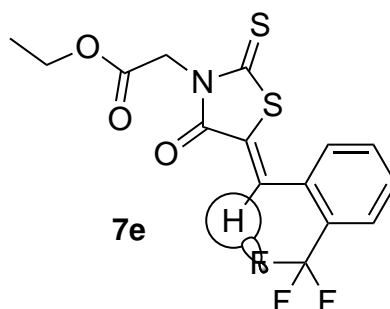


Figure 49: Long-range $^5J_{H,F}$ coupling observed in compound **7e**, possible induced by non-bonded orbital interactions

72.8 μM). Particularly remarkable was the effect of the esterification of the free carboxylic acid, resulting in low μM active compounds against *T. brucei* and *T. cruzi* (GI_{50} 1.3–17.6 μM and 4.7–94.6 μM respectively), whereas the free carboxylic analogues showed no activity at 100 μM . Reduction of the exo-cyclic double bond increased anti-trypanosomal activity, suggesting that Michael acceptor reactivity might not be part of the mode-of-action of these inhibitors.

Of particular interest were the rhodanine-N-acetic ester and thiazolidine-2,4-dione analogues displayed in Figure 50, as they showed low μM activity and selectivity against parasites.

The rhodanine-N-acetic ester derivatives **14b** and **14v** (Figure 50) both showed low μM activity against parasites, but furthermore the parent free carboxylic acid analogue of **14v** has been shown to inhibit DPMS, an essential enzyme in the GPI-anchor biosynthesis.^[68] Further modifications on the benzyloxy-substituent in **14v** increased anti-trypanosomal activity, but also toxicity against HL60 cells. The meta-methyl substituted *tert*-butyl ester **14b** showed broad anti-parasitic activity in the lower μM range against *T. brucei*, *T. cruzi* and *L. infantum* (GI_{50} 1.8, 5.1 and 2.4 μM respectively).

The para-*tert*-butyl derivative **14o** (Figure 50) showed excellent anti-trypanosomal activity against *T. brucei* at GI_{50} 1.7 μM , moderate activity at GI_{50} 23.4 μM against *L. infantum* and no activity against *T. cruzi*.

A 2-pyridinyl substituent on position 5 of the rhodanine moiety resulted in trypannocidal activity against *T. brucei* and *T. cruzi* (GI_{50} 1.5 μM and MIC 100 μM respectively) and had good selectivity indices for *T. brucei* (SI >67).

The ethyl esters of the meta-methyl (**14a**) and 3-benzyloxy (**14v**) derivatives were chosen for further mode-of-action studies. Using a myristic acid probe in combination with a fluorescent tag, allowed the identification of GPI-anchor biosynthesis as possible target, indicated by decreasing intensities of GPI-anchored proteins using in-gel fluorescence. In order to further evaluate GPI-anchor biosynthesis as potential target, flow cytometry experiments with FITC-

as the increased lipophilicity might aid membrane diffusion and possible result in low μM activity against *L. infantum*. Alternatively the N-3 side chain could be elongated to increase lipophilicity. In order to further optimise the anti-parasitic activity and to confirm the molecular target, a photo-affinity probe has been designed, where two azides, a photo-activable aromatic azide and an aliphatic azide for fluorophore-tagging, were attached to the 3-benzyloxy-moiety of **14v**. However, attempts to identify the target protein failed, most likely due to missing photo-reactivity of the probe with the target in 24 well plates. Once the reaction conditions are optimised and cross-labelling between the probe and the target protein occur, further mass spectrometry studies would help to identify the protein-sequence, the mass and potentially the amino-acid residues where the labelling occurred.

Another interesting class of rhodanine and thiazolidine-2,4-dione derivatives had a catechol moiety on position 5. The derivatives **14t**, **15f**, and **7k** were among the most potent inhibitors of *T. brucei* growth (GI_{50} 0.9-1.6 μM). **14ab** also showed anti-leishmanial activity at GI_{50} 45.9 μM , but unfortunately high toxicity against HL60 was also observed (GI_{50} 31.2 μM). However, **14t** and its thiazolidine-2,4-dione analogue **7k** showed no toxicity against HL60 at 100 μM . The free acid of **14t**, **2u** showed no activity against any enzymes of the GPI-anchor biosynthesis, suggesting a different mode-of-action. **2u** has previously been reported as probe for many dehydrogenases, possible by mimicking the cofactor NAD(P)H.^[107,108] The aldose reductase 14- α demethylase CYP51 plays an important role in sterol synthesis in *T. brucei*, *T. cruzi* and possible *L. infantum*.^[111] It would be possible that **14t** and **7k** act as inhibitors for this or similar NAD(P)H dependent enzymes in parasites, explaining their low μM activity. A possible strategy to confirm this hypothesis would be the use of in-gel protein-affinity binding of **2u**. A similar strategy has been employed previously, where **2u** has been shown to be a weak fluorophore, and this property in combination with target-affinity has led to the identification of lactate dehydrogenase isozymes and 1-deoxy-D-xylulose-5-phosphate reductoisomerase as targets of **2u** in *Escherichia coli*.^[108] Therefore in future experiments, crude protein extracts of *T. brucei* would be separated on a Western-blot gel, this gel would be stained with **2u**, washed with buffer and the fluorescent proteins visualised (λ_{ex} =465 nm, λ_{em} =535 nm emission).^[108]

3.7 Summary

130 rhodanine-N-acetic and related analogues have been synthesised and screened against *T. brucei*, *T. cruzi* and *L. infantum* in a whole cell activity assay.

At the same time all 130 derivatives were screened against HL60 cells for evaluation of toxicity against mammalian cells.

77 out of 130 derivatives were able to completely kill *T. brucei in vitro* at 100 μ M (MIC 100 μ M), a further 25 of them showed trypanocidal effects at 10 μ M (MIC 10 μ M).

27 out of 130 derivatives killed *T. cruzi* at 100 μ M (MIC 100 μ M).

8 out of 130 derivatives killed *L. infantum* at 100 μ M (MIC 100 μ M).

6 out of 130 derivatives showed anti-parasitic activity against *T. brucei*, *T. cruzi* and *L. infantum* in the whole cell activity screen, but only one compound (**14b**) had a good activity and selectivity profile. This *tert*-butyl ester analogue **14b** showed broad anti-parasitic activity against *T. brucei*, *T. cruzi* and *L. infantum* (GI₅₀ 1.8, 5.1 and 2.4 μ M, SI 14, 5 and 10 respectively).

Primary whole organism phenotypic screens allowed identification of inhibitors with low μ M anti-parasitic activity (GI₅₀ 0.9-17.6 μ M) and good selectivity (SI >62.5 - 2).

Target identification studies, comprising metabolic labelling with myristate analogues, flow cytometry with FITC-labelled transferrin and cell-free radio-label assays for GPI-synthesis in *T. brucei* allowed the identification of GPI-anchor synthesis as potential target, with DPMS and/or MT-1 as molecular targets.

Taken together, these results provide further evidence that GPI anchor biosynthesis is a drugable target for the development of novel anti-parasitic agents.

Catechol modified rhodanine-N-acetic ester analogues have been identified in a whole cell assay as low- μ M growth inhibitors of *T. brucei* (GI₅₀ 0.9-1.4 μ M, SI 21 - >75) with no activity in GPI-anchor biosynthesis and with unknown mode-of-action.

4 N-allyl rhodanine derivatives

4.1 Background on previous biological activities of N-allyl rhodanine and N-allyl thiazolidine-2,4-dione derivatives

The following introduction serves as an overview of previous reports about N-allyl rhodanine and related analogues. Previous biological studies on these inhibitor classes might have a similar effect in parasitic protozoa and therefore it is important to know about their mode-of-action in other organisms (Figure 51).

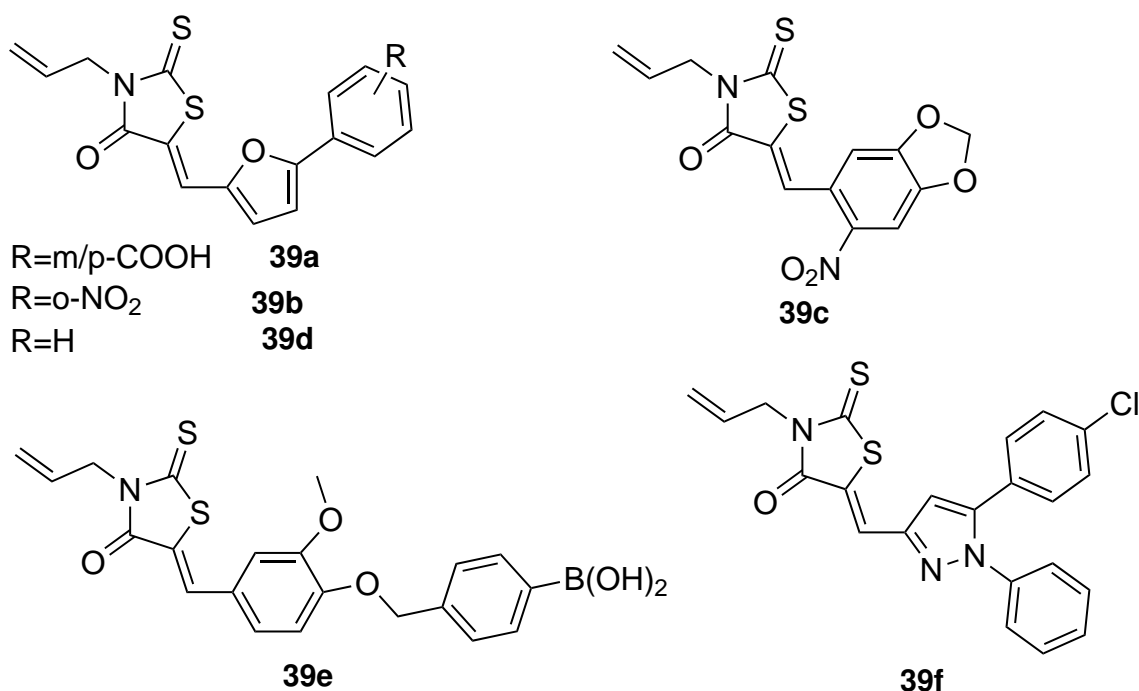


Figure 51: Examples of previously N-allyl rhodanine and N-allyl thiazolidine-2,4-dione derivatives.

N-allyl rhodanine and N-allyl thiazolidine-2,4-dione derivatives represent a compound class, which exhibits a broad activity spectrum and a low toxicity profile.^[114,226–233] N-allyl rhodanine derivatives from type **39a** have been described as anti-microbial agents, with activity against gram-positive bacteria including multi-drug resistant strains.^[226,227] Compound **39a** has furthermore been reported as an inhibitor of bacterial RNA polymerase and did not show any toxicity against growth of chinese hamster ovary cells, *Candida albicans* or *Aspergillus fumigatus*.^[226,231,232] However, a recent study on the inhibitory effect of **39a** and similar analogues showed inhibition of multiple enzymes in bacteria, such as malate dehydrogenase and chymotrypsin in addition to RNA polymerase.^[229] Using biomolecular approaches (bacterial mu-

tants exhibiting luciferase activity upon inhibition of particular targets), it was revealed that **39a** inhibit DNA biosynthesis and has membrane damaging effects.^[229] Consequently, **39a** was considered unattractive as an inhibitor of bacterial RNA polymerase.^[229] These studies indicate that rhodanine-N-allyl derivatives could also exhibit DNA damaging effects in parasites.

Furanyl rhodanine derivatives **39b** and **39c** have been reported as inhibitors of the non-structural protein 3 in Hepatitis C virus (HCV NS3).^[114] Although **39b** and **39c** are inhibitors against HCV NS3, they also showed activity against other serine proteases, namely chymotrypsin and plasmin.^[114] Furthermore, furanyl rhodanine derivatives **39d** have been shown to inhibit Sortase A, a trans-peptidase essential to attach surface proteins in *Staphylococcus aureus*.^[230]

Also the N-allyl thiazolidine-2,4-dione scaffold shows interesting pharmacological activity. Compound **39e** has been reported as an inhibitor of Autotaxin, a phosphodiesterase thought to have implications for tumor progression, metastasis, inflammation and fibrotic diseases.^[157] Compound **39e** has further been shown not to exhibit Michael addition reactivity to Autotaxin.^[157]

The pyrazole N-allyl thiazolidine-2,4-dione derivative **39f** has been studied for its anti-inflammatory and anti-neurotoxicity profile, showing that in particular NAD(P)H oxidase inhibition is effected.^[233] This hybrid molecule further showed no toxicity in animals at 300 mg/kg.^[233]

Recently thiazolidine-2,4-dione derivatives have been assessed as inhibitors against β -ketoacyl carrier protein synthase.^[228] While there have been reports of N-allyl rhodanine and N-allyl thiazolidine-2,4-dione derivatives as anti-bacterials, anti-viral, anti-inflammatory and anti-toxicity agents, there are no reports about their anti-parasitic activity.^[114,226–233] However, a patent about the use of these analogues as anti-parasitic agents against *Toxoplasma gondii* has been filed.^[234]

Rhodanine-N-allyl derivatives and analogues exhibit broad biological activity and were chosen as interesting candidates for the development as broad-spectrum anti-parasitic agents, as relatively little is yet known about their anti-trypanosomal and anti-leishmanial properties. Furthermore, it was of interest to compare this compound class with the rhodanine-N-acetic acid derivatives for their GPI anchor biosynthesis inhibition activity. The reported toxicity profile suggested low toxicity,^[226,231,232] but DNA damaging effects in bacteria were reported.^[229]

4.2 Synthesis of inhibitor library

In this chapter the synthesis of N-allyl rhodanine and N-allyl thiazolidine-2,4-dione derivatives as anti-parasitic agents is described.

The general molecular structure of N-allyl rhodanine and thiazolidine-2,4-dione derivatives is shown in Figure 52. This scaffold has large scope for modifications in order to improve

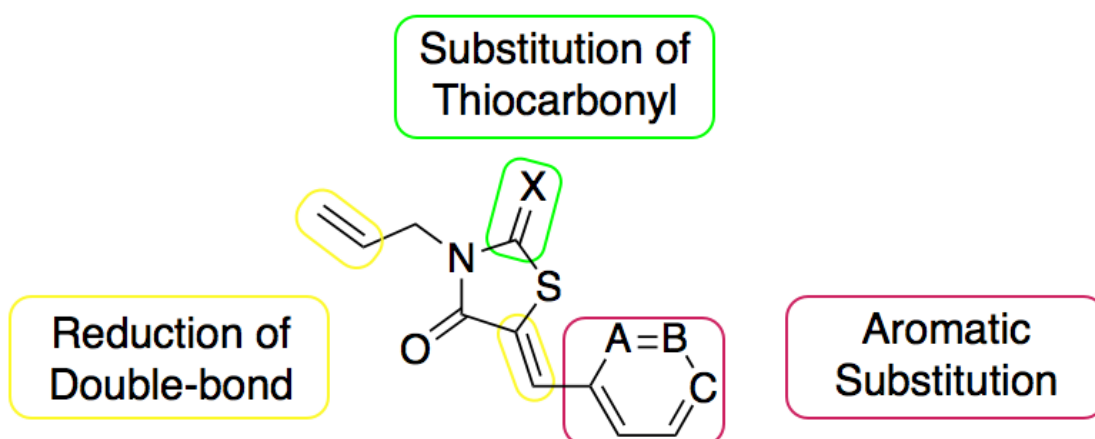
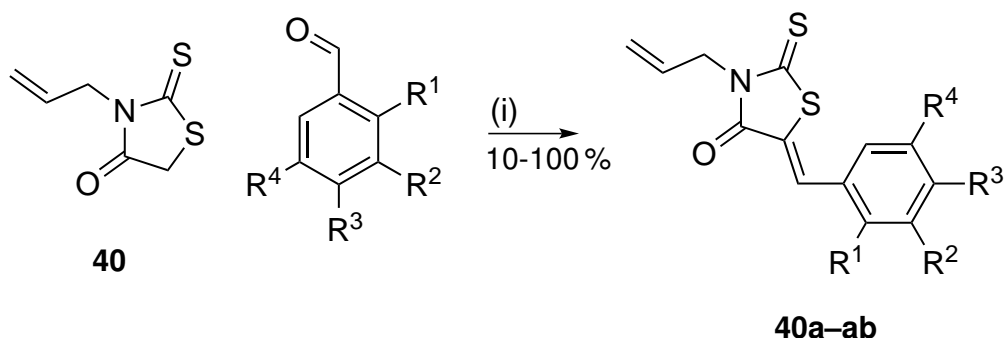


Figure 52: Synthetic strategy for N-allyl rhodanine and N-allyl thiazolidin-2,4-one derivatives as anti-parasitic agents; X=O,S; A,B,C: variable aromatic substitution.

anti-parasitic activity. Therefore several aromatic substitutions (A,B,C=N or CR) on the 5-position of this scaffold have been pursued (Figure 52). But also modifications on the exocyclic thiocarbonyl (X=S,O) have been explored. Furthermore, the influence of the exo-cyclic double bond was examined through the synthesis of saturated analogues.

4.2.1 Aromatic Substitution

The rhodanine derivatives were synthesised starting from N-allyl rhodanine **40**, which was subjected to Knoevenagel condensation reactions with various benzaldehyde derivatives in the presence of sodium acetate as the base (Scheme 22). The Knoevenagel reaction resulted in the formation of the desired 5-benzylidene modified N-allyl rhodanine derivatives **40a–ae** in good yields of 10-100 %.



Scheme 22: Knoevenagel condensation reaction of N-allyl rhodanine derivatives; (i) NaOAc, ethanol, 80 °C; for R¹-R³ substitutions see Table 28, see Table 28.

All products crystallised from the ethanol reaction mixture and were afforded by simple filtration, thus the yield of the reaction was dependant on the ability to form crystals. NMR analysis of the CH-signal in the N-allyl rhodanine derivatives **40a–ae** showed only the Z-isomer (δ_H 7.57–8.08 ppm, δ_C 128.6–135.3 ppm) of the exo-cyclic double bond. The configuration of the double bond was further validated by an X-ray structure of **40ac**. The X-ray structure showed the Z-configuration of the double bond (Figure 53). Molecules of **40ac** were stacked above each other, with the rhodanine core being in a plane of the 5-benzylidene moiety. The alternate arrangement of **40ac** along the stacked columns showed a slight offset in their alignment in the planes (Figure 53). The N-allyl group orientated in two distinct orientations alongside these planes. The crystal structure of **40ac** most likely represents a general representation of the crystal packing in compounds of the type **40a–ae**, explaining their tendency to form crystals. Although similar packing might be expected in other types of rhodanine derivatives, no other derivatives showed as facile crystallisation properties.

Another interesting observation in the ^1H - and ^{13}C -NMR spectra of **40e** (Table 28) was a $^5J_{H(C),F}$ -coupling constant of 1.9 Hz. This phenomenon was previously observed with similar rhodanine analogues in this research study (Chapter 3.2.5). The nature and underlying mechanism of the long-range coupling is discussed in Figure 20.

4.2.2 Replacement of the Thiocarbonyl X=O

The thiocarbonyl group in rhodanine derivatives have been shown to be in part responsible for their versatile ability to bind to different proteins (see also Chapter 3.2.6).^[83] Replacement of this group has previously been shown in this study to decrease toxicity against HL60 cells in rhodanine-N-acetic acid derivatives (Chapter 3.3.8). The replacement of the thiocarbonyl by a carbonyl group might potentially increase target selectivity and may result in decreased toxicity.

Synthesis of the N-allyl thiazolidine-2,4-dione precursor

The N-allyl or N-propargyl thiazolidine-2,4-dione derivatives **41** and **42** were synthesised starting from thiazolidine-2,4-dione. Two strategies have been chosen for the synthesis of substituted thiazolidine-2,4-dione derivatives **41** and **42** (Scheme 23, refnallyldionesynthesistable).

The first approach was nucleophilic substitution of thiazolidine-2,4-dione with allyl- or propargyl alcohol using Mitsunobu reaction conditions (method (i) in Scheme 23, Table 29). In the first reaction sequence the active reagent of the Mitsunobu reaction has to be prepared by addition of di-*tert*-butylazodicarboxylate (DEAD) to a -78°C cooled solution of triphenylphosphine (PPh_3) in anhydrous THF. In the consecutive step, the thiazolidine-2,4-dione and the corresponding alcohol were added and the reaction mixture was stirred subsequently at room

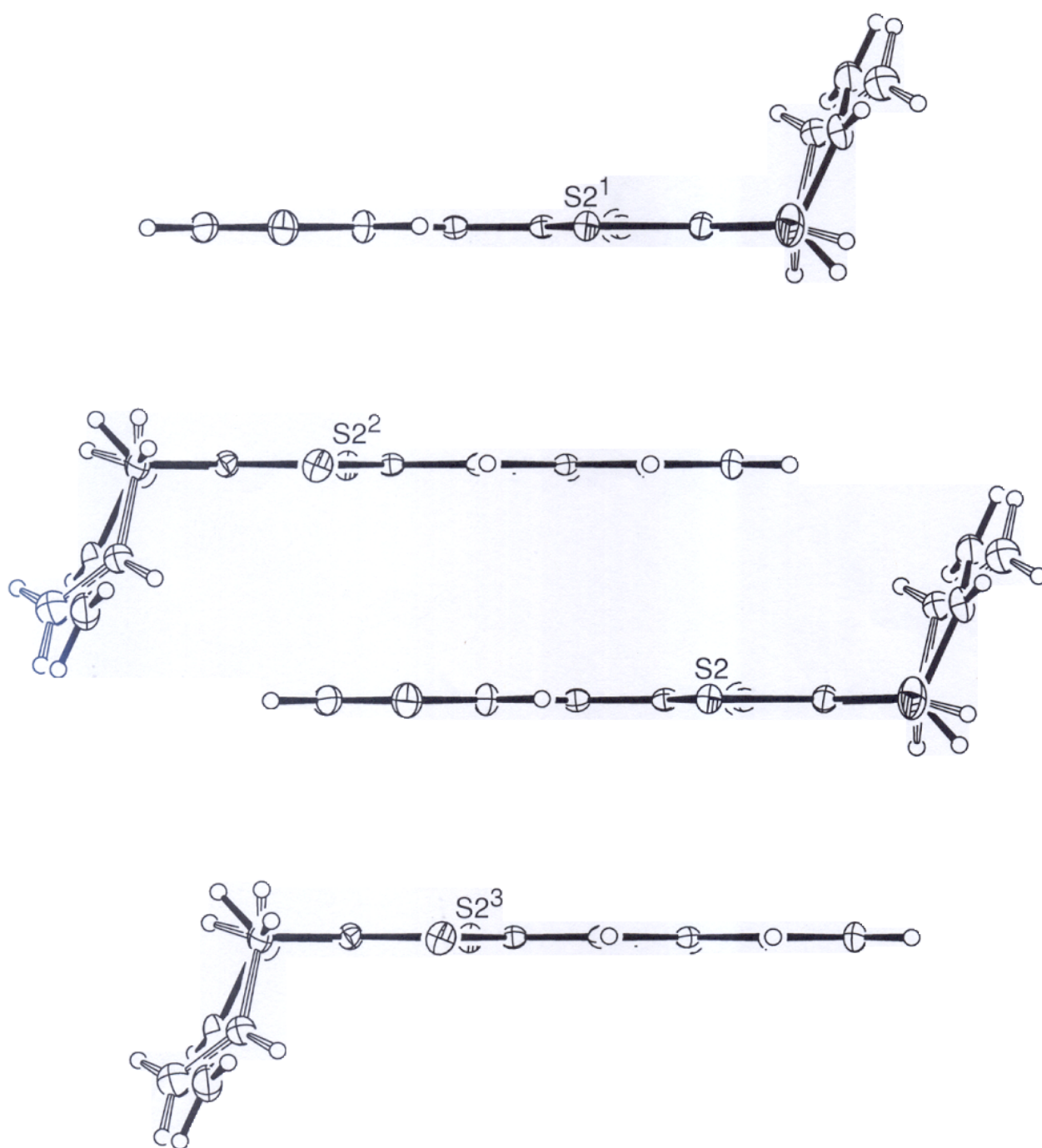
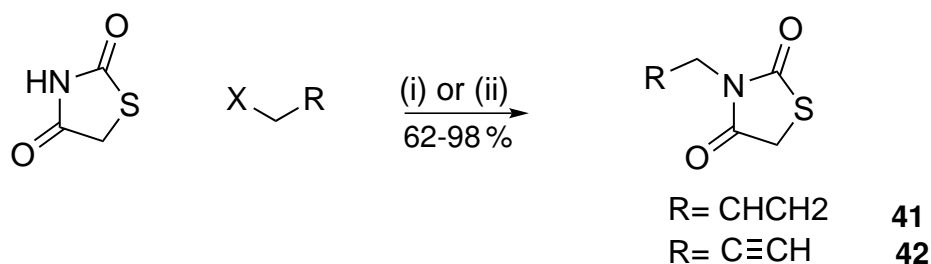


Figure 53: View of stacking of **40ac** along the b axis. The X-ray structure was kindly recorded by Dr. David Hughes (UEA, Norwich, UK).

Table 28: Knoevenagel condensation reaction of N-allyl rhodanine derivatives; R¹-R³ for rhodanine N-allyl derivatives **40a–ae**; yield and chemical shift of CH-signal, see Scheme 22.

#	R ¹	R ²	R ³	R ⁴	[%] yield	NMR chemical shifts of CH-signal [ppm]		
						δ_{solvent}	δ_H	δ_C
40a	H	H	H	H	31	CDCl ₃	7.74	133.4
40b	CH ₃	H	H	H	100	CDCl ₃	7.98	131.2
40c	H	CH ₃	H	H	49	CDCl ₃	7.70	133.7
40d	H	H	CH ₃	H	82	DMSO-d ₆	7.81	133.2
40e	CF ₃	H	H	H	22	CDCl ₃	8.01	128.6
40f	H	CF ₃	H	H	50	CDCl ₃	7.73	131.0
40g	H	H	CF ₃	H	70	CDCl ₃	7.73	130.9
40h	H	H	Cl	H	53	CDCl ₃	7.67	131.9
40i	H	H	CN	H	57	CDCl ₃	7.68	130.0
40j	H	H	CCH	H	49	CDCl ₃	7.69	132.0
40k	H	Br	OMe	H	66	CDCl ₃	7.79	129.6
40l	H	Br	F	H	52	CDCl ₃	7.61	130.2
40m	H	NO ₂	H	H	21	CDCl ₃	7.75	129.6
40n	H	H	Nme	H	32	CDCl ₃	7.68	n.a.
40o	H	H	NHAc	H	52	CDCl ₃	7.69	129.7
40p	OH	H	H	H	87	CDCl ₃	8.20	130.3
40q	H	OH	H	H	45	CDCl ₃	7.67	133.0
40r	H	H	OH	H	50	CDCl ₃	7.69	133.5
40s	OH	H	OH	H	47	CDCl ₃	8.08	131.1
40t	H	OH	OH	H	15	MeOD-d ₄	7.57	135.3
40u	H	OMe	OH	OMe	78	DMSO-d ₆	7.74	134.6
40v	H	H	SO ₂ Me	H	42	CDCl ₃ /DMSO-d ₆	7.72	130.0
40w	H	H	CHO	H	27	CDCl ₃	7.62	n.a.
40x	H	OBn	H	H	10	CDCl ₃	7.69	133.2
40y	H	H	OBn	H	69	CDCl ₃	7.69	133.4
40z	H	OBn	OBn	H	51	CDCl ₃	7.60	133.6
40aa	H	H	B(OH) ₂	H	decomposition			



Scheme 23: Synthesis of N-allyl thiazolidine-2,4-dione derivative **41** and analogue **42**; (i) allyl or propargyl alcohol, PPh_3 , DEAD, $-78^\circ\text{C} \rightarrow \text{rt}$, THF; (ii) allyl bromide, NaH, $0^\circ\text{C} \rightarrow \text{rt}$, DMF; for substituents of X and R see Table 29, see Table 29.

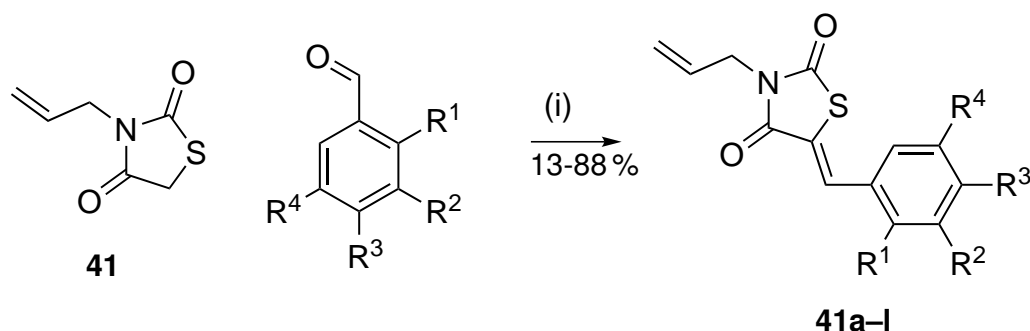
Table 29: Synthesis of N-allyl thiazolidine-2,4-dione derivative; X and R for synthesis of **41** and **42**; methods and yields, see Scheme 23.

#	x	R	Method	yield [%]
41	OH	CHCH_2	(i)	84
41	Br	CHCH_2	(ii)	62-86
42	OH	CCH	(i)	98

temperature. The products were obtained after column chromatography as clear oils and in good yields of 84-98 %. The second approach was the base-catalysed nucleophilic substitution with allyl bromide and thiazolidine-2,4-dione in the presence of sodium hydride (NaH) (method (ii) in Scheme 23). The reaction was carried out in DMF and under a nitrogen gas atmosphere. The yields of 62-67 % were slightly decreased compared to the Mitsunobu approach, but the reaction procedure was facilitated, as no reagents needed to be formed prior to reacting the substrates and the reaction could be carried out under ice-cooling compared to cooling to -78°C . In summary, both methods were suitable for the formation of the precursors **41** and **42**.

Knoevenagel reaction of thiazolidine-2,4-dione analogue **41** with benzaldehyde derivatives

The N-allyl thiazolidine-2,4-dione precursor **41** was subjected to various benzaldehyde derivatives in a Knoevenagel condensation reaction (Scheme 24). The condensation products were afforded in yields of 13-88 % mostly as white solids. The replacement of the thiocarbonyl group resulted in a complete loss of the previous yellow to red colour of the rhodanine analogue. The purification method of the previous reaction protocol for rhodanine derivatives needed to be adjusted, as most of the products **41a-m** did not precipitate from ethanol. However, alternative purification via extraction and column chromatography succeeded in the isolation of the desired products **41a-m** (Table 30). The low yield of the reaction might correspond to im-



Scheme 24: Synthesis of N-allyl thiazolidine-2,4-dione derivatives **41a-m** and **42**; (i) NaOAc, 80 °C, EtOH; for substitutions of R¹-R⁴ see Table 30.

proved water-solubility of the condensation products and therefore loss of product during the extraction process. The carbonyl group in thiazolidine-2,4-dione derivatives can form specific hydrogen-bonds to water molecules, which need to be disrupted, prior to binding to a molecular target, thus potentially leading to more target selectivity.^[83] In contrast the analogous thiocarbonyl derivatives undergoes less specific hydrogen bonds with water and desolvation is facilitated.^[83]

Compounds **41a** and **41e** (Table 30) showed a long-range $^5J_{H(C),F}$ -coupling of 1.5-1.9 Hz (discussed previously in chapter 4.2.1). The coupling constant of 1.5 Hz for **41e** is slightly lower compared to the previous observed long-range couplings of 1.9-2.0 Hz. This decrease is most likely due to the electron-withdrawing effect of the other trifluoromethyl group in the 5-benzylidene-residue. All products **41a-m** were afforded as the Z-double bond isomer as confirmed by the chemical shift of the CH-signal in 1H - and ^{13}C -NMR experiments. The chemical shifts were between 7.74-8.23 ppm depending on the deuterated solvent used and were in the same region as observed with all other analogues in Z-configuration.

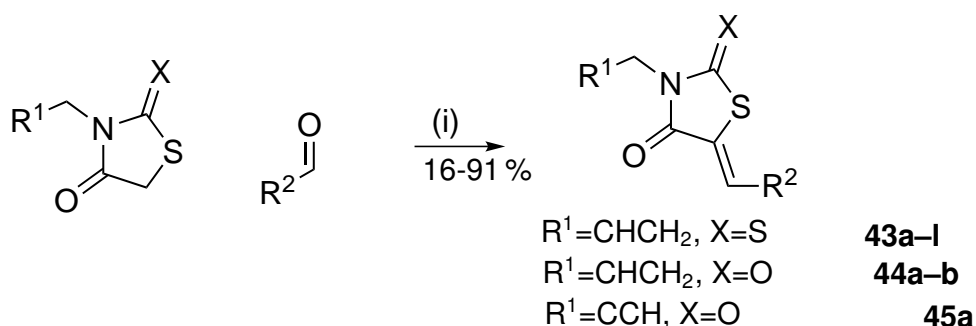
4.2.3 Introduction of 5-benzylidene-3-benzyloxy- and heterocyclic modifications on the N-allyl rhodanine 40 and thiazolidine-2,4-dione derivatives 41 and 42

In this chapter, the synthesis of condensation products, bearing heterocyclic modification on position 5 of the rhodanine or thiazolidine-2,4-dione moiety, is described. Furthermore, modifications on the 5-benzylidene-3-benzyloxy-substituent were explored and the condensation of non-aromatic aldehydes and difunctionalised aromatic aldehyde derivatives were investigated. The installation of further modifications on position 5 of the thiazolidine-4-one moiety possible helps the identification of compounds with improved anti-parasitic activity. In particular heterocyclic aldehydes have different electronic properties, such as charge or the ability to interact in hydrogen bonding than compared to simple benzylidene modifications. In a structure activity relationship study this important information would be invaluable.

Table 30: Synthesis of N-allyl thiazolidine-2,4-dione derivatives; R¹-R⁴ for derivatives **41a–m** and **42**; yield and NMR chemical shift of CH-signal, see Scheme 24.

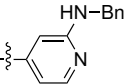
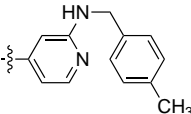
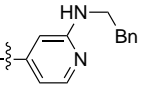
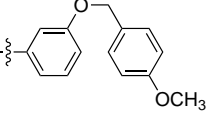
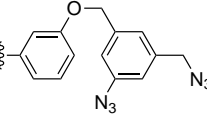
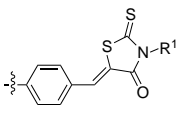
#	R ¹	R ²	R ³	R ⁴	[%] yield	NMR of CH-signal [ppm]		
						δ_{solvent}	δ_H	δ_C
41a	CF ₃	H	H	H	35	CDCl ₃	8.18	129.7
41b	H	CF ₃	H	H	14	CDCl ₃	7.92	132.0
41c	H	H	CF ₃	H	66	CDCl ₃	7.91	132.0
41d	H	CF ₃	H	CF ₃	no product			
41e	CF ₃	H	CF ₃	H	25	CDCl ₃	8.01	129.9
41f	OH	H	H	H	19	MeOD-d ₄	8.27	130.6
41g	H	OH	H	H	35	CDCl ₃	7.85	133.9
41h	H	H	OH	H	46	CDCl ₃	7.86	134.2
41i	H	OH	OH	H	13	MeOD-d ₄	7.74	135.6
41m	OH	H	OH	H	15	MeOD-d ₄	8.23	131.0
41j	H	OBn	H	H	88	CDCl ₃	7.83	133.9
41k	H	H	OBn	H	88	CDCl ₃	7.84	133.8
41l	H	OBn	OBn	H	72	CDCl ₃	7.75	134.0

Initially, simple pyridine-carboxaldehyde derivatives were subjected to **40**, **41**, and **42** in a Knoevenagel condensation reaction (Scheme 25). The products **43a**, **43b**, **43c**, **44a**, and **45a** (Table 31) were obtained in yields of 23-91 % after column chromatography. The chemical shift δ_H of the CH-signal (7.62-7.83 ppm) indicated the formation of the thermodynamically more stable Z-configuration of the double bond.^[158] Next, 2-halogen-substituted pyridinecar-

**Scheme 25:** Synthesis of modified N-allyl rhodanine and thiazolidine-2,4-dione derivatives; (i) NaOAc, 80 °C, EtOH, see Table 31.

boxaldehyde derivatives were reacted with **40**. The 2-chloro-substituted pyridine derivative **43d** (Table 31) was afforded in good yields of 44 %, while reaction of the 2-bromo-analogue resulted only in the formation of decomposition products. This observation was very similar to

Table 31: Synthesis of modified N-allyl rhodanine and thiazolidine-2,4-dione derivatives; X, R¹-R²; yields and chemical shift of CH-signal of modified N-allyl rhodanines and thiazolidine-2,4-dione derivatives, see Scheme 25.

#	X	R ¹	R ²	[%] yield	NMR shift of CH-signal [ppm]		
					δ_{solvent}	δ_H	δ_C
43a	S	Allyl	2-pyridinyl	91	CDCl ₃	7.62	128.0
43b	S	Allyl	3-pyridinyl	47	CDCl ₃	7.71	128.7
43c	S	Allyl	4-pyridinyl	42	CDCl ₃	7.62	129.2
44a	O	Allyl	4-pyridine	23	CDCl ₃	7.79	130.6
45a	O	Propagyl	4-pyridine	26	CDCl ₃	7.83	131.3
43d	S	Allyl	2-chloropyridinyl	44	CDCl ₃	7.55	n.a.
43e	S	Allyl	2-bromopyridine	no product			
43f	S	Allyl	25c 	54	CDCl ₃	7.41	n.a.
43g	S	Allyl	25g 	32	CDCl ₃	7.49	131
43h	S	Allyl	25a 	no product			
43i	S	Allyl	18c 	90	CDCl ₃	7.69	133.4
43j	S	Allyl	33f 	66	CDCl ₃	7.17	n.a.
43k	S	Allyl	hexanol	no reaction			
43l	S	Allyl		16	DMSO-d ₆	7.82-7.84	n.a.

the condensation reaction with the rhodanine-N-acetic ethyl ester **14**, as no product could be isolated in both cases after column chromatography (Scheme 14).

Previously, 2-amino-substituted aldehydes were synthesised to explore their structure activity relationship in comparison to 5-benzylidene-3-benzyloxy substituents (NHBn vs. OBn) and simple pyridine derivatives (Scheme 15). The aldehydes **25a**, **25c**, and **25g** were reacted with **40**. The 2-aminobenzyl aldehydes **25c** and **25g** led to the formation of the desired products **43f** and **43g** (Table 31) in yields of 32-54 %. In contrast, the 2-amino aldehyde **25a** (NHCH₂Bn) did not react with **40** and only starting materials were recovered.

In order to explore the anti-parasitic effect of 5-benzylidene-3-benzyloxy modified N-allyl rhodanine derivatives, the modified 3-benzyloxy benzaldehyde **18c** was subjected to Knoevenagel reaction conditions with **40**. The condensation product **43i** (Table 31) was isolated in very good yields of 90 %.

To study the anti-parasitic effect of 3-benzyloxy- and 2-amino- pyridines modified N-allyl rhodanine **43f**, **43g**, and **43i** (Table 31), a photo-affinity probe was introduced to the 3-benzyloxy-modification. The synthesis of this photo-affinity probe is described in Scheme 19. The Knoevenagel reaction was carried out under lower temperatures of 50 °C, to prevent decomposition of the newly formed product **43j** and the starting aldehyde **33f**. The photo-affinity probe for N-allyl rhodanine **43j** was obtained in yields of 66 % after simple filtration. The spectroscopic analysis (¹H-NMR) showed a chemical shift of the CH-signal at δ_H 7.17 ppm in CDCl₃. A chemical shift that up-field would indicate the E-configuration of the exo-cyclic double bond. Due to poor solubility of **43j** in CDCl₃, MeOH-d₄ and DMSO-d₆, further NMR spectroscopic analysis to reveal the double bond configuration could not be performed. Because of its poor solubility it was not expected, that the photo-affinity label would be active against living parasites and no further studies on the double bond configuration were pursued.

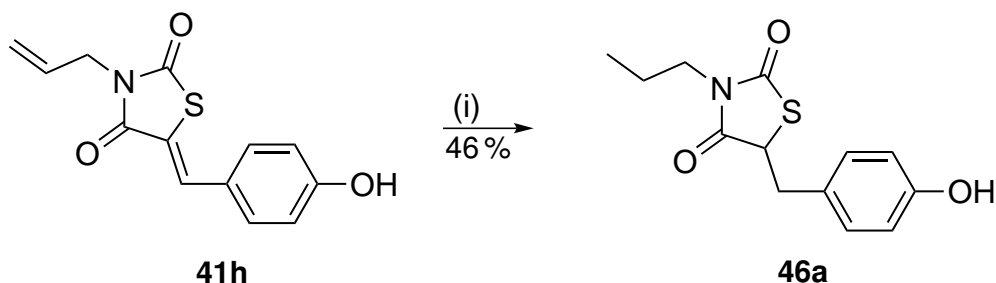
The aliphatic aldehyde 5-hydroxypentanal did not react to the desired condensation product **43k** (Table 31). The Knoevenagel reaction proceeded to a mixture of products, but no product was obtained after column chromatography.

Previously, terephthalaldehyde was reacted with N-allyl rhodanine to obtain **40w** as a 1:1 mixture of aldehyde and mono-condensated product. Here, two equivalents of N-allyl rhodanine **40** (Table 31) were used for the condensation reaction. The reaction proceeded to the desired bis-condensation product **43l** in poor yields of 16 %. The bis-substituted product **43l** was very poorly soluble, so synthesis was of minor importance and the reaction conditions were not optimised any further.

4.2.4 Reduction of the exo-cyclic double bond in N-allyl thiazolidine-2,4-dione derivatives

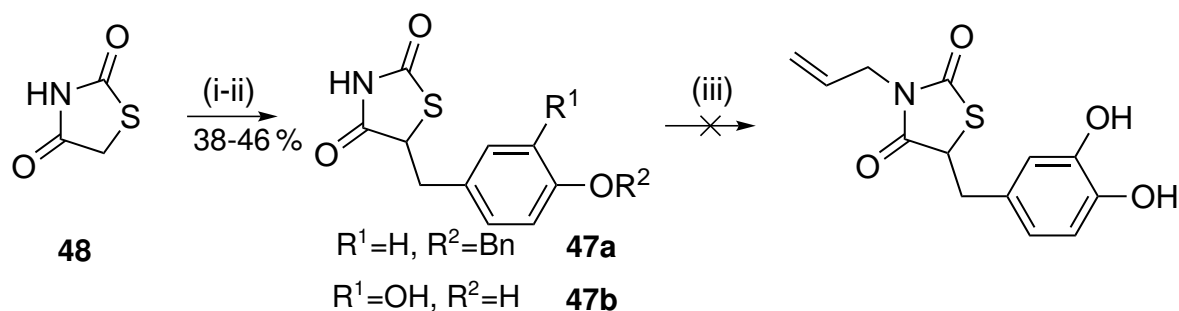
N-Allyl thiazolidine-2,4-dione derivatives are potentially prone to react with biological nucleophiles such as glutathione.^[82] The nucleophile could react with the Michael acceptor system and could covalently bind to the exo-cyclic double bond. Previous reports suggested that thiazolidine-2,4-dione derivatives were less reactive towards Michael addition reactions.^[157]

In order to exclude the possibility of covalent binding, it was desirable to reduce the double bond and compare the activity profile of both the saturated and unsaturated thiazolidine-2,4-dione derivatives. The reduction of thiazolidine-2,4-dione derivatives could easily be achieved by catalytic hydrogenation with Pd/C as the catalyst. Therefore, compound **41h** was subjected to catalytic hydrogenation conditions to yield the reduced analogue **46a** (Scheme 26).



Scheme 26: Synthesis of reduced N-allyl thiazolidine-2,4-dione analogue **46a**; (i) Pd/C, H₂ (30 psi), dioxane.

However, under these conditions also the allyl double bond of **41h** was reduced together with the double bond. Although the full reduction in **46a** was expected, sometimes the catalytic hydrogenation can give unpredicted outcomes. One such example was the hydrogenation product **47a**. Compound **47a** was synthesised starting from the unsubstituted thiazolidine-2,4-dione and 4-benzyloxybenzaldehyde in a Knoevenagel condensation reaction. The resulting Knoevenagel product was subjected to catalytic hydrogenation with Pd/C at 30 psi H₂. Surprisingly the 4-benzyl protecting group was not cleaved during the catalytic hydrogenation (Scheme 27, R¹=H, R²=Bn). Consequently, alternative strategies towards reduced N-allyl thiazolidine-2,4-dione derivatives were explored. The reduced catechol derivative **47b** was synthesised via a Knoevenagel reaction of catechol benzaldehyde and thiazolidine-2,4-dione. The condensation product was subjected to catalytic hydrogenation to afford the reduced analogue **47b** in quantitative yield. In order to introduce the N-allyl function, compound **47b** was reacted in a Mitsunobu reaction with allyl alcohol, but unfortunately the desired product could not be obtained via this route and only starting material was recovered. Therefore the derivative **46a** was used as a model compound for the comparison of the reduced versus the non-



Scheme 27: Alternative strategy toward reduced N-allyl thiazolidine-2,4-dione derivatives; (i) NaOAc, 80 °C, EtOH; (ii) Pd/C, 30 psi H₂, dioxane; (iii) allyl-alcohol, PPh₃, DEAD, THF, -78 °C → rt.

reduced analogue.

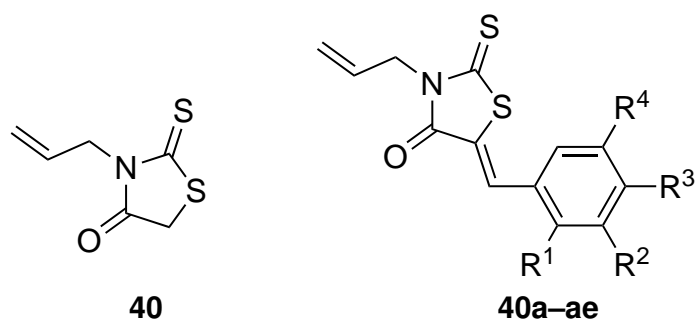
4.3 Anti-parasitic activity

4.3.1 Whole cell activity assay: simple N-allyl rhodanine derivatives

The biological activity against parasitic protozoa such as *T. brucei*, *T. cruzi* and *L. infantum* were assessed with the colorimetric and/or fluorometric viability dyes MTT and Alamar-Blue, as previously described in chapter 3.3.1.

Initially, N-allyl rhodanine **40** and its Knoevenagel condensation products **40a–ae** were screened for their activity as anti-parasitic agents. At the same time toxicity assays were performed to assess their toxicity against mammalian HL60 cells (Table 32).

The starting N-allyl rhodanine **40** had no effect on parasitic growth in *T. brucei*, but showed toxicity against HL60 cells (GI₅₀ 75.6 μM). However, the simple introduction of a benzyl group (**40a**) in position 5 of the rhodanine moiety led to a complete loss of toxicity at 100 μM. Although, **40a** did not show any effect on parasitic growth in *T. brucei*, *T. cruzi* or *L. infantum*, the introduction of hydroxy substituents on the 5-benzylidene moiety led to low μM inhibitors against *T. brucei* (**40t**) and moderate inhibitors against *T. cruzi* (**40r**). The inhibitor **40t** had a catechol motif on the benzylidene moiety. Similar catechol modifications in rhodanine-N-acetic ester derivatives (Table 16, Table 17, Table 18, Table 19 and Table 22) resulted in low μM inhibitors against *T. brucei* growth (GI₅₀ 0.9-14.2 μM) and moderate activity against *L. infantum* (GI₅₀ 45.9-75.7 μM). Derivative with only one hydroxy substituent in meta- (**40q**) or in para-position (**40r**) were 43- and 13-times less active against *T. brucei* than the catechol modified analogue with a meta- and para-substituent. However, the introduction of a para-hydroxy substituent in **40r** resulted in moderate activities against *T. brucei* and *T. cruzi* (GI₅₀ 15.1-27.8 μM). **40r** was the only inhibitor in this initial series to display activity against *T. cruzi*. N-allyl

Table 32: Anti-parasitic activity of N-allyl rhodanine derivatives; SI refers to *T. brucei* activity.

#	R ¹	R ²	R ³	R ⁴	GI ₅₀ [μM]			
					<i>T. brucei</i>	<i>T. cruzi</i>	<i>L. infantum</i>	HL60
40					338.7 ± 2.6	n.a.	n.a.	75.6 ± 15.1
40t	H	OH	OH	H	1.2 ± 0.1	n.a.	>100	>100
40e	CF ₃	H	H	H	1.7 ± 0.1	>100	22.4 ± 0.1	69.1 ± 4.3
40p	OH	H	H	H	1.5 ± 0.3	>100	>100	11.2 ± 3.5
40f	H	CF ₃	H	H	3.7 ± 1.2	>100	>100	15.1 ± 1.3
40l	H	Br	F	H	10.7 ± 0.2	>100	>100	12.3 ± 1.9
40v	H	H	SO ₂ Me	H	11.0 ± 0.6	>100	>100	20.8 ± 8.5
40b	CH ₃	H	H	H	12.4 ± 0.4	>100	>100	81.0 ± 2.9
40c	H	CH ₃	H	H	12.9 ± 0.8	>100	>100	81.0 ± 2.3
40u	H	OMe	OH	OMe	13.9 ± 0.9	n.a.	n.a.	>100
40s	OH	H	OH	H	14.0 ± 1.1	n.a.	>100	>100
40m	H	NO ₂	H	H	14.6 ± 0.5	>100	>100	18.3 ± 2.2
40x	H	OBn	H	H	14.9 ± 3.2	>100	>100	>100
40r	H	H	OH	H	15.1 ± 2.9	27.8 ± 1.9	>100	>100
40o	H	H	NHAc	H	16.3 ± 0.5	>100	>100	17.9 ± 2.5
40ad	H	H	CH ₃	H	16.5 ± 1.9	>100	>100	>100
40n	H	H	NMe ₂	H	17.5 ± 0.2	n.a.	n.a.	>100
40i	H	H	CN	H	41.3 ± 4.6	>100	>100	67.4 ± 0.4
40q	H	OH	H	H	52.1 ± 1.3	>100	>100	80.2 ± 3.1
40w	H	H	CHO	H	52.4 ± 2.7	>100	>100	>100
40a	H	H	H	H	>100	>100	>100	>100
40g	H	H	CF ₃	H	>100	>100	>100	>100
40y	H	H	OBn	H	>100	>100	>100	>100
40z	H	OBn	OBn	H	>100	>100	>100	>100
40h	H	H	Cl	H	>100	>100	>100	>100
40j	H	H	CCH	H	>100	>100	>100	>100
40k	H	Br	OMe	H	>100	>100	>100	>100
40d	H	H	tBu	H	n.a.	n.a.	n.a.	>100

rhodanine derivatives with a ortho- and para-hydroxy modification (**40s**) showed moderate activity against *T. brucei*, while the mono-ortho analogue **40p** was as potent (GI_{50} 1.5 μ M) as the previous identified catechol modified derivative **40t**. The ortho-hydroxy group might serve as a hydrogen-bond acceptor, as the ortho-trifluoromethyl substituted analogue **40e** was equipotent against *T. brucei* growth. Furthermore, **40e** was the only compound in this series to inhibit *L. infantum* growth at GI_{50} 22.4 μ M, while showing only moderate toxic against HL60 cells (GI_{50} 69.1 μ M) than the analogues hydroxy modified derivative **40p** (GI_{50} 11.2 μ M).

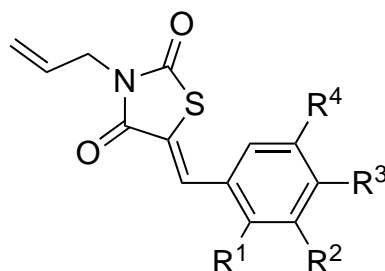
Substitutions of the meta position of the 5-benzylidene moiety with trifluoromethyl, methyl, methoxy, bromo and benzyloxy substitutions resulted in GI_{50} values of 3.7-14.9 μ M against *T. brucei*. However, large substituents in para-position (trifluoromethyl, benzyloxy, methoxy and *tert*-butyl groups) caused complete loss of anti-parasitic activity at 100 μ M.

4.3.2 Replacement of the thiocarbonyl

In order to further optimise activity of N-allyl rhodanine derivatives, the thiocarbonyl was replaced by a carbonyl group. This modification resulted in an improved toxicity profile in the rhodanine-N-acetic ester series (described in Chapter 3.3.8).

The best inhibitor of the first screening of rhodanine-N-allyl derivatives against *T. brucei*, *T. cruzi* and *L. infantum* had an activity of 1.2 μ M and displayed no toxicity against mammalian HL60 cells at 100 μ M. Replacing the thiocarbonyl group with a carbonyl group, decreased the activity of this catechol modified thiazolidine-2,4-dione derivative **41i** by a factor of 4 and an increased toxicity against HL60 cells was observed (GI_{50} 83.4 μ M, see Table 33). The ortho- and para-dihydroxy modified analogue **41m** displayed similar activity against *T. brucei* (GI_{50} 8.6 μ M) than its thiocarbonyl derivative **40s**. Both, the dione-modified analogue **41m** and the rhodanine derivative **40s** were non-toxic against HL60 cells at 100 μ M. The meta hydroxy modified derivative **41g** was 4 times as active against *T. brucei* (GI_{50} 12.9 μ M) than its thiocarbonyl analogue **40q**. The para-hydroxy modified thiazolidine-2,4-dione analogue **41h** was more than 4 times less active against *T. brucei* and *T. cruzi* than its rhodanine analogue **40r**. Particularly interesting was the ortho-hydroxy modified thiazolidine-2,4-dione analogue **41f**, which showed good activity against both *T. brucei* and *T. cruzi* (GI_{50} 15.7-49.4 μ M). The parent thiocarbonyl analogue **40p** was 10 fold more active against *T. brucei*, the selectivity SI 7 was relatively low towards *T. brucei* in comparison to HL60 cells. Additionally, compound **40p** did not show any activity against *T. cruzi*, whereas **41f** was moderately active.

A similar trend was observed in the trifluoromethyl series of the thiazolidine-2,4-dione derivatives. The meta-trifluoromethyl dione derivative **41b** (GI_{50} 14.4 μ M) was 4 fold less active against *T. brucei*, but did not show any toxicity against HL60 cells, compared to the analogous rhodanine derivative (GI_{50} 15.1 μ M). Ortho- and para-ditrifluoromethyl substituted thiazolidine-2,4-diones, such as **41e** were 10fold less active against *T. brucei* than the mono-

Table 33: N-allyl thiazolidine-2,4-dione derivatives and their anti-parasitic activity.

#	R ¹	R ²	R ³	R ⁴	GI ₅₀ [μM]				
					<i>T. brucei</i>	SI	<i>T. cruzi</i>	<i>L. infantum</i>	HL60
41i	H	OH	OH	H	5.0 ± 0.6	17	n.a.	>100	83.4 ± 0.3
41m	OH	H	OH	H	8.6 ± 0.4	>12	n.a.	n.a.	>100
41g	H	OH	H	H	12.9 ± 0.4	>8	>100	>100	>100
41e	CF ₃	H	CF ₃	H	14.2 ± 3.2	n.a.	>100	59.2 ± 6.0	n.a.
41b	H	CF ₃	H	H	14.4 ± 1.1	>7	>100	>100	>100
41f	OH	H	H	H	15.7 ± 0.1	>6	49.4 ± 4.6	>100	>100
41j	H	OBn	H	H	16.0 ± 1.9	n.a.	>100	>100	n.a.
41c	H	H	CF ₃	H	50.8 ± 4.0	>2	>100	>100	>100
41h	H	H	OH	H	58.2 ± 6.4	>2	n.a.	n.a.	>100
41l	H	OBn	OBn	H	>100	>1	>100	>100	>100
41k	H	H	OBn	H	>100	>1	>100	>100	>100

ortho trifluoromethyl substituted rhodanine derivative **40e**. However, both the dione **41e** and the rhodanine derivative **40e** displayed activity against *L. infantum*, indicating the importance of a ortho-trifluoromethyl substituent. A para-trifluoromethyl substituent in the dione series (**41c**) showed a 4 fold decreased activity against *T. brucei* and *T. cruzi*.

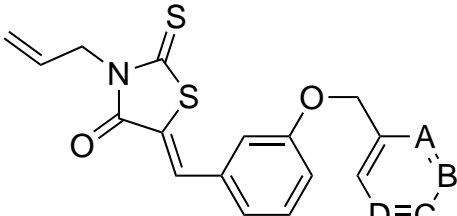
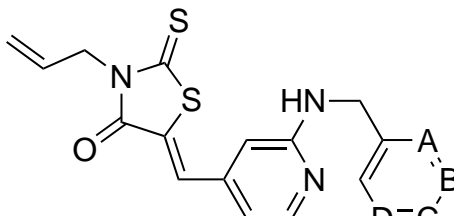
As expected from first screening results of rhodanine derivatives, bulky 4-benzyloxy derivatives, such as in compounds **41l** and **41k** did not show any effect on parasitic growth at 100 μM. Whereas the 3-benzyloxy analogue **41j** retained all of its activity against *T. brucei* (GI₅₀ 16.0 μM) then the thiocarbonyl (GI₅₀ 14.9 μM) was replaced by a carbonyl group.

4.3.3 Modification of the 3-benzyloxy-substituent

The N-allyl thiazolidine-2,4-dione derivative **41j** was the only derivative to retain its activity against *T. brucei*, if the thiocarbonyl group was replaced by a carbonyl group, whereas in general a decrease in activity by a factor 4-10 was observed. This outstanding observation led to further investigations of the importance of the 3-benzyloxy-substituent for anti-parasitic activity. Substitutions on the 3-benzyloxysubstituent in compounds **43i** and **43j** decreased anti-parasitic activity compared the unsubstituted analogue **40x** (Table 34). However, if the

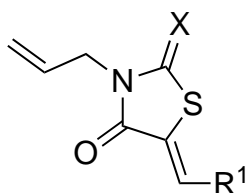
3-benzyloxy moiety was replaced by a 3-amino-benzyl group in the pyridine rhodanine derivatives **43f** and **43g** activity against *T. brucei* was retained (GI_{50} 12.7-15.0 μ M) from its parent derivative **40x**. But the modifications in **43f** and **43g** did not improve potency, as they showed increased toxicity against HL60 cells (GI_{50} 48.6-72.6 μ M). The derivative **43g** was also interesting for its activity against *L. infantum* (GI_{50} 46.1 μ M). The additional methyl group in meta-position of the 3-benzyloxy-substituent increased activity against *L. infantum* and decreased toxicity against HL60 cells, compared to the analogue without this methyl substituent.

Table 34: Activity of 3-benzyloxy modified N-allyl rhodanine derivatives.

									
40x, 43i, and 43j					43f and 43g				
GI_{50} [μ M]									
#	A	B	C	D	<i>T. brucei</i>	SI	<i>T. cruzi</i>	<i>L. infantum</i>	HL60
40x	CH	CH	CH	CH	14.9 ± 3.2	7	>100	>100	>100
43f	CH	CH	CH	CH	12.7 ± 0.5	4	>100	>100	48.6 ± 7.1
43g	CH	CH	CCH ₃	CH	15.0 ± 1.6	5	>100	46.1 ± 2.2	72.6 ± 22.1
43i	CH	CH	COCH ₃	CH	60.1 ± 10.7	2	>100	>100	>100
43j	CH	CN ₃	CH	CN ₃	>100	n.a.	>100	>100	n.a.

4.3.4 Heterocyclic modified N-allyl rhodanine and thiazolidine-2,4-dione derivatives

The 2-amino-pyridinyl-derivative **43g** in the previous chapter showed good activity against *T. brucei* (GI_{50} 15.0 μ M) and *T. cruzi* (GI_{50} 46.1 μ M). The derivative **43g** has been used to explore anti-parasitic activity of 3-benzyloxy-modified rhodanine derivatives (Table 34). Although structurally similar to 5-benzylidene-3-benzyloxy-substituents, additional effects of the 4-pyridinyl function in compound **43g** could not be excluded. Therefore, additional rhodanine and thiazolidine-2,4-dione derivatives bearing various heterocyclic modifications in position 5 have been tested for their anti-parasitic activity (Table 35). Indeed, the results of the screening of pyridinyl-derivatives showed that 4-pyridinyl modifications resulted in low μ M activity against *T. brucei* growth (GI_{50} 1.5-4.2 μ M). But these 4-pyridinyl derivative also showed high toxicity against HL60 cells. The 4-pyridinyl rhodanine derivative **43c** showed the highest toxicity of a GI_{50} 4.5 μ M against HL60 cells. However the introduction of an additional chloro-substituent in 2-position of the pyridinyl-moiety decreased toxicity to GI_{50} 11.0 μ M, without affecting anti-

Table 35: Activities of heterocyclic modified N-allyl rhodanine and thiazolidine-2,4-dione derivatives.

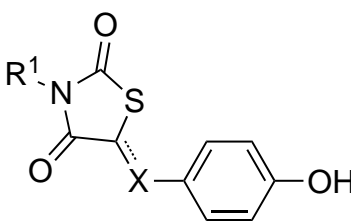
#	X	R ¹	GI ₅₀ [μM]			
			<i>T. brucei</i>	<i>T. cruzi</i>	<i>L. infantum</i>	HL60
43d	S	2-chloropyridin-4-yl	1.5 ± 0.1	>100	>100	11.0 ± 1.7
43b	S	3-pyridinyl	1.5 ± 0.2	>100	>100	29.3 ± 0.1
43c	S	4-pyridinyl	1.5 ± 0.2	n.a.	>100	4.5 ± 0.1
44a	O	4-pyridinyl	4.2 ± 0.2	>100	>100	63.7 ± 1.3
43a	S	2-pyridinyl	>100	>100	>100	>100
43l	S	benzylidene-4-(5-rhodanine-N-Allyl)	n.a.	>100	>100	n.a.

trypanosomal activity against *T. brucei*. The replacement of the thiocarbonyl group in the analogue **44a** decreased toxicity even further to GI₅₀ 63.7 μM, however also the anti-trypanosomal activity was slightly decreased to GI₅₀ 4.2 μM. Shifting the nitrogen in meta position in the 3-pyridinyl derivative **43b** resulted in equal potent anti-trypanosomal agents against *T. brucei* and only moderate toxicity (GI₅₀ 29.3 μM). Interestingly, the 2-pyridinyl-derivative **43a** showed no anti-trypanosomal activity at 100 μM.

The bis-benzylidene-N-allyl rhodanine derivative **43l** did not show any parasitic activity nor toxicity. However its activity evaluation was compromised due to insufficient solubility, resulting in precipitation under assay conditions with 0.5 % DMSO.

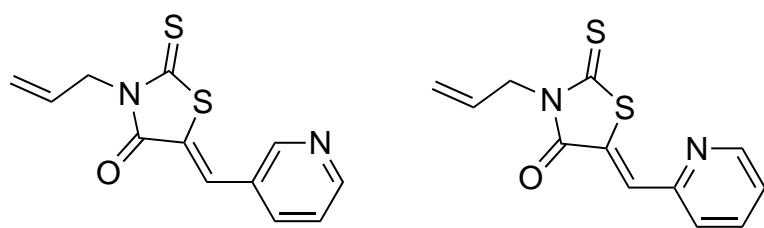
4.3.5 Effect of saturated N-propyl thiazolidine-2,4-dione derivative on anti-trypanosomal activity; reactivity assay towards glutathione

Attempts to synthesis a reduced N-allyl rhodanine derivative failed and the N-propyl thiazolidine-2,4-dione derivative **46a** was used to study the effect of a reduced double bond on anti-trypanosomal activity (Table 36). The reduced analogue **46a** showed no anti-trypanosomal activity at 100 μM, whereas its unsaturated precursor **41h** displayed moderate activity against *T. brucei*. This result may indicate, that the exo-cyclic double bond contributes towards the anti-parasitic activity. The reduction of the double bond increases flexibility and allows the molecule to adapt different conformations, possible reducing binding affinity towards the molecular target. But the double bond may also be involved in covalent binding towards biological nucleophiles, such as glutathione over its Michael acceptor system. For the following research

Table 36: Anti-trypanosomal activity of saturated N-propyl thiazolidine-2,4-dione derivative.


#	R ¹	X	GI ₅₀ [μM]	
			tb	hl
41h	allyl	CH	58.2 ± 6.4	>100
46a	propyl	CH ₂	>100	>100

study, the derivatives **43b** and **43a** have carefully been chosen for analysis of glutathione reactivity (Table 37). Compound **43b** possesses a low μM activity against *T. brucei*, whereas

Table 37: Glutathione reactivity of **43b** and **43a** measured by reaction with DTNB measured in 10 % DMSO in PBS.


#	GI ₅₀ [μM] <i>T. brucei</i>	RC ₅₀ [μM] against GSH			
		8min	15 min	42 min	50 min
Acrolein	n.a.	210.9 ± 15.7	196.8 ± 18.5	172.5 ± 6.4	83.7 ± 7.8
43b	1.5 ± 0.2	>2000	1642	803.1	552.2
43a	>100	>2000	>2000	>2000	>2000

43a did not show anti-parasitic activity. Furthermore, the nitrogen in the 3-pyridinyl would positively contribute towards Michael acceptor reactivity, as the nitrogens electronegativity results in a partially positive charge on the alkenyl-carbon atom, thus favouring possible addition of glutathione to the Michael acceptor system. This positive contribution is abandoned in **43a**, as the nitrogen partially changes the polarity of the alkenyl-carbon.

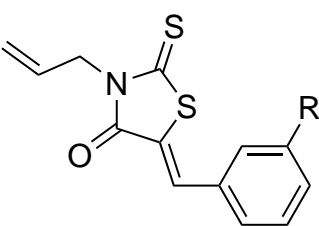
The reactivity towards glutathione was assessed by a published procedure using the Ellmanns reagent for measuring residual glutathione in solution.^[235] The reaction was carried

out in 10 % DMSO, to overcome the poor solubility of **43b** and **43a**, and PBS to ensure a buffered solution and physiological relevant conditions. Initially, the known Michael acceptor acrolein was screened for its ability to react with glutathione. It was pleasing to observe that the use of PBS-buffer instead of phosphate buffer had no influence on the reactivity constant for acrolein (RC_{50} 83.7 μ M), correlating well with previously published results (RC_{50} 84.5 μ M).^[235] In contrast to the previous published procedure, the RC_{50} values presented in this study were obtained in a 96 well plate assay format. Unfortunately, the absorbance of the 5,5'-dithiobis-(2-nitrobenzoic acid) (DTNB)-glutathione adduct at 412 nm interfered with the bright yellow coloured analogues **43b** and **43a**. However, at lower concentrations the background absorbance of the inhibitors was decreased, compared to the intense signal of the DTNB-glutathione adduct. For the evaluation of RC_{50} values for **43b** and **43a**, the absorbance of the inhibitor was measured prior to addition of DTNB and was subtracted from the final absorbance intensity. Indeed, the anti-trypanosomal inhibitor, which also showed moderate toxicity against HL60 cells (GI_{50} 29.3 μ M), reacted with glutathione and a RC_{50} of 552.2 μ M was measured. Although this concentration is much higher than concentrations used in the activity screens (100 μ M), it might explain **43b** general cytotoxicity against *T. brucei* and HL60 cells. The 2-pyridinyl analogue **43a** displayed no reactivity towards glutathione at 2 mM, possible explaining its missing anti-trypanosomal activity. It might be possible that the reactivity of these inhibitor against glutathione is reversible as it has previously been observed for similar derivatives in a UV-based assay.^[86] The assay for glutathione reactivity, used in this study is an endpoint assay, as DTNB addition results in consumption of all remaining glutathione. However, reversibility of the reaction with glutathione similarly as described by others is likely, as irreversible binding should lead to general cytotoxicity. However, **43b** did not show any activity against *T. cruzi* or *L. infantum* (GI_{50} >100).

4.4 Target identification studies

4.4.1 Myristate labelling of GPI anchor biosynthesis using YnC12

The previous analysed rhodanine-N-acetic ester derivatives **14v** and **14a** showed strong inhibitory effects on the incorporation of myristic acid derivative **YnC12** in *T. brucei*, most likely by inhibition of DPMS and/or the first mannosyltransferase as shown by a cell-free GPI-synthesis assay (Chapter 3.5.1 and 3.5.3). In this experiments, the analogous N-allyl rhodanine series (Table 38) was assessed for their ability to inhibit incorporation of the myristic acid **YnC12** in GPI-VSG proteins. Therefore, *T. brucei* was incubated with the N-allyl derivatives **40x** and **40c** for 3 h, before parasite density was adjusted to equal amounts for both inhibitors and **YnC12** was added. *T. brucei* was incubated for a further 4 h to ensure incorporation of the myristic acid in the GPI-anchor. Next, the crude proteins were precipitated and the fluorescent tag **38**

Table 38: Anti-parasitic activity of chosen N-allyl rhodanine derivatives.


GI ₅₀ [μM]					
#	R	<i>T. brucei</i>	<i>T. cruzi</i>	<i>L. infantum</i>	HL60
40x	OBn	14.9 ± 3.2	>100	>100	>100
40c	CH ₃	12.9 ± 0.8	>100	>100	81.0 ± 2.3

was introduced via Click-chemistry, followed by visualisation of fluorescent protein bands on a SDS-gel (Figure 54).

The positive control in the presence of DMSO and **YnC12** showed a strong fluorescent band at 50 kDa and a wide weak band at 57 kDa. As discussed previously it is assumed that the intense protein band at 50 kDa may represent a GPI-VSG precursor protein, which may not be fully glycosylated (Chapter 3.5.3). The allyl-derivative **40x** with a 3-benzyloxy substituent reduced the intensity of the 50 kDa band by about 50 %. However, in comparison to the analogous rhodanine-N-acetic ester derivative **14v** the effect of **40x** to inhibit myristate incorporation was reduced after incubation of 3 h. The methyl substituted N-allyl derivative **40c** showed comparable results to the analogous rhodanine-N-acetic ester **14a**, as both showed only weak inhibition of **YnC12** incorporation. Although, the fluorescent signal bands appeared reduced in Figure 54 for **40c**, Coomassie staining showed that a smaller quantity of protein was loaded to the SDS gel, explaining the reduced fluorescent intensity.

YnC12 labelling after 24 h incubation with 40x and 40c

The allyl-derivative **40x** had a moderate effect on incorporation of the myristic acid analogue **YnC12**⁹ in *T. brucei* after an incubation period of 3 h, as can be seen in Figure 54. The meta methyl substituted allyl derivative **40c** did not show any effect on myristate incorporation in GPI-VSG-proteins. In order to study the inhibition effect of **40x** and **40c** over a longer time period, the incubation time with *T. brucei* was increased to 24 h. After 24 h incubation with compound **40c** an increase in toxicity against *T. brucei* was observed, although earlier activity assays against *T. brucei* did not show any toxicity at this inhibitory concentration. Therefore, **40c** could not be evaluated for its inhibitory effect on **YnC12** labelling in the GPI bound VSG proteins. However, the remaining 3-benzyloxy derivative **40x** did not show any

⁹**YnC12** was kindly provided by Megan Wright and Dr. Ed Tate (Imperial College London, London, UK).

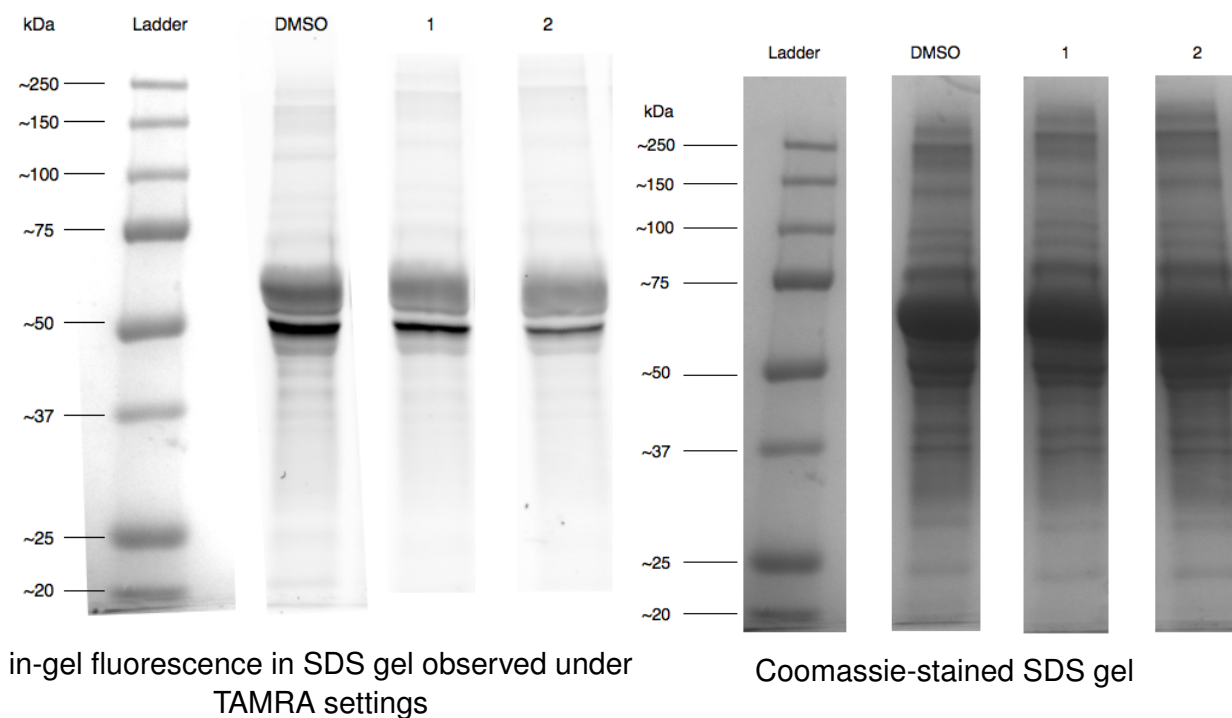


Figure 54: SDS gels after 3 h incubation with **40x** and **40c**; lane 1: **40x**, lane 2: **40c**, full gels see Chapter 11.

anti-trypansomal effects after 24 h and labelling with **YnC12** was performed. After lysis of the parasites and the introduction of the tamra-fluorophore **38**, the proteins were separated on a SDS gel and analysed by in-gel fluorescence and Coomassie staining.

The inhibitor **40x** resulted in a significant reduction of incorporation of **YnC12** in the GPI bound VSG proteins (Figure 55). However the rhodanine-N-acetic ester analogue **14v** showed a complete inhibition of **YnC12** incorporation, suggesting that the N-allyl functionality caused the reduction in activity and therefore suggesting that a carboxylic moiety is preferable for inhibiting **YnC12** incorporation in *T. brucei*.

YnC15 labelling in *T. brucei* and influence of N-allyl derivatives

The inhibitory effect of derivative **40c** on **YnC12** incorporation in *T. brucei* could not be studied after 24 h due to increased trypanocidal effects. Unfortunately, these experiments could not be repeated at lower concentrations of **40c** and **YnC12**, as all of the myristic acid analogue **YnC12** had been used. However, in order to overcome this problem, the pentadecylic fatty acid analogue **YnC15**¹⁰ was used in combination with lower concentration of **40c**.

Indeed, after 24 h of incubation with *T. brucei*, a decrease in anti-trypansomal activity was observed and labelling with **YnC15** could be performed with both **40x** and **40c** treated trypanosomes. However, the corresponding gel (Figure 55) showed only unspecific binding of

¹⁰**YnC15** was kindly provided by Megan Wright (Prof. Dr. Ed Tate, Imperial College London, London, UK).

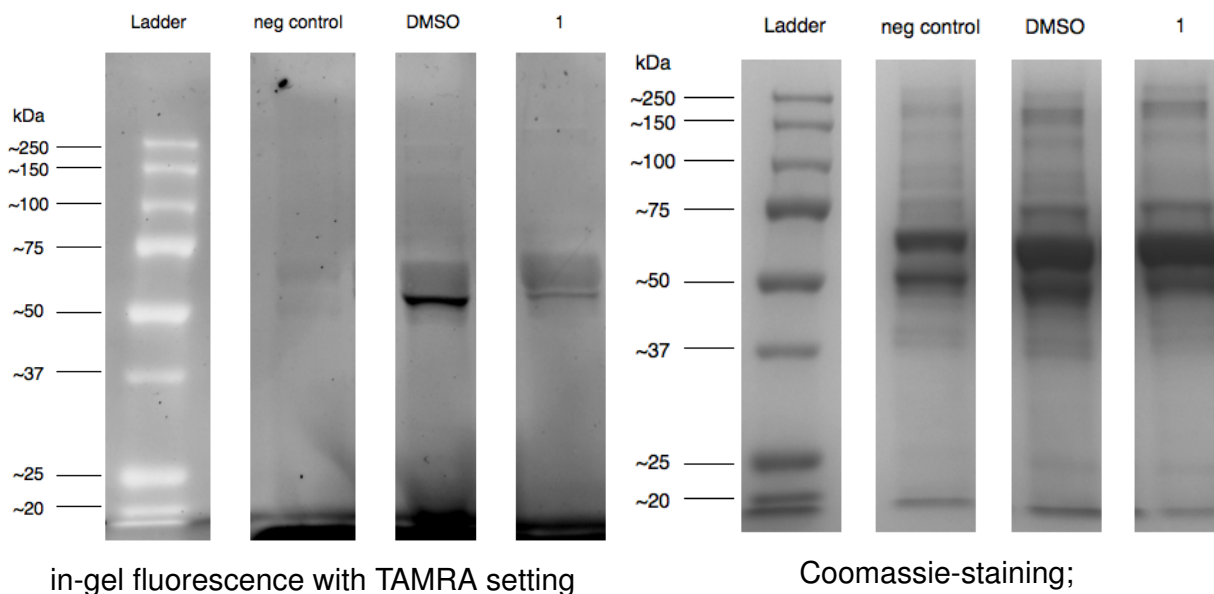


Figure 55: SDS gels after 24 h incubation with **40x**; lane 1: **40x**, full gels see Chapter 11.

the tamra-fluorophore with trypanosomal proteins in the negative control (absence of **YnC15**) and all treated trypanosome cultures. Therefore confirming the specificity of myristate incorporation in GPI-anchor bound VSG proteins.^[203,205]

YnC15 labelling in HL60 cells and influence of N-allyl derivatives **40x and **40c****

After showing that **40x** inhibited incorporation of the myristic acid analogue **YnC12** in the GPI bound VSG proteins in *T. brucei*, studies on the effect of **YnC12** in HL60 cells were performed. Therefore, *T. brucei* was incubated with the derivatives **40x** and **40c** for 24 h, after which cells were lysed, proteins tagged with the tamra-fluorophore **38** via Click-chemistry and visualised on a SDS gel using in-gel fluorescence and Coomassie staining. The negative control, which was performed in the absence of **YnC12** showed unspecific binding of the tamra-fluorophore with HL60 proteins (Figure 57). The same unspecific binding was observed in proteins treated with **YnC12** and inhibitors (DMSO, **40x** and **40c**).

This experiment could not provide an answer about the molecular target in HL60 cells of the N-allyl-derivatives **40x** and in particular **40c**, as this derivative showed toxicity at GI_{50} 81.0 μ M against HL60 cells.

4.4.2 Flow cytometry analysis of *T. brucei* transferrin receptors for indication of GPI anchor biosynthesis inhibition

The trypanosomal transferrin receptor (*TbTfR*) is bound through a GPI-anchor to the plasma membrane of *T. brucei*,^[128] therefore transferrin uptake was established as a measure of GPI-bound-transferrin receptors (Chapter 3.5.2). The uptake of transferrin can be quantified by the

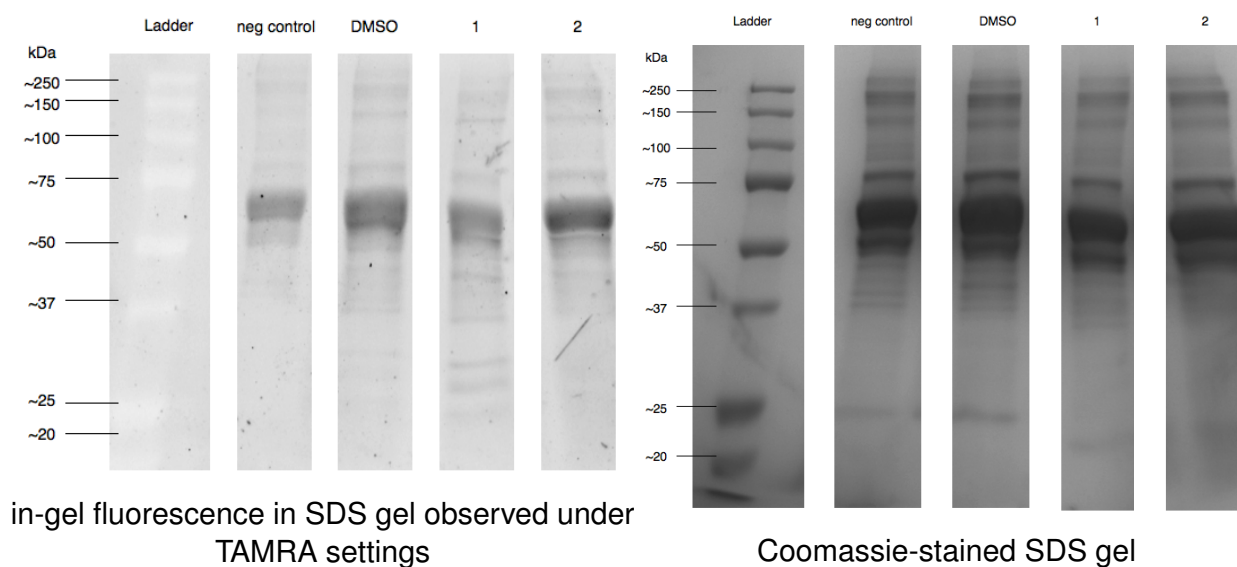


Figure 56: YnC15 SDS gels after 24 h incubation with **40x** and **40c**; lane 1: **40x**, lane 2: **40c** full gels see Chapter 11.

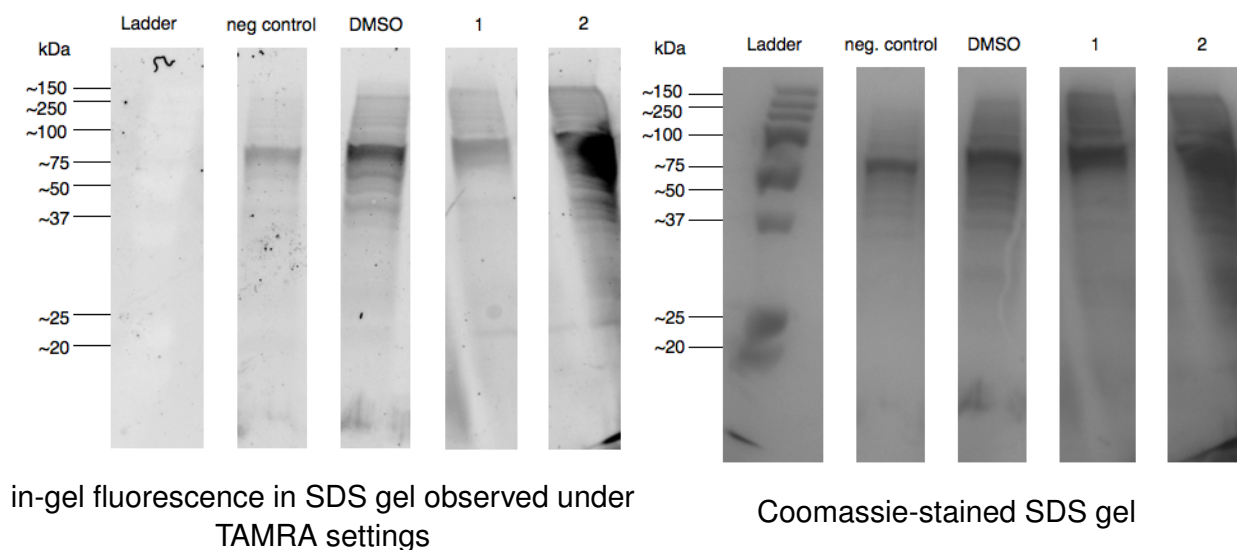


Figure 57: YnC12 SDS gels after 24 h incubation with **40x** and **40c** in HL60 cells; lane 1: **40x**, lane 2: **40c** full gels see Chapter 11.

use of FITC-labelled transferrin in combination with flow cytometry.

In this study, *T. brucei* was incubated with the N-allyl rhodanine derivatives **40x** and **40c** over a period of 24 h. Next, the trypanosomes were cultured in transferrin deprived media for another 4 h, causing an up-regulation of *TbTf* receptors and therefore increasing the uptake of FITC-labelled transferrin in the consecutive step.^[212] In the final step after 4 h, FITC-labelled transferrin was added and the uptake in *T. brucei* was measured by flow cytometry. The mean fluorescence intensity was measured and plotted in Figure 58.

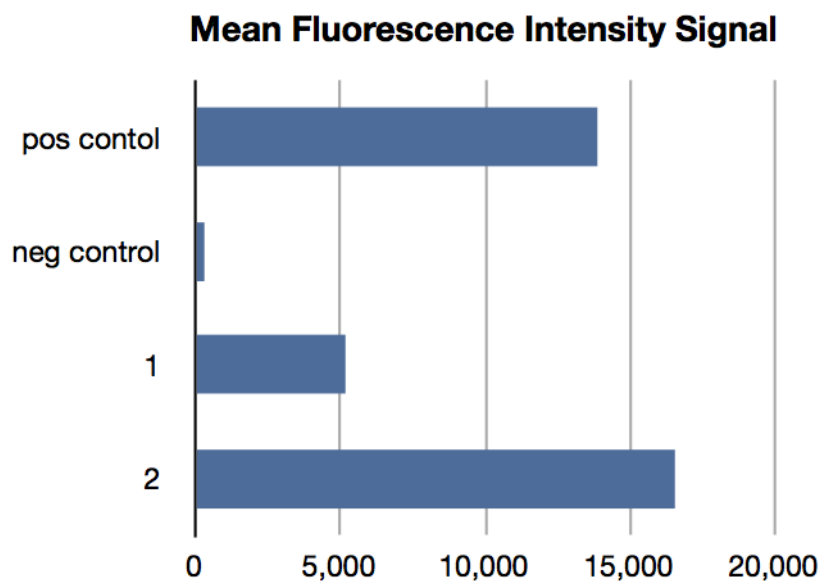


Figure 58: Mean fluorescence intensity of FITC-labelled transferrin after incubation with 1: **40x**, 2: **40c**.

Indeed the previous observation, that the 3-benzyloxy derivative **40x** inhibited uptake of the myristic acid analogue **YnC12** in GPI bound VSG proteins, was confirmed by a decrease in mean fluorescence intensity. In contrast, the meta-methyl derivative **40c** did not show any decrease in the mean fluorescence intensity, indicating that GPI-bound *TbTf* receptor synthesis in *T. brucei* was not effected. This observation was in agreement with previous experiments with the myristic acid analogue **YnC12** after 3 h of pre-incubation with **40c**. The myristate labelled GPI-VSG protein expression was similar to trypanosomes treated with DMSO only, indicating that **40c** did not inhibit GPI-anchor synthesis in GPI bound VSG proteins.

In addition to these experiments, fluorescence microscopy was performed in order to localise the FITC labelled transferrin in *T. brucei*. Therefore, trypanosomes, treated with DMSO, absence of FITC-labelled transferrin, **40x** and **40c** were co-stained with DAPI and analysed by fluorescence microscopy (Figure 59). The control experiments were discussed in chapter 3.5.2. The inhibitor **40c** showed a high FITC-fluorophore intensity, similar to the positive con-

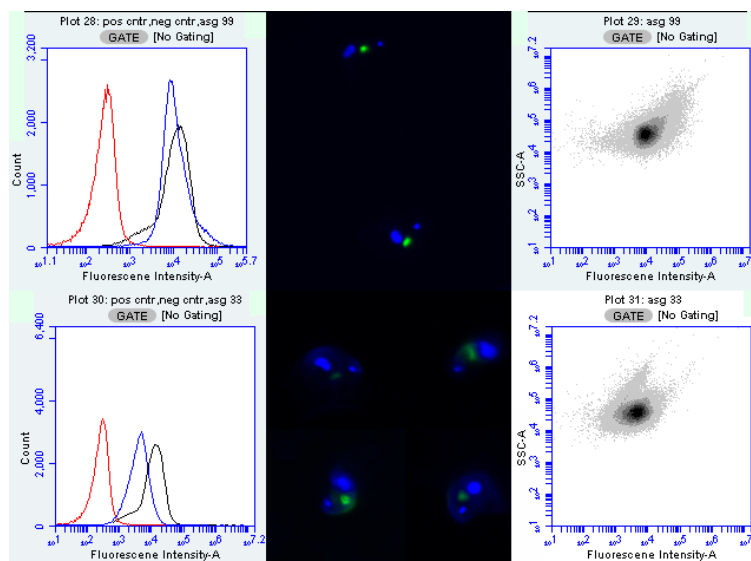


Figure 59: Flow cytometry analysis of derivatives **40x** and **40c**; Side-scattered light vs fluorescent intensity and Number of cells vs fluorescent intensity and fluorescence microscopy pictures of treated parasites.

trol with DMSO only (left upper blue graph in Figure 59) and morphological analysis with flow cytometry showed only intact trypanosomes (right upper plot Figure 59). As expected, fluorescence microscopy showed trypanosomes where the kinetoplast and nucleus were DAPI stained (blue in Figure 59) and an intense signal from the FITC fluorophore (green in Figure 59).

In contrast, the 3-benzyloxy derivative **40x** showed a low fluorescence intensity for FITC labelled transferrin (left blue graph in Figure 59), therefore fluorescence microscopy showed trypanosomes with intense DAPI signal and two types of FITC-fluorophore accumulations. Trypanosomes missing and weak FITC fluorophore intensities are most likely deficient in GPI-anchor biosynthesis.

Interestingly the myristate labelling and transferrin uptake experiments showed that the meta-benzyloxy-derivative **40x** in the N-allyl rhodanine series was as potent in inhibiting GPI-anchor biosynthesis than did the corresponding 3-benzyloxy N-acetic ester analogue **14v**. In contrast, the meta-methyl derivative **40c** was ineffective in GPI anchor biosynthesis, while the corresponding meta-methyl N-acetic ester analogue showed weak inhibition of GPI anchor biosynthesis in *T. brucei*.

Also this observation could be confirmed with the myristic acid labelling experiment, as there was no reduction in fluorescent labelled GPI-VSG-proteins. But even more interesting is the effect of compound **40x**, the structural analogue to **14v**. Pre-incubation with **40x** resulted in a 50 % reduction of uptake of transferrin. The FM pictures showed a reduction in fluorescent

intensity for the treated parasites. And indeed only one kind of population could be observed. Also these results are in agreement with previous experiments on the myristic acid labelling results, suggesting GPI-anchor biosynthesis inhibition.

From these experiments it can be concluded that the studied inhibitor classes of **14v**, **14a** and **40x**, **40c** are most likely inhibitors of the GPI anchor biosynthesis. The question of the exact molecular target remained and is elucidated in Chapter 4.4.3.

4.4.3 GPI cell-free radio-label assay

In order to confirm the hypothesis that the 3-benzyloxy derivative **40x** is active in GPI anchor synthesis in *T. brucei*, a cell-free assay was performed.¹¹ Further details on the assay are described in chapter 3.5.3. Briefly, this assay was performed with radioactive labelled [³H]-GDP-mannose and assay results are displayed in form of radioactive-labelled GPI synthesis substrates on a HPTLC.^[68] The intensity of the substrate bands on these HPTLC plate allow interpretation of potential targets in the GPI-anchor biosynthesis.^[68]

Initially, the 3-benzyloxy derivative together with other benzyloxy-modified and trifluoromethyl substituted rhodanine-N-allyl derivatives in this study were assessed for their ability to inhibit enzymatic steps in the cell-free GPI synthesis assay (Table 39). Indeed, the 3-benzyloxy derivative **40x** showed a weak inhibition of the M1 substrate band, suggesting inhibition of the first mannosyltransferase as potential target. However, the decrease in substrate intensity of M1 could be a synergistic effect of DPMS and MT-1 inhibition as previously described in chapter 3.5.3. Furthermore, **40x** has been shown to inhibit *T. brucei* growth at GI₅₀ 14.9 μM, without showing toxicity against HL60 cells.

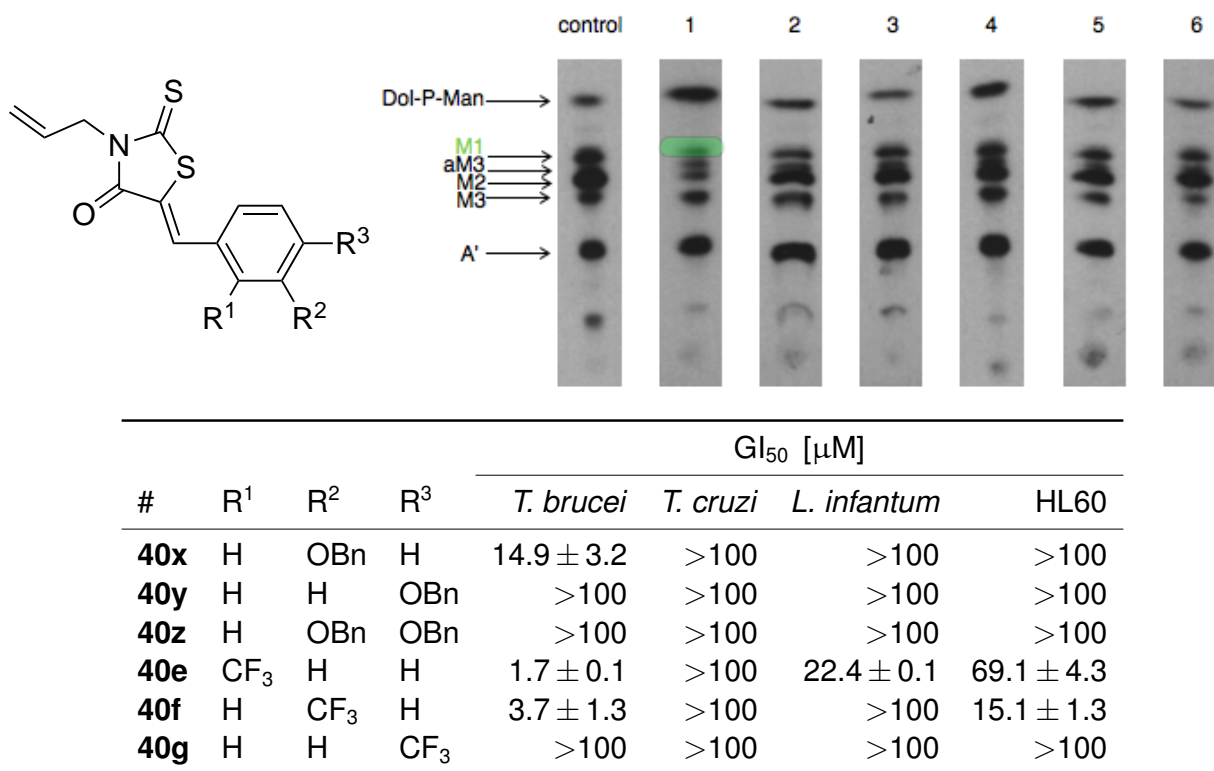
The 4-benzyloxy derivative **40y** showed a very weak decrease in the Dol-P-Man substrate band and the following M1 band, compared to the positive control with DMSO only. However, **40y** did not show anti-trypanosomal activity *in vitro*, suggesting that this derivative is possibly not reaching the molecular target, or that the inhibition effect was too weak to cause trypanocidal activity. In contrast, rhodanine-N-allyl derivatives with a trifluoromethyl substituent in ortho- and meta-position showed low μM activity against *T. brucei* *in vitro* (GI₅₀ 1.7 and 3.7 μM respectively) and moderate activity against *L. infantum* *in vitro*. But these derivatives did not show any inhibition of enzymes involved in the cell-free GPI-synthesis, indicating that other mode-of-actions are responsible for their anti-trypanosomal activity.

Anti-trypanosomal N-allyl rhodanine derivatives and activity against GPI-anchor synthesis

In this study, pyridine-substituted rhodanine-N-allyl derivatives have been identified as low μM inhibitors against *T. brucei* growth *in vitro* (Table 40).

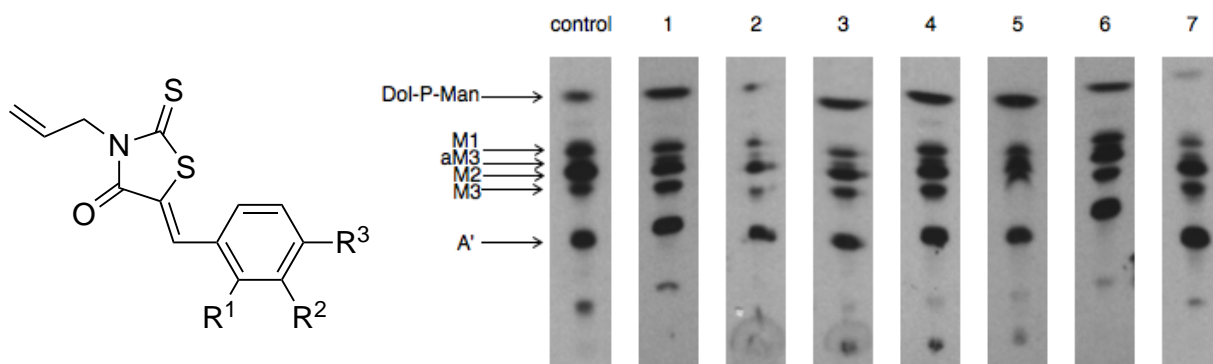
¹¹This assays were performed by Dr. Terry Smith from the University of St. Andrews, St Andrews, Scotland, UK

Table 39: cell-free GPI assay results for N-allyl rhodanine derivatives-1; line 1: **40x**, line 2: **40y**, line 3: **40z**, line 4: **40e**, line 5: **40f**, line 6: **40g**; *in vitro* activity against *T. brucei*; Blue highlighted bands: DPMS inhibition; Green highlighted bands: MT-1 inhibition.



In order to identify the mode-of-action of these derivatives, derivatives **43a**, **43b**, and **43c** were assessed for their ability to inhibit enzymes of the GPI-anchor synthesis in *T. brucei* using a cell-free radio-label assay. The 2-pyridinyl derivative **43a** did not show inhibitory activity in this assay, however these results were not surprising, as no trypanocidal activity against *T. brucei* *in vitro* was observed. The 3-pyridinyl derivative **43b** showed a reduction in the Dol-P-Man and the M1 substrate bands, however all subsequent GPI-intermediate appeared as intense bands, suggesting that Dol-P-Man and M1 was synthesised but consumed in later reaction steps. Based on this experiment no conclusions about GPI-synthesis inhibition can be drawn. However, **43b** has also been shown to react with glutathione under physiological relevant conditions (Table 37) and **43b** also displayed moderate toxicity against HL60 cells, suggesting possible un-selective binding to biological nucleophiles as mode-of-action. The 4-pyridinyl derivative **43c** displayed no activity in the cell-free GPI-synthesis assay, but showed a high toxicity against HL60 cells, possible indication similar Michael acceptor reactivity than displayed for derivative **43b**. In addition to these pyridine derivative several 5-benzylidene modified rhodanine-N-allyl derivative with low μM activity against *T. brucei* have been screened in

Table 40: Cell-free GPI assay results for N-allyl rhodanine derivatives-2; line 1: **43a**, line 2: **43b**, line 3: **43c**, line 4: **40v**, line 5: **40h**, line 6: **40i**, line 7: **40m**; *in vitro* activity against *T. brucei*; Blue highlighted bands: DPMS inhibition; Green highlighted bands: MT-1 inhibition.



#	R ¹	R ²	R ³	GI ₅₀ [μM]			
				<i>T. brucei</i>	<i>T. cruzi</i>	<i>L. infantum</i>	HL60
43a		2-pyridinyl		>100	>100	>100	>100
43b		3-pyridinyl		1.5 ± 0.2	>100	>100	29.3 ± 0.1
43c		4-pyridinyl		1.5 ± 0.2	n.a.	>100	4.5 ± 0.1
40v	H	H	SO ₂ Me	11.0 ± 0.6	>100	>100	20.8 ± 8.5
40h	H	H	Cl	>100	>100	>100	>100
40i	H	H	CN	41.3 ± 4.6	>100	>100	67.5 ± 0.4
40m	H	NO ₂	H	14.6 ± 0.5	>100	>100	18.3 ± 2.2

the cell-free GPI-synthesis assay (Table 40). None of these inhibitors showed any inhibitory activity against GPI-synthesis in this cell-free assay. But although these derivatives showed low μM activity against *T. brucei*, they also showed toxicity against HL60 cells. In all cases an electron-withdrawing group (SO₂Me, Cl, CN, NO₂) was present, suggesting that these groups may lead to general toxic derivatives, both against *T. brucei* and HL60 cells. Taking into account that N-allyl rhodanine derivatives have been shown to interfere with DNA synthesis in bacteria,^[229] this might be an alternative mode-of-action and possible explanation for their low selectivity profiles.

4.5 Discussion

The N-allyl rhodanine derivatives studied in this research project showed interesting anti-parasitic properties against *T. brucei*, but only moderate activities against *T. cruzi* and *L. infantum*. In particular three sub-classes displayed interesting activity as anti-trypanosomal agents.

The most interesting inhibitors discovered in this series were derivatives with a 3-benzyloxy-substituent on the 5-benzylidene-moiety of the N-allyl rhodanine or N-allyl thiazolidine-2,4-dione scaffold. The inhibitors showed promising anti-trypanosomal activity against *T. brucei* *in vitro* (GI_{50} 14.9-60.1) and had an excellent selectivity profile, as they showed no toxicity against HL60 cells at 100 μ M. Interestingly, replacement of the thiocarbonyl group in the rhodanine moiety retained anti-trypanosomal activity as compared to other modifications, there modifications of the thiocarbonyl group resulted in reduced anti-trypanosomal activity. The mode of anti-trypanosomal activity of these derivatives has been investigated in this study and these experiments suggested that GPI anchor biosynthesis and in particular the essential enzymes DPMS and MT-1 were inhibited by this subclass of rhodanine-N-allyl derivatives. This observation was further more significant as a similar 3-benzyloxy substituted N-acetic acid rhodanine showed similar mode-of-actions, but was 3 times more active against *T. brucei* *in vitro*. This observation showed that a 3-benzyloxy-substituent is important for inhibitory effects against DPMS and/or the first mannosyltransferase in the GPI-anchor biosynthesis pathway.

In order to validate DPMS inhibition as target by this substance subclass, a photo-affinity probe similar to the one described in chapter 3.5.5 has been designed and screened for its anti-trypanosomal activity. However, this photo-label-probe **43j** was insoluble in aqueous media and most likely therefore lost its anti-trypanosomal activity. The 3-benzyloxy-modification is a promising lead structure and further modification thereof might improve anti-trypanosomal activity.

The most potent anti-trypanosomal agent with a GI_{50} of 1.2 μ M was the catechol modified N-allyl rhodanine derivative **40t**. This subclass was particular interesting for its low toxicity against HL60 cells (GI_{50} >100 μ M). Similarly to the 3-benzyloxy-modification, substitution of the thiocarbonyl did not decrease anti-trypanosomal activity and the corresponding N-allyl thiazolidine-2,4-dione derivative retained its anti-trypanosomal activity at GI_{50} 5.0 μ M, while showing only moderate toxicity against HL60 cells (SI 17). The exact mode-of-action of this subclass is unknown, but similar catechol modified rhodanine derivatives were reported as probes for dehydrogenases.^[108]

Pyridinyl-substituted N-allyl rhodanine derivatives showed low μ M activity (GI_{50} 1.5 μ M) against *T. brucei*, but unfortunately this modifications also displayed increased toxicity against HL60 (GI_{50} 4.5-29.3 μ M). In order to decrease the observed toxicity the thiocarbonyl was re-

placed by a carbonyl group and indeed, this 4-pyridinyl derivative **44a** retained most of its anti-trypanosomal activity (GI_{50} 4.2 μ M) and displayed reduced toxicity against HL60 cells (GI_{50} 63.7 μ M). As these derivatives did not show activity against enzymes in the GPI anchor synthesis, alternative mode-of-actions such as general Michael acceptor reactivity were investigated. Indeed, the 3-pyridinyl N-allyl rhodanine-derivative **43b** reacted with glutathione under physiological conditions (PBS buffer pH 7.4), however its reactive dose was relatively high with 552.2 μ M, compared to the very reactive Michael acceptor acrolein (83.7 μ M), suggesting that only a small quantity of **43b** will effectively be covalently bound to glutathione *in vitro*. This small quantity most likely does not account for its low anti-trypanosomal activity and therefore validating further attempts to optimise this subclass for its anti-trypanosomal activity.

4.6 Summary

89 N-allyl rhodanine and thiazolidine-2,4-dione derivatives have been synthesised and screened for anti-parasitic activity against *T. brucei*, *T. cruzi* and *L. infantum*.

29 out of 89 N-allyl derivatives were able to kill *T. brucei* at 100 μ M (MIC 100 μ M), while a further 6 compounds showed trypanocidal effects at 10 μ M (MIC 10 μ M).

5 out of 89 N-allyl derivatives killed *T. cruzi* at 100 μ M (MIC 100 μ M).

2 out of 89 N-allyl derivatives killed *L. infantum* at 100 μ M (MIC 100 μ M).

No derivative showed inhibitory effects against all three parasites.

The whole cell phenotypic screening of N-allyl derivatives identified promising low μ M anti-trypanosomal (GI_{50} 1.2-14.9 μ M, SI 7 - >83) inhibitors with low toxicity against mammalian cells.

Target identification showed that with the exception of a meta-benzyloxy derivative **40x** GPI-anchor biosynthesis was not affected by this compound class.

The meta-benzyloxy substituted N-allyl rhodanine derivative **40x** showed low μ M activity against *T. brucei* (GI_{50} 14.9 μ M, SI >7). This derivative has been shown with metabolic labelling experiments, flow cytometry analysis and a cell-free radio-label assay to inhibit GPI-anchor biosynthesis *in vitro* and particularly to inhibit DPMS and/ or MT-1.

Further mode-of-action studies showed that a 3-pyridinyl derivative reacted as Michael acceptor with glutathione as nucleophile (RC_{50} 552.2 μ M), but the reactivity towards biological nucleophiles was very mild compared to acrolein (RC_{50} 83.7 μ M).

5 Rhodanine and thiazolidine-2,4-dione derivatives

This chapter analyses rhodanine and thiazolidine-2,4-dione derivatives and their analogues for their anti-parasitic activity. Therefore previous anti-parasitic biological applications or anti-parasitic related studies are reported. Furthermore, it was of interest to test active inhibitors of this series against enzymes of the GPI-anchor biosynthesis and compare these results to previous inhibitors in this thesis.

5.1 Rhodanine derivatives with an anti-parasitic application compared to structurally related inhibitors that had been reported previously

Numerous biological studies on rhodanine and thiazolidine-2,4-dione derivatives have been reported. This introduction gives an overview of rhodanine and thiazolidine-2,4-dione derivatives reported to have anti-parasitic activity to date (Figure 60).

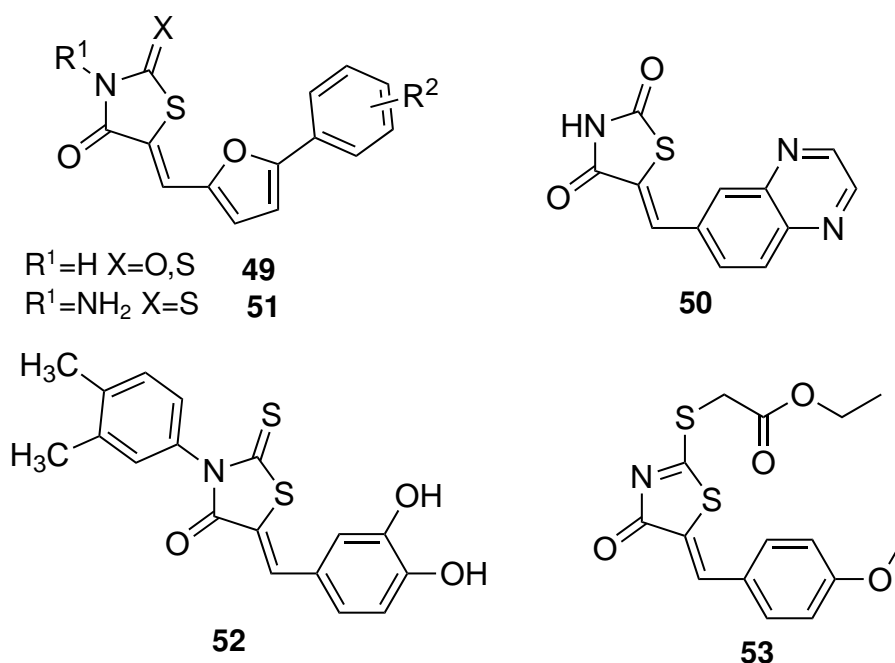


Figure 60: Examples of previous rhodanine and thiazolidine-2,4-dione derivatives and their biological application with relevance towards anti-parasitic agents; R^2 =variable.

Compounds of type **49** have been studied for their inhibitory effects on Phosphoinositide 3-Kinase γ (PI3K γ).^[236] PI3K γ is crucial in mediating leukocyte chemotaxis and mast cell degranulation.^[236] Therefore, it has been targeted for possible application as anti-inflammatory or auto-immune drugs.^[236] Compound **50** has been found to be a potent inhibitor for PI3K γ with no immediate toxicity in mice at 500 $\mu g/g$ and has further been shown to have a tumor-

static effect in PI3K γ exhibiting tumour cells and in tumour infected mice.^[117] Furthermore, **50** and therefore PI3K γ inhibition has been assessed for its role in parasite invasion and disease progression in cutaneous leishmaniasis.^[116] It has been proposed that inhibition of PI3K γ would be as effective as the drug Stibogluconate.^[116] PI3K activity has also been observed to play a critical role in host cell invasion by *T. cruzi*.^[237] However, derivatives of **49** and **50** have never been tested against parasitic protozoa, such as *T. brucei*, *T. cruzi* and *L. chagasi*. The above findings suggested that selective inhibitors of PI3K γ could potentially be active as broad-spectrum anti-parasitic agents.

Compounds of type **51** and **52** have been shown to be potent inhibitors against *Plasmodium falciparum* Enoyl-Acyl Carrier Protein Reductase (ACP).^[112] The type II fatty acid synthase (*P. falciparum*) and elongase pathway (*T. brucei*) have been validated for the development for drugs against both Malaria and Human African Trypanosomiasis (HAT).^[112,200] The etiological organism of HAT, *T. brucei* has a high demand for myristic acid in the GPI anchor biosynthesis.^[200] The myristic acid for the GPI anchor biosynthesis is partially salvaged from the host and *de novo* synthesised using the elongase pathway.^[200] Inhibitors of this pathway could prevent incorporation of myristic acid in the GPI anchor. *T. brucei* is dependant on numerous GPI anchored proteins, such as the transferrin receptor and the VSG proteins.^[65,128] Therefore, GPI anchor biosynthesis is essential for the survival of the bloodstream form of *T. brucei*.^[65] Compounds **51** and **52** have never been assessed for their activity against *T. brucei*, *T. cruzi* or *L. chagasi*.

Compound **53** was identified as a moderate inhibitor against *M. tuberculosis* growth, however, its macrophage toxicity was higher than the activity against *M. tuberculosis*.^[238] Besides this biological application, there is very little known about rhodanine derivatives of type **53**. Therefore, it would be very interesting to study this compound class for potential anti-parasitic use.

A further motivation was to study possible GPI anchor inhibition activity of this compound classes and compare them to previous results in this research project.

5.2 Synthesis of inhibitor library

In this chapter the synthesis of rhodanine derivatives with potential anti-parasitic effect is described. In the effort to synthesize anti-parasitic agents against *T. brucei*, *T. cruzi* and *L. infantum* simple 5-benzylidene modified rhodanine, thiazoidine-2,4-dione, N-amino rhodanine, N-phenyl rhodanine were investigated (blue box in Figure 61).

These derivatives were subjected to the Knoevenagel reaction to afford 5-modified analogues (R³, magenta box in Figure 61). Various benzylidene moieties were explored in 5-position, as well as modified pyridinyl substituents. Furthermore, unsubstituted rhodanine

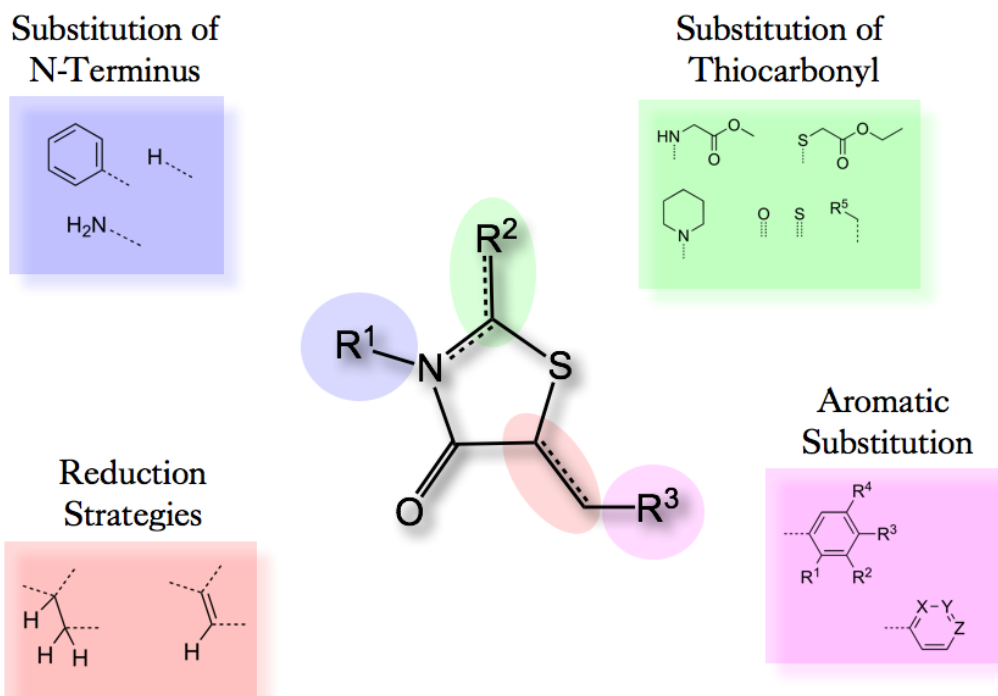
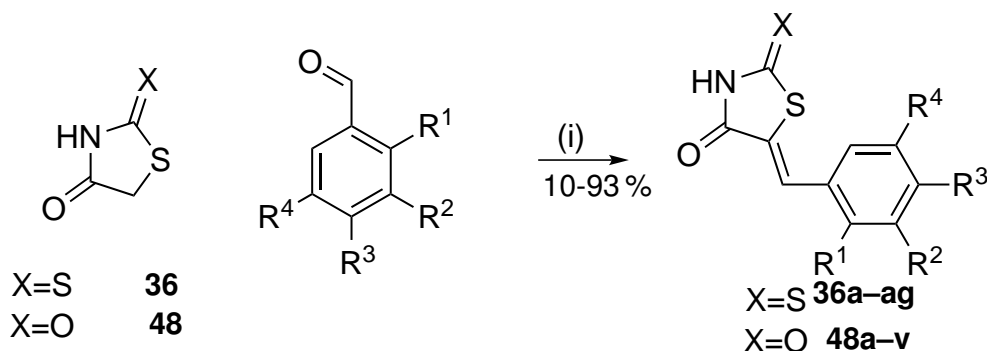


Figure 61: Strategy towards synthesis of rhodanine and thiazolidine-2,4-dione derivatives and analogues with anti-parasitic activity.

derivatives were modified on the thiocarbonyl function via alkylation with ethyl 2-bromoacetate, benzyl-bromide ($R^5 = \text{Bn}$) or methyl or ethyl iodide ($R^5 = \text{H}, \text{CH}_3$). Otherwise the thiocarbonyl was substituted with an amino-acetic methyl ester- or piperidine-moiety. Or in the simplest case, the thiocarbonyl was replaced with a carbonyl group (green box in Figure 61). In particular the latter replacement to a carbonyl group is of interest, as previous results in this thesis have shown, that this replacement resulted in reduced toxicity against HL60 cells and therefore might reduce promiscuous binding as reported for the thiocarbonyl group (see also Chapters 3.2.6, 4.2.2 and 3.3.8 for further explanation for the replacement of the thiocarbonyl).^[83] Lastly, the exo-cyclic double bond in rhodanine 5-benzylidene or thiazolidine-2,4-dione 5-benzylidene derivatives was reduced (red box in Figure 61).

5.2.1 Synthesis of 5-benzylidene modified rhodanine and thiazolidine-2,4-dione derivatives $R^1=H$, $R^2=S,O$ and $R^3=Aryl$

Unsubstituted rhodanine derivatives **36a–ag** were synthesised in a Knoevenagel reaction with various benzaldehyde derivatives (Scheme 28). The yield of the reaction varied from 10-



Scheme 28: Synthesis of rhodanine and thiazolidine-2,4-dione derivatives **36a–ag** and **48a–v**; (i) NaOAc, 80 °C, EtOH; for substitutions of X and R^1 - R^4 see Table 41, Table 42.

93 %. All rhodanine derivatives were synthesised on a parallel synthesiser in individual tubes. For this reason the reactions were not optimised for each single product, thus explaining the lower yields. The reaction was carried out over a time period of 4-5 h, at which TLC showed complete consumption of starting material. The crude reaction mixtures were filtered and washed with ethanol to obtain the desired unsubstituted 5-benzylidene rhodanine derivatives **36a–ag** in moderate yields. The products **36a–ag** were analysed by NMR spectroscopy to elucidate the configuration of the exo-cyclic double bond. The chemical shift for the CH-signal in 1H -NMR experiments varied from δ_H 7.16-8.21 ppm. The Z-configuration of the double bond is assigned by comparing the chemical shifts of the CH-signal with previous synthesised analogues. Usually, the thermodynamically more stable Z-isomer appears at lower fields, because of deshielding of the CH-signal from the neighbouring carbonyl function.^[158,162] The reported chemical shift of similar unsubstituted rhodanine derivatives was 7.30 ppm for the E-isomer and 7.74 ppm for the Z-isomer, where chemical shifts were measured in DMSO- d_6 .^[162] If previously published chemical shifts were to be used for the assignment of double bond configurations, only derivative **36v** would be assigned with an E-configured double bond, with all other derivatives in a Z-configuration. However, derivatives **36j** and **36o** were actually obtained as mixtures of E- and Z-configured products (Table 41), allowing the differentiation between both isomers. Both chemical shifts for the E- and the Z-configured double bond appeared downfield at δ_H 7.56-7.99 ppm for the E- and δ 7.70-8.21 ppm for the Z-isomer. In both cases there was a strong electron-withdrawing substituent (**36j** : CN; **36o** : NO₂), that most likely shifted the CH-signal further downfield. Therefore, it is very difficult to assign

Table 41: Synthesis of rhodanine and thiazolidine-2,4-dione derivatives; X, R¹-R⁴ for rhodanine derivatives **36a–ag**; yield and chemical shift of CH-signal; δ were recorded in DMSO-d₆, if not stated otherwise; (a) CDCl₃; (b) MeOD-d₄; n.a.: not available, see Scheme 28.

#	X	R ¹	R ²	R ³	R ⁴	yield [%]	NMR shift of CH-signal in [ppm]	
							δ_H	δ_C
36b	S	H	H	H	H	25	7.67	131.6
36c	S	CH ₃	H	H	H	23	7.74	129.3
36d	S	H	CH ₃	H	H	90	7.60	131.8
36e	S	H	H	CH ₃	H	78-86	7.58	131.7
36f	S	CF ₃	H	H	H	73	7.65-7.73	131.2
36g	S	H	CF ₃	H	H	42	8.00	129.5
36h	S	H	H	CF ₃	H	37-78	7.71	129.5
36i	S	H	H	Cl	H	63	7.61 ^(a)	n.a.
36j	S	H	H	CN	H	30	7.56(E), 7.70(Z)	129.1(Z), 133.7(E)
36k	S	H	Br	F	H	24	7.51	125.7
36l	S	H	Br	OMe	H	16	7.61	n.a.
36m	S	H	H	NHAc	H	22	7.57	n.a.
36n	S	H	H	NMe ₂	H	10	7.53	n.a.
36o	S	H	NO ₂	H	H	35	7.99(Z), 8.21(E)	129.0
36p	S	H	H	SO ₂ Me	H	12	7.73	n.a.
36q	S	H	H	CHO	H	32	7.67	n.a.
36r	S	OH	H	H	H	67	7.84	126.9
36s	S	H	OH	H	H	68	7.53	131.8
36t	S	H	H	OH	H	25	7.57	132.5
36u	S	OH	H	OH	H	15	7.97 ^(b)	n.a.
36a	S	H	OH	OH	H	14	7.47	132.8
36v	S	H	OMe	OH	OMe	93	7.16	125.4
36w	S	H	OBn	H	H	44	7.62	131.5
36y	S	H	H	OBn	H	41-89	7.62	131.7
36z	S	H	OBn	OBn	H	23	7.52 ^(a)	133.7
36ab	S	H	H	tBu	H	78	7.52	130.7

the double bond configuration only based on the chemical shift of the CH-signal. The best way would be to calculate each chemical shift based on their chemical environment. But generally, it can be assumed that the thermodynamically more stable Z-isomer is formed as the major product of the Knoevenagel reaction.^[158] The low chemical shift for **36v** is most likely explained by the two electron-donating methoxy groups in the aromatic ring. In the case of the E- and Z- mixtures in compounds **36j** and **36o**, there was a considerable difference in the chemical shift of the E- and Z-isomer ($\Delta > 0.2$ ppm). The Z/E-isomer-ratio for **36j** was 5:1, whereas the ratio for **36o** was 10:1. The higher isomerisation rate for **36j** is most likely explained by a electron withdrawing CN-group in para position in the 5-benzylidene moiety (Figure 62). The electron-withdrawing group in para position could stabilise the resonance

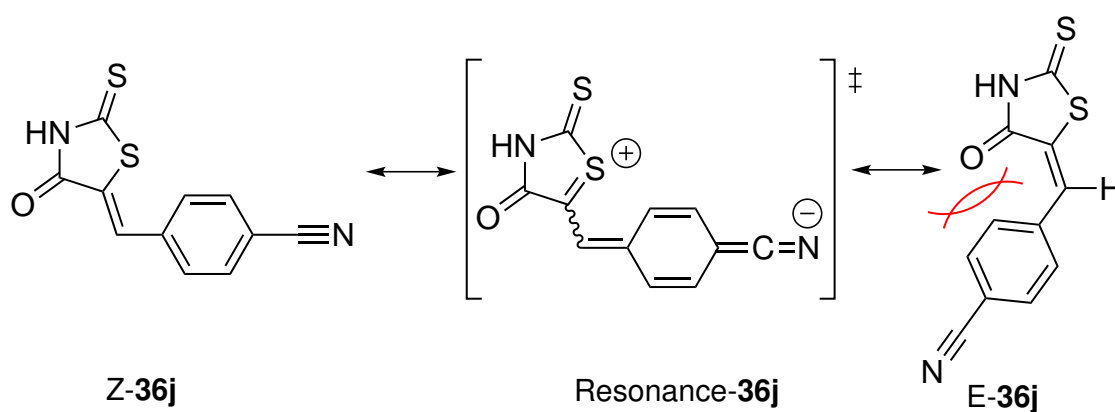


Figure 62: Resonance Structure of **36j** and possible isomerisation mechanism.

structure of **36j** (Resonance-**36j**, Figure 62). The conjugated aromatic system is interrupted and racemisation can occur. Steric hindrance of the 5-benzylidene group and the carbonyl moiety are most likely the cause for the excess of the Z-isomer (Scheme 4). whereas in the case of **36o**, a similar resonance structure can not be formed. However, in the case of **36o** electrostatic interactions between the carbonyl-group and the meta nitro-group could cause the formation of the E-isomer, although steric restrains would favour the formation of the Z-isomer (Figure 63). In comparison to **36j** this means that the isomer ratio is determined by the formation of the Knoevenagel product. The Knoevenagel reaction intermediate for the E-isomer of **36o** is shown as a Newman-projection (Figure 63). An electrostatic interaction between the carbonyl and the nitro-group would change the equilibrium slightly towards the formation of the E-isomer (Scheme 4).

The analogues thiazolidine-2,4-dione derivatives **48a–v** were obtained as a single regio-isomer (Table 42). The chemical shift of the CH-signal was δ_H 7.11–8.13 ppm. The chemical shift was dependant on the substitution of the aromatic ring, such that trifluoromethyl substituent led to a down-field shift of the CH-signal. Based on the chemical shifts, it can be

Table 42: Synthesis of thiazolidine-2,4-dione derivatives; X, R¹-R⁴ for thiazolidine-2,4-dione derivatives **48a–v**; yield and chemical shift of CH-signal; δ were recorded in DMSO-d₆, if not stated otherwise; (a) CDCl₃; (b) MeOD-d₄; n.a.: not available; see Scheme 28.

#	X	R ¹	R ²	R ³	R ⁴	yield [%]	NMR shift of CH-signal in [ppm]	
							δ_H	δ_C
48o	O	H	H	H	H	42	7.29	127.5
48a	O	CH ₃	H	H	H	31	7.89	129.6
48b	O	H	CH ₃	H	H	45	7.84 ^(a)	n.a.
48c	O	H	H	CH ₃	H	24	7.54 ^(b)	n.a.
48d	O	CF ₃	H	H	H	16	8.13 ^(a)	133.5
48e	O	H	CF ₃	H	H	45	7.93	130
48f	O	H	H	CF ₃	H	15	7.87	129.8
48g	O	OH	H	H	H	38	8.02	127
48h	O	H	OH	H	H	31	7.43	127.2
48i	O	H	H	OH	H	15	7.52 ^(b)	n.a.
48j	O	OH	H	OH	H	no product		
48p	O	H	OH	OH	H	46	7.11	123.1
48k	O	H	OMe	OH	OMe	47	7.21	123.2
48l	O	H	OBn	H	H	76	7.35	129.9
48m	O	H	H	OBn	H	38	7.74	131.1
48n	O	H	OBn	OBn	H	29	7.70 ^(a)	134.6 ^(a)

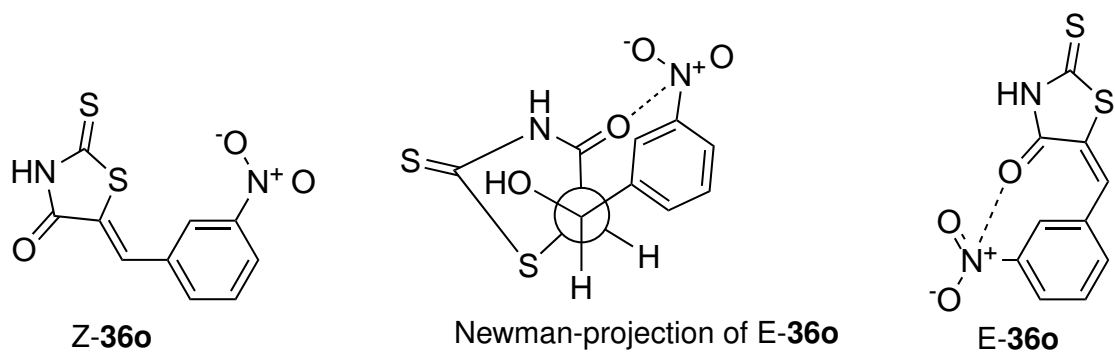


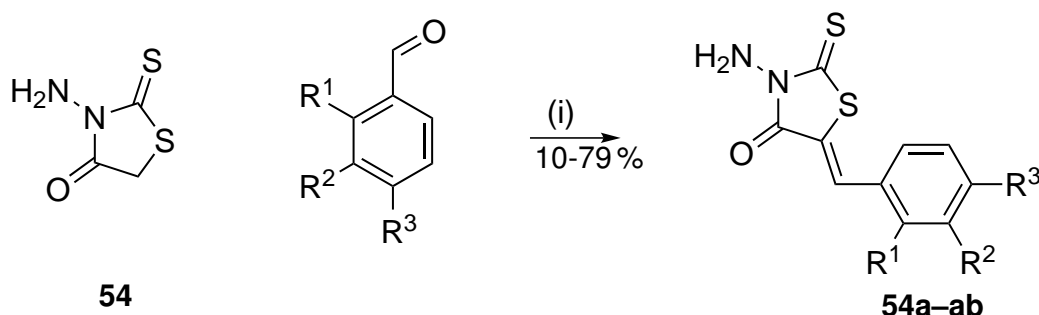
Figure 63: Formation of the E-isomer of **36o** shown in Newman-Projection.

assumed that only the thermodynamically more stable Z-isomer was formed.^[163]

Another interesting observation was the missing $^5J_{H,F}$ -long range coupling of compounds **36f** and **48d**. Analogous derivatives which were substituted on the N-3-position showed a long range coupling of the CH-signal and the trifluoromethyl group (Figure 20).

5.2.2 Synthesis of 5-benzylidene modified 3-amino rhodanine derivatives $R^1=NH_2$, $R^2=S$ and $R^3=Aryl$

N-amino rhodanine derivatives **54a–ab** (Scheme 29, Table 43) were synthesised via Knoevenagel reaction. The reaction was tolerated by a broad range of substituted benzaldehydes, however aldehydes substituted with labile groups such as boronic acid (**54y**), methyl sulfoxide (**54z**) or di-aldehydes (**54aa**) failed to react and no condensation product could be obtained. Otherwise, the reaction yielded the desired products in good yields of 10–79 %. The chemical



Scheme 29: Synthesis of 5-benzylidene modified N-amino rhodanine derivatives **54a–ab**; (i) NaOAc, 80 °C, EtOH, see Table 43.

shift of the CH-signal in the 1H -NMR experiment was in the range of δ_H 7.52–8.96 ppm, while unsubstituted derivatives had a chemical shift around δ_H 7.70–7.90 ppm. Only the Z-isomer has been observed for the condensation reaction with N-amino rhodanine and various benzaldehydes. Particularly interesting was **54p** as it showed a chemical shifts of the CH-signal at δ_H 8.96 ppm and δ_C 158.7 ppm. This was the first example, where the CH-signal was that far downfield, it could be possible that the ortho OH substituent of the 5-benzylidene moiety undergoes hydrogen-bond interactions with the carbonyl group, bringing the CH-signal in very close proximity to the carbonyl and the hydroxy group. The combined deshielding of the hydroxy group and the carbonyl group could account for the signal appearing at 8.96 ppm.

5.2.3 Synthesis of 5-benzylidene modified N-phenyl rhodanine derivatives $R^1=Ph$, $R^2=S$ and $R^3=Aryl$

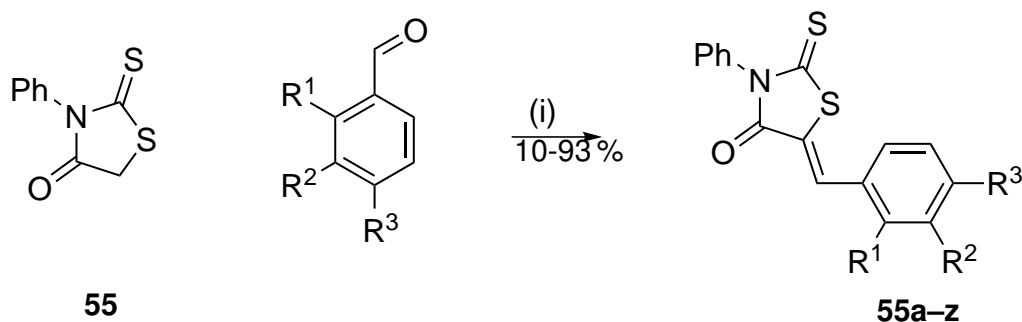
N-phenyl rhodanine derivatives **55a–z** were synthesised using the standard Knoevenagel conditions with NaOAc and various benzaldehydes in ethanol at 80 °C (Scheme 30). The products were obtained mostly after simple filtration in good yields of 10–93 % (Table 44). But the chosen reaction conditions were not tolerated with trifluoromethyl substituted aldehydes (**55t–v**), aldehydes bearing labile functional groups such as methyl sulfoxide and di-aldehydes (**55s** and **55y**), nor with the di-halogen or di-hydroxy benzaldehydes (**55w** and **55x**).

Table 43: Synthesis of 5-benzylidene modified N-amino rhodanine derivatives; R¹-R⁴ for N-amino rhodanine derivatives **54a–ab**; yield and chemical shift of CH-signal, see Scheme 29.

#	R ¹	R ²	R ³	yield [%]	NMR shift of CH-signal [ppm]		
					δ_{solvent}	δ_H	δ_C
54a	H	H	H	79	DMSO-d ₆	7.86	133.5
54b	CH ₃	H	H	32	DMSO-d ₆	7.93	131.2
54c	H	CH ₃	H	70	DMSO-d ₆	7.81	133.5
54d	H	H	CH ₃	74	DMSO-d ₆	7.81	133.5
54e	CF ₃	H	H	12	MeOD-d ₄	8.19	n.a.
54f	H	CF ₃	H	78	DMSO-d ₆	7.98	131.4
54g	H	H	CF ₃	41	CDCl ₃	7.82	130.7-132.1
54h	H	H	Cl	50	DMSO-d ₆	7.86	132
54i	H	Br	F	79	DMSO-d ₆	7.85	131.6
54j	H	Br	OMe	34	DMSO-d ₆	7.82	132.0
54k	H	H	CCH	28	DMSO-d ₆	7.86	132.1
54l	H	H	CN	42	DMSO-d ₆	7.90	130.9
54m	H	NO ₂	H	69	DMSO-d ₆	8.04	n.a.
54n	H	H	NHAc	68	DMSO-d ₆	7.73-7.78	133.4
54o	H	H	NMe ₂	21	DMSO-d ₆	7.74	135.0
54p	OH	H	H	65	DMSO-d ₆	8.96	158.7
54q	H	OH	H	32	DMSO-d ₆	7.74	133.7
54r	H	H	OH	31	DMSO-d ₆	7.74	133.7
54s	OH	H	OH	55	DMSO-d ₆	7.97	130.0
54t	H	OH	OH	14	MeOD-d ₄	7.67	n.a.
54u	H	H	OMe	62	DMSO-d ₆	7.82	133.7
54v	H	OBn	H	10	CDCl ₃	6.97-7.52	n.a.
54w	H	H	OBn	63	DMSO-d ₆	7.82	133.7
54x	H	OBn	OBn	31	DMSO-d ₆	7.76	133.7
54y	H	H	B(OH) ₂	no product			
54z	H	H	SO ₂ Me	32	DMSO-d ₆	8.85	n.a.
54aa	H	H	CHO	no product			

Table 44: Synthesis of 5-benzylidene modified N-phenyl rhodanine derivatives; R¹-R⁴ for N-phenyl rhodanine derivatives **55a–z**; yield and chemical shift of CH-signal, see Scheme 30.

#	R ¹	R ²	R ³	[%] yield	NMR shift of CH-signal [ppm]		
					δ_{solvent}	δ_H	δ_C
55a	H	H	H	60	CDCl ₃	7.80	133.6
55b	CH ₃	H	H	17	CDCl ₃	8.02	131.4
55c	H	CH ₃	H	32	CDCl ₃	7.78	133.9
55d	H	H	CH ₃	47	CDCl ₃	7.78	133.9
55e	H	H	Cl	46	CDCl ₃	7.74	n.a.
55f	H	H	CCH	18	CDCl ₃	7.76	n.a.
55g	H	H	CN	57	CDCl ₃	7.75	n.a.
55h	H	Br	OMe	36	CDCl ₃	7.67	n.a.
55i	H	H	NHAc	34	DMSO-d ₆	7.77	132.6
55j	H	H	NMe ₂	10	CDCl ₃	7.03(E), 7.73(Z)	134.9 (Z)
55k	H	NO ₂	H	19	CDCl ₃	7.81	n.a.
55l	OH	H	H	12	MeOD-d ₄	8.17	n.a.
55m	H	OH	H	15	CDCl ₃	7.73	n.a.
55n	H	H	OH	23	DMSO-d ₆	7.76	n.a.
55o	H	OH	OH	78	DMSO-d ₆	7.66	133.9
55p	H	OBn	H	93	CDCl ₃	7.75	133.2
55q	H	H	OBn	21	CDCl ₃	7.75	133.6
55r	H	OBn	OBn	60	CDCl ₃	7.59	133.8
55s	H	H	SO ₂ Me	no product			
55t	CF ₃	H	H	no product			
55u	H	CF ₃	H	no product			
55v	H	H	CF ₃	no product			
55w	H	Br	F	no product			
55x	OH	H	OH	no product			
55y	H	H	CHO	no product			



Scheme 30: Synthesis of 5-benzylidene modified N-phenyl rhodanine derivatives **55a–z**, (i) NaOAc, 80 °C, EtOH, see Table 44.

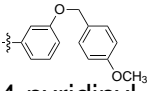
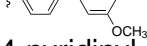
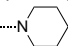
The chemical shift of the CH-signal was almost diagnostic for N-phenyl rhodanine derivatives **55a–z** with chemical shift of 7.70-7.80 indicated the thermodynamically more stable Z-isomer, whereas the chemical shift of the corresponding E-isomer was observed at 7.03 ppm (**55j**). The E-isomer was obtained in a mixture of 1:4 E to Z ratio. This E to Z ratio could possibly be explained through the electron-donating dimethylamino group. The electrons could be delocalised over the whole aromatic system (Figure 64), stabilising the negative charge through the carbonyl group in the rhodanine moiety. However there was no mixture of isomers observed, when the N-substituent was an allyl or acetic acid function. Therefore, it seems that an additional delocalisation of electron over the N-3-substituent is responsible for the isomerization (Figure 64). A possible resonance structure would involve a positive charge on the phenyl-amino substituent and a negative charge on the thiocarbonyl, stabilising all charges leading to the double bond isomerization (Figure 64). The equilibrium of this racemization should favour the Z-isomer because of steric clashes with the carbonyl group and the benzylidene moiety (Scheme 4, p. 35).

5.2.4 Synthesis of 5-benzylidene-3-benzyloxy- and heterocyclic-modified rhodanine **56a–d**, thiazolidine-2,4-dione, N-amino rhodanine **58a–i** and N-phenyl rhodanine **59a–c** derivatives.

Initially, the rhodanine and thiazolidine-2,4-dione derivatives were subjected to pyridine carboxaldehyde in the presence of NaOAc as a weak base (Scheme 31, Table 45).

This condensation reaction resulted in the synthesis of the pyridinyl-rhodanine derivatives **56a**, **56b**, and **56c** in good yields of 50-59% (Table 45). In contrast, the N-amino and N-phenyl substituted rhodanine derivatives yielded only the 2-pyridinyl-derivatives **58d** and **59c**, whereas in the case of the 3- or 4-pyridinylaldehydes no product was obtained. It was possible that the aldehydes and/ or the products decomposed under the reaction conditions used, while 2-pyridinyl-aldehyde was more stable to temperatures of 80 °C. The 2-pyridinyl derivative **59c**

Table 45: Synthesis of heterocyclic and 3-benzyloxy modified rhodanine derivatives; X, R¹-R² of 3-benzyloxy- and heterocyclic-modified rhodanine **56a–d**, thiazolidine-2,4-dione **57a–d**, N-amino rhodanine **58a–i** and N-phenyl rhodanine **59a–c** derivatives; yield and chemical shift of the CH-signal in DMSO-d₆, Scheme 31.

#	X	R ¹	R ²	[%] yield	NMR shift of CH-signal [ppm]	
					δ_H	δ_C
56a	S	H	4-pyridinyl	50- 96	7.57	n.a.
56b	S	H	3-pyridinyl	52	7.61	125.7
56c	S	H	2-pyridinyl	59	7.68	127.5
56d	S	H		85	7.59	131.3
57a	O	H		91	7.50	126.8
57b	O	H	4-pyridinyl	48	7.67	n.a.
57c	O	H	3-pyridinyl	53	7.56	123.3
57d	O	H	2-pyridinyl	24	7.54	n.a.
58a	S	NH ₂	CH ₂ Cl	no product		
58b	S	NH ₂	4-pyridinyl	no product		
58c	S	NH ₂	3-pyridinyl	no product		
58d	S	NH ₂	2-pyridinyl	57	7.87	128.8
58e	S	NH ₂	(CH ₂) ₄ OH	no product		
58f	S	NH ₂		no product		
58g	S	NH ₂	CH(CH ₃) ₂	no product		
58h	S	NH ₂	NH ₂	no product		
58i	S	NH ₂	H	no product		
59a	S	Ph	4-pyridinyl	no product		
59b	S	Ph	3-pyridinyl	no product		
59c	S	Ph	2-pyridinyl	72	8.85	149.6

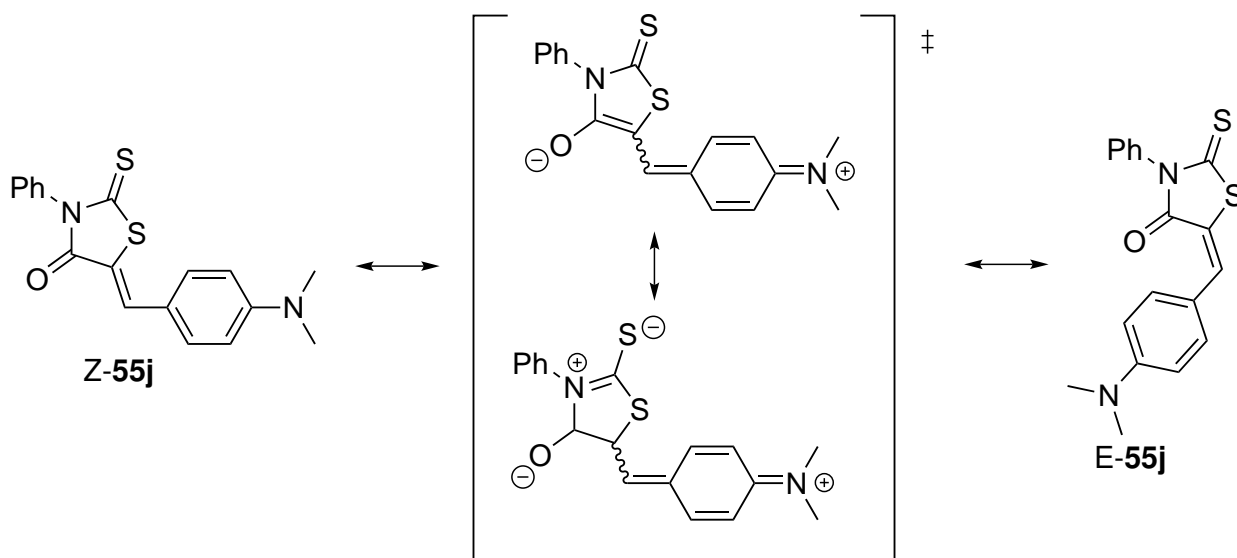
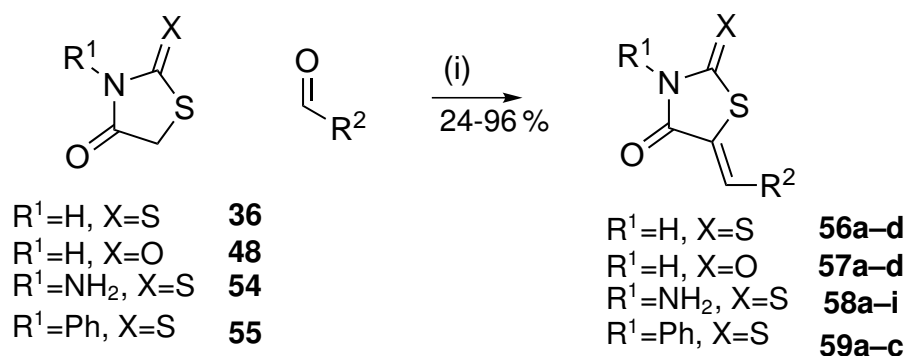


Figure 64: Resonance structures of **55j** to explain high Z/E isomer ration.

showed a very low field chemical shift of 8.85 ppm for the CH-signal. Similarly high values of 7.87-7.68 ppm for CH-signal in the presence of the 2-pyridinyl-group have been observed in the rhodanine derivatives **58d** and **56c**. The values for the CH-signal of 3- and 4-pyridinyl derivatives appeared at lower field at 7.57-7.61 ppm. It is possible that the 2-pyridinyl group in rhodanine derivatives performed a hydrogen-bonding interaction with the carbonyl-group and the CH-signal, resulting in a closer proximity of the CH to the two electronegative groups. A similar phenomena was observed in the case of the rhodanine derivative **54p**, which was modified with a 2-hydroxy aryl group in position 5 and had a chemical shift of the CH-signal at 8.96 ppm. It seemed that this interaction did not occur in thiazolidine-2,4-dione derivatives **57d**, **57c**, and **57b**, which had very similar CH chemical shifts of 7.54-7.67 ppm. All products were obtained as a single regio-isomer, which was most likely the Z-configured double bond isomer. Attempts to introduce aliphatic substituents on position 5 on the N-amino rhodanine moiety failed and no products could be obtained under the reaction conditions used.

5.2.5 Alkylation of the thiocarbonyl in rhodanine derivatives $R^2=SMe$, SEt , SBn , thio-acetic ester

Rhodanine derivatives, where the thiocarbonyl was substituted with alkyl groups were synthesised by nucleophilic substitution with alkyl-halides. These derivatives were of interest for their previous biological activity against *M. tuberculosis* growth,^[238] but also to study the effect of thiocarbonyl alkylation on the anti-parasitic activity of this inhibitor class. Particularly the introduction of a acetic ester functionality was interesting, as N-acetic ester derivatives have been identified as good inhibitors of DPMS and/ or the first mannosyltransferase in the GPI-



Scheme 31: Synthesis of heterocyclic and 3-benzyloxy modified rhodanine **56a-d**, thiazolidine-2,4-dione **57a-d**, N-aminorhodanine **58a-i** and N-phenyl rhodanine **59a-c** derivatives; (i) NaOAc, 80 °C, EtOH, see Table 45.

anchor biosynthesis in *T. brucei*, while having low μM activity against *T. brucei*, *T. cruzi* and *L. infantum* (Chapter 3.7). The substitution to a N-allyl functionality has been shown to decrease both DPMS and/ or MT-1 inhibition as well as *in vitro* anti-trypaosomal activity (Chapter 4.6). Therefore it was of interest to study the effect on shifting this essential functional group onto the thiocarbonyl position.

The reaction was carried out in the presence of a strong base, such as sodium hydroxide (NaOH). The NaOH deprotonates the rhodanine **36** and forms the sodium salt of the rhodanine **60a-b**, which now readily reacted with electrophiles such as alkyl-halides (Figure 65). This reaction can easily be visualised by the nucleophilic attack of **60b** and alkyl-halides

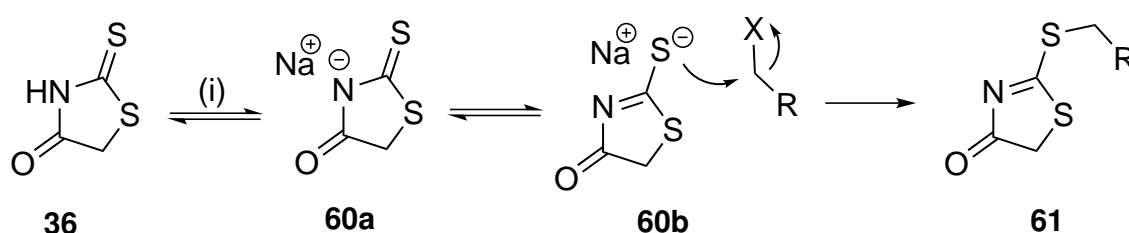
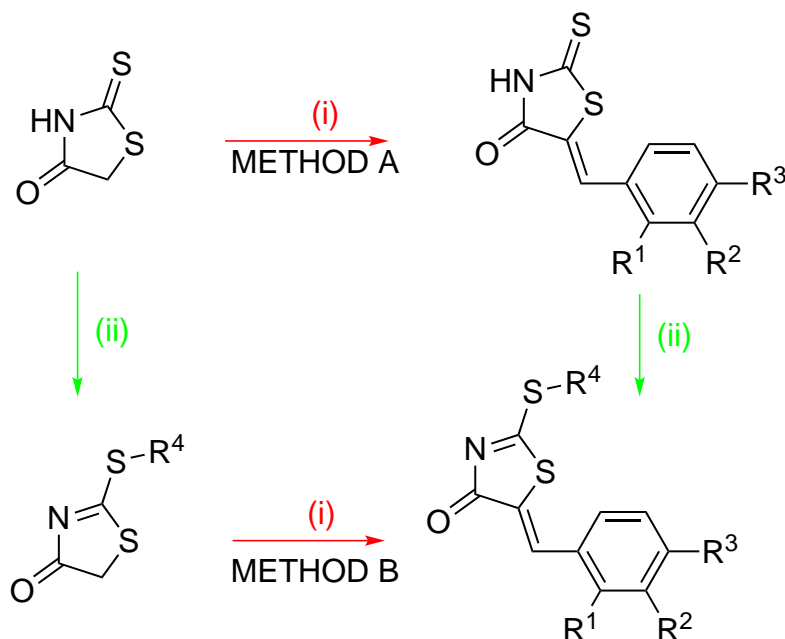


Figure 65: Electrophilic substitution of the thiocarbonyl group in rhodanine derivatives; (i) NaOH, see Scheme 32.

to form the alkylated thiocarbonyl **61** (Figure 65). Two strategies towards the synthesis of rhodanine-5-benzylidene derivatives, where the thiocarbonyl was alkylated by various aliphatic substituents, were employed. In the first approach (Method A (i), Scheme 32), rhodanine was subjected to Knoevenagel reactions with various benzaldehyde derivatives. In the subsequent step the condensation products were subjected to alkylating agents (Conditions (ii), Scheme 32). While in the second method (Method B, Scheme 32), the alkylation of the thio-

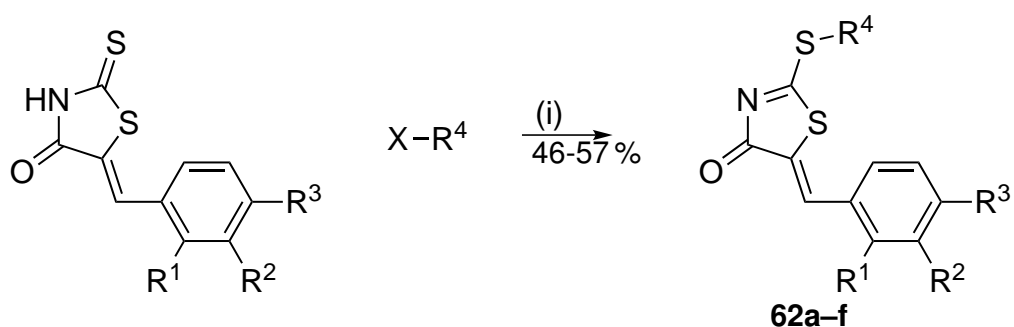
carbonyl was carried out prior to the condensation reaction.



Scheme 32: Two approaches towards alkylated thiocarbonyl derivatives; (i) Benzaldehyde derivatives, NaOAc, 80 °C, EtOH; (ii) NaOH_{aq} (2 %), R⁴-halide, see Figure 65.

Method A: Knoevenagel reaction followed by Alkylation

Ortho-, meta- or para-trifluoromethyl substituted rhodanine derivatives **36f**, **36g**, and **36h** were reacted with methyl iodide or benzyl bromide in the presence of NaOH as base (Scheme 33). The alkylation proceeded in good yields of 46-57% and the products were obtained after



Scheme 33: Alkylation of the thiocarbonyl group in benzylidene rhodanine derivatives; (i) NaOH_{aq} (2 %), see Table 46.

simple filtration. The chemical shift of the CH-signal in alkylated derivatives **62a-f** varied between δ_H 4.96-8.14 ppm. The alkylation of the thiocarbonyl group resulted in a change of

the steric demands of the rhodanine-moiety, most likely allowing the Knoevenagel reaction to proceed via the E-isomer transition state (Scheme 4). This is clearly shown in Table 46, the smaller the alkylation substituent R^4 , the bigger the ratio between E- and Z-isomer. But

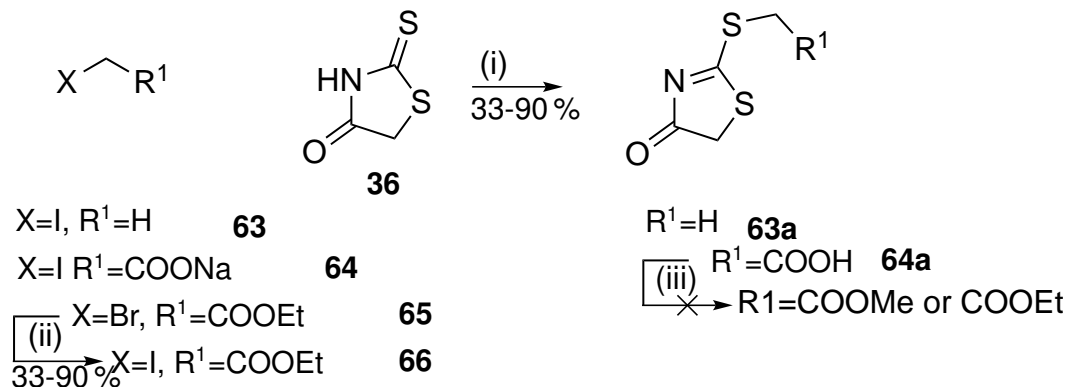
Table 46: Alkylation of the thiocarbonyl group in benzylidene rhodanine derivatives; X, R^1 - R^4 for alkylation products **62a–f**, yields and chemical shift of CH-signal, **62c** and **62f** in DMSO- d_6 , all other in $CDCl_3$, see Scheme 33.

#	X	R^1	R^2	R^3	R^4	yield [%]	NMR shift of CH-signal [ppm]		
							E:Z ratio	δ_H	δ_C
62a	I	CF_3	H	H	CH_3	48	0:1	8.14(Z)	131.2(Z)
62b	I	H	CF_3	H	CH_3	46	3:4	5.25(E), 7.81(Z)	n.a.
62c	I	H	H	CF_3	CH_3	48	10:1	4.96(E), 7.94(Z)	54.0(E)
62d	Br	CF_3	H	H	Bn	46	0:1	8.13(Z)	131.5
62e	Br	H	CF_3	H	Bn	54	0:1	7.85(Z)	133.9
62f	Br	H	H	CF_3	Bn	57	1:1	5.46(E), 7.96(Z)	57.5(E), 133.3(Z)

the steric considerations are not enough to explain the E:Z ratio. As described previously, the trifluoromethyl group is able to interact with the CH and the carbonyl-group (Figure 20). This interaction can be quantified by the long-range $^5J_{H(C),F}$ -coupling of the CH-signal and the trifluoromethyl group (Figure 20). Here, for the first time, this interaction could be brought into connection with the formation of double bond regio-isomers. An ortho-trifluoromethyl group interacts over space with the CH-group, establishing a preference for the Z-isomer. The further away the trifluoromethyl group in relation to the CH-group the greater the amount of E-isomer. In the para-trifluoromethyl substituted derivative **62c** the interaction can not be established and as a result the E-isomer occurred almost exclusively (ratio E:Z 10:1). However, if the R^4 group has a higher steric demand, as it is seen with the benzyl-group in **62d**, **62e**, and **62f**, the Z-isomer was favoured. The trifluoromethyl substituent and the steric demanding benzyl group both favour the Z-configuration over the E-isomer. Steric considerations on its own led to a formation of E:Z in a 1:1 ratio, as can be seen with **62f**. Here the trifluoromethyl group in para-position and therefore does not contribute to the formation of Z-isomer any longer. Compounds **62a–f** were ideal for the study of factors important for the formation of double bond isomers in rhodanine derivatives. But the chemical shift of the CH-signal for the E-isomer, suggested aliphatic characteristics, as the δ_H was around 4.96-5.46 ppm and the δ_C was 54.0-57.5 ppm. It was unclear as how this might effected the double bond isomerisation, so the above mentioned observation might only account for these types of derivatives.

Method B: Alkylation prior to Knoevenagel reaction

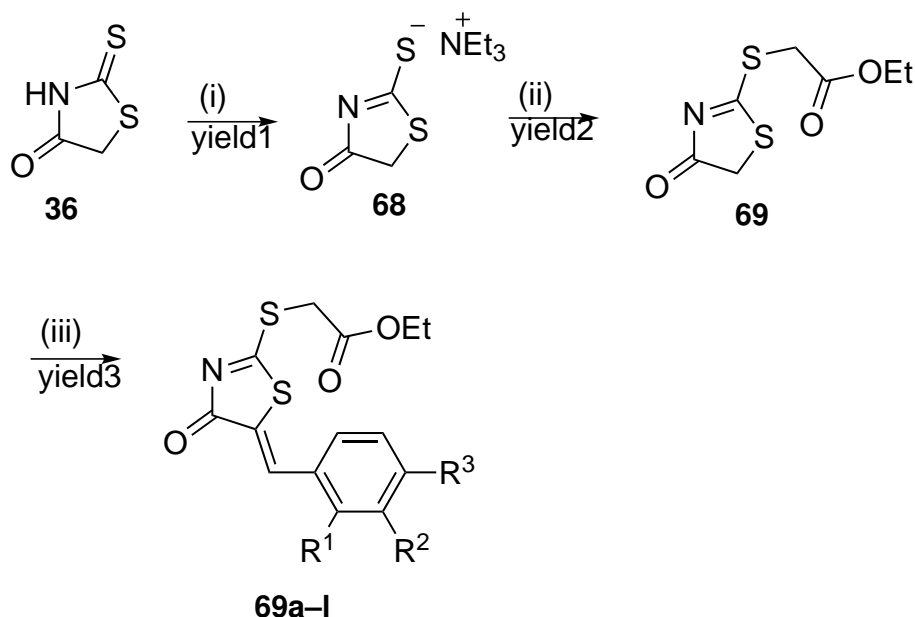
The alkylation of rhodanine derivatives was achieved by subjecting rhodanine **36** to various alkylating agents under slightly basic conditions (Scheme 34). Initially, the reaction conditions



Scheme 34: (i) 2 % NaOH_(aq), 16 h, rt; (ii) NaI, dark, acetone; (iii) DCC, DMAP, EtOH or MeOH, CHCl₃, rt.

were validated by using ethyl iodide as the alkylating agent.^[239] The reaction proceeded to the desired alkylation product **63a** with a 90 % yield after re-cystrallisation from methanol.^[239] After the validation of the reaction protocol, sodium iodoacetic acid **64** was subjected to rhodanine **36**. The alkylation occurred in moderate yields of 33 % after re-crystallisation from methanol. However, in order to obtain products which have previously been reported as anti-tuberculosis agents (**53** in Figure 60), the free carboxylic ester needed to be transformed to its ester.^[238] Here the previous protocol (Scheme 10) with DCC, DMAP and alcohol was applied to transform the free carboxylic ester of **64a** to its ethyl or methyl ester. However this resulted in decomposition products and no product could be isolated. An alternative strategy to the ester was employed. Performing the alkylation with the iodoacetate **66** would yield the desired ester in only one reaction step. But iodo ester **66** first had to be synthesised, starting from ethyl 2-bromoacetate **65**. The Finkelstein reaction between ethyl 2-bromoacetate **65** and sodium iodide in the dark yielded the desired iodo-substrate in excellent yields of 98 %, as confirmed by NMR and mass spectrometric analysis. The substitution product **66** was reacted with rhodanine **36** under NaOH catalysis, but these slightly basic conditions resulted in complete hydrolysis after 12 h.

This lack of success in the synthesis of S-modified acetic ester derivatives, meant that other approaches were subsequently investigated. One such approach was the pre-activation of the rhodanine precursor **36** with NEt₃ (Scheme 35).^[240] Treating rhodanine **36** with NEt₃ results in the formation of its triethylamine salt **68**. The base activated precursor **68** was easily alkylated by chloro- or bromo-alkyls.^[240] Here, ethyl 2-bromoacetate **65** was used as



Scheme 35: Synthesis of S-modified acetic ester analogues; (i) NEt_3 , isopropanol, $100\text{ }^\circ\text{C}$; (ii) **65**, acetone, $70\text{ }^\circ\text{C}$; (iii) NaOAc , EtOH , $80\text{ }^\circ\text{C}$.

the alkylating agent for **68**. The alkylation product **69** was afforded in excellent yields of 93–97 % after re-crystallisation.

In the consecutive step, the alkylated product **69** was subjected to various aromatic aldehydes in a Knoevenagel condensation reaction. The condensation products **69a–I** were afforded after simple filtration and were analysed by NMR and mass spectrometry (Table 47). While ^1H - and ^{13}C -NMR identified the products, the mass spectrometric analysis of compounds **69b**, **69c**, **69d**, and **69e** showed in addition to the molecular mass peak (M) another $M+100$ peak. It is likely, that under the conditions of the ionisation an adduct or different product was formed during spectrometric analysis. The instability in the mass analysis might also explain the overall low yield of the Knoevenagel reaction of 10–54 % for the benzylidene derivatives **69a–j**. The reaction with the 2-furanyl-aldehyde proceeded well and 84 % of product were isolated after filtration. The alkyl-ester derivative **69a** was analysed by mass spectrometry, but the Knoevenagel reaction yielded only traces of the desired product. The chemical shift of the CH-signal δ_{H} was between 7.00–8.05 ppm for all derivatives. Compound **69h** was obtained as a 1:1 mixture of E/Z-isomers, so it would seem that the formation of both isomers is facilitated if the thiocarbonyl group is alkylated. It is reasonable to assume that compounds **69d**, **69e**, **69f**, **69g**, and **69j** were obtained as the E-isomer as the only product. Compounds **69b** and **69c** were difficult to compare in these series, as the spectra were recorded in CDCl_3 , as other compounds were recorded in DMSO-d_6 . The CH-signal of previous NMR-experiments showed that the chemical shift is solvent dependant. However, in the ^{13}C -NMR

Table 47: Synthesis of S-modified acetic ester analogues; R¹-R³ for alkylation products **69a–l**; yield and chemical shift of the CH-signal.

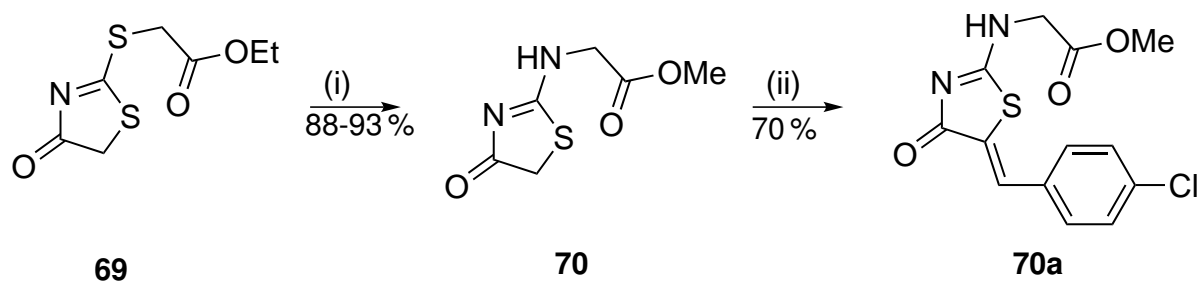
#	R ¹	R ²	R ³	yield [%]	NMR shift of CH-signal [ppm]		
					δ_{solvent}	δ_H	δ_C
69a	CH ₃	H	H	n.a.	n.a.	n.a.	n.a.
69b	H	CH ₃	H	30	CDCl ₃	7.81	134.6
69c	H	H	CH ₃	33	CDCl ₃	7.80	134.4
69d	H	OBn	H	21	DMSO-d ₆	7.32	130.0-136.9
69e	H	H	OBn	10	DMSO-d ₆	7.33	126.4
69f	H	OBn	OBn	14	DMSO-d ₆	7.27	127.7
69g	H	OH	H	16	DMSO-d ₆	7.00-7.05	121.0
69h	H	H	OH	14	DMSO-d ₆	7.29(E), 7.79(Z)	127.0(E), 136.5(Z)
69i	OH	H	OH	54	MeOD-d ₄	8.05	n.a.
69j	H	OH	OH	12	DMSO-d ₆	7.20	127.9
69k	OH	H	H	no product			
69l		2-furanyl		84	DMSO-d ₆	7.71	121.6

the changes in chemical shift were smaller and indeed the values of 123.6-134.4 ppm for compounds **69b** and **69c** were very similar to the reference chemical shift δ_C 136.5 ppm of **69h**.

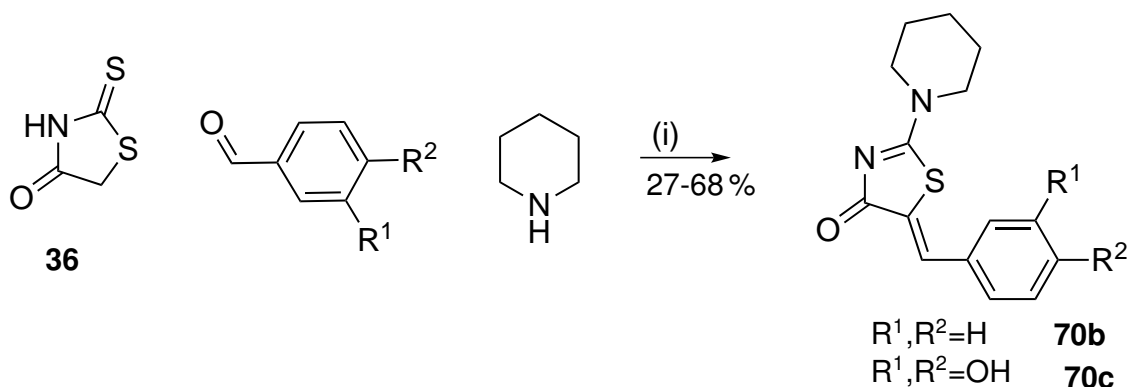
5.2.6 Replacement of thiocarbonyl group in rhodanine derivatives R²=NH-acetic ester or N-piperidyl

The alkylated thiocarbonyl derivatives **69a–l** have been shown to be unstable towards mass spectrometric analysis (Chapter 5.2.5). Indeed, the thio-alkyl group in derivatives of **69** were known to be good leaving groups.^[240] This thio-alkyl group can be substituted with primary amines in a nucleophilic substitution reaction.^[240] In order to show this experimentally, **69** was reacted with glycine methyl ester (NH₂-Gly-OMe) in the presence of N,N-diisopropylethylamine (DIPEA) as a base (Scheme 36). The amino substituted derivative **70** was obtained in excellent yields of 88-93 %. In the consecutive step **70** was reacted with 4-chloro-benzaldehyde in the presence of sodium acetate in methanol. Interestingly, the ethyl ester **70** was transformed to its methyl ester under Knoevenagel condensation conditions in methanol. The product **70a** was obtained in 70 % yield after column chromatography.

The nucleophilic substitution of the thiocarbonyl group in rhodanine derivatives can also be achieved in a one-pot reaction sequence.^[241] Therefore, rhodanine is reacted with piperidine and benzaldehyde in the presence of catalytic amounts of glacial acetic acid (Scheme 37). The products were obtained in good yields of 23-68 % after simple filtration. This was an interesting experiment, because the initial found reaction conditions for the Knoevenagel re-

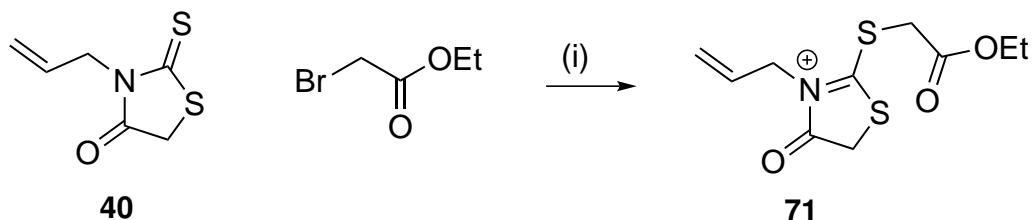


Scheme 36: (i) $\text{NH}_2\text{-Gly-OMe}$, DIPEA, EtOH, 80°C ; (ii) 4-chloro-benzaldehyde, NaOAc, EtOH, 80°C .



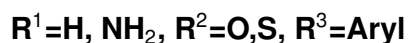
Scheme 37: Synthesis of thiocarbonyl substituted analogues; (i) AcOH, EtOH, 80°C .

action were piperidine in ethanol.^[68] Similar thiocarbonyl substitution reaction as well as the alkylation of N-modified rhodanine derivatives have previously been reported.^[242,243] However, attempts to repeat this claim failed (Scheme 38). N-allyl rhodanine **40** did not react with ethyl 2-bromoacetate towards the salt **71**, instead only starting materials were isolated. This suggests that these particular side reactions with N-substituted rhodanine derivatives are not very likely to occur.



Scheme 38: Attempts to alkylate N-substituted rhodanine derivatives; (i) 70°C , acetone.

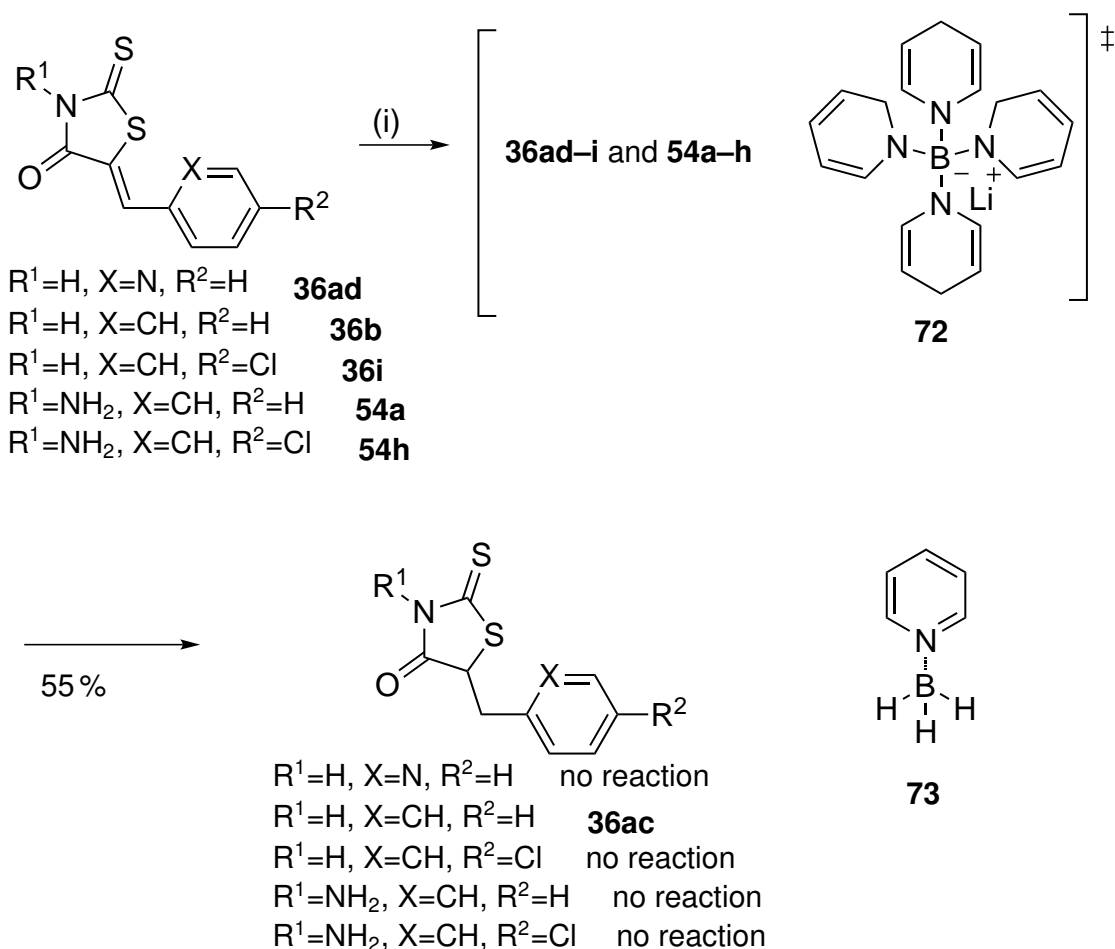
5.2.7 Reduction of double-bond in rhodanine and thiazolidine-2,4-dione derivatives



Representative compounds **36ad**, **36b**, **36i**, **54a**, **54a**, **54a**, and **54h** were chosen for the reduction of the exo-cyclic double bond. Similar derivatives in the N-acetic acid or N-allyl series showed low μM activity against *T. brucei* and reduction of analogous derivatives was therefore of interest in this series. The exo-cyclic double bond gives the molecule an essentially planar structure and is also part of a Michael acceptor system. Reduction of the double bond could be beneficial in terms of increased solubility by disruption of the planar configuration and loss of activity as a potential Michael acceptor. The reduction of rhodanine derivatives is complicated by the presence of a thiocarbonyl (S1) and carbonyl group. Catalytic hydrogenation would result in catalyst poisoning by the sulphur atoms contained in the rhodanine moiety.^[244] Indeed, catalytic hydrogenation with Pd/C and high H_2 pressure is used for the removal of the thiocarbonyl group, although a huge excess (300 eq) of Pd/C had to be used in the previous study to remove the thiocarbonyl.^[244] There are only few general methods reported for the reduction of rhodanine and thiazolidine-2,4-dione derivatives.^[176] One of these methods uses $LiBH_4$ and pyridine for the selective reduction of the double bond, without reduction of the carbonyl group.^[176] Another reduction procedure uses the Hantzsch ester as mild reducing agent for the exo-cyclic double bond.^[177] Initially, the first procedure with $LiBH_4$ and pyridine as the reducing agent was used for the reduction of the double bond in anhydrous THF. The reducing agent was proposed to be the pyridine-borane complex **72** (Scheme 39).^[176] The pyridine played a critical role for the selective reduction of the double bond, as in its absence unspecified mixtures were reported.^[176] 1H - and ^{13}C -NMR studies showed that pyridine does not undergo any interaction with the starting rhodanine or thiazolidine-2,4-dione, leaving only the complexation to $LiBH_4$ as an explanation for the regioselective reduction. Similar pyridine complexes have been reported with lithium aluminium hydride.^[176]

The reduction was carried out first using $NaBH_4$, LiCl and pyridine in anhydrous THF, for the *in situ* formation of $LiBH_4$ (Scheme 39). However, only compound **36b** was reduced to the desired product **36ac** and this reaction only proceeded in moderate yields of 55 %. In all other cases only starting material and the pyridine-boron complex **73** could be recovered from the reaction mixture after purification by flash column chromatography. The pyridine complex **73** has previously been reported to be ineffective in the reduction of rhodanine or thiazolidine-2,4-dione derivatives.^[176]

In the original procedure, N-1 substituted analogues have also been successfully reduced using $LiBH_4$ -pyridine procedure.^[176] In order to study the effect of N-1 substitution, the N-Allyl rhodanine derivative **40ae** (3-pyridine as 5-substituent) was used for the reduction with $LiBH_4$ and pyridine. However, only starting materials could be recovered. Taking the lengthy reaction protocol and the low reduction efficiency together, a different approach using the Hantzsch ester

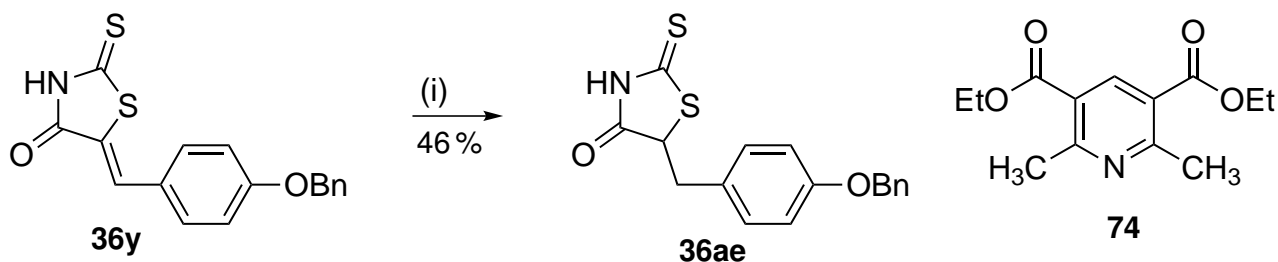


Scheme 39: Reduction of the exo-cyclic double bond in rhodanine derivatives; (i) $NaBH_4$, LiCl, pyridine, THF.

28 as a mild reducing agent was pursued.^[177] The reduction was carried out with the Hantzsch ester in the presence of activated SiO_2 solubilised in toluene in the dark.^[177] SiO_2 controls the regioselectivity of the reduction and is postulated to have a dual role in the reduction mechanism. Firstly, it could act as an acid catalyst and secondly as an adsorbent for the Hantzsch ester and the substrate, bringing them in close proximity.^[177]

Compound **36y** was subjected to the Hantzsch ester reduction protocol (Scheme 40).

The reaction was completed within 16 h and yielded the product **36ae** with the reduced Hantzsch ester **74** as the only side product. The R_f values of **36ae** and **74** were very similar, and multiple purifications attempts via flash column chromatography (Hexane/EtOAc 8:2 and DCM) had to be performed, thus explaining the low yield of 46 %.



Scheme 40: Reduction of exo-cyclic double bond using the Hantzsch-ester approach; (i) Hantzsch ester, activated SiO₂, toluene, dark, 110 °C.

5.3 Anti-parasitic activity

The activity of inhibitors has been assessed as previously described in Chapter 3.3.1

5.3.1 Anti-trypanosomal and anti-leishmanial activity of unsubstituted rhodanine derivatives

Initially, the starting material (rhodanine) was assessed for its activity against *T. brucei*. The starting material did not show any activity against *T. brucei*, *T. cruzi* or *L. infantum*. Similar results were obtained for the screening of the simple condensation product with benzaldehyde, however the derivative (**36b**) displayed toxicity against HL60 cells at GI₅₀ 95.3 μM (Table 48). Screening a variety of different substituted 5-benzylidene moieties a weak trend of anti-trypanosomal activity against *T. brucei* and the logP value has been discovered (Figure 66). Compounds following this trend, where a high logP value resulted in a decreased

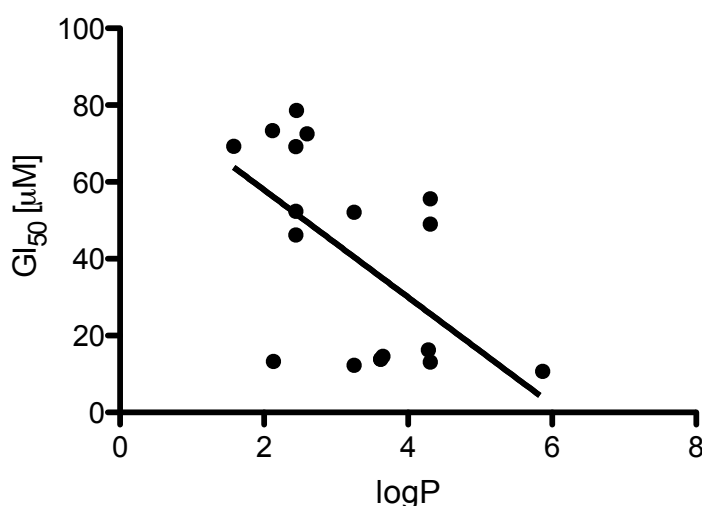
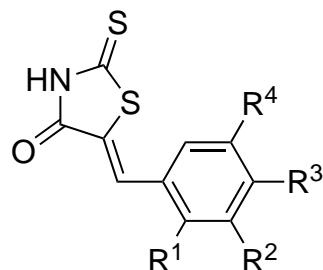


Figure 66: Rhodanine derivatives, their anti-parasitic activity and correlation to logP ($Y=85.9-14.0 \cdot x$, $r^2=0.3$).

Table 48: Anti-parasitic activity of rhodanine derivatives.

#	R ¹	R ²	R ³	R ⁴	logp	GI ₅₀ [μM]			
						<i>T. brucei</i>	<i>T. cruzi</i>	<i>L. inf.</i>	HL60
36					0.61	>100			
36z	H	OBn	OBn	H	5.87	10.7 ± 0.2	n.a.	>100	38.2 ± 2.7
36e	H	H	CH ₃	H	3.25	12.3 ± 0.2	>100	>100	>100
36w	H	OBn	H	H	4.31	13.1 ± 0.9	12.4 ± 0.2	>100	53.8 ± 0.2
36a	H	OH	OH	H	2.13	13.3 ± 1.1	>100	>100	45.0 ± 9.3
36h	H	H	CF ₃	H	3.62	13.9 ± 0.4	>100	>100	48.0 ± 3.6
36g	H	CF ₃	H	H	3.62	13.9 ± 1.7	n.a.	>100	>100
36k	H	Br	F	H	3.65	14.6 ± 2.7	23.7 ± 3.5	>100	70.8 ± 3.1
36ab	H	H	tBu	H	4.28	16.3 ± 2.3	n.a.	n.a.	25.7 ± 0.3
36r	OH	H	H	H	2.44	46.2 ± 2.1	n.a.	>100	>100
36y	H	H	OBn	H	4.31	49.0 ± 4.8	>100	>100	76.8 ± 9.9
36d	H	CH ₃	H	H	3.25	52.1 ± 8.0	>100	>100	>100
36t	H	H	OH	H	2.44	52.4 ± 0.6	n.a.	>100	>100
36s	H	OH	H	H	2.44	69.2 ± 13.7	>100	>100	n.a.
36p	H	H	SO ₂ Me	H	1.58	69.3 ± 8.9	>100	>100	>100
36j	H	H	CN	H	2.6	72.5 ± 8.3	>100	>100	91.7 ± 6.3
36v	H	OMe	OH	OMe	2.12	73.4 ± 20.5	n.a.	n.a.	>100
36q	H	H	CHO	H	2.45	78.6 ± 9.2	>100	>100	n.a.
36i	H	H	Cl	H	3.34	>100	>100	>100	59.8 ± 6.2
36m	H	H	NHAc	H	1.98	>100	>100	>100	>100
36l	H	Br	OMe	H	3.35	>100	>100	>100	90.0 ± 7.3
36u	OH	H	OH	H	2.13	>100	>100	>100	>100
36n	H	H	NMe ₂	H	2.85	>100	>100	>100	>100
36o	H	NO ₂	H	H	2.14	>100	>100	>100	>100
36b	H	H	H	H	2.74	>100	>100	>100	95.3 ± 3.3
36f	CF ₃	H	H	H	3.62	>100	24.9 ± 4.8	>100	87.5 ± 8.4
36c	CH ₃	H	H	H	3.25	>100	>100	>100	>100

anti-trypanosomal activity, are located close to the line drawn in Figure 66. However, there are a few exceptions from this linear correlation. The first exception is not surprising and arose from the catechol modified rhodanine analogue **36a**, this modification has previously been shown for rhodanine-N-acetic acid derivatives to result in low- μM activity (see Chapter 3.7). The other group of rhodanine derivatives not following this trend comprise of meta-substituted analogues (CH_3 , CF_3 , OBn). However, these derivatives are in close proximity to the line drawn in Figure 66, resulting in **36a** as the outlier of this trend.

Therefore most lipophilic compound, such as the 3,4-bis-benzyloxy moiety (**36z**), displayed a GI_{50} of $10.7 \mu\text{M}$ against *T. brucei*. However, also other lipophilic substitutions such as methyl, trifluoromethyl, fluoro, bromo or *tert*-butyl groups showed good anti-trypanosomal activity against *T. brucei* (GI_{50} 12.3 - $16.3 \mu\text{M}$). Particularly interesting was the 3-benzyloxy modified compound **36w** as it displayed similar activity against *T. cruzi* and *T. brucei*. But it is likely that other derivatives, such as the bis-benzyloxy **36z**, the trifluoromethyl **36g** and *tert*-butyl **36ab** derivative may show similar activities against *T. cruzi*, as they had a MIC value of $100 \mu\text{M}$. The exact GI_{50} value could not be measured due to interference with MTT.

Although this first series of inhibitors showed interesting anti-trypanosomal activity they were relatively toxic towards HL60 cells (GI_{50} 25.7 - $91.7 \mu\text{M}$) and showed no activity against *L. infantum*.

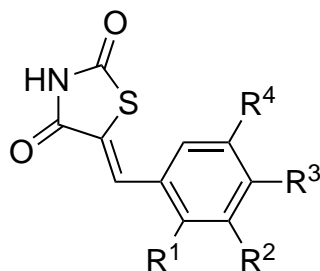
The catechol modified analogue **36a** represented an exception from the logP versus GI_{50} correlation. Although it has a low logP, it displayed a GI_{50} of $13.3 \mu\text{M}$ against *T. brucei*. But this result was not surprising, as similar catechol modified rhodanine analogues resulted in low μM active compounds against *T. brucei* (Chapter 4.3 and 3.3). But in contrast to previous results the derivative **36a** displayed a relatively high toxicity towards HL60 cells (GI_{50} $45 \mu\text{M}$).

Analogues with a hydrogen bond acceptor moiety (SO_2Me , CF_3 , CN , OBn , NHAc , OMe , NMe_2) in para-position of the benzyldiene moiety were characteristic for their weak anti-parasitic activity (GI_{50} $>100 \mu\text{M}$).

Analogues with an ortho-hydroxy group (**36r**) showed moderate activity against *T. cruzi*, while an ortho-trifluoromethyl group led to increased activity against *T. cruzi* (GI_{50} $24.9 \mu\text{M}$).

5.3.2 Strategies to decrease toxicity by screening of thiazolidine-2,4-dione derivatives against parasitic protozoa

Previous unsubstituted rhodanine derivatives showed promising anti-trypanosomal activity, but also possessed toxicity against HL60 cells (Table 48). In order to improve the toxicity profile the thiocarbonyl in the rhodanine moiety was substituted by a carbonyl group. Indeed, the resulting thiazolidine-2,4-dione derivatives did not show toxicity against HL60 cells at $100 \mu\text{M}$ (Table 49). The anti-trypanosomal activity still correlated with the logP of the derivatives, such that compounds with a high logP value showed improved anti-trypanosomal activity against

Table 49: Anti-parasitic activity of thiazolidine-2,4-dione derivatives.

#	R ¹	R ²	R ³	R ⁴	logp	GI ₅₀ [μM]			
						<i>T. brucei</i>	<i>T. cruzi</i>	<i>L. infantum</i>	HL60
48e	H	CF ₃	H	H	2.73	12.7 ± 1.3	n.a.	>100	>100
48f	H	H	CF ₃	H	2.73	15.3 ± 2.1	53.2 ± 0.7	>100	>100
48n	H	OBn	OBn	H	4.98	15.7 ± 2.5	>100	>100	>100
48b	H	CH ₃	H	H	2.36	65.9 ± 17.9	>100	>100	>100
48a	CH ₃	H	H	H	2.36	70.8 ± 15.5	>100	>100	>100
48l	H	OBn	H	H	3.42	87.6 ± 2.2	45.3 ± 0.8	>100	>100
48m	H	H	OBn	H	3.42	>100	>100	>100	>100
48d	CF ₃	H	H	H	2.73	>100	>100	>100	>100
48c	H	H	CH ₃	H	2.36	>100	>100	>100	>100
48o	H	H	H	H	1.85	>100	>100	>100	>100
48g	OH	H	H	H	1.55	>100	>100	>100	>100
48h	H	OH	H	H	1.55	>100	>100	>100	>100
48i	H	H	OH	H	1.55	>100	>100	>100	>100
48p	H	OH	OH	H	1.24	>100	n.a.	n.a.	>100
48k	H	OMe	OH	OMe	1.23	>100	n.a.	n.a.	>100

T. brucei. The meta- and para-trifluoromethyl substituted compounds **48e** and **48f** retained their activity against *T. brucei*, and additional **48f** showed moderate activity against *T. cruzi*. Replacement of the thiocarbonyl in compound **48f** led to a loss of toxicity compared to the rhodanine analogue **36h**.

Also the lipophilic 3,4-bis-benzyloxy modified thiazolidine-2,4-dione derivative **48n** was as active as the rhodanine **36z** (GI₅₀ 15.7 μM). The 3-benzyloxy-substituted analogue, although still trypanocidal against *T. brucei* and *T. cruzi*, lost most of its activity (GI₅₀ 87.6 and 45.3 μM). The 4-benzyloxy-substituted thiazolidine-2,4-dione derivative **48m** did not display any activity against *T. brucei* anymore.

Particularly interesting was the observation that all hydroxy substituted thiazolidine-2,4-dione did not show anti-parasitic activity at 100 μM. This was surprising, as the catechol modification independently from the rhodanine or thiazolidine-2,4-dione moiety so far always resulted in low μM active inhibitors against *T. brucei*.

In conclusion, the substitution strategy did improve the toxicity profile of lipophilic inhibitors **48e**, **48f**, and **48n** and retained anti-parasitic activity against *T. brucei*.

5.3.3 Anti-parasitic activity of N-phenyl rhodanine derivative

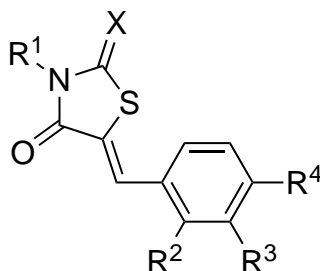
The rhodanine and thiazolidine-2,4-dione libraries screened against *T. brucei*, *T. cruzi* and *L. infantum*, showed a dependency of logP for anti-parasitic activity (Table 48 and Table 49). In order to exploit this dependency lipophilic N-phenyl rhodanine derivatives were evaluated for their anti-parasitic activity (Table 50). Initially, the starting N-phenyl rhodanine was evaluated for its anti-trypanosomal activity against *T. brucei*. N-phenyl rhodanine **55** showed a weak trypanocidal activity against *T. brucei* at GI₅₀ 122.3 μ M. The unsubstituted condensation product **55a** did not display anti-parasitic activity at 100 μ M. However the introduction of hydroxy groups in meta- and para-position of the 5-benzylidene moiety resulted in moderate activity against *T. brucei* (GI₅₀ 52.5-72.3 μ M). Shifting the hydroxy group in ortho-position resulted in low μ M active inhibitors against both *T. brucei* and *T. cruzi* (13.2 and 6.8 μ M). But installation of a catechol moiety further improved the anti-trypanosomal activity of **35d**. Replacement of the thiocarbonyl group to a carbonyl group had no influence on the activity against *T. brucei*, but decreased toxicity of **55o** to >100 μ M, compared to the ortho-hydroxy derivative **55l** (GI₅₀ 50.7 μ M). The acetylation of the free hydroxy groups furnished compound **35e**, which had the lowest anti-trypanosomal activity against *T. cruzi* in these series (GI₅₀ 0.8 μ M). Modifications in R¹, such as the dihydro-indene derivative **35c** were well tolerated and did not affect anti-parasitic activity against *T. brucei*.

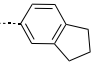
Modifications other than hydroxy groups were not tolerated on the 5-benzylidene moiety and these derivatives showed no anti-parasitic activity at 100 μ M.

5.3.4 Anti-parasitic activity of N-amino rhodanine derivatives

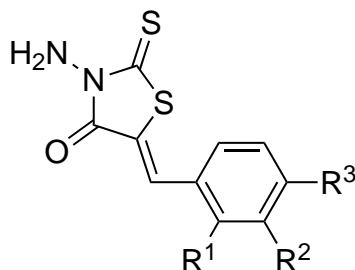
So far it has been established that lipophilicity in rhodanine (Table 48) and thiazolidine-2,4-dione (Table 49) derivatives played a critical role on their anti-parasitic activity, however too lipophilic derivatives such as in the phenyl rhodanine series (Table 50) showed diminished activity, if other than hydroxy modifications were introduced on the 5-benzylidene moiety. In this chapter, the more polar N-amino rhodanine derivatives have been evaluated for their anti-parasitic activity (Table 51). Firstly, the starting N-amino rhodanine was screened against its anti-trypanosomal activity against *T. brucei*, **54** showed no activity at 100 μ M (GI₅₀ 117.9 μ M).

The most promising inhibitors against *T. brucei* growth was the ortho- and meta-hydroxy derivatives **54p** and **54q** (GI₅₀ 12.9 and 19.3 μ M), as they showed no toxicity against HL60 cells at 100 μ M. Although, the bis-hydroxy substituted analogues **54s** and **54t** showed similar activities (GI₅₀ 12.8 and 17.5 μ M), they showed toxicity against HL60 cells.

Table 50: Screening results of N-phenyl rhodanine derivatives against *T. brucei*, *T. cruzi* and *L. infantum*.

#	X	R ¹	R ²	R ³	R ⁴	GI ₅₀ [μM]			
						<i>T. brucei</i>	<i>T. cruzi</i>	<i>L. infantum</i>	HL60
55	S	Ph				122.3 ± 2.2	n.a.	n.a.	n.a.
35c	O		H	OH	OH	1.4 ± 0.1	>100	>100	n.a.
35d	S	Ph	H	OH	OH	4.7 ± 0.9	n.a.	>100	n.a.
55o	O	Ph	H	OH	OH	5.5 ± 0.5	n.a.	>100	>100
35e	O	Ph	H	OAc	OAc	7.3 ± 1.1	0.8 ± 0.1	>100	n.a.
55l	S	Ph	OH	H	H	13.2 ± 1.7	6.8 ± 1.3	>100	50.7 ± 6.4
55n	S	Ph	H	H	OH	52.4 ± 6.2	>100	>100	37.7 ± 2.5
55b	S	Ph	CH ₃	H	H	62.4 ± 2.0	>100	>100	>100
55m	S	Ph	H	OH	H	72.3 ± 8.5	n.a.	>100	32.6 ± 5.0
55e	S	Ph	H	H	Cl	>100	>100	>100	>100
55g	S	Ph	H	H	CN	>100	>100	>100	>100
55f	S	Ph	H	H	CCH	>100	>100	>100	>100
55i	S	Ph	H	H	NHAc	>100	>100	>100	>100
55h	S	Ph	H	Br	OMe	>100	>100	>100	>100
55j	S	Ph	H	H	NMe ₂	>100	>100	>100	>100
55k	S	Ph	H	NO ₂	H	>100	>100	>100	>100
55c	S	Ph	H	CH ₃	H	>100	>100	>100	>100
55d	S	Ph	H	H	CH ₃	>100	>100	>100	>100
55r	S	Ph	H	OBn	OBn	>100	>100	>100	>100
55a	S	Ph	H	H	H	>100	>100	>100	>100
55q	S	Ph	H	H	OBn	>100	>100	>100	>100
55p	S	Ph	H	OBn	H	>100	>100	>100	>100

35a–k have been provided by Prof. Dr. M. Schlitzer, Phillips-Universität, Marburg, Germany.

Table 51: Anti-parasitic activity of N-amino rhodanine derivatives.

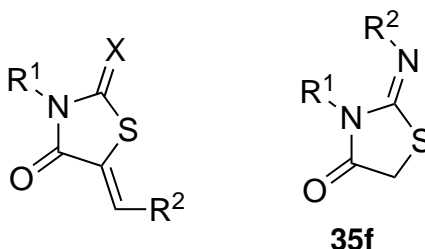
#	R ¹	R ²	R ³	<i>T. brucei</i>	GI ₅₀ [μM]		
					<i>T. cruzi</i>	<i>L. infantum</i>	HL60
54				117.9 ± 23.9	n.a.	n.a.	n.a.
54p	OH	H	H	12.9 ± 0.8	>100	>100	>100
54s	OH	H	OH	12.8 ± 2.2	>100	>100	57.0 ± 6.6
54g	H	H	CF ₃	13.0 ± 2.0	>100	>100	51.0 ± 0.9
54k	H	H	CCH	14.2 ± 2.5	>100	>100	>100
54j	H	Br	OMe	16.8 ± 4.4	>100	>100	>100
54t	H	OH	OH	17.5 ± 0.2	n.a.	>100	82.8 ± 10.1
54q	H	OH	H	19.3 ± 7.3	>100	>100	>100
54n	H	H	NHAc	21.0 ± 4.9	>100	>100	>100
54l	H	H	CN	47.2 ± 11.3	>100	>100	>100
54m	H	NO ₂	H	48.0 ± 3.4	>100	>100	>100
54w	H	H	OBn	58.3 ± 14.6	>100	>100	>100
54f	H	CF ₃	H	69.7 ± 29.6	n.a.	n.a.	n.a.
54v	H	OBn	H	>100	n.a.	n.a.	n.a.
54r	H	H	OH	>100	>100	>100	>100
54o	H	H	NMe ₂	>100	>100	>100	>100
54u	H	H	OMe	>100	>100	>100	>100
54b	CH ₃	H	H	>100	>100	>100	>100
54c	H	CH ₃	H	>100	>100	>100	>100
54d	H	H	CH ₃	>100	>100	>100	>100
54x	H	OBn	OBn	>100	>100	>100	>100
54a	H	H	H	>100	>100	>100	>100
54i	H	Br	F	>100	>100	>100	>100
54h	H	H	Cl	>100	>100	>100	>100
54e	CF ₃	H	H	>100	>100	>100	n.a.

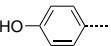
Large lipophilic substituents (CF₃, CCH, OMe, NHAc) led to improved activity against *T. brucei* (GI₅₀ 13.0-21.0 µM). Other modifications displayed in Table 51 showed no activity against parasitic protozoa.

5.3.5 Heterocyclic modifications on rhodanine and thiazolidine-2,4-dione derivatives and their anti-parasitic activity

A broad range of various benzylidene modifications have been explored in this research project. In this chapter, several heterocyclic modifications have been investigated for their anti-parasitic activity (Table 52). Pyridinyl groups in position 5 of the rhodanine or thiazolidine-

Table 52: Anti-parasitic activity of heterocyclic modified analogues.



#	R ¹	X	R ²	GI ₅₀ [µM]			
				<i>T. brucei</i>	<i>T. cruzi</i>	<i>L. infantum</i>	HL60
48q	H	O	3-pyridinyl	45.1	>100	>100	>100
54ab	NH ₂	S	2-pyridinyl	47.5 ± 2.5	12.1 ± 1.5	>100	82.5 ± 5.0
48r	H	O	2-pyridinyl	87.3	>100	>100	>100
36ad	H	S	2-pyridinyl	>100	>100	>100	>100
55z	Ph	S	2-pyridinyl	>100	>100	>100	>100
36af	H	S	3-pyridinyl	>100	>100	>100	>100
48s	H	O	4-pyridinyl	>100	>100	>100	n.a.
36ag	H	S	4-pyridinyl	>100	>100	>100	>100
35f		n.a.	see R ¹	>100	>100	>100	n.a.

35a–k were kindly donated by Prof. Dr. Schlitzer, Phillips-Universitat, Marburg, Germany

2,4-dione derivatives resulted only in moderate activity against *T. brucei* (GI₅₀ 45.1-87.3 µM). Particularly interesting was the N-amino rhodanine **54ab**, which was substituted with a 2-pyridinyl moiety. **54ab** showed anti-trypanosomal activity against both *T. brucei* and *T. cruzi*, with a preference against the last (GI₅₀ 12.1 µM). This derivative displayed toxicity against HL60 cells at GI₅₀ 82.5 µM. The unsubstituted thiazolidine-2,4-dione analogue **48r** was less toxic against HL60 cells (GI₅₀ >100 µM), but also displayed a diminished activity against both *T. brucei* and *T. cruzi*. However, the thiazolidine-2,4-dione derivative **48q**, where the 2-pyridinyl was substituted by a 3-pyridinyl moiety, regained its anti-trypanosomal activity against *T. brucei*

compared to **54ab**. Other combination, such as a phenyl-group in N-1 position and various rhodanine and thiazolidine-2,4-dione derivatives with other pyridinyl-moities than mentioned above displayed no activity against parasitic protozoa.

5.3.6 Anti-trypanosomal effects of 3-benzyloxy modified rhodanine and thiazolidine-2,4-diones

The 3-benzyloxy-substituted rhodanine derivative **36w** showed interesting anti-trypanosomal activity. In this chapter, it was shown that introduction of an additional methoxy-group in para-position of the 3-benzyloxy moiety (**36x**, Table 53) led to decreased trypanocidal activities against *T. brucei*. Similarly, in the thiazolidine-2,4-dione modification this additional substituent showed no improvement in anti-trypanosomal activity. The best inhibitor in this series remained the rhodanine derivative **36w**.

Table 53: Anti-trypanosomal effect of 3-benzoxo modifications.

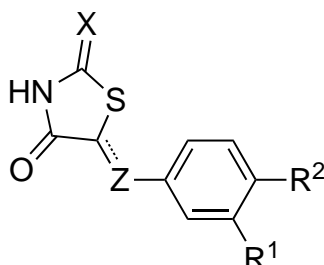
#	X	R ¹	GI ₅₀ [μM]	
			<i>T. brucei</i>	HL60
36w	S	CH	13.1 ± 0.9	53.8 ± 0.2
36x	S	OMe	57.9 ± 12.3	79.6 ± 13.3
48t	O	OMe	67.0 ± 30.6	>100
48l	O	CH	87.6 ppm 2.2	>100
18c		OMe	>100	n.a.

5.3.7 Activity of reduced rhodanine and thiazolidine-2,4-dione derivatives against *T. brucei*, *T. cruzi* and *L. infantum*

The 5-benzylidene rhodanine derivative **36b** did not show anti-trypanosomal activity at 100 μM, however its reduced analogue **36ac** was active against *T. brucei*, at a GI₅₀ of 13.3 μM (Table 54). Similarly reduction of the exo-cyclic double bond in the 4-benzyloxy rhodanine derivative **36y** improved activity against *T. brucei* by a factor of 4 and furthermore did not display

toxicity against HL60 cells. The reduction of the double bond in thiazolidine-2,4-dione derivatives in this series did not improve anti-trypanosomal activity.

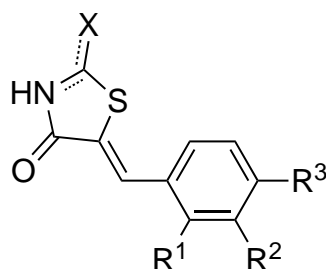
Table 54: Anti-parasitic activity of reduced rhodanine and thiazolidine-derivatives in comparison to their unsaturated analogues.



#	Z	X	R ¹	R ²	GI ₅₀ [μM]			
					<i>T. brucei</i>	<i>T. cruzi</i>	<i>L. infantum</i>	HL60
36ac	CH ₂	S	H	H	13.3	n.a.	n.a.	n.a.
75a	CH ₂	S	H	OBn	11.7 ± 0.2	>100	>100	>100
36y	CH	S	H	OBn	49.0 ± 4.8	>100	>100	76.8 ± 9.9
36b	CH	S	H	H	>100	>100	>100	95.3 ± 3.3
48m	CH	O	H	OBn	>100	>100	>100	>100
48u	CH ₂	O	H	OBn	>100	>100	>100	n.a.
48p	CH	O	OH	OH	>100	n.a.	n.a.	>100
48v	CH ₂	O	OH	OH	>100	n.a.	n.a.	n.a.

5.3.8 Modifications of the thiocarbonyl and anti-parasitic activity

5-Benzylidene rhodanine derivatives showed moderate activity against *T. brucei* and *T. cruzi*, if the benzylidene moiety was modified with lipophilic substituents (OBn, CH₃, CF₃), otherwise substituents showed a decrease in trypanosomal activity (Table 48). In this chapter, this trend was further examined, by focussing on lipophilic substituents in position 5 and modifications on the thiocarbonyl, such as alkylation or substitution with amino-groups (Table 55). This compound series is particularly interesting, as alkylation of the thiocarbonyl group resulted in racemisation of the exo-cyclic double bond, so that both E and Z isomers could be tested in varying ratios against their molecular target in parasites. One such example was the methylated thiocarbonyl derivative **62c** as it was composed as 10:1 mixture of E to Z double bond isomers. Usually, the thermodynamic more stable Z-isomer was obtained and was screened for their anti-parasitic activity.^[162] **62c** showed low anti-trypanosomal activity against *T. brucei* (GI₅₀ 13.6 μM) and *T. cruzi* (GI₅₀ 9.3 μM). Whereas the rhodanine-analogue **36h** did not display activity against *T. cruzi* at 100 μM. The anti-trypanosomal activity against *T. brucei* was similar for both derivatives. Similarly, compounds **62f**, **69h**, and **62b** were obtained

Table 55: Anti-parasitic activity of S-modified and S-substituted rhodanine analogues.

#	X	R ¹	R ²	R ³	GI ₅₀ [μM]			
					<i>T. brucei</i>	<i>T. cruzi</i>	<i>L. infantum</i>	HL60
69f	SCH ₂ CO ₂ Et	H	OBn	OBn	10.3 ± 0.5	n.a.	n.a.	n.a.
62d	SBn	CF ₃	H	H	13.1 ± 0.3	n.a.	n.a.	n.a.
62f	SBn	H	H	CF ₃	13.4 ± 0.1	n.a.	>100	n.a.
69e	SCH ₂ CO ₂ Et	H	H	OBn	13.4 ± 2.1	n.a.	>100	>100
62c	SMe	H	H	CF ₃	13.6 ± 0.1	9.3 ± 0.8	>100	31.9 ± 0.3
69a	SCH ₂ CO ₂ Et	CH ₃	H	H	14.8 ± 1.2	>100	>100	>100
69c	SCH ₂ CO ₂ Et	H	H	CH ₃	15.8 ± 1.3	n.a.	n.a.	>100
69b	SCH ₂ CO ₂ Et	H	CH ₃	H	15.8 ± 2.0	n.a.	>100	>100
62e	SBn	H	CF ₃	H	15.8 ± 2.2	n.a.	n.a.	n.a.
70b	NpiperidinyI	H	H	H	17.6	>100	>100	>100
70c	NpiperidinyI	H	OH	OH	18.2	>100	>100	>100
69l	SCH ₂ CO ₂ Et		2-furanyl		63.5 ± 9.5	>100	>100	56.6 ± 11.1
69d	SCH ₂ CO ₂ Et	H	OBn	H	65.9 ± 3.2	n.a.	n.a.	>100
69h	SCH ₂ CO ₂ Et	H	H	OH	97.1 ± 13.7	>100	>100	>100
62a	SMe	CF ₃	H	H	>100	>100	>100	n.a.
62b	SMe	H	CF ₃	H	>100	n.a.	n.a.	n.a.
69g	SCH ₂ CO ₂ Et	H	OH	H	>100	>100	>100	n.a.
69j	SCH ₂ CO ₂ Et	H	OH	OH	>100	>100	>100	>100
70a	NHCH ₂ CO ₂ Me	H	H	Cl	24.0	>100	>100	1.6 ± 0.1

in almost 1:1 ratios of both E and Z isomer. However, **62b** displayed a decrease in activity against *T. brucei*, whereas **62f** and **62b** showed similar activity values. All other derivatives screened in this series possessed a Z-configured double-bond. With the exception of derivatives **70c** and **69d**, analogues **69f**, **62d**, **62c**, **62e**, and **69e** retained their anti-trypanosomal activity against *T. brucei*, as compared to their rhodanine analogues.

In conclusion, modifications on the thiocarbonyl, such as alkylation and substitution did not improve anti-trypanosomal activity. Substitution of the thiocarbonyl to an amino-acetic ester moiety in compound **70a** resulted in high toxicity against HL60 cells and only moderate activity against *T. brucei*.

5.4 Target identification studies

5.4.1 GPI cell-free radio-label assay

In order to analyse the mode-of-action of rhodanine, N-amino rhodanine and N-phenyl rhodanine derivatives, a cell-free GPI synthesis assays was performed to assess their ability to inhibit enzymes within the GPI-anchor biosynthesis in *T. brucei*.¹² The assay is described in further detail in chapter 3.5.3.

GPI-inhibition of rhodanine derivatives

Initially selected rhodanine derivatives were evaluated for their ability to inhibit enzymes in the GPI-anchor biosynthesis using a cell-free GPI-synthesis assay. The derivatives have been chosen on the basis of previous N-acetic acid and N-allyl rhodanine derivatives which showed activity against enzymes of the GPI anchor biosynthesis.

Particularly interesting in this series was the 3-benzyloxy rhodanine derivative **36w**, as it was the first example of a derivative inhibiting MT-1 and possible DPMS, as could be seen by a diminished substrate band for Dol-P-Man and M1 (Table 56), and resulted in low μM activity against both *T. brucei* and *T. cruzi* *in vitro* (GI_{50} 13.1 and 12.4 μM respectively). But this derivative also showed an increased toxicity against HL60 cells (GI_{50} 53.8 μM), compared to its N-acetic acid (GI_{50} >100 μM) or N-allyl- rhodanine derivative (GI_{50} 100 μM).

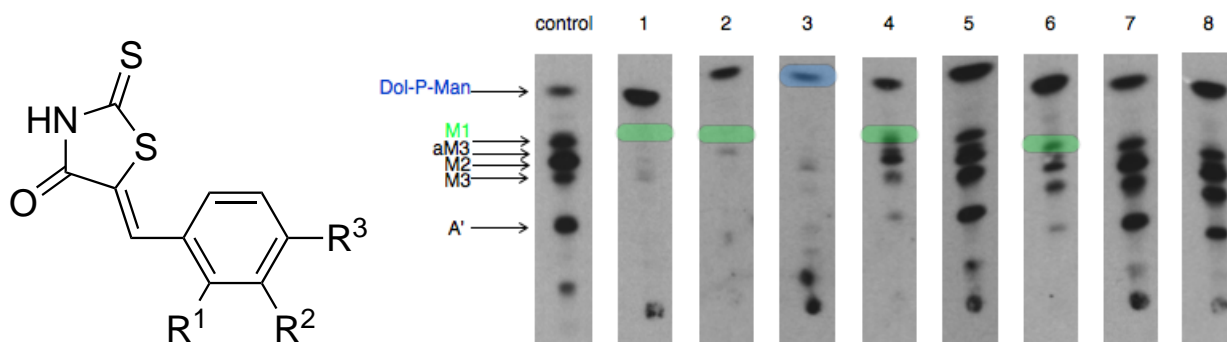
Rhodanine derivatives with an ortho methyl or trifluoromethyl group (**36c** and **36f**) were shown to be very good MT-1 inhibitors, as the substrate band for M1 and all subsequent GPI-substrates disappeared in the cell free GPI synthesis assay. The trifluoromethyl derivative **36f** showed moderate activity against *T. cruzi* (GI_{50} 24.9 μM), but did not display any activity against *T. brucei* or *L. infantum*. The methyl derivative **36c**, although a strong inhibitor of *T. brucei* MT-1 did not show anti-trypanosomal activity at 100 μM .

The rhodanine derivatives with a para-hydroxy group **36t** displayed good inhibitory activity against DPMS in the cell-free GPI synthesis assay. **36t** had moderate activity against *T. brucei* (GI_{50} 52.4 μM) and *T. cruzi* (MIC 100 μM). Benzylolation of the para-hydroxy group in derivative **36y** resulted in loss of its inhibitory function against enzymes of the GPI-synthesis assay, however its anti-trypanosomal activity against *T. brucei* was retained at GI_{50} 49.0 μM . But this derivative also displayed an increased toxicity against HL60 cells (76.8 μM), making it unattractive for further development.

A steric fluorine group in para position in combination with a meta bromo substituent in derivative **36k** resulted in a weak inhibitor for *T. brucei* MT-1 with low μM activity against both *T. brucei* and *T. cruzi* (GI_{50} 14.6 and 23.7 μM respectively). But the toxicity of this derivative was similar to the para-benzyloxy modified analogue (GI_{50} 70.8 μM). Pyridinyl substituted rho-

¹²This assays were performed by Dr. Terry Smith from the University of St. Andrews, St Andrews, Scotland, UK

Table 56: cell-free GPI assay for rhodanine derivatives; line 1: **36c**, line 2: **36f**, line 3: **36t**, line 4: **36w**, line 5: **36y**, line 6: **36k**, line 7: **36ad**, line 8: **36af**; *in vitro* activity against *T. brucei*; Blue highlighted bands: DPMS inhibition; Green highlighted bands: MT-1 inhibition.



#	R ¹	R ²	R ³	GI ₅₀ [μM]			
				<i>T. brucei</i>	<i>T. cruzi</i>	<i>L. infantum</i>	HL60
36c	CH ₃	H	H	>100	>100	>100	>100
36f	CF ₃	H	H	>100	24.9 ± 4.8	>100	87.5 ± 8.4
36t	H	H	OH	52.4 ± 0.6	n.a.	>100	>100
36w	H	OBn	H	13.1 ± 0.9	12.4 ± 0.2	>100	53.8 ± 0.2
36y	H	H	OBn	49.0 ± 4.8	>100	>100	76.8 ± 9.9
36k	H	Br	F	14.6 ± 2.7	23.7 ± 3.5	>100	70.8 ± 3.1
36ad		2-pyridinyl		>100	>100	>100	>100
36af		3-pyridinyl		>100	>100	>100	>100

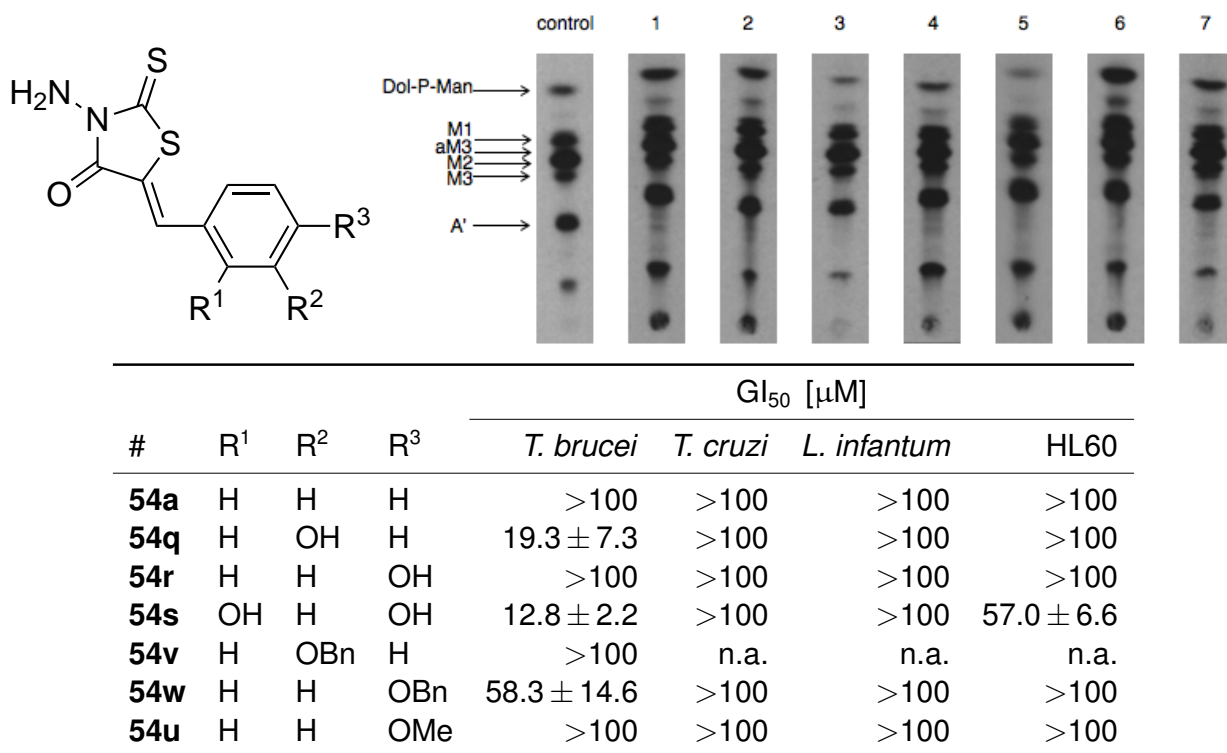
danine derivatives showed no activity in the cell-free GPI-synthesis assay or against parasites *in vitro*.

Particularly interesting was the cross-parasitic activity against *T. brucei* and *T. cruzi* of rhodanine derivatives. The cell-free GPI-synthesis assay suggests that GPI-biosynthesis might be responsible for anti-trypanosomal effects *in vitro*.

GPI synthesis inhibition by N-amino rhodanine derivatives

Rhodanine derivatives have been shown in the previous chapter, to be good inhibitors of MT-1 and/or DPMS, possible explaining the low μM anti-trypanosomal activity against *T. brucei* and *T. cruzi* (Table 56). In this chapter, the effect of N-amino substitution of the rhodanine moiety on GPI-synthesis was investigated using a cell-free GPI-synthesis assay. The derivatives were chosen based on their anti-trypanosomal activity against *T. brucei*, as many of the derivatives in Table 56 did not show anti-trypanosomal activity at 100 μM. However, although many of the chosen N-amino rhodanine derivatives showed good anti-trypanosomal activity (GI₅₀ 12.8–58.3 μM), they did not inhibit enzymes in the cell-free GPI-synthesis assay (Ta-

Table 57: cell-free GPI assay for N-amino rhodanine derivatives-1; line 1: **54a**, line 2: **54q**, line 3: **54r**, line 4: **54s**, line 5: **54v**, line 6: **54w**, line 7: **54u**; *in vitro* activity against *T. brucei*; Blue highlighted bands: DPMS inhibition; Green highlighted bands: MT-1 inhibition.



ble 57, Table 58). Although the ortho methyl substituted amino-derivative **54b** did not display anti-trypanosomal activity at 100 μM, **54b** showed an absence A' band in the GPI-synthesis assay, thus suggesting inhibition of the ethanol-amine-phosphate transferase. This was rather interesting as the ortho-methyl rhodanine analogue **36c** was identified as very good inhibitor of MT-1, the introduction of the additional amino-substituent caused inhibition of a complete different enzyme in the cell-free GPI synthesis assay. However, both the rhodanine (**36c**) and N-amino rhodanine (**54b**) derivative displayed no activity against *T. brucei*, *T. cruzi* or *L. infantum in vitro*.

GPI activity of phenyl rhodanine derivatives

Rhodanine derivatives and in particular N-acetic acid rhodanine derivatives have been identified as inhibitors of the GPI-anchor biosynthesis in *T. brucei* using a cell-free GPI synthesis assay. In order to study the importance of the N-1 substituent on GPI-anchor inhibition, N-phenyl rhodanine derivatives were assessed for their ability to inhibit enzymes in the GPI-anchor synthesis. However, none of the derivatives screened in the cell-free GPI synthesis showed inhibitory effects of enzymes within the ensemble of the GPI-anchor (Table 59).

Table 58: cell-free GPI assay for N-amino rhodanine derivatives-2; line 1: **54b**, line 2: **54c**, line 3: **54d**, line 4: **54i**, line 5: **54h**, line 6: **54l**, line 7: **54ab**; *in vitro* activity against *T. brucei*; Blue highlighted bands: DPMS inhibition; Green highlighted bands: MT-1 inhibition.

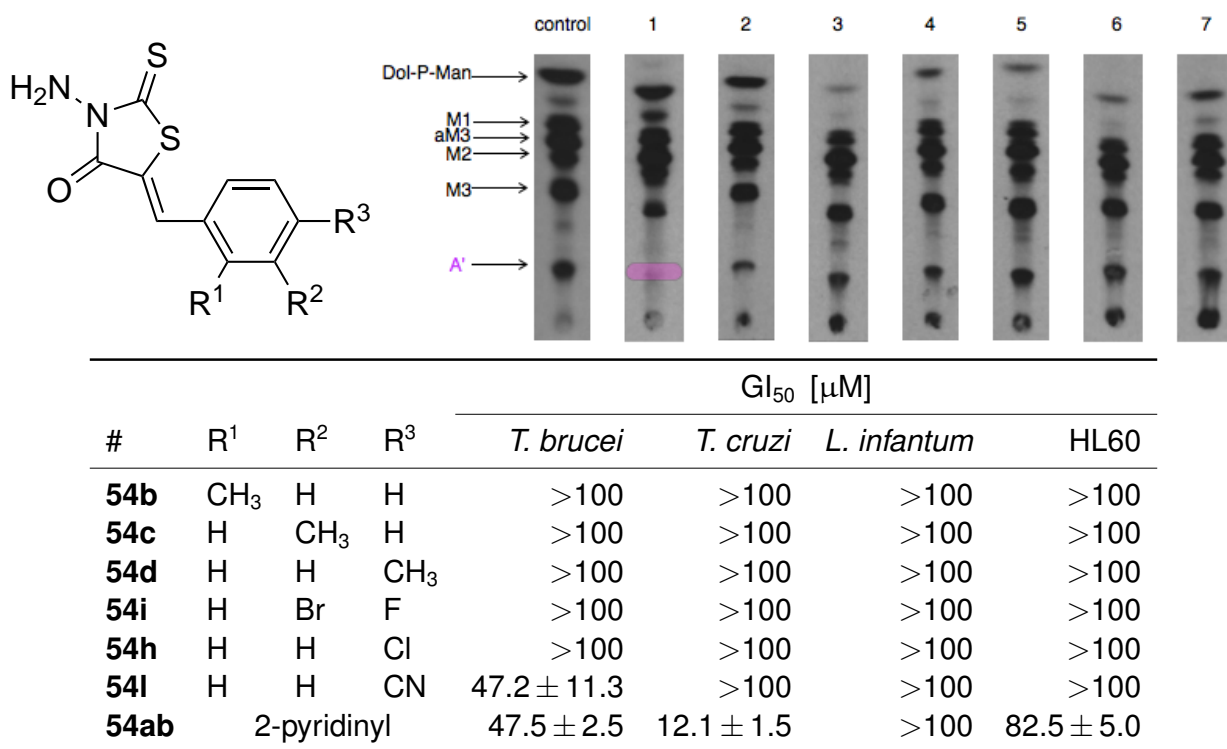
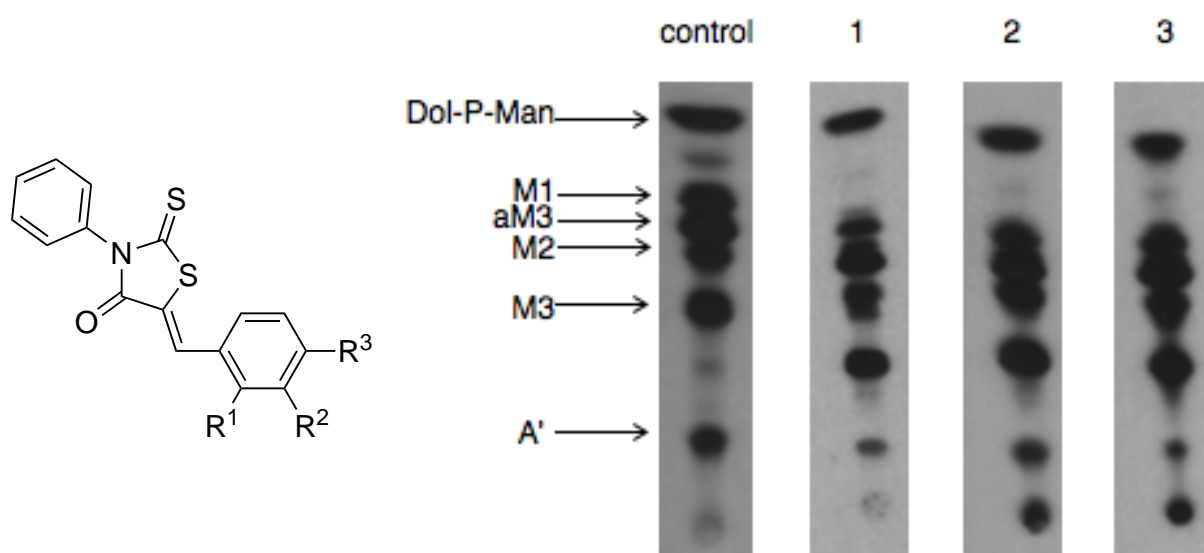


Table 59: cell-free GPI assay for N-phenyl rhodanine derivatives; line 1: **54b**, line 2: **54c**, line 3: **54d**, line 4: **54i**, line 5: **54h**, line 6: **54l**, line 7: **54ab**; *in vitro* activity against *T. brucei*; Blue highlighted bands: DPMS inhibition; Green highlighted bands: MT-1 inhibition.



#	R ¹	R ²	R ³	GI ₅₀ [μM]			
				<i>T. brucei</i>	<i>T. cruzi</i>	<i>L. infantum</i>	HL60
55q	H	H	OBn	>100	>100	>100	>100
55r	H	OBn	OBn	>100	>100	>100	>100
55z		2-pyridinyl		>100	>100	>100	>100

5.5 Discussion

Rhodanine derivatives in this study have been identified as good anti-trypanosomal agents. Interestingly compared to N-acetic acid (ester) and N-allyl rhodanine derivatives, which were mostly active against *T. brucei*, N-unsubstituted rhodanine showed broad activity against both *T. brucei* and *T. cruzi*. Although many GI_{50} for *T. cruzi* could not be measured due to interference with the viability dye MTT, N-unsubstituted analogues showed MIC values of 100 μ M against *T. cruzi* growth. But N-unsubstituted rhodanine derivatives also showed increased toxicity against HL60 cells (GI_{50} 25.7-91.7 μ M, Table 48). The activity against *T. brucei* of the unsubstituted rhodanines showed a correlation to the derivatives logP values (Figure 66). However, besides this observation, the structure activity relationship of the 5-benzylidene substituents was difficult to interpret as no clear trend could be observed in the screened series of unsubstituted rhodanine derivatives. Substitution of the thiocarbonyl to a carbonyl group in the thiazolidine-2,4-dione derivatives caused a decrease in anti-trypanosomal activity (Table 49). Substitution of the meta-benzyloxy substituent on the 5-benzylidene moiety did not improve anti-parasitic activity, as compared to the corresponding N-acetic rhodanine ester derivatives (Table 53). Reduction of the exo-cyclic double bond in the para-benzyloxy rhodanine derivative **36y** improved anti-trypanosomal activity against *T. brucei* by a factor of 4 and furthermore decreased toxicity against HL60 cells to $GI_{50} > 100$ μ M (Table 54), suggesting that these derivatives do not undergo un-selective Michael acceptor binding to biological nucleophiles such as glutathione. On the contrary, the reduction of the double bond might have improved the solubility of the rhodanine derivative due to increased flexibility and in conclusion caused an improvement in anti-parasitic activity against *T. brucei*.

Since the 5-benzylidene moiety showed limited information on a possible structure activity relationship, further modifications on the rhodanine moiety itself were carried out. One such modification was alkylation of the thiocarbonyl with various alkylating agents (Table 55). Particular interesting was the observation of racemisation of the exo-cyclic double bond configuration if the thiocarbonyl was subjected to alkylating agents (Table 46 and Table 47). Interestingly, these alkylated analogues showed comparable activities against *T. brucei* and *T. cruzi* (GI_{50} 9.3-65.9 μ M) than the not alkylated analogues. However, introduction of an amino-acetic ester group resulted in high toxicity against HL60 cells (GI_{50} 1.6 μ m).

Amino substitution of the N1-group in rhodanine moiety resulted in compounds with good activity against *T. brucei* (GI_{50} 12.9-69.7 μ M) and a good selectivity profile (SI 2-8, Table 51). However, this modification also caused decreased activity against *T. cruzi* and did not improve overall anti-parasitic activity, leading to the conclusion that an amino-modification on the rhodanine-N1-moiety was not favourable. Therefore, the lipophilic phenyl group was chosen for N-1 substitution. Indeed this modification in combination with a catechol motif on the 5-

benzylidene moiety resulted in the most active anti-trypanosomal agents in this series, with activity against both *T. brucei* and *T. cruzi*. Interestingly the acetylated catechol thiazolidine-2,4-dione derivative **35e** showed sub- μM activity against *T. cruzi* and μM activity against *T. brucei* (Table 50). Larger indene-modification on the N-1 position improved activity against *T. brucei*, if a catechol motif was present.

N-phenyl substituted rhodanine derivatives with other modifications than hydroxy groups on the 5-benzylidene moiety showed no anti-parasitic activity.

In order to determine the possible mode-of-action of the rhodanine derivatives discussed in this chapter, cell-free GPI synthesis were performed to identify possible inhibitors of the GPI-anchor biosynthesis.¹³ Further details on the assay are described in chapter 3.5.3 The unsubstituted rhodanine series was found to inhibit the first mannosyltransferase and DPMS of the cell-free GPI-synthesis assay (Table 56). Particularly interesting were derivatives with a ortho methyl or trifluoromethyl substituent, as they showed very strong inhibition effects on the first mannosyltransferase in *T. brucei*, but did not show any activity against *T. brucei* *in vitro*. The trifluoromethyl substituted derivative **36f**, a strong inhibitor of the first mannosyltransferase, showed moderate activity against *T. cruzi* (GI_{50} 24.9 μM). Whereas the methyl analogue showed no effect on *T. cruzi* growth, but retaining this methyl substituent and substituting the N-1 position with an amino-group resulted in a strong inhibitor for the ethanol-amine-phosphate transferase, an enzyme very late in GPI-anchor biosynthesis (Table 58). Other N-amino substituted rhodanine and N-phenyl amino rhodanine derivatives did not show any effect on enzymes of the cell-free GPI-synthesis assay.

The rhodanine and thiazolidine-2,4-dione series discussed in this chapter were very interesting for their anti-trypanosomal activity against both *T. brucei* and *T. cruzi*. They displayed good selectivity and further modifications could improve anti-parasitic activity. However, the alkylation strategy of the thiocarbonyl group generates good leaving groups for the attack of biological nucleophiles and indeed mass spectrometric analysis showed potential adducts with this compound class, so that this modification should not be pursued.

5.6 Summary

128 rhodanine, thiazolidine-2,4-dione derivatives and alkylation products have been synthesised and evaluated for anti-parasitic activity in a whole cell activity assay against *T. brucei*, *T. cruzi* and *L. infantum*.

30 out of 128 derivatives showed trypanocidal activity at 100 μM (MIC 100 μM) against *T. brucei*, while 2 showed a MIC value of 10 μM .

¹³This assays were performed by Dr. Terry Smith from the University of St. Andrews, St Andrews, Scotland, UK

22 out of the 30 compounds active against *T. brucei* showed anti-parasitic effects against *T. cruzi* at 100 μ M (MIC 100 μ M).

None of the 128 compounds showed any activity against *L. infantum* at 100 μ M.

Primary whole cell phenotypic screening of rhodanine, N-amino rhodanine, N-phenyl rhodanine and thiazolidine-2,4-dione derivatives, as well as their alkylation products showed promising anti-trypanosomal activity against both *T. brucei* and *T. cruzi* (GI₅₀ 1.4-16.3 μ M, SI 4-18).

Target identification assays on selected derivatives identified rhodanine derivatives as particular promising derivatives for inhibitors of GPI-anchor biosynthesis in *T. brucei*. A rhodanine-3-benzyloxy derivative showed good *in vitro* activities against both *T. brucei* and *T. cruzi* (GI₅₀ 13.1, 12.4 μ M, SI 4), while a cell-free radio-label assay showed very strong DPMS inhibition by this derivative.

Target identification studies on N-amino rhodanine derivatives identified the first small molecular inhibitor of ethanol-amine-phosphate transferase, a late enzyme in the GPI-anchor biosynthesis. But the same derivative did not show any activity in the whole cell assay against parasites *in vitro*.

N-phenyl rhodanine derivatives did not show any anti-parasitic activity in the whole cell assay and against isolated enzymes of the GPI-anchor biosynthesis. However, if the N-phenyl rhodanine moiety is conjugated to a catechol group, low μ M activity against *T. brucei* (GI₅₀ 1.4-7.3 μ M, SI 18) was observed.

Alkylation of the thiocarbonyl group resulted in inhibitors with good to moderate activity against *T. brucei*, but characterisation by mass spectrometry resulted in adducts of molecular weight + 100 Da, suggesting possible substitution reactivity of this inhibitor series. For this reason, this approach should not be pursued.

Replacing the rhodanine scaffold with a thiazolidine-2,4-dione moiety resulted in decreased toxicity against HL60 cells, while anti-trypanosomal activity was retained.

6 Pyrazolone derivatives

Pyrazolone derivatives (Figure 67) have been chosen as alternative inhibitor template to replace the thiazolidine-4-one moiety in rhodanine and thiazolidine-2,4-dione inhibitors. In the following introduction reasons for the need of an alternative template are described and the choice of the pyrazolone template is explained.

6.1 Introduction

Rhodanine have been shown in this study (Chapters 3.5.3, 4.4.3 and 5.4.1) to inhibit DPMS and the first MT-1 transferase in the GPI-anchor biosynthesis. Rhodanine inhibitors have been identified as low μM anti-parasitic compounds with promising selectivity profile in this study. However, the rhodanine inhibitor class has potential drawbacks, such as the ability to bind to many molecular targets, therefore compromising its selectivity profile.^[82] Furthermore, rhodanine derivative have been shown to undergo light-induced covalent binding interactions,^[87] and are potentially prone to nucleophilic attack on their Michael acceptor system.^[82]

Although the rhodanine derivatives in this study have shown promising anti-parasitic activity, some of these compounds in particular the unsubstituted rhodanine derivatives showed also an increased toxicity against HL60 cells. In order to improve this selectivity profile, the pyrazolone scaffold (Figure 67) was investigated as possible replacement of the rhodanine-moiety. Indeed, screening campaigns against bacterial sugar nucleotide transferases have

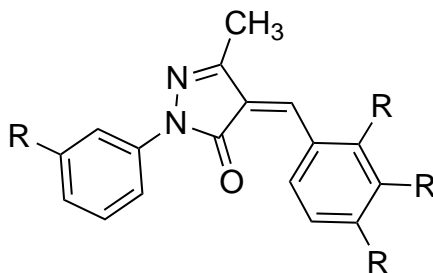


Figure 67: Pyrazolone derivatives as alternative inhibitor template.

identified similar 3-methylpyrazolone derivatives alongside rhodanine and thiazolidine-2,4-dione derivatives as potential inhibitors, justifying the use of this alternative scaffold for anti-parasitic glycosyltransferases.^[101,245] Furthermore, virtual screening identified all three substance classes (pyrazolone derivatives, rhodanine and thiazolidine-2,4-dione) as inhibitors of a bacterial GT-Pase,^[246] possibly supporting their resemblance to nucleobases (XDP with X=U,A,G) and phosphate mimics.

Pyrazolone derivatives are structurally very similar to rhodanine and thiazolidine-2,4-dione

derivative, they possess the same number of hydrogen-bond acceptors (2 donors) as the corresponding rhodanine and thiazolidine-2,4-dione derivatives and constitute of a similar molecular scaffold with a joined five- and six-membered ring system. Pyrazolone derivatives are joined by a Michael acceptor system to a benzylidene moiety. Similarly to rhodanine and thiazolidine-2,4-dione derivatives, this Michael acceptor system is susceptible towards thiol reactivity, but thiol reactivity for pyrazolone derivatives with the endoplasmic reticulum oxidase 1 in yeast has been reported to be selective and reversible.^[247]

Furthermore, pyrazolone derivatives have been studied as inhibitors for c-Met kinase activity.^[248] Similarly, rhodanine and thiazolidine-2,4-dione derivatives have been found as inhibitors of the kinase PI3K γ (Chapter 5.1),^[117,236] a potentially target for the development of anti-leishmanial and anti-trypanosomal agents.^[116,237] The previous biological studies suggested resemblance of the pyrazolone derivatives to the rhodanine class, as they showed similar activities against similar molecular targets.^[101,245]

6.2 Synthesis of inhibitor library

6.2.1 Synthetic strategies towards anti-parasitic pyrazolone derivatives

The pyrazolone derivatives in this study had the general structure displayed in Figure 68. Modification on the pyrazole-core were introduced over the R¹ and the R²-substituent. In the R¹ position two different aryl moieties have been introduced. An unsubstituted aryl-substituent (R=Ph) was introduced over phenyl hydrazine as reactant, whereas the corresponding meta-carboxylic acid aryl was introduced through 3-hydrazinylbenzoic acid. The unsubstituted (R=H) analogue was synthesised with hydrazine as reactant. In position R², substituted benzene-derivatives, furanyl- or other heterocyclic modification such as pyridines were introduced. Lastly, the double bond displayed in red was reduced.

The pyrazolone derivatives were synthesised via two synthetic approaches (Scheme 41, Route A or B). In the first approach (Route A) the hydrazine **76** is reacted with **77** in refluxing acetic acid (HOAc) to afford the pyrazolone **78** (Scheme 41, green arrows, conditions (i)),^[249] which can exist as its keto or enol-form. The pyrazolone **78** is purified and subsequently reacted with various benzaldehydes in the presence of NaOAc in HOAc (Scheme 41, conditions (ii)). Alternatively (Route B), the reagents can be combined in a one-pot reaction to obtain the desired **79** under microwave irradiation (Scheme 41, conditions (iii)).

6.2.2 Stereochemistry of pyrazole derivatives

The Knoevenagel reaction between pyrazolone **78** and various benzaldehydes can lead to two diastereoisomers (Figure 69). The isomers differ from each other through the configuration

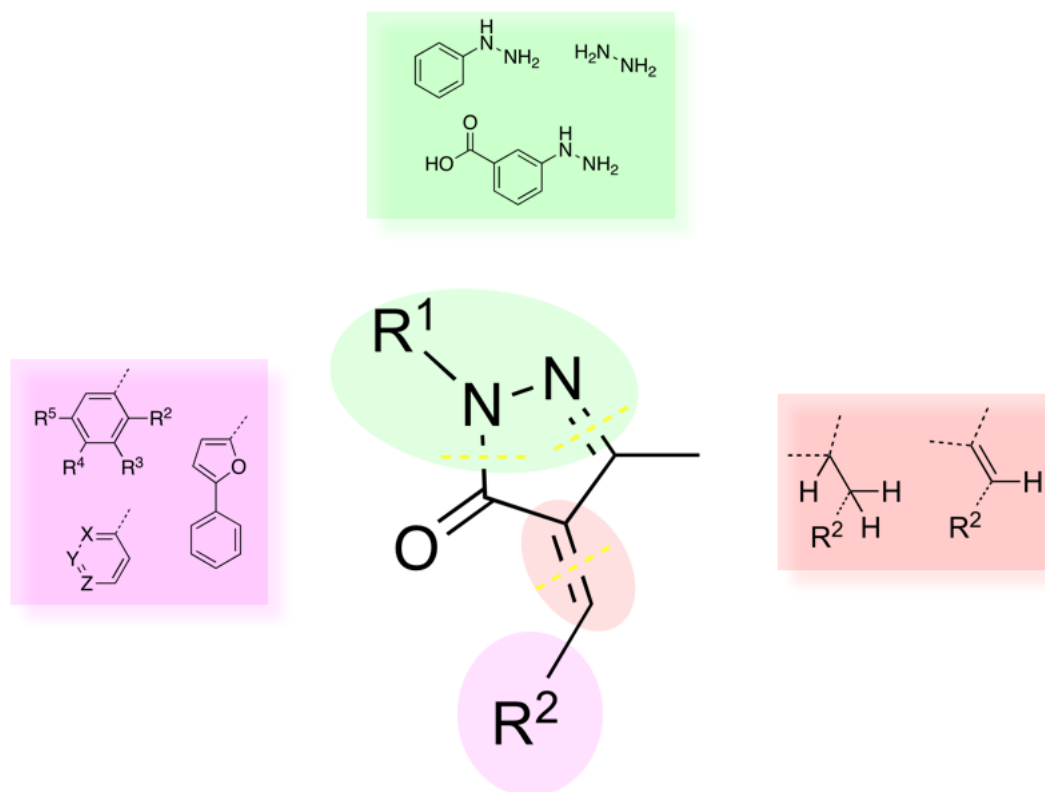


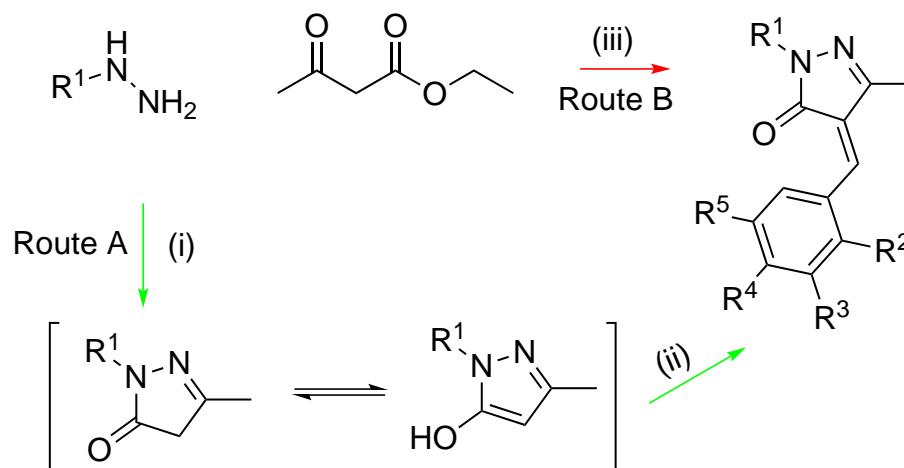
Figure 68: Synthetic strategies towards pyrazole-derivatives with anti-parasitic activity.

of the exo-cyclic double bond. Pyrazole derivatives were reported to preferentially react to its Z-isomer in Knoevenagel condensation reactions.^[152,250]

Two strategies are used to differentiate between both isomers with the aid of NMR spectroscopy.^[152,250] It has been observed that the chemical shift of the benzyldiene-protons appeared further downfield, if in proximity to the carbonyl function, as can be seen in the Z-configuration of the double bond (Figure 69, blue).

A further NMR experiment to distinguish between Z- and E-isomer is the nuclear Overhauser effect spectroscopy (NOESY) experiment. Here the proximity in space between the methyl group and the CH-moiety in the Z-configuration was measured. In the absence of a methyl group ^{13}C gated experiments can be performed to elucidate the double bond configuration (Figure 69, orange). The $^3J_{\text{C,H}}$ -coupling between the carbonyl group and the C-H-proton in rhodanine and rhodanine-like compounds have been reported between 5.52-7.21 Hz for the cis configuration and 10.0-12.3 Hz for the trans-configuration.^[106,163]

In this study NOESY experiments were performed for the correct assignment of the double bond configuration. Additionally, ^{13}C -CH-coupled experiments were performed, there specifically the gated coupling of the carbonyl and the CH-proton was measured. These tools allowed the assignment of the exo-cyclic double bond configuration. The assignment of the



Scheme 41: Two approaches pyrazolone-derivatives; (i) HOAc, reflux; (ii) NaOAc, HOAc; (iii) MWI 5 min, 420 W.

double bond configuration is essential for later structure activity relationship analysis. Different isomers could have different affinities towards a molecular target.

6.2.3 Synthesis of pyrazolone derivatives via Route A

Following the synthetic strategy outlined in Scheme 41, aryl hydrazine ($R^1 = \text{H}$ or COOH) was reacted with ethyl acetoacetate in acetic acid at 110°C .^[251] The condensation reaction yielded the cyclised products **80** and **81** in excellent yield of 81-97 % after column chromatography. The product was afforded as its keto form and no traces of the enol-form was seen in the NMR. However, the 3-benzoic acid analogue **81** was obtained as the enol form, as confirmed in the ^1H -NMR by the absence of the CH_2 signal and a signal further down field corresponding to the CH-proton of the enol form. N-phenyl pyrazole **80** was subjected to various benzaldehyde derivatives in the presence of sodium acetate as weak base (Scheme 42). These reaction conditions failed to produce the desired condensation product for 50 % of the used benzaldehyde derivatives. In all these cases, no product could be obtained after column chromatography and one side-products were purified. However, in the other 50 % of the cases the reaction yielded the desired condensation products **80a–f** after filtration in moderate yields of 13-80 %. The assignment of the double bond configuration was achieved with NOESY-NMR experiments for compounds **80a**, **80e**, and **80f**. The NOESY experiment showed a cross-coupling of the methyl group in the pyrazolone core structure and the CH-double bond proton, therefore confirming the formation of the Z-isomer as the major product. This observation is agreement with previous studies, suggesting that the pyrazolone derivatives of the type **80a–an** (Table 60) form preferably the Z-isomer.^[250] Compound **80c** was afforded as a 1:1 mixture of Z and E isomer. The chemical shift of the Ar-6-H proton in the Z-configuration ap-

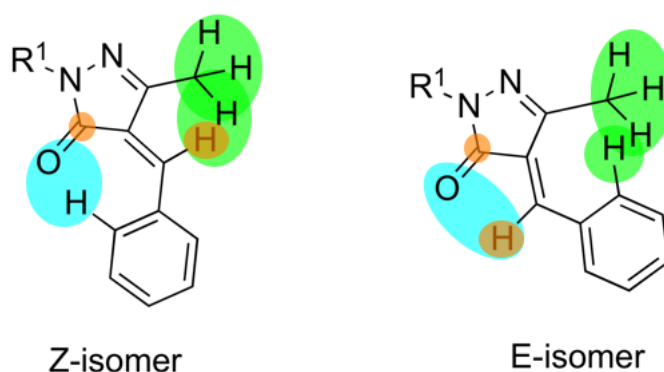
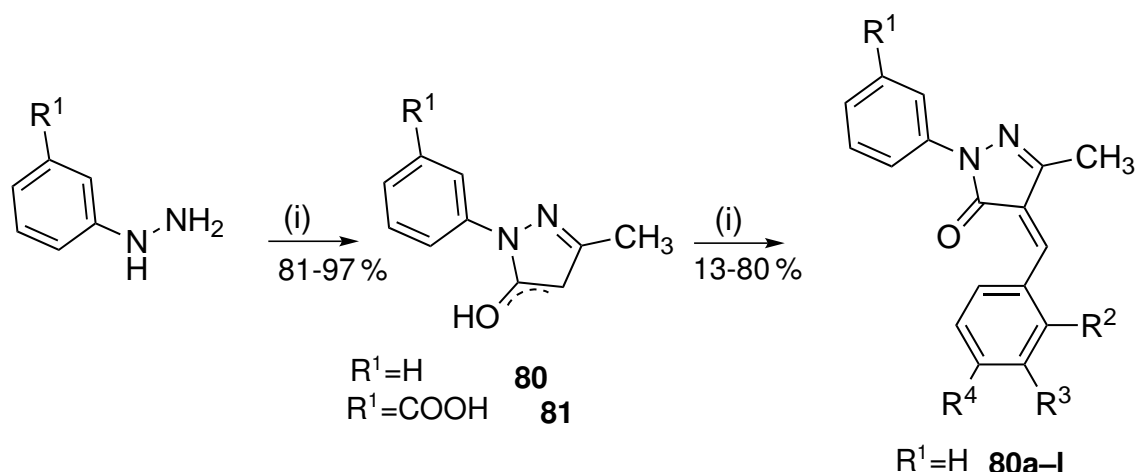


Figure 69: Z- and E-isomer of pyrazolone derivatives and their structural elucidation with NMR spectroscopy; green: NOESY; blue: δ_H of CH signal or H-6 on benzylidene-moiety; orange: $^3J_{C,H}$ coupling measurements.

peared further downfield δ_H 8.42 ppm in the ^1H -NMR experiment due to the proximity of the de-shielding carbonyl-group than the corresponding E-isomer δ_H 7.08-7.89 ppm. The signal for the CH-proton of the E-isomer appeared further downfield δ_H 8.11 ppm due to proximity of the carbonyl group compared to the Z-isomer δ_H 7.69-7.75 ppm. The assignment of the Z-configuration was further supported by a long-range $^5J_{C,F}$ coupling of 1.8 Hz for the CH-proton in the E-configuration. However, the $^5J_{C,F}$ -coupling for the Z-isomer was not found, as there was an overlap with other aromatic protons up-field in the ^1H -NMR. But it would be expected to see the long-range coupling only in the E-isomer, while in the Z-isomer the CH-proton and the CF_3 group are not in proximity any longer. In order to confirm this, the molecular structures of the E- and Z-isomer were generated with MOE2009.10 and the 3D coordinates were calculated after MMF94-forcefield optimisation (Figure 70). The generated 3D-structures suggested an intramolecular distance of 2.96 Å for the E-isomer, therefore explaining the observed long-range $^5J_{C,F}$ of 1.8 Hz (Figure 70, (b)). Whereas in the generated structure for the Z-isomer, the distance between the trifluoromethyl group and the CH-proton was 4.85-5.10 Å. However, the distance between the CH-proton and the methyl group was calculated to be only 2.52-2.53 Å, explaining the observed NOE effect in compounds **80a**, **80e**, and **80f** (Figure 70). It is possible that the trifluoromethyl group interacted as hydrogen bond acceptor with the CH-proton and caused the racemisation towards the E- and Z-isomer.

The remaining two products **80b** and **80d** were assigned the Z-configuration of the double bond based on the chemical shifts of the CH- and Ar-CH-signal. **80b** and **80d** showed a chemical shift δ_H 7.80-7.96 ppm for the CH-proton, while the Ar-CH signals in proximity to the carbonyl group appeared further downfield at 8.41-9.35 ppm. These values were similar to the



Scheme 42: Synthesis of pyrazolone derivatives through synthetic Route A; (i) Ethylacetoacetate, HOAc, 110 °C; (ii) NaOAc, EtOH, 110 °C; see Table 60.

ones observed for the Z-isomer of **80c** (δ_{CH} 7.69-7.75 ppm, δ_{ArCH} 8.42 ppm).

In summary, route A was suitable for the synthesis of pyrazolone derivatives, but the isolated yields and possible side-products made the investigation for improved methods necessary. For the corresponding aryl-pyrazolone **81** a different approach was employed for the condensation reaction with benzaldehyde derivatives.

6.2.4 Synthesis of pyrazolone derivatives via Route B

The alternative approach over route B was carried out under solvent free microwave irradiation of the aryl-hydrazine, ethyl aceto-acetate and various benzaldehydes. The reaction was carried out in a domestic microwave at 400-420 W at reaction times between 2-5 min. The yield of the reaction was slightly better compared to compounds obtained via Route A (Scheme 42). The microwave assisted one-pot three-component reaction with 3-hydrazinylbenzoic acid produced the condensation product **81a-I** in good yields of 13-80% (Scheme 43, Table 61). Derivatives **81h**, **81i**, **81j**, and **81k** could not be isolated. The major product for compounds **81j** and **81k** was the Schiff base of the reaction of 3-hydrazinylbenzoic acid and the corresponding aldehyde as confirmed by NMR spectroscopy. The one-pot reaction sequence using phenyl hydrazine yielded only the product **80m** in good yields of 60%. The reactions with any other aldehyde resulted in the formation of multiple products. It is possible that the starting aldehydes decomposed during microwave irradiation over a prolonged period, however reducing the reaction times from 5 min to 2-3 min (**80n**, **80p**, and **80q**) did not succeed in the desired product formation. All condensation products **81a-g** and **80m** were obtained as a single isomer. The chemical shift of the CH-signal δ_{H} 7.60-7.84 ppm and the Ar-CH δ_{H} 8.09-8.71 ppm confirmed the formation of the Z-isomer as the only product in the one-pot reaction sequence.

Table 60: Synthesis of pyrazolone derivatives through synthetic Route A; R¹=H and R²-R³ for pyrazole derivatives; yields and spectral analysis of double bond configuration; see Scheme 42.

#	R ²	R ³	R ⁴	yield [%]	NMR spectra for DB-configuration			
					δ	NOE	δ_{CH}	δ_{Ar-H}
80a	H	NO ₂	H	13	DMSO-d ₆	Z	8.02	9.61
80b	H	CH ₃	H	14	DMSO-d ₆	n.a.	7.80	8.41-8.45
80c	CF ₃	H	H	15	CDCl ₃	n.a.	7.69-7.75(Z) 8.11(E)	8.42(Z) 7.08-7.89(E)
80d	OH	H	OH	31	DMSO-d ₆	n.a.	7.96	9.35
80e	H	OBn	OBn	46	DMSO-d ₆	Z	7.73	8.9
80f	H	H	OH	80	DMSO-d ₆	Z	7.7	8.64
80g	H	OH	H	no product				
80h	OH	H	H	no product				
80i	H	H	CH ₃	no product				
80j	CH ₃	H	H	no product				
80k	H	CF ₃	H	no product				
80l	H	H	OMe	no product				

The reaction of 3-hydrazinylbenzoic acid, 2-carboxylic-benzaldehyde or 3-nitro benzaldehyde and excess ethyl aceto-acetate resulted in the formation of the Schiff-base product **82** (Scheme 44). In order to investigate the possible side-reaction in the microwave assisted one-pot three component reaction, ethyl-aceto acetate was reacted with 3-hydroxy-benzaldehyde in HOAc in the presence of NaOAc to catalyse the reaction. However, no reaction was observed. Although, method B improved the yields of the reaction towards pyrazolone derivatives, the formation of side-products was observed and phenyl-hydrazine were less tolerated. Therefore further optimisations were carried out for the synthesis of pyrazolone derivatives.

6.2.5 Improved reaction conditions for pyrazolone derivatives

The microwave assisted synthesis was not further optimised, because of the frequent side-reactions.

The reaction of ethyl 3-oxobutanoate with 3-hydroxy benzaldehyde did not yield any side product **83** (Scheme 44). These results and the good yields in the formation of the pyrazolone precursors **80** and **81** encouraged the use of HOAc as catalyst and solvent for the Knoevenagel reaction in the second step of the reaction sequence. The synthesis of pyrazolone derivatives was performed in a sequential one-pot reaction. The reaction was carried out in two steps. In the first step the pyrazolone precursor for the Knoevenagel reaction was synthesised via con-

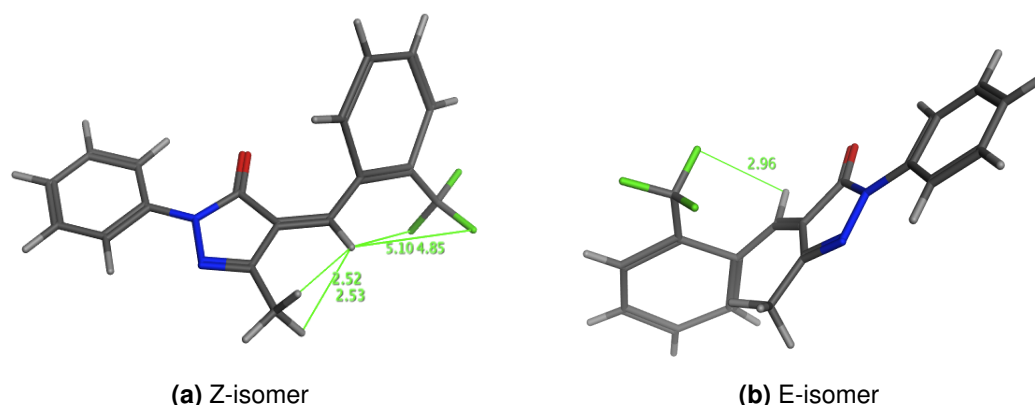
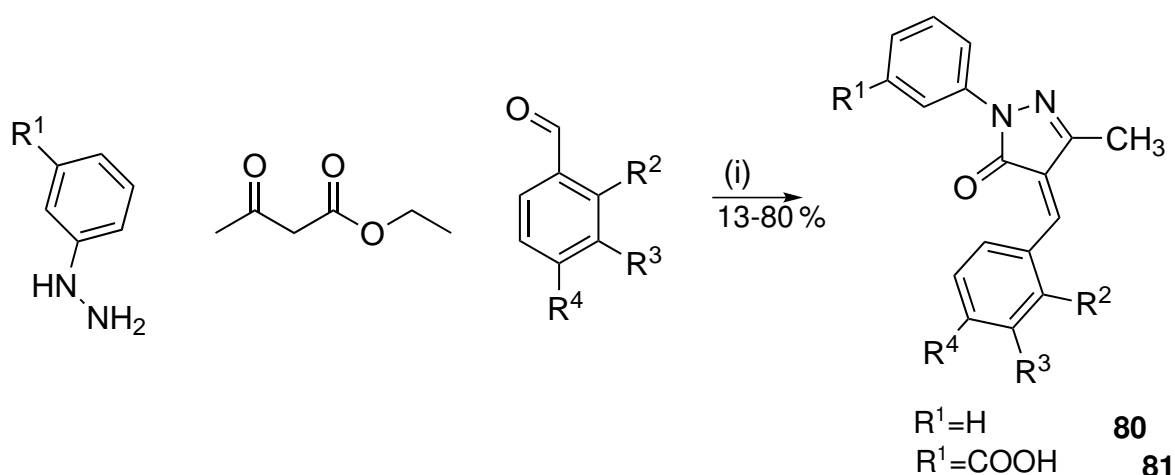


Figure 70: Measurement of distances of CH-proton and CF_3 -group in E-isomer and CH-proton and CF_3 and CH_3 -group in Z-isomer using MOE2009.10.

condensation of phenyl hydrazine or 3-benzoic acid hydrazine and ethyl-aceto acetate in HOAc. The reaction was stirred overnight (16 h), until which the starting material were completely converted to the desired phenylpyrazolone **80** or 3-benzoic acid pyrazolone **81**. In the following step, 1.5 eq. of benzaldehyde derivative were added and the reaction mixture was stirred until TLC showed complete consumption of **80** or **81**. The products were obtained in combined yields over two sequential steps of 15-93 % (??). The new reaction conditions resulted in higher yields and were tolerated by a broad range of benzaldehyde derivatives without the formation of side-products. Only compounds **80t** and **80u** could not be isolated under these reaction conditions. In the cases of **80t** and **80v** this might have been due to steric hindrance of the ortho substituent in the benzaldehyde moiety.

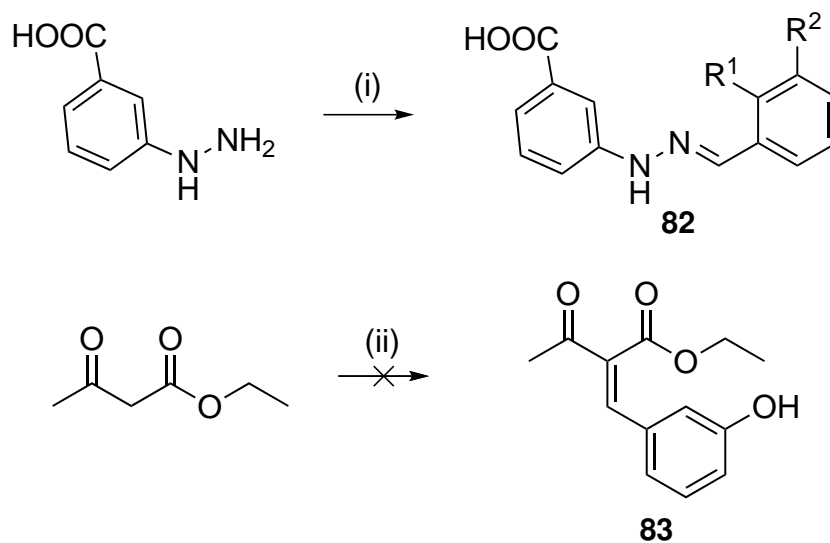
All products **80w–v** and **81m–n** showed the preferred Z-double bond configuration as the major product (Table 62).



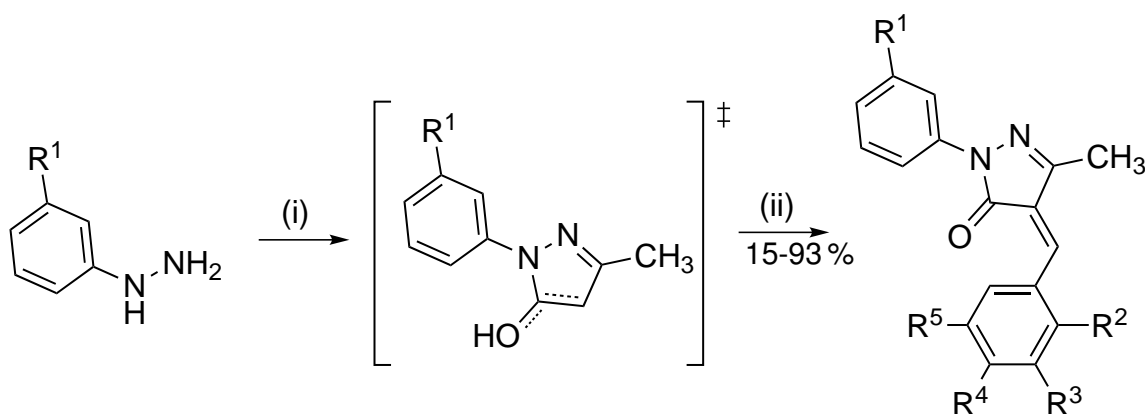
Scheme 43: Synthesis of pyrazolone derivatives using route B; microwave assistant one-pot three component reaction; (i) Microwave-irradiation (domestic), 400-420 W, 5 min.

Table 61: Synthesis of pyrazolone derivatives using route B; R^1 - R^4 for pyrazolone derivatives **81a–k** and **80s**; yields; section time and spectral analysis of double bond configuration; δ_H in DMSO- d_6 .

#	R^1	R^2	R^3	R^4	R-time [min]	yield [%]	NMR spectra for DB		
							NOE	δ_{CH} [ppm]	δ_{ArCH} [ppm]
81a	COOH	H	OBn	OBn	5	13	Z	7.75	8.21
81b	COOH	H	Br	OMe	5	24	n.a.	7.79	8.57
81c	COOH	H	OBn	H	5	25	n.a.	7.84	8.09
81d	COOH	H	H	CN	5	45	n.a.	7.83	8.64
81e	COOH	H	H	OH	5	64	n.a.	7.71	8.60-8.66
81f	COOH	H	H	OBn	5	72	n.a.	7.79	8.71
81g	COOH	H	H	NMe ₂	5	80	Z	7.60	8.65
81h	COOH	H	H	tBu	5	no product			
81i	COOH	H	H	SO ₂ Me	5	no product			
81j	COOH	COOH	H	H	5	schiff base			
81k	COOH	H	NO ₂	H	5	schiff base			
80m	H	H	H	OH	5	60	Z	7.70	8.64
80n	H	H	OH	H	2	no product			
80o	H	CF ₃	H	H	5	no product			
80p	H	H	OH	H	5	no product			
80q	H	H	OH	H	3	no product			
80r	H	H	H	OBn	5	no product			



Scheme 44: Side-reaction in the microwave assisted one-pot reaction; (i) ethyl acetoacetate, 2-carboxylic acid-benzaldehyde ($R^1=\text{COOH}$) or 3-nitro-benzaldehyde ($R^1=\text{H}$, $R^2=\text{NO}_2$), MWI, 400 W, 5 min; (ii) 3-hydroxy-benzaldehyde, NaOAc, HOAc.



Scheme 45: Improved reaction conditions towards pyrazolone derivatives; (i) ethyl 3-oxobutanoate, HOAc, 110 °C; (ii) benzaldehyde derivatives, HOAc.

Table 62: Improved reaction conditions towards pyrazolone derivatives; R¹-R⁵ for pyrazolone derivatives; yield; chemical shift δ_H for CH and 6-Ar-CH for double bond configuration.

#	R ¹	R ²	R ³	R ⁴	R ⁵	[%] yield	NMR spectra for DB conf. [ppm]			
							δ	NOE	δ_{CH}	δ_{ArCH}
80w	H	H	H	OMe	H	15	DMSO-d ₆	Z	7.71	8.71
80x	H	H	H	Ph	H	16	CDCl ₃	n.a.	7.39-7.45	8.61
80y	H	H	H	CN	H	22	DMSO-d ₆	n.a.	7.85-7.90	8.61-8.65
80z	H	H	H	Cl	H	24	DMSO-d ₆	n.a.	7.83	8.61
80aa	H	H	H	SO ₂ Me	H	44	DMSO-d ₆	n.a.	7.95	8.68
80ab	H	H	Br	OMe	H	46	DMSO-d ₆	Z	7.75	9.24
80ac	H	CF ₃	H	H	H	48	CDCl ₃	n.a.	7.62-7.65	8.37
80ad	H	H	Br	F	H	57	DMSO-d ₆	Z	7.84	9.20
80ae	H	H	CF ₃	H	H	62	DMSO-d ₆	Z	7.85-7.89	9.07
80af	H	H	OBn	H	H	62	CDCl ₃	Z	7.15(E), 7.22(Z)	6.98-7.89(E), 8.54(Z)
80ag	H	H	OMe	OH	OMe	72	DMSO-d ₆	n.a.	7.72	8.29
80ah	H	H	H	H	H	82	CDCl ₃	Z/E	7.27(Z), 7.92(E)	7.88(E), 8.37-8.41(Z)
80ai	H	H	OH	H	H	89	CDCl ₃	n.a.	7.33-7.43	8.52
80aj	H	H	H	CF ₃	H	93	DMSO-d ₆	n.a.	7.07	8.31
80ak	H	H	OH	OH	H	87	CDCl ₃	Z	7.34	9.19
80t	H	CF ₃	H	H	H	no product				
80al	H	H	H	CH ₃	H	no product				
80am	H	H	H	NMe ₂	H	56	CDCl ₃	n.a.	7.15	8.48
80v	H	OH	H	H	H	no product				
81m	COOH	OH	H	H	H	13	DMSO-d ₆	n.a.	8.07	9.07
81o	COOH	H	Br	F	H	58	DMSO-d ₆	Z	7.86	9.17
81p	COOH	H	H	H	H	78	DMSO-d ₆	Z	7.84	8.58
81n	COOH	H	H	OBn	H	64	DMSO-d ₆	n.a.	7.78	8.70

The double bond configuration of compounds **80w**, **80ab**, **80ad**, **80ae**, **80ak**, **81o**, and **81p** was determined by NOESY-NMR experiments. All these derivatives showed a cross peak of the methyl group in proximity to the CH-proton in the NOESY spectra. These Z-isomers had a chemical shift of the 6-Ar-CH-proton of δ_H 8.58-9.24 ppm due to the de-shielding effect of the neighbouring carbonyl group. Whereas the chemical shift of the CH-double bond proton is shifted towards higher fields δ_H 7.34-7.89 ppm. The chemical shifts of both the 6-Ar-CH- and CH-proton were compared with the remaining derivatives and the Z-configuration could be assigned. The chemical shifts of the 6-Ar-CH-proton in derivatives **80x**, **80y**, **80z**, **80aa**, **80ac**, **80ag**, **80ai**, **80am**, **81m**, and **81n** (Table 62) were δ 8.29-9.07 ppm and therefore in a similar range as previous observed aromatic CH-protons in proximity to a carbonyl group. The chemical shift of the CH-proton was δ_H 7.39-8.07 ppm and therefore were similar to Z-configured isomers, further supporting the Z-configuration. Compounds **80af** and **80ah** were afforded as mixtures of both Z- and E-isomer. The NMR spectra were recorded in $CDCl_3$ and the chemical shifts appeared therefore at slightly higher field compared to spectra recorded in $DMSO-d_6$. Both compounds were analysed by NOESY-NMR experiments and Z- and E-configuration were confirmed by cross peaks of the methyl and CH-proton for the Z-configuration and methyl and Ar-CH-proton cross peaks for the E-configuration. Compound **80af** was afforded as a mixture of isomers in a ratio of 5.5:1 (Z:E-isomer). It was most likely that steric hindrance of the 3-benzyloxy group was responsible for the racemisation. In the case of compound **80ah** the isomeric ratio was 6:1 (Z:E-isomer) and the absence of any substituents might be the reason for the racemisation. However, in both cases the Z-isomer was obtained as the major product.

The derivative **80z** was chosen for additional experiments to verify the Z-configuration of the double bond. The configuration of the Z-isomer was confirmed by NOESY and H-Jres experiments (Figure 71 (a)). Initially, NOESY-experiments were performed to show the Z-configuration of the double bond (Figure 71 (b)). The NOESY spectra showed the expected cross peak between the methyl and the CH-proton. Next, HPMC-experiments were performed to show the coupling of the CH-proton over multiple bonds in **80z** (Figure 71, (c)). In the HPMC-experiment the long range coupling of the CH-proton to the carbonyl function is visible. To quantify the long-range coupling of the CH-double-bond proton and the carbonyl group, a H-Jres-experiment was performed (Figure 71 (d)). The H-Jres experiment is a gated- ^{13}C - 1H -NMR coupling experiment, here the experiment is tuned to suppress all the signals except the signal of the CH-proton and the coupled ^{13}C -nuclei. The splitting at 161.4 ppm for the carbonyl function was measured to be $^3J_{CH,C=O} = 5.7$ Hz. This relatively small coupling constant was surprising, as rhodanine derivatives with a cis-configured double bond showed coupling constants of 10.0-12.3 Hz (Chapter 6.2.2).^[106,163] Attempts to find reference values for the long range coupling of the CH-double bond proton and the carbonyl group were unsuccessful. The double bond configuration is most conveniently determined by the chemical shift of the 6-Ar-

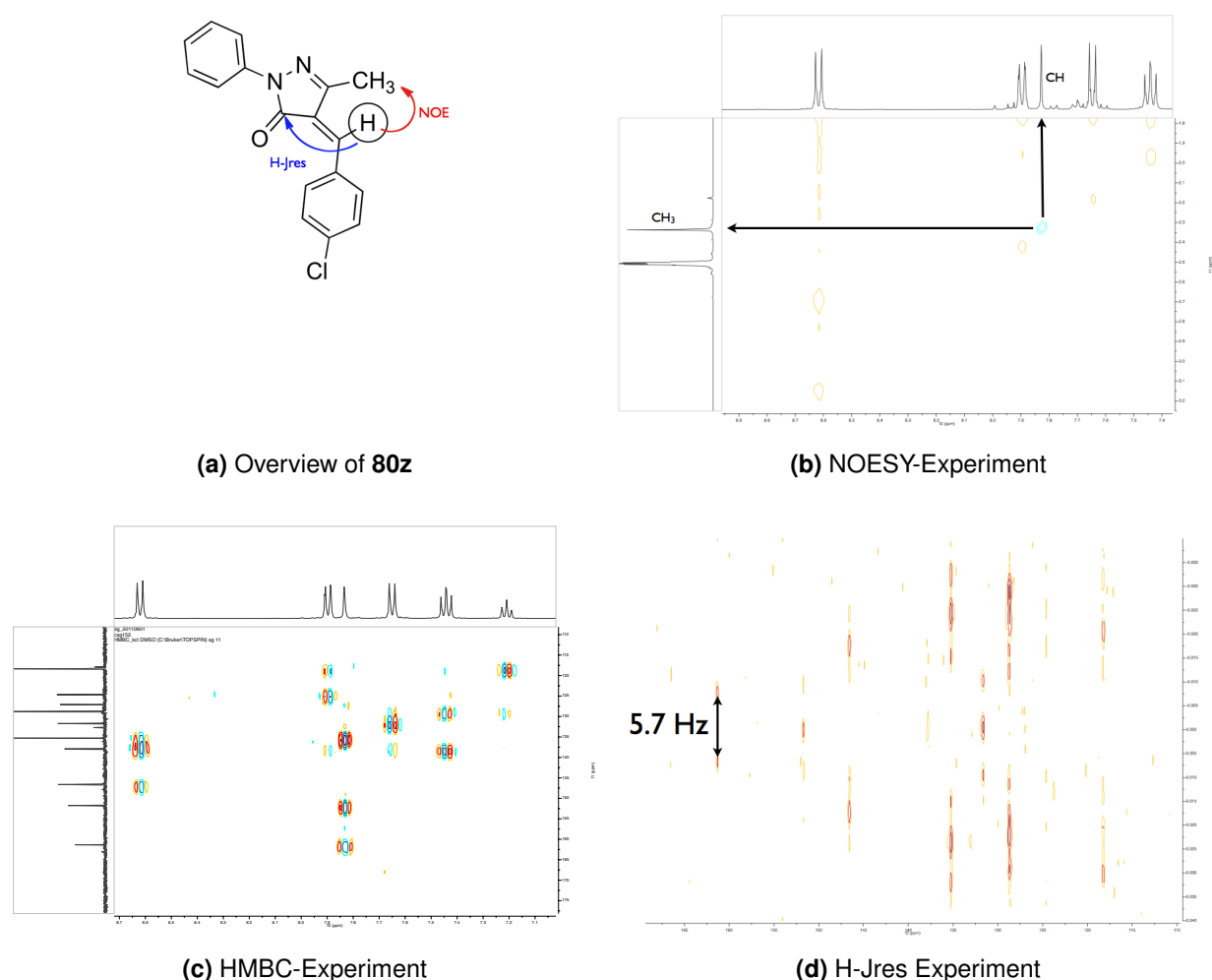


Figure 71: 2D-NMR Experiments for confirmation of the Z-configuration of double bond in **80z**.

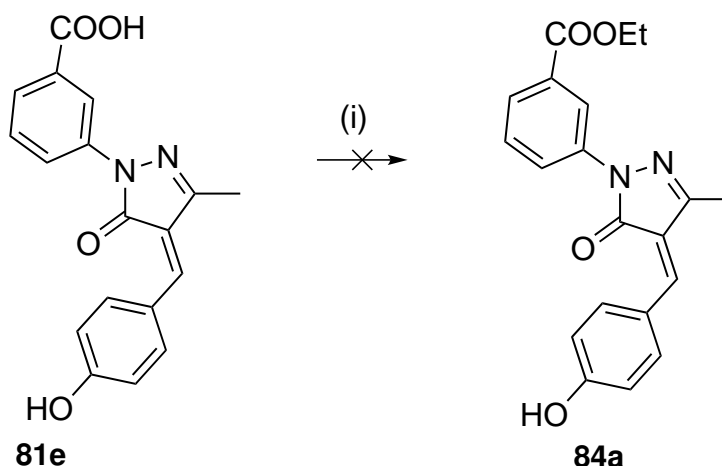
CH-shift in ^1H -NMR experiments.^[250] Therefore, it would be plausible that the $^3J_{\text{CH},\text{C}=\text{O}}$ coupling of 5.7 Hz would indicate the Z-configuration. The control experiment with the E-isomer was not performed, as access to the 700 MHz NMR was limited and the Z-configuration could undoubtedly be determined by other NMR experiments. But it would be expected that the coupling constant would be smaller than 5.7 Hz.

6.2.6 Synthesis of ester-analogues of **81e**

It has previously been reported that esterification of carboxylic acid could improve membrane permeability and efficiency of drugs in parasites.^[167] The beneficial aspect of the ester modification in thiazolidine-2,4-dione derivatives was described in chapter 3.2.6.

In order to study the importance of this ester modification in pyrazolone derivatives, attempts were made to synthesis the ester derivative **84a** via standard esterification conditions,

using DCC, DMAP in ethanol (Scheme 46). However, the esterification of the free carboxylic acid in **81e** failed and only starting material was recovered.



Scheme 46: Esterification reaction of **81e**; (i) DCC, DMAP, EtOH.

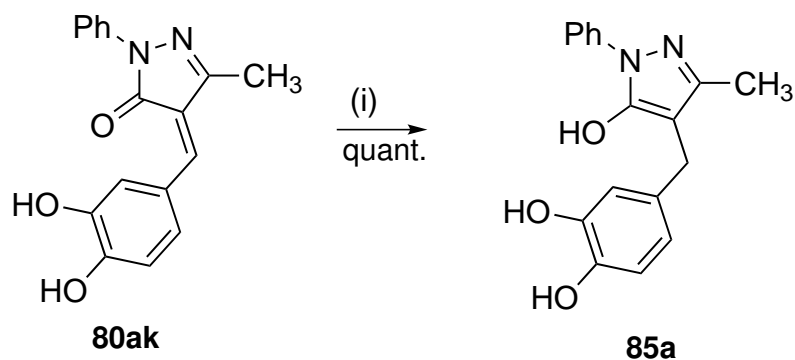
6.2.7 Reduction of exo-cyclic double bond in pyrazolone derivatives

Pyrazolones of the type **80ak** have an exo-cyclic double bond, which is in conjugation with the neighbouring carbonyl-group. This arrangement of conjugated double bond is possibly prone to 1,4-addition of nucleophiles to the carbonyl- and or double bond in pyrazolones. This Michael acceptor reactivity could potentially be a problem for compound selectivity and toxicity. Compound **80ak** could potentially bind nonselectively to biological nucleophiles (such as glutathione) or could covalently bind to multiple proteins with low affinity. In order to study the binding mode, the double bond in **80ak** was reduced (Scheme 47). The reduced analogue can be assessed for anti-parasitic activity and then compared to the activity of the parent non-reduced **80ak**. A drop in activity of the reduced analogue might be explained through a loss of covalent binding or through steric considerations, as the reduction of the double bond will lead to an increase in flexibility.

The double bond in **80ak** was reduced under catalytic hydrogenation, and the reduced product **85a** was obtained as the enol form. The ^1H -NMR and ^{13}C -NMR spectra showed no signal for the keto form, the CH-proton and the carbonyl signal were missing and the ^{13}C -NMR showed an additional un-saturated tertiary carbon-signal.

6.2.8 Synthesis of heterocyclic modified pyrazole derivatives

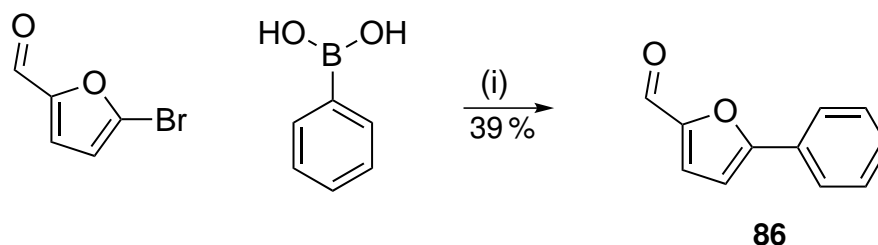
Pyrazolone derivatives have been studied as inhibitors of bacterial glycosyltransferases,^[101,245] a particularly good μM -molar inhibitor ($1\ \mu\text{M}$) against the bacterial heptosyltransferase WaaC,



Scheme 47: Reduction of pyrazole derivative **80ak**; (i) Pd/C, H₂, dioxane.

had a furanyl substituent in position 4 of the pyrazolone moiety.^[245] It was assumed that this furanyl pyrazolone might also inhibit glycosyltransferases involved in the GPI-anchor biosynthesis in parasites.

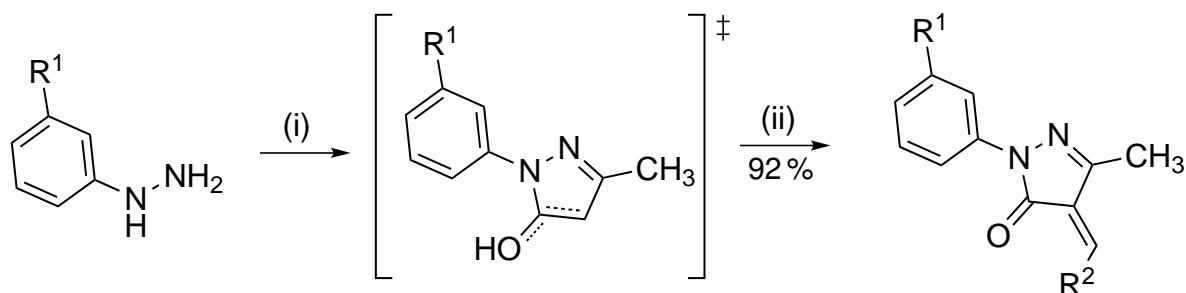
In this chapter, the synthesis of a similarly modified analogue is described, starting from the synthesis of the modified aldehyde for the Knoevenagel reaction. The corresponding aldehyde was synthesised via Suzuki cross coupling reaction between phenyl-boronic acid and bromo-furanyl-carbaldehyde. The C-C coupling reaction afforded the desired product **86** in moderate yields of 39 % (Scheme 48). The modified furanyl carbaldehyde **86** and various



Scheme 48: Synthesis of furanyl-carbaldehyde **86**; (i) Pd(PPh₃)₄, K₂CO_{3(aq)}, DMF, 110 °C.

other heteroaromatic-aldehydes were subjected to the improved sequential one-pot reaction procedure, described in Chapter 6.2.5 (Scheme 49, Table 63). The reaction of **86** and 3-benzoic-acid hydrazine and ethyl-aceto-acetate in HOAc failed and no product was obtained after column chromatography. However, the unsubstituted analogue **88a** produced the desired condensation product in excellent yields of 92 %. The double bond configuration was determined with NOESY experiments and through comparison with chemical shifts of the Ar-CH-proton in the Z-configuration. NOESY experiments showed a cross-peak between the methyl and CH-protons and the chemical shift of the furanyl-CH in proximity to the carbonyl was δ_H 8.64 ppm, thus indicating the Z-configuration of the double bond.

Attempts to subject various pyridine-carboxaldehydes to the one-pot reaction failed and no



Scheme 49: Synthesis of heterocyclic modified pyrazolone derivatives; (i) ethyl-aceto acetate, HOAc, 110 °C; (ii) benzaldehyde derivatives, HOAc.

Table 63: Synthesis of heterocyclic modified pyrazolone derivatives; R¹-R² for heterocyclic modified pyrazolone; yield and NMR Experiments for configuration of double bond.

#	R ¹	R ²	yield [%]	NMR for DB conf [ppm]			
				δ	NOE	δ_{CH}	δ_{ArCH}
87a	COOH		no product				
88a	H		92	DMSO-d ₆	Z	7.71	8.64
88b	H		no product				
88c	H		no product				
88d	H		no product				

products could be isolated (Table 63).

6.2.9 Synthesis of N-1 aliphatic modified pyrazolone

The previous N-1 aryl modified pyrazolone analogues **80a–an** and **81a–q** are potentially very lipophilic and might undergo unspecific binding to proteins. Lipophilicity can be quantified through measuring the partition coefficient in octanol and water. This partition coefficient, also known as logP, can be calculated by bioinformatic tools. Here, the logP has been calculated using the weighted logP function in MarvinSketch (Figure 72). The logP value for the N-1 benzoic acid derivatives **81p** was predicted to be logP 3.24, whereas the predicted value for the N-1 unsubstituted pyrazolone derivative **89a** was only logP 1.70. It would be very interesting to assess the activity of unsubstituted analogues, both in terms of lower logP values and lower molecular weights. N-1-unsubstituted analogues with a high anti-parasitic activity would give more opportunities for modifications, such as the introduction of additional substituents or

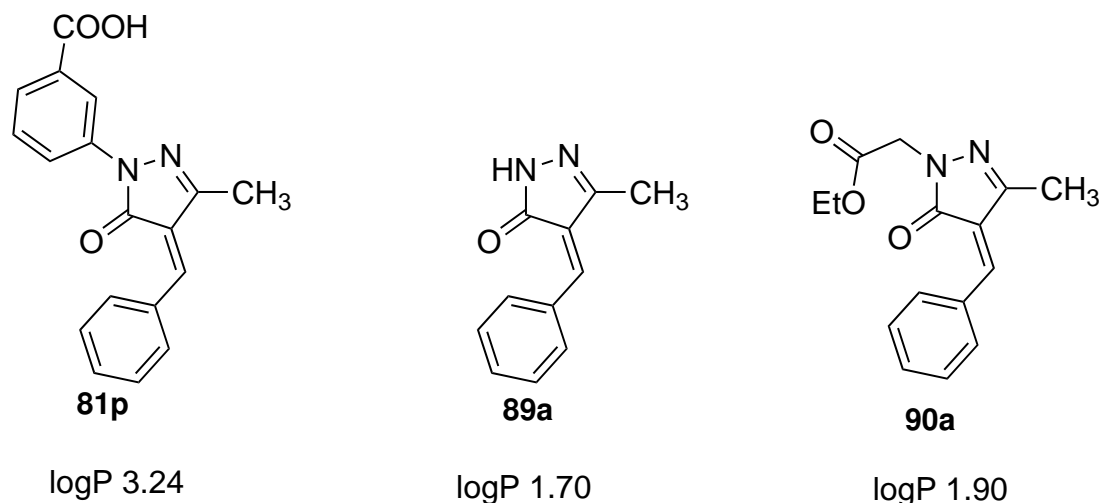


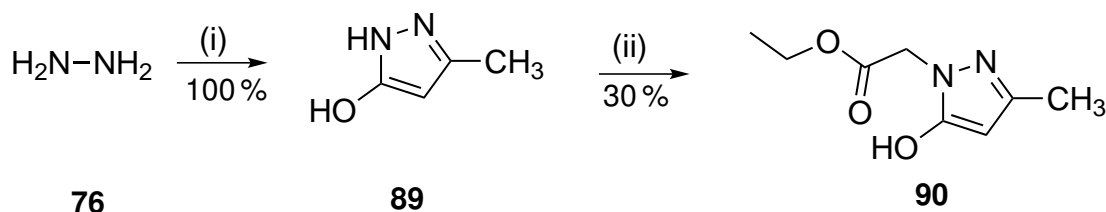
Figure 72: Calculated logP values using MarvinSketch (weighted method for calculation: VG, klogP, phys = 1).

bulkier substituents on the C-4-pyrazolone position.

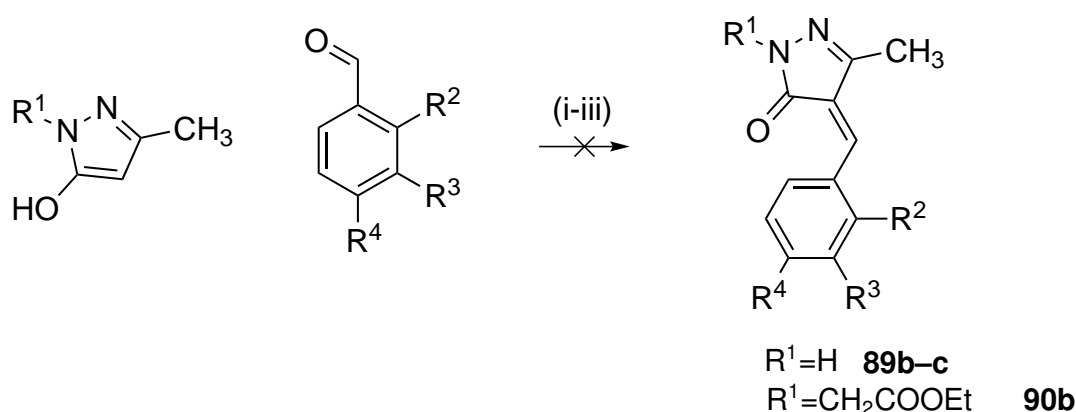
The aliphatic acetic acid ester modification in **90a** was calculated to have a logP value of 1.90, slightly higher than that of the unsubstituted analogue **89a**. If the ester was to be hydrolysed, the logP would be 1.40. As described previously in Chapter 3.2.6, the higher logP value of 1.70 could facilitate the diffusion through membranes. Once in the cell the free-acids can benefit both from better water solubility (logP 1.40) and possible specific interactions with the target protein(s). The precursors for the synthesis of N-1-modified pyrazolone derivatives were synthesised as outlined in Scheme 50. Hydrazine **76** was reacted with ethyl-aceto-acetate in HOAc to afford the precursor **89** in quantitative yields after simple filtration (Scheme 50).

The N-1-acetic ester modified analogue **90** was synthesised by reaction of the unsubstituted pyrazolone precursor **89** with ethyl 2-bromoacetate and NaH in DMF. The substitution product **90** was afforded in moderate yields of 30 % after column chromatography. ¹H-NMR spectral analysis of **90** confirmed the products enol-form, as well as substitution of the N-1 nitrogen. The NOESY experiment did not show any cross peak between the pyrazolone methyl substituent and the ester moiety, thus suggesting N-1 substitution (Scheme 50).

The unsubstituted and ester modified pyrazolone precursors **89** and **90** were subjected to Knoevenagel reaction conditions with benzaldehyde derivatives (Scheme 51). Initially, the condensation reaction was carried out with the unsubstituted pyrazolone **89**, 4-methylbenzaldehyde and NaOAc as base and in ethanol at 80 °C. However under these conditions no reaction was observed and only starting material was recovered. In an attempt to activate the substrates, the solvent was substituted to HOAc and the reaction mixture was heated to 110 °C (Table 64). But the reaction did not proceed and no conversion of starting materials was observed. The



Scheme 50: Synthesis of N-1-unsubstituted pyrazolone precursor **89** and ester analogue **90**; (i) ethyl aceto-acetate, HOAc, 110 °C; (ii) NaH, ethyl 2-bromoacetate, DMF, 0 ° → rt.



Scheme 51: Knoevenagel condensation reaction of N-1-aliphatic modified pyrazolone; (i) NaOAc, EtOH, 80 °C; (ii) NaOAc, HOAc, 110 °C; (iii) HOAc, 110 °C.

reaction with the 3-methylbenzaldehyde, the unsubstituted pyrazolone **89** in HOAc at 110 °C also failed to produce the desired condensation products. Next, the aldehyde was substituted to 4-chlorobenzaldehyde, as this aldehyde proved to be reactive in the Knoevenagel reaction of phenyl- or phenyl-3-benzoic acid pyrazolone derivatives. The reaction conditions with NaOAc in HOAc at 110 °C were chosen for the condensation reaction, but no product was obtained. The N-acetic acid ester analogue **90** was subjected to similar conditions with 4-chlorobenzaldehyde and sodium acetate in ethanol at 80 °C. Similar to previous attempts, the condensation product was not obtained. All reactions used the pyrazolone precursor in its enol form, so it might be that stronger bases are necessary to catalyse the condensation reaction with benzaldehyde derivatives. Another possibility would have been to substitute the solvent with DMF to stabilise the intermediates in the Knoevenagel reaction. The addition of TiCl_4 might also catalyse the reaction further and might lead to product formation.^[152] However, due to time constraints none of these alternatives could be investigated.

Table 64: Knoevenagel condensation reaction of N-1-aliphatic modified pyrazolone derivatives; R¹-R⁴ for N-1-substituted pyrazolone derivatives (Scheme 51); method of preparation and yield.

#	R ¹	R ²	R ³	R ⁴	method	yield [%]
89b	H	H	H	CH ₃	(i)	no reaction
89d	H	H	H	CH ₃	(iii)	no reaction
89e	H	H	CH ₃	H	(ii)	no reaction
89c	H	H	H	Cl	(iii)	no reaction
90b	CH ₂ COOEt	H	H	Cl	(i)	no reaction

6.3 Anti-parasitic activity

The anti-parasitic activity against *T. brucei*, *T. cruzi* and *L. infantum* was evaluated with the activity assays described in chapter 3.3.1.

6.3.1 Anti-parasitic activity of phenyl pyrazolones

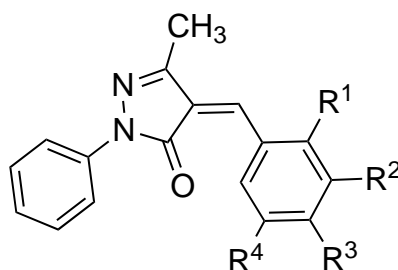
Initially, the starting phenyl pyrazolone derivative **80** was evaluated for its anti-parasitic activity. The derivative **80** showed no activity on *T. brucei*, *T. cruzi* nor *L. infantum* at 100 µM, however it displayed some toxicity against HL60 cells (GI₅₀ 151.7 µM).

The substitution product with benzaldehyde (**80ah**) was afforded as mixture of Z and E double bond isomers (ratio 6:1 Z to E). The condensation product **80ah** showed improved anti-trypanosomal activity (GI₅₀ 15.5 µM) compared to the starting pyrazolone **80**. Furthermore, **80ah** displayed an improved toxicity profile, as it did not show cytotoxicity against HL60 cells at 100 µM. The majority of substitutions on the 4-benzylidene moiety resulted in GI₅₀ values of 12.4-17.3 µM (Table 65). As for the *T. brucei* activity there was no clear trend, however the toxicity of the derivatives correlated well to the logP value. Therefore an increased logP value resulted in increased toxicity against HL60 cells in compounds **80ad**, **80a**, **80z**, **80e**, **80ac**, **80aj**, **80ak**, and **80ab**. Interestingly, the ortho- and para- dihydroxy derivative **80d** displayed no activity against *T. brucei*, indicating a possible preference for hydrogen bond acceptors or large lipophilic substituents, as the ortho-trifluoromethyl derivative **80ac** was active in the low µM range (GI₅₀ 15.4 µM) against *T. brucei*. This observation is further supported by low µM activity (GI₅₀ 17.1 µM) of the para-hydroxy derivative **80f**. Another interesting exception of the low µM activity of pyrazolone derivatives, was the para-dimethylamino derivative **80am**. Comparing this substituent to other para-substituted analogues with low µM activity showed that positive charged substituent (under physiological pH) resulted in loss of anti-trypanosomal activity. Whereas large substituents, such as benzyl, phenyl and trifluoromethyl showed low

μM activity against *T. brucei*. Furthermore, acceptor groups (CN, SO_2Me , OMe) were well tolerated and resulted in active reagents against *T. brucei* growth.

Heterocyclic modification, such as a furanyl group in derivative **88a** diminished anti-trypanosomal activity. The only derivative with moderate activity against *L. infantum* was compound **80ac**, however its high toxicity against HL60 cells (GI_{50} 41.6 μM) resulted in an undesirable toxicity profile.

Table 65: Anti-parasitic activity of phenyl pyrazolones derivatives.



#	R^1	R^2	R^3	R^4	GI_{50} [μM]				logP
					<i>T. brucei</i>	<i>T. cruzi</i>	<i>L. infantum</i>	HL60	
80					>100	>100	>100	151.7 \pm 8.3	1.53
80ag	H	OMe	OH	OMe	12.4 \pm 0.1	>100	>100	>100	2.96
80ad	H	Br	F	H	12.5 \pm 1.0	n.a.	>100	40.3 \pm 4.6	4.49
80y	H	H	CN	H	12.7 \pm 0.6	n.a.	n.a.	91.8 \pm 4.0	3.44
80a	H	NO_2	H	H	13.0 \pm 0.1	n.a.	>100	71.1 \pm 4.3	3.52
80af	H	OBn	H	H	13.6 \pm 0.3	n.a.	n.a.	n.a.	5.15
80x	H	H	Ph	H	13.7	n.a.	>100	20.7	5.23
80ae	H	CF_3	H	H	14.4 \pm 1.2	n.a.	>100	94.2 \pm 0.5	4.46
80z	H	H	Cl	H	14.4 \pm 1.3	n.a.	>100	67.8 \pm 1.8	4.19
80e	H	OBn	OBn	H	15.1 \pm 0.5	>100	>100	31.0 \pm 6.7	6.71
80aa	H	H	SO_2Me	H	15.2	n.a.	>100	>100	2.42
80ac	CF_3	H	H	H	15.4 \pm 1.9	n.a.	63.6 \pm 1.8	41.6 \pm 4.7	4.46
80w	H	H	OMe	H	15.5 \pm 1.8	>100	>100	>100	3.42
80aj	H	H	CF_3	H	15.5 \pm 2.8	n.a.	>100	48.7 \pm 6.1	4.46
80ah	H	H	H	H	15.5 \pm 3.2	>100	>100	>100	3.58
80f	H	H	OH	H	17.1 \pm 5.3	>100	>100	>100	3.28
80ak	H	OH	OH	H	17.3 \pm 0.1	n.a.	n.a.	47.3 \pm 8.9	2.97
80ab	H	Br	OMe	H	17.3 \pm 0.6	>100	>100	51.9 \pm 3.6	4.19
80ai	H	OH	H	H	27.5 \pm 13.9	>100	>100	n.a.	3.28
88a			2-furanyl		60.6 \pm 4.7	n.a.	n.a.	>100	2.64
80am	H	H	NMe_2	H	64.8 \pm 10.0	n.a.	n.a.	>100	3.69
80d	OH	H	OH	H	>100	>100	>100	>100	2.97

6.3.2 Anti-parasitic activity of 3-benzoic acid pyrazolones

Previous phenyl pyrazolone derivatives showed promising anti-trypanosomal activity against *T. brucei* (GI_{50} 12.4-17.3 μ M), however they also displayed toxicity against HL60 cells, resulting in low SI towards *T. brucei*. In order to increase selectivity, 3-benzoic acid pyrazolones were evaluated for their anti-parasitic activity. Although structurally very similar to previous pyrazolone inhibitors in this chapter, the additional carboxylic acid function may alter toxicity towards HL60 cells by introducing a substituent which could undergo other than lipophilic or π -stacking interactions. Indeed, derivatives **81a** and **81b** showed decreased toxicity against HL60 cells (GI_{50} >100 μ M), compared to their analogues **80e** and **80ab** (GI_{50} 31.0 and 51.9 μ M). However, only the bis-benzyloxy derivative **81a** retained its anti-trypanosomal activity against *T. brucei*, while the bromo-methoxy derivative **81b** showed no effect on *T. brucei* growth at 100 μ M. Interestingly, the 4-para-hydroxy derivative **81e** also showed no activity against *T. brucei* at 100 μ M, although its phenyl-analogue **80f** had a GI_{50} of 17.1 μ M. None of the inhibitors showed any activity against *L. infantum* at 100 μ M.

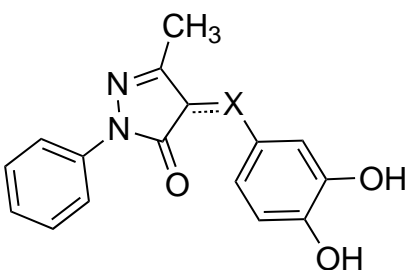
Table 66: Anti-parasitic activity of 3-benzoic acid pyrazole derivatives.

#	R ¹	R ²	R ³	R ⁴	GI_{50} [μ M]			
					<i>T. brucei</i>	<i>T. cruzi</i>	<i>L. infantum</i>	HL60
81p	H	H	H	H	11.7 \pm 0.2	n.a.	n.a.	>100
81o	H	Br	F	H	12.8 \pm 0.2	>100	>100	>100
81f	H	H	OBn	H	13.7 \pm 0.1	>100	>100	>100
81c	H	OBn	H	H	14.2 \pm 2.0	n.a.	>100	29.7 \pm 0.1
81a	H	OBn	OBn	H	14.3 \pm 3.5	n.a.	>100	79.8 \pm 7.0
81e	H	H	OH	H	>100	>100	>100	>100
81b	H	Br	OMe	H	>100	>100	>100	>100
81g	H	H	NMe ₂	H	>100	>100	>100	n.a.

6.3.3 Anti-trypanosomal effect of the reduction of the exo-cyclic double bond in pyrazolone derivatives

The exo-cyclic double bond of the catechol pyrazolone **80ak** (Table 67) was reduced and the racemic mixture was evaluated for its anti-parasitic activity. A broad range of different substituted pyrazolones showed anti-trypanosomal activity in the lower μM range against *T. brucei* (Table 65), while showing low selectivity then screened against mammalian HL60 cells. Therefore, it may be possible that these inhibitors bind covalently to biological targets over their Michael acceptor system and therefore displaying general cytotoxicity. However, reduction of the double in derivative **85a** (Table 67) did not effect its anti-trypanosomal activity, nor its toxicity against HL60 cells. This promising results validated the use of pyrazolones as anti-parasitic agents and further modification can be carried out to improve their anti-parasitic activity and toxicity towards HL60 cells. The retention of activity might suggest that pyrazolone derivatives are less susceptible to Michael addition reactions.

Table 67: Anti-trypanosomal effect on the reduction of the exo-cyclic double bond.



#	X	GI ₅₀ [μM]	
		<i>T. brucei</i>	HL60
85a	CH ₂	16.4 \pm 0.1	51.1 \pm 1.5
80ak	CH	17.3 \pm 0.1	47.3 \pm 8.9

6.4 Discussion

Pyrazolones are a promising class of inhibitors for the development of anti-parasitic agents, in particular against *T. brucei*. While substitutions on position 4 of the pyrazolone ring showed only minor alterations in their anti-trypanosomal activity (Table 65), the modification on the N-1 substituent improved selectivity without affecting trypanocidal activity (Table 66). The reduction of the exo-cyclic double bond did not affect its anti-trypanosomal activity, suggesting that covalent binding to the Michael acceptor system are less likely to occur in these inhibitor series. However, further optimisation of these promising compounds are necessary to increase

anti-parasitic activity. The phenyl pyrazolone derivatives **80a–an** showed considerable toxicity against HL60 cells, the best inhibitor **80ag** had a selectivity index of >8 for *T. brucei*, while showing no toxicity against HL60 cells at 100 μ M. The introduction of a 3-benzoic acid motif in position 1 resulted in improved selectivity for compound **81a** compared to its phenyl pyrazole analogue **80e**.

6.5 Summary

33 pyrazolone derivatives have been synthesised and evaluated against *T. brucei*, *T. cruzi* and *L. infantum* in a whole cell activity assay.

24 out of 33 derivatives were able to kill *T. brucei* at 100 μ M (MIC 100 μ M).

10 of the 24 active inhibitors against *T. brucei* growth also showed anti-trypanosomal effects against *T. cruzi* at 100 μ M (MIC 100 μ M).

None of the derivatives showed any effect on *L. infantum* growth at 100 μ M.

The whole cell activity screen was able to identify anti-trypanosomal inhibitors with good activity against *T. brucei* and *T. cruzi* (GI₅₀ 11.7-64.8 μ M, SI 2 - >9).

The meta-benzyloxy modified pyrazolone showed promising anti-trypanosomal activity (GI₅₀ 13.6-14.2 μ M), possibly indicating GPI-anchor biosynthesis inhibition, as all other meta-benzyloxy modified analogues in this thesis showed activity against enzymes in the GPI-anchor biosynthesis. But also increased toxicity against HL60 was observed (SI 2).

Scaffold replacement from a rhodanine to a pyrazolone moiety resulted in a loss of anti-parasitic activity. However, the toxicity in pyrazolone derivatives is also reduced.

In particular the N-1 substituent influenced anti-trypanosomal activity and less lipophilic substituents like aliphatic carboxylic acid might be a good starting point for improvement of anti-parasitic activity.

7 Iron chelating agents - hydroxypyridinones

7.1 Introduction

Iron is an ubiquitous element for growth in all living organisms, as such it is also essential for growth of *T. brucei*, *T. cruzi* and *L. infantum*.^[61–63] Iron, due to its redox properties and high affinity for oxygen, plays an important role in numerous biological processes.^[124] Consequently, iron chelation has been suggested as a potential strategy to combat infectious diseases.^[126]

The bacterial siderophore Deferoxamine (Figure 73) is a hexa-dentate iron-chelator with weak anti-parasitic activity.^[61–63] *T. brucei*, *T. cruzi* and *L. infantum* have been shown to have a high sensitivity for the iron chelator Deferoxamine, resulting in reduced parasitemia at concentration which did not interfere with the host iron metabolism.^[61–63] Deferoxamine has been studied in mouse models of visceral Leishmaniasis and acute and chronic Chagas disease, causing a reduction in parasite burden but no cure was observed.^[63] However, the clinical application of Deferoxamine is compromised due to its poor oral availability.^[252]

A more promising iron chelator is the orally available Deferiprone (Figure 73).^[253]

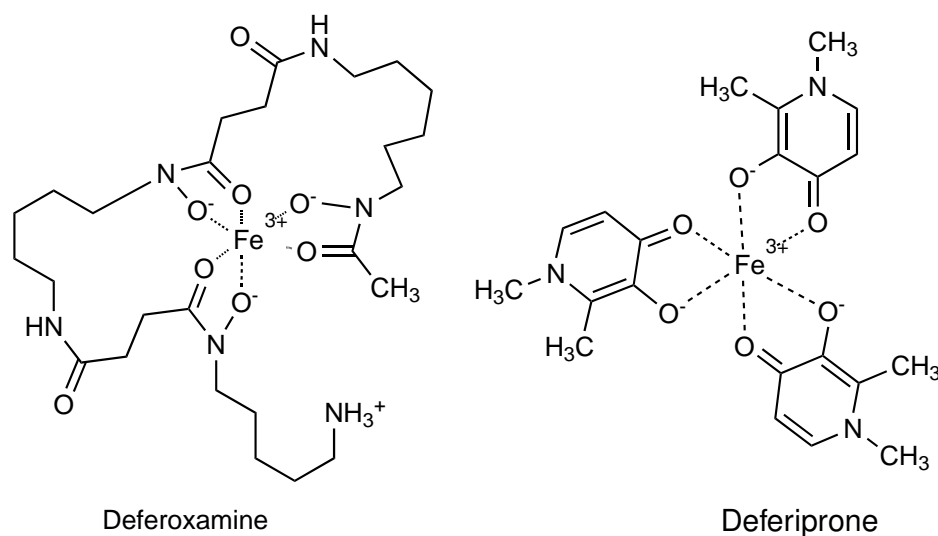


Figure 73: Iron chelators and their Fe(III)-complexes.

Deferiprone belongs to the class of hydroxypyridin-4-one and has a high affinity for Fe(III). Hydroxypyridin-4-one derivatives form a neutral 3:1 complex with Fe(III), where each hydroxypyridin-4-one is bi-dentate bound to Fe(III) (Figure 73).^[253] Deferiprone comprises a lower molecular weight of 139.15 g/mol than Deferoxamine (560.68 g/mol) and therefore might have a higher diffusion rate through cellular plasma membranes.^[253]

Deferiprone and similar hydroxypyridin-4-one (HPO) derivatives have previously been assessed as anti-malarial agents against *P. falciparum*.^[130–132] In particular, the N-1 position has been modified and these derivatives were evaluated for their anti-plasmodial activity and toxicity to mice or mammalian cells (K-562 cells).^[130–132] Several aliphatic and carboxylic acid functionalities have been introduced in position N-1, but all derivatives showed only moderate activities (IC₅₀ 53–650 μ M) against *P. falciparum*.^[131,132] However, anti-plasmodial activity of these derivatives correlated well with their lipophilicity, as increasing chain-lengths improved activity.^[132] However, all derivatives showed also a significant toxicity against mammalian cells.^[131,132]

Acidocalcisomes are important cellular storage compartments for essential elements like Ca(II), Fe(III) and Zn(II), as the free elements could cause the formation of radical species, thus killing *T. brucei*, *T. cruzi* and *L. infantum*.^[126,254] The 8-amino-quinoline Sitamaquine (Figure 5, p. 9), currently in clinical trials against visceral Leishmaniasis has been shown to accumulate within acidocalcisomes, although it has been shown not to be associated with its anti-leishmanial activity (Chapter 1).^[46] Molecules, which accumulate within acidocalcisomes are consequently of particular interest, as combined with the ability to chelate iron, would deprive these parasite from essential iron for its metabolic processes, leading to disruption of signal transduction and gene regulation.^[254] Chloroquine (Figure 74), the parent analogue of Sitamaquine, has previously been shown to accumulate in acidic compartments of procyclic trypomastigotes of *T. brucei* and consequently inhibited the uptake of essential lipids for growth.^[255] But the role of chloroquine is even more ubiquitous, as it is taken up into acidic acidocalcisomes of *Leishmania donovani* promastigotes, causing alkalinisation thereof and resulting in parasite death.^[256]

This encouraging observation led to the synthesis of chloroquine (CQ) conjugated HPO molecules, designed to accumulate within the acidocalcisome of protozoa. Here, a 4-amino-quinoline ring system was conjugated over the N-1 position to the HPO core (Figure 74). These CQ-HPO conjugates were designed to possess pK_a values which allow accumulation of the lysosomotropic chloroquine moiety into acidic compartments in parasites.^[255,256] All basic HPO-CQ derivatives possess three pK_a values. Where, pK_{a1} corresponds to the protonation of the 4-oxo group, pK_{a2} to the deprotonation of the nitrogen in the quinoline ring and pK_{a3} to the dissociation of the proton from the 3-hydroxyl group (Figure 75).^[257–259] The pK_a values have been estimated to be pK_{a1} 3 and pK_{a3} 10 based on similar substituted HPO derivatives.^[259] The pK_{a3} value was estimated based on the substituent in position 7 in CQ derivatives.^[258] Electron-withdrawing substituents such as chlorine (X=Cl) lower pK_{a3} to 7.6 (compared to the unsubstituted analogue (X=H) pK_{a3} 8.0).^[258] Under physiological pH (pH 7.4), the major species of the CQ-HPO conjugate exists in the neutral form **91c**, facilitating membrane diffusion. The pH in the acidic compartments in *T. brucei* is estimated to be between pH 4.6 -

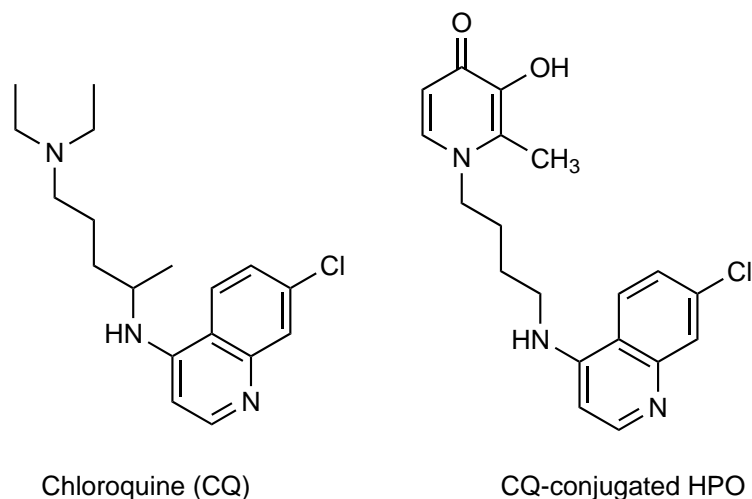


Figure 74: Conjugation strategy towards improved anti-parasitic HPO derivatives.

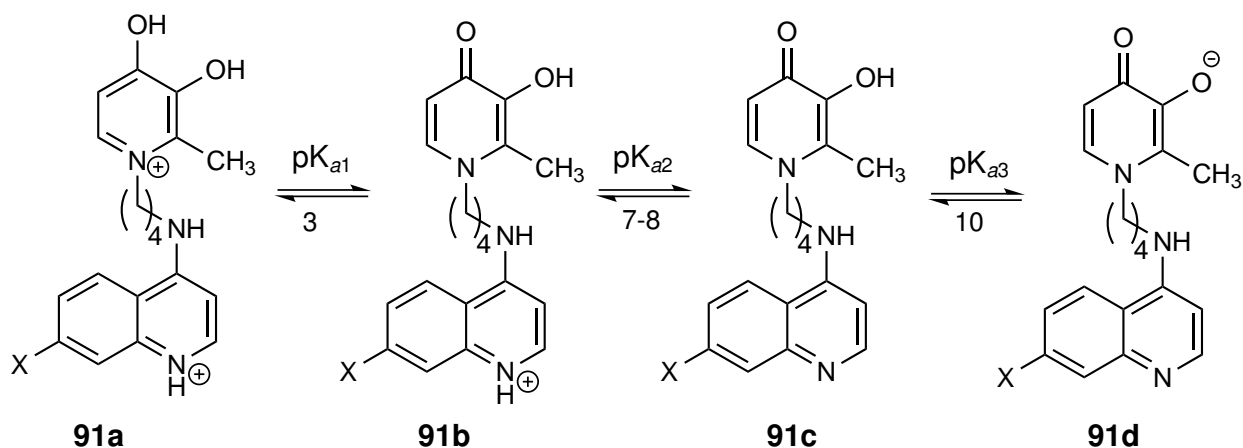


Figure 75: HPO-CQ at different pH values; X=Cl or H

5.6.^[255], favouring the protonation state of **91b** and therefore trapping the charged analogue within these acidic compartments.

In order to evaluate HPO derivatives against *T. brucei*, *T. cruzi* and *L. infantum*, modifications on the N-1 substituent were studied. Of particular interest were N-1 substituents with a CQ-like moiety, designed to accumulate within acidic compartments in parasites, possibly showing diminished toxicity towards mammalian cells.

Similar chloroquine conjugation strategies have previously been studied as anti-parasitic agents against Malaria, Leishmaniasis, and Trypanosomiasis.^[260] However, the previous chloroquine moieties were conjugated to an organo-metallic functionality, there a synergistic effect of lipophilicity and basicity from the CQ-moiety and toxicity from the organometallic complex led to low μM *in vitro* activity (IC_{50} 0.9-10.3 μM).^[260]

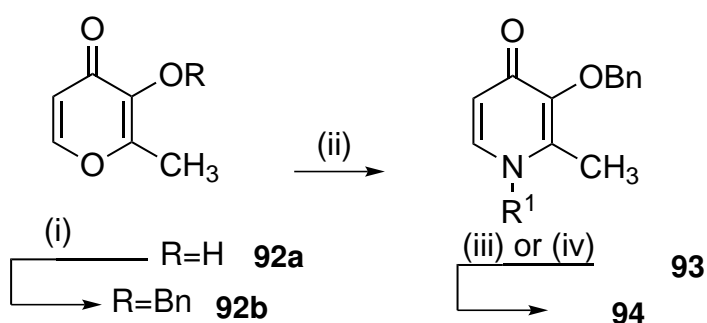
The activity of the CQ-HPO conjugates in this study was evaluated against a broad range of protozoa, including *T. brucei*, *T. cruzi*, *L. infantum* and their mode-of-action was analysed.

7.2 Synthesis of iron chelating agents

7.2.1 Previous synthesis of HPO iron chelators

This section describes the general synthetic strategy towards simple N-1 alkyl substituted HPO iron chelators as reported in the literature.^[261] This synthetic strategy is explained in detail because the synthesis of novel HPO-CQ conjugates followed a similar strategy.

Simple N-1-substituted HPO derivatives have previously been synthesised starting from maltol **92a**.^[261] In the first step, the hydroxy-group in maltol was protected as its benzyl ether (Scheme 52, (i)). Therefore maltol was subjected to benzyl bromide in the presence of NaOH (90 % in water).^[261] Subsequently, the benzyl protected maltol **92b** was conjugated to various primary amines under base-catalysed double Michael addition reaction conditions (Scheme 52, (ii)).^[261] In the final step of the reaction sequence the benzyl protection group of the double Michael addition product **93** was cleaved under acidic hydrolysis or catalytic hydrogenation to afford the final HPO iron chelator **94** (Scheme 52, (iii)).^[261] Simple N-1 alkyl substituted HPO derivatives were provided by Prof. Robert Hider (KCL, London, UK).

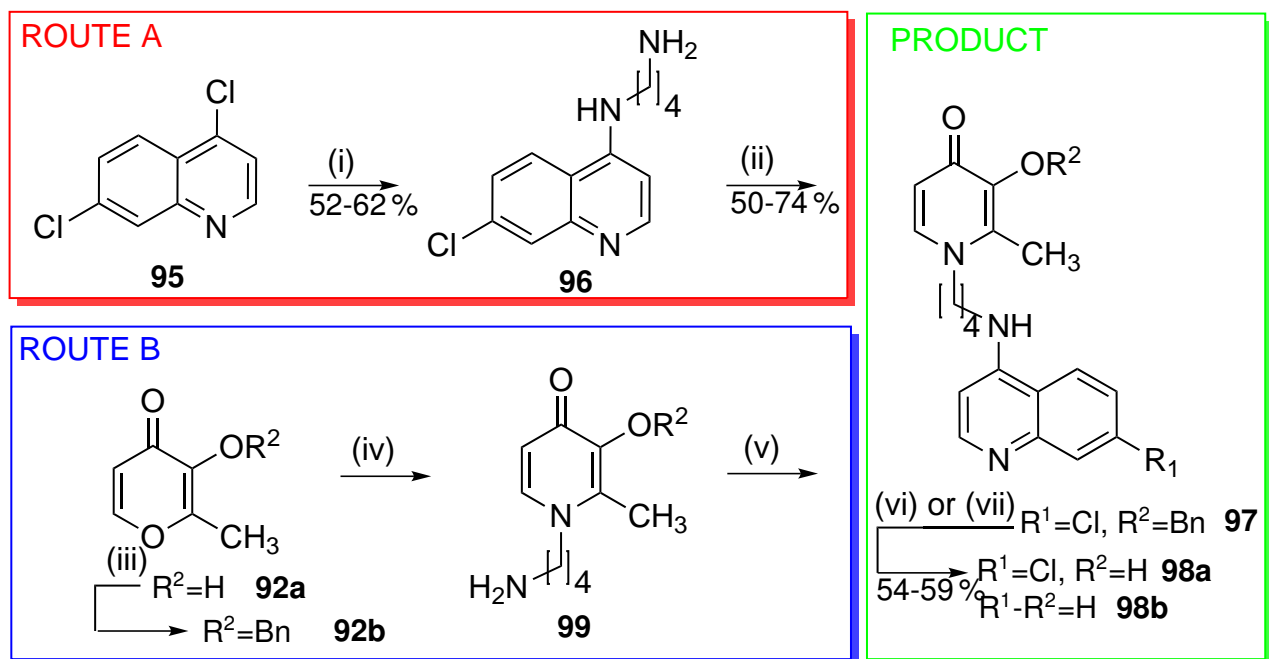


Scheme 52: Synthesis of simple N-1-substituted HPO derivatives as reported in the literature; R^1 =alkyl; (i) NaOH, MeOH (90 % in water), 100 °C; (ii) NaOH, pH 12, EtOH (50 % aqueous solution), 100 °C; (iii) HCl (6 N), 100 °C; (iv) Pd/C, H_2 , EtOH (aq, pH 1).

7.2.2 Synthesis of CQ-HPO conjugated derivatives

The novel CQ-HPO conjugated iron chelators were synthesised analogously to previously reported N-1-modifications of HPO derivatives.^[261] The key step of the synthesis was a double Michael addition reaction between various amines and the benzyl protected maltol **92b**. Two routes have been pursued for the synthesis of the CQ-HPO conjugates.

In the first route (Route A, Scheme 53), the amino linker was installed onto the chloroquinone fragment **95** prior to double Michael addition to **92b**. 4,7-Dichloroquinoline **95** was reacted with excess diaminobutane in neat solution at 160-180 °C (Scheme 53, (i)). The desired amino-quinoline **96** was afforded after re-crystallisation from methanol and diethyl ether as white crystals in good yields of 62 %. Alternatively, the amino-quinoline could be obtained after column chromatography of the crude reaction mixture, although the excess of 1,4-diaminobutane decreased the yield to 52 %.



Scheme 53: Synthesis of CQ-HPO conjugate derivatives; Reagents and conditions: (i) 1,4-diaminobutane (5 equiv.), 160-180 °C, 18h; (ii) **92b**, 2 N NaOH, pH 13, aqueous EtOH (25 %), reflux, 12h; (iii) NaOH (1.1 eq.), BnBr (1.1 eq.), aq. MeOH (50 %), reflux, 6h; (iv) 1,4-diaminobutane (1 equiv.), 10 N NaOH, pH 13, reflux, 18h; (v) **95**, (1 equiv.), DMSO, 100-110 °C, 12h; (vi) 6N HCl, reflux, 2h; (vii) 5% Pd/C, H₂, ethanol, aq. HCl.

The amino-quinoline **96** was subjected to double Michael addition reaction with the benzyl protected maltol **92b** (Scheme 53, (ii)). The reaction was carried out in aqueous ethanol (25 % H₂O) in the presence of catalytic amounts of NaOH. The base-catalysed double Michael addition reaction was pH sensitive. Therefore it was crucial to adjust the pH to 13 in order to improve the yield of reaction to 74 %. In the final step of the reaction towards the novel HPO-CQ conjugates, the precursor **97** was debenzylated under acidic hydrolysis in 6 N HCl_(aq) (Scheme 53, (vi)). The desired CQ-HPO conjugated iron chelator **98a** (R¹=Cl, R²=H) was afforded as its chloride salt, which was filtered, washed with acetone and recrystallised to

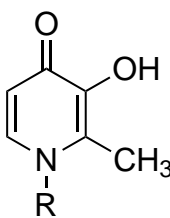
obtain the product **98a** in good yields of 54-59 %.

Alternatively, the double Michael addition can be executed prior to linking the amino-residue to the quinoline moiety (Route B, Scheme 53). Initially, maltol was protected with benzyl bromide in aqueous methanol ((v/v), 50 %) to yield **92b** in good yields of 81 % (Scheme 53, (iii)). **92b** was subjected to 1,4-diaminobutane to give access to the double Michael addition product **99** in good yields of 50 % (Scheme 53, (iv)). The amino-HPO **99** was conjugated to the quinoline moiety by nucleophilic substitution with 4,7-dichloroquinoline (Scheme 53, (v)). This alternative access to **97** gave a lower yield of only 20 % compared to Route A. The final deprotection of the benzyl group was achieved through catalytic hydrogenation (Scheme 53, (vii)), which also cleaved the 7-chloro substituent on the quinoline moiety. The desired iron chelator product ($R^1-R^2=H$) **98b** was obtained in quantitative yields after deprotection.¹⁴

In order to compare the activity of the novel CQ-HPO conjugates to previous simple N-alkyl modified analogues, several iron chelators have been kindly donated by Prof. Robert Hider (King's College London, London, UK) (Table 68). Simple N-alkyl HPO derivatives are synthesised under the same double Michael addition reaction between benzyl-protected maltol **92b** and various primary amines.^[261]

Table 68: Simple N-Alkyl HPO derivatives provided by Prof. Robert Hider (King's College London, London, UK).

(a)



(b)

#	R
101a	CH ₃
101b	(CH ₂) ₇ CH ₃
101c	(CH ₂) ₉ CH ₃
101d	(CH ₂) ₂ NH ₂

7.3 Anti-parasitic activity

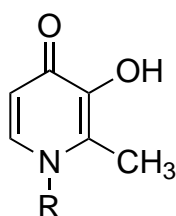
The iron-chelators were screened against *T. brucei*, *T. cruzi* trypomastigotes and *L. infantum* promastigotes using the activity assays described previously in chapter 3.3.1.

¹⁴The final iron chelating agent **100a** was synthesised by Karin Pleban and the synthesis described in this alternative approach was only carried out until the protected analogue **97** (Prof. Hider group, KCL, London, UK)

7.3.1 Anti-parasitic activity of simple aliphatic N-1-substitution of the HPO moiety

The simplest iron chelator **101a**, also known as Deferiprone, was substituted with a methyl group in N-1 position of the HPO core. **101a** did not display any anti-parasitic activity at 100 μM . However, substituting the N-1 aliphatic side chain to a octanyl (**101b**) or decanyl (**101c**) aliphatic substituent not only increased lipophilicity, but also cytotoxicity. The iron-chelators **101b** and **101c** displayed anti-parasitic activity against *T. brucei*, *T. cruzi* and *L. infantum* (GI_{50} 0.7-3.7 μM), but were also toxic against HL60 cells (GI_{50} 6.3-13.4 μM). Although, these HPO derivatives displayed general cytotoxicity against both parasitic and mammalian cells, they may possess great potential, if selectivity of these derivatives towards parasites could be improved.

Table 69: Anti-parasitic activity of simple N-alkyl modified HPO derivatives.



#	R	GI_{50} [μM]				
		<i>T. brucei</i>	SI <i>T. brucei</i>	<i>T. cruzi</i>	<i>L. infantum</i>	HL60
101c	$(\text{CH}_2)_9\text{CH}_3$	1.4 ± 0.1	5	0.9 ± 0.1	0.7 ± 0.1	6.3 ± 0.2
101b	$(\text{CH}_2)_7\text{CH}_3$	3.7 ± 0.2	4	3.0 ± 0.3	3.2 ± 0.4	13.4 ± 2.6
101a	CH_3	>100	>1	>100	>100	>100
101d	$(\text{CH}_2)_2\text{NH}_2$	>100	>1	>100	>100	>100

7.3.2 Improved selectivity through CQ conjugation strategy

Initially, the amino-quinoline precursor **96** was evaluated for its anti-parasitic activity. **96** displayed moderate activity against *T. brucei*, *T. cruzi* and *L. infantum* while showing no toxicity against HL60 cells 100 μM (Table 70). Conjugation of **96** with HPO improved anti-parasitic activity in *T. brucei* and *T. cruzi*, resulting in low μM inhibitors (GI_{50} 3.6-27.1 μM) compared to CQ activity alone. However in *L. infantum* the CQ-conjugation resulted in a decreased activity for **98a**. Removal of the 7-chloro substituent on the quinoline moiety in compound **98b** resulted in complete loss of activity in *L. infantum* and *T. cruzi* at 100 μM . Interestingly, anti-parasitic activity against *T. brucei* was retained at GI_{50} 7.6 μM .

Although **98b** is more basic than **98a**, as can be concluded by the substitution in position 7 in the quinoline ring, it was less active against *T. brucei*, *T. cruzi* and *L. infantum*.^[258] In-

deed, the pK_a values of **98b** and **98a** have been experimentally determined to be 7.90 and 7.77 respectively.¹⁵ Therefore, the fraction of membrane permeable CQ-HPO conjugates (unprotonated) is relatively small according to the Henderson-Hasselbalch equation (**98a**: 30%, **98b**: 24%) at physiological pH (7.4). Although the membrane-permeable fractions were relatively small, they were still 3 times better than for chloroquine itself (pK_a :8.5, 7.4%) at pH 7.4. However, optimisation of the quinoline pK_a could potentially improve anti-parasitic activity in this series. For example substitution of the 7-chloro to a nitro group would make these derivatives more acidic (pK_a 6.28)^[258], therefore improving their membrane permeability.

However, the weak activity of **98b** suggested other factors responsible for the weak anti-parasitic activity against *T. cruzi* and *L. infantum*.

Table 70: CQ-conjugated iron chelator and their anti-parasitic activity.

98a and 98b

96

		GI ₅₀ [μM]				
#	R	<i>T. brucei</i>	SI <i>T. brucei</i>	<i>T. cruzi</i>	<i>L. infantum</i>	HL60
98a	Cl	3.6 ± 0.9	14	6.5 ± 0.1	27.1 ± 7.0	50.5 ± 0.9
98b	H	7.6 ± 0.4	>13	>100	>100	>100
96	n.a.	15.8 ± 1.3	>6	39.2 ± 4.1	42.4 ± 4.8	>100
CQ		14.5 ± 1.3	>6	12.8 ± 2.9	3.6 ± 0.1	>100

7.4 Target identification studies

7.4.1 Transferrin uptake in *T. brucei*

The CQ moiety in derivatives **98a** and **98b** have been designed to selectively accumulate within parasitic compartments, while the HPO fragment chelates essential Fe(III), causing iron starvation of the protozoa. In order to validate this mode-of-action, the effect of **98a** was

¹⁵Personal Communication with Prof. Hider, King's College London, 2012

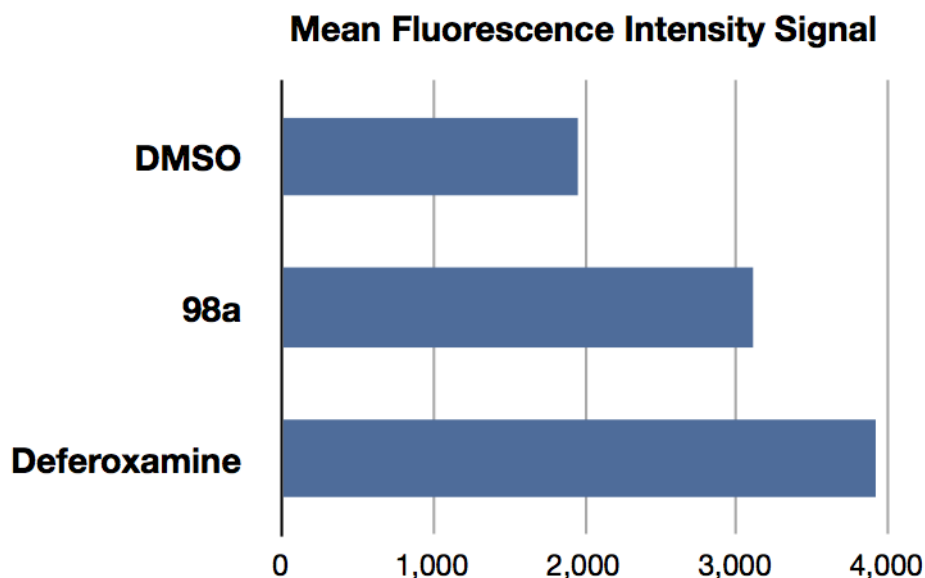


Figure 76: Mean Fluorescence Intensity of fluorescein labelled transferrin recorded by flow-cytometry using a DB Accuri C6 flow-cytometer.

studied in live trypanosomes. *T. brucei* is known to up-regulate transferrin receptor (*TbTfR*) expression if suffering from iron deprivation.^[212] Therefore, *TbTfR* can be used as an indicator for iron starvation in *T. brucei*.^[212] In order to quantify the uptake of transferrin, *T. brucei* was pre-incubated with the iron-chelator **98a** for 24 h. After this incubation time the parasites should have increased the number of *TbTf* receptors, if indeed suffering from iron starvation. Next, *T. brucei* was deprived from transferrin the main Fe(III) source by washing with transferrin-free Baltz-medium. Incubation with fluorescein-labelled transferrin allowed the quantification of transferrin-uptake by measuring of the mean fluorescence intensity with flow-cytometry (Figure 76). Iron starvation by the known iron chelator Deferoxamine resulted in an increase of transferrin uptake by a factor of 2 as compared to treatment with DMSO only. The uptake of fluorescence labelled transferrin for **98a** was increased by a factor of 1.6, suggesting iron starvation as possible contributor to trypanocidal activity of CQ-HPO conjugates in *T. brucei*.

7.4.2 Fe(III) saturation experiments

Measuring the uptake of fluorescence labelled transferrin after pretreatment of the CQ-HPO conjugate **98a** suggested Fe(III) chelation at least in part as contributor to trypanocidal activity against *T. brucei*. In order to further support the hypothesis that iron chelation is the major mode-of-action of CQ-HPO conjugates *T. brucei* was treated with pre-saturated **98a** in FeCl₃ solution (1:3 ratio). Similar experiments have been carried out for confirming iron chelation in Deferoxamine as major contributor to anti-trypanosomal activity.^[262] It was assumed,

that the CQ-HPO-Fe(III) complex would still be able to penetrate the parasitic membrane, as HPO-Fe(III) complexes do not have a formal charge and are known to cross through liposome membranes.^[253] Saturation of the CQ-HPO iron chelator with FeCl₃ solution resulted in a complete loss of trypanocidal activity against *T. brucei* consistent with the hypothesis that iron chelation is the major mode-of-action of CQ-HPO conjugates **98a** and **98b**. The excess Fe(III) ions most likely scavenge all the free iron chelator, leaving enough iron for parasite survival.

7.5 Discussion

Iron chelation is a good strategy for the development of novel anti-parasitic agents. Simple N-1 alkyl substituted HPO derivatives **101a–d** are generally cytotoxic against parasites and mammalian cells. In contrast, the CQ-HPO show selectivity against parasitic protozoa, while being only moderate toxic against HL60 cells. The activity of the CQ-HPO **98a** against *T. brucei* and *T. cruzi* is improved compared to the parent Deferiprone **101a** and CQ alone, thus suggesting a synergistic effect between the HPO and CQ fragments. Flow-cytometry experiments suggested iron-chelation was at least in part responsible for anti-trypanosomal activity of the CQ-HPO conjugate **98a**. Furthermore, saturation of the iron chelator **98a** with FeCl₃ resulted in a complete loss of trypanocidal activity, supporting the theory of iron chelation as mode-of-action. The novel CQ-HPO conjugates are promising leads for the development of more potent anti-parasitic agents. Changing the acidity of the quinone nitrogen might further improve membrane permeability of these derivatives and therefore increase anti-parasitic activity. Substitution of the quinoline nitrogen could result in a smaller percentage of the protonated iron-chelator conjugate and therefore could facilitate diffusion through the plasma membrane. A further experiment would be the localisation of the drug target within the parasites. Due to the basic pH of the HPO-CQ conjugated iron chelators, accumulations within acidic compartments such as acidocalcisome are possible. In order to confirm the accumulation of the HPO-CQ iron chelators a ligand displacement assay could be performed. Previously, the fluorescent probe LysoTracker Green, which accumulates in acidic organelles in live cells, was shown to be displaced by the chloroquine analogue Sitamaquine by alkalylation of this compartment in *Leishmania*.^[46] A similar experiment could be performed with the HPO-CQ iron chelators in this study, as the pH of this derivatives should be basic enough to displace LysoTracker Green, if accumulated within the acidocalcisome of *T. brucei*, *T. cruzi* or *L. infantum*. However, even without knowing the exact compartment of accumulation, the experiments in this study have shown, that iron chelation is a possible major contributor to the anti-parasitic activity.

7.6 Summary

1 iron HPO-CQ conjugated iron chelator (**102a**) has been synthesised.

8 derivatives have been assessed in a whole cell activity assay for anti-parasitic activity against *T. brucei*, *T. cruzi* and *L. infantum*.

Simple N-alkyl substituted HPO iron chelators showed low μM activity against all three protozoa (GI_{50} 0.7-3.7 μM , SI 4-9), but also high toxicity against HL60 cells.

The HPO-CQ conjugated iron chelator **98a** ($\text{R}^7=\text{Cl}$) retained low μM activity against *T. brucei*, *T. cruzi* and *L. infantum* (GI_{50} 3.6, 6.5 and 27.1 μM , SI 14, 8, 2 respectively), but displayed improved selectivity.

The replacement of the chloro-substituent in position 7 of the quinone moiety in the HPO-CQ iron chelator ($\text{R}^7=\text{H}$) abolished activity against *T. cruzi* and *L. infantum*, while activity against *T. brucei* was reduced by a factor of 2 (GI_{50} 7.6 μM , SI 13).

Mode-of-action studies with the HPO-CQ iron chelator **98a**, using flow- cytometry have shown an upregulation of *TbTf* receptors, indicating iron starvation as major course of anti-trypanosomal activity in *T. brucei*.^[212] Further iron saturation studies abolished anti-trypanosomal activity *in vitro*, thus supporting iron chelation as a possible mode-of-action.

8 Conclusion and outlook

The aim of this research study was to identify small molecular inhibitors with anti-parasitic activity against *T. brucei*, *T. cruzi* and *L. infantum*. Therefore whole cell phenotypic screening assays were performed to identify and optimise promising candidates, leading to low μM active inhibitors with good selectivity. Particular interesting targets studied in this thesis were GPI-anchor biosynthesis and iron chelation therapy.

The development of anti-parasitic agents against enzymes involved in GPI-anchor biosynthesis started with a lead structure (Figure 77), known to be a good inhibitor of DPMS in *T. brucei*.^[68] Although rhodanine-N-acetic acid derivatives were identified as small molecular inhibitors able to inhibit DPMS in *T. brucei*, the *in vitro* trypanocidal effect was negligible (ED_{50} 96 μM), compared to for example melarsoprol (1.7 nM). Therefore several modifications on this molecular scaffold were performed and their anti-parasitic activity was assessed in whole parasite activity assays against *T. brucei*, *T. cruzi* and *L. infantum*.

Analysis of the 379 thiazolidine-4-one and related pyrazole-5-one derivatives revealed a trend between the anti-trypanosomal activity and the N-3 substitution (Figure 77). Therefore derivatives carrying a N-carboxylic acid/ester or a N-allyl functional group showed low μM activity, whereas N-unsubstituted, N-amino or N-phenyl-substitution resulted in moderate activities against parasites. Scaffold replacement with a pyrazole-5-one moiety resulted in moderate inhibition of parasitic growth. However, there were some interesting exceptions from this general trend, such as a catechol or a benzylidene 3-benzyloxy motif in position 5 of the thiazolidine-4-one scaffold.

In the case of the catechol moiety, exactly the opposite trend was observed, where the catechol moiety was essential for low μM activity, while the thiazolidine-4-one moiety had a secondary role. Careful analysis of the logP values of all catechol derivatives elucidated a trend to the trypanocidal activity (Table 71), where an increased logP resulted in low- μM activity.

Compound **55o** was particularly interesting as it has previously been identified as nM inhibitor of enoyl acyl carrier protein reductase (IC_{50} 35.6 nM), an essential enzyme in the fatty acid synthesis II pathway, with *in vitro* activity against *P. falciparum* (IC_{50} 0.75 μM).^[263] However, *T. brucei*, *T. cruzi* and *L. infantum* do not have a fatty acid synthesis II pathway, instead these parasites salvage lipids from their hosts through an elongase (ELO) pathway.^[264] Elongation of fatty acids in these parasites involves the action of two flavin-cofactor dependant reductases (β -Ketoacyl-CoA reductase and Trans-2-enoyl-CoA reductase).^[264] Catechol rhodanine derivatives, previously been shown to mimic the NAD(P)H cofactor substrate and therefore described as a "privileged scaffold for dehydrogenases",^[107,108,265] would be potential inhibitors of the reductases in the ELO pathway. *T. brucei* is particularly dependant on *de novo* synthesis of myristate for the incorporation of the protective GPI-anchored VSG-proteins, which are essential for survival of the bloodstream form of *T. brucei*.^[64,264] Also *T. cruzi* and *L. infantum* are dependant on an ELO pathway to express lipid-functionalized proteins, responsible for virulence, on their plasma membrane.^[264] A possible strategy to monitor inhibition of the ELO-pathway as mode-of-action in living parasites would be the measurement of *de novo* synthesised myristate. This can potentially indirectly be achieved by the incubation of *T. brucei* in myristate-free media, inducing *de novo* synthesis of myristate for GPI-anchored VSG protein incorporation. One such GPI-anchored protein is the transferrin receptor of *T. brucei*, responsible for iron uptake via host-transferrin. The amount of uptake of FITC-labelled transferrin would be a measure for successful myristate incorporation in the GPI-anchored *TbTf* receptor. Inhibitors of the ELO-pathway would reduce the *de novo* synthesis of myristate and consequently lead to a reduction of GPI-anchored *TbTf* receptors, reducing the uptake of FITC-labelled transferrin. This could potentially be quantified by flow-cytometry analysis. This experiment would be analogous to the previously described experiments with DPMS and/or MT-1 inhibitors (Chapter 3.5.2).

Alternatively, an in-gel-affinity approach as described in Chapter 3.6 could be pursued. There the fluorescent catechol rhodanine-N-acetic acid **2u** could be applied to a western blot gel, washed and the remaining **2u** could be visualised via fluorescence. But this is not the only possible target for this kind of catechol derivative. Recently, catechol modified rhodanine derivatives have been studied as tyrosyl-DNA phosphodiesterase I inhibitors with μM activity (IC_{50} 2.6 μM).^[122] Interestingly Furamidine, the active reagent of the prodrug DB-289 (recently in clinical phase III against HAT until development was discontinued due to liver and

Table 71: Importance of catechol-modified inhibitors on antitrypanosomal activity.

#	R	logP	GI ₅₀ [μM]			
			<i>T. brucei</i>	<i>T. cruzi</i>	<i>L. infantum</i>	HL60
35c		4.13	1.4 ± 0.1	>100	>100	n.a.
35g		4.08	5.7 ± 0.1	>100	20.7 ± 7.4	n.a.
55o		4.01	4.7 ± 0.9	n.a.	>100	n.a.
35h		3.12	5.6 ± 0.8	n.a.	>100	n.a.
40t		3.09	1.2 ± 0.1	n.a.	>100	>100
80ak		2.97	17.3 ± 0.1	n.a.	n.a.	>100
35i		2.96	11.0 ± 0.6	>100	>100	n.a.
35j		2.89	4.6 ± 0.8	>100	>100	n.a.
16i		2.86	1.35 ± 0.3	n.a.	54.6 ± 0.4	29.0 ± 4.2
35k		2.83	5.2 ± 0.1	>100	>100	n.a.
15f		2.57	0.9 ± 0.1	n.a.	45.9 ± 15.1	31.2 ± 2.8
14t		2.34	1.6 ± 0.1	n.a.	n.a.	>100
70c		2.25	18.2	>100	>100	>100
41i		2.20	5.0 ± 0.6	n.a.	>100	83.4 ± 0.3
69j		2.18	>100	>100	>100	>100
36a		2.13	13.3 ± 1.1	>100	>100	45.0 ± 9.3
12m		2.07	14.2 ± 2.3	>100	>100	>100
14s		1.98	10.1 ± 1.6	>100	>100	23.6 ± 1.1
54t		1.84	17.5 ± 0.2	n.a.	>100	82.8 ± 10.1
2u		1.83	>100	>100	>100	
7k		1.45	1.4 ± 0.2	>100	>100	>100
48p		1.24	>100	n.a.	n.a.	>100
35a		1.03	17.7 ± 0.1	>100	>100	n.a.

35a–k were provided by Prof. Dr. Schlitzer, Germany.

renal-toxicity^[28,29]), has been shown to be an inhibitor for tyrosyl-DNA phosphodiesterase I in humans and therefore have potential as anti-cancer therapy.^[266]

These results imply that catechol modified rhodanine derivatives could potentially have a similar mode-of-action to those previously described for Pentamidine analogues. If this hypothesis is correct, then this would be significant, as Pentamidine analogues suffer from drug-resistance through loss of the P2 transporter in trypanosomes, which is essential for drug-uptake of Pentamidine and Melarsoprol.^[32] The diverse chemical scaffold of the catechol rhodanine could suggest a different drug transporter mechanism, possibly counter-acting resistance in *T. brucei*. Pentamidine analogues are not only excellent anti-trypanosomal agents, but are ideal to study drug accumulation through their fluorescent properties.^[267] Also the catechol rhodanine-N-acetic acid derivative **2u** has been identified as weak fluorophore,^[108] and depending on the possible accumulation of this fluorophore in cellular compartments of *T. brucei*, flow cytometry could be used to quantify the uptake in live trypanosomes and fluorescence microscopy might be used to localise these cellular compartments. A localisation close to the kinetoplast or nucleus would suggest a mode-of-action similar to Furamidine.^[267] Besides these possible advantages, catechol rhodanine derivatives are potentially also toxic to humans, as a study has shown that the catechol-rhodanine scaffold bound to many NAD(P)H dependant liver-proteins.^[265] But studies on catechol derivatives, described in this thesis showed that toxicity against HL60 cells depended on the type of rhodanine-scaffold used and in particular on the N-3 substitution of the rhodanine-moiety, implying that these inhibitors could be designed to be parasite specific. At this point no conclusion about the molecular target of catechol modified analogues can be drawn, but this compound class is very interesting for its anti-trypanosomal activity and high selectivity (Table 71).

In the case of the benzylidene-3-benzyloxy substituent, activity against parasites was observed to be similar to the catechol moiety. The benzylidene-3-benzyloxy modification resulted in low μM activity against *T. brucei*, independent from N-3-substitution of thiazolidine-4-one scaffold. Interestingly, scaffold replacement with a pyrazole-5-one moiety still resulted in good anti-trypanosomal activity (GI_{50} 13.6 and 13.7 μM). Furthermore, the benzylidene-3-benzyloxy rhodanine, N-allyl rhodanine and N-acetic acid rhodanine, have been shown in a radio-active HPTLC GPI-synthesis assay to inhibit the first mannosyltransferase and/or DPMS. Comparing the substrate band intensities of these HPTLC plates showed that the rhodanine-N-acetic acid derivative (GI_{50} 1.7 μM) was the most active inhibitor of DPMS and/ or MT-1, then the rhodanine-N-allyl (GI_{50} 14.9 μM), followed by the rhodanine derivative (GI_{50} 13.1 (*T. brucei*) and 12.4 μM (*T. cruzi*)). Metabolic labelling with myristate analogues revealed that the 3-benzyloxy rhodanine-N-acetic ester and the rhodanine-N-allyl rhodanine derivative inhibited incorporation of myristate in the GPI-VSG-proteins. With the aid of flow cytometry and FITC-labelling this inhibition could be quantified by a 1.6 and 2.7 fold reduction of transferrin uptake

respectively. However, the reduction with the rhodanine-N-acetic ester analogue is more significant, as could be seen in reduced FITC accumulations under the fluorescence microscope and using the metabolic labelling approach, resulting in a total abolishment of the myristate-VSG-proteins at 50 kDa. The rhodanine-N-acetic ester derivative showed trypanocidal activity at the chosen inhibitory concentration, resulting in reduced cell numbers and consequently an higher average of fluorescence signal, as fluorophore could accumulate within lysed cell compartments (see FM pictures Figure 41 and Figure 59). In an attempt to identify the molecular target, a homology model of DPMS was used to design a photo-affinity probe to identify the molecular target and potentially to identify active side residues via mass spectrometry.

The most interesting rhodanine derivative identified in this study was the 3-methyl benzylidene rhodanine-N-acetic *tert*-butyl ester **14b**, as it showed low μM activity against *T. brucei*, *T. cruzi* and *L. infantum* (GI_{50} 1.6, 5.1 and 2.4 μM , SI 14, 5, 10). Detailed mode-of-action studies for this derivative have been performed. The rhodanine-N-acetic ester derivative **14a** showed about 50 % reduction of labelled myristate-GPI-proteins, whereas the rhodanine-N-allyl derivative **40x** showed only about 25 % reduction, conferring GPI-biosynthesis as molecular target in both cases. The quantified FITC-labelled transferrin uptake showed a reduction in uptake by a factor of 1.3 for the rhodanine-N-acetic ester, whereas the rhodanine-N-allyl derivative did not show any reduction, supporting the previous results from the metabolic labelling with myristate analogues that GPI-synthesis is inhibited. The cell-free GPI-synthesis assay showed that the rhodanine-N-acetic acid derivative **2m** was a strong inhibitor of the first mannosyltransferase and possibly DPMS. Interestingly, only the *tert*-butyl ester **14b** was active against *L. infantum*, while the corresponding ethyl ester **14a** did not show any anti-leishmanial activity at 100 μM . It may be possible that the bulky and lipophilic *tert*-butyl ester is necessary to pass through the parasite plasma membrane, as a comparison of anti-leishmanial activity and logP in this study has shown that high logP values resulted in low μM anti-leishmanial activity. In order to confirm this hypothesis, several more *tert*-butyl ester analogues would need to be synthesised and screened against *L. infantum*. Particularly interesting would be the synthesis of the *tert*-butyl ester of the benzylidene-3-benzyloxy rhodanine-N-acetic acid, as the free acid (or ethyl ester) has already been shown to inhibit the same molecular targets in the GPI-biosynthesis in *T. brucei* (metabolic labelling (Figure 35), flow cytometry (Figure 39) and radio-labelling of GPI-substrates (Table 25)).

Rhodanine-N-allyl derivatives have been shown not to inhibit enzymes of the GPI-anchor biosynthesis in *T. brucei* in a cell-free GPI-synthesis assay. Instead, the 3-pyridinyl N-allyl rhodanine derivative has been shown to undergo unspecific binding over its Michael acceptor system to glutathione. Using the Ellman's reagent, this binding could be quantified to a reactivity constant RC_{50} , where half of the Michael acceptor reacted with glutathione, at 552.2 μM after 50 min. Over longer time periods this reactivity could account for the low anti-

trypanosomal activity (GI_{50} 1.5 μ M). But Michael acceptor reactivity in previous studies with rhodanine and thiazolidine-2,4-dione derivatives described the Michael addition reaction as reversible.^[85,86] The mode-of-action is unknown to this point, but Michael acceptor reactivity alone seems unlikely, as selectivity against parasites compared to mammalian HL60 cells has been observed.

In conclusion, GPI-anchor biosynthesis is a good target for the development of anti-parasitic agents, although it seems to be difficult to identify inhibitors which are active against all three parasites. In particular the carboxylic ester thiazolidine-4-one derivatives have great potential for the development of more active inhibitors against parasite growth.

In the search for broad anti-parasitic agents against HAT, Chagas disease and Leishmaniasis, iron chelation was studied as potential therapy. In this research study, oral available iron chelators from the 4-Hydroxy-pyridinone (HPO) class were studied for their anti-parasitic activity against *T. brucei*, *T. cruzi* and *L. infantum*. The results were compared to the bacterial iron-chelator Deferoxamine and showed significant improvements in clearing parasitaemia *in vitro*, but increased toxicity against HL60 was also observed. In order to improve selectivity, the HPO moiety was conjugated to an amino-chloroquine moiety, similar to chloroquine, which is known to accumulate within acidic compartments like acidocalcisomes in *T. brucei*, *T. cruzi* and *L. infantum*.^[46,254,254–256] These acidocalcisomes are important storage compartments for Zn^{2+} , Ca^{2+} and Fe^{3+} ,^[254] making them attractive targets for iron-chelating agents. Indeed, the chloroquine conjugated HPO iron chelator **98a** showed low μ M activity against *T. brucei* and *T. cruzi* (GI_{50} 3.6 and 6.5 μ M, SI 14 and 8) and moderate activity against *L. infantum* (GI_{50} 27.1 μ M, SI 2). Interestingly, substitution of the 7-quinoline substituent from a chlorine to a hydrogen, abolished activity in *T. cruzi* and *L. infantum*, while anti-trypanosomal activity against *T. brucei* was retained at GI_{50} 7.6 μ M (SI >13). Studies on the mode-of-action in *T. brucei* showed that trypanosomal transferrin receptors (*TbTfR*) were over expressed if subjected to the iron chelator **98a**, suggesting that *T. brucei* was indeed deprived of iron.^[212] Saturation experiments with $FeCl_3$ abolished anti-trypanosomal activity. Although this could potentially just mean that the $Fe(III)$ -complex with the CQ-HPO conjugate prevent membrane diffusion, studies on similar HPO- $Fe(III)$ complexes have shown membrane diffusion capabilities,^[253] conferring iron starvation as potential major contributor to anti-trypanosomal effects.

9 Methods

9.1 Reagents, Materials and Equipment

All chemical reagents were purchased from commercial sources and were used as received, unless otherwise noted. Dry solvents were obtained commercially or dried under standard procedures. The reactions were carried out under normal atmosphere unless otherwise stated in the procedure. Aqueous solutions and aqueous reaction solutions were prepared from Milli-Q water. For analytical applications such as HPLC, solvents and reagents of analytical purity had been used. The compounds were purified by flash chromatography and characterized by ^1H -NMR, ^{13}C -NMR, ESI-MS, HRMS-MS and TLC. **Flash chromatography:** Columns were packed wet and the separation was carried out under 1 bar. **^1H , ^{13}C and ^{31}P -NMR:** Spectras were recorded at 298 K on a Varian VXR 400 S spectrometer at 400 MHz, a Bruker Avance DPX-300 at 300 MHz, a Bruker BioSpin at 400 MHz. Chemical shifts (δ) are reported in ppm and coupling constants (J) in Hz. The signals are calibrated on the residual signals of CD_3OD , DMSO-d_6 or CDCl_3 (4.87 (49.00), 2.50 (39.52), 7.26 (77.16) respectively). **High Resolution Electrospray Ionization Mass Spectrometry:** ESI-MS and HRMS-MS were performed on a LTQ Orbitrap XL or on a Finnigan MAT 900 XLT mass spectrometer at the EPSRC National Mass Spectrometry Service Centre, Swansea. **Thin Layer Chromatography (TLC):** TLC was performed on precoated aluminium plates (Silica Gel 60 F₂₅₄, Merck). Compounds were visualized by exposure to UV light (254/365 nm) or by staining with Ninhydrin/Molobdic acid/ KMnO_4 solution. **Analytical HPLC** was carried out on a PerkinElmer Series 200 machine equipped with a SupelcosilTM LC-18-T column (5 μm , 25 cm x 4.6 mm), a column oven (set to 35 °C), and a diode array detector. Compound purity was determined under the following conditions: 0-100 % MeOH over 60 mins (flow rate: 1 mL/min); detection wavelengths: 280 and 354 nm.

9.2 General Procedures for Synthesis of 5-Benzylidene rhodanine

N-acetic acid derivatives 2a–ai

Rhodanine N-acetic acid (1.0 eq), corresponding benzaldehyde (1.1-1.5 eq) and piperidine (1-2 drops) or sodium acetate (1.0 eq) were dissolved in ethanol or methanol. The reaction mixture was stirred at 80 °C for 2-16 h. Upon cooling a yellow to orange solid precipitated and was filtered and washed with ethanol or methanol.

[(5Z)-4-oxo-5-(phenylmethylidene)-2-sulfanylidene-1,3-thiazolidin-3-yl] acetic acid **2a**^[268]

Reaction time: 2 h; **Purification:** Filtration from methanol; **Yield:** 71 mg of yellow solid (0.25 mmol, 72 %); **^1H -NMR** (400 MHz, DMSO-d_6) δ = 4.75 (s, 2 H, CH_2), 7.51-7.60 (m, 3 H, 3xAr-

$\underline{\text{CH}}$), 7.65-7.71 (m, 2 H, 2xAr- $\underline{\text{CH}}$), 7.91 (s, 1 H, $\underline{\text{CH}}$), 13.47 (s(br), 1 H, COOH) ppm; $^{13}\text{C-NMR}$ (400 MHz, DMSO- d_6) δ = 45.1 ($\underline{\text{CH}_2}$), 121.9 (Ar- $\underline{\text{C}}$), 129.6 (Ar- $\underline{\text{CH}}$), 130.8 (Ar- $\underline{\text{CH}}$), 131.3 (Ar- $\underline{\text{CH}}$), 132.8 (Ar- $\underline{\text{C}}$), 134.0 ($\underline{\text{CH}}$), 166.4 ($\underline{\text{C=O}}$), 167.3 ($\underline{\text{COOH}}$), 193.3 ($\underline{\text{C=S}}$) ppm; **HPLC-Analysis (Method B)**: 93 %, R_t = 17.7 min.

[(5Z)-5-[4-(benzyloxy)phenyl]methylidene-4-oxo-2-sulfanylidene-1,3-thiazolidin-3-yl] acetic acid **2b**^[68]

Reaction time: 4 h; **Purification**: Filtration from methanol; **Yield**: 52 mg of yellow solid (0.13 mmol, 24 %); $^1\text{H-NMR}$ (400 MHz, DMSO- d_6) δ = 4.73 (s, 2 H, $\underline{\text{CH}_2}$), 5.21 (s, 2 H, $\underline{\text{CH}_2}$), 7.21 (d, 2 H, $^3J_{\text{H,H}}$ = 8.8 Hz, 3,5-Ar- $\underline{\text{CH}}$), 7.32-7.49 (m, 5 H, 5xAr- $\underline{\text{CH}}$), 7.65 (d, 2 H, $^3J_{\text{H,H}}$ = 8.8 Hz, 2,6-Ar- $\underline{\text{CH}}$), 7.86 (s, 1 H, $\underline{\text{CH}}$), 13.32 (s(br), 1 H, COOH) ppm; $^{13}\text{C-NMR}$ (400 MHz, DMSO- d_6) δ = 45.0 ($\underline{\text{CH}_2}$), 69.6 ($\underline{\text{CH}_2}$), 116.0 (3,5-Ar- $\underline{\text{CH}}$), 118.6 (Ar- $\underline{\text{C}}$), 125.6 (Ar- $\underline{\text{C}}$), 127.9 (Ar- $\underline{\text{CH}}$), 128.1 (Ar- $\underline{\text{CH}}$), 128.5 (Ar- $\underline{\text{CH}}$), 133.1 (2,6-Ar- $\underline{\text{CH}}$), 134.1 ($\underline{\text{CH}}$), 136.4 (Ar- $\underline{\text{C}}$), 162.3 ($\underline{\text{C=O}}$), 167.4 ($\underline{\text{COOH}}$), 193.1 ($\underline{\text{C=S}}$) ppm; **ESI-MS** m/z (%) = 384.0 [M-H]⁻ (100 %), 769.1 [2M-H]⁻ (73 %); **HPLC-Analysis (Method B)**: 93 %, R_t = 17.7 min.

[(5Z)-5-[3-(benzyloxy)phenyl]methylidene-4-oxo-2-sulfanylidene-1,3-thiazolidin-3-yl] acetic acid **2c**^[68]

Reaction time: 2 h; **Purification**: Filtration from ethanol; **Yield**: 311 mg of yellow solid (0.81 mmol, 82 %); $^1\text{H-NMR}$ (400 MHz, DMSO- d_6) δ = 4.73 (s, 2 H, $\underline{\text{CH}_2}$), 5.19 (s, 2 H, $\underline{\text{CH}_2}$), 7.20 (dd, 1 H, $^{3,4}J_{\text{H,H}}$ = 8.3, 2.5 Hz, 4-Ar- $\underline{\text{CH}}$), 7.23-7.26 (m, 1 H, 6-Ar- $\underline{\text{CH}}$), 7.28-7.30 (m, 1 H, 2-Ar- $\underline{\text{CH}}$), 7.32-7.37 (m, 1 H, Ar- $\underline{\text{CH}}$), 7.38-7.43 (m, 2 H, 2xAr- $\underline{\text{CH}}$), 7.46-7.52 (m, 2 H, 3xAr- $\underline{\text{CH}}$), 7.86 (s, 1 H,) 13.54 (s(br), 1 H, COOH) ppm; $^{13}\text{C-NMR}$ (400 MHz, DMSO- d_6) δ = 45.1 ($\underline{\text{CH}_2}$), 69.5 ($\underline{\text{CH}_2}$), 116.6 (2-Ar- $\underline{\text{CH}}$), 118.1 (4-Ar- $\underline{\text{CH}}$), 122.3 (Ar- $\underline{\text{C}}$), 123.0 (6-Ar- $\underline{\text{CH}}$), 127.8 (Ar- $\underline{\text{CH}}$), 128.0 (Ar- $\underline{\text{CH}}$), 128.5 (Ar- $\underline{\text{CH}}$), 130.7 (Ar- $\underline{\text{CH}}$), 133.8 (Ar- $\underline{\text{C}}$), 134.2 ($\underline{\text{CH}}$), 136.6 (Ar- $\underline{\text{C}}$), 158.8 (Ar- $\underline{\text{C}}$), 166.3 ($\underline{\text{C=O}}$), 167.3 ($\underline{\text{COOH}}$), 193.2 ($\underline{\text{C=S}}$) ppm; **ESI-MS** m/z (%) = 343.1 [M+H]⁺ (90 %), 365.0 [M+Na]⁺ (30 %), 702.1 [2M+NH_4]⁺ (100 %), 707.1 [2M+Na]⁺ (50 %), 1044.2 [3M+NH_4]⁺ (30 %), 1049.1 [3M+Na]⁺ (20 %); **HR-MS** m/z = 343.0573 [M+H]⁺ (calculated: 343.0569); **HPLC-Analysis (Method B)**: 100 %, R_t = 20.2 min.

[(5Z)-5-[3,4-bis(benzyloxy)phenyl]methylidene-4-oxo-2-sulfanylidene-1,3-thiazolidin-3-yl] acetic acid **2d**^[68]

Reaction time: 2 h; **Purification**: Filtration from methanol; **Yield**: 403 mg of yellow solid (0.70 mmol, 54 %); $^1\text{H-NMR}$ (400 MHz, DMSO- d_6) δ = 1.48-1.56 (m, 2 H, Piperidine- $\underline{\text{CH}_2}$), 1.57-1.66 (m, 4 H, Piperidine- $\underline{\text{CH}_2}$), 2.95 (t, 4 H, $^3J_{\text{H,H}}$ = 6.0 Hz, Piperidine- $\underline{\text{CH}_2}$), 4.57 (s, 2 H, $\underline{\text{CH}_2\text{COOH}}$), 5.22 (s, 2 H, $\underline{\text{CH}_2}$), 5.24 (s, 2 H, $\underline{\text{CH}_2}$), 7.22-7.49 (m, 13 H, 13xAr- $\underline{\text{CH}}$), 7.74 (s, 1 H, $\underline{\text{CH}}$), 9.06 (s(br), 1 H, NH) ppm; $^{13}\text{C-NMR}$ (400 MHz, DMSO- d_6) δ = 21.8 (Piperidine- $\underline{\text{CH}_2}$), 22.2 (2xPiperidine- $\underline{\text{CH}_2}$), 43.5 (2xPiperidine- $\underline{\text{CH}_2}$), 46.2 ($\underline{\text{CH}_2\text{COOH}}$), 69.9 ($\underline{\text{CH}_2}$), 70.1 ($\underline{\text{CH}_2}$), 114.2 (Ar- $\underline{\text{CH}}$), 115.9 (Ar- $\underline{\text{CH}}$), 119.4 (Ar- $\underline{\text{C}}$), 125.4 (Ar- $\underline{\text{C}}$), 125.9 (Ar- $\underline{\text{CH}}$), 127.6 (2xAr-

$\underline{\text{CH}}$), 128.0 ($\text{Ar-}\underline{\text{CH}}$), 128.5 ($2\times\text{Ar-}\underline{\text{CH}}$), 133.5 ($\underline{\text{CH}}$), 136.6 ($\text{Ar-}\underline{\text{C}}$), 136.8 ($\text{Ar-}\underline{\text{C}}$), 148.3 ($\text{Ar-}\underline{\text{C}}$), 150.9 ($\text{Ar-}\underline{\text{C}}$), 166.6 ($\underline{\text{C=O}}$), 167.4 ($\underline{\text{COOH}}$), 193.1 ($\underline{\text{C=S}}$) ppm; **ESI-MS** m/z (%) = 490.1 [M-H][−] (100 %), 981.5 [2M-H][−] (25 %); **HPLC-Analysis (Method B)**: 96 %, R_t = 21.4 min.

[(5Z)-5-[(2-hydroxyphenyl)methylidene]-4-oxo-2- sulfanylidene-1,3-thiazolidin-3-yl] acetic acid **2e**^[68]

Reaction time: 2 h; **Purification**: Filtration from methanol; **Yield**: 202 mg of red solid (0.68 mmol, 45 %); **¹H-NMR** (400 MHz, DMSO- d_6) δ = 4.73 (s, 2 H, $\underline{\text{CH}_2}$), 6.95-7.01 (m, 2 H, $2\times\text{Ar-}\underline{\text{CH}}$), 7.35-7.41 (m, 2 H, $2\times\text{Ar-}\underline{\text{CH}}$), 8.04 (s, 1 H, $\underline{\text{CH}}$), 10.84 (s(br), 1 H, $\underline{\text{OH}}$), 13.45 (s(br), 1 H, $\underline{\text{COOH}}$) ppm; **¹³C-NMR** (400 MHz, DMSO- d_6) δ = 45.0 ($\underline{\text{CH}_2}$), 116.4 ($\text{Ar-}\underline{\text{C}}$), 119.8 ($\text{Ar-}\underline{\text{C}}$), 120.1 ($\text{Ar-}\underline{\text{CH}}$), 120.3 ($\text{Ar-}\underline{\text{CH}}$), 129.7 ($\text{Ar-}\underline{\text{CH}}$), 129.9 ($\underline{\text{CH}}$), 133.4 ($\text{Ar-}\underline{\text{CH}}$), 157.7 ($\text{Ar-}\underline{\text{C}}$), 166.6 ($\underline{\text{C=O}}$), 167.4 ($\underline{\text{COOH}}$), 193.8 ($\underline{\text{C=S}}$) ppm; **HPLC-Analysis (Method B)**: 100 %, R_t = 20.2 min.

[(5Z)-5-[(3-hydroxyphenyl)methylidene]-4-oxo-2- sulfanylidene-1,3-thiazolidin-3-yl] acetic acid **2f**^[68]

Reaction time: 3 h; **Purification**: Filtration from methanol; **Yield**: 205 mg of red solid (0.69 mmol, 84 %); **¹H-NMR** (400 MHz, DMSO- d_6) δ = 4.71 (s, 2 H, $\underline{\text{CH}_2}$), 6.93 (d, 1 H, $^3J_{\text{H,H}}$ = 7.9 Hz, 4-Ar- $\underline{\text{CH}}$), 7.01 (s, 1 H, 2-Ar- $\underline{\text{CH}}$), 7.09 (d, 1 H, $^3J_{\text{H,H}}$ = 7.4 Hz, 6-Ar- $\underline{\text{CH}}$), 7.35 (dd, 1 H, $^3J_{\text{H,H}}$ = 7.9, 7.4 Hz, 5-Ar- $\underline{\text{CH}}$), 7.77 (s, 1 H, $\underline{\text{CH}}$) ppm; **¹³C-NMR** (400 MHz, DMSO- d_6) δ = 45.1 ($\underline{\text{CH}_2}$), 116.5 (2-Ar- $\underline{\text{CH}}$), 118.7 (4-Ar- $\underline{\text{CH}}$), 121.7 ($\text{Ar-}\underline{\text{C}}$), 122.2 (6-Ar- $\underline{\text{CH}}$), 130.7 (5-Ar- $\underline{\text{CH}}$), 134.0 ($\text{Ar-}\underline{\text{C}}$), 134.2 ($\underline{\text{CH}}$), 158.1 ($\text{Ar-}\underline{\text{C}}$), 166.4 ($\underline{\text{C=O}}$), 167.4 ($\underline{\text{COOH}}$), 193.3 ($\underline{\text{C=S}}$) ppm; **ESI-MS** m/z (%) = 294.0 [M-H][−] (79 %), 589.0 [2M-H][−] (100 %); **HPLC-Analysis (Method B)**: 93 %, R_t = 15.8 min.

[(5Z)-5-[(4-hydroxyphenyl)methylidene]-4-oxo-2- sulfanylidene-1,3-thiazolidin-3-yl] acetic acid **2g**^[268]

Reaction time: 2 h; **Purification**: Filtration from methanol; **Yield**: 176 mg of red solid (0.60 mmol, 45 %); **¹H-NMR** (400 MHz, DMSO- d_6) δ = 4.72 (s, 2 H, $\underline{\text{CH}_2}$), 6.95 (d, 2 H, $^3J_{\text{H,H}}$ = 8.7 Hz, 3,5-Ar- $\underline{\text{CH}}$), 7.54 (d, 2 H, $^3J_{\text{H,H}}$ = 8.7 Hz, 2,6-Ar- $\underline{\text{CH}}$), 7.79 (s, 1 H, $\underline{\text{CH}}$) ppm; **¹³C-NMR** (400 MHz, DMSO- d_6) δ = 45.0 ($\underline{\text{CH}_2}$), 115.9 ($\text{Ar-}\underline{\text{C}}$), 116.7 (3,5-Ar- $\underline{\text{CH}}$), 123.9 ($\text{Ar-}\underline{\text{C}}$), 133.6 (2,6-Ar- $\underline{\text{CH}}$), 134.7 ($\underline{\text{CH}}$), 160.9 ($\text{Ar-}\underline{\text{C}}$), 166.5 ($\underline{\text{C=O}}$), 167.4 ($\underline{\text{COOH}}$), 193.1 ($\underline{\text{C=S}}$) ppm; **ESI-MS** m/z (%) = 294.0 [M-H][−] (100 %); **HR-MS** m/z = 293.9898 [M-H][−] (calculated: 293.9900); **HPLC-Analysis (Method B)**: 97 %, R_t = 16.9 min.

[(5Z)-5-[(4-chlorophenyl)methylidene]-4-oxo-2- sulfanylidene-1,3-thiazolidin-3-yl] acetic acid **2h**^[268]

Reaction time: 2 h; **Purification**: Filtration from methanol; **Yield**: 804 mg of red solid (2.56 mmol, 93 %); **¹H-NMR** (400 MHz, DMSO- d_6) δ = 4.71 (s, 2 H, $\underline{\text{CH}_2}$), 7.60 (d, 2 H, $^3J_{\text{H,H}}$ = 8.6 Hz, 3,5-Ar- $\underline{\text{CH}}$), 7.66 (d, 2 H, $^3J_{\text{H,H}}$ = 8.6 Hz, 2,6-Ar- $\underline{\text{CH}}$), 7.85 (s, 1 H, $\underline{\text{CH}}$), 13.71 (s(br), 1 H, $\underline{\text{COOH}}$) ppm; **¹³C-NMR** (400 MHz, DMSO- d_6) δ = 45.3 ($\underline{\text{CH}_2}$), 122.6 (3,5-Ar- $\underline{\text{CH}}$), 129.6 ($\text{Ar-}\underline{\text{C}}$), 131.7 ($\text{Ar-}\underline{\text{C}}$), 132.3 (2,6-Ar- $\underline{\text{CH}}$), 132.4 ($\underline{\text{CH}}$), 135.9 ($\text{Ar-}\underline{\text{C}}$), 166.3 ($\underline{\text{C=O}}$), 167.3 ($\underline{\text{COOH}}$), 192.9 ($\underline{\text{C=S}}$) ppm; **ESI-MS** m/z (%) = 312.0 [M-H][−] (100 %), 626.9 [2M-H][−] (57 %); **HPLC-Analysis**

(Method B): 99 %, $R_t = 18.8$ min.

[(5Z)-5-[(4-cyanophenyl)methylidene]-4-oxo-2-sulfanylidene-1,3-thiazolidin-3-yl] acetic acid **2i**^[68]

Reaction time: 8 h; **Purification:** Filtration from ethanol; **Yield:** 744 mg of yellow solid (2.44 mmol, 78 %); **¹H-NMR** (400 MHz, DMSO- d_6) $\delta = 4.70$ (s, 2 H, CH_2), 7.81 (d, 2 H, $^3J_{\text{H,H}} = 6.6$ Hz, 2,6-Ar-CH), 7.91 (s, 1 H, CH), 7.98 (d, 2 H, $^3J_{\text{H,H}} = 6.6$ Hz, 3,5-Ar-CH) ppm; **¹³C-NMR** (400 MHz, DMSO- d_6) $\delta = 45.5$ (CH_2), 112.6 (Ar-C), 118.3 (CN), 125.5 (Ar-C), 131.0 (2,6-Ar-CH), 131.4 (CH), 133.1 (3,5-Ar-CH), 137.1 (Ar-C), 166.3 (C=O), 167.2 (COOH), 192.7 (C=S) ppm; **ESI-MS** m/z (%) = 303.0 [M-H]⁻ (88 %), 607.0 [2M-H]⁻ (100 %); **HPLC-Analysis (Method B):** 99 %, $R_t = 18.8$ min.

[(5Z)-5-[(4-ethynylphenyl)methylidene]-4-oxo-2-sulfanylidene-1,3-thiazolidin-3-yl] acetic acid **2j**^[68]

Reaction time: 6 h; **Purification:** Filtration from ethanol; **Yield:** 872 mg of yellow solid (2.87 mmol, 87 %); **¹H-NMR** (400 MHz, DMSO- d_6) $\delta = 4.46$ (s, 1 H, CCH), 4.68 (s, 2 H, CH_2), 7.62 (d, 2 H, $^3J_{\text{H,H}} = 8.6$ Hz, 2,6-Ar-CH), 7.65 (d, 2 H, $^3J_{\text{H,H}} = 8.6$ Hz, 3,5-Ar-CH), 7.85 (s, 1 H, CH), 13.48 (s(br), 1 H, COOH) ppm; **¹³C-NMR** (400 MHz, DMSO- d_6) $\delta = 45.5$ (CH_2), 83.0 (CCH), 84.0 (CCH), 123.0 (Ar-C), 124.0 (Ar-C), 130.9 (3,5-Ar-CH), 132.5 (CH), 132.6 (2,6-Ar-CH), 133.1 (Ar-C), 166.4 (C=O), 167.3 (COOH), 192.9 (C=S) ppm; **ESI-MS** m/z (%) = 302.0 [M-H]⁻ (100 %), 605.0 [2M-H]⁻ (100 %); **HR-MS** $m/z = 301.9956$ [M-H]⁻ (calculated: 301.9951); **HPLC-Analysis (Method B):** 100 %, $R_t = 18.4$ min.

[(5Z)-5-[(3-nitrophenyl)methylidene]-4-oxo-2-sulfanylidene-1,3-thiazolidin-3-yl] acetic acid **2k**^[268]

Reaction time: 4 h; **Purification:** Filtration from ethanol; **Yield:** 673 mg of red solid (2.08 mmol, 67 %); **¹H-NMR** (400 MHz, DMSO- d_6) $\delta = 4.76$ (s, 2 H, CH_2), 7.80-7.89 (m, 1 H, 5-Ar-CH), 8.02-8.18 (m, 2 H, 6-Ar-CH, CH), 8.30-8.39 (m, 1 H, 4-Ar-CH), 8.53 (s, 1 H, 2-Ar-CH), 13.53 (s(br), 1 H, COOH) ppm; **¹³C-NMR** (400 MHz, DMSO- d_6) $\delta = 45.1$ (CH_2), 124.8 (Ar-C), 125.1 (4-Ar-CH), 125.3 (2-Ar-CH), 131.1 (5-Ar-CH), 131.5 (6-Ar-CH), 134.4 (Ar-C), 135.8 (CH), 148.3 (Ar-C), 166.1 (C=O), 167.2 (COOH), 192.7 (C=S) ppm; **ESI-MS** m/z (%) = 323.0 [M-H]⁻ (100 %), 647.0 [2M-H]⁻ (100 %); **HR-MS** $m/z = 322.9806$ [M-H]⁻ (calculated: 322.9802); **HPLC-Analysis (Method B):** 100 %, $R_t = 17.1$ min.

[(5Z)-5-[(3-bromo-4-methoxyphenyl)methylidene]-4-oxo-2-sulfanylidene-1,3-thiazolidin-3-yl] acetic acid **2l**^[269]

Reaction time: 8 h; **Purification:** Filtration from ethanol; **Yield:** 569 mg of yellow solid (1.47 mmol, 75 %); **¹H-NMR** (400 MHz, DMSO- d_6) $\delta = 3.95$ (s, 3 H, OCH_3), 4.74 (s, 2 H, CH_2), 7.32 (d, 1 H, $^3J_{\text{H,H}} = 8.8$ Hz, 5-Ar-CH), 7.67 (dd, 1 H, $^{3,4}J_{\text{H,H}} = 8.8, 2.3$ Hz, 6-Ar-CH), 7.87 (s, 1 H, CH), 7.97 (d, 1 H, $^4J_{\text{H,H}} = 2.3$ Hz, 2-Ar-CH) ppm; **ESI-MS** m/z (%) = 387.9 [M-H]⁻ (100 %), 774.8 [2M-H]⁻ (100 %), 796.8 [2M+Na-2H]⁻ (65 %); **HR-MS** $m/z = 385.9169$ [M-H]⁻ (calculated: 385.9162); **HPLC-Analysis (Method B):** 95 %, $R_t = 15.4$ min.

[(Z)-2-(5-(3-methylbenzylidene)-4-oxo-2-thioxothiazolidin-3-yl)] acetic acid **2m**^[160]

Reaction time: 6 h; **Purification:** Filtration from ethanol; **Yield:** 476 mg of yellow solid (1.62

mmol, 76 %); **¹H-NMR** (400 MHz, DMSO-*d*₆) δ = 2.39 (s, 3 H, CH₃), 4.74 (s, 2 H, CH₂), 7.35-7.39 (m, 1 H, Ar-CH), 7.45-7.48 (m, 3 H, 3 x Ar-CH), 7.85 (s, 1 H, CH); 13.50 (s(br), 1 H, COOH) ppm; **¹³C-NMR** (400 MHz, DMSO-*d*₆) δ = 19.4 (CH₃), 45.0 (CH₂), 123.4 (Ar-C), 127.0 (Ar-CH), 127.8 (Ar-CH), 131.1 (Ar-CH), 131.2 (Ar-CH), 131.7 (CH), 131.9 (Ar-C), 139.5 (Ar-C), 166.1 (C=O), 167.3 (COOH), 193.7 (C=S) ppm; **ESI-MS** m/z (%) = 294.0 [M+H]⁺ (100 %), 311.1 [M+NH₄]⁺ (85 %); **HR-MS** m/z = 294.0256 [M+H]⁺ (calculated: 294.0253); **HPLC-Analysis (Method B)**: 98 %, *R*_t = 18.8 min.

[(Z)-2-(5-(4-methylbenzylidene)-4-oxo-2-thioxothiazolidin-3-yl)] acetic acid **2n**^[268]

Reaction time: 6 h; **Purification**: Filtration from ethanol; **Yield**: 541 mg of yellow solid (1.84 mmol, 78 %); **¹H-NMR** (400 MHz, DMSO-*d*₆) δ = 2.38 (s, 3 H, CH₃), 4.74 (s, 2 H, CH₂), 7.39 (d, 2 H, ³*J*_{H,H} = 8.0 Hz, 3,5-Ar-CH), 7.58 (d, 2 H, ³*J*_{H,H} = 8.0 Hz, 2,6-Ar-CH), 7.87 (s, 1 H, CH); 13.48 (s(br), 1 H, COOH) ppm; **¹³C-NMR** (400 MHz, DMSO-*d*₆) δ = 21.2 (CH₃), 45.0 (CH₂), 120.6 (Ar-C), 130.1 (Ar-C), 130.2 (3,5-Ar-CH), 130.9 (2,6-Ar-CH), 134.1 (CH), 141.9 (Ar-C), 166.4 (C=O), 167.3 (COOH), 193.2 (C=S) ppm; **ESI-MS** m/z (%) = 294.0 [M+H]⁺ (100 %), 311.1 [M+NH₄]⁺ (85 %); **HR-MS** m/z = 294.0257 [M+H]⁺ (calculated: 294.0253); **HPLC-Analysis (Method B)**: 98 %, *R*_t = 18.8 min.

[(Z)-2-(5-(2-methylbenzylidene)-4-oxo-2-thioxothiazolidin-3-yl)] acetic acid **2o**

Reaction time: 6 h; **Purification**: Filtration from ethanol; **Yield**: 634 mg of yellow solid (2.16 mmol, 78 %); **¹H-NMR** (400 MHz, DMSO-*d*₆) δ = 2.43 (s, 3 H, Ar-CH₃), 4.74 (s, 2 H, CH₂), 7.35-7.47 (m, 4 H, 4xAr-CH), 7.96 (s, 1 H, CH), 13.50 (s(br), 1 H, COOH) ppm; **¹³C-NMR** (400 MHz, DMSO-*d*₆) δ = 19.4 (Ar-CH₃), 45.0 (CH₂), 123.4 (Ar-C), 127.0 (Ar-CH), 127.8 (Ar-CH), 131.1 (Ar-C), 131.2 (Ar-CH), 131.7 (Ar-CH), 131.9 (Ar-C), 139.5 (CH), 166.1 (C=O), 167.3 (COOH), 193.7 (C=S) ppm; **ESI-MS** m/z (%) = 294.0 [M+H]⁺ (100 %), 311.1 [M+NH₄]⁺ (85 %), 717.0 [2M+Na]⁺ (90 %); **HR-MS** m/z = 294.0258 [M+H]⁺ (calculated: 294.0253). **HR-MS** m/z = 365.0239 [M+NH₄]⁺ (calculated: 365.0236); **HPLC-Analysis (Method B)**: 97 %, *R*_t = 18.6 min.

[(Z)-2-(4-oxo-2-thioxo-5-(3-(trifluoromethyl)benzylidene)thiazolidin-3-yl)] acetic acid **2p**^[270]

Reaction time: 2 h; **Purification**: Filtration from ethanol; **Yield**: 361 mg of yellow solid (1.04 mmol, 94 %); **¹H-NMR** (400 MHz, DMSO-*d*₆) δ = 4.76 (s, 2 H, CH₂), 7.81 (at, 1 H, ³*J*_{H,H} = 7.8 Hz, 5-Ar-CH), 7.89 (d, 1 H, ³*J*_{H,H} = 7.8 Hz, 4-Ar-CH), 7.93 (d, 1 H, ³*J*_{H,H} = 7.8 Hz, 6-Ar-CH), 8.03 (s, 1 H, CH), 8.09 (s, 1 H, 2-Ar-CH), 13.51 (s(br), 1 H, COOH) ppm; **¹³C-NMR** (400 MHz, DMSO-*d*₆) δ = 45.1 (CH₂), 123.7 (q, ¹*J*_{C,F} = 272.7 Hz, CF₃), 124.1 (Ar-C), 127.3 (q, ³*J*_{C,F} = 3.7 Hz, 4-Ar-CH), 127.8 (q, ³*J*_{C,F} = 4.0 Hz, 2-Ar-CH), 130.1 (q, ²*J*_{C,F} = 32.3 Hz, 3-Ar-C), 130.7 (5-Ar-CH), 132.1 (CH), 133.3 (6-Ar-CH), 133.9 (Ar-C), 166.2 (C=O), 167.2 (COOH), 192.9 (C=S) ppm; **ESI-MS** m/z (%) = 348.0 [M+H]⁺ (40 %), 365.0 [M+NH₄]⁺ (100 %), 370.0 [M+Na]⁺ (30 %), **HR-MS** m/z = 365.0239 [M+NH₄]⁺ (calculated: 365.0236); **HPLC-Analysis (Method B)**: 99 %, *R*_t = 18.8 min.

(Z)-2-(4-oxo-2-thioxo-5-(4-(trifluoromethyl)benzylidene)thiazolidin-3-yl) acetic acid **2q**^[270]

Reaction time: 3 h; **Purification:** Filtration from ethanol; **Yield:** 643 mg of yellow solid (1.85 mmol, 73 %); **¹H-NMR** (400 MHz, DMSO-*d*₆) δ = 4.75 (s, 2 H, CH₂), 7.89 (d, 2 H, ³J_{H,H} = 8.8 Hz, 2,6-Ar-CH), 7.92 (d, 2 H, ³J_{H,H} = 8.8 Hz, 3,5-Ar-CH), 7.99 (s, 1 H, CH), 13.76 (s(br), 1 H, COOH) ppm; **¹³C-NMR** (400 MHz, DMSO-*d*₆) δ = 45.4 (CH₂), 123.8 (q, ¹J_{C,F} = 272.0 Hz, CF₃), 124.9 (Ar-C), 126.2 (q, ³J_{C,F} = 3.5 Hz, 3,5-Ar-CH) 130.2 (q, ²J_{C,F} = 33.3 Hz, 4-Ar-C), 131.2 (2,6-Ar-CH), 131.7 (CH), 136.7 (Ar-C), 166.3 (C=O), 167.3 (COOH), 192.9 (C=S) ppm; **ESI-MS** *m/z* (%) = 348.0 [M+H]⁺ (40 %), 365.0 [M+NH₄]⁺ (100 %), 717.0 [2M+Na]⁺ (90 %); **HR-MS** *m/z* = 365.0239 [M+NH₄]⁺ (calculated: 365.0236); **HPLC-Analysis (Method B):** 100 %, R_t = 19.2 min.

(Z)-2-(4-oxo-2-thioxo-5-(2-(trifluoromethyl)benzylidene)thiazolidin-3-yl) acetic acid **2r**

Reaction time: 4 h; **Purification:** Filtration from ethanol; **Yield:** 721 mg of yellow solid (2.08 mmol, 81 %); **¹H-NMR** (400 MHz, DMSO-*d*₆) δ = 4.75 (s, 2 H, CH₂), 7.74 (t, 1 H, ³J_{H,H} = 7.6 Hz, 5-Ar-CH), 7.78 (d, 1 H, ³J_{H,H} = 7.6 Hz, 6-Ar-CH), 7.89 (t, 1 H, ³J_{H,H} = 7.6 Hz, 4-Ar-CH), 7.89 (s, 1 H, CH), 7.95 (d, 1 H, ³J_{H,H} = 7.6 Hz, 3-Ar-CH), 13.55 (s(br), 1 H, COOH) ppm; **¹³C-NMR** (400 MHz, DMSO-*d*₆) δ = 45.1 (CH₂), 123.8 (q, ¹J_{C,F} = 274.3 Hz, CF₃), 127.0 (q, ³J_{C,F} = 5.3 Hz, 3-Ar-CH), 127.3 (Ar-C), 127.8 (CH), 128.0 (q, ²J_{C,F} = 29.0 Hz, 2-Ar-C), 129.6 (6-Ar-CH), 130.9 (Ar-C), 131.0 (5-Ar-CH) 133.6 (4-Ar-CH), 165.8 (C=O), 167.2 (COOH), 193.2 (C=S) ppm; **ESI-MS** *m/z* (%) = 348.0 [M+H]⁺ (40 %), 365.0 [M+NH₄]⁺ (100 %); **HR-MS** *m/z* = 365.0237 [M+NH₄]⁺ (calculated: 365.0236); **HPLC-Analysis (Method B):** 100 %, R_t = 18.4 min.

(Z)-2-(5-(4-(methylsulfonyl)benzylidene)-4-oxo-2-thioxothiazolidin-3-yl) acetic acid **2s**

Reaction time: 6 h; **Purification:** Filtration from ethanol; **Yield:** 167 mg of yellow solid (0.47 mmol, 29 %); **¹H-NMR** (400 MHz, DMSO-*d*₆) δ = 4.75 (s, 2 H, CH₂), 7.93 (d, 2 H, ³J_{H,H} = 8.5 Hz, 2,4-Ar-CH), 7.99 (s, 1 H, CH), 8.08 (d, 2 H, ³J_{H,H} = 8.5 Hz, 1,5-Ar-CH); **¹³C-NMR** (300 MHz, DMSO-*d*₆) δ = 45.2 (CH₂, CH₃), 125.4 (Ar-C or Ar-CH), 128.0 (Ar-C or Ar-CH), 131.3 (Ar-C or Ar-CH), 131.7 (Ar-C or Ar-CH), 137.5 (CH), 141.9 (Ar-C or Ar-CH), 166.3 (C=O), 166.3 (COOH), 193.01 (C=S); **ESI-MS** *m/z* (%) = 358.0 [M+H]⁺ (25 %), 375.0 [M+NH₄]⁺ (100 %), 380.0 [M+Na]⁺ (20 %); **HR-MS** *m/z* = 375.0140 [M+NH₄]⁺ (calculated: 375.0138); **HPLC-Analysis (Method B):** 91 %, R_t = 13.9 min.

(Z)-2-(5-(4-(dimethylamino)benzylidene)-4-oxo-2-thioxothiazolidin-3-yl) acetic acid **2t**^[268]

Reaction time: 6 h; **Purification:** Filtration from ethanol; **Yield:** 375 mg of yellow solid (1.16 mmol, 87 %); **¹H-NMR** (400 MHz, DMSO-*d*₆) δ = 3.06 (s, 6 H, 2 x CH₃), 4.72 (s, 2 H, CH₂), 6.85 (d, 2 H, ³J_{H,H} = 8.8 Hz, 2,4-Ar-CH), 7.51 (d, 2 H, ³J_{H,H} = 8.8 Hz, 1,5-Ar-CH), 7.75 (s, 1 H, CH); **¹³C-NMR** (300 MHz, DMSO-*d*₆) δ = 45.0 (CH₂, CH₃), 112.3 (2,4-Ar-CH), 119.7 (Ar-C), 133.5 (1,5-Ar-CH), 135.5 (CH), 152.1 (Ar-C), 161.9 (Ar-C), 166.4 (C=O), 167.5 (COOH); **ESI-MS** *m/z* (%) = 323.1 [M+H]⁺ (100 %), 345.0 [M+Na]⁺ (15 %), 645.1 [2M+H]⁺ (10 %); **HR-MS** *m/z* = 323.0522 [M+H]⁺ (calculated: 323.0519); **HPLC-Analysis (Method B):** 91 %, R_t = 13.9 min.

(Z)-2-(5-(3,4-dihydroxybenzylidene)-4-oxo-2-thioxothiazolidin-3-yl) acetic acid **2u**^[92]

Reaction time: 6 h; **Purification:** Filtration from ethanol; **Yield:** 189 mg of red solid (0.61 mmol, 76 %); **¹H-NMR** (400 MHz, DMSO-*d*₆) δ = 4.43 (s, 2 H, CH₂), 6.89 (d, 1 H, ³J_{H,H} = 8.0 Hz, 3-Ar-CH), 7.03 (dd, 1 H, ^{3,4}J_{H,H} = 8.1, 2.2 Hz, 4-Ar-CH), 7.04 (d, 1 H, ⁴J_{H,H} = 2.2 Hz, 1-Ar-CH), 7.65 (s, 1 H, CH); **¹³C-NMR** (300 MHz, DMSO-*d*₆) δ = 43.52 (CH₂), 100.2 (Ar-C or Ar-CH), 124.4 (Ar-C or Ar-CH), 126.7 (Ar-C or Ar-CH), 128.5 (Ar-C or Ar-CH), 129.1 (Ar-C or Ar-CH), 137.9 (Ar-C or Ar-CH), 149.8 (Ar-C or Ar-CH), 151.3 (Ar-C or Ar-CH), 166.8 (C=O), 167.5 (COOH), 199.9 (C=S); **ESI-MS** *m/z* (%) = 312.0 [M+H]⁺ (100 %), 329.0 [M+NH₄]⁺ (30 %), 640.0 [2M+NH₄]⁺ (30 %); **HR-MS** *m/z* = 311.9999 [M+H]⁺ (calculated: 311.9995); **HPLC-Analysis (Method B):** 99 %, R_t = 16.1 min.

(Z)-4-((3-(carboxymethyl)-4-oxo-2-thioxothiazolidin-5-ylidene)methyl) benzoic acid **2v**^[270]

Reaction time: 4 h; **Purification:** Filtration from ethanol; **Yield:** 29 mg of yellow (0.09 mmol, 17 %); **¹H-NMR** (400 MHz, DMSO-*d*₆) δ = 4.38 (s, 2 H, CH₂), 7.64-7.69 (m, 2 H, 2xAr-CH), 7.80 (s, 1 H, CH), 8.01 (d, 2 H, ³J_{H,H} = 7.4 Hz, 2xAr-CH) ppm; **APCI-MS** *m/z* (%) = 324.0 [M+H]⁺ (100 %); **HR-MS** *m/z* = 323.9995 [M+H]⁺ (calculated: 323.9995); **HPLC-Analysis (Method B):** 84 %, R_t = 16.0 min.

(Z)-2-(5-(2,4-dihydroxybenzylidene)-4-oxo-2-thioxothiazolidin-3-yl) acetic acid **2w**^[92]

Reaction time: 7 h; **Purification:** Filtration from ethanol; **Yield:** 153 mg of red solid (0.49 mmol, 52 %); **¹H-NMR** (400 MHz, DMSO-*d*₆) δ = 4.71 (s, 2 H, CH₂), 6.42-6.46 (m, 2 H, 3,4-Ar-CH), 7.24 (d, 1 H, ⁴J_{H,H} = 8.5 Hz, 1-Ar-CH), 7.99 (s, 1 H, CH), 10.47 (s, 1 H, OH), 10.83 (s, 1 H, OH); **ESI-MS** *m/z* (%) = 312.0 [M+H]⁺ (100 %), 640.0 [2M+NH₄]⁺ (40 %); **HR-MS** *m/z* = 311.9998 [M+H]⁺ (calculated: 311.9995); **HPLC-Analysis (Method B):** 84 %, R_t = 16.0 min.

[(5Z)-5-[2,5- bis(trifluoromethyl)phenyl]methylidene-4-oxo-2- sulfanylidene-1,3-thiazolidin-3-yl] acetic acid **2x**

TLC R_f = 0.4 (DCM/EtOAc 3:1); **Reaction time:** 4 h; **Purification:** Filtration from ethanol; **Yield:** 58 mg of yellow solid (0.14 mmol, 27 %); **¹H-NMR** (400 MHz, DMSO-*d*₆) δ = 4.36 (s, 2 H, CH₂), 7.77-7.80 (m, 1 H, Ar-CH), 8.01 (s, 1 H, Ar-CH), 8.10 (d, 1 H, ³J_{H,H} = 8.4 Hz, Ar-CH), 8.17 (d, 1 H, ³J_{H,H} = 8.4 Hz, Ar-CH) ppm; **ESI-MS** *m/z* (%) = 414.0 [M-H]⁻ (100 %), 828.9 [2M-H]⁻ (6 %); **HPLC-Analysis (Method B):** 82 %, R_t = 18.6 min.

[(5Z)-5-[2,4- bis(trifluoromethyl)phenyl]methylidene-4-oxo-2- sulfanylidene-1,3-thiazolidin-3-yl] acetic acid **2ag**

ESI-MS *m/z* (%) = 414.0 [M-H]⁻ (100 %), 850.9 [2M2Na-2H]⁻ (100 %); **HR-MS** *m/z* = 413.9702 [M-H]⁻ (calculated: 413.9699); **HPLC-Analysis (Method B):** 94 %, R_t = 20.5 min.

Piperidinium (Z)-2-(5-(4-tert-butylbenzylidene)-4-oxo-2-thioxothiazolidin-3-yl) acetate **2y**

TLC R_f = 0.2 (DCM/MeOH 9:1); **Reaction time:** 16 h; **Purification:** Filtration from ethanol; **Yield:** 96 mg of yellow solid (0.23 mmol, 20 %); **¹H-NMR** (400 MHz, MeOD) δ = 1.33 (s, 9 H, 3xCH₃), 1.62-1.69 (m, 2 H, 3-Pip-CH₂), 1.72-1.79 (m, 4 H, 2x2-Pip-CH₂), 3.09 (t, 4 H, J_{H,H} =

5.7 Hz, 2x1-Pip-CH₂), 4.62 (s, 2 H, CH₂), 7.50 (d, 2 H, ³J_{H,H} = 8.5 Hz, 2xAr-CH), 7.56 (d, 2 H, ³J_{H,H} = 8.5 Hz, 2xAr-CH), 7.70 (s, 1 H, CH) ppm; ¹³C-NMR (400 MHz, MeOD) δ = 23.1 (3-Pip-CH₂), 23.8 (2x2-Pip-CH₂), 31.5 (3xCH₃), 35.9 (CCH₃), 45.7 (2x1-Pip-CH₂), 48.4 (CH₂), 123.9 (Ar-C), 127.5 (2xAr-CH), 131.7 (2xAr-CH), 132.2 (Ar-C), 133.5 (CH), 155.7 (Ar-C), 169.0 (C=O), 172.8 (COOH), 195.2 (C=S) ppm; **HPLC-Analysis (Method B)**: 97 %, R_t = 20.7 min.

(Z)-2-(5-(4-tert-butylbenzylidene)-4-oxo-2-thioxothiazolidin-3-yl) acetic acid **2z**

Compound **2y** was extracted between 1 N HCl (15 mL) and EtOAc (3x15 mL), dried over MgSO₄, filtered and concentrated to afford the analogues free acid. **TLC** R_f = 0.1 (DCM/MeOH 9:1); **Yield**: 32 mg of yellow solid (0.10 mmol, 79 %); ¹H-NMR (400 MHz, MeOD) δ = 1.28 (s, 9 H, 3xCH₃), 4.74 (s, 2 H, CH₂), 7.44 (d, 2 H, ³J_{H,H} = 8.4 Hz, 2xAr-CH), 7.51 (d, 2 H, ³J_{H,H} = 8.4 Hz, 2xAr-CH), 7.68 (s, 1 H, CH) ppm; ¹³C-NMR (400 MHz, MeOD) δ = 31.4 (3xCH₃), 36.0 (CCH₃), 45.7 (CH₂), 122.8 (Ar-C), 127.6 (2xAr-CH), 131.9 (2xAr-CH), 134.7 (CH), 156.1 (Ar-C), 168.4 (C=O) 169.3 (C=OOH) 194.9 (C=S) ppm.

2-[(5Z)-3-(carboxymethyl)-4-oxo-2-sulfanylidene-1,3-thiazolidin-5-ylidene]methyl benzoic acid **2aa**^[271]

TLC R_f = 0.1 (DCM/MeOH 9:1); **Reaction time**: 4 h; **Purification**: Filtration from ethanol; **Yield**: 26 mg of yellow solid (0.08 mmol, 15 %); ¹H-NMR (400 MHz, DMSO-d₆) δ = 4.29 (s, 2 H, CH₂), 7.34-7.41 (m, 3 H, 3xAr-CH), 7.71-7.75 (m, 1 H, Ar-CH), 8.79 (s, 1 H, CH), ppm; ¹³C-NMR (400 MHz, DMSO-d₆) δ = 48.2 (CH₂), 121.7 (Ar-C), 127.2 (Ar-CH), 128.3 (Ar-CH), 129.8 (Ar-CH), 131.8 (Ar-CH), 136.0 (CH), 143.7 (Ar-C), 166.6 (C=O), 194.2 (C=S) ppm; **ESI-MS** m/z (%) = 322.0 [M-H]⁻ (100 %), 644.0 [2M-H]⁻ (55 %); **HR-MS** m/z = 321.9851 [M-H]⁻ (calculated: 321.9849); **HPLC-Analysis (Method B)**: 97 %, R_t = 16.3 min.

(Z)-2-(5-(2,4-bis(trifluoromethyl)benzylidene)-4-oxo-2-thioxothiazolidin-3-yl) acetic acid **2ab**

TLC R_f = 0.6 (DCM/MeOH 9:1); **Reaction time**: 4 h; **Purification**: Filtration from ethanol; **Yield**: 58 mg of yellow solid (0.14 mmol, 27 %); **Yield**: 84 mg of yellow solid (0.20 mmol, 39 %); ¹H-NMR (400 MHz, DMSO-d₆) δ = 4.30 (s, 2 H, CH₂), 7.77 (q, 1 H, ⁵J_{H,F} = 2.3 Hz, CH), 7.98 (d, 1 H, ³J_{H,H} = 8.1 Hz, 5-Ar-CH), 8.21 (s, 1 H, 3-Ar-CH), 8.25 (d, 1 H, ³J_{H,H} = 8.1 Hz, 6-Ar-CH) ppm; ¹³C-NMR (400 MHz, DMSO-d₆) δ = 48.0 (CH₂), 124.4 (3-Ar-CH) 124.6 (CH), 130.7 (5-Ar-CH), 130.8 (6-Ar-CH), 166.0 (C=O), 166.1 (COOH), 192.7 (C=S) ppm; **APCI-MS** m/z (%) = 416.0 [M+H]⁺ (100 %), 433.0 [M+NH₄]⁺ (20 %); **ESI-MS** m/z (%) = 414.0 [M-H]⁻ (100 %), 829.0 [2M-H]⁻ (100 %); 850.9 [2M+Na-2H]⁻ (100 %); **HR-MS** m/z = 413.9701 [M-H]⁻ (calculated: 413.9699); **HR-MS** m/z = 413.9702 [M-H]⁻ (calculated: 413.9699); **HR-MS** m/z = 415.9845 [M+H]⁺ (calculated: 415.9844); **HPLC-Analysis (Method B)**: 85 %, R_t = 20.2 min.

[(5Z)-5-[(4-methoxyphenyl)methylidene]-4-oxo-2-sulfanylidene-1,3-thiazolidin-3-yl] acetic acid **2ac**^[272]

Reaction time: 4 h **Purification**: Filtration from methanol; **Yield**: 174 mg of yellow solid (0.56 mmol, 31 %); ¹H-NMR (400 MHz, DMSO-d₆) δ = 2.08 (s, 3 H, CH₃) 4.48 (s, 2 H, CH₂) 7.55-

7.88 (m, 5 H, 4xAr-CH, CH) 10.37 (s, 1 H, COOH) ppm; **HPLC-Analysis (Method B)**: 91 %, R_t = 15.6 min.

(Z)-2-(5-(4-acetamidobenzylidene)-4-oxo-2-thioxothiazolidin-3-yl) acetic acid **2ad**

Reaction time: 4 h; **Purification**: Filtration from ethanol; **Yield**: 587 mg of yellow solid (1.75 mmol, 85 %); **$^1\text{H-NMR}$** (400 MHz, DMSO- d_6) δ = 2.09 (s, 1 H, CH₃), 4.74 (s, 2 H, CH₂), 7.64 (d, 2 H, $^3J_{\text{H,H}}$ = 8.9 Hz, 2,6-Ar-CH), 7.78 (d, 2 H, $^3J_{\text{H,H}}$ = 8.9 Hz, 3,5-Ar-CH), 7.82 (s, 1 H, CH), 10.36 (s, 1 H, NH), 13.46 (s(br), 1 H, COOH) ppm; **$^{13}\text{C-NMR}$** (400 MHz, DMSO- d_6) δ = 24.2 (CH₃), 45.0 (CH₂), 119.2 (Ar-C), 119.3 (3,5-Ar-CH), 127.2 (Ar-C), 132.2 (2,6-Ar-CH), 133.9 (CH), 142.1 (Ar-C), 166.5 (C=O), 167.4 (C=O), 169.0 (COOH), 193.2 (C=S) ppm; **ESI-MS** m/z (%) = 337.0 [M+H]⁺ (100 %), 354.1 [M+NH₄]⁺ (65 %), 690.1 [2M+NH₄]⁺ (20 %); **HR-MS** m/z = 337.0315 [M+H]⁺ (calculated: 337.0311); **ESI-MS** m/z (%) = 335.0 [M-H]⁻ (100 %), 671.0 [2M-H]⁻ (15 %); **HPLC-Analysis (Method B)**: 100 %, R_t = 17.1 min.

(Z)-2-(5-(3-bromo-4-fluorobenzylidene)-4-oxo-2-thioxothiazolidin-3-yl) acetic acid **2ai**

Reaction time: 6 h; **Purification**: Filtration from ethanol; **Yield**: 234 mg of yellow solid (0.62 mmol, 74 %); **$^1\text{H-NMR}$** (400 MHz, DMSO- d_6) δ = 4.75 (s, 2 H, CH₂), 7.59 (at, 1 H, $^3J_{\text{H,H(F)}}$ = 8.6 Hz, 5-Ar-CH), 7.71 (ddd, 1 H, $^{3,4}J_{\text{H,H(F)}}$ = 8.6, 4.7, 2.3 Hz, 6-Ar-CH), 7.91 (s, 1 H, CH), 8.10 (dd, 1 H, $^4J_{\text{C,F}}$ = 6.7, 2.3 Hz, 2-Ar-CH) ppm; **$^{13}\text{C-NMR}$** (400 MHz, DMSO- d_6) δ = 45.1 (CH₂), 109.4 (d, $^2J_{\text{C,F}}$ = 21.6 Hz, 3-Ar-C), 117.9 (5-Ar-CH), 123.2 (Ar-C), 131.4 (CH), 131.4 (d, $^4J_{\text{C,F}}$ = 8.1 Hz, 6-Ar-CH), 136.4 (2-Ar-CH), 158.1 (Ar-C), 166.2 (C=O), 167.3 (COOH), 192.9 (C=S) ppm; **ESI-MS** m/z (%) = 774.8 [2M+Na]⁺ (95 %); **HR-MS** m/z = 397.8926 [M+Na]⁺ (calculated: 397.8927), 421.8721 [M-H+2Na]⁺ (calculated: 421.8725), 774.7931 [2M+Na]⁺ (calculated: 774.7941), 796.7750 [2M-H+2Na]⁺ (calculated: 796.7761); **HPLC-Analysis (Method B)**: 92 %, R_t = 18.0 min.

(Z)-2-(5-(3,5-bis(trifluoromethyl)benzylidene)-4-oxo-2-thioxothiazolidin-3-yl) acetic acid **2ae**

TLC R_f = 0.6 (DCM/MeOH 9:1); **Reaction time**: 4 h; **Purification**: Filtration from ethanol; **Yield**: 86 mg of yellow solid (0.21 mmol, 40 %); **$^1\text{H-NMR}$** (400 MHz, DMSO- d_6) δ = 4.32 (s, 2 H, CH₂), 8.00 (s, 1 H, CH), 8.24-8.28 (m, 3 H, 3xAr-CH) ppm; **ESI-MS** m/z (%) = 414.0 [M-H]⁻ (100 %), 829.0 [2M-H]⁻ (100 %); **HR-MS** m/z = 413.9699 [M-H]⁻ (calculated: 413.9699); **HPLC-Analysis (Method B)**: 94 %, R_t = 20.7 min.

9.3 General Procedures for Synthesis of 5-Benzylidene thiazolidine-2,4-diones N-acetic ester derivatives 7a–l

Method 1: Alkylation of Thiazolidine-2,4-diones

Thiazolidine-2,4-diones (1.0 eq) was dissolved in minimum of dry DMF (2-5 mL) and NaH (1.0 eq) were added under ice cooling. The reaction mixture was stirred for 10 min and ethyl bromo acetate (1.0 eq) were added drop wise at 0 °C. The reaction was stirred at rt for 4 h or

until TLC shows complete consumption of starting Thiazolidine-2,4-diones. Next, the reaction was quenched with water (10 mL), extracted with EtOAc (3x10 mL), dried over MgSO₄, filtered and concentrated. Purification by flash column chromatography afforded ethyl 2-(2,4-dioxo-1,3-thiazolidin-3-yl) acetate **7**^[273] as a clear oil. **TLC** R_f = 0.1 (Hexane/EtOAc 9:1); **Reaction time**: 3 h; **Yield**: 450 mg of white solid (2.21 mmol, 86 %); **Yield**: 1423 mg of clear oil (7.00 mmol, 88 %); **Yield**: 3120 mg of clear oil (15.35 mmol, 90 %); **Purification**: Flash-Chromatography Hexane/ EtOAc 8:2 (R_f = 0.2); **¹H-NMR** (400 MHz, CDCl₃) δ = 1.26 (t, 3 H, $^3J_{H,H}$ = 7.1 Hz, CH₃), 4.02 (s, 2 H, CH₂), 4.19 (q, 2 H, $^3J_{H,H}$ = 7.1 Hz, CH₂CH₃), 4.30 (s, 2 H, CH₂) ppm; **¹³C-NMR** (400 MHz, CDCl₃) δ = 14.1 (CH₃), 33.9 (CH₂), 42.2 (CH₂), 62.2 (CH₂), 166.3 (C=O), 170.8 (C=O), 171.2 (C=O) ppm; **APCI-MS** m/z (%) = 204.0 [M+H]⁺ (100 %); **HR-MS** m/z = 204.0321 [M+H]⁺ (calculated: 204.0325).

Method 2: Alkylation of Thiazolidine-2,4-diones

Thiazolidine-2,4-diones (1325 mg, 10.18 mmol) was dissolved in 10 mL ethanol, potassium hydroxide (571 mg, 10.18 mmol) was added. The reaction mixture was stirred 1 h at 70 °C. Upon cooling 2,4-dioxo-1,3-thiazolidin-3-ide potassium salt **8**^[274] precipitated from the solution. The white solid was filtered and washed with acetone. **Yield**: 1113 mg of white solid (7.17 mmol, 100 %); **Purification**: Filtration from ethanol, washing with acetone. The crude potassium salt **8** (1.0 eq) was dissolved in 15 mL acetone. Ethyl bromo-acetate was added and the reaction mixture was heated 70 °C for 4 h. A white solid (KBr) crushed out and was filtered and washed with acetone. The crude was concentrated and extracted between water (10 mL) and EtOAc (3x10 mL). The combined organic fractions were dried over MgSO₄, filtered and concentrated. Crude **7** was pure enough for consecutive reactions. **Yield**: 346 mg of clear oil (1.70 mmol, 100 %); **Yield**: 205 mg of white solid (1.01 mmol, 100 %).

General Procedure for Knoevenagel condensation reaction

Ethyl 2-(2,4-dioxothiazolidin-3-yl) acetate **7** (1.0 eq), benzaldehyde derivatives (1.1-1.5 eq) and sodium acetate were dissolved in 10 mL ethanol. The reaction mixture was stirred at 80 °C until TLC showed complete consumption of starting **7**. The products were purified as described in the individual sections.

Ethyl 2-[(5Z)-2,4-dioxo-5-(phenylmethylidene)-1,3-thiazolidin-3-yl] acetate **7a**^[275]

TLC R_f = 0.6 (Hexane/EtOAc 8:2); **Reaction time**: 4 h; **Purification**: Filtration from ethanol; **Yield**: 324 mg of white solid (1.11 mmol, 46 %); **¹H-NMR** (400 MHz, CDCl₃) δ = 1.30 (t, 3 H, $^3J_{H,H}$ = 7.1 Hz, CH₃), 4.25 (q, 2 H, $^3J_{H,H}$ = 7.1 Hz, CH₂CH₃), 4.48 (s, 2 H, CH₂), 7.43-7.55 (m, 5 H, 5xAr-CH), 7.95 (s, 1 H, CH) ppm.

Ethyl 2-[(5Z)-5-[(2-methylphenyl)methylidene]-2,4-dioxo-1,3-thiazolidin-3-yl] acetate **7b**

TLC R_f = 0.6 (Hexane/EtOAc 8:2); **Reaction time**: 16 h; **Purification**: Flash-Chromatography Hexane/EtOAc 9:1 (R_f = 0.4), DCM; **Yield**: 211 mg of white solid (0.69 mmol, 69 %); **$^1\text{H-NMR}$** (400 MHz, CDCl_3) δ = 1.23 (t, 3 H, $^3J_{\text{H,H}}$ = 7.1 Hz, CH_3), 2.36 (s, 3 H, Ar- CH_3), 4.17 (q, 2 H, $^3J_{\text{H,H}}$ = 7.1 Hz, CH_2CH_3), 4.40 (s, 2 H, CH_2), 7.17-7.28 (m, 3 H, 3xAr-CH), 7.37-7.40 (m, 1 H, 1xAr-CH), 8.07 (s, 1 H, CH) ppm; **$^{13}\text{C-NMR}$** (400 MHz, CDCl_3) δ = 14.2 (CH_3), 20.0 (Ar- CH_3), 42.1 (CH_2), 62.3 (CH_2), 122.6 (Ar-C), 126.7 (Ar-CH), 127.7 (Ar-CH), 130.7 (Ar-CH), 131.2 (Ar-CH), 132.3 (Ar-C), 132.8 (CH), 139.3 (Ar-C) 165.5 ($\text{C}=\text{O}$), 166.4 ($\text{C}=\text{O}$), 168.0 (COOEt) ppm; **ESI-MS** m/z (%) = 306.1 $[\text{M}+\text{H}]^+$ (100 %), 323.1 $[\text{M}+\text{NH}_4]^+$ (35 %), 328.1 $[\text{M}+\text{Na}]^+$ (25 %), 344.0 $[\text{M}+\text{K}]^+$ (10 %), 628.2 $[2\text{M}+\text{NH}_4]^+$ (100 %), 633.1 $[2\text{M}+\text{Na}]^+$ (60 %), 649.1 $[2\text{M}+\text{K}]^+$ (15 %); **HR-MS** m/z = 306.0798 $[\text{M}+\text{H}]^+$ (calculated: 306.0795); **HPLC-Analysis (Method B)**: 85 %, R_t = 19.6 min.

Ethyl 2-[(5Z)-5-[(3-methylphenyl)methylidene]-2,4-dioxo-1,3-thiazolidin-3-yl] acetate **7c**

TLC R_f = 0.6 (Hexane/EtOAc 8:2); **Reaction time**: 16 h; **Purification**: Flash-Chromatography Hexane \rightarrow Hexane/EtOAc 95:5 (R_f = 0.2), ; **Yield**: 82 mg of white solid (0.27 mmol, 71 %); **$^1\text{H-NMR}$** (400 MHz, CDCl_3) δ = 1.30 (t, 3 H, $^3J_{\text{H,H}}$ = 7.1 Hz, CH_2CH_3), 2.41 (s, 3 H, CH_3), 4.25 (q, 2 H, $^3J_{\text{H,H}}$ = 7.1 Hz, CH_2CH_3), 4.48 (s, 2 H, CH_2), 7.25-7.28 (m, 1 H, Ar-CH), 7.31-7.40 (m, 3 H, 3xAr-CH), 7.91 (s, 1 H, CH) ppm; **$^{13}\text{C-NMR}$** (400 MHz, CDCl_3) δ = 14.2 (CH_2CH_3), 21.6 (CH_3) 42.3 (CH_2), 62.3 (CH_2CH_3), 120.9 (Ar-C), 127.5 (Ar-CH), 129.3 (Ar-CH), 131.2 (Ar-CH), 131.8 (Ar-CH), 133.2 (Ar-C), 135.1 (CH), 139.2 (Ar-C), 165.8 ($\text{C}=\text{O}$), 166.4 ($\text{C}=\text{O}$), 167.8 (COOEt) ppm; **ESI-MS** m/z (%) = 306.1 $[\text{M}+\text{H}]^+$ (100 %), 323.1 $[\text{M}+\text{NH}_4]^+$ (45 %), 633.1 $[2\text{M}+\text{Na}]^+$ (15 %); **HR-MS** m/z = 306.0798 $[\text{M}+\text{H}]^+$ (calculated: 306.0795); **HPLC-Analysis (Method B)**: 98 %, R_t = 18.5 min.

Ethyl 2-[(5Z)-5-[(4-methylphenyl)methylidene]-2,4-dioxo-1,3-thiazolidin-3-yl] acetate **7d**^[165]

TLC R_f = 0.6 (Hexane/EtOAc 8:2); **Reaction time**: 16 h; **Purification**: Flash-Chromatography Hexane/EtOAc 95:5 (R_f = 0.1); **Yield**: 211 mg of white solid (0.69 mmol, 71 %); **$^1\text{H-NMR}$** (400 MHz, CDCl_3) δ = 1.14 (t, 3 H, $^3J_{\text{H,H}}$ = 7.1 Hz, CH_2CH_3), 2.25 (s, 3 H, CH_3), 4.09 (d, 2 H, $^3J_{\text{H,H}}$ = 7.1 Hz, CH_2CH_3), 4.32 (s, 2 H, CH_2), 7.13 (d, 2 H, $^3J_{\text{H,H}}$ = 8.2 Hz, 2,6-Ar-CH), 7.26 (d, 2 H, $^3J_{\text{H,H}}$ = 8.2 Hz, 3,5-Ar-CH), 7.75 (s, 1 H, CH) ppm; **$^{13}\text{C-NMR}$** (400 MHz, CDCl_3) δ = 14.2 (CH_2CH_3), 21.7 (Ar- CH_3), 42.2 (CH_2), 62.2 (CH_2CH_3), 119.8 (Ar-C), 130.1 (2,6-Ar-CH), 130.4 (3,5-Ar-CH), 130.5 (Ar-C), 134.8 (CH), 141.6 (Ar-C), 165.8 ($\text{C}=\text{O}$), 166.4 ($\text{C}=\text{O}$), 167.7 ($\text{C}=\text{OOEt}$) ppm; **ESI-MS** m/z (%) = 306.1 $[\text{M}+\text{H}]^+$ (100 %), 323.1 $[\text{M}+\text{NH}_4]^+$ (60 %), 628.2 $[2\text{M}+\text{NH}_4]^+$ (25 %); **HR-MS** m/z = 306.0798 $[\text{M}+\text{H}]^+$ (calculated: 306.0795); **HPLC-Analysis (Method B)**: 98 %, R_t = 18.5 min.

Ethyl 2-[(5Z)-2,4-dioxo-5-[2-(trifluoromethyl)phenyl]methylidene-1,3-thiazolidin-3-yl] acetate **7e**

TLC R_f = 0.4 (Hexane/EtOAc 8:2); **Reaction time**: 8 h; **Purification**: Flash-Chromatography Hexane/EtOAc 9:1 (R_f = 0.3), loaded in DCM; **Yield**: 143 mg of white solid (0.40 mmol, 87 %); **$^1\text{H-NMR}$** (400 MHz, CDCl_3) δ = 1.31 (t, 3 H, $^3J_{\text{H,H}}$ = 7.1 Hz, CH_3), 4.26 (q, 2 H, $^3J_{\text{H,H}}$ = 7.1 Hz,

CH_2CH_3), 4.48 (s, 2 H, CH_2), 7.52-7.57 (m, 1 H, 4-Ar-CH), 7.62-7.70 (m, 2 H, 5,6-Ar-CH), 7.78 (d, 1 H, $^3J_{\text{H,H}} = 7.8$ Hz, 3-Ar-CH), 8.20 (q, 1 H, $^5J_{\text{H,F}} = 1.9$ Hz, CH) ppm; $^{13}\text{C-NMR}$ (400 MHz, CDCl_3) $\delta = 14.2$ (CH_3), 42.3 (CH_2), 62.4 (CH_2CH_3), 123.7 (q, $^1J_{\text{C,F}} = 274.1$ Hz, CF_3), 126.1 (Ar-C), 126.9 (q, $^3J_{\text{C,F}} = 5.4$ Hz, 3-Ar-CH), 129.0 (6-Ar-CH), 129.9 (q, $^2J_{\text{C,F}} = 30.7$ Hz, 2-Ar-C), 130.1 (4-Ar-CH), 130.6 (q, $^4J_{\text{C,F}} = 1.9$ Hz, CH), 132.1 (q, $^3J_{\text{C,F}} = 1.7$ Hz, 1-Ar-C), 132.5 (5-Ar-CH), 164.8 ($\text{C}=\text{O}$), 166.3 ($\text{C}=\text{O}$), 167.3 (COOEt) ppm; **ESI-MS** m/z (%) = 360.1 $[\text{M}+\text{H}]^+$ (100 %), 377.1 $[\text{M}+\text{NH}_4]^+$ (60 %), 382.0 $[\text{M}+\text{Na}]^+$ (30 %), 741.1 $[\text{2M}+\text{Na}]^+$ (100 %); **HR-MS** m/z = 360.0519 $[\text{M}+\text{H}]^+$ (calculated: 360.0512); **HPLC-Analysis (Method B)**: 98 %, $R_t = 18.8$ min. Ethyl 2-[(5Z)-2,4-dioxo-5-[3-(trifluoromethyl)phenyl]methylidene-1,3-thiazolidin-3-yl] acetate **7f** **TLC** $R_f = 0.5$ (Hexane/EtOAc 8:2); **Reaction time**: 72 h; **Purification**: Flash-Chromatography Hexane/EtOAc 9:1 ($R_f = 0.3$), loaded in DCM; **Yield**: 160 mg of yellow solid (0.45 mmol, 52 %); $^1\text{H-NMR}$ (400 MHz, CDCl_3) $\delta = 1.30$ (t, 3 H, $^3J_{\text{H,H}} = 7.1$ Hz, CH_3), 4.25 (q, 2 H, $^3J_{\text{H,H}} = 7.1$ Hz, CH_2CH_3), 4.49 (s, 2 H, CH_2), 7.60-7.63 (m, 1 H, 5-Ar-CCH), 7.68-7.71 (m, 2 H, 4,6-Ar-CH), 7.75 (s, 1 H, 2-Ar-CC), 7.94 (s, 1 H, CH) ppm; $^{13}\text{C-NMR}$ (400 MHz, CDCl_3) $\delta = 14.2$ (CH_3), 42.4 (CH_2), 62.4 (CH_2CH_3), 123.5 (Ar-C), 123.7 (q, $^1J_{\text{C,F}} = 272.8$ Hz, CF_3), 127.1 (q, $^3J_{\text{C,F}} = 3.9$ Hz, 2 or 4-CH), 127.2 (q, $^3J_{\text{C,F}} = 3.7$ Hz, 2 or 4-CH), 130.0 (5-Ar-CH), 132.0 (q, $^2J_{\text{C,F}} = 32.9$ Hz, 3-Ar-CCF₃), 132.7 (CH), 132.8 (6-Ar-CH), 134.0 (Ar-C), 165.4 ($\text{C}=\text{O}$), 166.2 ($\text{C}=\text{O}$), 166.9 (COOEt) ppm; **ESI-MS** m/z (%) = 360.1 $[\text{M}+\text{H}]^+$ (90 %), 377.1 $[\text{M}+\text{NH}_4]^+$ (100 %), 382.0 $[\text{M}+\text{Na}]^+$ (12 %), 736.1 $[\text{2M}+\text{H}]^+$ (11 %), 741.1 $[\text{2M}+\text{Na}]^+$ (18 %); **HPLC-Analysis (Method B)**: 98 %, $R_t = 18.8$ min.

Ethyl 2-[(5Z)-5-[3-(benzyloxy)phenyl]methylidene-2,4-dioxo-1,3-thiazolidin-3-yl] acetate **7h**^[276] **TLC** $R_f = 0.5$ (Hexane/EtOAc 8:2); **Reaction time**: 4 h; **Purification**: Flash-Chromatography Hexane/EtOAc 9:1 ($R_f = 0.3$), loaded in DCM; **Yield**: 430 mg of white solid (1.08 mmol, 88 %); $^1\text{H-NMR}$ (400 MHz, CDCl_3) $\delta = 1.28$ (t, 3 H, $^3J_{\text{H,H}} = 7.1$ Hz, CH_3), 4.23 (q, 2 H, $^3J_{\text{H,H}} = 7.1$ Hz, CH_2CH_3), 4.45 (s, 2 H, CH_2), 5.09 (s, 2 H, CH_2), 7.03-7.06 (m, 2 H, 2,4-Ar-CH), 7.09 (d, 1 H, $^3J_{\text{H,H}} = 8.1$ Hz, 6-Ar-CH), 7.30-7.45 (m, 6 H, 6xAr-CH), 7.86 (s, 1 H, CH) ppm; $^{13}\text{C-NMR}$ (400 MHz, CDCl_3) $\delta = 14.1$ (CH_3), 42.2 (CH_2), 62.2 (CH_2CH_3), 70.2 (CH_2), 116.0 (2-Ar-CH), 117.8 (4-Ar-CH), 121.4 (Ar-C), 123.1 (6-Ar-CH), 127.5 (2xAr-CH), 128.3 (Ar-CH), 128.8 (2xAr-CH), 130.4 (Ar-CH), 134.4 (Ar-C), 134.6 (CCH), 136.4 (Ar-C), 159.2 (Ar-C), 165.5 ($\text{C}=\text{O}$), 166.3 ($\text{C}=\text{O}$), 167.4 (COOEt) ppm; **ESI-MS** m/z (%) = 398.1 $[\text{M}+\text{H}]^+$ (100 %), 415.1 $[\text{M}+\text{NH}_4]^+$ (24 %), 420.1 $[\text{M}+\text{Na}]^+$ (4 %), 812.2 $[\text{2M}+\text{NH}_4]^+$ (13 %); **HPLC-Analysis (Method B)**: 99 %, $R_t = 20.3$ min.

Ethyl 2-[(5Z)-5-[4-(benzyloxy)phenyl]methylidene-2,4-dioxo-1,3-thiazolidin-3-yl] acetate **7i** **TLC** $R_f = 0.7$ (Hexane/EtOAc 8:2); **Reaction time**: 8 h; **Purification**: Filtration from Ethanol; **Yield**: 245 mg of white solid (0.62 mmol, 50 %); $^1\text{H-NMR}$ (400 MHz, CDCl_3) $\delta = 1.30$ (t, 3 H, $^3J_{\text{H,H}} = 7.1$ Hz, CH_2), 4.25 (q, 2 H, $^3J_{\text{H,H}} = 7.1$ Hz, CH_2CH_3), 4.48 (s, 2 H, CH_2), 5.14 (s, 2 H, CH_2), 7.07 (d, 2 H, $^3J_{\text{H,H}} = 8.8$ Hz, 3,5-Ar-CH), 7.33-7.46 (m, 5 H, 5xAr-CH), 7.48 (d,

2 H, $^3J_{\text{H,H}} = 8.8 \text{ Hz}$, 2,6-Ar-CH), 7.89 (s, 1 H, CH) ppm; $^{13}\text{C-NMR}$ (400 MHz, CDCl_3) $\delta = 14.2$ (CH₃), 42.2 (CH₂), 62.3 (CH₂CH₃), 70.4 (CH₂), 115.8 (3,5-Ar-CH), 118.2 (Ar-C), 126.1 (Ar-C), 127.6 (2xAr-CH), 128.5 (Ar-CH), 128.9 (2xAr-CH) 132.5 (2,6-Ar-CH), 134.7 (CH), 136.2 (Ar-C), 160.9 (Ar-C), 165.9 (Ar-C=O), 166.5 (C=O), 167.8 (COOEt) ppm; **ESI-MS** m/z (%) = 398.1 [M+H]⁺ (100 %), 415.1 [M+NH₄]⁺ (21 %), 420.1 [M+Na]⁺ (6 %), 812.2 [2M+NH₄]⁺ (34 %), 817.2 [2M+Na]⁺ (3 %); **HPLC-Analysis (Method B)**: 99 %, $R_t = 20.3 \text{ min}$.

Ethyl 2-[(5Z)-5-[3,4-bis(benzyloxy)phenyl]methylidene-2,4-dioxo-1,3-thiazolidin-3-yl] acetate **7j**
TLC $R_f = 0.5$ (Hexane/EtOAc 8:2); **Reaction time**: 16 h; **Purification**: Filtration from ethanol; **Yield**: 200 mg of white solid (0.40 mmol, 67 %); $^1\text{H-NMR}$ (400 MHz, CDCl_3) $\delta = 1.29$ (t, 3 H, $^3J_{\text{H,H}} = 7.1 \text{ Hz}$, CH₃), 4.23 (q, 2 H, $^3J_{\text{H,H}} = 7.1 \text{ Hz}$, CH₂), 4.45 (s, 2 H, CH₂), 5.23, 5.25 (0, s H, $^1J = \text{CH}_2$,) 6.97-7.09 (m, 3 H, 3xAr-CH), 7.31-7.48 (m, 11 H, 11xAr-CH), 7.79 (s, 1 H, CH) ppm; $^{13}\text{C-NMR}$ (400 MHz, CDCl_3) $\delta = 14.3$ (CH₃), 42.2 (CH₂), 62.3 (CH₂CH₃), 71.1 (OCH₂), 71.4 (OCH₂), 114.3 (Ar-CH), 116.0 (Ar-CH), 118.5 (Ar-C), 125.6 (Ar-CH), 126.4 (Ar-C), 127.3 (3xAr-CH), 128.8 (Ar-CH), 128.9 (2xAr-CH), 134.8 (CH), 136.5 (Ar-C), 136.6 (Ar-C), 149.0 (Ar-C), 151.4 (Ar-C), 166.4 (C=O), 167.6 (C=O) ppm; **ESI-MS** m/z (%) = 504.1 [M+H]⁺ (100 %), 521.2 [M+NH₄]⁺ (75 %), 526.1 [M+Na]⁺ (40 %), 542.1 [M+K]⁺ (10 %), 1024.3 [2M+NH₄]⁺ (100 %), 1029.3 [2M+Na]⁺ (40 %), 1045.2 [2M+K]⁺ (10 %); **HR-MS** $m/z = 504.1469$ [M+H]⁺ (calculated: 504.1475).

Ethyl 2-[(5Z)-5-[(3,4-dihydroxyphenyl)methylidene]-2,4-dioxo-1,3-thiazolidin-3-yl] acetate **7k**
TLC $R_f = 0.1$ ($\text{CHCl}_3/\text{MeOH}/\text{HOAc}$ 96:3:1); **Reaction time**: 1 h; **Purification**: Flash-Chromatography $\text{CHCl}_3/\text{MeOH}/\text{HOAc}$ 95:4:1 ($R_f = 0.2$); **Yield**: 465 mg of white solid (1.44 mmol, 58 %); **Yield**: 202 mg of white solid (0.62 mmol, 31 %); $^1\text{H-NMR}$ (400 MHz, MeOD) $\delta = 1.26$ (t, 3 H, $^3J_{\text{H,H}} = 7.1 \text{ Hz}$, CH₃), 4.21 (q, 2 H, $^3J_{\text{H,H}} = 7.1 \text{ Hz}$, CH₂), 4.44 (s, 2 H, CH₂), 6.85 (d, 1 H, $^3J_{\text{H,H}} = 8.2 \text{ Hz}$, 5-Ar-CH), 6.95 (d, 1 H, $^3,4J_{\text{H,H}} = 2.1, 8.2 \text{ Hz}$, 6-Ar-CH), 7.00 (d, 1 H, $^4J_{\text{H,H}} = 2.1 \text{ Hz}$, 2-Ar-CH), 7.73 (s, 1 H, CH) ppm; $^{13}\text{C-NMR}$ (400 MHz, CDCl_3) $\delta = 1.31$ (t, 3 H, $^3J_{\text{H,H}} = 7.1 \text{ Hz}$, CH₃), 4.26 (q, 2 H, $^3J_{\text{H,H}} = 7.1 \text{ Hz}$, CH₂CH₃), 4.48 (s, 2 H, CH₂), 5.70 (s(br), 1 H, OH), 5.95 (s(br), 1 H, OH), 6.95 (d, 1 H, $^3J_{\text{H,H}} = 8.5 \text{ Hz}$, 5-Ar-CH), 6.98-7.03 (m, 2 H, 2,6-Ar-CH), 7.78 (s, 1 H, CH) ppm; $^{13}\text{C-NMR}$ (400 MHz, MeOD) $\delta = 14.4$ (CH₃), 42.9 (CH₂), 63.1 (CH₂CH₃), 116.9 (5-Ar-CH), 117.6 (2-Ar-CH), 125.7 (6-Ar-CH), 126.2 (Ar-C), 136.2 (CH), 147.1 (Ar-C), 150.1 (Ar-C), 167.1 (Ar-C), 168.4 (C=O), 169.0 (C=O) ppm; **ESI-MS** m/z (%) = 324.1 [M+H]⁺ (100 %), 341.1 [M+NH₄]⁺ (20 %), 664.1 [2M+NH₄]⁺ (25 %); **HR-MS** $m/z = 324.0540$ [M+H]⁺ (calculated: 324.0536); **HPLC-Analysis (Method B)**: 95 %, $R_t = 14.3 \text{ min}$.

9.4 General procedure for 3-(4-oxo-2-sulfanylidene-1,3-thiazolidin-3-yl) propanoic/ butanoic acid **12** and **13**

β -alanine or γ -aminobutyric acid (30 mmol), carbon disulphide (30 mmol) and sodium acetate (30 mmol) were dissolved in 100 mL water. The reaction mixture was stirred 16 h at rt, after which bromo acetic acetate (30 mmol) were added. The reaction mixture turned red, while stirring was continued for another 3 h at rt. The mixture was acidified by addition of 30 mL HCl (6 N). The resulting red suspension was stirred 16 h at 100 °C. Upon cooling red crystals formed and were filtered then washed with water. The crude was concentrated and re-crystallized from HCl_{aq}. 3-(4-oxo-2-sulfanylidene-1,3-thiazolidin-3-yl) propanoic acid **12**^[277]

Purification: Re-crystallisation from HCl_{aq}; **Yield:** 8165 mg of red crystals (39.78 mmol, 80 %); **Yield:** 1655 mg of red crystals (8.06 mmol, 72 %); **Yield:** 3988 mg of red crystals (19.43 mmol, 65 %); **¹H-NMR** (400 MHz, CDCl₃) δ = 2.76 (t, 2 H, $^3J_{H,H}$ = 7.6 Hz, β -CH₂), 4.00 (s, 2 H, CH₂), 4.30 (t, 2 H, $^3J_{H,H}$ = 7.6 Hz, α -CH₂) ppm; **¹H-NMR** (400 MHz, DMSO-d₆) δ = 2.48-2.54 (m, 2 H, α -CH₂), 4.03-4.08 (m, 2 H, β -CH₂), 4.22 (s, 2 H, CH₂), 12.5 (s(br), 1 H, COOH) ppm; **¹³C-NMR** (400 MHz, DMSO-d₆) δ = 30.6 (α -CH₂), 36.0 (CH₂), 39.6 (β -CH₂), 171.8 (C=O), 174.3 (COOH), 203.0 (C=S) ppm; **ESI-MS** m/z (%) = 204.0 [M-H]⁻ (100 %); **HPLC-Analysis (Method B):** 98 %, R_t = 8.4 min.

4-(4-oxo-2-sulfanylidene-1,3-thiazolidin-3-yl)butanoic acid **103**butycooh^[278]

TLC R_f = 0.4 (Hexane/EtOAc/HOAc 1:1:0.01); **Purification:** Re-crystallisation from HCl_{aq}; **Yield:** 4461 mg of yellow solid (20.34 mmol, 68 %); **¹H-NMR** (400 MHz, DMSO-d₆) δ = 1.79 (ap, 2 H, $^3J_{H,H}$ = 7.0, 7.4 Hz, β -CH₂), 2.25 (t, 2 H, $^3J_{H,H}$ = 7.4 Hz, γ -CH₂), 3.90 (t, 2 H, $^3J_{H,H}$ = 7.0 Hz, α -CH₂), 4.22 (s, 2 H, CH₂), 12.12 (s, 1 H, COOH) ppm; **¹³C-NMR** (400 MHz, DMSO-d₆) δ = 21.9 (CH₂), 30.9 (CH₂), 35.9 (CH₂), 43.3 (CH₂), 173.8 (C=O), 174.6 (COOH), 203.5 (C=S) ppm; **ESI-MS** m/z (%) = 218.0 [M-H]⁻ (100 %).

Knoevenagel condensation of **12** and **13** with various benzaldehydes: Derivatives **12a–m** and **13a–d**

Compound **12** or **13** (1.0 eq), the benzaldehyde derivatives (1.1-1.5 eq) and sodium acetate (1.0 eq) were dissolved in 5-10 mL ethanol. The reaction mixture was stirred at 80 °C for 2-16 h. Upon cooling a precipitate formed and was filtered then washed with ethanol.

3-[(5Z)-4-oxo-5-(phenylmethylidene)-2-sulfanylidene-1,3-thiazolidin-3-yl] propanoic acid **12a**^[279]

TLC R_f = 0.6 (Hexane/EtOAc/HOAc 1:1:0.01); **Reaction time:** 4 h; **Purification:** Filtration from ethanol; **Yield:** 287 mg of orange solid (0.98 mmol, 80 %); **¹H-NMR** (400 MHz, DMSO-d₆) δ = 2.33-2.39 (m, 2 H, β -CH₂), 4.13-4.19 (m, 2 H, α -CH₂), 7.49-7.59 (m, 3 H, 3xAr-CH), 7.62-7.66 (m, 2 H, 2xAr-CH), 7.81 (s, 1 H, CH) ppm; **¹³C-NMR** (400 MHz, DMSO-d₆) δ = 32.8 (β -CH₂), 41.5 (α -CH₂), 122.6 (Ar-C), 129.5 (2xAr-CH), 130.6 (2xAr-CH), 130.9 (Ar-CH),

132.7 (CH), 133.1 (Ar-C), 166.8 (C=O), 172.4 (COOH), 193.2 (C=S) ppm; **ESI-MS** m/z (%) = 292.0 [$M-H$]⁻ (100 %), 585.0 [$2M-H$]⁻ (100 %), 607.0 [$2M+Na-2H$]⁻ (20 %); **HR-MS** m/z = 292.0113 [$M-H$]⁻ (calculated: 292.0108); **HPLC-Analysis (Method B)**: 98 %, R_t = 18.4 min. 3-[(5Z)-5-[(2-methylphenyl)methylidene]-4-oxo-2-sulfanylidene-1,3-thiazolidin-3-yl] propanoic acid **12b**^[280]

TLC R_f = 0.4 (Hexane/EtOAc/HOAc 1:1:0.01); **Reaction time**: 2h; **Purification**: Filtration from ethanol **Yield**: 326 mg of orange solid (1.06 mmol, 87 %); **¹H-NMR** (400 MHz, DMSO- d_6) δ = 2.22-2.27 (m, 2 H, β -CH₂), 2.43 (s, 3 H, CH₃), 4.11-4.17 (m, 2 H, α -CH₂), 7.34-7.43 (m, 4 H, 4xAr-CH), 7.88 (s, 1 H, CH) ppm; **¹³C-NMR** (400 MHz, DMSO- d_6) δ = 19.5 (CH₃), 34.3 (β -CH₂), 42.5 (α -CH₂), 124.2 (Ar-C), 126.9 (Ar-CH), 127.8 (Ar-CH), 130.3 (CH), 130.8 (Ar-CH), 131.2 (Ar-CH), 132.1 (Ar-C), 139.2 (Ar-C), 166.6 (C=O), 172.8 (COOH), 193.7 (C=S) ppm; **ESI-MS** m/z (%) = 306.0 [$M-H$]⁻ (100 %), 613.1 [$2M-H$]⁻ (71 %); **ESI-MS** m/z (%) = 306.0 [$M-H$]⁻ (54 %), 613.1 [$2M-H$]⁻ (100 %); **HPLC-Analysis (Method B)**: 96 %, R_t = 19.3 min.

3-[(5Z)-5-[(3-methylphenyl)methylidene]-4-oxo-2-sulfanylidene-1,3-thiazolidin-3-yl] propanoic acid **12c**^[280]

TLC R_f = 0.4 (Hexane/EtOAc/HOAc 1:1:0.01); **Reaction time**: 3.5 h; **Purification**: Filtration from ethanol; **Yield**: 367 mg of yellow solid (1.19 mmol, 98 %); **¹H-NMR** (400 MHz, DMSO- d_6) δ = 2.28-2.34 (m, 2 H, β -CH₂), 2.38 (s, 3 H, CH₃), 4.12-4.18 (m, 2 H, α -CH₂), 7.31-7.36 (m, 1 H, Ar-CH), 7.41-7.46 (m, 3 H, 3xAr-CH), 7.75 (s, 1 H, CH) ppm; **¹³C-NMR** (400 MHz, DMSO- d_6) δ = 20.9 (CH₃), 33.6 (β -CH₂), 42.0 (α -CH₂), 122.5 (Ar-C), 127.9 (Ar-CH), 129.4 (Ar-CH), 131.0 (Ar-CH), 131.7 (Ar-C), 132.8 (Ar-CH), 133.1 (CH), 138.9 (Ar-C), 166.8 (C=O), 172.6 (COOH), 193.3 (C=S) ppm; **ESI-MS** m/z (%) = 306.0 [$M-H$]⁻ (100 %), 613.1 [$2M-H$]⁻ (52 %); **HPLC-Analysis (Method B)**: 97 %, R_t = 17.6 min.

3-[(5Z)-5-[(4-methylphenyl)methylidene]-4-oxo-2-sulfanylidene-1,3-thiazolidin-3-yl] propanoic acid **12d**^[280]

TLC R_f = 0.5 (Hexane/EtOAc/HOAc 1:1:0.01); **Reaction time**: 3 h; **Purification**: Filtration from ethanol; **Yield**: 363 mg of yellow solid (1.18 mmol, 97 %); **¹H-NMR** (400 MHz, DMSO- d_6) δ = 2.36 (s, 3 H, CH₃), 2.42-2.48 (m, 2 H, β -CH₂), 4.14-4.20 (m, 2 H, α -CH₂), 7.37 (d, 2 H, ³ $J_{H,H}$ = 8.2 Hz, 3,5-Ar-CH), 7.54 (d, 2 H, ³ $J_{H,H}$ = 8.2 Hz, 2,6-Ar-CH), 7.77 (s, 1 H, CH) ppm; **¹³C-NMR** (400 MHz, DMSO- d_6) δ = 21.2 (CH₃), 32.3 (β -CH₂), 41.1 (α -CH₂), 121.3 (Ar-C), 130.2 (3,5-Ar-CH), 130.3 (Ar-C), 130.8 (2,6-Ar-CH), 133.0 (CH), 141.5 (Ar-C), 166.8 (C=O), 172.2 (COOH), 193.2 (C=S) ppm; **ESI-MS** m/z (%) = 306.0 [$M-H$]⁻ (86 %), 613.1 [$2M-H$]⁻ (100 %); **HPLC-Analysis (Method B)**: 98 %, R_t = 19.5 min.

3-[(5Z)-4-oxo-2-sulfanylidene-5-[2-(trifluoromethyl)phenyl]methylidene-1,3-thiazolidin-3-yl] propanoic acid **12e**

TLC R_f = 0.3 (Hexane/EtOAc/HOAc 6:4:0.01); **Reaction time**: 4 h; **Purification**: Filtration from ethanol; **Yield**: 257 mg of yellow solid (0.71 mmol, 58 %); **¹H-NMR** (400 MHz, DMSO- d_6)

δ = 2.23-2.30 (m, 2 H, β -CH₂), 4.11-4.17 (m, 2 H, α -CH₂), 7.68-7.75 (m, 2 H, 4,6-Ar-CH), 7.80 (q, 1 H, $^5J_{H,F}$ = 1.9 Hz, CH), 7.87 (at, 1 H, $^3J_{H,H}$ = 7.6, 7.7 Hz, 5-Ar-CH), 7.92 (d, 1 H, $^3J_{H,H}$ = 7.7 Hz, 3-Ar-CH) ppm; **¹³C-NMR** (400 MHz, DMSO-d₆) δ = 34.1 (β -CH₂), 42.5 (α -CH₂), 123.9 (q, $^1J_{C,F}$ = 274.2 Hz, CF₃), 126.2 (CH), 127.0 (q, $^3J_{C,F}$ = 5.7 Hz, 3-Ar-CH), 127.7 (Ar-C), 128.1 (Ar-C), 129.5 (6-Ar-CH), 130.8 (4-Ar-CH), 131.2 (Ar-C), 133.6 (5-Ar-CH), 163.3 (C=O), 172.7 (COOH), 193.2 (C=S) ppm; **ESI-MS** m/z (%) = 360.0 [M-H]⁻ (100 %), 721.0 [2M-H]⁻ (100 %); **HR-MS** m/z = 359.9974 [M-H]⁻ (calculated: 359.9981); **HPLC-Analysis (Method B)**: 96 %, R_t = 11.8 min.

3-[(5Z)-4-oxo-2-sulfanylidene-5-[3-(trifluoromethyl)phenyl]methylidene-1,3-thiazolidin-3-yl] propanoic acid **12f**

TLC R_f = 0.5 (DCM/MeOH/HOAc 9:1:0.01); **Reaction time**: 2 h; **Purification**: Filtration from ethanol; **Yield**: 305 mg of yellow solid (0.84 mmol, 69 %); **¹H-NMR** (400 MHz, DMSO-d₆) δ = 2.26-2.32 (m, 2 H, β -CH₂), 4.12-4.18 (m, 2 H, α -CH₂), 7.79 (at, 1 H, $^3J_{H,H}$ = 7.8 Hz, 5-Ar-CH), 7.84-7.91 (m, 2 H, 4,6-Ar-CH), 7.92 (s, 1 H, CH), 8.04 (s(br), 1 H, 2-Ar-CH) ppm; **¹³C-NMR** (400 MHz, DMSO-d₆) δ = 33.7 (β -CH₂), 42.2 (α -CH₂), 124.9 (4 or 6-Ar-CH), 127.5 (2-Ar-CH), 130.7 (CH and 4-Ar-CH), 133.2 (4 or 6-Ar-CH), 134.2 (Ar-C), 166.7 (C=O), 172.5 (COOH), 192.8 (C=S) ppm; **ESI-MS** m/z (%) = 360.0 [M-H]⁻ (100 %), 721.0 [2M-H]⁻ (100 %); **HR-MS** m/z = 359.9976 [M-H]⁻ (calculated: 359.9981); **HPLC-Analysis (Method B)**: 94 %, R_t = 18.8 min.

3-[(5Z)-5-[2,5-bis(trifluoromethyl)phenyl]methylidene-4-oxo-2-sulfanylidene-1,3-thiazolidin-3-yl] propanoic acid **12g**

TLC R_f = 0.6 (DCM/MeOH/HOAc 9:1:0.01); **Reaction time**: 2 h; **Purification**: Filtration from ethanol; **Yield**: 98 mg of yellow solid (0.23 mmol, 19 %); **¹H-NMR** (400 MHz, DMSO-d₆) δ = 2.18-2.24 (m, 2 H, β -CH₂), 4.10-4.16 (m, 2 H, α -CH₂), 7.77 (q, 1 H, $^5J_{H,F}$ = 2.1 Hz, CH), 7.99 (s, 1 H, 6-Ar-CH), 8.10 (d, 1 H, $^3J_{H,H}$ = 8.3 Hz, 4-Ar-CH), 8.16 (d, 1 H, $^3J_{H,H}$ = 8.3 Hz, 5-Ar-CH) ppm; **¹³C-NMR** (400 MHz, DMSO-d₆) δ = 34.3 (β -CH₂), 42.7 (α -CH₂), 124.9 (CH), 125.9 (6-Ar-CH), 127.4 (4-Ar-CH), 128.4 (5-Ar-CH) ppm; **ESI-MS** m/z (%) = 428.0 [M-H]⁻ (100 %), 857.0 [M-H]⁻ (20 %); **HPLC-Analysis (Method B)**: 84 %, R_t = 19.5 min.

3-[(5Z)-5-[4-(dimethylamino)phenyl]methylidene-4-oxo-2-sulfanylidene-1,3-thiazolidin-3-yl] propanoic acid **12h**^[281]

TLC R_f = 0.3 (Hexane/EtOAc/HOAc 6:4:0.01); **Reaction time**: 4 h; **Purification**: Filtration from ethanol; **Yield**: 330 mg of red solid (0.98 mmol, 80 %); **¹H-NMR** (400 MHz, DMSO-d₆) δ = 2.36-2.42 (m, 2 H, β -CH₂), 3.04 (s, 6 H, 2xCH₃), 4.13-4.18 (m, 2 H, α -CH₂), 6.83 (d, 2 H, $^3J_{H,H}$ = 9.1 Hz, 3,5-Ar-CH), 7.46 (d, 2 H, $^3J_{H,H}$ = 9.1 Hz, 2,6-Ar-CH), 7.67 (s, 1 H, CH) ppm; **¹³C-NMR** (400 MHz, DMSO-d₆) δ = 32.8 (β -CH₂), 39.6 (N(CH₃)₂), 41.2 (α -CH₂), 112.3 (3,5-Ar-CH), 114.1 (Ar-C), 119.9 (Ar-C), 133.2 (2,6-Ar-CH), 134.4 (CH), 151.9 (Ar-C), 166.8 (C=O), 172.3 (C=OOH), 192.4 (C=S) ppm; **ESI-MS** m/z (%) = 335.1 [M-H]⁻ (100 %), 671.1 [2M-H]⁻

(58 %); **HPLC-Analysis (Method B)**: 99 %, R_t = 21.2 min.

3-[(5Z)-5-[(4-chlorophenyl)methylidene]-4-oxo-2-sulfanylidene-1,3-thiazolidin-3-yl]propanoic acid **12i**

TLC R_f = 0.5 (Hexane/EtOAc/HOAc 1:1:0.01); **Reaction time**: 4 h; **Purification**: Filtration from ethanol; **Yield**: 333 mg of yellow solid (1.02 mmol, 83 %); **$^1\text{H-NMR}$** (400 MHz, DMSO- d_6) δ = 2.13-2.20 (m, 2 H, $\beta\text{-CH}_2$), 4.08-4.14 (m, 2 H, $\alpha\text{-CH}_2$), 7.62 (d, 2 H, $^3J_{\text{H,H}}$ = 8.7 Hz, 2,6-Ar-CH), 7.67 (d, 3 H, $^3J_{\text{H,H}}$ = 8.7 Hz, 3,5-Ar-CH), 7.81 (s, 1 H, CH) ppm; **$^{13}\text{C-NMR}$** (400 MHz, DMSO- d_6) δ = 34.6 ($\beta\text{-CH}_2$), 42.7 ($\alpha\text{-CH}_2$), 129.6 (2,6-Ar-CH), 131.1 (CH), 132.0 (Ar-C), 132.2 (3,5-Ar-CH), 135.5 (Ar-C), 166.8 (C=O), 171.9 (C=S) ppm; **ESI-MS** m/z (%) = 326.0 [M-H] $^-$ (100 %), 653.0 [2M-H] $^-$ (80 %), 674.9 [2M+Na-H] $^-$ (100 %); **HR-MS** m/z = 325.9724 [M-H] $^-$ (calculated: 325.9718); **HPLC-Analysis (Method B)**: 81 %, R_t = 17.5 min.

3-[(5Z)-5-[(2-hydroxyphenyl)methylidene]-4-oxo-2-sulfanylidene-1,3-thiazolidin-3-yl]propanoic acid **12j**^[281]

Reaction time: 2 h; **Purification**: Filtration from ethanol; **Yield**: 35 mg of red solid (0.11 mmol, 21 %); **$^1\text{H-NMR}$** (400 MHz, DMSO- d_6) δ = 2.15-2.25 (m, 2 H, $\beta\text{-CH}_2$), 3.16-3.26 (m, 2 H, $\alpha\text{-CH}_2$), 6.92-7.38 (m, 4 H, 4xAr-CH), 7.42 (s, 1 H, CH) ppm; **ESI-MS** m/z (%) = 308.0 [M-H] $^-$ (100 %), 617.0 [2M-H] $^-$ (100 %), 639.0 [2M+Na-2H] $^-$ (95 %); **HR-MS** m/z = 308.0062 [M-H] $^-$ (calculated: 308.0057).

3-[(5Z)-5-[(3-hydroxyphenyl)methylidene]-4-oxo-2-sulfanylidene-1,3-thiazolidin-3-yl]propanoic acid **12k**^[280]

TLC R_f = 0.3 (Hexane/EtOAc/HOAc 6:4:0.01); **Reaction time**: 4 h; **Purification**: Filtration from ethanol; **Yield**: 300 mg of yellow solid (0.97 mmol, 79 %); **$^1\text{H-NMR}$** (400 MHz, DMSO- d_6) δ = 2.21-2.29 (m, 2 H, $\beta\text{-CH}_2$), 4.10-4.18 (m, 2 H, $\alpha\text{-CH}_2$), 6.88-6.95 (m, 1 H, 4-Ar-CH), 7.00-7.07 (m, 2 H, 2,6-Ar-CH), 7.28-7.36 (m, 1 H, 5-Ar-CH), 7.69 (s, 1 H, CH) ppm; **$^{13}\text{C-NMR}$** (400 MHz, DMSO- d_6) δ = 34.3 ($\beta\text{-CH}_2$), 42.5 ($\alpha\text{-CH}_2$), 116.5 (2 or 6-Ar-CH), 118.5 (4-Ar-CH), 121.6 (Ar-C), 122.3 (2,6-Ar-CH), 130.5 (5-Ar-CH), 133.0 (CH), 134.2 (Ar-C), 158.5 (Ar-C), 166.9 (C=O), 172.7 (COOH), 193.3 (C=S) ppm; **ESI-MS** m/z (%) = 308.0 [HM] $^-$ (100 %); **HR-MS** m/z = 308.0051 [M-H] $^-$ (calculated: 308.0057); **HPLC-Analysis (Method B)**: 100 %, R_t = 16.6 min.

3-[(5Z)-5-[(4-hydroxyphenyl)methylidene]-4-oxo-2-sulfanylidene-1,3-thiazolidin-3-yl]propanoic acid **12l**^[280]

TLC R_f = 0.3 (Hexane/EtOAc/HOAc 6:4:0.01); **Yield**: 320 mg of yellow solid (1.03 mmol, 85 %); **Reaction time**: 4 h; **Purification**: Filtration from ethanol; **$^1\text{H-NMR}$** (400 MHz, DMSO- d_6) δ = 2.31-2.37 (m, 2 H, $\beta\text{-CH}_2$), 4.12-4.18 (m, 2 H, $\alpha\text{-CH}_2$), 6.85 (d, 2 H, $^3J_{\text{H,H}}$ = 8.7 Hz, 3,5-Ar-CH), 7.45 (d, 2 H, $^3J_{\text{H,H}}$ = 8.7 Hz, 2,6-Ar-CH), 7.68 (s, 1 H, CH) ppm; **$^{13}\text{C-NMR}$** (400 MHz, DMSO- d_6) δ = 33.0 ($\beta\text{-CH}_2$), 41.4 ($\alpha\text{-CH}_2$), 117.0 (3,5-Ar-CH), 133.4 (2,6-Ar-CH), 133.9 (CH), 166.9 (C=O), 172.4 (COOH), 192.8 (C=S) ppm; **ESI-MS** m/z (%) = 308.0 [HM] $^-$ (100 %); **HR-MS** m/z = 308.0051 [M-H] $^-$ (calculated: 308.0057).

MS m/z = 308.0060 $[M-H]^-$ (calculated: 308.0057); **HPLC-Analysis (Method B)**: 60 %, R_t = 16.6 min.

3-[(5Z)-5-[(3,4-dihydroxyphenyl)methylidene]-4-oxo-2-sulfanylidene-1,3-thiazolidin-3-yl] propionic acid **12m**^[280]

TLC R_f = 0.1 (Hexane/EtOAc 1:1); **Reaction time**: 4 h; **Purification**: Filtration from ethanol; **Yield**: 361 mg of red solid (1.11 mmol, 91 %); **¹H-NMR** (400 MHz, DMSO- d_6) δ = 2.36-2.42 (m, 2 H, β -CH₂), 4.12-4.18 (m, 2 H, α -CH₂), 6.50-6.61 (m, 1 H, 5-Ar-CH), 6.79-6.86 (m, 1 H, 2-Ar-CH), 6.98 (dd, 1 H, $^3J_{H,H}$ = 2.4, 8.5 Hz, 6-Ar-CH), 7.51 (s, 1 H, CH) ppm; **¹³C-NMR** (400 MHz, DMSO- d_6) δ = 33.0 (β -CH₂), 41.2 (α -CH₂), 114.2 (2-Ar-CH), 116.9 (5-Ar-CH), 129.2 (6-Ar-CH), 135.2 (CH) ppm; **ESI-MS** m/z (%) = 324.0 $[M-H]^-$ (100 %), 649.0 $[2M-H]^-$ (18 %); **HPLC-Analysis (Method B)**: 94 %, R_t = 15.1 min.

4-[(5Z)-4-oxo-5-(phenylmethylidene)-2-sulfanylidene-1,3-thiazolidin-3-yl] butanoic acid **13a**^[282]

TLC R_f = 0.7 (Hexane/EtOAc/HOAc 1:1:0.01); **Reaction time**: 4 h; **Purification**: Filtration from ethanol; **Yield**: 317 mg of orange solid (1.03 mmol, 90 %); **¹H-NMR** (400 MHz, DMSO- d_6) δ = 1.83 (p, 2 H, $^3J_{H,H}$ = 7.5 Hz, β -CH₂), 2.11 (t, 2 H, $^3J_{H,H}$ = 7.5 Hz, γ -CH₂), 4.05 (t, 2 H, $^3J_{H,H}$ = 7.5 Hz, α -CH₂), 7.48-7.58 (m, 3 H, 3xAr-CH), 7.62-7.66 (m, 2 H, 2xAr-CH), 7.80 (s, 1 H, CH) ppm; **¹³C-NMR** (400 MHz, DMSO- d_6) δ = 23.0 (β -CH₂), 33.2 (γ -CH₂), 44.3 (α -CH₂), 122.6 (Ar-C), 129.5 (Ar-CH), 130.7 (Ar-CH), 130.9 (Ar-CH), 132.7 (CH), 133.1 (Ar-C), 167.1 (C=O), 174.4 (COOH), 193.6 (C=S) ppm; **ESI-MS** m/z (%) = 306.0 $[M-H]^-$ (100 %), 613.0 $[2M-H]^-$ (100 %); **HR-MS** m/z = 306.0258 $[M-H]^-$ (calculated: 306.0264); **HPLC-Analysis (Method B)**: 100 %, R_t = 18.7 min.

4-[(5Z)-5-[(2-methylphenyl)methylidene]-4-oxo-2-sulfanylidene-1,3-thiazolidin-3-yl]butanoic acid **13b**^[283]

TLC R_f = 0.1 (Hexane/EtOAc/HOAc 6:4:0.01); **Reaction time**: 3 h; **Purification**: Filtration from ethanol; **Yield**: 222 mg of yellow solid (0.69 mmol, 61 %); **¹H-NMR** (400 MHz, DMSO- d_6) δ = 1.77-1.86 (m, 2 H, β -CH₂), 2.02-2.08 (m, 2 H, γ -CH₂), 4.01-4.07 (m, 2 H, α -CH₂), 7.34-7.44 (m, 4 H, 4xAr-CH), 7.88 (s, 1 H, CH) ppm; **¹³C-NMR** (400 MHz, DMSO- d_6) δ = 19.5 (CH₃), 23.4 (β -CH₂), 33.8 (γ -CH₂), 44.5 (α -CH₂), 124.1 (Ar-C), 126.9 (Ar-CH), 127.8 (Ar-CH), 130.4 (CH), 130.8 (Ar-CH), 131.2 (Ar-CH), 132.1 (Ar-C), 139.3 (Ar-C), 166.7 (C=O), 174.6 (COOH), 194.0 (C=S) ppm; **ESI-MS** m/z (%) = 320.0 $[M-H]^-$ (100 %), 641.1 $[2M-H]^-$ (25 %), 663.1 $[2M+Na-H]^-$ (10 %); **HR-MS** m/z = 320.0413 $[M-H]^-$ (calculated: 320.0421); **HPLC-Analysis (Method B)**: 98 %, R_t = 19.5 min.

4-[(5Z)-5-[(3-methylphenyl)methylidene]-4-oxo-2-sulfanylidene-1,3-thiazolidin-3-yl] butanoic acid **13c**^[283]

TLC R_f = 0.5 (Hexane/EtOAc/HOAc 6:4:0.01); **Reaction time**: 3 h; **Purification**: Filtration from ethanol; **Yield**: 259 mg of red solid (0.81 mmol, 71 %); **¹H-NMR** (400 MHz, DMSO- d_6) δ = 1.72-1.95 (m, 2 H,) 2.09-2.24 (m, 2 H,) 2.37 (s, 3 H, Ar-CH₃), 3.97-4.12 (m, 2 H, α -CH₂),

7.27-7.53 (m, 4 H, 4xAr-CH), 7.73 (s, 1 H, CH) ppm; $^{13}\text{C-NMR}$ (400 MHz, DMSO- d_6) δ = 20.9 (CH₃), 22.7 (β -CH₂), 32.5 (γ -CH₂), 44.1 (α -CH₂), 122.3 (Ar-C), 127.9 (Ar-CH), 129.4 (Ar-CH), 131.1 (Ar-CH), 131.7 (Ar-CH), 132.8 (CH), 133.0 (Ar-C), 138.9 (Ar-C), 167.1 (C=O), 174.4 (COOEt), 193.6 (C=S) ppm; **ESI-MS** m/z (%) = 320.0 [M-H]⁻ (100 %); **HR-MS** m/z = 320.0419 [M-H]⁻ (calculated: 320.0421); **HPLC-Analysis (Method B)**: 99 %, R_t = 19.8 min.

4-[(5Z)-5-[(4-methylphenyl)methylidene]-4-oxo-2-sulfanylidene-1,3-thiazolidin-3-yl] butanoic acid **13d**^[283]

TLC R_f = 0.4 (Hexane/EtOAc/HOAc 6:4:0.01); **Reaction time**: 3 h; **Purification**: Filtration from ethanol; **Yield**: 265 mg of red solid (0.82 mmol, 72 %); $^1\text{H-NMR}$ (400 MHz, DMSO- d_6) δ = 1.77-1.86 (m, 2 H, β -CH₂), 2.07-2.14 (m, 2 H, γ -CH₂), 2.36 (s, 3 H, CH₃), 4.04 (t, 2 H, $^3J_{\text{H,H}}$ = 7.1 Hz, α -CH₂), 7.36 (d, 2 H, $^3J_{\text{H,H}}$ = 8.2 Hz, 3,5-Ar-CH), 7.53 (d, 2 H, $^3J_{\text{H,H}}$ = 8.2 Hz, 2,6-Ar-CH), 7.76 (s, 1 H, CH) ppm; $^{13}\text{C-NMR}$ (400 MHz, DMSO- d_6) δ = 21.2 (CH₃), 23.1 (β -CH₂), 33.2 (γ -CH₂), 44.3 (α -CH₂), 121.3 (Ar-C), 130.2 (3,5-Ar-CH), 130.4 (Ar-C), 130.8 (2,6-Ar-CH), 132.9 (CH), 141.4 (Ar-C), 167.1 (C=O, COOH) 193.5 (C=S) ppm; **ESI-MS** m/z (%) = 320.0 [M-H]⁻ (34 %), 641.1 [2M-H]⁻ (100 %); **HPLC-Analysis (Method B)**: 99 %, R_t = 19.8 min.

9.5 General Procedure for the synthesis of ester derivatives

14a–ab, 15a–f, and 16a–j

Method 1: Knoevenagel condensation followed by esterification reaction

Rhodanine N-Acetic acid derivatives **14**, **15**, and **16** (1.0 eq), DCC (1.5 eq) and DMAP (0.3 eq) were dissolved in methanol, ethanol or *tert*-butanol. The reaction mixture was stirred at rt for 16 h or until TLC showed complete consumption of starting material. The crude was filtered and washed with DCM. The filtrate was concentrated and purified by flash column chromatography.

(E,Z)-ethyl 2-(5-(3-methylbenzylidene)-4-oxo-2-thioxothiazolidin-3-yl) acetate **14a**

Z to E 5:1 **TLC** R_f = 0.1 (Cyclohexane/EtOAc 9:1); **Reaction time**: 16 h; **Purification**: Flash-Chromatography Cyclohexane/EtOAc 9:1 (R_f = 0.1); **Yield**: 36 mg of yellow solid (0.11 mmol, 53 %); spectra for Z-isomer $^1\text{H-NMR}$ (400 MHz, DMSO- d_6) δ = 1.21 (t, 3 H, $^3J_{\text{H,H}}$ = 7.1 Hz, CH₃), 2.39 (s, 3 H, CH₃), 4.17 (q, 2 H, $^3J_{\text{H,H}}$ = 7.1 Hz, CH₂), 4.84 (s, 2 H, CH₂), 7.36-7.42 (m, 1 H, Ar-CH), 7.44-7.53 (m, 3 H, 2xAr-CH), 7.88 (s, 1 H, CH) ppm; E and Z isomer 1:5 $^1\text{H-NMR}$ (400 MHz, CDCl₃) δ = 1.28 (t, 3 H, $^3J_{\text{H,H}}$ = 7.1 Hz, E-CH₃), 1.29 (t, 3 H, $^3J_{\text{H,H}}$ = 7.1 Hz, Z-CH₃), 2.39 (s, 3 H, E-CH₃), 2.42 (s, 3 H, Z-CH₃), 4.22 (q, 2 H, $^3J_{\text{H,H}}$ = 7.1 Hz, E-CH₂CH₃), 4.24 (q, 2 H, $^3J_{\text{H,H}}$ = 7.1 Hz, Z-CH₂CH₃), 4.82 (s, 2 H, E-CH₂), 4.85 (s, 2 H, Z-CH₂), 7.14 (s, 1 H, E-CH), 7.27 (d, 1 H, $^3J_{\text{H,H}}$ = 7.4 Hz, E,Z-Ar-CH) 7.30-7.35 (m, 2 H, 2xE,Z-Ar-CH), 7.35-7.41 (m, 2 H, E,Z-Ar-CH), 7.76 (s, 1 H, Z-CH), 7.76-7.78 (m, 1 H, E-Ar-CH), 7.81 (d, 1 H, $J_{\text{H,H}}$ = 7.7 Hz, E-Ar-CH) ppm; $^{13}\text{C-NMR}$ (400 MHz, CDCl₃) δ = 14.3 (CH₃), 21.6 (Ar-CH₃), 45.0 (CH₂), 62.2

(CH₂CH₃), 122.5 (Z-Ar-C), 128.1 (Z-Ar-CH), 128.5 (E-Ar-CH), 128.9 (E-Ar-CH), 129.4 (Z-Ar-CH), 131.5 (Z-Ar-CH), 132.1 (Z-Ar-CH), 133.3 (Z-Ar-C), 134.5 (Z-CH), 138.7 (E-CH), 139.4 (Z-Ar-C), 166.0 (C=O), 167.3 (COOEt), 193.3 (C=S) ppm; **ESI-MS** m/z (%) = 322.1 [M+H]⁺ (100 %), 339.1 [M+NH₄]⁴⁵ (; %) **HR-MS** m/z = 322.0568 [M+H]⁺ (calculated: 322.0566); **HPLC-Analysis (Method B)**: 98 %, R_t = 16.1 min; **HPLC-Analysis** : 98 %, R_t = 20.6 min.

(Z)-tert-butyl 2-(5-(3-methylbenzylidene)-4-oxo-2-thioxothiazolidin-3-yl) acetate **14b**

TLC R_f = 0.1 (Cyclohexane/EtOAc 9:1); **Reaction time**: 4 h; **Purification**: Flash-Chromatography Cyclohexane/EtOAc 9:1 (R_f = 0.1); **Yield**: 50 mg of yellow solid (0.14 mmol, 72 %); **¹H-NMR** (400 MHz, DMSO-d₆) δ = 1.41 (s, 9 H, OC(CH₃)₃), 2.39 (s, 3 H, CH₃), 4.73 (s, 2 H, CH₂), 7.36-7.39 (m, 1 H, Ar-CH), 7.44-7.50 (m, 3 H, 3xAr-CH), 7.87 (s, 1 H, CH) ppm; **¹H-NMR** (400 MHz, CDCl₃) δ = 1.47 (s, 9 H, 3xCH₃), 2.42 (s, 3 H, CH₃), 4.76 (s, 2 H, CH₂), 7.25-7.29 (m, 1 H, Ar-CH), 7.30-7.34 (m, 2 H, 2xAr-CH), 7.35-7.42 (m, 1 H, Ar-CH), 7.75 (s, 1 H, CH) ppm; **¹³C-NMR** (400 MHz, CDCl₃) δ = 21.6 (CH₃), 28.1 (3xCH₃), 45.7 (CH₂), 83.4 (C(CH₃)₃), 122.6 (Ar-C), 128.1 (Ar-CH), 129.4 (Ar-CH), 131.4 (Ar-CH), 132.0 (Ar-CH), 133.4 (Ar-C), 134.3 (CH), 139.4 (Ar-C), 164.9 (C=O), 167.4 (COOtBu), 193.5 (C=S) ppm; **ESI-MS** m/z (%) = 350.1 [M+H]⁺ (100 %), 367.1 [M+NH₄]⁺ (85 %), 372.1 [M+Na]⁺ (10 %); **HR-MS** m/z = 367.1147 [M+NH₄]⁺ (calculated: 367.1145); **HR-MS** m/z = 350.0883 [M+H]⁺ (calculated: 350.0879); **HPLC-Analysis (Method B)**: 98 %, R_t = 20.6 min.

(Z)-methyl 2-(5-(3-methylbenzylidene)-4-oxo-2-thioxothiazolidin-3-yl) acetate **14c**

TLC R_f = 0.1 (Cyclohexane/EtOAc 9:1); **Reaction time**: 16 h; **Purification**: Flash-Chromatography Cyclohexane/EtOAc 9:1 (R_f = 0.1); **Yield**: 25 mg of yellow solid (0.08 mmol, 41 %); **¹H-NMR** (400 MHz, DMSO-d₆) δ = 2.38 (s, 3 H, CH₃), 3.71 (s, 3 H, Ar-CH₃), 4.86 (s, 2 H, CH₂), 7.33-7.40 (m, 1 H, Ar-CH), 7.42-7.50 (m, 3 H, 3xAr-CH), 7.86 (s, 1 H, CH) ppm; **ESI-MS** m/z (%) = 308.0 [M+H]⁺ (100 %), 325.0 [M+NH₄]⁺ (90 %), 330.0 [M+Na]⁺ (25 %), 346.0 [M+K]⁺ (10 %), 632.1 [2M+NH₄]⁺ (60 %), 637.1 [2M+Na]⁺ (100 %), 653.1 [2M+K]⁺ (70 %); **HR-MS** m/z = 308.0414 [M+H]⁺ (calculated: 308.0410); **HPLC-Analysis (Method B)**: 98 %, R_t = 21.7 min.

(Z)-ethyl 2-(4-oxo-2-thioxo-5-(4-(trifluoromethyl)benzylidene)thiazolidin-3-yl) acetate **14d**

TLC R_f = 0.1 (Cyclohexane/EtOAc 9:1); **Reaction time**: 16 h; **Purification**: Flash-Chromatography Cyclohexane/EtOAc 9:1 (R_f = 0.1); **Yield**: 36 mg of yellow solid (0.10 mmol, 69 %); **¹H-NMR** (400 MHz, DMSO-d₆) δ = 1.21 (t, 3 H, ³J_{H,H} = 7.0 Hz, CH₃), 4.18 (q, 2 H, ³J_{H,H} = 7.0 Hz, CH₂), 4.85 (s, 2 H, CH₂), 7.90 (d, 2 H, ³J_{H,H} = 8.5 Hz, 3,5-Ar-CH), 7.93 (d, 2 H, ³J_{H,H} = 8.5 Hz, 2,6-Ar-CH), 8.00 (s, 1 H, CH) ppm; **EI-MS** m/z (%) = 375.0 [M]⁺ (100 %), 202.0 [fragment]⁺ (100 %); **ESI-MS** m/z (%) = 391.3 [M+NH₄]⁺ (100 %), 773.0 [2M+Na]⁺ (100 %); **HR-MS** m/z = 375.0208 [M]⁺ (calculated: 375.0211); **HR-MS** m/z = 773.0312 [2M+Na]⁺ (calculated: 773.0314); **HPLC-Analysis (Method B)**: 99 %, R_t = 20.5 min.

(Z)-methyl 2-(4-oxo-2-thioxo-5-(4-(trifluoromethyl)benzylidene)thiazolidin-3-yl) acetate **14e**

TLC R_f = 0.1 (Cyclohexane/EtOAc 9:1); **Reaction time**: 16 h; **Purification**: Flash-Chroma-

tography Cyclohexane/EtOAc 9:1 ($R_f = 0.1$); **Yield**: 36 mg of yellow solid (0.10 mmol, 71 %); **$^1\text{H-NMR}$** (400 MHz, DMSO- d_6) $\delta = 3.71$ (s, 3 H, OCH $_3$), 4.88 (s, 2 H, CH $_2$), 7.86-7.95 (m, 4 H, 4xAr-CH), 8.00 (s, 1 H, CH) ppm; **ESI-MS** m/z (%) = 378.0 [M+NH $_4$] $^+$ (100 %), 400.0 [M+K] $^+$ (50 %); **EI-MS** m/z (%) = 361.0 [M] $^+$ (100 %), 202.0 [fragment] $^+$ (100 %). **HR-MS** $m/z = 361.0046$ [M] $^+$ (calculated: 361.0054). **HR-MS** $m/z = 378.0078$ [M+NH $_4$] $^+$ (calculated: 379.0392); **HPLC-Analysis (Method B)**: 99 %, $R_t = 20.5$ min.

(Z)-*tert*-butyl 2-(5-(3,4-bis(benzyloxy)benzylidene)-4-oxo-2-thioxothiazolidin-3-yl) acetate **14f**
TLC $R_f = 0.6$ (DCM); **Reaction time**: 16 h; **Purification**: Flash-Chromatography DCM ($R_f = 0.6$); **Yield**: 10 mg of yellow solid (0.02 mmol, 18 %); **$^1\text{H-NMR}$** (400 MHz, DMSO- d_6) $\delta = 1.41$ (s, 9 H, OC(CH $_3$) $_3$), 4.70 (s, 2 H, CH $_2$), 5.24 (s, 2 H, OCH $_2$ Ph), 5.26 (s, 2 H, OCH $_2$ Ph), 7.26-7.50 (m, 13 H, 13xAr-CH), 7.81 (s, 1 H, CH) ppm; **EI-MS** m/z (%) = 547.1 [M] $^+$ (100 %), 456.1 [fragment] $^+$ (25 %), 400.1 [fragment] $^+$ (15 %), 91.0 [fragment] $^+$ (100 %). **HR-MS** $m/z = 547.1478$ [M] $^+$ (calculated: 547.1487); **HPLC-Analysis (Method B)**: 94 %, $R_t = 19.9$ min.

Ethyl 2-[(5Z)-5-[(2-methylphenyl)methylidene]-4-oxo-2-sulfanylidene-1,3-thiazolidin-3-yl] acetate **14g**

TLC $R_f = 0.6$ (DCM); **Reaction time**: 16 h; **Purification**: Flash-Chromatography DCM ($R_f = 0.6$); **Yield**: 50 mg of yellow solid (0.16 mmol, 78 %); **$^1\text{H-NMR}$** (400 MHz, DMSO- d_6) $\delta = 1.07$ -1.33 (m, 3 H, CH $_3$), 2.45 (s, 3 H, Ar-CH $_3$), 4.06-4.26 (m, 2 H, CH $_2$ CH $_3$), 4.84 (s, 2 H, CH $_2$), 7.28-7.52 (m, 4 H, 4xAr-CH), 8.00 (s, 1 H, CH) ppm; **ESI-MS** m/z (%) = 322.1 [M+H] $^+$ (100 %), 339.1 [M+NH $_4$] $^+$ (45 %); **HR-MS** $m/z = 322.0571$ [M+H] $^+$ (calculated: 322.0566); **HPLC-Analysis (Method B)**: 99 %, $R_t = 20.4$ min.

(Z)-*tert*-butyl 2-(5-(2-methylbenzylidene)-4-oxo-2-thioxothiazolidin-3-yl) acetate **14h**

TLC $R_f = 0.7$ (DCM); **Yield**: 34 mg of yellow solid (0.10 mmol, 49 %); **Reaction time**: 16 h; **Purification**: Flash-Chromatography DCM ($R_f = 0.7$); **$^1\text{H-NMR}$** (400 MHz, DMSO- d_6) $\delta = 1.42$ (s, 9 H, OC(CH $_3$) $_3$), 2.45 (s, 3 H, Ar-CH $_3$), 4.73 (s, 2 H, CH $_2$), 7.37-7.49 (m, 4 H, 4xAr-CH), 7.99 (s, 1 H, CH) ppm; **ESI-MS** m/z (%) = 350.1 [M+H] $^+$ (100 %), 367.1 [M+NH $_4$] $^+$ (60 %), 716.2 [2M+NH $_4$] $^+$ (100 %), 721.1 [2M+Na] $^+$ (40 %), 737.1 [2M+K] $^+$ (10 %); **HR-MS** $m/z = 350.0883$ [M+H] $^+$ (calculated: 350.0879); **HR-MS** $m/z = 367.1145$ [M+NH $_4$] $^+$ (calculated: 367.1145); **HPLC-Analysis (Method B)**: 99 %, $R_t = 20.4$ min.

Method 2: Esterification followed by Knoevenagel condensation

The free carboxylic acid derivatives **2**, **12**, and **13** (1.0 eq), DCC (1.5 eq) and DMAP (0.3 eq) were dissolved in alcohol (methanol, ethanol or *tert*-butanol). The reaction mixture is stirred at rt for 4 h or until TLC showed complete consumption of starting material. After 1 h the reaction mixture turns from yellow to red. The reaction mixture was concentrated to half its' reaction volume, the DCU was filtered and washed with DCM. The crude was concentrated and purified by flash column chromatography. The ester derivatives **14**, **15**, and **16** (1.0 eq), benzaldehyde

derivatives (1.1-1.5 eq) and sodium acetate were dissolved in ethanol (5-10 mL). The reaction mixture was continued to stir at 80 °C for 2 h or until TLC showed complete consumption of starting material. The majority of products were purified by flash column chromatography. The individual purification method is stated for each compound below.

Methyl 2-(4-oxo-2-sulfanylidene-1,3-thiazolidin-3-yl) acetate : Methyl ester of **14**^[284]

TLC R_f = 0.2 (Hexane/EtOAc 8:2); **Reaction time**: 16 h; **Purification**: Flash-Chromatography Hexane/EtOAc 8:2 (R_f = 0.2), DCM; **Yield**: 4600 mg of yellow oil (22.41 mmol, 78 %); **¹H-NMR** (400 MHz, CDCl₃) δ = 3.69 (s, 3 H, CH₃), 4.03 (s, 2 H, CH₂), 4.65 (s, 2 H, CH₂) ppm; **¹³C-NMR** (400 MHz, CDCl₃) δ = 35.7 (CH₂), 44.7 (CH₂), 52.8 (CH₃), 166.3 (C=O), 173.1 (COOMe), 200.7 (C=S) ppm.

Ethyl 2-(4-oxo-2-sulfanylidene-1,3-thiazolidin-3-yl) acetate: Ethyl ester of **14**^[285]

TLC R_f = 0.3 (Hexane/EtOAc 8:2); **Reaction time**: 16 h; **Purification**: Flash-Chromatography Hexane/EtOAc 8:2 (R_f = 0.3), DCM; **Yield**: 1220 mg of red oil (5.56 mmol, 97 %); **Yield**: 1121 mg of red oil (5.11 mmol, 98 %); **Yield**: 1121 mg of red oil (5.11 mmol, 98 %); **¹H-NMR** (400 MHz, CDCl₃) δ = 1.29 (t, 3 H, ³ $J_{H,H}$ = 7.1 Hz, CH₃), 4.08 (s, 2 H, CH₂), 4.23 (q, 2 H, ³ $J_{H,H}$ = 7.1 Hz, CH₂CH₃), 4.72 (s, 2 H, CH₂) ppm; **¹³C-NMR** (400 MHz, CDCl₃) δ = 14.2 (CH₃), 35.7 (CH₂), 45.0 (CH₂), 62.2 (CH₂), 165.9 (C=O), 173.2 (COOEt), 200.6 (C=S) ppm; **ESI-MS** m/z (%) = 241.2 [M+Na]⁺ (100 %). **EI-MS** m/z (%) = 219.1 [M]⁺ (100 %), 173.0 [fragment]⁺ (45 %), 147.0 [fragment]⁺ (45 %), 118.0 [fragment]⁺ (85 %), 72.0 [fragment]⁺ (100 %), 6.07 [fragment]⁺ (100 %); **HR-MS** m/z = 219.0016 [M]⁺ (calculated: 219.0018); **HPLC-Analysis (Method B)**: 99 %, R_t = 9.9 min.

tert-Butyl 2-(4-oxo-2-sulfanylidene-1,3-thiazolidin-3-yl) acetate: *tert*-Butyl ester of **14**

TLC R_f = 0.8 (DCM/MeOH/AcOH 9:1:0.01); **Reaction time**: 16 h; **Purification**: Flash-Chromatography Hexane/EtOAc 8:2 → 7:3 (R_f = 0.4, 0.4); **Yield**: 225 mg of yellow oil (0.91 mmol, 17 %); **¹H-NMR** (400 MHz, CDCl₃) δ = 1.46 (s, 9 H, 3xCH₃), 4.09 (s, 2 H, CH₂), 4.60 (s, 2 H, CH₂) ppm; **¹³C-NMR** (400 MHz, CDCl₃) δ = 28.0 (3xCH₃), 74.6 (CH₂), 83.2 (CH₂), 164.8 (C=O), 173.2 (COOtBu), 200.8 (C=S) ppm.

Ethyl 3-(4-oxo-2-sulfanylidene-1,3-thiazolidin-3-yl)propanoate: Ethyl ester of **15**^[286]

TLC R_f = 0.6 (Hexane/EtOAc 1:1); **Reaction time**: 16 h; **Yield**: 256 mg of yellow oil (1.10 mmol, 41 %); **Yield**: 775 mg of yellow oil (3.32 mmol, 45 %); **Yield**: 5133 mg of yellow solid (22.00 mmol, 86 %) **Yield**: 1036 mg of yellow oil (4.44 mmol, 91 %); **Yield**: 347 mg of yellow oil (1.49 mmol, 31 %); **Yield**: 439 mg of yellow oil (1.88 mmol, 39 %); **Purification**: Flash-Chromatography Hexane/EtOAc 8:2 (R_f = 0.3); **¹H-NMR** (400 MHz, CDCl₃) δ = 1.24 (t, 3 H, ³ $J_{H,H}$ = 7.1 Hz, CH₃), 2.67 (t, 2 H, ³ $J_{H,H}$ = 7.5 Hz, α -CH₂), 3.99 (s, 2 H, CH₂), 4.12 (q, 2 H, ³ $J_{H,H}$ = 7.1 Hz, CH₂CH₃), 4.28 (t, 2 H, ³ $J_{H,H}$ = 7.5 Hz, β -CH₂) ppm; **¹³C-NMR** (400 MHz, CDCl₃) δ = 14.2 (CH₃), 31.2 (α -CH₂), 35.5 (CH₂), 40.2 (β -CH₂), 61.1 (CH₂CH₃), 170.5 (C=O), 173.6 (COOEt), 200.9 (C=S) ppm;

Ethyl 4-(4-oxo-2-sulfanylidene-1,3-thiazolidin-3-yl)butanoate: Ethyl ester of **16**^[287]

TLC R_f = 0.6 (Hexane/EtOAc/HOAc 6:4:0.01); **Yield**: 816 mg of orange oil (3.30 mmol, 72 %); **Yield**: 2083 mg of orange solid (8.42 mmol, 77 %) **Reaction time**: 16 h; **Purification**: Flash-Chromatography Hexane/EtOAc 9:1 → 8:2 (R_f = 0.3, 0.4), loaded in DCM; **¹H-NMR** (400 MHz, CDCl₃) δ = 1.25 (t, 3 H, $^3J_{H,H}$ = 7.1 Hz, CH₃), 1.98 (p, 2 H, $^3J_{H,H}$ = 7.3 Hz, β -CH₂), 2.35 (t, 2 H, $^3J_{H,H}$ = 7.3 Hz, γ -CH₂), 3.96 (s, 2 H, CH₂), 4.05 (t, 2 H, $^3J_{H,H}$ = 7.3 Hz, α -CH₂), 4.12 (q, 2 H, $^3J_{H,H}$ = 7.1 Hz, CH₂CH₃) ppm; **¹³C-NMR** (400 MHz, CDCl₃) δ = 14.3 (CH₃), 22.2 (β -CH₂), 31.6 (γ -CH₂), 35.4 (CH₂), 44.0 (α -CH₂), 60.7 (CH₂CH₃), 172.6 (C=O), 174.0 (COOEt), 201.4 (C=S) ppm.

Ethyl 2-[(9H-fluoren-9-ylmethoxy)carbonyl] amino-acetate^[288]

Starting was Fmoc-Gly-OH **TLC** R_f = 0.5 (Hexane/EtOAc 6:4); **Reaction time**: 16 h; **Purification**: Flash-Chromatography Hexane/EtOAc 9:1 → 8:2 (R_f = 0.2); **Yield**: 979 mg of white solid (3.01 mmol, 90 %); **¹H-NMR** (400 MHz, CDCl₃) δ = 1.22 (t, 3 H, $^3J_{H,H}$ = 7.1 Hz, CH₃), 3.92 (d, 2 H, $^3J_{H,H}$ = 5.5 Hz, CH₂COOEt), 4.13-4.20 (m, 3 H, CH₂CH₃, CH-Fmoc), 4.34 (d, 2 H, $^3J_{H,H}$ = 7.1 Hz, CH₂-Fmoc), 7.24 (at, 2 H, $^3J_{H,H}$ = 7.4, 7.5 Hz, Ar-CH), 7.33 (at, 2 H, $^3J_{H,H}$ = 7.4, 7.5 Hz, Ar-CH), 7.53 (d, 2 H, $^3J_{H,H}$ = 7.4 Hz, Ar-CH), 7.70 (d, 2 H, $^3J_{H,H}$ = 7.5 Hz, Ar-CH) ppm; **HPLC-Analysis (Method B)**: 99 %, R_t = 12.7 min.

Ethyl 2-[(5Z)-4-oxo-5-(phenylmethylidene)-2-sulfanylidene-1,3-thiazolidin-3-yl] acetate **14i**^[289]

TLC R_f = 0.6 (Hexane/EtOAc 8:2); **Reaction time**: 16 h; **Purification**: Filtration from ethanol; **Yield**: 175 mg of yellow solid (0.57 mmol, 50 %); **Yield**: 255 mg of yellow solid (0.30 mmol, 73 %); **¹H-NMR** (400 MHz, CDCl₃) δ = 1.29 (t, 3 H, $^3J_{H,H}$ = 7.1 Hz, CH₃), 4.25 (q, 2 H, $^3J_{H,H}$ = 7.1 Hz, CH₂CH₂), 4.86 (s, 2 H, CH₂), 7.45-7.55 (m, 5 H, 5xAr-CH), 7.79 (s, 1 H, CH) ppm; **¹³C-NMR** (400 MHz, CDCl₃) δ = 14.3 (CH₃), 45.0 (CH₂), 62.2 (CH₂CH₃), 122.9 (Ar-C), 129.6 (Ar-CH), 130.9 (Ar-CH), 131.1 (Ar-CH), 133.3 (Ar-C), 134.2 (CH), 166.0 (C=O), 167.3 (COOEt), 193.2 (C=S) ppm; **ESI-MS** m/z (%) = 308.0 [M+H]⁺ (100 %), 330.0 [M+Na]⁺ (25 %), 637.1 [2M+Na]⁺ (10 %); **HR-MS** m/z = 308.0415 [M+H]⁺ (calculated: 308.0410); **ESI-MS** m/z (%) = 308.0 [M+H]⁺ (79 %), 325.1 [M+NH₄]⁺ (16 %), 330.0 [M+Na]⁺ (84 %), 632.1 [2M+NH₄]⁺ (6 %), 637.1 [2M+Na]⁺ (100 %); **HPLC-Analysis (Method B)**: 96 %, R_t = 19.8 min.

tert-Butyl 2-[(5Z)-4-oxo-5-(phenylmethylidene)-2-sulfanylidene-1,3-thiazolidin-3-yl] acetate **14j**

TLC R_f = 0.3 (Hexane/EtOAc 9:1); **Purification**: Re-crystallisation from ethanol; **Yield**: 234 mg of yellow crystals (0.70 mmol, 77 %); 1:3 mixture of E:Z isomer: **¹H-NMR** (400 MHz, CDCl₃) δ = 1.47 (s, 9 H, 6xCH₃), 4.77 (s, 2 H, Z-CH₂), 4.84 (s, 2 H, E-CH₂), 7.43-7.55 (m, 5 H, 10xAr-CH), 7.78 (s, 1 H, Z-CH), 7.79 (s, 1 H, E-CH) ppm; **¹³C-NMR** (400 MHz, CDCl₃) δ = 28.1 (6xCH₃), 45.2 (E-CH₂), 45.7 (Z-CH₂), 83.4 (C(CH₃)₃), 123.0 (Ar-C), 129.5 (Ar-CH), 130.8 (Ar-CH), 131.0 (Ar-CH), 133.4 (Z-CH), 133.9 (E-CH), 164.9 (Z-C=O), 165.6 (E-C=O), 167.3 (E/Z-COOtBu), 193.2 (E-C=S), 193.3 (Z-C=S) ppm; **ESI-MS** m/z (%) = 336.1 [M+H]⁺ (48 %), 353.1 [M+NH₄]⁺ (51 %), 358.1 [M+Na]⁺ (30 %), 688.2 [2M+NH₄]⁺ (37 %), 693.1 [2M+Na]⁺ (52 %);

HPLC-Analysis (Method B): 98 %, R_t = 20.9 min.

(E/Z)-ethyl 2-(4-oxo-2-thioxo-5-(2-(trifluoromethyl)benzylidene)thiazolidin-3-yl) acetate **14k**

TLC R_f = 0.8 (DCM); **Yield:** 45 mg of yellow solid (0.12 mmol, 86 %); **Reaction time:** 16 h; **Purification:** Flash-Chromatography DCM (R_f = 0.8); mixture of Z to E (2:1) **¹H-NMR** (400 MHz, CDCl₃) δ = 1.26 (t, 3 H, $^3J_{H,H}$ = 7.1 Hz, CH₂CH₃), 1.30 (t, 3 H, $^3J_{H,H}$ = 7.1 Hz, CH₂CH₃), 4.21 (q, 2 H, $^3J_{H,H}$ = 7.1 Hz, CH₂CH₃), 4.26 (q, 2 H, $^3J_{H,H}$ = 7.1 Hz, CH₂CH₃), 4.73 (s, 2 H, CH₂), 4.86 (s, 2 H, CH₂), 7.45 (q, 1 H, $^5J_{H,F}$ = 2.2 Hz, E-CH), 7.48-7.74 (m, 7 H, 7xAr-CH), 7.79 (d, 1 H, $^3J_{H,H}$ = 7.8 Hz, Ar-CH), 8.05 (q, 1 H, $^5J_{H,F}$ = 2.2 Hz, Z-CH) ppm; **¹³C-NMR** (400 MHz, CDCl₃) δ = 14.2 (2xCH₃), 44.8 (CH₂), 45.0 (CH₂), 62.2 (CH₂CH₃), 62.3 (CH₂CH₃), 126.0 (Ar-CH), 127.0 (Ar-CH), 127.1 (Ar-CH), 127.7 (Ar-C), 129.3 (Ar-CH), 129.4 (E-CH), 129.7 (Ar-C), 130.3 (Ar-CH), 131.3 (Ar-CH), 132.1 (Ar-CH), 132.6 (Z-CH), 133.0 (Ar-C), 165.9 (C=O), 166.3 (C=O), 193.0 (2xC=S) ppm; **ESI-MS** m/z (%) = 376.0 [M+H]⁺ (100 %), 393.1 [M+NH₄]⁺ (50 %), 773.0 [2M+Na]⁺ (5 %); **HR-MS** m/z = 376.0287 [M+H]⁺ (calculated: 376.0283); **HPLC-Analysis (Method B):** 98 %, R_t = 21.8 min.

(Z)-ethyl 2-(4-oxo-2-thioxo-5-(3-(trifluoromethyl)benzylidene)thiazolidin-3-yl) acetate **14l**

TLC R_f = 0.6 (DCM); **Reaction time:** 16 h; **Purification:** Flash-Chromatography DCM (R_f = 0.6); **Yield:** 27 mg of yellow solid (0.07 mmol, 51 %); **¹H-NMR** (400 MHz, CDCl₃) δ = 1.30 (t, 3 H, $^3J_{H,H}$ = 7.1 Hz, OCH₂CH₃), 4.25 (q, 2 H, $^3J_{H,H}$ = 7.1 Hz, OCH₂CH₃), 4.87 (s, 2 H, CH₂), 7.61-7.76 (m, 4 H, 4xAr-CH), 7.79 (s, 1 H, CH) ppm; **¹³C-NMR** (400 MHz, CDCl₃) δ = 14.3 (CH₃), 45.1 (CH₂), 62.3 (CH₂CH₃) 123.6 (q, $^1J_{C,F}$ = 272.9 Hz, CF₃) 125.1 (Ar-C) 127.3 (q, $^3J_{C,F}$ = 3.7 Hz, Ar-CH), 127.4 (q, $^3J_{C,F}$ = 3.9 Hz, Ar-CH), 130.1 (Ar-CH), 131.8 (CH), 132.1 (q, $^2J_{C,F}$ = 33.0 Hz, 3-Ar-C), 133.2 (Ar-CH), 134.1 (Ar-C), 165.8 (C=O), 167.0 (COOEt), 192.3 (C=S) ppm; **ESI-MS** m/z (%) = 376.0 [M+H]⁺ (50 %), 393.1 [M+NH₄]⁺ (60 %), 398.0 [M+Na]⁺ (20 %), 768.1 [2M+NH₄]⁺ (60 %), 773.0 [2M+Na]⁺ (100 %), 789.0 [2M+K]⁺ (30 %); **HR-MS** m/z = 376.0287 [M+H]⁺ (calculated: 376.0283); **HPLC-Analysis (Method B):** 100 %, R_t = 20.5 min. Ethyl 2-[(3E)-3-[2,5-bis(trifluoromethyl)phenyl]methylidene-2-oxo-5-sulfanylidene]pyrrolidin-1-yl] acetate **14m**

TLC R_f = 0.8 (Hexane/EtOAc 9:1); **Reaction time:** 30 min; **Purification:** Flash-Chromatography Hexane/EtOAc 95:5 (R_f = 0.3); **Yield:** 303 mg of yellow solid (0.71 mmol, 62 %); **¹H-NMR** (400 MHz, CDCl₃) δ = 1.31 (t, 3 H, $^3J_{H,H}$ = 7.1 Hz, CH₃) 4.27 (q, 2 H, $^3J_{H,H}$ = 7.1 Hz, CH₂CH₃) 4.87 (s, 2 H, CH₂), 7.82 (d, 1 H, $^3J_{H,H}$ = 8.2 Hz, 4-Ar-CH), 7.87 (s, 1 H, 6-Ar-CH), 7.95 (d, 1 H, $^3J_{H,H}$ = 8.2 Hz, 3-Ar-CH), 8.00 (q, 1 H, $^5J_{H,F}$ = 1.9 Hz, CH) ppm; **¹³C-NMR** (400 MHz, CDCl₃) δ = 14.2 (CH₃), 45.1 (CH₂Ar) 62.4 (CH₂CH₃), 122.9 (q, $^1J_{C,F}$ = 273.3 Hz, CF₃), 123.0 (q, $^1J_{C,F}$ = 274.6 Hz, CF₃), 126.1 (q, $^3J_{C,F}$ = 3.7 Hz, 6-Ar-CH), 126.9 (q, $^3J_{C,F}$ = 3.6 Hz, 4-Ar-CH), 127.1 (q, $^4J_{C,F}$ = 1.9 Hz, CH), 127.8 (q, $^3J_{C,F}$ = 5.4 Hz, 3-Ar-CH), 129.7 (Ar-C) 132.9 (q, $^2J_{C,F}$ = 30.5 Hz, Ar-CCF₃), 133.3 (q, $^4J_{C,F}$ = 1.4 Hz, Ar-C), 134.9 (q, $^2J_{C,F}$ = 33.5 Hz, Ar-CCF₃), 165.7 (C=O), 166.1 (COOEt), 191.9 (C=S) ppm; **ESI-MS** m/z (%) = 444.0 [M+NH₄]⁺ (69 %);

HPLC-Analysis (Method B): 84 %, R_t = 20.9 min.

(Z)-ethyl 2-(5-(4-methylbenzylidene)-4-oxo-2-thioxothiazolidin-3-yl) acetate **14n**

TLC R_f = 0.6 (DCM); **Reaction time:** 3 h; **Purification:** Flash-Chromatography DCM (R_f = 0.6); **Yield:** 58 mg of yellow solid (0.18 mmol, 90 %); **$^1\text{H-NMR}$** (400 MHz, CDCl_3) δ = 1.29 (t, 3 H, $^3J_{\text{H,H}}$ = 7.1 Hz, OCH_2CH_3), 2.42 (s, 3 H, Ar- CH_3), 4.24 (q, 2 H, $^3J_{\text{H,H}}$ = 7.1 Hz, OCH_2CH_3), 4.86 (s, 2 H, CH_2), 7.30 (d, 2 H, $^3J_{\text{H,H}}$ = 8.1 Hz, 2,6-Ar-CH), 7.77 (s, 1 H, CH) ppm; **ESI-MS** m/z (%) = 322.1 $[\text{M}+\text{H}]^+$ (100 %); **HR-MS** m/z = 322.0571 $[\text{M}+\text{H}]^+$ (calculated: 322.0566); **HPLC-Analysis (Method B):** 100 %, R_t = 20.4 min.

(Z)-ethyl 2-(5-(4-tert-butylbenzylidene)-4-oxo-2-thioxothiazolidin-3-yl) acetate **14o**

TLC R_f = 0.4 (Cyclohexane/EtOAc 9:1); **Reaction time:** 4 h; **Purification:** Flash-Chromatography Cyclohexane/EtOAc 9:1 (R_f = 0.4), DCM; **Yield:** 18 mg of yellow solid (0.05 mmol, 55 %); **$^1\text{H-NMR}$** (400 MHz, CDCl_3) δ = 1.22 (t, 3 H, $^3J_{\text{H,H}}$ = 7.1 Hz, CH_3), 1.28 (s, 9 H, $3\times\text{CH}_3$), 4.17 (q, 2 H, $^3J_{\text{H,H}}$ = 7.1 Hz, CH_2), 4.79 (s, 2 H, CH_2), 7.39 (d, 2 H, $^3J_{\text{H,H}}$ = 8.5 Hz, $2\times\text{Ar-CH}$), 7.45 (d, 2 H, $^3J_{\text{H,H}}$ = 8.5 Hz, $2\times\text{Ar-CH}$), 7.71 (s, 1 H, CH) ppm; **$^{13}\text{C-NMR}$** (400 MHz, CDCl_3) δ = 14.2 (CH_3), 31.2 ($3\times\text{CH}_3$), 45.0 (CH_2), 62.2 (CH_2CH_3), 126.6 ($2\times\text{Ar-CH}$), 130.6 (Ar-C), 130.9 ($2\times\text{Ar-CH}$), 134.3 (CH), 155.1 (Ar-C), 166.1 (Ar-C), 167.4 (C=O), 193.3 (C=S) ppm; **ESI-MS** m/z (%) = 364.1 $[\text{M}+\text{H}]^+$ (68 %), 744.2 $[\text{M}+\text{NH}_4]^+$ (29 %); **HPLC-Analysis (Method B):** 99 %, R_t = 22.1 min.

Ethyl 2-[(5Z)-5-[(2-hydroxyphenyl)methylidene]-4-oxo-2-sulfanylidene-1,3-thiazolidin-3-yl] acetate **14p**

TLC R_f = 0.6 ($\text{CHCl}_3/\text{EtOAc}$ 9:1); **Reaction time:** 16 h; **Purification:** Flash-Chromatography $\text{CHCl}_3/\text{EtOAc}$ 1:0 \rightarrow 9:1 (R_f = 0.6); **Yield:** 210 mg of yellow solid (0.65 mmol, 84 %); **$^1\text{H-NMR}$** (400 MHz, CDCl_3) δ = 1.34 (t, 3 H, $^3J_{\text{H,H}}$ = 7.1 Hz, CH_3), 4.31 (q, 2 H, $^3J_{\text{H,H}}$ = 7.1 Hz, CH_2CH_3), 4.89 (s, 2 H, CH_2), 6.83 (d, 1 H, $^3J_{\text{H,H}}$ = 8.2 Hz, 3-Ar-CH), 6.94 (at, 1 H, $^3J_{\text{H,H}}$ = 7.5, 7.8 Hz, 5-Ar-CH), 7.16 (d, 1 H, $^3J_{\text{H,H}}$ = 7.8 Hz, 6-Ar-CH), 7.25-7.30 (m, 1 H, 4-Ar-CH), 7.48 (s(br), 1 H, OH), 8.19 (s, 1 H, CH) ppm; **$^{13}\text{C-NMR}$** (400 MHz, CDCl_3) δ = 14.2 (CH_3), 45.0 (CH_2), 62.8 (CH_2CH_3), 116.5 (3-Ar-CH), 120.6 (Ar-C), 121.1 (5-Ar-CH), 121.2 (Ar-C), 129.7 (6-Ar-CH), 130.1 (CH), 133.1 (4-Ar-CH), 156.8 (Ar-C), 167.6 (C=O, COOEt), 193.9 (C=S) ppm; **ESI-MS** m/z (%) = 324.0 $[\text{M}+\text{H}]^+$ (91 %), 341.1 $[\text{M}+\text{NH}_4]^+$ (17 %), 664.1 $[2\text{M}+\text{NH}_4]^+$ (100 %), 669.1 $[2\text{M}+\text{Na}]^+$ (6 %); **HPLC-Analysis (Method B):** 99 %, R_t = 18.2 min.

Ethyl 2-[(5Z)-5-[(3-hydroxyphenyl)methylidene]-4-oxo-2-sulfanylidene-1,3-thiazolidin-3-yl] acetate **14q**

TLC R_f = 0.3 ($\text{CHCl}_3/\text{EtOAc}$ 9:1); **Reaction time:** 3 h; **Purification:** Flash-Chromatography $\text{CHCl}_3/\text{EtOAc}$ 9:1 (R_f = 0.3), CHCl_3 ; **Yield:** 317 mg of yellow solid (0.98 mmol, 86 %); **$^1\text{H-NMR}$** (400 MHz, CDCl_3) δ = 1.23 (t, 3 H, $^3J_{\text{H,H}}$ = 7.1 Hz, CH_3), 4.29 (q, 2 H, $^3J_{\text{H,H}}$ = 7.1 Hz, CH_2CH_3), 4.88 (s, 2 H, CH_2), 6.84-6.87 (m, 1 H, 2-Ar-CH), 6.87 (dd, 1 H, 2.3, 7.8 Hz, 4-Ar-CH), 7.00 (d, 1 H, $^3J_{\text{H,H}}$ = 7.7 Hz, 6-Ar-CH), 7.30 (at, 1 H, $^3J_{\text{H,H}}$ = 7.7, 7.8 Hz, 5-Ar-CH), 7.55 (s, 1 H,

CH) ppm; $^{13}\text{C-NMR}$ (400 MHz, CDCl_3) δ = 14.2 (CH_3), 45.0 (CH_2), 62.6 (CH_2CH_3), 117.2 (2-Ar-CH), 118.4 (4-Ar-CH), 123.0 (Ar-C), 123.4 (6-Ar-CH), 130.7 (5-Ar-CH), 133.9 (CH), 134.6 (Ar-C), 156.7 (Ar-C), 166.8 (C=O) 167.3 (COOEt), 193.2 (C=S) ppm; **ESI-MS** m/z (%) = 324.0 $[\text{M}+\text{H}]^+$ (38 %), 341.1 $[\text{M}+\text{NH}_4]^+$ (16 %), 346.0 $[\text{M}+\text{Na}]^+$ (6 %), 664.1 $[\text{2M}+\text{NH}_4]^+$ (13 %), 669.1 $[\text{2M}+\text{Na}]^+$ (12 %); **HPLC-Analysis (Method B)**: 99 %, R_t = 18.2 min.

Ethyl 2-[(5Z)-5-[(4-hydroxyphenyl)methylidene]-4-oxo-2-sulfanylidene-1,3-thiazolidin-3-yl] acetate **14r**

TLC R_f = 0.1 (Hexane/EtOAc 8:2); **Reaction time**: 6 h; **Purification**: Flash-Chromatography Hexane/EtOAc 7:3 (R_f = 0.3); **Yield**: 330 mg of red crystals (1.02 mmol, 89 %); $^1\text{H-NMR}$ (400 MHz, MeOD) δ = 1.27 (t, 3 H, $^3J_{\text{H,H}}$ = 7.1 Hz, CH_3), 4.22 (q, 2 H, $^3J_{\text{H,H}}$ = 7.1 Hz, CH_2CH_3), 4.85 (s, 2 H, CH_2), 6.93 (d, 2 H, $^3J_{\text{H,H}}$ = 8.7 Hz, 2,6-Ar-CH), 7.47 (d, 2 H, $^3J_{\text{H,H}}$ = 8.7 Hz, 3,5-Ar-CH), 7.74 (s, 1 H, CH) ppm; $^{13}\text{C-NMR}$ (400 MHz, MeOD) δ = 14.4 (CH_3), 45.8 (CH_2), 63.0 (CH_2CH_3), 117.6 (2,6-Ar-CH), 119.4 (Ar-C), 126.0 (Ar-C), 134.5 (3,5-Ar-CH), 135.6 (CH), 162.2 (Ar-C), 167.9 (C=O), 168.5 (COOEt), 194.9 (C=S) ppm; $^1\text{H-NMR}$ (400 MHz, CDCl_3) δ = 1.32 (t, 3 H, $^3J_{\text{H,H}}$ = 7.1 Hz, CH_3), 4.27 (q, 2 H, $^3J_{\text{H,H}}$ = 7.1 Hz, CH_2CH_3), 4.88 (s, 2 H, CH_2), 5.97 (s(br), 1 H, OH), 6.90 (d, 2 H, $^3J_{\text{H,H}}$ = 8.6 Hz, 2,6-Ar-CH), 7.34 (d, 2 H, $^3J_{\text{H,H}}$ = 8.6 Hz, 3,5-Ar-CH), 7.61 (s, 1 H, CH) ppm; $^{13}\text{C-NMR}$ (400 MHz, CDCl_3) δ = 14.2 (CH_3), 45.0 (CH_2), 62.5 (CH_2CH_3), 116.7 (2,6-Ar-CH), 126.0 (Ar-C), 133.3 (3,5-Ar-CH), 134.3 (CH), 158.7 (Ar-C), 166.8 (C=O), 167.4 (COOEt), 193.1 (C=S) ppm; $^1\text{H-NMR}$ (400 MHz, DMSO-d_6) δ = 1.20 (t, 3 H, $^3J_{\text{H,H}}$ = 7.1 Hz, CH_3), 4.17 (q, 2 H, $^3J_{\text{H,H}}$ = 7.1 Hz, CH_2CH_3), 4.82 (s, 2 H, CH_2), 6.95 (d, 2 H, $^3J_{\text{H,H}}$ = 8.7 Hz, 2,6-Ar-CH), 7.56 (d, 2 H, $^3J_{\text{H,H}}$ = 8.7 Hz, 3,5-Ar-CH), 7.82 (s, 1 H, CH), 10.57 (s(br), 1 H, OH) ppm; **ESI-MS** m/z (%) = 341.2 $[\text{M}+\text{NH}_4]^+$ (20 %); **HPLC-Analysis (Method B)**: 90 %, R_t = 18.1 min.

Methyl 2-[(5Z)-5-[(3,4-dihydroxyphenyl)methylidene]-4-oxo-2-sulfanylidene-1,3-thiazolidin-3-yl] acetate **14s**

TLC R_f = 0.2 ($\text{CHCl}_3/\text{MeOH}/\text{HOAc}$ 97:2:1); **Reaction time**: 4 h; **Purification**: Filtration from ethanol; **Yield**: 35 mg of yellow solid (0.11 mmol, 32 %); $^1\text{H-NMR}$ (400 MHz, CDCl_3) δ = 3.79 (s, 3 H, CH_3), 4.87 (s, 2 H, CH_2), 6.94 (d, 1 H, $^3J_{\text{H,H}}$ = 8.1 Hz, Ar-CH), 6.96-7.03 (m, 2 H, 2xAr-CH), 7.64 (s, 1 H, CH) ppm; $^1\text{H-NMR}$ (400 MHz, MeOD) δ = 3.76 (s, 3 H, CH_3), 4.86 (s, 2 H, CH_2), 6.89 (d, 1 H, $^3J_{\text{H,H}}$ = 8.1 Hz, 5-Ar-CH), 6.97-7.03 (m, 2 H, 2,6-Ar-CH), 7.65 (s, 1 H, CH) ppm; $^{13}\text{C-NMR}$ (400 MHz, MeOD) δ = 45.6 (CH_2), 53.2 (OCH_3), 117.1 (5-Ar-CH), 117.9 (2-Ar-CH), 119.2 (Ar-C), 126.5 (6-Ar-CH), 136.0 (CH), 147.4 (Ar-C), 150.8 (Ar-C), 168.4 (C=O), 175.3 (COOMe), 194.8 (C=S) ppm; **HPLC-Analysis (Method B)**: 95 %, R_t = 15.8 min.

Ethyl 2-[(5Z)-5-[(3,4-dihydroxyphenyl)methylidene]-4-oxo-2-sulfanylidene-1,3-thiazolidin-3-yl] acetate **14t**

TLC R_f = 0.6 ($\text{CHCl}_3/\text{MeOH}$ 9:1); **Reaction time**: 4 h; **Purification**: Flash-Chromatography DCM/EtOAc 9:1 (R_f = 0.1); **Yield**: 192 mg of yellow solid (0.57 mmol, 58 %); $^1\text{H-NMR}$ (400

MHz, CDCl_3) δ = 1.32 (t, 3 H, $^3J_{\text{H,H}}$ = 7.1 Hz, CH_3), 4.27 (q, 2 H, $^3J_{\text{H,H}}$ = 7.1 Hz, CH_2CH_3), 4.87 (s, 2 H, CH_2), 5.98 (s(br), 1 H, OH), 6.28 (s(br), 1 H, OH), 6.91-7.00 (m, 2 H, 5,6-Ar-CH), 7.26 (s, 1 H, CH), 7.59 (s, 1 H, 2-Ar-CH) ppm; **$^1\text{H-NMR}$** (400 MHz, MeOD) δ = 1.25 (t, 3 H, $^3J_{\text{H,H}}$ = 7.1 Hz, CH_3), 4.20 (q, 2 H, $^3J_{\text{H,H}}$ = 7.1 Hz, CH_2CH_3), 4.78 (s, 2 H, CH_2), 6.85 (d, 1 H, $^3J_{\text{H,H}}$ = 8.2 Hz, 5-Ar-CH), 6.93 (dd, 1 H, $^{3,4}J_{\text{H,H}}$ = 2.1, 8.2 Hz, 6-Ar-CH), 6.96 (d, 1 H, $^4J_{\text{H,H}}$ = 2.1 Hz, 2-Ar-CH), 7.55 (s, 1 H, CH) ppm; **$^{13}\text{C-NMR}$** (400 MHz, MeOD) δ = 14.4 (CH_3), 45.7 (CH_2) 63.0 (CH_2CH_3), 117.1 (5-Ar-CH), 117.9 (2-Ar-CH), 119.1 (Ar-C), 126.4 (Ar-C), 126.6 (6-Ar-CH), 136.0 (CH), 147.2 (Ar-C), 150.6 (Ar-C), 167.9 (C=O), 168.4 (COOEt), 194.6 (C=S) ppm; **ESI-MS** m/z (%) = 340.0 $[\text{M}+\text{H}]^+$ (100 %), 357.1 $[\text{M}+\text{NH}_4]^+$ (15 %), 696.1 $[\text{2M}+\text{NH}_4]^+$ (20 %); **HR-MS** m/z = 340.0312 $[\text{M}+\text{H}]^+$ (calculated: 340.0308); **HPLC-Analysis (Method B)**: 95 %, R_t = 14.3 min.

Ethyl 2-[(5Z)-5-[(2,4-dihydroxyphenyl)methylidene]-4-oxo-2-sulfanylidene-1,3-thiazolidin-3-yl] acetate **14u**

TLC R_f = 0.2 ($\text{CHCl}_3/\text{MeOH}/\text{HOAc}$ 95:4:1); **Reaction time**: 1 h; **Purification**: Flash-Chromatography $\text{CHCl}_3/\text{MeOH}/\text{HOAc}$ 95:4:1 (R_f = 0.2); **Yield**: 342 mg of yellow solid (1.01 mmol, 86 %); **$^1\text{H-NMR}$** (400 MHz, DMSO-d_6) δ = 1.20 (t, 3 H, $^3J_{\text{H,H}}$ = 7.1 Hz, CH_3), 4.16 (q, 2 H, $^3J_{\text{H,H}}$ = 7.1 Hz, CH_2CH_3), 4.80 (s, 2 H, CH_2), 6.42-6.46 (m, 2 H, 3,5-Ar-CH), 7.25 (d, 1 H, $^3J_{\text{H,H}}$ = 8.4 Hz, 6-Ar-CH), 8.00 (s, 1 H, CH), 10.47 (s, 1 H, OH), 10.83 (s, 1 H, OH) ppm; **$^{13}\text{C-NMR}$** (400 MHz, DMSO-d_6) δ = 14.0 (CH_3), 44.9 (CH_2), 61.6 (CH_2CH_3), 102.5 (3-Ar-CH), 109.2 (5-Ar-CH), 111.8 (Ar-C), 114.8 (Ar-C), 130.6 (CH), 132.0 (6-Ar-CH), 160.2 (Ar-C), 163.1 (Ar-C), 166.2 (C=O), 166.6 (COOEt), 193.4 (C=S) ppm; **ESI-MS** m/z (%) = 340.0 $[\text{M}+\text{H}]^+$ (100 %), 696.1 $[\text{2M}+\text{NH}_4]^+$ (41 %); **HPLC-Analysis (Method B)**: 66 %, R_t = 17.4 min.

Ethyl 2-[(5Z)-5-[3-(benzyloxy)phenyl]methylidene-4-oxo-2-sulfanylidene-1,3-thiazolidin-3-yl] acetate **14v**

TLC R_f = 0.6 (Hexane/EtOAc 8:2); **Reaction time**: 2 h; **Purification**: Re-crystallisation from ethanol; **Yield**: 145 mg of yellow crystals (0.35 mmol, 54 %); **$^1\text{H-NMR}$** (400 MHz, CDCl_3) δ = 1.29 (t, 3 H, $^3J_{\text{H,H}}$ = 7.1 Hz, CH_3), 4.24 (q, 2 H, $^3J_{\text{H,H}}$ = 7.1 Hz, CH_2CH_3), 4.85 (s, 2 H, CH_2COOEt), 5.13 (s, 2 H, $\text{CH}_2\text{-Ar}$), 7.06-7.14 (m, 3 H, 3xAr-CH), 7.35-7.47 (m, 6 H, 6xAr-CH), 7.73 (s, 1 H, CH) ppm; **$^{13}\text{C-NMR}$** (400 MHz, CDCl_3) δ = 14.2 (CH_3), 45.0 (CH_2COOEt), 62.2 (CH_2CH_3), 70.4 (CH_2Ar), 116.2 (Ar-CH), 118.2 (Ar-CH), 123.2 (Ar-C), 123.8 (Ar-CH), 127.6 (Ar-CH), 128.4 (Ar-CH), 128.9 (Ar-CH), 130.6 (Ar-CH), 134.0 (CH), 134.6 (Ar-C), 136.4 (Ar-C), 159.4 (Ar-C), 166.0 (C=O), 167.2 (COOEt), 193.2 (C=S) ppm; **ESI-MS** m/z (%) = 414.1 $[\text{M}+\text{H}]^+$ (100 %), 431.1 $[\text{M}+\text{NH}_4]^+$ (33 %), 436.1 $[\text{M}+\text{Na}]^+$ (4 %); **HPLC-Analysis (Method B)**: 99 %, R_t = 21.6 min.

Ethyl 2-[(5Z)-5-[4-(benzyloxy)phenyl]methylidene-4-oxo-2-sulfanylidene-1,3-thiazolidin-3-yl] acetate **14w**

TLC R_f = 0.6 (Hexane/EtOAc 8:2); **Reaction time**: 2 h; **Purification**: Re-crystallisation from

ethanol; **Yield:** 340 mg of yellow crystals (0.82 mmol, 67 %); **¹H-NMR** (400 MHz, CDCl₃) δ = 1.29 (t, 3 H, $^3J_{\text{H,H}}$ = 7.1 Hz, CH₃), 4.24 (q, 2 H, $^3J_{\text{H,H}}$ = 7.1 Hz, CH₂CH₃), 4.86 (s, 2 H, CH₂COOEt), 5.14 (s, 2 H, CH₂Ar), 7.08 (d, 2 H, $^3J_{\text{H,H}}$ = 8.8 Hz, 2,6-Ar-CH), 7.33-7.45 (m, 5 H, 5xAr-CH), 7.48 (d, 2 H, $^3J_{\text{H,H}}$ = 8.8 Hz, 3,5-Ar-CH), 7.74 (s, 1 H, CH) ppm; **¹³C-NMR** (400 MHz, CDCl₃) δ = 14.3 (CH₃), 45.0 (CH₂COOEt), 62.2 (CH₂CH₃), 70.4 (CH₂Ar), 116.0 (2,6-Ar-CH), 119.9 (Ar-C), 126.3 (Ar-C), 127.6 (Ar-CH), 128.5 (Ar-CH), 128.9 (Ar-CH), 133.0 (3,5-Ar-CH), 134.1 (CH), 136.1 (Ar-C), 161.2 (Ar-C), 166.1 (C=O), 167.4 (COOEt), 193.2 (C=S) ppm; **ESI-MS** m/z (%) = 414.1 [M+H]⁺ (100 %), 436.1 [M+Na]⁺ (40 %), 452.0 [M+K]⁺ (15 %), 844.2 [2M+NH₄]⁺ (100 %), 849.1 [2M+Na]⁺ (95 %), 865.1 [2M+K]⁺ (70 %); **HR-MS** m/z = 414.0828 [M+H]⁺ (calculated: 414.0828); **HPLC-Analysis (Method B):** 99 %, R_t = 21.6 min.

Ethyl 2-[(5Z)-5-[3,4-bis(benzyloxy)phenyl]methylidene-4-oxo-2-sulfanylidene-1,3-thiazolidin-3-yl] acetate **14x**

TLC R_f = 0.3 (Hexane/EtOAc 8:2); **TLC** R_f = 0.5 (DCM); **Reaction time:** 1 h; **Purification:** Filtration from Ethanol; **Yield:** 513 mg of yellow solid (0.99 mmol, 87 %); **Yield:** 21 mg of yellow solid (0.04 mmol, 40 %); **¹H-NMR** (400 MHz, DMSO-d₆) δ = 1.20-1.23 (m, 3 H, OCH₂CH₃), 4.16 (q, 2 H, $^3J_{\text{H,H}}$ = 7.0 Hz, OCH₂), 4.82 (s, 2 H, CH₂), 5.24-5.26 (s, 2 H, OCH₂Ph), 7.25-7.49 (m, 13 H, 13xAr-CH), 7.82 (s, 1 H, CH) ppm; **¹H-NMR** (400 MHz, CDCl₃) δ = 1.28 (t, 3 H, $^3J_{\text{H,H}}$ = 7.1 Hz, CH₃), 4.23 (q, 2 H, $^3J_{\text{H,H}}$ = 7.1 Hz, CH₂CH₃), 4.84 (s, 2 H, CH₂), 5.24 (s, 2 H, CH₂Ar), 5.25 (s, 2 H, CH₂Ar), 6.99 (d, 1 H, $^3J_{\text{H,H}}$ = 8.4 Hz, 5-Ar-CH), 7.02 (d, 1 H, $^4J_{\text{H,H}}$ = 1.7 Hz, 2-Ar-CH), 7.08 (dd, 1 H, $^{3,4}J_{\text{H,H}}$ = 1.7, 8.4 Hz, 6-Ar-CH), 7.30-7.50 (m, 10 H, 10xAr-CH), 7.64 (s, 1 H, CH) ppm; **¹³C-NMR** (400 MHz, CDCl₃) δ = 14.3 (CH₃), 45.0 (CH₂), 62.2 (CH₂CH₃), 71.1 (CH₂), 71.4 (CH₂), 114.3 (5-Ar-CH), 116.1 (2-Ar-CH), 120.2 (Ar-C), 126.3 (6-Ar-CH), 127.3 (4xAr-CH), 127.4 (2xAr-CH), 128.3 (4xAr-CH), 128.9 (2xAr-C), 134.3 (CH), 136.4 (Ar-C), 149.1 (Ar-C), 151.7 (Ar-C), 166.1 (C=O), 167.3 (COOEt), 193.1 (C=S) ppm; **ESI-MS** m/z (%) = 520.1 [M+H]⁺ (100 %), 537.2 [M+NH₄]⁺ (75 %); **HR-MS** m/z = 520.1247 [M+H]⁺ (calculated: 520.1242); **HPLC-Analysis (Method B):** 98 %, R_t = 18.4 min.

Ethyl 2-[(5Z)-5-[(4-hydroxy-3,5-dimethoxyphenyl)methylidene]-4-oxo-2-sulfanylidene-1,3-thiazolidin-3-yl] acetate **14y**

TLC R_f = 0.6 (CHCl₃/MeOH 1:0.05); **Reaction time:** 16 h; **Purification:** Flash-Chromatography Toluene/MeOH 9:1 (R_f = 0.3); **Yield:** 279 mg of red solid (0.73 mmol, 64 %); **¹H-NMR** (400 MHz, CDCl₃) δ = 1.29 (t, 3 H, $^3J_{\text{H,H}}$ = 7.1 Hz, CH₃), 3.94 (s, 6 H, 2xOCH₃), 4.24 (q, 2 H, $^3J_{\text{H,H}}$ = 7.1 Hz, CH₂CH₃), 4.85 (s, 2 H, CH₂), 6.71 (s, 2 H, 2,6-Ar-CH), 7.65 (s, 1 H, CH) ppm; **¹³C-NMR** (400 MHz, CDCl₃) δ = 14.2 (CH₃), 44.9 (CH₂), 56.5 (2xOCH₃), 62.1 (CH₂CH₃), 108.0 (2,6-Ar-CH), 119.7 (Ar-C), 124.7 (Ar-C), 134.7 (CH), 138.1 (Ar-C), 147.6 (3,5-Ar-C), 166.0 (C=O), 167.1 (COOEt), 192.8 (C=S) ppm; **ESI-MS** m/z (%) = 384.1 [M+H]⁺ (20 %), 784.1 [2M+NH₄]⁺ (19 %), 789.1 [2M+Na]⁺ (3 %); **HPLC-Analysis (Method B):** 99 %, R_t = 22.6 min.

Ethyl 3-[(5Z)-4-oxo-5-(phenylmethylidene)-2-sulfanylidene-1,3-thiazolidin-3-yl] propanoate **15a**^[286]

TLC R_f = 0.3 (Hexane/EtOAc 8:2); **Reaction time**: 16 h; **Purification**: Flash-Chromatography DCM (R_f = 0.1); **Yield**: 211 mg of yellow solid (0.66 mmol, 72 %); **$^1\text{H-NMR}$** (400 MHz, CDCl_3) δ = 1.26 (t, 3 H, $^3J_{\text{H,H}}$ = 7.1 Hz, CH_3), 2.73-2.78 (m, 2 H, $\beta\text{-CH}_2$), 4.15 (q, 2 H, $^3J_{\text{H,H}}$ = 7.1 Hz, CH_2CH_3), 4.39-4.45 (m, 2 H, $\alpha\text{-CH}_2$), 7.42-7.51 (m, 5 H, 5xAr-CH), 7.73 (s, 1 H, CH) ppm; **$^{13}\text{C-NMR}$** (400 MHz, CDCl_3) δ = 14.2 (CH_3), 31.5 ($\beta\text{-CH}_2$), 40.1 ($\alpha\text{-CH}_2$), 61.1 (CH_2CH_3), 122.8 (Ar-C), 129.4 (2xAr-CH), 130.8 (2xAr-CH), 130.9 (Ar-CH), 133.3 (Ar-C), 133.5 (CH), 167.5 (C=O), 170.5 (COOEt), 193.1 (C=S) ppm; **ESI-MS** m/z (%) = 322.1 $[\text{M}+\text{H}]^+$ (100 %), 344.0 $[\text{M}+\text{Na}]^+$ (3 %), 660.1 $[\text{2M}+\text{NH}_4]^+$ (11 %); **HPLC-Analysis (Method B)**: 99 %, R_t = 20.4 min.
Ethyl 3-[(5Z)-5-[(2-methylphenyl)methylidene]-4-oxo-2-sulfanylidene-1,3-thiazolidin-3-yl] propionate **15b**

TLC R_f = 0.7 (Hexane/EtOAc 8:2); **Reaction time**: 30 min; **Purification**: Re-crystallisation from ethanol; **Yield**: 100 mg of orange crystals (0.30 mmol, 35 %); **$^1\text{H-NMR}$** (400 MHz, CDCl_3) δ = 1.27 (t, 3 H, $^3J_{\text{H,H}}$ = 7.1 Hz, CH_3), 2.47 (s, 3 H, Ar- CH_3), 2.77 (t, 2 H, $^3J_{\text{H,H}}$ = 7.6 Hz, $\beta\text{-CH}_2$), 4.16 (q, 2 H, $^3J_{\text{H,H}}$ = 7.1 Hz, CH_2CH_3), 4.44 (t, 2 H, $^3J_{\text{H,H}}$ = 7.6 Hz, $\alpha\text{-CH}_2$), 7.25-7.37 (m, 3 H, 3,4,5-Ar-CH), 7.41 (d, 1 H, $^3J_{\text{H,H}}$ = 7.5 Hz, 6-Ar-CH), 7.97 (s, 1 H, CH) ppm; **$^{13}\text{C-NMR}$** (400 MHz, CDCl_3) δ = 14.3 (CH_3), 20.2 (Ar- CH_3), 31.6 ($\beta\text{-CH}_2$), 40.1 ($\alpha\text{-CH}_2$), 61.1 (CH_2CH_3), 124.2 (Ar-C), 126.9 (Ar-CH), 128.2 (6-Ar-CH), 131.0 (Ar-CH), 131.4 (Ar-CH), 131.5 (CH), 132.5 (Ar-C), 139.7 (Ar-C), 167.4 (C=O), 170.6 (COOEt), 193.8 (C=S) ppm; **ESI-MS** m/z (%) = 336.1 $[\text{M}+\text{H}]^+$ (100 %), 353.0 $[\text{M}+\text{NH}_4]^+$ (7 %), 358.1 $[\text{M}+\text{Na}]^+$ (42 %), 688.3 $[\text{M}+\text{NH}_4]^+$ (13 %), 693.1 $[\text{2M}+\text{Na}]^+$ (33 %); **HPLC-Analysis (Method B)**: 99 %, R_t = 21.0 min.

Ethyl 3-[(5Z)-5-[(3-methylphenyl)methylidene]-4-oxo-2-sulfanylidene-1,3-thiazolidin-3-yl] propionate **15c**

TLC R_f = 0.4 (Hexane/EtOAc 9:1); **Reaction time**: 30 min; **Purification**: Filtration from ethanol; **Yield**: 132 mg of yellow solid (0.39 mmol, 61 %); **$^1\text{H-NMR}$** (400 MHz, CDCl_3) δ = 1.26 (t, 3 H, $^3J_{\text{H,H}}$ = 7.1 Hz, CH_3), 2.42 (s, 3 H, Ar- CH_3), 2.76 (t, 2 H, $^3J_{\text{H,H}}$ = 7.6 Hz, $\beta\text{-CH}_2$), 4.15 (q, 2 H, $^3J_{\text{H,H}}$ = 7.1 Hz, CH_2CH_3), 4.44 (t, 2 H, $^3J_{\text{H,H}}$ = 7.6 Hz, $\alpha\text{-CH}_2$), 7.25-7.29 (m, 1 H, 4-Ar-CH), 7.29-7.33 (m, 2 H, 2,6-Ar-CH), 7.35-7.40 (m, 1 H, 5-Ar-CH), 7.72 (s, 1 H, CH) ppm; **$^{13}\text{C-NMR}$** (400 MHz, CDCl_3) δ = 14.3 (CH_3), 21.6 (Ar- CH_3), 31.6 ($\beta\text{-CH}_2$), 40.1 ($\alpha\text{-CH}_2$), 61.1 (CH_2CH_3), 122.6 (Ar-C), 128.1 (2 or 6-Ar-CH), 129.4 (5-Ar-CH), 131.4 (2 or 6-Ar-CH), 131.9 (4-Ar-CH), 133.4 (Ar-C), 133.9 (CH), 139.4 (Ar-C), 167.7 (C=O), 170.6 (COOEt), 193.4 (C=S) ppm; **ESI-MS** m/z (%) = 336.1 $[\text{M}+\text{H}]^+$ (100 %), 353.1 $[\text{M}+\text{NH}_4]^+$ (6 %), 358.1 $[\text{M}+\text{Na}]^+$ (22 %), 688.2 $[\text{2M}+\text{NH}_4]^+$ (23 %), 693.1 $[\text{2M}+\text{Na}]^+$ (11 %); **HPLC-Analysis (Method B)**: 99 %, R_t = 21.0 min.

Ethyl 3-[(5Z)-5-[(4-methylphenyl)methylidene]-4-oxo-2-sulfanylidene-1,3-thiazolidin-3-yl] propionate **15d**

TLC R_f = 0.4 (Hexane/EtOAc 9:1); **Reaction time**: 30 min; **Purification**: Filtration from ethanol; **Yield**: 122 mg of yellow solid (0.36 mmol, 57 %); **$^1\text{H-NMR}$** (400 MHz, CDCl_3) δ =

1.26 (t, 3 H, $^3J_{\text{H,H}} = 7.1$ Hz, CH_3), 2.41 (s, 3 H, Ar- CH_3), 2.76 (t, 2 H, $^3J_{\text{H,H}} = 7.5$ Hz, $\beta\text{-CH}_2$), 4.15 (q, 2 H, $^3J_{\text{H,H}} = 7.1$ Hz, CH_2CH_3), 4.43 (t, 2 H, $^3J_{\text{H,H}} = 7.5$ Hz, $\alpha\text{-CH}_2$), 7.29 (d, 2 H, $^3J_{\text{H,H}} = 8.1$ Hz, 3,5-Ar- CH), 7.40 (d, 2 H, $^3J_{\text{H,H}} = 8.1$ Hz, 2,6-Ar- CH), 7.73 (s, 1 H, CH) ppm; $^{13}\text{C-NMR}$ (400 MHz, CDCl_3) $\delta = 14.3$ (CH_3), 21.8 (Ar- CH_3), 31.6 ($\beta\text{-CH}_2$), 40.1 ($\alpha\text{-CH}_2$), 61.1 (CH_2CH_3), 121.6 (Ar- C), 130.3 (3,5-Ar- CH), 130.7 (Ar- C), 131.0 (2,6-Ar- CH), 133.9 (CH), 170.6 (COOEt), 193.3 ($\text{C}=\text{S}$) ppm; **ESI-MS** m/z (%) = 336.1 $[\text{M}+\text{H}]^+$ (100 %), 358.1 $[\text{M}+\text{Na}]^+$ (35 %), 688.2 $[2\text{M}+\text{NH}_4]^+$ (5 %); **HR-MS** $m/z = 336.0728$ $[\text{M}+\text{H}]^+$ (calculated: 336.0723); **HPLC-Analysis (Method B)**: 99 %, $R_t = 21.2$ min.

Ethyl 3-[(5Z)-5-[(4-hydroxyphenyl)methylidene]-4-oxo-2-sulfanylidene-1,3-thiazolidin-3-yl] propanoate **15e**

TLC $R_f = 0.3$ ($\text{CHCl}_3/\text{EtOAc}$ 9:1); **Reaction time**: 1 h; **Purification**: Flash-Chromatography $\text{CHCl}_3/\text{EtOAc}$ 9:1 ($R_f = 0.3$); **Yield**: 334 mg of red solid (0.99 mmol, 93 %); $^1\text{H-NMR}$ (400 MHz, CDCl_3) $\delta = 1.28$ (t, 3 H, $^3J_{\text{H,H}} = 7.2$ Hz, CH_3), 2.77 (t, 2 H, $^3J_{\text{H,H}} = 7.3$ Hz, $\beta\text{-CH}_2$), 4.17 (q, 2 H, $^3J_{\text{H,H}} = 7.2$ Hz, CH_2CH_3), 4.44 (t, 2 H, $^3J_{\text{H,H}} = 7.3$ Hz, $\alpha\text{-CH}_2$), 6.91 (d, 2 H, $^3J_{\text{H,H}} = 8.6$ Hz, 2,6-Ar- CH), 7.33 (d, 2 H, $^3J_{\text{H,H}} = 8.6$ Hz, 3,5-Ar- CH), 7.61 (s, 1 H, CH) ppm; $^{13}\text{C-NMR}$ (400 MHz, CDCl_3) $\delta = 14.2$ (CH_3), 31.7 ($\beta\text{-CH}_2$), 40.2 ($\alpha\text{-CH}_2$), 61.3 (CH_2CH_3), 116.7 (2,6-Ar- CH), 119.7 (Ar- C), 126.1 (Ar- C), 133.2 (3,5-Ar- CH), 133.8 (CH), 158.6 (Ar- C), 167.8 ($\text{C}=\text{O}$), 171.0 (COOEt), 193.2 ($\text{C}=\text{S}$) ppm; **ESI-MS** m/z (%) = 338.1 $[\text{M}+\text{H}]^+$ (100 %), 355.1 $[\text{M}+\text{NH}_4]^+$ (5 %), 360.0 $[\text{M}+\text{Na}]^+$ (10 %), 692.1 $[2\text{M}+\text{NH}_4]^+$ (24 %), 696.1 $[2\text{M}+\text{Na}]^+$ (12 %); **HPLC-Analysis (Method B)**: 90 %, $R_t = 18.8$ min.

Ethyl 3-[(5Z)-5-[(3,4-dihydroxyphenyl)methylidene]-4-oxo-2-sulfanylidene-1,3-thiazolidin-3-yl] propanoate **15f**

TLC $R_f = 0.2$ ($\text{CHCl}_3/\text{MeOH}/\text{AcOH}$ 96:3:1); **Reaction time**: 2 h; **Purification**: Flash-Chromatography $\text{CHCl}_3/\text{MeOH}/\text{AcOH}$ 96:3:1 ($R_f = 0.1$); **Yield**: 195 mg of yellow solid (0.55 mmol, 52 %); $^1\text{H-NMR}$ (400 MHz, DMSO-d_6) $\delta = 1.16$ (t, 3 H, $^3J_{\text{H,H}} = 7.1$ Hz, CH_3), 2.69 (t, 2 H, $^3J_{\text{H,H}} = 7.4$ Hz, $\beta\text{-CH}_2$), 4.04 (q, 2 H, $^3J_{\text{H,H}} = 7.1$ Hz, CH_2CH_3), 4.25 (t, 2 H, $^3J_{\text{H,H}} = 7.4$ Hz, $\alpha\text{-CH}_2$), 6.89 (d, 1 H, $^3J_{\text{H,H}} = 8.0$ Hz, 5-Ar- CH), 7.03-7.05 (m, 1 H, 2-Ar- CH), 7.05 (dd, 1 H, $^3,4J_{\text{H,H}} = 2.2, 8.0$ Hz, 6-Ar- CH), 7.65 (s, 1 H, CH) ppm; $^{13}\text{C-NMR}$ (400 MHz, DMSO-d_6) $\delta = 14.0$ (CH_3), 31.0 ($\beta\text{-CH}_2$), 40.1 ($\alpha\text{-CH}_2$), 60.4 (CH_2CH_3), 116.5 (5-Ar- CH), 116.7 (2-Ar- CH), 117.3 (Ar- C), 124.4 (Ar- C), 125.4 (6-Ar- CH), 134.3 (CH), 146.2 (Ar- C), 149.6 (Ar- C), 166.8 ($\text{C}=\text{O}$), 170.2 ($\text{C}=\text{OOEt}$), 193.2 ($\text{C}=\text{S}$) ppm; **HPLC-Analysis (Method B)**: 97 %, $R_t = 17.6$ min.

Ethyl 4-[(5Z)-4-oxo-5-(phenylmethylidene)-2-sulfanylidene-1,3-thiazolidin-3-yl] butanoate **16a**^[287]

TLC $R_f = 0.5$ (Hexane/ EtOAc 8:2); **Reaction time**: 1 h; **Purification**: Filtration from ethanol; **Yield**: 310 mg of yellow solid (0.92 mmol, 91 %); $^1\text{H-NMR}$ (400 MHz, DMSO-d_6) $\delta = 1.17$ (t, 3 H, $^3J_{\text{H,H}} = 7.1$ Hz, CH_3), 1.92 (ap, 2 H, $^3J_{\text{H,H}} = 7.1, 7.0$ Hz, $\beta\text{-CH}_2$), 2.38 (t, 2 H, $^3J_{\text{H,H}} = 7.1$ Hz, $\gamma\text{-CH}_2$), 4.03 (q, 2 H, $^3J_{\text{H,H}} = 7.1$ Hz, CH_2CH_3), 4.07 (t, 2 H, $^3J_{\text{H,H}} = 7.0$ Hz, $\alpha\text{-CH}_2$), 7.48-7.66 (m, 5 H, 5xAr- CH), 7.80 (s, 1 H, CH) ppm; **ESI-MS** m/z (%) = 336.1 $[\text{M}+\text{H}]^+$ (100 %),

353.1 $[M+NH_4]^+$ (19 %); **HPLC-Analysis (Method B)**: 98 %, R_t = 20.8 min.

Ethyl 4-[(5Z)-5-[(2-methylphenyl)methylidene]-4-oxo-2-sulfanylidene-1,3-thiazolidin-3-yl] butanoate **16b** **TLC** R_f = 0.5 (Hexane/EtOAc 8:2); **Reaction time**: 1 h; **Purification**: Flash-Chromatography hexane/EtOAc 9:1 (R_f = 0.2); **Yield**: 320 mg of yellow solid (0.92 mmol, 92 %); **Yield**: 270 mg of yellow solid (0.77 mmol, 77 %); **1H -NMR** (400 MHz, $CDCl_3$) δ = 1.27 (t, 3 H, $^3J_{H,H}$ = 7.1 Hz, CH_2CH_3), 2.07 (p, 2 H, $^3J_{H,H}$ = 7.4 Hz, β - CH_2), 2.40 (t, 2 H, $^3J_{H,H}$ = 7.4 Hz, γ - CH_2), 2.46 (s, 3 H, CH_3), 4.14 (q, 2 H, $^3J_{H,H}$ = 7.1 Hz, CH_2CH_3), 4.20 (t, 2 H, $^3J_{H,H}$ = 7.4 Hz, α - CH_2), 7.25-7.35 (m, 3 H, 3xAr-CH), 7.38-7.41 (m, 1 H, 6-Ar-CH), 7.94 (s, 1 H, CH) ppm; **^{13}C -NMR** (400 MHz, $CDCl_3$) δ = 14.3 (CH_2CH_3), 20.0 (CH_3), 22.5 (β - CH_2), 31.6 (γ - CH_2), 43.7 (α - CH_2), 60.6 (Ar-C), 126.8 (Ar-CH), 128.1 (6-Ar-CH), 130.8 (Ar-CH), 131.0 (CH), 131.2 (Ar-CH), 132.4 (Ar-C), 139.5 (Ar-C), 167.6 (C=O), 172.5 (COOEt), 194.0 (C=S) ppm; **HPLC-Analysis (Method B)**: 98 %, R_t = 21.7 min.

Ethyl 4-[(5Z)-5-[(3-methylphenyl)methylidene]-4-oxo-2-sulfanylidene-1,3-thiazolidin-3-yl] butanoate **16c** **TLC** R_f = 0.5 (Hexane/EtOAc 8:2); **Reaction time**: 16 h; **Purification**: Flash-Chromatography Hexane/EtOAc 9:1 (R_f = 0.2); **Yield**: 340 mg of yellow solid (0.97 mmol, 97 %); **Yield**: 321 mg of yellow solid (0.92 mmol, 92 %); **1H -NMR** (400 MHz, $CDCl_3$) δ = 1.26 (t, 3 H, $^3J_{H,H}$ = 7.1 Hz, CH_2CH_3), 2.07 (p, 2 H, $^3J_{H,H}$ = 7.4 Hz, β - CH_2), 2.40 (t, 2 H, $^3J_{H,H}$ = 7.4 Hz, γ - CH_2), 2.41 (s, 3 H, CH_3), 4.14 (q, 2 H, $^3J_{H,H}$ = 7.1 Hz, CH_2CH_3), 4.19 (t, 2 H, $^3J_{H,H}$ = 7.4 Hz, α - CH_2), 7.24-7.39 (m, 4 H, 4xAr-CH), 7.68 (s, 1 H, CH) ppm; **^{13}C -NMR** (400 MHz, $CDCl_3$) δ = 14.3 (CH_2CH_3), 21.5 (CH_3), 22.5 (β - CH_2), 31.6 (γ - CH_2), 43.8 (α - CH_2), 60.7 (CH_2CH_3), 122.7 (Ar-C), 128.0 (Ar-CH), 129.3 (Ar-CH), 131.3 (Ar-CH), 131.8 (Ar-CH), 133.3 (Ar-C), 133.5 (CH), 139.3 (Ar-C), 167.9 (C=O), 172.5 (C=OOEt), 193.6 (C=S) ppm; **ESI-MS** m/z (%) = 350.1 $[M+H]^+$ (100 %), 716.2 $[2M+NH_4]^+$ (46 %); **HPLC-Analysis (Method B)**: 100 %, R_t = 21.6 min.

Ethyl 4-[(5Z)-5-[(4-methylphenyl)methylidene]-4-oxo-2-sulfanylidene-1,3-thiazolidin-3-yl] butanoate **16d** **TLC** R_f = 0.5 (Hexane/EtOAc 8:2); **Reaction time**: 1 h; **Purification**: Filtration from ethanol; **Yield**: 193 mg of yellow solid (0.55 mmol, 55 %); **Yield**: 247 mg of yellow crystals (0.71 mmol, 71 %); **1H -NMR** (400 MHz, $CDCl_3$) δ = 1.26 (t, 3 H, $^3J_{H,H}$ = 7.1 Hz, CH_2CH_3), 2.07 (p, 2 H, $^3J_{H,H}$ = 7.4 Hz, β - CH_2), 2.39 (t, 2 H, $^3J_{H,H}$ = 7.4 Hz, γ - CH_2), 2.41 (s, 3 H, CH_3), 4.14 (q, 2 H, $^3J_{H,H}$ = 7.1 Hz, CH_2CH_3), 4.20 (t, 2 H, $^3J_{H,H}$ = 7.4 Hz, α - CH_2), 7.29 (d, 2 H, $^3J_{H,H}$ = 8.2 Hz, 3,5-Ar-CH), 7.40 (d, 2 H, $^3J_{H,H}$ = 8.2 Hz, 2,6-Ar-CH), 7.71 (s, 1 H, CH) ppm; **^{13}C -NMR** (400 MHz, $CDCl_3$) δ = 14.4 (CH_2CH_3) 21.8 (CH_3), 22.6 (β - CH_2), 31.7 (γ - CH_2), 43.9 (α - CH_2), 60.8 (CH_2CH_3), 121.8 (Ar-C) 130.3 (3,5-Ar-CH), 130.8 (Ar-C), 130.9 (2,6-Ar-CH), 133.6 (CH), 141.9 (Ar-C), 168.1 (C=O), 172.6 (COOEt), 193.7 (C=S) ppm; **ESI-MS** m/z (%) = 350.1 $[M+H]^+$ (100 %), 372.1 $[M+Na]^+$ (7 %), 716.2 $[2M+NH_4]^+$ (44 %), 721.2 $[2M+Na]^+$ (7 %); **HPLC-Analysis (Method B)**: 98 %, R_t = 21.6 min.

Ethyl 4-[(5Z)-5-[2,5-bis(trifluoromethyl)phenyl]methylidene-4-oxo-2-sulfanylidene-1,3-thiazolidin-3-yl] butanoate **16e**

TLC R_f = 0.3 (Hexane/EtOAc 9:1); **Reaction time**: 1 h; **Purification**: Flash-Chromatography Hexane/EtOAc 95:5 (R_f = 0.2); **Yield**: 431 mg of yellow solid (0.91 mmol, 91 %); **$^1\text{H-NMR}$** (400 MHz, CDCl_3) δ = 1.28 (t, 3 H, $^3J_{\text{H,H}}$ = 7.1 Hz, CH_3), 2.09 (p, 2 H, $^3J_{\text{H,H}}$ = 7.2 Hz, $\beta\text{-CH}_2$), 2.42 (t, 2 H, $^3J_{\text{H,H}}$ = 7.1 Hz, $\gamma\text{-CH}_2$), 4.16 (q, 2 H, $^3J_{\text{H,H}}$ = 7.1 Hz, CH_2CH_3), 4.22 (t, 2 H, $^3J_{\text{H,H}}$ = 7.1 Hz, $\alpha\text{-CH}_2$), 7.81 (d, 1 H, $^3J_{\text{H,H}}$ = 8.2 Hz, 4-Ar-CH), 7.85 (s, 1 H, 6-Ar-CH), 7.92-7.96 (m, 2 H, 3-Ar-CH and CH) ppm; **$^{13}\text{C-NMR}$** (400 MHz, CDCl_3) δ = 14.3 (CH_3), 22.5 ($\beta\text{-CH}_2$), 31.6 ($\gamma\text{-CH}_2$), 44.1 ($\alpha\text{-CH}_2$), 60.8 (CH_2CH_3), 122.9 (q, $^1J_{\text{C,F}}$ = 273.3 Hz, CF_3), 123.0 (q, $^1J_{\text{C,F}}$ = 274.6 Hz, CF_3), 126.1 (q, $^3J_{\text{C,F}}$ = 3.6 Hz, 6-Ar-CH), 126.2 (q, $^5J_{\text{C,F}}$ = 1.9 Hz, CH) 126.7 (q, $^3J_{\text{C,F}}$ = 3.6 Hz, 4-Ar-CH), 127.8 (q, $^3J_{\text{C,F}}$ = 5.5 Hz, 3-Ar-CH), 129.9 (Ar-C), 132.8 (q, $^2J_{\text{C,F}}$ = 32.0 Hz, Ar-C), 133.5 (q, $^4J_{\text{C,F}}$ = 1.3 Hz, Ar-C), 134.8 (q, $^2J_{\text{C,F}}$ = 33.6 Hz, Ar-C), 166.8 (C=O), 172.5 (COOEt), 192.3 (C=S) ppm; **ESI-MS** m/z (%) = 472.1 $[\text{M}+\text{H}]^+$ (73 %), 489.0 $[\text{M}+\text{NH}_4]^+$ (100 %), 960.1 $[2\text{M}+\text{NH}_4]^+$ (51 %); **HPLC-Analysis (Method B)**: 97 %, R_t = 15.1 min.

Ethyl 4-[(5Z)-5-[(2-hydroxyphenyl)methylidene]-4-oxo-2-sulfanylidene-1,3-thiazolidin-3-yl] butanoate **16f**

TLC R_f = 0.3 (Hexane/EtOAc 7:3); **Reaction time**: 4 h; **Purification**: Flash-Chromatography Hexane/EtOAc 8:2 (R_f = 0.2); **Yield**: 330 mg of yellow solid (0.94 mmol, 94 %); **$^1\text{H-NMR}$** (400 MHz, CDCl_3) δ = 1.27 (t, 3 H, $^3J_{\text{H,H}}$ = 7.1 Hz, CH_3), 2.10 (ap, 2 H, $^3J_{\text{H,H}}$ = 7.4, 7.1 Hz, $\beta\text{-CH}_2$), 2.43 (t, 2 H, $^3J_{\text{H,H}}$ = 7.4 Hz, $\gamma\text{-CH}_2$), 4.15 (q, 2 H, $^3J_{\text{H,H}}$ = 7.1 Hz, CH_2CH_3), 4.23 (t, 2 H, $^3J_{\text{H,H}}$ = 7.1 Hz, $\alpha\text{-CH}_2$), 6.93 (d, 1 H, $^3J_{\text{H,H}}$ = 8.1 Hz, 3-Ar-CH), 7.00 (at, 1 H, $^3J_{\text{H,H}}$ = 7.6 Hz, 5-Ar-CH), 7.32 (atd, 1 H, $^{3,4}J_{\text{H,H}}$ = 8.1, 1.4 Hz, 4-Ar-CH), 7.37 (dd, 1 H, $^{3,4}J_{\text{H,H}}$ = 8.1, 1.4 Hz, 6-Ar-CH), 8.29 (s, 1 H, CH) ppm; **$^{13}\text{C-NMR}$** (400 MHz, CDCl_3) δ = 14.3 (CH_3), 22.6 ($\beta\text{-CH}_2$), 31.7 ($\gamma\text{-CH}_2$), 43.9 ($\alpha\text{-CH}_2$), 61.0 (CH_2CH_3), 116.6 (3-Ar-CH), 121.1 (Ar-C), 121.3 (5-Ar-C), 121.9 (Ar-C), 129.6 (CH), 129.8 (6-Ar-CH) 132.9 (4-Ar-CH), 156.5 (Ar-C), 168.8 (C=O), 173.0 (COOEt), 194.0 (C=S) ppm; **ESI-MS** m/z (%) = 352.1 $[\text{M}+\text{H}]^+$ (100 %), 369.1 $[\text{M}+\text{NH}_4]^+$ (16 %), 374.0 $[\text{M}+\text{Na}]^+$ (2 %), 720.1 $[2\text{M}+\text{NH}_4]^+$ (67 %), 725.1 $[2\text{M}+\text{Na}]^+$ (5 %); **HPLC-Analysis (Method B)**: 92 %, R_t = 20.0 min.

Ethyl 4-[(5Z)-5-[(3-hydroxyphenyl)methylidene]-4-oxo-2-sulfanylidene-1,3-thiazolidin-3-yl] butanoate **16g**

TLC R_f = 0.3 ($\text{CHCl}_3/\text{MeOH}/\text{HOAc}$ 97:2:1); **Reaction time**: 4 h; **Purification**: Flash-Chromatography $\text{CHCl}_3/\text{MeOH}/\text{HOAc}$ 97:2:1 (R_f = 0.3); **Yield**: 329 mg of yellow solid (0.94 mmol, 94 %); **$^1\text{H-NMR}$** (400 MHz, CDCl_3) δ = 1.27 (t, 3 H, $^3J_{\text{H,H}}$ = 7.1 Hz, CH_3), 2.03-2.12 (m, 2 H, $\beta\text{-CH}_2$), 2.42 (t, 2 H, $^3J_{\text{H,H}}$ = 7.4 Hz, $\gamma\text{-CH}_2$), 4.13-4.21 (m, 4 H, $\alpha\text{-CH}_2$, CH_2CH_3), 6.93-6.99 (m, 2 H, 2,4-Ar-CH), 7.03 (d, 1 H, $^3J_{\text{H,H}}$ = 7.6 Hz, 6-Ar-CH), 7.33 (at, 1 H, $^3J_{\text{H,H}}$ = 7.9 Hz, 5-Ar-CH), 7.64 (s, 1 H, CH) ppm; **$^{13}\text{C-NMR}$** (400 MHz, CDCl_3) δ = 14.3 (CH_3), 22.6 ($\beta\text{-CH}_2$), 31.7 ($\gamma\text{-CH}_2$), 43.8 ($\alpha\text{-CH}_2$), 61.1 (CH_2CH_3), 117.0 (2-Ar-CH), 118.5 (4-Ar-CH), 123.1 (Ar-C), 123.3 (6-Ar-CH), 130.7 (5-Ar-CH), 133.4 (CH), 134.7 (Ar-C), 156.8 (Ar-C), 168.1 (C=O), 173.2 (COOEt), 193.5 (C=S) ppm; **ESI-MS** m/z (%) = 352.1 $[\text{M}+\text{H}]^+$ (37 %), 369.1 $[\text{M}+\text{NH}_4]^+$ (8 %),

374.0 [M+Na]⁺ (19 %), 703.1 [2M+H]⁺ (100 %), 720.2 [2M+NH₄]⁺ (18 %), 725.1 [2M+Na]⁺ (27 %); **HPLC-Analysis (Method B)**: 91 %, R_t = 19.3 min.

Ethyl 4-[(5Z)-5-[(4-hydroxyphenyl)methylidene]-4-oxo-2-sulfanylidene-1,3-thiazolidin-3-yl] butanoate **16h**

TLC R_f = 0.3 (CHCl₃/MeOH/HOAc 97:2:1); **Reaction time**: 1 h; **Purification**: Filtration from ethanol; **Yield**: 145 mg of yellow solid (0.41 mmol, 71 %); **¹H-NMR** (400 MHz, DMSO-d₆) δ = 1.17 (t, 3 H, ³J_{H,H} = 7.1 Hz, CH₃), 1.92 (p, 2 H, ³J_{H,H} = 7.0 Hz, β-CH₂), 2.38 (t, 2 H, ³J_{H,H} = 7.2 Hz, γ-CH₂), 4.03 (q, 2 H, ³J_{H,H} = 7.1 Hz, CH₂CH₃), 4.08 (t, 2 H, ³J_{H,H} = 6.9 Hz, α-CH₂), 7.55 (d, 2 H, ³J_{H,H} = 7.5 Hz, 2xAr-CH), 7.65 (d, 2 H, ³J_{H,H} = 7.5 Hz, 2xAr-CH), 7.81 (s, 1 H, CH) ppm; **¹³C-NMR** (400 MHz, DMSO-d₆) δ = 14.1 (CH₃), 21.9 (CH₂), 30.8 (CH₂), 43.6 (CH₂), 59.9 (CH₂), 122.6 (Ar-C), 129.5 (2xAr-CH), 130.6 (2xAr-CH), 131.0 (Ar-C), 132.7 (CH), 167.2 (C=O), 172.2 (COOEt), 193.8 (C=S) ppm; **HPLC-Analysis (Method B)**: 99 %, R_t = 20.9 min.

Ethyl 4-[(5Z)-5-[(3,4-dihydroxyphenyl)methylidene]-4-oxo-2-sulfanylidene-1,3-thiazolidin-3-yl] butanoate **16i**

TLC R_f = 0.3 (Hexane/EtOAc 8:2); **Reaction time**: 1 h; **Purification**: Flash-Chromatography CHCl₃/MeOH/HOAc 96:3:1 (R_f = 0.1); **Yield**: 150 mg of yellow solid (0.41 mmol, 85 %); **¹H-NMR** (400 MHz, MeOD) δ = 1.14 (t, 3 H, ³J_{H,H} = 7.1 Hz, CH₃), 1.93 (ap, 2 H, ³J_{H,H} = 6.8, 7.2 Hz, β-CH₂), 2.29 (t, 2 H, ³J_{H,H} = 7.2 Hz, γ-CH₂), 4.00 (q, 2 H, ³J_{H,H} = 7.1 Hz, CH₂CH₃), 4.08 (t, 2 H, ³J_{H,H} = 6.8 Hz, α-CH₂), 6.78 (d, 1 H, ³J_{H,H} = 8.1 Hz, 5-Ar-CH), 6.86-6.92 (m, 2 H, 2,6-Ar-CH), 7.50 (s, 1 H, CH) ppm; **¹H-NMR** (400 MHz, DMSO-d₆) δ = 1.16 (H,H, tH, ³J_{7.1 Hz} = CH₃, 3) 1.91 (ap, 2 H, ³J_{H,H} = 6.8, 7.2 Hz, β-CH₂), 2.36 (t, 2 H, ³J_{H,H} = 7.2 Hz, γ-CH₂), 4.02 (q, 2 H, ³J_{H,H} = 7.1 Hz, CH₂CH₃), 4.07 (t, 2 H, ³J_{H,H} = 6.8 Hz, α-CH₂), 6.89 (d, 1 H, ³J_{H,H} = 8.1 Hz, 5-Ar-CH), 7.02-7.06 (m, 2 H, 2,6-Ar-CH), 7.62 (s, 1 H, CH) ppm; **¹³C-NMR** (400 MHz, DMSO-d₆) δ = 14.1 (CH₃), 21.9 (CH₂), 30.9 (CH₂), 43.5 (CH₂), 59.9 (CH₂), 116.5 (Ar-C or Ar-CH), 116.7 (Ar-C or Ar-CH), 117.5 (Ar-C or Ar-CH), 124.4 (Ar-C or Ar-CH), 125.4 (Ar-C or Ar-CH), 134.1 (CH), 146.1 (Ar-CH), 149.6 (Ar-C), 167.2 (C=O), 172.2 (COOEt), 193.6 (C=S) ppm; **ESI-MS** m/z (%) = 368.1 [M+H]⁺ (100 %), 752.1 [2M+NH₄]⁺ (41 %), 757.1 [2M+Na]⁺ (6 %); **HPLC-Analysis (Method B)**: 98 %, R_t = 20.9 min.

4-[(5Z)-5-[(4-hydroxy-3,5-dimethoxyphenyl)methylidene]-4-oxo-2-sulfanylidene-1,3-thiazolidin-3-yl] butanoic acid **16j**

ESI-MS m/z (%) = 406.0 [M+Na]⁺ (100 %); **HPLC-Analysis (Method B)**: 86 %, R_t = 16.5 min.

9.6 General procedure for the synthesis of modified benzyloxy benzaldehydes 18a–f and their condensation products 19a–l

3-Hydroxy benzaldehyde (1.0 eq), the corresponding benzylchloride (1.1 eq), potassium carbonate (1.0 eq) and sodium iodide (1.1 eq) were dissolved in anhydrous DMF. The reaction

mixture was stirred at 90 °C (50 °C for pyridine benzylchloride derivatives) until TLC showed complete consumption of starting material. The crude was concentrated and the remaining yellow oil was extracted between H₂O (20 mL) and EtOAc (3x25 mL). The combined organic fractions were washed with brine, dried over MgSO₄, filtered and concentrated. The crude extract was purified by flash column chromatography to obtain the desired modified benzyloxybenzaldehydes **18a–f**. In the consecutive reaction the aldehydes **18b–f** were subjected to Knoevenagel condensation conditions. Aldehydes **18b–f** (1.0 eq), sodium acetate (1.0 eq) and various rhodanine/ thiazolidine-2,4-dione derivatives (1.0 eq) were dissolved in ethanol (5-10 mL). The reaction mixture was stirred at 80 °C, until TLC showed complete consumption of starting material. The condensation products **19a–I** were obtained after re-crystallisation or column chromatography.

3-(benzyloxy)benzaldehyde **18a**^[290]

TLC R_f = 0.6 (Hexane/EtOAc 8:2); **Reaction time**: 4 h; **Purification**: Flash-Chromatography Hexane/EtOAc 95:5 (R_f = 0.1); **Yield**: 1462 mg of white solid (6.89 mmol, 84 %); **¹H-NMR** (400 MHz, CDCl₃) δ = 5.11 (s, 2 H, CH₂), 7.22-7.26 (m, 1 H, Ar-CH), 7.31-7.49 (m, 8 H, 8xAr-CH), 9.96 (s, 1 H, CHO) ppm; **¹³C-NMR** (400 MHz, CDCl₃) δ = 70.3 (CH₂), 113.3 (Ar-CH), 122.3 (Ar-CH), 123.8 (Ar-CH), 127.7 (Ar-CH), 128.3 (Ar-CH), 128.8 (Ar-CH), 130.2 (Ar-CH), 136.4 (Ar-C), 137.9 (Ar-C), 159.4 (Ar-C), 192.2 (CHO) ppm;

3-[(3-methoxyphenyl)methoxy] benzaldehyde **18b**

TLC R_f = 0.3 (Hexane/EtOAc 8:2); **Reaction time**: 8 h; **Purification**: Flash-Chromatography Hexane/EtOAc 8:2 (R_f = 0.3), loaded in DCM; **Yield**: 1628 mg of clear oil (6.72 mmol, 82 %); **Yield**: 60 mg of clear oil (0.25 mmol, 15 %) (without NaI); **¹H-NMR** (400 MHz, CDCl₃) δ = 3.71 (s, 3 H, OCH₃), 4.99 (s, 2 H, CH₂), 6.78 (dd, 1 H, ^{3,4} $J_{H,H}$ = 2.4, 8.1 Hz, Ar-CH), 6.88-6.90 (m, 1 H, Ar-CH), 6.92 (d, 1 H, ³ $J_{H,H}$ = 7.8 Hz, Ar-CH), 7.13-7.16 (m, 1 H, Ar-CH), 7.21 (at, 1 H, ³ $J_{H,H}$ = 7.8 Hz, Ar-CH), 7.32-7.39 (m, 3 H, 3xAr-CH), 9.86 (s, 1 H, CHO) ppm; **¹H-NMR** (400 MHz, CDCl₃) δ = 3.82 (s, 3 H, OCH₃), 5.10 (s, 2 H, CH₂), 6.88 (dd, 1 H, ^{3,4} $J_{H,H}$ = 2.3, 8.2 Hz, 4'-Ar-CH), 6.98-7.00 (m, 1 H, 2'-Ar-CH), 7.02 (d, 1 H, ³ $J_{H,H}$ = 7.5 Hz, 6'-Ar-CH), 7.25 (adt, 1 H, ^{3,4} $J_{H,H}$ = 1.8, 1.9, 7.7 Hz, 4-Ar-CH), 7.31 (at, 1 H, ³ $J_{H,H}$ = 7.5, 8.2 Hz, 5'-Ar-CH), 7.44 (at, 1 H, ³ $J_{H,H}$ = 7.7 Hz, 5-Ar-CH), 7.46-7.49 (m, 2 H, 2,6-Ar-CH), 9.97 (s, 1 H, CHO) ppm; **¹³C-NMR** (400 MHz, CDCl₃) δ = 55.4 (CH₃), 70.2 (CH₂), 113.1 (2'-Ar-CH), 113.4 (2-Ar-CH), 113.8 (4'-Ar-CH), 119.8 (6'-Ar-CH), 122.3 (4-Ar-CH), 123.8 (6-Ar-CH), 129.9 (5'-Ar-CH), 130.3 (5-Ar-CH), 137.9 (Ar-C), 138.0 (Ar-C), 159.4 (Ar-C), 160.0 (Ar-C), 192.2 (CHO) ppm; **APCI-MS** m/z (%) = 260.1 [M+NH₄]¹⁰⁰ (, %) 243.1 [M+H]⁺ (20 %); **HR-MS** m/z = 260.1281 [M+NH₄]⁺ (calculated: 260.1281).

3-[(4-methoxyphenyl)methoxy]benzaldehyde **18c**^[291]

TLC R_f = 0.6 (Hexane/EtOAc 8:2); **Reaction time**: 6 h; **Purification**: Flash-Chromatography Hexane/EtOAc 9:1 (R_f = 0.1); **Yield**: 211 mg of white solid (0.87 mmol, 53 %) (without NaI)

Yield: 66 mg of white solid (0.27 mmol, 30 %) (without NaI); **Yield:** 1688 mg of white solid (6.97 mmol, 85 %) (with addition of NaI); **¹H-NMR** (400 MHz, CDCl₃) δ = 3.75 (s, 3 H, CH₃), 4.98 (s, 2 H, CH₂), 6.86 (d, 2 H, ³J_{H,H} = 8.6 Hz, 2',6'-Ar-CH), 7.17 (adt, 1 H, ^{3,4}J_{H,H} = 2.4, 7.2 Hz, 4-Ar-CH), 7.30 (d, 2 H, ³J_{H,H} = 8.6 Hz, 3',5'-Ar-CH), 7.35-7.41 (m, 3 H, 2,5,6-Ar-CH), 9.90 (s, 1 H, CHO) ppm; **¹³C-NMR** (400 MHz, CDCl₃) δ = 55.5 (CH₃), 70.2 (CH₂), 113.3 (Ar-CH), 114.2 (2',6'-Ar-CH), 122.4 (4-Ar-CH), 123.8 (Ar-CH), 128.4 (Ar-C), 129.5 (3',5'-Ar-CH), 130.2 (Ar-CH), 137.9 (Ar-C), 159.5 (Ar-C), 159.8 (Ar-C), 192.3 (CHO) ppm; **EI-MS** m/z (%) = 242.0 [M]⁺ (100 %), 121.0 [fragment]⁺ (100 %); **HR-MS** m/z = 242.0933 [M]⁺ (calculated: 242.0937); **HPLC-Analysis (Method B):** 98 %, R_t = 15.1 min.

3-(pyridin-2-ylmethoxy)benzaldehyde **18d**^[292]

TLC R_f = 0.1 (Toluene/EtOAc 9:1); **Reaction time:** 16 h; **Purification:** Flash-Chromatography Toluene/EtOAc 9:1 (R_f = 0.1); **Yield:** 194 mg of white solid (0.91 mmol, 55 %) (without catalyst); **¹H-NMR** (400 MHz, CDCl₃) δ = 5.20 (s, 2 H, CH₂), 7.17-7.20 (m, 1 H, 5-Pyr-CH), 7.21 (ddd, 1 H, ^{3,4}J_{H,H} = 7.8, 2.7, 1.6 Hz, 6-Ar-CH), 7.39 (at, 1 H, ³J_{H,H} = 7.8 Hz, 5-Ar-CH), 7.41-7.43 (m, 2 H, 2,4-Ar-CH), 7.45 (d, 1 H, ³J_{H,H} = 7.7 Hz, 3-Pyr-CH), 7.67 (atd, 1 H, ^{3,4}J_{H,H} = 7.7, 1.8 Hz, 4-Pyr-CH), 8.55 (d(br), 1 H, ³J_{H,H} = 4.7 Hz, 6-Pyr-CH), 9.90 (s, 1 H, CHO) ppm; **¹³C-NMR** (400 MHz, CDCl₃) δ = 70.8 (CH₂), 114.2 (2 or 4-Ar-CH), 121.7 (3-Pyr-CH), 121.9 (5-Pyr-CH or 6-Ar-CH), 123.1 (5-Pyr-CH or 6-Ar-CH), 123.7 (2 or 4-Ar-CH), 130.4 (5-Ar-CH), 137.4 (4-Pyr-CCH), 138.0 (Ar-C), 149.3 (6-Pyr-CH), 156.5 (Ar-C), 159.1 (Ar-C), 192.1 (CHO) ppm; **APCI-MS** m/z (%) = 214.1 [M+H]⁺ (100 %); **HR-MS** m/z = 214.0858 [M+H]⁺ (calculated: 214.0863).

3-(pyridin-3-ylmethoxy)benzaldehyde **18e**^[293]

TLC R_f = 0.2 (Cyclohexane/EtOAc 7:3); **Reaction time:** 16 h; **Purification:** Flash-Chromatography Cyclohexane/EtOAc 7:3 (R_f = 0.2); **Yield:** 201 mg of white solid (0.94 mmol, 59 %) (with NaI); **Yield:** 136 mg of white solid (0.64 mmol, 16 %) (without catalyst); **APCI-MS** m/z (%) = 214.1 [M+H]⁺ (100 %), 427.16 [2M+H]⁺ (20 %); **HR-MS** m/z = 214.0860 [M+H]⁺ (calculated: 214.0863).

3-(pyridin-4-ylmethoxy)benzaldehyde **18f**

TLC R_f = 0.2 (Cyclohexane/EtOAc 6:4); **Reaction time:** 16 h; **Purification:** Flash-Chromatography Cyclohexane/EtOAc 6:4 (R_f = 0.2); **Yield:** 175 mg of white solid (0.82 mmol, 50 %) (with NaI); **Yield:** 1068 mg of white solid (5.01 mmol, 33 %) (without catalyst); **¹H-NMR** (400 MHz, CDCl₃) δ = 5.09 (s, 2 H, CH₂), 7.19 (ddd, 1 H, ^{3,4}J_{H,H} = 7.5, 2.0, 2.0 Hz, 6-Ar-CH), 7.32 (d, 2 H, ³J_{H,H} = 5.9 Hz, 3,5-Pyr-CH), 7.37-7.39 (m, 1 H, 2-Ar-CH), 7.39-7.47 (m, 2 H, 4,5-Ar-CH), 8.57 (d, 2 H, ³J_{H,H} = 5.9 Hz, 2,6-Pyr-CH), 9.91 (s, 1 H, CHO) ppm; **¹³C-NMR** (400 MHz, CDCl₃) δ = 68.4 (CH₂), 112.9 (2-Ar-CH), 121.7 (3,5-Pyr-CH), 122.2 (6-Ar-CH), 124.5, 130.5 (4,5-Ar-CH), 138.0 (Ar-C), 145.9 (Ar-C), 150.0 (2,6-Pyr-CH), 158.8 (Ar-C), 192.0 (CHO) ppm; **APCI-MS** m/z (%) = 214.1 [M+H]⁺ (100 %); **HR-MS** m/z = 214.0862 [M+H]⁺ (calculated: 214.0863).

Ethyl 3-[(5Z)-5-(3-[(3-methoxyphenyl)methoxy]phenylmethylidene)-4-oxo-2-sulfanylidene-1,3-thiazolidin-3-yl] propanoate **19a**

TLC R_f = 0.3 (Hexane/EtOAc 9:1); **Reaction time**: 1 h; **Purification**: Flash-Chromatography Hexane/EtOAc 9:1 (R_f = 0.3), loaded in DCM; **Yield**: 240 mg of yellow solid (0.52 mmol, 82 %); **$^1\text{H-NMR}$** (400 MHz, CDCl_3) δ = 1.26 (t, 3 H, $^3J_{\text{H,H}}$ = 7.1 Hz, CH_3), 2.74 (t, 2 H, $^3J_{\text{H,H}}$ = 7.6 Hz, $\beta\text{-CH}_2$), 3.82 (s, 3 H, OCH_3), 4.14 (q, 2 H, $^3J_{\text{H,H}}$ = CH_2CH_3 , 3), 4.40 (t, 2 H, $^3J_{\text{H,H}}$ = 7.6 Hz, $\alpha\text{-CH}_2$), 5.08 (s, 2 H, CH_2), 6.87 (dd, 1 H, $^{3,4}J_{\text{H,H}}$ = 8.2, 2.3 Hz, 4-Ar-CH), 6.98-7.00 (m, 1 H, 2-Ar-CH), 7.00-7.03 (m, 2 H, 2',4'-Ar-CH), 7.03-7.09 (m, 2 H, 6,6'-Ar-CH), 7.31 (at, 1 H, $^3J_{\text{H,H}}$ = 7.9 Hz, 5-Ar-CH), 7.37 (at, 1 H, $^3J_{\text{H,H}}$ = 7.9 Hz, 5'-Ar-CH), 7.66 (s, 1 H, CH) ppm; **$^{13}\text{C-NMR}$** (400 MHz, CDCl_3) δ = 14.2 (CH_3), 31.5 ($\beta\text{-CH}_2$), 40.1 ($\alpha\text{-CH}_2$), 55.4 (OCH_3), 61.1 (CH_2CH_3), 70.1 (CH_2Ar), 112.9 (2-Ar-CH), 113.7 (4-Ar-CH), 116.1 (2' or 4'-Ar-CH), 118.1 (6 or 6'-Ar-CH), 119.6 (2' or 4'-Ar-CH), 123.1 (Ar-C), 123.7 (6 or 6'-Ar-CH), 129.9 (5-Ar-CH), 130.5 (5'-Ar-CH), 133.4 (CH), 134.6 (Ar-C), 138.0 (Ar-C), 159.3 (Ar-C), 160.0 (Ar-C), 167.4 (C=O), 170.5 (COOEt), 193.1 (C=S) ppm; **ESI-MS** m/z (%) = 458.1 [$\text{M}+\text{H}$] $^+$ (100 %), 475.1 [$\text{M}+\text{NH}_4$] $^+$ (30 %), 480.1 [$\text{M}+\text{Na}$] $^+$ (50 %), 932.2 [$2\text{M}+\text{NH}_4$] $^+$ (75 %), 937.2 [$2\text{M}+\text{Na}$] $^+$ (100 %), 953.16 [$2\text{M}+\text{K}$] $^+$ (10 %); **HR-MS** m/z = 458.1096 [$\text{M}+\text{H}$] $^+$ (calculated: 458.1090); **HPLC-Analysis (Method B)**: 87 %, R_t = 22.2 min.

Ethyl 2-[5-(4-[(3-methoxyphenyl)methoxy]phenylmethyl)-2,4-dioxo-1,3-thiazolidin-3-yl] acetate **19b**

TLC R_f = 0.2 (Hexane/EtOAc 8:2); **Reaction time**: 8 h; **Purification**: Flash-Chromatography Hexane/EtOAc 8:2 (R_f = 0.2); **Yield**: 405 mg of white solid (0.94 mmol, 94 %); **$^1\text{H-NMR}$** (400 MHz, CDCl_3) δ = 1.29 (t, 3 H, $^3J_{\text{H,H}}$ = 7.1 Hz, CH_3), 3.81 (s, 3 H, OCH_3), 4.23 (q, 2 H, $^3J_{\text{H,H}}$ = 7.1 Hz, CH_2CH_3), 4.45 (s, 2 H, CH_2), 5.07 (s, 2 H, Ar- CH_2), 6.87 (d, 1 H, $^3J_{\text{H,H}}$ = 8.3 Hz, 4-Ar-CH), 6.97-7.06 (m, 4 H, 2,2',6,6'-Ar-CH), 7.09 (d, 1 H, $^3J_{\text{H,H}}$ = 7.3 Hz, 4'-Ar-CH), 7.30 (at, 1 H, $^3J_{\text{H,H}}$ = 7.9 Hz, 5-Ar-CH), 7.37 (at, 1 H, $^3J_{\text{H,H}}$ = 8.4 Hz, 5'-Ar-CH), 7.86 (s, 1 H, CH) ppm; **$^{13}\text{C-NMR}$** (400 MHz, CDCl_3) δ = 14.1 (CH_3), 42.2 (OCH_3), 55.3 (CH_2), 62.2 (CH_2CH_3), 70.1 (CH_2Ar), 112.9 (6 or 6'-Ar-CH), 113.6 (4-Ar-CH), 116.0 (2 or 2'-Ar-CH), 117.8 (2 or 2'-Ar-CH), 119.6 (6 or 6'-Ar-CH), 121.4 (Ar-C), 123.2 (4'-Ar-CH), 129.9 (5-Ar-CH), 130.4 (5'-Ar-CH), 134.4 (Ar-C), 134.6 (CH), 138.0 (Ar-C), 159.2 (Ar-C), 160.0 (Ar-C), 165.5 (C=O), 166.3 (C=O), 167.4 (COOEt) ppm; **HPLC-Analysis (Method B)**: 96 %, R_t = 20.1 min.

Ethyl 2-[(5Z)-5-(3-[(4-methoxyphenyl)methoxy]phenylmethylidene)-4-oxo-2-sulfanylidene-1,3-thiazolidin-3-yl] acetate **19c**

TLC R_f = 0.1 (Hexane/EtOAc 9:1); **Reaction time**: 4 h; **Purification**: Flash-Chromatography Hexane/EtOAc 9:1 (R_f = 0.1); **Yield**: 68 mg of yellow solid (0.15 mmol, 64 %); **$^1\text{H-NMR}$** (400 MHz, CDCl_3) δ = 1.21 (t, 3 H, $^3J_{\text{H,H}}$ = 7.1 Hz, CH_3), 3.74 (s, 3 H, OCH_3), 4.16 (q, 2 H, $^3J_{\text{H,H}}$ = 7.1 Hz, CH_2CH_3), 4.76 (s, 2 H, CH_2), 4.95 (s, 2 H, CH_2), 6.85 (d, 2 H, $^3J_{\text{H,H}}$ = 8.7 Hz, 3,5'-Ar-CH), 6.96 (s, 1 H, 2-Ar-CH), 6.95-7.00 (0, m H, 3J = 6-Ar-CH), 7.00 (at, 1 H, $^3J_{\text{H,H}}$ = 7.6 Hz, 5-Ar-

CH), 7.29 (d, 2 H, $^3J_{\text{H,H}} = 8.7$ Hz, 2,6'-Ar-H), 7.31 (d, 1 H, $^3J_{\text{H,H}} = 7.6$ Hz, 4-Ar-H), 7.63 (s, 1 H, CH) ppm; $^{13}\text{C-NMR}$ (400 MHz, CDCl_3) $\delta = 14.2$ (CH_3), 44.9 (CH_2), 55.4 (OCH_3), 62.2 (CH_2) 70.1 (CH_2CH_3), 114.2 (3,5'-Ar-CH), 116.1 (2-Ar-CH), 118.2 (6-Ar-CH), 123.0 (Ar-C), 123.7 (5-Ar-CH), 128.3 (2,6'-Ar-CH), 129.3 (Ar-C), 130.5 (Ar-C), 134.0 (CH), 134.5 (Ar-C), 159.4 (Ar-C), 159.7 (Ar-C), 165.9 ($\text{C}=\text{O}$), 167.1 (COOEt), 193.1 ($\text{C}=\text{S}$) ppm; **ESI-MS** m/z (%) = 461.1 $[\text{M}+\text{NH}_4]^+$ (100 %); **HR-MS** $m/z = 461.0892$ $[\text{M}+\text{NH}_4]^+$ (calculated: 461.0881); **HPLC-Analysis (Method B)**: 100 %, $R_t = 21.5$ min.

Ethyl 2-[(5Z)-5-(3-[(4-methoxyphenyl) methoxy] phenyl methylidene)-2,4-dioxo-1,3-thiazolidin-3-yl] acetate **19d**

TLC $R_f = 0.2$ (Hexane/EtOAc 8:2); **Reaction time**: 8 h; **Purification**: Flash-Chromatography Hexane/EtOAc 8:2 ($R_f = 0.2$); **Yield**: 401 mg of white solid (0.94 mmol, 94 %); $^1\text{H-NMR}$ (400 MHz, CDCl_3) $\delta = 1.29$ (t, 3 H, $^3J_{\text{H,H}} = 7.1$ Hz, CH_3), 3.81 (s, 3 H, OCH_3), 4.24 (q, 2 H, $^3J_{\text{H,H}} = 7.1$ Hz, CH_2CH_3), 4.47 (s, 2 H, CH_2), 5.03 (s, 2 H, CH_2Ar), 6.93 (d, 2 H, $^3J_{\text{H,H}} = 8.7$ Hz, 3',5'-Ar-CH), 7.03-7.08 (m, 2 H, 2,4-Ar-CH), 7.10 (d, 1 H, $^3J_{\text{H,H}} = 7.8$ Hz, 6-Ar-CH), 7.36 (d, 2 H, $^3J_{\text{H,H}} = 8.7$ Hz, 2',6'-Ar-CH), 7.34-7.40 (m, 1 H, 5-Ar-CH), 7.87 (s, 1 H, CH) ppm; $^{13}\text{C-NMR}$ (400 MHz, CDCl_3) $\delta = 14.2$ (CH_3), 42.2 (CH_2), 55.4 (OCH_3), 62.3 (CH_2CH_3), 70.1 (CH_2Ar), 114.2 (3',5'-Ar-CH), 116.0 (2-Ar-CH), 117.9 (4-Ar-CH), 121.4 (Ar-C), 123.1 (6-Ar-CH), 128.4 (Ar-C), 129.3 (2',6'-Ar-CH), 130.3 (5-Ar-CH), 130.4 (Ar-C), 134.4 (Ar-C), 134.7 (CH), 159.3 (Ar-C), 166.3 ($\text{C}=\text{O}$), 167.5 ($\text{C}=\text{O}$), 171.3 (COOEt) ppm; **ESI-MS** m/z (%) = 428.1 $[\text{M}+\text{H}]^+$ (53 %), 445.1 $[\text{M}+\text{NH}_4]^+$ (100 %), 855.2 $[2\text{M}+\text{H}]^+$ (2 %), 872.3 $[2\text{M}+\text{NH}_4]^+$ (59 %); **HPLC-Analysis (Method B)**: 86 %, $R_t = 20.1$ min.

Ethyl 3-[(5Z)-5-(3-[(4-methoxyphenyl)methoxy]phenylmethylidene)-4-oxo-2-sulfanylidene-1,3-thiazolidin-3-yl] propanoate **19e**

TLC $R_f = 0.4$ (Hexane/EtOAc 8:2); **Reaction time**: 1 h; **Purification**: Flash-Chromatography Hexane/EtOAc 9:1 ($R_f = 0.2$), loaded in DCM; **Yield**: 275 mg of yellow solid (0.60 mmol, 0.80 %); $^1\text{H-NMR}$ (400 MHz, CDCl_3) $\delta = 1.25$ (t, 3 H, $^3J_{\text{H,H}} = 7.1$ Hz, CH_3), 2.74 (t, 2 H, $^3J_{\text{H,H}} = 7.6$ Hz, $\beta\text{-CH}_2$), 3.81 (s, 3 H, OCH_3), 4.14 (q, 2 H, $^3J_{\text{H,H}} = 7.1$ Hz, CH_2CH_3), 4.39 (t, 2 H, $^3J_{\text{H,H}} = 7.6$ Hz, $\alpha\text{-CH}_2$), 5.02 (s, 2 H, CH_2), 6.92 (d, 2 H, $^3J_{\text{H,H}} = 8.7$ Hz, 3',5'-Ar-CH), 7.00-7.02 (m, 1 H, 2-Ar-CH), 7.02-7.08 (m, 2 H, 4,6-Ar-CH), 7.36 (d, 2 H, $^3J_{\text{H,H}} = 8.7$ Hz, 2',6'-Ar-CH), 7.36 (at, 1 H, $^3J_{\text{H,H}} = 7.9$ Hz, 5-Ar-CH), 7.65 (s, 1 H, CH) ppm; $^{13}\text{C-NMR}$ (400 MHz, CDCl_3) $\delta = 14.2$ (CH_3), 31.4 ($\beta\text{-CH}_2$), 40.0 ($\alpha\text{-CH}_2$), 55.3 (OCH_3), 61.0 (CH_2CH_3), 70.0 (CH_2), 114.1 (3',5'-Ar-CH), 116.1 (Ar-CH), 118.0 (Ar-CH), 123.0 (Ar-C), 123.6 (Ar-CH), 128.3 (Ar-C), 129.2 (2',6'-Ar-CH), 130.4 (5-Ar-CH), 133.4 (CH) 134.5 (Ar-C), 159.3 (Ar-C), 159.6 (Ar-C), 167.4 ($\text{C}=\text{O}$), 170.4 (COOEt) 193.0 ($\text{C}=\text{S}$) ppm; **ESI-MS** m/z (%) = 458.1 $[\text{M}+\text{H}]^+$ (8 %); **HPLC-Analysis (Method B)**: 87 %, $R_t = 22.0$ min.

Ethyl 2-[(5Z)-4-oxo-5-[3-(pyridin-2-ylmethoxy)phenyl]methylidene-2-sulfanylidene-1,3thiazolidin-3-yl] acetate **19j**

TLC $R_f = 0.1$ ($\text{CHCl}_3/\text{EtOAc}$ 9:1); **Reaction time:** 4 h; **Purification:** Flash-Chromatography $\text{CHCl}_3/\text{EtOAc}$ 9:1 ($R_f = 0.1$); **Yield:** 30 mg of yellow solid (0.07 mmol, 30 %); **$^1\text{H-NMR}$** (400 MHz, CDCl_3) $\delta = 1.22$ (t, 3 H, $^3J_{\text{H,H}} = 7.1$ Hz, CH_3), 4.17 (q, 2 H, $^3J_{\text{H,H}} = 7.1$ Hz, CH_2CH_3), 4.78 (s, 2 H, CH_2), 5.08 (s, 2 H, CH_2), 6.98 (s, 1 H, 2-Ar-CH), 6.97-7.00 (m, 1 H, $J = 6$ -Ar-CH), 7.08 (d, 1 H, $^3J_{\text{H,H}} = 7.6$ Hz, 4-Ar-CH), 7.34 (d, 2 H, $^3J_{\text{H,H}} = 6.4$ Hz, 4,5-Pyr-CH), 7.31-7.37 (m, 1 H, 5-Ar-CH), 7.65 (s, 1 H, CH), 8.59 (s(br), 2 H,); **$^{13}\text{C-NMR}$** (400 MHz, CDCl_3) $\delta = 14.2$ (CH_3), 45.0 (CH_2), 62.2 (CH_2CH_3), 68.4 (CH_2), 116.1 (2-Ar-CH), 117.8 (6-Ar-CH), 121.7 (4,5-Pyr-CH), 123.5 (Ar-C), 124.2 (4-Ar-CH), 130.7 (5-Ar-CH), 133.6 (CH), 134.8 (Ar-C), 146.0 (Ar-C), 149.9 (3,6-Pyr-CH), 158.7 (Ar-C), 165.9 ($\text{C}=\text{O}$), 167.1 (COOH), 192.8 ($\text{C}=\text{S}$) ppm; **APCI-MS** m/z (%) = 415.1 $[\text{M}+\text{H}]^+$ (100 %); **EI-MS** m/z (%) = 414.0 $[\text{M}]^+$ (100 %), 241.0 [fragment] $^+$ (100 %), 91.9 [fragment] $^+$ (50 %); **HR-MS** $m/z = 415.0772$ $[\text{M}+\text{H}]^+$ (calculated: 415.0781); **HPLC-Analysis (Method B):** 99 %, $R_t = 16.3$ min.

Ethyl 2-[(5Z)-4-oxo-5-[3-(pyridin-3-ylmethoxy)phenyl]methylidene-2-sulfanylidene-1,3-thiazolidin-3-yl] acetate **19l**

TLC $R_f = 0.1$ ($\text{CHCl}_3/\text{EtOAc}$ 9:1); **Reaction time:** 4 h; **Purification:** Flash-Chromatography $\text{CHCl}_3/\text{EtOAc}$ 9:1 ($R_f = 0.1$); **Yield:** 38 mg of yellow solid (0.09 mmol, 38 %); **$^1\text{H-NMR}$** (400 MHz, CDCl_3) $\delta = 1.22$ (t, 3 H, $^3J_{\text{H,H}} = 7.1$ Hz, CH_3), 4.17 (q, 2 H, $^3J_{\text{H,H}} = 7.1$ Hz, CH_2CH_3), 4.78 (s, 2 H, CH_2), 5.07 (s, 2 H, CH_2), 7.00 (s(br), 1 H, 2-Ar-CH), 6.98-7.02 (m, 1 H, 6-Ar-CH), 7.07 (d, 1 H, $^3J_{\text{H,H}} = 7.9$ Hz, 4-Ar-CH), 7.28-7.33 (m, 1 H, 5-Ar-CH), 7.35 (at, 1 H, $^3J_{\text{H,H}} = 7.8$ Hz, 5-Pyr-CH), 7.66 (s, 1 H, CH), 7.75 (d, 1 H, $^3J_{\text{H,H}} = 7.8$ Hz, 4-Pyr-CH), 8.56 (s(br), 1 H, 6-Pyr-CH), 8.65 (s(br), 1 H, 2-Pyr-CH) ppm; **$^{13}\text{C-NMR}$** (400 MHz, CDCl_3) $\delta = 14.2$ (CH_3), 45.0 (CH_2), 62.2 (CH_2CH_3), 67.8 (CH_2), 116.2 (2-Ar-CH), 117.9 (6-Ar-CH), 123.4 (5-Ar-CH), 124.1 (4-Ar-CH), 130.7 (5-Pyr-CH), 133.7 (CH), 134.7 (Ar-C), 135.6 (4-Pyr-CH), 148.8 (2-Pyr-CH), 149.6 (6-Pyr-CH), 158.9 (Ar-C), 165.9 ($\text{C}=\text{O}$), 167.1 ($\text{C}=\text{OOEt}$), 192.9 ($\text{C}=\text{S}$) ppm; **APCI-MS** m/z (%) = 415.1 $[\text{M}+\text{H}]^+$ (100 %); **HR-MS** $m/z = 415.0774$ $[\text{M}+\text{H}]^+$ (calculated: 415.0781); **HPLC-Analysis (Method B):** 99 %, $R_t = 16.3$ min.

Ethyl 2-[(5Z)-4-oxo-5-[3-(pyridin-4-ylmethoxy)phenyl]methylidene-2-sulfanylidene-1,3-thiazolidin-3-yl] acetate **19k**

TLC $R_f = 0.2$ (Toluene/ EtOAc 9:1); **Reaction time:** 4 h; **Purification:** Flash-Chromatography Toluene/ EtOAc 9:1 ($R_f = 0.2$); **Yield:** 50 mg of yellow solid (0.12 mmol, 50 %); **$^1\text{H-NMR}$** (400 MHz, CDCl_3) $\delta = 1.21$ (t, 3 H, $^3J_{\text{H,H}} = 7.1$ Hz, CH_3), 4.16 (q, 2 H, $^3J_{\text{H,H}} = 7.1$ Hz, CH_2CH_3), 4.77 (s, 2 H, CH_2), 5.07 (s, 2 H, CH_2), 6.97 (s, 1 H, 2-Ar-CH), 6.95-7.00 (m, 1 H, $J = 6$ -Ar-CH), 7.06 (d(br), 1 H, $^3J_{\text{H,H}} = 7.7$ Hz, 4-Ar-CH), 7.31 (d, 2 H, $^3J_{\text{H,H}} = 4.7$ Hz, 2,4-Pyr-CH), 7.34 (at, 1 H, $^3J_{\text{H,H}} = 7.7$ Hz, 5-Ar-CH), 7.64 (s, 1 H, CH), 8.58 (d, 2 H, $^3J_{\text{H,H}} = 4.7$ Hz, 1,5-Pyr-CH) ppm; **$^{13}\text{C-NMR}$** (400 MHz, CDCl_3) $\delta = 14.2$ (CH_3), 44.9 (CH_2), 62.2 (CH_2CH_3), 68.4 (CH_2), 116.1 (2-Ar-CH), 117.8 (6-Ar-CH), 121.6 (2,4-Pyr-CH), 123.4 (Ar-C), 124.1 (4-Ar-CH), 130.7 (5-Ar-CH), 133.5 (CH), 134.7 (Ar-C), 145.7 (Ar-C), 150.1 (1,5-Pyr-CH), 158.7 (Ar-C), 165.9 ($\text{C}=\text{O}$), 167.1

(COOH), 192.8 (C=S) ppm; **APCI-MS** m/z (%) = 415.1 [M+H]⁺ (100 %); **HR-MS** m/z = 415.0772 [M+H]⁺ (calculated: 415.0781); **HPLC-Analysis (Method B)**: 99 %, R_t = 14.9 min.

3-[(5Z)-4-oxo-5-[3-(pyridin-2-ylmethoxy)phenyl]methylidene-2-sulfanylidene-1,3-thiazolidin-3-yl]propanoic acid **19f**

TLC R_f = 0.3 (Hexane/EtOAc 1:1); **Reaction time**: 4 h; **Purification**: Filtration from ethanol; **Yield**: 205 mg of yellow solid (0.51 mmol, 75 %); **¹H-NMR** (400 MHz, DMSO- d_6) δ = 2.38-2.43 (m, 2 H, β -CH₂), 4.13-4.20 (m, 2 H, α -CH₂), 5.25 (s, 2 H, CH₂), 7.19 (dd, 1 H, ^{3,4} $J_{H,H}$ = 2.4, 8.0 Hz, 6-Ar-CH), 7.22 (d, 1 H, ³ $J_{H,H}$ = 8.1 Hz, 4-Ar-CH), 7.24-7.26 (m, 1 H, 2-Ar-CH), 7.36 (dd, 1 H, ^{3,4} $J_{H,H}$ = 5.0, 7.7 Hz, 4-Pyr-CH), 7.47 (at, 1 H, ³ $J_{H,H}$ = 8.0, 8.1 Hz, 5-Ar-CH), 7.53 (d, 1 H, ³ $J_{H,H}$ = 7.8 Hz, 6-Pyr-CH) 7.76 (s, 1 H, CH), 7.84 (atd, 1 H, ^{3,4} $J_{H,H}$ = 1.7, 7.7, 7.8 Hz, 5-Pyr-CH), 8.59 (d, 1 H, ³ $J_{H,H}$ = 5.0 Hz, 3-Pyr-CH) ppm; **¹³C-NMR** (400 MHz, DMSO- d_6) δ = 32.6 (β -CH₂), 41.3 (α -CH₂), 70.5 (CH₂), 116.3 (2-Ar-CH), 117.8 (6-Ar-CH), 121.8 (6-Pyr-CH), 123.1 (4-Ar-CH, 4-Pyr-CH), 130.7 (5-Ar-CH), 132.5 (CH), 134.4 (Ar-C), 137.1 (5-Pyr-CH), 149.2 (3-Pyr-CH), 156.3 (Ar-C), 158.6 (Ar-C), 166.7 (C=O), 172.4 (COOH), 193.2 (C=S) ppm; **ESI-MS** m/z (%) = 399.0 [M-H]⁻ (100 %); **HR-MS** m/z = 399.0468 [M-H]⁻ (calculated: 399.0479); **HPLC-Analysis (Method B)**: 99 %, R_t = 17.0 min.

3-[(5Z)-4-oxo-5-[3-(pyridin-3-ylmethoxy)phenyl]methylidene-2-sulfanylidene-1,3-thiazolidin-3-yl]propanoic acid **19g**

TLC R_f = 0.3 (Hexane/EtOAc 1:1); **Reaction time**: 4 h; **Purification**: Filtration from ethanol; **Yield**: 192 mg of yellow solid (0.48 mmol, 69 %); **¹H-NMR** (400 MHz, DMSO- d_6) δ = 2.38-2.43 (m, 2 H, β -CH₂), 4.13-4.20 (m, 2 H, α -CH₂), 5.23 (s, 2 H, CH₂), 7.17-7.23 (m, 2 H, 4,6-Ar-CH), 7.27-7.29 (m, 1 H, 2-Ar-CH), 7.44 (ddd, 1 H, ^{3,4} $J_{H,H}$ = 0.6, 4.8, 7.8 Hz, 5-Pyr-CH), 7.49 (at, 1 H, ³ $J_{H,H}$ = 8.0 Hz, 5-Ar-CH), 7.77 (s, 1 H, CH), 7.90 (dt, 1 H, ^{3,4} $J_{H,H}$ = 1.9, 7.8 Hz, 6-Pyr-CH), 8.56 (dd, 1 H, ^{3,4} $J_{H,H}$ = 1.6, 4.8 Hz, 4-Pyr-CH), 8.70 (ad, 1 H, ⁴ $J_{H,H}$ = 1.6, 1.9 Hz, 2-Pyr-CH) ppm; **¹³C-NMR** (400 MHz, DMSO- d_6) δ = 32.7 (β -CH₂), 41.4 (α -CH₂), 67.2 (CH₂), 116.6 (2-Ar-CH), 117.8 (6-Ar-CH), 123.0 (Ar-C), 123.1 (4-Ar-CH), 123.7 (5-Pyr-CH), 130.8 (5-Ar-CH), 132.3 (CH), 132.5 (Ar-C), 134.5 (6-Pyr-CH), 135.8 (Ar-C), 149.2 (2-Pyr-CH), 149.3 (4-Pyr-CH), 158.6 (Ar-C), 166.7 (C=O), 172.5 (C=OOEt), 193.2 (C=S) ppm; **ESI-MS** m/z (%) = 399.0 [M-H]⁻ (100 %); **HR-MS** m/z = 399.0469 [M-H]⁻ (calculated: 399.0479); **HPLC-Analysis (Method B)**: 99 %, R_t = 17.0 min.

3-[(5Z)-4-oxo-5-[3-(pyridin-4-ylmethoxy)phenyl]methylidene-2-sulfanylidene-1,3-thiazolidin-3-yl]propanoic acid **19h**

TLC R_f = 0.3 (Hexane/EtOAc 1:1); **Reaction time**: 4 h; **Purification**: Filtration from ethanol; **Yield**: 201 mg of yellow solid (0.50 mmol, 82 %); **¹H-NMR** (400 MHz, DMSO- d_6) δ = 2.29-2.35 (m, 2 H, β -CH₂), 4.12-4.18 (m, 2 H, α -CH₂), 5.27 (s, 2 H, CH₂), 7.19 (dd, 1 H, ^{3,4} $J_{H,H}$ = 2.2, 8.1 Hz, 6-Ar-CH), 7.23 (d, 1 H, ³ $J_{H,H}$ = 8.1 Hz, 4-Ar-CH), 7.25-7.27 (m, 1 H, 2-Ar-CH), 7.45-7.52 (m, 3 H, 5-Ar-CH, 2,6-Pyr-CH), 7.77 (s, 1 H, CH), 8.59 (d, 1 H, ³ $J_{H,H}$ = 6.0 Hz, 3,5-

Pyr-CH) ppm, $^{13}\text{C-NMR}$ (400 MHz, DMSO- d_6) δ = 32.9 (β -CH $_2$), 41.5 (α -CH $_2$), 67.6 (CH $_2$), 116.4 (2-Ar-CH), 117.7 (6-Ar-CH), 121.8 (2,6-Pyr-CH), 123.1 (4-Ar-CH), 123.2 (Ar-C), 130.7 (5-Ar-CH), 132.4 (CH), 134.5 (Ar-C), 145.7 (Ar-C), 149.7 (3,5-Pyr-CH), 158.3 (C=O), 166.7 (COOH), 193.1 (C=S) ppm; **ESI-MS** m/z (%) = 399.0 [M-H] $^-$ (100 %), 799.1 [2M-H] $^-$ (7 %); **HPLC-Analysis (Method B)**: 97 %, R_t = 13.5 min.

9.7 General procedure for the synthesis of 2-amino substituted pyridine carboxaldehyde derivatives 25a–g

Synthesis of the rhodanine condensed precursor 21a

The ethyl ester of **14** (44 mg, 0.20 mmol) and 2-chloroisonicotinaldehyde (31 mg, 0.22 mmol) were dissolved in ethanol (3 mL) and stirred under reflux for 48 h, until TLC (DCM, R_f 0.4) showed complete consumption of starting material. A yellow solid precipitated was filtered, washed with ethanol and dried *in vacuo* to afford **21a** as yellow solid (24 mg, 35 %).

(Z)-ethyl 2-(5-((2-chloropyridin-4-yl)methylene)-4-oxo-2-thioxothiazolidin-3-yl) acetate **21a**

Reaction time: 16 h; **TLC** R_f = 0.4 (DCM); **Purification**: Filtration from ethanol; **Yield**: 14 mg of yellow solid (0.04 mmol, 20 %); $^1\text{H-NMR}$ (400 MHz, DMSO- d_6) δ = 1.21 (t, 3 H, $^3J_{\text{H,H}}$ = 7.1 Hz, OCH $_2$ CH $_3$), 4.17 (q, 2 H, $^3J_{\text{H,H}}$ = 7.1 Hz, OCH $_2$ CH $_3$), 4.85 (s, 2 H, CH $_2$), 7.60 (d, 1 H, $^3J_{\text{H,H}}$ = 5.2 Hz, 4-Ar-CH), 7.81 (s, 1 H, 6-Ar-CH), 7.88 (s, 1 H, CH), 8.59 (d, 1 H, $^3J_{\text{H,H}}$ = 5.2 Hz, 3-Ar-CH) ppm; **ESI-MS** m/z (%) = 343.0 [M+H] $^+$ (100 %), 707.0 [2M+Na] $^+$ (15 %); **HR-MS** m/z = 342.9976 [M+H] $^+$ (calculated: 342.9972); **HPLC-Analysis (Method B)**: 92 %, R_t = 20.0 min.

General Procedure for the Synthesis of Acetal 23

2-bromoisonicotinaldehyde **20b** (1.0 eq) was dissolved in EtOH/CHCl $_3$ (1:1, 1 mL) and TFA (1.0 eq) was added. The reaction mixture was heated under reflux for 4.5 h, until TLC (hexane/EtOAc 9:1, R_f 0.4) showed complete consumption of starting material. The excess of TFA was neutralised with aqueous NaHCO $_{3\text{aq}}$ (sat.), extracted with DCM (3 x 5 mL). The combined organic layers were dried over MgSO $_4$, filtered and concentrated. The product can optionally be purified by flash chromatography, but the crude is satisfactory to proceed with the synthesis.

2-bromo-4-(diethoxymethyl)pyridine **23**

TLC R_f = 0.4 (Hexane/EtOAc 9:1); **Reaction time**: 4 h; **Purification**: Flash-Chromatography Hexane/EtOAc 9:1 \rightarrow 8:2 (R_f = 0.1, 0.2); **Yield**: 565 mg of clear oil (2.74 mmol, 51 %); $^1\text{H-NMR}$ (400 MHz, CDCl $_3$) δ = 1.17 (t, 6 H, $J_{\text{H,H}}$ = 7.0 Hz, (CH $_2$ CH $_3$) $_2$), 3.43-3.55 (m, 4 H, 2xCH $_2$ CH $_3$), 5.38 (s, 1 H, CH), 7.27 (ddd, 1 H, $^{3,4}J_{\text{H,H}}$ = 5.1, 1.3, 0.6 Hz, 4-Ar-CH), 7.53 (dd, 1 H, $^4J_{\text{H,H}}$ = 0.6, 1.3 Hz, 2-Ar-CH), 8.28 (d, 1 H, $^3J_{\text{H,H}}$ = 5.1 Hz, 5-Ar-CH) ppm; **ESI-MS** m/z (%) = 260.0 [M+H] $^+$ (100 %); **HR-MS** m/z = 260.0281 [M+H] $^+$ (calculated: 260.0285). $^{13}\text{C-NMR}$ (400 MHz, CDCl $_3$)

δ = 15.2 ($\underline{\text{CH}_3}$), 61.4 ($\underline{\text{CH}_2\text{CH}_3}$), 99.0 ($\underline{\text{CH}}$), 120.9 (6-Ar- $\underline{\text{CH}}$), 126.3 (2-Ar- $\underline{\text{CH}}$), 142.6 (Ar- $\underline{\text{C}}$), 150.2 (5-Ar- $\underline{\text{CH}}$), 150.8 (Ar- $\underline{\text{C}}$) ppm;

crude **23** after simple extraction:

TLC R_f = 0.2 (Hexane/EtOAc 9:1); **Yield**: 115 mg of clear oil (0.44 mmol, 82 %); **Yield**: 202 mg of clear oil (0.78 mmol, 71 %); **Yield**: 565 mg of clear oil (2.74 mmol, 51 %); **Yield**: 204 mg of clear oil (0.78 mmol, 91 %); **Yield**: 252 mg of clear oil (0.97 mmol, 88 %); **Yield**: 201 mg of clear oil (0.77 mmol, 80 %); **Reaction time**: 2.5-4.5 h; **$^1\text{H-NMR}$** (400 MHz, CDCl_3) δ = 1.25 (t, 3 H, $^3J_{\text{H,H}}$ = 7.1 Hz, $\underline{\text{CH}_3}$), 1.26 (t, 3 H, $^3J_{\text{H,H}}$ = 7.1 Hz, $\underline{\text{CH}_3}$), 3.52-3.62 (m, 4 H, $2\times\text{CH}_2\text{CH}_3$), 5.46 (s, 1 H, $\underline{\text{CH}}$), 7.34-7.37 (m, 1 H, 6-Ar- $\underline{\text{CH}}$), 7.61 (s, 1 H, 2-Ar- $\underline{\text{CH}}$), 8.34-8.38 (m, 1 H, 5-Ar- $\underline{\text{CH}}$) ppm; **$^1\text{H-NMR}$** (400 MHz, CDCl_3) δ = 1.11 (t, 6 H, $^3J_{\text{H,H}}$ = 7.1 Hz, $2\times\text{CH}_3$), 3.38-3.50 (m, 4 H, $2\times\text{CH}_2$), 5.34 (s, 1 H, $\underline{\text{CH}}$), 7.23 (d, 1 H, $^3J_{\text{H,H}}$ = 5.0 Hz, Pyr- $\underline{\text{CH}}$), 7.47 (s, 1 H, Pyr- $\underline{\text{CH}}$), 8.22 (d, 1 H, $^3J_{\text{H,H}}$ = 5.0 Hz, Pyr- $\underline{\text{CH}}$) ppm.

NaOtBu catalysed amination approach to compounds of the class 25

Representative Procedure for the Synthesis:

Acetal **23** (100 mg, 0.38 mmol) was dissolved in toluene (2 mL) and sodium-*tert*-butoxide (150 mg, 1.56 mmol), 2-phenylethanamine (191 μL , 2.52 mmol) were added. The reaction mixture was stirred under reflux for 48 h, until TLC (hexane,EtOAc 8:2, R_f 0.1) showed no change in the consumption of starting material (approx. 50 % conversion). The mixture was concentrated and extracted between brine and EtOAc (3 x 5 mL). The combined organic layers were dried over MgSO_4 , filtered and concentrated. Purification by column chromatography (hexane/EtOAc 8:2, R_f 0.1) afforded 4-(diethoxymethyl)-N-phenethylpyridin-2-amine **24i** (36 mg, 32 %) as a clear oil. The acetal **24i** was dissolved in H_2O (0.74 mL) and TFA (3 mL). The reaction mixture was stirred until TLC showed complete cleavage of acetal groups. The reaction mixture was neutralised with NaHCO_3 (sat, aq). The crude was extracted with DCM (4x5 mL), dried over MgSO_4 , filtered and concentrated. The crude was purified by flash column chromatography to afford the aldehyde **25a**.

4-(diethoxymethyl)-N-phenethylpyridin-2-amine **24i**

TLC R_f = 0.1 (hexane/EtOAc 8:2); **Reaction time**: 16 h; **Purification**: Flash-Chromatography hexane/EtOAc 8:2 (R_f = 0.1); **Yield**: 36 mg of clear oil (0.12 mmol, 32 %); **Yield**: 24 mg of clear oil (0.08 mmol, 21 %); **$^1\text{H-NMR}$** (400 MHz, CDCl_3) δ = 1.25 (t, 6 H, $^3J_{\text{H,H}}$ = 7.1 Hz, $(\text{OCH}_2\text{CH}_3)_2$), 2.94 (t, 2 H, $^3J_{\text{H,H}}$ = 7.0 Hz, $\text{CH}_2\text{CH}_2\text{Ph}$), 3.50-3.66 (m, 6 H, $(\text{OCH}_2\text{CH}_3)_2$, $\text{CH}_2\text{CH}_2\text{Ph}$), 4.63 (t(br), 1 H, $^3J_{\text{H,H}}$ = 5.4 Hz, NH), 5.39 (s, 1 H, $\underline{\text{CH}}$), 6.52 (s, 1 H, 2-Ar- $\underline{\text{CH}}$), 6.68 (dd, 1 H, $^3,4J_{\text{H,H}}$ = 1.3, 5.3 Hz, 4-Ar- $\underline{\text{CH}}$), 7.22-7.36 (m, 5 H, 5xAr- $\underline{\text{CH}}$), 8.08 (dd, 1 H, $^3,4J_{\text{H,H}}$ = 0.6, 5.3 Hz, 6-Ar- $\underline{\text{CH}}$) ppm;

2-(phenethylamino)isonicotinaldehyde **25a**

TLC R_f = 0.1 (CHCl_3 / EtOAc 9:1); **Reaction time**: 2 h; **Purification**: Flash-Chromatography

CHCl₃/EtOAc 9:1 (*R_f* = 0.1); **Yield**: 12 mg of white solid (0.05 mmol, 44 %); **Yield**: 18 mg of white solid (0.08 mmol, 100 %); **¹H-NMR** (400 MHz, CDCl₃) δ = 2.88 (t, 2 H, $^3J_{\text{H,H}}$ = 6.9 Hz, CH₂CH₂Ph), 3.56 (dt, 2 H, $^3J_{\text{H,H}}$ = 6.0, 6.9 Hz, CH₂CH₂Ph), 4.74 (t(br), 1 H, $^3J_{\text{H,H}}$ = 6.0 Hz, NH), 6.66 (s, 1 H, 2-Ar-CH), 6.89 (dd, 1 H, $^3J_{\text{H,H}}$ = 1.3 Hz, 5.1 Hz, 3,4) 7.13-7.28 (m, 5 H, 5xAr-CH), 8.22 (d, 1 H, $^3J_{\text{H,H}}$ = 5.1 Hz, 5-Ar-CH), 9.85 (s, 1 H, CHO) ppm; **APCI-MS** *m/z* (%) = 227.1 [M+H]⁺ (100 %); **HR-MS** *m/z* = 227.1172 [M+H]⁺ (calculated: 227.1179).

4-(diethoxymethyl)-N-(4-methylbenzyl)pyridin-2-amine **24j**

TLC *R_f* = 0.4 (DCM/EtOAc 9:1); **Reaction time**: 6.5 h; **Purification**: Flash-Chromatography hexane/EtOAc 9:1 (*R_f* = 0.1), ; **Yield**: 36 mg of white solid (0.12 mmol, 34 %); **¹H-NMR** (400 MHz, CDCl₃) δ = 1.14 (t, 6 H, $^3J_{\text{H,H}}$ = 7.1 Hz, (OCH₂CH₃)₂), 2.26 (s, 3 H, Ar-CH₃), 3.38-3.59 (m, 4 H, (OCH₂CH₃)₂), 4.40 (d, 2 H, $^3J_{\text{H,H}}$ = 5.7 Hz, CH₂Ph), 4.80 (t(br), 1 H, $^3J_{\text{H,H}}$ = 5.7 Hz, NH), 5.29 (s, 1 H, CH), 6.44 (s, 1 H, 2-Ar-CH), 6.61 (d, 1 H, $^3J_{\text{H,H}}$ = 5.3 Hz, 4-Ar-CH), 7.07 (d, 2 H, $^3J_{\text{H,H}}$ = 7.9 Hz, 2',6'-Ar-CH), 7.18 (d, 2 H, $^3J_{\text{H,H}}$ = 7.9 Hz, 3',5'-Ar-CH), 8.02 (d, 1 H, $^3J_{\text{H,H}}$ = 5.3 Hz, 5-Ar-CH) ppm; **ESI-MS** *m/z* (%) = 301.2 [M+H]⁺ (100 %); **HR-MS** *m/z* = 301.1914 [M+H]⁺ (calculated: 301.1911).

2-(4-methylbenzylamino)isonicotinaldehyde **25b**

TLC *R_f* = 0.6 (DCM/EtOAc 8:2); **Reaction time**: 2 h; **Purification**: Extraction between NaHCO₃ (aq., 10 mL) and DCM (3x10 mL). **Yield**: 6.4 mg of clear oil (0.03 mmol, 100 %); **¹H-NMR** (400 MHz, CDCl₃) δ = 2.28 (s, 3 H, Ar-CH), 4.45 (d, 2 H, $^3J_{\text{H,H}}$ = 5.1 Hz, CH₂Ar), 5.26 (s(br), 1 H, NH), 6.70 (s, 1 H, 2-Ar-CH), 6.92 (d, 1 H, $^3J_{\text{H,H}}$ = 5.0 Hz, 4-Ar-CH), 7.09 (d, 2 H, $^3J_{\text{H,H}}$ = 7.6 Hz, 3',5'-Ar-CH), 7.19 (d, 2 H, $^3J_{\text{H,H}}$ = 7.6 Hz, 2',6'-Ar-CH), 8.23 (d, 1 H, $^3J_{\text{H,H}}$ = 5.0 Hz, 5-Ar-CH), 9.84 (s, 1 H, CHO) ppm; **ESI-MS** *m/z* (%) = 227.1 [M+H]⁺ (100 %); **HR-MS** *m/z* = 227.1180 [M+H]⁺ (calculated: 227.1179).

Palladium catalyst amination approach to compounds of the class 25

The acetal **23** (100 mg, 0.38 mmol), Pd(OAc)₂ (8.4 mg, 3.8·10⁻² mmol), sodium-*tert*-butoxide (52 mg, 0.54 mmol) and DPPF (4.2 mg, 7.6·10⁻² mmol) were dissolved in dioxane/toluene (1:1, 5 mL). The reaction mixture was stirred under reflux for 12 h, until TLC (hexane/EtOAc 8:2, *R_f* 0.1) showed complete consumption of starting material. After concentration and extraction between brine (3 mL) and EtOAc (3 x 5 mL), the crude product was dried over MgSO₄, filtered and concentrated. Purification by flash chromatography (hexane/EtOAc 8:2, *R_f* 0.1) afforded the amino actual **24k** (20 mg, 18 %) as a white solid. The acetal **24k** (20 mg, 0.07 mmol) was dissolved in water (0.75 mL) and TFA (3 mL) and the reaction mixture was stirred for 4 h, until TLC (DCM/MeOH 9:1, *R_f* 0.3) showed complete consumption of starting material. The excess of TFA was neutralised with saturated aqueous NaHCO₃ solution and the mixture was extracted with DCM (4 x 5 mL). The combined organic layers were dried over MgSO₄, filtered and dried *in vacuo* to afford 2-(benzylamino)isonicotinaldehyde **25e** (15.0 mg, 100 %) as a

yellow solid.

N-benzyl-4-(diethoxymethyl)pyridin-2-amine **24k**

TLC R_f = 0.1 (hexane/EtOAc 8:2); **Reaction time**: 16 h; **Purification**: Flash-Chromatography hexane/EtOAc 8:2 (R_f = 0.1); **Yield**: 20 mg of white solid (0.07 mmol, 18 %); **¹H-NMR** (400 MHz, CDCl₃) δ = 1.12 (t, 6 H, $^3J_{\text{H,H}}$ = 7.0 Hz, (OCH₂CH₃)₂), 3.37-3.53 (m, 4 H, (OCH₂CH₃)₂), 4.44 (d, 2 H, $^3J_{\text{H,H}}$ = 5.6 Hz, CH₂Ph), 4.90 (t(br), 1 H, $^3J_{\text{H,H}}$ = 5.6 Hz, NH), 5.27 (s, 1 H, CH), 6.44 (s, 1 H, 2-Ar-CH), 6.60 (d, 1 H, $^3J_{\text{H,H}}$ = 5.2 Hz, 4-Ar-CH), 7.15-7.29 (m, 5 H, 5xAr-CH), 8.00 (d, 1 H, $^3J_{\text{H,H}}$ = 5.2 Hz, 5-Ar-CH) ppm;

2-(benzylamino)isonicotinaldehyde **25e**

TLC R_f = 0.3 (DCM/ MeOH 9:1); **Yield**: 19 mg of yellow solid (0.09 mmol, 100 %); **Reaction time**: 4 h; **Purification**: Extraction between NaHCO_{3aq} (10 mL) and DCM (3x10 mL). **¹H-NMR** (400 MHz, CDCl₃) δ = 4.49 (s, 2 H, CH₂), 6.38 (s(br), 1 H, NH), 6.74 (s, 1 H, 2-Ar-CH), 6.91 (dd, 1 H, $^{3,4}J_{\text{H,H}}$ = 1.3, 5.3 Hz, 4-Ar-CH), 7.15-7.29 (m, 5 H, 5xAr-CH), 8.13 (d, 1 H, $^3J_{\text{H,H}}$ = 5.3 Hz, 5-Ar-CH), 9.81 (s, 1 H, CHO) ppm; **ESI-MS** m/z (%) = 213.1 [M+H]⁺ (100 %); **HR-MS** m/z = 213.1023 [M+H]⁺ (calculated: 213.1022).

Ullman-type, Copper catalyst Amination

Acetal **23** (1.0 eq), the corresponding benzyl amine derivative (5 eq), and CsOAc (1.1 eq) were dissolved in 3 mL toluene. The reaction mixture was degassed for 5 min and CuI (1.1 eq) was added under N₂ atmosphere. The reaction mixture turned green. The crude was stirred at 110 °C and another 5 eq of benzyl amine derivative were added. The stirring was continued until TLC showed complete consumption of starting **23**. The crude was quenched with NH₄Cl_{aq} (5 mL, sat). The reaction mixture turned blue. The aqueous phase was extracted with toluene (5x 5 mL). The combined organic layers were dried over MgSO₄, filtered and concentrated. Purification by flash chromatography affords the desired amino acetal class **24**. The acetal was cleaved under acid hydrolysis as described above to afford the aldehyde **25f**.

4-(diethoxymethyl)-N-[(4-methylphenyl)methyl]pyridin-2-amine **24l**

TLC R_f = 0.1 (Cyclohexane/EtOAc 9:1); **Reaction time**: 16 h **Purification**: Flash-Chromatography Cyclohexane/EtOAc 9:1 (R_f = 0.1); **Yield**: 55 mg of yellow oil (0.18 mmol, 43 %); **¹H-NMR** (400 MHz, CDCl₃) δ = 1.18 (t, 6 H, $^3J_{\text{H,H}}$ = 7.1 Hz, 2xCH₃), 2.30 (s, 3 H, CH₃), 3.42-3.58 (m, 4 H, 2xCH₂CH₃), 4.42 (d, 2 H, $^3J_{\text{H,H}}$ = 5.6 Hz, CH₂NH), 5.16 (t, 1 H, $^3J_{\text{H,H}}$ = 5.6 Hz, NH), 5.32 (s, 1 H, CH), 6.48 (s, 1 H, 3-Pyr-CH), 6.64 (d, 1 H, $^3J_{\text{H,H}}$ = 5.3 Hz, 5-Pyr-CH), 7.09 (d, 2 H, $^3J_{\text{H,H}}$ = 7.8 Hz, 2xAr-CH), 7.21 (d, 2 H, $^3J_{\text{H,H}}$ = 7.8 Hz, 2xAr-CH), 8.04 (d, 1 H, $^3J_{\text{H,H}}$ = 5.3 Hz, 6-Pyr-CH) ppm; **¹³C-NMR** (400 MHz, CDCl₃) δ = 15.2 (2xCH₃), 21.2 (CH₃), 46.3 (CH₂NH), 61.2 (2xCH₂), 100.2 (CH), 104.8 (3-Pyr-CH), 111.4 (5-Pyr-CH), 127.6 (2xAr-CH), 129.4 (2xAr-CH), 136.0 (Ar-C), 136.9 (Ar-C), 148.4 (6-Pyr-CH), 149.1 (Ar-C), 158.9 (Ar-C) ppm;

2-(4-Methylbenzylamino)isonicotinaldehyde **25f**

TLC R_f = 0.1 (Hexane/EtOAc 8:2); **Reaction time**: 4 h; **Purification**: Flash-Chromatography hexane/EtOAc 8:2 (R_f = 0.1); **Yield**: 61 mg of yellow oil (0.27 mmol, 100 %); **$^1\text{H-NMR}$** (400 MHz, CDCl_3) δ = 2.33 (s, 3 H, CH_2), 4.51 (d, 2 H, $^3J_{\text{H,H}}$ = 5.5 Hz, CH_2), 5.46 (s(br), 1 H, NH), 6.76 (s, 1 H, 2-Pyr-H), 6.96 (d, 1 H, $^3J_{\text{H,H}}$ = 5.1 Hz, 4-Pyr-H), 7.15 (d, 2 H, $^3J_{\text{H,H}}$ = 7.9 Hz, 2xAr-H), 7.25 (d, 2 H, $^3J_{\text{H,H}}$ = 7.9 Hz, 2xAr-H), 8.26 (d, 1 H, $^3J_{\text{H,H}}$ = 5.1 Hz, 5-Pyr-H) 9.89 (s, 1 H, CHO); **$^{13}\text{C(DEPT)-NMR}$** (400 MHz, CDCl_3) δ = 21.1 (CH_3), 46.1 (CH_2), 106.4 (2-Pyr-CH), 111.0 (4-Pyr-CH), 127.4 (2xAr-CH), 129.4 (2xAr-CH), 149.6 (5-Pyr-CH), 192.2 (CHO) ppm; N-benzyl-4-(diethoxymethyl)pyridin-2-amine **24k**

TLC R_f = 0.1 (Hexane/EtOAc 8:2); **Reaction time**: 16 h; **Purification**: Flash-Chromatography hexane/EtOAc 8:2 (R_f = 0.1), loaded in DCM; **Yield**: 403 mg of white solid (1.41 mmol, 65 %); **$^1\text{H-NMR}$** (400 MHz, CDCl_3) δ = 1.20 (t, 6 H, $^3J_{\text{H,H}}$ = 7.1 Hz, 2x CH_3), 3.44-3.60 (m, 4 H, 2x CH_2CH_3), 4.50 (d, 2 H, $^3J_{\text{H,H}}$ = 5.7 Hz, CH_2NH), 5.25 (t(br), 1 H, $^3J_{\text{H,H}}$ = 5.7 Hz, NHCH_2), 5.34 (s, 1 H, CH), 6.51 (s, 1 H, 2-Ar-CH), 6.67 (dd, 1 H, $^{3,4}J_{\text{H,H}}$ = 5.3, 1.1 Hz, 6-Ar-CH), 7.21-7.36 (m, 5 H, 5xAr-CH), 8.04 (d, 1 H, $^3J_{\text{H,H}}$ = 5.3 Hz, 5-Ar-CH) ppm; **$^{13}\text{C-NMR}$** (400 MHz, CDCl_3) δ = 15.2 (2x CH_3), 46.4 (CH_2NH), 61.1 (2x CH_2CH_3), 100.2 (CH), 104.7 (2-Ar-CH), 111.4 (6-Ar-CH), 127.2 (Ar-CH), 127.5 (Ar-CH), 128.6 (Ar-CH), 139.2 (Ar-C), 148.3 (5-Ar-CH), 149.0 (Ar-C), 159.0 (Ar-C) ppm.

2-(4-(trifluoromethyl)benzylamino)isonicotinaldehyde **25d**

TLC R_f = 0.3 (Hexane/EtOAc 7:3); **Reaction time**: 2.5 h; **Purification**: Flash-Chromatography Cyclohexane/EtOAc 7:3 (R_f = 0.2); **Yield**: 17 mg of yellow crystals (0.08 mmol, 100 %); **$^1\text{H-NMR}$** (400 MHz, CDCl_3) δ = 4.67 (d, 2 H, $^3J_{\text{H,H}}$ = 6.0 Hz, Bn- CH_2), 5.41 (t(br), 1 H, $^3J_{\text{H,H}}$ = 6.0 Hz, NH), 6.79 (s, 1 H, 3-Pyr-CH), 7.01 (dd, 1 H, $^{3,4}J_{\text{H,H}}$ = 5.1, 1.2 Hz, 5-Pyr-CH), 7.48 (d, 2 H, $^3J_{\text{H,H}}$ = 8.2 Hz, 2xAr-CH), 7.60 (d, 2 H, $^3J_{\text{H,H}}$ = 8.2 Hz, 2xAr-CH), 8.31 (d, 1 H, $^3J_{\text{H,H}}$ = 5.1 Hz, 6-Pyr-CH), 9.92 (s, 1 H, CHO) ppm; **$^{13}\text{C-NMR}$** (400 MHz, CDCl_3) δ = 45.8 (CH_2), 106.7 (3-Pyr-CH), 111.9 (5-Pyr-CH), 125.8 (Ar-C), 125.9 (q, $^3J_{\text{C,F}}$ = 3.8 Hz, 2xAr-CH), 127.6 (2xAr-CH), 130.0 (Ar-C), 142.8 (Ar-C), 143.8 (Ar-C), 149.5 (6-Pyr-CH), 159.1 (Ar-C), 192.0 (CHO) ppm;

9.8 General procedure for the Synthesis of heterocyclic derivatives

26a–j

The derivatives **26a–j** were synthesised under standard Knoevenagel condensation conditions as described previously. Compounds **2**, **14**, and **7** (1.0 eq), the heterocyclic aldehyde (1.1 eq) and sodium acetate (1.0 eq) were dissolved in ethanol and stirred at 80 °C under TLC showed complete consumption of starting material.

[(5Z)-4-oxo-5-(pyridin-2-ylmethylidene)-2- sulfanylidene-1,3-thiazolidin-3-yl]acetic acid **26b**^[192]

Reaction time: 8 h; **Purification**: Filtration from ethanol; **Yield**: 105 mg of yellow solid (0.37

mmol, 54 %); **¹H-NMR** (400 MHz, DMSO-*d*₆) δ = 4.74 (s, 2 H, CH₂), 7.47 (ddd, 1 H, ^{3,4}*J*_{H,H} = 6.8, 4.8, 2.4 Hz, 4-Pyr-CH), 7.92 (s, 1 H, CH), 7.92-8.03 (m, 2 H, 5,6-Pyr-CH), 8.82 (d, 1 H, ³*J*_{H,H} = 4.8 Hz, 3-Pyr-CH), 13.43 (s(br), 1 H, COOH) ppm; **¹³C-NMR** (400 MHz, DMSO-*d*₆) δ = 44.6 (CH₂), 124.4 (4-Pyr-CH), 126.2 (Ar-C), 128.5 (6-Pyr-CH), 129.4 (CH), 137.8 (5-Pyr-CH), 149.6 (3-Pyr-CH), 150.9 (Ar-C), 166.5 (C=O), 167.4 (COOH), 199.7 (C=S) ppm; **ESI-MS** *m/z* (%) = 281.0 [M+H]⁺ (100 %); **HR-MS** *m/z* = 281.0052 [M+H]⁺ (calculated: 281.0049); **HPLC-Analysis (Method B)**: 99 %, *R*_t = 16.1 min.

(Z)-2-(4-oxo-5-(pyridin-3-ylmethylene)-2-thioxothiazolidin-3-yl)acetic acid **26c**^[192]

Reaction time: 6 h; **Purification**: Filtration from ethanol; **Yield**: 232 mg of yellow solid (0.83 mmol, 74 %); **¹H-NMR** (400 MHz, DMSO-*d*₆) δ = 4.76 (s, 2 H, CH₂), 7.60 (dd, 1 H, ^{3,4}*J*_{H,H} = 8.1, 4.7 Hz, 4-Ar-CH), 7.96 (s, 1 H, CH), 8.04 (ddd, 1 H, ³*J*_{H,H} = 1.2, 1.7, 8.0 Hz, 3-Ar-CH), 8.68 (dd, 1 H, ^{3,4}*J*_{H,H} = 1.2, 4.7 Hz, 5-Ar-CH), 8.92 (d, 1 H, ⁴*J*_{H,H} = 1.7 Hz, 1-Ar-CH), 13.52 (s(br), 1 H, COOH) ppm; **¹³C-NMR** (400 MHz, DMSO-*d*₆) δ = 45.1 (CH₂), 124.0 (4-Ar-CH), 124.4 (Ar-C), 129.0 (Ar-C), 130.6 (CH), 136.6 (3-Ar-CH), 151.2 (5-Ar-CH), 152.0 (1-Ar-CH), 166.2 (C=O), 167.3 (COOH), 192.9 (C=S) ppm; **ESI-MS** *m/z* (%) = 281.0 [M+H]⁺ (100 %), 583.0 [2M+Na]⁺ (10 %); **HR-MS** *m/z* = 281.0052 [M+H]⁺ (calculated: 281.0049); **HPLC-Analysis (Method B)**: 99 %, *R*_t = 12.2 min.

[(5Z)-4-oxo-5-(pyridin-4-ylmethylidene)-2- sulfanylidene-1,3-thiazolidin-3-yl]acetic acid **26d**^[192]

Reaction time: 6 h; **Purification**: Filtration from ethanol; **Yield**: 284 mg of yellow solid (1.01 mmol, 82 %); **¹H-NMR** (400 MHz, DMSO-*d*₆) δ = 4.63 (s, 2 H, CH₂), 7.47 (ddd, 1 H, ^{3,4}*J*_{H,H} = 6.2, 4.8, 6.2 Hz, 4-Ar-CH), 7.90 (s, 1 H, CH), 7.94-8.01 (m, 2 H, 2,3-Ar-CH), 8.82 (dd, 1 H, ^{3,4}*J*_{H,H} = 4.8, 1.2 Hz, 5-Ar-CH); **ESI-MS** *m/z* (%) = 281.0 [M+H]⁺ (100 %), 303.0 [M+Na]⁺ (25 %); **HR-MS** *m/z* = 281.0052 [M+H]⁺ (calculated: 281.0049); **HPLC-Analysis (Method B)**: 99 %, *R*_t = 12.2 min.

[(5Z)-4-oxo-5-[(2E)-3-phenylprop-2-en-1-ylidene]-2- sulfanylidene-1,3-thiazolidin-3-yl] acetic acid **26e**^[289]

Reaction time: 4 h; **Purification**: Filtration from ethanol; **Yield**: 32 mg of yellow solid (0.10 mmol, 20 %); **¹H-NMR** (400 MHz, DMSO-*d*₆) δ = ; 4.54 (s, 2 H, CH₂), 7.14 (dd, 1 H, ³*J*_{H,H} = 15.2, 11.6 Hz, CH), 7.41-7.48 (m, 3 H, 4xAr-CH), 7.58 (d, 1 H, ³*J*_{H,H} = 11.6 Hz, CH), 7.71-7.75 (m, 2 H, Ar-CH, CH) ppm; **ESI-MS** *m/z* (%) = 304.0 [M-H]⁻ (100 %); **HR-MS** *m/z* = 304.0105 [M-H]⁻ (calculated: 304.0108); **HPLC-Analysis (Method B)**: 82 %, *R*_t = 18.6 min.

(Z)-ethyl 2-(5-((2-(4-methylbenzylamino)pyridin-4-yl)methylene)-4-oxo-2-thioxothiazolidin-3-yl) acetate **26a**

TLC *R*_f = 0.5 (Hexane/EtOAc 7:3); **Reaction time**: 6 h; **Purification**: Flash-Chromatography DCM → DCM/EtOAc 9:1 (*R*_f = 0.1); **Yield**: 45 mg of yellow solid (0.11 mmol, 75 %); **¹H-NMR** (400 MHz, CDCl₃) δ = 1.29 (t, 3 H, ³*J*_{H,H} = 7.2 Hz, CH₃), 2.35 (s, 3 H, Ar-CH₃), 4.23 (q, 2 H, ³*J*_{H,H} = 7.2 Hz, CH₂), 4.49 (d, 2 H, ³*J*_{H,H} = 5.6 Hz, CH₂), 4.83 (s, 2 H, CH₂), 5.30 (t(br), 1 H,

$^3J_{\text{H,H}} = 5.6 \text{ Hz}$, NH), 6.33 (s, 1 H, 2-Pyr-CH), 6.64 (dd, 1 H, $^3,^4J_{\text{H,H}} = 5.3, 1.5 \text{ Hz}$, 4-Pyr-CH), 7.17 (d, 2 H, $J_{\text{H,H}} = 8.0 \text{ Hz}$, 2xAr-CH), 7.27 (d, 2 H, $J_{\text{H,H}} = 8.0 \text{ Hz}$, 2xAr-CH), 7.53 (s, 1 H, CH), 8.19 (d, 1 H, $^3J_{\text{H,H}} = 5.3 \text{ Hz}$, 5-Pyr-CH) ppm; $^{13}\text{C-NMR}$ (400 MHz, CDCl_3) $\delta = 14.1$ (OCH_2CH_3), 21.2 (Ar-CH₃), 44.8 (NCH_2COOEt), 46.2 (CH_2NH), 62.2 (OCH_2CH_3), 106.7 (2-Pyr-CH), 112.9 (4-Pyr-CH), 127.3 (2xAr-CH), 129.6 (2xAr-CH), 131.6 (CH), 149.4 (5-Pyr-CH) ppm; **ESI-MS** m/z (%) = 428.1 $[\text{M}+\text{H}]^+$ (100 %); **HR-MS** $m/z = 428.1098$ $[\text{M}+\text{H}]^+$ (calculated: 428.1097); **HPLC-Analysis** : 99.9 %, $R_t = 29.9 \text{ min}$.

Ethyl 2-[(5Z)-4-oxo-5-(pyridin-2-ylmethylidene)-2-sulfanylidene-1,3-thiazolidin-3-yl] acetate **26f**
TLC $R_f = 0.3$ (Hexane/EtOAc 6:4); **Reaction time**: 4 h; **Purification**: Re-crystallisation from ethanol; **Yield**: 395 mg of yellow crystals (1.28 mmol, 100 %); $^1\text{H-NMR}$ (400 MHz, CDCl_3) $\delta = 1.28$ (t, 3 H, $^3J_{\text{H,H}} = 7.1 \text{ Hz}$, CH_3), 4.23 (q, 2 H, $^3J_{\text{H,H}} = 7.1 \text{ Hz}$, CH_2CH_3), 4.87 (s, 2 H, CH_2), 7.29 (ddd, 1 H, $^3,^4J_{\text{H,H}} = 0.9, 4.8, 7.6 \text{ Hz}$, 4-Pyr-CH), 7.56 (d, 1 H, $^3J_{\text{H,H}} = 7.8 \text{ Hz}$, 6-Pyr-CH), 7.67 (s, 1 H, CH), 7.79 (adt, 1 H, $^3,^4J_{\text{H,H}} = 1.7, 7.6, 7.8 \text{ Hz}$, 5-Pyr-CH), 8.78 (d, 1 H, $^3J_{\text{H,H}} = 4.5 \text{ Hz}$, 3-Pyr-CH) ppm; $^{13}\text{C-NMR}$ (400 MHz, CDCl_3) $\delta = 14.3$ (CH_3), 44.6 (CH_2), 62.1 (CH_2CH_3), 123.8 (4-Pyr-CH), 127.5 (6-Pyr-CH), 128.6 (CH), 137.1 (5-Pyr-CH), 145.6 (Ar-C), 149.7 (3-Pyr-CH), 151.7 (Ar-C), 161.3 ($\text{C}=\text{O}$), 166.1 ($\text{C}=\text{O}$) ppm; **ESI-MS** m/z (%) = 309.0 $[\text{M}+\text{H}]^+$ (100 %), 331.0 $[\text{M}+\text{Na}]^+$ (5 %), 617.1 $[2\text{M}+\text{H}]^+$ (25 %); **HR-MS** $m/z = 309.0364$ $[\text{M}+\text{H}]^+$ (calculated: 309.0362); **HPLC-Analysis (Method B)**: 100 %, $R_t = 18.7 \text{ min}$.

Ethyl 2-[(5Z)-4-oxo-5-(pyridin-3-ylmethylidene)-2-sulfanylidene-1,3-thiazolidin-3-yl] acetate **26g**
TLC $R_f = 0.1$ (Hexane/EtOAc 8:2); **Reaction time**: 2 h; **Purification**: Filtration from ethanol; **Yield**: 31 mg of yellow solid (0.10 mmol, 14 %); $^1\text{H-NMR}$ (400 MHz, CDCl_3) $\delta = 1.29$ (t, 3 H, $^3J_{\text{H,H}} = 7.1 \text{ Hz}$, CH_3), 4.24 (q, 2 H, $^3J_{\text{H,H}} = 7.1 \text{ Hz}$, CH_2CH_3), 4.86 (s, 2 H, CH_2), 7.45 (dd, 1 H, $^3J_{\text{H,H}} = 4.8, 8.0 \text{ Hz}$, 5-Pyr-CH), 7.75 (s, 1 H, CH), 7.78-7.82 (m, 1 H, 6-Pyr-CH), 8.66 (dd, 1 H, $^3,^4J_{\text{H,H}} = 1.4, 4.8 \text{ Hz}$, 4-Pyr-CH), 8.79 (d, 1 H, $^4J_{\text{H,H}} = 2.2 \text{ Hz}$, 2-Pyr-CH) ppm; $^{13}\text{C-NMR}$ (400 MHz, CDCl_3) $\delta = 14.2$ (CH_3), 45.1 (CH_2), 62.3 (CH_2CH_3), 124.2 (5-Pyr-CH), 125.4 (Ar-C), 129.4 (Ar-C), 129.9 (CH), 136.5 (6-Pyr-CH), 151.2 (4-Pyr-CH), 152.1 (2-Pyr-CH), 165.8 ($\text{C}=\text{O}$), 166.9 (COOEt), 192.0 ($\text{C}=\text{S}$) ppm; **ESI-MS** m/z (%) = 309.0 $[\text{M}+\text{H}]^+$ (100 %), 639.0 $[2\text{M}+\text{Na}]^+$ (10 %); **HR-MS** $m/z = 309.0365$ $[\text{M}+\text{H}]^+$ (calculated: 309.0362); **HPLC-Analysis (Method B)**: 99 %, $R_t = 15.7 \text{ min}$.

Ethyl 2-[(5Z)-4-oxo-5-(pyridin-4-ylmethylidene)-2-sulfanylidene-1,3-thiazolidin-3-yl] acetate **26h**
TLC $R_f = 0.2$ ($\text{CHCl}_3/\text{EtOAc}$ 7:3); **Reaction time**: 16 h; **Purification**: Flash-Chromatography $\text{CHCl}_3/\text{EtOAc}$ 7:3 \rightarrow 6:4 ($R_f = 0.2$); **Yield**: 85 mg of yellow solid (0.28 mmol, 28 %); $^1\text{H-NMR}$ (400 MHz, $\text{DMSO}-d_6$) $\delta = 1.25$ (t, 3 H, $^3J_{\text{H,H}} = 7.1 \text{ Hz}$, CH_3), 4.21 (q, 2 H, $^3J_{\text{H,H}} = 7.1 \text{ Hz}$, CH_2), 7.05 (s, 1 H, CCH), 7.55 (d, 2 H, $^3J_{\text{H,H}} = 5.6 \text{ Hz}$, 2,6-Ar-CH), 8.60 (d, 2 H, $^3J_{\text{H,H}} = 5.6 \text{ Hz}$, 3,5-Ar-CH) ppm; **HPLC-Analysis (Method B)**: 94 %, $R_t = 18.6 \text{ min}$.

Ethyl 2-[(5Z)-2,4-dioxo-5-(pyridin-4-ylmethylidene)-1,3-thiazolidin-3-yl] acetate **26i**

TLC $R_f = 0.2$ ($\text{CHCl}_3/\text{MeOH}$ 95:5); **Reaction time**: 16 h; **Purification**: Flash-Chromatography

CHCl₃/MeOH 95:5 (*R_f* = 0.2); **Yield**: 84 mg of white solid (0.29 mmol, 21 %); **¹H-NMR** (400 MHz, CDCl₃) δ = 1.24 (t, 3 H, ³*J*_{H,H} = 7.1 Hz, CH₃), 4.11 (s, 2 H, CH₂), 4.18 (q, 2 H, ³*J*_{H,H} = 7.1 Hz, CH₂CH₃), 7.27 (d, 2 H, ³*J*_{H,H} = 5.9 Hz, 2xPyr-CH), 8.55 (d, 2 H, ³*J*_{H,H} = 5.9 Hz, 2xPyr-CH) ppm; **¹³C-NMR** (400 MHz, CDCl₃) δ = 14.3 (CH₃), 41.8 (CH₂), 61.9 (CH₂CH₃), 122.0 (2xPyr-CH), 142.3 (Ar-C), 150.4 (2xPyr-CH), 164.9 (C=O), 170.0 (C=O), 207.2 (COOEt) ppm; **APCI-MS** *m/z* (%) = 293.1 [M+H]⁺ (60 %); **HR-MS** APCI *m/z* = 293.0586 [M+H]⁺ (calculated: 293.0591); **HPLC-Analysis (Method B)**: 85 %, *R_t* = 19.6 min.

Ethyl 2-[(5Z)-5-(furan-2-ylmethylidene)-4-oxo-2-sulfanylidene-1,3-thiazolidin-3-yl] acetate **26j**^[289]

TLC *R_f* = 0.6 (Hexane/EtOAc 8:2); **Reaction time**: 4 h; **Purification**: Re-crystallisation from ethanol; **Yield**: 138 mg of yellow crystals (0.46 mmol, 38 %); **¹H-NMR** (400 MHz, CDCl₃) δ = 1.28 (t, 3 H, ³*J*_{H,H} = 7.1 Hz, CH₃), 4.23 (q, 2 H, ³*J*_{H,H} = 7.1 Hz, CH₂CH₃), 4.83 (s, 2 H, CH₂), 6.60 (dd, 1 H, ³*J*_{H,H} = 1.8, 3.5 Hz, 4-Ar-CH), 6.86 (d, 1 H, ³*J*_{H,H} = 3.5 Hz, 3-Ar-CH), 7.51 (s, 1 H, CH), 7.72 (d, 1 H, ³*J*_{H,H} = 1.8 Hz, 5-Ar-CH) ppm; **¹³C-NMR** (400 MHz, CDCl₃) δ = 14.2 (CH₃), 44.9 (CH₂), 62.1 (CH₂CH₃), 113.7 (4-Ar-CH), 119.1 (CH or 3-Ar-CH), 119.2 (CH or 3-Ar-CH), 120.7 (Ar-C), 147.4 (5-Ar-CH), 150.1 (Ar-C), 166.1 (C=O), 167.0 (COOEt), 194.3 (C=S) ppm; **ESI-MS** *m/z* (%) = 298.0 [M+H]⁺ (100 %), 320.0 [M+Na]⁺ (20 %), 617.0 [2M+Na]⁺ (10 %); **HR-MS** *m/z* = 298.0205 [M+H]⁺ (calculated: 298.0202); **HPLC-Analysis (Method B)**: 98 %, *R_t* = 18.1 min.

9.9 General Procedure for the reduction of rhodanine 14 and thiazolidine-2,4-dione derivatives 7

Hantzsch ester reduction

The rhodanine derivative **14i** (1.0 eq), Hantzsch ester **28** (1.3 eq) and activated SiO₂ (heat activated 120 °C for 5 h, 1 g/mmol) were dissolved in anhydrous toluene. The reaction mixture was stirred under a N₂ gas atmosphere at 85 °C for 24 h in the dark. After TLC showed complete consumption, the reaction mixture was concentrated, leaving the crude loaded on SiO₂. The product was purified by flash chromatography to afford the reduced analogue **27a**.

Ethyl 2-(5-benzyl-4-oxo-2-sulfanylidene-1,3-thiazolidin-3-yl)acetate **27a**

TLC *R_f* = 0.1 (Hexane/EtOAc 9:1); **Reaction time**: 16 h; **Purification**: Flash-Chromatography DCM (*R_f* = 0.4); **Yield**: 173 mg of white solid (0.56 mmol, 67 %); **¹H-NMR** (400 MHz, CDCl₃) δ = 1.27 (t, 3 H, ³*J*_{H,H} = 7.1 Hz, CH₃), 3.08 (dd, 1 H, ^{2,3}*J*_{H,H} = 14.0, 10.5 Hz, E-CHH), 3.62 (dd, 1 H, ^{2,3}*J*_{H,H} = 14.0, 4.0 Hz, Z-CHH), 4.21 (q, 2 H, ³*J*_{H,H} = 7.1 Hz, CH₂CH₃), 4.53 (dd, 1 H, ³*J*_{H,H} = 10.5, 4.0 Hz, CH), 4.69 (s, 2 H, CH₂) 7.21-7.36 (m, 5 H, 5xAr-CH) ppm; **¹³C-NMR** (400 MHz, CDCl₃) δ = 14.2 (CH₃), 38.7 (CH₂CH), 44.9 (CH₂), 53.2 (CH), 62.1 (CH₂CH₃), 127.8 (Ar-CH), 129.0 (4xAr-CH), 136.0 (Ar-C), 165.9 (C=O), 175.2 (COOEt), 199.8 (C=S) ppm; **ESI-MS** *m/z* (%) = 310.1 [M+H]⁺ (100 %), 327.1 [M+NH₄]⁺ (85 %); **HPLC-Analysis (Method B)**: 94 %, *R_t* = 18.1 min.

$R_t = 18.1$ min.

Catalytic hydrogenation of 27b and 27c on Pd/C (10 % on charcoal)

The thiazolidine-2,4-dione derivative (1.0 eq) was dissolved in dioxane (10-15 mL). Pd/C (xx eq) were added and the reaction mixture was placed in a hydrogenation chamber at 30 psi H_2 . The reaction mixture was shaken, until pressure valve equilibrated at a stable position, but for at least 4 h. The reaction mixture was filtered through celite and washed with EtOAc. The filtrate was concentrated and the products are afforded as white solids.

Ethyl 2-(5-benzyl-2,4-dioxo-1,3-thiazolidin-3-yl) acetate **27b**

Reaction time: 8 h; **1H -NMR** (400 MHz, $CDCl_3$) $\delta =$ **Yield:** 320 mg of white solid (1.09 mmol, 98 %); 1.28 (t, 3 H, $^3J_{H,H} = 7.1$ Hz, CH_3), 3.07 (dd, 1 H, $^{2,3}J_{H,H} = 14.0, 10.5$ Hz, E-CHH), 3.63 (dd, 1 H, $^{2,3}J_{H,H} = 14.0, 3.9$ Hz, Z-CHH), 4.21 (q, 2 H, $^3J_{H,H} = 7.1$ Hz, CH_2CH_3), 4.31 (s, 2 H, CH_2), 4.53 (dd, 1 H, $^3J_{H,H} = 10.5, 3.9$ Hz, CH), 7.22-7.36 (m, 5 H, 5xAr-CH) ppm; **^{13}C -NMR** (400 MHz, $CDCl_3$) $\delta =$ 14.1 (CH_3), 39.1 (E,Z-CHH), 42.1 (CH_2), 52.0 (CH), 62.2 (CH_2CH_3), 127.7 (Ar-CH), 129.0 (2xAr-CH), 129.1 (2xAr-CH), 136.1 (Ar-C), 166.3 (C=O), 170.5 (C=O), 173.3 (COOEt) ppm; **HPLC-Analysis (Method B):** 98 %, $R_t = 16.3$ min.

Ethyl 2-5-[(3,4-dihydroxyphenyl)methyl]-2,4-dioxo-1,3-thiazolidin-3-ylacetate **27c**

Reaction time: 4 h; **Yield:** 348 mg of white solid (1.07 mmol, 100 %); **1H -NMR** (400 MHz, $CDCl_3$) $\delta =$ 1.27 (t, 3 H, $^3J_{H,H} = 7.1$ Hz, CH_3), 2.93 (dd, 1 H, $^{2,3}J_{H,H} = 14.1, 10.1$ Hz, E-CHH), 3.44 (dd, 1 H, $^{2,3}J_{H,H} = 14.1, 3.9$ Hz, Z-CHH), 4.21 (q, 2 H, $^3J_{H,H} = 7.1$ Hz, CH_2CH_3), 4.32 (s, 2 H, CH_2), 4.47 (dd, 1 H, $^3J_{H,H} = 10.1, 3.9$ Hz, CH), 6.59 (dd, 1 H, $^{3,4}J_{H,H} = 8.1, 1.8$ Hz, 6-Ar-CH), 6.70 (d, 1 H, $^4J_{H,H} = 1.8$ Hz, 2-Ar-CH), 6.76 (d, 1 H, $^3J_{H,H} = 8.1$ Hz, 5-Ar-CH) ppm; **^{13}C -NMR** (400 MHz, $CDCl_3$) $\delta =$ 14.0 (CH_3), 38.1 (E,Z- CH_2), 42.1 (CH_2), 52.3 (C), 62.5 (CH_2CH_3), 115.6 (5-Ar-CH), 116.0 (2-Ar-CH), 121.4 (6-Ar-CH), 128.4 (Ar-C), 143.6 (Ar-C), 144.2 (Ar-C), 166.9 (C=O), 171.2 (C=O), 173.7 (COOEt) ppm; **ESI-MS** m/z (%) = 343.1 $[M+NH_4]^+$ (100 %), 668.2 $[2M+NH_4]^+$ (25 %), 673.1 $[2M+Na]^+$ (100 %); **HR-MS** $m/z = 326.0701$ $[M+H]^+$ (calculated: 326.0693); **HPLC-Analysis (Method B):** 97 %, $R_t = 11.5$ min.

9.10 Synthesis of N-allyl rhodanine and thiazolidine-2,4-dione derivatives

Synthesis of N-Allyl rhodanine derivatives 40a–ae with different 5-benzylidene moieties

N-Allyl rhodanine **40** (1.0 eq), benzaldehyde derivatives (1.1-1.5 eq) and sodium acetate (1.0 eq) are dissolved in ethanol (5-10 mL). The reaction mixture is stirred at 80 °C until TLC showed complete consumption of starting material. The products are purified by recrystallisation from ethanol or column chromatography.

(Z)-3-allyl-5-benzylidene-2-thioxothiazolidin-4-one **40a**^[294]

TLC R_f = 0.7 (DCM); **Reaction time**: 1.5 h; **Purification**: Re-crystallisation from methanol; **Yield**: 50 mg of yellow crystals (0.19 mmol, 31 %); **¹H-NMR** (400 MHz, DMSO- d_6) δ = 4.65 (ddd, 2 H, $^3J_{H,H}$ = 5.2, 1.6 Hz, $\underline{\text{CH}_2}$), 5.14 (ddd, 1 H, $^3J_{H,H}$ = 17.2, 2.9, 1.6 Hz, E-Allyl- $\underline{\text{CH}_2}$), 5.29 (ddd, 1 H, $^3J_{H,H}$ = 10.4, 2.9, 1.6 Hz, Z-Allyl- $\underline{\text{CH}_2}$), 5.85 (ddt, 1 H, $^3J_{H,H}$ = 17.2, 10.4, 5.2 Hz, Allyl- $\underline{\text{CH}}$), 7.51-7.61 (m, 3 H, 3 x Ar- $\underline{\text{CH}}$), 7.64-7.70 (m, 2 H, 2 x Ar- $\underline{\text{CH}}$), 7.85 (s, 1 H, C- $\underline{\text{H}}$); **¹H-NMR** (400 MHz, CDCl_3) δ = 4.75 (dt, 2 H, $^3J_{H,H}$ = 5.8, 1.2 Hz, $\underline{\text{CH}_2}$), 5.26 (ddd, 1 H, $^3J_{H,H}$ = 10.3, 2.5, 1.4 Hz, $\underline{\text{CHH}}$), 5.30 (ddd, 1 H, $^3J_{H,H}$ = 17.2, 2.5, 1.4 Hz, $\underline{\text{CHH}}$), 5.87 (ddt, 1 H, $^3J_{H,H}$ = 17.2, 10.3, 5.8 Hz, $\underline{\text{CH}}$), 7.42-7.53 (m, 5 H, 5xAr- $\underline{\text{CH}}$), 7.74 (s, 1 H, $\underline{\text{CH}}$) ppm; **¹³C-NMR** (400 MHz, CDCl_3) δ = 46.5 ($\underline{\text{CH}_2}$), 119.5 ($\underline{\text{CH}_2}$), 123.1 (Ar- $\underline{\text{C}}$), 129.5 (Ar- $\underline{\text{CH}}$), 129.6 (Allyl- $\underline{\text{CH}}$), 130.8 (Ar-C $\underline{\text{CH}}$), 130.9 (Ar- $\underline{\text{C}}$ or Ar-C $\underline{\text{CH}}$), 133.4 ($\underline{\text{CH}}$), 133.5 (Ar- $\underline{\text{C}}$), 167.6 ($\underline{\text{C=O}}$), 193.1 ($\underline{\text{C=S}}$) ppm; **ESI-MS** m/z (%) = 262.0 $[\text{M}+\text{H}]^+$ (100 %); **HR-MS** m/z = 262.0357 $[\text{M}+\text{H}]^+$ (calculated: 262.0355); **HPLC-Analysis (Method B)**: 99 %, R_t = 21.4 min.

(Z)-3-allyl-5-(2-methylbenzylidene)-2-thioxothiazolidin-4-one **40b**

Reaction time: 1 h; **Purification**: Re-crystallisation from methanol; **Yield**: 78 mg of yellow crystals (0.28 mmol, 100 %); **¹H-NMR** (400 MHz, CDCl_3) δ = 2.48 (s, 3 H, $\underline{\text{CH}_3}$), 4.76 (dt, 2 H, $^3J_{H,H}$ = 5.8, 1.3 Hz, $\underline{\text{CH}_2}$), 5.28 (ddd, 1 H, $^3J_{H,H}$ = 10.2, 2.3, 1.2 Hz, $\underline{\text{CHH}}$), 5.32 (ddd, 1 H, $^3J_{H,H}$ = 17.1, 2.3, 1.2 Hz, $\underline{\text{CHH}}$), 5.89 (ddt, 1 H, $^3J_{H,H}$ = 17.1, 10.2, 5.8 Hz, $\underline{\text{CH}}$), 7.26-7.37 (m, 3 H, 3xAr- $\underline{\text{CH}}$), 7.41-7.45 (m, 1 H, 1xAr- $\underline{\text{CH}}$), 7.98 (s, 1 H, $\underline{\text{CH}}$) ppm; **ESI-MS** m/z (%) = 276.1 $[\text{M}+\text{H}]^+$ (100 %); **¹³C-NMR** (400 MHz, CDCl_3) δ = 20.0 ($\underline{\text{CH}_3}$), 46.4 ($\underline{\text{CH}_2}$), 119.4 ($\underline{\text{CH}_2}$), 126.7 (Ar- $\underline{\text{CH}}$), 128.1 (Ar- $\underline{\text{CH}}$), 129.6 (Ar- $\underline{\text{CH}}$), 130.8 (Ar- $\underline{\text{CH}}$), 131.2 ($\underline{\text{CH}}$, Ar- $\underline{\text{CH}}$) ppm; 276.1 $[\text{M}+\text{H}]^+$ (100 %); **HR-MS** m/z = 276.0515 $[\text{M}+\text{H}]^+$ (calculated: 276.0511); **HPLC-Analysis** : 99.9 %, R_t = 37.7 min; **HPLC-Analysis (Method B)**: 100 %, R_t = 22.0 min.

(Z)-3-allyl-5-(3-methylbenzylidene)-2-thioxothiazolidin-4-one **40c**

TLC R_f = 0.6 (DCM/hexane 6:4); **Reaction time**: 3 h; **Purification**: Re-crystallisation from ethanol; **Yield**: 34 mg of yellow crystals (0.12 mmol, 49 %); **¹H-NMR** (400 MHz, CDCl_3) δ = 2.40 (s, 3 H, $\underline{\text{CH}_3}$), 4.74 (dt, 2 H, $^3J_{H,H}$ = 5.8, 1.3 Hz, $\underline{\text{CH}_2}$), 5.25 (ddd, 1 H, $^3J_{H,H}$ = 10.3, 2.3, 1.1 Hz, $\underline{\text{CHH}}$), 5.29 (ddd, 1 H, $^3J_{H,H}$ = 17.2, 2.5, 1.3 Hz, $\underline{\text{CHH}}$), 5.86 (ddt, 1 H, $^3J_{H,H}$ = 17.2, 10.3, 5.8 Hz, Allyl- $\underline{\text{CH}}$), 7.25 (d, 1 H, $^3J_{H,H}$ = 7.8 Hz, Ar- $\underline{\text{CH}}$), 7.28-7.32 (m, 2 H, 2xAr- $\underline{\text{CH}}$), 7.36 (at, 1 H, $^3J_{H,H}$ = 7.8 Hz, 5-Ar- $\underline{\text{CH}_3}$), 7.70 (s, 1 H, $\underline{\text{CH}}$) ppm; **¹³C-NMR** (400 MHz, CDCl_3) δ = 21.6 ($\underline{\text{CH}_3}$), 46.5 ($\underline{\text{CH}_2}$), 119.5 (Allyl- $\underline{\text{CH}_2}$), 122.8 (Ar- $\underline{\text{C}}$), 128.0 (Ar- $\underline{\text{CH}}$), 129.4 (5-Ar- $\underline{\text{CH}}$), 129.7 (Allyl- $\underline{\text{CH}}$), 131.4 (Ar- $\underline{\text{CH}}$), 131.9 (Ar- $\underline{\text{CH}}$), 133.4 (Ar- $\underline{\text{C}}$), 133.7 ($\underline{\text{CH}}$), 139.3 (Ar- $\underline{\text{C}}$), 167.6 ($\underline{\text{C=O}}$), 193.3 ($\underline{\text{C=S}}$) ppm; **APCI-MS** m/z (%) = 276.0 $[\text{M}+\text{H}]^+$ (100 %); **GCEI-MS** m/z (%) = 275.0 $[\text{M}]^+$ (100 %), 260.0 [fragment] $^+$ (50 %), 148.0 [fragment] $^+$ (100 %), 8.2 [fragment] $^+$ (100 %); **GCCI-MS** m/z (%) = 276.0 $[\text{M}+\text{H}]^+$ (100 %); **HR-MS** m/z = 276.0509 $[\text{M}+\text{H}]^+$ (calculated: 276.0511); **HPLC-Analysis (Method B)**: 100 %, R_t = 22.0 min.

(Z)-3-allyl-5-(4-methylbenzylidene)-2-thioxothiazolidin-4-one **40ad**^[295]

Reaction time: 1 h; **Purification:** Re-crystallisation from methanol; **Yield:** 43 mg of yellow crystals (0.16 mmol, 54 %); **¹H-NMR** (400 MHz, CDCl₃) δ = 2.35 (s, 3 H, CH₃), 4.69 (dt, 2 H, ^{3,4}J_{H,H} = 5.8, 1.3 Hz, CH₂), 5.20 (ddd, 1 H, ^{3,4}J_{H,H} = 10.2, 2.4, 1.2 Hz, CHH), 5.25 (ddd, 1 H, ^{3,4}J_{H,H} = 17.1, 2.6, 1.4 Hz, CHH), 5.82 (ddt, 1 H, ³J_{H,H} = 17.1, 10.2, 5.8 Hz, Allyl-CH), 7.23 (d, 2 H, ³J_{H,H} = 8.2 Hz, 2xAr-CH), 7.35 (d, 2 H, ³J_{H,H} = 8.2 Hz, 2xAr-CH), 7.66 (s, 1 H, CH) ppm; **¹³C-NMR** (400 MHz, CDCl₃) δ = 21.8 (CH₃), 46.5 (CH₂), 119.4 (Allyl-CH₂), 121.8 (Ar-C), 129.7 (Allyl-CH), 130.3 (2xAr-CH), 130.7 (Ar-C), 130.9 (2xAr-CH), 133.6 (CH), 141.8 (Ar-C), 167.7 (C=O), 193.1 (C=S) ppm; **APCI-MS** m/z (%) = 276.0 [M+H]⁺ (100 %); **GCEI-MS** m/z (%) = 275.0 [M]⁺ (100 %), 260.0 [fragment]⁺ (45 %), 148.0 [fragment]⁺ (100 %); **GCCI-MS** m/z (%) = 276.0 [M+H]⁺ (100 %); **HR-MS** m/z = 276.0512 [M+H]⁺ (calculated: 276.0511); **HPLC-Analysis (Method B):** 100 %, R_t = 32.1 min.

(Z)-3-allyl-2-thioxo-5-(2-(trifluoromethyl)benzylidene)thiazolidin-4-one **40e**

TLC R_f = 0.8 (DCM); **Reaction time:** 4 h; **Purification:** Filtration from methanol; **Yield:** 47 mg of yellow solid (0.14 mmol, 22 %); **¹H-NMR** (400 MHz, CDCl₃) δ = 4.75 (dt, 2 H, ^{3,4}J_{H,H} = 5.9, 1.3 Hz, CH₂), 5.28 (ddd, 1 H, ^{3,4}J_{H,H} = 10.2, 2.2, 1.1 Hz, CHH), 5.33 (ddd, 1 H, ^{3,4}J_{H,H} = 17.1, 2.5, 1.4 Hz, CHH), 5.87 (ddt, 1 H, ³J_{H,H} = 17.1, 10.2, 5.9 Hz, Allyl-CH), 7.54 (at, 1 H, ³J_{H,H} = 7.8, 7.7 Hz, 5-Ar-CH), 7.60 (d, 1 H, ³J_{H,H} = 7.5 Hz, 3-Ar-CH), 7.66 (at, 1 H, ³J_{H,H} = 7.7, 7.5 Hz, 4-Ar-CH), 7.78 (d, 1 H, ³J_{H,H} = 7.8 Hz, 6-Ar-CH), 8.01 (q, 1 H, ⁵J_{H,F} = 1.8 Hz, CH) ppm; **¹³C-NMR** (400 MHz, CDCl₃) δ = 46.7 (CH₂), 119.9 (Allyl-CH₂), 123.7 (q, ¹J_{C,F} = 274.1 Hz, CF₃), 127.0 (q, ³J_{C,F} = 5.5 Hz, 6-Ar-CH), 127.9 (Ar-C), 128.6 (q, ⁴J_{C,F} = 2.0 Hz, CH), 129.3 (3-Ar-CH), 129.5 (Allyl-CH), 130.0 (q, ²J_{C,F} = 30.6 Hz, 1-Ar-C), 130.2 (5-Ar-CH), 132.2 (q, ⁴J_{C,F} = 1.6 Hz, Ar-C), 132.5 (4-Ar-CH), 166.7 (C=O), 192.9 (C=S) ppm; **EI-MS** m/z (%) = 329.1 [M]⁺ (100 %), 314.1 [fragment]⁺ (30 %), 202.1 [fragment]⁺ (35 %), 86.1 [fragment]⁺ (60 %), 84.1 [fragment]⁺ (90 %), 48.9 [fragment]² (100 %); **HR-MS** m/z = 329.0147 [M]⁺ (calculated: 329.0156); **HPLC-Analysis (Method B):** 97 %, R_t = 21.1 min.

(Z)-3-allyl-2-thioxo-5-(3-(trifluoromethyl)benzylidene)thiazolidin-4-one **40f**

TLC R_f = 0.9 (DCM); **Reaction time:** 4 h; **Purification:** Re-crystallisation from ethanol; **Yield:** 114 mg of yellow crystals (0.35 mmol, 50 %); **¹H-NMR** (400 MHz, CDCl₃) δ = 4.75 (dt, 2 H, ^{3,4}J_{H,H} = 5.9, 1.3 Hz, CH₂), 5.27 (ddd, 1 H, ^{3,4}J_{H,H} = 10.3, 2.3, 1.2 Hz, CHH), 5.31 (ddd, 1 H, ^{3,4}J_{H,H} = 17.2, 2.6, 1.4 Hz, CHH), 7.63 (aq, 1 H, ^{3,4}J_{H,H} = 7.6 Hz, 5-Ar-CH), 7.67 (d, 1 H, ^{3,4}J_{H,H} = 7.6 Hz, 4-Ar-CH), 7.69 (d, 1 H, ^{3,4}J_{H,H} = 7.6 Hz, 6-Ar-CH), 7.73 (s, 2 H, CH₂-Ar-CH) ppm; **¹³C-NMR** (400 MHz, CDCl₃) δ = 46.7 (CH), 119.8 (Allyl-CH₂), 123.7 (q, ¹J_{C,F} = 272.7 Hz, CF₃), 125.4 (Ar-C), 127.1 (q, ³J_{C,F} = 3.7 Hz, 6-Ar-CH), 127.3 (q, ³J_{C,F} = 3.9 Hz, 2-Ar-CH), 129.5 (Allyl-CH), 130.1 (5-Ar-CH), 131.0 (CH), 132.1 (q, ³J_{C,F} = 32.8 Hz, 1-Ar-C), 133.2 (4-Ar-CH), 134.3 (Ar-C), 167.3 (C=O), 192.2 (C=S) ppm; **¹H-NMR** (400 MHz, DMSO-d₆) δ = 4.65 (dt, 2 H, ^{3,4}J_{H,H} = 5.2, 1.6 Hz, CH₂), 5.15 (ddd, 1 H, ^{3,4}J_{H,H} = 17.2, 2.9, 1.7 Hz, E-Allyl-CH₂), 5.19 (ddd, 1 H, ^{3,4}J_{H,H} = 10.4, 2.7, 1.4 Hz, Z-Allyl-CH₂), 5.85 (ddt, 1 H, ^{3,4}J_{H,H} = 17.2, 10.4, 5.2 Hz, Allyl-

CH), 7.80 (t, 1 H, $^3J_{\text{H,H}} = 7.8$ Hz, 4-Ar-CH), 7.86-7.93 (m, 2 H, 3,5-Ar-CH), 7.97 (s, 1 H, CH), 8.07 (s, 1 H, 1-Ar-CH) ppm; **EI-MS** m/z (%) = 329.0 [M]⁺ (100 %), 314.0 [fragment]⁺ (15 %), 202.0 [fragment]⁺ (100 %), 7.7 [fragment]⁺ (100 %); **HR-MS** $m/z = 329.0150$ [M]⁺ (calculated: 329.0156); **HPLC-Analysis (Method B)**: 98 %, $R_t = 21.7$ min.

(Z)-3-allyl-2-thioxo-5-(4-(trifluoromethyl)benzylidene)thiazolidin-4-one **40g**

TLC $R_f = 0.9$ (DCM); **Reaction time**: 4 h; **Purification**: Re-crystallisation from ethanol; **Yield**: 140 mg of yellow crystals (0.43 mmol, 70 %); **¹H-NMR** (400 MHz, CDCl₃) $\delta = 4.75$ (dt, 2 H, $^{3,4}J_{\text{H,H}} = 5.9, 1.3$ Hz, CH₂), 5.27 (ddd, 1 H, $^{3,4}J_{\text{H,H}} = 10.2, 2.3, 1.1$ Hz, CHH), 5.31 (ddd, 1 H, $^{3,4}J_{\text{H,H}} = 17.1, 2.4, 1.3$ Hz, CHH), 5.86 (ddt, 1 H, $^3J_{\text{H,H}} = 17.1, 10.2, 5.9$ Hz, Allyl-CH), 7.60 (d, 2 H, $^3J_{\text{H,H}} = 8.3$ Hz, 2xAr-CH), 7.73 (d, 2 H, $^3J_{\text{H,H}} = 8.3$ Hz, 2xAr-CH), 7.73 (s, 1 H, CH) ppm; **¹H-NMR** (400 MHz, DMSO-d₆) $\delta = 4.64$ -4.68 (m, 2 H, CH₂), 5.15 (ddd, 1 H, $^{3,4}J_{\text{H,H}} = 17.2, 2.9, 1.7$ Hz, E-Allyl-CH₂), 5.19 (ddd, 1 H, $^{3,4}J_{\text{H,H}} = 10.4, 2.7, 1.4$ Hz, Z-Allyl-CH₂), 5.85 (ddt, 1 H, $^{3,4}J_{\text{H,H}} = 17.2, 10.4, 5.2$ Hz, Allyl-CH), 7.86 (m, 5 H, CH₂, 4 x Ar-CH); **¹³C-NMR** (400 MHz, CDCl₃) $\delta = 46.7$ (CH₂), 119.8 (Allyl-CH₂), 123.6 (q, $^1J_{\text{C,F}} = 272.5$ Hz, CF₃), 126.0 (Ar-C), 126.4 (q, $^4J_{\text{C,F}} = 3.8$ Hz, 2,6-Ar-CH), 129.4 (Allyl-CH), 130.7 (3,5-Ar-CH), 130.9 (CH), 132.0 (q, $^3J_{\text{C,F}} = 33.0$ Hz, 1-Ar-CCF₃), 136.7 (Ar-C), 167.3 (C=O), 192.2 (C=S) ppm; **EI-MS** m/z (%) = 329.1 [M]⁺ (100 %), 314.1 [fragment]⁺ (75 %), 202.1 [fragment]⁺ (100 %); **HR-MS** $m/z = 329.0151$ [M]⁺ (calculated: 329.0156); **HPLC-Analysis (Method B)**: 100 %, $R_t = 21.6$ min.

(5Z)-5-[(4-tert-butylphenyl)methylidene]-3-(prop-2-en-1-yl)-2-sulfanylidene-1,3-thiazolidin-4-one **40d**

TLC $R_f = 0.9$ (DCM/EtOAc 9:1); **Reaction time**: 4 h; **Purification**: Re-crystallisation from ethanol; **Yield**: 240 mg of yellow solid (0.76 mmol, 82 %); **¹H-NMR** (400 MHz, DMSO-d₆) $\delta = 1.30$ (s, 9 H, 3xCH₃), 4.65 (d, 2 H, $^3J_{\text{H,H}} = 5.2$ Hz, CH₂), 5.11-5.17 (m, 1 H, E-CHH), 5.17-5.21 (m, 1 H, Z-CHH), 5.80-5.90 (m, 1 H, Allyl-CH), 7.59 (s, 4 H, 4xAr-CH), 7.81 (s, 1 H, CH) ppm; **¹³C-NMR** (400 MHz, DMSO-d₆) $\delta = 30.8$ (3xCH₃), 34.9 (C(CH₃)₃), 46.1 (CH₂), 117.9 (Allyl-CH₂), 121.3 (Ar-C), 126.5 (2xAr-CH), 130.3 (Allyl-CH, Ar-C), 130.7 (2xAr-CH), 133.2 (CH), 154.3 (Ar-C), 166.7 (C=O), 193.1 (C=S) ppm; **ESI-MS** m/z (%) = 318.1 [M+H]⁺ (100 %); **HPLC-Analysis (Method B)**: 100 %, $R_t = 23.1$ min.

(Z)-3-allyl-5-(4-chlorobenzylidene)-2-thioxothiazolidin-4-one **40h**^[295]

Reaction time: 4 h; **Purification**: Re-crystallisation from ethanol; **Yield**: 97 mg of yellow crystals (0.33 mmol, 53 %); **¹H-NMR** (400 MHz, CDCl₃) $\delta = 4.74$ (dt, 2 H, $^{3,4}J_{\text{H,H}} = 5.8, 1.3$ Hz, CH₂), 5.26 (ddd, 1 H, $^{3,4}J_{\text{H,H}} = 10.3, 2.5, 1.4$ Hz, CHH), 5.30 (ddd, 1 H, $^{3,4}J_{\text{H,H}} = 17.2, 2.5, 1.4$ Hz, CHH), 5.86 (ddt, 1 H, $^3J_{\text{H,H}} = 17.2, 10.3, 5.8$ Hz, CH), 7.42 (d, 2 H, $^3J_{\text{H,H}} = 8.8$ Hz, 2xAr-CH), 7.46 (d, 2 H, $^3J_{\text{H,H}} = 8.8$ Hz, 2xAr-CH), 7.67 (s, 1 H, CH) ppm; **¹H-NMR** (400 MHz, DMSO-d₆) $\delta = 4.65$ (dt, 2 H, $^{3,4}J_{\text{H,H}} = 5.2, 1.6$ Hz, CH₂), 5.17 (ddd, 1 H, $^{3,4}J_{\text{H,H}} = 17.2, 2.9, 1.5$ Hz, E-Allyl-CH₂), 5.20 (ddd, 1 H, $^{3,4}J_{\text{H,H}} = 10.4, 2.8, 1.3$ Hz, Z-Allyl-CH₂), 5.85 (ddt, 1 H, $^{3,4}J_{\text{H,H}} = 17.2, 10.4, 5.2$ Hz, Allyl-CH), 7.63 (ddd, 2 H, $^{3,4}J_{\text{H,H}} = 8.7, 2.1, 1.8, 2,4$ -Ar-CH), 7.69 (ddd, 2 H,

$^3,^4J_{\text{H,H}} = 8.7, 2.1, 1.8, 1,5\text{-Ar-CH}$), 7.84 (s, 1 H, CH) ppm; $^{13}\text{C-NMR}$ (400 MHz, CDCl_3) $\delta = 46.6$ (CH_2), 119.6 (Allyl- CH_2), 123.7 (C), 129.5 (Allyl-CH), 129.8 (3, 5-Ar-CH), 131.7 (4-Ar-C), 131.8 (2,6-Ar-CH), 131.9 (CH), 137.1 (1-Ar-C), 167.5 (C=O), 192.4 (C=S); ppm; **ESI-MS** m/z (%) = 318.0 $[\text{M}+\text{Na}]^+$ (100 %), 613.0 $[2\text{M}+\text{Na}]^+$ (100 %); **HR-MS** $m/z = 317.9789$ $[\text{M}+\text{Na}]^+$ (calculated: 317.9785); **HPLC-Analysis** : 99.9 %, $R_t = 38.3$ min.

(Z)-4-((3-allyl-4-oxo-2-thioxothiazolidin-5-ylidene)methyl)benzonitrile **40i**^[296]

Reaction time: 4 h; **Purification:** Re-crystallisation from ethanol; **Yield:** 107 mg of orange crystals (0.37 mmol, 57 %); $^1\text{H-NMR}$ (400 MHz, CDCl_3) $\delta = 4.74$ (d, 2 H, $^3J_{\text{H,H}} = 5.8$ Hz, CH_2), 5.24-5.33 (m, 2 H, Allyl- CH_2), 5.84 (ddt, 1 H, $^3J_{\text{H,H}} = 17.1, 10.3, 5.8$ Hz, Allyl-CH), 7.58 (d, 2 H, $^3J_{\text{H,H}} = 8.2$ Hz, 2xAr-CH), 7.68 (s, 1 H, CH), 7.76 (d, 2 H, $^3J_{\text{H,H}} = 8.2$ Hz, 2xAr-CH) ppm; $^{13}\text{C-NMR}$ (400 MHz, CDCl_3) $\delta = 46.7$ (CH_2), 113.6 (CN), 118.1 (Allyl- CH_2), 119.8 (Ar-C), 127.0 (Ar-C), 129.3 (Allyl-CH), 130.0 (CH), 130.7 (2xAr-CH), 133.0 (2xAr-CH), 137.5 (Ar-C), 167.1 (C=O), 191.6 (C=S) ppm; $^1\text{H-NMR}$ (400 MHz, DMSO-d_6) $\delta = 4.63$ -4.68 (m, 2 H, CH_2), 5.12-5.23 (m, 2 H, E(Z)-Allyl- CH_2), 5.79-5.91 (m, 1 H, Allyl-CH), 7.82 (d, 2 H, $^3J_{\text{H,H}} = 7.1$ Hz, 2,4-Ar-CH), 7.88 (s, 1 H, CH), 8.00 (d, 2 H, $^3J_{\text{H,H}} = 7.1$ Hz, 1,5-Ar-CH); ppm; **EI-MS** m/z (%) = 286.1 $[\text{M}]^+$ (100 %), 271.0 [fragment] $^+$ (15 %), 159.0 [fragment] $^+$ (80 %), 98.1 [fragment] $^+$ (40 %), 41.0 [fragment] $^+$ (95 %), 39.0 [fragment] $^+$ (100 %); **HR-MS** $m/z = 286.0231$ $[\text{M}]^+$ (calculated: 286.0235); **HPLC-Analysis (Method B)**: 99 %, $R_t = 19.5$ min.

(Z)-3-allyl-5-(4-ethynylbenzylidene)-2-thioxothiazolidin-4-one **40j**

Reaction time: 4 h; **Purification:** Filtration from ethanol; **Yield:** 86 mg of red solid (0.30 mmol, 49 %); $^1\text{H-NMR}$ (400 MHz, CDCl_3) $\delta = 3.26$ (s, 1 H, CCH), 4.74 (dt, 2 H, $^3,^4J_{\text{H,H}} = 5.8, 1.3$ Hz, CH_2), 5.26 (ddd, 1 H, $^3,^4J_{\text{H,H}} = 10.3, 2.3, 1.2$ Hz, CHH), 5.30 (ddd, 1 H, $^3,^4J_{\text{H,H}} = 17.2, 2.6, 1.4$ Hz, CHH), 5.86 (ddt, 1 H, $^3J_{\text{H,H}} = 17.2, 10.3, 5.8$ Hz, CH), 7.45 (d, 2 H, $^3J_{\text{H,H}} = 8.4$ Hz, 2xAr-CH), 7.58 (d, 2 H, $^3J_{\text{H,H}} = 8.4$ Hz, 2xAr-CH), 7.69 (s, 1 H, CH) ppm; $^1\text{H-NMR}$ (400 MHz, DMSO-d_6) $\delta = 4.49$ (s, 1 H, Acetylen-CH), 4.64 (dt, 2 H, $^3,^4J_{\text{H,H}} = 5.2, 1.6$ Hz, CH_2), 5.14 (ddd, 1 H, $^3,^4J_{\text{H,H}} = 17.2, 2.8, 1.6$ Hz, E-Allyl- CH_2), 5.19 (ddd, 1 H, $^3,^4J_{\text{H,H}} = 10.4, 2.7, 1.3$ Hz, Z-Allyl- CH_2), 5.84 (ddt, 1 H, $^3,^4J_{\text{H,H}} = 17.2, 10.4, 5.2$ Hz, Allyl-CH), 7.62-7.68 (m, 4 H, 4 x Ar-CH), 7.83 (s, 1 H, CH) ppm; $^{13}\text{C-NMR}$ (400 MHz, CDCl_3) $\delta = 46.6$ (CH_2), 80.5 (CCH), 83.0 (CCH), 119.6 (CH_2), 124.1 (Ar-C), 124.6 (Ar-C), 129.6 (CH), 130.5 (2xAr-CH), 132.0 (CH), 133.1 (2xAr-CH), 133.6 (Ar-C), 167.5 (C=O), 192.5 (C=S) ppm; **EI-MS** m/z (%) = 285.1 $[\text{M}]^+$ (100 %), 158.1 [fragment] $^+$ (100 %); **ESI-MS** m/z (%) = 286.0 $[\text{M}+\text{H}]^+$ (100 %), 308.0 $[\text{M}+\text{Na}]^+$ (60 %); **HR-MS** $m/z = 285.0272$ $[\text{M}]^+$ (calculated: 285.0282); **HR-MS** $m/z = 286.0358$ $[\text{M}+\text{H}]^+$ (calculated: 286.0355); **HPLC-Analysis** : 99.9 %, $R_t = 37.4$ min; **HPLC-Analysis (Method B)**: 99 %, $R_t = 19.5$ min.

(Z)-3-allyl-5-(3-bromo-4-methoxybenzylidene)-2-thioxothiazolidin-4-one **40k**

Reaction time: 4 h; **Purification:** Re-crystallisation from ethanol; **Yield:** 147 mg of yellow crystals (0.40 mmol, 66 %); $^1\text{H-NMR}$ (400 MHz, DMSO-d_6) $\delta = 3.94$ (s, 3 H, OCH_3), 4.62-

4.66 (m, 2 H, CH_2), 5.13 (ddd, 1 H, $^3,^4J_{\text{H,H}} = 17.2, 2.8, 1.6 \text{ Hz}$, E-Allyl- CH_2), 5.18 (ddd, 1 H, $^3,^4J_{\text{H,H}} = 10.4, 2.7, 1.3 \text{ Hz}$, Z-Allyl- CH_2), 5.84 (ddt, 1 H, $^3,^4J_{\text{H,H}} = 17.2, 10.4, 5.2 \text{ Hz}$, Allyl- CH), 7.30 (d, 1 H, $^3J_{\text{H,H}} = 8.7 \text{ Hz}$, 3-Ar- CH), 7.64 (dd, 1 H, $^3,^4J_{\text{H,H}} = 8.7, 2.2 \text{ Hz}$, 4-Ar- CH), 7.79 (s, 1 H, CH), 7.93 (d, 1 H, $^4J_{\text{H,H}} = 2.2 \text{ Hz}$, 1-Ar- CH); ppm; **$^1\text{H-NMR}$** (400 MHz, CDCl_3) $\delta = 3.96$ (s, 3 H, OCH_3), 4.73 (dt, 2 H, $^3,^4J_{\text{H,H}} = 5.8, 1.3 \text{ Hz}$, CH_2), 5.25 (ddd, 1 H, $^3,^4J_{\text{H,H}} = 10.3, 2.3, 1.2 \text{ Hz}$, CHH), 5.29 (ddd, 1 H, $^3,^4J_{\text{H,H}} = 17.2, 2.6, 1.4 \text{ Hz}$, CHH), 5.86 (ddt, 1 H, $^3J_{\text{H,H}} = 17.2, 10.3, 5.8 \text{ Hz}$, CH), 6.98 (d, 1 H, $^3J_{\text{H,H}} = 8.6 \text{ Hz}$, 3-Ar- CH), 7.42 (dd, 1 H, $^3,^4J_{\text{H,H}} = 8.6, 2.2 \text{ Hz}$, 4-Ar- CH), 7.59 (s, 1 H, CH), 7.68 (d, 1 H, $^4J_{\text{H,H}} = 2.2 \text{ Hz}$, 6-Ar- CH) ppm; **$^{13}\text{C-NMR}$** (400 MHz, CDCl_3) $\delta = 46.5$ (CH_2), 56.7 (OCH_3), 112.3 (3-Ar- CH), 113.0 (Ar- C), 119.5 (CH_2), 121.6 (Ar- C), 127.4 (Ar- C), 129.6 (Allyl- CH), 131.5 (4-Ar- CH and CH), 135.7 (6-Ar- CH), 157.9 (Ar- CBr), 167.5 (C=O), 192.5 (C=S) ppm; **ESI-MS** m/z (%) = 372.0 $[\text{M}+\text{H}]^+$ (100 %); **HR-MS** m/z = 369.9570 $[\text{M}+\text{H}]^+$ (calculated: 369.9566); **HPLC-Analysis (Method B)**: 98 %, $R_t = 21.9 \text{ min}$. (Z)-3-allyl-5-(3-bromo-4-fluorobenzylidene)-2-thioxothiazolidin-4-one **40I**

TLC $R_f = 0.9$ (DCM); **Reaction time**: 3 h; **Purification**: Re-crystallisation from methanol; **Yield**: 54 mg of yellow crystals (0.15 mmol, 52 %); **$^1\text{H-NMR}$** (400 MHz, CDCl_3) $\delta = 4.74$ (dt, 2 H, $^3,^4J_{\text{H,H}} = 5.8, 1.3 \text{ Hz}$, CH_2), 5.27 (ddd, 1 H, $^3,^4J_{\text{H,H}} = 10.3, 2.2, 1.1 \text{ Hz}$, CHH), 5.30 (ddd, 1 H, $^3,^4J_{\text{H,H}} = 17.1, 2.4, 1.3 \text{ Hz}$, CHH), 5.86 (ddt, 1 H, $^3J_{\text{H,H}} = 17.1, 10.3, 5.8 \text{ Hz}$, Allyl- CH), 7.23 (at, 1 H, $^3J_{\text{H,F}} = 8.4 \text{ Hz}$, 6-Ar- CH), 7.43 (ddd, 1 H, $^3,^4J_{\text{H,F(H)}} = 8.4, 4.5, 2.2 \text{ Hz}$, 5-Ar- CH), 7.61 (s, 1 H, CH), 7.70 (dd, 1 H, $^3,^4J_{\text{H,F(H)}} = 6.4, 2.2 \text{ Hz}$, 3-Ar- CH) ppm; **$^{13}\text{C-NMR}$** (400 MHz, CDCl_3) $\delta = 46.6$ (CH_2), 110.7 ($^2J_{\text{C,F}} = 21.8 \text{ Hz}$, 2-Ar- CBr), 117.7 ($^2J_{\text{C,F}} = 23.1 \text{ Hz}$, 6-Ar- CH), 119.7 (Allyl- CH_2), 124.4 ($^4J_{\text{C,F}} = 2.7 \text{ Hz}$, 4-Ar- C), 129.5 (Allyl- CH), 130.2 (CH), 131.2 ($^3J_{\text{C,F}} = 7.9 \text{ Hz}$, 5-Ar- CH , Ar- C), 135.7 ($^3J_{\text{C,F}} = 0.8 \text{ Hz}$, 3-Ar- CH) 160.1 ($^1J_{\text{C,F}} = 255.2 \text{ Hz}$, 1-Ar- CF) 167.3 (C=O), 192.1 (C=S) ppm; **EI-MS** m/z (%) = 358.9 $[\text{M}]^+$ (100 %), 343.9 $[\text{M-O}]^+$ (100 %), 231.9 [fragment] $^+$ (100 %); **HR-MS** m/z = 356.9282 $[\text{M}]^+$ (calculated: 356.9293); **HPLC-Analysis** : 99 %, $R_t = 37.6 \text{ min}$. (Z)-3-allyl-5-(3-nitrobenzylidene)-2-thioxothiazolidin-4-one **40m**^[297]

Reaction time: 4 h; **Purification**: Re-crystallisation from ethanol; **Yield**: 41 mg of red crystals (0.13 mmol, 21 %); **$^1\text{H-NMR}$** (400 MHz, CDCl_3) $\delta = 4.76$ (dt, 2 H, $^3,^4J_{\text{H,H}} = 5.9, 1.3 \text{ Hz}$, CH_2), 5.28 (ddd, 1 H, $^3,^4J_{\text{H,H}} = 10.3, 2.2, 1.1 \text{ Hz}$, CHH), 5.32 (ddd, 1 H, $^3,^4J_{\text{H,H}} = 17.1, 2.5, 1.4 \text{ Hz}$, CHH), 5.86 (ddt, 1 H, $^3J_{\text{H,H}} = 17.1, 10.3, 5.9 \text{ Hz}$, Allyl- CH), 7.69 (at, 1 H, $^3J_{\text{H,H}} = 8.2, 7.9 \text{ Hz}$, 5-Ar- CH), 7.75 (s, 1 H, CH), 7.80 (ddd, 1 H, $^3,^4J_{\text{H,H}} = 7.9, 1.8, 1.0 \text{ Hz}$, 4-Ar- CH), 8.29 (ddd, 1 H, $^3,^4J_{\text{H,H}} = 8.2, 2.1, 1.0 \text{ Hz}$, 6-Ar- CH), 8.36 (at, 1 H, $^4J_{\text{H,H}} = 2.1, 1.8 \text{ Hz}$, 2-Ar- CH) ppm; **$^1\text{H-NMR}$** (400 MHz, DMSO-d_6) $\delta = 4.66$ (dt, 2 H, $^3,^4J_{\text{H,H}} = 5.2, 1.6 \text{ Hz}$, CH_2), 5.15 (ddd, 1 H, $^3,^4J_{\text{H,H}} = 17.2, 2.9, 1.6 \text{ Hz}$, E-Allyl- CH_2), 5.19 (ddd, 1 H, $^3,^4J_{\text{H,H}} = 10.4, 2.8, 1.4 \text{ Hz}$, Z-Allyl- CH_2), 5.85 (ddt, 1 H, $^3,^4J_{\text{H,H}} = 17.2, 10.4, 5.2 \text{ Hz}$, Allyl- CH), 7.85 (t, 1 H, $^3J_{\text{H,H}} = 8.1 \text{ Hz}$, 4-Ar- CH), 8.01 (s, 1 H, CH), 8.06 (ddd, 1 H, $^3,^5J_{\text{H,H}} = 8.1, 1.7, 0.7 \text{ Hz}$, 3-Ar- CH), 8.33 (ddd, 1 H, $^3,^4,^5J_{\text{H,H}} = 8.1, 2.1, 0.7 \text{ Hz}$, 5-Ar- CH), 8.52 (dd, 1 H, $^4J_{\text{H,H}} = 2.1, 1.7 \text{ Hz}$, 1-Ar- CH) ppm; **$^{13}\text{C-NMR}$** (400 MHz, CDCl_3) $\delta = 46.7$ (CH_2), 119.9 (Allyl- CH_2), 124.8 (6-Ar- CH), 124.9 (2-Ar- CH), 126.7 (Ar- C),

129.4 (Allyl-CH), 129.6 (CH), 130.6 (5-Ar-CH), 135.1 (Ar-C), 135.6 (4-Ar-CH), 148.9 (Ar-C), 167.2 (C=O), 191.6 (C=S) ppm; **ESI-MS** m/z (%) = 307.0 [M+H]⁺ (100 %), 324.0 [M+NH₄]⁺ (60 %); **HR-MS** m/z = 307.0209 [M+H]⁺ (calculated: 307.0206); **HPLC-Analysis** : 99.9 %, R_t = 29.1 min; **HPLC-Analysis (Method B)**: 100 %, R_t = 21.6 min.

(5Z)-5-[4-(dimethylamino)phenyl]methylidene-3- (prop-2-en-1-yl)-2-sulfanylidene-1,3-thiazolidin-4-one **40n**^[298]

Reaction time: 4 h; **TLC** R_f = 0.6 (toluene/EtOAc 9:1); **Purification**: Flash-Chromatography toluene (R_f = 0.2); **Yield**: 61 mg of purple crystals (0.20 mmol, 32 %); **Purification**: Re-crystallisation from ethanol; **Yield**: 853 mg of red solid (2.80 mmol, 97 %); **¹H-NMR** (400 MHz, CDCl₃) δ = 3.09 (s, 6 H, 2xCH₃), 4.73-4.77 (m, 2 H, CH₂), 5.22-5.26 (m, 1 H, Z-CHH), 5.26-5.32 (m, 1 H, E-CHH), 5.82-5.94 (m, 1 H, Allyl-CH), 6.75 (d, 2 H, ³J_{H,H} = 9.0 Hz, 3,5-Ar-CH), 7.41 (d, 2 H, ³J_{H,H} = 9.0 Hz, 2,6-Ar-CH), 7.68 (s, 1 H, CH) ppm; **ESI-MS** m/z (%) = 305.1 [M+H]⁺ (100 %), 609.1 [2M+H]⁺ (15 %); **HR-MS** m/z = 305.0776 [M+H]⁺ (calculated: 305.0777); **HPLC-Analysis (Method B)**: 98 %, R_t = 21.9 min.

(Z)-N-(4-((3-allyl-4-oxo-2-thioxothiazolidin-5-ylidene)methyl)phenyl) acetamide **40o**

TLC R_f = 0.1 (DCM); **Reaction time**: 2 h; **Purification**: Filtration from methanol; **Yield**: 48 mg of yellow solid (0.15 mmol, 52 %); **¹H-NMR** (400 MHz, CDCl₃) δ = 2.22 (s, 3 H, CH₃), 4.75 (dt, 2 H, ^{3,4}J_{H,H} = 5.8, 1.3 Hz, CH₂), 5.25 (ddd, 1 H, ^{3,4}J_{H,H} = 10.3, 2.3, 1.2 Hz, CHH), 5.30 (ddd, 1 H, ^{3,4}J_{H,H} = 17.2, 2.6, 1.4 Hz, CHH), 5.87 (ddt, 1 H, ³J_{H,H} = 17.2, 10.3, 5.8 Hz, CH), 7.34 (s(br), 1 H, NH), 7.47 (d, 2 H, ³J_{H,H} = 8.7 Hz, 2xAr-CH), 7.65 (d, 2 H, ³J_{H,H} = 8.7 Hz, 2xAr-CH), 7.69 (s, 1 H, CH) ppm; **¹³C-NMR** (400 MHz, CDCl₃) δ = 25.0 (CH₃), 46.5 (CH₂), 119.5 (Allyl-CH₂), 120.0 (2xAr-CH), 121.6 (Ar-C), 129.1 (Ar-C), 129.7 (Allyl-CH), 132.1 (2xAr-CH), 132.8 (CH), 140.3 (Ar-C), 167.7 (C=O), 192.9 (C=S) ppm; **ESI-MS** m/z (%) = 319.1 [M+H]⁺ (100 %), 341.0 [M+Na]⁺ (75 %); **HR-MS** m/z = 319.0574 [M+H]⁺ (calculated: 319.0569); **HPLC-Analysis** : 100 %, R_t = 33.9 min; **HPLC-Analysis (Method B)**: 100 %, R_t = 18.3 min.

(Z)-3-allyl-5-(2-hydroxybenzylidene)-2-thioxothiazolidin-4-one **40p**^[297]

TLC R_f = 0.1 (DCM); **Reaction time**: 2.5 h; **Purification**: Re-crystallisation from H₂O; **Yield**: 70 mg of yellow crystals (0.25 mmol, 87 %); **¹H-NMR** (400 MHz, CDCl₃) δ = 4.76 (dt, 2 H, ^{3,4}J_{H,H} = 5.9, 1.3 Hz, CH₂), 5.26 (ddd, 1 H, ^{3,4}J_{H,H} = 10.2, 2.3, 1.3 Hz, Z-Allyl-CH₂), 5.30 (ddd, 1 H, ^{3,4}J_{H,H} = 17.1, 2.3, 1.3 Hz, E-Allyl-CH₂), 5.88 (ddt, 1 H, ³J_{H,H} = 17.1, 10.2, 5.9 Hz, Allyl-CH), 6.19 (s(br), 1 H, OH), 6.91 (d, 1 H, ³J_{H,H} = 8.4 Hz, 3-Ar-CH), 7.01 (at, 1 H, ³J_{H,H} = 7.6 Hz, 5-Ar-CH), 7.32 (dd, 1 H, ³J_{H,H} = 7.6, 8.4 Hz, 4-Ar-CH), 7.39 (d, 1 H, ³J_{H,H} = 7.6 Hz, 6-Ar-CH), 8.20 (s, 1 H, CH) ppm; **¹³C-NMR** (400 MHz, CDCl₃) δ = 47.2 (CH₂), 117.1 (5-ArCH), 118.9 (Allyl-CH₂), 121.1 (3-ArCH), 121.9 (Ar-C), 122.4 (Ar-C), 130.3 (CH), 130.8 (2-ArCH), 131.3 (Allyl-CH), 133.9 (4-ArCH), 159.1 (Ar-C), 168.8 (Ar-C), 173.0 (C=O), 195.2 (C=S) ppm; **¹H-NMR** (400 MHz, MeOD) δ = 4.71 (dt, 2 H, ^{3,4}J_{H,H} = 5.7, 1.4 Hz, CH₂), 5.20 (ddd, 1 H, ^{3,4}J_{H,H} = 10.1, 2.6, 1.3 Hz, CHH), 5.21 (ddd, 1 H, ^{3,4}J_{H,H} = 17.4, 2.6, 1.3 Hz, CHH), 5.87 (ddt, 1 H,

$^3J_{\text{H,H}} = 17.4, 10.1, 5.6 \text{ Hz, CH}$), 6.89 (d, 1 H, $^3J_{\text{H,H}} = 8.2 \text{ Hz, 5-Ar-CH}$), 6.94 (at, 1 H, $^3J_{\text{H,H}} = 7.8, 7.4 \text{ Hz, 3-Ar-CH}$), 7.30 (at, 1 H, $^3J_{\text{H,H}} = 8.2, 7.4 \text{ Hz, 4-Ar-CH}$), 7.35 (d, 1 H, $^3J_{\text{H,H}} = 7.8 \text{ Hz, 2-Ar-CH}$), 8.12 (s, 1 H, CH) ppm; $^{13}\text{C-NMR}$ (400 MHz, MeOD) $\delta = 47.2$ (CH₂), 117.1 (5-Ar-CH), 118.9 (Allyl-CH₂), 121.1 (3-Ar-CH), 121.9 (Ar-C), 130.3 (CH), 130.8 (2-Ar-CH), 131.3 (Allyl-CH), 133.9 (4-Ar-CH), 159.1 (Ar-C), 168.8 (Ar-C), 173.0 (C=O), 195.2 (C=S) ppm; **APCI-MS** m/z (%) = 278.0 [M+H]⁺ (100 %); **HR-MS** $m/z = 278.0303$ [M+H]⁺ (calculated: 278.0304); **HPLC-Analysis** : 99.9 %, $R_t = 34.0 \text{ min.}$

(Z)-3-allyl-5-(3-hydroxybenzylidene)-2-thioxothiazolidin-4-one **40q**

TLC $R_f = 0.1$ (DCM); **Reaction time**: 4 h; **Purification**: Flash-Chromatography DCM ($R_f = 0.1$); **Yield**: 36 mg of yellow solid (0.13 mmol, 45 %); $^1\text{H-NMR}$ (400 MHz, CDCl₃) $\delta = 1$ (, (, H H, $^7J_{\text{H}} = \text{,, } ^0J_{4.75} = 2, \text{ H,H Hz, 5.8, 1.3 Hz)CH}_2\text{3,4, 5.21 (s(br), 1 H, OH), 5.26 (ddd, 1 H, } ^{3,4}J_{\text{H,H}} = 10.3, 2.4, 1.2 \text{ Hz, Z-Allyl-CH}_2\text{), 5.30 (ddd, 1 H, } ^{3,4}J_{\text{H,H}} = 17.1, 2.4, 1.2 \text{ Hz, E-Allyl-CH}_2\text{), 5.87 (ddd, 1 H, } ^3J_{\text{H,H}} = 17.1, 10.3, 5.8 \text{ Hz, CH), 6.93 (dd, 1 H, } ^{3,4}J_{\text{H,H}} = 8.0, 2.4 \text{ Hz, 4-Ar-CH), 6.96 (at, 1 H, } ^{3,4}J_{\text{H,H}} = 2.4, 2.4 \text{ Hz, 2-Ar-CH), 7.09 (d, 1 H, } ^3J_{\text{H,H}} = 8.0 \text{ Hz, 6-Ar-CH), 7.36 (at, 1 H, } ^3J_{\text{H,H}} = 8.0, 8.0 \text{ Hz, 5-Ar-CH), 7.67 (s, 1 H, CH) ppm; } ^{13}\text{C-NMR}$ (400 MHz, CDCl₃) $\delta =$, 46.6 (CH₂), 117.1 (2-Ar-CH), 118.2 (4-Ar-CH), 119.6 (Alken-CH₂), 123.5 (6-Ar-CH), 123.6 (C), 129.6 (Alken-CH), 130.8 (5-Ar-CH), 133.0 (CH), 134.9 (C), 156.3 (C), 167.6 (C), 193.0 (CHO) ppm; **EI-MS** m/z (%) = 277.0 [M]⁺ (100 %), 262.0 [fragment]⁺ (70 %), 150.0 [fragment]⁺ (100 %); **HR-MS** $m/z = 277.0225$ [M]⁺ (calculated: 277.0226); **HPLC-Analysis** : 99.9 %, $R_t = 33.9 \text{ min.}$

(Z)-3-allyl-5-(4-hydroxybenzylidene)-2-thioxothiazolidin-4-one **40r**^[299]

TLC $R_f = 0.1$ (DCM/hexane 1:1); **Reaction time**: 4 h; **Purification**: Flash-Chromatography DCM/Hexane 1:1 ($R_f = 0.1$); **Yield**: 49 mg of red solid (0.18 mmol, 50 %); $^1\text{H-NMR}$ (400 MHz, CDCl₃) $\delta = 4.71\text{-}4.78$ (m, 2 H, CH₂), 5.23-5.33 (m, 2 H, Allyl-CH₂), 5.53 (s, 1 H, OH), 5.87 (ddt, 1 H, $^3J_{\text{H,H}} = 17.2, 10.4, 5.2 \text{ Hz, Allyl-CH}$), 6.95 (d, 2 H, $^3J_{\text{H,H}} = 8.3 \text{ Hz, 2,6-Ar-CH}$), 7.42 (d, 2 H, $^3J_{\text{H,H}} = 8.3 \text{ Hz, 3,5-Ar-CH}$), 7.69 (s, 1 H, CH) ppm; $^{13}\text{C-NMR}$ (400 MHz, CDCl₃) $\delta = 46.5$ (CH₂), 116.7 (2,6-Ar-CH), 119.4 (Allyl-CH₂), 120.2 (Ar-C), 126.4 (Ar-C) 129.7 (Allyl-CH), 133.2 (3,5-Ar-CH), 133.5 (CH), 158.3 (Ar-C), 167.9 (C=O), 193.1 (C=S) ppm; **EI-MS** m/z (%) = 277.0 [M]⁺ (100 %), 262.0 [fragment]⁺ (40 %), 150.0 [fragment]⁺ (100 %); **HR-MS** $m/z = 277.0226$ [M]⁺ (calculated: 277.0231); **HPLC-Analysis** : 91 %, $R_t = 38.1 \text{ min.}$

(Z)-3-allyl-5-(2,4-dihydroxybenzylidene)-2-thioxothiazolidin-4-one **40s**

Reaction time: red solid; **Purification**: Filtration from ethanol; **Yield**: 65 mg of red solid (0.22 mmol, 47 %); **Yield**: 30 mg of red solid (0.10 mmol, 35 %); $^1\text{H-NMR}$ (400 MHz, MeOD) $\delta = 4.69$ (dt, 2 H, $^{3,4}J_{\text{H,H}} = 5.6, 1.3 \text{ Hz, CH}_2\text{), 5.15-5.21 (m, 2 H, CH}_2\text{), 5.85 (ddt, 1 H, } ^3J_{\text{H,H}} = 17.4, 10.1, 5.6 \text{ Hz, CH), 6.34 (d, 1 H, } ^4J_{\text{H,H}} = 2.3 \text{ Hz, 2-Ar-CH), 6.42 (dd, 1 H, } ^{3,4}J_{\text{H,H}} = 8.7, 2.3 \text{ Hz, 4-Ar-CH), 7.20 (d, 1 H, } ^3J_{\text{H,H}} = 8.7 \text{ Hz, 5-Ar-CH), 8.08 (s, 1 H, CH) ppm; } ^{13}\text{C-NMR}$ (400 MHz, MeOD) $\delta = 47.1$ (CH₂), 103.4 (2-Ar-CH), 109.7 (4-Ar-CH), 114.2 (Ar-C), 117.6 (Ar-C), 118.7 (CH₂), 131.1 (CH), 131.4 (Allyl-CH), 132.7 (5-Ar-CH), 161.5 (Ar-C), 164.0 (Ar-C),

169.1 ($\text{C}=\text{O}$), 195.0 ($\text{C}=\text{S}$) ppm; **EI-MS** m/z (%) = 293.1 $[\text{M}]^+$ (100 %), 278.1 [fragment] $^+$ (20 %), 194.1 [fragment] $^+$ (75 %), 166.1 [fragment] $^+$ (100 %); **HR-MS** m/z = 293.0172 $[\text{M}]^+$ (calculated: 293.0180); **HPLC-Analysis (Method B)**: 97 %, R_t = 14.6 min.

(Z)-3-allyl-5-(3,4-dihydroxybenzylidene)-2-thioxothiazolidin-4-one **40t**

TLC R_f = 0.1 (DCM); **Reaction time**: 3 h; **Purification**: Re-crystallisation from DCM; **Yield**: 13 mg of yellow solid (0.04 mmol, 15 %); **$^1\text{H-NMR}$** (400 MHz, CDCl_3) δ = 4.83-4.87 (m, 2 H, CH_2), 5.29-5.41 (m, 2 H, Allyl- CH_2), 6.00-6.10 (m, 1 H, 3) 7.10 (d, 1 H, $^3J_{\text{H,H}}$ = 8.0 Hz, 5-Ar- CH), 7.25-7.29 (m, 1 H, Ar- CH), 7.43-7.50 (m, 1 H, Ar- CH), 7.87 (s, 1 H, CH), 9.74-10.38 (s(br), 2 H, 2xOH) ppm; **ESI-MS** m/z (%) = **$^1\text{H-NMR}$** (400 MHz, MeOD) δ = 4.68 (d, 2 H, $^3J_{\text{H,H}}$ = 5.5 Hz, CH_2), 5.15-5.21 (m, 2 H, Allyl- CH_2), 5.84 (ddt, 1 H, $^3J_{\text{H,H}}$ = 17.3, 10.2, 5.5 Hz, Allyl- CH), 6.86 (d, 1 H, $^3J_{\text{H,H}}$ = 8.2 Hz, 5-Ar- CH), 6.96 (d, 1 H, $^3J_{\text{H,H}}$ = 8.2 Hz, 6-Ar- CH), 6.98 (s, 1 H, 3-Ar- CH), 7.57 (s, 1 H, CH) ppm; **$^{13}\text{C-NMR}$** (400 MHz, MeOD) δ = 47.2 (CH_2), 117.1 (5-Ar- CH), 117.9 (6-Ar- CH), 118.9 (Allyl- CH_2), 119.6 (Ar- C), 126.4 (3-Ar- CH), 126.6 (Ar- C), 131.3 (Allyl- CH), 135.3 (CH), 147.3 (Ar- C), 150.5 ($\text{C}=\text{O}$), 168.8 ($\text{C}=\text{O}$) 193.0 ($\text{C}=\text{S}$) ppm; **ESI-MS** m/z (%) = 292.0 $[\text{M}-\text{H}]^-$ (100 %), 585.0 $[2\text{M}-\text{H}]^-$ (20 %); **HR-MS** m/z = 292.0105 $[\text{M}-\text{H}]^-$ (calculated: 292.0108); **HPLC-Analysis** : 99.9 %, R_t = 32.2 min.

(5Z)-5-[(4-hydroxy-3,5-dimethoxyphenyl)methylidene]-3-(prop-2-en-1-yl)-2-sulfanylidene-1,3-thiazolidin-4-one **40u**

TLC R_f = 0.7 (DCM/MeOH 9:1); **Reaction time**: 4 h; **Purification**: Re-crystallisation from ethanol; **Yield**: 280 mg of yellow solid (0.83 mmol, 78 %); **Yield**: 430 mg of yellow solid (1.27 mmol, 92 %); **$^1\text{H-NMR}$** (400 MHz, $\text{DMSO}-d_6$) δ = 3.83 (s, 6 H, 2xOCH₃), 4.64 (d, 2 H, $^3J_{\text{H,H}}$ = 5.2 Hz, CH_2), 5.11 (ddd, 1 H, $^3,4J_{\text{H,H}}$ = 17.2, 2.7, 1.1 Hz, E-Allyl- CHH), 5.18 (ddd, 1 H, $^3,4J_{\text{H,H}}$ = 10.4, 2.7, 1.1 Hz, Z-Allyl- CHH), 5.84 (ddt, 1 H, $^3J_{\text{H,H}}$ = 17.2, 10.4, 5.2 Hz, Allyl- CH), 6.92 (s, 2 H, 2,6-Ar- CH), 7.74 (s, 1 H, CH) ppm; **$^{13}\text{C-NMR}$** (400 MHz, $\text{DMSO}-d_6$) δ = 46.0 (CH_2), 56.1 (2xOCH₃), 108.8 (2,6-Ar- CH), 117.3 (Ar- C), 117.6 (Allyl- CH_2), 122.7 (Ar- C), 130.4 (Allyl- CH), 134.6 (CH), 140.6 (Ar- C), 148.5 (2xAr- C), 166.5 ($\text{C}=\text{O}$), 192.6 ($\text{C}=\text{S}$), ppm; **ESI-MS** m/z (%) = 338.1 $[\text{M}+\text{H}]^+$ (100 %), 360.0 $[\text{M}+\text{Na}]^+$ (23 %), 692.1 $[2\text{M}+\text{NH}_4]^+$ (28 %), 697.1 $[2\text{M}+\text{Na}]^+$ (100 %); **ESI-MS** m/z (%) = 338.1 $[\text{M}+\text{H}]^+$ (32 %), 360.0 $[\text{M}+\text{Na}]^+$ (4 %), 692.1 $[2\text{M}+\text{H}]^+$ (9 %), 697.1 $[2\text{M}+\text{Na}]^+$ (10 %); **HPLC-Analysis (Method B)**: 92 %, R_t = 19.3 min.

(Z)-3-allyl-5-(4-(methylsulfonyl)benzylidene)-2-thioxothiazolidin-4-one **40v**

Reaction time: 4 h; **Purification**: Re-crystallisation from ethanol; **Yield**: 88 mg of orange crystals (0.26 mmol, 42 %); **$^1\text{H-NMR}$** (400 MHz, CDCl_3) δ = 3.09 (s, 3 H, SO_2CH_3), 4.74 (dt, 2 H, $^3,4J_{\text{H,H}}$ = 5.9, 1.2 Hz, CH_2), 5.26 (ddd, 1 H, $^3,4J_{\text{H,H}}$ = 10.3, 2.3, 1.2 Hz, CHH), 5.30 (ddd, 1 H, $^3,4J_{\text{H,H}}$ = 17.2, 2.6, 1.3 Hz, CHH), 5.85 (ddt, 1 H, $^3J_{\text{H,H}}$ = 17.2, 10.3, 5.9 Hz, Allyl- CH), 7.66 (d, 1 H, $^3J_{\text{H,H}}$ = 8.4 Hz, 2xAr- CH), 7.72 (s, 1 H, CH), 8.04 (d, 1 H, $^3J_{\text{H,H}}$ = 8.4 Hz, 2xAr- CH) ppm; **$^1\text{H-NMR}$** (400 MHz, $\text{DMSO}-d_6$) δ = 3.29 (s, 3 H, CH_3), 4.66 (dt, 2 H, $^3,4J_{\text{H,H}}$ = 5.2, 1.6 Hz, CH_2), 5.17 (ddd, 1 H, $^3,4J_{\text{H,H}}$ = 17.2, 2.9, 1.5 Hz, E-Allyl- CH_2), 5.20 (ddd, 1 H, $^3,4J_{\text{H,H}}$ = 10.4,

2.8, 1.4 Hz, Z-Allyl-CH₂), 5.85 (ddt, 1 H, ^{3,4}J_{H,H} = 17.2, 10.4, 5.2 Hz, Allyl-CH), 7.91 (ddd, 2 H, ^{3,4}J_{H,H} = 8.6, 2.0, 2.0 Hz, 2,4-Ar-CH), 7.92 (s, 1 H, CH), 8.08 (ddd, 2 H, ^{3,4}J_{H,H} = 8.6, 2.0, 2.0 Hz, 1,5-Ar-CH); ¹³C-NMR (400 MHz, CDCl₃) δ = 44.5 (SO₂-CH₃), 46.7 (CH₂), 119.9 (Allyl-CH₂), 127.2 (Ar-C), 128.4 (2xAr-CH), 129.3 (Allyl-CH), 130.0 (CH), 131.0 (2xAr-CH), 138.5 (Ar-C), 141.6 (Ar-C), 167.1 (C=O), 191.7 (C=S) ppm; **ESI-MS** m/z (%) = 340.0 [M+H]⁺ (100 %), 362.0 [M+Na]⁺ (60 %); **HR-MS** m/z = 340.0133 [M+H]⁺ (calculated: 340.0130); **HPLC-Analysis** : 99.9 %, R_t = 31.7 min.

(Z)-4-((3-allyl-4-oxo-2-thioxothiazolidin-5-ylidene)methyl)benzaldehyde **40w**^[296]

TLC R_f = 0.4 (DCM); **Reaction time**: 4 h; **Purification**: Flash-Chromatography DCM (R_f = 0.4); **Yield**: 23 mg of yellow solid (0.08 mmol, 27 %); ¹H-NMR (400 MHz, CDCl₃) δ = 4.63-4.69 (m, 2 H, CH₂), 5.17-5.26 (m, 2 H, CH₂), 7.57 (d, 2 H, ³J_{H,H} = 8.3 Hz, 2xAr-CH), 7.62 (s, 1 H, CH), 7.90 (d, 2 H, ³J_{H,H} = 8.3 Hz, 2xAr-CH), 9.98 (s, 1 H, CHO) ppm; **EI-MS** m/z (%) = 288.9 [M]⁺ (100 %); **APCI-MS** m/z (%) = 290.0 [M+H]⁺ (100 %); **HR-MS** m/z = 290.0306 [M+H]⁺ (calculated: 290.0304); **HPLC-Analysis (Method B)**: 91 %, R_t = 14.8 min.

(Z)-3-allyl-5-(3-(benzyloxy)benzylidene)-2-thioxothiazolidin-4-one **40x**^[300]

TLC R_f = 0.6 (DCM); **Reaction time**: 3 h; **Purification**: Re-crystallisation from methanol/acetone; **Yield**: 25 mg of yellow crystals (0.07 mmol, 10 %); ¹H-NMR (400 MHz, CDCl₃) δ = 4.74 (dt, 2 H, ^{3,4}J_{H,H} = 5.8, 1.3 Hz, CH₂), 5.13 (s, 2 H, Bn-CH₂), 5.26 (ddd, 1 H, ^{3,4}J_{H,H} = 10.3, 2.4, 1.3 Hz, CHH), 5.30 (ddd, 1 H, ^{3,4}J_{H,H} = 17.2, 2.4, 1.3 Hz, CHH), 5.86 (ddt, 1 H, ³J_{H,H} = 17.2, 10.3, 5.8 Hz, Allyl-CH), 7.05-7.13 (m, 3 H, 3xAr-CH), 7.33-7.47 (m, 6 H, 6xAr-CH), 7.69 (s, 1 H, CH) ppm; ¹H-NMR (400 MHz, DMSO-d₆) δ = 4.62-4.67 (m, 2 H, CH₂), 5.10-5.22 (m, 4 H, E(Z)-Allyl-CH₂, OCH₂Ph), 5.80-5.90 (m, 1 H, Allyl-CH), 7.17-7.53 (m, 9 H, 9 x Ar-CH), 7.81 (s, 1 H, C-H); ¹³C-NMR (400 MHz, CDCl₃) δ = 46.5 (CH₂), 70.3 (Bn-CH₂), 116.2 (Ar-CH), 118.0 (Ar-CH), 119.5 (Allyl-CH₂), 123.4 (Ar-C), 123.7 (Ar-CH), 127.6 (Ar-CH), 128.4 (Ar-CH), 128.8 (Ar-CH), 128.9 (Ar-CH), 129.6 (Allyl-CH), 130.5 (Ar-CH), 133.2 (CH), 134.7 (Ar-C), 136.4 (Ar-C), 159.4 (Ar-C), 167.5 (C=O), 193.0 (C=S) ppm; **ESI-MS** m/z (%) = 368.1 [M+H]⁺ (100 %), 385.1 [M+NH₄]⁺ (35 %); **HR-MS** m/z = 368.0774 [M+H]⁺ (calculated: 368.0773). **HPLC-Analysis (Method B)**: 98 %, R_t = 21.9 min.

(Z)-3-allyl-5-(4-(benzyloxy)benzylidene)-2-thioxothiazolidin-4-one **40y**^[99]

Reaction time: 4 h; **Purification**: Re-crystallisation from ethanol; **Yield**: 154 mg of yellow crystals (0.42 mmol, 69 %); ¹H-NMR (400 MHz, DMSO-d₆) δ = 4.64 (dt, 2 H, ^{3,4}J_{H,H} = 5.2, 1.6 Hz, CH₂), 5.12 (ddd, 1 H, ^{3,4}J_{H,H} = 17.2, 2.9, 1.7 Hz, E-Allyl-CH₂), 5.19 (ddd, 1 H, ^{3,4}J_{H,H} = 10.4, 2.7, 1.5 Hz, Z-Allyl-CH₂), 5.21 (s, 2 H, OCH₂), 5.84 (ddt, 1 H, ^{3,4}J_{H,H} = 17.2, 10.4, 5.2 Hz, Allyl-CH), 7.21 (ddd, 2 H, ^{3,4,5}J_{H,H} = 8.9, 3.0, 2.0 Hz, 2,3-Ar-CH), 7.32-7.48 (m, 5 H, 5 x Ar-CH), 7.63 (ddd, 2 H, ^{3,4,5}J_{H,H} = 8.9, 3.0, 2.0 Hz, 1,4-Ar-CH), 7.81 (s, 1 H, CH) ppm; ¹H-NMR (400 MHz, CDCl₃) δ = 4.74 (dt, 2 H, ^{3,4}J_{H,H} = 5.8, 1.3 Hz, CH₂), 5.13 (s, 2 H, Bn-CH₂), 5.25 (ddd, 1 H, ^{3,4}J_{H,H} = 10.2, 2.3, 1.1 Hz, CHH), 5.30 (ddd, 1 H, ^{3,4}J_{H,H} = 17.2, 2.6, 1.3 Hz, CHH), 5.87

(ddt, 1 H, $^3J_{\text{H,H}} = 17.2, 10.2, 5.8 \text{ Hz}$, Allyl-CH), 7.07 (d, 2 H, $^3J_{\text{H,H}} = 8.9 \text{ Hz}$, 2xAr-CH), 7.46 (d, 2 H, $^3J_{\text{H,H}} = 8.9 \text{ Hz}$, 2xAr-CH), 7.33-7.48 (m, 5 H, 5xAr-CH), 7.69 (s, 1 H, CH) ppm; $^{13}\text{C-NMR}$ (400 MHz, CDCl_3) $\delta = 46.5$ (CH₂), 70.4 (Bn-CH₂), 115.9 (2xAr-CH), 119.4 (Allyl-CH₂), 120.2 (Ar/Bn-C), 126.4 (Ar/Bn-C), 127.6 (Bn-CH), 128.4 (Bn-CH), 128.9 (Ar/Bn-C), 129.7 (Allyl-CH), 132.9 (2xAr-CH), 133.4 (CH), 136.1 (Ar/Bn-C), 161.0 (Ar/Bn-C), 167.7 (C=O), 193.0 (C=S) ppm; **ESI-MS** m/z (%) = 368.1 [M+H]⁺ (100 %), 390.1 [M+Na]⁺ (40 %), 406.0 [M+K]⁺ (10 %), 757.1 [2M+Na]⁺ (35 %), 1124.2 [3M+Na]⁺ (10 %); **HR-MS** $m/z = 368.0773$ [M+H]⁺ (calculated: 368.0773); **HPLC-Analysis (Method B)**: 99 %, $R_t = 22.5 \text{ min}$.

(Z)-3-allyl-5-(3,4-bis(benzyloxy)benzylidene)-2-thioxothiazolidin-4-one **40z**

Reaction time: 4 h; **Purification**: Filtration from methanol; **Yield**: 138 mg of yellow solid (0.29 mmol, 51 %); $^1\text{H-NMR}$ (400 MHz, CDCl_3) $\delta = 4.73$ (dt, 2 H, $^{3,4}J_{\text{H,H}} = 5.8, 1.3 \text{ Hz}$, CH₂), 5.23 (s, 2 H, Bn-CH₂), 5.24 (s, 2 H, Bn-CH₂), 5.23-5.31 (m, 2 H, Allyl-CH₂), 5.85 (ddt, 1 H, $^3J_{\text{H,H}} = 17.1, 10.3, 5.8 \text{ Hz}$, CH), 6.99 (d, 1 H, $^3J_{\text{H,H}} = 8.5 \text{ Hz}$, 6-Ar-CH), 7.01 (d, 1 H, $^4J_{\text{H,H}} = 2.1 \text{ Hz}$, 3-Ar-CH), 7.07 (dd, 1 H, $^{3,4}J_{\text{H,H}} = 8.5, 2.1 \text{ Hz}$, 5-Ar-CH), 7.31-7.49 (m, 10 H, 10xBn-CH), 7.60 (s, 1 H, CH) ppm; $^1\text{H-NMR}$ (400 MHz, DMSO-d_6) $\delta = 4.62$ -4.65 (m, 2 H, CH₂), 5.12 (ddd, 1 H, $^{3,4}J_{\text{H,H}} = 17.2, 2.9, 1.7 \text{ Hz}$, E-Allyl-CH₂), 5.19 (ddd, 1 H, $^{3,4}J_{\text{H,H}} = 10.4, 2.7, 1.5 \text{ Hz}$, Z-Allyl-CH₂), 5.23 (s, 2 H, OCH₂Ph), 5.25 (s, 2 H, OCH₂Ph), 5.84 (ddt, 1 H, $^{3,4}J_{\text{H,H}} = 17.2, 10.4, 5.2 \text{ Hz}$, Allyl-CH), 7.23-7.50 (m, 13 H, 13 x Ar-CH), 7.74 (s, 1 H, CH) ppm; $^{13}\text{C-NMR}$ (400 MHz, CDCl_3) $\delta = 46.5$ (CH₂), 71.0 (Bn-CH₂), 71.4 (Bn-CH₂), 114.3 (6-Ar-CH), 116.0 (3-Ar-CH), 119.4 (Allyl-CH₂), 120.4 (Ar/Bn-C), 126.2 (5-Ar-CH), 126.7 (Ar/Bn-C or CH), 127.3 (Bn-CH), 127.4 (Bn-CH), 128.3 (2xBn-CH or Ar/Bn-C), 128.8 (Bn-CH), 128.9 (Bn-CH), 129.7 (Allyl-CH), 133.6 (CH), 136.4 (Ar/Bn-C), 136.6 (Ar/Bn-C), 149.1 (Ar/Bn-C), 151.6 (Ar/Bn-C), 167.6 (C=O), 193.0 (C=S) ppm; **ESI-MS** m/z (%) = 474.1 [M+H]⁺ (100 %), 491.1 [M+NH₄]⁺ (60 %), **HR-MS** $m/z = 474.1187$ [M+H]⁺ (calculated: 474.1192); **HPLC-Analysis (Method B)**: 99 %, $R_t = 22.5 \text{ min}$.

Synthesis of N-allyl-thiazolidine-2,4-dione **41** and N-Propagyl-thiazolidine-2,4-dione **42**

Synthesis of N-Allyl or N-Propagyl thiazolidine-2,4-dione via Mitsunobu reaction conditions

PPh₃ (2.56 mmol, 1.0 eq) was dissolved in anhydrous THF (20 mL) under a nitrogen atmosphere. DEAD (2.56 mmol, 1.0 eq) were added at -78 °C over a time period of 5 min. The thiazolidine-2,4-dione (2.56 mmol, 1.0 eq) and allyl or propagyl alcohol (2.56 mmol, 1.0 eq) were added to the reaction mixture. The reaction mixture was stirred at -78 °C for another 15 min and was subsequently allowed to stir at rt. After TLC showed complete consumption of starting material, the reaction mixture was concentrated and purified via flash column chromatography.

3-Allylthiazolidine-2,4-dione **41** ^[301]

TLC R_f = 0.6 (Toluene/EtOAc 8:2); **Reaction time**: 12 h; **Yield**: 126 mg of clear oil (0.80 mmol, 84 %); **Purification**: Flash-Chromatography toluene/EtOAc 8:2 (R_f = 0.6); **$^1\text{H-NMR}$** (400 MHz, CDCl_3) δ = 3.93 (s, 2 H, CH_2), 4.16 (dt, 2 H, $^3J_{\text{H,H}}$ = 5.9, 1.3 Hz, CH_2), 5.17 (ddd, 1 H, $^3J_{\text{H,H}}$ = 10.3, 2.3, 1.3 Hz, CHH), 5.21 (ddd, 1 H, $^3J_{\text{H,H}}$ = 17.2, 2.3, 1.3 Hz, CHH), 5.74 (ddt, 1 H, $^3J_{\text{H,H}}$ = 17.2, 10.3, 5.9 Hz, CH) ppm; **$^{13}\text{C-NMR}$** (400 MHz, CDCl_3) δ = 33.8 (($\text{C}=\text{O}$) CH_2S), 43.9 (CH_2), 119.0 (Allyl- CH_2), 130.0 (CH), 171.0 ($\text{C}=\text{O}$), 171.3 ($\text{C}=\text{O}$) ppm; **$^1\text{H-NMR}$** (400 MHz, CDCl_3) δ = 3.90 (s, 2 H, CH_2), 4.10 (dt, 2 H, $^3J_{\text{H,H}}$ = 5.9, 1.4 Hz, CH_2), 5.11 (ddd, 1 H, $^3J_{\text{H,H}}$ = 10.2, 2.3, 1.1 Hz, CHH), 5.15 (ddd, 1 H, $^3J_{\text{H,H}}$ = 17.2, 2.6, 1.4 Hz, CHH), 5.68 (ddt, 1 H, $^3J_{\text{H,H}}$ = 17.1, 10.2, 5.9 Hz, Allyl- CH) ppm; **$^{13}\text{C-NMR}$** (400 MHz, CDCl_3) δ = 33.7 (($\text{C}=\text{O}$) CH_2S), 43.6 (CH_2), 118.7 (Allyl- CH_2), 130.0 (CH), 170.9 ($\text{C}=\text{O}$), 171.2 ($\text{C}=\text{O}$) ppm; **$^1\text{H-NMR}$** (400 MHz, CDCl_3) δ = 3.97 (s, 2 H,) 4.22 (d, 2 H, $^3J_{\text{H,H}}$ = 5.9 Hz, CH_2), 5.20-5.29 (m, 2 H, CH_2), 5.73-5.84 (m, 1 H, CH) ppm;

3-(prop-2-yn-1-yl)thiazolidine-2,4-dione **42**^[302]

TLC R_f = 0.1 (Hexane/EtOAc 8:2); **Purification**: Flash-Chromatography Hexane/EtOAc 8:2 (R_f = 0.1); **Yield**: 388 mg of clear oil (2.50 mmol, 98 %); **$^1\text{H-NMR}$** (400 MHz, CDCl_3) δ = 2.23 (t, 1 H, $^4J_{\text{H,H}}$ = 2.5 Hz, CH), 4.00 (s, 2 H, 5- CH_2), 4.36 (d, 2 H, $^4J_{\text{H,H}}$ = 2.5 Hz, CH_2) ppm; **$^{13}\text{C-NMR}$** (400 MHz, CDCl_3) δ = 30.9 (CH_2), 34.0 (5- CH_2), 72.2 (CH), 76.1 (CCH), 170.2 ($\text{C}=\text{O}$), 170.6 ($\text{C}=\text{O}$) ppm;

Synthesis of N-allyl or N-Propagyl thiazolidine-2,4-dione via nucleophilic substitution

NaH (1.1 eq) was charged in a flask under N_2 atmosphere. Thiazolidone-2,4-dione (1.0 eq) in DMF (5 mL) were added at 0 °C. The reaction mixture was stirred for 5 min and allyl bromide was added at 0 °C. The reaction mixture was allowed to subsequently stir at rt. After TLC showed complete consumption of starting material, the reaction mixture was concentrated. The crude was extracted between H_2O (5 mL) and EtOAc (3x10 mL), dried over MgSO_4 , filtered and concentrated. Purification by flash column chromatography afforded **41** as clear oil.

3-(prop-2-en-1-yl)-1,3-thiazolidine-2,4-dione **41**^[301]

TLC R_f = 0.3 (Hexane/EtOAc 8:2), **Reaction time**: 2 h; **Purification**: Flash-Chromatography Hexane/EtOAc 8:2 (R_f = 0.3); **Yield**: 1161 mg of clear oil (7.39 mmol, 86 %); **Yield**: 251 mg of clear oil (1.60 mmol, 62 %); **Yield**: 371 mg of clear oil (2.36 mmol, 84 %); **Yield**: 297 mg of clear oil (1.89 mmol, 67 %); **$^1\text{H-NMR}$** (400 MHz, CDCl_3) δ = 3.98 (s, 2 H, CH), 4.22 (d, 2 H, $^3J_{\text{H,H}}$ = 5.9 Hz, CH_2), 5.23 (d, 1 H, $^3J_{\text{H,H}}$ = 10.3 Hz, CHH), 5.27 (d, 1 H, $^3J_{\text{H,H}}$ = 17.3 Hz, CHH), 5.79 (ddt, 1 H, $^3J_{\text{H,H}}$ = 5.9, 10.3, 17.3 Hz, CH) ppm. **EI-MS** m/z (%) = 157.0 [M]⁺ (50 %), 129.0 [fragment]⁺ (25 %), 97.1 [fragment]⁺ (70 %), 46.0 [fragment]⁺ (100 %), 4.20 [fragment]⁺ (100 %).

Knoevenagel condensation of 41 and 42 with various benzaldehydes

Compound **41** or **42** (1.0 eq), benzaldehyde derivative (1.1-1.5 eq) and sodium acetate (1.0 eq) were dissolved in ethanol (5-10 mL). The reaction mixture was stirred at 80 °C until TLC showed complete consumption of starting material. The compounds were purified as described below.

(5Z)-3-(prop-2-en-1-yl)-5-[2-(trifluoromethyl)phenyl]methylidene-1,3-thiazolidine-2,4-dione **41a**
TLC R_f = 0.6 (Hexane/EtOAc 8:2); **Reaction time**: 16 h; **Purification**: Flash-Chromatography Hexane/EtOAc 95:5 (R_f = 0.3); **Yield**: 123 mg of white solid (0.39 mmol, 35 %); **Purification**: Flash-Chromatography Cyclohexane/EtOAc 9:1 (R_f = 0.4); **Yield**: 49 mg of white solid (0.16 mmol, 46 %); **¹H-NMR** (400 MHz, CDCl₃) δ = 4.36 (dt, 2 H, $^3,4J_{H,H}$ = 6.0, 1.3 Hz, CH₂), 5.28 (ddd, 1 H, $^3,4J_{H,H}$ = 10.2, 2.2, 1.1 Hz, Allyl-CHH), 5.33 (ddd, 1 H, $^3,4J_{H,H}$ = 17.1, 2.4, 1.2 Hz, Allyl-CHH), 5.87 (ddt, 1 H, $^3J_{H,H}$ = 17.1, 10.2, 6.0 Hz, Allyl-CH), 7.50-7.56 (m, 1 H, 4-Ar-CH), 7.61-7.69 (m, 2 H, 5,6-Ar-CH), 7.78 (d, 1 H, $^3J_{H,H}$ = 7.9 Hz, 3-Ar-CH), 8.18 (q, 1 H, $^5J_{H,F}$ = 1.9 Hz, CH) ppm; **¹³C-NMR** (400 MHz, CDCl₃) δ = 44.1 (CH₂), 119.5 (Allyl-CH₂), 123.7 (q, $^1J_{C,F}$ = 274.1 Hz, CF₃), 126.4 (Ar-C), 126.8 (q, $^3J_{C,F}$ = 5.5 Hz, 3-Ar-CH), 129.0 (5 or 6-Ar-CH), 129.7 (q, $^4J_{C,F}$ = 1.9 Hz, CH), 129.8 (q, $^2J_{C,F}$ = 30.5 Hz, 2-Ar-C), 130.0 (4-Ar-CH), 130.1 (Allyl-CH), 132.2 (q, $^5J_{C,F}$ = 1.7 Hz, Ar-C), 132.4 (5 or 6-Ar-CH) 165.1 (C=O), 167.2 (C=O) ppm; **HPLC-Analysis (Method B)**: 100 %, R_t = 19.2 min.

(Z)-3-allyl-5-(3-(trifluoromethyl)benzylidene)thiazolidine-2,4-dione **41b**

TLC R_f = 0.3 (Hexane/EtOAc 9:1); **Reaction time**: 6 h; **Purification**: Re-crystallisation from ethanol; **Yield**: 17 mg of white crystals (0.05 mmol, 14 %); **¹H-NMR** (400 MHz, CDCl₃) δ = 4.37 (dt, 2 H, $^3,4J_{H,H}$ = 5.9, 1.3 Hz, CH₂), 5.27 (ddd, 1 H, $^3,4J_{H,H}$ = 10.2, 2.1, 1.1 Hz, CHH), 5.31 (ddd, 1 H, $^3,4J_{H,H}$ = 17.0, 2.5, 1.4 Hz, CHH), 5.86 (ddt, 1 H, $^3J_{H,H}$ = 17.0, 10.2, 5.0 Hz, Allyl-CH), 7.60-7.72 (m, 3 H, 3xAr-CH), 7.75 (s, 1 H, Ar-CH), 7.92 (s, 1 H, CH) ppm; **¹³C-NMR** (400 MHz, CDCl₃) δ = 44.2 (CH₂), 119.4 (Allyl-CH₂), 122.3 (Ar-C), 123.9 (Ar-C), 127.0 (2xAr-CH), 127.1 (Ar-C), 130.0 (Ar-CH), 130.1 (Allyl-CH), 132.0 (CH), 132.8 (Ar-CH), 134.2 (CF₃), 165.7 (C=O), 166.9 (C=O) ppm; **APCI-MS** m/z (%) = 314.0 [M+H]⁺ (100 %); **HR-MS** m/z = 314.0452 [M+H]⁺ (calculated: 314.0457); **HPLC-Analysis** : 99.9 %, R_t = 33.8 min.

(Z)-3-allyl-5-(4-(trifluoromethyl)benzylidene)thiazolidine-2,4-dione **41c**

TLC R_f = 0.7 (hexane/EtOAc 8:2); **Reaction time**: 5 h; **Purification**: Re-crystallisation from ethanol; **Yield**: 70 mg of white crystals (0.22 mmol, 66 %); **¹H-NMR** (400 MHz, CDCl₃) δ = 4.37 (dt, 2 H, $^3,4J_{H,H}$ = 5.9, 1.3 Hz, CH₂), 5.27 (ddd, 1 H, $^3,4J_{H,H}$ = 10.3, 2.2, 1.1 Hz, CHH), 5.32 (ddd, 1 H, $^3,4J_{H,H}$ = 17.2, 2.5, 1.4 Hz, CHH), 7.62 (d, 2 H, $^3J_{H,H}$ = 8.3 Hz, 2xAr-CH), 7.74 (d, 2 H, $^3J_{H,H}$ = 8.3 Hz, 2xAr-CH), 7.91 (s, 1 H, CH) ppm; **¹³C-NMR** (400 MHz, CDCl₃) δ = 44.2 (CH₂), 119.5 (Allyl-CH₂), 126.3 (2,6-Ar-CH), 130.1 (3,5-Ar-CH), 130.3 (Ar-C), 132.0 (CH), 165.7 (C=O), 167.0 (C=O); ppm; **APCI-MS** m/z (%) = 314.0 [M+H]⁺ (100 %); **HR-MS** m/z = 313.0380 [M]⁺ (calculated: 313.0379); **HR-MS** m/z = 314.0457 [M+H]⁺ (calculated: 314.0457); **HR-MS**

$m/z = 314.0454$ $[M+H]^+$ (calculated: 314.0457); **HPLC-Analysis** : 99.9 %, $R_t = 34.1$ min.

(Z)-3-allyl-5-(2,4-bis(trifluoromethyl)benzylidene)thiazolidine-2,4-dione **41e**

TLC $R_f = 0.7$ (Cyclohexan/EtOAc 8:2); **Reaction time**: 30 min; **Purification**: Flash-Chromatography Cyclohexan/EtOAc 95:5 ($R_f = 0.2$); **Yield**: 36 mg of white solid (0.09 mmol, 25 %); **1H -NMR** (400 MHz, $CDCl_3$) $\delta = 4.37$ (dt, 2 H, $^3,4J_{H,H} = 6.0, 1.2$ Hz, $\underline{CH_2}$), 5.27-5.31 (m, 1 H, \underline{CHH}), 5.31-5.37 (m, 1 H, \underline{CHH}), 5.86 (dt, 1 H, $^3J_{H,H} = 17.1, 10.2, 6.0$ Hz, Allyl- \underline{CH}), 7.77 (d, 1 H, $^3J_{H,H} = 8.1$ Hz, 3 o. 4-Ar- \underline{CH}), 7.92 (d, 1 H, $^3J_{H,H} = 8.1$ Hz, 3 o. 4-Ar- \underline{CH}), 8.01 (s, 1 H, 6-Ar- \underline{CH}), 8.13 (q, 1 H, $^4J_{H,F} = 1.5$ Hz, \underline{CH}) ppm; **^{13}C -NMR** (400 MHz, $CDCl_3$) $\delta = 44.4$ ($\underline{CH_2}$), 119.9 (Allyl- $\underline{CH_2}$), 123.0 (q, $^1J_{C,F} = 272.9$ Hz, $\underline{CF_3}$), 123.1 (q, $^2J_{C,F} = 272.9$ Hz, $\underline{CF_3}$), 124.1 (m, 6-Ar- \underline{CH}), 127.9 (\underline{CH}), 128.8 (Ar- \underline{C}) 129.4 (\underline{CH}) 129.7 (3 o. 4-Ar- \underline{CH}), 129.9 (\underline{CH}) 130.6 (q, $^2J_{C,F} = 31.6$ Hz, Ar- $\underline{C}-CF_3$), 131.9 (q, $^2J_{C,F} = 34.0$ Hz, Ar- $\underline{C}-CF_3$), 136.0 (Ar- \underline{C}), 164.7 ($\underline{C=O}$), 166.5 ($\underline{C=O}$) ppm; **APCI-MS** m/z (%) = 382.0 $[M+H]^+$ (100 %); **HR-MS** $m/z = 382.0337$ $[M+H]^+$ (calculated: 382.0331); **HPLC-Analysis (Method B)**: 98 %, $R_t = 20.5$ min.

(Z)-3-allyl-5-(2-hydroxybenzylidene)thiazolidine-2,4-dione **41f**

TLC $R_f = 0.2$ (Cyclohexane/EtOAc 8:2); **Reaction time**: 12 h; **Purification**: Filtration from Cyclohexane/EtOAc 8:2; **Yield**: 19 mg of white solid (0.07 mmol, 19 %); **1H -NMR** (400 MHz, MeOD) $\delta = 4.31$ (dt, 2 H, $^3,4J_{H,H} = 5.6, 1.4$ Hz, $\underline{CH_2}$), 5.19 (ddd, 1 H, $^3,4J_{H,H} = 10.3, 2.5, 1.2$ Hz, \underline{CHH}), 5.20 (ddd, 1 H, $^3,4J_{H,H} = 17.1, 2.7, 1.4$ Hz, \underline{CHH}), 5.86 (ddt, 1 H, $^3J_{H,H} = 17.1, 10.3, 5.6$ Hz, Allyl- \underline{CH}), 6.88 (d, 1 H, $^3J_{H,H} = 8.3$ Hz, 3-Ar- \underline{CH}), 6.92 (at, 1 H, $^3J_{H,H} = 7.7, 7.8$ Hz, 5-Ar- \underline{CH}), 7.27 (dd, 1 H, $^3J_{H,H} = 8.3, 7.7$ Hz, 4-Ar- \underline{CH}), 7.40 (d, 1 H, $^3J_{H,H} = 7.8$ Hz, 6-Ar- \underline{CH}), 8.27 (s, 1 H, \underline{CH}) ppm; **^{13}C -NMR** (400 MHz, MeOD) $\delta = 44.5$ ($\underline{CH_2}$), 117.0 (3-Ar- \underline{CH}), 118.4 (Allyl- $\underline{CH_2}$), 120.9 (5-Ar- \underline{CH}), 121.0 (Ar- \underline{C}), 121.8 (Ar- \underline{C}), 130.0 (6-Ar- \underline{CH}), 130.6 (\underline{CH}), 132.1 (Allyl- \underline{CH}), 133.5 (4-Ar- \underline{CH}), 158.9 (Ar- \underline{C}), 167.5 ($\underline{C=O}$), 169.2 ($\underline{C=O}$) ppm; **ESI-MS** m/z (%) = 262.1 $[M+H]^+$ (100 %), 279.1 $[M+NH_4]^+$ (26 %), 284.0 $[M+Na]^+$ (13 %), 523.1 $[2M+H]^+$ (2 %), 540.1 $[2M+NH_4]^+$ (15 %), 545.1 $[2M+Na]^+$ (30 %). **HPLC-Analysis** : 99.9 %, $R_t = 30.0$ min.

(5Z)-5-[(3-hydroxyphenyl)methylidene]-3-(prop-2-en-1-yl)-1,3-thiazolidine-2,4-dione **41g**

TLC $R_f = 0.1$ ($CHCl_3$ /MeOH 1:0.01); **Reaction time**: 6 h; **Purification**: Filtration from Ethanol; **Yield**: 144 mg of white crystals (0.55 mmol, 35 %); **1H -NMR** (400 MHz, $CDCl_3$) $\delta = 4.36$ (d, 2 H, $^3J_{H,H} = 5.9$ Hz, $\underline{CH_2}$), 5.21 (s(br), 1 H, \underline{OH}), 5.26 (d, 1 H, $^3J_{H,H} = 10.2$ Hz, \underline{CHH}), 5.30 (d, 1 H, $^3J_{H,H} = 17.1$ Hz, \underline{CHH}), 5.80-5.91 (m, 1 H, Allyl- \underline{CH}), 6.93 (dd, 1 H, $^3,4J_{H,H} = 1.4, 8.2$ Hz, 4-Ar- \underline{CH}), 6.99 (d, 1 H, $^4J_{H,H} = 1.4$ Hz, 2-Ar- \underline{CH}), 7.10 (d, 1 H, $^3J_{H,H} = 7.7$ Hz, 6-Ar- \underline{CH}), 7.35 (at, 1 H, $^3J_{H,H} = 7.7, 8.2$ Hz, 5-Ar- \underline{CH}), 7.85 (s, 1 H, \underline{CH}) ppm; **^{13}C -NMR** (400 MHz, $CDCl_3$) $\delta = 44.1$ ($\underline{CH_2}$), 116.7 (2-Ar- \underline{CH}), 118.0 (4-Ar- \underline{CH}), 119.3 (Allyl- $\underline{CH_2}$), 122.0 (Ar- \underline{C}), 123.1 (6-Ar- \underline{CH}), 130.2 (Allyl- \underline{CH}), 130.7 (5-Ar- \underline{CH}), 133.9 (\underline{CH}), 134.8 (Ar- \underline{C}), 156.3 (Ar- \underline{C}), 166.1 ($\underline{C=O}$), 167.7 ($\underline{C=O}$) ppm; **HPLC-Analysis (Method B)**: 97 %, $R_t = 16.5$ min.

(5Z)-5-[(4-hydroxyphenyl)methylidene]-3-(prop-2-en-1-yl)-1,3-thiazolidine-2,4-dione **41h**

TLC $R_f = 0.3$ (Hexane/EtOAc 8:2); **Reaction time**: 16 h; **Purification**: Flash-Chromatogra-

phy DCM ($R_f=0.1$); **Yield**: 160 mg of white solid (0.61 mmol, 46 %); **$^1\text{H-NMR}$** (400 MHz, CDCl_3) δ = 1.25 (s(br), 1 H, OH), 4.35 (adt, 2 H, $^3,^4J_{\text{H,H}} = 1.3, 5.8 \text{ Hz}$, 1-CH_2), 5.24 (ddd, 1 H, $^3,^4J_{\text{H,H}} = 1.1, 2.2, 10.2 \text{ Hz}$, Z-CHH), 5.29 (ddd, 1 H, $^3,^4J_{\text{H,H}} = 1.4, 2.5, 17.1 \text{ Hz}$, E-CHH), 5.86 (ddt, 1 H, $^3J_{\text{H,H}} = 5.8, 10.2, 17.1 \text{ Hz}$, Alken-CH), 5.90 (s(br), 1 H, OH), 6.94 (d, 2 H, $^3J_{\text{H,H}} = 8.7 \text{ Hz}$, $2,6\text{-Ar-CH}$), 7.43 (d, 2 H, $^3J_{\text{H,H}} = 8.7 \text{ Hz}$, $3,5\text{-Ar-CH}$), 7.86 (s, 1 H, CH) ppm; **$^{13}\text{C-NMR}$** (400 MHz, CDCl_3) δ = 44.0 (CH_2), 116.5 ($2,6\text{-Ar-CH}$), 118.4 (Ar-C), 119.0 (Allyl-CH_2), 126.1 (Ar-C), 130.4 (Allyl-CH), 132.7 ($3,5\text{-Ar-CH}$), 134.2 (CH), 158.2 (Ar-C), 166.4 (C=O), 168.0 (C=O) ppm; **APCI-MS** m/z (%) = 262.1 $[\text{M}+\text{H}]^+$ (100 %); **HR-MS** m/z = 262.0529 $[\text{M}+\text{H}]^+$ (calculated: 262.0532); **HPLC-Analysis (Method B)**: 98 %, R_t = 16.6 min.

(Z)-3-allyl-5-(3,4-dihydroxybenzylidene)thiazolidine-2,4-dione **41i**

TLC R_f = 0.2 (toluene/EtOAc 7:3); **Reaction time**: 6 h; **Purification**: Flash-Chromatography toluene/EtOAc 7:3 ($R_f=0.2$); **Yield**: 8 mg of white solid (0.03 mmol, 13 %); **$^1\text{H-NMR}$** (400 MHz, MeOD) δ = 4.29 (dt, 2 H, $^3,^4J_{\text{H,H}} = 5.6, 1.4 \text{ Hz}$, CH_2), 5.18 (m, 1 H, E-Allyl-CH_2), 5.19 (m, 1 H, Z-Allyl-CH_2), 5.85 (ddt, 1 H, $^3J_{\text{H,H}} = 17.2, 10.1, 5.5 \text{ Hz}$, Allyl-CH), 6.86 (d, 1 H, $^3J_{\text{H,H}} = 8.3 \text{ Hz}$, 6-Ar-CH), 6.96 (dd, 1 H, $^3,^4J_{\text{H,H}} = 8.3, 2.2 \text{ Hz}$, 5-ArCH), 7.01 (d, 1 H, $^4J_{\text{H,H}} = 2.2 \text{ Hz}$, 3-ArCH), 7.74 (s, 1 H, CH), **$^{13}\text{C-NMR}$** (400 MHz, MeOD) δ = 44.54 (CH_2), 116.9 (6-ArCH), 117.5 (3-ArCH), 118.1 (C), 118.3 (Allyl-CH_2), 132.1 (Allyl-C), 125.6 (5-ArCH), 126.4 (Ar-C), 132.1 (Ar-C), 135.6 (CH), 147.2 (ArC-OH), 150.1 (ArC-OH), 167.5 (C=O), 169.1 (C=O) ppm; **APCI-MS** m/z (%) = 278.0 $[\text{M}+\text{H}]^+$ (100 %); **HR-MS** m/z = 278.0480 $[\text{M}+\text{H}]^+$ (calculated: 278.0482); **HPLC-Analysis** : 99.9 %, R_t = 27.2 min.

(Z)-3-allyl-5-(2,4-dihydroxybenzylidene)-2-thioxothiazolidin-4-one **41m**

TLC R_f = 0.1 (Cyclohexane/EtOAc 7:3); **Reaction time**: 12 h; **Purification**: Flash-Chromatography Cyclohexane/EtOAc 8:2 \rightarrow 7:3 ($R_f=0.1$); **Yield**: 13 mg of white solid (0.05 mmol, 15 %); **$^1\text{H-NMR}$** (400 MHz, MeOD) δ = 4.28 (dt, 2 H, $^3,^4J_{\text{H,H}} = 5.6, 1.4 \text{ Hz}$, CH_2), 5.17 (ddd, 1 H, $^3,^4J_{\text{H,H}} = 10.1, 2.5, 1.3 \text{ Hz}$, CHH), 5.18 (ddd, 1 H, $^3,^4J_{\text{H,H}} = 17.2, 2.8, 1.5 \text{ Hz}$, CHH), 5.84 (ddt, 1 H, $^3J_{\text{H,H}} = 17.2, 10.1, 5.6 \text{ Hz}$, Allyl-CH), 6.34 (d, 1 H, $^4J_{\text{H,H}} = 2.3 \text{ Hz}$, 2-Ar-CH), 6.39 (dd, 1 H, $^3,^4J_{\text{H,H}} = 8.6, 2.3 \text{ Hz}$, 6-Ar-CH), 7.24 (d, 1 H, $^3J_{\text{H,H}} = 8.6 \text{ Hz}$, 5-Ar-CH), 8.23 (s, 1 H, CH) ppm; **$^{13}\text{C-NMR}$** (400 MHz, MeOD) δ = 44.4 (CH_2), 103.4 (2-Ar-CH), 109.2 (6-Ar-CH), 113.8 (Ar-C), 116.2 (Ar-C), 118.2 (Allyl-CH_2), 131.0 (CH), 131.7 (5-Ar-CH), 132.2 (Allyl-CH), 161.1 (Ar-C-OH), 163.4 (Ar-C-OH), 167.9 (C=O), 169.5 (C=O), ppm; **HPLC-Analysis (Method B)**: 97 %, R_t = 17.1 min.

(5Z)-5-[3-(benzyloxy)phenyl]-methylidene-3-(prop-2-en-1-yl)-1,3-thiazolidine-2,4-dione **41j**

TLC R_f = 0.7 (Hexane/EtOAc 8:2); **Reaction time**: 6 h; **Purification**: Flash-Chromatography Hexane/EtOAc 95:5 ($R_f=0.1$); **Yield**: 490 mg of white solid (1.39 mmol, 88 %); **$^1\text{H-NMR}$** (400 MHz, CDCl_3) δ = 4.32 (adt, 2 H, $^3,^4J_{\text{H,H}} = 1.1, 1.4, 5.9 \text{ Hz}$, CH_2), 5.09 (s, 2 H, CH_2Ar), 5.24 (ddd, 1 H, $^3,^4J_{\text{H,H}} = 1.0, 1.1, 10.2 \text{ Hz}$, CHH), 5.28 (ddd, 1 H, $^3,^4J_{\text{H,H}} = 1.0, 1.4, 17.1 \text{ Hz}$, CHH), 5.84 (ddt, 1 H, $^3J_{\text{H,H}} = 5.9, 10.2, 17.1 \text{ Hz}$, Allyl-CH), 7.01-7.06 (m, 2 H, $2,6\text{-Ar-CH}$), 7.08 (d,

1 H, $^3J_{\text{H,H}} = 7.9$ Hz, 4-Ar-CH), 7.30-7.45 (m, 6 H, 6xAr-CH), 7.83 (s, 1 H, CH) ppm; $^{13}\text{C-NMR}$ (400 MHz, CDCl_3) $\delta = 43.9$ (CH₂CH), 70.2 (CH₂Ar), 116.0 (2 or 6-Ar-CH), 117.6 (2 or 6-Ar-CH), 119.1 (Allyl-CH₂), 121.8 (Ar-C), 123.1 (4-Ar-CH), 127.5 (2xAr-CH), 128.3 (Ar-CH), 128.8 (2xAr-CH), 130.2 (Ar-CH), 130.3 (Allyl-CH), 133.9 (CH), 134.6 (Ar-C), 136.4 (Ar-C), 159.2 (Ar-C), 165.9 (C=O), 167.5 (C=O) ppm; **ESI-MS** m/z (%) = 352.1 [M+H]⁺ (28 %), 369.1 [M+NH₄]⁺ (16 %), 720.2 [2M+NH₄]⁺ (11 %), 725.2 [2M+Na]⁺ (2 %); **HPLC-Analysis (Method B)**: 99 %, $R_t = 21.1$ min.

(5Z)-5-[4-(benzyloxy)phenyl]methylidene-3-(prop-2-en-1-yl)-1,3-thiazolidine-2,4-dione **41k**
TLC $R_f = 0.6$ (Hexane/EtOAc 9:1); **Reaction time**: 16 h; **Purification**: Flash-Chromatography Hexane/EtOAc 95:5 ($R_f = 0.2$), loaded in DCM; **Yield**: 492 mg of white solid (1.40 mmol, 88 %); $^1\text{H-NMR}$ (400 MHz, CDCl_3) $\delta = 4.33$ (adt, 2 H, $^{3,4}J_{\text{H,H}} = 1.1, 1.4, 5.8$ Hz, CH₂), 5.11 (s, 2 H, CH₂Ar), 5.23 (ddd, 1 H, $^{3,4}J_{\text{H,H}} = 1.1, 1.2, 10.2$ Hz, CHH), 5.28 (ddd, 1 H, $^{3,4}J_{\text{H,H}} = 1.1, 1.4, 17.1$ Hz, CHH), 5.85 (ddt, 1 H, $^3J_{\text{H,H}} = 5.8, 10.2, 17.1$ Hz, Allyl-CH), 7.04 (d, 2 H, $^3J_{\text{H,H}} = 8.8$ Hz, 3,5-Ar-CH), 7.31-7.42 (m, 5 H, 5xAr-CH), 7.45 (d, 2 H, $^3J_{\text{H,H}} = 8.8$ Hz, 2,6-Ar-CH), 7.84 (s, 1 H, CH) ppm; $^{13}\text{C-NMR}$ (400 MHz, CDCl_3) $\delta = 43.8$ (CH₂CH), 70.3 (CH₂Ar), 115.7 (3,5-Ar-CH), 118.6 (Ar-C), 118.9 (Allyl-CH₂), 126.2 (Ar-C), 127.6 (2xAr-CH), 128.4 (Ar-CH), 128.8 (2xAr-CH), 130.4 (Allyl-CH), 132.4 (2,6-Ar-CH), 133.8 (CH), 136.2 (Ar-C), 160.7 (Ar-C), 166.2 (C=O), 167.7 (C=O) ppm; **ESI-MS** m/z (%) = 352.1 [M+H]⁺ (54 %), 369.1 [M+NH₄]⁺ (8 %), 720.2 [2M+NH₄]⁺ (17 %), 725.2 [2M+Na]⁺ (3 %); **HPLC-Analysis (Method B)**: 97 %, $R_t = 19.3$ min.

(5Z)-5-[3,4-bis(benzyloxy)phenyl]methylidene-3-(prop-2-en-1-yl)-1,3-thiazolidine-2,4-dione **41l**
TLC $R_f = 0.7$ (Hexane/EtOAc 8:2); **Reaction time**: 6 h; **Purification**: Flash-Chromatography DCM/CHCl₃ 9:1 ($R_f = 0.4$); **Yield**: 525 mg of white solid (1.15 mmol, 72 %); $^1\text{H-NMR}$ (400 MHz, CDCl_3) $\delta = 4.31$ (dt, 2 H, $^{3,4}J_{\text{H,H}} = 5.8, 1.2$ Hz, Allyl-CH₂), 5.21 (s, 2 H, CH₂Ar), 5.22 (s, 2 H, CH₂Ar), 5.20-5.24 (m, 1 H, CHHCH), 5.27 (ddd, 1 H, $^{3,4}J_{\text{H,H}} = 17.1, 2.5, 1.5$ Hz, CHH), 5.83 (ddt, 1 H, $^3J_{\text{H,H}} = 17.1, 10.3, 5.8$ Hz, Allyl-CH), 6.97 (d, 1 H, $^3J_{\text{H,H}} = 8.3$ Hz, 5-Ar-CH), 7.02 (d, 1 H, $^4J_{\text{H,H}} = 2.1$ Hz, 2-Ar-CH), 7.05 (dd, 1 H, $^{3,4}J_{\text{H,H}} = 8.3, 2.1$ Hz, 6-Ar-CH), 7.29-7.34 (m, 2 H, 2xAr-CH), 7.35-7.40 (m, 4 H, 4xAr-CH), 7.42-7.47 (m, 4 H, 4xAr-CH), 7.75 (s, 1 H, CH) ppm; $^{13}\text{C-NMR}$ (400 MHz, CDCl_3) $\delta = 43.9$ (Allyl-CH₂), 71.0 (CH₂Ar), 71.3 (CH₂Ar), 114.2 (5-Ar-CH), 115.9 (2-Ar-CH), 118.9 (CH-CH₂), 125.3 (6-Ar-CH), 126.5 (Ar-C), 127.2 (4xAr-CH), 127.3 (Ar-CH), 128.2 (4xAr-CH), 128.8 (Ar-C), 130.4 (Allyl-CH), 134.0 (CH), 136.5 (Ar-C), 136.6 (Ar-C), 148.9 (Ar-C), 151.2 (Ar-C), 166.1 (C=O), 167.7 (C=O) ppm; **HPLC-Analysis (Method B)**: 99 %, $R_t = 21.9$ min.

Synthesis of heterocyclic modification on N-allyl rhodanine and thiazolidine-2,4-dione derivatives; derivatives **43a–l**, **44a–b**, and **45a**

N-Allyl rhodanine **40** or the corresponding thiazolidine-2,4-dione derivative **41** and **42** (1.0 eq), the aldehyde (1.0-1.1 eq) and sodium acetate (1.0 eq) were dissolved in EtOH and stirred at 80 °C until TLC showed complete consumption of starting material. The products were purified

as stated below.

(Z)-3-allyl-5-(pyridin-2-ylmethylene)-2-thioxothiazolidin-4-one **43a**^[303]

TLC R_f = 0.7 (DCM); **Reaction time**: 4 h; **Purification**: Re-crystallisation from methanol; **Yield**: 155 mg of yellow crystals (0.59 mmol, 91 %); **¹H-NMR** (400 MHz, CDCl₃) δ = 4.75 (dt, 2 H, $^3J_{H,H}$ = 5.8, 1.4 Hz, CH₂), 5.24 (ddd, 1 H, $^3J_{H,H}$ = 10.3, 2.3, 1.2 Hz, CHH), 5.28 (ddd, 1 H, $^3J_{H,H}$ = 17.2, 2.6, 1.3 Hz, CHH), 5.87 (ddt, 1 H, $^3J_{H,H}$ = 17.2, 10.3, 5.8 Hz, CH), 7.28 (ddd, 1 H, $^3J_{H,H}$ = 7.7, 4.8, 1.0 Hz, 2-Pyr-CH), 7.54 (d(br), 1 H, $^3J_{H,H}$ = 7.7 Hz, 4-Pyr-CH), 7.62 (s, 1 H, CH), 7.77 (atd, 1 H, $^3J_{H,H}$ = 7.7, 1.8 Hz, 3-Pyr-CH), 8.77 (d(br), 1 H, $^3J_{H,H}$ = 4.8 Hz, 1-Pyr-CH) ppm; **¹H-NMR** (400 MHz, DMSO-d₆) δ = 4.65 (dt, 2 H, $^3J_{H,H}$ = 5.2, 1.6 Hz, CH₂), 5.11 (ddd, 1 H, $^3J_{H,H}$ = 17.2, 2.8, 1.6 Hz, E-Allyl-CH₂), 5.18 (ddd, 1 H, $^3J_{H,H}$ = 10.4, 2.8, 1.6 Hz, Z-Allyl-CH₂), 5.85 (ddt, 1 H, $^3J_{H,H}$ = 17.2, 10.4, 5.2 Hz, Allyl-CH), 7.46 (ddd, 1 H, $^3J_{H,H}$ = 6.9, 4.8, 2.2 Hz, 4-Ar-CH), 7.86 (s, 1 H, CH), 7.94-7.99 (m, 1 H, 5-Ar-CH), 7.94-8.00 (m, 1 H, 6-Ar-CH), 8.80-8.83 (m, 1 H, 3-Ar-CH) ppm; **¹³C-NMR** (400 MHz, CDCl₃) δ = 46.0 (CH₂), 119.2 (Allyl-CH₂), 123.6 (2-Pyr-CH), 127.5 (4-Pyr-CH), 128.0 (CH), 128.6 (Ar-C), 129.9 (Allyl-CH), 137.1 (3-Pyr-CH), 149.7 (1-Pyr-CH), 151.8 (Ar-C), 167.8 (C=O), 199.8 (C=S) ppm; **EI-MS** m/z (%) = 262.1 [M]⁺ (100 %), 247.1 [fragment]⁺ (65 %), 135.1 [fragment]⁺ (100 %); **HR-MS** m/z = 262.0231 [M]⁺ (calculated: 262.0235); **HPLC-Analysis (Method B)**: 99 %, R_t = 19.7 min.

(Z)-3-allyl-5-(pyridin-3-ylmethylene)-2-thioxothiazolidin-4-one **43b**^[303]

TLC R_f = 0.1 (DCM); **Reaction time**: 4 h; **Purification**: Re-crystallisation from ethanol; **Yield**: 75 mg of yellow crystals (0.29 mmol, 47 %); **¹H-NMR** (400 MHz, DMSO-d₆) δ = 4.65 (dt, 2 H, $^3J_{H,H}$ = 5.2, 1.6 Hz, CH₂), 5.15 (ddd, 1 H, $^3J_{H,H}$ = 17.2, 2.9, 1.7 Hz, E-Allyl-CH₂), 5.19 (ddd, 1 H, $^3J_{H,H}$ = 10.4, 2.7, 1.5 Hz, Z-Allyl-CH₂), 5.85 (ddt, 1 H, $^3J_{H,H}$ = 17.2, 10.4, 5.2 Hz, Allyl-CH), 7.59 (dddd, 1 H, $^3J_{H,H}$ = 8.0, 4.8, 0.8, 0.4 Hz, 4-Ar-CH), 7.89 (s, 1 H, CH), 8.01 (dddd, 1 H, $^3J_{H,H}$ = 8.0, 2.4, 1.6, 0.6 Hz, 3-Ar-CH), 8.66 (dd, 1 H, $^3J_{H,H}$ = 5.4, 1.6 Hz, 5-Ar-CH), 8.89-8.90 (m, 1 H, 1-Ar-CH) ppm; **¹H-NMR** (400 MHz, CDCl₃) δ = 4.75 (d, 2 H, $^3J_{H,H}$ = 5.9, 1.3 Hz, CH₂), 5.27 (ddd, 1 H, $^3J_{H,H}$ = 10.3, 2.2, 1.1 Hz, CHH), 5.31 (ddd, 1 H, $^3J_{H,H}$ = 17.2, 2.5, 1.4 Hz, CHH), 5.86 (ddt, 1 H, $^3J_{H,H}$ = 17.2, 10.3, 5.9 Hz, Allyl-CH), 7.48 (dd, 1 H, $^3J_{H,H}$ = 8.0, 4.9 Hz, 5-Pyr-CH), 7.71 (s, 1 H, CH), 7.82 (atd, 1 H, $^3J_{H,H}$ = 8.0, 2.2, 1.5 Hz, 4-Pyr-CH), 8.66 (dd, 1 H, $^3J_{H,H}$ = 4.9, 1.5 Hz, 6-Pyr-CH), 8.79 (d, 1 H, $^4J_{H,H}$ = 2.2 Hz, 2-Pyr-CH) ppm; **¹³C-NMR** (400 MHz, CDCl₃) δ = 46.7 (CH₂), 119.9 (Allyl-CH₂), 124.4 (5-Pyr-CH), 126.1 (Ar-C), 128.7 (CH), 129.4 (Allyl-CH), 129.8 (Ar-C), 136.9 (4-Pyr-CH), 150.4 (6-Pyr-CH), 151.4 (2-Pyr-CH), 167.2 (C=O), 191.8 (C=S) ppm; **ESI-MS** m/z (%) = 263.0 [M+H]⁺ (100 %); **HR-MS** m/z = 263.0310 [M+H]⁺ (calculated: 263.0307) **HPLC-Analysis (Method B)**: 98 %, R_t = 11.2 min.

(Z)-3-allyl-5-(pyridin-4-ylmethylene)thiazolidine-2,4-dione **43c**^[303]

TLC R_f = 0.3 (DCM); **Reaction time**: 2.5 h; **Purification**: Flash-Chromatography DCM (R_f = 0.3); **Yield**: 128 mg of yellow solid (0.49 mmol, 42 %); **Purification**: Re-crystallisation from ethanol;

Yield: 36 mg of orange crystals (0.14 mmol, 22 %); **¹H-NMR** (400 MHz, DMSO-*d*₆) δ = 4.65 (dt, 2 H, $^3J_{\text{H,H}}$ = 5.9, 1.3 Hz, CH₂), 5.15 (ddd, 1 H, $^3J_{\text{H,H}}$ = 17.5, 2.7, 1.3 Hz, E-Allyl-CH₂), 5.19 (ddd, 1 H, $^3J_{\text{H,H}}$ = 10.4, 2.7, 1.3 Hz, Z-Allyl-CH₂), 5.85 (ddt, 1 H, $^3J_{\text{H,H}}$ = 17.5, 10.4, 5.9 Hz, Allyl-CH), 7.59 (d, 2 H, $^3J_{\text{H,H}}$ = 5.6 Hz, 2,6-Ar-CH), 7.81 (s, 1 H, CH), 8.75 (d, 2 H, $^3J_{\text{H,H}}$ = 5.6 Hz, 3,5-Ar-CH) ppm; **¹H-NMR** (400 MHz, CDCl₃) δ = 4.75 (dt, 2 H, $^3J_{\text{H,H}}$ = 5.9, 1.3 Hz, CH₂), 5.26-5.35 (m, 2 H, Allyl-CH₂), 5.86 (ddt, 1 H, $^3J_{\text{H,H}}$ = 17.5, 10.4, 5.9 Hz, Allyl-CH), 7.36 (d, 2 H, $^3J_{\text{H,H}}$ = 5.6 Hz, 2,6-Pyr-CH), 7.62 (s, 1 H, CH), 8.76 (d, 2 H, $^3J_{\text{H,H}}$ = 5.6 Hz, 3,5-Pyr-CH) ppm; **¹³C-NMR** (400 MHz, CDCl₃) δ = 46.7 (CH₂), 120.0 (Allyl-CH₂), 123.8 (2,6-Pyr-CH), 128.6 (Allyl-CH), 129.2 (CH), 129.3 (Ar-C), 140.6 (Ar-C), 150.7 (3,5-Pyr-CH), 167.1 (C=O), 191.6 (C=S) ppm; **APCI-MS** m/z (%) = 263.0 [M+H]⁺ (100 %); **ESI-MS** m/z (%) = 263.0 [M+H]⁺ (100 %); **HR-MS** m/z = 263.0310 [M+H]⁺ (calculated: 263.0307); **HR-MS** m/z = 263.0306 [M+H]⁺ (calculated: 263.0307); **HPLC-Analysis (Method B)**: 97 %, R_f = 13.5 min.

(Z)-3-allyl-5-((2-chloropyridin-4-yl)methylene)-2-thioxothiazolidin-4-one **43d**

TLC R_f = 0.6 (DCM); **Reaction time:** 6 h; **Purification:** Re-crystallisation from ethanol; **Yield:** 75 mg of yellow solid (0.25 mmol, 44 %); **¹H-NMR** (400 MHz, CDCl₃) δ = 4.75 (dt, 2 H, $^3J_{\text{H,H}}$ = 5.9, 1.3 Hz, CH₂), 5.28 (ddd, 1 H, $^3J_{\text{H,H}}$ = 10.2, 2.3, 1.3 Hz, Z-Allyl-CH₂), 5.32 (ddd, 1 H, $^3J_{\text{H,H}}$ = 17.1, 2.3, 1.3 Hz, E-Allyl-CH₂), 5.85 (ddt, 1 H, $^3J_{\text{H,H}}$ = 17.1, 10.2, 5.9 Hz, Allyl-CH), 7.26 (ddd, 1 H, $^3J_{\text{H,H}}$ = 0.6, 1.6, 5.3 Hz, 4-Ar-CH), 7.38 (dd, 1 H, $^3J_{\text{H,H}}$ = 0.6, 1.6 Hz, 2-Ar-CH), 7.55 (0, 1 H, 1J = CH), 8.52 (d, 1 H, $^3J_{\text{H,H}}$ = 5.3 Hz, 5-Ar-CH) ppm; **ESI-MS** m/z (%) = 297.0 [M+H]⁺ (100 %); **HR-MS** m/z = 296.9921 [M+H]⁺ (calculated: 296.9918); **HPLC-Analysis** : 100 %, R_f = 34.4 min.

(Z)-3-allyl-5-((2-(benzylamino)pyridin-4-yl)methylene)-2-thioxothiazolidin-4-one **43f**

TLC R_f = 0.2 (CHCl₃/ EtOAc 9:1); **Reaction time:** 16 h; **Purification:** Flash-Chromatography CHCl₃/ EtOAc 9:1 (R_f = 0.2); **Yield:** 16 mg of orange solid (0.04 mmol, 54 %); **¹H-NMR** (400 MHz, CDCl₃) δ = 4.47 (d, 2 H, $^3J_{\text{H,H}}$ = 5.7 Hz, CH₂Ph), 4.64 (dt, 2 H, $^3J_{\text{H,H}}$ = 5.8, 1.3 Hz, CH₂), 5.18 (ddd, 1 H, $^3J_{\text{H,H}}$ = 10.2, 2.3, 1.3 Hz, Z-Allyl-CH₂), 5.22 (ddd, 1 H, $^3J_{\text{H,H}}$ = 17.1, 2.3, 1.3 Hz, E-Allyl-CH₂), 5.76 (ddt, 1 H, $^3J_{\text{H,H}}$ = 17.1, 10.2, 5.8 Hz, Allyl-CH), 7.18-7.33 (m, 6 H, 5xAr-CH), 7.41 (s, 1 H, CH), 8.12 (d, 1 H, $^3J_{\text{H,H}}$ = 5.4 Hz, 5-Ar-CH) ppm; **ESI-MS** m/z (%) = 368.1 [M+H]⁺ (100 %), 391.3 [M+Na]⁺ (10 %); **HR-MS** m/z = 368.0890 [M+H]⁺ (calculated: 368.0886); **HPLC-Analysis (Method B)**: 100 %, R_f = 20.5 min.

(Z)-3-allyl-5-((2-(4-methylbenzylamino)pyridin-4-yl)methylene)-2-thioxothiazolidin-4-one **43g**

TLC R_f = 0.4 (Hexane/EtOAc 6:4); **Reaction time:** 6 h; **Purification:** Flash-Chromatography hexane/EtOAc 8:2 (R_f = 0.2); **Yield:** 17 mg of yellow solid (0.04 mmol, 32 %); **¹H-NMR** (400 MHz, CDCl₃) δ = 2.35 (s, 3 H, CH₃), 4.49 (d, 2 H, $^3J_{\text{H,H}}$ = 5.7 Hz, Bn-CH₂), 4.72 (dt, 2 H, $^3J_{\text{H,H}}$ = 5.9, 1.3 Hz, CH₂), 5.15 (t(br), 1 H, $^3J_{\text{H,H}}$ = 5.7 Hz, NH₂), 5.26 (ddd, 1 H, $^3J_{\text{H,H}}$ = 10.3, 2.4, 1.2 Hz, CHH), 5.29 (ddd, 1 H, $^3J_{\text{H,H}}$ = 17.1, 2.4, 1.2 Hz, CHH), 5.84 (ddt, 1 H, $^3J_{\text{H,H}}$ = 17.1, 10.3, 5.9 Hz, CH), 6.32 (s, 1 H, 2-Pyr-CH), 6.63 (dd, 1 H, $^3J_{\text{H,H}}$ = 5.3, 1.2 Hz, 4-Pyr-CH),

7.17 (d, 2 H, $^3J_{\text{H,H}} = 8.0$ Hz, 2xAr-CH), 7.27 (d, 2 H, $^3J_{\text{H,H}} = 8.0$ Hz, 2x-Ar-CH), 7.49 (s, 1 H, CH), 8.19 (d, 1 H, $^3J_{\text{H,H}} = 5.3$ Hz, 5-Pyr-CH) ppm; $^{13}\text{C-NMR}$ (400 MHz, CDCl_3) $\delta = 21.3$ (CH_3), 46.4 (Allyl- CH_2), 46.6 (Bn- CH_2), 106.9 (2-Pyr-CH), 113.1 (4-Pyr-CH), 119.8 (Allyl- CH_2), 127.2 (Ar-C), 127.5 (2xAr-CH), 129.5 (Allyl-CH), 129.7 (2xAr-CH), 131.0 (CH), 135.4 (Ar-C), 137.4 (Ar-C), 141.8 (Ar-C), 149.6 (5-Pyr-CH), 159.4 (Ar-C), 167.3 ($\text{C}=\text{O}$), 192.5 ($\text{C}=\text{S}$), ppm; **ESI-MS** m/z (%) = 382.1 $[\text{M}+\text{H}]^+$ (100 %); **HR-MS** $m/z = 382.1046$ $[\text{M}+\text{H}]^+$ (calculated: 382.1042); **HPLC-Analysis (Method B)**: 99 %, $R_t = 19.1$ min.

(Z)-3-allyl-5-((2-(benzylamino)pyridin-4-yl)methylene)-2-thioxothiazolidin-4-one **43g**

TLC $R_f = 0.3$ (DCM/EtOAc 9:1); **Reaction time**: 6 h; **Purification**: Flash-Chromatography DCM/EtOAc 9:1 ($R_f = 0.3$); **Yield**: 8.0 mg of yellow solid (0.02 mmol, 70 %); $^1\text{H-NMR}$ (300 MHz, CDCl_3) $\delta = 2.35$ (s, 3 H, Ar- CH_3), 4.49 (d, 2 H, $^3J_{\text{H,H}} = 5.6$ Hz, CH_2Ar), 4.72 (dt, 2 H, $^3,4J_{\text{H,H}} = 5.8, 1.3$ Hz, CH_2), 5.23-5.32 (m, 2 H, E,Z-Allyl- CH_2), 5.77-5.91 (m, 1 H, Allyl-CH), 6.32 (s, 1 H, 2-Ar-CH), 6.62-6.65 (m, 1 H, 4-Ar-CH), 7.17 (d, 2 H, $^3J_{\text{H,H}} = 8.0$ Hz, 3',5'-Ar-CH), 7.27 (d, 2 H, $^3J_{\text{H,H}} = 8.0$ Hz, 2',6'-Ar-CH), 7.49 (s, 1 H, CH), 8.19 (d, 1 H, $^3J_{\text{H,H}} = 5.4$ Hz, 5-Ar-CH) ppm; **ESI-MS** m/z (%) = 382.1 $[\text{M}+\text{H}]^+$ (100 %), 763.2 $[2\text{M}+\text{H}]^+$ (10 %); **HR-MS** $m/z = 382.1043$ $[\text{M}+\text{H}]^+$ (calculated: 382.1042).

(5Z)-5-(3-[(4-methoxyphenyl)methoxy]phenylmethylidene)-3-(prop-2-en-1-yl)-2-sulfanylidene-1,3-thiazolidin-4-one **43i**

TLC $R_f = 0.7$ (Hexane/EtOAc 8:2); **Reaction time**: 4 h; **Purification**: Filtration from ethanol; **Yield**: 317 mg of yellow crystals (0.80 mmol, 90 %); $^1\text{H-NMR}$ (400 MHz, CDCl_3) $\delta = 3.83$ (s, 3 H, OCH_3), 4.74 (dt, 2 H, $^3,4J_{\text{H,H}} = 5.8, 1.3$ Hz, Allyl- CH_2), 5.05 (s, 2 H, CH_2Ar), 5.26 (ddd, 1 H, $^3,4J_{\text{H,H}} = 10.2, 2.3, 1.1$ Hz, CHH), 5.30 (ddd, 1 H, $^3,4J_{\text{H,H}} = 17.2, 2.5, 1.3$ Hz, CHH), 5.87 (ddt, 1 H, $^3J_{\text{H,H}} = 17.2, 10.2, 5.8$ Hz, Allyl-CH), 6.94 (d, 2 H, $^3J_{\text{H,H}} = 8.7$ Hz, 3',5'-Ar-CH), 7.04-7.08 (m, 2 H, 2,4-Ar-CH), 7.10 (d, 1 H, $^3J_{\text{H,H}} = 7.7$ Hz, 6-Ar-CH), 7.37 (d, 2 H, $^3J_{\text{H,H}} = 8.7$ Hz, 2',6'-Ar-CH), 7.39 (at, 1 H, $^3J_{\text{H,H}} = 7.7$ Hz, 5-Ar-CH), 7.69 (s, 1 H, CH) ppm; $^{13}\text{C-NMR}$ (400 MHz, CDCl_3) $\delta = 46.5$ (Allyl- CH_2), 55.5 (OCH_3), 70.2 (CH_2Ar), 114.3 (3',5'-Ar-CH), 116.2 (2-Ar-CH), 118.1 (4-Ar-CH), 119.6 (CH_2CH), 123.4 (Ar-C), 123.7 (6-Ar-CH), 128.4 (Ar-C), 129.4 (2',6'-Ar-CH), 129.6 (Allyl-CH), 130.5 (5-Ar-CH), 133.4 (CH) 134.7 (Ar-C), 159.5 (Ar-C), 159.8 (Ar-C), 167.6 ($\text{C}=\text{O}$), 193.1 ($\text{C}=\text{S}$) ppm; **ESI-MS** m/z (%) = 398.1 $[\text{M}+\text{H}]^+$ (5 %); **HPLC-Analysis (Method B)**: 99 %, $R_t = 22.6$ min.

(5Z)-5-[(3-[3-azido-5-(azidomethyl)phenyl]methoxyphenyl)methylidene]-3-(prop-2-en-1-yl)-2-sulfanylidene-1,3-thiazolidin-4-one **43j**

TLC $R_f = 0.7$ (DCM); **Reaction time**: 4 h; **Purification**: Flash-Chromatography Hexane/EtOAc 1:1 ($R_f = 0.2$); **Yield**: 260 mg of red solid (0.56 mmol, 66 %); $^1\text{H-NMR}$ (400 MHz, CDCl_3) $\delta = 4.39$ (s, 2 H, CH_2), 4.72 (dd, 2 H, $^3,4J_{\text{H,H}} = 1.0, 5.8$ Hz, Allyl- CH_2), 5.10 (s, 2 H, CH_2), 5.25 (d, 1 H, $^3J_{\text{H,H}} = 10.3$ Hz, Z-Allyl- CH_2), 5.29 (d, 1 H, $^3J_{\text{H,H}} = 17.3$ Hz, E-Allyl- CH_2), 5.85 (ddd, 1 H, $^3J_{\text{H,H}} = 5.8, 10.3, 17.3$ Hz, Allyl-CH), 6.95 (s, 1 H, Ar-CH), 6.99 (s, 1 H, Ar-CH), 7.05 (d,

1 H, $^3J_{\text{H,H}} = 8.3$ Hz, 4-Ar-CH), 7.06-7.08 (m, 1 H, 2-Ar-CH), 7.10 (d, 1 H, $^3J_{\text{H,H}} = 7.6$ Hz, 6-Ar-CH), 7.17 (s, 1 H, CH), 7.39 (at, 1 H, $^3J_{\text{H,H}} = 7.6, 8.3$ Hz, 5-Ar-CH), 7.65 (s, 1 H, CH) ppm; **HPLC-Analysis (Method B)**: 97 %, $R_f = 18.8$ min.

(5Z,5'Z)-5,5'-(1,4-phenylenebis(methan-1-yl-1-ylidene))bis(3-allyl-2-thioxothiazolidin-4-one) **43I**

Reaction time: 4 h; **Purification**: Re-crystallisation from ethanol; **Yield**: 41 mg of red crystals (0.09 mmol, 32 %); **$^1\text{H-NMR}$** (400 MHz, DMSO- d_6) $\delta = 4.65$ -4.68 (m, 4 H, CH₂), 5.12-5.22 (m, 4 H, E(Z)-Allyl-CH₂), 5.79-5.91 (m, 2 H, Allyl-CH), 7.82-7.84 (m, 3 H, CH₂ 2 x Ar-CH), 7.87-7.88 (m, 2 H, 2 x Ar-CH); **EI-MS** m/z (%) = 444.0 [M]⁺ (80 %), 429.0 [fragment]⁺ (70 %), 317.0 [fragment]⁺ (45 %), 221.0 [fragment]⁺ (65 %), 190.0 [fragment]⁺ (100 %); **HR-MS** $m/z = 444.0094$ [M]⁺ (calculated: 444.0095); **HPLC-Analysis (Method B)**: 64 %, $R_f = 23.9$ min.

(Z)-3-allyl-5-(pyridin-4-ylmethylene)thiazolidine-2,4-dione **44a**

TLC $R_f = 0.2$ (Toluene/EtOAc 7:3); **Reaction time**: 6 h; **Purification**: Flash-Chromatography toluene/EtOAc 7:3 ($R_f = 0.2$); **Yield**: 18 mg of white solid (0.07 mmol, 23 %); **$^1\text{H-NMR}$** (400 MHz, CDCl₃) $\delta = 4.36$ (dt, 2 H, $^3,4J_{\text{H,H}} = 6.0, 1.2$ Hz, CH₂), 5.27 (ddd, 1 H, $^3,4J_{\text{H,H}} = 10.3, 2.5, 1.3$ Hz, CHH), 5.31 (ddd, 1 H, $^3,4J_{\text{H,H}} = 17.1, 2.5, 1.3$ Hz, CHH), 5.85 (ddt, 1 H, $^3J_{\text{H,H}} = 17.1, 10.3, 6.0$ Hz, Allyl-CH), 7.34 (dd, 2 H, $^3,4J_{\text{H,H}} = 6.1, 1.6$ Hz, 2xPyr-CH), 7.79 (s, 1 H, CH), 8.74 (dd, 1 H, $^3,4J_{\text{H,H}} = 6.1, 1.6$ Hz, 2xPyr-CH) ppm; **$^{13}\text{C-NMR}$** (400 MHz, CDCl₃) $\delta = 44.3$ (CH₂), 119.6 (Allyl-CH₂), 123.5 (2xPyr-CH), 126.8 (Ar-C), 129.9 (Allyl-CH), 130.6 (CH), 140.4 (Ar-C), 150.9 (2xPyr-CH), 165.4 (C=O), 166.5 (C=O) ppm; **ESI-MS** m/z (%) = 247.1 [M+H]⁺ (100 %); **APCI-MS** m/z (%) = 247.1 [M+H]⁺ (100 %); **HR-MS** $m/z = 247.0533$ [M+H]⁺ (calculated: 247.0536); **HR-MS** $m/z = 247.0538$ [M+H]⁺ (calculated: 247.0536); **HPLC-Analysis** : 99.9 %, $R_f = 18.9$ min.

(Z)-3-(prop-2-yn-1-yl)-5-(pyridin-4-ylmethylene)thiazolidine-2,4-dione **44b**

TLC $R_f = 0.4$ (Hexane/EtOAc 1:1); **Reaction time**: 2 h; **Purification**: Re-crystallisation from ethanol; **Yield**: 40 mg of white crystals (0.16 mmol, 26 %); **$^1\text{H-NMR}$** (400 MHz, CDCl₃) $\delta = 2.29$ (t, 1 H, $^4J_{\text{H,H}} = 2.5$ Hz, CCH), 4.51 (d, 2 H, $^4J_{\text{H,H}} = 2.5$ Hz, CH₂), 7.34 (d, 2 H, $^3J_{\text{H,H}} = 5.6$ Hz, 2,6-Pyr-CH), 7.83 (s, 1 H, CH), 8.74 (d, 2 H, $^3J_{\text{H,H}} = 5.6$ Hz, 3,5-Pyr-CH) ppm; **$^{13}\text{C-NMR}$** (400 MHz, CDCl₃) $\delta = 31.1$ (CH₂), 72.7 (CCH), 75.8 (CCH), 123.4 (2,6-Pyr-CH), 126.3 (Ar-C), 131.3 (CH), 140.2 (Ar-C), 151.0 (3,5-Pyr-CH), 164.6 (C=O), 165.8 (C=O) ppm;

9.11 Reduction of compound 41h

Compound **41h** (124 mg, 0.47 mmol) was dissolved in 20 mL dioxane. Pd/C (300 mg, 2.02 mmol) was added and the hydrogenation was carried out under 30 psi H₂ atmosphere. After H₂ pressure stabilisation, the reaction mixture was filtered through celite and washed with EtOAc. The crude was purified by flash column chromatography (CHCl₃/EtOAc 100:5, R_f 0.2). The product was afforded as a white solid (130 mg, 0.49 mmol).

5-[(4-hydroxyphenyl)methyl]-3-propyl-1,3-thiazolidine-2,4-dione **46a**

TLC R_f = 0.1 (CHCl₃/EtOAc 100:5); **Reaction time**: 16 h; **Purification**: Flash-Chromatography CHCl₃/EtOAc 100:5 (R_f = 0.1); **Yield**: 130 mg of white solid (0.49 mmol, 100 %); **¹H-NMR** (400 MHz, CDCl₃) δ = 0.80 (t, 3 H, $^3J_{H,H}$ = 7.4 Hz, γ -CH₃), 1.51 (tq, 2 H, $^3J_{H,H}$ = 7.4, 7.2 Hz, β -CH₂), 3.07 (dd, 1 H, $^{2,3}J_{H,H}$ = 8.9, 14.1 Hz, cis-CHH), 3.39 (dd, 1 H, $^{2,3}J_{H,H}$ = 3.9, 14.1 Hz, anti-CHH), 3.50 (td, 2 H, $^{2,3}J_{H,H}$ = 3.5, 7.2 Hz, α -CH₂), 4.41 (dd, 1 H, $^3J_{H,H}$ = 3.9, 8.9 Hz, CH), 6.25 (s(br), 1 H, OH), 6.77 (d, 2 H, $^3J_{H,H}$ = 8.5 Hz, 2,6-Ar-CH), 7.06 (d, 2 H, $^3J_{H,H}$ = 8.5 Hz, 3,5-Ar-CH) ppm; **¹³C-NMR** (400 MHz, CDCl₃) δ = 11.1 (CH₃), 20.9 (β -CH₂), 37.8 (CH₂), 43.5 (α -CH₂), 51.7 (CH), 115.7 (2,6-Ar-CH), 127.3 (Ar-C), 130.8 (3,5-Ar-CH), 155.5 (Ar-C), 171.8 (C=O), 174.5 (C=O) ppm; **ESI-MS** m/z (%) = 264.1 [M-H]⁻ (85 %), 529.1 [2M-H]⁻ (100 %); **HR-MS** m/z = 264.0702 [M-H]⁻ (calculated: 264.0700); **HPLC-Analysis (Method B)**: 98 %, R_t = 16.6 min.

9.12 Synthesis of derivatives **36a–ag**, **48a–v**, **54a–ab**, and **55a–z**

The starting rhodanine or thiazolidine-2,4-dione **36**, **48**, **54**, and **55** (1.0 eq), the corresponding aldehyde (1.1–1.5 eq) and sodium acetate (1.0 eq) were dissolved in methanol or ethanol (5–10 mL). The reaction mixture was stirred at 80 °C until TLC showed complete consumption of starting material. The products were afforded after filtration, re-crystallisation or column chromatography as stated below.

(Z)-5-benzylidene-2-thioxothiazolidin-4-one **36b**^[304]

TLC R_f = 0.1 (DCM); **Reaction time**: 2 h; **Purification**: Filtration from methanol; **Yield**: 43 mg of yellow solid (0.19 mmol, 25 %); **¹H-NMR** (400 MHz, DMSO-d₆) δ = 7.48–7.64 (m, 5 H, 5 x Ar-CH), 7.67 (s, 1 H, CH) ppm; **¹³C-NMR** (400 MHz, DMSO-d₆) δ = 129.5 (Ar-CH), 130.5 (Ar-CH), 131.3 (Ar-C), 131.6 (CH), 133.0 (Ar-C), 202.5 (C=S) ppm; **EI-MS** m/z (%) = 221.0 [M]⁺ (100 %), 134.0 [fragment]⁺ (100 %). **HR-MS** m/z = 220.9962 [M]⁺ (calculated: 220.9969); **HPLC-Analysis (Method B)**: 100 %, R_t = 18.2 min.

(Z)-5-(2-methylbenzylidene)-2-thioxothiazolidin-4-one **36c**^[305]

TLC R_f = 0.1 (DCM); **Reaction time**: 4 h; **Purification**: Filtration from methanol; **Yield**: 41 mg of yellow solid (0.17 mmol, 23 %); **¹H-NMR** (400 MHz, DMSO-d₆) δ = 2.42 (s, 3 H, CH₃), 7.34–7.42 (m, 4 H, 4 x Ar-CH), 7.74 (s, 1 H, CH) ppm; **¹³C-NMR** (400 MHz, DMSO-d₆) δ = 19.4 (CH₃), 126.9 (Ar-CH), 127.6 (Ar-CH), 129.3 (CH), 130.7 (Ar-CH), 131.1 (Ar-CH), 132.0 (Ar-C), 139.1 (Ar-C), 169.1 (Ar-C), 196.1 (C=O), 206.5 (C=S) ppm; **EI-MS** m/z (%) = 235.1 [M]⁺ (100 %), 221.1 [fragment]⁺ (65 %), 147.1 [fragment]⁺ (100 %); **HR-MS** m/z = 235.0122 [M]⁺ (calculated: 235.0126); **HPLC-Analysis (Method B)**: 98 %, R_t = 17.1 min.

(5Z)-5-[(3-methylphenyl)methylidene]-2-sulfanylidene-1,3-thiazolidin-4-one **36d**^[295]

TLC R_f = 0.1 (Hexane/EtOAc 8:2); **Reaction time**: 16 h; **Purification**: Flash-Chromatography

Hexane/EtOAc 8:2 ($R_f = 0.1$); **Yield**: 400 mg of yellow solid (1.70 mmol, 90 %); **$^1\text{H-NMR}$** (400 MHz, DMSO- d_6) $\delta = 2.37$ (s, 3 H, CH_3), 7.33 (d, 1 H, $^3J_{\text{H,H}} = 7.1$ Hz, Ar-CH), 7.38-7.46 (m, 3 H, 3xAr-CH), 7.60 (s, 1 H, CH) ppm; **$^{13}\text{C-NMR}$** (400 MHz, DMSO- d_6) $\delta = 20.9$ (CH_3), 125.4 (Ar-C), 127.7 (Ar-CH), 129.4 (Ar-CH), 130.9 (Ar-CH), 131.6 (Ar-CH), 131.8 (CH), 133.0 (Ar-C), 138.9 (Ar-C), 169.4 (C=O), 195.8 (C=S) ppm; **APCI-MS** m/z (%) = 236.0 $[\text{M}+\text{H}]^+$ (100 %); **HR-MS** $m/z = 236.0199$ $[\text{M}+\text{H}]^+$ (calculated: 236.0198); **HPLC-Analysis (Method B)**: 93 %, $R_t = 19.4$ min.

(5Z)-5-[(4-methylphenyl)methylidene]-2-sulfanylidene-1,3-thiazolidin-4-one **36e**^[268]

TLC $R_f = 0.2$ (Hexane/EtOAc 8:2); **Reaction time**: 12 h; **Purification**: Flash-Chromatography Hexane/EtOAc 8:2 ($R_f = 0.2$), dry loaded on SiO_2 ; **Yield**: 380 mg of yellow solid (1.61 mmol, 86 %); **$^1\text{H-NMR}$** (400 MHz, DMSO- d_6) $\delta = 2.35$ (s, 3 H, CH), 7.33 (d, 2 H, $^3J_{\text{H,H}} = 8.2$ Hz, 3,5-Ar-CH), 7.47 (d, 2 H, $^3J_{\text{H,H}} = 8.2$ Hz, 2,6-Ar-CH), 7.58 (s, 1 H, CH) ppm; **$^{13}\text{C-NMR}$** (400 MHz, DMSO- d_6) $\delta = 21.2$ (CH_3), 124.4 (Ar-C), 130.1 (3,5-Ar-CH), 130.3 (Ar-C), 130.6 (2,6-Ar-CH), 131.7 (CH), 141.2 (Ar-C), 169.6 (C=O), 195.7 (C=S) ppm; **ESI-MS** m/z (%) = 236.0 $[\text{M}+\text{H}]^+$ (7 %), 253.0 $[\text{M}+\text{NH}_4]^+$ (3 %), 488.1 $[2\text{M}+\text{NH}_4]^+$ (3 %), 493.0 $[2\text{M}+\text{Na}]^+$ (2 %); **HPLC-Analysis (Method B)**: 99 %, $R_t = 21.9$ min.

(Z)-2-thioxo-5-(2-(trifluoromethyl)benzylidene)thiazolidin-4-one **36f**^[306]

TLC $R_f = 0.1$ (DCM); **Reaction time**: 4 h; **Purification**: Filtration from methanol; **Yield**: 205 mg of yellow solid (0.71 mmol, 73 %); **$^1\text{H-NMR}$** (400 MHz, DMSO- d_6) $\delta = 7.65$ -7.73 (m, 3 H, 2,3-Ar-CH, CH), 7.86 (t, 1 H, $^3J_{\text{H,H}} = 7.7$ Hz, 4-Ar-CH), 7.91 (d, 1 H, $^3J_{\text{H,H}} = 7.7$ Hz, 5-Ar-CH), 14.01 (s(br), 1 H, NH) ppm; **$^{13}\text{C-NMR}$** (400 MHz, DMSO- d_6) $\delta = 125.4$ (Ar-C), 126.9 (q, $^3J_{\text{C,F}} = 5.6$ Hz, 5-Ar-CH), 127.8 (q, $^2J_{\text{C,F}} = 29.8$ Hz, 6-Ar- CCF_3), 129.4 (Ar-CH), 130.6 (Ar-CH), 131.0 (Ar-C), 131.2 (CH), 133.6 (4-Ar-CH), 168.9 (C=O), 195.7 (C=S) ppm; **EI-MS** m/z (%) = 289.0 $[\text{M}]^+$ (100 %), 202.0 $[\text{fragment}]^+$ (60 %), 85.1 $[\text{fragment}]^+$ (70 %), 71.1 $[\text{fragment}]^+$ (90 %), 57.0 $[\text{fragment}]^+$ (100 %); **HR-MS** $m/z = 288.9831$ $[\text{M}]^+$ (calculated: 288.9843); **HPLC-Analysis** : 100 %, $R_t = 32.6$ min;

(5Z)-2-sulfanylidene-5-[3-(trifluoromethyl)phenyl]methylidene-1,3-thiazolidin-4-one **36g**^[307]

TLC $R_f = 0.1$ (DCM); **Reaction time**: 4 h; **Purification**: Flash-Chromatography DCM ($R_f = 0.1$); **Yield**: 113 mg of yellow solid (0.39 mmol, 42 %); **$^1\text{H-NMR}$** (400 MHz, DMSO- d_6) $\delta = 7.76$ (s, 1 H, CH), 7.76-7.80 (m, 1 H, 5-Ar-CH), 7.85 (d, 2 H, $^3J_{\text{H,H}} = 7.8$ Hz, 4,6-Ar-CH), 8.00 (s, 1 H, 2-Ar-CH), 13.95 (s(br), 1 H, NH); **$^{13}\text{C-NMR}$** (400 MHz, DMSO- d_6) $\delta = 123.8$ (q, $^1J_{\text{C,F}} = 272.5$ Hz, CF_3), 126.7 (q, $^3J_{\text{C,F}} = 3.7$ Hz, 4-Ar-CH), 127.3 (q, $^3J_{\text{C,F}} = 3.9$ Hz, 2-Ar-CH), 128.0 (Ar-C), 129.5 (CH), 130.0 (q, $^2J_{\text{C,F}} = 32.3$ Hz, 3-Ar- CCF_3), 130.6 (5-Ar-CH), 133.1 (6-Ar-CH), 134.2 (Ar-C), 169.6 (C=O), 195.5 (C=S) ppm; **$^1\text{H-NMR}$** (400 MHz, CDCl_3) $\delta = 7.61$ -7.66 (m, 2 H, 2xAr-CH), 7.68 (s, 1 H, CH), 7.69-7.73 (m, 2 H, 2xAr-CH), 9.59 (s(br), 1 H, NH) ppm; **EI-MS** m/z (%) = 289.0 $[\text{M}]^+$ (100 %), 202.0 $[\text{fragment}]^+$ (100 %); **HR-MS** $m/z = 288.9834$ $[\text{M}]^+$ (calculated: 288.9843); **HPLC-Analysis** : 98 %, $R_t = 34.1$ min.

(5Z)-2-sulfanylidene-5-[4-(trifluoromethyl)phenyl]methylidene-1,3-thiazolidin-4-one **36h**^[308]

TLC $R_f = 0.1$ (DCM); **Reaction time**: 4 h; **Purification**: Flash-Chromatography DCM ($R_f = 0.1$); **Yield**: 82 mg of yellow solid (0.28 mmol, 37 %); **¹H-NMR** (400 MHz, CDCl₃) $\delta = 7.59$ (d, 2 H, ³ $J_{H,H} = 8.2$ Hz, 2xAr-CH), 7.66 (s, 1 H, CH), 7.75 (d, 2 H, ³ $J_{H,H} = 8.2$ Hz, 2xAr-CH), 9.30 (s(br), 1 H, NH) ppm; **¹H-NMR** (400 MHz, DMSO-d₆) $\delta = 7.71$ (s, 1 H, CH), 7.81 (d, 2 H, ³ $J_{H,H} = 8.3$ Hz, 2,6-Ar-CH), 7.88 (d, 2 H, ³ $J_{H,H} = 8.3$ Hz, 3,5-Ar-CH), 13.95 (s(br), 1 H, NH) ppm; **¹³C-NMR** (400 MHz, DMSO-d₆) $\delta = 123.9$ (q, ¹ $J_{C,F} = 272.4$ Hz, CF₃), 126.2 (q, ³ $J_{C,F} = 3.7$ Hz, 2,6-Ar-H), 128.6 (Ar-C), 129.5 (CH), 129.8 (q, ² $J_{C,F} = 32.2$ Hz, Ar-CCF₃), 130.9 (3,5-Ar-CH), 136.9 (Ar-C), 169.3 (C=O), 195.5 (C=S) ppm; **EI-MS** m/z (%) = 289.0 [M]⁺ (100 %), 202.0 [fragment]⁺ (100 %); **HR-MS** $m/z = 288.9834$ [M]⁺ (calculated: 288.9843); **HPLC-Analysis (Method B)**: 98 %, $R_t = 21.7$ min.

(Z)-5-(4-chlorobenzylidene)-2-thioxothiazolidin-4-one **36i**^[268]

TLC $R_f = 0.3$ (DCM); **Reaction time**: 3 h; **Purification**: Flash-Chromatography DCM ($R_f = 0.3$); **Yield**: 61 mg of yellow solid (0.24 mmol, 63 %); **¹H-NMR** (400 MHz, CDCl₃) $\delta = 7.41$ (d, 2 H, ³ $J_{H,H} = 8.5$ Hz, 3,5-Ar-CH), 7.47 (d, 2 H, ³ $J_{H,H} = 8.5$ Hz, 2,6-Ar-CH), 7.61 (s, 1 H, CH), 9.13 (s(br), 1 H, NH) ppm; **ESI-MS** m/z (%) = 254.0 [M-H]⁻ (100 %); **HR-MS** $m/z = 253.9504$ [M-H]⁻ (calculated: 253.9507); **HPLC-Analysis**: 99.9 %, $R_t = 34.3$ min.

mixture of Z to E 5:1 (Z)-4-((4-oxo-2-thioxothiazolidin-5-ylidene)methyl)benzonitrile **36j**^[296]

Reaction time: 16 h; **Purification**: Filtration from methanol; **Yield**: 28 mg of yellow solid (0.11 mmol, 30 %); **¹H-NMR** (400 MHz, DMSO-d₆) $\delta = 7.56$ (s, 1 H, E-CH), 7.70 (s, 1 H, Z-CH), 7.78 (d, 2 H, ³ $J_{H,H} = 8.4$ Hz, Z-3,5-Ar-CH), 7.89 (d, 2 H, ³ $J_{H,H} = 8.4$ Hz, E-3,5-Ar-CH), 7.99 (d, 2 H, ³ $J_{H,H} = 8.4$ Hz, Z-2,6-Ar-CH), 8.03 (d, 2 H, ³ $J_{H,H} = 8.4$ Hz, E-2,6-Ar-CH), 13.94 (s(br), 1 H, NH) ppm; **¹³C-NMR** (400 MHz, DMSO-d₆) $\delta = 111.9$ (Ar-C), 112.2 (Ar-C), 118.4 (Ar-C), 129.1 (Z-CH), 129.4 (Ar-C), 130.8 (Z-3,5-Ar-CH), 131.3 (E-2,6-Ar-CH), 131.9 (E-3,5-Ar-CH), 133.1 (Z-2,6-Ar-CH), 133.7 (E-CH), 137.4 (Ar-C), 169.5 (C=O), 195.4 (C=S) ppm; **EI-MS** m/z (%) = 246 [M]⁺ (100 %), 202.0 [fragment]⁺ (30 %), 159.0 [fragment]⁺ (100 %); **HR-MS** $m/z = 245.9914$ [M]⁺ (calculated: 245.9916); **HPLC-Analysis (Method B)**: 97 %, $R_t = 18.7$ min.

(Z)-5-(3-bromo-4-fluorobenzylidene)-2-thioxothiazolidin-4-one **36k**

TLC $R_f = 0.2$ (DCM); **Reaction time**: 4 h; **Purification**: Filtration from methanol; **Yield**: 84 mg of yellow solid (0.26 mmol, 24 %); **¹H-NMR** (400 MHz, DMSO-d₆) $\delta = 7.51$ (s, 1 H, CH), 7.54 (t, 1 H, ³ $J_{H,H(F)} = 8.6$ Hz, 5-Ar-CH), 7.61 (ddd, 1 H, ^{3,4} $J_{H,H(F)} = 8.6, 4.7, 2.2$ Hz, 6-Ar-CH), 7.96 (dd, 1 H, ⁴ $J_{H,F(H)} = 6.7, 2.2$ Hz, 2-Ar-CH) ppm; **¹³C-NMR** (400 MHz, DMSO-d₆) $\delta = 109.0$ (d, ³ $J_{C,F} = 21.7$ Hz, 3-Ar-C), 117.6 (d, ³ $J_{C,F} = 23.1$ Hz, 5-Ar-CH), 125.7 (CH), 129.1 (Ar-C), 130.8 (d, $J_{C,F} = 8.1$ Hz, 6-Ar-CH), 132.4 (Ar-C), 135.2 (2-Ar-CH), 158.5 (d, ¹ $J_{C,F} = 250.3$ Hz, 4-Ar-CF), 181.6 (C=O), 198.1 (C=S) ppm; **EI-MS** m/z (%) = 318.9 [M]⁺ (100 %), 231.9 [fragment]⁺ (100 %), 151.0 [fragment]⁺ (40 %), 107.0 [fragment]⁺ (70 %); **HR-MS** $m/z = 316.8978$ [M]⁺ (calculated: 316.8980); **HPLC-Analysis (Method B)**: 100 %, $R_t = 32.6$ min.

(Z)-5-(3-bromo-4-methoxybenzylidene)-2-thioxothiazolidin-4-one **36l**^[309]

TLC R_f = 0.5 (DCM); **Reaction time**: 3 h; **Purification**: Filtration from methanol; **Yield**: 20 mg of yellow solid (0.06 mmol, 16 %); **¹H-NMR** (400 MHz, DMSO- d_6) δ = 3.93 (s, 3 H, OCH₃), 7.30 (d, 1 H, $^3J_{H,H}$ = 8.8 Hz, 4-Ar-CH), 7.60 (dd, 1 H, $^{3,4}J_{H,H}$ = 2.3, 8.8 Hz, 3-Ar-CH), 7.61 (s, 1 H, CH), 7.88 (d, 1 H, $^4J_{H,H}$ = 2.3 Hz, 6-Ar-CH) ppm; **EI-MS** m/z (%) = 330.9 [M]⁺ (100 %), 243.9 [fragment]⁺ (100 %), 228.9 [fragment]⁺ (50 %); **HR-MS** m/z = 328.9177 [M]⁺ (calculated: 328.9180); **HPLC-Analysis (Method B)**: 99 %, R_t = 18.3 min.

(Z)-N-(4-((4-oxo-2-thioxothiazolidin-5-ylidene)methyl)phenyl)acetamide **36m**^[310]

TLC R_f = 0.1 (DCM); **Reaction time**: 2 h; **Purification**: Filtration from methanol; **Yield**: 23 mg of yellow solid (0.08 mmol, 22 %); **¹H-NMR** (400 MHz, DMSO- d_6) δ = 2.08 (s, 3 H, CH₃), 7.56 (d, 2 H, $^3J_{H,H}$ = 8.7 Hz, 3,5-Ar-CH), 7.57 (s, 1 H, CH), 7.75 (d, 2 H, $^3J_{H,H}$ = 8.7 Hz, 2,6-Ar-CH), 10.31 (s(br), 1 H, NHAc) ppm; **EI-MS** m/z (%) = 278.0 [M]⁺ (100 %), 191.0 [fragment]⁺ (60 %), 149.0 [fragment]⁺ (95 %); **HR-MS** m/z = 278.0180 [M]⁺ (calculated: 278.0184); **HPLC-Analysis**: 99 %, R_t = 37.6 min.

(Z)-5-(4-(dimethylamino)benzylidene)-2-thioxothiazolidin-4-one **36n**^[268]

TLC R_f = 0.6 (DCM/EtOAc 9:1); **Reaction time**: 5 h; **Purification**: Filtration from methanol; **Yield**: 10 mg of red solid (0.04 mmol, 10 %); **¹H-NMR** (400 MHz, DMSO- d_6) δ = 3.04 (s, 6 H, N(CH₃)₂), 6.83 (d, 2 H, $^3J_{H,H}$ = 8.8 Hz, 3,5-Ar-CH), 7.44 (d, 2 H, $^3J_{H,H}$ = 8.8 Hz, 2,6-Ar-CH), 7.53 (s, 1 H, CH) ppm; **ESI-MS** m/z (%) = 265.0 [M+H]⁺ (100 %), 529.1 [2M+H]⁺ (30 %); **HR-MS** m/z = 265.0468 [M+H]⁺ (calculated: 265.0464); **HPLC-Analysis (Method B)**: 86 %, R_t = 18.6 min.

(Z)-5-(3-nitrobenzylidene)-2-thioxothiazolidin-4-one **36o**^[268]

Z to E 10:1 ratio; **Reaction time**: 3 h; **Purification**: Filtration from methanol; **Yield**: 35 mg of yellow solid (0.13 mmol, 35 %); **¹H-NMR** (400 MHz, DMSO- d_6) δ = 7.61 (s, 1 H, E-CH), 7.71 (at, 1 H, $^3J_{H,H}$ = 8.2, 7.9 Hz, E-5-Ar-CH), 7.79 (s, 1 H, Z-CH), 7.82 (at, 1 H, $^3J_{H,H}$ = 8.2, 7.9 Hz, Z-5-Ar-CH), 7.99 (d, 1 H, $^3J_{H,H}$ = 7.9 Hz, Z-6-Ar-CH), 8.21 (d, 1 H, $^3J_{H,H}$ = 7.9 Hz, E-6-Ar-CH), 8.25 (dd, 1 H, $^{3,4}J_{H,H}$ = 8.2, 2.1 Hz, E-4-Ar-CH), 8.30 (dd, 1 H, $^{3,4}J_{H,H}$ = 8.2, 2.1 Hz, Z-4-Ar-CH), 8.43 (at, 1 H, $^4J_{H,H}$ = 2.1 Hz, Z-2-Ar-CH), 8.91 (at, 1 H, $^4J_{H,H}$ = 2.1 Hz, Z-2-Ar-CH), 13.95 (s(br), 1 H, NH) ppm; **¹³C-NMR** (400 MHz, DMSO- d_6) δ = 124.7 (4-Ar-CH), 124.8 (2-Ar-CH), 128.6 (Ar-C), 129.0 (CH) 131.0 (5-Ar-CH), 134.7 (Ar-C), 135.7 (6-Ar-CH), 148.3 (Ar-C), 169.2 (C=O), 195.2 (C=S) ppm; **EI-MS** m/z (%) = 266.0 [M]⁺ (100 %), 179.0 [fragment]⁺ (100 %), 133.0 [fragment]⁺ (35 %), 89.0 [fragment]⁺ (40 %); **HR-MS** m/z = 265.9813 [M]⁺ (calculated: 265.9820); **HPLC-Analysis (Method B)**: 94 %, R_t = 17.6 min.

(Z)-5-(4-(methylsulfonyl)benzylidene)-2-thioxothiazolidin-4-one **36p**^[309]

TLC R_f = 0.4 (DCM/EtOAc 9:1); **Reaction time**: 6 h; **Purification**: Re-crystallisation from ethanol; **Yield**: 14 mg of yellow crystals (0.05 mmol, 12 %); **¹H-NMR** (400 MHz, DMSO- d_6) δ = 3.28 (s, 3 H, SO₂CH₃), 7.73 (s, 1 H, CH), 7.86 (d, 2 H, $^3J_{H,H}$ = 8.5 Hz, 3,5-Ar-CH), 8.05

(d, 2 H, $^3J_{\text{H,H}} = 8.5 \text{ Hz}$, 2,6-Ar-CH) ppm; **ESI-MS** m/z (%) = 317.0 $[\text{M}+\text{NH}_4]^+$ (100 %); **HR-MS** $m/z = 317.0087$ $[\text{M}+\text{NH}_4]^+$ (calculated: 317.0083); **HPLC-Analysis (Method B)**: 99 %, $R_t = 19.8 \text{ min}$.

(Z)-4-((4-oxo-2-thioxothiazolidin-5-ylidene)methyl)benzaldehyde **36q**^[311]

Reaction time: 3 h; **Purification**: Filtration from methanol; **Yield**: 30 mg of red solid (0.12 mmol, 32 %); **$^1\text{H-NMR}$** (400 MHz, DMSO- d_6) $\delta = 7.67$ (s, 1 H, CH), 7.81 (d, 2 H, $^3J_{\text{H,H}} = 8.0 \text{ Hz}$, 3,5-Ar-CH), 8.03 (d, 2 H, $^3J_{\text{H,H}} = 8.0 \text{ Hz}$, 2,6-Ar-CH) ppm; **APCI-MS** m/z (%) = 245.0 $[\text{M}+\text{H}]^+$ (100 %); **HR-MS** $m/z = 249.9991$ $[\text{M}+\text{H}]^+$ (calculated: 249.9995); **HPLC-Analysis (Method B)**: 97 %, $R_t = 16.1 \text{ min}$.

(Z)-5-(2-hydroxybenzylidene)-2-thioxothiazolidin-4-one **36r**^[268]

TLC $R_f = 0.3$ (DCM/EtOAc 9:1); **Reaction time**: 4 h; **Purification**: Filtration from H₂O; **Yield**: 60 mg of yellow solid (0.25 mmol, 67 %); **$^1\text{H-NMR}$** (400 MHz, CD₃OD) $\delta = 6.87$ -6.98 (m, 2 H, 2xAr-CH), 7.27-7.35 (m, 2 H, 2xAr-CH), 8.00 (s, 1 H, CH) ppm; **$^1\text{H-NMR}$** (400 MHz, DMSO- d_6) $\delta = 6.93$ -6.98 (m, 2 H, 2xAr-CH), 7.29-7.35 (m, 2 H, 2xAr-CH), 7.84 (s, 1 H, CH), 10.65 (s(br), 1 H, OH), 13.74 (s(br), 1 H, NH) ppm; **$^{13}\text{C-NMR}$** (400 MHz, DMSO- d_6) $\delta = 116.2$ (Ar-CH), 120.0 (Ar-CH), 124.3 (Ar-C), 126.9 (CH), 129.2 (Ar-CH), 132.7 (Ar-CH), 157.5 (C=O), 196.3 (C=S) ppm; **ESI-MS** m/z (%) = 236.0 $[\text{M}-\text{H}]^-$ (100 %); **HR-MS** $m/z = 235.9840$ $[\text{M}-\text{H}]^-$ (calculated: 235.9845); **HPLC-Analysis**: 99.9 %, $R_t = 30.6 \text{ min}$.

(5Z)-5-[(3-hydroxyphenyl)methylidene]-2-sulfanylidene-1,3-thiazolidin-4-one **36s**^[312]

TLC $R_f = 0.6$ (DCM/MeOH 9:1); **Reaction time**: 3 h; **Purification**: Flash-Chromatography DCM \rightarrow DCM/MeOH 9:1 ($R_f = 0.1, 0.6$); **Yield**: 102 mg of yellow solid (0.43 mmol, 68 %); **$^1\text{H-NMR}$** (400 MHz, MeOD) $\delta = 6.84$ (dd, 1 H, $^3,^4J_{\text{H,H}} = 8.1, 2.3 \text{ Hz}$, 4-Ar-CH), 6.89-6.91 (m, 1 H, 2-Ar-CH), 6.96 (d, 1 H, $^3J_{\text{H,H}} = 7.6 \text{ Hz}$, 6-Ar-CH), 7.27 (at, 1 H, $^3J_{\text{H,H}} = 8.1, 7.6$ (7.9) Hz, 5-Ar-CH), 7.47 (s, 1 H, CH) ppm; **$^1\text{H-NMR}$** (400 MHz, DMSO- d_6) $\delta = 6.89$ (dd, 1 H, $^3,^4J_{\text{H,H}} = 8.1, 2.4 \text{ Hz}$, 4-Ar-CH), 6.97 (at, 1 H, $^4J_{\text{H,H}} = 1.9 \text{ Hz}$, 2-Ar-CH), 7.05 (d, 1 H, $^3J_{\text{H,H}} = 7.7 \text{ Hz}$, 6-Ar-CH), 7.33 (at, 1 H, $^3J_{\text{H,H}} = 8.1, 7.7$ (7.9) Hz, 5-Ar-CH), 7.53 (s, 1 H, CH), 9.87 (s(br), 1 H, OH), 13.82 (s(br), 1 H, NH) ppm; **$^{13}\text{C-NMR}$** (400 MHz, DMSO- d_6) $\delta = 116.2$ (2-Ar-CH), 118.1 (4-Ar-CH), 121.9 (5-Ar-CH), 125.4 (Ar-C), 130.5 (5-Ar-CH), 131.8 (CH), 134.2 (Ar-C), 158.0 (Ar-C), 169.5 (C=O), 195.9 (C=S) ppm; **EI-MS** m/z (%) = 237.1 $[\text{M}]^+$ (100 %), 150.2 [fragment]⁺ (80 %), 121.2 [fragment]⁺ (40 %), 59.2 [fragment]⁺ (100 %); **ESI-MS** m/z (%) = 236.0 $[\text{M}-\text{H}]^-$ (100 %); 238.0 $[\text{M}+\text{H}]^+$ (80 %), 260.0 $[\text{M}+\text{Na}]^+$ (30 %), 734.0 $[\text{3M}+\text{Na}]^+$ (100 %); **ESI-MS** m/z (%) = 236.0 $[\text{M}-\text{H}]^-$ (100 %); **HR-MS** $m/z = 235.9843$ $[\text{M}-\text{H}]^-$ (calculated: 235.9845). **HR-MS** $m/z = 236.9913$ $[\text{M}]^+$ (calculated: 236.9918). **HR-MS** $m/z = 237.9981$ $[\text{M}+\text{H}]^+$ (calculated: 237.9991); **HR-MS** $m/z = 235.9843$ $[\text{M}-\text{H}]^-$ (calculated: 235.9845); **HPLC-Analysis (Method B)**: 26.3 %, $R_t = 100 \text{ min}$.

(Z)-5-(4-hydroxybenzylidene)-2-thioxothiazolidin-4-one **36t**^[268]

Reaction time: 2 h; **Purification**: Filtration from methanol; **Yield**: 51 mg of yellow solid (0.21

mmol, 25 %); **¹H-NMR** (400 MHz, DMSO-*d*₆) δ = 6.93 (d, 2 H, $^3J_{\text{H,H}}$ = 8.5 Hz, 3,5-Ar-CH), 7.47 (d, 2 H, $^3J_{\text{H,H}}$ = 8.5 Hz, 2,6-Ar-CH), 7.57 (s, 1 H, CH), 10.43 (s(br), 1 H, OH), 13.70 (s(br), 1 H, NH) ppm; **¹³C-NMR** (400 MHz, DMSO-*d*₆) δ = 116.6 (3,5-Ar-CH), 120.9 (Ar-C), 124.0 (Ar-C), 132.5 (CH), 133.1 (2,6-Ar-CH), 160.4 (Ar-C), 169.5 (C=O), 195.6 (C=S) ppm; **ESI-MS** m/z (%) = 238.0 [M+H]⁺ (100 %), 497.0 [2M+Na]⁺ (95 %), 734.0 [3M+Na]⁺ (100 %), 971.0 [4M+Na]⁺ (15 %); **HPLC-Analysis** : 97 %, R_t = 28.3 min; **EI-MS** m/z (%) = 237.2 [M]⁺ (100 %), 150.1 [fragment]⁺ (100 %), 121.2 [fragment]⁺ (50 %), 59.2 [fragment]⁺ (100 %); **HR-MS** m/z = 236.9913 [M]⁺ (calculated: 236.9918); **HR-MS** m/z = 237.9981 [M+H]⁺ (calculated: 237.9991); **HPLC-Analysis (Method B)**: 100 %, R_t = 18.2 min.

(Z)-5-(2,4-dihydroxybenzylidene)-2-thioxothiazolidin-4-one **36u**^[268]

TLC R_f = 0.1 (DCM/EtOAc 9:1); **Reaction time**: 2.5 h; **Purification**: Filtration from methanol; **Yield**: 14 mg of red solid (0.06 mmol, 15 %); **¹H-NMR** (400 MHz, CD₃OD) δ = 6.35 (d, 1 H, $^4J_{\text{H,H}}$ = 2.4 Hz, 2-Ar-CH), 6.42 (dd, 1 H, $^3,4J_{\text{H,H}}$ = 2.4, 8.6 Hz, 4-Ar-CH), 7.18 (d, 1 H, $^3J_{\text{H,H}}$ = 8.6 Hz, 5-Ar-CH), 7.97 (s, 1 H, CH) ppm; **EI-MS** m/z (%) = 253.0 [M]⁺ (100 %); **HPLC-Analysis (Method B)**: 99 %, R_t = 21.2 min.

(5Z)-5-[(3,4-dihydroxyphenyl)methylidene]-2-sulfanylidene-1,3-thiazolidin-4-one **36a**^[93]

TLC R_f = 0.7 (DCM/MeOH 9:1); **Reaction time**: 16 h; **Purification**: Filtration from methanol; **Yield**: 15 mg of yellow solid (0.06 mmol, 14 %); **¹H-NMR** (400 MHz, DMSO-*d*₆) δ = 6.88 (d, 1 H, $^3J_{\text{H,H}}$ = 8.8 Hz, 5-Ar-CH), 6.97-7.01 (m, 2 H, 2,6-Ar-CH), 7.47 (s, 1 H, CH), 9.54 (s(br), 1 H, OH), 9.96 (s(br), 1 H, OH), 13.67 (s(br), 1 H, NH) ppm; **¹³C-NMR** (400 MHz, DMSO-*d*₆) δ = 116.5 (5-Ar-CH), 116.6 (2- or 6-Ar-CH), 120.8 (Ar-C), 124.4 (Ar-C), 124.9 (2- or 6-Ar-CH), 132.8 (CH), 146.1 (Ar-C), 149.2 (Ar-C), 169.7 (C=O), 195.7 (C=S) ppm; **EI-MS** m/z (%) = 253.0 [M]⁺ (100 %), 166.0 [fragment]⁺ (100 %). **HR-MS** m/z = 252.9859 [M]⁺ (calculated: 252.9867); **HPLC-Analysis (Method B)**: 99 %, R_t = 21.0 min.

(5Z)-5-[(4-hydroxy-3,5-dimethoxyphenyl)methylidene]-2-sulfanylidene-1,3-thiazolidin-4-one **36v**^[313]

TLC R_f = 0.5 (DCM/EtOAc 9:1); **Reaction time**: 4 h; **Purification**: Filtration from ethanol; **Yield**: 460 mg of yellow solid (1.55 mmol, 93 %); **¹H-NMR** (400 MHz, DMSO-*d*₆) δ = 3.81 (s, 6 H, 2xOCH₃), 6.80 (s, 2 H, 2,6-Ar-CH), 7.16 (s, 1 H, CH), 9.00 (s(br), 1 H, NH) ppm; **¹³C-NMR** (400 MHz, DMSO-*d*₆) δ = 56.0 (2xOCH₃), 107.4 (2,6-Ar-CH), 125.4 (CH), 131.5 (Ar-C), 136.9 (Ar-C), 148.1 (2xAr-C), 182.6 (C=O), 201.9 (C=S) ppm; **ESI-MS** m/z (%) = 298.0 [M+H]⁺ (100 %), 320.0 [M+Na]⁺ (75 %), 617.0 [2M+Na]⁺ (100 %); **HR-MS** m/z = 298.0207 [M+H]⁺ (calculated: 298.0202); **HPLC-Analysis (Method B)**: 98 %, R_t = 15.5 min.

4-[(5Z)-4-oxo-2-sulfanylidene-1,3-thiazolidin-5-ylidene]methylbenzaldehyde **104**^[311]

Reaction time: 3 h; **Purification**: Filtration from EtOH; **Yield**: 30 mg of red solid (0.12 mmol, 32 %); **ESI-MS** m/z (%) = 250.0 [M+H]⁺ (100 %); **HR-MS** m/z = 249.9995 [M+H]⁺ (calculated: 249.9991).

(Z)-5-(3-(benzyloxy)benzylidene)-2-thioxothiazolidin-4-one **36w**^[110]

TLC R_f = 0.2 (DCM); **Reaction time**: 2 h; **Purification**: Re-crystallisation from methanol; **Yield**: 160 mg of yellow crystals (0.49 mmol, 44 %); **$^1\text{H-NMR}$** (400 MHz, DMSO- d_6) δ = 5.18 (s, 2 H, OCH₂), 7.08-7.24 (m, 3 H, 3xAr-CH), 7.29-7.53 (m, 7 H, 7xAr-CH), 7.62 (s, 1 H, CH), 13.84 (s(br), 1 H, NH) ppm; **$^{13}\text{C-NMR}$** (400 MHz, DMSO- d_6) δ = 69.40 (CH₂), 116.4 (Ar-CH), 117.6 (Ar-CH), 122.7 (Ar-CH), 125.9 (Ar-C), 127.8 (2xAr-CH), 128.0 (Ar-CH), 128.5 (2xAr-CH), 130.6 (Ar-CH), 131.5 (CH), 134.3 (Ar-C), 136.7 (Ar-C), 158.8 (Ar-C), 169.3 (C=O), 195.7 (C=S) ppm; **ESI-MS** m/z (%) = 328.1 [M+H]⁺ (25 %), 350.0 [M+Na]⁺ (15 %), **HR-MS** m/z = 328.0460 [M+H]⁺ (calculated: 328.0460); **HPLC-Analysis (Method B)**: 99 %, R_t = 21.4 min.

(Z)-5-(4-(benzyloxy)benzylidene)-2-thioxothiazolidin-4-one **36y**^[110]

TLC R_f = 0.2 (DCM); **Reaction time**: 2 h; **Purification**: Filtration from methanol; **Yield**: 123 mg of yellow solid (0.38 mmol, 41 %); **$^1\text{H-NMR}$** (400 MHz, DMSO- d_6) δ = 5.20 (s, 2 H, OCH₂), 7.19 (d, 2 H, $^3J_{\text{H,H}}$ = 8.9 Hz, 3,5-Ar-CH), 7.32-7.48 (m, 5 H, 5xAr-CH), 7.58 (d, 2 H, $^3J_{\text{H,H}}$ = 8.9 Hz, 2,6-Ar-CH), 7.62 (s, 1 H, CH); **$^{13}\text{C-NMR}$** (400 MHz, DMSO- d_6) δ = 69.6 (CH₂), 115.9 (3,5-Ar-CH), 122.5 (Ar-C), 125.7 (Ar-C), 127.8 (2xAr-CH), 128.1 (Ar-CH), 128.5 (2xAr-CH), 131.7 (CH), 132.7 (2,6-Ar-CH), 136.4 (Ar-C), 160.4 (Ar-C), 169.6 (C=O), 195.6 (C=S) ppm; **ESI-MS** m/z (%) = 328.0 [M+H]⁺ (100 %), 345.1 [M+NH₄]⁺ (50 %), 350.0 [M+Na]⁺ (55 %), 672.1 [2M+NH₄]⁺ (25 %), 677.1 [2M+Na]⁺ (25 %), 999.2 [3M+NH₄]⁺ (15 %); **HR-MS** m/z = 328.0464 [M+H]⁺ (calculated: 328.0460); **HPLC-Analysis (Method B)**: 85 %, R_t = 20.6 min.

(Z)-5-(3,4-bis(benzyloxy)benzylidene)-2-thioxothiazolidin-4-one **36z**^[314]

TLC R_f = 0.3 (Hexane/DCM 2:8); **Reaction time**: 4 h; **Purification**: Flash-Chromatography Hexane/DCM 2:8 (R_f = 0.3); **Yield**: 38 mg of yellow solid (0.09 mmol, 23 %); **$^1\text{H-NMR}$** (400 MHz, CDCl₃) δ = 5.24 (d, 4 H, $^2J_{\text{H,H}}$ = 6.8 Hz, 2xCH₂), 6.98 (s, 1 H, 1-Ar-CH), 6.99 (d, 1 H, $^3J_{\text{H,H}}$ = 8.1 Hz, 3-Ar-CH), 7.05 (d, 1 H, $^3J_{\text{H,H}}$ = 8.1 Hz, 4-Ar-CH), 7.31-7.49 (m, 10 H, 10xAr-CH), 7.52 (s, 1 H, CH), 9.33 (s(br), 1 H, NH) ppm; **$^{13}\text{C-NMR}$** (300 MHz, CDCl₃) δ = 70.9 (CH₂), 71.2 (CH₂), 114.1 (Ar-C or Ar-CH), 115.8 (Ar-C or Ar-CH), 126.0 (Ar-C or Ar-CH), 127.1 (Ar-C or Ar-CH), 127.2 (Ar-C or Ar-CH), 128.1 (Ar-C or Ar-CH), 128.2 (Ar-C or Ar-CH), 128.7 (Ar-C or Ar-CH), 133.7 (CH) ppm; **ESI-MS** m/z (%) = 434.1 [M+H]⁺ (60 %), 451.1 [M+NH₄]⁺ (100 %); **HR-MS** m/z = 451.1144 [M]^{+NH₄} (calculated: 451.1145); **HPLC-Analysis (Method B)**: 99 %, R_t = 22.0 min.

(5Z)-5-(phenylmethylidene)-1,3-thiazolidine-2,4- dione **48o**^[315]

TLC R_f = 0.4 (Toluene/EtOAc 8:2); **Reaction time**: 16 h; **Purification**: Re-crystallisation from ethanol; **Yield**: 81 mg of white crystals (0.39 mmol, 42 %); **$^1\text{H-NMR}$** (400 MHz, MeOD) δ = 7.29-7.59 (m, 5 H,), 7.90-7.951m0Ar-CH ppm; **$^1\text{H-NMR}$** (400 MHz, DMSO- d_6) δ = 7.29 (s, 1 H, CH), 7.42 (at, 2 H, $^3J_{\text{H,H}}$ = 7.7 Hz, 2xAr-CH), 7.52 (d, 2 H, $^3J_{\text{H,H}}$ = 7.6 Hz, 2xAr-CH), 7.87-7.92 (m, 1 H, Ar-CH) ppm; **$^{13}\text{C-NMR}$** (400 MHz, DMSO- d_6) δ = 122.0 (Ar-CH), 127.5 (CH) 127.7 (Ar-CH), 128.7 (Ar-CH), 129.0 (Ar-CH), 129.1 (Ar-CH), 135.9 (Ar-C), 136.4 (Ar-C), 175.6 (C=O), 182.9 (C=O) ppm; **EI-MS** m/z (%) = 205.0 [M]⁺ (100 %), 133.9 [fragment]⁺

(100 %); **HR-MS** m/z = 205.0192 $[M]^+$ (calculated: 205.0192); **HPLC-Analysis** : 100 %, R_t = 29.9 min;

(Z)-5-(2-methylbenzylidene)thiazolidine-2,4-dione **48a**^[316]

Reaction time: 16 h; **Purification**: Re-crystallisation from Ethanol/PE; **Yield**: 37 mg of white crystals (0.17 mmol, 31 %); **¹H-NMR** (400 MHz, $CDCl_3$) δ = 2.45 (s, 3 H, Ar-CH₃), 7.27-7.36 (m, 3 H, 3xAr-CH), 7.42-7.45 (m, 1 H, 6-Ar-CH), 8.07 (s, 1 H, CH) ppm; **¹H-NMR** (400 MHz, DMSO- d_6) δ = 2.39 (s, 3 H, CH₃), 7.32-7.38 (m, 3 H, 3xAr-CH), 7.39-7.43 (m, 1 H, Ar-CH), 7.89 (s, 1 H, CH), 12.63 (s(br), 1 H, NH) ppm; **¹³C-NMR** (400 MHz, DMSO- d_6) δ = 19.4 (CH₃), 125.2 (Ar-C), 126.6 (Ar-CH), 127.1 (Ar-CH), 129.6 (CH), 130.3 (Ar-CH), 131.0 (Ar-CH), 132.1 (Ar-C), 138.7 (Ar-C) 167.1 (C=O), 168.2 (C=O) ppm; **ESI-MS** m/z (%) = 237.1 $[M+NH_4]^+$ (100 %), 456.1 $[2M+NH_4]^+$ (25 %); **HR-MS** m/z = 237.0692 $[M+NH_4]^+$ (calculated: 237.0692); **HPLC-Analysis (Method B)**: 96 %, R_t = 30.2 min.

(Z)-5-(3-methylbenzylidene)thiazolidine-2,4-dione **48b**^[317]

Reaction time: 16 h; **Purification**: Re-crystallisation from PE; **Yield**: 58 mg of white crystals (0.26 mmol, 45 %); **¹H-NMR** (400 MHz, $CDCl_3$) δ = 2.41 (s, 3 H, Ar-CH₃), 7.25-7.41 (m, 4 H, 4xAr-CH), 7.84 (s, 1 H, CH), 8.45 (s(br), 1 H, NH) ppm; **ESI-MS** m/z (%) = 237.1 $[M+NH_4]^+$ (100 %), 456.1 $[2M+NH_4]^+$ (50 %), 675.1 $[3M+NH_4]^+$ (10 %); **HR-MS** m/z = 237.0696 $[M+NH_4]^+$ (calculated: 237.0692); **HPLC-Analysis** : 92 %, R_t = 30.7 min.

(Z)-5-(4-methylbenzylidene)thiazolidine-2,4-dione **48c**^[318]

TLC R_f = 0.5 (DCM/EtOAc 9:1); **Reaction time**: 16 h; **Purification**: Filtration from ethanol; **Yield**: 37 mg of white solid (0.17 mmol, 24 %); **¹H-NMR** (400 MHz, CD_3OD) δ = 2.31 (s, 3 H, Ar-CH₃), 7.22 (d, 2 H, $^3J_{H,H}$ = 8.1 Hz, 2,6-Ar-CH), 7.38 (d, 2 H, $^3J_{H,H}$ = 8.1 Hz, 3,5-Ar-CH), 7.54 (s, 1 H, CH) ppm; **ESI-MS** m/z (%) = 237.1 $[M+NH_4]^+$ (100 %), 242.0 $[M+Na]^+$ (10 %), 456.1 $[2M+NH_4]^+$ (50 %), 461.1 $[2M+Na]^+$ (30 %); **HR-MS** m/z = 237.0694 $[M+NH_4]^+$ (calculated: 237.0692); **HPLC-Analysis** : 99.9 %, R_t = 31.1 min; **HPLC-Analysis (Method B)**: 99 %, R_t = 12.4 min.

(Z)-5-(2-(trifluoromethyl)benzylidene)thiazolidine-2,4-dione **48d**

TLC R_f = 0.2 ($CHCl_3$ /EtOAc 9:1); **Reaction time**: 4 h; **Purification**: Re-crystallisation from petroleum ether; **Yield**: 20 mg of white solid (0.07 mmol, 16 %); **¹H-NMR** (400 MHz, $CDCl_3$) δ = 7.55 (at, 1 H, $^3J_{H,H}$ = 7.6 Hz, Ar-CH), 7.61 (d, 1 H, $^3J_{H,H}$ = 7.6 Hz, Ar-CH), 7.64-7.69 (m, 1 H, Ar-CH), 7.79 (d, 1 H, $^3J_{H,H}$ = 7.9 Hz, 6-Ar-CH), 8.13 (s, 1 H, CH), 8.23 (s(br), 1 H, NH) ppm; **¹H-NMR** (400 MHz, DMSO- d_6) δ = 7.65-7.74 (m, 2 H, 2xAr-CH), 7.82-7.88 (m, 2 H, Ar-CH, CH), 7.90 (d, 1 H, $^3J_{H,H}$ = 7.8 Hz, 3-Ar-CH), 12.83 (s(br), 1 H, NH) ppm; **¹³C-NMR** (400 MHz, DMSO- d_6) δ = 123.9 (q, $^1J_{C,F}$ = 273.9 Hz, CF₃), 126.1 (Ar-CH), 126.8 (q, $^3J_{C,F}$ = 5.6 Hz, 3-Ar-CH), 127.6 (Ar-C), 127.8 (Ar-C), 129.0 (Ar-CH), 130.4 (Ar-CH), 131.4 (Ar-C), 133.5 (CH), 166.8 (C=O), 167.6 (C=O) ppm; **APCI-MS** m/z (%) = 274.0 $[M+H]^+$ (100 %); **HR-MS** m/z = 274.0144 $[M+H]^+$ (calculated: 274.0139); **HPLC-Analysis** : 96 %, R_t = 30.2 min.

(Z)-5-(3-(trifluoromethyl)benzylidene)thiazolidine-2,4-dione **48e**^[317]

TLC R_f = 0.2 (CHCl₃/EtOAc 9:1); **Reaction time**: 6.5 h; **Purification**: Flash-Chromatography DCM/EtOAc 9:1 (R_f = 0.4); **Yield**: 58 mg of white solid (0.21 mmol, 45 %); **¹H-NMR** (400 MHz, CDCl₃) δ = 7.61-7.72 (m, 3 H, 3xAr-CH), 7.74 (s, 1 H, CH), 7.87 (s, 1 H, 2-CH) ppm; **¹H-NMR** (400 MHz, DMSO-d₆) δ = 7.70-7.85 (m, 3 H, 3xAr-CH), 7.87 (s, 1 H, 2-Ar-CH), 7.93 (s, 1 H, CH) 12.71 (s(br), 1 H, NH) ppm; **¹³C-NMR** (400 MHz, DMSO-d₆) δ = 123.8 (q, ¹J_{C,F} = 272.5 Hz, CF₃), 125.9 (Ar-CH), 126.7 (q, ³J_{C,F} = 32.9 Hz, 2-Ar-CH), 130.0 (q, J_{C,F} = 32.1 Hz, 4-Ar-C), 130.0 (CH), 130.5 (Ar-CH), 132.8 (Ar-CH) 134.2 (Ar-C), 167.1 (C=O), 167.5 (C=O) ppm; **APCI-MS** m/z (%) = 274.0 [M+H]⁺ (100 %), 547.0 [2M+H]⁺ (15 %); **HR-MS** m/z = 274.0144 [M+H]⁺ (calculated: 274.0141); **HPLC-Analysis (Method B)**: 100 %, R_t = 20.4 min.

(Z)-5-(4-(trifluoromethyl)benzylidene)thiazolidine-2,4-dione **48f**^[317]

Reaction time: 16 h; **Purification**: Re-crystallisation from PE; **Yield**: 23 mg of white crystals (0.08 mmol, 15 %); **¹H-NMR** (400 MHz, CDCl₃) δ = 7.61 (d, 2 H, ³J_{H,H} = 8.2 Hz, 3,5-Ar-CH), 7.74 (d, 2 H, ³J_{H,H} = 8.2 Hz, 2,6-Ar-CH), 7.87 (s, 1 H, CH), 8.37 (s(br), 1 H, NH) ppm; **¹H-NMR** (400 MHz, DMSO-d₆) δ = 7.81 (d, 2 H, ³J_{H,H} = 8.2 Hz, 3,5-Ar-CH), 7.87 (s, 1 H, CH), 7.89 (d, 2 H, ³J_{H,H} = 8.2 Hz, 2,6-Ar-CH), 12.76 (s(br), 1 H, NH) ppm; **¹³C-NMR** (400 MHz, DMSO-d₆) δ = 123.9 (q, ¹J_{C,F} = 272.4 Hz, CF₃), 126.1 (q, ³J_{C,F} = 3.9 Hz, 2,6-Ar-CH), 126.7 (Ar-C), 129.5 (Ar-C), 129.8 (CH), 130.5 (3,5-Ar-CH), 137.1 (Ar-C), 167.2 (C=O), 167.6 (C=O) ppm; **APCI-MS** m/z (%) = 274.0 [M+H]⁺ (100 %); **HR-MS** m/z = 274.0147 [M+H]⁺ (calculated: 274.0144); **HR-MS** m/z = 274.0143 [M+H]⁺ (calculated: 274.0144); **HPLC-Analysis** : 99.9 %, R_t = 32.0 min.

(Z)-5-(2-hydroxybenzylidene)thiazolidine-2,4-dione **48g**^[319]

TLC R_f = 0.1 (DCM/EtOAc 9:1); **Reaction time**: 16 h; **Purification**: Filtration from DCM; **Yield**: 50 mg of white solid (0.23 mmol, 38 %); **¹H-NMR** (400 MHz, CD₃OD) δ = 6.83 (dd, 1 H, ^{3,4}J_{H,H} = 1.2, 8.2 Hz, 3-Ar-CH), 6.88 (ddd, 1 H, ^{3,4}J_{H,H} = 1.2, 7.4, 8.2 Hz, 5-Ar-CH), 7.22 (ddd, 1 H, ^{3,4}J_{H,H} = 1.6, 7.4, 8.2 Hz, 4-Ar-CH), 7.34 (dd, 1 H, ^{3,4}J_{H,H} = 1.6, 8.2 Hz, 6-Ar-CH) 8.13 (s, 1 H, CH) ppm; **¹H-NMR** (400 MHz, DMSO-d₆) δ = 6.92-6.99 (m, 2 H, 2xAr-CH), 7.28-7.35 (m, 2 H, 2xAr-CH), 8.02 (s, 1 H, CH), 10.51 (s, 1 H, OH), 12.51 (s(br), 1 H, NH) ppm; **¹³C-NMR** (400 MHz, DMSO-d₆) δ = 116.1 (Ar-CH), 119.7 (Ar-CH), 119.9 (Ar-C), 121.9 (Ar-C), 127.0 (CH), 128.3 (Ar-CH), 132.3 (Ar-CH) 157.3 (Ar-C), 167.5 (C=O), 168.2 (C=S) ppm; **APCI-MS** m/z (%) = 222.0 [M+H]⁺ (100 %), 239.0 [M+NH₄]⁺ (5 %); **HR-MS** m/z = 222.0213 [M+H]⁺ (calculated: 222.0219); **HPLC-Analysis (Method B)**: 99 %, R_t = 13.0 min.

(Z)-5-(3-hydroxybenzylidene)thiazolidine-2,4-dione **48h**^[320]

TLC R_f = 0.3 (DCM/EtOAc 9:1); **Reaction time**: 16 h; **Purification**: Filtration from ethanol; **Yield**: 38 mg of white solid (0.17 mmol, 31 %); **¹H-NMR** (400 MHz, CD₃OD) δ = 6.76 (dd, 1 H, ^{3,4}J_{H,H} = 8.2, 2.4 Hz, 4-Ar-CH), 6.92-6.94 (m, 1 H, 2-Ar-CH), 6.96 (d, 1 H, ³J_{H,H} = 7.8 Hz, 6-Ar-CH), 7.21 (at, 1 H, ³J_{H,H} = 7.8 Hz, 5-Ar-CH), 7.50 (s, 1 H, CH) ppm; **¹H-NMR** (400 MHz, DMSO-d₆) δ = 6.79 (dd, 1 H, ^{3,4}J_{H,H} = 8.2, 2.4 Hz, 4-Ar-CH), 6.95-6.97 (m, 1 H, 2-Ar-CH), 6.98

(d, 1 H, $^3J_{\text{H,H}} = 7.8$ Hz, 6-Ar-CH), 7.26 (at, 1 H, $^3J_{\text{H,H}} = 7.8$ Hz, 5-Ar-CH), 7.43 (s, 1 H, CH), 9.68 (s(br), 1 H, NH) ppm; $^{13}\text{C-NMR}$ (400 MHz, DMSO- d_6) $\delta = 115.6$ (2-Ar-CH), 116.4 (4-Ar-CH), 120.9 (6-Ar-CH), 127.2 (CH), 130.0 (5-Ar-CH), 135.7 (Ar-C), 157.7 (Ar-C), 172.0 (C=O), 175.2 (C=O) ppm; **APCI-MS** m/z (%) = 222.0 $[\text{M}+\text{H}]^+$ (100 %); **HR-MS** $m/z = 222.0216$ $[\text{M}+\text{H}]^+$ (calculated: 222.0219); **HPLC-Analysis (Method B)**: 99 %, $R_t = 13.0$ min.

(Z)-5-(4-hydroxybenzylidene)thiazolidine-2,4-dione **48i**^[321]

Reaction time: 16 h; **Purification**: Filtration from ethanol; **Yield**: 19 mg of white solid (0.09 mmol, 15 %); $^1\text{H-NMR}$ (400 MHz, CD_3OD) $\delta = 6.81$ (d, 2 H, $^3J_{\text{H,H}} = 8.6$ Hz, 3,5-Ar-CH), 7.35 (d, 2 H, $^3J_{\text{H,H}} = 8.6$ Hz, 2,6-Ar-CH), 7.52 (s, 1 H, CH) ppm; **APCI-MS** m/z (%) = 222.0 $[\text{M}+\text{H}]^+$ (100 %), 239.0 $[\text{M}+\text{NH}_4]^+$ (5 %); **HR-MS** $m/z = 222.0216$ $[\text{M}+\text{H}]^+$ (calculated: 222.0219); **HPLC-Analysis (Method B)**: 99 %, $R_t = 12.4$ min.

(5Z)-5-[(3,4-dihydroxyphenyl)methylidene]-1,3-thiazolidine-2,4-dione **48p**^[322]

TLC $R_f = 0.2$ ($\text{CHCl}_3/\text{MeOH}$ 95:5); **Reaction time**: 16 h; **Purification**: Flash-Chromatography $\text{CHCl}_3/\text{MeOH}$ 95:5 ($R_f = 0.2$); **Yield**: 502 mg of white solid (2.12 mmol, 46 %); $^1\text{H-NMR}$ (400 MHz, DMSO- d_6) $\delta = 6.76$ (d, 1 H, $^3J_{\text{H,H}} = 8.2$ Hz, 5-Ar-CH), 6.81 (dd, 1 H, $^3J_{\text{H,H}} = 1.9, 8.2$ Hz, 6-Ar-CH), 6.96 (d, 1 H, $^4J_{\text{H,H}} = 1.9$ Hz, 2-Ar-CH), 7.11 (s, 1 H, CH) ppm; $^{13}\text{C-NMR}$ (400 MHz, DMSO- d_6) $\delta = 115.8$ (2,5-Ar-CH), 121.8 (6-Ar-CH), 123.1 (CH), 127.2 (Ar-C), 132.1 (Ar-C), 145.3 (Ar-C), 145.9 (Ar-C), 176.0 (C=O), 182.9 (C=O) ppm; **ESI-MS** m/z (%) = 236.0 $[\text{M}-\text{H}]^-$ (100 %), 473.0 $[2\text{M}-\text{H}]^-$ (60 %); **HR-MS** $m/z = 236.0023$ $[\text{M}-\text{H}]^-$ (calculated: 236.0023).

(5Z)-5-[(4-hydroxy-3,5-dimethoxyphenyl)methylidene]-1,3-thiazolidine-2,4-dione **48k**^[322]

TLC $R_f = 0.4$ (DCM/EtOAc 9:1); **Reaction time**: 4 h; **Purification**: Filtration from ethanol; **Yield**: 130 mg of white solid (0.46 mmol, 47 %); $^1\text{H-NMR}$ (400 MHz, DMSO- d_6) $\delta = 3.78$ (s, 6 H, $2\times\text{OCH}_3$), 6.82 (s, 2 H, 2,6-Ar-CH), 7.21 (s, 1 H, CH), 8.72 (s(br), 1 H, NH) ppm; $^{13}\text{C-NMR}$ (400 MHz, DMSO- d_6) $\delta = 55.9$ ($2\times\text{OCH}_3$), 106.8 (2,6-Ar-CH), 123.2 (CH), 126.4 (Ar-C), 133.0 (Ar-C), 135.9 (Ar-C), 148.0 ($2\times\text{Ar-C}$), 175.8 (C=O), 183.1 (C=O) ppm; **HPLC-Analysis (Method B)**: 99 %, $R_t = 12.7$ min.

(Z)-5-(3-(benzyloxy)benzylidene)thiazolidine-2,4-dione **48l**^[323]

TLC $R_f = 0.4$ (DCM/EtOAc 9:1); **Reaction time**: 7 h; **Purification**: Filtration from ethanol; **Yield**: 290 mg of white solid (0.93 mmol, 76 %); $^1\text{H-NMR}$ (400 MHz, CD_3OD) $\delta = 5.08$ (s, 2 H, CH_2), 6.95-6.98 (m, 1 H, Ar-CH), 7.06-7.09 (m, 2 H, $2\times\text{Ar-CH}$), 7.22-7.34 (m, 4 H, $4\times\text{Ar-CH}$), 7.38-7.41 (m, 2 H, $2\times\text{Ar-CH}$), 7.52 (s, 1 H, CH) ppm; $^1\text{H-NMR}$ (400 MHz, DMSO- d_6) $\delta = 5.14$ (s, 2 H, CH_2), 6.99 (dd, 1 H, $^3J_{\text{H,H}} = 8.2, 2.5$ Hz, 4-Ar-CH), 7.12 (d, 1 H, $^3J_{\text{H,H}} = 7.7$ Hz, 6-Ar-CH), 7.15-7.18 (m, 1 H, 2-Ar-CH), 7.35 (s, 1 H, CH), 7.30-7.42 (m, 4 H, $4\times\text{Ar-CH}$), 7.45-7.48 (m, 2 H, $2\times\text{Ar-CH}$) ppm; $^{13}\text{C-NMR}$ (400 MHz, DMSO- d_6) $\delta = 69.2$ (CH_2), 115.0 (4-Ar-CH), 115.2 (2-Ar-CH), 121.8 (6-Ar-CH), 123.9 (5-Ar-CH), 127.8 ($2\times\text{Ar-CH}$), 127.9 (Ar-CH), 128.5 ($2\times\text{Ar-CH}$), 129.9 (CH), 134.3 (Ar-C), 136.8 (Ar-C), 136.9 (Ar-C), 158.5 (Ar-C), 172.1 (C=O), 180.0 (C=O) ppm; **ESI-MS** m/z (%) = 329.1 $[\text{M}+\text{NH}_4]^+$ (100 %), 640.2 $[2\text{M}+\text{NH}_4]^+$ (60 %), 645.1

[2M+Na]⁺ (15 %); **HR-MS** m/z = 329.0959 [M+NH₄]⁺ (calculated: 329.0954); **HPLC-Analysis (Method B)**: 94 %, R_t = 17.0 min.

(Z)-5-(4-(benzyloxy)benzylidene)thiazolidine-2,4-dione **48m**^[320]

TLC R_f = 0.4 (DCM/EtOAc 9:1); **Reaction time**: 8 h; **Purification**: Filtration from ethanol; **Yield**: 112 mg of white solid (0.36 mmol, 38 %); **Yield**: 1189 mg of white solid (3.82 mmol, 89 %); **¹H-NMR** (400 MHz, CD₃OD) δ = 5.07 (s, 2 H, CH₂), 7.01 (d, 2 H, ³ $J_{H,H}$ = 8.9 Hz, 3,5-Ar-CH), 7.22-7.45 (m, 5 H, 5xAr-CH), 7.43 (d, 2 H, ³ $J_{H,H}$ = 8.9 Hz, 2,6-Ar-CH) ppm; **¹H-NMR** (400 MHz, DMSO-d₆) δ = 5.19 (s, 2 H, CH₂), 7.18 (d, 2 H, ³ $J_{H,H}$ = 8.9 Hz, 3,5-Ar-CH), 7.31-7.37 (m, 1 H, 4'-Ar-CH), 7.38-7.43 (m, 2 H, 3,5-Ar-CH), 7.44-7.48 (m, 2 H, 2',6'-Ar-CH), 7.56 (d, 2 H, ³ $J_{H,H}$ = 8.9 Hz, 2,6-Ar-CH), 7.74 (s, 1 H, CH), 12.53 (s(br), 1 H, NH) ppm; **¹³C-NMR** (400 MHz, DMSO-d₆) δ = 69.5 (CH₂), 115.7 (3,5-Ar-CH), 125.8 (Ar-C), 127.9 (2',6'-Ar-CH), 128.0 (4'-Ar-CH), 128.5 (3,5-Ar-CH), 131.1 (CH), 132.0 (2,6-Ar-CH), 136.5 (Ar-C), 160.0 (C=O), 168.2 (C=O) ppm; **ESI-MS** m/z (%) = 329.1 [M+NH₄]⁺ (100 %), 334.1 [M+Na]⁺ (20 %), 640.2 [2M+NH₄]⁺ (100 %), 645.1 [2M+Na]⁺ (55 %); **HR-MS** m/z = 329.0958 [M+NH₄]⁺ (calculated: 329.0954); **HPLC-Analysis (Method B)**: 99 %, R_t = 19.1 min.

(Z)-5-(3,4-bis(benzyloxy)benzylidene)thiazolidine-2,4-dione **48n**^[324]

TLC R_f = 0.3 (DCM/EtOAc 9:1); **Reaction time**: 6 h; **Purification**: Flash-Chromatography DCM/EtOAc 9:1 (R_f = 0.3); **Yield**: 94 mg of white solid (0.23 mmol, 29 %); **¹H-NMR** (400 MHz, CDCl₃) δ = 5.23 (s, 2 H, CH₂), 5.25 (s, 2 H, CH₂), 6.98 (d, 1 H, ³ $J_{H,H}$ = 8.5 Hz, 6-Ar-CH), 7.00 (d, 1 H, ⁴ $J_{H,H}$ = 2.1 Hz, 3-Ar-CH), 7.05 (dd, 1 H, ^{3,4} $J_{H,H}$ = 2.1, 8.5 Hz, 5-Ar-CH), 7.30-7.47 (m, 10 H, 10xAr-CH), 7.70 (s, 1 H, CH), 8.22 (s(br), 1 H, NH) ppm; **¹³C-NMR** (400 MHz, CDCl₃) δ = 71.0 (CH₂), 71.4 (CH₂), 114.2 (Ar-CH), 115.9 (Ar-CH), 119.7 (Ar-C), 125.5 (Ar-CH), 126.2 (Ar-C), 127.3 (2xAr-CH), 128.3 (2xAr-CH), 128.8 (2xAr-CH), 134.6 (CH), 136.4 (Ar-C), 136.6 (Ar-C), 148.9 (Ar-C), 151.4 (Ar-C), 166.8 (C=O), 167.4 (C=O) ppm; **ESI-MS** m/z (%) = 435.1 [M+NH₄]⁺ (100 %), 852.2 [2M+NH₄]⁺ (35 %), 858.2 [2M+Na]⁺ (10 %); **HR-MS** m/z = 435.1372 [M+NH₄]⁺ (calculated: 435.1373); **HPLC-Analysis**: 100 %, R_t = 31.1 min.

(5Z)-3-amino-5-(phenylmethylidene)-2-sulfanylidene-1,3-thiazolidin-4-one **54a**^[85]

TLC R_f = 0.3 (DCM/EtOAc 10:1); **Reaction time**: 4 h; **Purification**: Re-crystallisation from methanol; **Yield**: 629 mg of orange crystals (2.66 mmol, 79 %); **¹H-NMR** (400 MHz, DMSO-d₆) δ = 5.95 (s, 2 H, NH₂), 7.50-7.59 (m, 3 H, 3 x Ar-CH), 7.63-7.68 (m, 2 H, 2 x Ar-CH), 7.86 (s, 1 H, C-H) ppm; **¹³C-NMR** (300 MHz, DMSO-d₆) δ = 120.4 (C), 129.6 (2 x Ar-CH), 130.9 (2 x Ar-CH), 131.1 (Ar-CH), 133.1 (Ar-C), 133.5 (CH), 163.9 (C=O), 188.0 (C=S) ppm; **ESI-MS** m/z (%) = 237.0 [M+H]⁺ (55 %), 259.0 [M+Na]⁺ (45 %), 495.0 [2M+Na]⁺ (100 %), **HR-MS** m/z = 237.0153 [M+H]⁺ (calculated: 237.0151), 495.0043 [2M+Na]⁺ (calculated: 495.0048); **HPLC-Analysis (Method B)**: 97 %, R_t = 16.4 min.

(Z)-3-amino-5-(2-methylbenzylidene)-2-thioxothiazolidin-4-one **54b**

TLC R_f = 0.8 (DCM/MeOH 90:5); **Reaction time**: 4 h; **Purification**: Filtration from methanol;

Yield: 56 mg of yellow solid (0.22 mmol, 32 %); **¹H-NMR** (400 MHz, DMSO-*d*₆) δ = 2.43 (s, 3 H, CH₃), 5.95 (s, 2 H, NH₂), 7.35-7.45 (m, 4 H, 4xAr-CH), 7.93 (s, 1 H, CH) ppm; **¹³C-NMR** (400 MHz, DMSO-*d*₆) δ = 19.4 (CH₃), 121.8 (Ar-C), 126.9 (Ar-CH), 127.8 (Ar-CH), 130.9 (Ar-CH), 131.1 (Ar-CH), 131.2 (CH), 132.0 (Ar-C), 139.3 (Ar-C), 163.4 (C=O), 188.4 (C=S) ppm; **ESI-MS** m/z (%) = 251.0 [M+H]⁺ (75 %), 273.0 [M+Na]⁺ (50 %), 523.0 [2M+Na]⁺ (100 %). **HR-MS** m/z = 251.0310 [M+H]⁺ (calculated: 251.0307); **HPLC-Analysis (Method B)**: 99 %, *R*_t = 17.3 min.

(Z)-3-amino-5-(3-methylbenzylidene)-2-thioxothiazolidin-4-one **54c**

TLC *R*_f = 0.8 (DCM/MeOH 90:5); **Reaction time:** 20 min; **Purification:** Filtration from methanol; **Yield:** 125 mg of yellow solid (0.50 mmol, 70 %); **¹H-NMR** (400 MHz, DMSO-*d*₆) δ = 2.38 (0, 3 H, ¹*J* = 0, CH₃ Hz,) 5.95 (s, 2 H, NH₂), 7.30-7.51 (m, 4 H, 4xAr-CH), 7.81 (s, 1 H, C-H) ppm; **¹³C-NMR** (400 MHz, DMSO-*d*₆) δ = 20.9 (CH₃), 120.1 (Ar-C), 128.0 (Ar-CH), 129.4 (Ar-CH), 131.1 (Ar-CH), 131.8 (Ar-CH), 133.0 (Ar-C), 133.5 (CH), 138.9 (Ar-C) 163.7 (C=O), 187.8 (C=S) ppm; **ESI-MS** m/z (%) = 251.0 [M+H]⁺ (100 %), 268.1 [M+NH₄]⁺ (45 %), 518.1 [2M+NH₄]⁺ (70 %), 523.0 [2M+Na]⁺ (50 %), **HR-MS** m/z = 251.0309 [M+H]⁺ (calculated: 251.0307); **HPLC-Analysis (Method B)**: 99 %, *R*_t = 17.3 min.

(5Z)-3-amino-5-[(4-methylphenyl)methylidene]-2- sulfanylidene-1,3-thiazolidin-4-one **54d**^[85]

TLC *R*_f = 0.8 (DCM/MeOH 90:5); **Reaction time:** 20 min; **Purification:** Filtration from methanol; **Yield:** 124 mg of yellow solid (0.50 mmol, 74 %); **¹H-NMR** (400 MHz, DMSO-*d*₆) δ = 2.35 (s, 3 H, CH₃), 5.93 (s, 2 H, NH₂), 7.36 (d, 2 H, ³*J*_{H,H} = 8.0 Hz, 3,5-Ar-CH), 7.54 (d, 2 H, ³*J*_{H,H} = 8.0 Hz, 2,6-Ar-CH), 7.81 (s, 1 H, CH) ppm; **¹³C-NMR** (400 MHz, DMSO-*d*₆) δ = 21.2 (CH₃), 119.0 (Ar-C), 130.2 (3,5-Ar-CH), 130.3 (Ar-C), 130.9 (2,6-Ar-CH), 133.5 (CH), 141.6 (Ar-C), 163.8 (C=O), 187.6 (C=S) ppm; **ESI-MS** m/z (%) = 251.0 [M+H]⁺ (100 %), 268.1 [M+NH₄]⁺ (45 %), 518.1 [2M+NH₄]⁶⁰ (; %) **HR-MS** m/z = 251.0309 [M+H]⁺ (calculated: 251.0307); **HPLC-Analysis (Method B)**: 99 %, *R*_t = 17.8 min.

(Z)-3-amino-2-thioxo-5-(2-(trifluoromethyl)benzylidene)thiazolidin-4-one **54e**

TLC *R*_f = 0.6 (Cyclohexane/EtOAc 7:3); **Reaction time:** 16 h; **Purification:** Flash-Chromatography Cyclohexane/EtOAc 7:3 (*R*_f = 0.6); **Yield:** 12 mg of orange solid (0.04 mmol, 12 %); **¹H-NMR** (300 MHz, CD₃OD) δ = 6.89 (d, 1 H, ³*J*_{H,H} = 8.1 Hz, 2-Ar-CH), 6.94 (at, 1 H, ³*J*_{H,H} = 7.6, 8.1 Hz, 3-Ar-CH), 7.28 (at, 1 H, ³*J*_{H,H} = 7.6, 8.1 Hz, 4-Ar-CH), 7.40 (d, 1 H, ³*J*_{H,H} = 8,1 Hz, 5-Ar-CH), 8.19 (s, 1 H, CH) ppm; **HPLC-Analysis (Method B)**: 99 %, *R*_t = 11.5 min.

(5Z)-3-amino-2-sulfanylidene-5-[3-(trifluoromethyl)phenyl]methylidene-1,3-thiazolidin-4-one **54f**

TLC *R*_f = 0.3 (Hexane/EtOAc 6:4); **Yield:** 250 mg of yellow solid (0.82 mmol, 78 %); **Reaction time:** 12 h **Purification:** Flash-Chromatography Hexane/EtOAc 7.5:2.5 (*R*_f = 0.2); **¹H-NMR** (400 MHz, DMSO-*d*₆) δ = 5.96 (s, 2 H, NH₂), 7.77-7.82 (m, 1 H, Ar-CH), 7.83-7.93 (m, 2 H, 2xAr-CH), 7.98 (s, 1 H, CH), 8.06 (s, 1 H, Ar-CH) ppm; **¹³C-NMR** (400 MHz, DMSO-*d*₆) δ = 122.6 (Ar-CH), 123.8 (q, ¹*J*_{C,F} = 272.7 Hz, CF₃), 127.1 (q, ³*J*_{C,F} = 3.7 Hz, Ar-CH), 127.7

(q, $^3J_{C,F}$ = 3.8 Hz, Ar-CH), 130.1 (q, $^2J_{C,F}$ = 32.3 Hz, Ar-C), 130.7 (Ar-CH), 131.4 (CH) 163.7 (C=O), 187.6 (C=S) ppm; **ESI-MS** m/z (%) = 305.0 [M+H]⁺ (6 %); **HPLC-Analysis (Method B)**: 100 %, R_t = 18.2 min.

(Z)-3-amino-2-thioxo-5-(4-(trifluoromethyl)benzylidene)thiazolidin-4-one **54g**

TLC R_f = 0.1 (CHCl₃); **Reaction time**: 4 h; **Purification**: Flash-Chromatography CHCl₃ (R_f = 0.1); **Yield**: 50 mg of yellow solid (0.16 mmol, 41 %); **¹H-NMR** (400 MHz, CDCl₃) δ = 5.24 (s(br), 1 H, NH₂), 7.62 (d, 2 H, $^3J_{H,H}$ = 8.1 Hz, 3,5-Ar-CH), 7.75 (d, 2 H, $^3J_{H,H}$ = 8.1 Hz, 2,6-Ar-CH), 7.82 (s, 1 H, CH) ppm; **¹³C-NMR** (400 MHz, CDCl₃) δ = 123.1 (Ar-C or Ar-CH), 126.3 ($^2J_{1-ArC,CF_3}$ = 3.8 Hz, 1-ArC), 130.7 (Ar-C or Ar-CH), 132.0 (Ar-C or Ar-CH), 132.1 (Ar-C or Ar-CH), 136.3 (Ar-C or Ar-CH), 163.3 (C=O), 186.1 (C=S) ppm; **ESI-MS** m/z (%) = 322.0 [M+NH₄]⁺ (100 %); **HR-MS** m/z = 322.9936 [M+NH₄]⁺ (calculated: 322.0290); **HPLC-Analysis**: 99.9 %, R_t = 32.1 min; **HPLC-Analysis (Method B)**: 100 %, R_t = 21.1 min.

(Z)-3-amino-5-(4-chlorobenzylidene)-2-thioxothiazolidin-4-one **54h**^[325]

Reaction time: 4 h; **Purification**: Filtration from methanol; **Yield**: 227 mg of yellow solid (0.84 mmol, 50 %); **¹H-NMR** (400 MHz, DMSO-d₆) δ = 5.95 (s, 2 H, NH₂), 7.60-7.64 (m, 2 H, 2 x Ar-CH), 7.66-7.70 (m, 2 H, 2 x Ar-CH), 7.86 (s, 1 H, CH) ppm; **¹³C-NMR** (300 MHz, DMSO-d₆) δ = 121.2 (C), 129.7 (2 x Ar-CH), 132.0 (CH), 132.5 (2 x Ar-CH), 135.8 (Ar-C), 164.0 (C=O), 187.8 (C=S) ppm; **ESI-MS** m/z (%) = 293.0 [M+Na]⁺ (100 %), 562.9 [2M+Na]⁺ (100 %); **EI-MS** m/z (%) = 270.2 [M]⁺ (100 %), 170.2 [fragment]⁺ (40 %), 168.2 [fragment]⁺ (100 %); **HR-MS** m/z = 292.9586 [M+Na]⁺ (calculated: 292.9581); **HPLC-Analysis (Method B)**: 98 %, R_t = 18.5 min.

(5Z)-3-amino-5-[(3-bromo-4-fluorophenyl)methylidene]-2-sulfanylidene-1,3-thiazolidin-4-one **54i**

Reaction time: 4 h; **Purification**: Filtration from methanol; **Yield**: 444 mg of yellow solid (1.33 mmol, 79 %); **¹H-NMR** (400 MHz, DMSO-d₆) δ = 5.95 (s, 2 H, NH₂), 7.56 (t, 1 H, $^3J_{H,H}$ = 8.7 Hz, 5-Ar-CH), 7.67 (ddd, 1 H, $^{3,4}J_{H,H(F)}$ = 8.7, 4.7, 2.3 Hz, 6-Ar-CH), 7.85 (s, 1 H, CH), 8.05 (dd, 1 H, $^4J_{H,H(F)}$ = 6.7, 2.3 Hz, 2-Ar-CH); ppm; **¹³C-NMR** (300 MHz, DMSO-d₆) δ = 117.9 (Ar-C or Ar-CH), 121.7 (Ar-C or Ar-CH), 130.8 (Ar-C or Ar-CH), 131.6 (CH), 136.3 (Ar-C or Ar-CH), 163.7 (C=O), 187.6 (C=S), ppm; **ESI-MS** m/z (%) = 330.9 [M-H]⁻ (100 %), 664.8 [2M-H]⁻ (40 %); **EI-MS** m/z (%) = 334.1 [M]⁺ (100 %); **HR-MS** m/z = 332.9096 [M-H]⁻ (calculated: 332.8994), 664.8066 [2M-H]⁻ (calculated: 664.8084); **HR-MS** m/z = 331.9085 [M]⁻ (calculated: 331.9089); **HPLC-Analysis (Method B)**: 98 %, R_t = 18.5 min.

(Z)-3-amino-5-(3-bromo-4-methoxybenzylidene)-2-thioxothiazolidin-4-one **54j**

TLC R_f = 0.2 (DCM); **Reaction time**: 4 h; **Purification**: Flash-Chromatography DCM → DCM/MeOH 9:0.01 (R_f = 0.2, 0.3); **Yield**: 201 mg of yellow solid (0.58 mmol, 34 %); **¹H-NMR** (400 MHz, DMSO-d₆) δ = 3.94 (s, 3 H, OCH₃), 5.95 (s, 2 H, NH₂), 7.31 (d, 1 H, $^3J_{H,H}$ = 8.6 Hz, 5-Ar-CH), 7.65 (dd, 1 H, $^{3,4}J_{H,H}$ = 8.6, 2.3 Hz, 6-Ar-CH), 7.82 (s, 1 H, C-H), 7.93 (d, 1 H, $^3J_{H,H}$ = 2.3 Hz, 2-Ar-CH) ppm; **¹³C-NMR** (400 MHz, DMSO-d₆) δ = 56.8 (OCH₃), 111.6 (Ar-C), 113.4 (5-Ar-CH), 118.6 (Ar-C), 127.0 (Ar-C), 131.5 (6-Ar-CH), 132.0 (CH), 135.7 (2-Ar-CH), 157.4

(Ar-C), 163.7 (C=O), 187.2 (C=S) ppm; **EI-MS** m/z (%) = 344.1 [M]⁺ (100 %), 242.1 [fragment]⁺ (80 %), 120.2 [fragment]⁺ (50 %), 74.1 [fragment]⁺ (100 %); **HR-MS** m/z = 343.9279 [M]⁺ (calculated: 343.9289); **HPLC-Analysis (Method B)**: 95 %, R_t = 18.0 min.

(Z)-3-amino-5-(4-ethynylbenzylidene)-2-thioxothiazolidin-4-one **54k**

TLC R_f = 0.3 (DCM/MeOH 1:0.01); **Reaction time**: 4 h; **Purification**: Flash-Chromatography DCM/MeOH 1:0.01 (R_f = 0.3); **Yield**: 123 mg of red solid (0.47 mmol, 28 %); **¹H-NMR** (400 MHz, DMSO- d_6) δ = 4.48 (s, 1 H, Alkyne-CH), 5.95 (s, 2 H, NH₂), 7.64 (d, 2 H, ³J_{H,H} = 8.4 Hz, 2,6-Ar-CH), 7.67 (d, 2 H, ³J_{H,H} = 8.4 Hz, 3,5-Ar-CH), 7.86 (s, 1 H, CH) ppm; **¹³C-NMR** (400 MHz, DMSO- d_6) δ = 83.0 (CCH), 84.0 (CCH), 121.4 (Ar-C), 123.9 (Ar-C), 130.9 (3,5-Ar-CH), 132.1 (CH), 132.6 (2,6-Ar-CH), 133.3 (Ar-C), 163.7 (C=O), 187.6 (C=S) ppm; **ESI-MS** m/z (%) = 261.0 [M+H]⁺ (100 %), 278.0 [M+NH₄]⁺ (50 %), 283.0 [M+Na]⁺ (25 %), 538.0 [2M+NH₄]⁺ (45 %), 798.0 [3M+NH₄]⁺ (10 %); **HR-MS** m/z = 261.0148 [M]⁺ (calculated: 261.0151); **HPLC-Analysis (Method B)**: 100 %, R_t = 17.2 min.

4-[(5Z)-3-amino-4-oxo-2-sulfanylidene-1,3-thiazolidin-5-ylidene]methylbenzonitrile **54l**^[85]

TLC R_f = 0.1 (DCM); **Reaction time**: DCM; **Purification**: Flash-Chromatography DCM (R_f = 0.1); **Yield**: 187 mg of orange solid (0.72 mmol, 42 %); **¹H-NMR** (400 MHz, DMSO- d_6) δ = 5.95 (s, 2 H, NH₂), 7.80-7.86 (m, 2 H, 2xAr-CH), 7.90 (s, 1 H, C-H), 7.98-8.03 (m, 2 H, 2xAr-CH) ppm; **¹³C-NMR** (400 MHz, DMSO- d_6) δ = 112.4 (Ar-C), 118.3 (Ar-C), 124.0 (Ar-C), 130.9 (CH), 131.0 (2xAr-CH), 133.2 (2xAr-CH), 137.0 (Ar-C), 163.6 (C=O), 187.6 (C=S) ppm; **EI-MS** m/z (%) = 261.1 [M]⁺ (30 %), 159.1 [fragment]⁺ (100 %), 148.1 [fragment]⁺ (30 %), 74.1 [fragment]⁺ (100 %); **HR-MS** m/z = 261.0022 [M]⁺ (calculated: 261.0197); **HPLC-Analysis (Method B)**: 95 %, R_t = 14.2 min.

(Z)-3-amino-5-(3-nitrobenzylidene)-2-thioxothiazolidin-4-one **54m**^[85]

TLC R_f = 0.1 (DCM); **Reaction time**: 4 h; **Purification**: Flash-Chromatography DCM (R_f = 0.1); **Yield**: 327 mg of orange solid (1.16 mmol, 69 %); **¹H-NMR** (400 MHz, DMSO- d_6) δ = 5.97 (s, 2 H, NH₂), 7.84 (at, 1 H, ³J_{H,H} = 8.1 Hz, 5-Ar-CH), 8.04 (s, 1 H, C-H), 8.06 (d, 1 H, ³J_{H,H} = 8.1 Hz, 6-Ar-CH), 8.32-8.36 (m, 1 H, 4-Ar-CH), 8.51-8.53 (m, 1 H, 2-Ar-CH) ppm; **EI-MS** m/z (%) = 281.0 [M]⁺ (100 %), 179.0 [fragment]⁺ (100 %), 133.0 [fragment]⁺ (30 %), 89.0 [fragment]⁺ (40 %); **HR-MS** m/z = 280.9919 [M]⁺ (calculated: 280.9929); **HPLC-Analysis (Method B)**: 98 %, R_t = 15.7 min.

N-(4-[(5Z)-3-amino-4-oxo-2-sulfanylidene-1,3-thiazolidin-5-ylidene]methylphenyl)acetamide **54n**

Reaction time: 4 h; **Purification**: Filtration from methanol; **Yield**: 335 mg of red solid (1.14 mmol, 68 %); **¹H-NMR** (400 MHz, DMSO- d_6) δ = 2.08 (s, 3 H, CH₃), 5.93 (s, 2 H, NH₂), 7.58 (d, 2 H, ³J_{H,H} = 8.6 Hz, 2 x Ar-CH), 7.73-7.78 (m, 3 H, 2 x Ar-CH, CH), 10.31 (s, 1 H, NH) ppm; **¹³C-NMR** (300 MHz, DMSO- d_6) δ = 24.1 (CH₃), 117.8 (C), 119.3 (2 x Ar-CH), 127.5 (Ar-C), 132.2 (2 x Ar-CH), 133.4 (CH), 142.1 (Ar-C), 163.9 (C=O), 169.1 (C=O Ac), 187.5 (C=S), ppm; **ESI-MS** m/z (%) = 294.0 [M+H]⁺ (100 %), 316.0 [M+Na]⁺ (80 %), 609.0 [2M+Na]⁺

(65 %), 902.1 [3M+Na]⁺ (10 %); **HR-MS** m/z = 294.0369 [M+H]⁺ (calculated: 294.0365); **HPLC-Analysis (Method B)**: 97 %, R_t = 16.4 min.

(Z)-3-amino-5-(4-(dimethylamino)benzylidene)-2-thioxothiazolidin-4-one **54o**^[85]

Reaction time: 4 h; **Purification**: Filtration from methanol; **Yield**: 20 mg of red solid (0.07 mmol, 21 %); **¹H-NMR** (400 MHz, DMSO-*d*₆) δ = 3.05 (s, 6 H, N(CH₃)₂), 5.96 (s, 2 H, NH₂), 6.85 (d, 2 H, ³*J*_{H,H} = 9.0 Hz, 3,5-Ar-CH), 7.50 (d, 2 H, ³*J*_{H,H} = 9.0 Hz, 2,6-Ar-CH), 7.74 (s, 1 H, CH) ppm; **¹³C-NMR** (400 MHz, DMSO-*d*₆) δ = 39.6 (N(CH₃)₂), 111.7 (Ar-C), 112.3 (3,5-Ar-CH), 119.9 (Ar-C), 133.4 (2,6-Ar-CH), 135.0 (CH), 152.0 (Ar-C), 163.7 (C=O), 186.0 (C=S) ppm; **ESI-MS** m/z (%) = 280.1 [M+H]⁺ (100 %), 302.0 [M+Na]⁺ (15 %); **HR-MS** m/z = 280.0576 [M+H]⁺ (calculated: 280.0573); **HPLC-Analysis (Method B)**: 92 %, R_t = 17.2 min.

(5Z)-3-amino-5-[(2-hydroxyphenyl)methylidene]-2-sulfanylidene-1,3-thiazolidin-4-one **54p**^[305]

TLC R_f = 0.8 (DCM/EtOAc 9:1); **Reaction time**: 4 h; **Purification**: Filtration from ethanol; **Yield**: 276 mg of yellow solid (1.09 mmol, 65 %); **¹H-NMR** (400 MHz, DMSO-*d*₆) δ = 4.32 (s, 2 H, NH₂), 6.96 (at, 1 H, ³*J*_{H,H} = 7.8, 7.3 Hz, 5-Ar-CH), 6.99 (d, 1 H, ³*J*_{H,H} = 8.4 Hz, 3-Ar-CH), 7.47 (ddd, 1 H, ^{3,4}*J*_{H,H} = 8.4, 7.3, 1.7 Hz, 4-Ar-CH), 7.83 (dd, 1 H, ^{3,4}*J*_{H,H} = 7.8, 1.7 Hz, 6-Ar-CH), 8.96 (s, 1 H, CH), 10.69 (s, 1 H, OH) ppm; **¹³C-NMR** (400 MHz, DMSO-*d*₆) δ = 116.8 (3-Ar-CH), 117.7 (Ar-C), 119.7 (5-Ar-CH), 128.6 (6-Ar-CH), 134.8 (4-Ar-CH), 158.7 (CH), 167.1 (Ar-C), 169.8 (C=O), 197.2 (C=S) ppm; **ESI-MS** m/z (%) = 270.0 [M+NH₄]⁺ (100 %); **HR-MS** m/z = 270.0369 [M+NH₄]⁺ (calculated: 270.0365); **HPLC-Analysis (Method B)**: 100 %, R_t = 18.7 min.

(5Z)-3-amino-5-[(3-hydroxyphenyl)methylidene]-2-sulfanylidene-1,3-thiazolidin-4-one **54q**

Reaction time: 4 h; **Purification**: Re-crystallisation from methanol; **Yield**: 136 mg of orange crystals (0.54 mmol, 32 %); **¹H-NMR** (400 MHz, DMSO-*d*₆) δ = 5.94 (s, 2 H, NH₂), 6.92 (dd, 1 H, ^{3,4}*J*_{H,H} = 8.1, 1.7 Hz, Ar-CH), 7.01-7.04 (m, 1 H, Ar-CH), 7.09 (d, 1 H, ³*J*_{H,H} = 7.8 Hz, Ar-CH), 7.34 (at, 1 H, ³*J*_{H,H} = 7.8 Hz, Ar-CH), 7.74 (s, 1 H, C-H), 10.26 (s, 1 H, OH) ppm; **¹³C-NMR** (300 MHz, DMSO-*d*₆) δ = 116.5 (C), 118.5 (Ar-C o. Ar-CH), 120.2 (Ar-C o. Ar-CH), 122.3 (Ar-C o. Ar-CH), 130.7 (Ar-CH), 133.7 (CH), 134.3 (Ar-C o. Ar-CH), 158.2 (3-Ar-C), 163.9 (C=O), 188.0 (C=S) ppm; **ESI-MS** m/z (%) = 251.0 [M-H]⁻ (75 %), 503.0 [2M-H]⁻ (100 %), 755.0 [3M-H]⁻ (20 %); **HR-MS** m/z = 250.9950 [M-H]⁻ (calculated: 250.9954); **HPLC-Analysis (Method B)**: 98 %, R_t = 15.7 min.

(5Z)-3-amino-5-[(4-hydroxyphenyl)methylidene]-2-sulfanylidene-1,3-thiazolidin-4-one **54r**^[305]

Reaction time: 4 h; **Purification**: Re-crystallisation from methanol; **Yield**: 134 mg of red crystals (0.53 mmol, 31 %); **¹H-NMR** (400 MHz, DMSO-*d*₆) δ = 5.94 (s, 2 H, NH₂), 6.89 (d, 2 H, ³*J*_{H,H} = 8.7 Hz, 2 x Ar-CH), 7.49 (d, 2 H, ³*J*_{H,H} = 8.7 Hz, 2 x Ar-CH), 7.74 (s, 1 H, C-H) ppm; **¹³C-NMR** (300 MHz, DMSO-*d*₆) δ = 114.2 (Ar-CH or Ar-C), 117.1 (C), 123.5 (Ar-CH or Ar-C), 133.7 (CH), 133.9 (Ar-CH or Ar-C), 134.5 (Ar-CH or Ar-C), 134.8 (Ar-CH or Ar-C), 162.0 (4-Ar-C), 163.9 (C=O), 187.1 (C=S) ppm; **EI-MS** m/z (%) = 252.0 [M]⁺ (100 %), 150.0 [fragment]⁺

(100 %); **HPLC-Analysis (Method B)**: 97 %, $R_t = 13.9$ min.

(5Z)-3-amino-5-[(2,4-dihydroxyphenyl)methylidene]-2-sulfanylidene-1,3-thiazolidin-4-one **54s**
Reaction time: 4 h; **Purification**: Filtration from methanol; **Yield**: 251 mg of red solid (0.94 mmol, 55 %); **$^1\text{H-NMR}$** (400 MHz, DMSO- d_6) $\delta = 5.93$ (s, 2 H, NH_2), 6.42-6.43 (m, 1 H, 3-Ar-CH), 6.43 (dd, 1 H, $^3,^4J_{6,5(3)} = 2.3, 7.5$ Hz, 6-Ar-CH), 7.22 (dd, 1 H, $^3,^4J_{5,6(3)} = 7.5, 2.1$ Hz, 5-Ar-CH), 7.97 (s, 1 H, C-H), 10.48 (s, 1 H, OH), 10.69 (s, 1 H, OH) ppm; **$^{13}\text{C-NMR}$** (300 MHz, DMSO- d_6) $\delta = 102.6$ (3-Ar-CH), 109.1 (6-Ar-CH), 112.1 (1-Ar-C o. C), 113.4 (1-Ar-C o. C), 130.0 (CH), 131.9 (5-Ar-CH), 160.2 (2- o. 4-Ar-C), 163.0 (2- o. 4-Ar-C), 164.1 (C=O), 187.2 (C=S) ppm; **ESI-MS** m/z (%) = 267.0 $[\text{M}-\text{H}]^-$ (100 %), 535.0 $[2\text{M}-\text{H}]^-$ (85 %), 803.0 $[3\text{M}-\text{H}]^-$ (10 %), 269.0 $[\text{M}+\text{H}]^+$ (100 %), 559.0 $[2\text{M}+\text{Na}]^+$ (30 %); **HR-MS** $m/z = 266.9900$ $[\text{M}-\text{H}]^-$ (calculated: 266.9904), **HR-MS** $m/z = 269.0051$ $[\text{M}+\text{H}]^+$ (calculated: 269.0049); **HPLC-Analysis (Method B)**: 98 %, $R_t = 16.2$ min.

(Z)-3-amino-5-(3,4-dihydroxybenzylidene)-2-thioxothiazolidin-4-one **54t**

TLC $R_f = 0.2$ (DCM/MeOH 9:1); **Purification**: Filtration from methanol; **Yield**: 13 mg of yellow solid (0.05 mmol, 14 %); **$^1\text{H-NMR}$** (400 MHz, CD_3OD) $\delta = 6.89$ (d, 1 H, $^3J_{\text{H,H}} = 8.1$ Hz, 5-Ar-CH), 7.01 (dd, 1 H, $^1J_{\text{H,H}} = 2.1, 8.1$ Hz, 3,4), 7.03 (d, 1 H, $^4J_{\text{H,H}} = 2.1$ Hz, 3-Ar-CH), 7.67 (s, 1 H, CH) ppm; **EI-MS** m/z (%) = 268.0 $[\text{M}]^+$ (100 %), 166.0 [fragment] $^+$ (100 %); **HR-MS** $m/z = 267.9971$ $[\text{M}]^+$ (calculated: 267.9976); **HPLC-Analysis** : 99 %, $R_t = 32.3$ min.

(5Z)-3-amino-5-[(4-methoxyphenyl)methylidene]-2-sulfanylidene-1,3-thiazolidin-4-one **54u**^[85]

Reaction time: 4 h; **Purification**: Filtration from methanol; **Yield**: 277 mg of yellow solid (1.04 mmol, 62 %); **$^1\text{H-NMR}$** (400 MHz, DMSO- d_6) $\delta = 3.84$ (s, 3 H, OCH_3), 5.94 (s, 2 H, NH_2), 7.10-7.15 (m, 2 H, 2,6-Ar-CH), 7.60-7.65 (m, 2 H, 3,5-Ar-CH), 7.82 (s, 1 H, C-H) ppm; **$^{13}\text{C-NMR}$** (300 MHz, DMSO- d_6) $\delta = 55.6$ (OCH_3), 115.3 (2,6-Ar-CH), 117.0 (C), 125.7 (1-Ar-C), 133.2 (3,5-Ar-CH), 133.7 (CH), 161.8 (4-Ar-C), 164.0 (C=O), 187.4 (C=S) ppm; **ESI-MS** m/z (%) = 284.1 $[\text{M}+\text{NH}_4]^+$ (40 %), 550.1 $[2\text{M}+\text{NH}_4]^+$ (100 %); **HR-MS** $m/z = 284.0524$ $[\text{M}+\text{NH}_4]^+$ (calculated: 284.0522), 550.0701 $[2\text{M}+\text{NH}_4]^+$ (calculated: 550.0706); **HPLC-Analysis (Method B)**: 100 %, $R_t = 17.2$ min.

(5Z)-3-amino-5-[3-(benzyloxy)phenyl]methylidene-2-sulfanylidene-1,3-thiazolidin-4-one **54v**

TLC $R_f = 0.3$ (DCM/EtOAc 10:1); **Reaction time**: 1 h; **Purification**: Flash-Chromatography DCM/EtOAc 10:1 ($R_f = 0.3$); **Yield**: 22 mg of yellow solid (0.06 mmol, 10 %); **$^1\text{H-NMR}$** (400 MHz, CDCl_3) $\delta = 3.97$ (s(br), 1 H, NH_2), 5.08 (s, 2 H, CH_2), 6.97-7.52 (m, 10 H, 10xCH) ppm; **ESI-MS** m/z (%) = 343.1 $[\text{M}+\text{H}]^+$ (100 %), 365.0 $[\text{M}+\text{Na}]^+$ (30 %), 702.1 $[2\text{M}+\text{NH}_4]^+$ (100 %), 707.1 $[2\text{M}+\text{Na}]^+$ (50 %), 1044.2 $[3\text{M}+\text{NH}_4]^+$ (25 %), 1049.1 $[3\text{M}+\text{Na}]^+$ (85 %); **HR-MS** $m/z = 343.0573$ $[\text{M}+\text{H}]^+$ (calculated: 343.0569); **HPLC-Analysis (Method B)**: 19.6 %, $R_t = 94$ min.

(5Z)-3-amino-5-[4-(benzyloxy)phenyl]methylidene-2-sulfanylidene-1,3-thiazolidin-4-one **54w**

TLC $R_f = 0.5$ (DCM/EtOAc 10:1); **Reaction time**: 30 min; **Purification**: Filtration from methanol; **Yield**: 145 mg of yellow solid (0.42 mmol, 63 %); **$^1\text{H-NMR}$** (400 MHz, DMSO- d_6) $\delta = 5.21$ (s,

2 H, CH_2), 5.94 (s, 2 H, NH_2), 7.18-7.23 (m, 2 H, 2,6-Ar-CH), 7.32-7.49 (m, 5 H, Ar-CH), 7.61-7.66 (m, 2 H, 3,5-Ar-CH), 7.82 (s, 1 H, C-H) ppm; $^{13}\text{C-NMR}$ (300 MHz, DMSO-d_6) δ = 69.6 (CH_2), 100.1 (Ar-C), 116.1 (2,6-Ar-underlineCH), 117.2 (C), 125.9 (Ar-C), 128.0, 128.2, 128.6 (5 x Ar-CH), 133.2 (3,5-Ar-CH), 133.7 (CH), 136.6 (Ar-C), 160.9 (4-Ar-C), 164.0 (C=O), 187.5 (C=S) ppm; **EI-MS** m/z (%) = 342.2 $[\text{M}]^+$ (100 %); **ESI-MS** m/z (%) = 343.1 $[\text{M}+\text{H}]^+$ (100 %), 365.0 $[\text{M}+\text{Na}]^+$ (50 %), 707.1 $[\text{2M}+\text{Na}]^+$ (100 %), 1049.1 $[\text{3M}+\text{Na}]^+$ (40 %); **HR-MS** m/z = 343.0573 $[\text{M}+\text{H}]^+$ (calculated: 343.0569); **HR-MS** m/z = 365.0393 $[\text{M}+\text{Na}]^+$ (calculated: 365.0389), 707.0889 $[\text{2M}+\text{Na}]^+$ (calculated: 707.0892); **HPLC-Analysis (Method B)**: 94 %, R_t = 19.6 min.

(Z)-3-amino-5-(4-(methylsulfonyl)benzylidene)-2-thioxothiazolidin-4-one **54z**

Reaction time: 20 min; **Purification**: Filtration from EtOH; **Yield**: 76 mg of yellow solid (0.24 mmol, 32 %); $^1\text{H-NMR}$ (400 MHz, DMSO-d_6) δ = 3.29 (s, 3 H, SO_2CH_3), 8.07 (d, 2 H, $^3J_{\text{H,H}}$ = 8.5 Hz, 3,5-Ar-CH), 8.15 (d, 2 H, $^3J_{\text{H,H}}$ = 8.5 Hz, 2,6-Ar-CH), 8.85 (s, 1 H, CH) ppm.

(Z)-3-amino-5-(3,4-bis(benzyloxy)benzylidene)-2-thioxothiazolidin-4-one **54x**

TLC R_f = 0.9 (DCM/MeOH 90:5); **Reaction time**: 20 min; **Purification**: Filtration from methanol; **Yield**: 202 mg of yellow solid (0.45 mmol, 31 %); $^1\text{H-NMR}$ (400 MHz, DMSO-d_6) δ = 5.23 (s, 2 H, CH_2), 5.25 (s, 2 H, CH_2), 5.93 (s, 2 H, NH_2), 7.23-7.51 (m, 13 H, 13xAr-CH), 7.76 (s, 1 H, CH) ppm; $^{13}\text{C-NMR}$ (400 MHz, DMSO-d_6) δ = 69.9 (CH_2), 70.0 (CH_2), 114.2 (Ar-CH), 116.0 (Ar-CH), 117.3 (Ar-C), 125.4 (Ar-C), 125.9 (Ar-CH), 127.5 (Ar-CH), 127.6 (Ar-CH), 127.9 (Ar-CH), 128.0 (Ar-CH), 128.5 (Ar-CH), 133.7 (CH), 136.6 (Ar-C), 136.7 (Ar-C), 148.3 (Ar-C), 150.9 (Ar-C), 163.7 (C=O), 187.2 (C=S) ppm; **ESI-MS** m/z (%) = 449.1 $[\text{M}+\text{H}]^+$ (100 %), 471.1 $[\text{M}+\text{Na}]^+$ (20 %), 914.2 $[\text{2M}+\text{NH}_4]^+$ (20 %); **HR-MS** m/z = 449.0991 $[\text{M}+\text{H}]^+$ (calculated: 449.0988); **HPLC-Analysis (Method B)**: 99 %, R_t = 17.8 min.

(Z)-5-benzylidene-3-phenyl-2-thioxothiazolidin-4-one **55a**^[326]

TLC R_f = 0.5 (DCM); **Reaction time**: 55 min; **Purification**: Filtration from methanol; **Yield**: 80 mg of yellow solid (0.27 mmol, 60 %); $^1\text{H-NMR}$ (400 MHz, DMSO-d_6) δ = 7.41-7.77 (m, 10 H, Ar-CH), 7.86 (s, 1 H, C-H) ppm; $^1\text{H-NMR}$ (400 MHz, CDCl_3) δ = 7.27-7.32 (m, 2 H, 2xAr-CH), 7.44-7.61 (m, 8 H, 8xAr-CH), 7.80 (s, 1 H, CH) ppm; $^{13}\text{C-NMR}$ (400 MHz, CDCl_3) δ = 123.5 (Ar-C), 128.5 (2xAr-CH), 129.5 (2xAr-CH), 129.7 (2xAr-CH), 129.9 (Ar-CH), 130.8 (2xAr-CH), 131.0 (Ar-CH), 133.5 (Ar-C), 133.6 (CH), 135.0 (Ar-C), 167.7 (C=O), 193.6 (C=S) ppm; **ESI-MS** m/z (%) = 298.0 $[\text{M}+\text{H}]^+$ (100 %), 320.0 $[\text{M}+\text{Na}]^+$ (30 %), 336.0 $[\text{M}+\text{K}]^+$ (25 %), 617.0 $[\text{2M}+\text{Na}]^+$ (60 %); **HR-MS** m/z = 298.0358 $[\text{M}+\text{H}]^+$ (calculated: 298.0355); **HPLC-Analysis (Method B)**: 99 %, R_t = 20.2 min.

(Z)-5-(2-methylbenzylidene)-3-phenyl-2-thioxothiazolidin-4-one **55b**

TLC R_f = 0.7 (DCM); **Reaction time**: 5 h; **Purification**: Filtration from methanol; **Yield**: 13 mg of yellow solid (0.04 mmol, 17 %); $^1\text{H-NMR}$ (400 MHz, CDCl_3) δ = 2.49 (s, 3 H, CH_3), 7.28-7.37 (m, 5 H, 5xAr-CH), 7.47-7.59 (m, 4 H, 4xAr-CH), 8.02 (s, 1 H, CH) ppm; $^{13}\text{C-NMR}$ (400 MHz, CDCl_3) δ = 20.2 (CH_3), 124.8 (Ar-C), 126.9 (Ar-CH), 128.2 (Ar-CH), 128.5 (2xAr-CH), 129.7

(2xAr-CH), 129.9 (Ar-CH), 131.0 (Ar-CH), 131.4 (CH), 131.6 (Ar-CH) 132.6 (Ar-C), 135.0 (Ar-C), 139.7 (Ar-C) ppm; **ESI-MS** m/z (%) = 312.1 [M+H]⁺ (100 %), 329.1 [M+NH₄]⁺ (20 %), 334.0 [M+Na]⁺ (10 %), 645.1 [2M+Na]⁺ (100 %); **HR-MS** m/z = 312.0515 [M+H]⁺ (calculated: 312.0511); **HPLC-Analysis (Method B)**: 99 %, R_t = 20.9 min.

(Z)-5-(3-methylbenzylidene)-3-phenyl-2-thioxothiazolidin-4-one **55c**^[327]

Reaction time: 5 h; **Purification**: Filtration from ethanol; **Yield**: 24 mg of yellow solid (0.08 mmol, 32 %); **¹H-NMR** (400 MHz, CDCl₃) δ = 2.44 (s, 3 H, CH₃), 7.27-7.31 (m, 3 H, 3xAr-CH), 7.35-7.43 (m, 3 H, 3xAr-CH), 7.50-7.60 (m, 3 H, 3xAr-CH), 7.78 (s, 1 H, CH) ppm; **¹³C-NMR** (400 MHz, CDCl₃) δ = 21.6 (CH₃), 123.1 (Ar-C), 128.1 (Ar-CH), 128.5 (2xAr-CH), 129.4 (Ar-CH), 129.7 (2xAr-CH), 129.9 (Ar-CH), 131.5 (Ar-CH), 131.9 (Ar-CH), 133.4 (Ar-C), 133.9 (CH), 135.0 (Ar-C), 139.4 (Ar-C), 167.8 (C=O), 193.8 (C=S) ppm; **ESI-MS** m/z (%) = 312.1 [M+H]⁺ (100 %), 329.1 [M+NH₄]³⁰ (, %) 645.1 [2M+Na]⁺ (20 %), 956.1 [3M+Na]⁺ (5 %); **HR-MS** m/z = 312.0515 [M+H]⁺ (calculated: 312.0511); **HPLC-Analysis (Method B)**: 99 %, R_t = 20.9 min.

(Z)-5-(4-methylbenzylidene)-3-phenyl-2-thioxothiazolidin-4-one **55d**^[328]

Z to E ratio 1:17 **Reaction time**: 4.5 h; **Purification**: Filtration from methanol; **Yield**: 35 mg of yellow solid (0.11 mmol, 47 %); **¹H-NMR** (400 MHz, CDCl₃) δ = 2.38 (s, 3 H, E-CH₃) 2.43 (s, 3 H, Z-CH₃), 7.16 (s, 1 H, E-CH), 7.20 (d, 2 H, ³J_{H,H} = 8.0 Hz, E-3,5-Ar-CH), 7.30 (d, 2 H, ³J_{H,H} = 8.0 Hz, 3,5-Ar-CH), 7.28-7.34 (m, 2 H, 2xAr-CH), 7.45 (d, 2 H, ³J_{H,H} = 8.0 Hz, 2,6-Ar-CH), 7.48-7.59 (m, 8 H, 8xAr-CH), 7.78 (s, 1 H, CH), 7.97 (d, 2 H, ³J_{H,H} = 8.0 Hz, E-2,6-Ar-CH) ppm; **¹³C-NMR** (400 MHz, CDCl₃) δ = 21.8 (CH₃), 122.2 (Ar-C), 128.5 (3,5-Ar-CH), 129.7 (2xAr-CH), 129.8 (Ar-CH), 130.3 (2xAr-CH), 130.8 (Ar-C), 131.0 (2,6-Ar-CH), 133.9 (CH), 135.1 (Ar-C), 142.0 (Ar-C), 167.9 (C=O), 193.7 (C=S) ppm; **ESI-MS** m/z (%) = 312.1 [M+H]⁺ (100 %), 329.1 [M+NH₄]⁺ (25 %), 640.1 [2M+NH₄]⁺ (15 %); **HR-MS** m/z = 312.0513 [M+H]⁺ (calculated: 312.0511); **HPLC-Analysis (Method B)**: 99 %, R_t = 21.0 min.

(Z)-5-(4-chlorobenzylidene)-3-phenyl-2-thioxothiazolidin-4-one **55e**^[329]

TLC R_f = 0.7 (DCM); **Reaction time**: 2 h; **Purification**: Filtration from methanol; **Yield**: 37 mg of yellow solid (0.11 mmol, 46 %); **¹H-NMR** (400 MHz, CDCl₃) δ = 7.29 (d, 2 H, ³J_{H,H} = 7.6 Hz, 3,5-Ar-CH), 7.47-7.60 (m, 5 H, 5xAr-CH), 7.56 (d, 2 H, ³J_{H,H} = 7.6 Hz, 2,6-Ar-CH), 7.74 (s, 1 H, CH) ppm; **¹³C-NMR** (400 MHz, DMSO-d₆) δ = 124.1 (Ar-C) 128.8 (2xAr-CH), 129.4 (2xAr-CH), 129.5 (Ar-C), 129.7 (2xAr-CH), 131.2 (Ar-CH), 132.0 (Ar-CH), 132.2 (2xAr-CH), 135.2 (Ar-C), 135.6 (Ar-C), 166.9 (C=O), 193.7 (C=S) ppm; **ESI-MS** m/z (%) = 332.0 [M+H]⁺ (100 %), 685.0 [2M+Na]⁺ (50 %); **HR-MS** m/z = 331.9969 [M+H]⁺ (calculated: 331.9965); **HPLC-Analysis (Method B)**: 99 %, R_t = 21.1 min.

(Z)-5-(4-ethynylbenzylidene)-3-phenyl-2-thioxothiazolidin-4-one **55f**

TLC R_f = 0.8 (DCM); **Reaction time**: 3 h; **Purification**: Flash-Chromatography CHCl₃ (R_f = 0.5); **Yield**: 14 mg of yellow solid (0.04 mmol, 18 %); **¹H-NMR** (400 MHz, CDCl₃) δ = 3.27 (s, 1 H, Alkyne-CH), 7.27-7.32 (m, 2 H, 2xAr-CH), 7.51 (d, 2 H, ³J_{H,H} = 8.4 Hz, 2,6-Ar-CH), 7.50-7.60

(m, 3 H, 3xAr-CH), 7.61 (d, 2 H, $^3J_{H,H} = 8.4$ Hz, 3,5-Ar-CH), 7.76 (s, 1 H, CH) ppm; **EI-MS** m/z (%) = 321.0 [M]⁺ (100 %), 158.0 [fragment]⁺ (100 %); **HR-MS** $m/z = 321.0277$ [M]⁺ (calculated: 321.0282); **HPLC-Analysis (Method B)**: 99 %, $R_t = 18.8$ min.

(Z)-4-((4-oxo-3-phenyl-2-thioxothiazolidin-5-ylidene)methyl)benzonitrile **55g**^[112]

TLC $R_f = 0.7$ (DCM); **Reaction time**: 3 h; **Purification**: Filtration from ethanol; **Yield**: 44 mg of yellow solid (0.14 mmol, 57 %); **¹H-NMR** (400 MHz, CDCl₃) $\delta = 7.27$ -7.30 (m, 2 H, 2xAr-CH), 7.51-7.60 (m, 3 H, 3-Ar-CH), 7.64 (d, 2 H, $^3J_{H,H} = 8.4$ Hz, 3,5-Ar-CH), 7.75 (s, 1 H, CH), 7.79 (d, 2 H, $^3J_{H,H} = 8.4$ Hz, 2,6-Ar-CH) ppm; **EI-MS** m/z (%) = 322.0 [M]⁺ (100 %), 159.0 [fragment]⁺ (100 %); **HR-MS** $m/z = 322.0228$ [M]⁺ (calculated: 322.0235); **HPLC-Analysis (Method B)**: 99 %, $R_t = 18.8$ min.

(Z)-5-(3-bromo-4-methoxybenzylidene)-3-phenyl-2-thioxothiazolidin-4-one **55h**^[112]

TLC $R_f = 0.6$ (DCM); **Reaction time**: 4 h; **Purification**: Filtration from methanol; **Yield**: 35 mg of yellow solid (0.09 mmol, 36 %); **¹H-NMR** (400 MHz, CDCl₃) $\delta = 3.99$ (s, 3 H, OCH₃), 7.02 (d, 1 H, $^3J_{H,H} = 8.6$ Hz, 4-Ar-CH), 7.27-7.31 (m, 2 H, 2xAr-CH), 7.48-7.59 (m, 3 H, 3xAr-CH), 7.54-7.57 (m, 1 H, 3-Ar-CH), 7.67 (s, 1 H, CH), 7.76 (d, 1 H, $^4J_{H,H} = 2.3$ Hz, 6-Ar-CH) ppm; **ESI-MS** m/z (%) = 408.0 [M+H]⁺ (100 %), 425.0 [M+NH₄]⁺ (50 %), 829.9 [2M+NH₄]⁺ (100 %), 1241.8 [3M+Na]⁺ (10 %); **HR-MS** $m/z = 405.9563$ [M+H]⁺ (calculated: 405.9566); **HPLC-Analysis (Method B)**: 99 %, $R_t = 21.2$ min.

(Z)-N-(4-((4-oxo-3-phenyl-2-thioxothiazolidin-5-ylidene)methyl)phenyl)acetamide **55i**^[330]

TLC $R_f = 0.1$ (DCM); **Reaction time**: 3 h; **Purification**: Filtration from methanol; **Yield**: 29 mg of yellow solid (0.08 mmol, 34 %); **¹H-NMR** (400 MHz, DMSO-d₆) $\delta = 2.10$ (s, 3 H, CH₃), 7.40-7.43 (m, 2 H, 2xAr-CH), 7.49-7.59 (m, 3 H, 3xAr-CH), 7.66 (d, 2 H, $^3J_{H,H} = 8.8$ Hz, 3,5-Ar-CH), 7.77 (s, 1 H, CH), 7.79 (d, 2 H, $^3J_{H,H} = 8.8$ Hz, 2,6-Ar-CH), 10.35 (s(br), 1 H, NHAc) ppm; **¹³C-NMR** (400 MHz, DMSO-d₆) $\delta = 24.2$ (CH₃) 119.3 (2,6-Ar-CH), 120.7 (Ar-C), 127.5 (Ar-C), 128.8 (2xAr-CH) 129.3 (2xAr-CH), 129.4 (Ar-CH), 132.0 (3,5-Ar-CH), 132.6 (CH), 135.3 (Ar-C), 141.8 (Ar-C), 167.1 (C=O), 169.0 (C=O), 193.9 (C=S) ppm; **ESI-MS** m/z (%) = 355.1 [M+H]⁺ (100 %), 709.1 [2M+H]⁺ (15 %), 1085.1 [3M+Na]⁺ (5 %); **HR-MS** $m/z = 355.0573$ [M+H]⁺ (calculated: 355.0569); **HPLC-Analysis (Method B)**: 99 %, $R_t = 18.3$ min; **HPLC-Analysis** : 100 %, $R_t = 33.9$ min.

(Z)-5-(4-(dimethylamino)benzylidene)-3-phenyl-2-thioxothiazolidin-4-one **55j**^[329]

mixture of Z to E 4:1 ratio **Reaction time**: 5 h; **Purification**: Filtration from methanol; **Yield**: 8 mg of red solid (0.02 mmol, 10 %); **¹H-NMR** (400 MHz, CDCl₃) $\delta = 3.08$ (s, 6 H, E-N(CH₃)₂), 3.11 (s, 6 H, Hz,)6.732dH,H9.0 HzE-3,5-Ar-CH₃, 6.80 (d, 2 H, $^3J_{H,H} = 9.0$ Hz, Z-3,5-Ar-CH), 7.03 (s, 1 H, E-CH), 7.28-7.31 (m, 2 H, 2xAr-CH), 7.46 (d, 2 H, $^3J_{H,H} = 9.0$ Hz, Z-2,6-Ar-CH), 7.49-7.58 (m, 3 H, 8xAr-CH), 7.73 (s, 1 H, CH), 8.16 (d, 2 H, $^3J_{H,H} = 9.0$ Hz, E-2,6-Ar-CH) ppm; **¹³C-NMR** (400 MHz, CDCl₃) $\delta = 40.5$ (CH₃) 112.6 (Z-3,5-Ar-CH), 128.6 (Ar-CH), 129.6 (Ar-CH), 133.4 (Z-2,6-Ar-CH), 134.9 (Z-CH) ppm; **ESI-MS** m/z (%) = 341.1 [M+H]⁺ (100 %),

681.1 [2M+H]⁺ (30 %); **HR-MS** m/z = 341.0781 [M+H]⁺ (calculated: 341.0777); **HPLC-Analysis (Method B)**: 83 %, R_t = 18.4 min.

(Z)-5-(3-nitrobenzylidene)-3-phenyl-2-thioxothiazolidin-4-one **55k**

Reaction time: 4 h; **Purification**: Filtration from methanol; **Yield**: 16 mg of yellow solid (0.05 mmol, 19 %); **¹H-NMR** (400 MHz, CDCl₃) δ = 7.27-7.32 (m, 2 H, 2xAr-CH), 7.52-7.61 (m, 3 H, 3xAr-CH), 7.72 (at, 1 H, ³J_{H,H} = 8.0 Hz, 5-Ar-CH), 7.81 (s, 1 H, CH), 7.86 (d, 1 H, ³J_{H,H} = 8.0 Hz, 4-Ar-CH), 8.32 (d, 1 H, ³J_{H,H} = 8.0 Hz, 6-Ar-CH), 8.41 (s, 1 H, 2-Ar-CH) ppm; **EI-MS** m/z (%) = 342.0 [M]⁺ (100 %), 179.0 [fragment]⁺ (100 %); **HR-MS** m/z = 342.0129 [M]⁺ (calculated: 342.0133); **HPLC-Analysis (Method B)**: 99 %, R_t = 19.8 min.

(Z)-5-(2-hydroxybenzylidene)-3-phenyl-2-thioxothiazolidin-4-one **55l**^[331]

TLC R_f = 0.5 (DCM); **Reaction time**: 3 h; **Purification**: Filtration from DCM; **Yield**: 9 mg of yellow solid (0.03 mmol, 12 %); **¹H-NMR** (400 MHz, CD₃OD) δ = 6.93 (d, 1 H, ³J_{H,H} = 8.4 Hz, 3-Ar-CH), 6.99 (at, 1 H, ³J_{H,H} = 7.6 Hz, 5-Ar-CH), 7.29-7.37 (m, 3 H, 3xAr-CH), 7.42-7.45 (m, 1 H, Ar-CH), 7.48-7.60 (m, 3 H, 3xAr-CH), 8.17 (s, 1 H, CH) ppm; **EI-MS** m/z (%) = 313.0 [M]⁺ (100 %), 178.0 [fragment]⁺ (90 %), 150.0 [fragment]⁺ (100 %). **HR-MS** m/z = 313.0224 [M]⁺ (calculated: 313.0231); **HPLC-Analysis (Method B)**: 98 %, R_t = 19.9 min.

(Z)-3-amino-2-thioxo-5-(3-(hydroxy)benzylidene)thiazolidin-4-one **55m**^[112]

TLC R_f = 0.2 (DCM); **Reaction time**: 3 h; **Purification**: Flash-Chromatography DCM (R_f = 0.2); **Yield**: 11 mg of yellow solid (0.04 mmol, 15 %); **¹H-NMR** (400 MHz, CDCl₃) δ = 5.22 (s(br), 1 H, OH), 6.95 (dd, 1 H, ^{3,4}J_{H,H} = 2.1, 8.1 Hz, 6-Ar-CH), 7.01 (s, 1 H, 2-Ar-CH), 7.14 (d, 1 H, ³J_{H,H} = 8.1 Hz, 4-Ar-CH), 7.27-7.31 (m, 2 H, 2-Ar-CH), 7.38 (t, 1 H, ³J_{H,H} = 8.1 Hz, 5-Ar-CH), 7.49-7.59 (m, 3 H, 3xAr-CH), 7.73 (s, 1 H, CH) ppm; **ESI-MS** m/z (%) = 314.0 [M+H]⁺ (100 %), 331.1 [M+NH₄]⁺ (30 %), 649.0 [2M+Na]⁺ (80 %), 962.1 [3M+Na]⁺ (20 %); **HR-MS** m/z = 314.0307 [M+H]⁺ (calculated: 314.0304); **HPLC-Analysis (Method B)**: 98 %, R_t = 18.7 min.

(Z)-5-(4-hydroxybenzylidene)-3-phenyl-2-thioxothiazolidin-4-one **55n**^[112]

Reaction time: 2 h; **Purification**: Filtration from methanol; **Yield**: 17 mg of yellow solid (0.05 mmol, 23 %); **¹H-NMR** (400 MHz, DMSO-d₆) δ = 6.97 (d, 2 H, ³J_{H,H} = 8.4 Hz, 3,5-Ar-CH), 7.40 (d, 2 H, ³J_{H,H} = 8.4 Hz, 2,6-Ar-CH), 7.49-7.60 (m, 5 H, 5 x Ar-CH), 7.76 (s, 1 H, CH), 10.52 (s, 1 H, OH) ppm; **ESI-MS** m/z (%) = 312.0 [M-H]⁻ (100 %); **HR-MS** m/z = 312.0155 [M-H]⁻ (calculated: 312.0158); **ESI-MS** m/z (%) = 314.0 [M+H]⁺ (100 %), 649.0 [2M+Na]⁺ (60 %); **HR-MS** m/z = 314.0308 [M+H]⁺ (calculated: 314.0304); **HPLC-Analysis** : 100 %, R_t = 34.3 min.

(5Z)-5-[(3,4-dihydroxyphenyl)methylidene]-3-phenyl-2-sulfanylidene-1,3-thiazolidin-4-one **55o**^[332]

TLC R_f = 0.3 (DCM/EtOAc 9:1); **Reaction time**: 4 h; **Purification**: Filtration from ethanol; **Yield**: 190 mg of yellow solid (0.58 mmol, 78 %); **¹H-NMR** (400 MHz, DMSO-d₆) δ = 6.91 (d, 1 H, ³J_{H,H} = 8.8 Hz, 5-Ar-CH), 7.07-7.12 (m, 2 H, 2,6-Ar-CH), 7.36-7.43 (m, 2 H, 2xAr-CH), 7.46-7.59 (m, 3 H, 3xAr-CH), 7.66 (s, 1 H, CH), 9.80 (s(0), 2 H, 2xOH) ppm; **¹³C-NMR** (400 MHz, DMSO-d₆) δ = 116.6 (Ar-CH), 124.4 (Ar-C), 125.4 (Ar-CH), 128.8 (Ar-CH), 129.3

(Ar-CH), 133.9 (CH), 135.4 (Ar-CH), 137.9 (Ar-C), 146.2 (Ar-CH), 167.0 (C=O), 193.8 (C=S), ppm; **ESI-MS** m/z (%) = 330.0 [M+H]⁺ (100 %), 347.1 [M+NH₄]⁺ (27 %), 676.1 [2M+NH₄]⁺ (32 %), 681.0 [2M+Na]⁺ (10 %); **HPLC-Analysis (Method B)**: 92 %, R_t = 17.4 min.

(Z)-5-(3-(benzyloxy)benzylidene)-3-phenyl-2-thioxothiazolidin-4-one **55p**

TLC R_f = 0.3 (Hexane/DCM 2:8); **Reaction time**: 4 h; **Purification**: Flash-Chromatography Hexane/DCM 2:8 (R_f = 0.3); **Yield**: 90 mg of yellow solid (0.23 mmol, 93 %); **¹H-NMR** (400 MHz, CDCl₃) δ = 5.15 (s, 2 H, CH₂), 7.08-7.12 (m, 2 H, 2xAr-CH), 7.14-7.17 (m, 1 H, 1xAr-CH), 7.27-7.59 (m, 11 H, 11xAr-CH), 7.75 (s, 1 H, CH) ppm; **¹³C-NMR** (300 MHz, CDCl₃) δ = 46.5 (CH₂), 100.4 (Ar-C or Ar-CH), 116.7 (Ar-C or Ar-CH), 119.5 (Ar-C or Ar-CH), 129.9 (Ar-C or Ar-CH), 133.2 (CH), 158.3 (C=O), 193.3 (C=S) ppm; **ESI-MS** m/z (%) = 404.1 [M+H]⁺ (100 %), 824.2 [2M+NH₄]⁺ (75 %), 1232.2 [3M+Na]⁺ (25 %), 1636.3 [4M+Na]⁺ (10 %); **HR-MS** m/z = 404.0774 [M]^H (calculated: 404.0773); **HPLC-Analysis (Method B)**: 99 %, R_t = 22.0 min.

(Z)-5-(4-(benzyloxy)benzylidene)-3-phenyl-2-thioxothiazolidin-4-one **55q**

TLC R_f = 0.6 (DCM); **Reaction time**: 1 h; **Purification**: Re-crystallisation from DCM/ethanol; **Yield**: 41 mg of yellow solid (0.10 mmol, 21 %); **¹H-NMR** (400 MHz, DMSO-d₆) δ = 5.22 (s, 2 H, CH₂Ph), 7.23 (d, 2 H, ³J_{3(5),2(6)} = 9.0 Hz, 3,5-Ar-CH), 7.33-7.45 (m, 5 H, 5xAr-CH), 7.46-7.59 (m, 5 H, 5xAr-CH), 7.68 (d, 2 H, ³J_{2(6),3(5)} = 9.0 Hz, 2,6-Ar-CH), 7.82 (s, 1 H, C-H) ppm; **¹H-NMR** (400 MHz, CDCl₃) δ = 4.15 (s, 2 H, CH₂), 7.10 (d, 2 H, ³J_{H,H} = 8.6 Hz, 3,5-Ar-CH), 7.27-7.31 (m, 2 H, 2xAr-CH), 7.33-7.47 (m, 5 H, 5xAr-CH), 7.51 (d, 2 H, ³J_{H,H} = 8.6 Hz, 2,6-Ar-CH), 7.53-7.59 (m, 3 H, 3xAr-CH), 7.75 (s, 1 H, CH) ppm; **¹³C-NMR** (400 MHz, CDCl₃) δ = 70.4 (CH₂), 100.1 (Ar-C), 109.2 (Ar-C), 116.0 (3,5-Ar-CH), 120.5 (Ar-C), 126.4 (Ar-CH), 127.6 (Ar-CH), 128.5 (2xAr-CH), 128.9 (Ar-CH), 129.7 (Ar-CH), 129.8 (Ar-CH), 133.0 (2,6-Ar-CH), 133.6 (CH), 135.1 (Ar-C), 136.2 (Ar-CH), 161.1 (Ar-C), 167.9 (C=O), 193.6 (C=S) ppm; **ESI-MS** m/z (%) = 404.1 [M+H]⁺ (100 %), 426.1 [M+Na]⁺ (70 %), 442.0 [M+K]⁺ (10 %), **HR-MS** m/z = 404.0774 [M+H]⁺ (calculated: 404.0773); **HPLC-Analysis (Method B)**: 99 %, R_t = 20.2 min.

(Z)-5-(3,4-bis(benzyloxy)benzylidene)-3-phenyl-2-thioxothiazolidin-4-one **55r**^[314]

TLC R_f = 0.9 (DCM); **Reaction time**: 1 h; **Purification**: Filtration from methanol; **Yield**: 144 mg of yellow solid (0.28 mmol, 60 %); **¹H-NMR** (400 MHz, DMSO-d₆) δ = 5.25 (s, 2 H, CH₂Ph), 5.27 (s, 2 H, CH₂Ph), 7.27-7.58 (m, 18 H, Ar-CH), 7.75 (s, 1 H, C-H) ppm; **¹H-NMR** (400 MHz, CDCl₃) δ = 5.19 (s, 4 H, 2xCH₂), 6.90-7.06 (m, 3 H, 3xAr-CH), 7.14-7.51 (m, 15 H, 15xAr-CH), 7.59 (s, 1 H, CH) ppm; **¹³C-NMR** (400 MHz, CDCl₃) δ = 71.1 (CH₂), 71.4 (CH₂), 114.3 (Ar-CH), 116.1 (Ar-CH), 120.8 (Ar-C), 126.2 (Ar-CH), 126.7 (Ar-C), 127.3 (Ar-CH), 127.4 (Ar-CH), 128.3 (Ar-CH), 128.5 (Ar-CH), 128.8 (Ar-CH), 128.9 (Ar-CH), 129.7 (Ar-CH), 129.8 (Ar-CH), 133.8 (CH), 135.1 (Ar-C), 136.4 (Ar-C), 136.6 (Ar-C), 149.1 (Ar-C), 151.6 (Ar-C), 167.8 (C=O), 193.5 (C=S) ppm; **ESI-MS** m/z (%) = 510.1 [M+H]⁺ (100 %), 532.1 [M+Na]⁺ (30 %), 548.1 [M+K]⁺

(10 %); **HR-MS** m/z = 510.1185 $[M+H]^+$ (calculated: 510.1192); **ESI-MS** m/z (%) = 510.1 $[M+H]^+$ (100 %), 527.1 $[M+NH_4]^+$ (8 %), 532.6 $[M+Na]^+$ (12 %); **HPLC-Analysis (Method B)**: 89 %, R_t = 20.8 min.

9.13 Synthesis of heterocyclic modified rhodanine, thiazolidine-2,4-dione, N-amino rhodanine and N-phenyl rhodanine derivatives 56a–d, 57a–d, 58a–i, and 59a–c

(Z)-5-(pyridin-4-ylmethylene)-2-thioxothiazolidin-4-one **36ag**^[333]

Reaction time: 4–16 h; **TLC** R_f = 0.1 (hexane/EtOAc 6:4); **Purification**: Filtration from methanol; **Yield**: 93 mg of yellow solid (0.42 mmol, 50 %); **Yield**: 400 mg of green solid (1.80 mmol, 96 %); **¹H-NMR** (400 MHz, DMSO- d_6) δ = 7.55 (d, 2 H, $^3J_{H,H}$ = 6.2 Hz, 2,6-Pyr-CH), 7.60 (s, 1 H, CH), 8.73 (d, 2 H, $^3J_{H,H}$ = 6.2 Hz, 3,5-Pyr-CH) ppm; **ESI-MS** m/z (%) = 223.0 $[M+H]^+$ (100 %), 445.1 $[2M+H]^+$ (4 %), 462.2 $[2M+NH_4]^+$ (5 %); **HPLC-Analysis (Method B)**: 92 %, R_t = 16.7 min.

(Z)-5-(pyridin-3-ylmethylene)-2-thioxothiazolidin-4-one **36af**^[334]

TLC R_f = 0.4 (DCM); **Reaction time**: 4 h; **Purification**: Filtration from methanol; **Yield**: 97 mg of yellow solid (0.44 mmol, 52 %); **¹H-NMR** (400 MHz, DMSO- d_6) δ = 7.56 (dd, 1 H, $^3J_{H,H}$ = 4.7, 7.9 Hz, 4-Ar-CH), 7.61 (s, 1 H, CH), 7.93 (d, 1 H, $^3J_{H,H}$ = 7.9 Hz, 3-Ar-CH), 8.61 (dd, 1 H, $^{3,4}J_{H,H}$ = 4.7, 1.0 Hz, 5-Ar-CH), 8.82 (d, 1 H, $^4J_{H,H}$ = 1.7 Hz, 1-Ar-CH) ppm; **¹³C-NMR** (400 MHz, DMSO- d_6) δ = 124.2 (4-Ar-CH), 125.7 (CH), 129.8 (Ar-C), 130.8 (Ar-C), 136.1 (3-Ar-CH), 150.1 (5-Ar-CH), 151.5 (1-Ar-CH), 172.0 (C=O), 197.3 (C=S) ppm; **EI-MS** m/z (%) = 222.0 $[M]^+$ (100 %), 135.0 [fragment] $^+$ (100 %); **HR-MS** m/z = 221.9916 $[M]^+$ (calculated: 221.9922); **HPLC-Analysis (Method B)**: 98 %, R_t = 11.2 min.

(Z)-5-(pyridin-2-ylmethylene)-2-thioxothiazolidin-4-one **36ad**^[335]

TLC R_f = 0.1 (DCM); **Reaction time**: 4 h; **Purification**: Re-crystallisation from methanol; **Yield**: 145 mg of yellow crystals (0.65 mmol, 59 %); **¹H-NMR** (400 MHz, DMSO- d_6) δ = 7.44 (ddd, 1 H, $^{3,4}J_{2\text{-Ar-CH},1(3,4)\text{Ar-CH}}$ = 4.8, 7.2, 1.3 Hz, 4-Ar-CH), 7.68 (s, 1 H, C-H), 7.90 (dd, 1 H, $^{3,4}J_{H,H}$ = 7.5, 0.5 Hz, 6-Ar-CH), 7.94 (ddd, 1 H, $^{3,4}J_{H,H}$ = 7.5, 7.2, 1.3 Hz, 5-Ar-CH), 8.79 (ddd, 1 H, $^{3,4}J_{H,H}$ = 4.8, 0.5, 0.5 Hz, 3-Ar-CH), 13.67 (s(br), 1 H, NH) ppm; **¹³C-NMR** (400 MHz, DMSO- d_6) δ = 124.0 (4-Ar-CH), 127.5 (CH), 128.2 (6-Ar-CH), 129.7 (Ar-C), 137.6 (5-Ar-CH), 149.5 (3-Ar-CH), 151.1 (Ar-C), 169.4 (C=O), 202.0 (C=S) ppm; **ESI-MS** m/z (%) = 222.9 $[M+H]^+$ (100 %), 445.0 $[2M+H]^+$ (10 %); **HR-MS** m/z = 222.9996 $[M+H]^+$ (calculated: 222.9994); **HPLC-Analysis (Method B)**: 99 %, R_t = 16.2 min.

(5Z)-5-[(4-tert-butylphenyl)methylidene]-2-sulfanylidene-1,3-thiazolidin-4-one **36ab**^[336]

TLC R_f = 0.8 (DCM/EtOAc 9:1); **Reaction time**: 4 h; **Purification**: Filtration from ethanol; **Yield**: 380 mg of yellow solid (1.37 mmol, 78 %); **¹H-NMR** (400 MHz, DMSO- d_6) δ = 1.29

(s, 9 H, 3xCH₃), 7.51 (d, 2 H, ³J_{H,H} = 8.6 Hz, 3,5-Ar-CH), 7.52 (s, 1 H, CH), 7.55 (H,H, 2 H, ³J_{8.6 Hz} = 2,6-Ar-CH, 3) 13.80 (s(br), 1 H, NH) ppm; ¹³C-NMR (400 MHz, DMSO-d₆) δ = 30.8 (3xCH₃), 34.8 (C(CH₃)₃), 125.4 (Ar-C), 126.3 (2,6-Ar-CH), 129.2 (Ar-C), 130.0 (Ar-C), 130.3 (3,5-Ar-CH), 130.7 (CH), 153.4 (C=O), 197.1 (C=S) ppm; **ESI-MS** m/z (%) = 278.1 [HM+]¹⁰⁰ (, %) 295.1 [NH₄M+]⁴⁵ (; %) **HR-MS** m/z = 278.0672 [M+H]⁺ (calculated: 278.0668); **HPLC-Analysis (Method B)**: 84 %, R_t = 21.4 min.

(5Z)-5-(3-[(4-methoxyphenyl)methoxy]phenylmethylidene)-2-sulfanylidene-1,3-thiazolidin-4-one **36x**

TLC R_f = 0.8 (DCM/EtOAc 9:1); **Reaction time**: 4 h; **Purification**: Filtration from ethanol; **Yield**: 380 mg of yellow solid (1.06 mmol, 85 %); ¹H-NMR (400 MHz, DMSO-d₆) δ = 3.75 (s, 3 H, OCH₃), 5.08 (s, 2 H, CH₂), 6.95 (d, 2 H, ³J_{H,H} = 8.7 Hz, 3',5'-Ar-CH), 7.12-7.17 (m, 2 H, 4,6-Ar-CH), 7.19-7.21 (m, 1 H, 2-Ar-CH), 7.40 (d, 2 H, ³J_{H,H} = 8.7 Hz, 2',6'-Ar-CH), 7.45 (at, 1 H, ³J_{H,H} = 8.0 Hz, 5-Ar-CH), 7.59 (s, 1 H, CH), 13.85 (s(br), 1 H, NH) ppm; ¹³C-NMR (400 MHz, DMSO-d₆) δ = 55.1 (OCH₃), 69.2 (CH₂), 113.9 (3',5'-Ar-CH), 116.4 (2-Ar-CH), 117.6 (4 or 6-Ar-CH), 122.6 (4 or 6-Ar-CH), 126.3 (Ar-C), 128.5 (Ar-C), 129.6 (2',6'-Ar-CH), 130.6 (5-Ar-CH), 131.3 (CH), 134.4 (Ar-C), 158.8 (Ar-C), 159.1 (C=O), 196.0 (C=S) ppm; **ESI-MS** m/z (%) = 358.1 [M+H]⁺ (100 %), 375.1 [M+NH₄]⁺ (75 %), 380.0 [M+Na]⁺ (80 %), 732.1 [2M+NH₄]⁺ (100 %), **HR-MS** m/z = 358.0571 [M+H]⁺ (calculated: 358.0566); **HPLC-Analysis (Method B)**: 100 %, R_t = 20.7 min.

(5Z)-5-(3-[(4-methoxyphenyl)methoxy]phenylmethylidene)-1,3-thiazolidine-2,4-dione **48t**

TLC R_f = 0.5 (Hexane/EtOAc 8:2); **Reaction time**: 4 h; **Purification**: Filtration from ethanol; **Yield**: 440 mg of white solid (1.29 mmol, 91 %); ¹H-NMR (400 MHz, DMSO-d₆) δ = 3.75 (s, 3 H, OCH₃), 5.06 (s, 2 H, CH₂), 6.95 (d, 2 H, ³J_{H,H} = 8.5 Hz, 3',5'-Ar-CH), 7.02 (d, 1 H, ³J_{H,H} = 7.7 Hz, 4-Ar-CH), 7.13 (d, 1 H, ³J_{H,H} = 7.5 Hz, 6-Ar-CH), 7.17 (s, 1 H, 2-Ar-CH), 7.35-7.42 (m, 1 H, 5-Ar-CH), 7.39 (d, 2 H, ³J_{H,H} = 8.5 Hz, 2',6'-Ar-CH), 7.50 (s, 1 H, CH) ppm; ¹³C-NMR (400 MHz, DMSO-d₆) δ = 55.1 (OCH₃), 69.0 (CH₂Ar), 113.9 (3',5'-Ar-CH), 115.6 (2-Ar-CH), 115.8 (4-Ar-CH), 121.8 (6-Ar-CH), 126.8 (CH), 128.7 (Ar-C), 129.6 (2',6'-Ar-CH), 130.1 (5-Ar-CH), 135.9 (Ar-C), 158.6 (C=O), 159.1 (C=O) ppm; **HPLC-Analysis (Method B)**: 88 %, R_t = 19.1 min.

(Z)-5-(pyridin-4-ylmethylene)thiazolidine-2,4-dione **48s**^[315]

Reaction time: 16 h; **Purification**: Filtration from ethanol; **Yield**: 70 mg of white solid (0.34 mmol, 48 %); ¹H-NMR (400 MHz, DMSO-d₆) δ = 7.53 (dd, 2 H, ^{3,5}J_{H,H} = 1.5, 4.6 Hz, 3,5-Ar-CH), 7.67 (s, 1 H, CH), 8.70 (dd, 2 H, ^{3,5}J_{H,H} = 1.5, 4.6 Hz, 2,6-Ar-CH) ppm; **ESI-MS** m/z (%) = 207.0 [M+H]⁺ (100 %); **HR-MS** m/z = 207.0223 [M+H]⁺ (calculated: 207.0223); **HPLC-Analysis (Method B)**: 97 %, R_t = 2.7 min.

(Z)-5-(pyridin-3-ylmethylene)thiazolidine-2,4-dione **48q**^[315]

Reaction time: 16 h; **Purification**: Filtration from ethanol; **Yield**: 51 mg of white solid (0.25

mmol, 53 %); **¹H-NMR** (400 MHz, DMSO-*d*₆) δ = 7.51 (dd, 1 H, $^3J_{\text{H,H}}$ = 8.1, 4.8 Hz, 5-Pyr-CH), 7.56 (s, 1 H, CH), 7.93 (adt, 1 H, $^{3,4}J_{\text{H,H}}$ = 8.1, 2.0 Hz, 6-Pyr-CH), 8.54 (dd, 1 H, $^{3,4}J_{\text{H,H}}$ = 4.8, 1.6 Hz, 4-Pyr-CH), 8.78 (d, 1 H, $^4J_{\text{H,H}}$ = 2.1 Hz, 2-Pyr-CH) ppm; **¹³C-NMR** (400 MHz, DMSO-*d*₆) δ = 123.3 (CH), 124.0 (5-Pyr-CH), 130.6 (Ar-C), 135.4 (6-Pyr-CH), 149.3 (4-Pyr-CH), 150.9 (2-Pyr-CH), 171.3 (C=O), 175.0 (C=O) ppm; **ESI-MS** m/z (%) = 207.0 [M+H]⁺ (100 %); **HR-MS** m/z = 207.0223 [M+H]⁺ (calculated: 207.0223); **HPLC-Analysis (Method B)**: 99 %, R_t = 11.5 min.

(Z)-5-(pyridin-2-ylmethylene)thiazolidine-2,4-dione **48r**^[315]

Reaction time: 16 h; **Purification**: Filtration from ethanol; **Yield**: 26 mg of brown solid (0.13 mmol, 24 %); **¹H-NMR** (400 MHz, DMSO-*d*₆) δ = 7.31 (ddd, 1 H, $^{3,4}J_{\text{H,H}}$ = 1.2, 4.8, 7.5 Hz, 4-Ar-CH), 7.54 (s, 1 H, CH), 7.69 (dd, 1 H, $^3J_{\text{H,H}}$ = 1.2, 7.8 Hz, 2-Ar-CH), 7.85 (ddd, 1 H, $^{3,4}J_{\text{H,H}}$ = 1.8, 7.5, 7.8 Hz, 3-Ar-CH), 8.69 (d, 1 H, $^3J_{\text{H,H}}$ = 4.8 Hz, 5-Ar-CH) ppm; **ESI-MS** m/z (%) = 207.0 [M+H]⁺ (100 %); **HR-MS** m/z = 207.0223 [M+H]⁺ (calculated: 207.0223); **HPLC-Analysis** : 99.9 %, R_t = 24.8 min; **HPLC-Analysis (Method B)**: 99 %, R_t = 11.5 min.

(Z)-3-amino-5-(pyridin-2-ylmethylene)-2-thioxothiazolidin-4-one **54ab**

TLC R_f = 0.1 (DCM); **Reaction time**: 4 h; **Purification**: Filtration from methanol; **Yield**: 105 mg of yellow solid (0.44 mmol, 57 %); **¹H-NMR** (400 MHz, DMSO-*d*₆) δ = 5.91 (s, 2 H, NH₂), 7.46 (ddd, 1 H, $^{3,4}J_{\text{H,H}}$ = 4.8, 6.8, 1.9 Hz, 4-Ar-CH), 7.87 (s, 1 H, C-H), 7.94 (dd, 1 H, $^{3,4}J_{\text{H,H}}$ = 7.8, 1.9 Hz, 6-Ar-CH), 7.96 (ddd, 1 H, $^{3,4}J_{\text{H,H}}$ = 7.8, 6.8, 1.7 Hz, 5-Ar-CH), 8.79-8.81 (m, 1 H, 3-Ar-CH) ppm; **¹³C-NMR** (400 MHz, DMSO-*d*₆) δ = 124.2 (4-Ar-CH), 124.8 (Ar-C), 128.3 (6-Ar-CH), 128.8 (CH), 137.7 (5-Ar-CH), 149.5 (3-Ar-CH), 151.3 (Ar-C), 163.8 (C=O), 194.2 (C=S) ppm; **ESI-MS** m/z (%) = 238.0 [M+H]⁺ (100 %), 260.0 [M+Na]⁺ (10 %); **HR-MS** m/z = 238.0104 [M+H]⁺ (calculated: 238.0103); **HPLC-Analysis** : 99.9 %, R_t = 27.2 min; **HPLC-Analysis (Method B)**: 99 %, R_t = 16.2 min.

(Z)-3-phenyl-5-(pyridin-2-ylmethylene)-2-thioxothiazolidin-4-one **55z**^[337]

TLC R_f = 0.7 (DCM); **Reaction time**: 4 h; **Purification**: Filtration from methanol; **Yield**: 97 mg of yellow solid (0.33 mmol, 72 %); **¹H-NMR** (400 MHz, DMSO-*d*₆) δ = 7.23-7.77 (m, 6 H, 6 x Ar-CH), 7.81-8.10 (m, 3 H, 3xAr-CH), 8.85 (s, 1 H, CH) ppm; **¹³C-NMR** (400 MHz, DMSO-*d*₆) δ = 124.1 (Ar-CH), 127.7 (Ar-C), 128.3 (2xAr-CH), 128.8 (2xAr-CH), 129.2 (2xAr-CH), 129.4 (Ar-CH), 135.2 (Ar-C), 137.7 (Ar-CH), 149.6 (CH), 151.3 (Ar-C), 167.0 (C=O), 200.4 (C=S) ppm; **ESI-MS** m/z (%) = 299.1 [M+H]⁺ (100 %); **HR-MS** m/z = 299.0310 [M+H]⁺ (calculated: 299.0307); **HPLC-Analysis (Method B)**: 99 %, R_t = 19.7 min.

9.14 Reduction of the rhodanine derivative 36b

Sodium borohydrite (10 mg, 0.27 mmol) was dissolved in pyridine (0.2 mL). The mixture was stirred at 30 °C for 15 min, then the temperature was increased to 65 °C and lithium chlo-

rid (17.2 mg, 0.41 mmol) in pyridine (0.2 mL) was added. After 2 h, THF (2 mL) was added and the reaction mixture was heated under reflux for 30 min. After the reaction mixture has reached ambient temperature **36b** (20 mg, 0.09 mmol) was added in 3 portions. The mixture was heated to reflux for 2.5 h, until TLC (DCM/EtOAc 9:1, R_f 0.9) showed complete consumption of starting material. The cooled crude was quenched with 1 N HCl (pH 6), extracted with EtOAc (3x5 mL), dried over $MgSO_4$, filtered and concentrated. Purification by flash chromatography (DCM, R_f 0.6) afforded **36ac** (11.0 mg, 55 %) as a yellow oil.

5-benzyl-2-thioxothiazolidin-4-one **36ac**^[338]

TLC R_f = 0.3 (Cyclohexane/EtOAc 8:2); **Reaction time**: 2.5 h; **Purification**: Flash-Chromatography DCM (R_f = 0.4); **Yield**: 11 mg of white solid (0.05 mmol, 55 %); **1H -NMR** (400 MHz, $CDCl_3$) δ = 3.07 (dd, 1 H, $^1J_{H,H}$ = 9.7, 14.0 Hz, 2,3), 3.49 (dd, 1 H, $^1J_{H,H}$ = 3.9, 14.0 Hz, 2,3), 4.38 (dd, 1 H, $J_{H,H}$ = 3.9, 9.7 Hz, CH), 7.59 (dd, 2 H, $^{3,4}J_{H,H}$ = 6.6, 7.6 Hz, 3,5-Ar-CH), 8.05 (ddd, 1 H, $^{3,4}J_{H,H}$ = 1.5, 7.7 Hz, 4-Ar-CH), 8.76 (dd, 2 H, $^{3,4}J_{H,H}$ = 1.5, 6.6 Hz, 2,3-Ar-CH) ppm; **ESI-MS** m/z (%) = 222.0 $[M-H]^-$ (100 %); **HR-MS** m/z = 222.0054 $[M-H]^-$ (calculated: 222.0053); **HPLC-Analysis (Method B)**: 64 %, R_t = 18.4 min.

pyridine-borane **73**

1H -NMR (400 MHz, $CDCl_3$) δ = 2.56 (q, 3 H, $^1J_{B,H}$ = 92.3 Hz, BH_3), 7.45-7.52 (m, 2 H, 3,5-Pyr-CH), 7.86-7.99 (m, 1 H, 4-Pyr-CH), 8.57 (d, 2 H, $^3J_{H,H}$ = 5.7 Hz, 2,6-Pyr-CH) ppm.

Reduction of Compound 36y using Hantzsch ester reduction

The general procedure is as described for **27a**.

5-[4-(benzyloxy)phenyl]methyl-2-sulfanylidene-1,3-thiazolidin-4-one **75a**

TLC R_f = 0.3 (Hexane/EtOAc 8:2); **Reaction time**: 16 h; **Purification**: Flash-Chromatography Hexane/EtOAc 8:2 (R_f = 0.3); **Yield**: 122 mg of yellow solid (0.37 mmol, 46 %); **1H -NMR** (400 MHz, $CDCl_3$) δ = 3.10 (dd, 1 H, $^{2,3}J_{H,H}$ = 14.2, 9.8 Hz, E-CHH), 3.44 (dd, 1 H, $^{2,3}J_{H,H}$ = 14.2, 4.0 Hz, Z-CHH), 4.56 (dd, 1 H, $^3J_{H,H}$ = 9.8, 4.0 Hz, CH), 5.03 (s, 2 H, CH_2), 6.92 (d, 2 H, $^3J_{H,H}$ = 8.6 Hz, 3,5-Ar-CH), 7.13 (d, 2 H, $^3J_{H,H}$ = 8.6 Hz, 2,6-Ar-CH), 7.29-7.44 (m, 5 H, 5xAr-CH) 9.89 (s(br), 1 H, NH) ppm; **^{13}C -NMR** (400 MHz, $CDCl_3$) δ = 37.5 (E,Z- CH_2), 57.1 (CH), 70.1 (CH_2 Ar), 115.3 (3,5-Ar-CH), 127.6 (Ar-CH), 127.9 (Ar-C), 128.1 (Ar-CH), 128.7 (Ar-CH), 130.3 (2,6-Ar-CH), 136.8 (Ar-C), 158.4 (Ar-C), 176.9 (C=O), 200.4 (C=S) ppm; **HPLC-Analysis (Method B)**: 98 %, R_t = 16.3 min.

3,5-diethyl 2,6-dimethylpyridine-3,5-dicarboxylate **74**^[339]

TLC R_f = 0.3 (Hexane/EtOAc 8:2); **1H -NMR** (400 MHz, $CDCl_3$) δ = 1.42 (t, 6 H, $^3J_{H,H}$ = 7.1 Hz, 2x CH_3), 2.85 (s, 6 H, 2x CH_3), 4.40 (q, 4 H, $^1J_{H,H}$ = 7.1 Hz, 2x CH_2CH_3) 8.68 (s, 1 H, Ar-CH) ppm; **ESI-MS** m/z (%) = 252.1 $[M+H]^+$ (100 %).

9.15 Reduction of thiazolidine-2,4-dione derivatives 48p and 48m

The procedure is as described for **27b** and **27c**.

5-[(3,4-dihydroxyphenyl)methyl]-1,3-thiazolidine-2,4-dione **48v**^[340]

TLC R_f = 0.2 (CHCl₃/MeOH 95:5); **Reaction time**: 16 h; **Purification**: Flash-Chromatography CHCl₃/MeOH 95:5 (R_f = 0.2); **Yield**: 201 mg of white solid (0.84 mmol, 100 %); **¹H-NMR** (400 MHz, DMSO-d₆) δ = 2.91 (dd, 1 H, ^{2,3} $J_{H,H}$ = 9.3, 14.1 Hz, anti-CHH), 3.19 (dd, 1 H, ^{2,3} $J_{H,H}$ = 4.2, 14.1 Hz, syn-CHH), 4.78 (dd, 1 H, ³ $J_{H,H}$ = 4.2, 9.3 Hz, CH), 6.47 (dd, 1 H, ^{3,4} $J_{H,H}$ = 2.1, 8.0 Hz, 6-Ar-CH), 6.60 (d, 1 H, ⁴ $J_{H,H}$ = 2.1 Hz, 2-Ar-CH), 6.64 (d, 1 H, ³ $J_{H,H}$ = 8.0 Hz, 5-Ar-CH), 8.83 (s(br), 1 H, OH), 8.87 (s(br), 1 H, OH), 11.98 (s(br), 1 H, NH) ppm; **¹³C-NMR** (400 MHz, DMSO-d₆) δ = 36.7 (CH₂), 53.3 (CH), 115.5 (5-Ar-CH), 116.5 (2-Ar-CH), 119.9 (6-Ar-CH), 127.5 (Ar-C), 144.3 (Ar-C), 145.1 (Ar-C), 172.0 (C=O), 175.9 (C=O) ppm; **ESI-MS** m/z (%) = 238.0 [M-H]⁻ (100 %), 477.0 [2M-H]⁻ (40 %); **HR-MS** m/z = 238.0177 [M-H]⁻ (calculated: 238.0180).

5-[4-(benzyloxy)phenyl]methyl-1,3-thiazolidine-2,4-dione **48u**^[341]

Reaction time: 4 h; **Yield**: 63 mg of white solid (0.20 mmol, 100 %); **¹H-NMR** (400 MHz, CDCl₃) δ = 3.08 (dd, 1 H, ^{2,3} $J_{H,H}$ = 14.2, 9.6 Hz, E-CHH), 3.45 (dd, 1 H, ^{2,3} $J_{H,H}$ = 14.2, 3.9 Hz, Z-CHC), 3.71 (s, 1 H, NH), 4.49 (dd, 1 H, ³ $J_{H,H}$ = 9.6, 3.9 Hz, CH), 5.03 (s, 2 H, CH₂), 6.92 (d, 2 H, ³ $J_{H,H}$ = 8.6 Hz, 3,5-Ar-CH), 7.14 (d, 2 H, ³ $J_{H,H}$ = 8.6 Hz, 2,6-Ar-CH), 7.30-7.44 (m, 5 H, 5xAr-CH) ppm; **¹³C-NMR** (400 MHz, CDCl₃) δ = 37.9 (E,ZCH₂), 53.9 (CH), 70.1 (CH₂), 115.3 (3,5-Ar-CH), 127.6 (2xAr-CH), 128.1 (Ar-C), 128.2 (Ar-CH), 128.7 (2xAr-CH), 130.5 (2,6-Ar-CH), 136.9 (Ar-C), 158.4 (Ar-C), 171.1 (C=O), 174.8 (C=O) ppm; **ESI-MS** m/z (%) = 331.1 [M+NH₄]⁺ (13 %); **HPLC-Analysis (Method B)**: 64 %, R_t = 17.3 min.

9.16 Alkylation of the thiocarbonyl in rhodanine derivatives

Representative procedure for the alkylation of the thiocarbonyl in rhodanine derivatives

Rhodanine (666 mg, 5 mmol, 1.0 eq) were dissolved in NaOH_(aq) (2 %, 12 mL). Ethyl-iodide **63** (342 mg, 5.5 mmol, 1.1 eq) were added and the reaction mixture was stirred at rt for 16 h. The crude was extracted with DCM (3x15 mL). The combined organic fractions were washed with NaHCO₃ (sat, 10 mL), dried over MgSO₄, filtered and concentrated. Re-crystallisation from methanol yields the substituted thiocarbonyl **63a** as yellow solid.

2-(ethylsulfanyl)-5H-1,3-thiazol-4-one **67a**^[342]

TLC R_f = 0.3 (Hexane/EtOAc 8:2); **Purification**: Re-crystallisation from methanol; **Yield**: 726 mg of yellow solid (4.50 mmol, 90 %); **¹H-NMR** (400 MHz, MeOD) δ = 1.48 (t, 3 H, ³ $J_{H,H}$ = 7.4 Hz, CH₃), 3.37 (q, 2 H, ³ $J_{H,H}$ = 7.4 Hz, CH₂CH₃), 4.18 (s, 2 H, CH₂) ppm.

Alkylating agent: iodo-acetic acid sodium salt: [(4-oxo-5H-1,3-thiazol-2-yl)sulfanyl]acetic acid **64a**^[343]

TLC R_f = 0.2 (DCM/MeOH 7:3); **Reaction time**: 12 h; **Purification**: Filtration from methanol; **Yield**: 638 mg of white solid (3.34 mmol, 33 %); **¹H-NMR** (400 MHz, DMSO- d_6) δ = 3.78 (s, 2 H, $\underline{\text{CH}_2}$), 4.18 (s, 2 H, $\underline{\text{CH}_2}$) ppm; **¹³C-NMR** (400 MHz, DMSO- d_6) δ = 33.8 ($\underline{\text{CH}_2}$), 45.0 ($\underline{\text{CH}_2}$), 168.1 ($\underline{\text{C}}$), 171.9 ($\underline{\text{C=O}}$), 172.1 ($\underline{\text{C=O}}$) ppm;

Finkelstein reaction to iodo-acetic acetate **66**: To a solution of NaI (7683 mg, 51.26 mmol, 1.2 eq) in acetone (150 mL) was added ethyl 2-bromoacetate **65** (4.83 mL, 42.78 mmol, 1.0 eq). The reaction mixture was stirred 12 h in the dark. After 12 h, sodium bromide was filtered and the filtrate was concentrated. The crude was extracted between H₂O (40 mL) and EtOAc (3x50 mL). The combined organic fraction were washed with Na₂S₂O₃ (sat, 20 mL), brine (20 mL) and was dried over MgSO₄, filtered and concentrated. The changed NMR shift and mass spec confirmed the product.

Ethyl iodoacetate **66**^[344]

TLC R_f = 0.5 (Hexane/EtOAc 9:1); **Reaction time**: 12 h; **Yield**: 8988 mg of clear oil (42.01 mmol, 98 %); **¹H-NMR** (400 MHz, CDCl₃) δ = 1.27 (t, 3 H, $^3J_{\text{H,H}}$ = 7.1 Hz, $\underline{\text{CH}_3}$), 3.67 (s, 2 H, $\underline{\text{CH}_2}$), 4.19 (q, 2 H, $^3J_{\text{H,H}}$ = 7.1 Hz, $\underline{\text{CH}_2\text{CH}_3}$) ppm; **APCI-MS** m/z (%) = 215.0 [$\text{M}+\text{H}$]⁺ (100 %), 428.9 [$2\text{M}+\text{H}$]⁺ (45 %), **HR-MS** m/z = 214.9561 [$\text{M}+\text{H}$]⁺ (calculated: 214.9563).

Procedure as describes for **105a** with iodo-acetic acetate **66** as alkylating agent.

(4-oxo-5H-1,3-thiazol-2-yl)sulfanyl acetic acid **67b**^[343]

TLC R_f = 0.1 (Hexane/EtOAc 95:5); **Yield**: 1012 mg of white solid (5.29 mmol, 53 %); **Reaction time**: 16 h; **Purification**: Flash-Chromatography Hexane/EtOAc 95:5 (R_f = 0.1); **¹H-NMR** (400 MHz, DMSO- d_6) δ = 3.78 (s, 2 H, $\underline{\text{CH}_2}$), 4.18 (s, 2 H, $\underline{\text{CH}_2}$) ppm; **¹³C-NMR** (400 MHz, DMSO- d_6) δ = 33.8 ($\underline{\text{CH}_2}$), 45.0 ($\underline{\text{CH}_2}$), 168.1 ($\underline{\text{C}}$), 171.9 ($\underline{\text{C=O}}$), 172.1 ($\underline{\text{C=OOH}}$) ppm; **ESI-MS** m/z (%) = 190.0 [$\text{M}-\text{H}$]⁻ (100 %), 380.9 [$2\text{M}-\text{H}$]⁻ (15 %); **HR-MS** m/z = 189.9638 [$\text{M}-\text{H}$]⁻ (calculated: 189.9638).

(4-oxo-5H-1,3-thiazol-2-yl)sulfanide TEAH salt **68**^[345]

Rhodanine **36** (6.65 g, 0.05 mol, 1.0 eq) was dissolved in iso-propanol (25 mL). NEt₃ (7 mL, 0.05 mol, 1.0 eq) was added to the reaction mixture. The yellow mixture was stirred at 100 °C for 15 min. Upon cooling, yellow crystals were forming. The crystals were filtered and re-crystallised from toluene to afford **68** as purple crystals. **Reaction time**: 15 min; **Purification**: Re-crystallisation from isopropanol, toluene; **Yield**: 8006 mg of purple crystals (34.16 mmol, 68 %); **¹H-NMR** (400 MHz, DMSO- d_6) δ = 1.14 (t, 9 H, $^3J_{\text{H,H}}$ = 7.3 Hz, 3x $\underline{\text{CH}_3}$), 3.02 (q, 6 H, $^3J_{\text{H,H}}$ = 7.3 Hz, 3x $\underline{\text{CH}_2}$), 3.82 (s, 2 H, $\underline{\text{CH}_2}$) ppm; **¹³C-NMR** (400 MHz, CDCl₃) δ = 9.0 (3x $\underline{\text{CH}_3}$), 42.3 ($\underline{\text{CH}_2}$), 45.6 (3x $\underline{\text{CH}_2}$) ppm; **ZQ-Nano-EI-MS** m/z (%) = 131.9 [M] (100 %); **HR-MS** m/z = 131.9587 [M] (calculated: 131.9583).

Ethyl 2-[(4-oxo-5H-1,3-thiazol-2-yl)sulfanyl] acetate **69**^[346]

Compound **68** (4.00 g, 0.02 mol, 1.0 eq) and ethyl 2-bromoacetate **65** (1.9 mL, 0.02 mol, 1.0 eq) were dissolved in acetone (20 mL) and stirred at 70 °C for 2 h. A white solid precipitated from the mixture and was filtered and washed with acetone. The filtrate was concentrated and re-crystallised from iso-propanol or acetone to afford **67c**. **TLC** R_f = 0.1 (Hexane/EtOAc 9:1); **Reaction time**: 2 h; **Purification**: Re-crystallisation from acetone; **Yield**: 3465 mg of pink crystals (15.80 mmol, 93 %); **Yield**: 901 mg of orange solid (4.11 mmol, 97 %); **¹H-NMR** (400 MHz, DMSO- d_6) δ = 1.20 (t, 3 H, $^3J_{H,H}$ = 7.1 Hz, $\underline{\text{CH}_3}$), 4.15 (q, 2 H, $^3J_{H,H}$ = 7.1 Hz, $\underline{\text{CH}_2}$), 4.25 (s, 2 H, $\underline{\text{CH}_2}$), 4.28 (s, 2 H, $\underline{\text{CH}_2}$) ppm; **¹³C-NMR** (400 MHz, DMSO- d_6) δ = 14.0 ($\underline{\text{CH}_3}$), 35.1 ($\underline{\text{CH}_2}$), 40.4 ($\underline{\text{CH}_2}$), 61.6 ($\underline{\text{CH}_2\text{CH}_3}$), 167.2 ($\underline{\text{C=O}}$), 187.4 ($\underline{\text{C=N}}$), 200.3 ($\underline{\text{COOEt}}$) ppm; **ESI-MS** m/z (%) = 220.0 $[\text{M}+\text{H}]^+$ (100 %), 237.0 $[\text{M}+\text{NH}_4]^+$ (15 %), 242.0 $[\text{M}+\text{Na}]^+$ (25 %), 461.0 $[2\text{M}+\text{Na}]^+$ (15 %); **HR-MS** m/z = 220.0099 $[\text{M}+\text{H}]^+$ (calculated: 220.0097).

Synthesis of S-modified analogues 69

The alkylated analogue **69** (1.0 eq), various cyclic aldehydes (1.1 eq) and sodium acetate (1.0 eq) were dissolved in ethanol (5 mL) and stirred at 70 °C until TLC showed complete consumption of starting material.

Ethyl 2-[(5Z)-5-[(2-methylphenyl)methylidene]-4-oxo-1,3-thiazol-2-yl]sulfanylacetate **69a**

TLC R_f = 0.4 (Toluene/MeOH 8:2); **Reaction time**: 1 h; **Purification**: Re-crystallisation from isopropanol; **HR-MS APCI** m/z = 322.0557 $[\text{M}+\text{H}]^+$ (calculated: 322.0566); **HPLC-Analysis (Method B)**: 67 %, R_t = 19.0 min.

Ethyl 2-[(5Z)-5-[(3-methylphenyl)methylidene]-4-oxo-1,3-thiazol-2-yl]sulfanylacetate **69b**

TLC R_f = 0.1 (Toluene/MeOH 9:1); **Reaction time**: 2 h; **Purification**: Flash-Chromatography Toluene/MeOH 9:1 (R_f = 0.1); **Yield**: 110 mg of yellow solid (0.34 mmol, 30 %); **¹H-NMR** (400 MHz, CDCl_3) δ = 1.31 (t, 3 H, $^3J_{H,H}$ = 7.1 Hz, $\underline{\text{CH}_3}$), 2.44 (s, 3 H, Ar-CH_3), 4.22 (s, 2 H, $\underline{\text{CH}_2}$), 4.25 (q, 2 H, $^3J_{H,H}$ = 7.1 Hz, $\underline{\text{CH}_2\text{CH}_3}$), 7.26-7.42 (m, 4 H, $4\times\text{Ar-CH}$), 7.81 (s, 1 H, $\underline{\text{CH}}$) ppm; **¹³C-NMR** (400 MHz, CDCl_3) δ = 14.2 ($\underline{\text{CH}_3}$), 21.6 (Ar-CH_3), 35.5 ($\underline{\text{CH}_2}$), 62.7 ($\underline{\text{CH}_2\text{CH}_3}$), 118.4 ($\text{Ar-}\underline{\text{C}}$), 127.3 (Ar-CH), 129.4 (Ar-CH), 131.0 (Ar-CH), 132.0 (Ar-CH), 134.6 ($\underline{\text{CH}}$), 139.4 ($\text{Ar-}\underline{\text{C}}$), 147.5 ($\text{Ar-}\underline{\text{C}}$), 165.9 ($\underline{\text{C=O}}$), 167.2 ($\underline{\text{C=N}}$), 184.7 ($\underline{\text{COOEt}}$) ppm; **HPLC-Analysis (Method B)**: 100 %, R_t = 18.7 min.

Ethyl 2-[(5Z)-5-[(4-methylphenyl)methylidene]-4-oxo-1,3-thiazol-2-yl]sulfanylacetate **69c**^[346]

TLC R_f = 0.1 (Toluene/MeOH 95:5); **Reaction time**: 2 h; **Purification**: Flash-Chromatography Toluene/MeOH 95:5 (R_f = 0.1); **Yield**: 120 mg of yellow solid (0.37 mmol, 33 %); **¹H-NMR** (400 MHz, CDCl_3) δ = 1.30 (t, 3 H, $^3J_{H,H}$ = 7.1 Hz, $\underline{\text{CH}_3}$), 2.42 (s, 3 H, Ar-CH_3), 4.21 (s, 2 H, $\underline{\text{CH}_2}$), 4.24 (q, 2 H, $^3J_{H,H}$ = 7.1 Hz, $\underline{\text{CH}_2\text{CH}_3}$), 7.30 (d, 2 H, $^3J_{H,H}$ = 8.1 Hz, 3,5- Ar-CH), 7.42 (d, 2 H, $^3J_{H,H}$ = 8.1 Hz, 2,6- Ar-CH), 7.80 (s, 1 H, $\underline{\text{CH}}$) ppm; **¹³C-NMR** (400 MHz, CDCl_3) δ = 14.2 ($\underline{\text{CH}_3}$), 21.8 (Ar-CH_3), 35.5 ($\underline{\text{CH}_2}$), 62.7 ($\underline{\text{CH}_2\text{CH}_3}$), 117.4 ($\underline{\text{C}}$), 130.3 ($4\times\text{Ar-CH}$), 134.4 ($\underline{\text{CH}}$), 142.0 ($\text{Ar-}\underline{\text{C}}$), 147.6 ($\text{Ar-}\underline{\text{C}}$), 167.2 ($\underline{\text{C=O}}$), 178.2 ($\underline{\text{C=N}}$), 184.6 ($\underline{\text{COOEt}}$) ppm; **HPLC-Analysis**

(Method B): 98 %, R_t = 19.1 min.

Ethyl 2-[(5Z)-5-[3-(benzyloxy)phenyl]methylidene-4-oxo-1,3-thiazol-2-yl]sulfanylacetate **69d**

TLC R_f = 0.4 (Toluene/MeOH 8:2); **Reaction time:** 1 h; **Purification:** Filtration from ethanol;

Yield: 97 mg of yellow solid (0.23 mmol, 21 %); **$^1\text{H-NMR}$** (400 MHz, DMSO- d_6) δ = 1.21 (t, 3 H, $^3J_{\text{H,H}}$ = 7.1 Hz, CH_3), 4.15 (q, 2 H, $^3J_{\text{H,H}}$ = 7.1 Hz, CH_2CH_3), 4.19 (s, 2 H, CH_2), 5.17 (s, 2 H, $\text{OCH}_2\text{-Ar}$), 7.03 (dd, 1 H, $^{3,4}J_{\text{H,H}}$ = 2.2, 8.1 Hz, 6-Ar-CH), 7.21 (d, 1 H, $^3J_{\text{H,H}}$ = 7.8 Hz, 4-Ar-CH), 7.24 (d, 1 H, $^4J_{\text{H,H}}$ = 2.2 Hz, 2-Ar-CH), 7.32 (s, 1 H, CH), 7.32-7.36 (m, 1 H, 4'-Ar-CH), 7.38-7.44 (m, 3 H, 3',5',5-Ar-CH), 7.50 (d, 2 H, $^3J_{\text{H,H}}$ = 7.7 Hz, 2',6'-Ar-CH) ppm; **$^{13}\text{C-NMR}$** (400 MHz, DMSO- d_6) δ = 14.0 (CH_3), 33.9 (CH_2), 61.4 (CH_2), 69.3 (CH_2), 114.9 (Ar-C or CH), 115.9 (Ar-C or CH), 121.8 (Ar-C or CH), 126.2 (Ar-C or CH), 127.9 (2xAr-CH), 128.5 (2xAr-CH), 130.0 (Ar-C or CH), 131.7 (Ar-C or CH), 136.8 (Ar-C or CH), 136.9 (Ar-C or CH), 158.6 (Ar-C or CH), 164.5 (Ar-C or CH), 167.8 (Ar-C or CH), 176.4 (C=O), 177.1 (C=N), 180.0 (COOEt) ppm; **ESI-MS** m/z (%) = 513.1 [$\text{M}+99$] $^+$ (100 %); **HPLC-Analysis (Method B):** 98 %, R_t = 20.8 min.

Ethyl 2-[(5Z)-5-[4-(benzyloxy)phenyl]methylidene-4-oxo-1,3-thiazol-2-yl]sulfanylacetate **69e**

TLC R_f = 0.7 (Toluene/MeOH 8:2); **Reaction time:** 1 h; **Purification:** Filtration from ethanol;

Yield: 49 mg of yellow solid (0.12 mmol, 10 %); **$^1\text{H-NMR}$** (400 MHz, DMSO- d_6) δ = 1.22 (t, 3 H, $^3J_{\text{H,H}}$ = 7.1 Hz, CH_3), 4.15 (q, 2 H, $^3J_{\text{H,H}}$ = 7.1 Hz, CH_2CH_3), 4.18 (s, 2 H, CH_2), 5.17 (s, 2 H, CH_2Ar), 7.16 (d, 2 H, $^3J_{\text{H,H}}$ = 8.8 Hz, 2,6-Ar-CH), 7.33 (s, 1 H, CH), 7.32-7.37 (m, 1 H, 4'-Ar-CH), 7.39 (d, 1 H, $^3J_{\text{H,H}}$ = 7.5 Hz, 3',5'-Ar-CH), 7.48 (d, 1 H, $^3J_{\text{H,H}}$ = 7.5 Hz, 2',6'-Ar-CH), 7.57 (d, 1 H, $^3J_{\text{H,H}}$ = 8.8 Hz, 3,5-Ar-CH) ppm; **$^{13}\text{C-NMR}$** (400 MHz, DMSO- d_6) δ = 14.0 (CH_3), 33.9 (CH_2), 61.4 (CH_2CH_3), 69.4 (CH_2Ar), 115.4 (2,6-Ar-CH), 126.4 (CH), 127.9 (2',6'-Ar-CH), 128.5 (3',5'-Ar-CH), 131.1 (3,5-Ar-CH), 136.8 (Ar-C), 158.6 (Ar-C), 164.9 (Ar-C), 167.9 (Ar-C), 175.7 (C=O), 176.9 (C=N), 180.3 (COOEt) ppm; **ESI-MS** m/z (%) = 414.1 [$\text{M}+\text{H}$] $^+$ (90 %); **HR-MS** m/z = 414.0829 [$\text{M}+\text{H}$] $^+$ (calculated: 414.0828); **HPLC-Analysis (Method B):** 98 %, R_t = 20.8 min.

Ethyl 2-[(5Z)-5-[3,4-bis(benzyloxy)phenyl]methylidene-4-oxo-1,3-thiazol-2-yl]sulfanylacetate **69f**

TLC R_f = 0.8 (Hexane/EtOAc 6:4); **Reaction time:** 1.5 h; **Purification:** Filtration from ethanol;

Yield: 84 mg of yellow solid (0.16 mmol, 14 %); **$^1\text{H-NMR}$** (400 MHz, DMSO- d_6) δ = 1.22 (t, 3 H, $^3J_{\text{H,H}}$ = 7.1 Hz, CH_3), 4.15 (q, 2 H, $^3J_{\text{H,H}}$ = 7.1 Hz, CH_2CH_3), 4.18 (s, 2 H, CH_2), 5.20 (s, 4 H, 2x CH_2), 7.17 (dd, 1 H, $^{3,4}J_{\text{H,H}}$ = 1.9, 8.5 Hz, 6-Ar-CH), 7.22 (d, 1 H, $^3J_{\text{H,H}}$ = 8.5 Hz, 5-Ar-CH), 7.27 (s, 1 H, CH), 7.30 (d, 1 H, $^4J_{\text{H,H}}$ = 1.9 Hz, 2-Ar-CH), 7.29-7.35 (m, 2 H, 2xAr-CH), 7.36-7.42 (m, 4 H, 4xAr-CH), 7.46-7.53 (m, 4 H, 4xAr-CH) ppm; **$^{13}\text{C-NMR}$** (400 MHz, DMSO- d_6) δ = 14.0 (CH_3), 33.9 (CH_2), 61.4 (CH_2CH_3), 70.0 (CH_2Ar), 70.1 (CH_2Ar), 114.4 (5-Ar-CH), 115.9 (2-Ar-CH), 122.7 (6-Ar-CH), 127.7 (CH), 127.8 (Ar-CH), 127.9 (Ar-CH), 128.4 (Ar-CH), 128.5 (Ar-CH), 129.1 (Ar-CH), 137.0 (Ar-C), 137.1 (Ar-C), 148.1 (Ar-C), 164.8 (Ar-C), 167.9 (Ar-C), 173.6 (Ar-C), 175.8 (C=O), 176.9 (C=N), 180.2 (COOEt) ppm; **HPLC-Analysis (Method B):**

69 %, R_t = 20.5 min.

Ethyl 2-[(5Z)-5-[(3-hydroxyphenyl)methylidene]-4-oxo-1,3-thiazol-2-yl]sulfanylacetate **69g**

TLC R_f = 0.3 (Hexane/EtOAc 6:4); **Reaction time**: 1 h; **Purification**: Filtration from ethanol; **Yield**: 59 mg of yellow solid (0.18 mmol, 16 %); **$^1\text{H-NMR}$** (400 MHz, DMSO- d_6) δ = 1.22 (t, 3 H, $^3J_{\text{H,H}}$ = 7.1 Hz, CH_3), 4.15 (q, 2 H, $^3J_{\text{H,H}}$ = 7.1 Hz, CH_2CH_3), 4.19 (s, 2 H, CH_2), 6.74-6.78 (m, 1 H, 6-Ar-CH), 7.00-7.05 (m, 2 H, 4-Ar-CH, CH), 7.25-7.30 (2,5-Ar-CH, 2 H, $^9,^{73}J$ = „) (s, 1 H, OH) ppm; **$^{13}\text{C-NMR}$** (400 MHz, DMSO- d_6) δ = 14.0 (CH_3), 33.9 (CH_2), 61.4 (CH_2CH_3), 115.3 (4-Ar-CH), 115.9 (6-Ar-CH), 121.0 (CH), 126.6 (5 or 2-Ar-CH), 129.9 (5 or 2-Ar-CH), 136.5 (Ar-C), 157.8 (Ar-C), 167.9 (Ar-C) 176.2 (C=O), 177.0 (C=N), 180.1 (COOEt) ppm; **ESI-MS** m/z (%) = 421.0 $[\text{M}+99]^-$ (100 %), 423.0 $[\text{M}+99]^+$ (100 %); **HPLC-Analysis (Method B)**: 46 %, R_t = 14.5 min.

Ethyl 2-[(5Z/E)-5-[(4-hydroxyphenyl)methylidene]-4-oxo-1,3-thiazol-2-yl]sulfanyl acetate **69h**^[346]
1:1 ratio E to Z

TLC R_f = 0.1 (Toluene/MeOH 8:2); **Reaction time**: 2 h; **Purification**: Filtration from ethanol; **Yield**: 103 mg of yellow solid (0.16 mmol, 14 %); **$^1\text{H-NMR}$** (400 MHz, DMSO- d_6) δ = 1.21 (t, 6 H, $^3J_{\text{H,H}}$ = 7.1 Hz, 2x CH_3), 4.15 (q, 4 H, $^3J_{\text{H,H}}$ = 7.1 Hz, 2x CH_2CH_3), 4.18 (s, 2 H, CH_2), 4.36 (s, 2 H, CH_2), 6.89 (d, 2 H, $^3J_{\text{H,H}}$ = 8.6 Hz, 2,6 or 2',6'-Ar-CH), 6.93 (d, 2 H, $^3J_{\text{H,H}}$ = 8.6 Hz, 2,6 or 2',6'-Ar-CH), 7.29 (s, 1 H, E-CH), 7.46 (d, 2 H, $^3J_{\text{H,H}}$ = 8.6 Hz, 3,5- or 3',5'-Ar-CH), 7.53 (d, 2 H, $^3J_{\text{H,H}}$ = 8.6 Hz, 3,5- or 3',5'-Ar-CH), 7.79 (s, 1 H, Z-CH), 9.97 (s(br), 2 H, 2xOH) ppm; **$^{13}\text{C-NMR}$** (400 MHz, DMSO- d_6) δ = , 13.9 (CH_3), 14.0 (CH_3), 33.9 (CH_2), 34.8 (CH_2), 61.4 (CH_2CH_3), 61.7 (CH_2CH_3), 116.0, 116.5 (2,6 or 2',6'-Ar-CH), 121.6 (Ar-C), 124.0 (Ar-C), 126.3 (Ar-C), 127.0 (E-CH), 131.3 (3,5 or 3',5'-Ar-CH), 133.1 (3,5 or 3',5'-Ar-CH), 136.5 (Z-CH), 138.8 (Ar-C), 158.1 (Ar-C), 160.7 (Ar-C), 167.1 (C=O), 167.9 (C=O), 176.8 (C=N), 178.8 (C=N), 189.0 (COOEt), 189.9 (COOEt) ppm; **HPLC-Analysis (Method B)**: 46 %, R_t = 14.5 min; **HPLC-Analysis (Method B)**: 55 %, R_t = 15.3 min.

Ethyl 2-[(5Z)-5-[(2,4-dihydroxyphenyl)methylidene]-4-oxo-1,3-thiazol-2-yl]sulfanylacetate **69i**

TLC R_f = 0.2 (Toluene/MeOH 7:3); **Reaction time**: 1 h; **Purification**: Filtration from ethanol; **Yield**: 210 mg of red solid (0.62 mmol, 54 %); **$^1\text{H-NMR}$** (400 MHz, MeOD) δ = 1.29 (t, 3 H, $^3J_{\text{H,H}}$ = 7.1 Hz, CH_3), 4.22 (q, 2 H, $^3J_{\text{H,H}}$ = 7.1 Hz, CH_2CH_3), 6.33 (d, 1 H, $^4J_{\text{H,H}}$ = 2.4 Hz, 3-Ar-CH), 6.41 (dd, 1 H, $^{3,4}J_{\text{H,H}}$ = 2.4, 8.6 Hz, 4-Ar-CH), 7.52 (d, 1 H, $^3J_{\text{H,H}}$ = 8.6 Hz, 6-Ar-CH), 8.05 (s, 1 H, CH) ppm;

Ethyl 2-[(5Z)-5-[(3,4-dihydroxyphenyl)methylidene]-4-oxo-1,3-thiazol-2-yl]sulfanylacetate **69j**

TLC R_f = 0.1 (Hexane/EtOAc 6:4); **Reaction time**: 2 h; **Purification**: Filtration from ethanol; **Yield**: 46 mg of red solid (0.14 mmol, 12 %); **$^1\text{H-NMR}$** (400 MHz, DMSO- d_6) δ = 1.22 (t, 3 H, $^3J_{\text{H,H}}$ = 7.1 Hz, CH_3), 4.15 (q, 2 H, $^3J_{\text{H,H}}$ = 7.1 Hz, CH_2CH_3), 4.18 (s, 2 H, CH_2), 6.78 (d, 1 H, $^3J_{\text{H,H}}$ = 8.2 Hz, 5-Ar-CH), 6.90 (d, 1 H, $^{3,4}J_{\text{H,H}}$ = 2.1, 8.2 Hz, 6-Ar-CH), 7.04 (d, 1 H, $^4J_{\text{H,H}}$ = 2.1 Hz, 2-Ar-CH), 7.20 (s, 1 H, CH) ppm; **$^{13}\text{C-NMR}$** (400 MHz, DMSO- d_6) δ = 14.0 (CH_3), 33.9

(CH₂), 61.4 (CH₂CH₃), 116.1 (2,5-Ar-CH), 122.9 (6-Ar-CH), 126.3 (Ar-C), 127.9 (CH), 146.0 (Ar-C), 165.4 (Ar-C), 167.9 (Ar-C), 175.0 (C=O), 176.7 (C=N), 180.6 (COOEt) ppm; **HPLC-Analysis (Method B)**: 93 %, R_t = 21.5 min.

Ethyl 2-[(5Z)-5-(furan-2-ylmethylidene)-4-oxo-1,3-thiazol-2-yl]sulfanylacetate **69I**^[347]

TLC R_f = 0.4 (Hexane/EtOAc 7:3); **Reaction time**: 4 h; **Purification**: Filtration from ethanol; **Yield**: 285 mg of yellow solid (0.96 mmol, 84 %); **¹H-NMR** (400 MHz, DMSO-d₆) δ = 1.21 (t, 3 H, ³J_{H,H} = 7.1 Hz, CH₃), 4.17 (q, 2 H, ³J_{H,H} = 7.1 Hz, CH₂CH₃), 4.35 (s, 2 H, CH₂), 6.79 (dd, 1 H, ³J_{H,H} = 1.8, 3.5 Hz, 4-Ar-CH), 7.22 (d, 1 H, ³J_{H,H} = 3.5 Hz, 3-Ar-CH), 7.71 (s, 1 H, CH), 8.11 (d, 1 H, ³J_{H,H} = 1.8 Hz, 5-Ar-CH) ppm; **¹³C-NMR** (400 MHz, DMSO-d₆) δ = 14.0 (CH₃), 34.8 (CH₂), 61.7 (CH₂CH₃), 114.1 (4-Ar-CH), 120.5 (3-Ar-CH), 121.6 (CH), 122.9 (Ar-C), 148.4 (5-Ar-CH), 149.2 (Ar-C), 167.2 (C=O), 178.4 (C=N), 191.2 (COOEt) ppm; **ESI-MS** m/z (%) = 296.0 [M-H]⁻ (22 %), 298.0 [M+H]⁺ (100 %), 595.0 [2M+H]⁺ (3 %), 612.1 [2M+NH₄]⁺ (3 %); **HPLC-Analysis (Method B)**: 84 %, R_t = 15.1 min.

Substitution of thio-alkyl group in 67c

Thio-alkyl **69** (250 mg, 1.14 mmol, 1.0 eq), glycine methyl ester (143 mg, 1.14 mmol, 1.0 eq, HCl salt) and DIPEA (397 μL, 2.28 mmol, 2.0 eq) were dissolved in ethanol (4 mL). The reaction mixture was stirred at 80 °C. After 24 h, TLC showed complete consumption of starting **67c**. The crude was concentrated and purified by flash column chromatography to afford **70** as white solid.

Ethyl 2-[(4-oxo-5H-1,3-thiazol-2-yl)amino] acetate **70**

TLC R_f = 0.2 (Hexane/EtOAc 1:9); **Reaction time**: 16 h; **Purification**: Flash-Chromatography Hexane/EtOAc 1:9 (R_f = 0.2); **Yield**: 202 mg of white solid (1.00 mmol, 88 %); **Yield**: 892 mg of white solid (4.41 mmol, 93 %); **¹H-NMR** (400 MHz, MeOD) δ = 1.28 (t, 3 H, ³J_{H,H} = 7.2 Hz, CH₃), 4.03 (s, 2 H, CH₂), 4.21 (q, 2 H, ³J_{H,H} = 7.2 Hz, CH₂CH₃), 4.28 (s, 2 H, CH₂) ppm; **¹³C-NMR** (400 MHz, MeOD) δ = 14.4 (CH₃), 40.3 (CH₂), 46.9 (CH₂), 62.6 (CH₂CH₃), 169.9 (C=O), 185.1 (C=N), 190.7 (COOEt) ppm.

The amino-derivative **67d** (250 mg, 1.24 mmol, 1.0 eq), 4-chloro-benzaldehyde (209 mg, 1.48 mmol, 1.2 eq) and sodium acetate (101 mg, 1.24 mmol, 1.0 eq) were dissolved in methanol. The reaction mixture was stirred at 80 °C, until TLC showed complete consumption of starting **67d**.

Methyl 2-[(5Z)-5-[(4-chlorophenyl)methylidene]-4-oxo-1,3-thiazol-2-yl]aminoacetate **70a**

TLC R_f = 0.2 (Hexane/EtOAc 4:6); **Reaction time**: 16 h; **Purification**: Flash-Chromatography Hexane/EtOAc 4:6 (R_f = 0.2); **Yield**: 267 mg of white solid (0.86 mmol, 70 %); **¹H-NMR** (400 MHz, DMSO-d₆) δ = 3.70 (s, 3 H, OCH₃), 4.38 (s, 2 H, CH₂), 7.59 (as, 4 H, 4xAr-CH), 7.63 (s, 1 H, CH), 10.12 (s(br), 1 H, NH) ppm; **¹³C-NMR** (400 MHz, DMSO-d₆) δ = 45.3 (CH₂), 52.3 (CH₃), 128.7 (Ar-C), 129.3 (2xAr-CH or CH), 131.2 (2xAr-CH or CH), 132.9 (Ar-C), 134.2

(Ar-C), 169.0 (C=O), 174.6 (C=N), 179.2 (C=OMe) ppm; **ESI-MS** m/z (%) = 309.0 [M-H]⁻ (100 %), 311.0 [M+H]⁺ (100 %), 333.0 [M+Na]⁺ (58 %); **HPLC-Analysis (Method B)**: 81 %, R_t = 15.5 min.

One-pot reaction sequence to compounds of the class 70

Rhodanine **36** (499 mg, 3.75 mmol, 1.0 eq), benzaldehyde (1.042 mL, 7.50 mmol, 2.0 eq) and piperidine (408 μ L, 4.13 mmol, 1.1 eq) were dissolved in ethanol (3 mL). Glacial acetic acid (21 μ L, 0.38 mmol, 0.1 eq) was added to the reaction mixture and stirring was continued at 80 °C until TLC showed complete consumption of starting **36**. Upon cooling, a white crystalline solid was forming. The solid was filtered and washed with ethanol and dried *in vacuo*.

(5Z)-5-(phenylmethylidene)-2-(piperidin-1-yl)-1,3-thiazol-4-one **70b**^[348]

TLC R_f = 0.3 (Hexane/EtOAc 8:2); **Reaction time**: 5 h; **Purification**: Filtration from ethanol; **Yield**: 691 mg of white solid (2.54 mmol, 68 %); **¹H-NMR** (400 MHz, DMSO-d₆) δ = 1.57-1.71 (m, 6 H, 3xCH₂), 3.60-3.64 (m, 2 H, CH₂), 3.88-3.92 (m, 2 H, CH₂), 7.41-7.54 (m, 3 H, 3xAr-CH), 7.61-7.65 (m, 3 H, 2xAr-CH, CH) ppm; **¹³C-NMR** (400 MHz, DMSO-d₆) δ = 23.4 (CH₂), 25.1 (CH₂), 25.8 (CH₂), 49.1 (CH₂), 49.9 (CH₂), 128.8 (Ar-C), 129.2 (2xAr-CH), 129.5 (3xAr-CH), 129.7 (Ar-CH), 133.9 (Ar-C), 173.3 (C=O), 179.4 (C=N), ppm; **ESI-MS** m/z (%) = 273.1 [M+H]⁺ (100 %), 545.2 [2M+H]⁺ (25 %); **HPLC-Analysis (Method B)**: 82 %, R_t = 16.3 min.

(5Z)-5-[(3,4-dihydroxyphenyl)methylidene]-2-(piperidin-1-yl)-1,3-thiazol-4-one **70c**

TLC R_f = 0.2 (Hexane/EtOAc 7:3); **Reaction time**: 5 h; **Purification**: Filtration from ethanol; **Yield**: 312 mg of white solid (1.03 mmol, 27 %); **¹H-NMR** (400 MHz, DMSO-d₆) δ = 1.57-1.63 (m, 2 H, CH₂), 1.63-1.69 (m, 4 H, 2xCH₂), 3.56-3.60 (m, 2 H, CH₂), 3.85-3.90 (m, 2 H, CH₂), 6.85 (d, 1 H, ³J_{H,H} = 8.2 Hz, 5-Ar-CH), 6.96 (dd, 1 H, ^{3,4}J_{H,H} = 2.2, 9.2 Hz, 6-Ar-CH), 7.04 (d, 1 H, ⁴J_{H,H} = 2.2 Hz, 2-Ar-CH), 7.44 (s, 1 H, CH), 9.50 (s(br), 2 H, 2xOH) ppm; **¹³C-NMR** (400 MHz, DMSO-d₆) δ = 23.5 (CH₂), 25.2 (CH₂), 25.7 (CH₂), 48.9 (CH₂), 49.8 (CH₂), 116.2 (2,5-Ar-CH), 122.9 (6-Ar-CH), 124.5 (Ar-C), 125.2 (Ar-C), 130.5 (CH), 145.8 (Ar-C), 147.8 (Ar-C), 173.4 (C=O), 179.8 (C=N) ppm; **ESI-MS** m/z (%) = 305.1 [M+H]⁺ (96 %), 609.2 [2M+H]⁺ (41 %); **HPLC-Analysis (Method B)**: 99 %, R_t = 12.6 min.

General Procedure for methylation/ Benzylation of 36f, 36g, and 36h

The rhodanine derivative (1.0 eq), iodo methane or benzyl bromide (1.4 eq) and NaOH (1.2 eq) were dissolved in ethanol (10 mL). The reaction mixture was stirred at rt for 2 h. After 2 h, the products were afforded by filtration.

(5Z)-2-(methylsulfanyl)-5-[2-(trifluoromethyl)phenyl]methylidene-1,3-thiazol-4-one **62a**

Reaction time: 2 h; **Purification**: Filtration from ethanol **Yield**: 24 mg of white solid (0.08 mmol, 48 %); only Z-isomer: **¹H-NMR** (400 MHz, CDCl₃) δ = 2.83 (s, 3 H, CH₃), 7.49-7.55 (m,

1 H, 4-Ar-CH), 7.61-7.67 (m, 2 H, 5,6-Ar-CH), 7.76 (d, 1 H, $^3J_{H,H} = 7.8$ Hz, 3-Ar-CH), 8.14 (q, 1 H, $^5J_{H,F} = 2.0$ Hz, CH) ppm; $^{13}\text{C-NMR}$ (400 MHz, CDCl_3) $\delta = 16.3$ (CH₃), 100.1 (Ar-C), 126.8 (q, $^3J_{C,F} = 5.5$ Hz, 3-Ar-CH), 129.3 (5(6)-Ar-CH), 130.0 (4-Ar-CH), 131.2 (CH), 132.4 (5(6)-CH), 178.6 (C=O), 193.8 (C=N) ppm; **ESI-MS** m/z (%) = 304.0 [M+H]⁺ (100 %), 607.0 [2M+H]⁺ (2 %); **HR-MS** $m/z = 304.0072$ [M+H]⁺ (calculated: 304.0072); **HPLC-Analysis (Method B)**: 96 %, $R_t = 17.7$ min.

(5E/Z)-2-(methylsulfanyl)-5-[3- (trifluoromethyl)phenyl]methylidene-1,3-thiazol-4- one **62b**

Reaction time: 2 h; **Purification**: Filtration from ethanol; **Yield**: 21 mg of white solid (0.07 mmol, 46 %); 4:3 Z to E isomer ratio: $^1\text{H-NMR}$ (400 MHz, CDCl_3) $\delta = 2.69$ (s, 3 H, CH₃), 2.79 (s, 3 H, CH₃), 5.25 (s, 1 H, E-CH), 6.79 (d, 1 H, $^3J_{H,H} = 8.0$ Hz, E-Ar-CH), 7.00 (s, 1 H, E-2-Ar-CH), 7.30 (at, 1 H, $^3J_{H,H} = 7.8$ Hz, E-Ar-CH), 7.43-7.47 (m, 1 H, Ar-CH), 7.43-7.47 (m, 1 H, Ar-CH), 7.52-7.57 (m, 1 H, Ar-CH), 7.59-7.65 (m, 2 H, 2xZ-Ar-CH), 7.69 (s, 1 H, Z-2-Ar-CH), 7.81 (s, 1 H, Z-CH) ppm; **ESI-MS** m/z (%) = 304.0 [M+H]⁺ (100 %), 607.0 [2M+H]⁺ (100 %), 624.0 [2M+NH₄]⁺ (50 %), 910.0 [3M+H]⁺ (100 %), 932.0 [3M+Na]⁺ (60 %), 1213.0 [4M+H]⁺ (30 %), 1230.0 [4M+NH₄]⁺ (45 %); **HR-MS** $m/z = 304.0070$ [M+H]⁺ (calculated: 304.0072); **HPLC-Analysis (Method B)**: 96 %, $R_t = 17.7$ min.

(5Z)-2-(methylsulfanyl)-5-[4- (trifluoromethyl)phenyl]methylidene-1,3-thiazol-4- one **62c**

Reaction time: 2 h **Purification**: Filtration from ethanol; **Yield**: 25 mg of white solid (0.08 mmol, 48 %); $^1\text{H-NMR}$ (400 MHz, DMSO-d_6) $\delta = 2.84$ (s, 3 H, E-CH₃), 2.85 (s, 3 H, Z-CH₃) 4.96 (s, 1 H, E-CH), 6.87 (d, 2 H, $^3J_{H,H} = 8.2$ Hz, E-3,5-Ar-CH), 7.77 (d, 2 H, $^3J_{H,H} = 8.2$ Hz, E-2,6-Ar-CH) 7.86-7.93 (m, 4 H, 4xZ-Ar-CH), 7.94 (s, 1 H, Z-CH) ppm; $^{13}\text{C-NMR}$ (400 MHz, DMSO-d_6) $\delta = 16.5$ (CH₃), 54.0 (CH), 72.2 (Ar-C), 125.9 (2,6-Ar-CH), 127.3 (3,5-Ar-CH), 186.6 (C=O), 201.2 (C=N) ppm; **ESI-MS** m/z (%) = 304.0 [M+H]⁺ (100 %), 607.0 [2M+H]⁺ (100 %), 624.0 [2M+NH₄]⁺ (10 %), 629.0 [2M+Na]⁺ (20 %); **HR-MS** $m/z = 304.0075$ [M+H]⁺ (calculated: 304.0072); **HPLC-Analysis (Method B)**: 87 %, $R_t = 20.5$ min.

(5Z)-2-(benzylsulfanyl)-5-[2- (trifluoromethyl)phenyl]methylidene-1,3-thiazol-4- one **62d**

Reaction time: 3 h **Purification**: Filtration from ethanol; **Yield**: 36 mg of white solid (0.09 mmol, 46 %); only Z-isomer: $^1\text{H-NMR}$ (400 MHz, CDCl_3) $\delta = 4.67$ (s, 2 H, CH₂), 7.26-7.40 (m, 5 H, 5xAr-CH), 7.46-7.52 (m, 1 H, 4-Ar-CH), 7.58-7.62 (m, 2 H, 5,6-Ar-CH), 7.73 (d, 1 H, $^3J_{H,H} = 7.8$ Hz, 3-Ar-CH), 8.13 (q, 1 H, $^5J_{H,F} = 2.1$ Hz, CH) ppm; $^{13}\text{C-NMR}$ (400 MHz, CDCl_3) $\delta = 38.2$ (CH₂), 126.8 (q, $^4J_{C,F} = 5.5$ Hz, 3-Ar-CH), 128.5 (Ar-CH), 129.1 (Ar-CH), 129.3 (5(6)-Ar-CH), 129.5 (Ar-CH), 129.8 (Ar-C), 130.1 (4-Ar-CH), 131.5 (q, $^4J_{C,F} = 2.2$ Hz, CH), 131.7 (Ar-C), 132.4 (5(6)-Ar-CH), 133.2 (Ar-C), 134.7 (Ar-C), 178.7 (C=O), 192.7 (C=N) ppm; **ESI-MS** m/z (%) = 380.0 [M+H]⁺ (100 %), 402.0 [M+Na]⁺ (15 %), 759.1 [2M+H]⁺ (30 %); **HR-MS** $m/z = 380.0384$ [M+H]⁺ (calculated: 380.0385).

(5Z)-2-(benzylsulfanyl)-5-[3- (trifluoromethyl)phenyl]methylidene-1,3-thiazol-4- one **62e**

Reaction time: 3 h; **Purification**: Filtration from ethanol; **Yield**: 42 mg of white solid (0.11

mmol, 54 %); only Z-isomer: **¹H-NMR** (400 MHz, CDCl₃) δ = 4.68 (s, 2 H, CH₂), 7.28-7.41 (m, 5 H, 5xAr-CH), 7.54-7.70 (m, 3 H, 3xAr-CH), 7.72 (s, 1 H, 2-Ar-CH), 7.85 (s, 1 H, CH) ppm; **¹³C-NMR** (400 MHz, CDCl₃) δ = 38.3 (CH₂), 126.9 (2-Ar-CH), 127.1 (4-Ar-CH), 128.5 (Ar-CH), 128.6 (Ar-C), 129.2 (Ar-CH), 129.5 (Ar-CH), 130.0 (Ar-CH), 130.1 (Ar-C), 133.3 (Ar-CH), 133.9 (CH), 134.6 (q, ⁴J_{C,F}=3.1 Hz, 5-Ar-CH), 179.7 (C=O), 192.1 (C=N), ppm; **ESI-MS** m/z (%) = 380.0 [M+H]⁺ (100 %), 402.0 [M+Na]⁺ (20 %), 759.1 [2M+H]⁺ (100 %), 781.1 [2M+Na]⁺ (100 %), 797.0 [2M+K]⁺ (40 %); **HR-MS** m/z = 380.0388 [M+H]⁺ (calculated: 380.0385). (5Z)-2-(benzylsulfanyl)-5-[4-(trifluoromethyl)phenyl]methylidene-1,3-thiazol-4-one **62f**
Z to E 1:1 mixture **Reaction time**: 3 h; **Purification**: Filtration from ethanol; **Yield**: 52 mg of white solid (0.14 mmol, 57 %); **¹H-NMR** (400 MHz, DMSO-d₆) δ = 4.61 (s, 2 H, CH₂), 4.75 (s, 2 H, CH₂), 5.46 (s, 1 H, E-CH), 7.27-7.42 (m, 10 H, 10xAr-CH), 7.48-7.52 (m, 2 H, 2xAr-H), 7.72 (d, 2 H, ³J_{H,H} = 8.2 Hz, 2xAr-CH), 7.87 (d, 2 H, ³J_{8.6 Hz} = 2xAr-CH, 3) 7.90 (d, 2 H, ³J_{8.6 Hz} = 2xAr-CH, 3) 7.96 (s, 1 H, Z-CH) ppm; **¹³C-NMR** (400 MHz, DMSO-d₆) δ = 36.9 (CH₂), 37.0 (CH₂), 57.5 (E-CH), 125.3 (q, ⁴J_{C,F} = 4.1 Hz, 2xAr-CH), 126.2 (q, ⁴J_{C,F} = 3.8 Hz, 2xAr-CH), 128.0 (2xAr-CH), 128.7 (Ar-CH), 128.8 (Ar-CH), 128.9 (Ar-CH), 129.2 (Ar-CH), 129.3 (Ar-CH), 129.4 (Ar-CH), 130.9 (2xAr-CH), 133.3 (CH), 135.2 (Ar-C), 135.5 (Ar-C), 178.7 (C=O), 186.9 (C=O), 192.0 (C-S), 200.2 (C-S) ppm; **ESI-MS** m/z (%) = 380.0 [M+H]⁺ (100 %), 402.0 [M+Na]⁺ (15 %), 418.0 [M+K]⁺ (10 %), 759.1 [2M+H]⁺ (85 %), 781.1 [2M+Na]⁺ (100 %), 797.0 [2M+K]⁺ (40 %); **HR-MS** m/z = 380.0388 [M+H]⁺ (calculated: 380.0385); **HPLC-Analysis (Method B)**: 48 %, R_t = 20.9 min.

9.17 Synthesis of photo-label affinity probe

Synthesis of phosphorochloridate 31

Prior to reaction, phosphoryl trichloride (8.75 mL, 94 mmol) was distilled. The clear solution of phosphoryl trichloride was subjected to 2,4-dichlorophenol (24.45 g, 150 mmol) and magnesium turnings (80 mg, 3.3 mmol). The reaction mixture was slowly heated to 120 °C. HCl fumes were collected in a cooling trap and neutralised with concentrated NaOH_{aq}. After 3 h, the reaction temperature was increased to 160 °C and stirring was continued for another 3 h. The product was afforded via fractionated distillation (bp 200 °C, 0.02 mm Hg). The first fraction of the destination (bp 180 °C, 0.02 mm Hg) was the dichloro-mono-ester and this fraction was recovered and subjected to fresh 2,4-dichlorophenol and magnesium turnings (same equivalents as described above). The combined yield and product characterisation is stated below.

Bis(2,4-dichlorophenyl) chlorophosphonate **31a**^[182]

Purification: Fractionated distillation of product. **Yield**: 15230 mg of white solid (37.50 mmol, 80 %); **Yield**: 34000 mg of white solid (83.66 mmol, 89 %); **¹H-NMR** (400 MHz, CDCl₃) δ =

7.27 (dd, 2 H, $^3,^4J_{\text{H,H}} = 2.4, 8.9 \text{ Hz}$, 5,5'-Ar-CH), 7.46-7.49 (m, 2 H, 3,3'-Ar-CH), 7.49 (dd, 2 H, $^3,^4J_{\text{H,H}} = 1.2, 8.9 \text{ Hz}$, 6,6'-Ar-CH) ppm; $^{31}\text{P-NMR}$ (400 MHz, CDCl_3) $\delta = 18.84$ (P=OCl) ppm; $^{13}\text{C-NMR}$ (400 MHz, CDCl_3) $\delta = 122.4$ (6-Ar-CH) 122.5 (6'-Ar-CH), 126.7 (Ar-C), 126.8 (Ar-C), 128.3 (5,5'-Ar-CH), 130.8 (3,3'-Ar-CH), 132.0 (Ar-C), 145.0 (Ar-C), 145.1 (Ar-C) ppm; 2,4-dichlorophenoxyphosphonoyl dichloride **31b**^[182]
 $^1\text{H-NMR}$ (400 MHz, CDCl_3) $\delta = 7.21$ (dd, 1 H, $^3,^4J_{\text{H,H}} = 1.6, 8.8 \text{ Hz}$, 5-Ar-CH), 7.33 (dd, 1 H, $^3,^4J_{\text{H,H}} = 2.2, 8.8 \text{ Hz}$, 6-Ar-CH), 7.41-7.43 (m, 1 H, 3-Ar-CH) ppm; $^{31}\text{P-NMR}$ (400 MHz, CDCl_3) $\delta = 4.38$ (P=OCl) ppm;

Representative procedure for the synthesis of diol-amine 33b

Dimethyl 5-aminoisophthalate (10 g, 47.8 mmol) was dissolved in THF (anhydrous, 200 mL) under a nitrogen gas atmosphere. LiAlH_4 (4.9 g, 143 mmol) was added in small portions at 0 °C. The reaction mixture was stirred 8 h at rt and then cooled to 0 °C. The reaction was quenched with NaOH_{aq} (w/v %: 20 %, 20 mL). The crude was filtered through cellite, washed with EtOAc and concentrated. Purification by flash column chromatography (EtOAc \rightarrow EtOAc/MeOH 9:1, R_f 0.2) afforded the product (6.45 g, 88 %) as a yellow solid.

[3-amino-5-(hydroxymethyl)phenyl]methanol^[349]

TLC $R_f = 0.2$ (EtOAc); **Purification**: Flash-Chromatography EtOAc \rightarrow EtOAc/MeOH 9:1 ($R_f = 0.2$); **Yield**: 695 mg of yellow solid (4.54 mmol, 95 %) (1 g scale); **Yield**: 717 mg of yellow solid (4.68 mmol, 98 %) (1 g scale); **Yield**: 6454 mg of yellow solid (42.13 mmol, 88 %) (10 g scale); $^1\text{H-NMR}$ (400 MHz, DMSO-d_6) $\delta = 4.32$ (d, 4 H, $^3J_{\text{H,H}} = 5.8 \text{ Hz}$, CH_2), 4.94 (s(br), 2 H, NH_2), 4.96 (t, 2 H, $^3J_{\text{H,H}} = 5.8 \text{ Hz}$, OH), 6.40 (s, 3 H, 3xAr-CH) ppm; $^{13}\text{C-NMR}$ (400 MHz, DMSO-d_6) $\delta = 63.3$ (CH_2), 110.6 (2,6-Ar-CH) 112.4 (4-Ar-CH), 142.8 (Ar-C), 148.3 (Ar-C) ppm; $^1\text{H-NMR}$ (400 MHz, MeOD) $\delta = 4.48$ (s, 4 H, 2x CH_2), 6.63 (s, 2 H, 2,6-Ar-CH), 6.67 (s, 1 H, 4-Ar-CH) ppm; $^{13}\text{C-NMR}$ (400 MHz, MeOD) $\delta = 65.4$ (CH_2), 114.2 (2,6-Ar-CH), 116.6 (4-Ar-CH), 143.7 (Ar-C), 148.9 (Ar-C) ppm.

Representative protocol for the synthesis of azido-diol 33c

The amino-diol **33b** (1.00 g, 6.53 mmol, 1.0 eq) and t-BuONO (815 μL , 7.69 mmol, 1.2 eq) were dissolved in anhydrous acetonitrile (20 mL) under a N_2 gas atmosphere. TMS-N_3 (1110 μL , 9.23 mmol, 1.4 eq) was added in five portions to the reaction mixture. The mixture was stirred 2 h at rt. The crude was concentrated and purified by flash column chromatography. Conditions, yields and analytical data below.

[3-azido-5-(hydroxymethyl)phenyl]methanol **33c**^[349]

TLC $R_f = 0.3$ (Hexane/EtOAc 3:7); **Purification**: Flash-Chromatography Hexane/EtOAc 3:7 ($R_f = 0.3$); **Yield**: 1150 mg of yellow solid (6.42 mmol, 98 %); **Yield**: 2170 mg of yellow solid

(12.11 mmol, 98 %); **¹H-NMR** (400 MHz, MeOD) δ = 4.58 (s, 4 H, 2xCH₂), 6.95 (s, 2 H, 2,6-Ar-CH), 7.10 (s, 1 H, 4-Ar-CH) ppm; **¹³C-NMR** (400 MHz, MeOD) δ = 64.5 (CH₂), 116.9 (2,6-Ar-CH), 122.7 (Ar-C), 141.6 (4-Ar-CH), 145.2 (Ar-C-N₃) ppm.

Representative reaction for the synthesis of the di-azido alcohol **33d**

[3-azido-5-(azidomethyl)phenyl]methanol **33d**^[349]

TLC R_f = 0.4 (Hexane/EtOAc 7:3); **Purification**: Flash-Chromatography Hexane/EtOAc 7:3 → 1:1 (R_f = 0.4); **Yield**: 843 mg of yellow oil (4.13 mmol, 74 %); **Yield**: 1481 mg of yellow oil (7.26 mmol, 65 %); **Yield**: 943 mg of yellow oil (4.62 mmol, 75 %); **Yield**: 634 mg of yellow oil (3.11 mmol, 54 %); **Yield**: 388 mg of yellow oil (1.90 mmol, 73 %); **¹H-NMR** (400 MHz, CDCl₃) δ = 2.57 (s(br), 1 H, OH), 4.32 (s, 2 H, CH₂N₃), 4.65 (s, 2 H, CH₂OH), 6.87 (s, 1 H, 6-Ar-CH), 6.98 (s, 1 H, 2-Ar-CH), 7.05 (s, 1 H, 4-Ar-CH) ppm; **¹³C-NMR** (400 MHz, CDCl₃) δ = 54.3 (CH₂), 64.3 (CH₂), 117.0 (Ar-CH), 117.7 (Ar-C), 122.7 (Ar-CH), 137.7 (Ar-C), 141.0 (Ar-C), 143.6 (Ar-CH) ppm; **¹H-NMR** (400 MHz, MeOD) δ = 4.33 (s, 2 H, CH₂), 4.59 (s, 2 H, CH₂), 6.89 (s, 1 H, Ar-CH), 7.01 (s, 1 H, Ar-CH), 7.10 (s, 1 H, Ar-CH) ppm.

Installation of the tosyl-leaving group, synthesis of

The azido-alcohol **33d** (500 mg, 2.45 mmol, 1.0 eq) was dissolved in DCM (20 mL). NEt₃ (849 μ L, 6.09 mmol, 2.5 eq) was added to the reaction mixture, followed by TsCl (529 mg, 2.78 mmol, 1.1 eq) at 0 °C. The reaction mixture was maintained at 0 °C until TLC (hexane/EtOAc 7:3, R_f 0.6) showed complete consumption of **33d**. The reaction mixture was quenched with water (20 mL). The crude was extracted with DCM (3x30 mL), washed with brine (10 mL), dried over MgSO₄, filtered and concentrated. Purification by flash column chromatography afforded the tosylated di-azido compound **33e**.

[3-azido-5-(azidomethyl)phenyl]methyl 4-methylbenzenesulfonate **33e**^[349]

TLC R_f = 0.6 (Hexane/EtOAc 7:3); **Purification**: Flash-Chromatography Hexane/EtOAc 9:1 → 7:3 (R_f = 0.2), DCM; **Yield**: 396 mg of yellow oil (1.10 mmol, 45 %) (500 mg scale); **Yield**: 1533 mg of yellow oil (4.28 mmol, 76 %)(1150 mg scale); **Yield**: 402 mg of yellow oil (1.12 mmol, 35 %) 655.1 mg scale); **¹H-NMR** (400 MHz, CDCl₃) δ = 2.45 (s, 3 H, CH₃), 4.31 (s, 2 H, CH₂), 5.03 (s, 2 H, CH₂), 6.82 (s, 1 H, Ar-CH), 6.91 (s, 1 H, Ar-CH), 6.97 (s, 1 H, Ar-CH), 7.34 (d, 2 H, ³J_{H,H} = 8.3 Hz, 3,5-Ts-CH), 7.80 (d, 2 H, ³J_{H,H} = 8.3 Hz, 2,6-Ts-CH) ppm; **¹³C-NMR** (400 MHz, CDCl₃) δ = 21.8 (CH₃), 54.1 (CH₂), 70.8 (CH₂), 118.5 (Ar-CH), 119.0 (Ar-CH), 124.2 (Ar-CH), 128.1 (2,6-Ts-CH), 130.1 (3,5-Ts-CH), 133.1 (Ar-C), 136.2 (Ar-C), 138.2 (Ar-C), 141.4 (Ar-C), 145.3 (Ar-C) ppm;

Synthesis of modified photo-affinity aldehyde 33f

3-Hydroxybenzaldehyde (151 mg, 1.23 mmol, 1.1 eq) and potassium carbonate (346 mg, 2.50 mmol, 2.2 eq) were dissolved in DMF (10 mL). Tosyl derivative **33f** (402 mg, 1.12 mmol, 1.0 eq) was added to the reaction mixture. The mixture was stirred at 50 °C for 4 h. The reaction mixture was concentrated and purified by flash column chromatography. See below for conditions, yields and analytical details.

3-[3-azido-5-(azidomethyl)phenyl]methoxybenzaldehyde **33f**

TLC R_f = 0.7 (Hexane/EtOAc 7:3); **Reaction time**: 2-4 h; **Purification**: Flash-Chromatography Hexane/EtOAc 9:1 → 7:3 (R_f = 0.2), DCM; **Yield**: 267 mg of clear oil (0.87 mmol, 86 %) (396 mg of **33f** scale); **Yield**: 262 mg of clear oil (0.85 mmol, 69 %) (402 mg of **33f** scale); **¹H-NMR** (400 MHz, CDCl₃) δ = 4.34 (s, 2 H, CH₂), 5.06 (s, 2 H, CH₂), 6.92 (s, 1 H, Ar-CH), 7.05 (s, 1 H, Ar-CH), 7.14 (s, 1 H, Ar-CH), 7.21-7.24 (m, 1 H, Ar-CH), 7.41-7.48 (m, 3 H, 3xAr-CH) ppm; **¹³C-NMR** (400 MHz, CDCl₃) δ = 54.1 (CH₂), 69.2 (CH₂), 113.1 (Ar-CH), 117.5 (Ar-CH), 118.1 (Ar-CH), 122.0 (Ar-CH), 123.1 (Ar-CH), 124.0 (Ar-CH), 130.2 (Ar-CH), 137.9 (Ar-C), 138.0 (Ar-C), 139.1 (Ar-C), 141.1 (Ar-C), 158.9 (Ar-C), 191.8 (CHO) ppm;

Synthesis of rhodanine-N-acetic ethyl ester photo-affinity probe 34

Rhodanine-N-acetic ethyl ester **14** (189 mg, 0.86 mmol, 1.0 eq), the aldehyde **33f** (266 mg, 0.86 mmol, 1.0 eq) and sodium acetate (71 mg, 0.86 mmol, 1.0 eq) were dissolved in EtOH (10 mL) and stirred at 50 °C for 2 h. The reaction mixture was concentrated and purified by flash column chromatography.

Ethyl 2-[(5Z)-5-[(3-[3-azido-5-(azidomethyl)phenyl]methoxyphenyl) methylidene] 4-oxo-2-sulfanylidene-1,3-thiazolidin-3-yl] acetate **34**

TLC R_f = 0.5 (Hexane/EtOAc 8:2); **Reaction time**: 2 h; **Purification**: Flash-Chromatography Hexane/EtOAc 95:5 → 9:1 (R_f = 0.3), DCM; **Yield**: 168 mg of red solid (0.33 mmol, 38 %); **¹H-NMR** (400 MHz, CDCl₃) δ = 1.29 (t, 3 H, $^3J_{H,H}$ = 7.1 Hz, CH₃), 4.23 (q, 2 H, $^3J_{H,H}$ = 7.1 Hz, CH₂CH₃), 4.39 (s, 2 H, CH₂), 4.83 (s, 2 H, CH₂), 5.10 (s, 2 H, CH₂), 6.95 (s, 1 H, Ar-CH), 6.98-7.01 (m, 1 H, Ar-CH), 7.04-7.08 (m, 2 H, 2,4-Ar-CH), 7.11 (d, 1 H, $^3J_{H,H}$ = 7.8 Hz, 6-Ar-CH), 7.17 (s, 1 H, Ar-CH), 7.39 (at, 1 H, $^3J_{H,H}$ = 7.8, 8.0 Hz, 5-Ar-CH), 7.69 (s, 1 H, CH) ppm; **¹³C-NMR** (400 MHz, CDCl₃) δ = 14.2 (CH₃), 44.9 (CH₂), 54.2 (CH₂), 62.2 (CH₂CH₃), 69.4 (CH₂), 115.8 (Ar-CH), 117.5 (2-Ar-CH), 118.2 (4-Ar-CH), 118.3 (Ar-CH), 123.1 (Ar-CH), 123.2 (Ar-C), 124.2 (6-Ar-CH), 130.6 (5-Ar-CCH), 133.7 (CH), 134.6 (Ar-C), 138.2 (Ar-C), 139.2 (Ar-C), 141.3 (Ar-C), 158.9 (Ar-C), 165.9 (C=O), 167.0 (COOEt), 192.9 (C=S) ppm; **ESI-MS** m/z (%) = 527.1 [M+NH₄]⁺ (100 %), 532.1 [M+Na]⁺ (50 %), 548.1 [M+K]⁺ (25 %), 1036.2 [2M+NH₄]⁺ (100 %), 1041.2 [2M+Na]⁺ (100 %), 1057.2 [2M+K]⁺ (75 %); **HR-MS** m/z = 527.1275 [M+NH₄]⁺ (calculated: 527.1278); **HPLC-Analysis (Method B)**: 90 %, R_t = 18.8 min.

9.18 Synthesis of pyrazole derivatives

Synthesis of Pyrazole derivatives using traditional heating and NaOAc/HOAc

Representative procedure for the synthesis of N-phenyl-pyrazole precursor **80** for Knoevenagel reaction

Phenylhydrazine (200 μ L, 2.03 mmol), ethyl 3-oxobutanoate (260 μ L, 2.03 mmol) were dissolved in glacial HOAc (5 mL). The reaction mixture was stirred at 100-110 °C for 12 h or until TLC showed complete consumption of starting material.

edaravone **80**^[350]

TLC R_f = 0.3 (Hexane/EtOAc 1:1); **Reaction time**: 12 h; **Purification**: Flash-Chromatography Cyclohexan/EtOAc 7:3 (R_f = 0.1); **Yield**: 343 mg of white solid (1.97 mmol, 97 %) (scale: 2.03 mmol); **Yield**: 650 mg of white solid (3.73 mmol, 92 %) (scale: 4.06 mmol); **¹H-NMR** (400 MHz, CDCl₃) δ = 2.26 (s, 3 H, CH₃), 3.49 (s, 2 H, CH₂), 7.27-7.32 (m, 1 H, 1xAr-CH), 7.48-7.54 (m, 2 H, 2xAr-CH), 7.96-8.01 (m, 2 H, 2xAr-CH) ppm; **¹³C-NMR** (400 MHz, CDCl₃) δ = 16.9 (CH₃), 43.0 (CH₂), 118.8 (2x-Ar-CH), 125.0 (Ar-CH), 128.8 (2x-Ar-CH), 138.0 (Ar-C), 156.4 (Ar-C), 170.6 (C=O) ppm; **HPLC-Analysis (Method B)**: 96 %, R_t = 8.2 min.

Representative procedure for the synthesis of N-(3-benzoic-acid)-pyrazole precursor **81** for Knoevenagel reaction

3-Hydrazinylbenzoic acid (128 mg, 0.84 mmol), ethyl 3-oxobutanoate (108 μ L, 0.84 mmol) were dissolved in glacial HOAc (6 mL). The orange reaction mixture was stirred at 100-110 °C until TLC showed complete consumption of starting material.

3-(3-methyl-5-oxo-4H-pyrazol-1-yl)benzoic acid **81**^[351]

TLC R_f = 0.1 (Toluene/MeOH 8:2); **TLC** R_f = 0.5 (DCM/MeOH 9:1); **Reaction time**: 16 h **Purification**: Flash-Chromatography Toluene/MeOH 8:2 (R_f = 0.1); **Yield**: 150 mg of white solid (0.69 mmol, 81 %); **Yield**: 23 mg of white solid (0.11 mmol, 20 %); **¹H-NMR** (400 MHz, MeOD) δ = 2.24 (s, 3 H,) 7.56 (at, 1 H, ³J_{H,H} = 8.0 Hz, 5-Ar-CH), 7.89-7.95 (m, 2 H, 4,6-Ar-CH), 8.30 (at, 1 H, ⁴J_{H,H} = 1.9 Hz, 2-Ar-CH) ppm; **¹H-NMR** (400 MHz, DMSO-d₆) δ = 2.46 (d, 3 H, ⁴J_{H,H} = 1.0 Hz, CH₃), 5.98 (q, 1 H, ⁴J_{H,H} = 1.0 Hz, CH), 7.71 (at, 1 H, ³J_{H,H} = 8.1, 7.8 Hz, 5-Ar-CH), 7.93-7.96 (m, 1 H, 6-Ar-CH), 8.06 (ddd, 1 H, ^{3,4}J_{H,H} = 8.1, 2.2, 0.9 Hz, 4-Ar-CH), 8.37 (at, 1 H, ⁴J_{H,H} = 1.9, 1.8 Hz, 2-Ar-CH), 13.32 (s(br), 1 H, COOH) ppm; **HPLC-Analysis (Method B)**: 99 %, R_t = 8.6 min.

Knoevenagel reaction with N-phenyl pyrazole **80** and benzaldehyde derivatives

N-phenyl pyrazole **80** (0.29 mmol, 1.0 eq)), benzaldehyde derivative (0.58 mmol, 2.0 eq) and NaOAc (0.29 mmol, 1.0 eq) were dissolved in EtOH (5 mL) and stirred at 100 °C until TLC showed complete consumption of starting material.

(4Z)-3-methyl-4-[(3-nitrophenyl)methylidene]-1-phenyl-4,5-dihydro-1H-pyrazol-5-one **80a**^[352]

TLC R_f = 0.6 (Hexane/EtOAc 7:3); **Reaction time**: 4 h; **Purification**: Filtration from methanol; **Yield**: 17 mg of red solid (0.55 mmol, 13 %); NOESY ($\text{CH}_3, \text{CH} \rightarrow \text{Z}$) **¹H-NMR** (400 MHz, CDCl_3) δ = 2.38 (s, 3 H, CH_3), 7.21 (at, 1 H, $^3J_{\text{H,H}} = 7.5$ Hz, 4-Ar-CH), 7.39-7.45 (m, 3 H, 2xAr-CH, CH), 7.70 (dd, 1 H, $^3J_{\text{H,H}} = 8.1, 7.9$ Hz, 5'-Ar-CH), 7.91-7.96 (m, 2 H, 2,6-Ar-CH), 8.37 (ddd, 1 H, $^{3,4}J_{\text{H,H}} = 8.1, 2.0, 1.0$ Hz, 4'-Ar-CH), 8.95 (d, 1 H, $^3J_{\text{H,H}} = 7.9$ Hz, 6'-Ar-CH), 9.18 (at, 1 H, $^4J_{\text{H,H}} = 2.0$ Hz, 2'-Ar-CH) ppm; **¹H-NMR** (400 MHz, DMSO-d_6) δ = 2.36 (s, 3 H, CH_3), 7.22 (at, 1 H, $^3J_{\text{H,H}} = 7.5$ Hz, 4-Ar-CH), 7.46 (dd, 2 H, $^3J_{\text{H,H}} = 7.5, 7.8$, 3,5-Ar-CH), 7.84 (at, 1 H, $^3J_{\text{H,H}} = 7.9$ Hz, 5'-Ar-CH), 7.88 (d, 2 H, $^3J_{\text{H,H}} = 7.8$ Hz, 2,6-Ar-CH), 8.02 (s, 1 H, CH), 8.43 (dd, 1 H, $^{3,4}J_{\text{H,H}} = 8.2, 1.8$ Hz, 4'-Ar-CH), 8.84 (d, 1 H, $^3J_{\text{H,H}} = 7.9$ Hz, 6'-Ar-CH), 9.61 (dd, 1 H, $^4J_{\text{H,H}} = 1.8$ Hz, 2'-Ar-CH) ppm; **¹³C-NMR** (400 MHz, DMSO-d_6) δ = 13.1 (CH_3), 118.5 (2,6-Ar-CH), 124.9 (4-Ar-CH), 126.9 (4'-Ar-CH), 127.4 (2'-Ar-CH), 128.8 (3,5-Ar-CH), 128.9 (5'-Ar-CH), 130.2 (Ar-C), 134.1 (Ar-C), 137.9 (Ar-C), 139.4 (6'-Ar-CH), 145.4 (CH), 147.8 (Ar-C), 151.8 (Ar-C), 161.3 (C=O) ppm; **ESI-MS** m/z (%) = 308.1 $[\text{M}+\text{H}]^+$ (80 %), 340.1 $[\text{M}+\text{CH}_3\text{OH}+\text{H}]^+$ (100 %); **HR-MS** m/z = 308.1032 $[\text{M}+\text{H}]^+$ (calculated: 308.1030); **HPLC-Analysis (Method B)**: 66 %, R_t = 19.7 min.

(4Z)-5-methyl-4-[(3-methylphenyl)methylidene]-2-phenylpyrazol-3-one **80b**^[353]

Reaction time: 4 h **Purification**: Filtration from EtOAc **Yield**: 26 mg of yellow solid (0.09 mmol, 14 %); **¹H-NMR** (400 MHz, DMSO-d_6) δ = 2.35 (s, 3 H, CH_3), 2.40 (s, 3 H, CH_3), 7.18-7.23 (m, 1 H, Ar-CH), 7.41-7.48 (m, 4 H, 4xAr-CH), 7.80 (s, 1 H, CH), 7.88-7.92 (m, 2 H, 2xAr-CH), 8.41-8.45 (m, 2 H, 2xAr-CH) ppm.

5-methyl-2-phenyl-4-[2-(trifluoromethyl)phenyl]methylidenepyrazol-3-one **80c**

1:1 mixture of E to Z

TLC R_f = 0.5 (Hexane/EtOAc 8:2); **Reaction time**: 20 min; **Purification**: Flash-Chromatography Hexane/EtOAc 95:5 (R_f = 0.1); **Yield**: 30 mg of red solid (0.08 mmol, 15 %); **¹H-NMR** (400 MHz, CDCl_3) δ = 1.80 (s, 3 H, CH_3), 2.29 (s, 3 H, CH_3), 7.08-7.16 (m, 2 H, 2xAr-CH), 7.29-7.39 (m, 5 H, 5xAr-CH), 7.50-7.61 (m, 4 H, 4xAr-CH), 7.69-7.75 (m, 3 H, Z-CH, 2xAr-CH), 7.81-7.84 (m, 2 H, 2xAr-CH), 7.86-7.89 (m, 2 H, 2xAr-CH), 8.11 (q, 1 H, $^5J_{\text{H,F}} = 1.8$ Hz, E-CH), 8.42 (d, 1 H, $^3J_{\text{H,H}} = 7.7$ Hz, Ar-CH) ppm.

(Z)-4-(2,4-dihydroxybenzylidene)-3-methyl-1-phenyl-1H-pyrazol-5(4H)-one **80d**^[354]

TLC R_f = 0.1 (Hexane/EtOAc 7:3); **Reaction time**: 1 h; **Purification**: Filtration from HOAc; **Yield**: 60 mg of red solid (0.20 mmol, 31 %); **¹H-NMR** (400 MHz, DMSO-d_6) δ = 2.28 (s, 3 H, CH_3), 6.39 (dd, 1 H, $^{3,4}J_{\text{H,H}} = 2.4, 8.9$ Hz, 4-Ar-CH), 6.43 (d, 1 H, $^4J_{\text{H,H}} = 2.4$ Hz, 2-Ar-CH), 7.16 (at, 1 H, $^3J_{\text{H,H}} = 7.5$ Hz, 4'-Ar-CH), 7.41 (at, 2 H, $^3J_{\text{H,H}} = 7.9$ Hz, 3',5'-Ar-CH), 7.93 (d, 2 H, $^3J_{\text{H,H}} = 7.7$ Hz, 2',6'-Ar-CH), 7.96 (s, 1 H, CH), 9.35 (d, 1 H, $^3J_{\text{H,H}} = 8.9$ Hz, 5-Ar-CH), 10.88 (s, 2 H, 2xOH) ppm; **¹³C-NMR** (400 MHz, DMSO-d_6) δ = 13.2 (CH_3), 101.8 (2-Ar-CH), 108.5 (4-Ar-CH), 113.1 (Ar-C), 118.2 (2',6'-Ar-CH), 119.8 (Ar-C), 124.2 (4'-Ar-CH), 128.7 (3',5'-Ar-CH),

132.3 (Ar-C), 135.8 (5-Ar-CH), 138.7 (Ar-C), 141.3 (CH), 151.8 (Ar-C), 162.3 (Ar-C), 162.6 (Ar-C), 165.9 (Ar-C) ppm; **ESI-MS** m/z (%) = 293.1 [M-H]⁻ (100 %); **HR-MS** m/z = 293.0928 [M-H]⁻ (calculated: 293.0932); **HPLC-Analysis (Method B)**: 92 %, R_t = 17.0 min.

(4Z)-4-[3,4-bis(benzyloxy)phenyl]methylidene-5-methyl-2-phenylpyrazol-3-one **80e**

TLC R_f = 0.3 (Hexane/EtOAc 8:2); **Reaction time**: 30 min; **Purification**: Re-crystallisation from ethanol; **Yield**: 130 mg of red crystals (0.27 mmol, 46 %); NOESY (CH₃,CH → Z) **¹H-NMR** (400 MHz, DMSO-d₆) δ = 2.32 (s, 3 H, CH₃), 5.22 (s, 2 H, CH₂), 5.30 (s, 2 H, CH₂), 7.19 (at, 1 H, ³J_{H,H} = 7.6 Hz, 4-Ar-CH), 7.28 (d, 1 H, ³J_{H,H} = 8.6 Hz, 6'-Ar-CH), 7.30-7.52 (m, 12 H, 12xAr-CH), 7.73 (s, 1 H, CH), 7.93 (d, 2 H, ³J_{H,H} = 7.6 Hz, 3,5-Ar-CH), 8.12 (dd, 1 H, ^{3,4}J_{H,H} = 1.9, 8.6 Hz, 5'-Ar-CH), 8.90 (d, 1 H, ⁴J_{H,H} = 1.9 Hz, 3'-Ar-CH), **¹³C-NMR** (400 MHz, DMSO-d₆) δ = 13.2 (CH₃), 69.9 (CH₂), 70.1 (CH₂), 113.3 (6'-Ar-CH), 118.4 (3,5-Ar-CH or 3'-Ar-CH), 188.5 (3,5-Ar-CH or 3'-Ar-CH), 123.9 (Ar-C), 124.5 (4-Ar-CH), 126.5 (Ar-C), 127.7 (Ar-CH), 128.0 (Ar-CH), 128.5 (Ar-CH), 128.9 (Ar-CH), 130.7 (5'-Ar-CH), 136.5 (Ar-C), 136.7 (Ar-C), 138.4 (Ar-C), 147.4 (Ar-C), 148.5 (CH), 151.8 (Ar-C), 153.1 (Ar-C), 161.9 (C=O) ppm; **APCI-MS** m/z (%) = 475.2 [M+H]⁺ (100 %); **HR-MS** m/z = 475.2008 [M+H]⁺ (calculated: 475.2016); **HPLC-Analysis (Method B)**: 90 %, R_t = 22.5 min.

(Z)-4-(4-hydroxybenzylidene)-3-methyl-1-phenyl-1H-pyrazol-5(4H)-one **80f**^[355]

TLC R_f = 0.3 (Hexane/EtOAc 6:4); **Purification**: Filtration from Cyclohexan/EtOAc 9:1; **Yield**: 65 mg of red solid (0.23 mmol, 80 %); NOESY (CH₃,CH → Z) **¹H-NMR** (400 MHz, DMSO-d₆) δ = 2.32 (s, 3 H, CH₃), 6.94 (d, 2 H, ³J_{H,H} = 8.9 HZ, 3,5-Ar-CH), 7.18 (at, 1 H, ³J_{H,H} = 7.4 Hz, 4'-Ar-CH), 7.43 (dd, 2 H, ³J_{H,H} = 7.4, 8.4 Hz, 3,5'-Ar-CH), 7.70 (s, 1 H, CH), 7.93 (dd, 2 H, ³J_{H,H} = 7.4, 8.4 Hz, 2,6'-Ar-CH), 8.64 (d, 2 H, ³J_{H,H} = 8.9 Hz, 2,6-Ar-CH) 10.84 (s(br), 1 H, OH), ppm; **¹³C-NMR** (400 MHz, DMSO-d₆) δ = 13.2 (CH₃), 115.9 (3,5-Ar-CH), 118.3 (2,6'-Ar-CH), 122.5 (Ar-C), 124.4 (4'-Ar-CH), 124.9 (Ar-C), 128.8 (3,5'-Ar-CH), 137.5 (2,6-Ar-CH), 138.5 (Ar-C), 148.5 (CH), 151.8 (Ar-C), 162.0 (Ar-C), 163.2 (Ar-C), ppm; **ESI-MS** m/z (%) = 277.1 [M-H]⁻ (100 %); **HR-MS** m/z = 277.0985 [M-H]⁻ (calculated: 277.0983); **HPLC-Analysis (Method B)**: 94 %, R_t = 17.5 min.

(4Z)-4-[(2-hydroxyphenyl)methylidene]-5-methyl-2-phenylpyrazol-3-one **80an**^[356]

ESI-MS m/z (%) = 279.1 [M+H]⁺ (65 %), 557.2 [2M+H]⁺ (36 %), 579.2 [2M+Na]⁺ (2 %).

Synthesis of pyrazole derivatives using microwave-assisted three-component one-pot reaction

Aryl hydrazine (0.30 mmol, 1.0 eq), ethyl-aceto-acetate (0.45 mmol, 1.5 eq) and benzaldehyde derivative (0.3 mmol) were placed in microwave proof glass tube and heated 5 min at 400 W. Ethylacetate was added to the cooled reaction mixture and the products were afforded after simple filtration.

3-[(4Z)-4-[3,4-bis(benzyloxy)phenyl]methylidene-3-methyl-5-oxopyrazol-1-yl] benzoic acid **81a**

TLC R_f = 0.1 (Toluene/MeOH 9:1); **Reaction time**: 5 min (MWI, 400 W); **Purification**: Filtration from EtOAc; **Yield**: 37 mg of red solid (0.07 mmol, 13 %); **NOESY** ($\text{CH}_3, \text{CH} \rightarrow \text{Z}$) **$^1\text{H-NMR}$** (400 MHz, DMSO-d_6) δ = 2.34 (s, 3 H, CH_3), 5.23 (s, 2 H, CH_2), 5.30 (s, 2 H, CH_2), 7.27-7.60 (m, 12 H, 12xAr-CH), 7.75 (s, 1 H, CH), 7.73-7.78 (m, 1 H,) 8.16 (d, 1 H, $^3J_{\text{H,H}}$ = 8.5 Hz, Ar-CH), 8.21 (d, 1 H, $^3J_{\text{H,H}}$ = 8.5 Hz, Ar-CH), 8.54 (s, 1 H, Ar-CH), 8.84 (s, 1 H, Ar-CH), 13.11 (s(br), 1 H, COOH) ppm; **$^{13}\text{C-NMR}$** (400 MHz, DMSO-d_6) δ = 13.2 (CH_3), 70.1 (2x CH_2), 113.3 (Ar-CH), 118.5 (Ar-CH), 118.8 (Ar-CH), 122.1 (Ar-CH), 123.6 (Ar-C or Ar-CH), 125.1 (Ar-C or Ar-CH), 126.5 (Ar-C or Ar-CH), 127.7 (Ar-CH), 127.9 (Ar-CH), 128.0 (Ar-CH), 128.1 (Ar-CH), 128.4 (Ar-CH), 128.5 (Ar-CH) 129.2 (Ar-CH), 130.7 (Ar-CH), 136.4 (Ar-C or Ar-CH), 136.7 (Ar-C or Ar-CH), 138.5 (Ar-C or Ar-CH), 147.4 (Ar-C or Ar-CH), 148.9 (CH), 152.3 (Ar-C or Ar-CH), 153.2 (Ar-C or Ar-CH), 162.1 (Ar-C), 167.1 (C=O), ppm; **ESI-MS** m/z (%) = 517.2 $[\text{M-H}]^-$ (100 %), 1035.4 $[2\text{M-H}]^-$ (20 %); **HR-MS** m/z = 517.1775 $[\text{M-H}]^-$ (calculated: 517.1769); **HPLC-Analysis (Method B)**: 74 %, R_t = 21.5 min.

3-[(4Z)-4-[(3-bromo-4-methoxyphenyl)methylidene]-3- methyl-5-oxopyrazol-1-yl] benzoic acid **81b**

TLC R_f = 0.5 (DCM/MeOH 9:1); **Reaction time**: 5 min (MWI, 400W); **Purification**: Filtration from ethanol; **Yield**: 53 mg of red solid (0.13 mmol, 24 %); **$^1\text{H-NMR}$** (400 MHz, DMSO-d_6) δ = 2.33 (s, 3 H, CH_3), 3.99 (s, 3 H, OCH_3), 7.33 (d, 1 H, $^3J_{\text{H,H}}$ = 8.8 Hz, 5-Ar-CH), 7.56 (at, 1 H, $^3J_{\text{H,H}}$ = 8.2, 7.7 Hz, 5'-Ar-CH), 7.76 (adt, 1 H, $^{3,4}J_{\text{H,H}}$ = 7.7, 1.3 Hz, 4'-Ar-CH), 7.79 (s, 1 H, CH), 8.18 (ddd, 1 H, $^{3,4}J_{\text{H,H}}$ = 8.2, 2.3, 1.1 Hz, 6'-Ar-CH), 8.53 (at, 1 H, $^4J_{\text{H,H}}$ = 1.9 Hz, 2'-Ar-CH), 8.57 (dd, 1 H, $^{3,4}J_{\text{H,H}}$ = 8.8, 2.1 Hz, 6-Ar-CH), 9.23 (d, 1 H, $^4J_{\text{H,H}}$ = 2.1 Hz, 2-Ar-CH), 13.09 (s(br), 1 H, COOH) ppm; **$^{13}\text{C-NMR}$** (400 MHz, DMSO-d_6) δ = 13.1 (CH_3), 56.9 (OCH_3), 110.8 (Ar-C), 112.6 (5-Ar-CH), 118.7 (2'-Ar-CH), 122.1 (6'-Ar-CH), 124.7 (Ar-C), 125.2 (4'-Ar-CH), 127.3 (Ar-C), 129.3 (5'-Ar-CH), 131.4 (Ar-C), 136.7 (6-Ar-CH), 138.1 (2-Ar-CH), 138.4 (Ar-C), 147.0 (CH), 152.3 (Ar-C), 159.3 (Ar-C), 161.9 (C=O), 167.0 (COOH) ppm; **ESI-MS** m/z (%) = 413.0 $[\text{M-H}]^-$ (100 %), 829.0 $[2\text{M-H}]^-$ (25 %); **HR-MS** m/z = 413.0151 $[\text{M-H}]^-$ (calculated: 413.0142); **HR-MS** m/z = 413.0148 $[\text{M-H}]^-$ (calculated: 413.0142); **HPLC-Analysis (Method B)**: 73 %, R_t = 19.0 min.

3-[(4Z/E)-4-[3-(benzyloxy)phenyl]methylidene-3- methyl-5-oxopyrazol-1-yl] benzoic acid **81c**

TLC R_f = 0.1 (DCM/MeOH 9:1); **Reaction time**: 5 min (MWI, 400 W); **Purification**: Filtration from EtOAc; **Yield**: 56 mg of red solid (0.14 mmol, 25 %); **$^1\text{H-NMR}$** (400 MHz, DMSO-d_6) δ = 2.36 (s, 3 H, CH_3), 5.20 (s, 2 H, CH_2), 7.30 (dd, 1 H, $^{3,4}J_{\text{H,H}}$ = 2.4, 8.0 Hz, Ar-CH), 7.32-7.37 (m, 1 H, Ar-CH), 7.39-7.44 (m, 2 H, 2xAr-CH), 7.46-7.53 (m, 3 H, 3xAr-CH), 7.57 (at, 1 H, $^3J_{\text{H,H}}$ = 8.0 Hz, Ar-CH), 7.77 (ddd, 1 H, $^{3,4}J_{\text{H,H}}$ = 1.3, 7.8 Hz, Ar-CH), 7.84 (s, 1 H, CH), 8.09 (d, 1 H, $^3J_{\text{H,H}}$ = 8.0 Hz, Ar-CH), 8.18 (ddd, 1 H, $^{3,4}J_{\text{H,H}}$ = 1.0, 2.2, 8.2 Hz, Ar-CH), 8.51-8.53 (m, 2 H, 2,2'-Ar-CH), 13.07 (s(br), 1 H, COOH) ppm; **$^{13}\text{C-NMR}$** (400 MHz, DMSO-d_6) δ = 13.2 (CH_3), 69.5 (CH_2), 118.8 (2 or 2'-Ar-CH), 119.0 (2 or 2'-Ar-CH), 120.3 (Ar-CH) 122.2 (Ar-CH) 125.3

(Ar-CH) 126.7 (Ar-CH), 127.0 (Ar-C), 128.0 (2xAr-CH) 128.5 (Ar-CH) 129.3 (Ar-CH) 129.8 (Ar-CH) 131.5 (Ar-C), 134.1 (Ar-C), 136.7 (Ar-C), 138.3 (Ar-C), 148.7 (CH), 152.3 (Ar-C), 158.2 (Ar-C), 161.6 (Ar-C=O), 167.0 (COOH) ppm; **ESI-MS** m/z (%) = 411.1 [M-H]⁻ (100%); **HR-MS** m/z = 411.1352 [M-H]⁻ (calculated: 411.1350); **HPLC-Analysis (Method B)**: 73 %, R_t = 19.0 min.

3-[(4Z)-4-[(4-cyanophenyl)methylidene]-3-methyl-5-oxopyrazol-1-yl] benzoic acid **81d**

5:1 mixture with starting aldehyde **Reaction time**: 5 min **Purification**: Filtration from EtOAc

Yield: 46 mg of red solid (0.14 mmol, 45 %); **¹H-NMR** (400 MHz, DMSO-d₆) δ = 2.37 (s, 3 H, CH₃), 7.34-7.40 (m, 2 H, 2xAldehyde-Ar-CH), 7.57 (at, 1 H, ³J_{H,H} = 8.0 Hz, Ar-CH), 7.75-7.80 (m, 1 H, Ar-CH), 7.83 (s, 1 H, CH), 7.90-7.95 (m, 1 H, Ar-CH), 8.03 (d, 2 H, ³J_{H,H} = 8.5 Hz, 2xAr-CH), 8.06-8.17 (m, 2 H, 2xAldehyde-Ar-CH), 8.51-8.53 (m, 1 H, Ar-CH) 8.64 (d, 2 H, ³J_{H,H} = 8.5 Hz, 2xAr-CH), 13.10 (s(br), 1 H, COOH) ppm.

3-[(4Z)-4-[(4-hydroxyphenyl)methylidene]-3-methyl-5-oxo-4,5-dihydro-1H-pyrazol-1-yl] benzoic acid **81e**

TLC R_f = 0.5 (DCM/MeOH 9:1); **Reaction time**: 5min under MWI (400 W); **Purification**: Filtration from EtOAc; **Yield**: 111 mg of red solid (0.34 mmol, 64 %); **¹H-NMR** (400 MHz, DMSO-d₆) δ = 2.33 (s, 3 H, CH₃), 6.92-6.98 (m, 2 H, 3,5-Ar-CH), 7.52-7.58 (m, 1 H, 5'-Ar-CH), 7.69-7.77 (m, 1 H, Ar-CH), 7.71 (s, 1 H,), 8.13-8.20 (m, 1 H, 6'-Ar-CH), 8.59 (s, 1 H, 2'-Ar-CH), 8.60-8.66 (m, 1 H, 2,6-Ar-CH), 10.91 (s(br), 1 H, OH), 13.06 (s(br), 1 H, COOH), ppm; **¹³C-NMR** (400 MHz, DMSO-d₆) δ = 13.2 (CH₃), 99.6 (Ar-C or Ar-CH), 115.9 (Ar-C or Ar-CH), 118.6 (Ar-C or Ar-CH), 121.9 (Ar-C or Ar-CH), 122.4 (Ar-C or Ar-CH), 124.9 (Ar-C or Ar-CH), 124.9 (Ar-C or Ar-CH), 129.2 (Ar-C or Ar-CH), 131.4 (Ar-C or Ar-CH), 137.6 (Ar-C or Ar-CH), 138.6 (Ar-C or Ar-CH), 149.0 (Ar-C or Ar-CH), 152.3 (Ar-C or Ar-CH), 162.2 (Ar-C or Ar-CH), 163.3 (C=O), 167.1 (COOH) ppm; **ESI-MS** m/z (%) = 321.1 [M-H]⁻ (100 %), 365.1 [M+FA-H]⁻ (10 %); **HR-MS** m/z = 321.0878 [M-H]⁻ (calculated: 321.0881); **HPLC-Analysis (Method B)**: 89 %, R_t = 16.5 min.

3-[(4Z)-4-[4-(benzyloxy)phenyl]methylidene-3-methyl-5-oxopyrazol-1-yl] benzoic acid **81f**

TLC R_f = 0.6 (DCM/MeOH 9:1); **Reaction time**: 10min, MWI (400 W); **Purification**: Filtration from EtOAc; **Yield**: 160 mg of red solid (0.39 mmol, 72 %); NOESY (CH₃,CH → Z) **¹H-NMR** (400 MHz, DMSO-d₆) δ = 2.35 (s, 3 H, CH₃), 5.26 (s, 2 H, CH₂), 7.22 (d, 2 H, ³J_{H,H} = 8.8 Hz, 3,5''-Ar-CH), 7.35-7.51 (m, 5 H, 5xAr-CH), 7.55 (H,H, dd H, ³J_{7.8, 8.1 Hz} = 5'-Ar-CH, 3) 7.75 (d, 1 H, ³J_{H,H} = 7.8 Hz, 4'-Ar-CH), 7.79 (s, 1 H, CH), 8.18 (d, 1 H, ³J_{H,H} = 8.1 Hz, 6'-Ar-CH), 8.57 (s, 1 H, 2'-Ar-CH), 8.71 (d, 2 H, ³J_{H,H} = 8.8 Hz, 2,6''-Ar-CH), 13.08 (s(br), 1 H, COOH) ppm; **¹³C-NMR** (400 MHz, DMSO-d₆) δ = 13.2 (CH₃), 69.7 (CH₂), 115.1 (3,5''-Ar-CH), 118.7 (CH), 122.0 (6'-Ar-CH), 123.6 (Ar-C), 125.0 (4'-Ar-CH), 126.3 (Ar-C), 128.0 (''Ar-CH), 128.2 (''Ar-CH), 128.5 (''-Ar-CH), 129.2 (''-Ar-CH), 131.4 (Ar-C), 136.3 (Ar-C), 136.9 (2,6''-Ar-CH), 138.5 (Ar-C), 148.5 (2'-Ar-CH), 152.3 (Ar-C), 162.0 (Ar-C), 162.8 (Ar-C), 167.1 (C=O),

185.1 (COOH) ppm; **ESI-MS** m/z (%) = 411.1 $[\text{M}-\text{H}]^-$ (100 %), 823.3 $[2\text{M}-\text{H}]^-$ (11 %); **HPLC-Analysis (Method B)**: 89 %, R_t = 16.5 min.

3-[(4Z)-4-[4-(dimethylamino)phenyl]methylidene-3-methyl-5-oxopyrazol-1-yl] benzoic acid **81g**^[357]

TLC R_f = 0.5 (DCM/MeOH 9:1); **Reaction time**: 5 min (MWI, 400 W); **Purification**: Filtration from EtOAc; **Yield**: 151 mg of red solid (0.43 mmol, 80 %); NOESY ($\text{CH}_3, \text{CH} \rightarrow \text{Z}$) **¹H-NMR** (400 MHz, DMSO- d_6) δ = 2.31 (s, 3 H, CH_3), 3.13 (s, 6 H, $\text{N}(\text{CH}_3)_2$), 6.85 (d, 2 H, $^3J_{\text{H,H}}$ = 9.2 Hz, 2,6-Ar-CH), 7.53 (at, 1 H, $^3J_{\text{H,H}}$ = 7.9, 8.2 Hz, 5'-Ar-CH), 7.60 (s, 1 H, CH), 7.72 (adt, 1 H, $^{3,4}J_{\text{H,H}}$ = 1.2, 7.9 Hz, 4'-Ar-CH), 8.22 (ddd, 1 H, $^{3,4}J_{\text{H,H}}$ = 1.2, 2.0, 8.2 Hz, 6'-Ar-CH), 8.61 (m, 1 H, 2'-Ar-CH), 8.65 (d, 2 H, $^3J_{\text{H,H}}$ = 9.2 Hz, 3,5-Ar-CH), 13.02 (s(br), 1 H, COOH) ppm; **¹³C-NMR** (400 MHz, DMSO- d_6) δ = 13.2 (CH_3), 39.6 ($\text{N}(\text{CH}_3)_2$), 111.4 (2,6-Ar-CH), 118.5 (Ar-C), 118.6 (2'-Ar-CH), 121.2 (6'-Ar-CH), 121.8 (Ar-C), 124.5 (4'-Ar-CH), 129.1 (5'-Ar-CH), 131.3 (Ar-C), 137.6 (3,5-Ar-CH), 139.1 (Ar-C), 148.6 (CH), 152.1 (Ar-C), 154.0 (Ar-C), 162.6 ($\text{C}=\text{O}$), 167.2 (COOH) ppm; **ESI-MS** m/z (%) = 348.1 $[\text{M}-\text{H}]^-$ (100 %), 697.3 $[2\text{M}-\text{H}]^-$ (60 %); **HR-MS** m/z = 348.1356 $[\text{M}-\text{H}]^-$ (calculated: 348.1354); **HPLC-Analysis (Method B)**: 99 %, R_t = 14.9 min.

2-[(1Z)-[2-(3-carboxyphenyl)hydrazin-1-ylidene]methyl] benzoic acid **81j**^[358]

TLC R_f = 0.3 (DCM/MeOH 9:1); **Reaction time**: 5 min (MWI, 400 W); **Purification**: Flash-Chromatography $\text{CHCl}_3/\text{MeOH}$ 9:1 (R_f = 0.1); **Yield**: 70 mg of red solid (0.25 mmol, 46 %); **¹H-NMR** (400 MHz, DMSO- d_6) δ = 6.69 (s(br), 1 H, NH), 7.52-7.66 (m, 4 H, 4xAr-CH), 7.75-7.82 (m, 2 H, 2xAr-CH), 7.90 (d, 1 H, $^3J_{\text{H,H}}$ = 7.6 Hz, Ar-CH), 7.99 (dd, 1 H, $^{3,4}J_{\text{H,H}}$ = 8.1, 1.3 Hz, Ar-CH), 8.29 (s, 1 H, Ar-CH) ppm.

3-[(E)-2-[(3-nitrophenyl)methylidene]hydrazin-1-yl] benzoic acid **81k**^[359]

TLC R_f = 0.1 (Hexane/EtOAc 8:2); **Reaction time**: 10 min (MWI, 400 W); **Purification**: Flash-Chromatography DCM/MeOH 9:1 (R_f = 0.3); **Yield**: 52 mg of ; (0.18 mmol, 34 %) **¹H-NMR** (400 MHz, DMSO- d_6) δ = 7.34-7.40 (m, 3 H, 3xAr-CH), 7.67-7.71 (m, 2 H, 2xAr-CH), 8.00 (s, 1 H, CH), 8.09-8.15 (m, 2 H, 2xAr-CH), 8.46 (at, 1 H, $^4J_{\text{H,H}}$ = 1.8 Hz, Ar-CH), 10.87 (s, 1 H, NH), 12.91 (s(br), 1 H, COOH) ppm; **¹³C-NMR** (400 MHz, DMSO- d_6) δ = 112.9 (Ar-CH), 116.5 (Ar-CH), 119.8 (Ar-CH), 120.3 (Ar-CH), 122.3 (Ar-CH), 129.5 (Ar-CH), 130.3 (Ar-CH), 131.7 (Ar-CH), 131.7 (Ar-CH), 134.9 (Ar-CH), 137.6 (Ar-C), 145.0 (Ar-C), 148.3 (Ar-C), 167.5 (Ar-COOH), ppm; **ESI-MS** m/z (%) = 284.1 $[\text{M}-\text{H}]^-$ (100 %), 320.0 $[\text{M}+\text{Cl}]^-$ (10 %), 569.1 $[2\text{M}-\text{H}]^-$ (70 %); **HR-MS** m/z = 284.0675 $[\text{M}-\text{H}]^-$ (calculated: 284.0677); **HR-MS** m/z = 284.0679 $[\text{M}-\text{H}]^-$ (calculated: 284.0677); **HPLC-Analysis (Method B)**: 74 %, R_t = 21.5 min. (Z)-4-(4-hydroxybenzylidene)-3-methyl-1-phenyl-1H-pyrazol-5(4H)-one **80f**^[360]

TLC R_f = 0.3 (Hexane/EtOAc 6:4); **Purification**: Filtration from Cyclohexan/EtOAc 9:1; **Yield**: 50 mg of red solid (0.18 mmol, 60 %); NOESY ($\text{CH}_3, \text{CH} \rightarrow \text{Z}$); **¹H-NMR** (400 MHz, DMSO- d_6) δ = 2.32 (s, 3 H, CH_3), 6.94 (d, 2 H, $^3J_{\text{H,H}}$ = 8.9 HZ, 3,5-Ar-CH), 7.18 (at, 1 H, $^3J_{\text{H,H}}$ = 7.4 Hz, 4'-Ar-CH), 7.43 (dd, 2 H, $^3J_{\text{H,H}}$ = 7.4, 8.4 Hz, 3,5'-Ar-CH), 7.70 (s, 1 H, CH), 7.93 (dd, 2 H, $^3J_{\text{H,H}}$ =

7.4, 8.4 Hz, 2,6'-Ar-CH), 8.64 (d, 2 H, $^3J_{\text{H,H}} = 8.9$ Hz, 2,6-Ar-CH) 10.84 (s(br), 1 H, OH), ppm; $^{13}\text{C-NMR}$ (400 MHz, DMSO- d_6) $\delta = 13.2$ (CH₃), 115.9 (3,5-Ar-CH), 118.3 (2,6'-Ar-CH), 122.5 (Ar-C), 124.4 (4'-Ar-CH), 124.9 (Ar-C), 128.8 (3,5'-Ar-CH), 137.5 (2,6-Ar-CH), 138.5 (Ar-C), 148.5 (CH), 151.8 (Ar-C), 162.0 (Ar-C), 163.2 (Ar-C), ppm; **ESI-MS** m/z (%) = 277.1 [M-H]⁻ (100 %); **HR-MS** $m/z = 277.0985$ [M-H]⁻ (calculated: 277.0983).

Synthesis of pyrazole derivatives with improved sequential one-pot reaction

Phenylhydrazine or 3-hydrazinylbenzoic acid (2.03 mmol, 1.0 eq), ethyl aceto-acetate (2.03 mmol, 1.0 eq) were dissolved in 5 mL HOAc. The reaction mixture was stirred at 110 °C for 16 h. Benzaldehyde derivative (2.44 mmol, 1.2 eq) was added to the yellow reaction mixture. The reaction mixture was continued to stir at 110 °C, until TLC showed complete consumption of intermediate formed pyrazole precursor. The reaction mixture was cooled and the product was isolated by simple filtration or column chromatography.

(Z)-4-(4-methoxybenzylidene)-3-methyl-1-phenyl-1H-pyrazol-5(4H)-one **80w**^[361]

TLC $R_f = 0.1$ (Hexane/EtOAc 8:2); **Reaction time**: 17 h; **Purification**: Re-crystallisation from ethanol; **Yield**: 40 mg of red crystals (0.14 mmol, 15 %); **NOESY** (CH₃,CH → Z) $^1\text{H-NMR}$ (400 MHz, DMSO- d_6) $\delta = 2.33$ (s, 3 H, CH₃), 3.89 (s, 3 H, OCH₃), 7.14 (d, 2 H, $^3J_{\text{H,H}} = 9.0$ Hz, 3,5-Ar-CH), 7.19 (att, 1 H, $^3,4J_{\text{H,H}} = 7.4$, 1.2 Hz, 4'-Ar-CH), 7.43 (at, 2 H, $^3J_{\text{H,H}} = 7.6$, 7.4 Hz, 3',5'-Ar-CH), 7.77 (s, 1 H, CH), 7.92 (dd, 2 H, $^3,4J_{\text{H,H}} = 7.6$, 1.2 Hz, 2',6'-Ar-CH), 8.71 (d, 2 H, $^3J_{\text{H,H}} = 9.0$ Hz, 2,6-Ar-CH) ppm; $^{13}\text{C-NMR}$ (400 MHz, DMSO- d_6) $\delta = 13.2$ (CH₃), 55.8 (OCH₃), 114.4 (3,5-Ar-CH), 118.3 (2',6'-Ar-CH), 123.8 (Ar-C), 124.5 (4'-Ar-CH), 126.2 (Ar-C), 128.8 (3',5'-Ar-CH), 136.9 (2,6-Ar-CH), 138.4 (Ar-C), 148.2 (CH), 151.9 (Ar-C), 161.9 (Ar-C), 163.7 (C=O) ppm; **ESI-MS** m/z (%) = 293.1 [M+H]⁺ (100 %), 585.2 [2M+H]⁺ (20 %); **HR-MS** $m/z = 293.1286$ [M+H]⁺ (calculated: 293.1285); **HPLC-Analysis (Method B)**: 98 %, $R_t = 19.2$ min.

(4Z)-5-methyl-2-phenyl-4-[(4-phenylphenyl)methylidene]pyrazol-3-one **80x**^[362]

TLC $R_f = 0.1$ (Hexane/EtOAc 9:1); **Reaction time**: 17 h; **Purification**: Filtration from HOAc; **Yield**: 113 mg of red solid (0.33 mmol, 16 %); $^1\text{H-NMR}$ (400 MHz, CDCl₃) $\delta = 2.38$ (s, 3 H, CH₃), 7.20 (att, 1 H, $^3,4J_{\text{H,H}} = 1.0$, 7.4 Hz, 4'-Ar-CH), 7.39-7.45 (m, 4 H, 3',5,4''-Ar-CH, CH), 7.49 (at, 2 H, $^3J_{\text{H,H}} = 7.4$ Hz, 3'',5''-Ar-CH), 7.66-7.69 (m, 2 H, 2'',6''-Ar-CH), 7.75 (d, 2 H, $^3J_{\text{H,H}} = 8.5$ Hz, 3,5-Ar-CH), 7.98 (d, 2 H, $^3J_{\text{H,H}} = 7.7$ Hz, 2',6'-Ar-CH), 8.61 (d, 2 H, $^3J_{\text{H,H}} = 8.5$ Hz, 2,6-Ar-CH) ppm; $^{13}\text{C-NMR}$ (400 MHz, CDCl₃) $\delta = 13.5$ (CH₃), 119.3 (2',6'-Ar-CH), 125.0 (4'-Ar-CH), 127.4 (2'',6'',3,5-Ar-CH), 127.6 (Ar-C) 128.6 (Ar-CH), 128.9 (Ar-CH) 129.2 (Ar-CH) 132.1 (Ar-C), 134.5 (2,6-Ar-CH), 138.5 (Ar-C), 139.9 (Ar-C), 145.8 (Ar-C), 146.5 (CH), 151.0 (Ar-C), 162.1 (C=O) ppm; **ESI-MS** m/z (%) = 339.1 [M+H]⁺ (100 %), 677.3 [2M+H]⁺ (5 %); **HPLC-Analysis (Method B)**: 96 %, $R_t = 21.5$ min.

4-[(4Z)-3-methyl-5-oxo-1-phenylpyrazol-4-ylidene]methylbenzonitrile **80y**^[363]

TLC $R_f = 0.1$ (Hexane/EtOAc 8:2); **Reaction time**: 20 h; **Purification**: Filtration from HOAc;

Yield: 126 mg of red solid (0.44 mmol, 22 %); **¹H-NMR** (400 MHz, DMSO-*d*₆) δ = 2.34 (s, 3 H, CH₃), 7.18-7.24 (m, 1 H, 4'-Ar-CH), 7.40-7.46 (m, 2 H, 3',5'-Ar-CH), 7.85-7.90 (m, 3 H, CH, 2',6'-Ar-C), 7.99-8.04 (m, 2 H, 3,5-Ar-CH), 8.61-8.65 (m, 2 H, 2,6-Ar-CH) ppm; **¹³C-NMR** (400 MHz, DMSO-*d*₆) δ = 13.1 (CH₃), 114.1 (CN), 118.4 (2',6'-Ar-CH), 124.9 (4'-Ar-CH), 128.9 (3',5'-Ar-CH), 129.1 (Ar-C), 132.3 (2,6-Ar-CH), 133.4 (3,5-Ar-CH), 136.7 (Ar-C), 137.9 (Ar-C), 145.5 (CH), 151.7 (C=N), 161.1 (C=O) ppm; **APCI-MS** m/z (%) = 288.1 [M+H]⁺ (100 %); **HR-MS** m/z = 288.1134 [M+H]⁺ (calculated: 288.1131); **HPLC-Analysis (Method B):** 82 %, R_t = 16.3 min.

(4Z)-4-[(4-chlorophenyl)methylidene]-5-methyl-2-phenylpyrazol-3-one **80z**^[353]

TLC R_f = 0.6 (Hexane/EtOAc 8:2); **Reaction time:** 17 h; **Purification:** Re-crystallisation from ethanol; **Yield:** 144 mg of red crystals (0.49 mmol, 24 %); **¹H-NMR** (400 MHz, DMSO-*d*₆) δ = 2.33 (s, 3 H, CH₃), 7.20 (at, 1 H, ³*J*_{H,H} = 1.0, 7.4 Hz, 4'-Ar-CH), 7.44 (dd, 2 H, ³*J*_{H,H} = 7.4, 8.6 Hz, 3',5'-Ar-CH), 7.64 (d, 2 H, ³*J*_{H,H} = 8.6 Hz, 3,5-Ar-CH), 7.83 (s, 1 H, CH), 7.89 (dd, 2 H, ^{3,4}*J*_{H,H} = 1.0, 8.6 Hz, 2',6'-Ar-CH), 8.61 (d, 2 H, ³*J*_{H,H} = 8.6 Hz, 2,6-Ar-CH) ppm; **¹³C-NMR** (400 MHz, DMSO-*d*₆) δ = 13.1 (CH₃), 118.4 (2',6'-Ar-CH), 124.7 (4'-Ar-CH), 127.1 (Ar-C), 128.8 (2,6-Ar-CH), 128.9 (3',5'-Ar-CH), 131.8 (Ar-C), 135.3 (3,5-Ar-CH), 137.9 (Ar-C), 138.0 (Ar-C), 146.7 (CH), 151.8 (Ar-C), 161.4 (C=O) ppm; **APCI-MS** m/z (%) = 297.1 [M+H]⁺ (100 %); **HR-MS** m/z = 297.0796 [M+H]⁺ (calculated: 297.0789); H-Jresqf-Experiment: ³*J*_{CH,C=O} = 5.7 Hz; **HPLC-Analysis (Method B):** 98 %, R_t = 18.1 min.

(4Z)-4-[(4-methanesulfonylphenyl)methylidene]-5-methyl-2-phenylpyrazol-3-one **80aa**

TLC R_f = 0.1 (DCM); **Reaction time:** 20 h; **Purification:** Filtration from ethanol; **Yield:** 306 mg of red solid (0.90 mmol, 44 %); **¹H-NMR** (400 MHz, DMSO-*d*₆) δ = 2.36 (s, 3 H, CH₃), 3.31 (s, 3 H, SO₂CH₃), 7.21 (att, 1 H, ^{3,4}*J*_{H,H} = 1.0, 7.4 Hz, 4'-Ar-CH), 7.45 (dd, 2 H, ³*J*_{H,H} = 7.4, 8.8 Hz, 3',5'-Ar-CH), 7.88 (dd, 2 H, ^{3,4}*J*_{H,H} = 8.8, 1.0 Hz, 2',6'-Ar-CH), 7.95 (s, 1 H, CH), 8.08 (d, 2 H, ³*J*_{H,H} = 8.6 Hz, 3,5-Ar-CH), 8.68 (d, 2 H, ³*J*_{H,H} = 8.6 Hz, 2,6-Ar-CH) ppm; **¹³C-NMR** (400 MHz, DMSO-*d*₆) δ = 13.1 (CH₃), 43.2 (SO₂CH₃), 118.4 (2',6'-Ar-CH), 124.9 (4'-Ar-CH), 126.9 (3,5-Ar-CH), 128.9 (3',5'-Ar-CH), 129.1 (Ar-C), 133.6 (2,6-Ar-CH), 137.0 (Ar-C), 137.9 (Ar-C), 143.3 (Ar-C), 145.7 (CH), 151.8 (Ar-C), 161.1 (C=O) ppm; **ESI-MS** m/z (%) = 341.1 [M+H]⁺ (87 %), 358.1 [M+NH₄]⁺ (4 %); **HPLC-Analysis (Method B):** 96 %, R_t = 21.5 min.

(4Z)-4-[(3-bromo-4-methoxyphenyl)methylidene]-5-methyl-2-phenylpyrazol-3-one **80ab**

TLC R_f = 0.2 (Hexane/EtOAc 8:2); **Reaction time:** 20 h; **Purification:** Filtration from HOAc; **Yield:** 346 mg of red solid (0.93 mmol, 46 %); NOESY (CH₃,CH → Z) **¹H-NMR** (400 MHz, DMSO-*d*₆) δ = 2.31 (s, 3 H, CH₃), 3.98 (s, 3 H, O-CH₃), 7.20 (at, 1 H, ³*J*_{H,H} = 7.4 Hz, 4'-Ar-CH), 7.31 (d, 1 H, ³*J*_{H,H} = 8.8 Hz, 5-Ar-CH), 7.43 (at, 2 H, ³*J*_{H,H} = 7.4, 7.6 Hz, 3',5'-Ar-CH), 7.75 (s, 1 H, CH), 7.91 (d, 2 H, ³*J*_{H,H} = 7.6 Hz, 2',6'-Ar-CH), 8.55 (dd, 1 H, ³*J*_{H,H} = 1.7, 8.8 Hz, 6-Ar-CH), 9.24 (d, 1 H, ⁴*J*_{H,H} = 1.7 Hz, 2-Ar-CH) ppm; **¹³C-NMR** (400 MHz, DMSO-*d*₆) δ = 13.1 (CH₃), 56.9 (OCH₃), 110.8 (Ar-C), 112.6 (5-Ar-CH), 118.4 (2',6'-Ar-CH), 124.6 (Ar-C), 124.9

(4'-Ar-CH), 127.3 (Ar-C), 128.9 (3',5'-Ar-CH), 136.6 (6-Ar-CH), 138.1 (Ar-C or 2-Ar-CH), 138.2 (Ar-C or 2-Ar-CH), 146.6 (CH), 151.8 (Ar-C), 159.2 (Ar-C), 161.8 (C=O) ppm; **ESI-MS** m/z (%) = 372.0 [M+H]⁺ (22 %), 743.1 [2M+H]⁺ (8 %); **HPLC-Analysis (Method B)**: 90 %, R_t = 18.0 min.

(4Z)-5-methyl-2-phenyl-4-[2-(trifluoromethyl)phenyl]methylidenepyrazol-3-one **80ac**

TLC R_f = 0.1 (Hexane/EtOAc 95:5); **Reaction time**: 20 h; **Purification**: Flash-Chromatography Hexane/EtOAc 95:5 (R_f = 0.1); **Yield**: 320 mg of red solid (0.97 mmol, 48 %); **¹H-NMR** (400 MHz, CDCl₃) δ = 2.20 (s, 3 H, CH₃), 7.05 (att, 1 H, ^{3,4} $J_{H,H}$ = 1.1, 7.4 Hz, 4'-Ar-CH), 7.26 (at, 2 H, ³ $J_{H,H}$ = 7.4, 8.7 Hz, 3',5'-Ar-CH), 7.44 (at, 1 H, ³ $J_{H,H}$ = 7.6 Hz, 5-Ar-CH), 7.52 (at, 1 H, ³ $J_{H,H}$ = 7.6, 8.1 Hz, 4-Ar-CH), 7.62-7.65 (m, 2 H, CH, 6-Ar-CH), 7.80 (dd, 2 H, ^{3,4} $J_{H,H}$ = 1.1, 8.7 Hz, 2',6'-Ar-CH), 8.37 (d, 1 H, ³ $J_{H,H}$ = 8.1 Hz, 3-Ar-CH) ppm; **¹³C-NMR** (400 MHz, CDCl₃) δ = 13.0 (CH₃), 118.9 (2',6'-Ar-CH), 124.1 (q, ¹ $J_{C,F}$ = 273.9 Hz, CF₃), 125.0 (4'-Ar-CH), 126.0 (q, ⁴ $J_{C,F}$ = 5.5 Hz, 6-Ar-CH), 128.8 (3',5'-Ar-CH), 129.4 (q, ³ $J_{C,F}$ = 30.2 Hz, Ar-C), 130.4 (q, ² $J_{C,F}$ = 66.1 Hz, Ar-C), 131.3 (5-Ar-CH), 131.5 (4-Ar-CH), 132.7 (3-Ar-CH), 138.1 (Ar-C), 141.3 (CH), 150.5 (Ar-C), 161.0 (C=O) ppm; **ESI-MS** m/z (%) = 331.1 [M+H]⁺ (100 %), 348.1 [M+NH₄]⁺ (8 %), 661.2 [2M+H]⁺ (3 %); **APCI-MS** m/z (%) = 331.1 [M+H]⁺ (100 %); **HR-MS** m/z = 331.1058 [M+H]⁺ (calculated: 331.1053); **HPLC-Analysis (Method B)**: 98 %, R_t = 19.8 min.

(Z)-4-(3-bromo-4-fluorobenzylidene)-3-methyl-1-phenyl-1H-pyrazol-5(4H)-one **80ad**

TLC R_f = 0.6 (Hexane/EtOAc 7:3); **Reaction time**: 2 h; **Purification**: Filtration from HOAc/ethanol; **Yield**: 189 mg of red solid (0.53 mmol, 57 %); **NOESY** (CH₃,CH → Z) **¹H-NMR** (400 MHz, DMSO-d₆) δ = 2.33 (s, 3 H,) 7.21 (at, 1 H, ³ $J_{H,H}$ = 7.4 Hz, 4'-Ar-CH), 7.45 (at, 2 H, ³ $J_{H,H}$ = 7.4, 7.6 Hz, 3',5'-Ar-CH), 7.60 (at, 1 H, ³ $J_{H,H(F)}$ = 8.7 Hz, 6-Ar-CH), 7.84 (s, 1 H, CH), 7.89 (d, 2 H, ³ $J_{7.6\text{ Hz}}$ = H,H, 2',6'-Ar-CH), 8.57 (ddd, 1 H, ^{3,4} $J_{H,H(F)}$ = 2.1, 5.0, 8.7 Hz, 5-Ar-CH), 9.20 (dd, 1 H, ^{3,4} $J_{H,H(F)}$ = 2.1, 7.0 Hz, 3-Ar-CH), **¹³C-NMR** (400 MHz, DMSO-d₆) δ = 13.1 (CH₃), 117.1 (d, ² $J_{C,F}$ = 22.8 Hz, 6-Ar-CH) 118.5 (2',6'-Ar-CH), 124.8 (4'-Ar-CH), 127.3 (Ar-C), 128.9 (3',5'-Ar-CH), 131.2 (Ar-C), 136.0 (d, ² $J_{C,F}$ = 8.6 Hz, 5-Ar-CH), 138.0 (Ar-C), 138.4 (3-Ar-CH), 145.4 (CH), 151.8 (Ar-C), 161.4 (C=O) ppm; **¹H-NMR** (400 MHz, CDCl₃) δ = 2.23 (s, 3 H, CH₃), 3.02 (s, 6 H, 2xCH₃), 6.62 (d, 2 H, ³ $J_{H,H}$ = 9.0 Hz, 3,5-Ar-CH), 7.07 (at, 1 H, ³ $J_{H,H}$ = 7.4 Hz, 4'-Ar-CH), 7.15 (s, 1 H, CH), 7.32 (at, 2 H, ³ $J_{H,H}$ = 7.4, 7.9 Hz, 3',5'-Ar-CH), 7.93 (d, 2 H, ³ $J_{H,H}$ = 7.9 Hz, 2',6'-Ar-CH), 8.48 (d, 2 H, ³ $J_{H,H}$ = 9.0 Hz, 2,6-Ar-CH) ppm; **¹³C-NMR** (400 MHz, CDCl₃) δ = 13.5 (CH₃), 40.1 (2xCH₃), 111.4 (3,5-Ar-CH), 119.2 (2',6'-Ar-CH), 121.0 (Ar-C), 121.9 (Ar-C), 124.4 (4'-Ar-CH), 128.7 (3',5'-Ar-CH), 137.4 (2,6-Ar-CH), 139.1 (Ar-C), 147.4 (CH), 151.3 (Ar-C), 153.7 (Ar-C), 163.0 (C=O) ppm; **ESI-MS** m/z (%) = 359.0 [M+H]⁺ (100 %), 719.0 [2M+H]⁺ (45 %); **HR-MS** m/z = 359.0195 [M+H]⁺ (calculated: 359.0190); **HPLC-Analysis (Method B)**: 66 %, R_t = 18.4 min.

(4Z)-5-methyl-2-phenyl-4-[3-(trifluoromethyl)phenyl]methylidenepyrazol-3-one **80ae**

TLC R_f = 0.1 (Hexane/EtOAc 9:1); **Reaction time**: 4 h; **Purification**: Re-crystallisation from ethanol; **Yield**: 416 mg of red crystals (1.26 mmol, 62 %); **NOESY** (CH₃,CH → Z) **¹H-NMR**

(400 MHz, DMSO- d_6) δ = 2.30 (s, 3 H, $\underline{\text{CH}_3}$), 7.18 (at, 1 H, $^3J_{\text{H,H}}$ = 7.4 Hz, Ar- $\underline{\text{CH}}$), 7.39-7.46 (m, 2 H, 2xAr- $\underline{\text{CH}}$), 7.72 (d, 1 H, $^3J_{\text{H,H}}$ = 8.6 Hz, Ar- $\underline{\text{CH}}$), 7.76 (d, 1 H, $^3J_{\text{H,H}}$ = 7.9 Hz, Ar- $\underline{\text{CH}}$), 7.85-7.89 (m, 3 H, 2xAr- $\underline{\text{CH}}$, $\underline{\text{CH}}$), 7.92 (d, 1 H, $^3J_{\text{H,H}}$ = 7.7 Hz, Ar- $\underline{\text{CH}}$), 8.69 (d, 1 H, $^3J_{\text{H,H}}$ = 7.9 Hz, Ar- $\underline{\text{CH}}$), 9.07 (s, 1 H, 2-Ar- $\underline{\text{CH}}$) ppm; $^{13}\text{C-NMR}$ (400 MHz, DMSO- d_6) δ = 13.0 ($\underline{\text{CH}_3}$), 118.4 (2xAr- $\underline{\text{CH}}$), 120.5 (Ar- $\underline{\text{CH}}$), 123.9 (q, $^1J_{\text{C,F}}$ = 272.6 Hz, $\underline{\text{CF}_3}$), 128.2 (Ar- $\underline{\text{CH}}$), 128.8 (2xAr- $\underline{\text{CH}}$), 128.9 (Ar- $\underline{\text{CH}}$), 129.7 (2-Ar- $\underline{\text{CH}}$), 133.5 (Ar- $\underline{\text{C}}$), 137.1 (Ar- $\underline{\text{CH}}$), 137.9 (Ar- $\underline{\text{C}}$) 146.0 ($\underline{\text{CH}}$), 151.6 (Ar- $\underline{\text{C}}$), 161.2 ($\underline{\text{C=O}}$) ppm; **ESI-MS** m/z (%) = 331.1 [$\text{M}+\text{H}$] $^+$ (83 %); **HPLC-Analysis (Method B)**: 88 %, R_t = 18.5 min.

(E/Z)-4-(3-(benzyloxy)benzylidene)-3-methyl-1-phenyl-1H-pyrazol-5(4H)-one **80af**

ratio 5.5 to 1 (Z to E) not isolated

TLC R_f = 0.4 (Hexane/EtOAc 9:1); **Reaction time**: 4 h; **Purification**: Flash-Chromatography Hexane/EtOAc 95:5 (R_f = 0.3); **Yield**: 192 mg of yellow solid (0.52 mmol, 62 %); NOESY ($\text{CH}_3, \text{CH} \rightarrow \text{Z}$); $^1\text{H-NMR}$ (400 MHz, CDCl_3) δ = 2.05 (s, 3 H, Z- $\underline{\text{CH}_3}$), 2.22 (s, 3 H, E- $\underline{\text{CH}_3}$), 5.01 (s, 2 H, E- $\underline{\text{CH}_2}$), 5.09 (s, 2 H, Z- $\underline{\text{CH}_2}$), 6.98-7.02 (m, 2 H,) 7.05-7.11 (m, 2 H,) 7.15 (s, 1 H, E- $\underline{\text{CH}}$), 7.22 (s, 1 H, Z- $\underline{\text{CH}}$), 7.22-7.35 (m, 6 H,) 7.37-7.41 (m, 2 H, 2xZ-Ar- $\underline{\text{CH}}$), 7.60-7.63 (m, 1 H,) 7.67 (d, 1 H, $^3J_{\text{H,H}}$ = 7.7 Hz, 6-Z-Ar- $\underline{\text{CH}}$), 7.85-7.89 (m, 2 H, 2xE-Ar- $\underline{\text{CH}}$), 7.85-7.89 (m, 3 H,) 8.54 (at, 1 H, $^4J_{\text{H,H}}$ = 1.9 Hz, 2-Z-Ar- $\underline{\text{CH}}$) ppm; $^{13}\text{C-NMR}$ (400 MHz, CDCl_3) δ = 13.4 ((E)- $\underline{\text{CH}_3}$), 17.6 ((Z)- $\underline{\text{CH}_3}$), 70.3 ((E,Z)- $\underline{\text{CH}_2}$), 116.3 (Ar- $\underline{\text{CH}}$), 117.9 ((E)-2-Ar- $\underline{\text{CCH}}$), 118.7 (Ar- $\underline{\text{C}}$), 119.3 (2xAr- $\underline{\text{CH}}$), 121.2 (Ar- $\underline{\text{CH}}$), 121.8 (Ar- $\underline{\text{CH}}$), 123.2 (Ar- $\underline{\text{CH}}$), 125.0, 127.3, 127.5, 127.6, 127.9, 128.0, 128.2, 128.3, 128.7, 2x128.8, 128.9, 129.0, 129.6, 129.9 (Ar- $\underline{\text{CH}}$ or Ar- $\underline{\text{C}}$), 134.3, 134.5, 136.5, 136.8, 138.3, 138.5, 145.5 (Ar- $\underline{\text{C}}$), 147.0 ((E)- $\underline{\text{CH}}$), 147.6, 150.9, 158.8, 159.0, 161.9, 163.8 (Ar- $\underline{\text{C}}$), ppm; **ESI-MS** m/z (%) = 369.2 [$\text{M}+\text{H}$] $^+$ (100 %), 391.3 [$\text{M}+\text{Na}$] $^+$ (35 %); **HR-MS** m/z = 369.1599 [$\text{M}+\text{H}$] $^+$ (calculated: 369.1598); **HPLC-Analysis (Method B)**: 98 %, R_t = 19.2 min.

(4Z)-4-[(4-hydroxy-3,5-dimethoxyphenyl)methylidene]-5-methyl-2-phenylpyrazol-3-one **80ag**^[364]

TLC R_f = 0.1 (Hexane/EtOAc 6:4); **Reaction time**: 16 h; **Purification**: Filtration from ethanol; **Yield**: 496 mg of red crystals (1.47 mmol, 72 %); NOESY ($\text{CH}_3, \text{CH} \rightarrow \text{Z}$); $^1\text{H-NMR}$ (400 MHz, DMSO- d_6) δ = 2.32 (s, 3 H, $\underline{\text{CH}_3}$), 3.87 (s, 6 H, 2xAr- $\underline{\text{CH}_3}$), 7.19 (att, 1 H, $^{3,4}J_{\text{H,H}}$ = 1.0, 7.4 Hz, 4'-Ar- $\underline{\text{CH}}$), 7.44 (dd, 1 H, $^3J_{\text{H,H}}$ = 7.4, 8.7 Hz, 3',5'-Ar- $\underline{\text{CH}}$), 7.72 (s, 1 H, $\underline{\text{CH}}$), 7.92 (dd, 1 H, $^{3,4}J_{\text{H,H}}$ = 1.0, 8.7 Hz, 2',6'-Ar- $\underline{\text{CH}}$), 8.29 (s, 2 H, 2,6-Ar- $\underline{\text{CH}}$) ppm; $^{13}\text{C-NMR}$ (400 MHz, DMSO- d_6) δ = 13.2 ($\underline{\text{CH}_3}$), 56.1 (2xO $\underline{\text{CH}_3}$), 112.7 (2,6-Ar- $\underline{\text{CH}}$), 118.5 (2',6'-Ar- $\underline{\text{CH}}$), 122.8 (4'-Ar- $\underline{\text{CH}}$), 124.0 (Ar- $\underline{\text{C}}$), 124.5 (Ar- $\underline{\text{C}}$), 128.8 (3',5'-Ar- $\underline{\text{CH}}$), 138.5 (Ar- $\underline{\text{C}}$), 142.3 (Ar- $\underline{\text{C}}$), 147.5 (Ar- $\underline{\text{C}}$), 149.4 ($\underline{\text{CH}}$), 151.8 (Ar- $\underline{\text{C}}$), 162.1 ($\underline{\text{C=O}}$) ppm; **ESI-MS** m/z (%) = 339.1 [$\text{M}+\text{H}$] $^+$ (100 %), 677.3 [$2\text{M}+\text{H}$] $^+$ (24 %); **HPLC-Analysis (Method B)**: 95 %, R_t = 17.8 min.

(4Z/E)-5-methyl-2-phenyl-4-(phenylmethylidene)pyrazol-3-one **80ah**^[365]

Is a mixture of E to Z of 1 to 6 **TLC** R_f = 0.1 (Hexane/EtOAc 9:1); **Reaction time**: 16 h; **Purification**: Flash-Chromatography hexane/EtOAc 9:1 (R_f = 0.1); **Yield**: 438 mg of yellow solid (1.67 mmol, 82 %); NOESY ($\text{CH}_3, \text{CH} \rightarrow \text{Z}$); NOESY ($\text{CH}_3, \text{ArCH} \rightarrow \text{E}$); $^1\text{H-NMR}$ (400

MHz, CDCl_3) δ = 2.12 (s, 3 H, E- CH_3), 2.24 (s, 3 H, Z- CH_3), 7.09 (att, 1 H, $^3J_{\text{H,H}}$ = 1.0, 7.4 Hz, 4'-(E+Z)-Ar-CH), 7.27 (s, 1 H, Z-CH), 7.32 (dd, 2 H, $^3J_{\text{H,H}}$ = 7.4, 8.6 Hz, 3',5'-(E+Z)-Ar-CH), 7.37-7.47 (m, 3 H, 3,4,5-Z-Ar-CH), 7.37-7.47 (m, 5 H, 2,3,4,5,6-E-Ar-CH), 7.88 (dd, 2 H, $^3,4J_{\text{H,H}}$ = 1.0, 8.6 Hz, 2',6'-(E+Z)-Ar-CH), 7.92 (s, 1 H, E-CH), 8.37-8.41 (m, 2 H, 2,6-Z-Ar-CH) ppm; $^{13}\text{C-NMR}$ (400 MHz, CDCl_3) δ = 13.4 (Z- CH_3), 17.7 (E- CH_3), 118.7 (2',6'-E-Ar-CH), 119.2 (2',6'-Z-Ar-CH), 125.0 (4'-(E+Z)-Ar-CH), 127.8 (Ar-C), 128.7, 128.8, 128.9, 129.0 (3,4,5-Z-Ar and 2-6-E-Ar and 3',5'-(E+Z)-Ar-CH), 130.5 (Ar-C or Ar-CH), 131.2 (Ar-C), 133.0, 133.1 (3,4,5-Z-Ar- and 2-6-Ar-CH), 133.8 (2,6-Z-Ar-CH), 138.4 (Ar-C), 145.8 (E-CH), 147.0 (Z-Ar-CH), 147.6 (Ar-C), 150.9 (Ar-C), 161.9 (C=O) ppm; **ESI-MS** m/z (%) = 263.1 $[\text{M}+\text{H}]^+$ (100 %), 280.1 $[\text{M}+\text{NH}_4]^+$ (3 %); **HPLC-Analysis (Method B)**: 88 %, R_t = 18.5 min.

(4Z)-4-[(3-hydroxyphenyl)methylidene]-5-methyl-2-phenylpyrazol-3-one **80ai**^[366]

TLC R_f = 0.2 ($\text{CHCl}_3/\text{MeOH}/\text{HOAc}$ 96:3:1); **Reaction time**: 16 h; **Purification**: Flash-Chromatography $\text{CHCl}_3/\text{MeOH}/\text{HOAc}$ 97:2:1 (R_f = 0.1); **Yield**: 501 mg of red solid (1.80 mmol, 89 %); $^1\text{H-NMR}$ (400 MHz, CDCl_3) δ = 2.34 (s, 3 H, CH_3), 7.07 (dd, 1 H, $^3J_{\text{H,H}}$ = 8.2, 1.8 Hz, 6-Ar-CH), 7.19 (at, 1 H, $^3J_{\text{H,H}}$ = 7.4 Hz, 4'-Ar-CH), 7.33-7.43 (m, 4 H, 3',5,5'-Ar-CH, CH), 7.60 (d, 1 H, $^3J_{\text{H,H}}$ = 7.7 Hz, 4-Ar-CH), 7.90 (d, 2 H, $^3J_{\text{H,H}}$ = 7.6 Hz, 2',6'-Ar-CH), 8.52 (s, 1 H, 2-Ar-CH) ppm; $^{13}\text{C-NMR}$ (400 MHz, CDCl_3) δ = 13.4 (CH_3), 119.2 (2-Ar-CH), 119.7 (2',6'-Ar-CH), 121.1 (6-Ar-CH), 125.4 (4'-Ar-CH), 127.2 (4-Ar-CH), 127.8 (Ar-C), 129.0 (3',5'-Ar-CH), 129.1 (Ar-C), 130.0 (5-Ar-CH), 134.2 (Ar-C), 138.2 (Ar-C), 147.5 (CH) 151.3 (Ar-C), 156.2 (C=O), 161.9 (C=O) ppm; **ESI-MS** m/z (%) = 279.1 $[\text{M}+\text{H}]^+$ (100 %), 296.1 $[\text{M}+\text{NH}_4]^+$ (4 %), 557.2 $[2\text{M}+\text{H}]^+$ (2 %); **HPLC-Analysis (Method B)**: 95 %, R_t = 17.3 min.

(4Z)-4-[(3,4-dihydroxyphenyl)methylidene]-5-methyl-2-phenylpyrazol-3-one **80ak**

Reaction time: 20 h; **Purification**: Filtration from HOAc; **Yield**: 310 mg of red solid (1.05 mmol, 87 %); NOESY ($\text{CH}_3, \text{CH} \rightarrow \text{Z}$); $^1\text{H-NMR}$ (400 MHz, CDCl_3) δ = 2.33 (s, 3 H, CH_3), 6.96 (d, 1 H, $^3J_{\text{H,H}}$ = 8.3 Hz, 5-Ar-CH), 7.19-7.24 (m, 1 H, 4'-Ar-CH), 7.33 (dd, 1 H, $^3,4J_{\text{H,H}}$ = 8.3, 2.1 Hz, 6-Ar-CH), 7.34 (s, 1 H, CH), 7.40 (at, 2 H, $^3J_{\text{H,H}}$ = 7.9 Hz, 3',5'-Ar-CH), 7.78-7.81 (m, 2 H, 2',6'-Ar-CH), 9.19 (d, 1 H, $^4J_{\text{H,H}}$ = 2.1 Hz, 2-Ar-CH) ppm; $^{13}\text{C-NMR}$ (400 MHz, CDCl_3) δ = 13.4 (CH_3), 115.2 (5-Ar-CH), 119.3 (2-Ar-CH), 120.5 (2',6'-Ar-CH), 123.8 (Ar-C), 125.8 (4'-Ar-CH), 126.4 (Ar-C), 128.9 (3',5'-Ar-CH), 131.7 (6-Ar-CH), 138.0 (Ar-C), 143.8 (Ar-C), 149.6 (CH), 151.2 (Ar-C), 152.0 (Ar-C), 162.4 (C=O) ppm; **ESI-MS** m/z (%) = 295.1 $[\text{M}+\text{H}]^+$ (92 %), 589.2 $[2\text{M}+\text{H}]^+$ (17 %); **HPLC-Analysis (Method B)**: 87 %, R_t = 16.3 min.

(4Z)-4-[4-(dimethylamino)phenyl]methylidene-5-methyl-2-phenylpyrazol-3-one **80am**^[361]

Reaction time: 20 h; **Purification**: Filtration from HOAc; **Yield**: 85 mg of yellow solid (0.28 mmol, 56 %); $^1\text{H-NMR}$ (400 MHz, CDCl_3) δ = 2.23 (s, 3 H, CH_3), 3.02 (s, 6 H, 2x CH_3), 6.62 (d, 2 H, $^3J_{\text{H,H}}$ = 9.0 Hz, 3,5-Ar-CH), 7.07 (at, 1 H, $^3J_{\text{H,H}}$ = 7.4 Hz, 4'-Ar-CH), 7.15 (s, 1 H, CH), 7.32 (at, 2 H, $^3J_{\text{H,H}}$ = 7.9, 7.4 Hz, 3',5'-Ar-CH), 7.93 (d, 2 H, $^3J_{\text{H,H}}$ = 7.9 Hz, 2',6'-Ar-CH), 8.48 (d, 2 H, $^3J_{\text{H,H}}$ = 9.0 Hz, 2,6-Ar-CH) ppm; $^{13}\text{C-NMR}$ (400 MHz, CDCl_3) δ = 13.5 (CH_3), 40.1

(2xCH₃), 111.4 (3,5-Ar-CH), 119.2 (2',6'-Ar-CH), 121.0 (Ar-C), 121.9 (Ar-C), 124.4 (4'-Ar-CH), 128.7 (3',5'-Ar-CH), 137.4 (2,6-Ar-CH), 139.1 (Ar-C), 147.4 (CH), 151.3 (Ar-C), 153.7 (Ar-C), 163.0 (C=O) ppm; **ESI-MS** m/z (%) = 306.2 [M+H]⁺ (100 %), 611.3 [2M+H]⁺ (30 %), 1238.6 [3M+NH₄]⁺ (10 %); **HR-MS** m/z = 306.1602 [M+H]⁺ (calculated: 306.1601); **HPLC-Analysis (Method B)**: 66 %, R_t = 18.4 min.

(4Z)-5-methyl-2-phenyl-4-[4-(trifluoromethyl)phenyl]methylidenepyrazol-3-one **80aj**

TLC R_f = 0.1 (Hexane/EtOAc 9:1); **Reaction time**: 4 h; **Purification**: Flash-Chromatography Hexane/EtOAc 9:1 (R_f = 0.1), DCM; **Yield**: 621 mg of red solid (1.88 mmol, 93 %); **¹H-NMR** (400 MHz, CDCl₃) δ = 2.08 (s, 3 H, CH₃), 7.02 (at, 1 H, ³ $J_{H,H}$ = 7.4 Hz, 4'-Ar-CH), 7.07 (s, 1 H, CH), 7.24 (at, 2 H, ³ $J_{H,H}$ = 7.4, 8.5 Hz, 3',5'-Ar-CH), 7.52 (d, 2 H, ³ $J_{H,H}$ = 8.2 Hz, 3,5-Ar-CH), 7.78 (d, 2 H, ³ $J_{H,H}$ = 8.5 Hz, 2',6'-Ar-CH), 8.31 (d, 2 H, ³ $J_{H,H}$ = 8.2 Hz, 2,6-Ar-CH), ppm; **¹³C-NMR** (400 MHz, CDCl₃) δ = 13.1 (CH₃), 118.8 (2',6'-Ar-CH), 120.4 (q, ¹ $J_{C,F}$ = 393.1 Hz, CF₃), 125.0 (4'-Ar-CH), 125.4 (q, ³ $J_{C,F}$ = 3.7 Hz, 3,5-Ar-CH), 128.8 (3',5'-Ar-CH), 129.5 (Ar-C), 133.3 (q, ² $J_{C,F}$ = 32.8 Hz, 4-Ar-CCF₃), 133.4 (2,6-Ar-CH), 135.7 (Ar-C), 138.1 (Ar-C), 144.2 (CH), 150.6 (Ar-C), 161.2 (C=O) ppm; **ESI-MS** m/z (%) = 331.1 [M+H]⁺ (100 %), 348.1 [M+NH₄]⁺ (1 %); **HPLC-Analysis (Method B)**: 98 %, R_t = 19.8 min.

3-[(4Z)-4-[(2-hydroxyphenyl)methylidene]-3-methyl-5-oxopyrazol-1-yl] benzoic acid **81m**^[367]

TLC R_f = 0.5 (CHCl₃/MeOH 8:2); **Reaction time**: 16 h; **Purification**: Flash-Chromatography CHCl₃/MeOH 95:5 (R_f = 0.3); **Yield**: 22 mg of red solid (0.07 mmol, 13 %); **¹H-NMR** (400 MHz, DMSO-d₆) δ = 2.34 (s, 3 H, CH₃), 6.93 (at, 1 H, ³ $J_{H,H}$ = 7.3, 8.0 Hz, 5-Ar-CH), 7.01 (dd, 1 H, ^{3,4} $J_{H,H}$ = 0.7, 8.6 Hz, 3-Ar-CH), 7.47 (ddd, 1 H, ^{3,4} $J_{H,H}$ = 1.6, 7.3, 8.6 Hz, 4-Ar-CH), 7.55 (at, 1 H, ³ $J_{H,H}$ = 8.0 Hz, 5'-Ar-CH), 7.74-7.77 (m, 1 H, 6'-Ar-CH), 8.07 (s, 1 H, CH), 8.14-8.18 (m, 1 H, 4'-Ar-CH), 8.55 (at, 1 H, ⁴ $J_{H,H}$ = 1.8 Hz, 2'-Ar-CH), 9.07 (dd, 1 H, ^{3,4} $J_{H,H}$ = 1.6, 8.0 Hz, 6-Ar-CH) ppm; **¹³C-NMR** (400 MHz, DMSO-d₆) δ = 13.1 (CH₃), 116.0 (3-Ar-CH), 118.9 (2'-Ar-CH), 119.8 (5-Ar-CH), 122.0 (4'-Ar-CH), 124.4 (Ar-C), 125.1 (6'-Ar-CH), 129.3 (5'-Ar-CH), 133.0 (6-Ar-CH), 136.1 (Ar-C), 138.5 (Ar-C), 142.2 (CH), 152.3 (Ar-C), 159.4 (Ar-C), 162.0 (Ar-C), 167.1 (C=O), 184.6 (COOH) ppm.

3-[(4Z)-4-[(3-bromo-4-fluorophenyl)methylidene]-3-methyl-5-oxopyrazol-1-yl] benzoic acid **81o**

TLC R_f = 0.1 (Hexane/EtOAc 7:3); **Reaction time**: 2 h; **Purification**: Filtration from HOAc; **Yield**: 126 mg of red solid (0.31 mmol, 58 %); NOESY (CH₃,CH → Z); **¹H-NMR** (400 MHz, DMSO-d₆) δ = 2.35 (s, 3 H, CH₃), 7.57 (at, 1 H, ³ $J_{H,H}$ = 7.8, 8.2 Hz, 5-Ar-CH), 7.61 (at, 1 H, ³ $J_{H,H(F)}$ = 8.7 Hz, 5'-Ar-CH), 7.77 (adt, 1 H, ^{3,4} $J_{H,H}$ = 1.3, 7.8 Hz, 4-Ar-CH), 7.86 (s, 1 H, CH), 8.15 (ddd, 1 H, ^{3,4} $J_{H,H}$ = 1.3, 1.9, 8.2 Hz, 6-Ar-CH), 8.52 (at, 1 H, ⁴ $J_{H,H}$ = 1.9 Hz, 2-Ar-CH), 8.59 (ddd, 1 H, ^{3,4} $J_{H,H(F)}$ = 2.1, 4.9, 8.7 Hz, 6'-Ar-CH), 9.17 (dd, 1 H, ^{3,4} $J_{H,H(F)}$ = 2.1, 7.0 Hz, 3'-Ar-CH), 13.13 (s(br), 1 H, COOH) ppm; **¹³C-NMR** (400 MHz, DMSO-d₆) δ = 13.1 (CH₃), 117.3 (5'-Ar-CH), 118.8 (6'-Ar-CH), 122.2 (6-Ar-CH), 125.4 (4-Ar-CH), 127.2 (Ar-C), 129.3 (5-Ar-CH), 131.2 (Ar-C), 131.5 (Ar-C), 136.1 (2-Ar-CH), 138.2 (Ar-C), 138.5 (3'-Ar-CH), 145.8 (CH)

152.3 (Ar-C), 161.6 (Ar-C), 167.0 (C=O) ppm; **ESI-MS** m/z (%) = 401.0 [M-H]⁻ (20 %), 436.0 [M+Cl-H]⁻ (100 %), 460.0 [M+HAc-H]⁻ (55 %), **HR-MS** m/z = 400.9935 [M-H]⁻ (calculated: 400.9943); **HPLC-Analysis (Method B)**: 92 %, R_t = 17.0 min.

3-[(4Z)-3-methyl-5-oxo-4- (phenylmethylidene)pyrazol-1-yl] benzoic acid **81p**^[368]

Reaction time: 6 h; **Purification**: Filtration from HOAc; **Yield**: 173 mg of yellow solid (0.56 mmol, 78 %); **NOESY** (CH₃,CH → Z); **¹H-NMR** (400 MHz, DMSO-d₆) δ = 2.35 (s, 3 H, CH₃), 7.52-7.65 (m, 4 H, 3,4,5,5'-Ar-CH), 7.76 (d, 1 H, ³J_{H,H} = 7.7 Hz, 4'-Ar-CH), 7.84 (s, 1 H, CH), 8.13-8.17 (m, 1 H, 6'-Ar-CH), 8.55 (at, 1 H, ⁴J_{H,H} = 1.8 Hz, 2'-Ar-CH), 8.58 (d, 2 H, ³J_{H,H} = 7.5 Hz, 2,6-Ar-CH), 13.07 (s(br), 1 H, COOH) ppm; **¹³C-NMR** (400 MHz, DMSO-d₆) δ = 13.1 (CH₃), 118.7 (2'-Ar-CH), 122.0 (6'-Ar-CH), 125.2 (4'-Ar-CH), 126.5 (Ar-C), 128.7 (3,5-Ar-CH), 129.2 (4, 5'-Ar-CH), 131.4 (Ar-C), 132.9 (Ar-C), 133.3 (4 or 5'-Ar-CH), 133.8 (2,6-Ar-CH), 138.3 (Ar-C), 148.7 (CH), 152.3 (Ar-C), 161.6 (C=O), 167.0 (COOH) ppm; **HPLC-Analysis (Method B)**: 82 %, R_t = 17.7 min.

3-[(4Z)-4-[4-(benzyloxy)phenyl]methylidene-3- methyl-5-oxopyrazol-1-yl] benzoic acid **81n**

Reaction time: 18 h **Purification**: Filtration from HOAc **Yield**: 176 mg of yellow solid (0.43 mmol, 64 %); **¹H-NMR** (400 MHz, DMSO-d₆) δ = 1.91 (s, 3 H, CH₃), 5.25 (s, 2 H, CH₂), 7.20-7.24 (m, 2 H, 2xAr-CH), 7.34-7.58 (m, 7 H, 7xAr-CH), 7.73-7.77 (m, 1 H, 1xAr-CH), 7.78 (s, 1 H, CH), 8.57 (at, 1 H, ⁴J_{H,H} = 2.0 Hz, Ar-CH), 8.70 (d, 2 H, ³J_{H,H} = 9.0 Hz, 2xAr-CH), 12.62 (s(br), 2 H, 2xOH) ppm; **¹³C-NMR** (400 MHz, DMSO-d₆) δ = 21.1 (CH₃), 69.7 (CH₂), 115.1 (Ar-CH), 115.3 (Ar-CH), 118.7 (Ar-CH), 122.0 (Ar-CH), 123.6 (Ar-C), 125.0 (Ar-CH), 126.3 (Ar-CH), 127.9 (Ar-CH), 128.0 (Ar-CH), 128.1 (Ar-CH), 128.5 (Ar-CH), 129.2 (Ar-CH), 136.3 (Ar-C), 136.9 (2xAr-CH), 138.5 (Ar-C), 148.5 (CH), 152.3 (Ar-C), 162.0 (Ar-C), 162.8 (Ar-C), 167.1 (C=O), 172.0 (COOH) ppm; **ESI-MS** m/z (%) = 411.1 [M-H]⁻ (53 %) **HPLC-Analysis (Method B)**: 46 %, R_t = 20.1 min.

3-[(4Z)-4-[(3,4-dihydroxyphenyl)methylidene]-3- methyl-5-oxopyrazol-1-yl] benzoic acid **81q**^[369]
ESI-MS m/z (%) = 337.1 [M-H]⁻ (100 %), 675.2 [2M-H]⁻ (22 %).

Synthesis of phenyl-furanyl-carbaldehyde **86**

5-Bromofuran-2-carbaldehyde (100 mg, 0.57 mmol), phenyl-boronic acid (105 mg, 0.86 mmol), Pd(PPh₃)₄ (13 mg, 0.01 mmol) and potassium carbonate (197 mg, 1.425 mmol) were dissolved in DMF under a N₂-gas protection atmosphere. H₂O (0.5 mL) were added so the suspension and the reaction mixture was heated to 110 °C. After 4 h, TLC showed complete consumption of starting material and the reaction mixture was concentrated and subjected to column chromatography.

5-phenylfuran-2-carbaldehyde **86**^[370]

TLC R_f = 0.5 (Hexane/EtOAc 8:2); **Reaction time**: 4 h **Yield**: 38 mg of yellow oil (0.22 mmol, 39 %); **Purification**: Flash-Chromatography Cyclohexan/EtOAc 95:5 (R_f = 0.1); **¹H-NMR** (400

MHz, CDCl₃) δ = 6.58 (d, 1 H, $^3J_{\text{H,H}}$ = 3.7 Hz, Furan-CH), 7.06 (d, 1 H, $^3J_{\text{H,H}}$ = 3.7 Hz, Furan-CH), 7.11-7.21 (m, 3 H, 3xAr-CH), 7.54-7.58 (m, 2 H, 2xAr-CH), 9.39 (s, 1 H, CHO).

Reduction of double bond in pyrazole derivatives

The pyrazole derivative **80ak** (253 mg, 0.86 mmol) was dissolved in 25 mL dioxane and Pd/C (360 mg) was added. The reaction mixture was placed in a hydrogenation chamber and the hydrogenation was carried out at 30 psi H₂ under gently shaking. The crude was filtered, washed with EtOAc and concentrated to afford the reduced analogue **85a** as a white solid.

4-[(5-hydroxy-3-methyl-1-phenylpyrazol-4-yl)methyl]benzene-1,2-diol **85a**

Reaction time: 4 h; **Purification:** Filtration from EtOAc; **Yield:** 255 mg of white solid (0.86 mmol, 100 %); **¹H-NMR** (400 MHz, MeOD-d₄) δ = 2.10 (s, 3 H, CH₃), 3.51 (s, 2 H, CH₂), 6.56 (dd, 1 H, $^3,^4J_{\text{H,H}}$ = 8.1, 2.0 Hz, 6-Ar-CH), 6.64-6.71 (m, 2 H, 2,5-Ar-CH), 7.25 (at, 1 H, $^3J_{\text{H,H}}$ = 7.4 Hz, 4'-Ar-CH), 7.42 (at, 2 H, $^3J_{\text{H,H}}$ = 7.9, 7.4 Hz, 3',5'-Ar-CH), 7.62 (d, 2 H, $^3J_{\text{H,H}}$ = 7.9 Hz, 2',6'-Ar-CH) ppm; **¹³C-NMR** (400 MHz, MeOD-d₄) δ = 11.2 (CH₃), 27.8 (CH₂), 106.9 (Ar-C), 116.2 (2(5)-Ar-CH), 116.3 (2(5)-Ar-CH), 120.4 (6-Ar-CH), 122.1 (2',6'-Ar-CH), 127.2 (4'-Ar-CH), 130.1 (3',5'-Ar-CH), 133.4 (Ar-C), 137.8 (Ar-C), 144.4 (Ar-C), 146.2 (Ar-C), 148.7 (Ar-C) ppm; **ESI-MS** m/z (%) = 297.1 [M+H]⁺ (100 %).

Synthesis of heterocyclic modified pyrazole derivatives

The Phenylhydrazine or the 3-hydrazinyl benzoic acid (2.03 mmol, 1.0 eq), ethyl 3-oxobutanoate (2.03 mmol, 1.0 eq) were dissolved in 5 mL HOAc. The reaction mixture was stirred at 110 °C for 16 h. The heterocyclic modified aldehyde (2.44 mmol, 1.2 eq) was added to the yellow reaction mixture. The reaction mixture was continued to stir at 110 °C, until TLC showed complete consumption of intermediate formed pyrazole precursor. The reaction mixture was cooled and the product was isolated by simple filtration or column chromatography.

(4Z)-4-(furan-2-ylmethylidene)-5-methyl-2-phenylpyrazol-3-one **88a**^[353]

TLC R_f = 0.3 (Hexane/EtOAc 8:2); **Reaction time:** 4 h; **Purification:** Flash-Chromatography Hexane/EtOAc 8:2 (R_f = 0.3); **Yield:** 472 mg of red solid (1.87 mmol, 92 %); **¹H-NMR** (400 MHz, DMSO-d₆) δ = 2.33 (s, 3 H, CH₃), 6.94 (dd, 1 H, $^3J_{\text{H,H}}$ = 1.6, 3.7 Hz, 4-Furan-CH), 7.19 (at, 1 H, $^3J_{\text{H,H}}$ = 7.4 Hz, 4'-Ar-CH), 7.41-7.47 (m, 2 H, 3',5'-Ar-CH), 7.71 (s, 1 H, CH), 7.90-7.93 (m, 2 H, 2',6'-Ar-CH), 8.27 (d, 1 H, $^3J_{\text{H,H}}$ = 1.6 Hz, 5-Furan-CH), 8.64 (d, 1 H, $^3J_{\text{H,H}}$ = 3.7 Hz, 3-Furan-CH) ppm; **¹³C-NMR** (400 MHz, DMSO-d₆) δ = 12.8 (CH₃), 115.0 (4-Furan-CH), 117.8 (2',6'-Ar-CH), 118.2 (Ar-C), 121.4 (4'-Ar-CH or 3-Furan-CH), 124.5 (4'-Ar-CH or 3-Furan-CH), 128.9 (3',5'-Ar-CH), 130.5 (CH), 138.3 (Ar-C), 150.2 (Ar-C), 150.5 (Ar-C), 161.6 (C=O) ppm; **HPLC-Analysis (Method B):** 99 %, R_t = 12.6 min.

Synthesis of N-1-modified pyrazole derivatives

Synthesis of N-1-unsubstituted precursor 89

Ethyl 3-oxobutanoate (1275 μ L, 10 mmol) was added to ethanol and hydrazine (973 μ L, 20 mmol) was added drop wise to the reaction mixture. The temperature was maintained at 60 °C with ice-cooling. After complete addition of hydrazine the reaction mixture was continued to stir for 1 h until TLC showed complete consumption of starting ethyl-aceto-acetate. Upon cooling the product crystallised from the ethanol solution and was filtered and washed with ethanol.

5-methyl-2H-pyrazol-3-ol **89**^[371]

TLC R_f = 0.1 (DCM/MeOH 9:1); **Reaction time**: 1 h; **Purification**: Filtration from ethanol; **Yield**: 1066 mg of white solid (10.87 mmol, 100 %); **Yield**: 791 mg of white solid (8.06 mmol, 81 %); **¹H-NMR** (400 MHz, DMSO- d_6) δ = 2.08 (s, 3 H, $\underline{\text{CH}_3}$), 5.21 (s, 1 H, $\underline{\text{CH}}$), 10.28 (s(br), 1 H, $\underline{\text{OH}}$) ppm; **¹³C-NMR** (400 MHz, DMSO- d_6) δ = 11.2 ($\underline{\text{CH}_3}$), 88.9 ($\underline{\text{CH}}$), 139.3 (Ar- $\underline{\text{C}}$), 161.0 ($\underline{\text{C=O}}$) ppm; **HPLC-Analysis (Method B)**: 100 %, R_t = 1.9 min.

Synthesis of N-1-acetic ester pyrazole precursor 90

Compound **89** (250 mg, 2.55 mmol) in DMF (5 mL) was added to NaH (102 mg, 2.55 mmol) under ice-cooling at 0 °C and N_2 gas atmosphere. The reaction mixture was stirred for 10 min and ethyl 2-bromoacetate (283 μ L, 2.55 mmol) was added drop wise. The reaction mixture was continued to stir at rt until TLC showed complete consumption of starting materials. The reaction was quenched with water (20 mL), extracted with EtOAc (3x20 mL), dried over MgSO_4 , filtered and concentrated. The crude was purified by flash column chromatography.

Ethyl 2-(5-hydroxy-3-methylpyrazol-1-yl) acetate **90**^[372]

TLC R_f = 0.1 ($\text{CHCl}_3/\text{MeOH}$ 1:0.02); **Reaction time**: 6 h; **Purification**: Flash-Chromatography $\text{CHCl}_3/\text{MeOH}$ 1:0.02 \rightarrow 1:0.05 (R_f = 0.1, 0.3) **Purification**: Flash-Chromatography $\text{CHCl}_3/\text{MeOH}$ 1:0.02 (R_f = 0.1); **Yield**: 140 mg of white solid (0.76 mmol, 30 %); **¹H-NMR** (400 MHz, CDCl_3) δ = 1.25 (t, 3 H, $^3J_{\text{H,H}}$ = 7.1 Hz, $\text{CH}_2\underline{\text{CH}_3}$), 2.14 (s, 3 H, $\underline{\text{CH}_3}$), 4.19 (q, 2 H, $^3J_{\text{H,H}}$ = 7.1 Hz, $\text{CH}_2\underline{\text{CH}_3}$), 4.55 (s, 2 H, $\underline{\text{CH}_2}$), 5.44 (s, 1 H, $\underline{\text{CH}}$), 10.99 (s(br), 1 H, $\underline{\text{OH}}$) ppm; **¹³C-NMR** (400 MHz, CDCl_3) δ = 11.2 ($\underline{\text{CH}_3}$), 14.2 ($\text{CH}_2\underline{\text{CH}_3}$), 49.6 ($\underline{\text{CH}_2}$), 61.9 ($\underline{\text{CH}_2\underline{\text{CH}_3}}$), 92.1 ($\underline{\text{CH}}$), 141.7 (Ar- $\underline{\text{C}}$), 162.0 ($\underline{\text{C=O}}$), 167.8 ($\underline{\text{COOEt}}$) ppm;

9.19 Synthesis of CQ-HPO conjugated iron chelators

Synthesis of amino-quinoline precursor 96

4,7-dichloroquinoline **95** (5 g, 0.025 mmol) and 1,4-diaminobutane (11.02 g, 0.125 mol) was heated to reflux for 18 h at 160-180 °C until TLC showed complete consumption of **95**. DMF was added to the reaction mixture and a white solid was filtered and washed with chloroform.

Recrystallization from MeOH/Et₂O gave 3.85 g of the amino-quinoline **96** as white crystals (62 % yield).

N-(4-aminobutyl)-7-chloroquinolin-4-amine **96**^[373]

TLC R_f = 0.3 (Toluene/MeOH 7:3); **Purification**: Flash-Chromatography Toluene/MeOH 8:2 (R_f = 0.2); **Yield**: 3246 mg of white solid (13.00 mmol, 52 %) (column chromatography); **Yield**: 3850 mg of white solid (15.42 mmol, 62 %) (precipitation and recrystallisation); **Melting point**: 242.2-244.8 °C; **¹H-NMR** (400 MHz, DMSO-*d*₆) δ = 1.49-1.57 (m, 2 H, β -CH₂), 1.61-1.70 (m, 2 H, γ -CH₂), 3.11-3.16 (m, 2 H, δ -CH₂), 3.24-3.30 (m, 2 H, α -CH₂), 6.48 (d, 1 H, $^3J_{H,H}$ = 5.5 Hz, 3-Ar-CH), 7.37 (t(br), 1 H, $^3J_{H,H}$ = 5.1 Hz, NH), 7.77 (d, 1 H, $^4J_{H,H}$ = 2.2 Hz, 8-Ar-CH), 7.97-8.05 (m, 2 H, NH₂), 8.28 (d, 1 H, $^3J_{H,H}$ = 9.0 Hz, 5-Ar-CH), 8.39 (d, 1 H, $^3J_{H,H}$ = 5.5 Hz, 2-Ar-CH) ppm; **¹³C-NMR** (400 MHz, DMSO-*d*₆) δ = 25.2 (γ -CH₂), 26.7 (β -CH₂), 36.8 (δ -CH₂), 42.0 (α -CH₂), 98.7 (3-Ar-CH), 117.4 (Ar-C), 124.1 (6-Ar-CH), 124.2 (5-Ar-CH), 127.3 (8-Ar-CH), 133.5 (Ar-C), 150.2 (Ar-C), 151.7 (2-Ar-CH), 161.0 (Ar-C), ppm; **HPLC-Analysis (Method B)**: 81 %, R_t = 16.6 min.

Synthesis of HPO-CQ-conjugated iron chelators

Synthesis following Route A: Installation of amino-linker prior to Michael addition reaction

Benzyl protected maltol **92b** (1.300 g, 0.006 mol) was dissolved in EtOH (83 % v/v, 30 mL). The amino-quinoline **96** (1.000 g, 0.004 mol) was added, followed by NaOH (2 N) until pH 13 was reached. The reaction mixture was stirred at 100 °C until TLC showed complete consumption of starting materials. The crude was concentrated, extracted between water (20 mL) and EtOAc (3x50 mL). The combined organic fractions were dried over MgSO₄, filtered and concentrated. Purification by flash chromatography (CHCl₃/MeOH 8:2 + 0.25-0.30 % aq. NH₃) afforded 0.9 g of the protected iron-chelator **97** as a yellow-orange solid. This material was dissolved in aq. HCl (6 N, 30 mL) and the solution was heated to reflux until TLC showed complete consumption of starting material to remove the protecting group. The reaction mixture was concentrated in vacuo, and the resulting precipitate was recrystallized from ethanol/acetone, to give the title compound **98a** as a white solid.

3-(benzyloxy)-1-(4-((7-chloroquinolin-4-yl)amino)butyl)-2-methylpyridin-4(1H)-one **97**

TLC R_f = 0.4 (CHCl₃/MeOH/NH₃ 8:2:0.25); **Purification**: Flash-Chromatography CHCl₃/ MeOH/ NH₃ (R_f = 0.4); **Yield**: 188 mg of white solid (0.42 mmol, 74 %) (Route A); **Yield**: 900 mg of yellow-orange solid (2.01 mmol, 50 %) (Route A); **Yield**: 200 mg of white solid (0.45 mmol, 20 %) (Route B); **¹H-NMR** (400 MHz, DMSO-*d*₆) δ = 1.61-1.74 (m, 4 H, β, γ -CH₂), 2.16 (s, 3 H,) 3.38-3.44 (m, 2 H, δ -CH₂), 3.94 (t, 2 H, $^3J_{H,H}$ = 6.8 Hz, α -CH₂), 5.00 (s, 2 H, CH₂), 6.16 (d, 1 H, $^3J_{H,H}$ = 7.4 Hz, 3-HPO-CH), 6.65 (d, 1 H, $^3J_{H,H}$ = 6.3 Hz, 3-Ar-CH), 7.29-7.39 (m, 5 H, 5xAr-CH), 7.56 (dd, 1 H, $^{3,4}J_{H,H}$ = 2.2, 9.0 Hz, 6-Ar-CH), 7.68 (d, 1 H, $^3J_{H,H}$ = 7.4 Hz, 2-HPO-

CH), 7.91-7.97 (m, 1 H, 8-Ar-CH), 8.45 (d, 1 H, $^3J_{H,H} = 6.3$ Hz, 2-Ar-CH), 8.58 (d, 1 H, $^3J_{H,H} = 9.0$ Hz, 5-Ar-CH), 8.69-8.74 (m, 1 H,) ppm; $^{13}\text{C-NMR}$ (400 MHz, DMSO- d_6) $\delta = 11.9$ (CH₃), 24.4, 27.7 (β,γ -CH₂), 42.2 (δ -CH₂), 52.4 (α -CH₂), 71.8 (CH₂), 98.6 (3-Ar-CH), 116.0 (3-HPO-CH), 116.5 (Ar-C), 123.1 (8-Ar-CH), 125.3 (5-Ar-CH), 125.4 (6-Ar-CH), 127.8 (Ar-CH), 128.2 (Ar-CH), 128.4 (Ar-CH), 135.7 (Ar-C), 137.7 (Ar-C), 139.6 (2-HPO-CH), 140.8 (Ar-C), 143.7 (Ar-C), 145.3 (Ar-C), 147.1 (2-Ar-CH), 152.8 (Ar-C), 171.8 (C=O) ppm; **ESI-MS** m/z (%) = 447.1 [M-H]⁻ (50 %), **HR-MS** $m/z = 447.0729$ [M-H]⁻ (calculated: 447.1714).

1-(4-((7-chloroquinolin-4-yl)amino)butyl)-3-hydroxy-2-methylpyridin-4(1H)-one **98a**

TLC $R_f = 0.1$ (CHCl₃/MeOH 8:2); **Purification**: Re-crystallisation from EtOH/Acetone; **Yield**: 47 mg of white solid (0.13 mmol, 59 %); $^1\text{H-NMR}$ (400 MHz, DMSO- d_6) $\delta = 1.68$ -1.79 (m, 2 H, γ -CH₂), 1.83-1.92 (m, 2 H, β -CH₂), 2.53 (s, 3 H, CH₃), 3.54-3.61 (m, 2 H, δ -CH₂), 4.38 (t, 2 H, $^3J_{H,H} = 7.4$ Hz, α -CH₂), 6.89 (d, 1 H, $^3J_{H,H} = 7.2$ Hz, 3-HPO-CH), 7.18 (d, 1 H, $^3J_{H,H} = 7.0$ Hz, 3-Ar-CH), 7.77 (dd, 1 H, $^{3,4}J_{H,H} = 2.1, 9.1$ Hz, 6-Ar-CH) 8.07 (d, 1 H, $^4J_{H,H} = 2.1$ Hz, 8-Ar-CH), 8.26 (d, 1 H, $^3J_{H,H} = 7.0$ Hz, 2-Ar-CH), 8.55 (d, 1 H, $^3J_{H,H} = 7.2$ Hz, 2-HPO-CH), 8.77 (d, 1 H, $^3J_{H,H} = 9.1$ Hz, 5-Ar-CH) 9.56 (t, 1 H, $^3J_{H,H} = 5.4$ Hz, NH), 14.27 (s(br), 1 H, OH) ppm; $^1\text{H-NMR}$ (400 MHz, D₂O) $\delta = 1.76$ -1.84 (m, 2 H, γ -CH₂), 1.94-2.02 (m, 2 H, β -CH₂), 2.45 (s, 3 H, CH₃), 3.55-3.60 (m, 2 H, δ -CH₂), 4.35 (t, 2 H, $J_{H,H} = 7.0$ Hz, α -CH₂), 6.69 (d, 1 H, $^3J_{H,H} = 7.2$ Hz, 3-Ar-HPO-CH), 6.91 (d, 1 H, $^3J_{H,H} = 7.0$ Hz, 3-Ar-CH), 7.64 (dd, 1 H, $^{3,4}J_{H,H} = 1.9, 9.0$ Hz, 6-Ar-CH), 7.86 (d, 1 H, $^4J_{H,H} = 1.9$ Hz, 8-Ar-CH), 7.95 (d, 1 H, $^3J_{H,H} = 7.0$ Hz, 2-Ar-CH), 8.08 (d, 1 H, $^3J_{H,H} = 9.0$ Hz, 5-Ar-CH), 8.22 (d, 1 H, $^{ppm}J_{H,H} = 7.2$ Hz, 2-Ar-HPO-CH); $^{13}\text{C-NMR}$ (400 MHz, DMSO- d_6) $\delta = 12.5, 24.2, 26.9, 42.5, 55.3, 98.6, 110.7, 115.5, 119.1, 125.9, 126.9, 138.0, 138.5, 142.9, 143.2, 155.4$ () ppm; **IR (cm-1)**: 2500-3300 (OH, NH); **EI-MS** m/z (%) = 358.0 [M]⁺ (100 %), 233.0 [fragment]⁺ (75 %), 154 [fragment]⁺ (38 %); **HPLC-Analysis** : 99.9 %, $R_t = 20.6$ min.

Synthesis following Route B: Double Michael addition prior to quinoline conjugation

Maltol (50 g, 0.397 mol) was dissolved in methanol (450 mL). NaOH (8.7 M, 50 mL) was added, followed by benzylbromide (74.66 g, 0.437 mmol). The reaction mixture was heated to 100 °C for 6 h. The crude was concentrated, extracted between NaOH_(aq) (5 %, 400 mL) and DCM (2x200 mL). The combined organic fractions were washed with water (190 mL) and dried over MgSO₄, filtered and concentrated. Recrystallisation from Et₂O gave 69.9 g of **92b** as colourless needles (81 % yield). The benzyl protected maltol (346 mg, 1.60 mmol) was dissolved in EtOH_(aq) (50 %, 15 mL) and 1,4-diaminobutane (141 mg, 1.60 mmol) was added. The pH of the reaction mixture was adjusted to pH 13 with aq. sodium hydroxide (10 N) and stirring was continued at 100 °C for 18 h. The reaction mixture was concentrated and the crude was extracted between water (10 mL) and CHCl₃ (3x10 mL). The combined organic fractions were dried over MgSO₄, filtered and concentrated. The amino-HPO **99** was obtained after column chromatography (CHCl₃/MeOH/NH₃ 8:2:0.01, R_f 0.1) as white solid (230 mg, 50 %). The amino-HPO

(1.00 g, 3.50 mmol) and 4,7-dichloroquinoline (693 mg, 3.50 mmol) were dissolved in DMSO (10 mL) and heated to 100 °C for 16 h. The reaction mixture was concentrated and purified as described in chapter 9.19. The protected iron chelator was obtained in 20 % yield. The protected reaction product **97** (22 mg, 0.05 mmol) was dissolved in ethanol, the pH was adjusted to 1 with HCl_(aq), and hydrogenation was carried out in the presence of 5 % Pd/C to give the title compound **98b** as a white solid.

2-Methyl-3-benzyloxy-4-(4H)-pyranone **92b**^[261]

Reaction time: 6 h; **Purification:** Re-crystallisation from Et₂O; **Yield:** 69.9 mg of colourless needles (0.32 mmol, 81 %); **¹H-NMR** (400 MHz, DMSO-d₆) δ = 1.99 (s, 3 H, CH₃), 5.00 (s, 2 H, CH₂), 6.14-6.24 (m, 1 H, Ar-CH), 7.20 (m, 5 H, 5xAr-CH), 7.39-7.49 (m, 1 H, Ar-CH) ppm.

1-(4-aminobutyl)-3-(benzyloxy)-2-methylpyridin-4(1H)-one **99**^[374]

TLC R_f = 0.1 (CHCl₃/MeOH/NH₃ 8:2:0.01); **Reaction time:** 18 h; **Purification:** Flash-Chromatography CHCl₃/MeOH/NH₃ 8:2:0.01 (R_f = 0.1); **Yield:** 230 mg of white solid (0.80 mmol, 50 %); **¹H-NMR** (400 MHz, MeOD) δ = 1.36-1.47 (m, 2 H, β -CH₂), 1.55-1.64 (m, 2 H, γ -CH₂), 2.65 (t, 2 H, ³J_{H,H} = 7.3 Hz, α -CH₂), 3.87 (t, 2 H, ³J_{H,H} = 7.4 Hz, δ -CH₂), 4.98 (s, 3 H, CH₃), 6.39 (d, 1 H, ³J_{H,H} = 7.4 Hz, 3-HPO-CH), 7.23-7.33 (m, 5 H, 5xAr-CH), 7.61 (d, 1 H, ³J_{H,H} = 7.4 Hz, 2-HPO-CH) ppm; **¹³C-NMR** (400 MHz, MeOD) δ = 12.8 (CH₃), 28.8 (CH₂), 41.3 (CH₂), 54.9 (CH₂), 74.4 (CH₂), 117.3 (Ar-C or Ar-underlineCH), 129.4 (Ar-C or Ar-underlineCH), 129.4 (Ar-C or Ar-underlineCH), 130.3 (Ar-C or Ar-underlineCH), 138.3 (Ar-C or Ar-underlineCH), 141.2 (Ar-C or Ar-underlineCH), 144.0 (Ar-C or Ar-underlineCH), 146.9 (Ar-C or Ar-underlineCH), 174.6 (C=O) ppm;

4-((4-(3,4-dihydroxy-2-methylpyridin-1-ium-1-yl)butyl)amino)quinolin-1-ium **98b**

Reaction time: 4 h **Purification:** Filtration from EtOH; **Yield:** 15 mg of white solid (0.05 mmol, 100 %); **¹H-NMR** (400 MHz, D₂O) δ = 1.80-1.89 (m, 2 H, CH₂), 1.98-2.06 (m, 2 H, CH₂), 2.50 (s, 3 H, CH₃), 3.58 (t, 2 H, ³J_{H,H} = 6.6 Hz, CH₂), 4.38 (t, 2 H, ³J_{H,H} = 6.9 Hz, CH₂), 6.65 (d, 1 H, ³J_{H,H} = 7.0 Hz, 3-HPO-Ar-CH), 6.93 (d, 1 H, ³J_{H,H} = 6.9 Hz, 3-Ar-CH), 7.65 (at, 1 H, ³J_{H,H} = 7.6, 8.4 Hz, 7-Ar-CH), 7.75 (d, 1 H, ³J_{H,H} = 8.4 Hz, 5-Ar-CH), 7.90 (at, 1 H, ³J_{H,H} = 7.6, 8.4 Hz, 6-Ar-CH), 7.99 (d, 1 H, ³J_{H,H} = 6.9 Hz, 2-Ar-CH), 8.03 (d, 1 H, ³J_{H,H} = 8.4 Hz, 8-Ar-CH), 8.21 (d, 1 H, ³J_{H,H} = 7.0 Hz, 2-HPO-Ar-CH), ppm; **¹³C-NMR** (400 MHz, D₂O) δ = 15.1 (CH₃), 26.1 (CH₂), 29.3 (CH₂), 45.1 (CH₂), 59.2 (CH₂), 100.8 (3-HPO-Ar-CH), 113.6 (3-Ar-CH), 119.4 (Ar-C), 122.8 (5-Ar-CH), 124.7 (8-Ar-CH), 130.0 (7-Ar-CH), 136.6 (6-Ar-CH), 140.1 (Ar-C), 141.5 (2-Ar-CH), 144.2 (2-HPO-Ar-CH), 145.7 (Ar-C), 158.5 (Ar-C), 161.6 (C=O), ppm; **EI-MS** m/z (%) = 324.0 [M]⁺ (45 %), 233.0 [fragment]⁺ (100 %); **HPLC-Analysis** : 100 %, R_t = 20.6 min.

Synthesis of CatL inhibitor CAA0225

Synthesis of building block A

2-(tert-butoxycarbonylamino)-3-phenylpropanoic acid **106** (500 mg, 1.88 mmol) was dissolved in DCM and TBTU (605 mg, 1.88 mmol) was added. After 5 min, DIPEA (445 μ L, 1.88 mmol) and benzyl-amine (206 μ L, 1.88 mmol) were added subsequently. The reaction mixture was stirred for 16 h at rt. The mixture was diluted with DCM and washed with brine. The organic phase was further washed with 1 N HCl (2 x 5 mL), dried over MgSO_4 , filtered and concentrated. Purification by flash chromatography (cyclohexane/EtOAc 6:4, R_f 0.5) afforded tert-butyl 1-(benzylamino)-1-oxo-3-phenylpropan-2-ylcarbamate **107a** (662 mg, 99 %) as a white solid. The Boc protected amide **107a** (100 mg, 0.28 mmol) was dissolved in DCM (5 mL) and TFA (408 mg, 4.21 mmol) was subsequently added. The reaction mixture was allowed to stir for another 2 h and was concentrated. The crude mixture was redissolved in DCM and cooled to 0°C, while it was neutralised with Na_2CO_3 solution. The organic layer was washed with conc. NaHCO_3 solution (3 x 5 mL) and dried over MgSO_4 , filtered and dried in vacuo to afford 2-amino-N-benzyl-3-phenylpropanamide **107b** (69 mg, 98 %) as a white solid.

tert-Butyl 1-(benzylamino)-1-oxo-3-phenylpropan-2-ylcarbamate **107a**^[375]

TLC R_f = 0.5 (Cyclohexane/EtOAc 6:4); **Purification:** Flash-Chromatography Cyclohexane/EtOAc 6:4 (R_f = 0.5); **Yield:** 662 mg of white solid (1.87 mmol, 99 %); **$^1\text{H-NMR}$** (400 MHz, CDCl_3) δ = 1.39 (s, 9 H, $(\text{CH}_3)_3\text{Boc}$), 3.02-3.15 (m, 2 H, CH_2CH), 4.35, 4.36 (2xs, 3 H, CH_2NH , HC , NH), 5.05 (s(br), 1 H, NHBoc), 6.06 (s(br), 1 H, NHCO), 7.05-7.30 (m, 10 H, 10xAr-CH) ppm; **$^{13}\text{C-NMR}$** (400 MHz, CDCl_3) δ = 28.3 (3x CH_3), 38.8 (CH_2), 43.4 (CH_2), 56.1 (CH), 80.2 (CtBu), 126.9 (Ar-CH), 127.4 (Ar-CH), 127.7 (Ar-CH), 128.6 (Ar-CH), 128.7 (Ar-CH), 129.4 (Ar-CH), 136.8 (Ar-C), 137.8 (Ar-C), 155.6 (C=O), 171.3 (COOtBu) ppm; **ESI-MS** m/z (%) = 355.2 $[\text{M}+\text{H}]^+$ (100 %), 377.2 $[\text{M}+\text{Na}]^+$ (10 %), 709.4 $[\text{2M}+\text{H}]^+$ (15 %), 731.4 $[\text{2M}+\text{Na}]^+$ (10 %); **HR-MS** m/z = 355.2020 $[\text{M}+\text{H}]^+$ (calculated: 355.2016); **HPLC-Analysis (Method B):** 87 %, R_f = 17.5 min.

2-amino-N-benzyl-3-phenylpropanamide **107b**^[375]

Reaction time: 2 h; **Yield:** 69 mg of white solid (0.27 mmol, 98 %); **$^1\text{H-NMR}$** (400 MHz, CDCl_3) δ = 1.53 (s(br), 2 H, NH_2), 2.74 (dd, 1 H, $^3J_{\text{H,H}}$ = 9.1, 13.7 Hz, CH_2CH), 3.28 (dd, 1 H, $^3J_{\text{H,H}}$ = 4.2, 13.7 Hz, CH_2CH), 3.59-3.69 (m, 1 H, αH), 4.40 (dd, 1 H, $^3J_{\text{H,H}}$ = 6.1, 14.8 Hz, CH_2NH), 4.45 (dd, 1 H, $^3J_{\text{H,H}}$ = 6.1, 14.8 Hz, CH_2NH), 7.12-7.33 (m, 10 H, 10xAr-CH), 7.58 (s(br), 1 H, NH) ppm. **ESI-MS** m/z (%) = 255.1 $[\text{M}+\text{H}]^+$ (100 %), 277.1 $[\text{M}+\text{Na}]^+$ (35 %), 509.3 $[\text{2M}+\text{H}]^+$ (25 %), 531.3 $[\text{2M}+\text{Na}]^+$ (85 %), **HR-MS** m/z = 255.1495 $[\text{M}+\text{H}]^+$ (calculated: 255.1492); **HR-MS** m/z = 255.1496 $[\text{M}+\text{H}]^+$ (calculated: 255.1492).

Synthesis of CAA0225, assembly of building blocks

(2S,3S)-diethyl oxirane-2,3-dicarboxylate **108a** (99 mg, 0.53 mmol) in EtOH (0.5 mL) was cooled to 4 °C and KOH (5.25 mL, 0.1 M) was added over a period of 3 h. The mixture was then stored over night in the freezer. After warming to rt, the mixture was concentrated, the residue was taken up between NaHCO₃ (aqueous, 50 mM) and EtOAc. The aqueous layer was extracted with EtOAc (2 x 2 mL). The pH of the aqueous layer was adjusted to 2.5 using NaHSO₄ (50 mM) and was extracted with EtOAc (5 x 5 mL). The combined of organic layers of the second extraction were dried over MgSO₄, filtered and concentrated to afford (2S,3S)-3-(ethoxycarbonyl)oxirane-2-carboxylic acid **108b** (60 mg, 70 %) as a clear oil. To a solution of cmpdepoxy.oh (53 mg, 0.33 mmol), tyramine (55 mg, 0.40 mmol) and HOBt (51 mg, 0.33 mmol) in CHCl₃ (1 mL) at 0 °C was added EDC (57 mg, 0.36 mmol) slowly in 5 portions. The reaction mixture was stirred for 1 h at 0 °C and then subsequently at rt for 24 h. The mixture was concentrated, and the residue was taken up between EtOAc and water. The organic layer was washed with 0.5 N HCl (2 x 5 mL) and saturated NaHCO₃ (2 x 5 mL), dried over MgSO₄, filtered and concentrated. Purification by flash chromatography (Cyclohexane/EtOAc 1:1, R_f 0.1) afforded (2S,3S)-ethyl 3-(4-hydroxyphenethylcarbamoyl)oxirane-2-carboxylate **109a** (30 mg, 33 %) as a white solid. Compound **109a** was dissolved in EtOH (2 mL) and KOH (1.3 mL, 0.1 M) was added over a period of 3 h. The mixture was then stored over night in the freezer. After warming to rt, the mixture was concentrated, the residue was taken up between NaHCO₃ (aqueous, 50 mM) and EtOAc. The aqueous layer was extracted with EtOAc (2 x 2 mL). The pH of the aqueous layer was adjusted to 2.5 using NaHSO₄ (50 mM) and was extracted with EtOAc (5 x 5 mL). The combined of organic layers of the second extraction were dried over MgSO₄, filtered and concentrated to afford (2S,3S)-3-(4-hydroxyphenethylcarbamoyl)oxirane-2-carboxylic acid **109b** (15 mg, 54 %) as a white solid. Compound **109b** (19 mg, 0.07 mmol), **107b** (15 mg, 0.06 mmol) and HOBt (10 mg, 0.06 mmol) were dissolved in CHCl₃ (1 mL) and NMM (9 µL) was added. The reaction mixture was cooled to 0 °C and EDC (11 mg, 0.07 mmol) was added in 5 small portions. The mixture was stirred for 16 h subsequently at rt. The crude reaction mixture was diluted with DCM and washed with 1 N HCl (2 x 1 mL) and NaHCO₃ (conc, 2 x 1 mL). The organic phase was dried over MgSO₄, filtered and concentrated. Purification by flash chromatography (DCM/MeOH 1:0.05, R_f 0.1) afforded (2S,3S)-N2-(1-(benzylamino)-1-oxo-3-phenylpropan-2-yl)-N3-(4-hydroxyphenethyl)oxirane-2,3-dicarboxamide **CAA0225** (5 mg, 17 %) as a white solid.

(2S,3S)-3-(ethoxycarbonyl)oxirane-2-carboxylic acid **108b**^[375]

TLC R_f = 0.1 (DCM/MeOH 9:1); **Purification:** The crude was dissolved in NaHCO_{3aq} (4 mL, 50 mM), extracted with EtOAc (2x4 mL). The pH of the aqueous layer was adjusted to 2.5 using KHSO₄ (2 M) and was extracted with EtOAc (5x3 mL). The combined organic fractions from the 2nd extraction were dried over MgSO₄, filtered and concentrated. **Yield:** 60 mg of

clear oil (0.37 mmol, 71 %); **¹H-NMR** (400 MHz, DMSO-*d*₆) δ = 1.22 (t, 3 H, $^3J_{\text{H,H}}$ = 7.1 Hz, CH₂CH₃), 3.61 (d, 1 H, $^3J_{\text{H,H}}$ = 1.8 Hz, CH), 3.70 (d, 1 H, $^3J_{\text{H,H}}$ = 1.8 Hz, CH), 4.17 (q, 2 H, $^3J_{\text{H,H}}$ = 7.1 Hz, CH₂CH₃) ppm; **ESI-MS** m/z (%) = 159.0 [M–H][–] (100 %), 177.0 [M+H₂O–H][–] (30 %), 319.1 [2M–H][–] (50 %), 337.1 [2M+H₂O–H][–] (10 %); **HR-MS** m/z = 159.0302 [M–H][–] (calculated: 159.0299).

(2S,3S)-ethyl 3-(4-hydroxyphenethylcarbamoyl)oxirane-2-carboxylate **109c**^[375]

TLC R_f = 0.4 (Cyclohexane/EtOAc 1:1); **Reaction time**: 16 h; **Purification**: Flash-Chromatography Cyclohexane/EtOAc 1:1 (R_f = 0.4); **Yield**: 60 mg of white solid (0.21 mmol, 65 %); **¹H-NMR** (400 MHz, CDCl₃) δ = 1.28 (t, 3 H, $^3J_{\text{H,H}}$ = 7.1 Hz, CH₂CH₃), 2.69–2.75 (m, 2 H, NHCH₂), 3.35 (d, 1 H, $^3J_{\text{H,H}}$ = 1.8 Hz, CH), 3.42–3.53 (m, 2 H, CH₂), 3.64 (d, 1 H, $^3J_{\text{H,H}}$ = 1.8 Hz, CH), 4.18–4.27 (m, 2 H, CH₂), 6.20 (t(br), 1 H, $^3J_{\text{H,H}}$ = 5.7 Hz, NHCH₂), 6.39 (s(br), 1 H, Ar-OH), 6.78 (d, 2 H, $^3J_{\text{H,H}}$ = 8.5 Hz, 3,5-Ar-CH), 6.99 (d, 2 H, $^3J_{\text{H,H}}$ = 8.5 Hz, 2,6-Ar-CH) ppm.

(2S,3S)-3-(4-hydroxyphenethylcarbamoyl)oxirane-2-carboxylic acid **109b**

TLC R_f = 0.1 (Cyclohexane/EtOAc 1:1); **Yield**: 15 mg of white solid (0.06 mmol, 54 %); **Reaction time**: 3 h; **¹H-NMR** (400 MHz, CD₃OD) δ = 2.63 (t, 2 H, $^3J_{\text{H,H}}$ = 7.4 Hz, CH₂CH₂Ar), 3.27–3.35 (m, 2 H, CH₂CH₂Ar), 3.37 (d, 1 H, $^3J_{\text{H,H}}$ = 1.8 Hz, CH), 3.45 (d, 1 H, $^3J_{\text{H,H}}$ = 1.8 Hz, CH), 6.64 (d, 2 H, $^3J_{\text{H,H}}$ = 8.5 Hz, 3,5-Ar-CH), 6.95 (d, 2 H, $^3J_{\text{H,H}}$ = 8.5 Hz, 2,6-Ar-CH), 8.19 (t(br), 1 H, $^3J_{\text{H,H}}$ = 5.5 Hz, NH) ppm. **ESI-MS** m/z (%) = 367.1 [M–H][–] (100 %); **HR-MS** m/z = 367.1300 [M–H][–] (calculated: 367.1299).

(2S,3S)-N2-(1-(benzylamino)-1-oxo-3-phenylpropan-2-yl)-N3-(4-hydroxyphenethyl)oxirane-2,3-dicarboxamide **CAA0225**^[375]

TLC R_f = 0.1 (DCM/MeOH 100:5); **Reaction time**: 16 h; **Purification**: Flash-Chromatography DCM/MeOH 100:5 (R_f = 0.1); **Yield**: 5 mg of white solid (0.01 mmol, 17 %); **¹H-NMR** (400 MHz, CD₃OD) δ = 2.64 (t, 2 H, $^3J_{\text{CH}_2, \text{CH}_2}$ = 7.4 Hz, tyramine-CH₂), 2.89 (dd, 1 H, $^{2,3}J_{\beta\text{H}, \beta\text{H}(\alpha\text{H})}$ = 8.5, 13.7 Hz, βH), 3.09 (dd, 1 H, $^{2,3}J_{\beta\text{H}, \beta\text{H}(\alpha\text{H})}$ = 6.8, 13.7 Hz, βH), 3.25 (d, 1 H, $J_{\text{H,H}}$ = 1.9 Hz, CH), 3.32 (dt, 2 H, $^3J_{\text{H,H}}$ = 1.5, 7.4 Hz, tyramine-NHCH₂), 3.43 (d, 1 H, $J_{\text{H,H}}$ = 1.9 Hz, CH), 4.24 (d, 1 H, $^2J_{\text{H,H}}$ = 15.0 Hz, CH₂Ph), 4.31 (d, 1 H, $^2J_{\text{H,H}}$ = 15.0 Hz, CH₂Ph), 4.61 (dd, 1 H, $^3J_{\alpha\text{H}, \beta\text{H}}$ = 6.8, 8.5 Hz, αH), 6.66 (d, 2 H, $^3J_{\text{H,H}}$ = 8.5 Hz, tyramine-3,5-Ar-CH), 6.97 (d, 2 H, $^3J_{\text{H,H}}$ = 8.5 Hz, tyramine-2,6-Ar-CH), 7.06–7.25 (m, 10 H, 10xAr-CH) ppm; **APCI-MS** m/z (%) = 488.2 [M+H]⁺ (100 %); **HR-MS** m/z = 488.2168 [M+H]⁺ (calculated: 488.2180).

Table 72: Reagents for Baltz-Media preparation

Reagent	Supplier	Order-No	CAS-No	Molecular Formula	FW [$\frac{g}{mol}$]
HEPES	Sigma	H3375-100G	7365-45-9	C ₈ H ₁₈ N ₂ O ₄ S	238.30
D-(+)-Glucose	Sigma	G8270-1006	50-99-7	C ₆ H ₁₂ O ₆	180.16
L-Glutamine	Sigma	G8540-25G	56-85-9	C ₅ H ₁₀ N ₂ O ₃	146.15
Hypoxanthine	Sigma	H9636-1G	68-94-0	C ₅ H ₄ N ₄ O	136.11
Thymidine	Sigma	T1895-1G	50-89-5	C ₁₀ H ₁₄ N ₂ O ₅	242.23
BCDS	Sigma	B-1125		C ₂₆ H ₁₈ N ₂ O ₆ S ₂ Na ₂	564.50
Sodium pyruvate	Sigma	P-5280-25G	113-24-6	C ₃ H ₃ NaO ₃	110.04
Adenosine	Sigma	A4036-5G	58-61-7	C ₁₀ H ₁₃ N ₅ O ₄	267.25
MEM	GIBCO	51200-087			
NEAA	Sigma	M7145			

Table 73: Reagents for Baltz-Media-completion

Reagent	Supplier	Order-No
Fetal Bovine Serum (heat inactivated)	Sigma	F4135-500ML
Penicillin-Streptomycin	Sigma	P4333-100ML
β-ME	Sigma	63689-25ML-F

9.20 Preparation of media

Preparation of incomplete-Baltz-Media

HEPES (3.00 g), glucose (0.45 g), glutamine (146.00 mg), sodium pyruvate (100.00 mg), hypoxanthine (7.00 mg), thymidine (2.00 mg), adenosine (10.70 mg) and Bathocuproinedisulfonic acid disodium salt (Na-BCDS, 14.10 mg) were dissolved in Earls' medium without phenol red (50 mL). The solution was stirred 15 min at rt and the pH was adjusted to 7.5 using NaOH (1aq, 1 M). The neutralised solution was sterile filtered and transferred back to the remaining 450 mL of media. The media was supplemented with 5 mL non-essential amino acid solution (NEAA).

Preparation of complete-Baltz-Medium

In order to prepare complete-Baltz-Medium for the culturing of *T. brucei*, 100 mL of incomplete-Baltz-medium was supplemented with 20 mL heat-inactivated FBS, 1 mL β-mercapto-ethanol (β-ME) solution (14.1 μL β-ME in 10 mL dd-H₂O) and 1 mL of PenStrep (1000 $\frac{U}{mL}$).

Table 74: Reagents for RPMI-media

Reagent	Supplier	Order-No
Fetal Bovine Serum (heat inactivated)	Sigma	F4135-500ML
Penicillin-Streptomycin	Sigma	P4333-100ML
L-Glutamine solution (200 mM)	Sigma	G7513-100ML

Preparation of RPMI-1640 media

RPMI-1640 media was prepared by adding heat-inactivated FBS (20 mL), PenStrep (1 mL) and L-glutamine (2 mL) to 100 mL RPMI 1640 media.

9.21 Culturing of parasites and mammalian cells

Culturing of *T. brucei*

T. brucei bloodstream form 427-221a was cultured in Baltz-medium (complete) at 37 °C and 5 % CO₂. The parasite density was adjusted to not exceed $10^6 \frac{\text{cells}}{\text{ml}}$.^[189]

Culturing of *T. cruzi*

The trypomastigotes forms of *Trypanosoma cruzi* (Y strain) were grown in LLC-MK2 cells in RPMI-1640 supplemented with 2 % FBS, at 37 °C in an incubator with 5 % CO₂.^[136,376]

Culturing of *L. infantum*

Promastigotes of *Leishmania (Leishmania) infantum chagasi* (MHOM/BR/1972/LD) were cultured in M-199 supplemented with 10 % FCS and 0.25 % hemine, without addition of antibiotics in an incubator at 24 °C. Amastigotes of *L. infantum* were obtained by infection of golden hamsters (*Mesocricetus auratus*). All animals were obtained from the vivarium of the Adolfo Lutz Institute in Sao Paulo and kept in sterile boxes with absorbent material, receiving food and water *ad libitum*. All procedures performed on animals were previously approved by the Research Ethics Committee (CEP) of the Adolfo Lutz Institute.^[136]

Amastigotes of *L. (L.) infantum chagasi* were purified from the spleen of golden hamsters by differential centrifugation and the number of parasites was determined by weight of the infected spleen and counting of a representative sample 60 to 70 days after infection.^[377]

Culturing of *HL-60* cells

Human Caucasian promyelocytic leukaemia cells were obtained from European Collection of Cell Cultures (ECACC, Catalogue No: 98070106) *HL-60* cells were propagated in RPMI-

medium, supplemented with L-glutamine (2mM) and FBS (20 %) at 37 °C and 5 % CO₂. The cells were obtained at passage P+8 and were first frozen in 10 % DMSO in FBS after P+10. Toxicity assays were performed with cells with a passage number of lower P+20. HL60 cells grow in suspension and cells were suspended at 100-150xg in a centrifuge for maximum 5 min. Cultures were maintained between $1-9 \times 10^5 \frac{\text{cells}}{\text{mL}}$. Cells were counted with the aid of trypan blue in a Neubauer counting chamber (20 μL sample and 20 μL trypanblue).

9.22 Anti-parasitic activity and toxicity assays

AlamarBlue assay for *T. brucei* activity and HL-60 cell toxicity

The AlamarBlue assay was performed in a 24 well plate (Figure 78). The columns (1-6) represent different concentrations of inhibitor, with the highest concentration of 100 μM in column 1. **A1** contains 995.5 μL of media and 5.5 μL of inhibitor (20 mM in DMSO). For the next dilution in **A2**, 100 μL of **A1** were given to 900 μL of media (0.5 % DMSO). This procedure was repeated for all subsequent columns, so that 1:10 dilutions were achieved. **B1** would represent the next drug tested in this assay. To each well with the exception of wells **C6** and **D6**, 100 μL of *T. brucei* $10^5 \frac{\text{cells}}{\text{mL}}$ were added, so that the final parasite concentration in each well was $10^4 \frac{\text{cells}}{\text{mL}}$. The positive controls contained only media with 0.5 % DMSO and *T. brucei*, there as the negative controls constituted of media (0.5 % DMSO) alone. The cells were incubated for 24 h, at 37 °C and 5 % CO₂, before 100 μL AlamarBlue (11.11 mg resazurin in 100 mL PBS) were added. The colour reaction was allowed to proceed for another 48 h and the plates were read at 570 nm with 630 nm as the reference wavelength. MIC values were obtained after visual inspection of the wells after 72 h of incubation. In order to keep the DMSO concentration throughout the assay constant, the media was prepared with a concentration of 0.5 % DMSO (110.6 μL DMSO in 20 mL media). Melarsoprol was used as positive control for *T. brucei*.

The toxicity assay with HL-60 cells was performed analogues to the *T. brucei* activity assay. The final cell density was adjusted to $10^5 \frac{\text{cells}}{\text{mL}}$ and all other steps were as described above. Alternatively, the HL-60 toxicity assay was performed in a 96 well plate (Figure 79). Here, the inhibitors were arranged in the columns 1-12. Each inhibitor was tested in duplicate on each plate (inhibitor 1: column 1+2). The rows represent the tested concentrations. The highest concentration was 100 μM (row A). This concentration was diluted 1:1 with media in each subsequently row, till the lowest concentration of 0.78125 μM was reached. *H9* and *H10* represented the positive control with *T. brucei* in media only, there as *H11* and *H12* represented the negative controls with only media. In detail, each well in row A was loaded with 198 μL media, followed by 2 μL of inhibitor (20 mM in DMSO) to give a starting concentration of 200 μM . Rows B-H were charged with 100 μL of media. 100 μL of row A were taken from each well and mixed with 100 μL of media from the well below (red arrows, Figure 79). This was

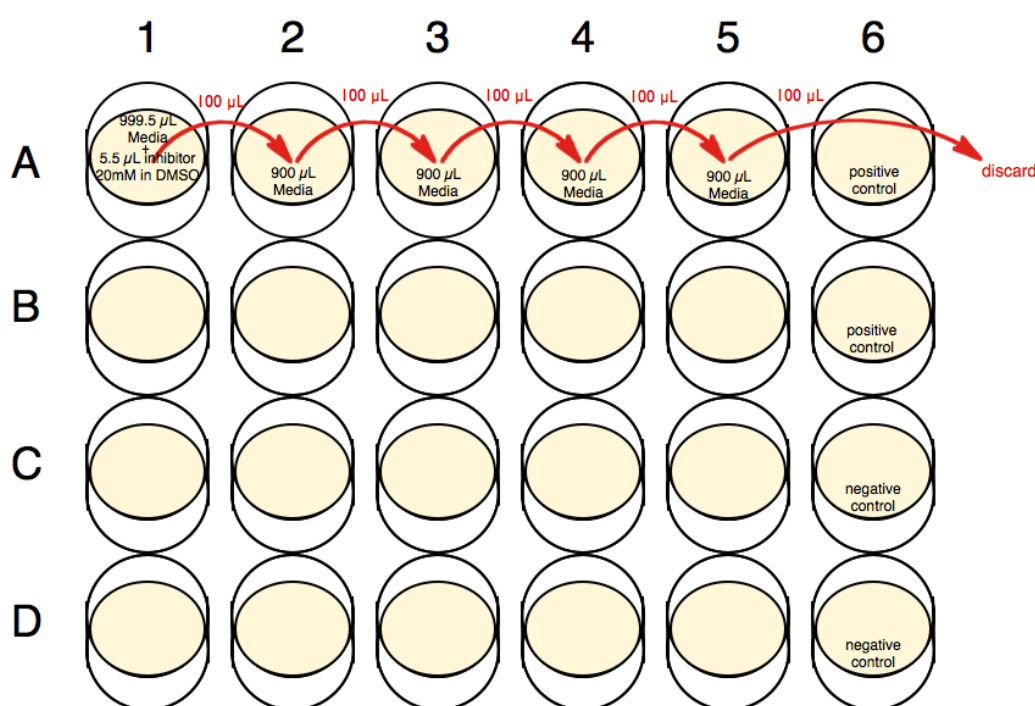


Figure 78: Pipette scheme for AlamarBlue assay in 24 well plate

repeated for all the wells and the last 100 μL were discarded. To each well, except the negative control, 100 μL of $2 \cdot 10^5 \frac{\text{cells}}{\text{mL}}$ HL60 cells were added. The negative control, was supplemented with 100 μL of media. While in the 24 well plate assay the DMSO concentration was constant, here the DMSO concentration decreased from row to row. However, both methods did not have any effect on parasitic or mammalian cell growth. After 44 h, 20 μL AlamarBlue (11.11 mg in 100 mL PBS) was added and incubation was continued for another 4 h. The emission at 585 nm (excitation wavelength 570 nm) was read and the cell viability was estimated.

The cell densities for both the 24 and 96 well plate assay were estimated by counting of a representative culture sample in a Neubauer counting chamber. In detail, each side of the neubauer counting chamber was filled with 10 μL of *T. brucei* culture solution prior to mixing. All 20 middle squares were counted under a light microscope and averaged for both side of the counting chamber. The cell density was calculated according to the volume of the counting chamber (2). HL60-cells were visualised with trypan blue solution prior to counting. 20 μL of HL60-cell culture were added to 20 μL of trypan blue. The cells were counting similarly to

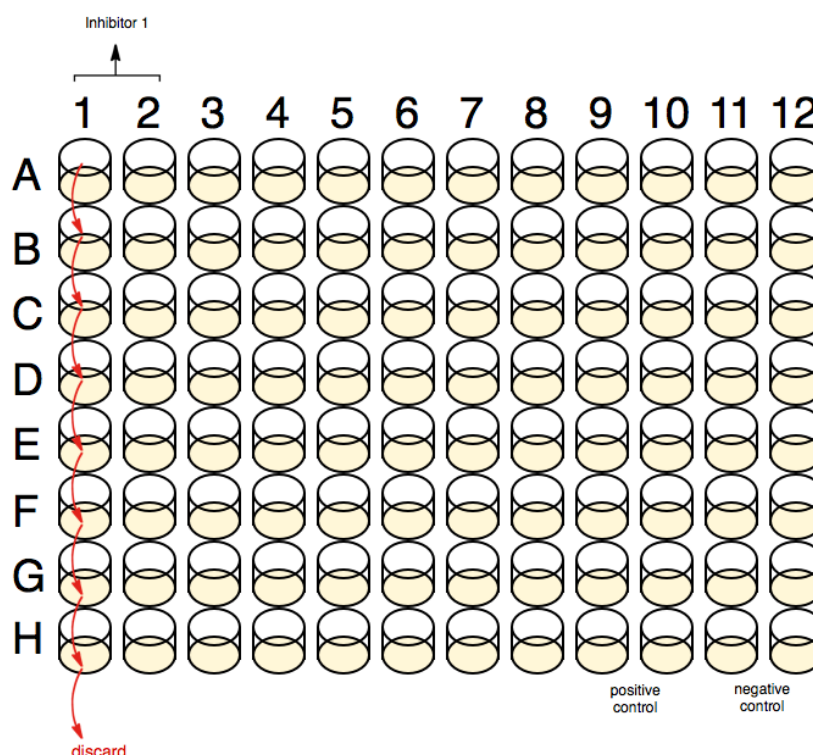


Figure 79: Pipette scheme for AlamarBlue/MTT assay in 96 well plate

T. brucei, but the individual counts were not average, because of the 1:1 dilution in the initial preparation step.

$$\text{viable cell count} \left[\frac{\text{cells}}{\text{mL}} \right] = \frac{\text{Number of living cells counted}}{\text{Number of counted squares} \cdot 2 \text{ (from 1:1 dilution)}} \cdot 10^4 \quad (2)$$

For the 24 well plate assay, the density of the cells was adjusted by dilution of the *T. brucei* or *HL60* cell culture. In the case of the 96 well assay format, the cells were concentrated by centrifugation (*T. brucei* 3000 rpm for 5 min; *HL60* 1000 rpm for 5-10 min). The volume of media to resuspend the cells was estimated by calculating the dilution factor from the first count (3).

$$\text{Dilution factor} = \frac{\text{initial cell count}}{2 \cdot 10^5} \quad (3)$$

MTT activity assay for *T. cruzi* and *L. chagasi*

Inhibitors were dissolved in DMSO, diluted in culture medium and incubated with parasites at different concentrations in order to determine its GI_{50} . The solvent concentration did not exceed 0.5 % to avoid damage of parasites. The GI_{50} of different compounds was determined using promastigotes of *L. infantum*, applied to $1 \times 10^6 \frac{\text{cells}}{\text{well}}$ for 48 hours (in BOD incubator at 24 °C) in 96 well plates. After an incubation period of 24 h, the viability of the promastigotes was verified by mitochondrial oxidative activity using the colorimetric viability dye MTT (3 - (4,5 - dimethylthiazol-2-yl)-bromide 2,5-di-fenoltetrazolio). Therefore, 20 μ l of MTT were added and the cells were incubated for 4 h, followed by the addition of 80 μ L of sodium dodecyl sulphate (SDS). After 24 or 48 hours, the supernatant was read at 550nm on a plate reader (Multiskan reader 30). The drug amphotericin B was used as the assay positive control. Trypomastigotes, taken on the first day of culture LLC-MK2 cells were applied at a concentration of $1 \times 10^6 \frac{\text{cells}}{\text{well}}$ in 96-well plates containing the various compounds in RPMI-1640 medium supplemented with 2 % fetal bovine serum. The plates were incubated at 37 °C and 5 % CO_2 for 24 hours and viability of trypomastigotes was determined by the MTT as previously described for Leishmania. The drug benznidazole was used as the assay positive control.

Amastigote assay for *L. infantum*

Macrophages were collected from the peritoneal cavity of BALB/c mice by washing with RPMI-1640 medium supplemented with 10 % FCS and were incubated at 37 °C at 5 % CO_2 . Macrophages were seeded to $4 \times 10^5 \frac{\text{cells}}{\text{mL}}$ in 16-well Nunc plates and were incubated at 37°C for 24 hours. Amastigotes of *L. infantum* were extracted from the spleen of an infected golden hamster and were separated by differential centrifugation.^[377] Amastigotes were added to the macrophages in a ratio of 10:1 (amastigotes/macrophage), and incubated with inhibitors at 37°C and 5 % CO_2 for 120 h. Following, staining of the slides with Giemsa and microscopically inspection. The EC_{50} was determined by counting 200 macrophages/well, evaluating the number of infected macrophages, using as positive control (100 % infected) and macrophages treated with glucantime as negative control (0 % infected).

9.23 Metabolic labelling of GPI-anchor proteins with myristate analogues

T. brucei was pre-incubated with various inhibitors over a course of 24 h. The concentrations of the inhibitors were chosen based on the minimum inhibitory concentration (MIC). The parasites for the labelling experiment should be cultured at a concentration of inhibitor which inhibits growth but does not show any toxic effects. To determine the effective doses, *T. brucei* was

Table 75: P: parasitaemia count; %-P: percent parasitaemia; AB-%-P: Alamar Blue; seeding concentration of *T. brucei*: $5 \cdot 10^5$ cells/mL

#	c [μ M]	P $\cdot 10^5$ cells/mL	%-P	AB-%-P
40x	50.0	17.5	56	74
	25.0	31.5	100	93
40c	50.0	27.5	93	72
	25.0	29.5	100	98
14v	50.0	11.0	40	36
	25.0	18.5	67	41
14a	5.0	25.0	63	83
	0.5	40.0	100	100

Table 76: P: parasitaemia count; P_{label} : cell density for labelling experiment with YNC12; seeding concentration of *T. brucei*: $1 \cdot 10^6$ cells/mL

#	c [μ M]	$P_{24\ h}$ 10^5 cells/mL	P_{label} 10^5 cells/mL
40x	75.0	9.35	37.4
40c	100	0.50	excluded
14v	50	8.30	37.4
14a	7.5	31.7	37.4

incubated at concentrations below the MICs of inhibitors over a time course of 24 h (Table 75). Following this initial time course experiment *T. brucei* was incubated at the estimated effective dose over a course of 24 h. After the incubation period the parasites were counted and the cell density adapted to the lowest growth density after 24 h (Table 76). The effective doses for **14v** and **40c** were too high and therefore showed increased toxicity against *T. brucei*. However there were sufficient amounts of parasites to continue with the labelling with **YnC12**. **YnC12** and the corresponding inhibitor were added to *T. brucei* at a final concentration of 100 μ M for an incubation period of 4 h. After 4 h, the cells were lysed in ice-cold RIPA buffer (50 mM Tris pH 7.4, 1 % (v/v) NP-40, 1 % (w/v) sodium deoxycholate, 150 mM NaCl, 0.5 % (w/v) SDS and 1 x EDTA-free Complete protease inhibitor cocktail (Roche)), sonicated, then centrifuged at 15,000 g for 30 minutes at 4°C.^[378] A total of 25 μ g protein from each sample were diluted to 1 mg/mL with lysis buffer. Then 4 volumes of ice-cold acetone (stored at -20) were added, vortexed and left at -20 °C for 1 hour. Pelleted by centrifugation at 15,000 x g for 10 mins and acetone was removed and the pellet was air-dried. The pellet was resuspended in 25 μ L 2 %

P: parasitaemia count; seeding concentration of *HL60* cells: $2.5 \cdot 10^5 \text{ cells/mL}$

#	c [μM]	$P_{24 \text{ h}}$ 10^5 cells/mL
40x	75.0	4.1
40c	100	2.4
14a	7.5	4.4
14v	50	4.5

SDS in PBS to give a $1 \frac{\text{mg}}{\text{mL}}$ solution. For the click chemistry reaction, premix the click reagents before use. Therefore $0.25 \mu\text{L}$ **38** reagent ($100 \mu\text{L}$ final concentration, 10 mM stock in DMSO), $0.5 \mu\text{L}$ CuSO_4 (1 mM final concentration, 50 mM stock in water), $0.5 \mu\text{L}$ TCEP (1 mM final concentration, 50 mM stock in water), $0.25 \mu\text{L}$ TBTA ($100 \mu\text{L}$ final concentration, 10 mM stock in DMSO). The reagents were vortexed between each addition and after addition of the TCEP solution, 2 min incubation were performed prior to addition of the TBTA solution. Add $1.5 \mu\text{L}$ premix solution to each protein ($25 \mu\text{g}$ protein) sample and shake for 1 h at rt. To stop the reaction, $5 \mu\text{L}$ of 100 mM EDTA stock (in water) were added to each sample, giving a 10 mM final concentration. 2xSDS Page sample loading buffer was added ($10 \mu\text{L}$) and the mixture was vortexed. $10 \mu\text{g}$ crude protein were loaded on a SDS gel and run at 80 V . The gel was fixed with 50% aqueous methanol solution (10% AcOH, 40% MeOH; this helps clean up the gel and fixes it) for 10 min to 1 h and imaged using TAMRA-settings. Next the gel was stained with Coomassie to confirm equal loading with protein sample.

The labelling with **YnC15** was carried out at a final concentration of $100 \mu\text{M}$ for 4 h . The proteins were labelled with TB-Az as described for **YnC12**. The crude proteins were subjected to a SDS gel. The overall efficiency of the labelling with YNC15 was lower than for YNC12.

GPI-Labelling with myristate analogue YNC12 *HL-60*

The GPI-anchored VSG proteins in *HL-60* cells were labelled analogues to *T. brucei*. The inhibitors **40x**, **40c**, **14a** and **14v** were incubated at the same concentrations as used for the *T. brucei* settings (??). Compound **40c** did show some toxicity in *HL60* cells, while all the other compounds did not have any influence on *HL60* cell growth. In contrast to the previous protocol, the cell density was not adjusted prior addition of **YnC12**. **YnC12** was added at a final concentration of $100 \mu\text{M}$. After a further 4 h , the cells were lysed and the proteins purified. The proteins were subjected to TB-Az (**38**) in the following Click-chemistry reaction. According to there cell density after 24 h equal amounts of $10 \mu\text{g}$ protein sample was loaded onto a SDS gel.

P: parasitaemia count; P_{label} ; seeding concentration of *T. brucei*: $1 \cdot 10^6$ cells/mL

#	c [μ M]	$P_{24\ h}$ 10^5 cells/mL	$P_{starvation}$ 10^5 cells/mL
40x	75.0	10.6	20.3
40c	50	20.4	20.3
14a	7.5	36.2	20.3
14v	25	4.05	20.3

9.24 Transferrin uptake after iron starvation

Trypanosomes ($5 \cdot 10^5$ $\frac{\text{cells}}{\text{ml}}$) were incubated with 50 μ M **100a**, 25 μ M Deferoxamine or DMSO in Baltz medium supplemented with 16.7 % heat-inactivated FBS. After 24 h incubation, trypanosomes were harvested and washed three times with Baltz medium supplemented with 2 % BSA. The cells were incubated with 50 $\frac{\mu\text{g}}{\text{ml}}$ fluorescein-labelled transferrin in Baltz medium with 2 % BSA and 100 μ M benzyloxycarbonyl-phenylalanyl-arginyl-diazomethyl ketone (Z-FA-DMK) for 2 h. After washing twice with PBS/1 % glucose, cells were fixed with 2 % formaldehyde/0.05 % glutaraldehyde, and analysed by flow cytometry using a DB Accuri C6 flow cytometer

9.25 Flow cytometry

In order to study the effect on FITC-conjugated transferrin of compounds **14v**, **14a**, **40x** and **40c**, *T. brucei* was pre incubated for 24 h in the presence of the inhibitors (??).^[379] After 24 h, the parasites were starved on transferrin for 2 h, before the FITC-conjugated transferrin was added. Pre-incubation with the inhibitor **14a** resulted only in a minor change on the mean fluorescent intensity. The fluorescence microscopy pictures show that there is still fluorescent signal for the FITC conjugated transferrin (Figure Figure 41).

T. brucei (1×10^6 $\frac{\text{cells}}{\text{mL}}$) were subjected to FITC-labelled transferrin in Baltz-Media containing 2 % BSA and 100 μ M benzyloxycarbonyl-phenylalanyl-arginyl-diazomethyl ketone (Z-FA-DMK). After 2 h of incubation, the parasites were washed two times with PBS supplemented with 1 % glucose. Lastly, the cells were fixed with 2 % formaldehyde/0.05 % glutaraldehyde in PBS. The cells were analysed by flow cytometry using a BD Accuri C6 flow cytometer. The excitation wavelength was set to 488 nm (Filter 530 ± 30 nm). The gates were set to exclude cell fragments and debris from the analysis, if possible 50.000 events were counted.

9.26 Fluorescence microscopy

FITC-labelled cells were applied to poly-L-lysine-coated microscope slides, and treated with 0.0001 % 4,6-diamidino-2-phenylindole (DAPI) in PBS. The slides were washed 6 times with PBS and imaged with a Zeiss Axioplan 2 fluorescence microscope using a Plan-Apochromat 100x/1.4 oil objective.^[379]

9.27 Photo-labelling of *T. brucei* proteins

Lysis of parasites: 1 % Triton X-100 sodiumphosphate pH 8, 0.1 % DSD, 1 % NP40, 50 mM Tris pH 7.4, 150 mM NaCl and 1xEDTA-free protease inh

Abbreviations

L. infantum *Leishmania infantum* spp.

T. brucei *Trypanosoma brucei* spp..

T. cruzi *Trypanosoma cruzi* spp..

AD Alzheimer's disease.

ADME absorption, distribution, metabolism, and excretion.

CHCl₃ chloroform.

CNS central nervous system.

CQ chloroquine.

DAPI 4',6-diamidino-2-phenylindole.

DCC N',N'-dicyclohexylcarbodiimide.

DCU dicyclohexylurea.

DEAD di-*tert*-butylazodicarboxylate.

DIPEA N,N-Diisopropylethylamine.

DMAP 4-dimethylaminopyridine.

DMF dimethylformamide.

DMSO dimethyl sulfoxide.

Dol-P dolichol phosphate.

DPMS dolichol phosphate mannanose synthase.

DTNB 5,5'-dithiobis-(2-nitrobenzoic acid).

DTT dithiothreitol.

ESI electron spray ionisation.

EtOAc ethyl acetate.

EtOH ethanol.

FBS foetal bovine serum.

FITC fluorescein isothiocyanate.

GDP guanosine diphosphate.

GI₅₀ (growth inhibition)₅₀.

GPI Glycosyl Phosphatidyl Innositol.

HAT Human african trypanosomiasis.

HCl hydrochloric acid.

HCV hepatitis C virus.

HOAc acetic acid.

HOMO highest occupied molecular orbital.

HPO hydroxypyridin-4-one.

HPTLC high performance thin layer chromatography.

LiAlH₄ lithium aluminium hydride.

MIC minimum inhibitory concentration.

MMFF94x Merck molecular force field 94x.

MPGS mannosyl-3-phosphoglycerate synthase.

MTT 3-(4,5-dimethylthiazol-2-yl)-2,5-diphenyltetrazolium bromide.

NAD(P)H nicotinamide adenine dinucleotide phosphate.

NaH sodium hydride.

NaN₃ sodium azide.

NaOAc sodium acetate.

NaOH sodium hydroxide.

NEt₃ triethylamine.

NMR Nuclear magnetic resonance.

NOESY nuclear overhauser effect spectroscopy.

PBS phosphate buffered saline.

RPMI Roswell Park Memorial Institute.

rt room temperature.

SCC side scatter.

SDS sodium dodecyl sulphate.

TAMRA tetramethylrhodamine.

tBuONO *tert*-butyl nitrite.

TLC thin layer chromatography.

TsCl tosyl chloride.

UGM UDP-galactopyranose mutase.

UV ultraviolet.

VSG variant surface glycoprotein.

WHO world health organisation.

10 References

- [1] Pink, R.; Hudson, A.; Mouriès, M.-A.; Bendig, M. *Nat. Rev. Drug Discov.* **2005**, *4*, 727–740.
- [2] WHO; *WHO / Chagas disease (American trypanosomiasis)*; 2012. <http://www.who.int/mediacentre/factsheets/fs340/en/index.html>.
- [3] World Health Organization; *The World Health Report 2004: Changing History, Annex Table 3: Burden of disease in DALYs by cause, sex, and mortality stratum in WHO regions, estimates for 2002*; 2004.
- [4] WHO; *Leishmaniasis: The disease and its epidemiology*; 2012. http://www.who.int/leishmaniasis/disease_epidemiology/en/index.html.
- [5] Crompton, D. W. T. *Working to overcome the global impact of neglected tropical diseases*; First WHO report on neglected tropical diseases; Who, 2010.
- [6] WHO; *Human African trypanosomiasis (sleeping sickness)*; 2012. <http://www.who.int/mediacentre/factsheets/fs259/en/>.
- [7] González, M.; Cerecetto, H. *Expert Opin. Ther. Pat.* **2011**, *21*, 699–715.
- [8] Croft, S. L.; Coombs, G. H. *Trends Parasitol.* **2003**, *19*, 502–508.
- [9] Seifert, K. *Open Med. Chem. J.* **2011**, *5*, 31–39.
- [10] Doyle, P. S.; Zhou, Y. M.; Engel, J. C.; McKerrow, J. H. *Antimicrob. Agents Chemother.* **2007**, *51*, 3932–3939.
- [11] Torreele, E.; Bourdin Trunz, B.; Tweats, D.; Kaiser, M.; Brun, R.; Mazué, G.; Bray, M. A.; Pécou, B. *PLoS Negl. Trop. Dis.* **2010**, *4*, e923.
- [12] Mäser, P.; Wittlin, S.; Rottmann, M.; Wenzler, T.; Kaiser, M.; Brun, R. *Curr. Opin. Pharmacol.* **2012**, *12*, 562–566.
- [13] Stuart, K.; Brun, R.; Croft, S.; Fairlamb, A. *J. Clin. Invest.* **2008**, *118*, 1301–1310.
- [14] Barrett, M. P.; Burchmore, R.; Stich, A.; Lazzari, J. O. *The Lancet* **2003**, *362*, 1469–1480.
- [15] Welburn, S. C.; Fèvre, E. M.; Coleman, P. G.; Odiit, M. *Trends Parasitol.* **2001**, *17*, 20–24.

- [16] Tomlinson, S.; Raper, J. *Nat. Biotechnol.* **1996**, *14*, 717–721.
- [17] Tyler, K. M.; Engman, D. M. *Int. J. Parasitol.* **2001**, *31*, 472–481.
- [18] Chandra, S.; Ruhela, D.; Deb, A.; Vishwakarma, R. A. *Expert Opin. Ther. Targets* **2010**, *14*, 739–757.
- [19] Le Blancq, S. M. S.; Peters, W. W. *T. Roy. Trop. Med. H.* **1986**, *80*, 367–377.
- [20] Delespaulx, V.; de Koning, H. P. *Drug Resist. Updat.* **2007**, *10*, 30–50.
- [21] Urbina, J. A.; Docampo, R. *Trends Parasitol.* **2003**, *19*, 495–501.
- [22] Kennedy, P. G. E. *Ann. Neurol.* **2008**, *64*, 116–126.
- [23] Simarro, P. P.; Diarra, A.; Postigo, J.; Franco, J. R. *PLoS Negl. Trop. Dis.* **2011**, *5*, 1–7.
- [24] Jurado, J.; Alejandre-Durán, E.; Pueyo, C. *Mutagenesis* **1993**, *8*, 527–532.
- [25] Moraga, A. A.; Graf, U. *Mutagenesis* **1989**, *4*, 105–110.
- [26] Trouiller, P.; Olliaro, P.; Torreele, E.; Orbinski, J.; Laing, R.; Ford, N. *Lancet* **2002**, *359*, 2188–2194.
- [27] Steverding, D. *Parasit Vectors* **2008**, *1*, 1–8.
- [28] Burri, C.; et al. *57th Meet. Am. Soc. Trop. Med. Hyg* **2008**, Abstract No 542.
- [29] Wenzler, T.; Boykin, D. W.; Ismail, M. A.; Hall, J. E.; Tidwell, R. R.; Brun, R. *Antimicrob. Agents Chemother.* **2009**, *53*, 4185–4192.
- [30] Denise, H.; Barrett, M. P. *Biochem. Pharmacol.* **2001**, *61*, 1–5.
- [31] Mathis, A. M. A.; Bridges, A. S. A.; Ismail, M. A. M.; Kumar, A. A.; Francesconi, I. I.; Anbazhagan, M. M.; Hu, Q. Q.; Tanious, F. A. F.; Wenzler, T. T.; Saulter, J. J.; Wilson, W. D. W.; Brun, R. R.; Boykin, D. W. D.; Tidwell, R. R. R.; Hall, J. E. J. *Antimicrob. Agents Chemother.* **2007**, *51*, 2801–2810.
- [32] Ward, C. P.; Wong, P. E.; Burchmore, R. J.; de Koning, H. P.; Barrett, M. P. *Antimicrob. Agents Chemother.* **2011**, *55*, 2352–2361.
- [33] Kaiser, M.; Bray, M. A.; Cal, M.; Bourdin Trunz, B.; Torreele, E.; Brun, R. *Antimicrob. Agents Chemother.* **2011**, *55*, 5602–5608.
- [34] Brun, R.; Don, R.; Jacobs, R. T.; Wang, M. Z.; Barrett, M. P. *Future Microbiol.* **2011**, *6*, 677–691.

- [35] Moreno, S. N.; Docampo, R. *Environ. Health Perspect.* **1985**, *64*, 199–208.
- [36] Enanga, B.; Ariyanayagam, M. R.; Stewart, M. L.; Barrett, M. P. *Antimicrob. Agents Chemother.* **2003**, 3368–3370.
- [37] Wyllie, S.; Patterson, S.; Stojanovski, L.; Simeons, F. R. C.; Norval, S.; Kime, R.; Read, K. D.; Fairlamb, A. H. *Sci. Transl. Med.* **2012**, *4*, 119re1.
- [38] Jacobs, R. T.; et al. *PLoS Negl. Trop. Dis.* **2011**, *5*, e1151.
- [39] Nare, B.; et al. *Scynexis* **2009**, Poster No. 1.
- [40] Thorens, I.; *Oxaborole Phase I*; 2012. <http://www.dndi.org/press-releases/1169-oxa-phasei.html>.
- [41] Dorlo, T. P. C.; Balasegaram, M.; Beijnen, J. H.; de Vries, P. J. *J. Antimicrob. Chemother.* **2012**, *67*, 2576–2597.
- [42] Croft, S. L.; Engel, J. T. *Roy. Trop. Med. H.* **2006**, *100*, S4–S8.
- [43] Croft, S.; Neal, R. A.; Pendergast, W.; Chan, J. H. *Biochem. Pharmacol.* **1987**, *36*, 2633–2636.
- [44] Saraiva, V. B.; Gibaldi, D.; Previato, J. O.; Mendonça-Previato, L.; Bozza, M. T.; Freire-de Lima, C. G.; Heise, N. *Antimicrob. Agents Chemother.* **2002**, *46*, 3472–3477.
- [45] Yeates, C. *Curr. Opin. Investig. Drugs* **2002**, *3*, 1446–1452.
- [46] Lopez-Martin, C.; Perez-Victoria, J. M.; Carvalho, L.; Castanys, S.; Gamarro, F. *Antimicrob. Agents Chemother.* **2008**, *52*, 4030–4036.
- [47] Garnier, T.; Brown, M. B.; Lawrence, M. J.; Croft, S. L. *J. Pharm. Pharmacol.* **2006**, *58*, 1043–1054.
- [48] Singh, N.; Kumar, M.; Singh, R. K. *Asian Pac. J. Trop. Med.* **2012**, *5*, 485–497.
- [49] Berman, J. *Expert Opin. Investig. Drugs* **2005**, *14*, 1337–1346.
- [50] Coimbra, E. S.; Libong, D.; Cojean, S.; Saint-Pierre-Chazalet, M.; Solgadi, A.; Le Moyec, L.; Duenas-Romero, A. M.; Chaminade, P.; Loiseau, P. M. *J. Antimicrob. Chemother.* **2010**, *65*, 2548–2555.
- [51] A E Vercesi, R. D. *Biochem. J.* **1992**, *284*, 463–467.

- [52] De Vas, M. G.; Portal, P.; Alonso, G. D.; Schlesinger, M.; Flawiá, M. M.; Torres, H. N.; Fernández Villamil, S.; Paveto, C. *Int. J. Parasitol.* **2011**, *41*, 99–108.
- [53] Coura, J. R.; Castro, S. L. d. *Mem. Inst. Oswaldo Cruz* **2002**, *97*, 3–24.
- [54] Buckner, F. S.; Urbina, J. A. *Int. J. Parasitol. Drugs Drug Resist.* **2012**, *2*, 236–242.
- [55] Clayton, J. *Nature* **2010**, *465*, S12–S15.
- [56] Urbina, J. A. *Mem. Inst. Oswaldo Cruz* **2009**, *104 Suppl 1*, 311–318.
- [57] Walker, K. A.; Kertesz, D. J.; Rotstein, D. M.; Swinney, D. C.; Berry, P. W.; So, O. Y.; Webb, A. S.; Watson, D. M.; Mak, A. Y.; Burton, P. M. *J. Med. Chem.* **1993**, *36*, 2235–2237.
- [58] McKerrow, J. H.; Doyle, P. S.; Engel, J. C.; Podust, L. M.; Robertson, S. A.; Ferreira, R.; Saxton, T.; Arkin, M.; Kerr, I. D.; Brinen, L. S.; Craik, C. S. *Mem. Inst. Oswaldo Cruz* **2009**, *104*, 263–269.
- [59] Eakin, A. E.; Mills, A. A.; Harth, G.; McKerrow, J. H.; Craik, C. S. *J. Biol. Chem.* **1992**, *267*, 7411–7420.
- [60] Alvarez, V. E.; Niemirowicz, G. T.; Cazzulo, J. J. *Biochim. Biophys. Acta* **2012**, *1824*, 195–206.
- [61] Steverding, D. *Parasitol. Res.* **1997**, *84*, 59–62.
- [62] Arantes, J. M.; Francisco, A. F.; de Abreu Vieira, P. M.; Silva, M.; Araújo, M. S. S.; de Carvalho, A. T.; Pedrosa, M. L.; Carneiro, C. M.; Tafuri, W. L.; Martins-Filho, O. A.; Elói-Santos, S. M. *Exp. Parasitol.* **2011**, *128*, 401–408.
- [63] Malafaia, G.; Marcon, L. d. N.; Pereira, L. d. F.; Pedrosa, M. L.; Rezende, S. A. *Exp. Parasitol.* **2011**, *127*, 719–723.
- [64] Ferguson, M. A.; Brimacombe, J. S.; Brown, J. R.; Crossman, A.; Dix, A.; Field, R. A.; Güther, M. L.; Milne, K. G.; Sharma, D. K.; Smith, T. K. *Biochim. Biophys. Acta* **1999**, *1455*, 327–340.
- [65] Smith, T. K.; Crossman, A.; Brimacombe, J. S.; Ferguson, M. A. J. *EMBO J.* **2004**, *23*, 4701–4708.
- [66] Neres, J.; Bryce, R. A.; Douglas, K. T. *Drug Discov Today* **2008**, *13*, 110–117.

- [67] Garg, N.; Postan, M.; Mensa-Wilmot, K.; Tarleton, R. L. *Infect. Immun.* **1997**, *65*, 4055–4060.
- [68] Smith, T. K.; Young, B. L.; Denton, H.; Hughes, D. L.; Wagner, G. K. *Bioorg. Med. Chem. Lett.* **2009**, *19*, 1749–1752.
- [69] Ferguson, M. A.; Haldar, K.; Cross, G. A. *J. Biol. Chem.* **1985**, *260*, 4963–4968.
- [70] Nagamune, K.; Nozaki, T.; Maeda, Y.; Ohishi, K.; Fukuma, T.; Hara, T.; Schwarz, R. T.; Sutterlin, C.; Brun, R.; Riezman, H.; Kinoshita, T. *Proc. Natl. Acad. Sci. U.S.A.* **2000**, *97*, 10673–10675.
- [71] Chang, T.; Milne, K. G.; Güther, M. L. S.; Smith, T. K.; Ferguson, M. A. J. *J. Biol. Chem.* **2002**, *277*, 50176–50182.
- [72] Cross, G. A. G. *BioEssays* **1996**, *18*, 283–291.
- [73] Adkin, C.; Butt, T.; Sheader, K.; Rudenko, G. *Mol. Microbiol.* **2005**, *57*, 1608–1622.
- [74] Lillico, S. *Mol. Biol. Cell* **2002**, *14*, 1182–1194.
- [75] Urbaniak, M. D.; Yashunsky, D. V.; Crossman, A.; Nikolaev, A. V.; Ferguson, M. A. J. *ACS Chem. Biol.* **2008**, *3*, 625–634.
- [76] Urbaniak, M. D.; Crossman, A.; Chang, T.; Smith, T. K.; van Aalten, D. M. F.; Ferguson, M. A. J. *J. Biol. Chem.* **2005**, *280*, 22831–22838.
- [77] Abdelwahab, N. Z.; Crossman, A. T.; Sullivan, L.; Ferguson, M. A. J.; Urbaniak, M. D. *Chem. Biol. Drug. Des.* **2012**, *79*, 270–278.
- [78] Helenius, A.; Aebi, M. *Annu. Rev. Biochem.* **2004**, *73*, 1019–1049.
- [79] Herscovics, A.; Orlean, P. *FASEB J.* **1993**, *7*, 540–550.
- [80] Schutzbach, J. S. J. *Glycoconj. J.* **1997**, *14*, 175–182.
- [81] Tomašić, T.; Peterlin Mašič, L. *Expert Opin. Drug Discov.* **2012**, *7*, 549–560.
- [82] Baell, J. B.; Holloway, G. A. *J. Med. Chem.* **2010**, *53*, 2719–2740.
- [83] Mendgen, T.; Steuer, C.; Klein, C. D. *J. Med. Chem.* **2012**, *55*, 743–753.
- [84] Lowe, D. *Chemistry World* **2012**, 21–21.

- [85] Powers, J. P.; Piper, D. E.; Li, Y.; Mayorga, V.; Anzola, J.; Chen, J. M.; Jaen, J. C.; Lee, G.; Liu, J.; Peterson, M. G.; Tonn, G. R.; Ye, Q.; Walker, N. P. C.; Wang, Z. *J. Med. Chem.* **2006**, *49*, 1034–1046.
- [86] Carlson, E. E.; May, J. F.; Kiessling, L. L. *Chem. Biol.* **2006**, *13*, 825–837.
- [87] Carter, P. H.; et al. *Proc. Natl. Acad. Sci. U.S.A.* **2001**, *98*, 11879–11884.
- [88] Huth, J. R.; Mendoza, R.; Olejniczak, E. T.; Johnson, R. W.; Cothron, D. A.; Liu, Y.; Lerner, C. G.; Chen, J.; Hajduk, P. J. *J. Am. Chem. Soc.* **2005**, *127*, 217–224.
- [89] Jacks, A.; Babon, J.; Kelly, G.; Manolaridis, I.; Cary, P. D.; Curry, S.; Conte, M. R. *Structure* **2003**, *11*, 833–843.
- [90] Huth, J. R.; Song, D.; Mendoza, R. R.; Black-Schaefer, C. L.; Mack, J. C.; Dorwin, S. A.; Lador, U. S.; Severin, J. M.; Walter, K. A.; Bartley, D. M.; Hajduk, P. J. *Chem. Res. Toxicol.* **2007**, *20*, 1752–1759.
- [91] Tomašić, T.; Masic, L. P. *Curr. Med. Chem.* **2009**, *16*, 1596–1629.
- [92] Tomašić, T.; Zidar, N.; Kovač, A.; Turk, S.; Simčič, M.; Blanot, D.; Müller Premru, M.; Filipič, M.; Grdadolnik, S. G.; Zega, A.; Anderluh, M.; Gobec, S.; Kikelj, D.; Peterlin Mašič, L. *ChemMedChem* **2010**, *5*, 286–295.
- [93] Tomašić, T.; Zidar, N.; Mueller-Premru, M.; Kikelj, D.; Mašič, L. P. *Eur. J. Med. Chem.* **2010**, *45*, 1667–1672.
- [94] Zidar, N.; Tomašić, T.; Šink, R.; Rupnik, V.; Kovač, A.; Turk, S.; Patin, D.; Blanot, D.; Contreras Martel, C.; Dessen, A.; Müller Premru, M.; Zega, A.; Gobec, S.; Peterlin Mašič, L.; Kikelj, D. *J. Med. Chem.* **2010**, *53*, 6584–6594.
- [95] Tomašić, T.; Kovač, A.; Simčič, M.; Blanot, D.; Grdadolnik, S. G.; Gobec, S.; Kikelj, D.; Mašič, L. P. *Eur. J. Med. Chem.* **2011**, *46*, 3964–3975.
- [96] Zidar, N.; Tomašić, T.; Šink, R.; Kovač, A.; Patin, D.; Blanot, D.; Contreras-Martel, C.; Dessen, A.; Premru, M. M.; Zega, A.; Gobec, S.; Mašič, L. P.; Kikelj, D. *Eur. J. Med. Chem.* **2011**, *46*, 5512–5523.
- [97] Hotta, N.; Kawamori, R.; Fukuda, M.; Shigeta, Y. *Diabetic Med.* **2012**.
- [98] Orchard, M. G.; Neuss, J. C.; Galley, C. M. S.; Carr, A.; Porter, D. W.; Smith, P.; Scopes, D. I. C.; Haydon, D.; Vousden, K.; Stubberfield, C. R.; Young, K.; Page, M. *Bioorg. Med. Chem. Lett.* **2004**, *14*, 3975–3978.

- [99] Pesnot, T.; Palcic, M. M.; Wagner, G. K. *Chembiochem* **2010**, *11*, 1392–1398.
- [100] Soltero-Higgin, M.; Carlson, E. E.; Phillips, J. H.; Kiessling, L. L. *J. Am. Chem. Soc.* **2004**, *126*, 10532–10533.
- [101] Hu, Y.; Helm, J. S.; Chen, L.; Ginsberg, C.; Gross, B.; Kraybill, B.; Tiyanont, K.; Fang, X.; Wu, T.; Walker, S. *Chem. Biol.* **2004**, *11*, 703–711.
- [102] Huang, N.; Nagarsekar, A.; Xia, G.; Hayashi, J.; MacKerell, A. D. *J. Med. Chem.* **2004**, *47*, 3502–3511.
- [103] Helm, J. S.; Hu, Y.; Chen, L.; Gross, B.; Walker, S. *J. Am. Chem. Soc.* **2003**, *125*, 11168–11169.
- [104] Irvine, M. W.; Patrick, G. L.; Kewney, J.; Hastings, S. F.; MacKenzie, S. J. *Bioorg. Med. Chem. Lett.* **2008**, *18*, 2032–2037.
- [105] Nottbohm, A. C.; Hergenrother, P. J. *Phosphate Mimics: Cyclic Compounds*; John Wiley & Sons, Inc.: Hoboken, NJ, USA, 2007.
- [106] Fresneau, P.; Cussac, M.; Morand, J.-M.; Szymonski, B.; Tranqui, D.; Leclerc, G. *J. Med. Chem.* **1998**, *41*, 4706–4715.
- [107] Sem, D. S.; et al. *Chem. Biol.* **2004**, *11*, 185–194.
- [108] Ge, X.; Sem, D. S. *Anal. Biochem.* **2007**, *370*, 171–179.
- [109] Soni, L. K.; Kaskhedikar, S. G. *Chem. Pharm. Bull.* **2007**, *55*, 72–75.
- [110] Maccari, R.; Del Corso, A.; Giglio, M.; Moschini, R.; Mura, U.; Ottanà, R. *Bioorg. Med. Chem. Lett.* **2011**, *21*, 200–203.
- [111] Lepesheva, G. I.; Hargrove, T. Y.; Kleshchenko, Y.; Nes, W. D.; Villalta, F.; Waterman, M. R. *Lipids* **2008**, *43*, 1117–1125.
- [112] Kumar, G.; Banerjee, T.; Kapoor, N.; Surolia, N.; Surolia, A. *IUBMB Life* **2010**, *62*, 204–213.
- [113] Sudo, K.; Matsumoto, Y.; Matsushima, M.; Fujiwara, M.; Konno, K.; Shimotohno, K.; Shigeta, S.; Yokota, T. *Biochem. Biophys. Res. Commun.* **1997**, *238*, 643–647.
- [114] Sing, W. T.; Lee, C. L.; Yeo, S. L.; Lim, S. P.; Sim, M. M. *Bioorg. Med. Chem. Lett.* **2001**, *11*, 91–94.

- [115] Steverding, D.; Baldisserotto, A.; Wang, X.; Marastoni, M. *Exp. Parasitol.* **2011**, *128*, 444–447.
- [116] Cummings, H. E.; et al. *Proc. Natl. Acad. Sci. U.S.A.* **2012**, *109*, 1251–1256.
- [117] Spitzenberg, V.; König, C.; Ulm, S.; Marone, R.; Röpke, L.; Müller, J. P.; Grün, M.; Bauer, R.; Rubio, I.; Wymann, M. P.; Voigt, A.; Wetzker, R. *J. Cancer Res. Clin. Oncol.* **2010**, *136*, 1881–1890.
- [118] Bird, L. *Nat. Rev. Immunol.* **2005**, *5*, 748–748.
- [119] Diaz-Gonzalez, R.; Kuhlmann, F. M.; Galan-Rodriguez, C.; Madeira da Silva, L.; Saldivia, M.; Karver, C. E.; Rodriguez, A.; Beverley, S. M.; Navarro, M.; Pollastri, M. P. *PLoS Negl. Trop. Dis.* **2011**, *5*, e1297.
- [120] Hall, B. S.; Gabernet-Castello, C.; Voak, A.; Goulding, D.; Natesan, S. K.; Field, M. C. *J. Biol. Chem.* **2006**, *281*, 27600–27612.
- [121] Compain, P.; Martin, O. R. *Bioorg. Med. Chem.* **2001**, *9*, 3077–3092.
- [122] Sirivolu, V. R.; Vernekar, S. K. V.; Marchand, C.; Naumova, A.; Chergui, A.; Renaud, A.; Stephen, A. G.; Chen, F.; Sham, Y. Y.; Pommier, Y.; Wang, Z. *J. Med. Chem.* **2012**, *55*, 8671–8684.
- [123] Dakin, L. A.; et al. *Bioorg. Med. Chem. Lett.* **2012**, *22*, 4599–4604.
- [124] Hershko, C.; Peto, T. *J. Exp. Med.* **1988**, *168*, 375–387.
- [125] Atkinson, C. T.; Bayne, M. T.; Gordeuk, V. R.; Brittenham, G. M.; Aikawa, M. *Am. J. Trop. Med. H.* **1991**, *45*, 593–601.
- [126] Taylor, M. C.; Kelly, J. M. *Parasitol.* **2010**, *137*, 899–917.
- [127] Ajayi, W. U.; Chaudhuri, M.; Hill, G. C. *J. Biol. Chem.* **2002**, *277*, 8187–8193.
- [128] Steverding, D. *Parasitol. Int.* **2000**, *48*, 191–198.
- [129] Cohen, A. R. *Blood* **2003**, *102*, 1583–1587.
- [130] Hershko, C.; Gordeuk, V. R.; Thuma, P. E.; Theanacho, E. N.; Spira, D. T.; Hider, R. C.; Peto, T. E.; Brittenham, G. M. *J. Inorg. Biochem.* **1992**, *47*, 267–277.
- [131] Hider, R. C.; LIU, Z. *J. Pharm. Pharmacol.* **1997**, *49*, 59–64.

- [132] Hershko, C.; Theanacho, E. N.; Spira, D. T.; Peter, H. H.; Dobbin, P.; Hider, R. C. *Blood* **1991**, *77*, 637–643.
- [133] Gupta, S.; Nishi *Indian J. Med. Res.* **2011**, *133*, 27–39.
- [134] Bodley, A. L.; McGarry, M. W.; Shapiro, T. A. *J. Inf. Dis.* **1995**, *172*, 1157–1159.
- [135] Keita, M.; Bouteille, B.; Enanga, B.; Vallat, J. M.; Dumas, M. *Exp. Parasitol.* **1997**, *85*, 183–192.
- [136] Grecco, S. S.; Reimão, J. Q.; Tempone, A. G.; Sartorelli, P.; Romoff, P.; Ferreira, M. J. P.; Fávero, O. A.; Lago, J. H. G. *Parasitol. Res.* **2010**, *106*, 1245–1248.
- [137] Reimão, J. Q.; Scotti, M. T.; Tempone, A. G. *Bioorg. Med. Chem.* **2010**, *18*, 8044–8053.
- [138] Vermeersch, M.; da Luz, R. I.; Tote, K.; Timmermans, J. P.; Cos, P.; Maes, L. *Antimicrob. Agents Chemother.* **2009**, *53*, 3855–3859.
- [139] Bonse, S.; Santelli-Rouvier, C.; Barbe, J.; Krauth-Siegel, R. L. *J. Med. Chem.* **1999**, *42*, 5448–5454.
- [140] Dumas, C.; Ouellette, M.; Tovar, J.; Cunningham, M. L.; Fairlamb, A. H.; Tamar, S.; Olivier, M.; Papadopoulou, B. *EMBO J.* **1997**, *16*, 2590–2598.
- [141] Tovar, J.; Cunningham, M. L.; Smith, A. C.; Croft, S.; Fairlamb, A. H. *Proc. Natl. Acad. Sci. U.S.A.* **1998**, *95*, 5311–5316.
- [142] Krieger, S.; Schwarz, W.; Ariyanayagam, M. R.; Fairlamb, A. H.; Krauth-Siegel, R. L.; Clayton, C. *Mol. Microbiol.* **2000**, *35*, 542–552.
- [143] Andres, C. J.; Bronson, J. J.; D’Andrea, S. V.; Deshpande, M. S.; Falk, P. J.; Grant-Young, K. A.; Harte, W. E.; Ho, H. T.; Misco, P. F.; Robertson, J. G.; Stock, D.; Sun, Y. X.; Walsh, A. W. *Bioorg. Med. Chem. Lett.* **2000**, *10*, 715–717.
- [144] Forino, M.; et al. *Proc. Natl. Acad. Sci. U.S.A.* **2005**, *102*, 9499–9504.
- [145] Johnson, S. L.; Jung, D.; Forino, M.; Chen, Y.; Satterthwait, A.; Rozanov, D. V.; Strongin, A. Y.; Pellecchia, M. *J. Med. Chem.* **2006**, *49*, 27–30.
- [146] Bulic, B.; Pickhardt, M.; Khlistunova, I.; Biernat, J.; Mandelkow, E.-M.; Mandelkow, E.; Waldmann, H. *Angew. Chem. Int. Ed.* **2007**, *46*, 9215–9219.
- [147] Ono, M.; Hayashi, S.; Matsumura, K.; Kimura, H.; Okamoto, Y.; Ihara, M.; Takahashi, R.; Mori, H.; Saji, H. *ACS Chem. Neurosci.* **2011**, *2*, 269–275.

- [148] Pocsi, I.; Taylor, S. A.; Richardson, A. C.; Aamlid, K. H.; Smith, BV; Price, R. G. *Clin. Chem.* **1990**, *36*, 1884–1888.
- [149] Gould, S. W. J.; Chadwick, M.; Cuschieri, P.; Easmon, S.; Richardson, A. C.; Price, R. G.; Fielder, M. D. *FEMS Microbiol. Lett.* **2009**, *297*, 10–16.
- [150] Roychoudhury, S. *J. Biomol. Screen.* **2003**, *8*, 555–558.
- [151] Maeda, Y.; Kinoshita, T. *Biochim. Biophys. Acta* **2008**, *1780*, 861–868.
- [152] Tietze, L. F.; Beifuss, U. *Compr Org Syn* **1991**, *2*, 341–392.
- [153] Knoevenagel, E. *Ber. Dtsch. Chem. Ges.* **1898**, *31*, 2596–2619.
- [154] Tanaka, M.; Oota, O.; Hiramatsu, H.; Fujiwara, K. *Bull. Chem. Soc. Jpn.* **1988**, *61*, 2473–2479.
- [155] Hann, R. A. *J. Chem. Soc., Perkin Trans. 1* **1974**, 1379.
- [156] Kunz, F. J.; Margaret, P.; Polansky, O. E. *Chimia* **1970**, *24*, 165–165.
- [157] Albers, H. M. H. G.; van Meeteren, L. A.; Egan, D. A.; van Tilburg, E. W.; Moolenaar, W. H.; Ovaa, H. *J. Med. Chem.* **2010**, *53*, 4958–4967.
- [158] Ohishi, Y.; Mukai, T.; Nagahara, M.; Yajima, M.; Kajikawa, N.; Miyahara, K.; Takano, T. *Chem. Pharm. Bull.* **1990**, *38*, 1911–1919.
- [159] Clayden, J.; Greeves, N.; Warren, S. *Organic Chemistry*, 1st ed.; Oxford University Press, 2012.
- [160] Lee, C. L.; Sim, M. M. *Tetrahedron Lett.* **2000**, *41*, 5729–5732.
- [161] Cutshall, N. S.; ODay, C.; Prezhdo, M. *Bioorg. Med. Chem. Lett.* **2005**, *15*, 3374–3379.
- [162] Momose, Y.; Meguro, K.; Ikeda, H.; Hatanaka, C.; Oi, S.; Sohda, T. *Chem. Pharm. Bull.* **1991**, *39*, 1440–1445.
- [163] Fresneau, P.; Morand, J. M.; Thomasson, F.; Cussac, M. *Spectrochim Acta Part A* **1999**, *55*, 2893–2898.
- [164] Lipinski, C. A.; Lombardo, F.; Dominy, B. W.; Feeney, P. J. *Adv. Drug Deliv. Rev.* **2001**, *46*, 3–26.
- [165] Bhat, B. A.; Ponnala, S.; Sahu, D. P.; Tiwari, P.; Tripathi, B. K.; Srivastava, A. K. *Bioorg. Med. Chem.* **2004**, *12*, 5857–5864.

- [166] Rida, S. M.; Salama, H. M.; Labouta, I. M.; Ghany, Y. S. A. *Pharmazie* **1985**, *40*, 727–728.
- [167] Ohkanda, J.; Buckner, F. S.; Lockman, J. W.; Yokoyama, K.; Carrico, D.; Eastman, R.; de Luca-Fradley, K.; Davies, W.; Croft, S. L.; Van Voorhis, W. C.; Gelb, M. H.; Sebt, S. M.; Hamilton, A. D. *J. Med. Chem.* **2004**, *47*, 432–445.
- [168] Bondi, A. *J. Phys. Chem.* **1964**, *68*, 441–451.
- [169] Gakh, Y. G.; Gakh, A. A.; Gronenborn, A. M. *Magn. Reson. Chem.* **2000**, *38*, 551–558.
- [170] Mallory, F. B. *J. Am. Chem. Soc.* **1973**, 7747–7752.
- [171] Mallory, F. B.; Mallory, C. W.; Baker, M. B. *J. Am. Chem. Soc.* **1990**, *112*, 2577–2581.
- [172] Jaime-Figueroa, S.; Kurz, L. J.; Liu, Y.; Cruz, R. *Spectrochim Acta Part A* **2000**, *56*, 1167–1178.
- [173] Tomita, K.; Oishi, S.; Ohno, H.; Fujii, N. *Biopolymers* **2008**, *90*, 503–511.
- [174] Zuber, F.; Sorkin, E. *Helv. Chim. Acta* **1952**, *35*, 1744–1747.
- [175] Frey, L. F.; Marcantonio, K.; Frantz, D. E.; Murry, J. A.; Tillyer, R. D.; Grabowski, E. J. J.; Reider, P. J. *Tetrahedron Lett.* **2001**, *42*, 6815–6818.
- [176] Giles, R.; Lewis, N.; Quick, J.; Sasse, M.; Urquhart, M.; Youssef, L. *Tetrahedron* **2000**, *56*, 4531–4537.
- [177] Nakamura, K.; Fujii, M.; Ohno, A.; Oka, S. *Tetrahedron Lett.* **1984**, *25*, 3983–3986.
- [178] He, B.; Velaparthi, S.; Pieffet, G.; Pennington, C.; Mahesh, A.; Holzle, D. L.; Brunsteiner, M.; van Breemen, R.; Blond, S. Y.; Petukhov, P. A. *J. Med. Chem.* **2009**, *52*, 7003–7013.
- [179] Weber, P. J. P.; Beck-Sickinger, A. G. A. *J. Pept. Res.* **1997**, *49*, 375–383.
- [180] Fleming, S. A. *Tetrahedron* **1995**, *51*, 12479–12520.
- [181] Neelarapu, R.; Holzle, D. L.; Velaparthi, S.; Bai, H.; Brunsteiner, M.; Blond, S. Y.; Petukhov, P. A. *J. Med. Chem.* **2011**, *54*, 4350–4364.
- [182] Nakayama, K.; Thompson, W. J. *J. Am. Chem. Soc.* **1990**, *112*, 6936–6942.
- [183] Mikus, J.; Steverding, D. *Parasitol. Int.* **2000**, *48*, 265–269.
- [184] Tada, H. H.; Shiho, O. O.; Kuroshima, K. K.; Koyama, M. M.; Tsukamoto, K. K. *J. Immunol. Methods* **1986**, *93*, 157–165.

- [185] Raz, B.; Iten, M.; Grether-Buhler, Y.; Kaminsky, R.; Brun, R. *Acta Tropica* **1997**, *68*, 139–147.
- [186] Collins, S. J. *Blood* **1987**, *70*, 1233–1244.
- [187] Schoonen, W. G. E. J.; Westerink, W. M. A.; de Roos, J. A. D. M.; Débiton, E. *Toxicol. In Vitro* **2005**, *19*, 505–516.
- [188] Ekwall, B.; Silano, V.; Paganuzzi-Stammati, A.; Zucco, F. In *Short-term Toxicity Tests for Non-genotoxic Effects*; John Wiley & Sons Ltd, 1990; pp 75–97.
- [189] Steverding, D.; Wang, X. *Parasit Vectors* **2009**, *2*, 29–33.
- [190] Caffrey, C. R.; et al. *Antimicrob. Agents Chemother.* **2007**, *51*, 2164–2172.
- [191] Croft, S.; Seifert, K.; Yardley, V. *Ind. J. Med. R.* **2012**, 1–12.
- [192] Dolezel, J.; Hirsova, P.; Opletalova, V.; Dohnal, J.; Marcela, V.; Kunes, J.; Jampilek, J. *Molecules* **2009**, *14*, 4197–4212.
- [193] Mikami, K.; Itoh, Y.; Yamanaka, M. *Chem. Rev.* **2004**, *104*, 1–16.
- [194] Exner, O.; Böhm, S. *New J. Chem.* **2008**, *32*, 1449–1453.
- [195] Müller, K.; Faeh, C.; Diederich, F. *Science* **2007**, *317*, 1881–1886.
- [196] Filler, R.; Saha, R. *Future Med. Chem.* **2009**, *1*, 777–791.
- [197] Wang, H.; Hammoudeh, D. I.; Follis, A. V.; Reese, B. E.; Lazo, J. S.; Metallo, S. J.; Prochownik, E. V. *Mol. Cancer Ther.* **2007**, *6*, 2399–2408.
- [198] Stanwell, C.; Ye, B.; Yuspa, S. H.; Burke, T. R. *Biochem. Pharmacol.* **1996**, *52*, 475–480.
- [199] Costi, R.; Santo, R. D.; Artico, M.; Massa, S.; Ragno, R.; Loddò, R.; La Colla, M.; Tramontano, E.; La Colla, P.; Pani, A. *Bioorg. Med. Chem.* **2004**, *12*, 199–215.
- [200] Roberts, C. W.; McLeod, R.; Rice, D. W.; Ginger, M.; Chance, M. L.; Goad, L. J. *Mol. Biochem. Parasitol.* **2003**, *126*, 129–142.
- [201] Scott, A.; Robbins, T. *Ind. Eng. Chem. Anal. Ed.* **1942**, *14*, 206–207.
- [202] Richard, J. V.; Werbovetz, K. A. *Current Opin. Chem. Biol.* **2010**, *14*, 447–455.
- [203] Ferguson, M. A.; Cross, G. A. *J. Biol. Chem.* **1984**, *259*, 3011–3015.
- [204] Cross, G. A. *BioEssays* **1996**, *18*, 283–291.

- [205] Paul, K. S.; Jiang, D.; Morita, Y. S.; Englund, P. T. *Trends Parasitol.* **2001**, *17*, 381–387.
- [206] Heal, W. P.; Jovanovic, B.; Bessin, S.; Wright, M. H.; Magee, A. I.; Tate, E. W. *Chem. Commun. (Camb.)* **2011**, *47*, 4081–4083.
- [207] Buxbaum, L. U.; Milne, K. G.; Werbovetz, K. A.; Englund, P. T. *Proc. Natl. Acad. Sci. U.S.A.* **1996**, *93*, 1178–1183.
- [208] Engstler, M. *J. Cell Sci.* **2004**, *117*, 1105–1115.
- [209] Sheader, K.; Vaughan, S.; Minchin, J.; Hughes, K.; Gull, K.; Rudenko, G. *Proc. Natl. Acad. Sci. U.S.A.* **2005**, *102*, 8716–8721.
- [210] Rudenko, G. *Biochem. Soc. Trans* **2005**, *33*, 981–982.
- [211] Seyfang, A.; Mecke, D.; Duszenko, M. *J. Protozool.* **1990**, *37*, 546–552.
- [212] Fast, B.; Kremp, K.; Boshart, M.; Steverding, D. *Biochem. J.* **1999**, *342 Pt 3*, 691–696.
- [213] Mazhari-Tabrizi, R.; Eckert, V.; Blank, M.; Müller, R.; Mumberg, D.; Funk, M.; Schwarz, R. T. *Biochem. J.* **1996**, *316 (Pt 3)*, 853–858.
- [214] Datta, A. K.; Lehrman, M. A. *J. Biol. Chem.* **1993**, *268*, 12663–12668.
- [215] Lamani, E.; Mewbourne, R. B.; Fletcher, D. S.; Maltsev, S. D.; Danilov, L. L.; Veselovsky, V. V.; Lozanova, A. V.; Grigorieva, N. Y.; Pinsker, O. A.; Xing, J.; Forsee, W. T.; Cheung, H. C.; Schutzbach, J. S.; Shibaev, V. N.; Jedrzejewski, M. J. *Glycobiology* **2006**, *16*, 666–678.
- [216] Chivian, D.; Kim, D. E.; Malmström, L.; Bradley, P.; Robertson, T.; Murphy, P.; Strauss, C. E. M.; Bonneau, R.; Rohl, C. A.; Baker, D. *Proteins* **2003**, *53 Suppl 6*, 524–533.
- [217] Altschul, S. F.; Madden, T. L.; Schäffer, A. A.; Zhang, J.; Zhang, Z.; Miller, W.; Lipman, D. J. *Nucleic Acids Res.* **1997**, *25*, 3389–3402.
- [218] Lundström, J.; Rychlewski, L.; Bujnicki, J. *Protein Sci.* **2001**, 2354–2362.
- [219] Empadinhas, N.; Pereira, P. J. B.; Albuquerque, L.; Costa, J.; Sá-Moura, B.; Marques, A. T.; Macedo-Ribeiro, S.; da Costa, M. S. *Mol. Microbiol.* **2011**, *79*, 76–93.
- [220] Wiederstein, M.; Sippl, M. J. *Nucleic Acids Res.* **2007**, *35*, W407–W410.
- [221] Eisenberg, D. D.; Lüthy, R. R.; Bowie, J. U. J. *Methods Enzymol.* **1997**, *277*, 396–404.
- [222] Wallner, B.; Fang, H.; Elofsson, A. *Proteins* **2003**, *53*, 534–541.

- [223] Chemical Computing Group Inc.; *Molecular Operating Environment (MOE)*, 2011.10; 2011.
- [224] Welsch, M. E.; Snyder, S. A.; Stockwell, B. R. *Current Opin. Chem. Biol.* **2010**, *14*, 347–361.
- [225] Hennig, M.; Munzarova, M. L.; Bermel, W.; Scott, L. G.; Sklenar, V.; Williamson, J. R. *J. Am. Chem. Soc.* **2006**, *128*, 5851–5858.
- [226] Andre, E. *J. Antimicro. Chemother.* **2006**, *57*, 245–251.
- [227] Gualtieri, M. *J. Antimicro. Chemother.* **2006**, *58*, 778–783.
- [228] Lee, J.-Y.; Jeong, K.-W.; Lee, J.-U.; Kang, D.-I.; Kim, Y.-M. *Bull. Korean Chem. Soc.* **2011**, *32*, 1645–1649.
- [229] Mariner, K. R.; Trowbridge, R.; Agarwal, A. K.; Miller, K.; O'Neill, A. J.; Fishwick, C. W. G.; Chopra, I. *Antimicrob. Agents Chemother.* **2010**, *54*, 4506–4509.
- [230] Suree, N.; Yi, S. W.; Thieu, W.; Marohn, M.; Damoiseaux, R.; Chan, A.; Jung, M. E.; Clubb, R. T. *Bioorg. Med. Chem.* **2009**, *17*, 7174–7185.
- [231] Villain-Guillot, P.; Gualtieri, M.; Bastide, L.; Leonetti, J. P. *Antimicrob. Agents Chemother.* **2007**, *51*, 3117–3121.
- [232] Villain-Guillot, P.; Gualtieri, M.; Bastide, L.; Roquet, F.; Martinez, J.; Amblard, M.; Pugniere, M.; Leonetti, J.-P. *J. Med. Chem.* **2007**, *50*, 4195–4204.
- [233] Youssef, A. M.; White, M. S.; Villanueva, E. B.; El-Ashmawy, I. M.; Klegeris, A. *Bioorg. Med. Chem.* **2010**, *18*, 2019–2028.
- [234] Lee, B. *U.S. Pat. Appl. Publ.* **2011**, US2011032336.
- [235] Schultz, T.; Yarbrough, J.; Johnson, E. L. *SAR QSAR Environ Res* **2005**, *16*, 313–322.
- [236] Pomel, V.; et al. *J. Med. Chem.* **2006**, *49*, 3857–3871.
- [237] Wilkowsky, S. E.; Barbieri, M. A.; Stahl, P.; Isola, E. *Exp. Cell Res.* **2001**, *264*, 211–218.
- [238] Stanley, S. A.; Grant, S. S.; Kawate, T.; Iwase, N.; Shimizu, M.; Wivagg, C.; Silvis, M.; Kazyanskaya, E.; Aquadro, J.; Golas, A. *ACS Chem. Biol.* **2012**.
- [239] Khodair, A. I. *J. Heterocyclic Chem.* **2002**, *39*, 1153–1160.

- [240] Lesyk, R.; Zimenkovsky, B.; Subtelna, I.; Nektegayev, I.; Kazmirchuk, G. *Acta Pol. Pharm.* **2009**, *60*, 457–466.
- [241] Anderluh, M.; Jukič, M.; Petrič, R. *Tetrahedron* **2009**, *65*, 344–350.
- [242] Takasu, K.; Inoue, H.; Kim, H.-S.; Suzuki, M.; Shishido, T.; Wataya, Y.; Ihara, M. *J. Med. Chem.* **2002**, *45*, 995–998.
- [243] Klebanov, B. M.; Mikitenko, E. K.; Mogilevich, S. E.; Romanov, N. N. *U.S.S.R. Patent* **1990**, SU1334670A1.
- [244] Hansen, M. M.; Harkness, A. R. *Tetrahedron Lett.* **1994**, *35*, 6971–6974.
- [245] Moreau, F.; Desroy, N.; Genevard, J. M.; Vongsouthi, V.; Gerusz, V.; Le Fralliec, G.; Oliveira, C.; Floquet, S.; Denis, A.; Escaich, S.; Wolf, K.; Busemann, M.; Aschenbrenner, A. *Bioorg. Med. Chem. Lett.* **2008**, *18*, 4022–4026.
- [246] Hwang, J.; Tseitlin, V.; Ramnarayan, K.; Shenderovich, M. D.; Inouye, M. *J. Antibiot.* **2012**, *65*, 237–243.
- [247] Blais, J. D.; Chin, K.-T.; Zito, E.; Zhang, Y.; Heldman, N.; Harding, H. P.; Fass, D.; Thorpe, C.; Ron, D. *J. Biol. Chem.* **2010**, *285*, 20993–21003.
- [248] Liang, Z.; Ding, X.; Ai, J.; Kong, X.; Chen, L.; Chen, L.; Luo, C.; Geng, M.; Liu, H.; Chen, K.; Jiang, H. *Org. Biomol. Chem.* **2012**, *10*, 421–430.
- [249] Huang, H.; Yu, Y.; Gao, Z.; ZHANG, Y.; Li, C.; Xu, X.; Jin, H.; Yan, W.; Ma, R.; Zhu, J. *J. Med. Chem.* **2012**, *55*, 7037–7053.
- [250] Tietze, L. F.; Brumby, T.; Pretor, M.; Remberg, G. *J. Org. Chem.* **1988**, *53*, 810–820.
- [251] Duffy, K. J.; et al. *J. Med. Chem.* **2001**, *44*, 3730–3745.
- [252] Scott, M. D.; Ranz, A.; Kuypers, F. A.; Lubin, B. H.; Meshnick, S. R. *Br. J. Haematol.* **1990**, *75*, 598–602.
- [253] Hider, R. C.; Singh, S.; Porter, J. B.; Huehns, E. R. *Ann. N. Y. Acad. Sci.* **1990**, *612*, 327–338.
- [254] Corrêa, A. F. S.; Andrade, L. R.; Soares, M. J. *Parasitol. Res.* **2002**, *88*, 875–880.
- [255] Coppens, I.; Baudhuin, P.; Opperdoes, F. R.; Courtoy, P. J. *Mol. Biochem. Parasitol.* **1993**, *58*, 223–232.

- [256] Vercesi, A. E.; Rodrigues, C. O.; Catisti, R.; Docampo, R. *FEBS Letters* **2000**, *473*, 203–206.
- [257] Chen, Y.-L.; Barlow, D. J.; Kong, X.-L.; Ma, Y.-M.; Hider, R. C. *Dalton Trans.* **2012**, *41*, 6549–6557.
- [258] Kaschula, C. H.; Egan, T. J.; Hunter, R.; Basilico, N.; Parapini, S.; Taramelli, D.; Pasini, E.; Monti, D. *J. Med. Chem.* **2002**, *45*, 3531–3539.
- [259] Rai, B. L.; Dekhordi, L. S.; Khodr, H.; Jin, Y.; LIU, Z.; Hider, R. C. *J. Med. Chem.* **1998**, *41*, 3347–3359.
- [260] Glans, L.; Hu, W.; Jöst, C.; de Kock, C.; Smith, P. J.; Haukka, M.; Bruhn, H.; Schatzschneider, U.; Nordlander, E. *Dalton Trans.* **2012**, *41*, 6443–6450.
- [261] Dobbin, P. S.; Hider, R. C.; Hall, A. D.; Taylor, P. D.; Sarpong, P.; Porter, J. B.; Xiao, G.; van der Helm, D. *J. Med. Chem.* **1993**, *36*, 2448–2458.
- [262] Breidbach, T.; Scory, S.; Krauth-Siegel, R. L.; Steverding, D. *Int. J. Parasitol.* **2002**, *32*, 473–479.
- [263] Kumar, G.; Parasuraman, P.; Sharma, S. K.; Banerjee, T.; Karmodiya, K.; Surolia, N.; Surolia, A. *J. Med. Chem.* **2007**, *50*, 2665–2675.
- [264] Hee Lee, S.; Stephens, J. L.; Englund, P. T. *Nat. Rev. Micro.* **2007**, *5*, 287–297.
- [265] Ge, X.; Wakim, B.; Sem, D. S. *J. Med. Chem.* **2008**, *51*, 4571–4580.
- [266] Antony, S.; Marchand, C.; Stephen, A. G.; Thibaut, L.; Agama, K. K.; Fisher, R. J.; Pommier, Y. *Nucleic Acids Res.* **2007**, *35*, 4474–4484.
- [267] Ward, C. P.; Burgess, K. E. V.; Burchmore, R. J. S.; Barrett, M. P.; de Koning, H. P. *Mol. Biochem. Parasitol.* **2010**, *174*, 145–149.
- [268] Zhou, J.-F.; Song, Y.-Z.; Zhu, F.-X.; Zhu, Y.-L. *Synth. Commun.* **2006**, *36*, 3297–3303.
- [269] Cantley, L. C.; Vander Matthew G, H.; Christofk, H. R. *PCT Int. Appl.* **2008**, WO2008019139A2.
- [270] Talele, T. T.; Arora, P.; Kulkarni, S. S.; Patel, M. R.; Singh, S.; Chudayeu, M.; Kaushik-Basu, N. *Bioorg. Med. Chem.* **2010**, *18*, 4630–4638.
- [271] Tadao, T.; Masanori, K.; Akio, A.; Tetsuya, M.; Masaki, H.; Hiroshi, T.; Fumio, H.; Takeshi, M. *Eur. Pat. Appl.* **1982**, EP47109A1.

- [272] Hardej, D.; Ashby, C. R., Jr; Khadtare, N. S.; Kulkarni, S. S.; Singh, S.; Talele, T. T. *Eur. J. Med. Chem.* **2010**, *45*, 5827–5832.
- [273] Lo, C.-P.; Shropshire, E. Y. *J. Org. Chem.* **1957**, *22*, 999–1001.
- [274] D'Amico, J. J.; Harman, M. W.; Cooper, R. H. *J. Am. Chem. Soc.* **1957**, *79*, 5270–5276.
- [275] Demchuk, O. G. *Farm. Zh. (Kiev)* **1972**, *27*, 33–35.
- [276] Wilkerson, W. W. *U.S. Pat. Appl. Publ.* **1994**, US5326770A.
- [277] Brooker, L. G. S.; White, F. L.; Keyes, G. *Eur. Pat. Appl.* **1948**, GB606141.
- [278] Kallenberg, S. *Ber. Dtsch. Chem. Ges. B* **1919**, *52B*, 2057–2071.
- [279] Demchuk, I. L.; Horishny, V. Y.; Nektehayev, I. O. *Farm. Zh. (Kiev)* **2010**, 64–68.
- [280] Dasgupta, R.; Gonsalves, F. *PCT Int. Appl.* **2009**, WO2009097113A2.
- [281] Turkevich, B. M. *Khim. Geterotsikl. Soedin.* **1966**, 212–215.
- [282] Sato, M.; Matsumoto, T.; Ushiki, Y.; Nishimura, K. *Jpn. Kokai Tokkyo Koho* **2003**, 8–10.
- [283] Mckee, T. D.; Suto, R. K.; Tibbitts, T.; Sowadski, J. *PCT Int. Appl.* **2004**, WO2004028535A1.
- [284] Francis, C. V.; White, K. M.; Newmark, R. A.; Stephens, M. G. *Macromolecules* **1993**, *26*, 4379–4380.
- [285] Taniyama, H.; Yasui, B.; Takehara, N.; Uchida, H. *Yakugaku Zasshi* **1959**, *79*, 1465–1468.
- [286] Turkevich, B. M. *Khim. Geterotsikl. Soedin.* **1967**, 476–80.
- [287] Kovalev, Y. D. *Farm. Zh. (Kiev)* **1972**, *27*, 38–41.
- [288] Carpino, L. A.; Han, G. Y. *J. Org. Chem.* **1972**, *37*, 3404–3409.
- [289] Turkevich, N. M.; Ganitkevich, M. I. *Zh. Obshch. Khim.* **1959**, *29*, 1699–702.
- [290] Rapson, W. S.; Robinson, R. *J. Chem. Soc.* **1935**, 1533–1533.
- [291] Hodgetts, K. J.; Wallace, T. W. *Synth. Commun.* **1994**, *24*, 1151–1155.
- [292] Soll, R. M.; Dollings, P. J.; Mitchell, R. D.; Hafner, D. A. *Eur. J. Med. Chem.* **1994**, *29*, 223–232.

- [293] Shih, N. Y.; Blythin, D. J. *U.S. Pat. Appl. Publ.* **1990**, US4897397A.
- [294] Gabillet, S.; Lecerclé, D.; Loreau, O.; Carboni, M.; Dézard, S.; Gomis, J.-M.; Taran, F. *Org Lett* **2007**, *9*, 3925–3927.
- [295] Brown, F. C.; Bradsher, C. K.; Bond, S. M.; Potter, M. *J. Am. Chem. Soc.* **1951**, *73*, 2357–2359.
- [296] Allan, F. J.; Allan, G. G. *J. Heterocyclic Chem.* **1970**, *7*, 1091–1094.
- [297] Zubenko, V. G.; Turkevich, N. M. *Zh. Obshch. Khim.* **1957**, *27*, 3275–3278.
- [298] Turkevich, B. M. *Farm. Zh. (Kiev)* **1960**, *15*, 15–20.
- [299] Kiprianov, A. I.; Mushkalo, I. L. *Zh. Org. Khim.* **1965**, *1*, 750–755.
- [300] Smith, J. W.; Richardson, R. D. *U.S. Pat. Appl. Publ.* **2007**, US20070203236A1.
- [301] Eberly, F. A.; Dains, F. B. *J. Am. Chem. Soc.* **1936**, *58*, 2544–2547.
- [302] Mousseron, M. J. *U.S. Pat. Appl. Publ.* **1972**, US3704296A.
- [303] Allan, F. J.; Allan, G. G.; Thomson, J. B. *Recl. Trav. Chim. Pays-Bas Belg.* **1961**, *80*, 403–408.
- [304] Wang, K. K.; Yuen, P.-w. *U.S. Pat. Appl. Publ.* **1996**, US5554767A.
- [305] Russell, A. J.; Westwood, I. M.; Crawford, M. H. J.; Robinson, J.; Kawamura, A.; Redfield, C.; Laurieri, N.; Lowe, E. D.; Davies, S. G.; Sim, E. *Bioorg. Med. Chem.* **2009**, *17*, 905–918.
- [306] Ootake, Y.; Horio, Y.; Matsumoto, J.; Takahashi, T.; Agata, M.; Goto, M. *Jpn. Kokai Tokkyo Koho* **1993**, 13–15.
- [307] Cetenko, W. A.; Connor, D. T.; Sorenson, R. J.; Unangst, P. C.; Stabler, S. R. *Eur. Pat. Appl.* **1989**, EP343643A2.
- [308] Kulkarni, Y. D.; Kumar, B. *Biol. Mem.* **1984**, *9*, 200–203.
- [309] Kidd, D. A. A.; Wright, D. E. *J. Chem. Soc.* **1962**, 1420–1420.
- [310] Taniyama, H.; Takemura, S. *Yakugaku Zasshi* **1953**, *73*, 164–165.
- [311] Hu, B.; Jetter, J.; Kaufman, D.; Singhaus, R.; Bernotas, R.; Unwalla, R.; Quinet, E.; Savio, D.; Halpern, A.; Basso, M.; Keith, J. *Bioorg. Med. Chem.* **2007**, *15*, 3321 – 3333.

- [312] Pinson, J.-A.; Schmidt-Kittler, O.; Zhu, J.; Jennings, I. G.; Kinzler, K. W.; Vogelstein, B.; Chalmers, D. K.; Thompson, P. E. *ChemMedChem* **2011**, *6*, 514–522.
- [313] Lilly, Eli *U.S. Pat. Appl. Publ.* **1996**, US5523314.
- [314] Bursavich, M. G.; Gilbert, A. M.; Lombardi, S.; Georgiadis, K. E.; Reifenberg, E.; Flannery, C. R.; Morris, E. A. *Bioorg. Med. Chem. Lett.* **2007**, *17*, 1185–1188.
- [315] Alegaon, S. G.; Alagawadi, K. R. *Med. Chem. Res.* **2012**, *21*, 3214–3223.
- [316] Graef, I. A.; Alhamadsheh, M. *U.S. Pat. Appl. Publ.* **2011**, WO2011–140333.
- [317] Bruno, G.; Costantino, L.; Curinga, C.; Maccari, R.; Monforte, F.; Nicolo, F.; Ottanà, R.; Vigorita, M. G. *Bioorg. Med. Chem.* **2002**, *10*, 1077 – 1084.
- [318] Ginak, A. I.; Aronova, E. V.; Rutto, M. V. *Russ. J. Appl. Chem.* **2001**, *74*, 1604 – 1605.
- [319] Sarkar, A.; Banerjee, P.; Hossain, S. U.; Bhattacharya, S.; Bhattacharya, S. C. *Spectrochim Acta Part A* **2009**, *72*, 1097 – 1102.
- [320] Maccari, R.; Ottanà, R.; Curinga, C.; Vigorita, M. G.; Rakowitz, D.; Steindl, T.; Langer, T. *Bioorg. Med. Chem.* **2005**, *13*, 2809–2823.
- [321] Luo, Y.; Ma, L.; Zheng, H.; Chen, L.; Li, R.; He, C.; Yang, S.; Ye, X.; Chen, Z.; Han, J.; He, G.; Yang, L.; Wei, Y.; Li, Z.; Gao, Y. *J. Med. Chem.* **2010**, *53*, 273 – 281.
- [322] Jeong, T.-S.; Kim, J.-R.; Kim, K. S.; Cho, K.-H.; Bae, K.-H.; Lee, W. S. *Bioorg. Med. Chem.* **2004**, *12*, 4017–4023.
- [323] Maccari, R.; Paoli, P.; Ottanà, R.; Jacomelli, M.; Ciurleo, R.; Manao, G.; Steindl, T.; Langer, T.; Vigorita, M. G.; Camici, G. *Bioorg. Med. Chem.* **2007**, *15*, 5137 – 5149.
- [324] Kaarsholm, N. C.; Madsen, P.; Schlein, M.; Olsen, H. B.; Havelund, S.; Steensgaard, D. B.; Ludvigsen, S.; Jakobsen, P.; Petersen, A. K.; Schluckebier, G. *U.S. Pat. Appl. Publ.* **2005**, US2005–65066.
- [325] Fan, C.; Vederas, J. C.; Clay, M. D.; Deyholos, M. K. *Bioorg. Med. Chem.* **2010**, *18*, 2141 – 2151.
- [326] Bourahla, K.; Derdour, A. Ä.; Rahmouni, M.; Carreaux, F. o.; Bazureau, J. P. *Tetrahedron Lett.* **2007**, *48*, 5785–5789.
- [327] Naegele, H. *Monatsh Chem* **1912**, *33*, 941–965.

- [328] Hassaneen, H. M.; Shawali, A. S.; Farag, D. S.; Ahmed, E. M. *Phosphorus Sulfur Silicon Relat. Elem.* **1996**, *113*, 53 – 58.
- [329] Khan, M. H.; Haque, R.; Safi, A.; Nizamuddin *Indian J. Chem. Sect. B* **1998**, *37*, 1069 – 1074.
- [330] Turkewitsch; Wladimirskaja *Zh. Obshch. Khim.* **1957**, *27*, 1348–1349.
- [331] Nizamuddin, M.; Mishra, M.; Srivastava, M. K.; Khan, M. H. *Indian J. Chem. Sect. B* **2001**, *40*, 49 – 53.
- [332] Smirnova, N. A.; Rakhman, I.; Moroz, N.; Basso, M.; Payappilly, J.; Ratan, R. R.; Gazaryan, I. G.; Kazakov, S.; Hernandez-Guzman, F.; Gaisina, I. N.; Kozikowski, A. P. *Chem. Biol.* **2010**, *17*, 380 – 391.
- [333] Carroll, R. T.; Dluzen, D. E.; Stinnett, H.; Awale, P. S.; Geldenhuys, W. J.; Funk, M. O. *Bioorg. Med. Chem. Lett.* **2011**, *21*, 4798 – 4803.
- [334] Zvarec, O.; Tieu, W.; Kuan, K.; Pedersen, D. S.; Abell, A. D.; Polyak, S. W.; Morona, R.; Booker, G. W.; Dai, H.; Zhang, L. *Bioorg. Med. Chem. Lett.* **2012**, *22*, 2720 – 2722.
- [335] Sortino, M.; Delgado, P.; Juárez, S.; Quiroga, J.; Abonía, R.; Insuasty, B.; Noguerras, M.; Rodero, L.; Garibotto, F. M.; Enriz, R. D.; Zacchino, S. A. *Bioorg. Med. Chem.* **2007**, *15*, 484–494.
- [336] Subasi, E.; Ercag, A.; Sert, S.; Senturk, O. S. *Synth. React. Inorg. Met.-Org. Nan.* **2006**, *36*, 705 – 712.
- [337] Ibrahim, T. M.; Donia, S. G.; Essawy, S. A. *Egypt. J. Chem.* **1994**, *37*, 405 – 412.
- [338] Joshi, M.; Vargas, C.; Boisguerin, P.; Diehl, A.; Krause, G.; Schmieder, P.; Moelling, K.; Hagen, V.; Schade, M.; Oschkinat, H. *Angew. Chem. Int. Ed.* **2006**, *45*, 3790 – 3795.
- [339] Wang, Y.; Ji, K.; Lan, S.; Zhang, L. *Angew. Chem. Int. Ed.* **2012**, *51*, 1915 – 1918.
- [340] Sohda, T.; Mizuno, K.; Hirata, T.; Maki, Y.; Kawamatsu, Y. *Chem. Pharm. Bull.* **1983**, *31*, 560 – 569.
- [341] Rakowitz, D.; Maccari, R.; Ottanà, R.; Vigorita, M. G. *Bioorg. Med. Chem.* **2006**, *14*, 567 – 574.
- [342] Vyunov, K. A.; Ginak, A. I.; Sochilin, E. G. *Chem. Heterocycl. Compd.* **1971**, *7*, 175–176.
- [343] Girard, M. L.; Dreux, C. *Bull. Soc. Chim. Fr.* **1968**, 3461 – 3468.

- [344] Jawale, D. V.; Pratap, U. R.; Mane, R. A. *Bioorg. Med. Chem. Lett.* **2012**, *22*, 924 – 928.
- [345] Lo, C.-P. *J. Am. Chem. Soc.* **1958**, *80*, 3466–3468.
- [346] Kambe, S. *Bull. Chem. Soc. Jpn.* **1973**, *46*, 2926–2928.
- [347] Hashimoto, N. *JP Patent* **1964**, JP39010345B4.
- [348] Besyadets'ka, O. I. *Farm. Zh. (Kiev)* **1967**, *22*, 9–11.
- [349] Neelarapu, R.; Holzle, D. L.; Velaparthi, S.; Bai, H.; Brunsteiner, M.; Blond, S. Y.; Petukhov, P. A. *J. Med. Chem.* **2011**, *54*, 4350–4364.
- [350] Ren, T.; Wang, L.; Zhang, J.; Li, G. *Faming Zhuanli Shenqing* **2012**, 16–18.
- [351] Moreau, F.; Desroy, N.; Genevard, J. M.; Vongsouthi, V.; Gerusz, V.; Le Fralliec, G.; Oliveira, C.; Floquet, S.; Denis, A.; Escaich, S.; Wolf, K.; Busemann, M.; Aschenbrenner, A. *Bioorg. Med. Chem. Lett.* **2008**, *18*, 4022–4026.
- [352] Lugovkin, B. P. *Zh. Obshch. Khim.* **1974**, *44*, 1038–1041.
- [353] Liu, L.; Zhong, Y.; Zhang, P.; Jiang, X.; Wang, R. *J. Org. Chem.* **2012**, *77*, 10228–10234.
- [354] Tanaka, N.; Yamagata, M.; Tanabe, T. *Jpn. Kokai Tokkyo Koho* **2007**, 18–20.
- [355] Nayak, A.; Mittra, A. S. *J. Indian Chem. Soc.* **1978**, *55*, 593–597.
- [356] Beiles, R. G.; Beiles, E. M. *Zh. Obshch. Khim.* **1963**, *33*, 190–192.
- [357] Fukawa, J.; Kobayashi, A.; Hosoi, J. *Jpn. Kokai Tokkyo Koho* **1992**, 21–23.
- [358] Johnson, S. M.; Petrassi, H. M.; Palaninathan, S. K.; Mohamedmohaideen, N. N.; Purkey, H. E.; Nichols, C.; Chiang, K. P.; Walkup, T.; Sacchettini, J. C.; Sharpless, K. B.; Kelly, J. W. *J. Med. Chem.* **2005**, *48*, 1576–1587.
- [359] Chattaway, F. D.; Clemo, G. R. *J. Chem. Soc., Trans.* **1923**, *123*, 3041–3041.
- [360] Nanda, S.; Pati, D.; Mitra, A. S.; Rout, M. K. *J. Indian Chem. Soc.* **1963**, *40*, 833–838.
- [361] Kedia, P.; Singh, V.; Singh, P.; Singh, M.; Upadhyay, V.; Singh, D. *J. Ultra Chem.* **2009**, *5*, 271–278.
- [362] Trusevich, N. D.; Pravotorova, L. A.; Pivnenko, N. S.; Lavrushin, V. F. *Ukr. Khim. Zh. (Russ. Ed.)* **1980**, *46*, 642–645.

- [363] Zea, A.; Alba, A.-N. R.; Mazzanti, A.; Moyano, A.; Rios, R. *Org. Biomol. Chem.* **2011**, *9*, 6519–6523.
- [364] Mauthner, F. *Ann.* **1913**, *395*, 273–281.
- [365] Huang, H.; Yu, Y.; Gao, Z.; Zhang, Y.; Li, C.; Xu, X.; Jin, H.; Yan, W.; Ma, R.; Zhu, J.; Shen, X.; Jiang, H.; Chen, L.; Li, J. *J. Med. Chem.* **2012**, *55*, 7037–7053.
- [366] Gemzova, I.; Gemza, E. *Chem. Prum.* **1972**, *22*, 621–614.
- [367] Thomas, M. C.; Zauli, G.; Secchiero, P.; Fabris, B.; Bernardi, S. *PCT Int. Appl.* **2012**, WO2012117336A2.
- [368] Michaelis, A.; Horn, H. *Justus Liebigs Ann. Chem.* **1910**, *373*, 213–218.
- [369] Huang, H.; Yu, Y.; Gao, Z.; Zhang, Y.; Li, C.; Xu, X.; Jin, H.; Yan, W.; Ma, R.; Zhu, J.; Shen, X.; Jiang, H.; Chen, L.; Li, J. *J. Med. Chem.* **2012**, *55*, 7037–7053.
- [370] Jung, M. E.; Ku, J.-M.; Du, L.; Hu, H.; Gatti, R. A. *Bioorg. Med. Chem. Lett.* **2011**, *21*, 5842–5848.
- [371] Abdelhamid, A. O.; Abdel-Riheem, N. A.; El-Idreesy, T. T.; Rashdan, H. R. M. *Eur. J. Chem.* **2012**, *3*, 322–331.
- [372] Liu, M.; Xin, Z.; Clampit, J. E.; Wang, S.; Gum, R. J.; Haasch, D. L.; Trevillyan, J. M.; Abad-Zapatero, C.; Fry, E. H.; Sham, H. L.; Liu, G. *Bioorg. Med. Chem. Lett.* **2006**, *16*, 2590–2594.
- [373] Aminake, M. N.; Mahajan, A.; Kumar, V.; Hans, R.; Wiesner, L.; Taylor, D.; de Kock, C.; Grobler, A.; Smith, P. J.; Kirschner, M.; Rethwilm, A.; Pradel, G.; Chibale, K. *Bioorg. Med. Chem.* **2012**, *20*, 5277–5289.
- [374] Chaves, S.; Marques, S. M.; Matos, A. M. F.; Nunes, A.; Gano, L.; Tuccinardi, T.; Martinelli, A.; Santos, M. A. *Chem. Eur. J.* **2010**, *16*, 10535–10545.
- [375] Steverding, D.; Sexton, D. W.; Wang, X.; Gehrke, S. S.; Wagner, G. K.; Caffrey, C. R. *Int. J. Parasitol.* **2012**, *42*, 481–488.
- [376] Kesper, N.; de Almeida, K. A.; Stolf, A. M.; Umezawa, E. S. *J. Parasitol.* **2000**, *86*, 862–867.
- [377] Stauber, L. A.; Franchino, E. M.; Grun, J. *J. Eukaryotic Microbiol.* **1958**, *5*, 269–273.

- [378] Price, H. P.; Hodgkinson, M. R.; Wright, M. H.; Tate, E. W.; Smith, B. A.; Carrington, M.; Stark, M.; Smith, D. F. *Biochim. Biophys. Acta* **2012**, 1823, 1178–1191.
- [379] Steverding, D.; Sexton, D. W.; Chrysochoidi, N.; Cao, F. *Mol. Biochem. Parasitol.* **2012**, 1–30.

11 Appendices

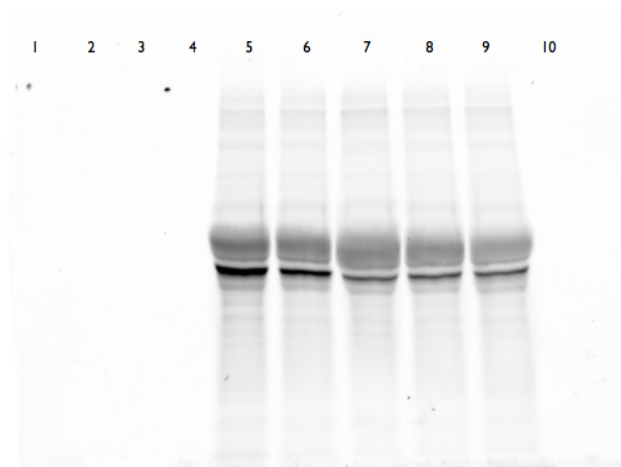


Figure 80: SDS gel visualised with Tamra-Channel settings; lane 1:SB, lane 2: SD, lane 3: SB, lane 4: DMSO, lane 5: **40x**, lane 6: **14v**, lane 7: **40c**, lane 8: **14a**, lane 9+10: SB

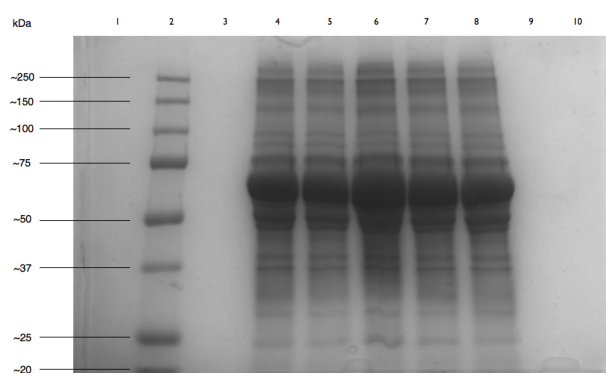


Figure 81: SDS gel visualised with Coomassie stain; lane 1:SB, lane 2: SD, lane 3: SB, lane 4: DMSO, lane 5: **40x**, lane 6: **14v**, lane 7: **40c**, lane 8: **14a**, lane 9+10: SB

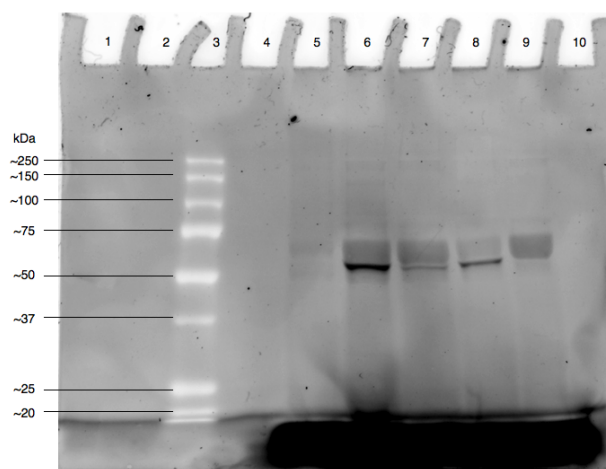


Figure 82: in-gel fluorescence after 24 h incubation with inhibitors and 4 h **YnC12** labelling using TAMRA settings; lane 1: SB, lane 2: SB, lane 3: SD, lane 4: SB, lane 5: negative control (-**YnC12**), lane 6: positive control (DMSO), lane 7: **40x**, lane 8: **14a**, lane 9: **14v**, lane 10: SB.

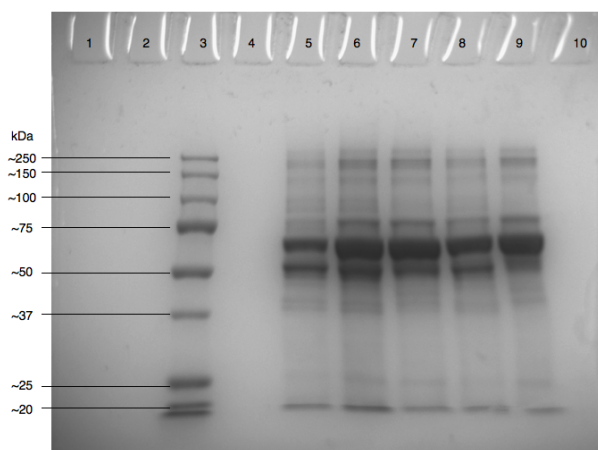


Figure 83: Coomassie stain after 24 h incubation with inhibitors and 4 h **YnC12** labelling using TAMRA settings; lane 1: SB, lane 2: SB, lane 3: SD, lane 4: SB, lane 5: negative control (-**YnC12**), lane 6: positive control (DMSO), lane 7: **40x**, lane 8: **14a**, lane 9: **14v**, lane 10: SB.

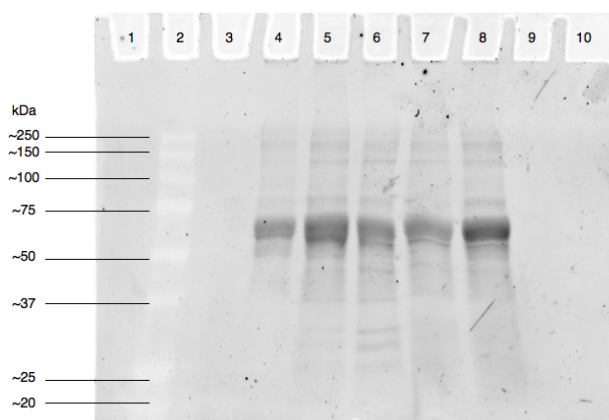


Figure 84: in-gel fluorescence: Tamra settings; lane 1: SB, lane 2: SD, lane 3: SB, lane 4: negative control, lane 5: DMSO, lane 6: **40x**, lane 7: **14a**, lane 8: **40c**, lane 9: SB, lane 10: SB.

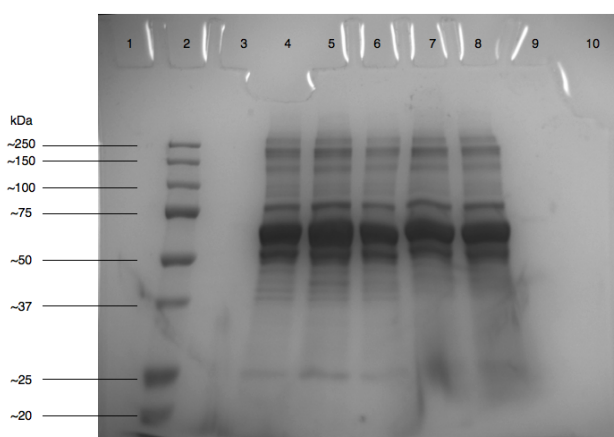


Figure 85: Coomassie staining; lane 1: SB, lane 2: SD, lane 3: SB, lane 4: negative control, lane 5: DMSO, lane 6: **40x**, lane 7: **14a**, lane 8: **40c**, lane 9: SB, lane 10: SB.

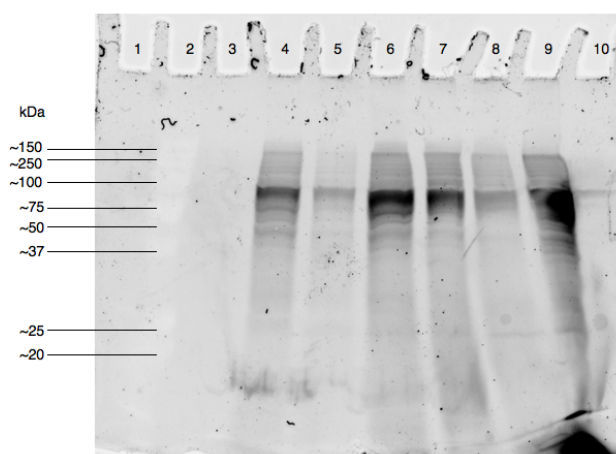


Figure 86: in-gel fluorescence: Tamra setting; lane 1: SB, lane 2: SD, lane 3: SB, lane 4: negative control (absence of **YnC15**), lane 5: DMSO, lane 6: **14a**, lane 7: **14v**, lane 8: **40x**, lane 9: **40c**, lane 10: SB.

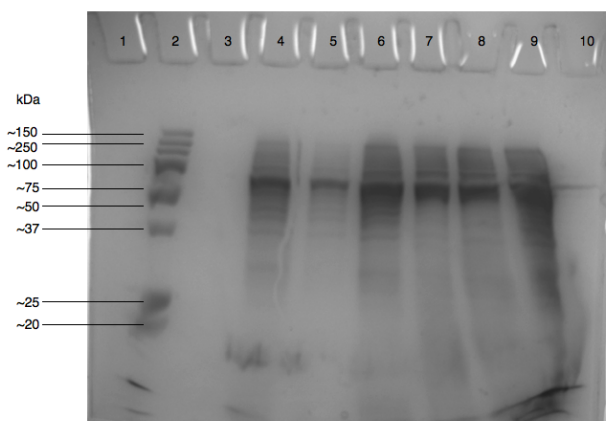


Figure 87: Coomassie stain; lane 1: SB, lane 2: SD, lane 3: SB, lane 4: negative control (absence of **YnC15**), lane 5: DMSO, lane 6: **14a**, lane 7: **14v**, lane 8: **40x**, lane 9: **40c**, lane 10: SB.

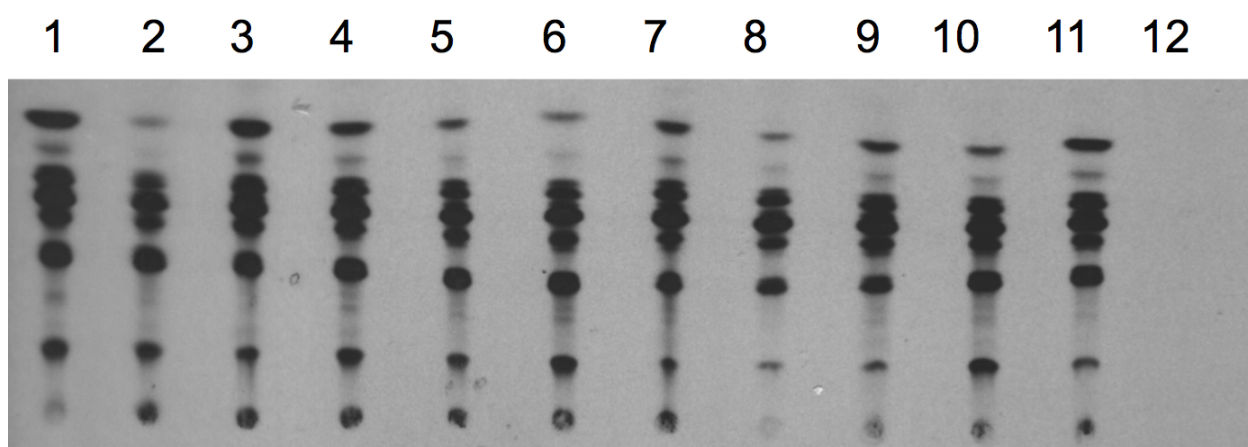


Figure 88: HPTLC of GPI synthesis radio-label assay (Plate 1); lane 1: control; lane 2 **54v**; lane 3: **54w**; lane 4: **54a**; lane 5: **54i**; lane 6: **54h**; lane 7: **54q**; lane 8: **54r**; lane 9: **54u**; lane 10: **54s**; lane 11: **54c**; lane 12: **54x** (failed).

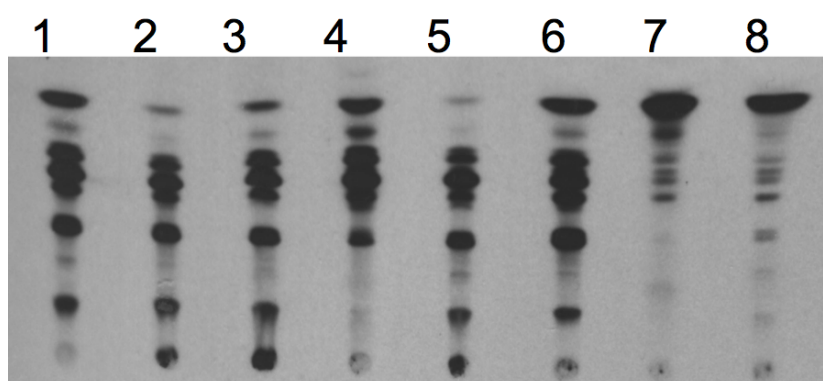


Figure 89: HPTLC of GPI synthesis radio-label assay (Plate 2); lane 1: control; lane 2 **54l**; lane 3: **54ab**; lane 4: **54b**; lane 5: **54d**; lane 6: unknown; lane 7: unknown; lane 8: unknown.

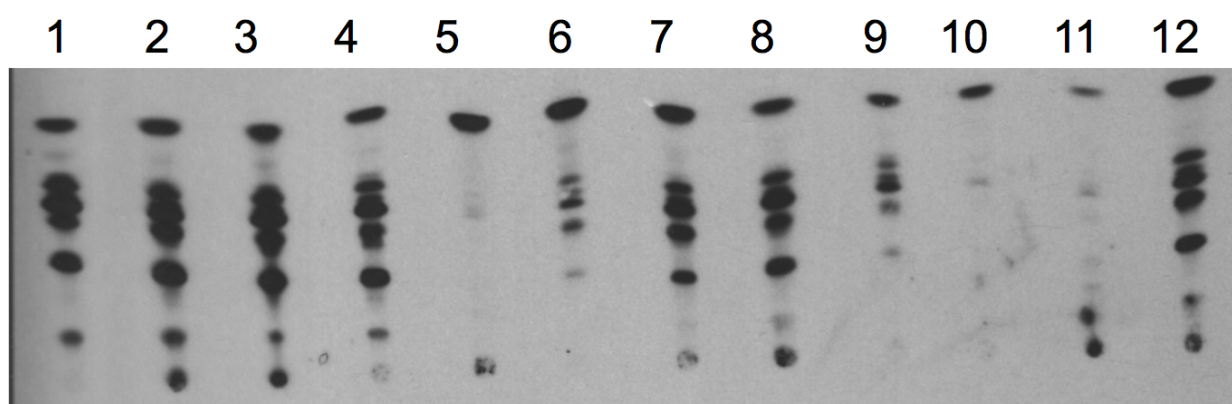


Figure 90: HPTLC of GPI synthesis radio-label assay (Plate 3); lane 1: control; lane 2: **55r**; lane 3: **55z**; lane 4: **55q**; lane 5: **36c**; lane 6: **36k**; lane 7: **36af**; lane 8: **36ad**; lane 9: **36w**; lane 10: **36f**; lane 11: **36t**; lane 12: **36y**.

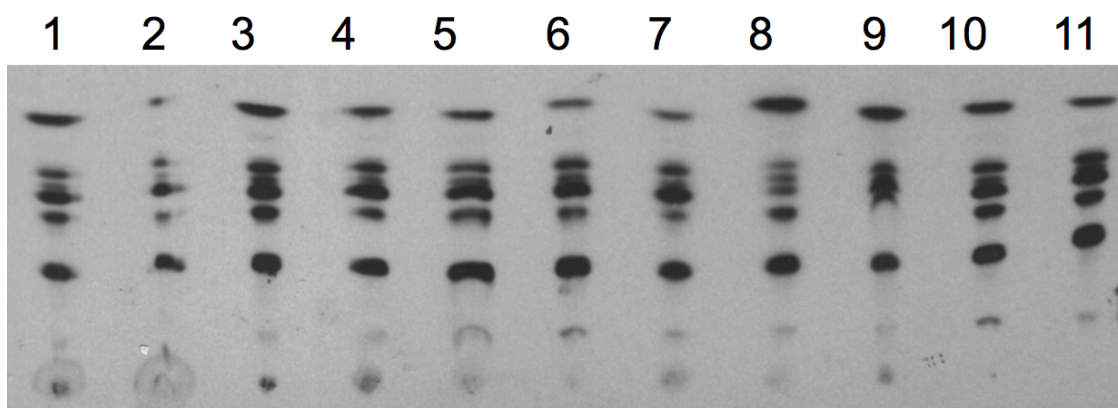


Figure 91: HPTLC of GPI synthesis radio-label assay (Plate 4); lane 1: **43c**; lane 2: **43b**; lane 3: **40v**; lane 4: **40f**; lane 5: **40y**; lane 6: **40z**; lane 7: **40g**; lane 8: **40x**; lane 9: **40h**; lane 10: **43a**; lane 11: **40i**.

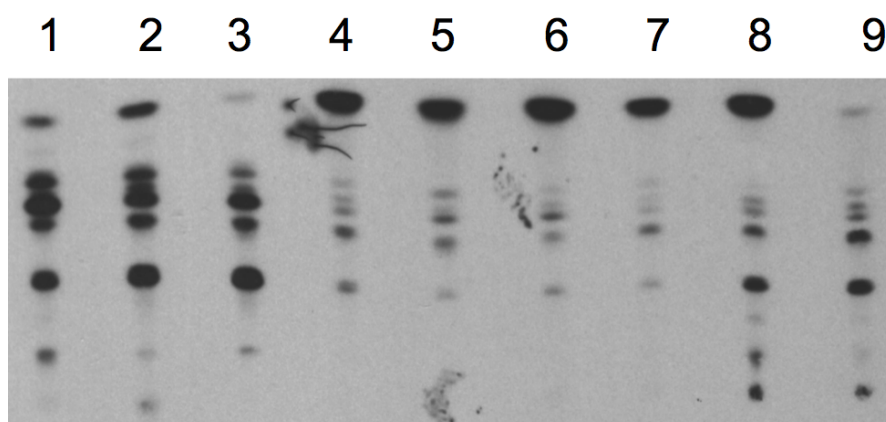


Figure 92: HPTLC of GPI synthesis radio-label assay (Plate 5); lane 1: control; lane 2: **40e**; lane 3: **40m**; lane 4: **2a**; lane 5: **2b**; lane 6: **2c**; lane 7: **2e**; lane 8: **2g**; lane 9: **2f**.

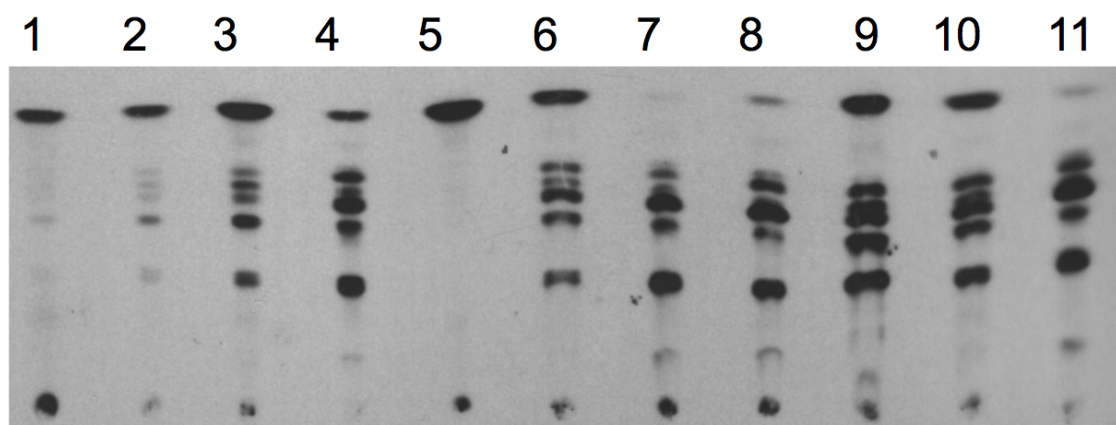


Figure 93: HPTLC of GPI synthesis radio-label assay (Plate 6); lane 1: **2q**; lane 2: **2p**; lane 3: **2o**; lane 4: **2r**; lane 5: **2m**; lane 6: **2h**; lane 7: **26d**; lane 8: **26c**; lane 9: **2u**; lane 10: **2s**; lane 11: **2n**.

Crystal and structure refinement data for
 3-allyl-5-(3-pyridinylmethylene)-2-thioxo-1,3-thiazolidin-4-one

Identification code	sebasg1
Elemental formula	C12 H10 N2 O S2
Formula weight	262.3
Crystal system	Triclinic
Space group	P-1
Unit cell dimensions	a = 6.7307(2) Å α = 83.733(2) ° b = 7.1089(2) Å β = 76.293(3) ° c = 13.3937(4) Å γ = 71.237(3) °
Volume	589.14(3) Å ³
No. of formula units, Z	2
Calculated density	1.479 Mg/m ³
F(000)	272
Absorption coefficient	0.435 mm ⁻¹
Temperature	140(1) K
Wavelength	0.71073 Å
Crystal colour, shape	pale yellow prism
Crystal size	0.38 x 0.13 x 0.10 mm
Crystal mounting	on a glass fibre, in oil, fixed in cold N ₂ stream
On the diffractometer:	
Theta range for data collection	3.1 to 27.5 °
Limiting indices	-8<=h<=8, -9<=k<=9, -17<=l<=17
Completeness to theta = 27.5	99.9 %
Absorption correction	Semi-empirical from equivalents
Max. and min. transmission	1.044 and 0.972
Reflections collected (not including absences)	13507
No. of unique reflections	2708 [R(int) for equivalents = 0.044]
No. of 'observed' reflections (I > 2 σ _I)	2135
Structure determined by:	direct methods, in SHELXS
Refinement:	Full-matrix least-squares on F ² , in SHELXL
Data / restraints / parameters	2708 / 0 / 163

Goodness-of-fit on F^2	1.012
Final R indices ('observed' data)	$R_1 = 0.034$, $wR_2 = 0.082$
Final R indices (all data)	$R_1 = 0.054$, $wR_2 = 0.086$
Reflections weighted: $w = [\sigma^2(F_o^2) + (0.0515P)^2]^{-1}$ where $P = (F_o^2 + 2F_c^2)/3$	
Largest diff. peak and hole	0.36 and -0.22 e. \AA^{-3}
Location of largest difference peak	on S(2)-C(3) bond

Table 1. Atomic coordinates ($\times 10^4$) and equivalent isotropic displacement parameters ($\text{\AA}^2 \times 10^4$). $U(\text{eq})$ is defined as one third of the trace of the orthogonalized U_{ij} tensor. E.s.ds are in parentheses.

	x	y	z	$U(\text{eq})$	S.o.f.#
C(1)	6637(2)	7693(2)	3965.5(13)	211(3)	
C(10)	6327(2)	7093(2)	4963.4(13)	219(3)	
C(11)	4315(3)	7204(2)	5703.1(12)	221(3)	
C(12)	2272(3)	8011(3)	5486.3(14)	292(4)	
N(13)	434(2)	8126(2)	6176.6(13)	390(4)	
C(14)	612(3)	7395(3)	7123.7(16)	389(5)	
C(15)	2544(3)	6553(3)	7419.3(14)	379(5)	
C(16)	4414(3)	6463(2)	6703.5(14)	291(4)	
S(2)	4766.7(6)	8820.3(6)	3203.9(3)	246.7(12)	
C(3)	6758(3)	8953(2)	2120.7(13)	263(4)	
S(3)	6170.4(9)	9909.9(8)	1020.6(4)	450(2)	
N(4)	8752(2)	8189.7(19)	2337.8(11)	244(3)	
C(41)	10738(3)	8093(3)	1556.6(14)	348(4)	
C(42)	11172(5)	6477(5)	811(2)	338(9)	0.668(7)
C(43)	12819(6)	4884(5)	767(3)	431(10)	0.668(7)
C(42X)	11970(10)	5964(9)	1210(6)	312(18)*	0.332(7)
C(43X)	12091(11)	5516(11)	298(7)	444(21)*	0.332(7)
C(5)	8846(3)	7431(2)	3340.7(13)	228(3)	
O(5)	10511.1(18)	6672.1(17)	3623.3(10)	312(3)	

- site occupancy, if different from 1.

* - $U(\text{iso})$ ($\text{\AA}^2 \times 10^4$)

Table 2. Molecular dimensions. Bond lengths are in Ångstroms, angles in degrees. E.s.ds are in parentheses.

C(1)-C(10)	1.346(2)	S(2)-C(3)	1.7436(17)
C(1)-S(2)	1.7458(16)	C(3)-S(3)	1.6353(17)
C(1)-C(5)	1.487(2)	C(3)-N(4)	1.365(2)
C(10)-C(11)	1.461(2)	N(4)-C(41)	1.477(2)
C(11)-C(12)	1.397(2)	N(4)-C(5)	1.400(2)
C(11)-C(16)	1.394(2)	C(41)-C(42)	1.517(3)
C(12)-N(13)	1.342(2)	C(42)-C(43)	1.300(6)
N(13)-C(14)	1.335(3)	C(41)-C(42X)	1.535(6)
C(14)-C(15)	1.378(3)	C(42X)-C(43X)	1.273(13)
C(15)-C(16)	1.377(2)	C(5)-O(5)	1.2076(19)
C(10)-C(1)-S(2)	129.89(12)	S(3)-C(3)-S(2)	121.70(10)
C(10)-C(1)-C(5)	120.52(14)	N(4)-C(3)-S(2)	110.99(12)
C(5)-C(1)-S(2)	109.59(12)	N(4)-C(3)-S(3)	127.31(13)
C(1)-C(10)-C(11)	129.13(15)	C(3)-N(4)-C(41)	122.53(15)
C(12)-C(11)-C(10)	124.82(15)	C(3)-N(4)-C(5)	116.73(13)
C(16)-C(11)-C(10)	118.37(15)	C(5)-N(4)-C(41)	120.71(15)
C(16)-C(11)-C(12)	116.80(15)	N(4)-C(41)-C(42)	109.95(16)
N(13)-C(12)-C(11)	124.23(17)	C(43)-C(42)-C(41)	121.5(3)
C(14)-N(13)-C(12)	116.73(17)	N(4)-C(41)-C(42X)	112.1(2)
N(13)-C(14)-C(15)	123.89(17)	C(43X)-C(42X)-C(41)	119.4(7)
C(16)-C(15)-C(14)	118.62(17)	N(4)-C(5)-C(1)	109.90(14)
C(15)-C(16)-C(11)	119.73(17)	O(5)-C(5)-C(1)	126.88(15)
C(3)-S(2)-C(1)	92.77(8)	O(5)-C(5)-N(4)	123.22(15)

Table 3. Anisotropic displacement parameters ($\text{\AA}^2 \times 10^4$) for the expression:

$$\exp \{-2\pi^2(h^2a^{*2}U_{11} + \dots + 2hka^*b^*U_{12})\}$$

E.s.ds are in parentheses.

	U_{11}	U_{22}	U_{33}	U_{23}	U_{13}	U_{12}
C(1)	185(8)	204(7)	263(8)	-18(6)	-73(6)	-66(6)
C(10)	196(8)	188(7)	275(9)	-16(6)	-72(6)	-43(6)
C(11)	252(8)	170(7)	243(8)	-21(6)	-36(6)	-73(6)
C(12)	246(9)	363(9)	255(9)	22(7)	-38(7)	-98(7)
N(13)	299(9)	449(9)	390(10)	-35(7)	13(7)	-127(7)
C(14)	362(11)	346(10)	408(12)	-72(8)	98(9)	-149(8)
C(15)	579(13)	315(9)	206(9)	18(7)	16(8)	-167(9)
C(16)	315(9)	258(8)	285(9)	11(7)	-76(7)	-67(7)
S(2)	193(2)	315(2)	246(2)	21(2)	-78(2)	-84(2)
C(3)	284(9)	321(8)	234(9)	4(7)	-72(7)	-151(7)
S(3)	464(3)	697(4)	260(3)	112(2)	-159(2)	-258(3)
N(4)	221(7)	291(7)	238(7)	-19(6)	-31(5)	-116(6)
C(41)	302(10)	427(10)	313(10)	-32(8)	59(8)	-191(8)
C(42)	269(16)	462(18)	241(16)	-27(13)	-5(12)	-87(13)
C(43)	443(19)	446(19)	334(19)	11(14)	-11(14)	-100(16)
C(5)	221(8)	217(7)	263(9)	-23(6)	-52(6)	-84(6)
O(5)	201(6)	369(7)	358(7)	29(5)	-75(5)	-80(5)

Table 4. Hydrogen coordinates ($\times 10^4$) and isotropic displacement parameters ($\text{\AA}^2 \times 10^3$). All hydrogen atoms were included in idealised positions with $U(\text{iso})$'s set at $1.2 \cdot U(\text{eq})$ of the parent carbon atom.

	x	y	z	U(iso)	S.o.f.#
H(10)	7568	6528	5218	26	
H(12)	2178	8500	4821	35	
H(14)	-643	7457	7613	47	
H(15)	2586	6057	8088	45	
H(16)	5737	5910	6887	35	
H(41A)	11938	7813	1891	42	0.668(7)
H(41B)	10589	9364	1185	42	0.668(7)
H(41X)	11656	8604	1838	42	0.332(7)
H(41Y)	10372	8934	965	42	0.332(7)
H(42)	10239	6628	374	41	0.668(7)
H(43A)	13763	4716	1200	52	0.668(7)
H(43B)	13052	3913	304	52	0.668(7)
H(42X)	12623	5010	1663	37	0.332(7)
H(43X)	11437	6475	-152	53	0.332(7)
H(43Y)	12835	4230	82	53	0.332(7)

- Site occupancy, if different from 1.

Table 5. Torsion angles, in degrees. E.s.ds are in parentheses.

C(5)-C(1)-C(10)-C(11)	-179.71(14)	S(2)-C(3)-N(4)-C(5)	1.22(18)
S(2)-C(1)-C(10)-C(11)	0.3(3)	S(3)-C(3)-N(4)-C(41)	-1.3(2)
C(1)-C(10)-C(11)-C(16)	179.64(15)	S(2)-C(3)-N(4)-C(41)	179.26(12)
C(1)-C(10)-C(11)-C(12)	-0.6(3)	C(3)-N(4)-C(41)-C(42)	-73.1(2)
C(16)-C(11)-C(12)-N(13)	0.6(3)	C(5)-N(4)-C(41)-C(42)	104.8(2)
C(10)-C(11)-C(12)-N(13)	-179.16(16)	N(4)-C(41)-C(42)-C(43)	-113.1(3)
C(11)-C(12)-N(13)-C(14)	-0.7(3)	C(3)-N(4)-C(41)-C(42X)	-106.6(4)
C(12)-N(13)-C(14)-C(15)	0.1(3)	C(5)-N(4)-C(41)-C(42X)	71.4(4)
N(13)-C(14)-C(15)-C(16)	0.4(3)	N(4)-C(41)-C(42X)-C(43X)	111.7(5)
C(14)-C(15)-C(16)-C(11)	-0.5(3)	C(3)-N(4)-C(5)-O(5)	178.17(15)
C(12)-C(11)-C(16)-C(15)	0.0(2)	C(41)-N(4)-C(5)-O(5)	0.1(2)
C(10)-C(11)-C(16)-C(15)	179.77(15)	C(3)-N(4)-C(5)-C(1)	-1.29(19)
C(10)-C(1)-S(2)-C(3)	179.84(15)	C(41)-N(4)-C(5)-C(1)	-179.37(13)
C(5)-C(1)-S(2)-C(3)	-0.11(12)	C(10)-C(1)-C(5)-O(5)	1.4(3)
C(1)-S(2)-C(3)-N(4)	-0.59(13)	S(2)-C(1)-C(5)-O(5)	-178.67(14)
C(1)-S(2)-C(3)-S(3)	179.90(11)	C(10)-C(1)-C(5)-N(4)	-179.19(13)
S(3)-C(3)-N(4)-C(5)	-179.31(12)	S(2)-C(1)-C(5)-N(4)	0.76(15)

Crystal structure analysis of 3-allyl-5-(3-pyridinylmethylene)-2-thioxo-1,3-thiazolidin-4-one

Crystal data: C₁₂H₁₀N₂OS₂, M = 262.3. Triclinic, space group P-1 (no. 2), a = 6.7307(2), b = 7.1089(2), c = 13.3937(4) Å, α = 83.733(2), β = 76.293(3), γ = 71.237(3)°, V = 589.14(3) Å³. Z = 2, D_c = 1.479 g cm⁻³, F(000) = 272, T = 140(1) K, μ(Mo-Kα) = 4.4 cm⁻¹, λ(Mo-Kα) = 0.71069 Å.

Crystals are pale yellow prisms. From a sample under oil, one, ca 0.38 x 0.13 x 0.10 mm, was mounted on a glass fibre and fixed in the cold nitrogen stream on an Oxford Diffraction Xcalibur-3 CCD diffractometer equipped with Mo-Kα radiation and graphite monochromator. Intensity data were measured by thin-slice ω- and φ-scans. Total no. of reflections recorded, to θ_{max} = 27.5°, was 13507 of which 2708 were unique (R_{int} = 0.044); 2135 were 'observed' with I > 2σ_I.

Data were processed using the CrysAlisPro-CCD and -RED (1) programs. The structure was determined by the direct methods routines in the SHELXS program (2A) and refined by full-matrix least-squares methods, on F²'s, in SHELXL (2B). The non-hydrogen atoms were refined with anisotropic thermal parameters. Hydrogen atoms were included in idealised positions and their U_{iso} values were set to ride on the U_{eq} values of the parent carbon atoms. At the conclusion of the refinement, wR₂ = 0.086 and R₁ = 0.054 (2B) for all 2708 reflections weighted w = [σ²(F_o²) + (0.0515P)²]⁻¹ with P = (F_o² + 2F_c²)/3; for the 'observed' data only, R₁ = 0.034.

In the final difference map, the highest peak (ca 0.36 eÅ⁻³) was on the S(2)-C(3) bond.

Scattering factors for neutral atoms were taken from reference (3). Computer programs used in this analysis have been noted above, and were run through WinGX (4) on a Dell Precision 370 PC at the University of East Anglia.

References

- (1) Programs CrysAlisPro-CCD and -RED, Oxford Diffraction Ltd., Abingdon, UK (2008).
- (2) G. M. Sheldrick, SHELX-97 – Programs for crystal structure determination (SHELXS) and refinement (SHELXL), *Acta Cryst.* (2008) A64, 112-122.
- (3) 'International Tables for X-ray Crystallography', Kluwer Academic Publishers, Dordrecht (1992). Vol. C, pp. 500, 219 and 193.

- (4) L. J. Farrugia, *J. Appl. Cryst.*, (1999) **32**, 837-838 .

Legends for Figures

- Figure 1. View of a molecule of 3-allyl-5-(3-pyridinylmethylene)-2-thioxo-1,3-thiazolidin-4-one, indicating the atom numbering scheme. Thermal ellipsoids are drawn at the 50% probability level.
- Figure 2. Stacking of molecules up the *b* axis.
- Figure 3. Overlap of the stacked molecules of Figure 2, viewed on to the plane of the pyridine ring.
- Figure 4a and b. Overlap of pairs of molecules, above and below the principal molecule, projected on to the plane of the pyridine ring.

Notes on the structure

Except for part of the allyl group, the molecule is essentially planar.

The allyl group is disordered in two distinct (and resolved) orientations, Figure 1.

There is stacking of molecules along the *b* axis, Figure 2. On each side of the principal molecule, there is a molecule related by a centre of symmetry. There is an offset in the alignment of alternate molecules along the stacked columns, as shown in Figure 3, *e.g.* between the atoms labelled S3 and S3³. The distances between the overlapping ring systems are *ca* 3.41 Å (as in the pair in Figure 4a) and 3.45 Å (for the pair in Figure 4b).

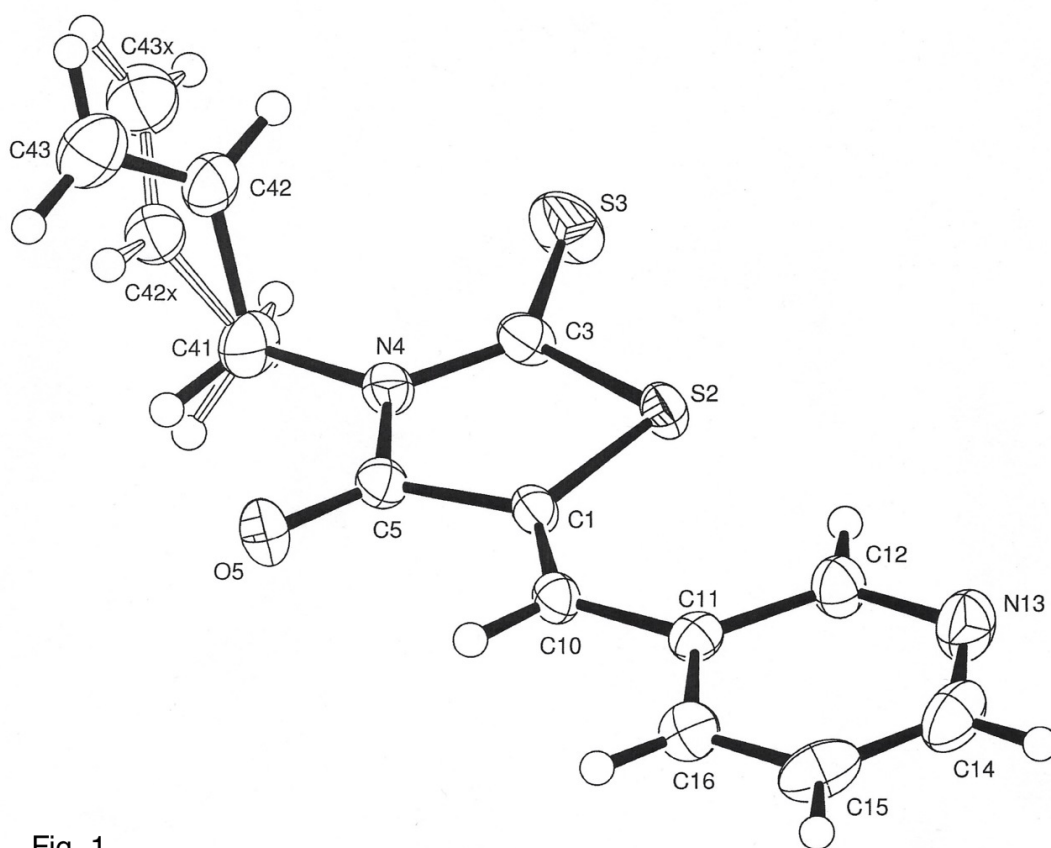


Fig. 1

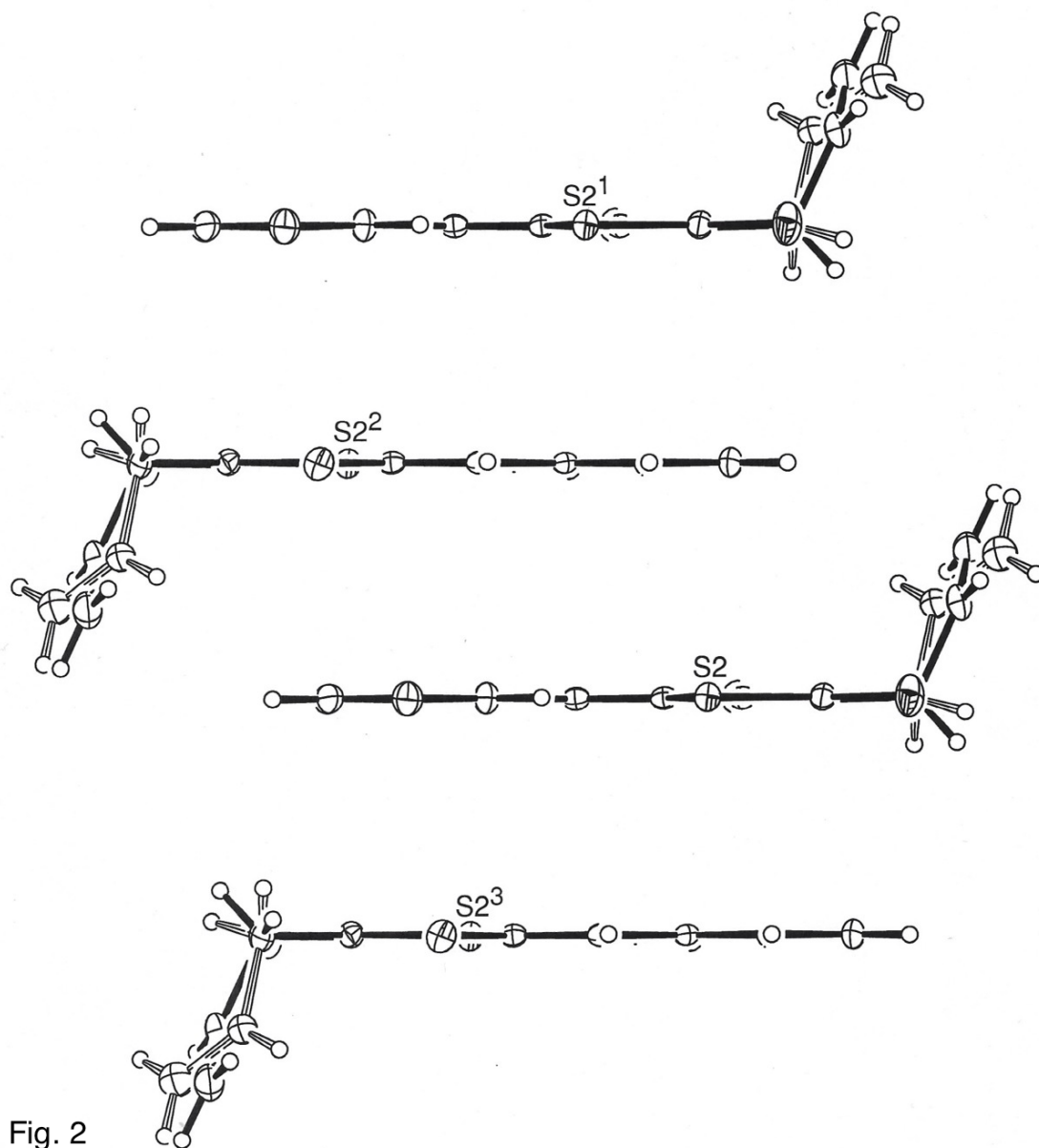


Fig. 2

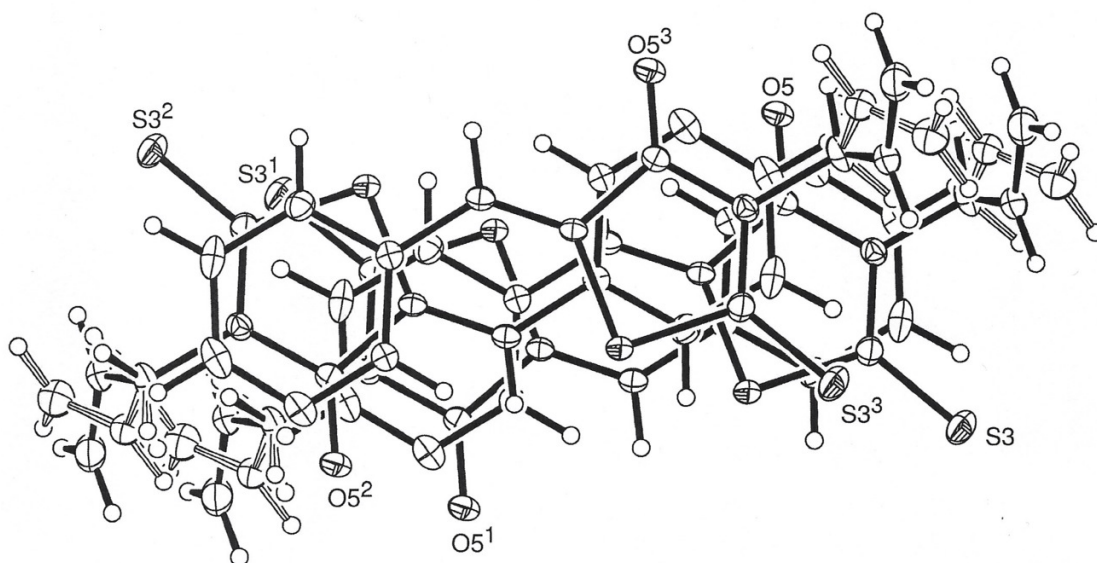


Fig. 3

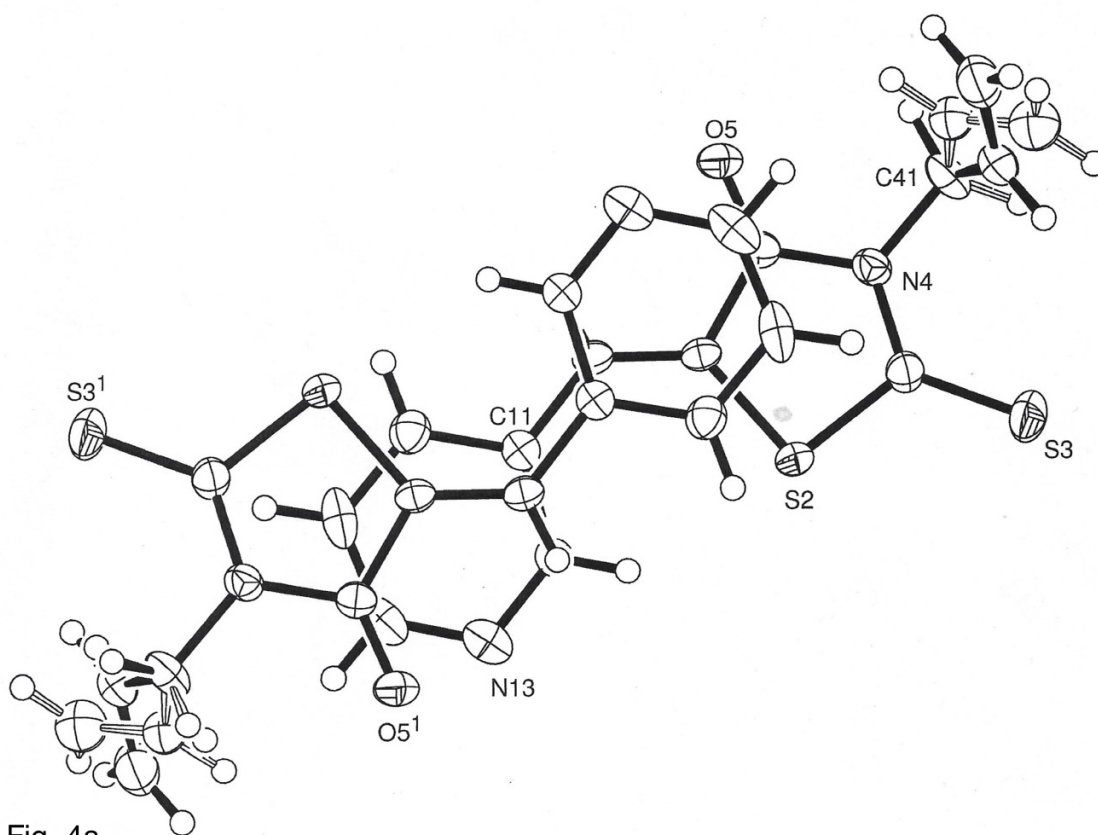


Fig. 4a

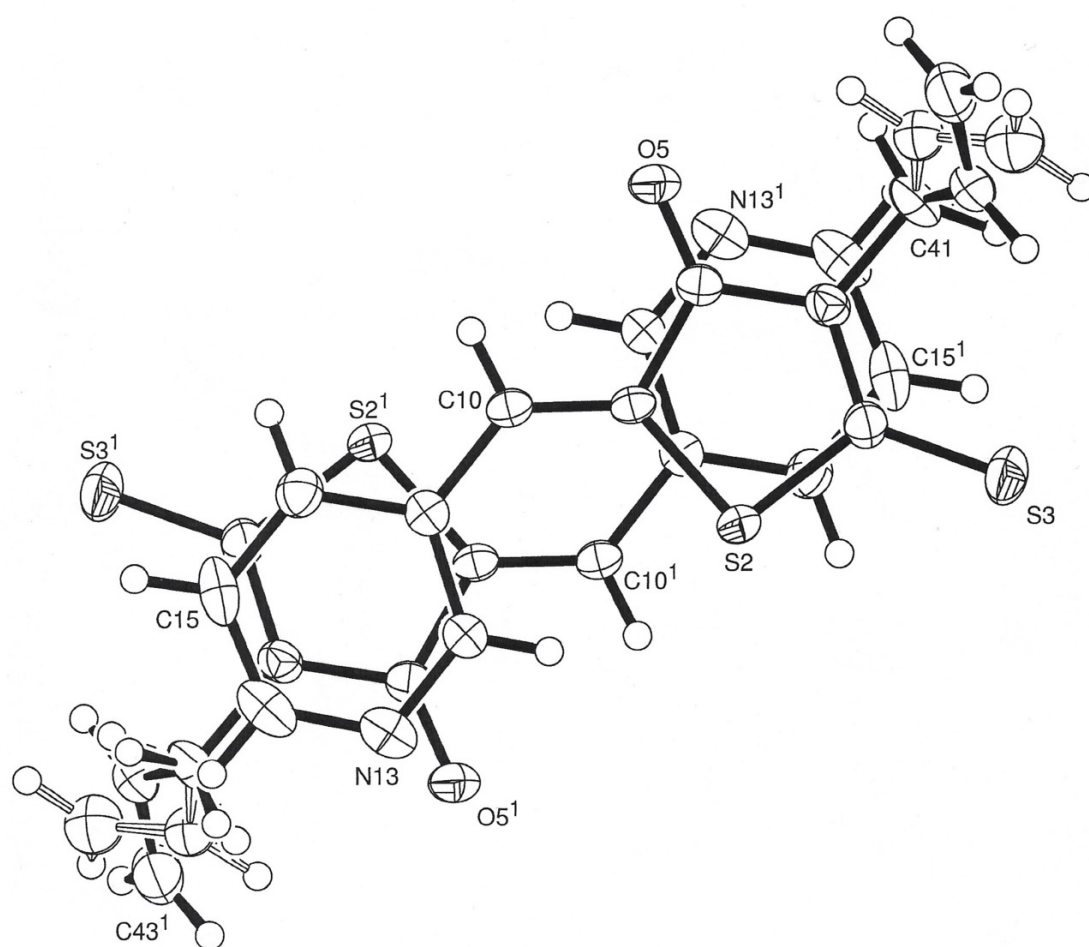


Fig. 4b